Complexation of Various Fragrance Materials with 2-Hydroxypropyl-β-cyclodextrin

Hajime MATSUDA,*[,a] Kenzo ITO,[a] Yumiko FUJIWARA,[a] Muneo TANAKA,[a] Akio TAKI,[b] Osamu UEJIMA[b] and Hideyuki SUMIYOSHI[b]

Shiseido Research Laboratories,[a] 1050, Nippa-cho, Kohoku-ku, Yokohama 223, Japan and Nihon Shokuhin Kako Co., Ltd.,[b] 30, Tajima, Fuji, Shizuoka 417, Japan. *Received May 9, 1990*

2-Hydroxypropyl-β-cyclodextrin (2HP-β-CD) is more soluble in water than α, β, or γ cyclodextrin. Although water-insoluble substances are dissolved by surfactants, the surfactants induced a number of problems. Therefore, we have studied a method for dissolving water-insoluble perfumes using 2HP-β-CD, without the need of a surfactant.

First, complexes of various perfumes with 2HP-β-CD were prepared, and the solubilized amount of the perfumes was determined by high-performance liquid chromatography (HPLC). As a result, water-insoluble perfumes were dissolved in water by 2HP-β-CD, even though a surfactant was not used.

The use of proton nuclear magnetic resonance (^{1}H-NMR) confirmed that these dissolution phenomena were based on the inclusion mechanism.

Next, factors which caused differences in the inclusion among perfumes were discussed. Among the perfumes with a hydroxide (OH) group and an aromatic ester group and perfumes of low molecular weight (150—160), some perfumes were highly soluble. Obtaining the stability constant (*Ke'*) through Higuchi's formula confirmed that the solubilization of perfumes was dependent on the concentration. It was proven that the solubilized amount of perfumes is in close relation with the addition of 2HP-β-CD, in other words, the apparent stability constant.

Keywords 2-hydroxypropyl-β-cyclodextrin; 2HP-β-CD; fragrance material; cosmetic; ^{1}H-NMR; solubility; solubilized amount; substitution degree; stability constant

Surfactants in cosmetic preparations have been regarded as important raw materials for use in emulsion, dispersion, and solubilization techniques for many years. However, studies on surfactants used as a solubilizing agent (such as polyoxy ethylene octyl dodecyl ether and polyoxy ethylene hydrogenated castor oil) reveal different problems. These problems involve high sensitivity to human skin,[1,2] poor appearance due to cloudiness or turbidity caused when surfactants dissolve water-insoluble substances, and an uncomfortable feeling due to a foam residue like that of soap. To eliminate these problems, the authors tried to use cyclodextrin derivatives to solubilize any water-insoluble substances.

It is well known that cyclodextrin, in which 6—8 glycose molecules are circularly connected by an α-1,4 glycoside bond, is capable of including water-insoluble substances.[3] However, β-cyclodextrin $(C_6H_{10}O_5)_7$ scarcely dissolves in water, so it is difficult to use β-cyclodextrin instead of a surfactant. Cyclodextrin derivatives have been intensely studied in recent years. Among them the authors selected 2-hydroxypropyl-β-cyclodextrin (2HP-β-CD), because it is easily soluble in water, inexpensive, convenient to use in manufacturing, and safe. The authors conducted an experiment to dissolve water-insoluble substances in water using 2HP-β-CD. They selected perfumes as the water-insoluble substances. Most perfumes have low molecular weights. Since some perfumes have a functional group, they are essential raw materials in cosmetic components and are suitable hosts. By producing complexes of different perfumes with 2HP-β-CD, the authors obtained solubilized amounts of each and studied the difference between the amount of perfume included. As a result, some interesting facts were observed.

Experimental

Materials Host experiments were performed using 2HP-β-CD made by Nihon Shokuhin Kako Ltd. Eight typical fragance materials were used as the guest material.

We calculated the degree of substitution using the average number of 2-hydroxypropyl groups per molecule of 2HP-β-CD estimated by proton nuclear magnetic resonance (^{1}H-NMR). We allowed them to stand for 12 h at 25 °C. Table I shows the list of guest materials.

Specimen Preparation Method The discrete fragrance material used as a guest was directly and gradually added to an aqueous solution in which 2HP-β-CD was dissolved. The mixture was stirred at 25 °C for 12 h with a magnetic stirrer. Later, the concentration of the guest in the filtrate was determined.

Figure 1 shows the flow chart for this preparation method.

Determination of the Degree of Substitution The degree of substitution was calculated from the ^{1}H-NMR integration ratio of anomeric protons and methyl protons at the terminal of the hydroxypropyl. However, the degree of substitution was expressed as the number of hydroxypropyl group per mol of cyclodextrin.

Solubility Studies Solubility measurements were carried out according to Higuchi and Connors.[4] Excess amounts of fragrance materials were added to aqueous solutions containing 2HP-β-CD (degree of substitution (DS) = 4.3) at various concentrations, and the mixtures were equilibrated by shaking at 25 °C for about 2 weeks. Thereafter, the mixtures were filtered and after appropriate dilution with methanol, the concentration of the fragrance materials in the filtrate was measured by high-performance liquid chromatography (HPLC).

Determination Method The concentration of fragrance materials in the solution was determined by HPLC with the calibration curve method.

The HPLC equipment (Nihon Bunko 860-CO) used and the conditions are as follows: Column; CAPCELLPAK C_{18} SG 4.6 × 250 mm (Shiseido), pump flow rate; 1 ml/min, quantity of the solution; 4.0 μl.

Table II gives the solvent and λ_{max} for each fragrance material in the HPLC.

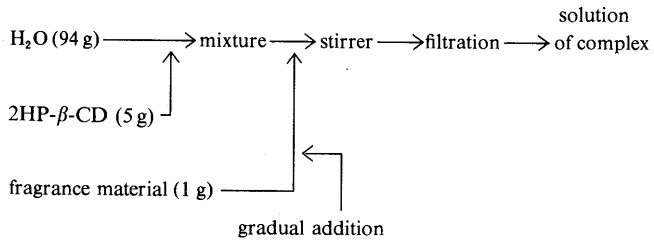

Fig. 1. Flow Chart

Add 2HP-β-CD to water, mix together and slowly add the fragrance to the mixture, stir using a stirrer and filter. Use the filtrate as the inspection body.

TABLE I. List of Guests Used

Fragrance materials	Structural formula	Molecular weight
Linalool	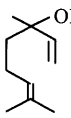	154.25
Citronellol	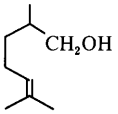	156.27
Citral	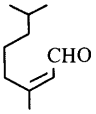	152.24
Limonene	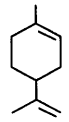	136.24
Methyl ionone	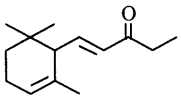 α Type	206.33
Benzyl acetate	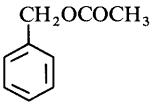	150.17
Linalyl acetate	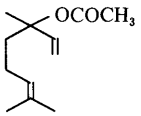	196.29
Methyl dihydro-jasmonate	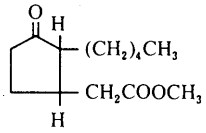	226.32

Calculation of the Stability Constant By preparing a solubility phase plot of the concentration of fragrance material *versus* the 2HP-β-CD according to the method of Higuchi *et al.*,[4] the authors used the least square method for linear regression and calculated the apparent stability constant (*Ke'*) using the following formula.

$$Ke' = \frac{S_i - S_0}{[S_i - (S_i - S_0)][L_i - (S_i - S_0)]}$$

where S_i and L_i are the guest and CD addition concentrations, respectively. S_0 is the solubility of the guest alone.

NMR Spectra NMR spectra were taken on a JEOL-GX-400 spectrometer (^{1}H, 400 MHz). Samples (10 mg) were dissolved in 10 mg of the solvent.

Results and Discussion

Solubilized Amount Using HPLC, we determined the solubilized amount for each of the eight types of fragrance materials in water in the absence of 2HP-β-CD. Next, we similarly determined the solubilized amount for each type of fragrance material in a solution containing 5% 2HP-β-CD. We then determined the solubilized amount for each type of the fragrance materials from the difference between the solubilities in solutions of 2HP-β-CD and the solubilities in water alone. Thereafter, we calculated the ratio of the guest to the host. Table III shows these results.

TABLE II. The Solvents and Ultraviolet Spectrum (UV) λ_{max} for Each Fragrance Material in the HPLC

Fragrance material	λ_{max} (nm)	Solvent water : methanol
Linalool	215	3 : 7
Citronellol	215	3 : 7
Citral	280	3 : 7
Limonene	215	1 : 9
Methyl ionone	260	1 : 9
Benzyl acetate	256	2 : 8
Linalyl acetate	215	1 : 9
Methyl dihydro-jasmonate	215	3 : 7

TABLE III. The Solubilized Amount of the Fragrance Materials

Fragrance material	Solubility (%) 25 °C		Molar ratio guest/host
	Water	2HP-β-CD 5% soln.	
Linalool	0.15	0.58	0.82
Citronellol	0.02	0.47	0.83
Citral	0.03	0.41	0.71
Limonene	0.003	0.08	0.17
Methyl ionone	0.002	0.25	0.38
Benzyl acetate	0.15	0.63	0.94
Linalyl acetate	0.05	0.30	0.37
Methyl dihydro-jasmonate	0.04	0.42	0.49

TABLE IV. The Relationship between Substitution Degree and Solubilized Amount

Degree of substitution	Benzyl acetate (%)		Linalool (%)	
	2HP-β-CD 5% soln.	2HP-β-CD 10% soln.	2HP-β-CD 5% soln.	2HP-β-CD 10% soln.
3.6	0.55	1.16	0.56	1.08
4.6	0.60	1.11	0.59	1.17
5.5	0.55	1.04	0.56	1.09
8.1	0.52	0.97	0.48	0.97

Substitution Degree and Solubilization of 2HP-β-CD The solubilization was measured using 2HP-β-CD with a substitution degree of 4.3. However, when producing 2HP-β-CD, scattering occurs in the degree of the substitution. Therefore, we conducted an experiment to examine the change in the solubilization concerning the four lots of the actually produced samples. We selected benzyl acetate and linalool with a relatively large solubilization, and we examined the relationship between substitution degree and solubilization (Table IV).

This result shows that in the substitution degree range of 3.5—8.1 (Nihon Shokuhin Kako), as the substitution degree increases, the solubilization tends to decrease, though only slightly, and there is a peak at 3.5—4.6.

Confirmation of Clathration by ^{1}H-NMR By using 2HP-β-CD, it was possible to solubilize a considerable amount of the fragrance materials without using a surfactant. We examined them with ^{1}H-NMR in order to determine whether or not this solubilization phenomenon was based on clathration. In our experiment, we used benzyl acetate as a kind of fragrance material. We prepared the sample to

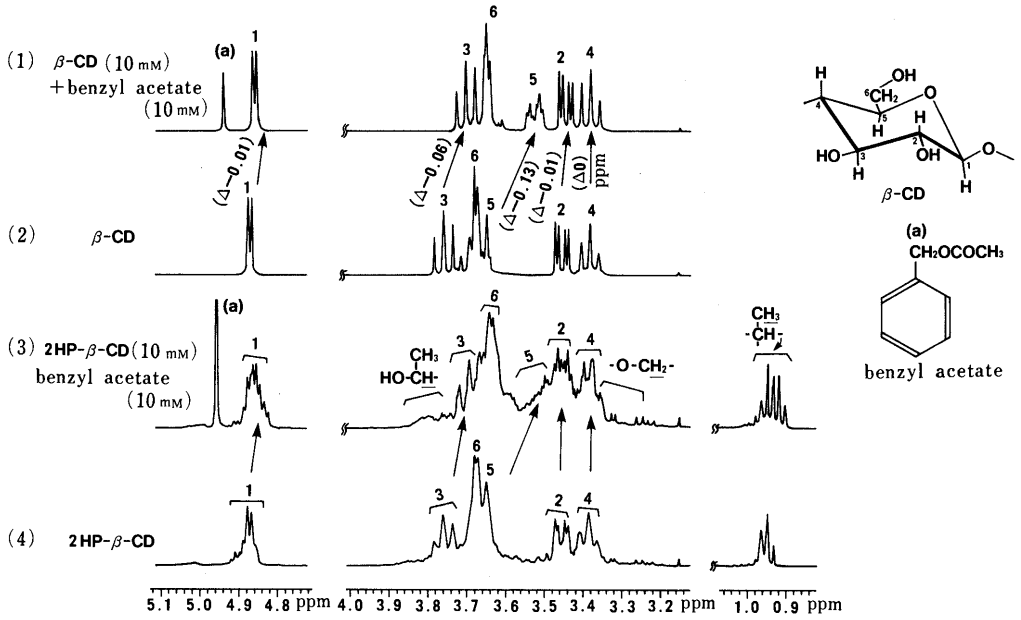

Fig. 2. The Shift ^{1}H-NMR Spectra of β-CD and 2HP-β-CD by Solubilizing Fragrance Material

(1) Spectra obtained when 10 mM of benzyl acetate was added to 10 mM of β-CD. (2) Spectra of β-CD. (3) Spectra obtained when 10 mM of benzyl acetate was added to 10 mM of 2HP-β-CD. (4) Spectra of 2HP-β-CD.

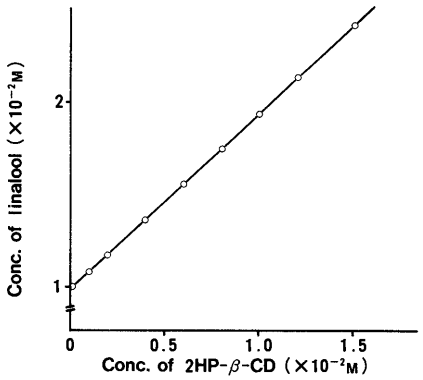

Fig. 3. Solubility Phase

Linalool is used to compose the solubility phase.

determine whether equal moles of the host and the guest were contained in each milliliter of heavy water. First, as a model we used β-CD which is known to produce a clathration phenomenon, mixed it with benzyl acetate, and compared its spectrum and that of the β-CD not mixed with a guest. As a result, we confirmed that C_2-H, C_3-H and C_6-H shifted to a high magnetic field compared with the other protons.[5-7] Next, we conducted an experiment using 2HP-β-CD in the same way. Also in 2HP-β-CD, C_2-H, C_3-H and C_6-H shifted to a high magnetic field due to the guest mixture as in the case of the β-CD (Fig. 2). These results indicate that the solubilization of the fragrance materials used in this experiment is based on clathration.

Stability Constant The stability constant is considered to be an important parameter for predicting the clathration phenomenon. According to the usual method[3,4] we obtained the apparent stability constant for each fragrance material.

Figure 3 shows the phase solubility diagram of linalool in water with 2HP-β-CD (DS=4.3). The solubility of linalool increased with CD concentration, showing an A_L type solubility diagram according to Higuchi and Connors.[4] Assuming that a 1:1 complex is initially formed, the apparent stability constant (Ke') of the complex was calculated in terms of Eq. 1,[4] using the slope and intercept of the straight line of the diagram.

$$Ke' = \frac{\text{slope}}{\text{intercept}(1-\text{slope})} \quad (1)$$

Also, apparent stability constants of the complexes of other fragrance materials with 2HP-β-CD could be calculated by the same method, because of their similar behavior in aqueous solution containing 2HP-β-CD. As Table V demonstrates, we found a relatively high correlation between the solubilized amount of the fragrance materials in water and 5% 2HP-β-CD aq.

A stability constant is one of the parameter which explains the degree of the contribution of 2HP-β-CD added to raise the solubility of a guest.

Table V. Solubilized Amounts and the Apparent Stability Constant

Fragrance material	Apparent stability constant (M^{-1})$K'_{1:1}$	Solubility 2HP-β-CD 5% soln./water
Linalool	1610	+
Citronellol	3740	+ + +
Citral	1560	+ +
Limonene	3350	+ + +
Methyl ionone	29500	+ + + +
Benzyl acetate	306	+
Linalyl acetate	137	+
Methyl dihydro-jasmonate	712	+

+; The value obtained by dividing the solubility of the perfume in the presence of 2HP-β-CD 5% by the solubility of the perfume dissolved in water is small. + +; The value of the ratio is slightly high. + + +; The value of the ratio is quite high. + + + +; The value of the ratio is very high.

For instance, although the stability constant of methyl ionone is very high, methyl ionone hardly dissolves in water, so that the calculated value of the solubility of a guest in a 2HP-β-CD 5% solution and the solubility of a guest in water are very high.

Thus, the comparison between the value of the stability constant and the value obtained by dividing the solubility of the guest in the presence of 2HP-β-CD by the value of the guest dissolved in water shows a considerable correlationship.

Although we have omitted details because of space limitations, we also found a considerable correlation in the fragrance material molecular weight, the polarity value, and the amount solubilized.

Conclusions

By using 2HP-β-CD, it was possible to solubilize a considerable amount of fragrance materials without using a surface active agent. We examined them with ^{1}H-NMR in order to determine whether or not this solubilization phenomenon was based on inclusion. The results of the ^{1}H-NMR study indicate that the solubilization of the fragrance materials used in this experiment is dependant on formation of an inclusion complex.

The relationship between solubility of guests and degree of substitution on 2HP-β-CD shows that in the substitution degree range of 3.5—8.1, as the substitution degree increases, the solubilized amount tends to decrease, though only slightly, and there is a peak at 3.5—4.6.

From the measured solubilities of the fragrance materials, it has been found that a fragrance material of lower molecular weight or higher polarity tends to be more soluble in water and that solubility correlated fairly well with the apparent stability constant.

Acknowledgement The authors are very grateful to Professor Kaneto Uekama of Kumamoto University for his kind advice. The authors are also indebted to Mr. Ryuichiro Nanba and Mr. Kazuo Komatsu for the ^{1}H-NMR measurements.

References

1) J. F. Treon, *Am. Perf. Cosmet.*, **77**, 35 (1962).
2) H. Stupel, *Soap Perf. Cosmet.*, **28**, 300 (1955).
3) K. Uekama, *Yakugaku Zasshi*, **101**, 10 (1981).
4) T. Higuchi and K. A. Connors, *Adv. Anal. Chem. Instrum.*, **4**, 117 (1966).
5) R. Bergeron and Rowan, *Bioorg. Chem.*, **5**, 425 (1976).
6) R. Bergeron and M. A. Channing, *Bioorg. Chem.*, **5**, 437 (1976).
7) J. Szejtli, "Cyclodextrins and Their Inclusion Complexes," Akademiai Kiado, Budapest, 1982.

Catalytic Effect of Buffers on Degradation of Imipenem (*N*-Formimidoylthienamycin) in Aqueous Solution

Rosa MÉNDEZ, Teresa ALEMANY and Javier MARTÍN-VILLACORTA*

Departamento de Bioquímica y Biología Molecular, Facultades de Biología y Veterinaria, Universidad de León, 24071 León, Spain.
Received September 17, 1990

The catalytic effect of various buffer systems on the degradation of imipenem (*N*-formimidoylthienamycin) in aqueous solution at 35°C and at an ionic strength of 0.5 mol·dm^{-3} has been studied. Changes in the concentration of intact imipenem in the solutions were determined by reverse-phase high-performance liquid chromatography (HPLC) with UV-detection. The observed degradation rates at various pH's were found to follow pseudo-first-order kinetics with regard to imipenem concentrations (2×10^{-4} mol·dm^{-3}) and were significantly influenced by general acid and general base catalysis. Of the buffer systems employed in the kinetic studies the citrate buffer and borate buffer systems showed the greatest catalytic effects. The pH-rate profile obtained from non-buffer-catalyzed rate constants, k_{pH}, showed a minimum at a pH of 6.40. The calculated theoretical pH-rate profile and the experimental points coincide, thus supporting the hypothesis presented[1] concerning the reactions involved in the degradation of imipenem in solution. The Arrhenius activation energies at pH 4.21, 6.58 and 8.64 were estimated as 12.47, 15.22 and 17.49 kcal/mol, respectively.

Keywords imipenem (*N*-formimidoylthienamycin); β-lactam antibiotic; aqueous solution stability; degradation kinetics; catalytic effect; pH-rate profile

Introduction

Carbapenem antibiotics are, in general, unstable compounds in aqueous solution, exhibiting maximum stability only over a narrow pH range. Special effort is required during isolation to minimize losses. Thienamycin (I), the first member of the family to be isolated, presented particular problems. Between pH 2 and pH 5 thienamycin is reported to have a stability comparable with that of benzylpenicillin[2]; however, at pH 7 and higher, the decomposition rate of thienamycin is significantly greater than that of the penicillin.[3]

Imipenem (*N*-formimidoyl thienamycin) (II) is a derivative of thienamycin. Chemical structures are shown in Fig. 1. It has an unusually high degree of activity against a broad spectrum of bacteria.[4,5]

It is known that the hydrolysis of the β-lactam ring of penicillins is catalyzed by certain buffers; this is also the case with imipenem. A limited number of papers have described kinetic[6,7] and chemical[8,9] features of this drug in aqueous solution, but only over a narrow pH range. The present research deals with kinetic aspects of the degradation of imipenem in buffer solutions of various pH's.

Experimental

Materials Imipenem (*N*-formimidoylthienamycin) was supplied by Merck, Sharp & Dohme of Spain, S. A.

Buffer salts used and other chemicals were commercial products of analytical grade. All the water used was purified by a Milli-Q-Reagent Water System (Millipore Bedford, MA, U.S.A.).

Buffer Solutions The buffer systems used in the kinetic studies were: citrate buffer (pH 3.90—4.75), acetate (pH 4.20—5.50), phosphate (pH 5.84—7.95), borate (pH 8.10—9.40) and carbonate (pH 10.00 and 10.50). Buffers were adjusted to an ionic strength of 0.5 mol·dm^{-3} with sodium perchlorate monohydrate and a 1×10^{-4} mol·dm^{-3} concentration of ethylenediaminetetraacetic acid (EDTA) was used in order to avoid the catalytic effect induced by small amounts of metal ions possibly present as impurities. The buffers were prepared by dissolving the citric acid, acetic acid, sodium phosphate, boric acid and sodium bicarbonate together with sodium perchlorate monohydrate and EDTA in distilled water and adjusting the pH with concentrated sodium hydroxide. The solutions were freshly prepared and the pH's measured at 35°C using a pH meter equipped with a combination electrode.

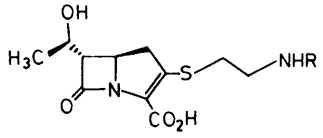

I thienamycin : R=H
II imipenem : R=CH=NH

Fig. 1. Chemical Structures of Thienamycin and Imipenem

Analytical Precedure The residual imipenem concentration was determined using a reverse-phase high-performance liquid chromatographic (RP-HPLC) method. The HPLC system consisted of a Konik KNK-500-A liquid chromatograph, a Rheodyne 7125 loop injector (volume 20 μl), a Water 441 UV detector and a Varian 4290 computing integrator. The detector was set at 313 nm. The separation was carried out using a Spherisorb ODS-2 RP-18 column (10 μm; 25 × 0.4 cm i.d.) with a phosphate (0.1 mol·dm^{-3}, pH 7.0): methanol (93 : 7) mobile phase. A pre-column (3 × 0.4 cm i.d.) packed with μ-Bondapak C18 (30 μm) was used to guard the main column. The flow-rate was 1.5 ml·min^{-1} and the capacity factor 1.79. All chromatographic operations were carried out under ambient conditions.

Analyses of the experimental reproducibility and of the various time plots indicate the relative uncertainty of the observed rate constant, k_{obs}, to be 10% at the 95% confidence level.

Kinetic Procedure Weighed amounts of imipenem were dissolved in the buffer solutions to make concentrations of 2×10^{-4} mol·dm^{-3}. Aliquots (10 ml) of the solutions were each sealed in a glass vial. To avoid possible changes in the pH of the kinetic solution during the reaction, it was maintained with a pH-stat. All reactions were conducted at 35.0 ±0.1 °C with the total buffer concentration greatly exceeding the reacting substrate concentration to maintain pseudo-first-order kinetics. Aliquots of the solution were withdrawn at appropriate time intervals and immediately analyzed by HPLC.

Ionization Constants The apparant pK_a of each buffer system was determined at 35.0 °C and an ionic strength of 0.5 mol·dm^{-3} by potentiometric titration.

Results and Discussion

Order of Reaction and Observed Rate Constants The degradation kinetics of imipenem were investigated at various pH values and buffer concentrations at a constant temperature (35 °C) and ionic strength ($\mu = 0.5$ mol·dm^{-3}). The time *versus* log (residual %) plot, given in Fig. 2, indicates that the degradation in the pH range examined followed apparent pseudo-first-order kinetics with respect to the concentrations of imipenem. The observed rate constants, k_{obs}, were estimated by means of the least-squares method from the slopes of the plots.

Catalytic Effect of Buffer Systems The catalytic effect of the buffer systems used in the kinetic studies was determined by experiments at constant pH, temperature, ionic strength and imipenem concentration, the only variation being in the buffer concentration at a given pH. This was repeated at several pH values within the effective range of the buffer employed.

The results of these studies are summarized in Figs. 3—7, where the observed rate constants are plotted against buffer concentration.

Figure 3 shows the catalytic effect of citrate buffers between pH 3.90 and 4.75, which increased linearly with the buffer concentration. Therefore, the rates of degradation of imipenem in the citrate buffer at constant pH and 35 °C were shown to be significantly affected by general acid catalysis.

In this pH region approximately 3% of total citrate exists as citrate ion (A^{3-}). Therefore, the observed rate constant is a summation of several catalytic rate constants catalyzed by the buffer species plus the rate at zero buffer concentration, and may be expressed by the following equation:

$$k_{obs}=k_{pH}+k_{H_3A}[H_3A]+k_{H_2A^-}[H_2A^-]+k_{HA^{2-}}[HA^{2-}] \quad (1)$$

where k_{pH} is the rate constant at zero buffer concentration; the other k's are the catalytic rate constants due to the citrate buffer species; $[H_3A]$ is the concentration of nondissociated citric acid; $[H_2A^-]$ is the concentration of dihydrogen citrate ion; and $[HA^{2-}]$ is the concentration of monohydrogen citrate ion.

The total citrate concentration, c_T, is

$$c_T=[H_3A]+[H_2A^-]+[HA^{2-}] \quad (2)$$

From the dissociation constants, $pK_1=2.85$ and $pK_2=4.40$

$$K_1=\frac{[H^+][H_2A^-]}{[H_3A]} \quad (3)$$

$$K_2=\frac{[H^+][HA^{2-}]}{[H_2A^-]} \quad (4)$$

and from Eqs. 1 and 2 the following overall rate expression, k_{obs}, was obtained.

$$k_{obs}=k_{pH}+c_T\frac{k_{H_3A}[H^+]^3+k_{H_2A^-}[H^+]^2K_1+k_{AH^{2-}}[H^+]K_1K_2}{[H^+]^3+[H^+]^2K_1+[H^+]K_1K_2} \quad (5)$$

A plot of k_{obs} *versus* the total citrate concentration will yield a straight line with an intercept of k_{pH} and a slope of

$$\text{slope}=\frac{k_{H_3A}[H^+]^3+k_{H_2A^-}[H^+]^2K_1+k_{HA^{2-}}[H^+]K_1K_2}{[H^+]^3+[H^+]^2K_1+[H^+]K_1K_2} \quad (6)$$

From the slopes, the citrate buffer catalytic rate constants on degradation of imipenem at 35 °C were calculated:

$k_{H_3A}=1.96\,l\cdot mol^{-1}\cdot h^{-1}$

$k_{H_2A^-}=0.527\,l\cdot mol^{-1}\cdot h^{-1}$

$k_{HA^{2-}}=0.402\,l\cdot mol^{-1}\cdot h^{-1}$

Figure 4 shows the catalytic effect of acetate buffers of pH 4.20 to pH 5.50. The observed rate constant may be expressed by the following equation:

$$k_{obs}=k_{pH}+k_{AcH}[AcH]+k_{Ac^-}[Ac^-] \quad (7)$$

where AcH is the undissociated acetic acid and Ac^- is the acetate ion. Combining Eq. 7 and the equations

$$K_a=\frac{[H^+][Ac^-]}{[AcH]} \quad (8)$$

$$c_T=[AcH]+[Ac^-] \quad (9)$$

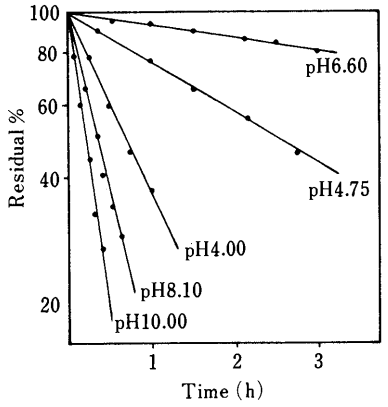

Fig. 2. Plots of the Observed Pseudo-First-Order Kinetic Degradation of Imipenem in Aqueous Solution at Different pH's at 35 °C ($\mu=0.5$ mol·dm^{-3})

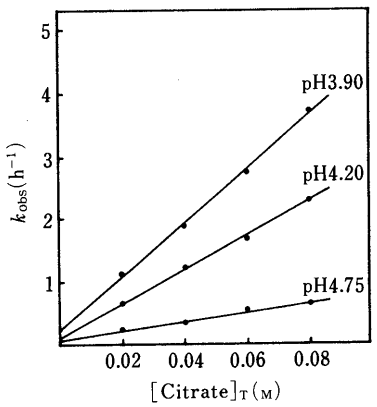

Fig. 3. Plots of the Pseudo-First-Order Rate Constants *versus* the Total Citrate Buffer Concentration at Several pH's for the Degradation of Imipenem at 35 °C and $\mu=0.5$ mol·dm^{-3}

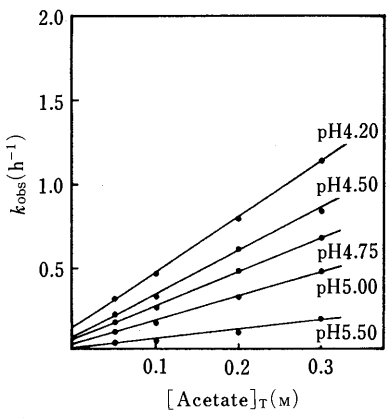

Fig. 4. Plots of the Pseudo-First-Order Rate Constants *versus* the Total Acetate Buffer Concentration at Several pH's for the Degradation of Imipenem at 35 °C and $\mu=0.5$ mol·dm^{-3}

we find

$$k_{obs}=k_{pH}+c_T\frac{k_{AcH}[H^+]+k_{Ac^-}K_a}{[H^+]+K_a} \quad (10)$$

where k_{pH} is the rate constant at zero buffer concentration and $pK_a=4.55$. Plotting the rate constant against the total acetate concentration for each pH allows us to obtain the k_{pH} value and the catalytic rate constants

$k_{AcH}=0.279\,l\cdot mol^{-1}\cdot h^{-1}$

$k_{Ac^-}=0.0191\,l\cdot mol^{-1}\cdot h^{-1}$

For phosphate buffers the observed rate constants were also shown to increase as buffer concentrations increased. Figure 5 shows the catalytic effect of phosphate buffers on the degradation of imipenem at 35 °C, pH 5.84 to pH 7.95. In this region only di- and mono-hydrogen phosphate ions are important. Accordingly, the total phosphate concentration and the overall rate may be written as:

$$k_{obs}=k_{pH}+k_{H_2PO_4^-}[H_2PO_4^-]+k_{HPO_4^{2-}}[HPO_4^{2-}] \quad (11)$$

$$c_T=[H_2PO_4^-]+[HPO_4^{2-}] \quad (12)$$

The dissociation constant of dihydrogen phosphate ion ($pK_2=6.58$) is

$$K_2=\frac{[H^+][HPO_4^{2-}]}{[H_2PO_4^-]} \quad (13)$$

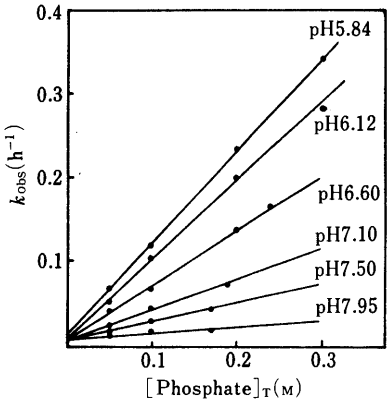

Fig. 5. Plots of the Pseudo-First-Order Rate Constants *versus* the Total Phosphate Buffer Concentration at Several pH's for the Degradation of Imipenem at 35 °C and $\mu=0.5\,mol\cdot dm^{-3}$

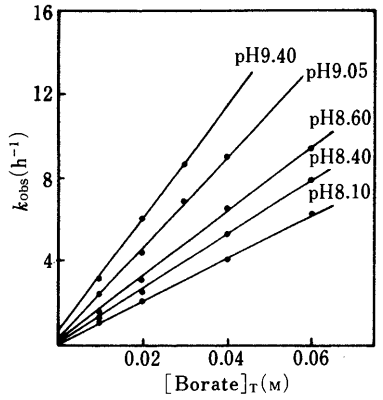

Fig. 6. Plots of the Pseudo-First-Order Rate Constants *versus* the Total Borate Buffer Concentration at Several pH's for the Degradation of Imipenem at 35 °C and $\mu=0.5\,mol\cdot dm^{-3}$

and the overall rate may be shown as:

$$k_{obs}=k_{pH}+c_T\frac{k_{H_2PO_4^-}[H^+]+k_{HPO_4^{2-}}K_2}{[H^+]+K_2} \quad (14)$$

The following catalytic constants were found:

$k_{H_2PO_4^-}=2.32\times10^{-2}\,l\cdot mol^{-1}\cdot h^{-1}$

$k_{HPO_4^{2-}}=2.24\times10^{-2}\,l\cdot mol^{-1}\cdot h^{-1}$

It is obvious from Fig. 6 that borate buffers, from pH 8.10 to 9.40, have a catalytic effect on the degradation of imipenem. If the assumption is made that boric acid in this pH region exists mainly as H_3BO_3 and $H_2BO_3^-$ ($pK_a=8.90$), an equation (Eq. 15) similar to Eq. 14 may be derived.

$$k_{obs}=k_{pH}+c_T\frac{k_{H_3BO_3}[H^+]+k_{H_2BO_3^-}K_a}{[H^+]+K_a} \quad (15)$$

The following catalytic constants were found:

$k_{H_3BO_3}=8.13\,l\cdot mol^{-1}\cdot h^{-1}$

$k_{H_2BO_3^-}=39.4\,l\,mol^{-1}\cdot h^{-1}$

Figure 7 shows the small catalytic effect of carbonate

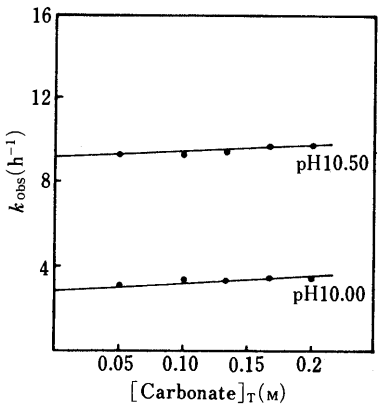

Fig. 7. Plots of the Pseudo-First-Order Rate Constants *versus* the Total Carbonate Buffer Concentration at Several pH's for the Degradation of Imipenem at 35 °C and $\mu=0.5\,mol\cdot dm^{-3}$

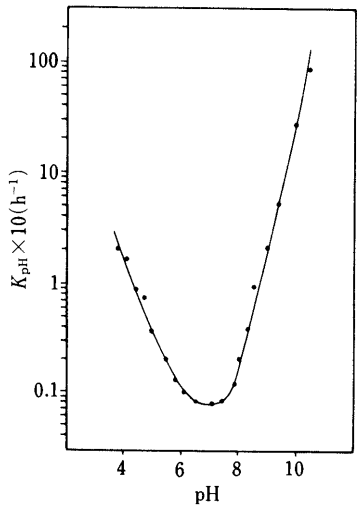

Fig. 8. $\log k_{pH}$–pH Profile of Imipenem Degradation in Aqueous Solution at 35 °C and $\mu=0.5\,mol\cdot dm^{-3}$

The closed circles indicate experimental values and the solid line shows the theoretical curve according to Eq. 17.

buffers at pH 10.00 and 10.50. In this pH region only bicarbonate and carbonate ions are important ($pK_2 = 10.02$). Accordingly, the overall rate may be written as:

$$k_{obs} = k_{pH} + c_T \frac{k_{HCO_3^-}[H^+] + k_{CO_3^{2-}} K_2}{[H^+] + K_2} \quad (16)$$

The plot of Eq. 16 allows us to obtain the carbonate buffer catalytic rate constants.

$$k_{HCO_3^-} = 0.0831\ l \cdot mol^{-1} \cdot h^{-1}$$

$$k_{CO_3^{2-}} = 1.91\ l \cdot mol^{-1} \cdot h^{-1}$$

pH-Rate Profile The rate constants at zero buffer concentration were obtained from the intercepts of the lines in Figs. 3—7. In Fig. 8, the logarithms of these rate constants are plotted *versus* pH in the pH range 3.90—10.50. In this pH region imipenem ($pK_1 = 3.18$, $pK_2 = 9.91$)[6] is found mainly in the zwitterionic form. The pH-rate profile has a U-shape which is characteristic of reactions susceptible to specific acid–base catalysis.

The catalytic constants of the water species in imipenem hydrolysis are grouped under the constant k_{pH} according to the following equation:

$$k_{pH} = k_{H_2O} + k_H[H^+] + k_{OH}[OH^-] \quad (17)$$

where k_H and k_{OH} represent second-order rate constants of proton- and hydroxide ion-catalyzed degradation, respectively, and k_{H_2O} is the rate constant of spontaneous or water-catalyzed degradation. The values of these constants, computed by means of a non-linear least-squares method, were

$$k_{H_2O} = 6.61 \times 10^{-3} \pm 1.63 \times 10^{-3} h^{-1}$$

$$k_H = 1207 \pm 220\ l \cdot mol^{-1} \cdot h^{-1}$$

$$k_{OH} = 8916 \pm 1731\ l \cdot mol^{-1} \cdot h^{-1}$$

These values were in good agreement with those obtained by interpolation at 35°C from the values calculated by other investigators[6] for imipenem at 25 and 40 °C in the pH range 5—8.

The pH for maximal stability of imipenem, which is given by

$$pH_{min} = 1/2(pk_{OH} - pk_H + pK_w) \quad (18)$$

is estimated to be 6.40.

The pH-rate profile can be interpreted kinetically as follows: There were three important pH regions. One where a hydrogen-ion-catalyzed reaction took place (pH < 6.00), a pH-independent region (pH 6.50—7.50) where the predominating reaction is the attack of water molecule and a region where the reaction was hydroxide ion catalyzed (pH > 8.00).

A comparison of the values of the catalytic constants of the water species used in imipenem hydrolysis with those obtained for several penicillins and cephalosporins[10] and clavulanic acid[11] shows those of imipenem to be greater than those relative to the other β-lactamic antibiotics. Thus, the acid catalysis constant k_H for imipenem, a carbapenem, is almost double that of clavulanic acid, from 2 (for penicillin G) to 600 (for ampicillin) times higher than that of penicillins and about 6000 times higher than that of cephalosporins. The basic catalysis constant, k_{OH}, is between 2 and 8 times greater for imipenem than for penicillins and cephalosporins and almost twice that of clavulanic acid.

TABLE I. Rate Constants and Arrhenius Activation Parameters for Degradation of Imipenem at $\mu = 0.5\ mol \cdot dm^{-3}$

pH	k_{obs} ($h^{-1} \times 10$) (40 °C)	k_{obs} ($h^{-1} \times 10^2$) (30 °C)	k_{obs} ($h^{-1} \times 10^2$) (20 °C)	E_a (kcal/mol)	$\log A$ (h^{-1})
4.21	15.67	82.34	39.46	12.47	8.88
6.58	2.033	9.13	3.78	15.22	9.90
8.64	20.38	81.55	29.46	17.49	12.49

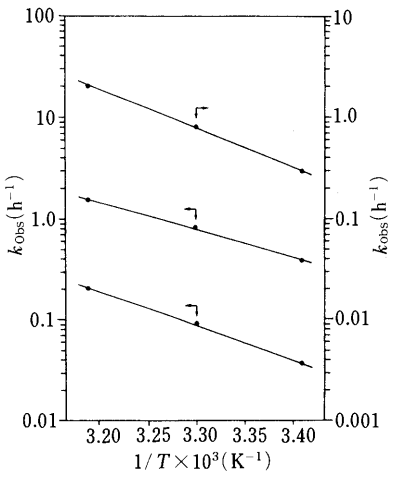

Fig. 9. Arrhenius Plots of the Degradation of Imipenem at pH 4.21 (Acetate Buffer), pH 6.58 (Phosphate Buffer) and pH 8.64 (Borate Buffer)

If we compare the catalytic effects of buffer solutions of citrates, acetates, phosphates, borates and carbonates on the degradation of imipenem with those found in the literature for penicillin G,[3] ampicillin,[1] cephazolin, cephalexin[12] and clavulanic acid[11] in some of these buffer solutions, we find that the catalytic constants for the degradation of these antibiotics are much lower than for imipenem. Thus, for example, the citrate buffer catalytic rate constants k_{H_3A} and $k_{HA^{2-}}$ for imipenem are about 5 times higher than those of ampicillin and the catalytic rate constant $k_{H_2A^-}$ for imipenem is double that of ampicillin.

The high reactivity of imipenem in relation to the hydrolysis catalysed by buffer solution species and water species may be due to the high grade of inhibition of amide resonance present in its structure and to the strain of the five-member ring which possesses no heteroatom in position 1. These affirmations are supported by the X-ray crystallographic data of thienamycin which indicate that this β-lactam antibiotic is the most folded fused β-lactam ring system.[13]

Stress should be laid on the great catalytic effect presented by the acid species of the citrates and the basic species on borates, which may be up to 300 times greater than the catalytic effect of phosphates.

Effect of Temperature The temperature effect on the degradation of imipenem was determined at three different pH values in the acidic, neutral and alkaline regions with $\mu = 0.5\ mol \cdot dm^{-3}$. The observed rate constants at 20, 30 and 40 °C are given in Table I and Arrhenius plots of the data at pH 4.21, 6.58 and 8.64 are shown in Fig. 9. The

apparent activation energies (E_a) estimated from the lines in Fig. 9 are also listed in the table together with the values of the frequency factor (log A).

References

1) J. P. Hou and J. W. Poule, *J. Pharm. Sci.*, **58**, 447 (1969).
2) R. Brodersen, *Trans. Faraday Soc.*, **43**, 351 (1947).
3) P. Finholt, G. Jurgensen and H. Kristiansen, *J. Pharm. Sci.*, **54**, 387 (1965).
4) H. Kropp, J. G. Sundelof, J. S. Kahan, F. M. Kahan and J. Birnbaum, *Antimicrob. Agents Chemother.*, **17**, 993 (1980).
5) T. Kesado, T. Hashizume and Y. Asashi, *Antimicrob. Agents Chemother.*, **17**, 912 (1980).
6) G. B. Smith and E. F. Schoenewaldt, *J. Pharm. Sci.*, **70**, 272 (1981).
7) D. J. Swanson, C. DeAngelis, I. L. Smith and J. J. Schentag, *Antimicrob. Agents Chemother.*, **29** 936 (1986).
8) W. J. Leanza, K. J. Wildonger, T. W. Miller and B. G. Christensen, *J. Med. Chem.*, **22**, 1435 (1979).
9) D. A. Gravallese, D. G. Musson, L. T. Pauliukonis and W. F. Bayne, *J. Chromatogr.*, **310**, 71 (1984).
10) T. Yamana and A. Tsuji, *J. Pharm. Sci.*, **65**, 1563 (1976).
11) J. Haginaka, T. Nakagawa and T. Uno, *Chem Pharm. Bull.*, **29**, 3334 (1981).
12) E. S. Rattie, D. E. Guttman and L. J. Ravin, *Drug Res.*, **28**, 944 (1978).
13) G. Albers-Schönberg, B. H. Arison, O. D. Hensens, J. Hirshfield, K. Hoogsteen, E. A. Kaczka, R. E. Rhodes, J. S. Kahan, R. W. Ratcliffe, E. Walton, L. J. Ruswinkle, R. B. Morin and B. G. Christensen, *J. Am. Chem. Soc.*, **100**, 6491 (1978).

Organometallic Reactions Characteristic of Chiral Heterocyclic Compounds: Synthesis and Stereoselective Grignard Reaction of Chiral 4-Oxa-7,7a-diazaperhydroindans

Hiroshi TAKAHASHI,* Takashi SENDA, and Kimio HIGASHIYAMA

Faculty of Pharmaceutical Science, Hoshi University, 2-4-41, Ebara, Shinagawa, Tokyo 142, Japan. *Received June 26, 1990*

New heterocyclic compounds, 6-phenyl-4-oxa-7,7a-diazaperhydroindans (5 and 6), were synthesized by condensation of chiral 2-hydroxyethylhydrazines prepared from (*R*)-phenylglycinol with γ-chlorobutyraldehyde. The stereoselective Grignard reaction of 5 and 6 proceeded to give chiral 2-substituted 1-[*N*-(2-hydroxy-1-phenylethyl)amino]pyrrolidines (7a—d and 8a—d). The structures of these products were determined by comparison with authentic samples, and the reaction mechanism is proposed to involve an intermediate iminium salt.

Keywords 1-aminopyrrolidine; chiral iminium intermediate; chiral 2-substituted pyrrolidine; chiral heterocyclic compound; Grignard reaction; 4-oxa-7,7a-diazaperhydroindan; (*R*)-phenylethylhydrazine; (*R*)-phenylglycinol; stereoselective reaction; X-ray analysis

We have recently reported the syntheses and stereoselective organometallic reactions of 1,3-oxazolidines[1] and 5-oxa-7,8a-diazaperhydroazulen-8-ones.[2] In this paper, we wish to describe the synthesis and stereoselective reactions of compounds having a new ring system, *i.e.*, chiral 7-alkyl-6-phenyl-4-oxa-7,7a-diazaperhydroindans (**5** and **6**).

The synthesis of (*R*)-*N*-alkyl-2-hydroxy-1-phenylethylhydrazines (**3** and **4**) was achieved by *N*-amination of (*R*)-*N*-alkyl-2-hydroxy-1-phenylethylamines (**1**[1,3] and **2**[1,4]), and the new heterocyclic compounds (**5** and **6**) were synthesized by condensation of **3** and **4** with γ-chlorobutyraldehyde in 80% and 66% yields, respectively. Compound **5** was found to consist exclusively of one isomer by proton nuclear magnetic resonance (^{1}H-NMR) spectral (270 MHz) analysis.

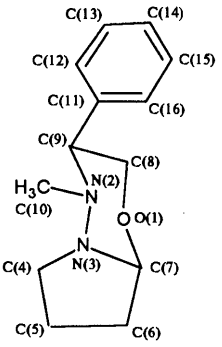

Fig. 1. Atomic Numbering of (3a*S*,6*R*)-**3a**

The absolute configuration of a newly created asymmetric carbon atom at the 3a-position of the heterocyclic ring of **5** was established by X-ray analysis. The atomic numbering is shown in Fig. 1, and the crystal data are summarized in Table I. The positional and thermal parameters with their standard deviations are listed in Table II. The intramolecular bond distances and bond angles for nonhydrogen atoms are given in Table III. Stereoscopic drawings of the molecular structure are shown in Fig. 2. It was determined that the hydrogen atom at the 3a-position of the ring is attached in a *cis* relationship to the phenyl group at the 6-position.

On the other hand, **6** was obtained as a mixture of two isomers, and the ratio of the major to the minor components was estimated as 55:45 by ^{1}H-NMR spectral analysis. Diastereomerically pure **6** could not be isolated from the

TABLE I. Crystal Data

Chemical formula	$C_{13}H_{18}N_2O$
Formula weight	218.30
Crystal system	Orthorhombic
Cell dimensions	a= 7.050 (2) (Å)
	b=25.586 (6) (Å)
	c= 6.641 (5) (Å)
Cell volume (Å^3)	1197.9 (10)
Space group	$P2_12_12_1$
Z	4
D_c (g cm^{-3})	1.12

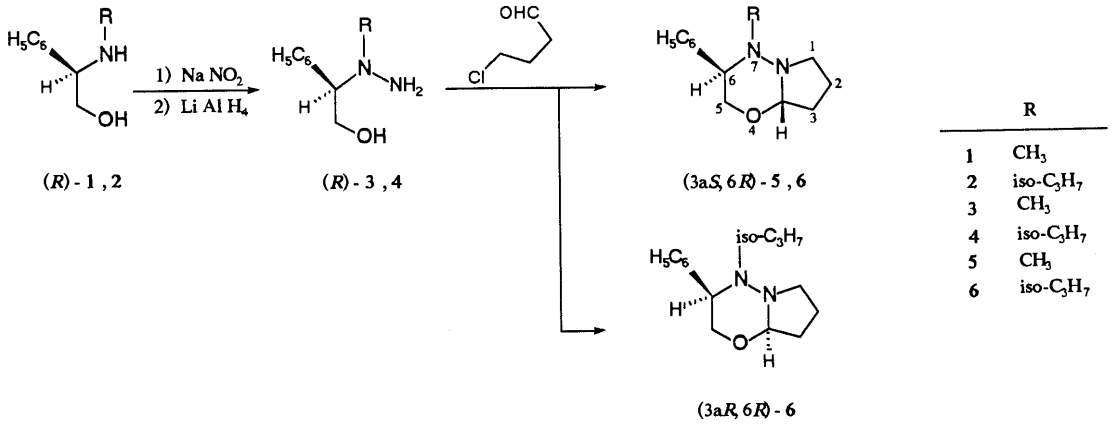

Chart 1

TABLE II. Positional and Thermal Parameters of (3a*S*,6*R*)-**3a** for Nonhydrogen Atoms with Their Standard Deviations in Parentheses

Atom	*X*	*Y*	*Z*	B_{eq} (Å^2)[a]
O(1)	0.973 (1)	0.1014 (3)	0.418 (1)	2.6
N(2)	0.871 (1)	0.1386 (2)	0.537 (1)	2.4
N(3)	0.680 (1)	0.0634 (2)	0.307 (1)	3.5
C(4)	0.856 (1)	0.0861 (4)	0.245 (1)	3.3
C(5)	1.092 (2)	0.0166 (4)	0.335 (2)	5.4
C(6)	0.975 (2)	0.0404 (4)	0.148 (2)	4.7
C(7)	0.997 (1)	0.1571 (4)	0.697 (2)	3.5
C(8)	0.369 (1)	0.1851 (4)	1.001 (2)	3.6
C(9)	0.485 (1)	0.1470 (4)	0.901 (1)	3.2
C(10)	0.577 (1)	0.1594 (3)	0.719 (1)	2.5
C(11)	0.619 (1)	0.1175 (3)	0.613 (1)	2.7
C(12)	0.352 (1)	0.2348 (4)	0.915 (2)	3.4
C(13)	0.444 (1)	0.2471 (4)	0.736 (2)	3.8
C(14)	1.040 (1)	0.0523 (3)	0.521 (2)	3.5
C(15)	0.578 (1)	0.1000 (4)	0.425 (2)	3.6
C(16)	0.558 (1)	0.2097 (3)	0.635 (2)	3.2

a) $B_{eq}=(4/3)\sum_i\sum_j \beta_{ij}\boldsymbol{a}_i\boldsymbol{a}_j$.

TABLE III. Bond Distances (Å) and Bond Angles (°) of (3a*S*,6*R*)-**3a** for Nonhydrogen Atoms with Their Standard Deviations in Parentheses

Bond distance (Å)			
O(1)–C(7)	1.432 (13)	C(6)–C(7)	1.573 (16)
O(1)–C(8)	1.416 (12)	C(8)–C(9)	1.543 (14)
N(2)–N(3)	1.428 (10)	C(9)–C(11)	1.514 (13)
N(2)–C(9)	1.469 (12)	C(11)–C(12)	1.407 (13)
N(2)–C(10)	1.463 (12)	C(11)–C(16)	1.409 (13)
N(3)–C(4)	1.506 (13)	C(12)–C(13)	1.419 (15)
N(3)–C(7)	1.470 (13)	C(13)–C(14)	1.393 (15)
C(4)–C(5)	1.580 (18)	C(14)–C(15)	1.397 (15)
C(5)–C(6)	1.613 (19)	C(15)–C(16)	1.435 (14)
Bond angle (°)			
C(7)–O(1)–C(8)	109.3 (8)	O(1)–C(8)–C(9)	112.3 (8)
N(3)–N(2)–C(9)	112.3 (7)	N(2)–C(9)–C(8)	106.0 (7)
N(3)–N(2)–C(10)	108.2 (7)	N(2)–C(9)–C(11)	111.1 (7)
C(9)–N(2)–C(10)	113.3 (7)	C(8)–C(9)–C(11)	107.9 (8)
N(2)–N(3)–C(4)	117.5 (7)	C(9)–C(11)–C(12)	121.0 (8)
N(2)–N(3)–C(7)	109.3 (7)	C(9)–C(11)–C(16)	118.8 (8)
C(4)–N(3)–C(7)	108.2 (7)	C(12)–C(11)–C(16)	120.2 (8)
N(3)–C(4)–C(5)	101.5 (9)	C(11)–C(12)–C(13)	119.0 (9)
C(4)–C(5)–C(6)	105.4 (10)	C(12)–C(13)–C(14)	121.0 (10)
C(5)–C(6)–C(7)	103.8 (9)	C(13)–C(14)–C(15)	120.7 (10)
O(1)–C(7)–N(3)	111.3 (8)	C(14)–C(15)–C(16)	118.9 (9)
O(1)–C(7)–C(6)	106.1 (8)	C(11)–C(16)–C(15)	120.3 (9)
N(3)–C(7)–C(6)	102.7 (8)		

mixture by column chromatography. It was considered that the two diastereomeric isomers are equilibrated during column chromatography owing to the cleavage of the carbon–oxygen bond of the 4-oxa-7,7a-diazaperhydroindan ring, since cleavage of the carbon–oxygen bond of the chiral 1,3-oxazolidine ring during column chromatography been reported.[1)]

The Grignard reaction of diastereomerically pure 7-methyl-6-phenyl-4-oxa-7,7a-diazaperhydroindan (**5**) with methyl, ethyl, benzyl, and phenylmagnesium halides gave diastereomeric mixtures of 1-[*N*-(2-hydroxy-1-phenylethyl)-*N*-methylamino]pyrrolidine (**7a**—**d**) in 81—88% yields. On the other hand, a diastereomeric mixture of 7-isopropyl-6-phenyl-4-oxa-7,7a-diazaperhydroindan (**6**) gave diastereomerically pure 1-[*N*-(2-hydroxy-1-phenylethyl)-*N*-isopropylamino]pyrrolidines (**8a**—**d**) in the same reaction, in

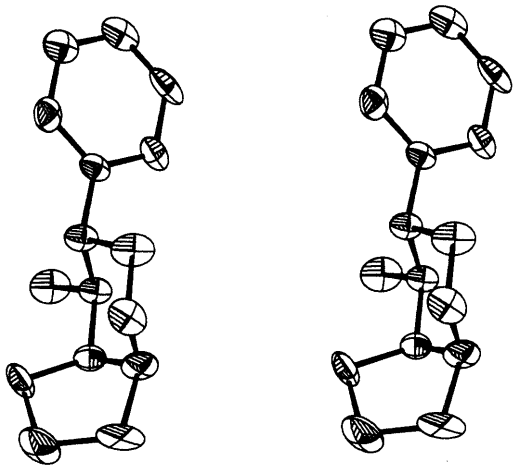

Fig. 2. Stereoscopic Drawings of the Structure of (3a*S*,6*R*)-**3a**

TABLE IV. Reaction of 7-Alkyl-6-phenyl-4-oxa-7,7a-diazaperhydroindans (**5** and **6**) with Grignard Reagent at 0 °C for 12 h

Reactant	Reagent (eq mol)	Solvent	Product	Yield[a] (%)	Ratio of[b] (1′*R*,2*R*):(1′*R*,2*S*)
5[c]	CH_3MgBr	(3) Et_2O–THF	**7a**	83	75:25
5[c]	C_2H_5MgBr	(3) Et_2O–THF	**7b**	86	58:42
5[c]	$C_6H_5CH_2MgCl$	(4) THF	**7c**	88	46:54
5[c]	C_6H_5MgBr	(4) THF	**7d**	81	25:75
6[d]	CH_3MgBr	(3) Et_2O–THF	**8a**	81	— : >98
6[d]	C_2H_5MgBr	(3) Et_2O–THF	**8b**	80	— : >98
6[d]	$C_6H_5CH_2MgCl$	(4) THF	**8c**	82	>98 : —
6[d]	C_6H_5MgBr	(4) Et_2O–THF	**8d**	62	>98 : —

a) Isolated yield. b) Estimated by ^{1}H-NMR (270 MHz) spectral analysis. c) Diastereomerically pure compound was used. d) Diastereomeric mixture (ratio, 55:45) was used.

62—82% yields, as shown in Chart 2. Thus, it was found that the stereoselectivity of these Grignard reactions does not correlate with the configuration at the 3a-position of 4-oxa-7,7a-diazaperhydroindans. The ratios of the major to the minor components of **7a**—**d** were estimated by ^{1}H-NMR spectral analysis, and **8a**—**d** were confirmed to consist of a single isomer by ^{1}H-NMR spectral analysis. These experimental data are summarized in Table IV.

The absolute configurations at the 2-position of **8c**, **7a**, and **7c** were elucidated as follows. (*R*)-2-Benzylpyrrolidine (**9**)[5)] was converted to (*R*)-1-amino-2-benzylpyrrolidine (**10**), and (*R*)-2-benzyl-1-isopropylaminopyrrolidine (**11**) was obtained by *N*-isopropylation of (*R*)-**10**. Alternatively, (*R*)-**11** was also obtained by hydrogenolysis of **8c** using a palladium–carbon catalyst. Both products were identical on ^{1}H-NMR spectral and specific rotation comparisons. Consequently, the absolute configuration of **8c** was determined as (1′*R*,2*R*), and those of **8a**, **8b**, and **8d** were deduced to be the same as that of **8c**, form a in Chart 2, on the assumption that these compounds might have been formed by a similar reaction mechanism.

(*R*)-2-Methylpyrrolidine hydrochloride (**12**)[6)] was converted to (*R*)-1-amino-2-methylpyrrolidine (**13**), followed by condensation of ethyl phenylglyoxylate to give 1-(α-ethoxycarbonylbenzylideneamino)-2-methylpyrrolidines (**14**). Reduction of **14** with lithium aluminum hydride gave

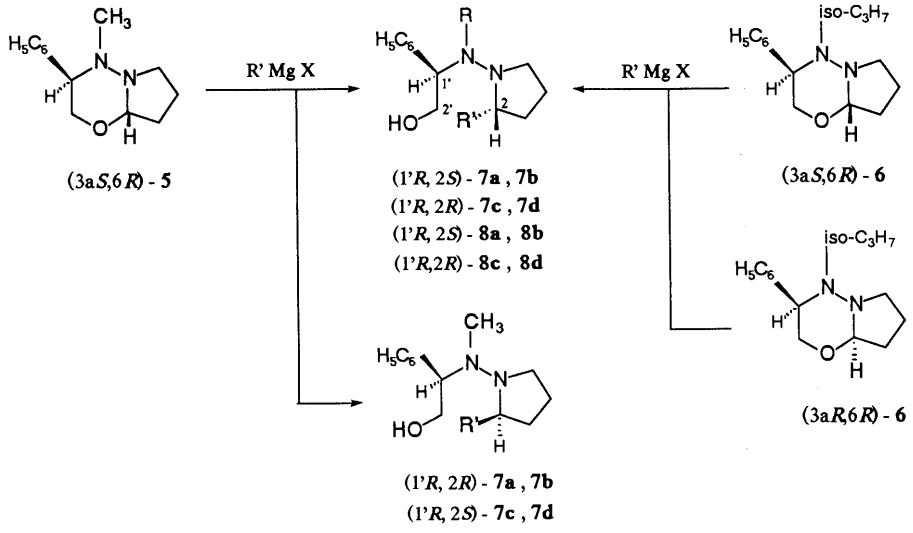

7	R	R'
a	CH_3	CH_3
b	CH_3	C_2H_5
c	CH_3	$CH_2C_6H_5$
d	CH_3	C_6H_5

8	R	R'
a	iso - C_3H_7	CH_3
b	iso-C_3H_7	C_2H_5
c	iso-C_3H_7	$CH_2C_6H_5$
d	iso-C_3H_7	C_6H_5

Chart 2

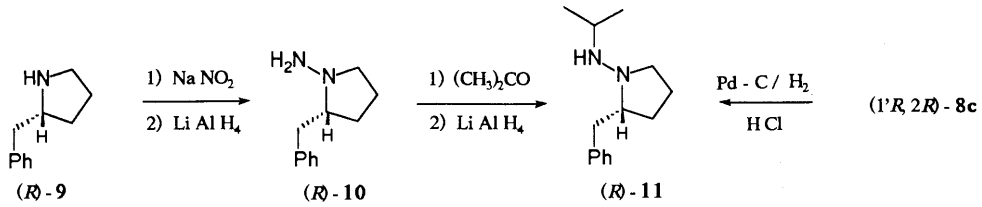

Chart 3

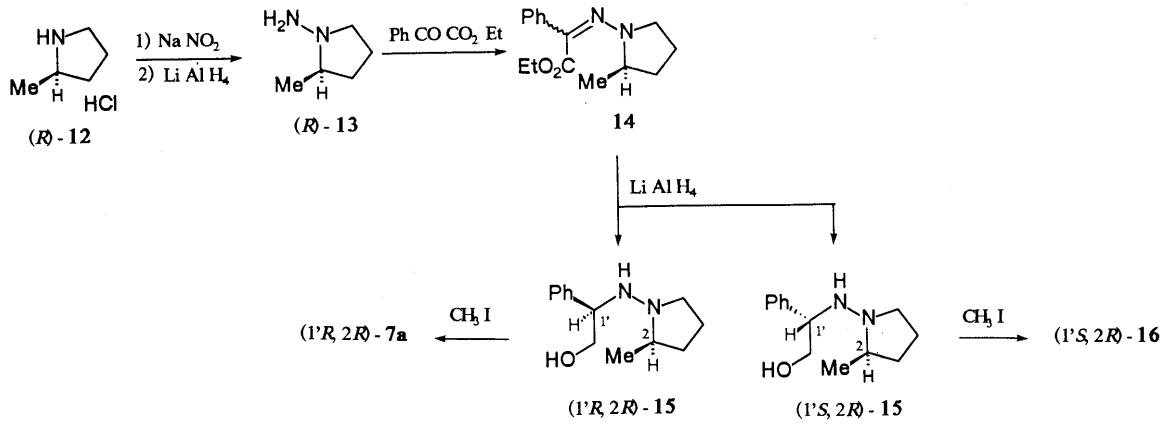

Chart 4

a mixture of (1′*R*,2*R*)- and (1′*S*,2*R*)-1-[*N*-(2-hydroxy-1-phenylethyl)amino]-2-methylpyrrolidines (**15**), and the diastereomerically pure compound was isolated by column chromatography on silica gel. Compounds (1′*R*,2*R*)-**15** and (1′*S*,2*R*)-**15** were converted to the *N*-methyl products [(1′*R*,2*R*)-**7a** and (1′*S*,2*R*)-**16**]. Then, the ^{1}H-NMR spectra and specific rotations of **7a** (ratio of diastereomers, 75 : 25), (1′*R*,2*R*)-**7a**, and (1′*S*,2*R*)-**16** were compared with each other. The specific rotation of (1′*R*,2*S*)-**7a** may be estimated as $[\alpha]_D + 111.7°$ if (1′*R*,2*S*)-**7a** is the minor component, whereas it is $[\alpha]_D + 31.9°$ if (1′*R*,2*S*)-**7a** is the major component. Consequently, it was concluded that (1′*R*,2*S*)-**7a** is the minor component, since the specific rotation of (1′*S*,2*R*)-**16** was $[\alpha]_D - 121.8°$.

Similarly, the condensation of (*R*)-**10** with ethyl phenylglyoxylate gave a mixture of 2-benzyl-1-[*N*-(α-ethoxycarbonylbenzylidene)amino]pyrrolidines (**17**), which was converted to a mixture of 2-benzyl-1-[*N*-(2-hydroxy-1-phenylethyl)amino]pyrrolidines (**18**) by reduction with lithium aluminum hydride. The diastereomerically pure

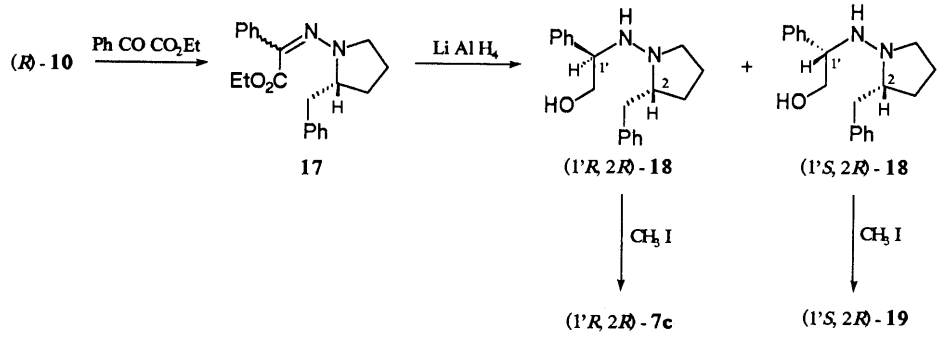

Chart 5

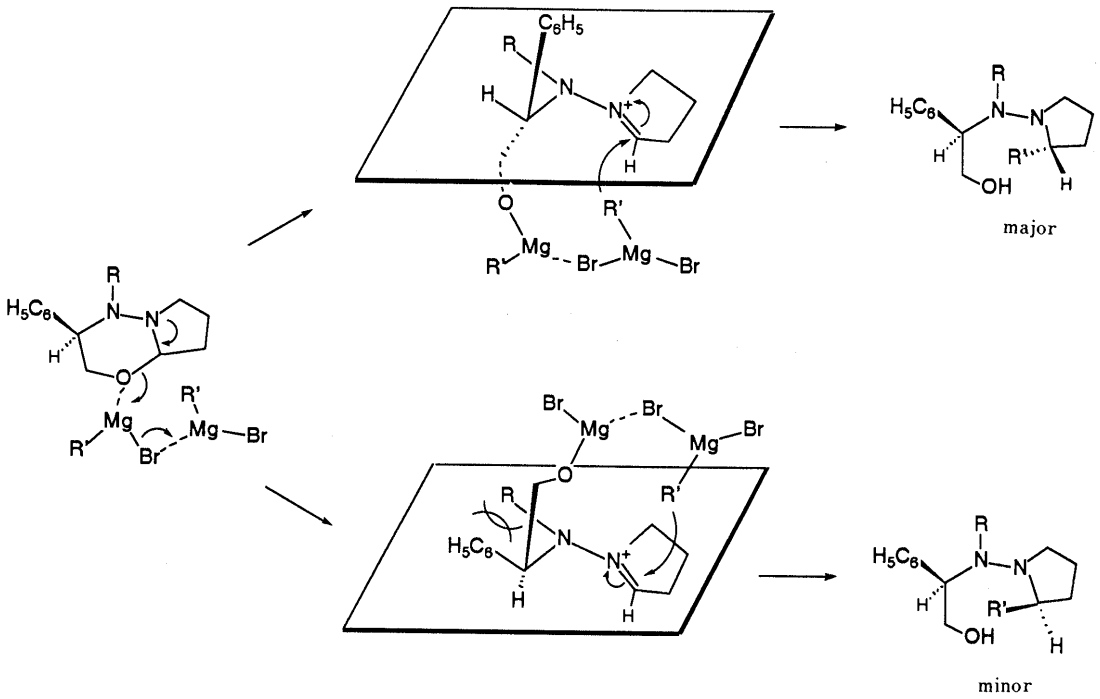

Chart 6

compound was isolated by column chromatography on silica gel. Compounds (1′*R*,2*R*)-**18** and (1′*S*,2*R*)-**18** were converted to (1′*R*,2*R*)-**7c** and (1′*S*,2*R*)-**19**, respectively. The ^{1}H-NMR spectra and the specific rotations of **7c** (ratio of diastereomers, 54:46), (1′*R*,2*R*)-**7c**, (1′*S*,2*R*)-**19** were compared with each other, and the configuration of the minor component of **7c** may be assumed as (1′*R*,2*R*).

We have reported the stereoselective Grignard reaction of 3-alkyl-4-phenyl-1,3-oxazolidines prepared from (*R*)-*N*-alkylphenylglycinol, and proposed a possible reaction mechanism, *i.e.*, the Grignard reagent approaches the oxygen atom of the 1,3-oxazolidine ring to give a favorable intermediate iminium salt, and nucleophilic attach occurs from the *si*-face of the carbon–nitrogen double bond of the intermediate.[1] Thus, it was considered that the Grignard reaction of 7-alkyl-6-phenyl-4-oxa-7,7a-diazaperhydroindans (**5** and **6**) prepared from (*R*)-*N*-alkylphenylglycinol occurs by a similar reaction mechanism to that of 3-alkyl-4-phenyl-1,3-oxazolidines, as shown in Chart 6. Furthermore, the extremely highly diastereoselective reaction presumably proceeded by nucleophilic attack from the *si*-face of the intermediate in the *N*-isopropyl compound (**6**), because steric hindrance is considered to occur between the isopropyl group at the *N*-position and the phenyl group at the 1′-position.

Experimental

The ^{1}H-NMR spectra were obtained with a JEOL JNM-GSX270 spectrometer. The mass spectra (MS) were recorded with a JEOL JMS-D300 spectrometer by using the electron impact (EI) and the chemical ionization (CI) (isobutane) methods. The melting points were measured with a Yanagimoto micro melting point apparatus and are uncorrected. The optical rotations were measured at 20—23°C with a JASCO DIP-360 digital polarimeter.

(*R*)-*N*-(2-Hydroxy-1-phenylethyl)-*N*-methylhydrazine (3a) An aqueous solution of $NaNO_2$ (2.76 g, 40 mmol) in H_2O (6 ml) was added dropwise to a suspension of (*R*)-*N*-(2-hydroxy-1-phenylethyl)-*N*-methylamine (**1**)[3] (3.02 g, 20 mmol) in H_2O (6 ml) with vigorous stirring on an ice-cold bath, and then acetic acid (1.80 g, 30 mmol) was added. The mixture was stirred at room temperature for 4 h, the whole was extracted with ether, and the ethereal solution was dried over Na_2SO_4 and concentrated under reduced pressure to give the *N*-nitroso compound as a colorless oil. The *N*-nitroso compound was slowly added to a stirred suspension of $LiAlH_4$ (1.14 g, 30 mmol) in tetrahydrofuran (THF) (60 ml), and the mixture was refluxed for 3 h. After treatment with a small amount of water, the resulting white precipitate was filtered off, and the filtrate was dried over Na_2SO_4 and concentrated under reduced pressure. The residue was distilled *in vacuo* to give a colorless oil (2.66 g, 80%), bp 165—170 °C (1.2 mmHg). $[\alpha]_D$ −40.0° (c=1.98, EtOH). MS *m/z*: Calcd for $C_9H_{14}N_2O$, 166.1103 (M^+); Found, 166.1101. EI, 166 (M^+), 135 (M^+-CH_2OH); CI, 167 (M^++1),

135 ($M^+ - CH_2OH$), 121 ($M^+ - CH_3NNH_2$). ^{1}H-NMR ($CDCl_3$) δ: 2.45 (3H, s, NCH_3), 3.2—3.3 (2H, br s, NH_2), 3.56 (1H, dd, J=2.4, 8.6 Hz, $NC\underline{H}CH_2O$), 3.69 (1H, dd, J=2.4, 11.0 Hz, $NCHC\underline{H}_2O$), 4.15 (1H, dd, J=8.6, 11.0 Hz, $NCHC\underline{H}_2O$), 4.8—5.1 (1H, br s, OH), 7.36—7.48 (5H, m, aromatic H).

(*R*)-*N*-(2-Hydroxy-1-phenylethyl)-*N*-isopropylhydrazine (4) *N*-Amination of (*R*)-*N*-(2-hydroxy-1-phenylethyl)-*N*-isopropylamine (**2**)[4] (3.59 g, 20 mmol) was achieved in a similar manner to that described for the preparation of (*R*)-**3** to give (*R*)-**4** (2.37 g, 61%) as a colorless oil, bp 146—150 °C (1.3 mmHg). $[\alpha]_D$ −24.7° (c=1.40, EtOH). MS *m/z*: Calcd for $C_{11}H_{18}N_2O$, 194.1413 (M^+); Found, 194.1408. EI, 194 (M^+), 163 ($M^+ - CH_2OH$); CI, 195 ($M^+ + 1$), 163 ($M^+ - CH_2OH$). ^{1}H-NMR ($CDCl_3$) δ: 0.89 (3H, d, J=6.7 Hz, $CHC\underline{H}_3$), 1.00 (3H, d, J=6.7 Hz, $CHC\underline{H}_3$), 1.5—1.7 (2H, br s, NH_2), 2.82 (1H, septet, J=6.7 Hz, $C\underline{H}(CH_3)_2$), 3.54 (1H, dd, J=2.4, 11.0 Hz, $NCHC\underline{H}_2O$), 3.80 (1H, dd, J=2.4, 8.5 Hz, $NC\underline{H}CH_2O$), 4.0—4.1 (1H, br s, OH), 4.02 (1H, dd, J=8.5, 11.0 Hz, $NCHC\underline{H}_2O$), 7.21—7.35 (5H, m, aromatic H).

(3a*S*,6*R*)-7-Methyl-6-phenyl-4-oxa-7,7a-diazaperhydroindan (5) A solution of (*R*)-**3** (3.32 g, 20 mmol) in CH_2Cl_2 (20 ml) was added dropwise to a solution of γ-chlorobutyraldehyde (2.34 g, 22 mmol) in CH_2Cl_2 (30 ml) in the presence of anhydrous $MgSO_4$ (6 g), and the reaction mixture was stirred at room temperature for 1 h. The precipitate was filtered off and the solvent was evaporated under reduced pressure. The residue thus obtained was dissolved in benzene (40 ml) and the solution was refluxed in the presence of K_2CO_3 (6 g) for 24 h. After removal of the solid, the reaction mixture was concentrated under pressure and the residue was subjected to column chromatography on silica gel with a solution of ether–hexane (1 : 1) to give (3a*S*,6*R*)-**5** (3.49 g, 80%). Colorless columns, mp 79 °C (hexane). $[\alpha]_D$ −193.9° (c=1.10, EtOH). *Anal.* Calcd for $C_{13}H_{18}N_2O$: C, 71.52; H, 8.31; N, 12.83. Found: C, 71.64; H, 8.45; N, 12.80. MS *m/z*: EI, 218 (M^+); CI, 219 ($M^+ + 1$). ^{1}H-NMR ($CDCl_3$) δ: 1.67—2.10 (4H, m, CH_2CH_2), 2.32 (3H, s, NCH_3), 2.93 (1H, dt, J=2.4, 8.5 Hz, $NC\underline{H}_2CH_2$), 3.30 (1H, q, J=8.5 Hz, $NC\underline{H}_2CH_2$), 3.61—3.83 (3H, m, $NCHCH_2$), 4.86 (1H, d, J=3.7 Hz, NCHO), 7.26—7.39 (5H, m, aromatic H).

Diastereomeric Mixture of 7-Isopropyl-6-phenyl-4-oxa-7,7a-diazaperhydroindans (6) The condensation of (*R*)-**4** (20 mmol) with γ-chlorobutyraldehyde (2.34 g, 22 mmol) gave a diastereomeric mixture of **6** (3.25 g, 66%) as a colorless oil in a similar manner to the preparation of (3a*S*,6*R*)-**5**, bp 67—70°C (1.3 mmHg). The ratio of the major to the minor components was estimated as 55 : 45 by ^{1}H-NMR spectrometric analysis. MS *m/z*: EI, 246 (M^+), 203 ($M^+ - C_3H_7$); CI, 247 ($M^+ + 1$). ^{1}H-NMR ($CDCl_3$) δ: Major component; 0.86 (3H, d, J=6.7 Hz, $CHC\underline{H}_3$), 1.09 (3H, d, J=6.7 Hz, $CHC\underline{H}_3$), 1.58—2.08 (4H, m, CH_2CH_2), 2.99 (1H, septet, J=6.7 Hz, $C\underline{H}(CH_3)_2$), 3.12 (1H, q, J=8.5 Hz, NCH_2), 3.26 (1H, dt, J=3.7, 8.5 Hz, NCH_2), 3.62—3.88 (2H, m, $NC\underline{H}CH_2O$), 4.18—4.25 (1H, m, $NCHC\underline{H}_2O$), 4.80 (1H, d, J=3.1 Hz, NCHO), 7.22—7.46 (5H, m, aromatic H). Minor component; 1.02 (6H, d, J=6.1 Hz, $CH(C\underline{H}_3)_2$), 2.73 (1H, septet, J=6.1 Hz, $C\underline{H}(CH_3)_2$), 2.78 (1H, dt, J=3.1, 7.9 Hz, NCH_2), 3.40 (1H, q, J=7.9 Hz, NCH_2), 5.07 (1H, d, J=3.7 Hz, NCHO), 7.22—7.46 (5H, m, aromatic H).

Crystallographic Measurements A single crystal of (3a*S*,6*R*)-**5** was grown in hexane solution as a colorless column with dimensions of 0.4 × 0.3 × 0.4 mm. All the measurements were performed on a Rigaku AFC-5 diffractometer using graphite-monochromated CuK_α radiation. The unit cell dimensions were determined by least-squares calculation with 24 high-angle reflections.

Intensity data were collected by using the $2\theta/\omega$ scan technique with an average scan rate of 4°/min. In total, 1248 independent reflections with $0° < 2\theta < 130°$ were collected, of which 1183 that satisfied the condition $F_0 > 3\sigma(F)$ were used for calculations.

Structure Analysis and Refinement The structure was solved by the direct method using MULTAN[7] and the Rigaku crystallographic package RASA-II. The structure was refined by the block-diagonal least-squares technique with anisotropic thermal factors for all nonhydrogen atoms. The *R* factor was finally reduced to 0.102.

General Procedure for the Reaction of (3a*S*,6*R*)-5 with Grignard Reagents Grignard reagent (CH_3MgBr or C_2H_5MgBr, 3 mmol; $C_6H_5CH_2MgCl$ or C_6H_5MgBr, 4 mmol) was added dropwise to a stirred solution of (3a*S*,6*R*)-**5** (0.22 g, 1 mmol) in THF (2 ml) at 0 °C under a nitrogen atmosphere. After being stirred at 0 °C for 12 h, the reaction mixture was treated with a small amount of water. The resulting white precipitate was filtered off, and the filtrate was diluted with CH_2Cl_2 (10 ml). The organic layer was dried over Na_2SO_4 and concentrated under reduced pressure to give a colorless oily residue. The ratios of the major to the minor components were estimated by ^{1}H-NMR spectrometric analysis. The residues were subjected to column chromatography on silica gel with a solution of ether–hexane (1 : 1) to give the corresponding diastereomeric mixture of **7a—d** as a colorless oil. The experimental data are summarized in Table IV.

1-[*N*-(2-Hydroxy-1-phenylethyl)-*N*-methylamino]-2-methylpyrrolidine (**7a**): CH_3MgBr (1 ml of a 3 M solution in ether) was used. Specific rotation of this mixture (ratio, 75 : 25) was $[\alpha]_D$ +22.0° (c=1.12, EtOH). ^{1}H-NMR ($CDCl_3$) δ: Major component, (1′*R*,2*R*); 1.36 (3H, d, J=6.1 Hz, $CH_2CHC\underline{H}_3$), 1.69—1.90 (4H, m, CH_2CH_2), 2.02 (3H, s, NCH_3), 2.74 (1H, dq, J=2.6, 6.1 Hz, $C\underline{H}CH_3$), 2.80 (1H, q, J=9.2 Hz, NCH_2), 3.05 (1H, dt, J=3.7, 9.2 Hz, NCH_2), 3.48 (1H, dd, J=2.0, 11.5 Hz, $NCHC\underline{H}_2O$), 3.72 (1H, dd, J=2.0, 9.2 Hz, $NC\underline{H}CH_2O$), 3.98 (1H, dd, J=9.2, 11.5 Hz, $NCHC\underline{H}_2O$), 6.3—6.5 (1H, br s, OH), 7.24—7.32 (5H, m, aromatic H). Minor component, (1′*R*,2*S*); 1.31 (3H, d, J=6.1 Hz, $CHC\underline{H}_3$), 2.24 (3H, s, NCH_3), 2.74—2.92 (2H, m, $CH_3C\underline{H}CH_3$ and NCH_2), 3.05—3.10 (1H, m, NCH_2), 3.60 (1H, dd, J=2.0, 10.8 Hz, $NCHC\underline{H}_2O$), 3.94 (1H, dd, J=2.0, 9.0 Hz, $NC\underline{H}CH_2O$), 4.04 (1H, dd, J=9.0, 10.8 Hz, $NCHC\underline{H}_2O$), 7.22—7.31 (5H, m, aromatic H).

2-Ethyl-1-[*N*-(2-hydroxy-1-phenylethyl)-*N*-methylamino]pyrrolidine (**7b**): C_2H_5MgBr (1 ml of a 3 M solution in ether) was used. ^{1}H-NMR ($CDCl_3$) δ: Major component, (1′*R*,2*R*); 0.98 (3H, t, J=7.3 Hz, $CH_2C\underline{H}_3$), 1.34—1.95 (4H, m, CH_2CH_2), 1.97—2.01 (2H, m, $C\underline{H}_2CH_3$), 2.03 (3H, s, NCH_3), 2.64—2.81 (2H, m, NCH_2, $C\underline{H}CH_2CH_3$), 2.84—2.92 (1H, m, NCH_2), 3.47 (1H, t, J=9.8 Hz, $NCHC\underline{H}_2O$), 3.73 (1H, dd, J=2.4, 9.8 Hz, $NC\underline{H}CH_2O$), 3.90—4.07 (1H, m, $NCHC\underline{H}_2O$), 6.4 (1H, br s, OH), 7.23—7.31 (5H, m, aromatic H). Minor component, (1′*R*,2*S*); 0.92 (3H, t, J=7.3 Hz, $CH_2C\underline{H}_3$), 2.20—2.29 (2H, m, $C\underline{H}_2CH_3$), 2.25 (3H, s, NCH_3), 3.02—3.09 (1H, m, NCH_2), 3.63 (1H, t, J=6.1 Hz, $NCHC\underline{H}_2O$), 3.90—4.07 (2H, m, $NC\underline{H}CH_2O$), 5.9 (1H, br s, OH), 7.23—7.31 (5H, m, aromatic H).

2-Benzyl-1-[*N*-(2-hydroxy-1-phenylethyl)-*N*-methylamino]pyrrolidine (**7c**): $C_6H_5CH_2MgCl$ (4 ml of a 1 M solution in THF) was used. Specific rotation of this mixture (ratio, 54 : 46) was $[\alpha]_D$ +10.0° (c=1.32, EtOH). ^{1}H-NMR ($CDCl_3$) δ: Major component, (1′*R*,2*S*); 1.41—1.81 (4H, m, CH_2CH_2), 2.10 (3H, s, NCH_3), 2.55 (1H, dd, J=10.1, 13.4 Hz, $PhCH_2$), 2.76—2.86 (1H, m, NCH_2), 2.99—3.07 (1H, m, NCH_2), 3.09—3.14 (1H, m, $PhCH_2C\underline{H}$), 3.52 (1H, dd, J=1.8, 11.8 Hz, $NCHC\underline{H}_2O$), 3.70 (1H, dd, J=3.7, 13.4 Hz, $PhCH_2$), 3.73 (1H, dd, J=1.8, 9.2 Hz, $NC\underline{H}CH_2O$), 4.05 (1H, dd, J=9.2, 11.6 Hz, $NCHC\underline{H}_2O$), 6.3 (1H, br s, OH), 7.19—7.36 (10H, m, aromatic H). Minor component, (1′*R*,2*R*); 1.21—1.78 (4H, m, CH_2CH_2), 2.38 (3H, s, NCH_3), 2.58 (1H, dd, J=10.7, 13.4 Hz, $PhCH_2$), 2.69—2.79 (1H, m, NCH_2), 2.86—2.94 (1H, m, NCH_2), 3.19—3.29 (1H, m, $PhCH_2C\underline{H}$), 3.39 (1H, dd, J=3.7, 13.4 Hz, $PhCH_2$), 3.68 (1H, dd, J=2.4, 10.4 Hz, $NCHC\underline{H}_2O$), 3.97 (1H, dd, J=2.4, 9.5 Hz, $NC\underline{H}CH_2O$), 4.08 (1H, dd, J=9.5, 10.4 Hz, $NCHC\underline{H}_2O$), 7.18—7.36 (10H, m, aromatic H).

1-[*N*-(2-Hydroxy-1-phenylethyl)-*N*-methylamino]-2-phenylpyrrolidine (**7d**): C_6H_5MgBr (4 ml of a 1 M solution in THF) was used. ^{1}H-NMR ($CDCl_3$) δ: Major component, (1′*R*,2*S*); 1.92—2.15 (4H, m, CH_2CH_2), 2.10 (3H, s, NCH_3), 2.89 (1H, q, J=8.5 Hz, NCH_2), 3.14 (1H, dt, J=3.7, 8.5 Hz, NCH_2), 3.25 (1H, d, J=7.3 Hz, $PhC\underline{H}$), 3.63 (1H, dd, J=4.3, 8.3 Hz, $NC\underline{H}CH_2O$), 3.78—3.84 (2H, m, $NCHC\underline{H}_2O$), 5.5 (1H, br s, OH), 6.93—7.25 (10H, m, aromatic H). Minor component, (1′*R*,2*R*); 1.92—2.15 (4H, m, CH_2CH_2), 2.41 (3H, s, NCH_3), 2.45—2.53 (1H, m, NCH_2), 3.33 (1H, dd, J=3.7, 8.7 Hz, $NC\underline{H}CH_2O$), 3.71—3.81 (2H, m, $NCHC\underline{H}_2O$), 5.9 (1H, br s, OH), 6.93—7.25 (10H, m, aromatic H).

General Procedure for the Reaction of a Diastereomeric Mixture of 6 with Grignard Reagents Grignard reagent (CH_3MgBr or C_2H_5MgBr, 3 mmol; $C_6H_5CH_2MgCl$ or C_6H_5MgBr, 4 mmol) was added dropwise to a stirred solution of the diastereomeric mixture (ratio, 55 : 45) of **6** (0.25 g, 1 mmol) in THF (2 ml) at 0°C under a nitrogen atmosphere. After being stirred at 0 °C for 12 h, the reaction mixture was worked up in a similar manner to that employed in the reaction of (3a*S*,6*R*)-**5** to give the corresponding product (**8a—d**) as a colorless crystaline solid. The experimental data are summarized in Table IV.

(1′*R*,2*S*)-1-[*N*-(2-Hydroxy-1-phenylethyl)-*N*-isopropylamino]-2-methylpyrrolidine (**8a**): CH_3MgBr (1 ml of a 3 M solution in ether) was used. Colorless plates, mp 109—110 °C (hexane). $[\alpha]_D$ +64.9° (c=0.82, EtOH). *Anal.* Calcd for $C_{16}H_{26}N_2O$: C, 73.24; H, 9.99; N, 10.68. Found: C, 73.54; H, 10.15; N, 10.68. MS *m/z*: CI, 263 ($M^+ + 1$), 121 ($M^+ - PhCHCH_2OH$). ^{1}H-NMR ($CDCl_3$) δ: 0.60 (3H, d, J=6.7 Hz, $CHC\underline{H}_3$), 1.08 (3H, d, J=6.7 Hz, $CHC\underline{H}_3$), 1.38 (3H, d, J=6.1 Hz, $CHC\underline{H}_3$), 1.62—1.92 (4H, m, CH_2CH_2), 2.63 (1H, q, J=8.6 Hz, NCH_2), 2.83 (1H, ddq, J=1.8, 14.0, 6.1 Hz, $CH_3C\underline{H}CH_2$), 3.07 (1H, septet, J=6.7 Hz, $C\underline{H}(CH_3)_2$), 3.17 (1H,

dt, J=8.6, 3.7 Hz, NCH_2), 3.34 (1H, m, $NCHCH_2O$), 3.94 (1H, dd, J=8.6, 11.6 Hz, $NCHCH_2O$), 4.15 (1H, dd, J=1.8, 8.6 Hz, $NCHCH_2O$), 5.9 (1H, br s, OH), 7.19—7.39 (5H, m, aromatic H).

(1′*R*,2*S*)-2-Ethyl-1-[*N*-(2-hydroxy-1-phenylethyl)-*N*-isopropylamino]-pyrrolidine (**8b**): C_2H_5MgBr (1 ml of a 3 M solution in ether) was used. Colorless columns, mp 123—124 °C (ether–hexane). $[\alpha]_D$ +71.8° (c=0.94, EtOH). *Anal.* Calcd for $C_{17}H_{28}N_2O$: C, 73.86; H, 10.21; N, 10.14. Found: C, 74.11; H, 10.57; N, 10.15. MS *m/z*: CI, 277 (M^++1), 155 (M^+−$PhCHCH_2OH$). ^{1}H-NMR ($CDCl_3$) δ: 0.60 (3H, d, J=7.3 Hz, $CHCH_3$), 0.97 (3H, t, J=7.3 Hz, CH_2CH_3), 1.08 (3H, d, J=7.3 Hz, $CHCH_3$), 1.35 (2H, m, CH_2CH_3), 1.60—1.89 (4H, m, CH_2CH_2), 2.37 (1H, m, CH_3CH_2CH), 2.65 (1H, q, J=9.2 Hz, NCH_2), 3.09 (1H, septet, J=7.3 Hz, $CH(CH_3)_2$), 3.19 (1H, dt, J=9.2, 3.1 Hz, NCH_2), 3.33 (1H, dd, J=2.4, 11.6 Hz, $NCHCH_2O$), 3.93 (1H, dd, J=9.1, 11.6 Hz, $NCHCH_2O$), 4.16 (1H, dd, J=2.4, 9.1 Hz, $NCHCH_2O$), 5.9 (1H, br s, OH), 7.20—7.39 (5H, m, aromatic H).

(1′*R*,2*R*)-2-Benzyl-1-[*N*-(2-hydroxy-1-phenylethyl)-*N*-isopropylamino]-pyrrolidine (**8c**): $C_6H_5CH_2MgCl$ (4 ml of a 1 M solution in THF) was used. Colorless columns, mp 106—106.5 °C (ether–hexane). $[\alpha]_D$ +28.7° (c=1.03, EtOH). *Anal.* Calcd for $C_{22}H_{30}N_2O$: C, 78.06; H, 8.93; N, 8.28. Found: C, 78.21; H, 9.13; N, 8.30. MS *m/z*: CI, 339 (M^++1), 217 (M^+−$PhCHCH_2OH$). ^{1}H-NMR ($CDCl_3$) δ: 0.72 (3H, d, J=6.7 Hz, $CHCH_3$), 1.13 (3H, d, J=6.7 Hz, $CHCH_3$), 1.43—1.75 (4H, m, CH_2CH_2), 2.47 (1H, dd, J=10.4, 12.8 Hz, $PhCH_2$), 2.70 (1H, q, J=8.6 Hz, NCH_2), 2.98 (1H, m, $PhCH_2CH$), 3.18 (1H, septet, J=6.7 Hz, $CH(CH_3)_2$), 3.23 (1H, dt, J=8.6, 4.3 Hz, NCH_2), 3.39 (1H, dd, J=2.4, 11.6 Hz, $NCHCH_2O$), 3.86 (1H, d, J=10.4 Hz, $PhCH_2$), 4.03 (1H, dd, J=9.2, 11.6 Hz, $NCHCH_2O$), 4.22(1H, dd, J=2.4, 9.2 Hz, $NCHCH_2O$), 5.8 (1H, br s, OH), 7.18—7.43 (10H, m, aromatic H).

(1′*R*,2*R*)-1-[*N*-(2-Hydroxy-1-phenylethyl)-*N*-isopropylamino]-2-phenylpyrrolidine (**8d**): C_6H_5MgBr (4 ml of a 1 M solution in THF) was used. Colorless plates, mp 63—64 °C (hexane). $[\alpha]_D$ +114.3° (c=1.45, EtOH). MS *m/z*: Calcd for $C_{12}H_{28}N_2O$: 324.2202 (M^+); Found: 324.2202. CI, 325 (M^++1), 203 (M^+−$PhCHCH_2OH$). ^{1}H-NMR ($CDCl_3$) δ: 0.50 (3H, d, J=6.7 Hz, $CHCH_3$), 1.10 (3H, d, J=6.7 Hz, $CHCH_3$), 1.89—2.17 (4H, m, CH_2CH_2), 2.82 (1H, q, J=8.5 Hz, NCH_2), 3.05 (1H, t, J=9.2 Hz, $PhCH$), 3.20—3.30 (3H, m, NCH_2, $CH(CH_3)_2$, and $NCHCH_2O$), 3.82 (1H, dd, J=4.3, 8.5 Hz, $NCHCH_2O$), 4.04 (1H, dd, J=2.4, 8.5 Hz, $NCHCH_2O$), 5.3 (1H, br s, OH), 6.80—7.47 (10H, m, aromatic H).

(*R*)-1-Amino-2-benzylpyrrolidine (10) (*R*)-2-Benzylpyrrolidine (**9**)[5] (3.2 g, 20 mmol) was converted into the *N*-nitroso compound by treatment with $NaNO_2$ and acetic acid, and the product was reduced with $LiAlH_4$ as described for the preparation of (*R*)-**3** to give (*R*)-**10** (2.5 g, 70%). Colorless oil, bp 119—120 °C (3 mmHg). $[\alpha]_D$ +64.5° (c=1.25, EtOH). MS *m/z*: CI, 177 (M^++1), 85 (M^+−$PhCH_2$). ^{1}H-NMR ($CDCl_3$) δ: 1.45—1.86 (4H, m, CH_2CH_2), 2.26—2.42 (2H, m, NCH_2), 2.54 (1H, dd, J=9.3, 13.1 Hz, $PhCH_2$), 2.9 (2H, br s, NH_2), 3.17 (1H, dd, J=4.3, 13.1 Hz, $PhCH_2$), 3.27—3.34 (1H, m, $PhCH_2CH$), 7.16—7.31 (5H, m, aromatic H).

(*R*)-2-Benzyl-1-isopropylaminopyrrolidine (11) i) From (*R*)-**10**: A solution of (*R*)-**10** (0.18 g, 1 mmol) in acetone (10 ml) was refluxed for 3 h, and then the solvent was removed. A solution of the residue in THF (1 ml) was added dropwise to a stirred suspension of $LiAlH_4$ (0.038 g, 1 mmol) in THF (10 ml), and the reaction mixture was refluxed for 20 h. A small amount of water was added, and the resulting white precipitate was filtered off. The filtrate was dried over Na_2SO_4 and concentrated under reduced pressure. The residue was subjected to column chromatography on silica gel with a solution of ether–hexane (1 : 3) to give (*R*)-**11** (0.17 g, 78%) as a colorless oil. $[\alpha]_D$ +101.1° (c=1.00, EtOH). MS *m/z*: Calcd for $C_{14}H_{22}N_2$: 218.1782 (M^+); Found: 218.1744. ^{1}H-NMR ($CDCl_3$) δ: 1.04 (3H, d, J=6.1 Hz, $CHCH_3$), 1.07 (3H, d, J=6.1 Hz, $CHCH_3$), 1.37—1.79 (1H, m, CH_2CH_2), 2.0 (1H, br s, NH), 2.08—2.18 (1H, m, NCH_2), 2.38 (1H, dd, J=9.8, 13.1 Hz, $PhCH_2$), 2.50—2.60 (1H, m, NCH_2), 3.04 (1H, septet, J=6.1 Hz, $CH(CH_3)_2$), 3.29 (1H, dd, J=3.7, 13.1 Hz, $PhCH_2$), 3.44—3.51 (1H, m, $PhCH_2CH$), 7.13—7.29 (5H, m, aromatic H).

ii) From (1′*R*,2*R*)-**8c**: A solution of (1′*R*,2*R*)-**8c** (0.18 g, 0.5 mmol) in methanol (5 ml) was treated with 10% Pd–carbon (0.91 g) and concentrated HCl (0.5 ml), and the mixture was shaken in a hydrogen atmosphere at room temperature for 3 h under a pressure of 3 kg/cm^2. The catalyst was then filtered off and the filtrate was concentrated under reduced pressure. The phenylethanol thus prepared was extracted into ether, and the residual solution was made alkaline with 1 N NaOH aqueous solution and extracted with ether. The ethereal solution was concentrated and the residue was subjected to column chromatography on silica gel with a solution of ether–hexane (1 : 3) to give (*R*)-**11** (0.04 g, 39%). $[\alpha]_D$ +96.1° (c=1.27, EtOH). This compound was identical with (*R*)-**11** prepared from (*R*)-**10** on the basis of ^{1}H-NMR spectral comparison.

(*R*)-1-Amino-2-methylpyrrolidine (13) (*R*)-2-Methylpyrrolidine hydrochloride (**12**)[6] (2.4 g, 20 mmol) was converted into the *N*-nitroso compound by treatment with $NaNO_2$ and acetic acid, and the product was reduced with $LiAlH_4$ as described for the preparation of (*R*)-**3** to give (*R*)-**13** (1.3 g, 65%). Colorless oil, bp 62—67 °C (62 mmHg). $[\alpha]_D$ −35.7° (c=1.23, EtOH). MS *m/z*: CI, 101 (M^++1). ^{1}H-NMR ($CDCl_3$) δ: 1.16 (3H, d, J=6.1 Hz, $CHCH_3$), 1.36—2.02 (4H, m, CH_2CH_2), 2.17 (1H, dq, J=9.2, 6.1 Hz, $CHCH_3$), 2.30 (1H, q, J=9.2 Hz, NCH_2), 2.9 (2H, br s, NH_2), 3.27 (1H, dt, J=9.2, 3.1 Hz, NCH_2).

1-(α-Ethoxycarbonylbenzylideneamino)-2-methylpyrrolidines (14) A mixture of (*R*)-**13** (1.0 g, 10 mmol) and ethyl phenylglyoxylate (2.0 g, 11 mmol) was stirred at 60 °C for 2 h, and the reaction mixture was diluted with CH_2Cl_2 (20 ml). The organic layer was dried over Na_2SO_4 and evaporated under reduced pressure. The residue was subjected to column chromatography on silica gel with a solution of ether–hexane (1 : 3) to give a mixture of two isomers as a pale yellow oil (2.5 g, 95%; 62 : 38 mixture), which was unstable at room temperature. ^{1}H-NMR ($CDCl_3$) δ: Major component; 1.11 (3H, d, J=6.1 Hz, $CHCH_3$), 1.40 (3H, t, CH_2CH_3), 1.56—1.97 (4H, m, CH_2CH_2), 2.13—2.25 (1H, m, NCH_2), 2.95—2.99 (1H, m, NCH_2), 3.01—3.73 (1H, m, $CHCH_3$), 4.38 (2H, q, J=6.7 Hz, CH_2CH_3), 7.41—8.07 (5H, m, aromatic H). Minor component; 1.29 (3H, t, J=7.3 Hz, CH_2CH_3), 1.33 (3H, d, J=6.1 Hz, $CHCH_3$), 1.35—2.01 (4H, m, CH_2CH_2), 2.59 (1H, q, J=7.9 Hz, NCH_2), 2.77 (1H, dt, J=7.9, 4.3 Hz, NCH_2), 3.80 (1H, sextet, J=6.1 Hz, $CHCH_3$), 4.24 (2H, q, J=7.3 Hz, CH_2CH_3), 7.23—7.45 (5H, m, aromatic H).

(1′*R*,2*R*)- and (1′*S*,2*R*)-1-[*N*-(2-Hydroxy-1-phenylethyl)amino]-2-methylpyrrolidines (15) A solution of the mixture of two isomers of **14** (2.3 g, 9 mmol) in THF (10 ml) was added dropwise to a stirred suspension of $LiAlH_4$ (0.7 g, 18 mmol) in THF (20 ml), and stirring was continued at room temperature for 20 h. The reaction mixture was worked up with a small amount of water, and the resulting precipitate was filtered off. The filtrate was dried over Na_2SO_4 and concentrated under reduced pressure. The residue was subjected to column chromatography on silica gel with CH_2Cl_2. The first fraction gave (1′*R*,2*R*)-**15** (0.61 g, 28%) as a colorless oil. $[\alpha]_D$ −23.9° (c=1.30, EtOH). MS *m/z*: CI, 221 (M^++1), 189 (M^+−CH_2OH). ^{1}H-NMR ($CDCl_3$) δ: 1.34 (3H, d, J=6.1 Hz, $CHCH_3$), 1.61—1.99 (4H, m, CH_2CH_2), 2.03 (1H, q, J=9.2 Hz, NCH_2), 2.43—2.51 (1H, m, NCH_2), 2.5—2.6 (1H, br s, NH or OH), 2.8—3.0 (1H, br s, NH or OH), 3.68 (1H, dd, J=1.8, 4.2 Hz, $NCHCH_2O$), 3.73—3.79 (1H, m, $CHCH_3$), 3.91 (1H, dd, J=4.2, 9.2 Hz, $NCHCH_2O$), 4.28 (1H, dd, J=1.8, 9.2 Hz, $NCHCH_2O$), 7.23—7.38 (5H, m, aromatic H).

The second fraction gave (1′*S*,2*R*)-**15** (0.42 g, 19%) as a pale yellow oil. $[\alpha]_D$ −162.2° (c=0.20, EtOH). MS *m/z*: CI, 221 (M^++1), 189 (M^+−CH_2OH). ^{1}H-NMR ($CDCl_3$) δ: 1.25 (3H, d, J=6.7 Hz, $CHCH_3$), 1.38—2.01 (4H, m, CH_2CH_2), 2.8—2.9 (2H, br, NH and OH), 2.66—2.76 (1H, m, NCH_2), 2.73 (1H, q, J=8.5 Hz, NCH_2), 3.12—3.20 (1H, m, $CHCH_3$), 3.72 (1H, dd, J=3.1, 10.4 Hz, $NCHCH_2O$), 3.94 (1H, dd, J=8.6, 10.4 Hz, $NCHCH_2O$), 4.32 (1H, dd, J=3.1, 8.6 Hz, $NCHCH_2O$), 7.23—7.38 (5H, m, aromatic H).

Preparation of (1′*R*,2*R*)-7a CH_3I (2.27 g, 16 mmol) and anhydrous K_2CO_3 (0.2 g) were added to a solution of (1′*R*,2*R*)-**15** (0.22 g, 1 mmol) in *N*,*N*-dimethylformamide (DMF, 4 ml). After being stirred at room temperature for 20 h, the reaction mixture was poured into water and extracted with ether. The organic layer was dried over Na_2SO_4 and evaporated under reduced pressure, and the residue was subjected to column chromatography on silica gel with a solution of ether–hexane (1 : 3) to give (1′*R*,2*R*)-**7a** (0.16 g, 68%) as a colorless oil. $[\alpha]_D$ −7.9° (c=0.44, EtOH). This compound was identical with the major component [(1′*R*,2*R*)] of **7a** on the basis of ^{1}H-NMR spectral comparison.

Preparation of (1′*S*,2*R*)-16 (1′*S*,2*R*)-**15** (0.22 g, 1 mmol) gave (1′*S*,2*R*)-**16** (0.18 g, 77%) as a colorless oil in a similar manner to that described for the preparation of (1′*R*,2*R*)-**7a**. $[\alpha]_D$ −121.8° (c=1.21, EtOH). This compound was identical with the minor component [(1′*R*,2*S*)] of **7a** on the basis of ^{1}H-NMR spectral comparison.

2-Benzyl-1-(α-ethoxycarbonylbenzylideneamino)pyrrolidines (17) (*R*)-**10** (1.8 g, 10 mmol) was condensed with ethyl phenylglyoxylate (2.0 g, 11 mmol) to give a pale yellow oil (2.0 g, 86%) in a similar manner to that employed in the preparation of (*R*)-**14**. This product was a mixture of two isomers (ratio, 64 : 36) and was unstable at room temperature. ^{1}H-NMR ($CDCl_3$) δ: Major component; 1.31 (3H, t, J=7.3 Hz, CH_2CH_3), 1.44—1.80 (4H, m, CH_2CH_2), 2.54—2.75 (2H, m, NCH_2), 2.82 (1H, dd, J=9.6, 13.4 Hz, $PhCH_2$), 3.29 (1H, dd, J=3.7, 13.4 Hz, $PhCH_2$), 3.98—4.05 (1H, m, $PhCH_2CH$), 4.22 (1H, dq, J=11.0, 7.3 Hz, CH_2CH_3),

4.31 (1H, dq, J=11.0, 7.3 Hz, CH_2CH_3), 7.19—7.34 (10H, m, aromatic H). Minor component; 1.37 (3H, t, J=7.0 Hz, CH_2CH_3), 1.54—1.89 (4H, m, CH_2CH_2), 2.78 (1H, dd, J=9.2, 13.4 Hz, $PhCH_2$), 3.02—3.11 (1H, m, NCH_2), 3.30 (1H, dd, J=4.3, 13.4 Hz, $PhCH_2$), 3.35—3.44 (1H, m, NCH_2), 3.82—3.91 (1H, m, $PhCH_2CH$), 4.31—4.41 (2H, m, CH_2CH_3), 7.18—7.35 (10H, m, aromatic H).

(1′*R*,2*R*)- and (1′*S*,2*R*)-2-Benzyl-1-[*N*-(2-hydroxy-1-phenylethyl)amino]-pyrrolidines (18) A solution of the mixture of two isomers of **17** (3.0 g, 8.9 mmol) was reduced with $LiAlH_4$ (0.7 g, 18 mmol) in a similar manner to that employed in the preparation of (1′*R*,2*R*)- and (1′*S*,2*R*)-**15**. The first fraction gave (1′*S*,2*R*)-**18** (1.05 g, 40%) as a colorless oil. $[\alpha]_D$ +56.9° (c=1.18, EtOH). MS m/z: CI, 297 (M^++1), 205 (M^+−$PhCH_2$), 175 (M^+−$PhCHCH_2OH$). ^{1}H-NMR ($CDCl_3$) δ: 1.5—1.6 (2H, br, NH and OH), 1.43—1.81 (4H, m, CH_2CH_2), 2.03—2.13 (1H, m, NCH_2), 2.55 (1H, dd, J=9.8, 12.2 Hz, $PhCH_2$), 2.16—2.66 (1H, m, NCH_2), 3.67 (1H, dd, J=3.1, 12.2 Hz, $PhCH_2$), 3.69 (1H, dd, J=2.4, 11.0 Hz, $NCHCH_2O$), 3.80—3.87 (1H, m, $PhCH_2CH$), 4.00 (1H, dd, J=9.2, 11.0 Hz, $NCHCH_2O$), 4.34 (1H, dd, J=2.4, 9.2 Hz, $NCHCH_2O$), 7.18—7.41 (10H, m, aromatic H).

The second fraction gave (1′*R*,2*R*)-**18** (1.02 g, 39%) as colorless needles, mp 107—108 °C (ether–hexane). $[\alpha]_D$ +124.6° (c=1.24, EtOH). MS m/z: CI, 297 (M^++1), 265 (M^+−CH_2OH). ^{1}H-NMR ($CDCl_3$) δ: 1.6—1.8 (2H, m, NH and OH), 1.41—1.80 (4H, m, CH_2CH_2), 2.51 (1H, dd, J=10.1, 12.8 Hz, $PhCH_2$), 2.65—2.75 (1H, m, NCH_2), 2.81—2.92 (1H, m, NCH_2), 3.30 (1H, dd, J=4.3, 12.8 Hz, $PhCH_2$), 3.74 (1H, dd, J=3.1, 10.4 Hz, $NCHCH_2O$), 3.90 (1H, dd, J=8.9, 10.4 Hz, $NCHCH_2O$), 4.27 (1H, dd, J=3.1, 8.9 Hz, $NCHCH_2O$), 7.14—7.39 (10H, m, aromatic H).

Preparation of (1′*R*,2*R*)-7c CH_3I (2.27 g, 16 mmol) and anhydrous K_2CO_3 (0.2 g) were added to a solution of (1′*R*,2*R*)-**18** (0.30 g, 1 mmol) in DMF (4 ml) in a similar manner to that described for the preparation of (1′*R*,2*R*)-**7a** to give (1′*R*,2*R*)-**7c** (0.21 g, 69%) as a colorless oil. $[\alpha]_D$ +22.0° (c=0.07, EtOH). This compound was identical with the minor component [(1′*R*,2*R*)] of **7c** on the basis of ^{1}H-NMR spectral comparison.

Preparation of (1′*S*,2*R*)-19 (1′*S*,2*R*)-**18** (0.30 g, 1 mmol) gave (1′*S*,2*R*)-**19** (0.16 g, 53%) as a colorless oil in the same manner as employed in the preparation of (1′*R*,2*R*)-**7c**. $[\alpha]_D$ −5.9° (c=0.06, EtOH). This compound was identical with the major component [(1′*R*,2*S*)] of **7c** on the basis of ^{1}H-NMR spectral comparison.

Acknowledgment We are grateful to Miss Y. Takahashi and Mrs. T. Ogata of Hoshi University for MS and elemental analysis.

References and Notes

1) H. Takahashi, B. C. Hsieh, and K. Higashiyama, *Chem. Pharm. Bull.*, **38**, 2429 (1990).
2) H. Takahashi, I. Morimoto, and K. Higashiyama, *Heterocycles*, **30**, 287 (1990); *idem*, *Chem. Pharm. Bull.*, **38**, 2627 (1990).
3) Y. Ito, Y. Amino, M. Nakatsuka, and T. Saegusa, *J. Am. Chem. Soc.*, **105**, 1586 (1983).
4) A. Ando and T. Shioiri, *J. Chem. Soc., Chem. Commun.*, **1987**, 656.
5) C. C. Tseng, S. Terashima, and S. Yamada, *Chem. Pharm. Bull.*, **25**, 29 (1977).
6) L. A. Paquette, J. P. Freeman, and S. Mariorana, *Tetrahedron*, **27**, 2599 (1977).
7) P. Main, M. M. Woolfson, and G. Germin, *Acta Crystallogr., Sect. A*, **27**, 368 (1971).

A Series of Sesquiterpenes with a 7α-Isopropyl Side Chain and Related Compounds Isolated from *Curcuma wenyujin*

Kenzo HARIMAYA,[a] Ji-Fu GAO,[a,1)] Tamiko OHKURA,[a] Takeshi KAWAMATA,[a] Yoichi IITAKA,[b] Yong-Tian GUO[c] and Seiichi INAYAMA*,[a]

Pharmaceutical Institute, School of Medicine, Keio University,[a] 35 Shinanomachi, Shinjuku-ku, Tokyo 160, Japan, Department of Biological Sciences, Nishi-Tokyo Science University,[b] Uenohara-cho, Yamanashi 409-01, Japan and Dalian Institute of Medicinal and Pharmaceutical Sciences,[c] Zhong Shan Qu, Dalian, China. *Received August 8, 1990*

Sesquiterpenoids possessing a 7α-isopropyl group, such as curcumol (1a), curdione (2a), curcumalactone (3), and a new epoxy germacrane, (1*R*,10*R*)-epoxy-(−)-1,10-dihydrocurdione (5a), were isolated from the essential oil of *Curcuma wenyujin*. Other related new sesquiterpenes, neocurdione (4) and (1*S*,10*S*),(4*S*,5*S*)-germacrone-1(10),4-diepoxide (6) were also isolated from this plant. The stereostructures and absolute configurations of these sesquiterpenes were established on the basis of spectroscopic and chemical data as well as X-ray crystallographic analyses.

Keywords *Curcuma wenyujin*; Zingiberaceae; curcumol; curdione; curcumalactone; germacrone-epoxide; neocurdione; germacrone-diepoxide

Of the eight Chinese species of the genus *Curcuma* (Zingiberaceae), the rhizomes of five have been used medicinally in China.[2)] In particular, the essential oil of *Curcuma wenyujin* is currently used as a clinical remedy for uterus cancer in China.[3)] Major constituents of the essential oil of this plant are found to be curcumol (**1a**)[4)] and curdione (**2a**),[5,6)] both of which are sesquiterpenes that were first isolated from *C. zedoaria*.[7)] However the stereochemistry of **1a** and **2a** has not been established.

In our continuing investigation of active constituents of *C. wenyujin*,[8)] we now wish to report in detail the absolute stereostructures of **1a**, **2a**, curcumalactone (**3**)[6)] and (1*R*,10*R*)-(−)-1,10-dihydrocurdione (**5a**).[9)] These sesquiterpenoids have a 7α-isopropyl side chain, which is uncommon among constituents of higher plants.[10)] Other related sesquiterpenes such as neocurdione (**4**)[11)] and (1*S*,10*S*),(4*S*,5*S*)-germacrone-1(10),4-diepoxide (**6**)[12)] were also isolated from this plant. The elucidation of their stereostructures and absolute configurations is also described.

Results and Discussion

Steam distillation of the rhizome of *C. wenyujin* gave an essential oil (1.2%). Silica gel chromatography of this oil eluting with petroleum ether–ether afforded curcumol (**1a**) (7.7%) and curdione (**2a**) (14.8%).

Other sesquiterpenes were isolated from this plant under the following mild extractive conditions. The air-dried rhizomes were soaked in ether for 5 d at about 5 °C. After evaporation of the solvent *in vacuo* at room temperature, the oil obtained was subjected to silica gel chromatography by using a gradient solvent system of petroleum ether and ether. After the separation of the major constituents, *i.e.* curdione (**2a**) and neocurdione (**4**), the fractions eluted with petroleum ether and ether (1 : 1) gave a crystalline compound. Recrystallization from the solvent mixture of petroleum ether and ether gave (1*R*,10*R*)-epoxy-(−)-1,10-dihydrocurdione (**5a**). The epoxy germacranoid compounds, *i.e.* (1*R*,10*R*)-epoxy-(−)-1,10-dihydrocurdione (**5a**),[9)] (4*S*,5*S*)-epoxy-(+)-4,5-dihydrogermacrone (**4b**),[13)] and (1*S*,10*S*),(4*S*,5*S*)-germacrone-1(10),4-diepoxide (**6**),[12)] were separated from the fractions eluted with petroleum ether and ether (4 : 5).

The physical data of **1a** accorded with those of curcumol isolated from *C. zedoaria*.[7)] Because the stereochemistry of curcumol had not been defined, the relative stereostructure of **1a** was determined by X-ray analysis as illustrated in Fig. 1.[4b)]

The absolute configuration was elucidated by examination of the circular dichroism (CD) spectrum of the ozonolysate.[4b)] This spectrum showed a negative Cotton effect ($[\theta]_{25}$ −1423, dioxane). Application of the octant rule suggested that the absolute structure of curcumol should be expressed as **1a** in Chart 1. The α-configuration

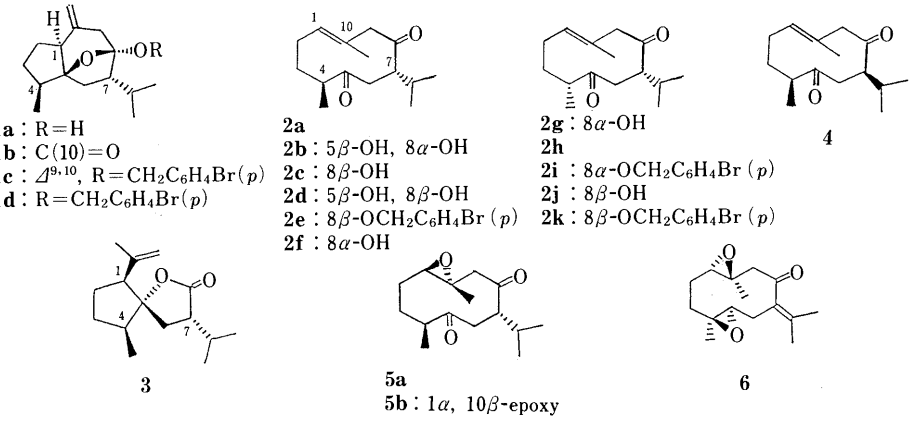

Chart 1

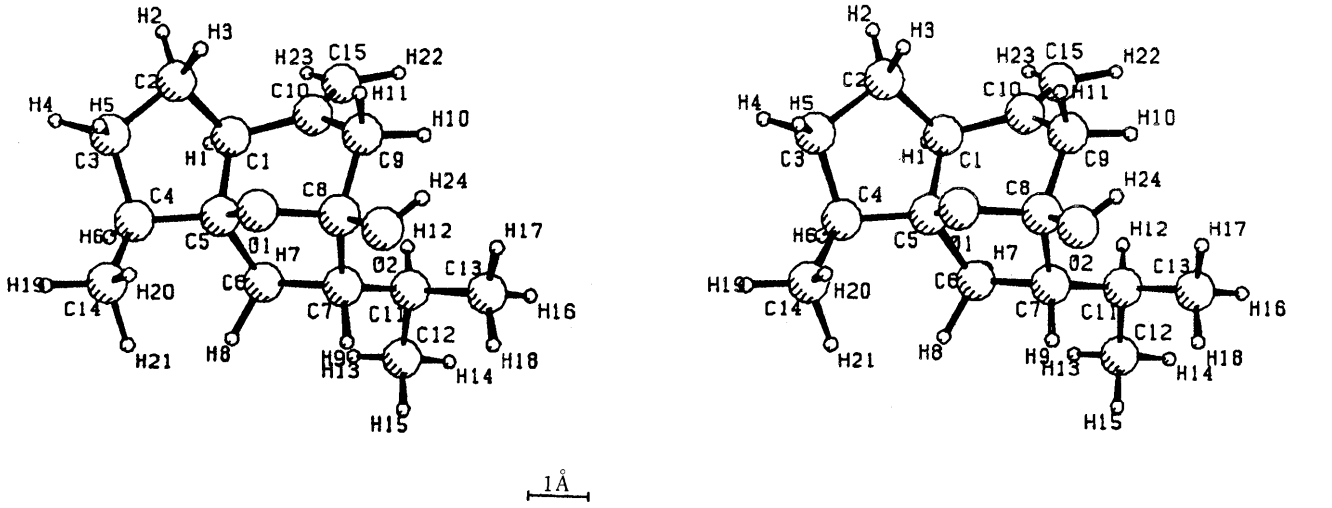

Fig. 1. Stereoview of Curcumol (**1a**)

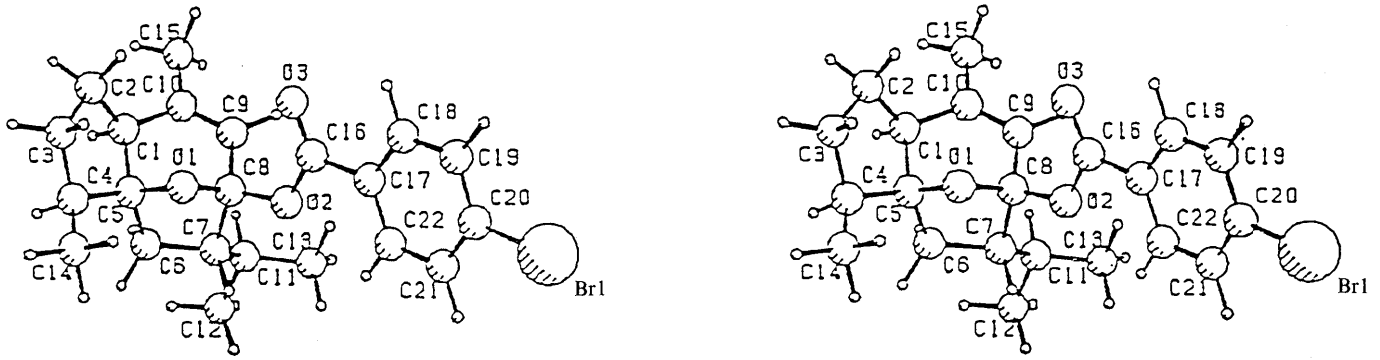

Fig. 2. Stereoview of the *p*-Bromobenzoate (**1c**) of the Δ^9-Isomer of **1a**

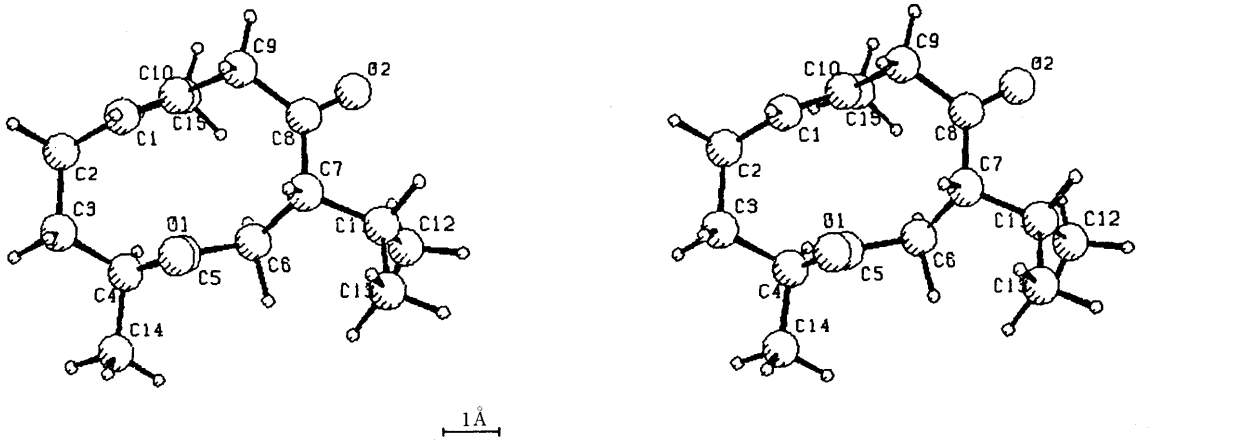

Fig. 3. Stereoview of Curdione (**2a**)

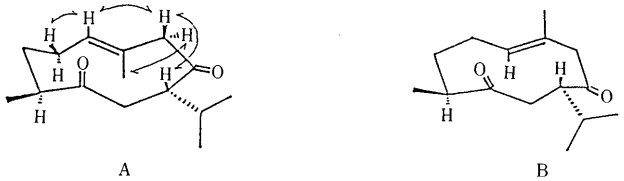

Chart 2. Conformer A and Conformer B of Curdione (**2a**)

of the isopropyl side chain seen in **1a** is not often found in higher plant constituents, for biogenetic reasons.[10] In order to obtain conclusive proof of the absolute structure of **1a**, its *p*-bromobenzoate (**1c**) was prepared and was submitted to X-ray crystal diffraction analysis. The absolute configuration of **1c** was determined from the anomalous dispersion of CuK_α radiation by the bromine-atom. The crystal data and the final atomic coordinates are given in the experimental section. The absolute structure and stereoview of **1c** are depicted in Chart 1 and in Fig. 2, respectively.

Thus, the absolute structure of curcumol must be expressed as **1a** and is in agreement with that deduced from the CD analysis.

Curdione (**2a**), a germacrane first isolated from *C. zedoaria*,[7] was also isolated from *C. wenyujin* by our group.[5b,6a] Physical data of **2a** were all coincident with those of curdione.[7] As the stereostructure of curdione had not been proved, we undertook the X-ray analysis of **2a** in order to determine its relative structure and conformation.[5b] The structure of **2a** is depicted in Fig. 3. Curdione (**2a**) exists in a chair–chair conformation, possessing a *trans* relationship between the C(4)-methyl group and C(7)-isopropyl side chain.

A variable temperature proton nuclear magnetic resonance (^{1}H-NMR) study of **2a** was performed to verify its conformation in solution. The spectrum showed a set of broad signals at $-30\,^\circ$C in spite of exhibiting sharp signals at room temperature. As the temperature was decreased below less than $-50\,^\circ$C, two sets of signals with an intensity ratio of approximately 5:1 (*e.g.* C(1)-H 5.06 and 5.63; C(10)-CH_3 1.76 and 1.48 ppm) were observed. These signals presumably arose from two chair–chair conformers, *i.e.* conformation A and conformation B (Chart 2), of which the latter takes the *syn*-arrangement of C(5)=O and C(10)-CH_3. Nuclear Overhauser effect (NOE) measurements of curdione (**2a**) at $-70\,^\circ$C also suggest that the major conformer is conformer A [C(5)=O/C(10)-CH_3: *anti*] and the minor one is conformer B [C(5)=O/C(10)-CH_3: *syn*].

Since curcumol (**1a**) was exclusively produced by heating of **2a** at 200 °C in ethanol (EtOH),[5] it seems that **2a** mainly existing in conformation A could transform *via* conformation B to **1a** with retention of the C(7) configuration.

In order to confirm the absolute configuration of **2a**, the bromobenzoate of 8αH-dihydrocurdione (**2c**) was prepared from **2a** and was subjected to X-ray diffraction analysis.

The stereoselective lithium aluminum hydride ($LiAlH_4$) reduction of **2a** afforded a ketol. This compound was treated with *p*-bromobenzoyl chloride (*p*-BrC_6H_4COCl)–dichloromethane (CH_2Cl_2) in the presence of 4-dimethylaminopyridine (DMAP) at room temperature to afford the *p*-bromobenzoate (**2e**).[6a] The absolute structure of **2e** was determined by the anomalous dispersion method and is shown in Fig. 4.

Curdione (**2a**) was converted to a cyclopentanolide (**3**) in quantitative yield in chloroform containing a catalytic amount of hydrochloric acid at room temperature. Compound **3** was identical with curcumalactone obtained from the essential oil of *C. wenyujin*. It is noteworthy that dehydrocurdione isolated from *C. zedoaria* was converted to a mixture of two dehydrocyclopentenolides[14] under

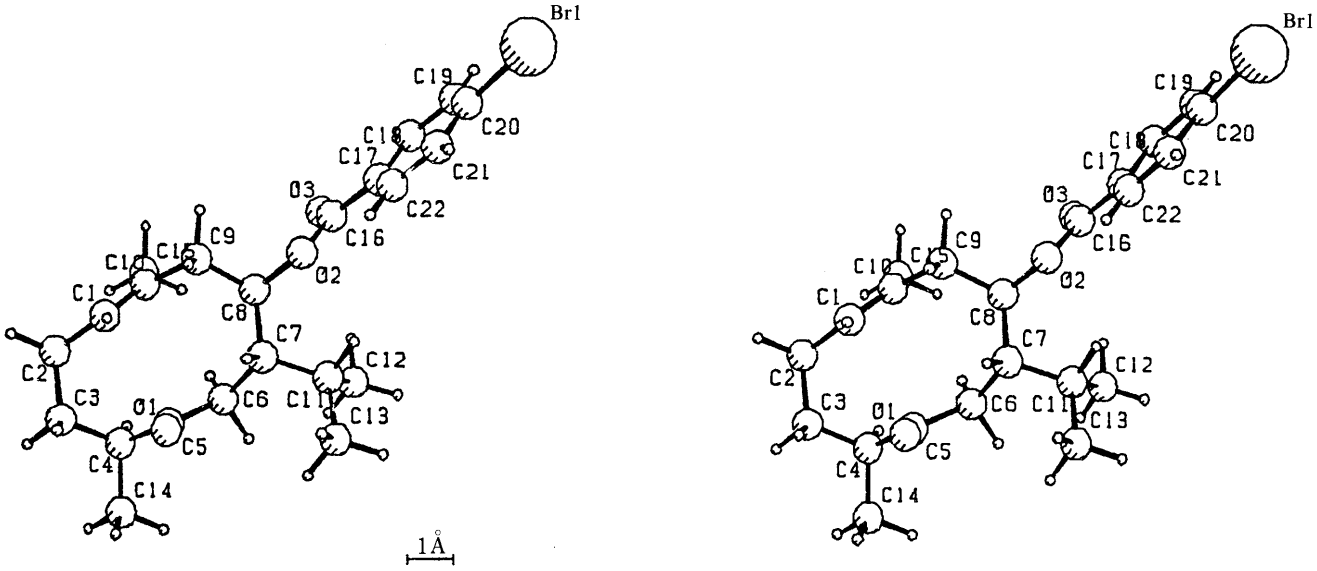

Fig. 4. Stereoview of the *p*-Bromobenzoate (**2e**) of 8αH-Dihydrocurdione (**2j**)

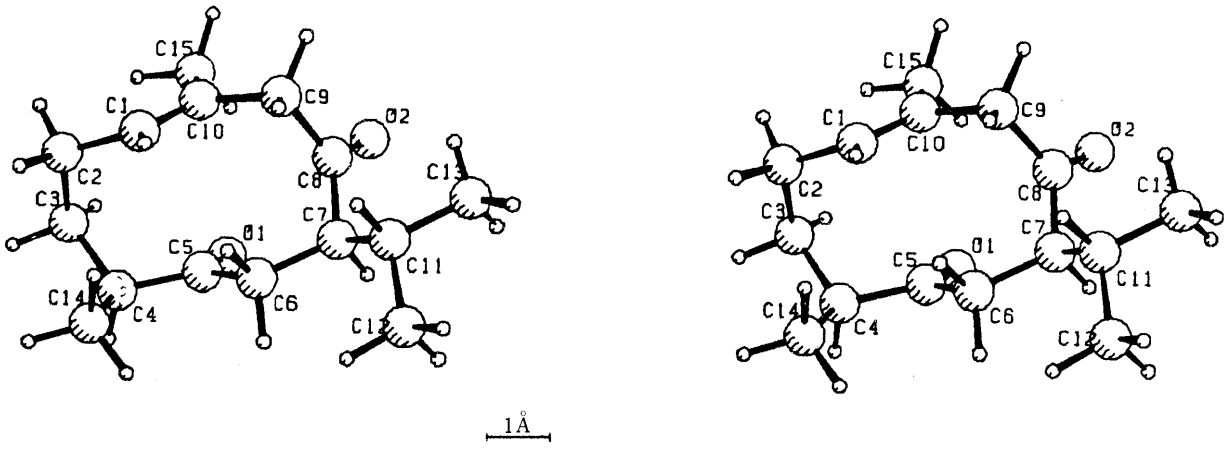

Fig. 5. Stereoview of Neocurdione (**4**)

acidic conditions.

Neocurdione (**4**)[8,11] was the second germacrane compound isolated from *C. wenyujin*. The very close similarity of the spectroscopic data of **4** to those of **2a** (^{1}H-NMR, infrared (IR) and mass (MS) fragmentation) and the opposite sign of the optical rotation and CD absorption suggested that **4** is an epimer of **2a** either at C(4) or at C(7). In order to solve the stereostructure of **4**, an X-ray diffraction analysis of **4** was carried out.[11b] The relative stereostructure is shown in Fig. 5. Neocurdione (**4**) was thus found to have an unusual twisted chair–boat conformation, wherein the C(10) and the C(5) substituents are on the same side of the average molecular plane (*syn*). It is of interest that **4** takes an unstable *syn* conformation of C(10)-CH_3/C(5)=O, in sharp contrast to curdione (**2a**), which possesses a rather stable *anti* conformation as described above. The low temperature ^{1}H-NMR study of **3** showed two sets of signals at $-60\,^\circ$C in the ratio of 26:74. A further NOE study at $-60\,^\circ$C suggested that the major conformation of **4** in solution is a chair–chair conformation, which is different from the one in the solid state. This observation prompted us to apply molecular mechanics calculations to these flexible germacranes, curdione (**2a**) and neocurdione (**4**).[15] The calculated ratios of conformations of *anti* and *syn* type [C(5)=O/C(10)-CH_3] are in reasonably good accordance with the ratios which were estimated from low temperature NMR studies.

In order to determine the absolute structure of **4**, the following chemical transformation was carried out. Compound **2a** was reduced with sodium borohydride ($NaBH_4$) in methanol (MeOH) at room temperature for 4 h to give a ketol, which was assigned as 8βH-dihydrocurdione (**2f**) by ^{1}H-NMR spectroscopy. This ketol was then treated with potassium *tert*-butoxide (*tert*-BuOK) in benzene to afford a 4:1 mixture of the starting material and its C(4)-epimer, *i.e.* 8βH-dihydro-4-epicurdione (**2g**). This epimer was oxidized with chromic anhydride (CrO_3) in pyridine to give 4-epicurdione (**2h**) ($[\alpha]_D$ $+65.9^\circ$, $CHCl_3$). The physical properties of **2h** were identical with those of neocurdione (**4**) except for the optical rotation ($[\alpha]_D$ -65.8°) and the sign of CD Cotton effect {$[\theta]_{299.5}$ -36060; $[\theta]_{223}$ $+12368$ ($c=5.08$, MeOH)}. Neocurdione (**4**) is thus considered to be the antipode of 4-epicurdione (**2h**).

We decided to confirm the absolute structure of **2h**, since the availability of **4** was very limited. The first attempted preparation of *p*-bromobenzoate (**2i**) from the oily ketol (**2g**) gave no crystalline compound suitable for the X-ray diffraction study. When **2h** was rapidly treated with $LiAlH_4$ in tetrahydrofuran (THF), an oily ketol mixture was obtained. Separation of this mixture by silica gel chromatography as usual afforded 8βH- (**2g**) and 8αH-dihydro-4-epicurdione (**2j**) in yields of 80% and 8%, respectively. The latter crystalline ketol (**2j**) was converted to the corresponding crystalline *p*-bromobenzoate (**2k**) (*p*-BrC_6H_4COCl–pyridine–DMAP), which was suitable for X-ray crystallographic analysis. The absolute structure of **2k** was then determined from the anomalous dispersion of CuK_α radiation by the bromine atom. A stereoview of **2k** is shown in Fig. 6.

Since the absolute structure of 4-epicurdione (**2h**) was established, the absolute configuration of neocurdione (**4**) can be expressed as shown in Chart 1.

Heating of **4** in EtOH solution at 230 °C in a sealed tube afforded neocurcumol (**1b**) in 50% yield.[10] The stereostructure was deduced from the spectroscopic data and the analogy of the similar reaction of curdione (**2a**) to give curcumol (**1a**).

The third germacrane, (1*R*,10*R*)-epoxy-(−)-1,10-dihydrocurdione (**5a**), has the formula $C_{15}H_{24}O_3$. Both the IR spectrum (1705 cm^{-1}) and the ultraviolet (UV) absorption (288 nm) of **5a** suggest the presence of a saturated cyclic ketone. Its ^{1}H-NMR spectrum is similar to that of **2a** except that the signal of C(1)-hydrogen of **5a** appeared at δ 2.89, while that of **2a** was observed at δ 5.17 in the olefinic region. On the other hand, in the ^{13}C-NMR spectrum of **5a**, two signals appeared at δ 64.1 and 58.9, while in **2a** two olefinic carbon signals were observed at δ 131.6 and 129.9. This suggests that each of these two carbons is attached to oxygen in **5a**. As the IR spectrum of **5a** showed no hydroxyl absorption, **5a** was deduced to be the 1,10-epoxy derivative of either **2a** or its 7αH-epimer. No NOE was observed

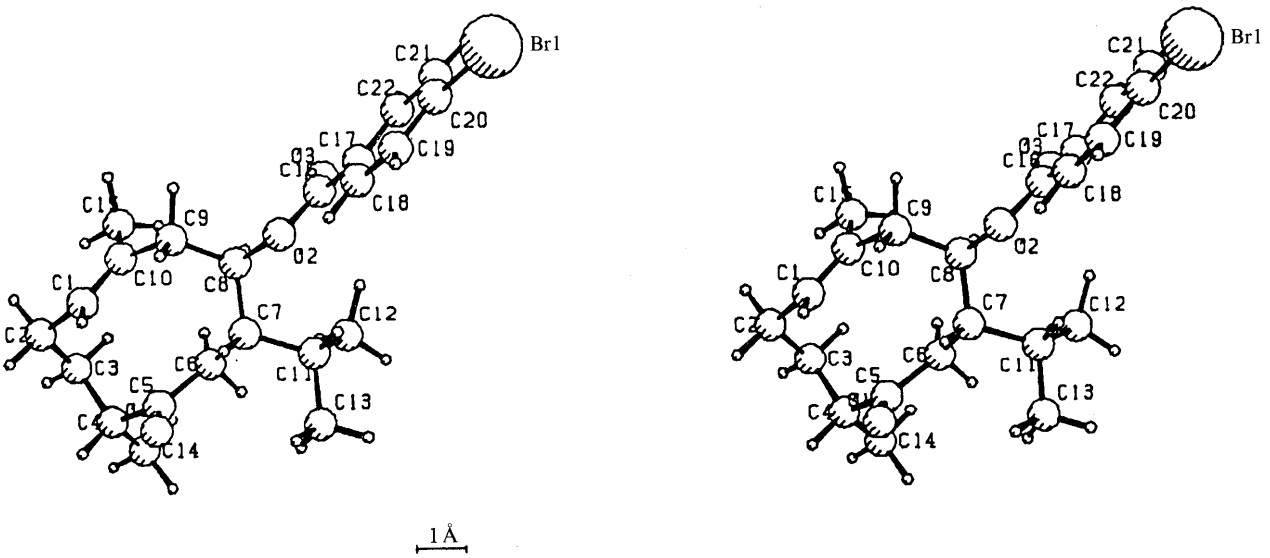

Fig. 6. Stereoview of the *p*-Bromobenzoate (**2k**) of 8αH-Dihydro-4-epicurdione (**2j**)

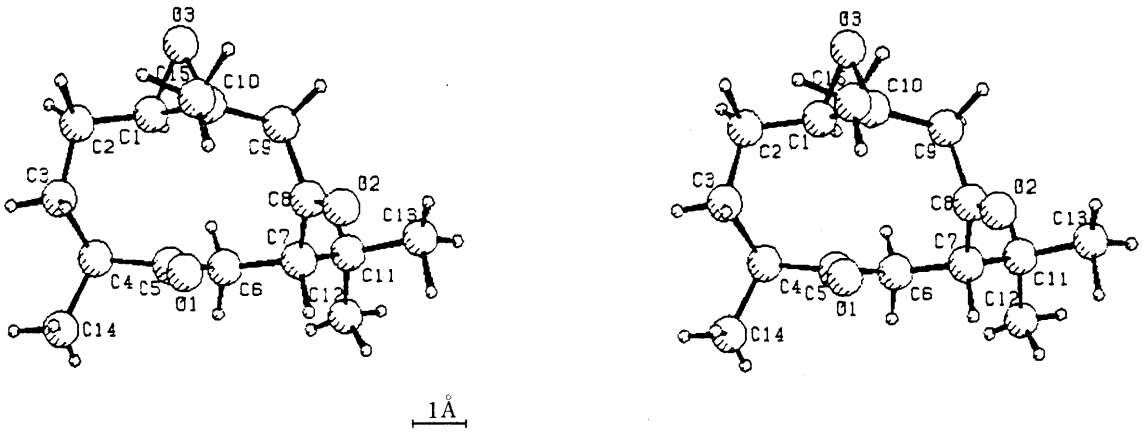

Fig. 7. Stereoview of (1*R*,10*R*)-Epoxy-(−)-1,10-dihydrocurdione (**5a**)

between the C(10)-CH_3 and C(4)-H. The relative stereostructure of **5a** was determined by X-ray analysis and is shown in Fig. 7.

In order to determine the absolute configuration of **5a**, epoxidation of **2a** was examined. Epoxidation of **2a** with *m*-chloroperbenzoic acid (MCPBA) afforded **5a** and its 1(10)-epoxy isomer in a ratio of 1.3:1. This conversion proved that the epoxy group in **5a** must have the same (4*S*,7*S*) configuration as that in **2a**. The ten-membered ring *trans*-fused with the oxirane group at C(1)–C(10) exists in a chair–boat conformation.[14,15] The C(4)-β-methyl and C(7)-α-isopropyl groups in **2a** and **5a** are on opposite sides of the average molecular plane.

The spectroscopic properties of the monoepoxide (**5c**) isolated from this plant were in accord with those of (4*S*,5*S*)-germacrone-4,5-epoxide isolated from *C. zedoaria*[13a] and *C. aromatica*.[13b] It is of interest from the biogenetic point of view that the enantiomer of **5c** was isolated from a higher plant, *Asarum caulescens* (Aristolochiacae).[16]

The next epoxy germacrane (**6**) (mp 84—86 °C) has the formula $C_{15}H_{22}O_3$. The physical and spectroscopic properties of **6** suggested that **6** has two epoxy rings and an α,β-unsaturated ketone moiety. From the ^{1}H- and ^{13}C-NMR spectral comparison between **6** and **5c**, compound **6** seemed to be a 1,10-epoxide of **5c**. The relative stereochemistry of the oxirane moieties of **6** was deduced to be *cis*, based on the observation of 3.6% NOE between the C(4)-Me and C(10)-Me. Epoxidation of **5c** with MCPBA (1 eq) in CH_2Cl_2 at room temperature afforded the diepoxide **6** in 86% yield. Thus the absolute structure of **6** was established to be (1*S*,10*S*),(4*S*,5*S*)-germacrone-1(10),4-diepoxide.[12]

A biogenetic hypothesis concerning sesquiterpenoids in *C. wenyujin*, including those described in this paper, will be presented elsewhere.[10]

Experimental

Melting points were determined on a Yanagimoto micromelting point apparatus and are uncorrected. Optical rotations were measured with a JASCO DIP-360 digital polarimeter, and IR spectra were obtained with a Hitachi EPI-G3 spectrometer. ^{1}H-NMR spectra were obtained with JEOL GSX-270 and GX-400 spectrometers at 270 and 400 MHz, respectively, using tetramethylsilane as an internal standard. Mass spectra such as electron impact (EI-), chemical ionization (CI-) and high resolution (HR-) were measured with a JEOL JMS-D300 spectrometer. Column chromatography was carried out on Kieselgel 60 (70—230 mesh).

Isolation of Curcumol (1a) and Curdione (2a) The air-dried rhizomes of *C. wenyujin* (7.5 kg) collected in Wechow (China) were powdered and submitted to steam distillation to yield 100 g of a dark brown essential oil. This oil was kept in a refrigerator several days to afford 25 g of a crystalline mixture of curcumol (**1a**) and curdione (**2a**). This mixture was subjected to silica gel column chromatography with a gradient solvent system of petroleum ether and ether. The fractions eluted with petroleum ether–ether (20:1) were collected and evaporation of the solvent yielded a crystalline material. Recrystallization of this from EtOH afforded 7.7 g of curcumol (**1a**) as white needles (0.1%). Curdione (**2a**) (14.8 g, 0.21%) was also isolated from the above mixture.

Curcumol (**1a**): $C_{15}H_{24}O_2$. mp 141—142 °C. $[\alpha]_D^{30}$ −32.26° (*c*=2.13, $CHCl_3$). HR-MS *m/z*: 236.1777 (Theor. 236.1770 for $C_{15}H_{24}O_2$). IR ν_{max}^{KBr} cm^{-1}: 3420 (OH), 3070, 1647, 882 (>C=CH_2). ^{1}H-NMR ($CDCl_3$) δ: 0.87 (3H, d, *J*=6.8, 4-CH_3), 1.00, 1.01 (3H×2, each d, *J*=6.8, 11-CH_3), 2.51, 2.57 (1H, ×2, each d, *J*=14.8, 9-H), 4.88 (2H, br s, 15-H).

Curdione (**2a**): $C_{15}H_{24}O_2$. mp 61—62 °C. $[\alpha]_D^{25}$ +26.0° (*c*=1.00, $CHCl_3$). IR ν_{max}^{KBr} cm^{-1}: 1704 (C=O), 1667 (C=C). EI-MS *m/z*: 236 (M^+). HR-MS *m/z*: 236.1778 (Theor. 236.1770). ^{1}H-NMR ($CDCl_3$) δ: 5.17 (1H, s, 1-H), 3.07 (1H, d, *J*=11, 9α-H), 2.94 (1H, d, *J*=11, 9α-H), 2.85 (1H, ddd, *J*=8.8, 8.8, 2.2, 7β-H), 2.69 (1H, m, 6α-H), 2.40 (1H, dd, *J*=18, 2.2, 6β-H), 2.34 (1H, m, 4α-H), 2.09—2.15 (3H, br, 3α-H, 2α-H, 2β-H), 1.88 (1H, m, 12-H), 1.66 (3H, s, 10-CH_3), 1.57 (1H, m, 3α-H), 0.98 (3H, d, *J*=6.6, 4-CH_3), 0.88, 0.95 [3H×2, each d, *J*=6.6, 11-CH_3].

X-Ray Analysis of Curcumol (1a) A direct X-ray analysis of **1a** was carried out with a single crystal, a prism elongated along the *c* axis. The crystal data are: $C_{15}H_{24}O_2$; M.W.=236; trigonal; space group $P3_2$; lattice constants: *a*=*b*=12.387(6), *c*=7.866(4) Å, α=β=90°, γ=120°, *U*=1045 Å^3, *Z*=3, D_{calc}=1.125 g cm^{-3}. The intensity data were collected on a Philips PW1100 diffractometer using graphite monochromated CuK_α radiation. Of the total of 2323 reflections within the 2θ range of 6° through 156°, 1951 reflections observed above the 2σ(I) level were used for the X-ray analysis. The structure was solved by the direct method using a MULTAN program, and refined by the least-squares method with the block-diagonal matrix approximation. The final *R* value was 0.046 including 24 hydrogen atoms with isotropic temperature factors. The relative structure of curcumol (**1a**) is illustrated in Fig. 1.

X-Ray Analysis of Curdione (2a) The crystal data are: $C_{15}H_{24}O_2$; M.W.=236; orthorhombic, space group $P2_12_12_1$; lattice constant: *a*=10.758(5), *b*=13.164(7), *c*=10.176(5) Å, *U*=1441.1 Å^3, *Z*=4, D_{calc}=1.0895 g cm^{-3}. The intensity data were collected on a Philips PW 1100 diffractometer using graphite monochromated CuK_α radiation and 1229 reflections up to 155° (2θ) were used. The structure was solved by the direct method using a MULTAN program and refined by the least-squares method with the block-diagonal matrix approximation. The final *R* value was 0.05 including 24 hydrogen atoms with isotropic temperature factors. The relative stereostructure of **2a** is shown in Fig. 2.

Ozonolysis of Curcumol (1a) A solution of **1a** (17 mg) in ethyl acetate (EtOAc) (6 ml) in an ice-salt bath was saturated with ozone. Water (1 ml), zinc powder (40 mg), $AgNO_3$ (trace) and hydroquinone (trace) were added to the reaction mixture. Then this mixture was refluxed for 1 h. Excess zinc powder was filtered off, the organic layer was washed with water and dried over anhydrous Na_2SO_4. After evaporation of the solvent at room temperature *in vacuo*, the residue was submitted to silica gel column chromatography to give 11 mg of the 14-norketone (**1b**) (65%).

TABLE I. Atomic Coordinates of Curcumol (**1a**)

No.	Atom	$x \cdot 10^4$	$y \cdot 10^4$	$z \cdot 10^4$	B_{eq} (Å^2)
1	C1	6123 (4)	−895 (4)	−714 (0)	3.76 (0.09)
2	C2	7065 (5)	−619 (5)	738 (7)	5.12 (0.12)
3	C3	8324 (5)	−185 (5)	−166 (8)	5.44 (0.13)
4	C4	8133 (5)	−35 (5)	−2081 (7)	4.55 (0.11)
5	C5	6943 (4)	41 (4)	−2113 (6)	3.43 (0.09)
6	C6	6236 (5)	−134 (4)	−3797 (6)	3.93 (0.10)
7	C7	5723 (4)	784 (4)	−3639 (6)	3.33 (0.09)
8	C8	6113 (4)	1303 (4)	−1814 (5)	3.24 (0.09)
9	C9	5224 (4)	555 (4)	−366 (6)	3.69 (0.09)
10	C10	5001 (4)	−770 (4)	−327 (6)	3.77 (0.09)
11	C11	4354 (4)	252 (5)	−4112 (6)	4.33 (0.10)
12	C12	4130 (6)	−234 (7)	−5948 (7)	6.67 (0.16)
13	C13	3948 (6)	1231 (7)	−3902 (8)	6.16 (0.15)
14	C14	9255 (5)	1068 (6)	−2934 (9)	5.83 (0.14)
15	C15	3881 (5)	−1748 (5)	−12 (6)	5.06 (0.11)
16	O1	7242 (3)	1272 (2)	−1554 (4)	3.09 (0.05)
17	O2	6405 (3)	2551 (3)	−1647 (4)	3.79 (0.06)

No.	Atom	$x \cdot 10^3$	$y \cdot 10^3$	$z \cdot 10^3$	B_{eq} (Å^2)
18	HCl	583 (4)	−181 (4)	−116 (5)	4.0 (1.0)
19	HC2	675 (5)	−138 (5)	161 (7)	7.0 (2.0)
20	H′C2	720 (5)	14 (5)	165 (6)	5.0 (1.0)
21	HC3	866 (5)	−88 (5)	1 (6)	6.0 (1.0)
22	H′C3	901 (5)	69 (5)	37 (6)	6.0 (1.0)
23	HC4	796 (5)	−90 (5)	−276 (6)	6.0 (1.0)
24	HC6	551 (5)	−109 (5)	−396 (7)	6.0 (1.0)
25	H′C6	688 (5)	10 (5)	−491 (6)	6.0 (1.0)
26	HC7	622 (5)	155 (5)	−454 (6)	6.0 (1.0)
27	HC9	433 (4)	54 (4)	−50 (5)	4.0 (1.0)
28	H′C9	561 (4)	104 (4)	72 (6)	5.0 (1.0)
29	HC11	386 (4)	−46 (4)	−343 (6)	4.0 (1.0)
30	HC12	437 (5)	−93 (5)	−613 (7)	7.0 (1.0)
31	H′C12	318 (5)	−55 (5)	−630 (6)	6.0 (1.0)
32	H″C12	467 (5)	50 (5)	−678 (7)	7.0 (1.0)
33	HC13	298 (6)	81 (5)	−427 (7)	8.0 (2.0)
34	H′C13	409 (5)	162 (5)	−270 (7)	7.0 (1.0)
35	H″C13	440 (6)	194 (6)	−473 (8)	8.0 (2.0)
36	HC14	1007 (6)	100 (6)	−289 (8)	9.0 (2.0)
37	H′C14	947 (5)	190 (5)	−242 (7)	6.0 (1.0)
38	H″C14	903 (5)	110 (5)	−435 (7)	7.0 (1.0)
39	HC15	310 (5)	−162 (5)	17 (7)	7.0 (1.0)
40	H′C15	373 (5)	−270 (5)	−2 (7)	7.0 (1.0)
41	HO2	593 (7)	266 (7)	−102 (9)	12.0 (2.0)

14-Norketocurcumol (**1b**): Colorless oil, $C_{14}H_{22}O_3$. $[\alpha]_D^{30}$ −62.76° (c=0.81, $CHCl_3$). IR ν_{max}^{KBr} cm^{-1}: 3568 (OH), 3378 (br, OH), 1708 (C=O). ^{1}H-NMR ($CDCl_3$, 400 MHz) δ: 2.78, 2.66 (each 1H, d, J=17, 9α, 9β-H), 1.05 (3H, d, J=6.8, 11-CH_3), 0.99 (3H, d, J=6.8, 11-CH_3), 0.91 (3H, d, J=6.4, 14-H).

Esterification of Curcumol (1a) A solution of **1a** (15 mg) and *p*-BrC_6H_4COCl (102 mg) in pyridine (2 ml) was refluxed for 17 h. Evaporation of the solvent and subsequent silica gel chromatography of the residue afforded 9 mg of curcumol *p*-bromobenzoate (**1d**), as a syrup and 5 mg of the *p*-bromobenzoate (**1c**) of the Δ^9-*endo* isomer of **1a** as crystals, the overall yield being 52%.

The *p*-Bromobenzoate (**1c**): $C_{22}H_{27}O_3Br$. mp 122.5—124.5 °C. $[\alpha]_D^{29}$ −7.42° (c=1.89, $CHCl_3$). IR ν_{max}^{KBr} cm^{-1}: 1740 (C=O), 1594 (aromatic). CI-MS m/z: 419, 421 (each MH^+). EI-MS m/z: 418, 420 (each M^+). HR-MS m/z: 418.1137, 420.1112, (Theor. 418.3663 for $C_{22}H_{27}O_3Br$, 420.3643 for $C_{22}H_{27}O_3Br$). ^{1}H-NMR ($CDCl_3$) δ: 0.94 (3H, d, J=6.4, 14-H), 0.99, 1.01 (3H, each d, J=6.4, 13-H, 12-H), 1.74 (3H, d, J=1.2, 15-H), 5.65 (1H, s, 10H), 7.57, 7.90 (2H×2, each d, J=8.4, aromatic).

The *p*-Bromobenzoate (**1d**): $C_{22}H_{27}O_3Br$. $[\alpha]_D^{30}$ +46.2° (c=1.30, $CHCl_3$). IR ν_{max}^{KBr} cm^{-1}: 3080 (C=C–H), 1742 (C=O), 1648 (C=C), 1595 (aromatic). CI-MS (isobutane) m/z: 419 (MH^+), 421 (MH^+). EI-MS m/z: 418, 420 (M^+). HR-MS m/z: 418.1159, 420.1110 (Theor. 418.3663 for $C_{22}H_{27}O_3Br$, 420.3643 for $C_{22}H_{27}O_3Br$). ^{1}H-NMR ($CDCl_3$) δ: 0.91 (3H,

TABLE II. Atomic Coordinates of the *p*-Bromobenzoate (**1c**) of the Δ^9-Isomer of **1a**

No.	Atom	$x \cdot 10^5$	$y \cdot 10^5$	$z \cdot 10^5$	B_{eq} (Å^2)
1	Br1	−23417 (6)	−19492 (7)	−6388 (6)	8.10 (0.01)

No.	Atom	$x \cdot 10^4$	$y \cdot 10^4$	$z \cdot 10^4$	B_{eq} (Å^2)
2	C1	2628 (5)	−3402 (5)	6383 (5)	6.54 (0.11)
3	C2	1986 (6)	−4225 (6)	6958 (7)	9.05 (0.16)
4	C3	1117 (7)	−3679 (7)	7574 (7)	10.35 (0.19)
5	C4	1275 (5)	−2570 (6)	7430 (5)	7.43 (0.13)
6	C5	1905 (4)	−2502 (5)	6349 (5)	5.64 (0.10)
7	C6	2461 (5)	−1523 (4)	6087 (5)	6.02 (0.10)
8	C7	2303 (4)	−1381 (4)	4789 (4)	4.69 (0.08)
9	C8	1861 (4)	−2416 (4)	4468 (4)	4.73 (0.08)
10	C9	2680 (4)	−3196 (4)	4318 (5)	5.02 (0.08)
11	C10	3081 (4)	−3642 (4)	5230 (5)	5.75 (0.10)
12	C11	3258 (4)	−1031 (4)	4172 (6)	5.57 (0.10)
13	C12	3703 (5)	−65 (5)	4684 (7)	7.47 (0.13)
14	C13	3046 (5)	−882 (5)	2912 (6)	7.12 (0.12)
15	C14	295 (5)	−1976 (7)	7477 (6)	8.93 (0.15)
16	C15	3941 (5)	−4376 (5)	5196 (7)	7.95 (0.14)
17	C16	755 (4)	−3085 (4)	3023 (4)	4.66 (0.08)
18	C17	82 (3)	−2765 (4)	2083 (4)	3.99 (0.07)
19	C18	−461 (4)	−3514 (4)	1516 (5)	4.94 (0.09)
20	C19	−1154 (4)	−3265 (4)	681 (5)	5.55 (0.09)
21	C20	−1306 (4)	−2283 (4)	423 (4)	5.07 (0.09)
22	C21	−761 (4)	−1525 (4)	939 (4)	4.92 (0.08)
23	C22	−59 (4)	−1779 (4)	1777 (4)	4.47 (0.08)
24	O1	1212 (3)	−2656 (3)	5394 (3)	4.92 (0.06)
25	O2	1231 (3)	−2281 (2)	3497 (3)	4.65 (0.05)
26	O3	858 (3)	−3930 (3)	3339 (4)	6.29 (0.07)

No.	Atom	$x \cdot 10^3$	$y \cdot 10^3$	$z \cdot 10^3$	B_{eq} (Å^2)
27	HC1	329 (4)	−322 (4)	697 (4)	7.0 (1.0)
28	HC2	167 (4)	−475 (4)	639 (5)	8.0 (2.0)
29	H′C2	244 (5)	−464 (4)	763 (5)	9.0 (2.0)
30	HC3	36 (4)	−391 (4)	715 (5)	9.0 (2.0)
31	H′C3	106 (5)	−388 (5)	845 (5)	10.0 (2.0)
32	HC4	171 (4)	−229 (4)	813 (4)	7.0 (1.0)
33	HC6	327 (4)	−160 (4)	629 (4)	6.0 (1.0)
34	H′C6	214 (4)	−93 (4)	663 (4)	7.0 (2.0)
35	HC7	173 (4)	−81 (4)	461 (4)	6.0 (1.0)
36	HC9	301 (4)	−338 (4)	347 (4)	7.0 (1.0)
37	HC11	388 (3)	−160 (3)	426 (4)	5.0 (1.0)
38	HC12	378 (4)	−16 (4)	561 (5)	7.0 (1.0)
39	H′C12	320 (4)	53 (4)	448 (5)	9.0 (2.0)
40	H″C12	447 (4)	9 (4)	433 (5)	8.0 (2.0)
41	HC13	253 (5)	−26 (3)	281 (4)	7.0 (1.0)
42	H′C13	374 (4)	−78 (4)	245 (4)	7.0 (1.0)
43	H″C13	265 (4)	−155 (4)	258 (4)	8.0 (2.0)
44	HC14	47 (4)	−115 (5)	736 (5)	9.0 (2.0)
45	H′C14	−13 (4)	−203 (5)	827 (5)	9.0 (2.0)
46	H″C14	−23 (4)	−216 (4)	678 (5)	9.0 (2.0)
47	HC15	372 (5)	−505 (4)	484 (5)	9.0 (2.0)
48	H′C15	456 (5)	−408 (5)	471 (5)	11.0 (2.0)
49	H″C15	422 (5)	−453 (4)	601 (5)	10.0 (2.0)
50	HC18	−31 (4)	−426 (4)	175 (4)	6.0 (1.0)
51	HC19	−161 (4)	−384 (4)	25 (4)	6.0 (1.0)
52	HC21	−86 (4)	−74 (4)	72 (5)	7.0 (1.0)
53	HC22	36 (4)	−120 (4)	220 (4)	6.0 (1.0)

Equivalent positions:

x	y	z
1/2−x	−y	1/2+z
1/2+x	1/2−y	−z
−x	1/2+y	1/2−z.

TABLE III. Atomic Coordinates of Curdione (**2a**)

No.	Atom	$x\cdot10^4$	$y\cdot10^4$	$z\cdot10^4$	B_{eq} (Å^2)
1	C1	1035 (4)	−1670 (3)	1295 (5)	4.92 (0.08)
2	C2	−8 (4)	−1019 (3)	1817 (6)	5.62 (0.09)
3	C3	288 (4)	116 (3)	1587 (5)	4.85 (0.07)
4	C4	1534 (3)	434 (3)	2198 (4)	3.54 (0.06)
5	C5	2624 (4)	33 (3)	1416 (4)	3.33 (0.05)
6	C6	3725 (3)	−394 (3)	2176 (4)	3.29 (0.05)
7	C7	4519 (4)	−1179 (3)	1404 (4)	3.51 (0.06)
8	C8	4190 (4)	−2264 (3)	1762 (5)	4.34 (0.07)
9	C9	2939 (4)	−2695 (3)	1331 (5)	5.24 (0.08)
10	C10	1839 (4)	−2198 (3)	2024 (5)	4.42 (0.07)
11	C11	5939 (4)	−973 (3)	1532 (5)	4.23 (0.07)
12	C12	6365 (4)	−833 (4)	2948 (5)	5.37 (0.08)
13	C13	6294 (5)	−73 (4)	662 (6)	6.08 (0.09)
14	C14	1647 (4)	1592 (3)	2255 (6)	5.55 (0.08)
15	C15	1770 (5)	−2347 (3)	3503 (5)	5.47 (0.08)
16	O1	2658 (3)	124 (3)	229 (3)	5.10 (0.05)
17	O2	4919 (3)	−2814 (2)	2319 (5)	7.50 (0.07)

No.	Atom	$x\cdot10^3$	$y\cdot10^3$	$z\cdot10^3$	B_{eq} (Å^2)
18	HC1	110 (4)	−158 (3)	15 (4)	5.1 (1.0)
19	HC2	−25 (4)	−109 (3)	305 (4)	6.8 (1.1)
20	H′C2	−86 (4)	−123 (3)	125 (5)	7.7 (1.3)
21	HC3	35 (4)	27 (3)	47 (4)	7.3 (1.2)
22	H′C3	−47 (4)	58 (3)	196 (4)	7.2 (1.2)
23	HC4	152 (3)	7 (3)	324 (4)	4.9 (0.9)
24	HC6	347 (3)	−68 (3)	315 (4)	4.5 (0.9)
25	H′C6	419 (3)	37 (3)	230 (4)	5.6 (1.0)
26	HC7	432 (4)	−111 (3)	34 (4)	5.0 (1.0)
27	HC9	292 (4)	−350 (3)	154 (4)	7.2 (1.2)
28	H′C9	282 (4)	−257 (3)	27 (4)	5.5 (1.1)
29	HC11	645 (4)	−164 (3)	113 (4)	6.1 (1.1)
30	HC12	738 (4)	−93 (3)	303 (5)	7.9 (1.3)
31	H′C12	617 (4)	−8 (3)	330 (4)	7.6 (1.2)
32	H″C12	595 (4)	−142 (3)	359 (4)	7.3 (1.3)
33	HC13	730 (4)	6 (4)	70 (4)	7.5 (1.2)
34	H′C13	603 (4)	−19 (3)	−34 (4)	5.7 (1.1)
35	H″C13	584 (4)	62 (3)	103 (4)	6.6 (1.2)
36	HC14	247 (4)	182 (3)	280 (5)	7.6 (1.3)
37	H′C14	173 (5)	191 (3)	121 (5)	8.4 (1.4)
38	H″C14	83 (4)	193 (3)	268 (5)	8.0 (1.3)
39	HC15	92 (5)	−200 (4)	393 (5)	10.1 (1.6)
40	H′C15	180 (5)	−312 (4)	380 (5)	9.4 (1.5)
41	H″C15	255 (5)	−193 (4)	401 (5)	9.9 (1.6)

Equivalent positions:

x	y	z
$1/2-x$	$-y$	$1/2+z$
$1/2+x$	$1/2-y$	$-z$
$-x$	$1/2+y$	$1/2-z$.

d, J=6.8, 14-H), 1.03, 0.99 (3H × 2, each d, J=6.8, 12-H, 13-H), 2.62, 3.30 (1H × 2, each d, J=14.4, 9-H), 4.91 (2H, br s, 15-H), 7.56, 7.79 (2H × 2, each d, J=8.4, aromatic).

X-Ray Analysis of *p*-Bromobenzoate (1c) The absolute configuration of **1c** was determined from the anomalous dispersion of CuK_α radiation by the bromine atom. The crystal data are: $C_{22}H_{27}O_3Br$; mp 122.5—124.5 °C; M.W.=419.4; orthorhombic; space group $P2_12_12_1$; lattice constants: a=13.004(7), b=13.442(8), c=11.875(6) Å, U=2076 Å^3, Z=4, D_{calc}=1.342 g cm^{-3}. Intensity data were collected by using graphite monochromated CuK_α radiation, and of the total of 2311 reflections measured within the 2θ angle of 156°, 1908 that exceeded the 2σ(I) level were used for the structure determination. The structure was determined by the heavy atom method and refined by the least-squares method. Of the total of 76 Friedel pairs, 66 pairs clearly showed the absolute configuration. The final R value was 0.043 taking into account the contributions of 27 hydrogen atoms and dispersion corrections. The absolute configuration of **1c** is depicted in Chart 1 and in Fig. 3 (drawn by the PLUTO program).

Preparation of 5α,8βH-Tetrahydrocurdione (2b) A solution of $LiAlH_4$

TABLE IV. Atomic Coordinates of the *p*-Bromobenzoate (**2e**) of 8αH-Dihydrocurdione (**2j**)

No.	Atom	$x\cdot10^4$	$y\cdot10^4$	$z\cdot10^4$	B_{eq} (Å^2)
1	Br1	20107 (8)	100000 (0)	110893 (7)	10.24 (0.02)

No.	Atom	$x\cdot10^4$	$y\cdot10^4$	$z\cdot10^4$	B_{eq} (Å^2)
2	C1	−2765 (5)	8198 (16)	2604 (5)	4.7 (0.1)
3	C2	−3384 (6)	7564 (20)	1482 (6)	6.6 (0.2)
4	C3	−4434 (5)	7104 (19)	1274 (5)	5.9 (0.2)
5	C4	−4532 (4)	5211 (19)	2019 (4)	4.7 (0.1)
6	C5	−4178 (4)	6277 (16)	3115 (5)	4.5 (0.1)
7	C6	−3529 (4)	4625 (15)	4018 (4)	3.9 (0.1)
8	C7	−2878 (4)	6026 (12)	5026 (4)	3.2 (0.1)
9	C8	−1822 (4)	5923 (13)	5164 (4)	3.7 (0.1)
10	C9	−1602 (4)	7664 (13)	4440 (5)	3.8 (0.1)
11	C10	−2049 (5)	6870 (14)	3311 (5)	4.2 (0.1)
12	C11	−2981 (4)	5036 (16)	5984 (4)	3.6 (0.1)
13	C12	−2761 (6)	2292 (16)	6179 (6)	5.4 (0.2)
14	C13	−3991 (5)	5693 (16)	5911 (6)	5.3 (0.2)
15	C14	−5595 (5)	4450 (27)	1664 (6)	8.3 (0.2)
16	C15	−1622 (5)	4562 (18)	3083 (6)	5.8 (0.2)
17	C16	−427 (4)	5537 (16)	6789 (5)	4.4 (0.1)
18	C17	124 (4)	6599 (14)	7841 (5)	3.8 (0.1)
19	C18	1005 (4)	5542 (17)	8488 (5)	5.1 (0.1)
20	C19	1551 (5)	6502 (18)	9466 (5)	5.7 (0.2)
21	C20	1237 (5)	8541 (19)	9760 (5)	6.0 (0.2)
22	C21	361 (5)	9686 (20)	9148 (5)	5.5 (0.1)
23	C22	−184 (4)	8650 (16)	8174 (5)	4.8 (0.1)
24	O1	−4438 (3)	8262 (12)	3266 (4)	5.8 (0.1)
25	O2	−1223 (3)	6810 (9)	6218 (3)	3.8 (0.1)
26	O3	−178 (4)	3726 (12)	6477 (5)	7.4 (0.1)

No.	Atom	$x\cdot10^3$	$y\cdot10^3$	$z\cdot10^3$	B_{eq} (Å^2)
27	HC1	−297 (4)	993 (16)	286 (5)	5.0 (1.0)
28	HC2	−308 (5)	585 (17)	131 (6)	9.0 (2.0)
29	H′C2	−333 (5)	911 (17)	99 (7)	9.0 (3.0)
30	HC3	−487 (5)	651 (14)	49 (5)	6.0 (2.0)
31	H′C3	−473 (5)	880 (14)	140 (6)	7.0 (2.0)
32	HC4	−413 (4)	358 (13)	202 (5)	5.0 (2.0)
33	HC6	−398 (5)	325 (18)	416 (7)	9.0 (2.0)
34	H′C6	−310 (4)	337 (14)	375 (5)	6.0 (2.0)
35	HC7	−311 (4)	788 (13)	493 (5)	4.0 (1.0)
36	HC8	−164 (5)	393 (15)	505 (6)	8.0 (2.0)
37	HC9	−83 (5)	778 (16)	470 (6)	8.0 (2.0)
38	H′C9	−190 (4)	945 (14)	448 (5)	6.0 (2.0)
39	HC11	−247 (4)	597 (11)	663 (4)	4.0 (1.0)
40	HC12	−202 (5)	188 (16)	629 (6)	7.0 (2.0)
41	H′C12	−282 (5)	176 (15)	684 (6)	7.0 (2.0)
42	H″C12	−321 (5)	124 (17)	550 (7)	9.0 (2.0)
43	HC13	−456 (5)	483 (21)	521 (6)	9.0 (2.0)
44	H′C13	−406 (5)	495 (20)	660 (6)	8.0 (2.0)
45	H″C13	−410 (5)	770 (15)	588 (5)	6.0 (2.0)
46	HC14	−588 (5)	372 (17)	89 (7)	9.0 (3.0)
47	H′C14	−566 (6)	312 (21)	222 (8)	12.0 (3.0)
48	H″C14	−604 (6)	605 (10)	168 (7)	10.0 (3.0)
49	HC15	−168 (6)	308 (20)	353 (8)	11.0 (3.0)
50	H′C15	−195 (6)	400 (19)	231 (7)	11.0 (3.0)
51	H″C15	−90 (5)	474 (21)	334 (6)	9.0 (2.0)
52	HC18	122 (5)	419 (16)	828 (6)	8.0 (2.0)
53	HC19	215 (4)	574 (15)	988 (5)	7.0 (2.0)
54	HC21	16 (4)	1100 (14)	939 (5)	6.0 (2.0)
55	HC22	−77 (4)	934 (13)	773 (5)	5.0 (2.0)

Equivalent positions:

x	y	z
$-x$	$1/2+y$	$-z$.

(70 mg) in ether (5 ml) was added at 0 °C to a solution of **2a** (100 ml) in ether (2 ml), and the mixture was stirred for 1 h. The reaction mixture was worked up treated as usual. The residue thus obtained was subjected to silica gel column chromatography to afford 100 mg of colorless prisms (98%).

Compound **2b**: mp 107—109 °C. $[\alpha]_D^{19}$ 16.60° ($c=2.0$, $CHCl_3$). IR ν_{max}^{KBr} cm^{-1}: 3309 (OH), 1660 (C=C). EI-MS *m/z*: 240 (M^+).

Preparation of 5α,8βH-Tetrahydrocurdione (2b) 8αH-Dihydrocurdione (2c) and 5α,8αH-Tetrahydrocurdione (2d) A mixture of $LiAlH_4$ (150 mg) and ether (5 ml) was added to a solution of **2a** (203 mg) in ether (5 ml). The solution was stirred for 10 min at room temperature. After the usual work-up, 206 mg of crude products was chromatographed on a silica gel column using a gradient solvent mixture of petroleum ether and ether to give successively 27 mg of 8αH-dihydrocurdione (**2c**) as needles, 100 mg of 5α,8βH-tetrahydrocurdione (**2b**) as prisms and 20 mg of 5α,8αH-tetrahydrocurdione (**2d**) as prisms.

8αH-Dihydrocurdione (**2c**): mp 162—163 °C. $[\alpha]_D^{24}$ +3.07° ($c=3.85$, $CHCl_3$). IR ν_{max}^{KBr} cm^{-1}: 3474 (OH), 1698 (C=O). EI-MS *m/z*: 238 (M^+). CI-MS *m/z*: 239 (MH^+). HR-MS *m/z*: 238.1930 for $C_{15}H_{26}O_2$. ^{1}H-NMR ($CDCl_3$) δ: 4.94 (1H, d, $J=8.3$, 1-H), 3.63 (1H, m, 8α-H), 2.53 (1H, d, $J=12.2$), 2.23—2.36 (2H, m), 2.05—2.19 (5H, m), 1.95 (1H, d, $J=11.7$), 1.76 (3H, s, 15-H), 1.57—1.61 (2H, m), 1.25 (1H, d, $J=6.3$), 0.96, 0.76 (3H × 2, each d, $J=6.83$, 12-H, 13-H), 0.85 (3H, d, $J=7.08$, 14-H).

5α,8αH-Tetrahydrocurdione (**2d**): mp 70—72 °C. $[\alpha]_D^{18}$ +13.66° ($c=0.85$, $CHCl_3$). IR ν_{max}^{KBr} cm^{-1}: 3390, 3300 (br, OH). EI-MS *m/z*: 240 (M^+).

Esterification of 8αH-Dihydrocurdione (2c) A solution of **2c** (20 mg), *p*-BrC_6H_4COCl (40 mg) and pyridine (0.1 ml) in CH_2Cl_2 was stirred at room temperature for 3 h. After evaporation of the solvent at room temperature, the residue was submitted to silica gel column chromatography to give 27 mg of the *p*-bromobenzoate (**2e**) as needles (84%). Recrystallization from pentane afforded a single crystal suitable for X-ray analysis.

The *p*-Bromobenzoate (**2e**): mp 132—134 °C. $[\alpha]_D^{24}$ −23.52° ($c=0.77$, $CHCl_3$). IR ν_{max}^{KBr} cm^{-1}: 1720 (C=O), 1595 (aromatic). ^{1}H-NMR ($CDCl_3$) δ: 6.21 (1H, ddd, $J=10$, 10, 4, 8α-H), 5.04 (1H, d, $J=10$, 1-H), 2.52—2.72 (2H, m), 1.96—2.48 (7H, m), 1.86 (3H, s, 15-H), 1.51—1.78 (2H, m), 1.01, 0.86, 0.67 (each 3H, d, $J=7$, 12-H, 13-H, 14-H).

X-Ray Analysis of the *p*-Bromobenzoate (2e) Crystal data for **2e** are as follows: $C_{22}H_{29}O_3Br$; M.W. = 421.4; monoclinic; space group $P2_1$; lattice constant: $a=15.394(8)$, $b=5.451(3)$, $c=14.225(8)$ Å, $\beta=115.61(6)$, $U=1076$ Å^3, $Z=2$, $D_{calc}=1.300$ g cm^{-3}. A single crystal of approximate dimensions 0.03 × 0.01 × 0.5 mm was chosen for the X-ray study. Of the total of 2343 reflections observed within the 2θ range of 6° through 70°, 1620 reflections were crystallographically independent and 519 were Friedel reflections. The remaining 204 were equivalent reflections which agree with the original ones with an approximate $R'=\sum||F01(hkl)|-|F01(hkl)||/\sum|F01|$ of 0.03. The R' value for the Friedel reflections was 0.055. The structure was determined by the heavy atom method and refined by the block-diagonal matrix least-squares method to an R value of 0.06. All the hydrogen atoms were included with isotropic temperature factors. The absolute configuration was determined by the anomalous dispersion method allowing for the dispersion terms of Br, O and C atoms for CuK_α radiation. Of the total of 135 Friedel pairs, for which the value $=\sum||F_O(hkl)|-|F_O(h\bar{k}\bar{l})||$ was estimated to be greater than $2\delta(F_O)$, 120 pairs showed the same configuration as given in Fig. 4. The final refinement in which the dispersion corrections were adequately made, gave the R value of 0.053. Hence the absolute configuration of curdione (**2a**) was deduced to be as mentioned above.

Isolation of (1*R*,10*R*)-Epoxy-(−)-1,10-dihydrocurdione (5a) Air-dried rhizomes (75 g) of *C. wenyujin* were extracted with 4 l of ether at 5 °C for a week. After filtration, the solvent was evaporated off at room temperature. The residue obtained was chromatographed on a silica gel column using a gradient solvent system of petroleum ether and ether. The fractions eluted with petroleum ether–ether (10:8) were collected. Evaporation of the solvent afforded 200 mg of oil. Crystallization from petroleum ether and ether, subsequent repeated silica gel chromatography and final recrystallization from ether gave a pure sample of the (1*R*,10*R*)-epoxide (**5a**) (40 mg, 0.07%).

(1*R*,10*R*)-Epoxy-(−)-1,10-dihydrocurdione (**5a**): $C_{15}H_{24}O_3$. mp 133—134 °C. $[\alpha]_D^{24}$ −235.0° ($c=0.68$, $CHCl_3$). UV $\lambda_{max}^{CHCl_3}$ nm (ε): 288 (52). EI-MS *m/z*: 252 (M^+). CI-MS *m/z*: 253 (MH^+). HR-MS *m/z*: 252.1745 (Theor. 252.3528) for $C_{15}H_{24}O_3$. IR ν_{max}^{KBr} cm^{-1}: 1705 (C=O). ^{1}H-NMR ($CDCl_3$) δ: 3.08 (1H, dd, $J=18.3$, 11.9, 6-H), 2.89 (1H, dd, $J=9.9$, 3.8, 1-H), 2.83 (1H, m, 4-H), 2.81 (1H, dd, $J=18.3$, 4.0, 6-H), 2.69 (1H, d, $J=11.2$, 9-H), 2.66 (1H, dd, $J=11.9$, 4.0, 7-H), 2.07 (1H, m, 2-H), 1.73 (1H, m, 11-H), 1.69 (1H, m, 2-H), 1.34 (1H, m, 3-H), 1.17 (3H, s, 15-H), 1.07 (3H, d, $J=6.8$, 14-H), 0.97 (3H, d, $J=6.6$, 13-H), 0.87 (3H, d, $J=6.6$, 12-H). ^{13}C-NMR ($CDCl_3$) δ: 213.1 (C-5), 208.9 (C-8), 64.1 (C-1), 58.9 (C-10), 56.0 (C-7), 50.9 (C-9), 44.5 (C-4), 42.5 (C-6), 30.1 (C-11), 29.6 (C-3), 24.8 (C-2), 21.1 (C-12), 20.6 (C-13), 18.9 (C-14), 16.1 (C-15).

TABLE V. Atomic Coordinates of Neocurdione (**4**)

No.	Atom	$x\cdot10^4$	$y\cdot10^4$	$z\cdot10^4$	B_{eq} (Å^2)
1	C1	1143 (3)	7651 (0)	5594 (6)	3.5 (0.0)
2	C2	−41 (3)	7071 (3)	4154 (7)	4.5 (0.1)
3	C3	321 (3)	6316 (3)	2188 (6)	4.2 (0.1)
4	C4	1584 (3)	5663 (3)	3129 (6)	3.4 (0.0)
5	C5	2808 (3)	6340 (3)	3281 (5)	2.8 (0.0)
6	C6	3837 (3)	6414 (2)	5724 (5)	2.8 (0.0)
7	C7	4839 (3)	7305 (3)	5810 (5)	3.1 (0.0)
8	C8	4221 (3)	8371 (3)	5080 (6)	3.5 (0.0)
9	C9	3127 (3)	8763 (3)	6278 (6)	3.9 (0.1)
10	C10	1793 (3)	8416 (3)	4750 (5)	3.4 (0.0)
11	C11	5736 (3)	7391 (3)	8519 (6)	4.0 (0.1)
12	C12	6476 (4)	6380 (4)	9305 (9)	7.1 (0.1)
13	C13	6709 (4)	8293 (4)	8707 (9)	7.4 (0.1)
14	C14	1558 (4)	5021 (3)	5461 (7)	4.5 (0.1)
15	C15	1349 (4)	8934 (3)	2218 (6)	4.8 (0.1)
16	O1	2981 (2)	6771 (2)	1402 (4)	3.7 (0.0)
17	O2	4625 (3)	8915 (2)	3595 (5)	5.3 (0.0)

No.	Atom	$x\cdot10^3$	$y\cdot10^3$	$z\cdot10^3$	B_{eq} (Å^2)
18	HC1	146 (3)	739 (3)	754 (6)	6.0 (1.0)
19	HC2	−46 (3)	661 (3)	551 (7)	6.0 (1.0)
20	H'C2	−78 (4)	761 (3)	325 (6)	6.0 (1.0)
21	HC3	47 (3)	677 (3)	56 (6)	6.0 (1.0)
22	H'C3	−48 (3)	576 (3)	154 (6)	6.0 (1.0)
23	HC4	164 (3)	506 (3)	169 (6)	5.0 (1.0)
24	HC6	333 (3)	651 (3)	724 (6)	5.0 (1.0)
25	H'C6	434 (3)	566 (3)	597 (6)	5.0 (1.0)
26	HC7	546 (3)	711 (3)	449 (6)	4.0 (1.0)
27	HC9	316 (4)	962 (3)	638 (7)	7.0 (1.0)
28	H'C9	328 (3)	845 (3)	822 (6)	5.0 (1.0)
29	HC11	511 (4)	755 (3)	989 (7)	6.0 (1.0)
30	HC12	502 (4)	571 (3)	922 (8)	8.0 (1.0)
31	H'C12	710 (4)	643 (3)	1120 (7)	7.0 (1.0)
32	H''C12	715 (4)	622 (4)	799 (8)	9.0 (1.0)
33	HC13	613 (3)	891 (3)	847 (6)	6.0 (1.0)
34	H'C13	739 (4)	829 (3)	1048 (8)	8.0 (1.0)
35	H''C13	724 (4)	820 (3)	718 (7)	8.0 (1.0)
36	HC14	147 (3)	555 (3)	702 (7)	6.0 (1.0)
37	H'C14	246 (4)	457 (3)	608 (7)	7.0 (1.0)
38	H''C14	72 (3)	449 (3)	513 (7)	7.0 (1.0)
39	HC15	127 (4)	970 (4)	244 (7)	8.0 (1.0)
40	H'C15	37 (4)	864 (4)	123 (7)	8.0 (1.0)
41	H''C15	204 (4)	877 (4)	104 (7)	7.0 (1.0)

Equivalent positions:

x	y	z
$-x$	$1/2+y$	$-z$.

X-Ray Analysis of (1*R*,10*R*)-Epoxy-(−)-1,10-dihydrocurdione (5a) The relative structure of **5a** was determined by X-ray analysis. The crystal data were as follows: $C_{15}H_{24}O_3$; M.W. = 252.4; orthorhombic; space group $P2_12_12_1$; lattice constants : $a=10.605(3)$, $b=13.503(1)$, $c=10.429$ (9) Å, $U=1493.4$ Å^3, $Z=4$, $D_{calc}=1.24$. The intensity data were collected on Philips PW 1100 diffractometer using graphite monochromated CuK_α radiation; 777 reflections up to 150° (2θ) were used. The crystal structure was determined by the direct method using the MULTAN program and refined by means of the block-diagonal least-squares method. The final R value was 0.051 including 24 hydrogen atoms with isotropic temperature factors. The crystal structure and relative stereostructure of **5a** were thus revealed to be as shown in Fig. 5.

Epoxidation of Curdione (2a) MCPBA (52 mg) in CH_2Cl_2 (1 ml) was added dropwise to a solution of **2a** (60 mg) in CH_2Cl_2 (1 ml) cooled in an ice-bath. The mixture was stirred for 2 h in the ice bath and for 3 h at

room temperature. Then it was washed with saturated aqueous Na_2CO_3 solution, dried over anhydrous Na_2SO_4 and evaporated to give 107 mg of crude products, which were separated by silica gel chromatography to afford 36 mg of (1*R*,10*R*)-epoxy-(−)-1,10-dihydrocurdione (**5a**) and (1*S*,10*S*)-epoxy-(+)-1,10-dihydrocurdione (**5b**) (27 mg). The overall yield was 98%.

(1*S*,10*S*)-Epoxy-(+)-1,10-dihydrocurdione (**5b**): $C_{15}H_{24}O_3$. mp 117—119°C. $[\alpha]_D^{24}$ +99.80° (c=0.95, $CHCl_3$). UV $\lambda_{max}^{CHCl_3}$ nm (ε): 288 (49). IR ν_{max}^{KBr} cm^{-1}: 1705 (C=O). EI-MS *m/z*: 252 (M^+). ^{1}H-NMR ($CDCl_3$) δ: 2.91 (1H, dt, J=15.3, 8.9, 7-H), 2.81 (1H, d, J=10.3, 9-H), 2.80 (1H, dd, J=15.3, 8.9, 6-H), 2.70 (1H, dd, J=10.3, 2.2, 1-H), 2.48 (1H, dd, J=15.3, 1.8, 6-H), 2.44 (1H, m, 4-H), 2.26 (1H, d, J=10.3, 9-H), 2.24 (2H, m, 2-H, 3-H), 1.91 (1H, m, 11-H), 1.56 (1H, m, 3-H), 1.29 (3H, s, 15-H), 1.25 (1H, m, 2-H), 1.09 (3H, d, J=6.0, 14-H), 0.94 (3H, d, J=6.6, 13-H), 0.89 (3H, J=6.6, 12-H). ^{13}C-NMR ($CDCl_3$) δ: 214.3 (C-5), 212.0 (C-8), 62.5 (C-1), 58.5 (C-10), 55.6 (C-7), 55.9 (C-9), 46.8 (C-4), 42.4 (C-6), 30.4 (C-11), 29.1 (C-3), 35.8 (C-2), 21.2 (C-12), 20.2 (C-13), 18.2 (C-14), 17.3 (C-15).

Isolation of Neocurdione (4) Dried rhizomes of *C. wenyujin* (450 g) were cut into small pieces and the chips were percolated with ether for four days in a refrigerator. After the filtration of this ether extract, evaporation of the solvent *in vacuo* afforded 16.8 g of essential oil (3.7%), which was submitted to silica gel chromatography with *n*-hexane–ether. The fractions eluted with *n*-hexane–ether (1:1) were collected. Preparative thin layer chromatography (TLC) (*n*-hexane–ether) and finally recrystallization from *n*-pentane afforded 220 mg (1.3%) of neocurdione (**4**) as colorless prisms.

Neocurdione (**4**): $C_{15}H_{24}O_2$. mp 45—47°C. $[\alpha]_D^{22}$ −65.80° (c=1.20, $CHCl_3$). CD [θ] −36060 (300), +12368 (223). IR ν_{max}^{KBr} cm^{-1}: 1702 (C=O), 1662 (C=C). EI-MS *m/z*: 236 (M^+). CD [θ] (c=0.05, MeOH). ^{1}H-NMR ($CDCl_3$, 400 MHz) δ: 0.91, 0.97 (6H, d, J=6.6, 12 or 13-H), 1.25 (3H, d, J=7.1, 14-H), 1.65 (3H, s, 15-H), 1.75 (1H, m, 3β-H), 1.91 (1H, m, 3α-H), 1.93 (1H, m, 11-H), 2.09 (1H, m, 2β-H), 2.16 (1H, m, 2α-H), 2.39 (1H, dd, J=14.9, 2.7, 6β-H), 2.88 (1H, d, J=12.5, 9α-H), 2.89 (1H, ddd, J=6.8, 3.2, 1.0, 7β-H), 3.04 (1H, d, J=12.5, 9β-H), 5.17 (1H, s, 1-H).

X-Ray Analysis of Neocurdione (4) The relative structure of neocurdione (**4**) was determined by X-ray analysis. The crystal data were as follows: $C_{15}H_{24}O_2$; M.W.=236.4; monoclinic; space group $P2_1$; lattice constants: a=10.446(7), b=12.785(7) Å, β=103.19(6)°, U=714 Å^3, Z=2, D_{calc}=1.099 g cm^{-3}. The intensity data were collected on a Philips PW 1100 diffractometer using graphite monochromated CuK_α radiation; 1387 reflections up to 156° (2θ) were used. The crystal structure was determined by the direct method using the MULTAN program, and refined by means of the block diagonal least squares method. The final R value was 0.04 including 24 hydrogen atoms with isotropic temperature factors.

Transformation of Curdione (2a) to 8βH-Dihydrocurdione (2f) Compound **2a** (28 mg) was dissolved in 2 ml of methanol. After addition of $NaBH_4$ (3.4 mg), the mixture was stirred for 3 h. After evaporation of the solvent, the residue was extracted with ether. Evaporation of the solvent afforded 28 mg of crude residue. This residue was submitted to silica gel column chromatography to yield 25 mg (89%) of 8βH-dihydrocurdione (**2f**) as colorless prisms.

Compound **2f**: $C_{15}H_{26}O_2$. mp 55—58°C. $[\alpha]_D^{19}$ +70.25° (c=2.10, $CHCl_3$). IR ν_{max}^{KBr} cm^{-1}: 3460 (OH), 1695 (C=O). CI-MS *m/z*: 239 (MH^+). ^{1}H-NMR ($CDCl_3$) δ: 4.90 (1H, d, J=12.1, 1-H), 4.20 (1H, t, J=3.3, 8-H), 3.02 (1H, dd, J=18.0, 5.1), 2.41 (1H, m), 2.38 (1H, m), 2.18 (1H, dd, J=13.8, 3.7), 2.15 (1H, dd, J=13.9, 2.6), 1.90 (3H, s, 10-CH_3), 1.86—1.96 (2H, m), 1.60—1.68 (2H, m), 0.98 (3H, d, J=7.0, 14-CH_3), 0.95 (3H, d, J=6.6, 11-CH_3), 0.94 (3H, d, J=6.6, 11-CH_3).

Transformation of 8βH-Dihydrocurdione (2f) to 8βH-Dihydro-4-epicurdione (2g) Compound **2f** was dissolved in 2 ml of benzene and a catalytic amount of *tert*-BuOK was added. The reaction mixture was refluxed for 2 h, then the solvent was evaporated off. The residue was submitted to silica gel chromatography by using a *n*-hexane–ether gradient solvent system to afford 41 mg of 8βH-dihydrocurdione (**2f**) and 10 mg of 8βH-dihydro-4-epicurdione (**2g**) in the ratio of 4:1.

Compound **2g**: $C_{15}H_{26}O_2$. Oil. $[\alpha]_D^{20}$ −0.26° (c=3.82, $CHCl_3$). IR ν_{max}^{KBr} cm^{-1}: 3470 (–OH), 1690 (C=O). EI-MS *m/z*: 238 (M^+), ^{1}H-NMR ($CDCl_3$) δ: 5.10 (1H, brs, 1-H), 4.15 (1H, brs, 8β-H), 3.07 (1H, dd, J=17.3, 5.4), 2.47 (1H, brs), 2.09 (1H, dd, J=13.4, 2.4), 1.83 (3H, s, 10-CH_3), 1.12 (3H, d, J=7.1, 14-CH_3), 1.12 (3H, d, J=7.1, 4-CH_3), 0.95 (3H, d, J=6.8, 11-CH_3), 0.94 (3H, d, J=6.6, 11-CH_3).

Transformation of 8βH-Dihydro-4-epicurdione (2g) to 4-Epicurdione (2h) Compound **2g** (10 mg) was dissolved in 1.5 ml of pyridine and CrO_3

TABLE VI. Atomic Coordinates of the *p*-Bromobenzoate (**2k**) of 8αH-Dihydro-4-epicurdione (**2j**)

No.	Atom	$x\cdot10^5$	$y\cdot10^5$	$z\cdot10^5$	B_{eq} (Å^2)
1	Br1	−43040 (6)	56556 (6)	−3610 (16)	9.88 (0.02)

No.	Atom	$x\cdot10^4$	$y\cdot10^4$	$z\cdot10^4$	B_{eq} (Å^2)
2	C1	3158 (5)	7854 (3)	−2103 (8)	4.5 (0.1)
3	C2	4251 (5)	8016 (3)	−2320 (9)	6.0 (0.1)
4	C3	4798 (4)	7400 (3)	−3119 (9)	5.0 (0.1)
5	C4	4472 (4)	7239 (3)	−4833 (8)	4.8 (0.1)
6	C5	3359 (4)	7079 (3)	−4986 (7)	4.1 (0.1)
7	C6	2965 (4)	6431 (3)	−4162 (7)	3.5 (0.1)
8	C7	1824 (4)	6433 (3)	−3922 (7)	3.3 (0.1)
9	C8	1568 (4)	6434 (3)	−2147 (7)	3.7 (0.1)
10	C9	1712 (4)	7147 (3)	−1300 (8)	4.4 (0.1)
11	C10	2777 (4)	7363 (3)	−1158 (8)	4.2 (0.1)
12	C11	1337 (4)	5820 (3)	−4853 (8)	4.3 (0.1)
13	C12	1674 (4)	5088 (3)	−4303 (10)	5.6 (0.1)
14	C13	1505 (5)	5900 (4)	−6671 (9)	6.2 (0.1)
15	C14	5069 (5)	6618 (4)	−5514 (11)	7.0 (0.1)
16	C15	3375 (5)	6974 (3)	105 (8)	5.5 (0.1)
17	C16	187 (4)	5767 (3)	−1099 (7)	4.1 (0.1)
18	C17	−910 (4)	5747 (3)	−996 (7)	3.9 (0.1)
19	C18	−1509 (4)	6203 (3)	−1833 (7)	3.9 (0.1)
20	C19	−2524 (4)	6179 (3)	−1666 (8)	4.7 (0.1)
21	C20	−2910 (4)	5696 (3)	−655 (9)	5.7 (0.1)
22	C21	−2345 (5)	5234 (4)	240 (11)	7.1 (0.1)
23	C22	−1324 (4)	5262 (3)	39 (10)	6.4 (0.1)
24	O1	2856 (3)	7446 (2)	−5832 (5)	5.5 (0.1)
25	O2	499 (3)	6306 (2)	−2015 (5)	4.1 (0.1)
26	O3	723 (3)	5357 (2)	−409 (6)	5.9 (0.1)

No.	Atom	$x\cdot10^3$	$y\cdot10^3$	$z\cdot10^3$	B_{eq} (Å^2)
27	HC1	271 (4)	814 (3)	−281 (8)	7.0 (2.0)
28	HC2	434 (5)	849 (3)	−302 (8)	9.0 (2.0)
29	H'C2	456 (5)	812 (3)	−117 (8)	8.0 (2.0)
30	HC3	467 (3)	692 (2)	−241 (6)	4.0 (1.0)
31	H'C3	556 (4)	751 (3)	−310 (7)	6.0 (1.0)
32	HC4	462 (5)	769 (3)	−555 (8)	8.0 (2.0)
33	HC6	319 (3)	599 (2)	−492 (6)	5.0 (1.0)
34	H'C6	332 (4)	621 (3)	−313 (7)	5.0 (1.0)
35	HC7	155 (3)	692 (2)	−445 (6)	4.0 (1.0)
36	HC8	199 (4)	603 (3)	−159 (7)	6.0 (1.0)
37	HC9	140 (4)	711 (3)	−10 (7)	6.0 (1.0)
38	H'C9	131 (4)	756 (3)	−192 (7)	5.0 (1.0)
39	HC11	56 (4)	585 (3)	−468 (7)	6.0 (1.0)
40	HC12	128 (5)	493 (3)	−317 (8)	7.0 (2.0)
41	H'C12	243 (5)	507 (3)	−400 (8)	7.0 (2.0)
42	H''C12	151 (5)	473 (3)	−516 (9)	9.0 (2.0)
43	HC13	227 (5)	584 (3)	−695 (9)	9.0 (2.0)
44	H'C13	129 (5)	642 (3)	−710 (8)	8.0 (2.0)
45	H''C13	113 (4)	550 (3)	−731 (7)	6.0 (2.0)
46	HC14	498 (4)	616 (3)	−477 (8)	8.0 (2.0)
47	H'C14	584 (4)	675 (3)	−560 (7)	6.0 (2.0)
48	H''C14	481 (5)	648 (3)	−674 (8)	8.0 (2.0)
49	HC15	335 (4)	644 (3)	−2 (8)	7.0 (2.0)
50	H'C15	311 (6)	709 (4)	130 (9)	11.0 (2.0)
51	H''C15	415 (5)	714 (3)	6 (10)	11.0 (2.0)
52	HC18	−123 (4)	655 (3)	−257 (7)	6.0 (2.0)
53	HC19	−294 (4)	650 (3)	−228 (7)	6.0 (2.0)
54	HC21	−264 (6)	486 (4)	93 (9)	10.0 (2.0)
55	HC22	−91 (4)	494 (3)	64 (7)	6.0 (1.0)

Equivalent positions:

x	y	z
1/2−x	−y	1/2+z
1/2+x	1/2−y	−z
−x	1/2+y	1/2−z.

(12 mg) was added. This mixture was stirred at room temperature for 4 h. After filtration and evaporation of the reaction mixture, the residue obtained was submitted to silica gel chromatography to afford 5 mg (50%) of 4-epicurdione (**2h**) as colorless prisms. The physical properties of this compound were in accord with those of neocurdione (**4**) except for the optical rotations.

4-Epicurdione (**2h**): $C_{15}H_{24}O_2$. mp 45—47 °C. $[\alpha]_D^{24}$ +65.88° (c=3.88, $CHCl_3$). CD (c=3.88, MeOH) [θ] (nm): +36100 (259). IR ν_{max}^{KBr} cm^{-1}: 1700 (C=O), 1663 (C=C). EI-MS m/z: 236 (M^+). ^{1}H-NMR ($CDCl_3$) δ: 5.16 (1H, s, 1-H), 2.15 (1H, m, 2α-H), 2.09 (1H, m, 2β-H), 1.98 (1H, m, 3α-H), 1.76 (1H, m, 3β-H), 2.49 (1H, m, 4β-H), 2.69 (1H, dd, J=14.9, 2.7, 6β-H), 2.87 (1H, ddd, J=6.8, 2.7, 7-H), 2.88 (1H, d, J=12.5, 9α-H), 3.04 (1H, d, J=12.5, 9β-H), 1.05 (3H, d, J=7.1, 4-CH_3), 1.93 (1H, m, 11-H), 0.91 (3H, d, J=6.6, 11-CH_3), 0.97 (3H, d, J=6.6, 11-CH_3), 1.66 (3H, s, 10-CH_3).

Esterification of 8βH-Dihydro-4-epicurdione (2f) Compound **2f** (7 mg), p-BrC_6H_4COCl (30 mg) and DMAP (30 mg) were dissolved in 2 ml of pyridine. This mixture was stirred at room temperature for 2 d. After evaporation of the solvent *in vacuo*, the oil obtained was submitted to silica gel chromatography to yield 13 mg (quantitative yield, oil) of the benzoate (**2i**).

Compound **2i**: $C_{22}H_{29}O_3Br$. Oil. $[\alpha]_D^{20}$ +24.50° (c=0.53, $CHCl_3$). IR ν_{max}^{KBr} cm^{-1}: 1720 (C=O), 1700 (benzoate >C=O), 1595 (arom.). CI-MS m/z: 423, 421 (MH^+).

Transformation of 4-Epicurdione (2h) to 8αH-Dihydro-4-epicurdione (2j) $LiAlH_4$ (5 mg) in dry THF (5 ml) was added to a solution of compound 2h (50 mg) in THF (5 ml). The reaction mixture was stirred for 10 min and worked up to afford 40 mg of oil. Silica gel chromatography of this oil afforded 4 mg (8%) of **2j** as colorless prisms and 40 mg (80%) of **2g**.

Compound **2j**: $C_{15}H_{26}O_2$. mp 102—103 °C. IR ν_{max}^{KBr} cm^{-1}: 3400 (OH), 1682 (C=O). EI-MS m/z: 238 (M^+). CI-MS m/z: 239 (MH^+). HR-MS m/z: 238.1930 (Theor. 238.1928). ^{1}H-NMR ($CDCl_3$) δ: 5.07 (1H, br s, 1-H), 3.66 (1H, br s, 8α-H), 2.46 (1H, br s, 4-H), 1.76 (3H, s, 10-CH_3), 1.11 (3H, d, J=7.3, 4-CH_3), 0.83 (3H, d, J=7.1, 11-CH_3), 0.77 (3H, d, J=6.8, 11-CH_3).

Esterification of 8αH-Dihydro-4-epicurdione (2j) Compound **2j** (4 mg), p-BrC_6H_4COCl (15 mg) and DMAP (15 mg) were dissolved in 1 ml of pyridine, and the mixture was stirred overnight at room temperature. The solvent was evaporated off *in vacuo* to yield a colorless oil. This oil was submitted to silica gel chromatography. After usual work-up, 7 mg of the p-bromobenzoate (**2k**) was obtained as colorless prisms.

Compound (**2k**): $C_{29}H_{29}O_3Br$. mp 123—124 °C. $[\alpha]_D^{20}$ −11.36° (c=0.35, $CHCl_3$). IR ν_{max}^{KBr} cm^{-1}: 1718 (C=O), 1700 (benzoate C=O), 1593 (arom.). EI-MS m/z: 220 ($M^+ - BrC_6H_4COOH$). ^{1}H-NMR ($CDCl_3$) δ: 7.90 (2H, d, J=7.0, arom.-H), 7.59 (2H, d, J=6.5, arom.-H), 5.13 (2H, br s, 1-H and 8α-H), 2.63 (1H, br s, 4-H), 1.86 (3H, s, 10-CH_3), 1.15 (3H, d, J=7.3, 4-CH_3), 0.83 (3H, d, J=6.8, 11-CH_3), 0.67 (3H, d, J=6.6, 11-CH_3).

X-Ray Analysis of Compound (2k) The absolute configuration of **2k** was determined from the anomalous dispersion of CuK_α radiation by the bromine atom. The crystal data are as follows: $C_{29}H_{29}O_3Br$; M.W. = 421.4; orthorhombic; space group $P2_12_12_1$; lattice constants: a=13.569(1), b=18.887(2), c=8.382(0) Å, $\alpha=\beta=\gamma=90°$, U=2151.4 Å^3, Z=4, D_{calc}=1.289 g cm^{-3}. The intensity data of a total of 1720 reflections were collected within the 2θ angle of 156° by using graphite monochromated CuK_α radiation. The structure was determined by the heavy atom method and refined by the least-squares method as usual. The final R-value was 0.047.

Isolation of (1S,10S),(4S,5S)-Germacrone-1(10),4-diepoxide (6) Air-dried and chipped rhizomes of *Curcuma wenyujin* (875 g) were percolated with ether (4 l) at 5 °C for a week. Evaporation of the solvent *in vacuo* afforded 28.5 g, of essential oil. This oil was submitted to silica gel column chromatography with petroleum ether–ether solvent system to collect fifteen fractions. The eighth fraction (petroleum ether–ether; 5:4) was evaporated to give a residue (100 mg), which was purified by silica gel chromatography. Recrystallization of the oil from ether afforded 6 mg of (1S,10S),(4S,5S)-germacrone-1(10),4-diepoxide (**6**) as colorless needles.

(1S,10S),(4S,5S)-Germacrone-1(10),4-diepoxide (**6**): $C_{15}H_{22}O_3$. mp 84—86 °C. $[\alpha]_D^{23}$ +69.0° (c=0.51, $CHCl_3$). UV λ_{max}^{MeOH} nm (ε): 256 (1660), 315 (203). IR ν_{max}^{KBr} cm^{-1}: 1678, 1645 (enone). HR-MS m/z: 250.3524 for $C_{15}H_{20}O_3$(Theor. 250.3528). ^{1}H-NMR ($CDCl_3$, 270 MHz) δ: 3.02 (1H, d, J=11.6, 9-H), 2.94 (1H, dd, J=10.7, 1.1, 1-H), 2.88 (1H, dd, J=12.1, 1.8, 5-H), 2.67 (1H, dd, J=11.0, 2.0, 6-H), 2.66 (1H, d, J=11.6, 9-H), 2.30 (1H, dd, J=12.1, 11.0, 6-H), 2.22 (1H, m, 2-H), 2.08 (1H, m, 3-H), 1.88, 1.81 (each 3H, s, 11-CH_3), 1.46 (3H, s, 10-CH_3), 1.21 (3H, s, 4-CH_3). ^{13}C-NMR ($CDCl_3$) δ: 207.0 (C-8), 137.4 (C-11), 133.8 (C-7), 63.9 (C-5), 61.2 (C-1), 60.0 (C-4), 57.4 (C-10), 54.4 (C-9), 35.5 (C-3), 29.1 (C-6), 22.8 (C-2), 22.6 (C-12), 20.6 (C-13), 17.2 (C-15), 15.4 (C-6).

TABLE VII. Atomic Coordinates of (1R,10R)-Epoxy-(−)-1,10-dihydrocurdione (**5a**)

No.	Atom	$x\cdot10^4$	$y\cdot10^4$	$z\cdot10^4$	B_{eq} (Å^2)
1	C1	−54 (7)	−2716 (6)	−1980 (7)	4.6 (0.1)
2	C2	−325 (8)	−3575 (6)	−2830 (8)	5.3 (0.1)
3	C3	−1343 (8)	−4270 (6)	−2313 (7)	4.7 (0.1)
4	C4	−1283 (7)	−4480 (5)	−860 (7)	3.6 (0.1)
5	C5	−1792 (7)	−3578 (5)	−122 (7)	3.5 (0.1)
6	C6	−1033 (6)	−3164 (5)	980 (7)	3.6 (0.1)
7	C7	−1507 (7)	−2158 (5)	1472 (7)	3.4 (0.1)
8	C8	−1756 (7)	−1427 (5)	405 (7)	4.0 (0.1)
9	C9	−732 (7)	−1216 (5)	−610 (8)	4.4 (0.1)
10	C10	−850 (7)	−1807 (6)	−1833 (7)	4.4 (0.1)
11	C11	−566 (7)	−1725 (6)	2478 (8)	4.7 (0.1)
12	C12	−476 (9)	−2400 (7)	3645 (8)	6.5 (0.2)
13	C13	−957 (11)	−670 (7)	2870 (10)	8.3 (0.2)
14	C14	−2089 (9)	−5368 (6)	−515 (9)	6.1 (0.2)
15	C15	−2026 (9)	−1643 (6)	−2629 (9)	6.1 (0.2)
16	O1	−2821 (4)	−3230 (4)	−389 (5)	4.4 (0.1)
17	O2	−2742 (5)	−955 (4)	374 (5)	5.5 (0.1)
18	O3	324 (5)	−1785 (4)	−2571 (6)	5.9 (0.1)

No.	Atom	$x\cdot10^3$	$y\cdot10^3$	$z\cdot10^3$	B_{eq} (Å^2)
19	HC1	66 (6)	−285 (4)	−129 (6)	5.0 (2.0)
20	HC2	70 (9)	−396 (6)	−303 (8)	12.0 (3.0)
21	H'C2	−60 (9)	−328 (7)	−382 (9)	13.0 (3.0)
22	HC3	−227 (6)	−405 (5)	−254 (6)	6.0 (2.0)
23	H'C3	−130 (6)	−488 (4)	−273 (6)	5.0 (2.0)
24	HC4	−38 (5)	−466 (4)	−59 (5)	4.0 (1.0)
25	HC6	−2 (6)	−315 (5)	68 (6)	6.0 (2.0)
26	H'C6	−103 (6)	−371 (5)	172 (6)	5.0 (2.0)
27	HC7	−243 (5)	−235 (4)	194 (5)	3.0 (1.0)
28	HC9	13 (6)	−122 (4)	−17 (5)	4.0 (1.0)
29	H'C9	−85 (7)	−41 (5)	−85 (7)	8.0 (2.0)
30	HC11	59 (7)	−171 (6)	217 (7)	8.0 (2.0)
31	HC12	17 (8)	−205 (6)	441 (7)	10.0 (2.0)
32	H'C12	−13 (6)	−301 (5)	368 (6)	7.0 (2.0)
33	H''C12	−130 (6)	−232 (5)	401 (7)	5.0 (2.0)
34	HC13	−116 (8)	−21 (7)	222 (9)	10.0 (3.0)
35	H'C13	−43 (8)	−35 (6)	371 (8)	12.0 (3.0)
36	H''C13	−192 (8)	−88 (6)	336 (7)	9.0 (2.0)
37	HC14	−300 (8)	−515 (6)	−114 (8)	9.0 (2.0)
38	H'C14	−194 (8)	−558 (5)	27 (7)	9.0 (2.0)
39	H''C14	−168 (8)	−604 (6)	−82 (8)	10.0 (3.0)
40	HC15	−288 (8)	−177 (6)	−219 (7)	9.0 (2.0)
41	H'C15	−198 (8)	−203 (6)	−358 (8)	12.0 (3.0)
42	H''C15	−193 (7)	−89 (5)	−298 (7)	8.0 (2.0)

Equivalent positions:

x	y	z
1/2−x	−y	1/2+z
1/2+x	1/2−y	−z
−x	1/2+y	1/2−z.

Synthesis of (1S,10S),(4S,5S)-Germacrone-1(10),4-diepoxide (6) and (1S,10S),(4S,5S),(7ξ,11ξ)-(−)-1(10),4,7(11)-Triepoxide (7) from (4S,5S)-Germacrone-4,5-epoxide (5c) A mixture of (4S,5S)-germacrone-4,5-epoxide (**5c**) (500 mg) isolated from *C. wenyujin* and MCPBA (400 mg) in 4 ml of CH_2Cl_2 was stirred at room temperature for 24 h. The reaction mixture was washed twice with saturated Na_2SO_4. The organic layer was concentrated under reduced pressure, and the residue was subjected to a column chromatography over silica gel with a gradient solvent of petroleum ether and ether to afford 450 mg of **2a** (86%) and 20 mg of (1S,10S),(4S,5S),(7ξ,11ξ)-(−)-1(10),4,7(11)-triepoxide (**7**) (4%). **7**: $C_{15}H_{22}O_4$. mp 138—140 °C. $[\alpha]_D^{20}$ +228° (c=0.90, $CHCl_3$). IR ν_{max}^{KBr} cm^{-1}: 1705 (C=O). CI-MS m/z: 267 (MH^+). EI-MS m/z: 266 (M^+). HR-MS m/z: 266.3595 for $C_{15}H_{22}O_4$ (Theor. 266.3522). ^{1}H-NMR ($CDCl_3$, 270 MHz) δ: 3.07 (1H, d, J=9.9), 3.04 (1H, d, J=10.6), 3.00 (1H, dd, J=10.3, 0.7), 2.43 (1H, d, J=10.6), 2.25—2.15 (2H, m), 2.10 (1H, dd,

J=13.9, 1.1), 1.98 (1H, dd, J=13.9, 2.0), 1.44, 1.42, 1.19, 1.14 (each 3H, s), 1.28—1.35 (2H, m).

Acknowledgements The authors are grateful to Dr. Moroi and Mr. Hirota of Daiichi Pharmaceutical Co., Ltd. and to Dr. Akita of the Physical and Chemical Institute for Measurements of 400 MHz NMR spectra. Our thanks are due to Miss S. Takei, Mr. H. Yamanaka and Mr. M. Nakamura, Joint Laboratory of the School of Medicine, Keio University, for UV, IR and MS measurements, respectively.

References and Notes

1) Visiting Research Associate of Keio University on leave from Dalian Institute of Medicinal and Pharmaceutical Sciences.
2) H.-J. Fang, J.-G. Yu, Y.-H. Chen and Q. Hu, *Acta Pharmaceutica Sinica*, **17**, 441 (1982).
3) H.-X. Xu, *Zhong Cao Yao Tong Xun*, **10**, 433 (1979).
4) *a*) H. Hikino, K. Meguro, Y. Sakurai and T. Takemoto, *Chem. Pharm. Bull.*, **27**, 275 (1979); *b*) S. Inayama, J.-F. Gao, K. Harimaya, T. Kawamata, Y. Iitaka and Y.-T. Guo, *ibid.*, **32**, 3783 (1984).
5) *a*) H. Hikino, K. Meguro, Y. Sakurai and T. Takemoto, *Chem. Pharm. Bull.*, **14**, 1341 (1966); *b*) S. Inayama, J.-F. Gao, K. Harimaya, Y. Iitaka, Y.-T. Guo and T. Kawamata, *ibid.*, **33**, 1323 (1985).
6) *a*) S. Inayama, J.-F. Gao, K. Harimaya, M. Hikichi, Y. Iitaka, Y.-T. Guo and T. Kawamata, *Chem. Pharm. Bull.*, **33**, 2179 (1985); *b*) J.-F. Gao, T. Ohkura, K. Harimaya, M. Hikichi, T. Kawamata, X.-Y. Wu, Y. Iitaka and S. Inayama, *ibid.*, **34**, 5122 (1986).
7) H. Hikino, Y. Sakurai, S. Takahashi and T. Takemoto, *Chem. Pharm. Bull.*, **15**, 1390 (1967).
8) *a*) T. Ohkura, J.-F. Gao, T. Nishishita, K. Harimaya, T. Kawamata and S. Inayama, *Shoyakugaku Zasshi*, **41**, 102 (1987); *b*) T. Ohkura, J-F. Gao, J.-H. Xie and S. Inayama, *ibid.*, **44**, 171 (1990).
9) J.-F. Gao, J.-H. Xie, Y. Iitaka and S. Inayama, *Shoyakugaku Zasshi*, **42**, 347 (1988).
10) T. Ohkura, J.-F. Gao, K. Harimaya and S. Inayama, *Shoyakugaku Zasshi*, submitted (1991).
11) *a*) T. Ohkura, J.-F. Gao, K. Harimaya, M. Hikichi, T. Kawamata, Y. Iitaka, X.-Y. Wu, T. Nishishita and S. Inayama, *Shoyakugaku Zasshi*, **40**, 352 (1986); *b*) T. Ohkura, J.-F. Gao, K. Harimaya, M. Hikichi, Y. Iitaka, T. Kawamata, M. Kuroyanagi, S. Fukushima and S. Inayama, *Chem. Pharm. Bull.*, **34**, 4435 (1986).
12) *a*) J.-F. Gao, J.-H. Xie, Y. Iitaka and S. Inayama, *Chem. Pharm. Bull.*, **37**, 233 (1989); *b*) J.-F. Gao, J.-H. Xie, K. Harimaya, T. Kawamata, Y. Iitaka and S. Inayama, *ibid.*, **39**, 854 (1991).
13) *a*) M. Yoshibara, H. Shibuya, E. Kitano, K. Yanagi and Y. Kitagawa, *Chem. Pharm. Bull.*, **32**, 2058 (1984); *b*) M. Kuroyanagi, A. Ueno, K. Ujiie and S. Sata, *ibid.*, **35**, 53 (1987). Note: (4*S*,5*S*)-germacrane-4,5-epoxide (**5c**) in ref. 15 should be better designated as (4*S*,5*S*)-germacrone-4-epoxide for comparison with compounds, *e.g.* (1*S*,-10*S*),(4*S*,5*S*)-germacrone-1(10),4-diepoxide-1(10),4-diepoxide (**6**) and (1*S*,10*S*),(4*S*,5*S*),(7ξ,11ξ)-germacrone-1(10),4,7(11)-triepoxide (**7**), in this paper.
14) See Note **10** in ref. 6*a* and ref. 14*c* in ref. 8*a* [Y. Shiobara, T. Iwata, M. Kodama, Y. Asakawa, T. Takemoto and Y. Fukazawa, *Tetrahedron Lett.*, **26**, 913 (1985)].
15) K. Harimaya, T. Ohkura, J.-F. Gao, Y. Iitaka, E. Osawa and S. Inayama, *Chem. Pharm. Bull.*, **35**, 3866 (1987).
16) *a*) J. Endo and M. Nagasawa, *Yakugaku Zasshi*, **94**, 1574 (1974); *b*) J. Endo, M. Nagasawa, H. Itogawa and Y. Iitaka, *Chem. Pharm. Bull.*, **27**, 275 (1979).

The Absolute Structure and Synthesis of Wenjine Isolated from *Curcuma wenyujin*

Ji-Fu GAO,[a,1)] Ji-Hong XIE,[a] Kenzo HARIMAYA,[a] Takeshi KAWAMATA,[a] Yoichi IITAKA[b] and Seiichi INAYAMA*,[a]

Pharmaceutical Institute, School of Medicine, Keio University,[a] 35 Shinanomachi, Shinjuku-ku, Tokyo 160, Japan and Department of Biological Sciences, Nishi-Tokyo Science University,[b] Uenohara-cho, Yamanashi 409-01, Japan. *Received August 8, 1990*

A novel highly oxygenated sesquiterpenoid named wenjine (1) was isolated from *Curcuma wenyujin*. The relative structure was established on the basis of spectroscopic data and X-ray analysis. The absolute structure of 1 was determined by photooxygenation of (+)-(1*S*,10*S*),(4*S*,5*S*)-germacrone-1(10),4-diepoxide (2).

Keywords wenjine; *Curcuma wenyujin*; Zingiberaceae; sesquiterpene; germacrone diepoxide; photooxidation; hemiacetal dioxalone

In our continuing study of bioactive constituents of *Curcuma wenyujin* (Zingiberaceae), seven sesquiterpenes, curcumol,[2)] curdione,[3,4a)] curcumalactone,[4)] (1*R*,10*R*)-(−)-1,10-dihydrocurione,[5)] neocurdione,[6)] (1*S*,10*S*),(4*S*,5*S*)-germacrone-1(10),4-diepoxide (**2**),[7)] and (4*S*,5*S*)-(+)-germacrone-4,5-epoxide (**3**),[7,8)] have been isolated from the essential oil[9)] of the rhizome. In this paper, we wish to describe the absolute structure of a new sesquiterpene dioxalane hemiacetal named wenjine (**1**) and chemical correlations of the monoepoxide (**3**) and diepoxide (**2**).[7,8)]

Air-dried chipped rhizomes of *C. wenyujin* were percolated with ether at 5 °C for a week. Evaporation of the solvent afforded an essential oil. This oil was submitted to silica gel chromatography with petroleum ether and ether solvent system. The fractions eluted with petroleum ether–ether (5:4) afforded (1*S*,10*S*),(4*S*,5*S*)-germacrone-1(10),4-diepoxide (**2**). The 5:6 fractions were collected and evaporated to dryness to yield an oily substance. This oil was submitted to silica gel chromatography (petroleum ether–ether; 5:1) to yield a crystalline material. Recrystallization from methanol–chloroform (1:1) afforded wenjine (**1**) as colorless prisms.

Wenjine (**1**), mp 230—231 °C, $[\alpha]_D$ +54.3° (c=0.37, dimethylformamide (DMF)), has the same protons and carbons as the diepoxide **2**, as deduced from the nuclear magnetic resonance (NMR) studies. Comparison of the ^{1}H- and ^{13}C-NMR data of **1** with those of **2**[10)] is informative. The ^{1}H-NMR methyl singlet signals of **2** at δ 1.88 and 1.81 due to the isopropylidene group are shifted to higher field in the spectrum of **1**. Another signal appeared at lower field at δ 5.26 and this signal is coupled with the H_5 proton in the spectrum of **1**. The ^{13}C-NMR signal of **1** at δ 156.5 appears instead of that at δ 29.1 due to the C(6) allylic methylene in the spectrum of **2**. In addition, the signal of **2** at δ 207.0 due to the C(8) ketone moved to δ 156.5 in the spectrum of **1**. The olefinic C(11) signal of **2** at δ 137.4 shifted to higher field at δ 86.7 (allyl alcoholic carbon) in the spectrum of **1**.

Based on the above data, one can deduce that **1** probably has an oxirane moiety and a 6,7-*endo* double bond, providing that the C(8) ketone and a hydroxyl group at C(11) are condensed, instead of the 7,11-*exo* double bond in **2**.

Dreiding models showed that, while the C(8) ketone is difficult to condense with a C(11)-hydroxyl group to form a hemiacetal oxetene, a C(11)-hydroperoxyl group seems to be better suited for forming a 1,2-dioxalane.

A direct X-ray analysis of **1** was carried out in order to determine its relative stereostructure, which was established to be as shown in Fig. 1. The ten-membered ring in **1** is fused in *trans*-relationship with two oxirane moieties at

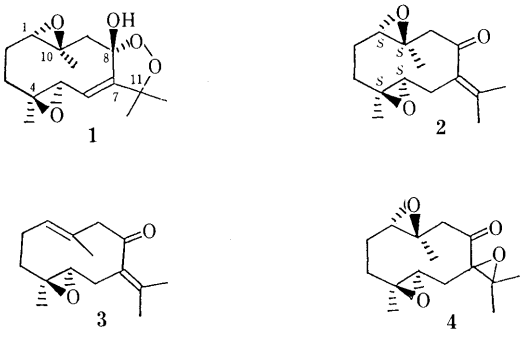

Chart 1

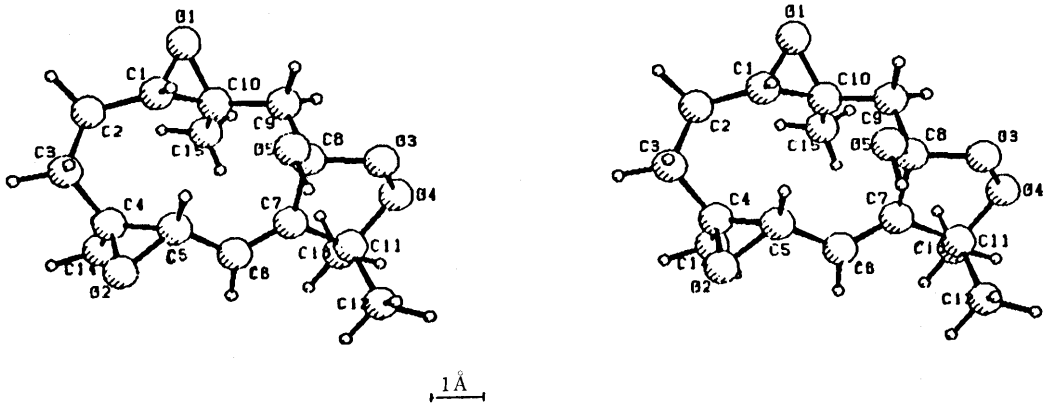

Fig. 1. Stereoview of Wenjine (**1**)

C(1)–C(10) and C(4)–C(5), and a hemiacetal 1,2-dioxalane is attached at the C(7) and C(8) positions. Wenjine (**1**) has a relatively stable diepoxy peroxyhemiacetal moiety, which seems to be rare in nature.

In order to estimate the absolute configuration, stereospecific transformation of (4*S*,5*S*)-(+)-germacrone-4,5-epoxide (**3**)[8] to **1** was undertaken.

Oxidation of **3** with *m*-chloroperbenzoic acid (MCPBA) provided (1*S*,10*S*),(4*S*,5*S*)-germacrone-1(10),4-diepoxide (**2**) in 86% yield accompanied with a trace amount of germacrone-1(10),4,7(11)-triepoxide (**4**). Compound **4** has the molecular formula $C_{15}H_{22}O_4$. The triepoxide structure of **4** was supported by the comparison of the ^{1}H-NMR data of **4** with those of the diepoxide (**2**). Photo-oxidation of **2** using rose bengal or hematoporphyrin as a photosensitizer gave **1** in 25% yield under controlled conditions.[10]

The synthetic wenjine shows the same physical and spectral properties as those of the natural product isolated from *C. wenyujin*.[7] Thus, the absolute configuration of **1** was unequivocally established to be (1*S*,4*S*,5*S*,8*S*,10*S*).

Experimental

Melting points were determined on a Buchi melting point apparatus and are uncorrected. Optical rotations were measured with a JASCO DIP-360 spectrometer. Infrared (IR) spectra were recorded on a Hitachi EPI-G3 spectrophotometer. Mass spectra (MS) were obtained on a JEOL LMS-D300 spectrometer. ^{1}H- and ^{13}C-NMR spectra were measured with a JEOL GS-270 using tetramethylsilane as an internal standard unless otherwise stated. The coupling patterns are indicated as follows: singlet = s, doublet = d, triplet = t, quartet = q, multiplet = m, and broad = br. The coupling constant J values are expressed in hertz (Hz).

Isolation of Wenjine (1) Air-dried and cut rhizomes of *Curcuma wenyujin* (875 g) were percolated with ether (4 l) at 5 °C for a week. Evaporation of the solvent *in vacuo* afforded 28.5 g of the ether extract as an oil. This oil was submitted to silica gel column chromatography with a petroleum ether–ether solvent system, and fifteen fractions were collected. The eighth fraction (petroleum ether–ether; 5 : 4) was evaporated. The residue obtained (100 mg) was purified by silica gel chromatography. Recrystallization of the oil from ether afforded 6 mg of (1*S*,10*S*),(4*S*,5*S*)-germacrone-1(10),4-diepoxide (**2**) (0.0016%) as colorless needles. The twelfth fraction (petroleum ether–ether; 5 : 6) was evaporated *in vacuo* to yield 150 mg of residue. This material was submitted to repeated silica gel chromatography and the fractions eluted with petroleum ether–ether (10 : 2) were collected. Evaporation of these fractions yielded a crystalline material. This product was recrystallized from methanol–chloroform (1 : 1) to afford 8 mg (0.001%) of wenjine (**1**) as colorless prisms.

Wenjine (**1**): Colorless prisms; mp 230—231 °C (dec.). $[\alpha]_D^{22}$ +54.3° (c = 0.37, DMF). IR ν_{max}^{KBr} cm^{-1}: 3425, 3330 (OH). EI-MS m/z: 264 ($M^+ - H_2O$). ^{1}H-NMR ($CDCl_3$, 400 MHz) δ: 5.26 (1H, d, J = 8.2, H_6), 4.08 (1H, d, J = 8.3, H_5), 3.26 (1H, br s, –OH), 3.15 (1H, d, J = 10.4, H_1), 2.74 (1H, d, J = 15.0, H_9), 1.46, 1.43, 1.35, 1.30 (each 3H, s, $C_{11}(CH_3)_2$, C_4-CH_3, C_{10}-CH_3), 1.41—1.43 (2H, m, H_2, H_3). ^{13}C-NMR ($CDCl_3$) δ: 156.5 (C_8), 120.8 (C_2), 106.9 (C_3), 86.7 (C_4), 62.5 (C_5), 62.0 (C_6), 59.1 (C_7), 59.0 (C_5), 50.6 (C_9), 36.7 (C_{10}), 26.5 (C_{11}), 25.2 (C_{13}), 20.4 (C_{14}), 16.8 (C_{15}).

(1*S*,10*S*),(4*S*,5*S*)-Germacrone-1(10),4-diepoxide (**2**): Colorless needles. mp 84—86 °C. $[\alpha]_D^{23}$ +69° (c = 0.51, $CHCl_3$). UV λ_{max}^{MeOH} nm (ε): 256 (1660), 315 (203). IR ν_{max}^{KBr} cm^{-1}: 1678, 1645 (enone). CD [θ] (nm): +41900 (250), −7400 (325), −7800 (332), HR-MS m/z: 250.3524 for $C_{15}H_{22}O_3$ (Theor. 250.3528). ^{1}H-NMR ($CDCl_3$, 270 MHz) δ: 3.02 (1H, d, J = 11.6, H_9), 2.94 (1H, dd, J = 10.7, 1.1, H_1), 2.88 (1H, dd, J = 12.1, 1.8, H_5), 2.67 (1H, dd, J = 11.0, 2.0, H_6), 2.66 (1H, d, J = 11.6, H_9), 2.30 (1H, dd, J = 12.1, 11.0, H_6), 2.22 (1H, m, H_2), 2.08 (1H, m, H_3), 1.88 and 1.81 (each 3H, s, H_{12}, H_{13}), 1.46 (3H, s, H_{15}), 1.21 (3H, s, H_{14}).

X-Ray Analysis of Wenjine (1) The relative structure of wenjine (**1**) was determined by X-ray analysis. The crystal data were as follows: $C_{15}H_{22}O_5$: M.W. = 282.3; orthorhombic; space group $P2_12_12_1$; lattice constants a = 11.542(6), b = 14.305(9), c = 8.759(2) Å, $\alpha = \beta = \gamma = 90°$, U = 1446 Å^3, Z = 4, D_{calc} = 1.296 g cm^{-3}. The intensity data were collected on a Philips PW 1100 diffractometer using graphite monochromated CuK_α radiation. We used 1391 reflections up to 155° (2θ). The structure was solved by the MULTAN program and refined by the least-squares method with the block-diagonal matrix approximation. The final R value was 0.050 including 22 hydrogen atoms with isotropic temperature factors.

TABLE I. Atomic Coordinates and Equivalent Isotropic Temperature Factors of Wenjine (**1**)

No.	Atom	$x \cdot 10^4$	$y \cdot 10^4$	$z \cdot 10^4$	B_{eq} (Å^2)
1	C1	6474 (3)	7324 (2)	−2464 (5)	3.8 (0.1)
2	C2	6822 (4)	7580 (3)	−4038 (5)	4.3 (0.1)
3	C3	7485 (4)	8515 (3)	−4119 (5)	3.9 (0.1)
4	C4	6751 (3)	9305 (3)	−3512 (4)	3.2 (0.1)
5	C5	6696 (3)	9393 (2)	−1831 (4)	2.8 (0.0)
6	C6	5673 (3)	9755 (2)	−1009 (4)	2.7 (0.0)
7	C7	5140 (3)	9281 (2)	84 (4)	2.5 (0.0)
8	C8	5501 (3)	8348 (3)	765 (4)	3.3 (0.1)
9	C9	5130 (4)	7459 (3)	−86 (5)	3.9 (0.1)
10	C10	5284 (3)	7414 (2)	−1791 (5)	3.3 (0.1)
11	C11	4089 (3)	9618 (3)	958 (4)	3.4 (0.1)
12	C12	4327 (4)	10511 (3)	1834 (5)	4.9 (0.1)
13	C13	3000 (4)	9691 (4)	6 (6)	5.1 (0.1)
14	C14	5810 (4)	9662 (3)	−4521 (4)	4.0 (0.1)
15	C15	4283 (3)	7767 (3)	−2733 (5)	4.4 (0.1)
16	O1	5727 (3)	6510 (2)	−2308 (4)	5.0 (0.1)
17	O2	7391 (2)	10048 (2)	−2725 (3)	3.7 (0.0)
18	O3	4936 (3)	8381 (2)	2245 (4)	5.5 (0.1)
19	O4	3865 (3)	8843 (2)	1982 (4)	5.7 (0.1)
20	O5	6676 (2)	8268 (2)	1122 (3)	4.2 (0.0)

No.	Atom	$x \cdot 10^3$	$y \cdot 10^3$	$z \cdot 10^3$	B_{eq} (Å^2)
21	HC1	719 (4)	733 (3)	−158 (5)	6.0 (1.0)
22	HC2	735 (4)	705 (3)	−462 (5)	6.0 (1.0)
23	H′C2	620 (3)	761 (2)	−475 (4)	3.0 (1.0)
24	HC3	778 (3)	866 (3)	−529 (4)	4.0 (1.0)
25	H′C3	824 (3)	847 (3)	−341 (4)	5.0 (1.0)
26	HC5	719 (3)	894 (2)	−120 (4)	2.0 (1.0)
27	HC6	535 (3)	1039 (2)	−132 (4)	4.0 (1.0)
28	HC9	555 (4)	696 (3)	46 (5)	6.0 (1.0)
29	H′C9	429 (4)	734 (3)	22 (6)	7.0 (1.0)
30	HC12	500 (4)	1049 (3)	261 (6)	7.0 (1.0)
31	H′C12	442 (3)	1106 (3)	101 (5)	5.0 (1.0)
32	H″C12	364 (4)	1071 (3)	268 (6)	8.0 (1.0)
33	HC13	237 (4)	985 (3)	71 (5)	7.0 (1.0)
34	H′C13	301 (4)	1024 (3)	−81 (6)	8.0 (1.0)
35	H″C13	283 (4)	909 (3)	−60 (5)	6.0 (1.0)
36	HC14	526 (4)	917 (3)	−506 (5)	6.0 (1.0)
37	H′C14	542 (4)	1010 (3)	−416 (5)	6.0 (1.0)
38	H″C14	615 (4)	990 (3)	−558 (5)	8.0 (1.0)
39	HC15	408 (4)	837 (3)	−248 (5)	6.0 (1.0)
40	H′C15	432 (4)	770 (3)	−393 (5)	6.0 (1.0)
41	H″C15	363 (4)	746 (3)	−249 (5)	6.0 (1.0)
42	HO5	687 (5)	887 (4)	161 (6)	10.0 (2.0)

Equivalent positions:

x	y	z
1/2−x	−y	1/2+z
1/2+x	1/2−y	−z
−x	1/2+y	1/2−z.

Synthesis of (1*S*,10*S*),(4*S*,5*S*)-Germacrone-1(10),4-diepoxide (2) and (1*S*,10*S*),(4*S*,5*S*),(7ξ,11ξ)-(−)-1(10),4,7(11)-Triepoxide (4) from (4*S*,5*S*)-(+)-Germacrone-4-epoxide (3) A mixture of (4*S*,5*S*)-(+)-germacrone-4,5-epoxide (**3**) (500 mg) isolated from *C. wenyujin*,[7] and MCPBA (400 mg) in 4 ml of CH_2Cl_2 was stirred at room temperature for 24 h. The reaction mixture was washed twice with saturated Na_2SO_4. The organic layer was concentrated under reduced pressure and the residue was subjected to column chromatography over silica gel with a gradient system of petroleum ether and ether to afford 450 mg of **2** (86%) and 20 mg of **4** (4%). **4**: $C_{15}H_{22}O_4$: colorless powder. mp 138—140 °C; $[\alpha]_D^{20}$ +228° (c = 0.90, $CHCl_3$). IR ν_{max}^{KBr} cm^{-1}: 1705 (C=O). CI-MS m/z: 267 (MH^+). EI-MS m/z: 266 (M^+). HR-MS m/z: 266.3595 for $C_{15}H_{22}O_4$ (Theor. 266.3522). ^{1}H-NMR ($CDCl_3$, 270 MHz) δ: 3.07 (1H, d, J = 9.9), 3.04 (1H,

d, $J=10.6$), 3.00 (1H, dd, $J=10.3$, 0.7), 2.43 (1H, d, $J=10.6$), 2.25—2.15 (2H, m), 2.10 (1H, dd, $J=13.9$, 1.1), 1.98 (1H, dd, $J=13.9$, 2.0), 1.44, 1.42, 1.19, 1.14 (each 3H, s), 1.28—1.35 (2H, m).

Synthesis of Wenjine (1) from (1*S*,10*S*),(4*S*,5*S*)-Germacrone-1(10),4-diepoxide (2) A solution of **2** (15 mg) and rose bengal (1 mg) in EtOH (12 ml) was irradiated with a bank of tungsten lamps (200 W × 3) under bubbling with oxygen for 70 h. The reaction mixture was concentrated under reduced pressure, and the residue was subjected to silica gel column chromatography, wherein was obtained 4 mg (25%) of wenjine (**1**). When hematoporphyrin was used as the sensitizer, the photooxygenation for only 10 h afforded 4 mg (25%) of **1**, mp 230—231 °C.[10] Irradiation for one week was required to provide the same yield of **1** when eosine was used. **1**: ^{13}C-NMR ($CDCl_3$) δ: 207.0 (C_8), 137.4 (C_{11}), 133.8 (C_7), 63.9 (C_4), 61.2 (C_1), 60.0 (C_4), 57.4 (C_{10}), 54.4 (C_9), 35.5 (C_3), 29.1 (C_6), 22.8 (C_2), 22.6 (C_{12}), 20.6 (C_{13}), 17.2 (C_{15}), 15.4 (C_6).

(±)-Wenjine from (±)-Germacrone-1(10),4-epoxide (±)-Germacrone-1(10),4-epoxide (15 mg) was photooxygenated according to the same procedure as described above for the synthesis of wenjine (**1**), giving 3 mg (17%) of (±)-wenjine. mp 244—246 °C.

Acknowledgement The authors are grateful to Dr. R. Moroi and Mr. Hirota of Daiichi Pharmaceutical Co., Ltd., and to Dr. H. Akita of the Physical and Chemical Institute for 400 MHz NMR spectral measurements. Thanks are also due to Miss S. Takei, Mr. H. Yamanaka and Mr. M. Nakamura, Joint Laboratory of the School of Medicine, Keio University, for MS and IR measurements, respectively.

References and Notes

1) Visiting Research Associate of Keio University on leave from Dalian Institute of Medicinal and Pharmaceutical Sciences, China.
2) S. Inayama, J.-F. Gao, K. Harimaya, T. Kawamata, Y. Iitaka and Y.-T. Guo, *Chem. Pharm. Bull.*, **32**, 3783 (1984).
3) S. Inayama, J.-F. Gao, K. Harimaya, Y. Iitaka, Y.-T. Guo and T. Kawamata, *Chem. Pharm. Bull.*, **33**, 1323 (1985).
4) *a*) S. Inayama, J.-F. Gao, K. Harimaya, M. Hikichi, Y. Iitaka, Y.-T. Guo and T. Kawamata, *Chem. Pharm. Bull.*, **33**, 2179 (1985); *b*) J.-F. Gao, T. Ohkura, K. Harimaya, M. Hikichi, T. Kawamata, X.-Y. Wu, Y. Iitaka and S. Inayama, *ibid.*, **34**, 5122 (1986).
5) J.-F. Gao, J.-H. Xie, Y. Iitaka and S. Inayama, *Shoyakugaku Zasshi*, **42**, 347 (1988).
6) *a*) T. Ohkura, J.-F. Gao, K. Harimaya, M. Hikichi, T. Kawamata, Y. Iitaka, X.-Y. Wu, T. Nishishita and S. Inayama, *Shoyakugaku Zasshi*, **40**, 352 (1986); *b*) T. Ohkura, J.-F. Gao, K. Harimaya, M. Hikichi, Y. Iitaka, T. Kawamata, M. Kuroyanagi, S. Fukushima and S. Inayama, *Chem. Pharm. Bull.*, **34**, 4435 (1986).
7) *a*) J.-F. Gao, J.-H. Xie, Y. Iitaka and S. Inayama, *Chem. Pharm. Bull.*, **37**, 233 (1989); *b*) K. Harimaya, J.-F. Gao, T. Ohkura, T. Kawamata, Y. Iitaka, Y.-T. Guo and S. Inayama, *ibid.*, **39**, 843 (1991).
8) *a*) M. Yoshihara, H. Shibuya, E. Kitano, K. Yanagi and I. Kitagawa, *Chem. Pharm. Bull.*, **32**, 2059 (1984); *b*) (4*S*,5*S*)-Germacrane-4,5-epoxide (**3**) in their paper would be better designated as (4*S*,5*S*)-germacrone-4-epoxide for comparison with compounds, *e.g.* (1*S*,10*S*),(4*S*,5*S*)-germacrone-1(10),4-diepoxide (**2**) and (1*S*,10*S*),-(4*S*,5*S*),(7ξ,11ξ)-germacrone-1(10),4,7(11)-triepoxide (**4**), in this paper.
9) *a*) T. Okura, J.-F. Gao, T. Nishishita, K. Harimaya, T. Kawamata and S. Inayama, *Shoyakugaku Zasshi*, **41**, 102 (1987); *b*) T. Ohkura, J.-F. Gao, J.-H. Xie and S. Inayama, *ibid.*, **44**, 171 (1990).
10) The photosensitized reaction of **2** (32 mg) using hematoporphyrin (1 mg) was conducted for 40 h to afford 9-hydroxygermacrone-1(10),4-diepoxide (**5**) (5 mg, 5%) together with **1** (2 mg, 6%). **5**: $C_{15}H_{22}O_5$. mp 179—180 °C. $[\alpha]_D^{20}$ +5.98° ($c=1.00$, $CHCl_3$). IR ν_{max}^{KBr} (cm^{-1}): 3435 (OH), 1682, 1632 (enone). CI-MS *m/z*: 276 (M^+-O). ^{1}H-NMR ($CDCl_3$, 270 MHz) δ: 3.73 (1H, s), 3.18 (1H, dt, $J=10.6$, 2.6), 3.08 (1H, dd, $J=13.6$, 1.8), 3.07 (1H, dd, $J=9.2$, 1.8), 2.33 (1H, d, $J=2.5$), 2.28 (1H, dq, $J=5.9$, 2.9), 2.08 (1H, dd, $J=2.0$).

Synthetic Anthracyclines: Total Synthesis of D-Ring Pyridine and Pyrazine Analogues of 11-Deoxydaunomycin

Yasuyuki KITA,*[,a] Masayuki KIRIHARA,[a] Yuji FUJII,[a] Ryuichi OKUNAKA,[a] Shuji AKAI,[a] Hiroshi MAEDA,[a] Yasumitsu TAMURA,[a] Kin-o SHIMOOKA,[b] Hirofumi OHISHI,[c] and Toshimasa ISHIDA[c]

Faculty of Pharmaceutical Sciences, Osaka University,[a] 1–6, Yamada-oka, Suita, Osaka 565, Japan, New Product Development Center, Pfizer Pharmaceutical Inc., Ltd.,[b] 5-gochi, Taketoyo-cho, Chita-gun, Aichi 470–23, Japan, and Osaka University of Pharmaceutical Sciences,[c] 2–10–65, Kawai, Matsubara, Osaka 580, Japan. *Received August 30, 1990*

Treatment of sodium salts generated from tetrahydrohomophthalic anhydrides (6a, b) with 5,8-dihydro-5,8-dioxoquinoline (9) gave cycloadducts (7 and 8), regioselectively. These adducts were converted to the D-ring pyridine analogue (21) of 11-deoxydaunomycin. The D-ring pyrazine analogue (27) of 11-deoxydaunomycin was also prepared by a similar method.

Keywords 11-deoxydaunomycin analogue; heteroanthracycline; azatetrahydronaphthacene; cycloaddition; antitumor agent

The anthracycline antibiotics such as daunomycin (**1a**) and adriamycin (**1b**) are powerful antitumor agents used to treat a wide range of human cancers.[1,2] However, their severe cardiotoxicity often presents a serious problem.[3] The cardiotoxicity may in part be explained by the easy one-electron reduction of these agents to the corresponding radical anion, which is able to react with oxygen to afford reactive oxygen species such as $O_2^{\cdot-}$, H_2O_2, and $OH^{\cdot}$.[4] The C-ring quinone moiety of anthracyclines plays an important role in this redox reaction, and some C-ring modified anthracyclines show antitumor activity with low cardiotoxicity.[5] Modification of the redox potential may be of importance to obtain more information about the structure–activity relationships. The B and/or D-ring modification of the chromophore is also known to influence the C-ring quinone moiety.[6,7] As part of our continuing studies on synthetic anthracyclines, we have recently reported a total synthesis of the D-ring indole[8] and thiophene[9] analogues of **1a**, which showed inhibitory activity against L-1210 cell growth (*in vitro*) comparable to that of **1a**. Furthermore, 11-deoxyanthracyclines such as 11-deoxydaunomycin (**2a**),[7a] 4-demethoxy-11-deoxydaunomycin (**2b**),[7b] and aclacinomycin A (**3**)[7c] show stronger antitumor activity and/or weaker cardiotoxicity than ordinary agents (**1**). We have already succeeded in the total synthesis of **2a**, **2b**, and their analogues.[10]

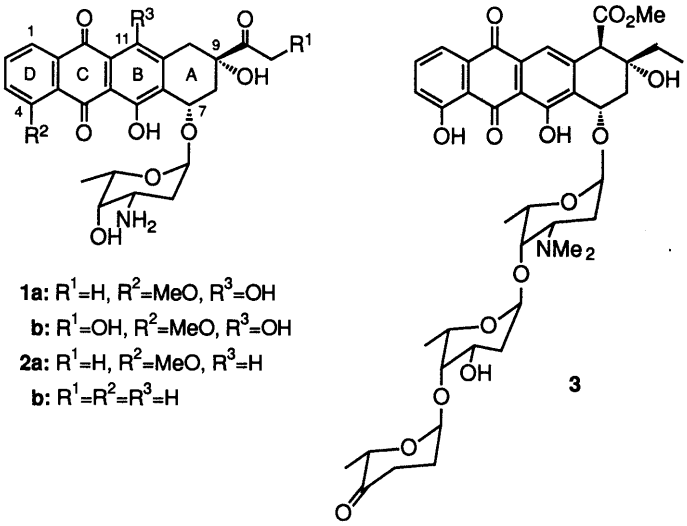

Fig. 1

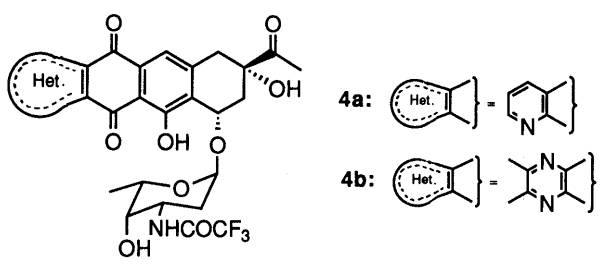

Fig. 2

Therefore, our attention has been focused on the synthesis of D-ring hetero analogues of 11-deoxydaunomycin (**4**). We have briefly reported an effective total synthesis of the D-ring pyridine analogue of 11-deoxydaunomycin.[11] We now report in detail the total synthesis of D-ring pyridine and pyrazine analogues of 11-deoxydaunomycin.

We first investigated an effective synthesis of the pivotal intermediates (**7**, **8**) for the D-ring pyridine analogue (**4a**), since 11-deoxydaunomycin could be synthesized from similar key intermediates.[10] However, attempted cycloaddition of tetrahydrohomophthalic anhydrides (**6a**, **b**)[10] to 7-halo-5,8-dihydro-5,8-dioxoquinolines (**5a**, **b**)[12] in the presence of sodium hydride failed to afford the tetracyclic compounds (**7**, **8**), probably owing to the instability of the quinones (**5a**, **b**) under the strongly basic conditions employed. Next, we used the unsubstituted quinone (**9**),[13] which is stable under basic conditions, instead of **5**. Treatment of the sodium salt generated from tetrahydrohomophthalic anhydride (**6a**) and 1.1 eq of sodium hydride in tetrahydrofuran (THF) with 5,8-dihydro-5,8-dioxoquinoline (**9**) at room temperature gave a single cycloadduct (**7** or **7'**) in 62% yield, regioselectively (Chart 1).

It was difficult to establish that the structure of the adduct is **7** [not the regioisomer (**7'**)] from the normal spectral data. This problem could be resolved by application of the long-range selective proton decoupling (LSPD) technique and also by X-ray analysis. In the carbon-13 nuclear magnetic resonance (^{13}C-NMR) spectrum of **7** obtained by the LSPD method irradiating at the H-4 proton, a carbonyl carbon signal at 181.75 ppm was observed as a doublet (J=4.3 Hz). When the H-6 proton was irradiated, the carbonyl carbon signal was also observed as a doublet (J=4.3 Hz). Another carbonyl carbon signal was observed at 186.37 ppm as a singlet, which did not change in the

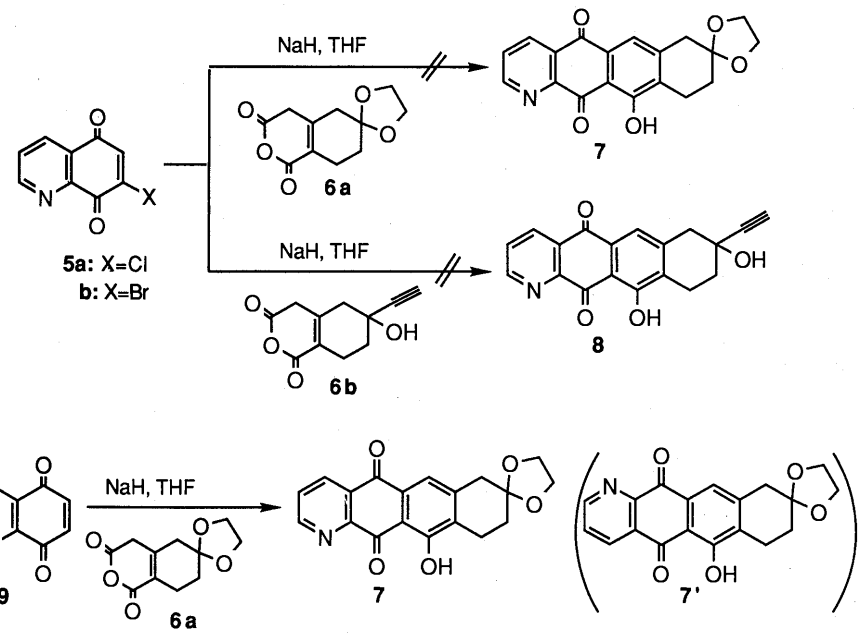

Chart 1

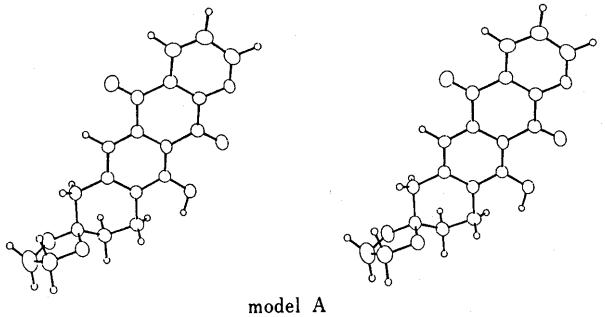

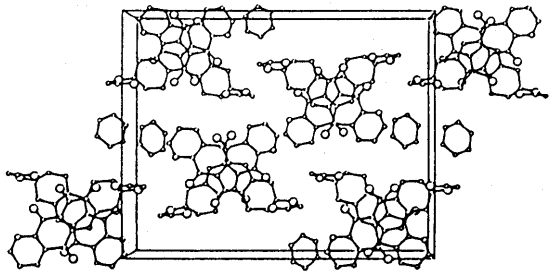

Fig. 4. Stereoscopic Packing Diagrams of Cycloadduct (7)

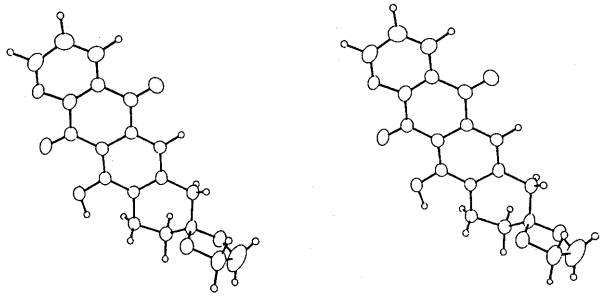

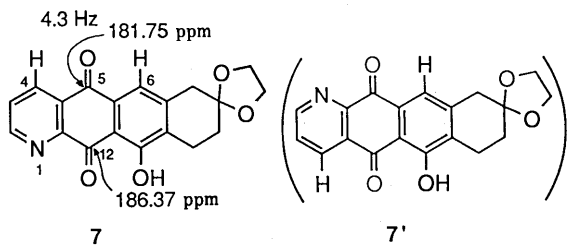

Fig. 3. Stereoscopic Diagrams of Cycloadduct (7)

above experiment. These results show that the C-5 carbonyl carbon at 181.8 ppm is coupled with both H-4 and H-6, suggesting that the cycloadduct has the structure **7**, not the regioisomeric structure **7'**. Finally, the structure was confirmed by X-ray crystallographic analysis. Transparent and well-formed crystals were obtained from the benzene solution. Intensity data were collected with graphite-monochromated CuK_α radiation, employing the ω–2θ scan mode. The structure was solved by the direct method, and the parameters of nonhydrogen atoms were refined by the block-diagonal least-squares method with anisotropic temperature factors (Figs. 3 and 4).

Similarly, reaction of the sodium salt generated from compound **6b** with **9** gave the cycloadduct (**8**) regioselectively (60% yield), and this product was identical with the compound obtained from **7**. Compound **7** was hydrolyzed with trifluoroacetic acid (TFA) and treated with (trimethylsilyl)ethynylcerium(III) chloride[14] to give **10**. Treatment of **10** with tetrabutylammonium fluoride (TBAF) gave **8** in a quantitative yield. Conversion of the ethynyl group of **8** into the methyl ketone group was accomplished by treatment with mercury(II) oxide and diluted sulfuric acid in boiling THF to give the α-hydroxyketone (**11**) in 91% yield. Ketalization of **11** with ethylene glycol in the presence of a catalytic amount of *p*-toluenesulfonic acid in boiling benzene gave **12** in 51% yield (Chart 2).

Bromination of **12** with bromine and 2,2'-azobisisobutyronitrile (AIBN) in a mixture of water, carbon tetrachloride, and chloroform at room temperature[15] did

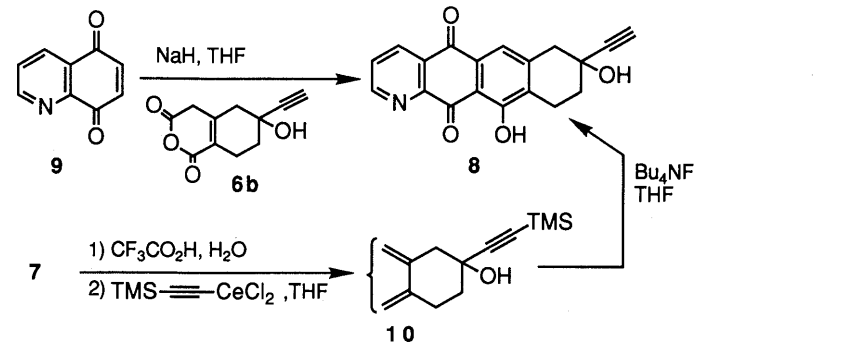

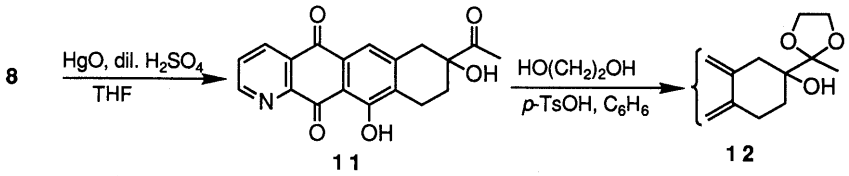

Chart 2

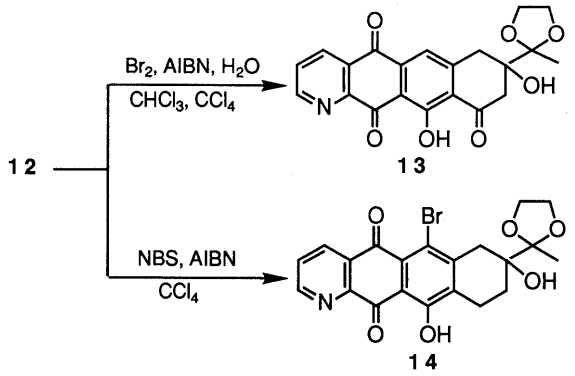

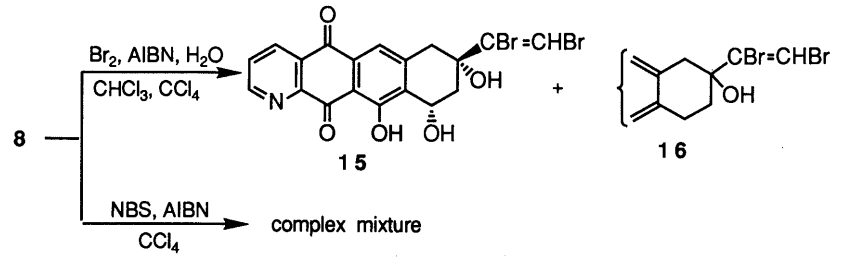

Chart 3

not give the 8,10-diol but the 10-oxo compound (**13**) in 55% yield. Another bromination of **12** with *N*-bromosuccinimide (NBS) and AIBN in refluxing anhydrous carbon tetrachloride[10] resulted in the formation of the 6-bromo compound (**14**) in 80% yield. Next, we examined the introduction of the C-10 hydroxy group into **8**. Bromination of **8** with bromine and AIBN in a mixture of water, carbon tetrachloride, and chloroform at room temperature gave the 8,10-*cis*-diol (**15**) which has the 1,2-dibromoethylene side chain at C-8 in 32% yield, accompanied with **16** in 26% yield. However, treatment of **8** with NBS and AIBN in refluxing anhydrous carbon tetrachloride gave a complex mixture (Chart 3).

We finally obtained the desired compound (**17**) from **11** by the following method. Bromination of **11** with bromine and AIBN in a mixture of water, carbon tetrachloride, and chloroform at room temperature gave the *cis*-diol (**17**) in 16% yield and the *trans*-diol (**18**) in 63% yield. The *trans*-diol (**18**) was epimerized to **17** *via* the *cis*-boronate intermediate (**19**).[16] Thus, compound **18** was treated with benzeneboronic acid in the presence of TFA and the resulting *cis*-boronate (**19**) was deprotected with 2-methylpentane-2,4-diol and acetic acid, giving the pure **17** in 86% yield. Condensation of **17** with the appropriately protected L-daunosamine (**20**) was performed under the conditions developed by Terashima *et al.*[17] The racemic aglycone (**17**) and **20** were treated with trimethylsilyl trifluoromethanesulfonate (TMSOTf) and molecular sieves 4A in a mixed

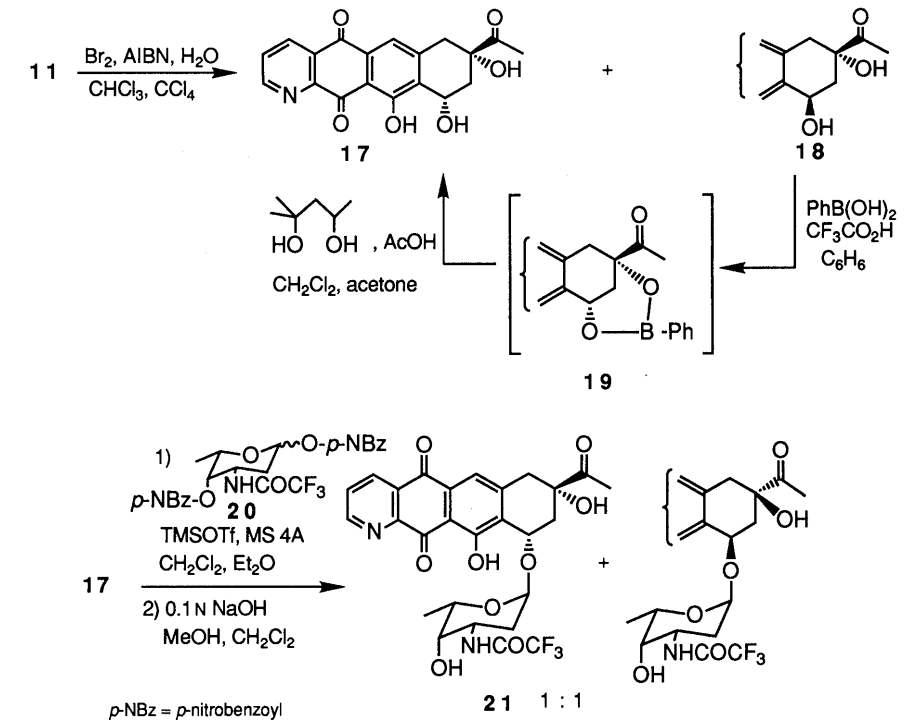

Chart 4

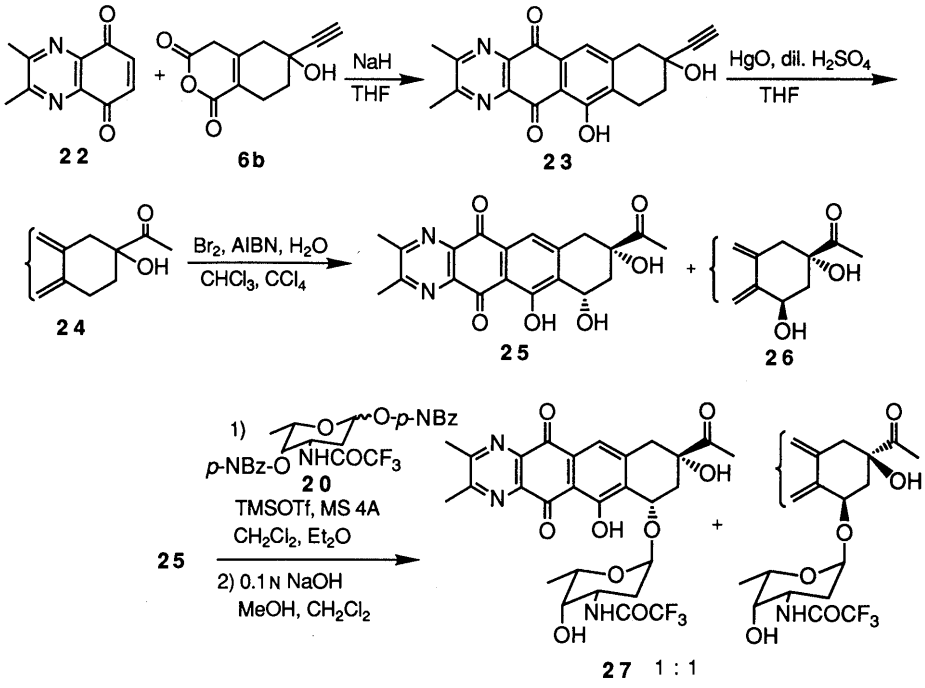

Chart 5

solvent of anhydrous dichloromethane and anhydrous ether at $-15°C$ for 4 h to give two inseparable α-glycosides. These were deprotected with one equivalent of 0.1 N sodium hydroxide at 0 °C to give an inseparable 1 : 1 mixture of two diastereomers (**21**) in 52% yield (Chart 4).

Next, we tried to synthesize the D-ring pyrazine analogue of 11-deoxydaunomycin. Treatment of the sodium salt generated from **6b** and 1.1 eq of sodium hydride in THF with 5,8-dihydro-5,8-dioxoquinoxaline (**22**)[18] at room temperature for 4 h gave **23** in 63% yield. Treatment of **23** with mercury(II) oxide and diluted sulfuric acid in boiling THF gave **24** in 99% yield. Bromination of **24** with bromine and AIBN in a mixture of water, carbon tetrachloride, and chloroform at room temperature gave the *cis*-diol (**25**) in 28% yield and the *trans*-diol (**26**) in 27% yield. The relative configurations of **25** and **26** were determined from the proton nuclear magnetic resonance (^{1}H-NMR) spectral data.[19] Condensation of racemic **25** with **20** by the same procedure as described for the preparation of **21** followed by base hydrolysis gave the α-glycosides (**27**) as an inseparable 1 : 1 mixture of two diastereomers in 48% yield (Chart 5).

The D-ring pyridine and pyrazine analogues (**21** and **27**) show inhibiting activity against L-1210 cell growth (*in vitro*) comparable to that of adriamycin (**1b**). The results will be described in detail elsewhere.

Experimental

All melting points are uncorrected. Infrared (IR) absorption spectra were recorded on a JASCO HPIR-102 spectrophotometer. ^{1}H- and ^{13}C-NMR spectra were determined on a Hitachi R-22 (90 MHz), a JEOL JNM FX-90Q (90 MHz), or a JEOL JNM-GX500 (500 MHz) spectrometer with tetramethylsilane as an internal standard. Mass spectra (MS) were obtained by the electron impact (EI) method unless otherwise noted on an ESCO EMD-05A (for EI-MS), a JEOL JMS-D300 (for EI- and exact MS), or a JEOL HX-100 [for fast atom bombardment mass spectra (FAB-MS)] mass spectrometer. E. Merck Silica gel 60 (0.063—0.200 mm, 70—230 mesh ASTM) and E. Merck pre-coated TLC plates, Silica gel 60 F_{254} were used for column chromatography and for preparative thin layer chromatography (preparative TLC), respectively.

X-Ray Crystal Analysis Intensity data were collected on a Rigaku automated four-circle diffractometer with graphite-monochromated CuK_α radiation, employing the ω–2θ scan mode. Three thousand four hundred and ninety-one unique reflections up to $2\theta = 130°$ were measured, of which 2719 ($F_O > 0.0$) were used for the structure determination. The intensities were corrected for Lorentz and polarization factors but not for absorption. The structure was solved by the direct method using the MULTAN-87 program, and the parameters of nonhydrogen atoms were refined by the block-diagonal least-squares method with anisotropic temperature factors. The positions of hydrogen atoms were calculated based on stereochemical considerations, and refined with isotropic temperature parameters. The position of the nitrogen atom in the pyridine ring was finally determined based on (i) the bond lengths (Table I) and angles (Table II) and (ii) the hydrogen bonds (Table III) formed in the crystal structure.

1-Aza-8,8-ethylenedioxy-11-hydroxy-7,8,9,10-tetrahydronaphthacene-5,12-dione (7) Under a nitrogen atmosphere, a solution of **6a** (180 mg, 0.80 mmol) in dry THF (8 ml) was added to a stirred suspension of NaH (60% in mineral oil, 34 mg, 0.85 mmol) in dry THF (8 ml) at 0 °C, and the mixture was stirred for 3 min. A solution of **9** (140 mg, 0.88 mmol) in dry THF (8 ml) was added to this mixture, and the whole was stirred at room temperature for 3 h. The reaction mixture was quenched with saturated aqueous NH_4Cl (8 ml), and extracted with CH_2Cl_2 (40 ml × 3). The extract was washed with brine, dried over $MgSO_4$, and concentrated *in vacuo*. The residue was subjected to column chromatography on silica gel (hexane : AcOEt = 1 : 3) to give a 62% yield of **7** (166 mg) as yellow crystals. mp 223—225 °C (C_6H_6). IR ($CHCl_3$) ν: 1675, 1640, 1605, 1580 cm^{-1}. ^{1}H-NMR ($CDCl_3$) δ: 2.02 (t, 2H, J=7 Hz, H-9), 3.06 (t, 2H, J=7 Hz, H-10), 3.09 (s, 2H, H-7), 4.06 (s, 4H, OCH_2CH_2O), 7.55 (s, 1H, H-6), 7.73 (dd, 1H, J=8.0, 5.0 Hz, H-3), 8.60 (dd, 1H, J=8.0, 1.5 Hz, H-4), 9.10 (dd, 1H, J=5.0, 1.5 Hz, H-2), 12.96 (s, 1H, OH-11). ^{13}C-NMR ($CDCl_3$) δ: 22.35 (t, C-9), 30.33 (t, C-10), 39.95 (t, C-7), 64.65 (t, OCH_2CH_2O), 107.06 (s), 113.41 (s), 120.63 (s, C-6), 128.01 (d, C-3), 129.74 (s), 130.76 (s), 133.20 (s), 135.39 (d, C-4), 145.34 (s), 148.82 (s), 154.79 (d, C-2), 161.28 (s), 181.70 (s, C-5), 186.33 (s, C-12). MS m/z: 337 (M^+). *Anal.* Calcd for $C_{19}H_{15}NO_5$: C, 67.65; H, 4.48; N, 4.15. Found: C, 67.72; H, 4.28; N, 3.99. Crystal data: $C_{19}H_{15}NO_5$, M_r=337.33, orthorhombic, $Pna2_1$, a=24.923(5), b=19.865(3), c=7.155(2) Å, V=3452(1) Å^3, Z=8, D_{cal}=1.2651 g cm^{-3}, μ(CuK_α)=7.32 cm^{-1}, crystal size 0.40 mm × 0.45 mm × 0.30 mm. Transparent and well-formed crystals were obtained from the

Table I. Bond Lengths (Å) with Their e.s.d.s in Parentheses

Bond	Distance	Bond	Distance
C(1)A–C(2)A	1.35 (1)	C(3)B–N(4)B	1.31 (1)
C(1)A–C(13)A	1.402 (9)	N(4)B–C(14)B	1.352 (9)
C(2)A–C(3)A	1.37 (1)	C(5)B–O(5)B	1.224 (9)
C(3)A–N(4)A	1.322 (9)	C(5)B–C(13)B	1.484 (9)
N(4)A–C(14)A	1.334 (8)	C(5)B–C(15)B	1.496 (9)
C(5)A–O(5)A	1.204 (8)	C(6)B–O(6)B	1.228 (7)
C(5)A–C(13)A	1.502 (8)	C(6)B–C(14)B	1.501 (9)
C(5)A–C(15)A	1.505 (8)	C(6)B–C(16)B	1.442 (8)
C(6)A–O(6)A	1.239 (7)	C(7)B–C(15)B	1.367 (8)
C(6)A–C(14)A	1.474 (8)	C(7)B–C(17)B	1.414 (8)
C(6)A–C(16)A	1.476 (8)	C(8)B–C(9)B	1.495 (9)
C(7)A–C(15)A	1.359 (8)	C(8)B–C(17)B	1.510 (9)
C(7)A–C(17)A	1.414 (8)	C(9)B–C(10)B	1.495 (9)
C(8)A–C(9)A	1.535 (9)	C(9)B–O(19)B	1.426 (7)
C(8)A–C(17)A	1.499 (9)	C(9)B–O(22)B	1.401 (8)
C(9)A–C(10)A	1.510 (9)	C(10)B–C(11)B	1.554 (9)
C(9)A–O(19)A	1.433 (7)	C(11)B–C(18)B	1.514 (8)
C(9)A–O(22)A	1.384 (8)	C(12)B–O(12)B	1.350 (7)
C(10)A–C(11)A	1.542 (9)	C(12)B–C(16)B	1.412 (8)
C(11)A–C(18)A	1.521 (9)	C(12)B–C(18)B	1.377 (8)
C(12)A–O(12)A	1.337 (7)	C(13)B–C(14)B	1.358 (9)
C(12)A–C(16)A	1.392 (8)	C(15)B–C(16)B	1.428 (8)
C(12)A–C(18)A	1.401 (8)	C(17)B–C(18)B	1.395 (8)
C(13)A–C(14)A	1.385 (8)	O(19)B–C(20)B	1.396 (9)
C(15)A–C(16)A	1.416 (8)	C(20)B–C(21)B	1.39 (1)
C(17)A–C(18)A	1.399 (8)	C(21)B–O(22)B	1.39 (1)
O(19)A–C(20)A	1.400 (9)	C(1)–C(3)	1.36 (1)
C(20)A–C(21)A	1.47 (1)	C(1)–C(4)	1.31 (1)
C(21)A–O(22)A	1.42 (1)	C(2)–C(3)	1.41 (2)
C(1)B–C(2)B	1.36 (1)	C(2)–C(6)	1.24 (2)
C(1)B–C(13)B	1.37 (1)	C(4)–C(5)	1.33 (2)
C(2)B–C(3)B	1.42 (1)	C(5)–C(6)	1.41 (2)

Table II. Bond Angles (°) with Their e.s.d.s in Parentheses

Bond	Angle	Bond	Angle
C(2)A–C(1)A–C(13)A	117.9 (2)	C(3)B–N(4)B–C(14)B	116.2 (3)
C(1)A–C(2)A–C(3)A	119.6 (2)	O(5)B–C(5)B–C(13)B	121.6 (2)
C(2)A–C(3)A–N(4)A	124.0 (2)	O(5)B–C(5)B–C(15)B	120.1 (2)
C(3)A–N(4)A–C(14)A	117.0 (2)	C(13)B–C(5)B–C(15)B	118.3 (2)
O(5)A–C(5)A–C(13)A	122.3 (2)	O(6)B–C(6)B–C(14)B	120.6 (2)
O(5)A–C(5)A–C(15)A	120.8 (2)	O(6)B–C(6)B–C(16)B	121.7 (2)
C(13)A–C(5)A–C(15)A	116.9 (1)	C(14)B–C(6)B–C(16)B	117.7 (2)
O(6)A–C(6)A–C(14)A	120.1 (2)	C(15)B–C(7)B–C(17)B	120.8 (2)
O(6)A–C(6)A–C(16)A	120.5 (2)	C(9)B–C(8)B–C(17)B	112.3 (2)
C(14)A–C(6)A–C(16)A	119.4 (2)	C(8)B–C(9)B–C(10)B	111.6 (2)
C(15)A–C(7)A–C(17)A	121.0 (2)	C(8)B–C(9)B–O(19)B	110.5 (2)
C(9)A–C(8)A–C(17)A	112.9 (1)	C(8)B–C(9)B–O(22)B	110.1 (2)
C(8)A–C(9)A–C(10)A	111.1 (2)	C(10)B–C(9)B–O(19)B	109.2 (2)
C(8)A–C(9)A–O(19)A	109.9 (2)	C(10)B–C(9)B–O(22)B	108.9 (2)
C(8)A–C(9)A–O(22)A	110.2 (2)	O(19)B–C(9)B–O(22)B	106.4 (1)
C(10)A–C(9)A–O(19)A	109.3 (2)	C(9)B–C(10)B–C(11)B	111.4 (2)
C(10)A–C(9)A–O(22)A	110.1 (2)	C(10)B–C(11)B–C(18)B	113.1 (1)
O(19)A–C(9)A–O(22)A	106.1 (2)	O(12)B–C(12)B–C(16)B	120.4 (2)
C(9)A–C(10)A–C(11)A	112.3 (2)	O(12)B–C(12)B–C(18)B	117.6 (2)
C(10)A–C(11)A–C(18)A	112.9 (2)	C(16)B–C(12)B–C(18)B	122.0 (2)
O(12)A–C(12)A–C(16)A	122.7 (2)	C(1)B–C(13)B–C(5)B	119.4 (2)
O(12)A–C(12)A–C(18)A	116.5 (2)	C(1)B–C(13)B–C(14)B	119.9 (2)
C(16)A–C(12)A–C(18)A	120.8 (2)	C(5)B–C(13)B–C(14)B	120.5 (2)
C(1)A–C(13)A–C(5)A	119.4 (2)	N(4)B–C(14)B–C(6)B	114.3 (2)
C(1)A–C(13)A–C(14)A	118.6 (2)	N(4)B–C(14)B–C(13)B	123.4 (2)
C(5)A–C(13)A–C(14)A	121.8 (2)	C(6)B–C(14)B–C(13)B	122.3 (2)
N(4)A–C(14)A–C(6)A	116.5 (2)	C(5)B–C(15)B–C(7)B	118.7 (2)
N(4)A–C(14)A–C(13)A	122.8 (2)	C(5)B–C(15)B–C(16)B	119.6 (2)
C(6)A–C(14)A–C(13)A	120.6 (2)	C(7)B–C(15)B–C(16)B	121.5 (2)
C(5)A–C(15)A–C(7)A	118.6 (2)	C(6)B–C(16)B–C(12)B	122.3 (2)
C(5)A–C(15)A–C(16)A	120.6 (2)	C(6)B–C(16)B–C(15)B	121.3 (2)
C(7)A–C(15)A–C(16)A	120.8 (2)	C(12)B–C(16)B–C(15)B	116.4 (2)
C(6)A–C(16)A–C(12)A	120.9 (2)	C(7)B–C(17)B–C(8)B	119.0 (2)
C(6)A–C(16)A–C(15)A	120.4 (2)	C(7)B–C(17)B–C(18)B	118.4 (2)
C(12)A–C(16)A–C(15)A	118.7 (2)	C(8)B–C(17)B–C(18)B	122.6 (2)
C(7)A–C(17)A–C(8)A	118.8 (2)	C(11)B–C(18)B–C(12)B	118.2 (2)
C(7)A–C(17)A–C(18)A	118.8 (2)	C(11)B–C(18)B–C(17)B	121.0 (2)
C(8)A–C(17)A–C(18)A	122.3 (2)	C(12)B–C(18)B–C(17)B	120.7 (2)
C(11)A–C(18)A–C(12)A	118.2 (2)	C(9)B–O(19)B–C(20)B	106.9 (2)
C(11)A–C(18)A–C(17)A	121.9 (2)	O(19)B–C(20)B–C(21)B	106.4 (3)
C(12)A–C(18)A–C(17)A	119.9 (2)	C(20)B–C(21)B–O(22)B	109.9 (2)
C(9)A–O(19)A–C(20)A	107.6 (2)	C(9)B–O(22)B–C(21)B	106.9 (3)
O(19)A–C(20)A–C(21)A	105.1 (2)	C(3)–C(1)–C(4)	121.5 (4)
C(20)A–C(21)A–O(22)A	105.9 (2)	C(3)–C(2)–C(6)	121.5 (5)
C(9)A–O(22)A–C(21)A	109.5 (2)	C(1)–C(3)–C(2)	117.4 (4)
C(2)B–C(1)B–C(13)B	118.8 (2)	C(1)–C(4)–C(5)	119.9 (4)
C(1)B–C(2)B–C(3)B	117.5 (3)	C(4)–C(5)–C(6)	119.7 (4)
C(2)B–C(3)B–N(4)B	124.2 (2)	C(2)–C(6)–C(5)	119.7 (5)

TABLE III. Possible Hydrogen Bond Distances (Å) and Short Contacts (Less than 3.5 Å) with Their e.s.d.s in Parentheses

Atom 1	Atom 2[a]	Distance	Symmetry operation[b]
C(5)A	O(5)B	3.471 (8)	$x, y, z-1.00$
O(5)A	C(1)B	3.361 (9)	$x, y, z-1.00$
C(6)A	C(7)B	3.463 (8)	$x, y, z-1.00$
O(6)A	C(7)B	3.495 (7)	$x, y, z-1.00$
O(6)A	O(19)B	3.244 (6)	$x, y, z-1.00$
O(6)A	C(20)B	3.460 (9)	$x, y, z-1.00$
C(7)A	C(13)B	3.443 (8)	$x, y, z-1.00$
C(7)A	C(14)B	3.305 (8)	$x, y, z-1.00$
C(12)A	C(16)B	3.469 (8)	$x, y, z-1.00$
O(12)A	C(18)B	3.335 (7)	$x, y, z-1.00$
O(12)A	O(19)B	3.087 (6)	$x, y, z-1.00$
C(15)A	C(5)B	3.388 (9)	$x, y, z-1.00$
C(16)A	C(15)B	3.390 (8)	$x, y, z-1.00$
C(17)A	C(6)B	3.408 (8)	$x, y, z-1.00$
C(1)B	O(5)A	3.361 (9)	$x, y, z+1.00$
C(5)B	C(15)A	3.388 (9)	$x, y, z+1.00$
O(5)B	C(5)A	3.471 (8)	$x, y, z+1.00$
C(6)B	C(17)A	3.408 (8)	$x, y, z+1.00$
C(7)B	C(6)A	3.463 (8)	$x, y, z+1.00$
C(7)B	O(6)A	3.495 (7)	$x, y, z+1.00$
C(13)B	C(7)A	3.443 (8)	$x, y, z+1.00$
C(14)B	C(7)A	3.305 (8)	$x, y, z+1.00$
C(15)B	C(16)A	3.390 (8)	$x, y, z+1.00$
C(16)B	C(12)A	3.469 (8)	$x, y, z+1.00$
C(18)B	O(12)A	3.335 (7)	$x, y, z+1.00$
O(19)B	O(6)A	3.244 (6)	$x, y, z+1.00$
O(19)B	O(12)A	3.087 (6)	$x, y, z+1.00$
C(20)B	O(6)A	3.460 (9)	$x, y, z+1.00$
N(4)A	C(2)A	3.276 (9)	$-x+1.00, -y+1.00, z-0.50$
N(4)A	C(3)A	3.427 (9)	$-x+1.00, -y+1.00, z-0.50$
C(2)A	N(4)A	3.276 (9)	$-x+1.00, -y+1.00, z+0.50$
C(3)A	N(4)A	3.427 (9)	$-x+1.00, -y+1.00, z+0.50$
C(20)A	O(22)B	3.456 (9)	$x-0.50, -y+0.50, z$
C(21)A	O(22)B	3.46 (1)	$x-0.50, -y+0.50, z$
N(4)B	C(4)	3.37 (1)	$x-0.50, -y+0.50, z$
O(22)B	C(20)A	3.456 (9)	$x+0.50, -y+0.50, z$
O(22)B	C(21)A	3.46 (1)	$x+0.50, -y+0.50, z$
C(4)	N(4)B	3.37 (1)	$x+0.50, -y+0.50, z$
O(19)A	C(1)B	3.432 (9)	$-x+0.50, y-0.50, z-0.50$
C(20)A	O(5)B	3.439 (9)	$-x+0.50, y-0.50, z-0.50$
C(21)A	O(5)B	3.45 (1)	$-x+0.50, y-0.50, z-0.50$
C(1)B	O(19)A	3.432 (9)	$-x+0.50, y+0.50, z+0.50$
O(5)B	C(20)A	3.439 (9)	$-x+0.50, y+0.50, z+0.50$
O(5)B	C(21)A	3.45 (1)	$-x+0.50, y+0.50, z+0.50$

a) Atom 2 is translated by the symmetry operation. *b*) Except for the self-symmetry (x, y, z).

TABLE IV. Crystal Data for the Cycloadduct (**7**)

Chemical formula	$C_{19}O_5NH_{15}\cdot 1/2C_6H_6$
Molecular weight	337
Crystal system	Orthorhombic
Space group	*Pna*2 (1)
Cell constants	$a=24.923$ (5) Å
	$b=19.865$ (3) Å
	$c=7.155$ (2) Å
Volume	3542 (1) Å^3
Z	8
Final R-value	0.079

benzene solution (Table IV).

(±)-1-Aza-8-ethynyl-8,11-dihydroxy-7,8,9,10-tetrahydronaphthacene-5,12-dione (8) (i) Preparation from **9**: By a similar procedure to that described for the preparation of **7**, the crude product was obtained from **6b** (164 mg, 0.80 mmol), **9** (128 mg, 0.80 mmol) and NaH (60% in mineral oil, 32 mg, 0.80 mmol). It was purified by column chromatography on silica gel (AcOEt) to give a 60% yield of **8** (141 mg) as yellow crystals, mp 177 °C (dec.) (C_6H_6–AcOEt). IR ($CHCl_3$) ν: 1670, 1635, 1600, 1575 cm^{-1}. ^{1}H-NMR ($CDCl_3$) δ: 2.13—2.30 (m, 2H, H-9), 2.49 (s, 1H, C≡CH), 3.00—3.14 (m, 2H, H-10), 3.18 (d, 1H, $J=17$ Hz, H-7), 3.33 (d, 1H, $J=17$ Hz, H-7), 7.61 (s, 1H, H-6), 7.74 (dd, 1H, $J=8.0$, 5.0 Hz, H-3), 8.62 (dd, 1H, $J=8.0$, 2.0 Hz, H-4), 9.11 (dd, 1H, $J=5.0$, 2.0 Hz, H-2), 12.99 (s, 1H, OH-11). Exact MS Calcd for $C_{19}H_{13}NO_4$: 319.0844. Found: 319.0854.

(ii) Preparation from **10**: A solution of **10** (6.2 mg, 0.016 mmol) and $Bu_4NF\cdot 3H_2O$ (10 mg) in THF (4 ml) was stirred at room temperature for 30 min. The reaction mixture was diluted with water (4 ml) and extracted with CH_2Cl_2 (10 ml × 2). The extract was washed with brine, dried over Na_2SO_4, and concentrated *in vacuo*. The residue was purified by preparative TLC (AcOEt) to give a quantitative yield (5.0 mg) of **8** as yellow crystals. This product was identical with an authentic sample obtained from **9**.

(±)-1-Aza-8,11-dihydroxy-8-(trimethylsilyl)ethynyl-7,8,9,10-tetrahydronaphthacene-5,12-dione (10) A solution of **7** (41.9 mg, 0.124 mmol) in CF_3CO_2H (4 ml) and water (1 ml) was heated at 50 °C for 40 h, then concentrated *in vacuo*, and the residue was partitioned between CH_2Cl_2 (45 ml) and water. The organic layer was separated, washed with water and brine, dried over Na_2SO_4, and concentrated *in vacuo*. Under a nitrogen atmosphere, the residue was dissolved in dry CH_2Cl_2 (12 ml), and a dry THF solution of (trimethylsilyl)ethynylcerium(III) chloride [prepared from (trimethylsilyl)acetylene (0.37 ml, 2.6 mmol), BuLi (1.6 M, 1.8 ml, 3 mmol), anhydrous $CeCl_3$ (867 mg, 3.5 mmol), and dry THF (3 ml) according to the literature[10,13]] was added at −78 °C over 3 h. After being stirred for 1 h under the same conditions, the reaction mixture was quenched with saturated aqueous NH_4Cl (5 ml), and extracted with CH_2Cl_2 (25 ml). The organic layer was washed with brine, dried over $MgSO_4$, and concentrated *in vacuo*. The residue was purified by preparative TLC (CH_2Cl_2 : AcOEt = 3 : 1) to give a 24% yield (11.5 mg) of **10** as yellow crystals. mp 76—79 °C (CCl_4–CH_2Cl_2). IR ($CHCl_3$) ν: 1670, 1640, 1590 cm^{-1}. ^{1}H-NMR ($CDCl_3$) δ: 0.13 (s, 9H, $SiMe_3$), 2.16 (t, 2H, $J=6.5$ Hz, H-9), 3.03 (t, 2H, $J=6.5$ Hz, H-10), 3.16 (d, 1H, $J=17.5$ Hz, H-7), 3.30 (d, 1H, $J=17.5$ Hz, H-7), 7.59 (s, 1H, H-6), 7.73 (dd, 1H, $J=8.0$, 4.5 Hz, H-3), 8.61 (dd, 1H, $J=8.0$, 1.5 Hz, H-4), 9.10 (dd, 1H, $J=4.5$, 1.5 Hz, H-2), 12.98 (s, 1H, OH-11). Exact MS Calcd for $C_{22}H_{21}NO_4Si$: 391.1237. Found: 391.1222.

(±)-8-Acetyl-1-aza-8,11-dihydroxy-7,8,9,10-tetrahydronaphthacene-5,12-dione (11) A solution of **8** (50 mg, 0.157 mmol), HgO (68 mg, 0.314 mmol), and 3 M H_2SO_4 (1.8 ml) in THF (8.5 ml) was heated under reflux for 1.5 h and then cooled to room temperature. The reaction mixture was diluted with 10% HCl (5 ml) and extracted with AcOEt (30 ml × 3). The aqueous layer was saturated with NaCl and extracted with AcOEt (30 ml × 2). The combined organic layer was washed with brine, dried over $MgSO_4$, and concentrated *in vacuo*. The residue was purified by column chromatography on silica gel (AcOEt) to give a 98% yield (52 mg) of **11** as orange crystals, mp 177—180 °C (C_6H_6). IR (KCl) ν: 1705, 1670, 1640, 1600, 1575 cm^{-1}. ^{1}H-NMR ($CDCl_3$) δ: 1.80—2.08 (m, 2H, H-9), 2.38 (s, 3H, $COCH_3$), 2.82—3.50 (m, 4H, H-7 and H-10), 7.61 (s, 1H, H-6), 7.80 (dd, 1H, $J=8.0$, 3.5 Hz, H-3), 8.62 (dd, 1H, $J=8.0$, 2.0 Hz, H-4), 9.04 (dd, 1H, $J=3.5$, 2.0 Hz, H-2), 12.95 (s, 1H, OH-11). Exact MS Calcd for $C_{19}H_{15}NO_5$: 337.0950. Found: 337.0953.

(±)-1-Aza-8-[1,1-(ethylenedioxy)ethyl]-8,11-dihydroxy-7,8,9,10-tetrahydronaphthacene-5,12-dione (12) A mixture of **11** (51.1 mg, 0.135 mmol), ethylene glycol (100 mg, 1.6 mmol), and *p*-toluenesulfonic acid (12 mg) in C_6H_6 (15 ml) was refluxed for 2 h with azeotropic removal of water formed using a Dean–Stark apparatus. After being cooled, the mixture was partitioned between AcOEt (20 ml) and saturated aqueous $NaHCO_3$ (7 ml), and the organic layer was separated. The aqueous layer was extracted with AcOEt (20 ml × 2), and the combined organic layer was washed with brine, dried over $MgSO_4$, and concentrated *in vacuo*. The residue was purified by column chromatography on silica gel (AcOEt) to give a 51% yield (29.8 mg) of **12** as yellow crystals. mp 240—242 °C (C_6H_6). IR (KCl) ν: 1670, 1640, 1600, 1580 cm^{-1}. ^{1}H-NMR ($CDCl_3$) δ: 1.44 (s, 3H, H-14), 1.80—1.87 (m, 1H, H-9), 2.04—2.12 (m, 1H, H-9), 2.84—2.92 (m, 1H, H-10), 2.96 (dd, 1H, $J=17.5$, 2.0 Hz, H-7), 3.08—3.13 (m, 1H, H-10), 3.13 (d, 1H, $J=17.5$ Hz, H-7), 4.07 (br s, 4H, OCH_2CH_2O), 7.62 (s, 1H, H-6), 7.72 (dd, 1H, $J=8.0$, 4.5 Hz, H-3), 8.60 (dd, 1H, $J=8.0$, 1.5 Hz, H-4), 9.10 (dd, 1H, $J=4.5$, 1.5 Hz, H-2), 13.00 (s, 1H, OH-11). Exact MS Calcd for $C_{21}H_{19}NO_6+H$: 382.1288. Found: 382.1265.

(±)-1-Aza-8-[1,1-(ethylenedioxy)ethyl]-8,11-dihydroxy-7,8,9,10-tetrahydronaphthacene-5,10,12-trione (13) A solution of bromine (38 mg, 0.238 mmol) in CCl_4 (0.95 ml) was added to the two-phase solution of **12** (10 mg, 0.026 mmol) and AIBN (19 mg, 0.116 mmol) in a mixture of $CHCl_3$

(3 ml), CCl_4 (0.6 ml), and water (0.6 ml). The reaction mixture was stirred at room temperature for 20 h. After being cooled, the mixture was quenched with saturated aqueous $Na_2S_2O_3$ (5 ml), and extracted with $CHCl_3$ (15 ml × 2). The combined organic layer was washed with brine, dried over $MgSO_4$, and concentrated *in vacuo*. The residue was subjected to preparative TLC (CH_2Cl_2 : AcOEt = 1 : 1) to give a 55% yield (5.7 mg) of **13** as yellow crystals. mp 150—155 °C (CCl_4–$CHCl_3$). IR ($CHCl_3$) *v*: 1685, 1680, 1640, 1600, 1580 cm^{-1}. ^{1}H-NMR ($CDCl_3$) δ: 1.44 (s, 3H, H-14), 2.92 (dd, 1H, J = 17.0, 2.0 Hz, H-7), 3.02 (d, 1H, J = 17.0 Hz, H-7), 3.27 (dd, 1H, J = 17.5, 2.0 Hz, H-9), 3.41 (d, 1H, J = 17.5 Hz, H-9), 4.06 (br s, 4H, OCH_2CH_2O), 7.73 (s, 1H, H-6), 7.74 (dd, 1H, J = 8.0, 5.0 Hz, H-3), 8.59 (dd, 1H, J = 8.0, 1.5 Hz, H-4), 9.15 (dd, 1H, J = 5.0, 1.5 Hz, H-2), 13.87 (s, 1H, OH-11). MS *m/z*: 377 ($M^+ - H_2O$).

(±)-1-Aza-6-bromo-8-[1,1-(ethylenedioxy)ethyl]-8,11-dihydroxy-7,8,9,10-tetrahydronaphthacene-5,12-dione (14) Under a nitrogen atmosphere, a mixture of **12** (10 mg, 0.026 mmol), NBS (11.2 mg, 0.064 mmol), and AIBN (4 mg, 0.024 mmol) in dry CCl_4 (3 ml) was stirred at room temperature for 14 h. The reaction mixture was quenched with water (5 ml) and extracted with $CHCl_3$ (15 ml × 2). The combined organic layer was washed with brine, dried over $MgSO_4$, and concentrated *in vacuo*. The residue was subjected to preparative TLC (CH_2Cl_2 : AcOEt = 1 : 1) to give an 80% yield (9.7 mg) of **14** as yellow crystals. mp 228—232 °C (CCl_4–$CHCl_3$). IR ($CHCl_3$) *v*: 1670, 1640, 1580 cm^{-1}. ^{1}H-NMR ($CDCl_3$) δ: 1.46 (s, 3H, H-14), 1.7—1.8 (m, 1H, H-9), 2.0—2.1 (m, 1H, H-9), 2.9—3.3 (m, 4H, H-7 and H-10), 4.10 (s, 4H, OCH_2CH_2O), 7.74 (dd, 1H, J = 8.0, 5.0 Hz, H-3), 8.63 (dd, 1H, J = 8.0, 2.0 Hz, H-4), 9.09 (dd, 1H, J = 5.0, 2.0 Hz, H-2), 13.72 (s, 1H, OH-11). Exact MS Calcd for $C_{21}H_{18}{}^{79}BrNO_6$: 459.0315. Found: 459.0293; Calcd for $C_{21}H_{18}{}^{81}BrNO_6$: 461.0295. Found: 461.0274.

(8*RS*,10*RS*)-1-Aza-8-(1,2-dibromoethylene)-8,10,11-trihydroxy-7,8,9,10-tetrahydronaphthacene-5,12-dione (15) and (±)-1-Aza-8-(1,2-dibromoethylene)-8,11-dihydroxy-7,8,9,10-tetrahydronaphthacene-5,12-dione (16) A solution of bromine (50 mg, 0.625 mmol) in CCl_4 (1.25 ml) was added to the two-phase solution of **8** (20 mg, 0.063 mmol) and AIBN (25 mg, 0.128 mmol) in a mixture of $CHCl_3$ (10 ml), CCl_4 (2 ml), and water (2 ml). The reaction mixture was stirred for 2 h at room temperature. The mixture was quenched with saturated aqueous $Na_2S_2O_3$ (5 ml), and the organic phase was separated. The aqueous layer was extracted with $CHCl_3$ (20 ml × 2). The combined organic layer was washed with brine, dried over Na_2SO_4, and concentrated *in vacuo*. The residue was purified by preparative TLC (CH_2Cl_2 : AcOEt = 1 : 1) to give a 32% yield (10 mg) of **15** and a 26% yield (7.8 mg) of **16**, each as yellow crystals. **15**: mp 137—143 °C (CCl_4–CH_2Cl_2). IR ($CHCl_3$) *v*: 1670, 1640, 1620, 1600, 1580 cm^{-1}. ^{1}H-NMR ($CDCl_3$) δ: 2.38 (dt, 1H, J = 14.5, 2.0 Hz, H-9), 2.60 (dd, 1H, J = 14.5, 5.0 Hz, H-9), 3.10 (dd, 1H, J = 17.5, 2.0 Hz, H-7), 3.41 (br s, 1H, OH-8), 3.56 (d, 1H, J = 17.5 Hz, H-7), 4.63 (s, 1H, OH-10), 5.43 (br d, J = 5.0 Hz, $v_{1/2}$ = 9 Hz, H-10), 7.45 (s, 1H, 14-CHBr), 7.67 (s, 1H, H-6), 7.78 (dd, 1H, J = 8.0, 5.0 Hz, H-3), 8.63 (dd, 1H, J = 8.0, 2.0 Hz, H-4), 9.14 (dd, 1H, J = 5.0, 2.0 Hz, H-2), 13.18 (s, 1H, OH-11). Exact MS Calcd for $C_{19}H_{13}{}^{79}Br_2NO_5 - 2H_2O$: 456.8950. Found: 456.8968; Calcd for $C_{19}H_{13}{}^{79}Br^{81}BrNO_5 - 2H_2O$: 458.8930. Found: 458.8950; Calcd for $C_{19}H_{13}{}^{81}Br_2NO_5 - 2H_2O$: 460.8911. Found: 460.8949. **16**: mp 250—255 °C (CCl_4–CH_2Cl_2). IR ($CHCl_3$) *v*: 1670, 1640, 1620, 1600, 1580 cm^{-1}. ^{1}H-NMR ($CDCl_3$) δ: 2.10—2.15 (m, 1H, H-9), 2.31—2.37 (m, 1H, H-9), 3.00 (q, 2H, J = 6.0 Hz, H-10), 3.10 (d, 1H, J = 17.0 Hz, H-7), 3.42 (d, 1H, J = 17.0 Hz, H-7), 7.14 (s, 1H, 14-CHBr), 7.55 (s, 1H, H-6), 7.74 (dd, 1H, J = 8.0, 5.0 Hz, H-3), 8.60 (dd, 1H, J = 8.0, 1.5 Hz, H-4), 9.11 (dd, 1H, J = 5.0, 1.5 Hz, H-2), 12.94 (s, 1H, OH-11). Exact MS Calcd for $C_{19}H_{13}{}^{79}Br_2NO_4$: 476.9212. Found: 476.9228; Calcd for $C_{19}H_{13}{}^{79}Br^{81}BrNO_4$: 478.9193. Found: 478.9264; Calcd for $C_{19}H_{13}{}^{81}Br_2NO_4$: 480.9394. Found: 480.9366.

(8*RS*,10*RS*)-8-Acetyl-1-aza-8,10,11-trihydroxy-7,8,9,10-tetrahydronaphthacene-5,12-dione (17) and (8*RS*,10*SR*)-8-Acetyl-1-aza-8,10,11-trihydroxy-7,8,9,10-tetrahydronaphthacene-5,12-dione (18) By a similar procedure to that described for the preparation of **15**, the crude product which was obtained from **11** (28 mg, 0.08 mmol), AIBN (10 mg, 0.061 mmol), and bromine (30 mg, 0.91 mmol) was purified by preparative TLC ($CHCl_3$: MeOH = 15 : 1) to give a 16% yield (4.4 mg) of **17** and a 63% yield (17.9 mg) of **18**, each as yellow crystals. **17**: mp 218 °C (dec.) (CCl_4–$CHCl_3$). IR ($CHCl_3$) *v*: 1720, 1675, 1670, 1640, 1580 cm^{-1}. ^{1}H-NMR ($CDCl_3$) δ: 2.21 (dd, 1H, J = 15.0, 5.0 Hz, H-9), 2.39 (dt, 1H, J = 15.0, 2.0 Hz, H-9), 2.43 (s, 3H, $COCH_3$), 3.05 (dd, 1H, J = 17.5, 2.0 Hz, H-7), 3.31 (d, 1H, J = 17.5 Hz, H-7), 5.40 (m, 1H, $v_{1/2}$ = 11 Hz, H-10), 7.69 (s, 1H, H-6), 7.77 (dd, 1H, J = 8.0, 5.0 Hz, H-3), 8.63 (dd, 1H, J = 8.0, 1.5 Hz, H-4), 9.14 (dd, 1H, J = 5.0, 1.5 Hz, H-2), 13.21 (s, 1H, OH-11). Exact MS Calcd for $C_{19}H_{15}NO_6$: 353.0898. Found: 353.0898. **18**: mp 119—123 °C (CCl_4–$CHCl_3$). IR ($CHCl_3$) *v*: 1720, 1670, 1640, 1600, 1580 cm^{-1}. ^{1}H-NMR ($CDCl_3$) δ: 2.25 (dd, 1H, J = 13.0, 9.0 Hz, H-9), 2.35—2.44 (m, 1H, H-9), 2.40 (s, 3H, $COCH_3$), 2.80 (dd, 1H, J = 17.0, 2.0 Hz, H-7), 3.43 (d, 1H, J = 17.0 Hz, H-7), 3.82 (br s, 1H, OH-8), 4.10 (br s, 1H, OH-10), 5.45 (m, 1H, $v_{1/2}$ = 18.0 Hz, H-10), 7.65 (s, 1H, H-6), 7.77 (dd, 1H, J = 8.0, 5.0 Hz, H-3), 8.62 (dd, 1H, J = 8.0, 1.5 Hz, H-4), 9.14 (dd, 1H, J = 5.0, 1.5 Hz, H-2), 13.42 (s, 1H, OH-11). Exact MS Calcd for $C_{19}H_{15}NO_6 - 2H_2O$: 317.0689. Found: 317.0694.

The Transformation of 18 into 17 Under a nitrogen atmosphere, a mixture of **18** (5.2 mg, 0.015 mmol), benzeneboronic acid (5.5 mg, 0.045 mmol), CF_3CO_2H (1 ml), and dry toluene (2 ml) were stirred at room temperature for 5 d. The reaction mixture was quenched with saturated aqueous $NaHCO_3$ (4 ml) at 0 °C, and extracted with CH_2Cl_2 (15 ml). The extract was washed with water, dried over Na_2SO_4, and concentrated *in vacuo*. The residue was dissolved in CH_2Cl_2 (1.5 ml) and acetone (1.5 ml). 2-Methyl-2,4-pentanediol (0.1 ml) and AcOH (0.05 ml) were added to this solution, and the mixture was stirred for 12 h at room temperature. The reaction mixture was poured into a mixture of saturated aqueous $NaHCO_3$ (8 ml) and CH_2Cl_2 (15 ml). The organic layer was separated, washed with water, dried over Na_2SO_4, and concentrated *in vacuo*. The residue was washed with pentane (4 ml × 2) and purified by preparative TLC (CH_2Cl_2 : Et_2O = 10 : 1) to give an 86% yield (4.5 mg) of **17**, which was identical with an authentic sample obtained from **11**.

4-Aza-4-demethoxy-11-deoxy-3′-*N*-trifluoroacetyldaunomycin (21) Under a nitrogen atmosphere, TMSOTf (19.1 mg, 0.086 mmol) was added to a stirred suspension of molecular sieves 4A (150 mg) and **20** (23 mg, 0.043 mmol) in dry CH_2Cl_2 (6 ml) and dry Et_2O (2 ml) at −40 °C. The mixture was stirred at −5 °C for 1 h and then cooled to −15 °C, and a solution of **17** (11 mg, 0.031 mmol) in dry CH_2Cl_2 (5 ml) was added to it. After being stirred for 4 h under the same conditions, the mixture was poured into a vigorously stirred mixture of AcOEt (18 ml) and saturated aqueous $NaHCO_3$ (16 ml). The organic layer was separated and the aqueous layer was extracted with AcOEt (18 ml). The combined organic layer was washed with brine, dried over Na_2SO_4, and concentrated *in vacuo*. The residue was dissolved in CH_2Cl_2 (1 ml) and MeOH (10 ml) under a nitrogen atmosphere, and 0.1 N NaOH (0.3 ml) was added to this solution at 0 °C. The mixture was stirred for 30 min under the same conditions, then one drop of AcOH was added. The resulting mixture was partitioned between AcOEt (15 ml) and brine (8 ml), and the organic layer was separated. The aqueous layer was extracted with AcOEt (8 ml), and the combined organic layer was washed with brine, dried over $MgSO_4$, and concentrated *in vacuo*. The residue was purified by preparative TLC ($CHCl_3$: MeOH = 10 : 1) to give a 52% yield (9.3 mg) of **21** as an inseparable 1 : 1 mixture of two diastereomers. mp 161—165 °C (CCl_4–$CHCl_3$). IR ($CHCl_3$) *v*: 1720, 1680, 1670, 1640, 1600, 1580 cm^{-1}. ^{1}H-NMR ($CDCl_3$) δ: 1.26 (d, 3H × 1/2, J = 6.5 Hz, H-6′), 1.29 (d, 3H × 1/2, J = 6.5 Hz, H-6′), 2.41 (s, 3H × 1/2, $COCH_3$), 2.46 (s, 3H × 1/2, $COCH_3$), 5.35 (br t, 1H × 1/2, J = 2.0 Hz, $v_{1/2}$ = 7.0 Hz, H-10), 5.38 (br d, 1H × 1/2, J = 3.0 Hz, $v_{1/2}$ = 7.0 Hz, H-1′), 5.55 (br d, 1H × 1/2, J = 3.0 Hz, $v_{1/2}$ = 7.0 Hz, H-1′), 5.62 (br t, 1H × 1/2, J = 2.0 Hz, $v_{1/2}$ = 7.0 Hz, H-10), 6.68 (br d, 1H × 1/2, J = 8.0 Hz, 3′-NH), 6.71 (br d, 1H × 1/2, J = 8.0 Hz, 3′-NH), 7.67 (s, 1H × 1/2, H-6), 7.69 (s, 1H × 1/2, H-6), 13.22 (s, 1H × 1/2, ArOH), 13.35 (s, 1H × 1/2, ArOH). FAB-MS (negative) *m/z*: 577 [(M − H)$^-$].

(±)-1,4-Diaza-9-ethynyl-6,9-dihydroxy-2,3-dimethyl-7,8,9,10-tetrahydronaphthacene-5,12-dione (23) By a similar procedure to that described for the preparation of **7**, the crude product which was obtained from NaH (60% in mineral oil, 32 mg, 0.80 mmol), **6b** (82 mg, 0.40 mmol), and **22** (75 mg, 0.40 mmol) was purified by column chromatography to give a 63% yield (87 mg) of **23** as yellow crystals. mp 293—295 °C ($CHCl_3$–Et_2O). IR (KCl) *v*: 1680, 1630 cm^{-1}. ^{1}H-NMR ($CDCl_3$) δ: 2.10—2.26 (m, 2H, H-8), 2.49 (s, 1H, C≡CH), 2.83 (s, 6H, CH_3 × 2), 2.99—3.28 (m, 4H, H-7 and H-10), 7.67 (s, 1H, H-11), 12.83 (s, 1H, OH-6). Exact MS Calcd for $C_{20}H_{16}N_2O_4$: 348.1108. Found: 348.1103.

(±)-9-Acetyl-1,4-diaza-6,9-dihydroxy-2,3-dimethyl-7,8,9,10-tetrahydronaphthacene-5,12-dione (24) By a similar procedure to that described for the preparation of **11**, the crude product which was obtained from **23** (29 mg, 0.083 mmol), HgO (35 mg, 0.162 mmol), and 3 N H_2SO_4 (0.5 ml) was purified by column chromatography (CH_2Cl_2 : Et_2O = 1 : 1) to give a 99% yield (30 mg) of **24** as yellow crystals. mp 209—211 °C (CH_2Cl_2–Et_2O). IR (KCl) *v*: 1700, 1670, 1630 cm^{-1}. ^{1}H-NMR ($CDCl_3$) δ: 1.95—2.12 (m, 2H, H-8), 2.39 (s, 3H, $COCH_3$), 2.83 (s, 6H, CH_3 × 2), 2.80—3.20 (m, 4H, H-7 and H-10), 7.59 (s, 1H, H-11), 12.75 (s, 1H, OH-6). FAB-MS (negative) *m/z*: 365 [(M − H)$^-$].

(7*RS*,9*RS*)-9-Acetyl-1,4-diaza-6,7,9-trihydroxy-2,3-dimethyl-7,8,9,10-

tetrahydronaphthacene-5,12-dione (25) and (7*RS*,9*SR*)-9-Acetyl-1,4-diaza-6,7,9-trihydroxy-2,3-dimethyl-7,8,9,10-tetrahydronaphthacene-5,12-dione (26) By a similar procedure to that described for the preparation of **17**, the crude product which was obtained from **24** (32 mg, 0.087 mmol), bromine (64 mg, 0.4 mmol), and AIBN (10 mg, 0.061 mmol) was purified by preparative TLC ($CHCl_3$: MeOH = 15 : 1) to give a 28% yield (9.3 mg) of **25** and a 27% yield (9.0 mg) of **26**, each as yellow crystals. **25**: mp 199—202 °C (CCl_4–CH_2Cl_2). IR ($CHCl_3$) ν: 1710, 1680, 1630, 1600 cm^{-1}. ^{1}H-NMR ($CDCl_3$) δ: 2.22 (dd, 1H, J = 14.5, 5.0 Hz, H-8), 2.39 (dt, 1H, J = 14.5, 2.0 Hz, H-8), 2.42 (s, 3H, $COCH_3$), 2.84 (s, 6H, $CH_3 \times 2$), 3.05 (dd, 1H, J = 17.5, 2.0 Hz, H-10), 3.31 (d, 1H, J = 17.5 Hz, H-10), 5.39 (m, 1H, $\nu_{1/2}$ = 7.0 Hz, H-7), 7.76 (s, 1H, H-11), 13.05 (s, 1H, ArOH). FAB-MS (negative) m/z: 381 [$(M-H)^-$]. **26**: mp 136—138 °C (CCl_4–CH_2Cl_2). IR ($CHCl_3$) ν: 1710, 1680, 1630, 1600 cm^{-1}. ^{1}H-NMR ($CDCl_3$) δ: 2.25 (dd, 1H, J = 13.0, 9.0 Hz, H-8), 2.34—2.44 (m, 1H, H-8), 2.40 (s, 3H, $COCH_3$), 2.78—2.90 (m, 1H, H-10), 2.84 (s, 6H, $CH_3 \times 2$), 3.43 (d, 1H, J = 17.0 Hz, H-10), 3.82 (s, 1H, OH-9), 4.06 (s, 1H, OH-7), 5.44 (m, 1H, $\nu_{1/2}$ = 16.0 Hz, H-7), 7.73 (s, 1H, H-11), 13.25 (s, 1H, OH-6). FAB-MS (negative) m/z: 381 [$(M-H)^-$].

1,4-Diaza-4-demethoxy-2,3-dimethyl-11-deoxy-3′-*N*-trifluoroacetyldaunomycin (27) By a similar procedure to that described for the preparation of **21**, a 41% yield (7.1 mg) of **27** was obtained from **20** (16.9 mg, 0.031 mmol), **25** (9.3 mg, 0.024 mmol), TMSOTf (13.8 mg, 0.062 mmol), and molecular sieves 4A (100 mg) as an inseparable 1 : 1 mixture of two diastereomers. mp 178—180 °C (CCl_4–CH_2Cl_2). IR ($CHCl_3$) ν: 1710, 1680, 1630, 1600 cm^{-1}. ^{1}H-NMR ($CDCl_3$) δ: 1.20 (d, 3H × 1/2, J = 6.5 Hz, H-6′), 1.25 (d, 3H × 1/2, J = 6.5 Hz, H-6′), 1.75—2.0 (m, 2H, H-2′), 2.05—2.45 (m, 2H, H-8), 2.32 (s, 3H × 1/2, $COCH_3$), 2.33 (s, 3H × 1/2, $COCH_3$), 2.78 (s, 6H, $CH_3 \times 2$), 3.05—3.30 (m, 2H, H-10), 3.53 (br s, 1H × 1/2, H-4′), 3.62 (br s, 1H × 1/2, H-4′), 4.01—4.40 (m, 2H, H-3′ and H-5′), 5.23 (br t, 1H × 1/2, J = 2.0 Hz, $\nu_{1/2}$ = 7.0 Hz, H-7), 5.28 (br d, 1H × 1/2, J = 3.0 Hz, $\nu_{1/2}$ = 7.0 Hz, H-1′), 5.43 (br d, 1H × 1/2, J = 3.0 Hz, $\nu_{1/2}$ = 7.0 Hz, H-1′), 5.51 (br t, 1H × 1/2, J = 2.0 Hz, $\nu_{1/2}$ = 7.0 Hz, H-7), 7.68 (s, 1H × 1/2, H-11), 7.70 (s, 1H × 1/2, H-11), 12.97 (s, 1H × 1/2, OH-6), 13.11 (s, 1H × 1/2, OH-6). FAB-MS (negative) m/z: 606 [$(M-H)^-$].

References and Notes

1) Reviews on biological activities: S.T. Crooke and S. D. Reich (eds.), "Anthracyclines: Current Status and New Developments," Academic Press, New York, 1980; H. S. E. Khadem (ed.), "Anthracycline Antibiotics," Academic Press, New York, 1982; T. Oki and T. Takeuchi, *Yuki Gosei Kagaku Kyokai Shi*, **40**, 2 (1982); F. Arcamone, *Med. Res. Rev.*, **4**, 153 (1984).
2) Reviews on synthetic studies: *a*) S. Terashima, *Yuki Gosei Kagaku Kyokai Shi*, **40**, 20 (1982); Tetrahedron Symposia-in-Print Number 17, T. R. Kelly (ed.), *Tetrahedron*, **40**, 4537 (1984); M. J. Broadhurst, C. H. Hassall, and G. J. Thomas, *Chem. Ind.* (London), **1985**, 106; K. Krohn, *Angew. Chem. Int. Ed. Engl.*, **25**, 790 (1986); *b*) Y. Tamura and Y. Kita, *Yuki Gosei Kagaku Kyokai Shi*, **46**, 205 (1988).
3) G. Bonadonna and S. Monfardini, *Lancet*, i, **1969**, 837; B. Smith, *Br. Heart J.*, **31**, 607 (1969).
4) N. R. Bachur, S. L. Gordon, and M. V. Gee, *Molec. Pharmacol.*, **13**, 901 (1977); R. A. Newman and M. P. Hacker, "Anthracyclines-Current Status and Future Developments," ed. by G. Mathe, R. Maral and R. DeJager, Masson Publishing USA, Inc., New York, 1983, p. 55.
5) G. L. Tong, D. W. Henry, and E. M. Acton, *J. Med. Chem.*, **22**, 36 (1979); E. M. Acton and G. L. Tong, *ibid.*, **24**, 669 (1981); J. W. Lown, H.-H. Chen, J. A. Plambeck, and E. M. Acton, *Biochem. Pharmacol.*, **28**, 2563 (1979); *idem*, *ibid.*, **31**, 575 (1982); D. W. Cameron, G. I. Feutrill, and P. G. Griffiths, *Tetrahedron Lett.*, **29**, 4629 (1988).
6) F. Arcamone, *Lloydia*, **40**, 45 (1977); S. Neidle, *Nature* (London), **268**, 195 (1977).
7) *a*) F. Arcamone, G. Cassinelli, F. DiMatteo, S. Forenza, M. C. Ripamonti, G. Rivola, A. Vigevani, J. Clardy, and T. McCabe, *J. Am. Chem. Soc.*, **102**, 1462 (1980); G. Cassinelli, F. DiMatteo, S. Forenza, M. C. Ripamonti, G. Rivola, F. Arcamone, A. D. Marco, A. M. Casazza, C. Soranzo, and G. Pratesi, *J. Antibiot.*, **33**, 1468 (1980); *b*) H. Umezawa, Y. Takahashi, M. Kinoshita, H. Naganawa, K. Tatsuta, and T. Takeuchi, *ibid.*, **33**, 1581 (1980); *c*) T. Oki, Y. Matsuzawa, A. Yoshimoto, K. Numata, I. Kitamura, S. Hori, A. Takamatsu, H. Umezawa, M. Ishizuka, H. Naganawa, H. Suda, M. Hamada, and T. Takeuchi, *ibid.*, **28**, 830 (1975); S. Hori, M. Shirai, S. Hirano, T. Oki, T. Inui, S. Tsukagoshi, M. Ishizuka, T. Takeuchi, and H. Umezawa, *Gann*, **68**, 685 (1977).
8) Y. Tamura, M. Kirihara, M. Sasho, S. Akai, J. Sekihachi, R. Okunaka, and Y. Kita, *J. Chem. Soc., Chem. Commun.*, **1987**, 1474; Y. Kita, M. Kirihara, M. Sasho, Y. Fujii, J. Sekihachi, R. Okunaka, Y. Tamura, and K. Shimooka, *Chem. Pharm. Bull.*, **38**, 585 (1990).
9) Y. Tamura, M. Kirihara, J. Sekihachi, R. Okunaka, S. Mohri, T. Tsugoshi, S. Akai, M. Sasho, and Y. Kita, *Tetrahedron Lett.*, **28**, 3971 (1987); Y. Kita, M. Kirihara, J. Sekihachi, R. Okunaka, M. Sasho, S. Mohri, T. Honda, S. Akai, Y. Tamura, and K. Shimooka, *Chem. Pharm. Bull.*, **38**, 1836 (1990).
10) Y. Tamura, M. Sasho, S. Akai, A. Wada, and Y. Kita, *Tetrahedron*, **40**, 4539 (1984); Y. Tamura, M. Sasho, H. Ohe, S. Akai, and Y. Kita, *Tetrahedron Lett.*, **26**, 1549 (1985); Y. Tamura, S. Akai, H. Kishimoto, M. Kirihara, M. Sasho, and Y. Kita, *ibid.*, **28**, 4583 (1987); *idem*, *Chem. Pharm. Bull.*, **36**, 3897 (1988).
11) Y. Kita, M. Kirihara, Y. Fujii, R. Okunaka, S. Akai, H. Maeda, and Y. Tamura, *J. Chem. Soc., Chem. Commun.*, **1990**, 136.
12) Y. T. Pratt and N. L. Drake, *J. Am. Chem. Soc.*, **82**, 1155 (1960).
13) V. Petrow and B. Sturgeon, *J. Chem. Soc.*, **1954**, 570.
14) The weakly basic alkylcerium(III) reagents were shown to be useful for the alkylation of enolizable ketones; T. Imamoto, T. Kusumoto, and M. Yokoyama, *J. Chem. Soc., Chem. Commun.*, **1982**, 1042; T. Imamoto, N. Takiyama, K. Nakamura, T. Hatajima, and Y. Kamiya, *J. Am. Chem. Soc.*, **111**, 4392 (1989).
15) A. S. Kende, Y. Tsay, and J. E. Mills, *J. Am. Chem. Soc.*, **98**, 1967 (1976).
16) For the use of a benzeneboronate intermediate in anthracycline synthesis, see: M. J. Broadhurst, C. H. Hassall, and G. J. Thomas, *J. Chem. Soc., Perkin Trans. 1*, **1982**, 2239; K. Ravichandran, F. A. J. Kerdesky, and M. P. Cava, *J. Org. Chem.*, **51**, 2044 (1986).
17) Y. Kimura, M. Suzuki, M. Matsumoto, R. Abe, and S. Terashima, *Chem. Lett.*, **1984**, 501; *idem*, *Bull. Chem. Soc. Jpn.*, **50**, 423 (1986).
18) J. D. Warren, V. J. Lee, and R. B. Angier, *J. Heterocycl. Chem.*, **16**, 1617 (1979).
19) Relatively small $\nu_{1/2}$ values (7—12 Hz) for 7,9-*cis*-diols and larger $\nu_{1/2}$ values (18—20 Hz) for 7,9-*trans*-diols were reported for the C-7 proton; N. Tanno and S. Terashima, *Chem. Pharm. Bull.*, **31**, 821 (1983); D. Dominguez, R. J. Ardecky, and M. P. Cava, *J. Am. Chem. Soc.*, **105**, 1608 (1983).

Studies on the Constituents of the Bark of *Kalopanax pictus* NAKAI[1)]

Kazuko SANO, Shuichi SANADA, Yoshiteru IDA* and Junzo SHOJI

School of Pharmaceutical Sciences, Showa University, Hatanodai, Shinagawa-ku, Tokyo 142, Japan. *Received September 20, 1990*

Five new compounds, kalopanaxsaponin G (2) and kalopanaxins A (6), B (8), C (11) and D (13), were isolated from the bark of *Kalopanax pictus* together with nine known compounds, kalopanaxsaponins A (1) and B (5), pericarpsaponin P_{J3} (3), hederasaponin B (4), syringin (7), protocatechuic acid (9), coniferin (10), liriodendrin (=*dl*-syringaresinol di-*O*-glucopyranoside) (12), glucosyringic acid (14) and chlorogenic acid (15). The structures of the new compounds were characterized as hederagenin 28-*O*-α-L-rhamnopyranosyl(1→4)-β-D-glucopyranosyl(1→6)-β-D-glucopyranoside (2), ferulylaldehyde (=coniferylaldehyde) 4-*O*-β-D-glucopyranoside (6), coniferin 6′-*O*-(4-*O*-α-L-rhamnopyranosyl)-syringate (8), 2-methoxyhydroquinone 4-*O*-[6-*O*-(4-*O*-α-L-rhamnopyranosyl)-syringyl]-β-D-glucopyranoside (11) and coniferyl alcohol 4-*O*-β-D-apiofuranosyl(1→2)-β-D-glucopyranoside (=coniferin 2′-*O*-β-D-apiofuranoside) (13).

Keywords Araliaceae; *Kalopanax pictus*; saponin; glycoside; triterpenoid; hederagenin; oleanolic acid; kalopanaxin; phenolic compound; phenylpropanoid

The dried bark of *Kalopanax pictus* NAKAI (Japanese name: harigiri) (Araliaceae) has been used as a medicine in China for expelling so-called wind-evil, eliminating wetness, destroying intestinal parasites, promoting blood circulation, and treating paralysis caused by wind and damp, pain along the knee and spine, and pain owing to necrosis and cutaneous fungus.[2)] As for the constituents of this plant, the substances reported so far are as follows: polyacetylenic compounds,[3)] tannin, flavonoid and coumarin glycosides, small amounts of alkaloid, essential oil, resin and starch,[2)] and two hederagenin glycosides, kalopanaxsaponins A and B.[4)] Recently, Shao *et al.* isolated seven triterpenoid saponins including four new ones, namely kalopanaxsaponins C—F, from *K. septemlobus* root collected in China[5a)]: this plant has been thought to be of the same species as *K. pictus* in Japan, as described in their paper. In the course of our phytochemical investigations on Araliaceous plants, we studied the constituents of the bark of *K. pictus* collected in Yamanashi prefecture, Japan. The present paper deals with the isolation and characterization of fifteen compounds from the plant bark.

The fresh bark was extracted with methanol and the extract was treated to afford a saponin fraction (fr-2) and a phenolic fraction (fr-3), and repeated chromatography of the fractions furnished fifteen compounds, **1**—**15**, as described in the experimental section.

Five compounds, **1**—**5**, obtained from fr-2 tested positive in the Liebermann–Burchard reaction and showed strong hydroxyl absorption in the infrared (IR) spectra. Further, the IR spectra of **2**—**5** showed ester absorption (1725 cm^{-1}),

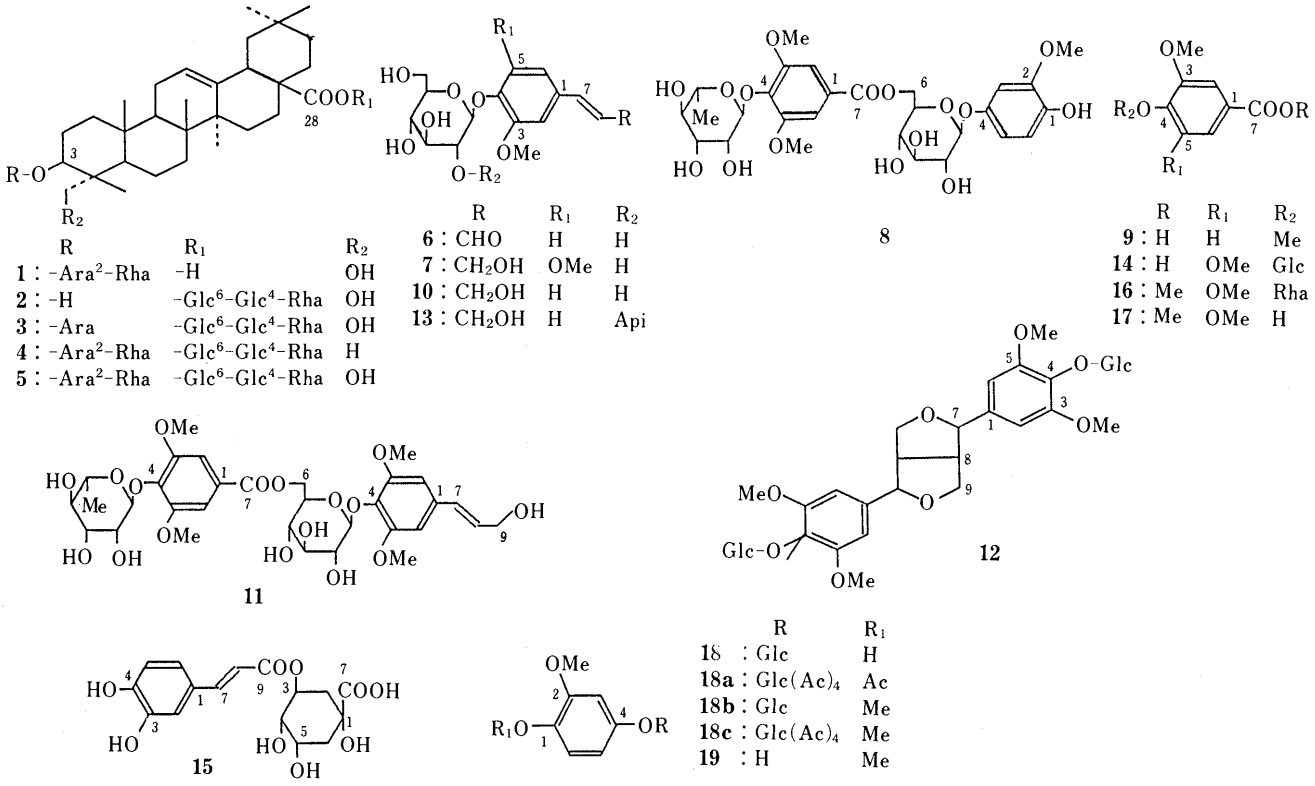

Chart 1. Structures of the Compounds

TABLE I. ^{13}C-NMR Signals of Saponins **1**—**5** in Pyridine-d_5

	1	2	3	4	5
Aglycone					
C-1	39.0	38.9	38.8	38.9	39.1
2	26.2	27.7	26.0	28.1	26.2
3	81.1	73.5	82.0	88.8	81.1
4	43.5	42.9	43.5	39.5	43.5
5	47.8	48.7	47.6	55.9	47.8
6	18.2	18.7	18.2	18.5	18.2
7	32.9	32.6	32.6	32.7	32.6
8	39.8	39.9	39.9	39.9	39.9
9	48.2	48.2	48.2	48.1	48.2
10	36.9	37.3	36.9	37.1	36.9
11	23.8	23.8	23.7	23.7	23.7
12	122.6	122.9	122.9	122.4	122.9
13	144.8	144.1	144.1	144.1	144.1
14	42.2	42.2	42.1	42.2	42.2
15	28.4	28.4	28.3	28.1	28.3
16	23.8	23.5	23.4	23.4	23.4
17	46.7	47.0	47.0	47.1	47.1
18	42.0	41.7	41.7	41.7	41.7
19	46.4	46.2	46.2	46.4	46.2
20	31.0	30.7	30.7	30.8	30.8
21	34.3	34.1	34.0	34.1	34.1
22	33.3	32.9	32.6	33.2	32.8
23	64.1	67.9	64.5	28.1	64.0
24	14.0	13.1	13.6	17.0	14.0
25	16.1	16.1	16.3	15.7	16.2
26	17.4	17.6	17.6	17.5	17.6
27	26.2	26.1	26.0	26.0	26.0
28	180.0	176.5	176.5	176.5	176.5
29	33.3	33.1	33.1	33.2	33.1
30	23.8	23.7	23.7	23.7	23.7

	1	2	3	4	5
Sugars at C-3 of aglycone					
Ara-1	104.3	—	106.6	104.7	104.3[a]
2	75.8	—	73.1	75.9	75.9
3	74.7	—	74.7	73.6	74.6
4	69.3	—	69.6	68.5	69.2
5	65.7	—	67.0	64.7	65.5
Rha-1	101.7	—	—	101.2	101.7
2	72.4	—	—	72.3	72.3[b]
3	72.6	—	—	72.5	72.5[b]
4	74.1	—	—	73.9	74.1
5	69.7	—	—	69.9	69.7
6	18.6	—	—	18.5	18.5
Sugars at C-28 of aglycone					
Glc-1		95.6	95.6	95.6	95.6
2		75.3	75.3	75.3	75.3
3		78.3	78.2	78.3	78.4
4		70.3	70.3	70.3	70.3[c]
5		76.5	76.5	76.5	76.5
6		70.9	70.9	70.9	70.9
Glc-1		104.8	104.8	104.7	104.8[a]
2		73.9	73.9	73.9	74.0
3		78.0	78.1	78.1	78.0
4		78.7	78.7	78.7	78.7
5		77.1	77.1	77.1	77.1
6		61.3	61.3	61.3	61.3
Rha-1		102.7	102.7	102.7	102.7
2		72.5	72.6	72.5	72.5[b]
3		72.7	72.7	72.7	72.5[b]
4		73.8	73.9	73.9	74.0
5		69.2	69.2	69.3	69.2[c]
6		18.5	18.5	18.5	18.5

a—*c*) Assignments with the same superscript in each column may be interchanged.

while that of **1** showed carboxylic absorption (1700 cm^{-1}). On acid hydrolysis, they provided the following aglycones and sugar components: arabinose, rhamnose and hederagenin from **1**; glucose, rhamnose and hederagenin from **2**; arabinose, rhamnose, glucose and hederagenin from **3** and **5**; arabinose, rhamnose, glucose and oleanolic acid from **4**. Their ^{13}C-nuclear magnetic resonance (^{13}C-NMR) spectra indicated that there are two sugar units in **1**, three in **2**, four in **3**, and five in **4** and **5** (Table I). Further, the C-3 signal of **1**, **3**, **4** and **5** appeared at lower field and the C-28 signal of **2**, **3**, **4** and **5** at higher field than those of oleanolic acid, because of glycosylation shifts. Hence, they were deduced to be hederagenin 3- and 28-monodesmoside (**1** and **2**), and hederagenin and oleanolic acid 3,28-bisdesmosides (**3**, **5** and **4**).

On alkaline hydrolysis, **5** afforded **1** as its prosapogenin and an oligosaccharide, which afforded glucose and rhamnose on acidic hydrolysis. In addition, analysis of the ^{13}C-NMR spectra of the saponins was carried out, and the saponins **1**, **5**, **3** and **4** were deduced to be identical with kalopanaxsaponins A and B,[4,6] pericarpsaponin P_{J3}[7] and hederasaponin B,[8] respectively. Of them, saponin **5** was shown to be identical with pericarpsaponin P_K[7] (=kalopanaxsaponin B) by direct comparison.

The new saponin named kalopanaxsaponin G (**2**) was shown to be a hederagenin trisaccharide composed of glucose and rhamnose as described above. In the ^{13}C-NMR spectrum of **2**, with respect to those of **1**, **3**, **4** and **5**, the C-28 carboxyl carbon signal appeared at the lower field (−3.9 ppm) than that of hederagenin due to the glycosylation shift although the C-3 and C-23 signals showed no such down-field shift, and the carbon signals due to the sugar moiety were superimposable on those of the trisaccharide moiety in **4** and **5** (Table I). Hence, the structure of **2** was characterized as hederagenin 28-*O*-α-L-rhamnopyranosyl(1→4)-β-D-glucopyranosyl(1→6)-β-D-glucopyranoside.

The remaining ten compounds (**6**—**15**) showed hydroxyl and aromatic absorptions in their IR spectra. Of them, seven were characterized as follows, mainly on the basis of coincidence of their physical and chemical properties with those reported: syringin (**7**),[9] protocatechuic acid (**9**), coniferin (**10**),[10] (±)-syringaresinol di-*O*-glucopyranoside (=liriodendrin, **12**),[11] glucosyringic acid (**14**)[9] and chlorogenic acid (**15**). The other four were found to be new compounds, and were named kalopanaxins A (**6**), B (**8**), C (**11**) and D (**13**).

Kalopanaxin A (**6**) showed hydroxyl, aldehyde and aromatic absorptions in its IR spectrum. The ^{13}C-NMR spectrum of **6** exhibited signals due to a methoxyl, an aldehyde, two vinylic and six aromatic carbon atoms, and six signals ascribable to a β-D-glucopyranosyl moiety (Table II), as seen in the spectrum of **12**. The ^{1}H-NMR spectrum showed a methoxyl signal at δ 3.83 and two sets of AMX-type signals, one at δ 7.14 (d, J=8 Hz), 7.29 (dd, J=1, 8 Hz) and 7.40 (d, J=1 Hz), and the other at δ 6.83 (dd, J=8, 16 Hz), 7.66 (d, J=16 Hz) and 9.63 (d, J=8 Hz). Therefore, **6** appeared to be feruloyl (=coniferyl) aldehyde

4-*O*-*β*-D-glucopyranoside. This was proved by chemical conversion of **6** to **10**.

Kalopanaxin B (**8**) showed IR absorption bands due to hydroxyl, ester and aromatic groups. On alkaline treatment in methanol, **8** afforded two products. One was identical with **10**. The other (**16**) showed similar IR absorptions to **8**. The ^{13}C-NMR spectrum of **16** exhibited signals due to an α-L-rhamnopyranosyl moiety, a syringoyl group and a methoxyl carbon (Table II). On acid hydrolysis, **16** gave rhamnose and an aglycone (**17**), which was identical with methyl syringate prepared from **14**.[5b] Accordingly, **16** was identified as methyl syringate 4-*O*-α-L-rhamnopyranoside. On comparison of the ^{13}C-NMR spectra of **8** and **10**, the glucosyl C-6 signal (δ 64.7) of **8** appeared at lower field by 4 ppm than that of **10** (Table II). Consequently, **8** was deduced to be coniferin 6′-*O*-(4-*O*-α-L-rhamnopyranosyl)-syringate.

Kalopanaxin C (**11**) also showed hydroxyl, ester and aromatic absorption bands in its IR spectrum. On alkaline treatment, **11** gave two products. One was identified as **16**. The other (**18**) tested positive in the ferric chloride reaction, and its ^{1}H-NMR spectrum showed the presence of a methoxyl group (δ 3.73) and a 1,2,4-trisubstituted benzene ring (AMX-type signals at δ 6.45, 6.67 and 6.69) in the molecule. The ^{13}C-NMR spectrum of **18** exhibited signals due to a *β*-D-glucopyranosyl moiety (Table II). On acetylation, **18** afforded a penta-acetate (**18a**), which showed no hydroxyl absorption in its IR spectrum. On methylation with diazomethane, **18** gave a dimethyl ether (**18b**), which gave a tetra-acetate (**18c**) under usual acetylation conditions. Accordingly, **18** was concluded to be the glucoside of a monomethylether of 1,2,4-trihydroxybenzene. The location of the substituents on the benzene ring was established by means of the nuclear Overhauser effect (NOE) between aromatic and methoxyl protons of **18a** and **18c**. In the case of **18a**, irradiation of the methoxyl protons at δ 3.79 (3H, s) caused enhancement (18%) of a doublet signal with a *meta*-couping value (J=3 Hz) at δ 6.65 due to the C-3 proton of the benzene ring. For **18c**, irradiation of the methoxyl protons at δ 3.84 (6H, s) caused enhancements (20% each) of the doublet signals at δ 6.61 (J=2 Hz) and δ 6.77 (J=8 Hz) due to the C-3 and C-6 protons, respectively. Hence, **18** was assumed to be 2-methoxy-1,4-hydroquinone 4-*O*-*β*-D-glucopyranoside. This was proved as follows. On acidic hydrolysis, **18b** afforded glucose and an aglycone (**19**), which was identical with 3,4-dimethoxyphenol prepared from vanillin by the Beyer–Villiger oxidation.[12] On comparison of the ^{13}C-NMR spectrum of **11** with that of **18**,

Table II. ^{13}C-NMR Signals of Phenolic Compounds in DMSO-d_6

	7	6	10	13	8	16	14	11	18	15
	SRN	CNA	CNI	CNI	CNI			HDQ	HDQ	FRA
C-1	132.9	128.5	131.1	131.0	131.4			141.5	141.4	125.7
2	104.6	112.0	110.1	109.7	110.2			150.5	150.8	114.4
3	152.8	149.1	149.1	148.9	149.1			102.7	102.6	148.4
4	134.0	148.8	146.0	145.8	145.8			147.8	147.8	145.6
5	152.8	115.6	115.4	115.1	115.3			115.1	115.3	115.8
6	104.6	123.2	119.1	118.9	118.8			107.7	108.1	121.4
7	130.3	153.8	129.0	129.0	129.3			—	—	145.0
8	128.7	126.7	128.5	128.4	128.5			—	—	114.8
9	61.7	195.6	61.7	61.6	61.8			—	—	165.8
OMe	56.6[a]	56.0	55.8	55.6	55.9			55.5	55.6	—
	Glc	Glc	Glc	Glc	Glc			Glc	Glc	QNA
1	102.8	99.9	100.1	98.5	99.9			104.4	101.8	73.6
2	77.3	73.1	73.3	76.9	73.4			73.3	73.4	36.4
3	74.4	76.2	76.9	75.1	76.7			76.4	76.8	70.9
4	70.1	69.7	69.8	70.0	70.5			70.3	70.1	68.2
5	76.7	76.6	77.0	77.2	74.1			73.8	77.4	70.5
6	61.1	60.8	60.8	60.7	64.7			64.7	60.9	37.3
7										174.9
	Api				SGA	SGA	SGA	SGA		
C-1	108.3				125.5	126.3	132.9	125.3		
2	76.1				106.9	107.2	107.7	106.6		
3	79.4				153.2	153.7	152.8	153.0		
4	74.0				138.7	138.8	138.6	138.5		
5	64.5				153.2	153.7	152.8	153.0		
6	—				106.9	107.2	107.7	106.6		
7	—				165.3	167.3	167.6	165.2		
OMe	—				56.5	57.0	56.9	56.2		
OMe	—				56.5	57.0	56.9	56.2		
						53.4				
					Rha	Rha	Glc	Rha		
1					102.3	102.7	102.5	102.2		
2					70.5	71.0	74.6	70.3		
3					70.5	71.0	76.9	70.3		
4					71.9	71.3	70.3	71.7		
5					70.8	71.3	77.6	70.6		
6					18.0	18.3	61.3	17.8		

SRN, syringin; CNA, coniferyl aldehyde; CNI, coniferyl alcohol; SGN, 5-OMe-coniferin; SGA, syringic acid; HDQ, 2-OMe-hydroquinone; FRA, ferulic acid.
a) Doubled.

an acylation shift was observed at the glucosyl C-6 signal (+3.8 ppm), as in the case of **8**. Consequently, the structure of **11** was characterized as 2-methoxyhydroquinone 4-*O*-[6-*O*-(4-*O*-α-L-rhamnopyranosyl)-syringoyl]-β-D-glucopyranoside.

Kalopanaxin D (**13**) showed IR absorption bands due to hydroxyl and aromatic moieties, and ^{13}C-NMR signals due to a coniferyl moiety and two anomeric carbons (Table II), showing **13** to be a glycoside of coniferyl alcohol with two monosaccharide units. Enzymatic hydrolysis of **13** with pectinase furnished glucose and apiose, while mild acid hydrolysis of **13** provided coniferin (**10**). Therefore, **13** was supposed to be an apioside of coniferin. The carbon signal due to the glucopyranosyl C-2 in **13** appeared at lower field by 4 ppm than that of **10**, and the apiosyl group was supposed to be located at C-2 of the glucopyranosyl moiety, as in the case of apiin (=apigenin 7-*O*-β-D-apiofuranosyl-(1→2)-β-D-glucopyranoside).[13] In the ^{13}C-NMR spectra of **13** and apiin, the signals due to the sugar moieties resembled each other quite closely. Accordingly, **13** was deduced to be coniferyl alcohol 4-*O*-β-D-apiofuranosyl-(1→2)-β-D-glucopyranoside.

As mentioned above, five saponins and ten phenolic compounds including five new compounds (**2**, **6**, **8**, **11** and **13**) were isolated from the bark of *K. pictus* and were characterized. The new saponin (**2**) is a very rare example of an ester glycoside of oleanolic acid possessing no sugar moiety at the C-3 hydroxyl group, and two of the new phenolic glycosides (**8** and **11**) are remarkable in that they consist of two phenolic glycoside moieties linked together by an ester linkage. Compounds **12** and **7**, obtained in good yield here, were reported to show preventive activity against the stress-induced changes in mice.[14]

It is still necessary to survey the saponin constituents of the root of *K. pictus* and the bark of *K. septemlobus* from the chemotaxonomical point of view.

Experimental

The melting points were determined on a Yanaco micro-melting point apparatus (hot-stage type) and are uncorrected. Optical rotations were measured with a JASCO DIP-140 polarimeter at room temperature (20—25 °C). The IR spectra were taken with a Hitachi EPI-2 spectrometer. The NMR spectra were recorded with a JEOL JNM FX-100 apparatus (100 MHz for ^{1}H-NMR, 25MHz for ^{13}C-NMR) and chemical shifts are given on the δ (ppm) scale with tetramethylsilane as an internal standard. Gas-liquid chromatography (GLC) was run on a Shimadzu GC-6A unit equipped with a flame ionization detector. GLC conditions: column, 5% SE-52 on Chromosorb W (3 mm × 2 m); column temperature, 175 °C; injection temperature, 220 °C; carrier gas, N_2 (1.0 kg/cm^2). Thin-layer chromatography (TLC) was performed on precoated Kieselgel 60 F_{254} plates (Merck) using $CHCl_3$–MeOH–H_2O (70 : 30 : 5, v/v), and detection was achieved by spraying 10% H_2SO_4 followed by heating. Silica gel used for column chromatography was Wako-gel C-200 (Wako Pure Chemical Ind. Co.).

Extraction and Isolation of Saponins from the Bark The fresh bark (without the cork layer, 11.0 kg) of *K. pictus* collected at Narusawa in Yamanashi prefecture, Japan, in June 1982, was chopped after being dried in the air for one week, and extracted with 70% MeOH (15 l × 3) under reflux. The MeOH extract was evaporated to dryness *in vacuo*. The residue (1.96 kg) was suspended in water, and the suspension was extracted with Et_2O and then with BuOH saturated with H_2O. The extracts were concentrated *in vacuo* to give an Et_2O extract (362 g) and a BuOH extract (859 g), respectively. The aqueous layer was subjected to column chromatography on Amberlite XAD-2 eluted first with water and then with MeOH. The MeOH eluate (220 g) and the BuOH extract were combined, followed by evaporation of the solvent, and the residue was subjected to column chromatography on Sephadex LH-20 with MeOH to yield four fractions: fr-**1** (13 g), **2** (595 g) **3** (334 g) and **4** (87 g). Fraction-**2** was repeatedly chromatographed on silica gel columns ($CHCl_3$–MeOH–H_2O (70 : 30 : 5, v/v)) or on Lichroprep RP-8 columns (Merck) (aqueous MeOH) to afford five saponins **1** (50.8 g), **2** (365 mg), **3** (12.9 g), **4** (10.3 g) and **5** (400 g). Fraction-**3** was chromatographed on a silica gel column with $CHCl_3$–MeOH–H_2O (70 : 20 : 2) to give **6** (0.35 g), **7** (1.58 g), **8** (0.71 g), **10** (1.60 g), **11** (1.50 g), **12** (28.9 g), **13** (2.80 g) and **14** (0.17 g). Fraction-**4** was subjected to Toyopearl HW-40 column chromatography with 30% MeOH to give **9** (1.10 g) and **15** (0.54 g).

1: Colorless needles (MeOH), mp 265—268 °C (dec.), $[\alpha]_D$ +18.2° (c=0.3, MeOH) [lit.[6] mp 256—259 °C (dec.), $[\alpha]_D$ +15°]. IR (KBr) cm^{-1}: 3400 (OH), 1700 (COOH). ^{13}C-NMR (Table I): the signals were identical with those reported for clematissaponin CP_{3b} (=kalopanaxsaponin A).[6a] *Anal.* Calcd for $C_{41}H_{66}O_{12}\cdot H_2O$: C, 64.04, H, 8.91. Found: C, 63.46; H, 8.71.

2: Colorless needles (aqueous EtOH), mp 213—215 °C (dec.), $[\alpha]_D$ −2.8° (c=0.3, MeOH). IR (KBr) cm^{-1}: 3300 (OH), 1725 (COOR). ^{13}C-NMR: Table I. *Anal.* Calcd for $C_{48}H_{78}O_{18}\cdot 0.5H_2O$: C, 60.55; H, 8.36. Found: C, 60.78; H, 8.50.

3: A white powder (iso-PrOH), (mp 210—215 °C (dec.)), $[\alpha]_D$ −0.2° (c=0.3, MeOH) [lit.[6d] mp 211—213 °C]. IR (KBr) cm^{-1}: 3400 (OH), 1725 (COOR). ^{13}C-NMR (Table I): the signals due to the sugar moiety at C-28 were super-imposable on those of **5**, and those due to the arabinosyl moiety at C-3 were coincident with those reported for clematissaponin CP_1 (=pericarpsaponin P_{J3}).[6a] *Anal.* Calcd for $C_{53}H_{86}O_{22}\cdot 2H_2O$: C, 57.28; H, 8.16. Found: C, 57.46; H, 8.26.

4: A white powder (iso-PrOH), (mp 210—220 °C (dec.)), $[\alpha]_D$ −29.3° (c=0.8, MeOH). IR (KBr) cm^{-1}: 3400 (OH), 1725 (COOR). ^{13}C-NMR (Table I): the signals resembled those reported for hederasaponin B.[5b] *Anal.* Calcd for $C_{59}H_{96}O_{25}\cdot 2.5H_2O$: C, 56.67; H, 8.14. Found: C, 56.68; H, 8.06.

5: A white powder (iso-PrOH), (mp 226—229 °C (dec.)), $[\alpha]_D$ +20.0° (c=0.7, MeOH) [lit.[6] mp 212—215 °C (dec.), $[\alpha]_D$ +18°]. IR (KBr) cm^{-1}: 3400 (OH), 1725 (COOR). ^{13}C-NMR (Table I): the signals were in accordance with those reported for kalopanaxsaponin B.[5a] Compound **5** was identified as pericarpsaponin P_K (=kalopanaxsaponin B)[7] by direct comparison. *Anal.* Calcd for $C_{59}H_{96}O_{26}\cdot 2.5H_2O$: C, 55.95; H, 8.04. Found: C, 56.04; H, 8.05.

6: Colorless needles (H_2O), mp 209—211 °C, $[\alpha]_D$ −39.3° (c=0.3, pyridine). IR (KBr) cm^{-1}: 3360, 1660, 1590, 1510, 1460. ^{1}H-NMR (DMSO-d_6): 3.83 (3H, s), 6.83 (1H, dd, J=8, 16 Hz), 7.14 (1H, d, J=8 Hz), 7.29 (1H, dd, J=1, 8 Hz), 7.40 (1H, d, J=1 Hz), 7.66 (1H, d, J=16 Hz), 9.63 (1H, d, J=8 Hz). ^{13}C-NMR: Table II. *Anal.* Calcd for $C_{16}H_{20}O_8$: C, 56.47; H, 5.92. Found: C, 56.08; H, 5.85. Reduction of **6** with $NaBH_4$ yielded an alcohol, mp 192—193 °C, which was identified as **10**.

7: Colorless needles (H_2O), mp 192—193 °C, $[\alpha]_D$ −21.4° (c=1.3, MeOH) [lit.[9] mp 190—191 °C, $[\alpha]_D$ −21.8°]. ^{1}H-NMR (DMSO-d_6): 3.77 (3H, s), 4.11 (2H, br t, J=5 Hz), 6.30 (1H, dt, J=5, 17 Hz), 6.50 (1H, d, J=17 Hz), 6.73 (2H, s). ^{13}C-NMR: Table II. *Anal.* Calcd for $C_{17}H_{24}O_9$: C, 54.83; H, 6.50. Found: C, 54.75; H, 6.50. **7** Acetate: Colorlss needles (dil. MeOH), mp 112—114 °C. MS: m/z 582 (M^+, $C_{27}H_{34}O_{14}$). Compound **7** was identified as syringin by direct comparison with an authentic specimen.

8: Colorless needles (H_2O), mp 183 °C, $[\alpha]_D$ −74.9° (c=0.3, pyridine). IR (KBr) cm^{-1}: 3360, 1705, 1590, 1510. ^{1}H-NMR (DMSO-d_6): 1.40 (2H, d, J=6.3 Hz), 3.76 (3H, s), 3.78 (6H, s), 4.09 (2H, t, J=5 Hz), 6.18 (1H, dt, J=16, 5 Hz), 6.43 (1H, d, J=16 Hz), 6.57 (1H, dd, J=1.5, 8 Hz), 6.99 (1H, d, J=8 Hz), 7.03 (1H, d, J=1.5 Hz), 7.24 (2H, s). ^{13}C-NMR: Table II. *Anal.* Calcd for $C_{31}H_{40}O_{16}$: C, 55.69; H, 6.03. Found: C, 55.77; H, 6.04.

9: Colorless needles (H_2O), mp 196—198 °C (dec.). Positive in the $FeCl_3$ reaction: Bluish green. MS: m/z 154 (M^+, $C_7H_6O_4$). IR (KBr) cm^{-1}: 3200, 1670, 1595, 1520, 1460. ^{1}H-NMR (DMSO-d_6): 6.78 (1H, d, J=8 Hz), 7.29 (1H, dd, J=2, 8 Hz), 7.34 (1H, d, J=2 Hz), 9.45 (2H, br s). *Anal.* Calcd for $C_7H_6O_4$: C, 54.55; H, 3.92. Found: C, 54.35; H, 3.86. **9** Acetate: Colorless needles (dil. MeOH), mp 159—160 °C. MS: m/z 238 (M^+, $C_{11}H_{10}O_6$). ^{1}H-NMR ($CDCl_3$): 2.31 (6H, s), 7.41 (1H, d, J=8 Hz), 7.82 (1H, d, J=1.5 Hz), 7.86 (1H, dd, J=8, 1.5 Hz). Compound **9** was identified as protocatechuic acid by direct comparison with a commercially available sample [Wako Pure Chemical Ind. Co.].

10: Colorless needles (H_2O), mp 186—188 °C, $[\alpha]_D$ −63.9° (c=0.3, MeOH) [lit.[10] mp 187 °C, $[\alpha]_D$ −60.0°]. IR (KBr) cm^{-1}: 3300, 1595, 1510, 1460. ^{1}H-NMR (DMSO-d_6): 3.78 (3H, s), 4.09 (2H, br t, J=5 Hz), 4.52 (1H, t, J=5 Hz), 6.25 (1H, dt, J=17, 5 Hz), 6.50 (1H, d, J=17 Hz), 6.89 (1H, dd, J=1.5, 8 Hz), 7.03 (1H, d, J=8 Hz), 7.05 (1H, d, J=1.5 Hz). ^{13}C-NMR: Table II. *Anal.* Calcd for $C_{16}H_{22}O_8$: C, 56.14; H, 6.48. Found: C, 56.14; H, 6.43. **10** Acetate: Colorless needles (dil. MeOH), mp 105—

107 °C [lit.[11b] mp 115 °C]. MS: *m/z* 552 (M^+, $C_{26}H_{32}O_{13}$). Compound **10** was identified as coniferin by direct comparison with an authentic sample.

11: Colorless needles (H_2O), mp 129—130 °C, $[\alpha]_D$ −65.1° (*c*=0.3, pyridine). IR (KBr) cm^{-1}: 3400, 1700, 1690, 1505, 1455. ^{1}H-NMR (DMSO-d_6): 1.08 (3H, d, *J*=6 Hz), 3.66 (3H, s), 3.79 (3H, s), 6.48 (2H, br s), 6.56 (1H, br s), 7.23 (2H, s), 8.49 (1H, s). ^{13}C-NMR: Table II. *Anal.* Calcd for $C_{28}H_{36}O_{16}$: C, 53.50; H, 5.77. Found: C, 53.24; H, 5.80.

12: Colorless needles (H_2O), mp 255 °C. IR (KBr) cm^{-1}: 3340, 1592, 1502, 1420. ^{13}C-NMR: the signals resemble those reported for (+)-syringaresinol di-*O*-β-D-glucopyranoside.[7,11a] *Anal.* Calcd for $C_{34}H_{46}O_{18}\cdot 2H_2O$: C, 52.44: H, 6.44. Found: C, 52.43; H, 6.47. Compound **12** was characterized as a mixture of di-*O*-β-D-glucopyranosides of (+)- and (−)-syringaresinol based on the following evidence. Fractional recrystallization of **12** from water afforded two isomeric compounds, **12a**, mp 248—258 °C, $[\alpha]_D$ +3.2° (*c*=0.3, pyridine) [lit.[11a] mp 258 °C, $[\alpha]_D$ ±0°] and **12b**, mp 210—220 °C, $[\alpha]_D$ −65.2° (*c*=0.2, pyridine) [lit.[11b] mp 245—47 °C, $[\alpha]_D$ −33°]. Enzymatic hydrolysis of **12a** and **12b** with pectinase gave **12a-ag** and **12b-ag** as the individual aglycone, which showed similar spectral data (IR and NMR) to those reported for (+)-syringaresinol.[7,11a] **12a-ag**, colorless needles (MeOH), mp 185—190 °C, $[\alpha]_D$ +50.6° (*c*=0.3, $CHCl_3$) [(+)-syringaresinol,[11a] mp 183.5 °C, $[\alpha]_D$ +44.0°]. **12b-ag**, colorless needles (MeOH), mp 185—190 °C, $[\alpha]_D$ −39.5° (*c*=0.4, $CHCl_3$) [(−)-syringaresinol,[11b] mp 170—172 °C, $[\alpha]_D$ −21.5°].

13: Colorless needles (H_2O), mp 128—130 °C, $[\alpha]_D$ +110.8° (*c*=0.3, pyridine). IR (KBr) cm^{-1}: 3300, 1585, 1510, 1460. ^{1}H-NMR (DMSO-d_6): 3.77 (3H, s), 4.07 (2H, d, *J*=5 Hz), 4.94 (1H, br d, *J*=7 Hz), 5.41 (1H, s), 6.24 (1H, dt, *J*=17, 5 Hz), 6.49 (1H, d, *J*=17 Hz), 6.87 (1H, dd, *J*=2, 8 Hz), 7.00 (1H, d, *J*=8 Hz), 7.05 (1H, d, *J*=2 Hz). ^{13}C-NMR: Table II. *Anal.* Calcd for $C_{21}H_{30}O_{12}\cdot H_2O$: C, 51.22; H, 6.55. Found: C, 51.42; H, 6.08.

14: Colorless needles (MeOH–Et_2O), mp 219—221 °C (dec.) [lit.[9a] mp 212 °C (dec.)], $[\alpha]_D$ −15.2° (*c*=0.3, MeOH). IR (KBr) cm^{-1}: 3400, 1660, 1590, 1500, 1460. ^{1}H-NMR (DMSO-d_6): 3.81 (3H, s), 5.14 (1H, br d, *J*=4 Hz), 7.23 (2H, s), ^{13}C-NMR (DMSO-d_6): Table II. *Anal.* Calcd for $C_{15}H_{20}O_{10}$: C, 50.0; H, 5.60. Found; C, 50.01; H, 5.59. **14** was identical with authentic glucosyringic acid, mp 218—221 °C (dec.), prepared from **7**.[9b]

15: Colorless needles (H_2O), mp 208—209 °C, $[\alpha]_D$ −36.6° (*c*=0.3, MeOH). Positive in the $FeCl_3$ reaction (bluish green). IR (KBr) cm^{-1}: 3280, 1680, 1630, 1590, 1510, 1440. ^{1}H-NMR (DMSO-d_6): 1.89 (4H, m), 3.57 (1H, dd, *J*=3, 7 Hz), 3.93 (1H, m), 5.07 (1H, br d, *J*=7 Hz), 6.14 (1H, d, *J*=16 Hz), 6.76 (1H, d, *J*=8 Hz), 7.00 (1H, dd, *J*=2, 8 Hz), 7.03 (1H, d, *J*=2 Hz), 7.42 (1H, d, *J*=16 Hz), 9.13, 9.57, 12.40 (1H each, s). ^{13}C-NMR: Table II. *Anal.* Calcd for $C_{16}H_{18}O_9$: C, 54.24; H, 5.12. Found: C, 54.13; H, 5.18. Compound **15** was identified as chlorogenic acid by direct comparison with an authentic sample commercially available [Aldrich Chem. Co.].

Acid Hydrolysis of the Saponins (1—5) The saponins were individually subjected to hydrolysis under heating in 2 N HCl in 50% aqueous dioxane on a boiling water bath for 4 h. The reaction mixture was extracted with $CHCl_3$. The $CHCl_3$ layer was worked up in the usual manner, followed by evaporation of the solvent to afford an aglycone. The aglycone (colorless prisms, mp >300 °C; diacetate: colorless needles, mp 172—174 °C) obtained from **1**, **2**, **3** and **5** was identified as hederagenin, and the aglycone (colorless needles, mp 294—295 °C) from **4** was identified as oleanolic acid, by direct comparison with authentic samples. The aqueous layer of the hydrolysate was neutralized with Ag_2CO_3 followed by filtration, and the filtrate was concentrated to dryness *in vacuo*. The residue was examined both on TLC and GLC, and the following sugar components were detected: arabinose (ara), rhamnose (rha) and glucose (glc) from **3**, **4** and **5**; rha and glc from **2**; ara and rha from **1**. TLC, *Rf*: 0.31 (rha), 0.19 (ara), 0.14 (glc). GLC of the tetramethylsilane derivatives, t_R: 3.6, 4.8 (rha), 3.5, 4.0, 4.5 (ara), 11.4, 17.5 (glc).

Alkaline Hydrolysis of 5 Compound **5** (400 mg) was heated at 90 °C with 5% aqueous KOH (20 ml) for 2 h. The reaction mixture was neutralized with 2 N HCl and extracted with BuOH. The BuOH layer was concentrated to dryness *in vacuo*, and the residue was purified by silica gel column chromatography ($CHCl_3$–MeOH–H_2O (80 : 20 : 1, v/v)) to give a prosapogenin (210 mg), colorless needles from MeOH, mp 265—268 °C, $[\alpha]_D$ −10.3° (*c*=0.3, MeOH), which was identified as **1**. Inorganic compounds in the aqueous layer were removed by Sephadex LH-20 column chromatography (MeOH) and the eluate was evaporated to dryness *in vacuo*. The residue was hydrolyzed and the products were examined as described above, and glucose and rhamnose were detected.

Methanolysis of 8 Compound **8** (100 mg) was treated with 0.2% methanolic potassium carbonate under stirring for 30 min at room temperature. After removal of inorganic salts by Sephadex LH-20 chromatography (MeOH), the reaction product was partitioned between EtOAc and water. The product (45 mg), colorless needles (H_2O), mp 186—187 °C, obtained from the aqueous layer was identified as **10**. The product (**16**, 52 mg) from the EtOAc layer: colorless needles (EtOAc), mp 89—91 °C, $[\alpha]_D$ −102.0° (*c*=0.3, pyridine). *Anal.* Calcd for $C_{16}H_{22}O_9$: C, 53.63; H, 6.19. Found: C, 53.44; H, 6.15. IR (KBr) cm^{-1}: 3250, 1705, 1590, 1500, 1460. ^{1}H-NMR (DMSO-d_6+D_2O, 400 MHz): 1.01 (3H, d, *J*=5.2 Hz), 3.29 (1H, t, *J*=9.5 Hz), 3.70 (1H, dd, *J*=3.3, 9.5 Hz), 3.83 (6H, s), 3.86 (3H, s), 3.92 (1H, m), 3.96 (1, dd, *J*=1.5, 3.3 Hz), 3.99 (1H, dd, *J*=5.2, 9.5 Hz), 5.21 (1H, dd, *J*=1.5 Hz), 7.27 (2H, s). ^{13}C-NMR: Table II.

Acid Hydrolysis of 16 Compound **16** (30 mg) was refluxed wih 2 N HCl in 50% aqueous dioxane for 1 h to provide a sugar and an aglycone (**17**, 15 mg), colorless needles, mp 104—105 °C. MS: *m/z* 212 (M^+, $C_{10}H_{12}O_5$). IR (KBr) cm^{-1}: 3400, 1710, 1600, 1500. ^{1}H-NMR (DMSO-d_6): 3.60 (3H, s), 3.95 (6H, s), 5.92 (1H, s), 7.33 (2H, s). Compound **17** was identified as methyl syringate prepared from **14** by methylation with diazomethane, followed by acidic hydrolysis. The sugar was identified as rhamnose, as described above.

Methanolysis of 11 Compound **11** (100 mg) was treated in the same way as described for **8** to afford two products from the EtOAc and the aqueous layers. The one (59 mg), colorless needles (EtOAc), mp 89—91 °C, obtained from the EtOAc layer was identified as **16**. The other (**18**, 38 mg) from the aqueous layer, colorless needles (MeOH), mp 207 °C. IR (KBr) cm^{-1}: 3400, 1610, 1510, 1450. ^{1}H-NMR (DMSO-d_6): 3.73 (3H, s), 6.45 (1H, dd, *J*=2.5, 9 Hz), 6.67 (1H, d, *J*=9 Hz), 6.69 (1H, d, *J*=2.5 Hz), 8.54 (1H, br s). ^{13}C-NMR: Table II.

18 Acetate (**18a**): Colorless needles (MeOH), mp 118—120 °C. MS: *m/z* 512 (M^+, $C_{23}H_{28}O_{13}$). IR (KBr) cm^{-1}: OH (nil), 1720. ^{1}H-NMR ($CDCl_3$): 2.03, 2.05, 2.06, 2.07, 2.29, 3.79 (3H each, s), 6.55 (1H, dd, *J*=3, 9 Hz), 6.59 (1H, d, *J*=9 Hz), 6.65 (1H, d, *J*=3 Hz). Methylation of **18** with diazomethane etherate provided **18b** (37 mg), colorless needles (EtOH), mp 159—161 °C. On acetylation, **18b** provided an acetate (**18c**), colorless needles (EtOH), mp 121—123 °C. MS: *m/z* 484 (M^+, $C_{22}H_{28}O_{12}$). IR (KBr) cm^{-1}: OH (nil), 1720. ^{1}H-NMR ($CDCl_3$): 2.03,2.04, 2.07, 2.08 (3H each, s), 3.84 (6H, s), 6.11 (1H, d, *J*=2 Hz), 6.53 (1H, dd, *J*=2, 8 Hz), 6.77 (1H, d, *J*=8 Hz).

Acid Hydrolysis of 18b Compound **18b** (15 mg) was heated in 2 N HCl in 50% aqueous dioxane (2 ml) at 80 °C for 2 h to give glucose and an aglycone (**19**), colorless syrup. MS: *m/z* 154 (M^+, $C_8H_{10}O_3$). ^{1}H-NMR ($CDCl_3$): 3.82 (6H, s), 6.35 (1H, dd, *J*=3, 9 Hz), 6.48 (1H, d, *J*=3 Hz), 6.74 (1H, d, *J*=9 Hz). ^{13}C-NMR ($CDCl_3$): 55.8 (q), 56.6 (q), 100.7 (d), 105.8 (d), 112.5 (d), 143.2 (s), 149.9 (s), 150.1 (s). Compound **19** was identical with authentic 1,2,4-tri-hydroxybenzene 2,4-dimethylether prepared from vanillin methylether by the Beyer–Villiger oxidation.[12]

Enzymatic Hydrolysis of 13 Compound **13** (5 mg) was incubated with pectinase (0.3 mg) in water (1 ml) at 37 °C for 24 h. The reaction mixture was examined on TLC and GLC, and glucose and apiose were detected. TLC, *Rf*: 0.14 (glc), 0.33 (api). GLC, t_R: 7.3, 11.0 (glc), 1.8, 2.1, 2.4 (api).

Acidic Hydrolysis of 13 Compound **13** (2 mg) was heated in 0.1 N H_2SO_4 at 60 °C for 10 min to give **10** and apiose.

Acknowledgement The authors are grateful to Mr. S. Isoda (Medicinal Plant Garden of this school) for providing the plant material, and to Dr. R. Higuchi (Kyushu University) for providing authentic samples and ^{1}H-NMR data, as well as to Prof. H. Itokawa and Dr. Y. Kumekawa (Tokyo College of Pharmacy) for providing relevant IR and mass spectra. Thanks are also due to the Analytical Lab. of this school for the elemental analysis and spectral measurements.

References and Notes

1) This work was presented orally at the 31st Annual Meeting of the Japanese Scoeity of Pharmacognosy, Tokyo, Sept. 1984, Abstract of Papers, p. 47.
2) Jiangsu Medical College (ed.), "Zhong-yao-da-ci-dian" (The dictionary of Chinese Crude Drugs), Shanghai Scientific Technologic Publisher, Shanghai, 1977, p. 1277.
3) I. Yoshioka, T. Kimura, H. Imagawa and K. Kohra, *Yakugaku Zasshi*, **86**, 1216 (1966).
4) *a*) A. Y. Khorlin, A. G. Ven'yaminova and N. K. Kochetokov, *Izu. Akad. Nauk SSSR, Ser Khim*, **1966**, 1588; *b*) *Idem, Dokl, Akad. Nauk SSSR*, **155**, 619 (1964).

5) *a*) C. Shao, R. Kasai, J. Xu and O. Tanaka, *Chem. Pharm. Bull.*, **37**, 311 (1989); *b*) *Idem*, *ibid.*, **36**, 601 (1988).
6) *a*) H. Kizu and T. Tomimori, *Chem. Pharm. Bull.*, **30**, 3340 (1982); *b*) *Idem*, *ibid.*, **28**, 3555 (1980); *c*) *Idem*, *ibid.*, **28**, 2827 (1980); *d*) *Idem*, *ibid.*, **26**, 655 (1980).
7) R. Higuchi and T. Kawasaki, *Chem. Pharm. Bull.*, **24**, 1021 (1976). P_{J2} and P_{J3} were isolated as the permethylates.
8) R. Tschesche, W. Schmidt and G. Wulff, *Z. Naturforsch.*, **20b**, 708 (1965).
9) *a*) Y. Yoneiti and H. Sawada, *Yakugaku Zasshi*, **79**, 1226 (1959). *Cf.* K. Shima, S. Hisada and I. Inagaki, *ibid.*, **91**, 1121 (1971).
10) C. P. Falshaw, K. L. Ormand, S. Mongkolsuk and V. Podimuang, *Phytochemistry*, **8**, 913 (1969).
11) *a*) T. Deyama, *Chem. Pharm. Bull.*, **31**, 2993 (1983); *b*) L. A. Elyakova, A. K. Dzizenko and G. B. Elyakov, *Dokl. Akad. Nauk SSSR*, **165**, 562 (1965); *c*) M. S. Tempesta and R. B. Bate, *J. Org. Chem.*, **45**, 1327 (1980).
12) D. G. Grosby, *J. Org. Chem.*, **26**, 1215 (1961).
13) K. R. Markham, B. Ternai, R. Stanley, H. Geiger and T. J. Mabry, *Tetrahedron*, **34**, 1389 (1978).
14) N. Takasugi, T. Moriguchi, T. Fuwa, S. Sanada, Y. Ida, J. Shoji and H. Saito, *Shoyakugaku Zasshi*, **39**, 232 (1985); N. Nishiyama, T. Kamegaya, A. Iwai, H. Saito, S. Sanada, Y. Ida and J. Shoji, *ibid.*, **39**, 238 (1985).

A Series of Novel Acyclic Nucleosides. IV.[1] Synthesis of N^1-Sulfur Analogues of Acyclovir, Directed toward Improved Antiviral Activities

Chisato KANEKO*,[a] Sumiko HARA,[a] Hiroatsu MATSUMOTO,[a] Tadao TAKEUCHI,[a] Takeo MORI,[a] Kazuyoshi IKEDA,[b] and Yoshihisa MIZUNO[a]

Research Laboratory, Minophagen Pharmaceutical Co.,[a] 2–5233, Komatsubara, Zama, Kanagawa 228 and The Center for Instrumental Analysis of Hokkaido University,[b] Kita 11, Nishi 8, Kita-ku, Sapporo, Hokkaido 060, Japan. *Received October 8, 1990*

Novel imidazothiazine acyclic nucleoside analogues (9a—d, 12a—d and 3c, d) in which N^1 of the purine base is replaced by a sulfur atom were synthesized. 5-Substituted imidazo[4,5-*d*][1,3]thiazine-7(3*H*)-thiones (7a—d) were prepared from 5(4)-substituted amino-4(5)-ethoxycarbonyl-1(3*H*)-imidazoles with Lawesson reagent and then 7a—d were alkylated with 2-oxa-1,4-butanediol diacetate or with 2-acetoxyethoxymethyl halide to give 9a—d and 10a, d in moderate yields. Compounds 9a—d were led to the corresponding 7-one derivatives (12a—d) by $KMnO_4$ oxidation. Deprotection of the acetyl group in 9a—d and 12c, d was achieved by means of the Zemplen procedure.

Keywords antiviral agent; acyclonucleoside; oxidative desulfuration; imidazo[4,5-*d*][1,3]thiazin-7(3*H*)-one; Lawesson reagent

Some acyclic nucleosides such as Acyclovir (**1**),[2] and 9-[(1,3-dihydroxy-2-propoxy)methyl]guanine (DHPG),[3] modified in the carbohydrate portion of the ribonucleosides, exhibit selective and potent antiviral activity against herpes viruses. These acyclic nucleosides are viewed as prodrugs in terms of the mode of action, because they are initially phosphorylated by virus-encoded thymidine kinase, not by a kinase originated from the host, and are further phosphorylated to the corresponding triphosphates, which are specific inhibitors of DNA-polymerase (deoxyribonucleic acid-polymerase), associated with the multiplication of viruses.

There have been only a few papers[4] dealing with synthesis of acyclic nucleosides having modified purine rings. Some of the products showed antiviral activities.

We have been concerned with acyclic nucleosides in which N^1 of purine bases is replaced by O, S, Se or sp^2 carbon because of our interest in the relationship between structure and antiviral activity, and to examine the substrate specificity of viral thymidine kinases. As part of this program, we recently reported the synthesis of acyclic oxanosine (**2**), and it was found that the replacement of N^1 of acyclovir with an oxygen atom resulted in a dramatic reduction in antiviral activity against herpes simplex virus (HSV-I).[5] Compound **2** also showed no activity against human immunodeficiency virus (HIV-I).[5]

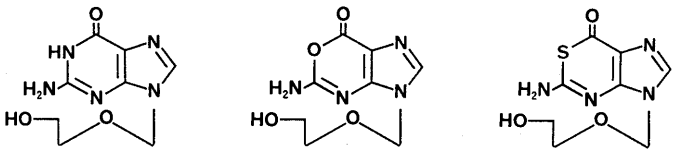

1 2 3d

Chart 1

This paper describes syntheses of acyclic 5-substituted (amino, benzylamino, methyl, and phenyl) imidazo [4,5-*d*]-[1,3]thiazine-7(3*H*)-thiones (**9a—d**) and also their 7(3*H*)-one derivatives (**12a—d**), that is, the N^1-sulfur analogues of acyclovir.[6]

5(4)-Substituted amino-4(5)-ethoxycarbonyl-1(3*H*)-imidazoles (**4a—c**) were synthesized from 5(4)-amino-4(5)-ethoxycarbonyl-1(3*H*)-imidazole by the use of acetic anhydride, benzoyl chloride, and benzyl isocyanate, respectively. They were treated with an excess amount of Lawesson reagent[7] in refluxing xylene to give the thiazine derivatives (**7a—c**) in good yields. It was found that the cyclization yield depended on the reaction time. For example, when the mixture was refluxed for 8 h, **4c** gave **5c**, **6**, and **7c** in 15%, 64%, and 9% yields, respectively, and when refluxing was continued for another 8 h, **7c** was the predominant product (86% yield). Treatment of the pu-

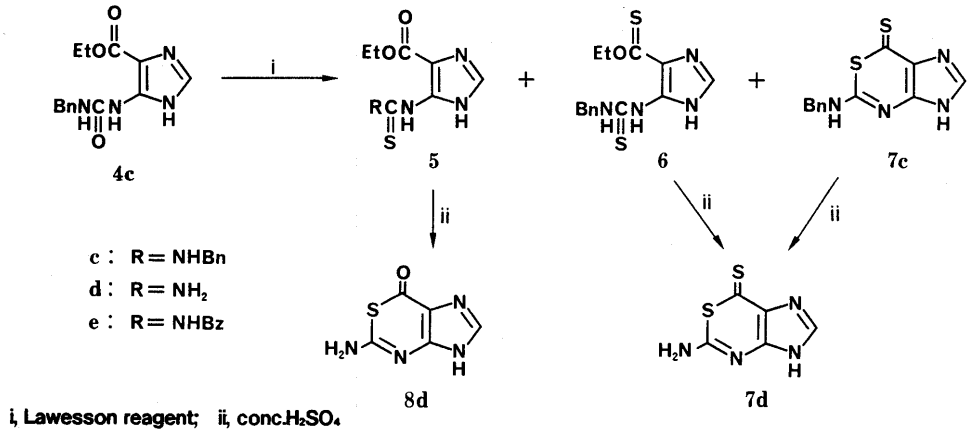

4c 5 6 7c 8d 7d

Chart 2

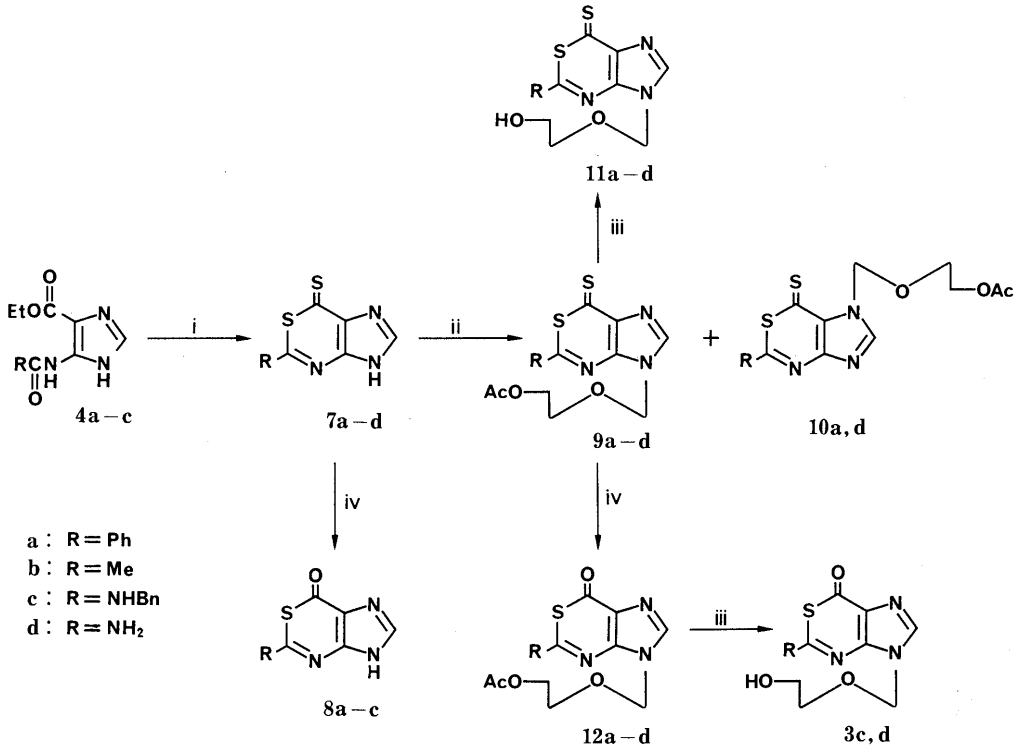

i, Lawesson reagent; ii, $AcOCH_2CH_2OCH_2X$, X=Cl or OAc; iii, NaOMe/MeOH; iv, $KMnO_4$/acetone

Chart 3

rified dithione compound (**6**) with more Lawesson reagent in refluxing xylene afforded **7c** in 60% yield. These results suggested that 5(4)-thioureido-4(5)-ethoxycarbonyl-1(3*H*)-imidazole (**5c**) was initially formed and this further reacted with Lawesson reagent to give the dithione derivative (**6**), which cyclized to form the thiazine ring either spontaneously or by catalysis of the reagent. On treatment with concentrated sulfuric acid, **6** was also cyclized, with simultaneous debenzylation to give **7d**; debenzylation of **7c** was effected with concentrated sulfuric acid to give **7d** in 75% yield. Compounds **7a**—**c** were oxidatively desulfurized by the use of potassium permanganate to afford **8a**—**c** without damage to the imidazothiazine ring. Compounds **5d**, **e** could be directly cyclized to **8d** on treatment with concentrated sulfuric acid. This procedure, however, has the following drawbacks; the yields of these products were quite poor and the purification was difficult because of instability.

These thiazine compounds (**7a**, **b**, and **7c**) were converted to the corresponding (2-acetoxyethoxymethyl)imidazothiazine derivatives (**9a**, **b**, **c** and **10a**) by fusion with 2-oxa-1,4-butanediol diacetate in the absence of a catalyst. The 5-phenyl derivative (**7a**) gave a mixture of positional isomers, whereas **7b** and **7c** gave only the 3-substituted derivatives as isolable products. Compounds **9d** and **10d** were synthesized via silylation that is, **7d** was firstly trimethylsilylated using hexamethyldisilazane and then alkylated with 2-acetoxyethoxymethyl chloride in the presence of cesium iodide according to Kim and coworkers[8] in moderate yield (33%). The alkylation of **7a** and **7d** took place on both N^1 and N^3 in the imidazole ring. In the cases of **7b** and **7c**, the N^3-alkylated compounds **9b** and **9c** were isolated as the only products (99% and 56%).

The alkylated sites of the isomers (**9** and **10**) were determined by proton and carbon-13 nuclear magnetic resonance (^{1}H- and ^{13}C-NMR) spectrometry. Chemical shift values are listed in Table I, together with long-range (two or three bonds) ^{1}H–^{13}C-connectivity. Namely, the ^{1}H-NMR signals of 1′-methylene protons in the N^1-isomers were always observed at lower field than those of the N^3-isomers, because the N^1-isomers are exposed to the anisotropic effect of thiocarbonyl groups at the peri-position. Further, the ^{13}C chemical shifts for C-3a or C-7a were shifted upfield by 10 ppm in most cases, when the adjacent nitrogen in the imidazole ring was alkylated. Similarly, compounds **10a** and **10d** having the substituent at position N^1 caused a shielding of carbon 7a by the same order of magnitude. These shift values are in agreement with reported values in imidazole ring systems.[9] Compound **9a** and **9d** also exhibited a connectivity between 1′-methylene protons and two carbons (C-3a and C-2) in ^{1}H–^{13}C-heteronuclear multiple bond connectivity (HMBC).[10] Protons of the 1′-methylene group in **10a** and **10d** showed a connectivity with C-7a and C-2 carbons, respectively. No connectivity was observed between carbon 3a and the 1′-methylene group in **10a** and **10d**, or between carbon 7a and the methylene protons in **9a** and **9d**. These results support the conclusion that the acyclic side chain in **9a** and **9d** is attached to N^3 of the imidazole ring, whereas **10a** and **10d** are alkylated at the N^1 position.

Compounds **9a**—**d** were then desulfurized with potassium permanganate in acetone to give colorless products (**12a**—**d**) (46—85% yields). These products showed a new carbonyl absorption band at around 1690 cm^{-1} in the infrared (IR) spectra, and the absorption maxima in the ultraviolet (UV) spectra of the former were shifted hypsochro-

TABLE I. ^{1}H- and ^{13}C-NMR Chemical Shifts of Acyclic Imidazo[4,5-*d*][1,3]thiazines

	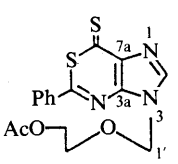 **9a**	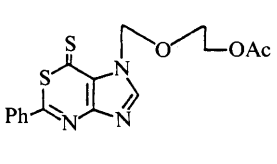 **10a**		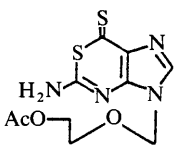 **9d**	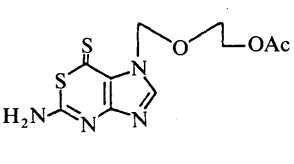 **10d**		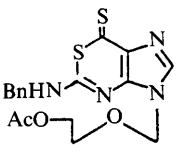 **9c**
^{1}H-NMR H-1′	5.73	(0.54)[a]	6.27	5.48	(0.72)	6.20	5.38
δ: ppm H-2	8.09	(0.20)	8.29	8.04	(0.24)	8.28	7.75
$CDCl_3$							
^{13}C-NMR C-2	141.94		146.69	140.17		148.25	139.40
δ: ppm C-3a	142.04	(11.29)	153.33	147.51	(9.99)	157.50	146.82
$CDCl_3$ C-7a	134.60	(9.62)	124.98	129.51	(7.34)	122.17	131.07
or							
DMSO-d_6 C-1′	73.52	(4.22)	77.74	72.93	(3.92)	76.85	72.45
^{1}H–^{13}C-NMR HMBC							
1′-CH_2: C-2	+		+	+		+	+
1′-CH_2: C-3a	+		−	+		−	+
1′-CH_2: C-7a	−		+	−		+	−

a) Values in parentheses are differences of NMR chemical shift values between N^1- and N^3-alkylated derivatives. +, connectivity; −, no connectivity.

mically by *ca.* 85 nm compared with those of the latter. Attempts at direct formation of **12a—c** from **8a—c** were abandoned because of the low yields of **8a—c** from **7a—c**, respectively.

Deprotection of the acetyl group in **9a—d** and **12c, d** was achieved by treatment with a catalytic amount of sodium methoxide in methanol at low temperature (Zemplen procedure)[11] to afford **11a—d** and **3c, d** in good yields, though these compounds were unstable on prolonged treatment with a strongly alkaline medium. New sulfur analogues of acyclovir and their thione derivatives were successively prepared in moderate yields through several reaction steps.

These new compounds (**3d, 9c, 11a, b, d,** and **12a, b**) were found to be inactive against HIV and HSV-I. Details of the bioassay will be the subject of a separate paper.

Experimental

All melting points were determined on a Yanagimoto micro melting point apparatus and are uncorrected. ^{1}H- and ^{13}C-NMR spectra were obtained on a JEOL GX-270 spectrometer using tetramethylsilane as an internal standard. Unless otherwise stated, deuteriodimethyl sulfoxide (DMSO-d_6) was used as a solvent. Chemical shifts are given on the δ scale (ppm). ArH-*o*, *p* and ArH-*m* refer to *ortho*, *para*, and *meta* aromatic hydrocarbon atoms. Mass and high resolution mass spectra (MS and HR-MS) measurements were run on a JMS-DX303 spectrometer. IR spectra were recorded with a JASCO IRA-1 spectromerer in KBr disks. UV spectra were measured on a Hitachi 200-20 spectrophotometer. Column chromatography was performed on Silica gel 60 (E. Merck, 70–230 mesh).

5-Phenylimidazo[4,5-*d*][1,3]thiazine-7(3*H*)-thione (7a) Lawesson reagent (5.24 g, 13.0 mmol) was added to a solution of **4a** (2.80 g, 10.8 mmol) in xylene (80 ml), and the reaction mixture was refluxed for 1.5 h, then allowed to cool. Yellow-colored precipitates were collected by filtration and then washed with MeOH to give **7a** (1.58 g, 60%), mp 250—260 °C. MS *m/z*: 245 (M^+). ^{1}H-NMR: 7.62—7.66 (3H, m, ArH-*m*, *p*), 8.04—8.07 (2H, m, ArH-*o*), 8.56 (1H, s, 2-H). UV $\lambda_{max}^{H_2O}$ nm: 261, 290 (sh), 340, 405.

5-Methylimidazo[4,5-*d*][1,3]thiazine-7(3*H*)-thione (7b) Lawesson reagent (4.90 g, 12.0 mmol) was added to a solution of **4b** (1.96 g, 10.0 mmol) in xylene (80 ml), and the reaction mixture was worked up as above to give **7b** (1.38 g, 76%), mp 276—277 °C (dec). MS *m/z*: 183 (M^+) HR-MS Calcd for $C_6H_5N_3S_2$: 182.9925. Found *m/z*: 182.9921. ^{1}H-NMR: 2.66 (3H, s, CH_3), 8.46 (1H, br s, 2-H), 13.86 (1H, br s, NH). UV $\lambda_{max}^{H_2O}$ nm: 270, 313, 383.

5-Benzylaminoimidazo[4,5-*d*][1,3]thiazine-7(3*H*)-thione (7c) Lawesson reagent (2.48 g, 6.4 mmol) was added to a solution of **4c** (885 mg, 3.1 mmol) in xylene (60 ml), and the reaction mixture was refluxed for 16 h, then allowed to cool. Yellow-colored precipitates were collected by filtration, and purified by silica gel column chromatography using 3% MeOH–$CHCl_3$ as an eluant to give **7c** (725 mg, 86%), mp 245–246 °C. MS *m/z*: 274 (M^+). HR-MS Calcd for $C_{12}H_{10}N_4S_2$: 274.0347. Found *m/z*: 274.0331. ^{1}H-NMR (20% DMSO-d_6–$CDCl_3$): 4.66 (2H, d, CH_2, J=4.95 Hz), 7.85 (1H, br s, 2-H), 7.28—7.35 (5H, m, ArH). UV $\lambda_{max}^{H_2O}$ nm ($\varepsilon \times 10^3$): 238 (22.4), 300 (3.3), 412 (10.2). When the refluxing time was only 8 h, the reaction mixture gave **5c** (15%), **6** (64%) and **7c** (9%) after purification by silica gel column chromatography using 3% MeOH–$CHCl_3$ as an eluant. **5c**: mp 198—200 °C. MS *m/z*: 304 (M^+). ^{1}H-NMR (10% DMSO-d_6–$CDCl_3$): 1.44 (3H, t, CH_3, J=7.14 Hz), 4.39 (2H, q, CH_2, J=7.15 Hz), 4.96 (2H, d, $ArCH_2$, J=5.49 Hz), 7.24—7.41 (6H, m, ArH and 2-H), 9.02 (1H, s $NHCH_2$), 11.00 (1H, s, NHC=S), 12.71 (1H, br s, 1H, NH). UV λ_{max}^{MeOH} nm: 252, 293. **6**: mp 147—148 °C. MS *m/z*: 320 (M^+). ^{1}H-NMR ($CDCl_3$): 1.52 (3H, br t, CH_3), 4.67 (2H, q, CH_2, J=7.14 Hz), 4.96 (2H, d, $ArCH_2$, J=5.49 Hz), 7.26—7.41 (6H, m, ArH and 2-H), 9.86 (1H, br s, $NHCH_2$), 10.89 (1H, br s, NHC=S).

5-Aminoimidazo[4,5-*d*][1,3]thiazine-7-(3*H*)-thione (7d) a) Compound **7c** (282 mg, 1.0 mmol) was added to cooled, concentrated H_2SO_4 (3 ml) at 0 °C, and the reaction mixture was kept overnight at 60 °C. After neutralization with aqueous NaOH solution, the reaction mixture was concentrated to dryness under reduced pressure. The residue was triturated with EtOH (100 ml) and salts were filtered off. The filtrate was evaporated and the residue was purified by silica gel column chromatography using 6% MeOH–$CHCl_3$ as an eluant to give **7d** (114 mg, 75%), mp > 300 °C. MS *m/z*: 184 (M^+). HR-MS Calcd for $C_5H_4N_4S_2$: 183.9877. Found *m/z*: 183.9862. ^{1}H-NMR: 8.11 (1H, s, 2-H), 8.27 (2H, s, NH_2). UV $\lambda_{max}^{H_2O}$: 232, 255, 290 (sh), 408. b) **6** (100 mg, 0.3 mmol) was added to concentrated H_2SO_4 (1 ml) at 0 °C and the reaction mixture was kept overnight at 60 °C. After work-up as above, the title compound (**7d**) was obtained (50 mg, 95%).

5-Phenylimidazo[4,5-*d*][1,3]thiazin-7-(3*H*)-one (8a) $KMnO_4$ (160 mg) was added slowly to a solution of **7a** (60 mg, 0.3 mmol) in acetone (2 ml) at 60 °C in a water bath until the color of the reaction mixture became violet, and the excess $KMnO_4$ was decomposed with MeOH. The solution was filtered, the filtrate was evaporated, and the residue was recrystallized from MeOH to give **8a** (12 mg, 21%), mp > 300 °C. MS *m/z*: 229 (M^+). ^{1}H-NMR: 7.55—7.62 (3H, q, ArH-*m*, *p*), 8.00—8.03 (2H, t, ArH-*o*), 8.33 (1H, s, 2-H), 13.90 (1H, br s, NH). UV λ_{max}^{MeOH} nm: 280 (sh), 300 (sh), 330. IR (KBr): 1676 cm^{-1} (C=O).

5-Methylimidazo[4,5-*d*][1,3]thiazin-7(3*H*)-one (8b) $KMnO_4$ (172 mg)

was added slowly to a solution of **7b** (67 mg, 0.4 mmol) in acetone (2 ml) at 60 °C in a water bath, and the reaction mixture was worked up as above to give **8b** (29 mg, 47%, viscous oil). MS *m/z*: 167 (M^+). ^{1}H-NMR: 2.60 (3H, s, CH_3), 7.96 (1H, s, 2-H). UV λ_{max}^{MeOH} nm: 265 (sh), 302. IR (KBr): 1688 cm^{-1} (C=O).

5-Benzylaminoimidazo[4,5-*d*][1,3]thiazin-7(3*H*)-one (8c) $KMnO_4$ (53 mg) was added slowly to a solution of **7c** (37 mg, 0.14 mmol) in acetone (20 ml) at room temperature, and the reaction mixture was kept for 1.5 h, then concentrated. The residue was purified by silica gel column chromatography using 5% MeOH–$CHCl_3$ as an eluant to give **8c** (5 mg, 14%), mp 195 °C. MS *m/z*: 258 (M^+). HR-MS Calcd for $C_{12}H_{10}N_4OS$ 258.0575. Found *m/z*: 258.0565. ^{1}H-NMR: 4.57 (2H, d, $ArCH_2$, J=5.49 Hz), 7.21—7.35(5H, m, ArH), 7.73 (1H, s, 2-H), 9.07 (1H, t, CH_2NH), 12.83 (1H, s, NH). UV $\lambda_{max}^{H_2O}$ nm: 220 (sh), 264, 332.

5-Aminoimidazo[4,5-*d*][1,3]thiazin-7(3*H*)-one (8d) a) **5d** (50 mg, 0.23 mmol) was added to concentrated H_2SO_4 (0.5 ml) at 0 °C and the solution was kept at 60 °C for 2 d. After cooling, the reaction mixture was poured onto ice, then neutralized with aqueous NaOH solution and evaporated. The residue was purified by silica gel column chromatography using 5% MeOH–$CHCl_3$ as an eluant to give **8d** (3 mg, 8%), mp>280 °C. MS *m/z*: 168 (M^+). ^{1}H-NMR: 7.72 (1H, s, 2-H), 7.91 (2H, s, NH_2), 12.66 (1H, br s, NH). UV $\lambda_{max}^{H_2O}$ nm: 275, 330. IR (KBr): 1643 cm^{-1} (C=O). b) **5e** (100 mg, 0.31 mmol) was added to concentrated H_2SO_4 (1 ml) at 0 °C and the reaction mixture was kept overnight at 60 °C. Work-up as above gave **8d** (12 mg, 23%).

3-(2-Acetoxyethoxymethyl)-5-phenylimidazo[4,5-*d*][1,3]thiazine-7(3*H*)-thione (9a) and 1-(2-Acetoxyethoxymethyl)-5-phenylimidazo-[4,5-*d*][1,3]-thiazine-7-(1*H*)-thione (10a) A mixture of **7a** (167 mg, 0.68 mmol) and 2-oxa-1,4-butanediol diacetate (1 ml, 2.5 mmol) was fused at 150 °C for 20 min. The reaction mixture was purified by silica gel column chromatography using $CHCl_3$ as an eluant to give **9a** (406 mg, 55%) and **10a** (276 mg, 38%). **9a**: mp 100—105 °C. MS *m/z*: 361 (M^+). ^{1}H-NMR ($CDCl_3$): 2.05 (3H, s, $COCH_3$), 3.80–3.83 (2H, m, 4′-CH_2), 4.21—4.25 (2H, m, 3′-CH_2), 5.73 (2H, s, 1′-CH_2), 7.51—7.64 (3H, m, ArH-*m*, *p*), 8.02—8.05 (2H, m, ArH-*o*), 8.09 (1H, br s, 2-H). ^{13}C-NMR ($CDCl_3$): 73.5 (C-1′), 134.6 (C-7a), 141.9 (C-2), 142.0 (C-3a). UV $\lambda_{max}^{H_2O}$ nm ($\varepsilon\times10^3$): 262 (33.49), 339 (12.77), 405 (11.56). *Anal.* Calcd for $C_{16}H_{15}N_3O_3S_2$: C, 53.17; H, 4.18; N, 11.63; S, 17.74. Found: C, 52.93; H, 4.17; N, 11.61; S, 17.50. **10a**: mp 95–100 °C. MS *m/z*: 361 (M^+). ^{1}H-NMR ($CDCl_3$): 2.08 (3H, s, $COCH_3$), 3.87—3.90 (2H, m, 4′-CH_2), 4.22—4.26 (2H, m, 3′-CH_2), 6.27 (2H, s, 1′-CH_2), 7.58—7.59 (3H, m, ArH-*m*, *p*), 8.09—8.12 (2H, m, ArH-*o*), 8.29 (1H, br s, 2-H). ^{13}C-NMR ($CDCl_3$): 77.7 (C-1′), 125.0 (C-7a), 153.3 (C-3a), 146.7 (C-2). UV λ_{max}^{MeOH} nm ($\varepsilon\times10^3$): 410, 340, 280. *Anal.* Calcd for $C_{16}H_{15}N_3O_3S_2$: C, 53.17; H, 4.18; N, 11.63; S, 17.74. Found: C, 52.93; H, 4.17; N, 11.61; S, 17.50.

3-(2-Hydroxyethoxymethyl)-5-phenylimidazo[4,5-*d*][1,3]thiazine-7(3*H*)-thione (11a) A catalytic amount of sodium methoxide was added to a solution of **9a** (90 mg, 0.25 mmol) in absolute MeOH (30 ml), and the reaction mixture was kept for 5 min at room temperature. The precipitates were collected by filtration and washed with EtOAc to give **11a** (79 mg, 99%), mp 209—210 °C. MS *m/z*: 319. ^{1}H-NMR: 3.61—3.71 (4H, m, 3′ and 4′-CH_2), 4.61 (1H, t, OH), 5.80 (2H, s, 1′-CH_2), 7.53—7.64 (3H, m, ArH-*m*, *p*), 8.06—8.09 (2H, m, ArH-*o*), 8.40 (1H, s, 2-H). UV $\lambda_{max}^{H_2O}$ nm ($\varepsilon\times10^3$): 261 (12.10), 338 (4.59), 403 (4.24).

3-(2-Acetoxyethoxymethyl)-5-methylimidazo[4,5-*d*][1,3]thiazine-7(3*H*)-thione (9b) A mixture of **7b** (120 mg, 0.66 mmol) and 2-oxa-1,4-butanediol diacetate (1 ml, 2.5 mmol) was fused at 150 °C for 20 min. The reaction mixture was purified by silica gel column chromatography using 0.2% MeOH–$CHCl_3$ as an eluant to give **9b** (194 mg, 94%), mp 80—81 °C. MS *m/z*: 299 (M^+). ^{1}H-NMR ($CDCl_3$): 2.11 (3H, s, $COCH_3$), 2.65 (3H, s, CH_3), 3.75 (2H, m, 4′-CH_2), 4.21 (2H, m, 3′-CH_2), 5.62 (2H, s, 1′-CH_2), 8.02 (1H, s, 2-H). UV λ_{max}^{MeOH} nm: 222, 261, 318, 380. *Anal.* Calcd for $C_{11}H_{13}N_3O_3S_2$: C, 44.10; H, 4.38; N, 14.04; S, 21.42. Found: C, 43.99; H, 4.33; N, 13.97; S, 21.46.

3-(2-Hydroxyethoxymethyl)-5-methylimidazo[4,5-*d*][1,3]thiazine-7(3*H*)-thione (11b) A catalytic amount of sodium methoxide was added to a solution of **9b** (100 mg, 0.3 mmol) in absolute MeOH (3 ml), and the reaction mixture was kept for 5 min at room temperature. The precipitates were collected by filtration and washed with EtOAc to give **8b** (48 mg, 56%), mp 217—217.5 °C. MS *m/z*: 257 (M^+). ^{1}H-NMR: 2.68 (2H, s, CH_3), 3.46—3.66 (4H, m, 3′ and 4′-CH_2), 4.65 (1H, br t, OH), 5.62 (2H, s, 1′-CH_2), 8.49 (1H, s, 2-H). UV $\lambda_{max}^{H_2O}$ nm ($\varepsilon\times10^3$): 224 (14.71), 262 (10.43), 318 (6.85), 378 (10.62).

3-(2-Acetoxyethoxymethyl)-5-benzylaminoimidazo[4,5-*d*][1,3]-thiazine-7(3*H*)-thione (9c) A mixture of **7c** (50 mg, 0.2 mmol) and 2-oxa-1,4-butanediol diacetate (1 ml) was fused at 160 °C for 20 min. The reaction mixture was worked up as above to give **9c** (40 mg, 56%), mp 147—148 °C. MS *m/z*: 390 (M^+). HR-MS Calcd for $C_{17}H_{18}N_4O_3S_2$ 390.0802. Found *m/z*: 390.0801. ^{1}H-NMR ($CDCl_3$): 2.02 (3H, s, $COCH_3$), 3.51 (2H, m, 4′-CH_2), 4.04 (2H, m, 3′-CH_2), 4.65 (2H, d, $ArCH_2$, J=5.49 Hz), 5.38 (2H, s, 1′-CH_2), 7.32—7.33 (5H, m, ArH), 7.55 (1H, s, 2-H), 8.86 (1H, br s, NH). ^{13}C-NMR ($CDCl_3$): 46.1 ($ArCH_2$), 62.5 (C-4′), 67.2 (C-3′), 72.5 (C-1′), 131.1 (C-7a), 139.4 (C-2), 146.8 (C-3a), 166.8 (C-5), 214.8 (C=S). UV $\lambda_{max}^{H_2O}$ nm ($\varepsilon\times10^3$): 240 (28.92), 296 (8.23), 410 (24.86).

5-Benzylamino-3-(2-hydroxyethoxymethyl)imidazo[4,5-*d*][1,3]thiazine-7-(3*H*)-thione (11c) A catalytic amount of sodium methoxide was added to a solution of **9c** (0.01 g, 0.03 mmol) in absolute MeOH (8 ml), and the reaction mixture was kept for 90 min at 0 °C. It was neutralized with 1.4% AcOH and evaporated. The residue was purified by silica gel column chromatography using 1% MeOH–$CHCl_3$ as an eluant to give **11c** (3.8 mg, 43%), mp 173—174 °C. MS *m/z*: 348 (M^+). HR-MS Calcd for $C_{15}H_{16}N_4O_2S_2$ 348.0715. Found *m/z*: 348.0704. ^{1}H-NMR: 3.42—3.47 (4H, m, 3′ and 4′-CH_2), 4.63 (2H, m, $ArCH_2$), 5.43 (2H, s, 1′-CH_2), 7.25—7.39 (5H, m, ArH), 8.25 (1H, s, 2-H), 9.71 (1H, br NH). UV λ_{max}^{MeOH} nm: 253, 296, 390 (sh), 410.

3-(2-Acetoxyethoxymethyl)-5-aminoimidazo[4,5-*d*][1,3]thiazine-7(3*H*)-thione (9d) A solution of **7d** (90 mg, 0.49 mmol) in 1,1,1,3,3,3-hexamethyldisilazane (HMDS) (20 ml) and CH_3CN (5 ml) was refluxed in the presence of a catalytic amount of $(NH_4)_2SO_4$ for 3 h. The reaction mixture was concentrated under vacuum with exclusion of moisture and the silylated base was treated with 2-acetoxyethoxymethyl chloride (149 mg, 1.0 mmol) in the presence of CsI (141 mg, 0.5 mmol) in CH_3CN (25 ml) under reflux for 4 h. After cooling of the reaction mixture, pyridine (2 ml) was added and the whole was evaporated. The residue was purified by silica gel column chromatography using $CHCl_3$ to give **9d** (27 mg, 18%) and **10d** (23 mg, 15%). **9d**: mp 170—171 °C. MS *m/z*: 300 (M^+). HR-MS Calcd for $C_{10}H_{12}N_4O_3S_2$: 300.0351. Found *m/z*: 300.0321. ^{1}H-NMR: 2.03 (3H, s, $COCH_3$), 3.75—3.79 (2H, m, 4′-CH_2), 4.16—4.20 (2H, m, 3′-CH_2), 5.48 (2H, m, 1′-CH_2), 8.04 (1H, s, 2-H), 8.14 (1H, s, NH_2). ^{13}C-NMR: 20.7 (CH_3), 62.7 (C-4′), 67.4 (C-3′), 72.9 (C-1′), 129.5 (C-7a), 40.2 (C-2), 147.5 (C-3a). UV λ_{max}^{MeOH} nm ($\varepsilon\times10^3$): 232, 251, 295, 407. **10d**: mp 163—165 °C. MS *m/z*: 300 (M^+). HR-MS Found *m/z*: 300.0372. ^{1}H-NMR: 2.04 (3H, s, $COCH_3$), 3.83—3.85 (2H, m, 4′-CH_2), 4.16—4.18 (2H, m, 3′-CH_2), 6.20 (2H, s, 1′-CH_2), 7.88 (2H, s, NH_2), 8.28 (1H, s, 2-H). ^{13}C-NMR: 76.9 (C-1′), 122.2 (C-7a), 148.3 (C-2), 157.8 (C-3a). UV λ_{max}^{MeOH} nm: 229, 252, 320 (sh), 418.

5-Amino-(2-hydroxyethoxymethyl)imidazo[4,5-*d*][1,3]thiazine-7(3*H*)-thione (11d) A catalytic amount of sodium methoxide was added to a solution of **9d** (12.5 mg, 0.04 mmol) in absolute MeOH (10 ml) at 0 °C. The reaction mixture was kept for 1 h at 0 °C and worked up as above give **11b** (11 mg, 99%), mp 211 °C. MS *m/z*: 258 (M^+). HR-MS Calcd for $C_8H_{10}N_4O_2S_2$: 258.0245. Found *m/z*: 258.0240. ^{1}H-NMR: 3.50 (4H, m, 3′ and 4′-CH_2), 4.66 (1H, t, OH), 5.39 (2H, s, 1′-CH_2), 8.12 (1H, s, 2-H), 8.62 (2H, s, NH_2). UV $\lambda_{max}^{H_2O}$ nm ($\varepsilon\times10^3$): 233 (2.2), 254 (16.5), 296 (6.8), 406 (22.9).

3-(2-Hydroxyethoxymethyl)-5-phenylimidazo[4,5-*d*][1,3]thiazin-7(3*H*)-one (12a) $KMnO_4$ (57 mg) was added gradually to a solution of **9a** (40 mg, 0.1 mmol) in acetone (8 ml) at room temperature until the color of the reaction mixture changed to violet. Silica gel column chromatography of the mixture using 5% MeOH–$CHCl_3$ gave **12a** (31 mg, 81%), mp 144—145 °C. MS *m/z*: 345 (M^+). ^{1}H-NMR ($CDCl_3$): 2.05 (3H, s, $COCH_3$), 3.79—3.83 (2H, t, 4′-CH_2), 4.20—4.24 (2H, t, 3′-CH_2), 5.74 (2H, s, 1′-CH_2), 7.26—7.59 (3H, m, ArH-*m*, *p*), 8.00—8.02 (2H, t, ArH-*o*), 8.05 (1H, s, 2-H). UV $\lambda_{max}^{H_2O}$ nm ($\varepsilon\times10^3$): 228 (25.18), 239 (sh) (20.80), 270 (10.44), 337 (12.80). *Anal.* Calcd for $C_{16}H_{15}O_4N_3S$: C, 55.64; H, 4.38; N, 12.17; S, 9.28. Found: C, 55.48; H, 4.36; N, 12.27, S; 9.36.

3-(2-Acetoxyethoxymethyl)-5-methylimidazo[4,5-*d*][1,3]thiazin-7(3*H*)-one (12b) $KMnO_4$ (325 mg) was added gradually to a solution of **9b** (100 mg, 0.3 mmol) in acetone (2 ml) at room temperature until the color of the reaction mixture changed to violet. Work-up as above gave **12b** as an amorphous powder (80 mg, 85%). mp 217—217.5 °C. MS *m/z*: 283 (M^+). ^{1}H-NMR ($CDCl_3$): 2.05 (3H, s, $COCH_3$), 2.71 (3H, s, CH_3), 3.77 (2H, m, 4′-CH_2), 4.21 (2H, m, 3′-CH_2), 5.64 (2H, s, 1′-CH_2), 7.94 (1H, s, 2-H). UV $\lambda_{max}^{H_2O}$ nm ($\varepsilon\times10^3$): 303 (4.08), 266 (4.50), 258 (4.41), 228 (23.70).

3-(2-Acetoxyethoxymethyl)-5-benzylaminoimidazo[4,5-*d*][1,3]thiazin-7(3*H*)-one (12c) $KMnO_4$ (58 mg) was added gradually to a solution of **9c** (0.25 g, 0.06 mmol) in acetone (8 ml) at room temperature until the color of the reaction mixture changed to violet. Work-up as above gave **12c** (11 mg, 46%), mp 146—148 °C. MS *m/z*: 374 (M^+). HR-MS Calcd for $C_{17}H_{18}N_4O_4S$: 374.1049. Found *m/z*: 374.1030. ^{1}H-NMR ($CDCl_3$): 2.03

(3H, s, $COCH_3$), 3.56 (2H, t, 4′-CH_2), 4.09 (2H, q, 3′-CH_2), 4.69 (2H, d, $ArCH_2$, $J=5.5$ Hz), 5.42 (2H, s, 1′-CH_2), 7.26—7.37 (5H, m, ArH), 7.67 (1H, s, 2-H). UV λ_{max}^{MeOH} nm: 264, 272 (sh), 330.

5-Benzylamino-3-(2-hydroxyethoxymethyl)imidazo[4,5-*d*][1,3]thiazin-7(3*H*)-one (3c) A catalytic amount of sodium methoxide was added to a solution of **12c** (0.01 g, 0.03 mmol) in absolute MeOH (6 ml) at 0 °C, and the reaction mixture was kept at 0 °C for 2 h. It was neutralized with 1.5% aqueous AcOH solution and evaporated to dryness. The residue was purified by silica gel column chromatography using 2% MeOH–$CHCl_3$ to give **3c** (6 mg, 68%) as a viscous oil. MS *m/z*: 332 (M^+). HR-MS Calcd for $C_{15}H_{16}N_4O_3S$: 332.0943. Found *m/z*: 332.0917. ^{1}H-NMR: 3.51 (2H, d, 4′-CH_2), 3.59 (2H, d, 3′-CH_2), 4.67 (2H, d, $ArCH_2$, $J=5.49$ Hz), 5.46 (2H, s, 1′-CH_2), 7.26 (3H, s, ArH-*m*, *p*), 7.33—7.38 (2H, q, ArH-*o*), 7.67 (1H, s, 2-H). UV $\lambda_{max}^{H_2O}$ nm: 266, 275 (sh), 332.

3-(2-Acetoxyethoxymethyl)-5-Aminoimidazo[4,5-*d*][1,3]thiazin-7(3*H*)-one (12d) $KMnO_4$ (47 mg) was added gradually to a solution of **9d** (0.014 g, 0.05 mmol) in acetone (3 ml) at room temperature until the color of the reaction mixture changed to violet. Work-up as above gave **12d** (11 mg, 83%), mp 112—113 °C. MS *m/z*: 284 (M^+). HR-MS calcd for $C_{10}H_{12}N_4O_4$: 284.0579. Found *m/z*: 284.0565. ^{1}H-NMR: 1.66 (3H, s, $COCH_3$), 3.67–3.71 (2H, m, 4′-CH_2), 4.07—4.10 (2H, m, 3′-CH_2), 5.40 (2H, s, 1′-CH_2), 7.97 (1H, s, 2-H), 8.33 (2H, s, NH_2). UV $\lambda_{max}^{H_2O}$ nm: 265, 274 (Sh), 322.

5-Amino-3-(2-hydroxyethoxymethyl)imidazo[4,5-*d*][1,3]thiazin-7(3*H*)-one (3d) A catalytic amount of sodium methoxide was added to a solution of **12d** (0.009 g, 0.03 mmol) in absolute MeOH (4 ml) at 0 °C, and the reaction mixture was kept for 40 min in an ice bath. The reaction mixture was neutralized with 1.5% aqueous AcOH solution and evaporated to dryness. The residue was purified by silica gel column chromatography using 8% MeOH–$CHCl_3$ as an eluant to give **3d** as colorless crystals (5 mg, 60%), mp 204—205 °C. MS *m/z*: 242 (M^+). HR-MS Calcd for $C_8H_{10}N_4O_3S$: 242.0473. Found *m/z*: 242.0480. ^{1}H-NMR: 3.51 (4H, s, 3′ and 4′-CH_2), 4.67 (1H, br s, OH), 5.39 (2H, s, 1′-CH_2), 7.96 (1H, s, 2-H), 8.31 (2H, s, NH_2). UV $\lambda_{max}^{H_2O}$ nm ($\varepsilon \times 10^3$): 265 (11.5), 326 (9.3).

Acknowledgement The authors are indebted to the staff of the Center for Instrumental Analysis of Hokkaido University for elemental analysis and measurements of MS and NMR spectra.

References and Notes

1) Paper III in this series, H. Matsumoto, C. Kaneko, T. Mori, and Y. Mizuno, *J. Heterocycl. Chem.*, **27**, 1307 (1990).
2) H. J. Schaeffer, L. M. Beauchamp, G. B. Miranda, D. J. Bauer, and P. Collins, *Nature* (London), **272**, 583 (1978).
3) K. O. Smith, K. S. Galloway, W. L. Kennell, K. K. Ogilvie, and R. K. Radatus, *Antimicrob. Agents Chemother.*, **22**, 55 (1982).
4) N. K. Saxana, L. A. Coleman, J. C. Drach, and L. B. Townsend, *J. Med. Chem.*, **33**, 1980 (1990); J. S. Pudlo, M. R. Nassiri, E. R. Kern, L. L. Wotring, J. C. Drach, and L. B. Townsend, *ibid.*, **33**, 1984 (1980).
5) H. Matsumoto, C. Kaneko, T. Mori, and Y. Mizuno, *Chem. Pharm. Bull.*, **37**, 229 (1989).
6) The numberings of the purine ring, imidazo [4,5-*d*] [1,3]thiazine and the acyclic side chain are as follows:

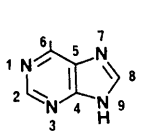

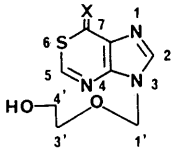

7) K. Klausen and S. O. Lawesson, *Bull. Soc. Chem. Belg.*, **88**, 305 (1979).
8) Y. H. Kim, J. Y. Kim, and C. H. Lee, *Chem. Lett.*, **1988**, 1045.
9) A. Parkin and M. R. Harnden, *J. Heterocycl. Chem.*, **19**, 33 (1982).
10) M. F. Summers, L. G. Marzilli, and A. Bax, *J. Am. Chem. Soc.*, **108**, 4285, (1985).
11) G. Zemplen and E. Pacsu, *Ber.*, **62**, 1613 (1929).

Tannins of Theaceous Plants. III.[1] Camelliatannins A and B, Two New Complex Tannins from *Camellia japonica* L.

Tsutomu HATANO, Shoko SHIDA, Li HAN and Takuo OKUDA*

Faculty of Pharmaceutical Sciences, Okayama University, Tsushima, Okayama 700, Japan. *Received October 11, 1990*

Two new complex tannins, camelliatannins A (1) and B (2), were isolated from the leaves of *Camellia japonica* L. (Theaceae). The structures of these tannins, each consisting of a *C*-glucosidic ellagitannin and (−)-epicatechin (9), were established by means of chemical degradation, synthesis from casuariin (4) and 9, and rotating frame Overhauser enhancement spectroscopy (ROESY). Gemin D (3), 4, pedunculagin (5) and 2,3-(*S*)-hexahydroxydiphenoyl-D-glucose (6) were also isolated from the leaves.

Keywords tannin; complex tannin; *C*-glucosidic ellagitannin; casuariin; epicatechin; camelliatannin A; camelliatannin B; *Camellia japonica*; Theaceae; ROESY

Isolation and structure elucidation of several dimeric and monomeric hydrolyzable tannins including camelliin B, which has a macrocyclic structure, from flowers of *Camellia japonica* L. were reported previously.[1,2] Further investigation of tannins of this species has led to the isolation of six compounds from the leaves. This paper deals with two new tannins named camelliatannins A (**1**) and B (**2**),[3] which belong to the category of complex tannins,[4] each consisting of a hydrolyzable tannin unit and a condensed tannin unit.

Results and Discussion

Fresh leaves of *Camellia japonica* were homogenized in aqueous acetone, and the concentrated filtrate from the homogenate was extracted with Et_2O, EtOAc and *n*-BuOH, successively. The *n*-BuOH extract was subjected to centrifugal partition chromatography (CPC),[5] and the fractions from CPC were further subjected to column chromatography on Toyopearl HW-40 and/or MCI-gel CHP-20P, which afforded camelliatannins A and B, along with gemin D (**3**),[2] casuariin (**4**),[6] pedunculagin (**5**)[6,7] and 2,3-(*S*)-hexahydroxydiphenoyl-D-glucose (**6**).[7-9]

Camelliatannin A (**1**) was obtained as an off-white powder. The positive-ion and negative-ion fast-atom bombardment mass spectra (FAB-MS) showed the $[M+H]^+$ ion peak at *m/z* 1057 and $[M-H]^-$ ion peak at *m/z* 1055, respectively. These ion peaks and the microanalytical data indicated that **1** has the molecular formula $C_{49}H_{36}O_{27}$. Methylation of **1** afforded a hexadeca-*O*-methyl derivative (**7**). The constituent sugar of **1** was glucose, as shown by its liberation upon the treatment of **1** with diluted sulfuric acid.

The proton nuclear magnetic resonance (^{1}H-NMR)

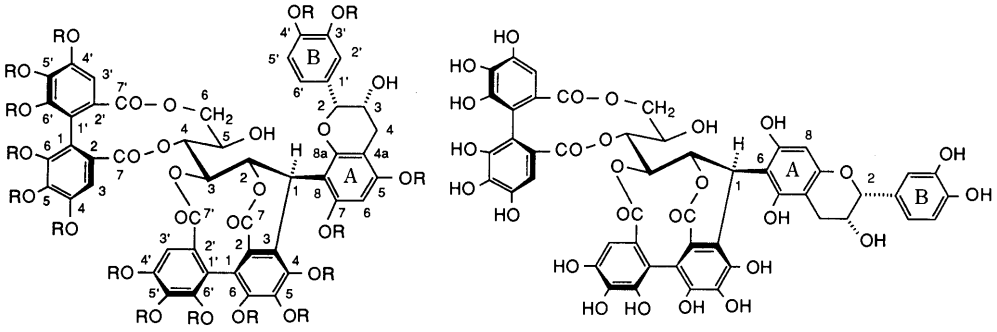

1: R=H
7: R=Me

2

Chart 1

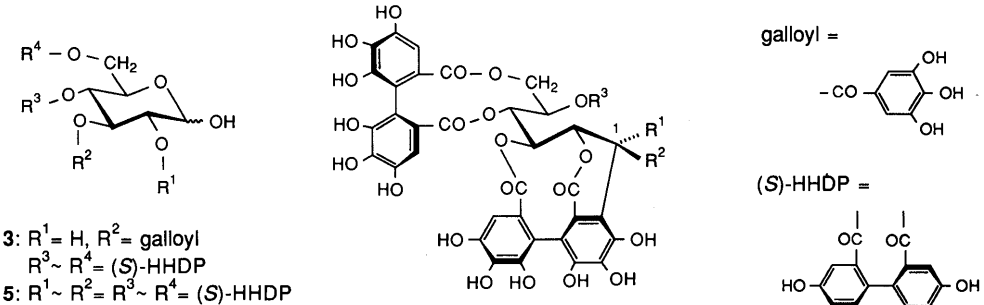

3: R^1= H, R^2= galloyl
R^3~ R^4= (*S*)-HHDP
5: R^1~ R^2= R^3~ R^4= (*S*)-HHDP
6: R^1~ R^2= (*S*)-HHDP
R^3= R^4= H

4: R^1= OH, R^2= R^3= H
8: R^1= H, R^2= OH, R^3= galloyl

Chart 2

spectrum (500 MHz, in acetone-d_6 + D_2O) showed that **1** consists of two hexahydroxydiphenoyl (HHDP) groups (one forms a *C*-glucosidic HHDP group) [δ 6.65, 6.47 and 6.26 (1H each, s)], a glucose moiety in open-chain form [δ 4.71 (br s, H-1), 4.93 (br s, H-2), 4.99 (br d, J=3 Hz, H-3), 5.07 (br dd, J=3, 7 Hz, H-4), 3.81 (d-like, J=7 Hz, H-5), 4.48 (br d, J=12 Hz, H-6) and 3.38 (br d, J=12 Hz, H-6)] and an epicatechin residue [δ 7.18 (br s, H-2'), 6.93 (br d, J=8 Hz, H-5'), 6.83 (br d, J=8 Hz, H-6'), 5.91 (br s, A-ring H), 5.03 (br s, H-2), 4.24 (br s, H-3), 2.85 (br dd, J=3.5, 16 Hz, H-4), 2.73 (br d, J=16 Hz, H-4)]. The presence of the epicatechin residue was proved by the release of (−)-epicatechin (**9**) upon the treatment of **1** with acetic acid.[10] The chemical shifts of the glucose protons indicate that O-2, O-3, O-4 and O-6 of the glucose residue in **1** are acylated, and O-5 is unacylated. Although the precise coupling constants of the glucose protons are obscured by broadening of the peaks, the splitting patterns observed for H-3—H-6 of the glucose residue in **1** are very similar to those of the corresponding protons in several *C*-glucosidic tannins, such as **4** and stachyurin (**8**),[6] both of which have two HHDP groups at O-2/O-3 and O-4/O-6. This spectral similarity suggests that the locations of the two HHDP groups on the glucose moiety of **1** are the same as those of **4** and **8**. The circular dichroism (CD) spectrum of **1** showed a positive Cotton effect with a large amplitude in the short-wavelength region ($[\theta]_{234}$ $+2.2\times10^5$), indicating[9] the (*S*)-configuration for both of the HHDP groups. These findings suggest that **1** consists of **4** (or its epimer at C-1 of the glucose core) and **9**.

Although most of the signals in the carbon-13 nuclear magnetic resonance (^{13}C-NMR) spectrum of **1** are superimposable on the combined ^{13}C signals of **4** and **9** (Table I), differences of the chemical shifts were observed for several signals between **1** and the sum of **4** and **9**. The presence of a C–C bond between glucose C-1 and epicatechin C-8 (or C-6) in **1** is indicated by the large upfield shifts of the signals of these two carbons, relative to the corresponding carbon signals of **4**. The chemical shift (δ 80.3) of the glucose C-2 signal of **1** is analogous to those of the corresponding signals of the complex tannins in which the orientation of glucose H-1 is the same as that in **8**,[11] and suggests that the stereostructure at glucose C-1 in **1** is the same as that in these complex tannins.

TABLE I. ^{13}C-NMR Spectral Data for **1**, **2**, **4** and **9**

Carbons	**1**[a,b]	**2**[c]	**4**[a,b]	**9**[a,d]
Glucose residue				
C-1	38.2	38.1	67.7	
C-2	80.3	81.5	76.9	
C-3	76.5	76.4	70.7	
C-4	75.8	75.9	77.1	
C-5	69.2	68.6	68.4	
C-6	67.1	67.9	68.1	
Hexahydroxydiphenoyl				
C-1,1'	115.4, 115.6	115.4, 115.8	115.1, 115.9	
	115.7, 116.9	115.9, 117.0	116.3, 116.6	
C-2,2'	122.2, 124.2	122.4, 124.0	120.5, 125.5	
	125.9, 127.2	125.6, 127.4	127.4, 127.6	
C-3,3'	105.2, 107.4	105.8, 107.3	105.1, 106.9	
	108.6, 128.0	108.9, 128.1	108.3, 115.9	
C-4,4'	145.0,[e] 145.2[e]	145.1,[f] 145.2[f]	145.0, 145.1	
	145.2,[e] 145.4[e]	145.2,[f] 145.7[f]	145.7, 146.2	
C-5,5'	134.9, 135.8	135.2, 135.9	134.8, 135.6	
	136.3, 137.5	136.5, 137.6	136.5, 138.4	
C-6,6'	142.7,[e] 143.3[e]	143.1,[f] 143.2[f]	143.6, 143.8	
	144.2,[e] 144.2[e]	144.3,[f] 144.4[f]	144.3, 144.5	
C-7,7'	167.2, 167.8	167.9, 168.7	164.7, 168.6	
	169.1, 170.4	169.6, 170.6	169.3, 170.2	
Epicatechin moiety				
C-2	79.4	79.0		79.2
C-3	66.5	66.6		66.7
C-4	29.1	29.3		28.7
C-4a	99.6	100.1		99.5
C-5	156.4	155.6		157.4
C-6	96.6	107.2		95.9
C-7	155.9	155.6		157.3
C-8	105.2	96.5		95.3
C-8a	153.9	155.2		156.8
C-1'	132.0	131.9		131.6
C-2'	115.0	115.2		115.0
C-3'	145.0[e]	145.2[f]		145.2
C-4'	144.3[e]	144.3[f]		145.1
C-5'	115.7	115.4		115.3
C-6'	119.4	119.2		119.0

125.7 MHz, in acetone-d_6 + D_2O. *a*) Recorded at ambient temperature. *b*) The assignments are based on the (one-bond) ^{1}H–^{13}C heteronuclear shift correlation spectrum. *c*) Recorded at 40 °C. *d*) The assignments are based on the one-bond and long-range ^{1}H–^{13}C heteronuclear shift correlation spectra. *e,f*) The values with the same superscript may be interchanged.

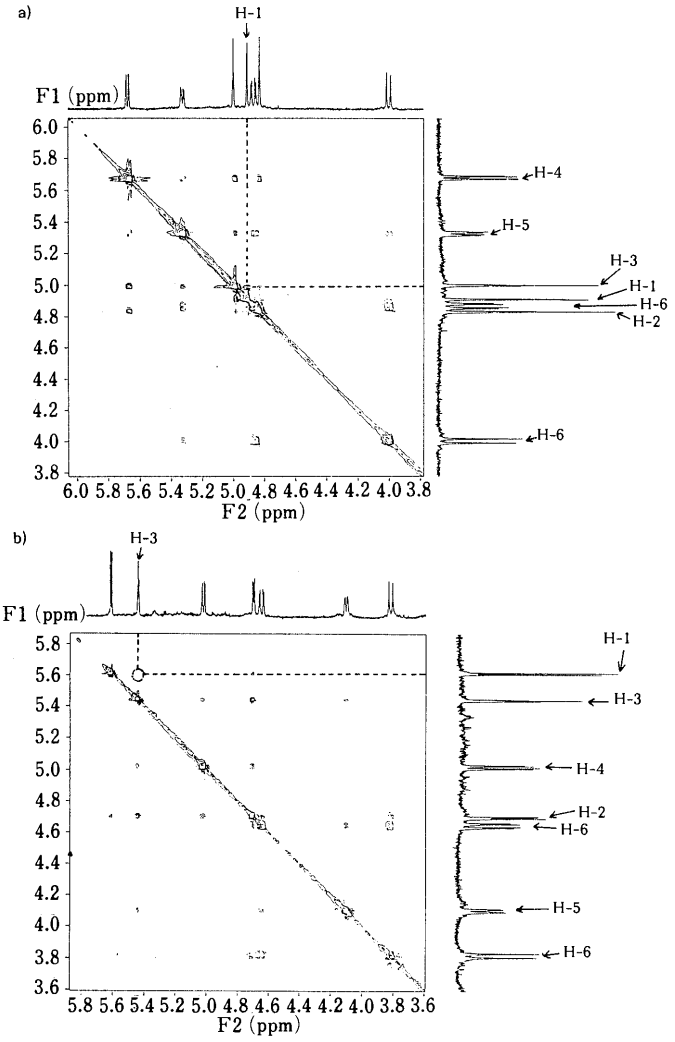

Fig. 1. The ROESY Spectra of a) Stachyurin (**8**) and b) Casuariin (**4**)

In acetone-d_6 + D_2O, 27 °C. The regions of the glucose protons are shown. The dotted circle in the spectrum of **4** (b) indicates the absence of the cross peak between H-1 and H-3.

The rotating frame Overhauser enhancement spectroscopy (ROESY) spectrum of **8** showed a cross peak due to the nuclear Overhauser effect (NOE) between glucose H-1 and H-3 (Fig. 1a), indicating the α-orientation of H-1 as reported recently,[12] while this cross peak was absent in the spectrum of **4**, which is the C-1 epimer of degalloylated **8** (Fig. 1b).

Since the glucose protons H-1 and H-2 in the ^{1}H-NMR spectrum of **1** are somewhat broadened, the coupling constant between these two protons is not clear enough for determining the orientation of the hydrogen on C-1. However, the ROESY spectrum of **1** (Fig. 2) showed the presence of an NOE between H-1 and H-3. Therefore, H-1 in **1** is α-oriented.

The ROESY spectrum of **1** also showed an NOE between H-1 of the glucose residue and H-2′ of the epicatechin residue. Molecular models of the two possible structures for **1** (one has a bond between epicatechin C-8 and glucose C-1, and the other between epicatechin C-6 and glucose C-1) show that only the former structure allows approach of the B-ring of the epicatechin residue to glucose H-1 (Fig. 2). The H-2 signal (δ 5.03) of the epicatechin moiety in **1** showed a downfield shift, relative to the corresponding signals of **9** (δ 4.89). This downfield shift is analogous to that observed for the corresponding H-2 signal (δ 4.96) of the lower epicatechin moiety in procyanidin B-2 (**10**),[13] which possesses a C-4—C-8 linkage. As noted for the glucose protons, the signals of most of the other protons in the ^{1}H-NMR spectrum of **1** are also broadened, and this broadening is attributable to the presence of the C-8 substituted epicatechin residue. Namely, the "folded" structure of **1** may induce not only restricted rotation[14] around the epicatechin-glucose linkage, but also hindrance of the conformational change of the ellagitannin residue.

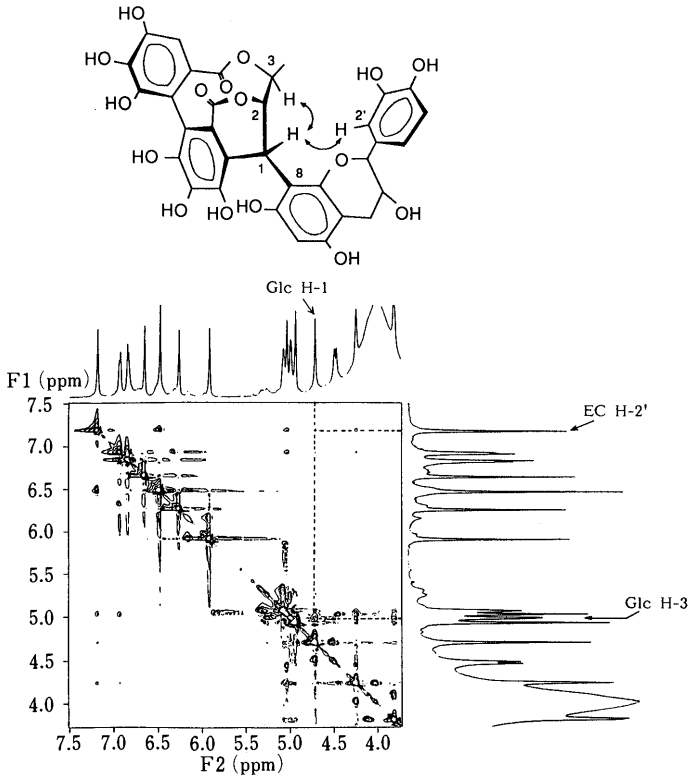

Fig. 2. The ROESY Spectrum of Camelliatannin A (**1**)

In acetone-d_6+D_2O, 30 °C. Glc and EC respectively represent glucose and epicatechin moieties in **1**.

Camelliatannin B (**2**) was obtained as an off-white powder. The positive-ion FAB-MS of **2** showed the $[M+H]^+$ ion peak at *m/z* 1057, which is consistent with the molecular formula $C_{49}H_{36}O_{27}$. The presence of glucose and an epicatechin moiety in the molecule of **2** was shown by their formation upon the treatment of **2** with diluted sulfuric acid or ethanolic acetic acid.

The ^{1}H-NMR spectrum (500 MHz, at 40 °C, in acetone-d_6+D_2O) showed that **2** has two HHDP groups (one has a *C*-glucosidic linkage) [δ 6.80, 6.53 and 6.47 (1H each, s)], a glucose moiety in the open-chain form [δ 4.66 (d, *J*=1 Hz, H-1), 4.82 (dd, *J*=1, 2.5 Hz, H-2), 5.21 (t, *J*=2.5 Hz, H-3), 5.27 (dd, *J*=2.5, 8 Hz, H-4), 4.12 (ddd, *J*=1, 3, 8 Hz, H-5), 4.73 (dd, *J*=3, 12 Hz, H-6) and 3.83 (dd, *J*=1, 12 Hz, H-6)] and an epicatechin moiety [δ 7.01 (d, *J*=1.5 Hz, H-2′), 6.79 (dd, *J*=1.5, 8.5 Hz, H-6′), 6.74 (d, *J*=8.5 Hz, H-5′), 5.98 (br s, A-ring H), 4.78 (br s, H-2), 4.15 (m, H-3), 2.82 (br dd, *J*=3.5, 16 Hz, H-4), 2.67 (br d, *J*=16 Hz, H-4)]. The CD spectrum of **2** showed a positive Cotton effect ($[\theta]_{236}$ $+2.3\times10^5$) reflecting the (*S*)-configuration of the two HHDP groups.[9] These two (*S*)-HHDP groups in **2** are at O-2/O-3 and O-4/O-6 as indicated by the chemical shifts and the coupling constants of the glucose protons. The ^{13}C-NMR spectrum of **2** was closely similar to that of **1** (Table I). These findings indicate that **2** is also composed of **4** (or its C-1 epimer) and **9**.

The orientation of glucose H-1 in **2** is also α, since the coupling constant between H-1 and H-2 is similar to that of **8**. The presence of an NOE between H-1 and H-3 of the glucose residue, which was shown by a cross peak in the ROESY spectrum of **2** (Fig. 3), also substantiated α-orientation of H-1.

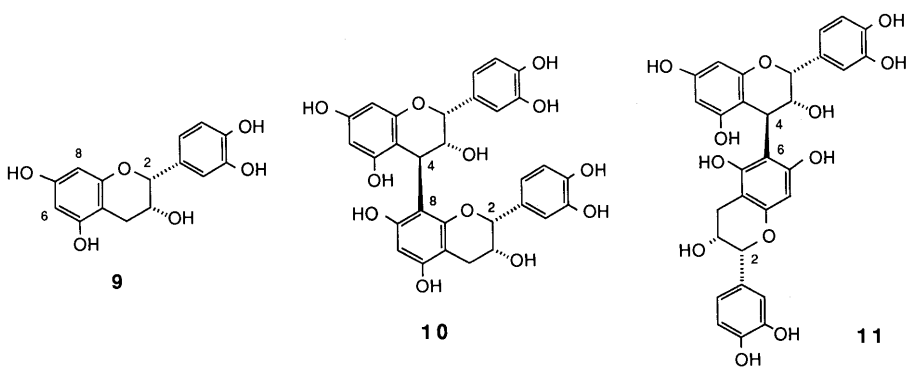

Chart 3

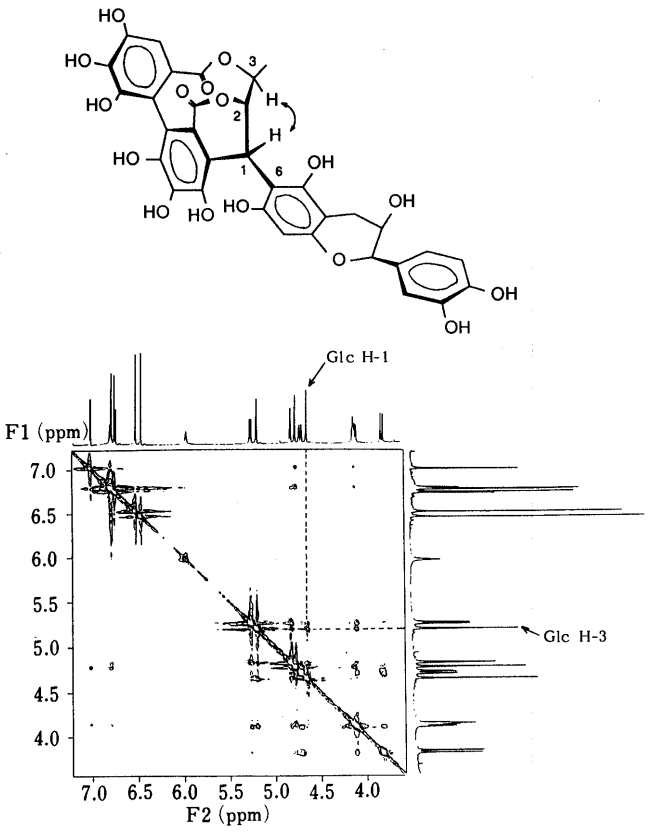

Fig. 3. The ROESY Spectrum of Camelliatannin B (**2**)
In acetone-d_6 + D_2O, 40 °C. Glc: glucose moiety in **2**.

This ROESY spectrum, however, did not show any cross peaks between the protons of the epicatechin moiety and those of the other parts of the molecule (glucose and HHDP). Unlike in **1**, the downfield shift of H-2 of the epicatechin moiety [relative to the corresponding proton of **9** (δ 4.89)] was not observed in **2**, and this absence of the downfield shift is analogous to that of H-2 in the C-6 substituted epicatechin (the lower half) of procyanidin B-5 (**11**) (δ 4.84).[13] These spectral data indicate C-6 substitution in the epicatechin moiety in **2**. Among the ^1H signals of **2**, only H-8 of the epicatechin moiety showed distinctive broadening due to the presence of the glucose-epicatechin linkage, and this supports the "unfolded" structure **2** having the less-hindered C-6-substituted epicatechin.

The structures **1** and **2** of camelliatannins A and B, thus assigned to be complex tannins,[4] were confirmed by acid-catalyzed condensation of **4** and **9**, followed by fractionation of the products by gel-column chromatography, which afforded **1** and **2**. Biogenetically, these two complex tannins may have been formed by the C–C oxidative coupling of these two constituent units.

Experimental

Optical rotations were measured on a JASCO DIP-4 polarimeter. Ultraviolet (UV) and infrared (IR) spectra were recorded on a Hitachi 200-10 spectrophotometer and a JASCO A-102 spectrometer, respectively. ^1H- and ^{13}C-NMR spectra were recorded on a Varian VXR-500 instrument (500 MHz for ^1H-NMR and 125.7 MHz for ^{13}C-NMR) in acetone-d_6 or in acetone-d_6 containing D_2O (*ca.* 3%). Chemical shifts are given in δ values (ppm), based on those of the ^1H and ^{13}C signals of acetone-d_6 (δ_H 2.04; δ_C 29.8) in the solvents. CD spectra were recorded on a JASCO J-500A spectrometer, equipped with a DP-501N data processor. FAB-MS were recorded on a JEOL JMS-D300 mass spectrometer. Gas liquid chromatography (GLC) was performed on a Hitachi 163 gas chromatograph equipped with a CITI G-250 WCOT column (1.2 mm × 40 m). The injection temperature and column temperature were 200 °C and 180 °C, respectively. Normal-phase high-performance liquid chromatography (HPLC) was performed on a Merck Superspher SI60 column (4 × 125 mm) with *n*-hexane–MeOH–tetrahydrofuran–formic acid (55:33:11:1) containing oxalic acid (450 mg/l) (flow rate, 1.5 ml/min). Reversed-phase HPLC was performed on a LiChrospher RP-18 (5 μm) column (4 × 250 mm) at 40 °C, with solvent system (A) 10 mM H_3PO_4–10 mM KH_2PO_4–MeOH (2:2:1) (flow rate, 1.1 ml/min), (B) 10 mM H_3PO_4–10 mM KH_2PO_4–EtOH–EtOAc (17:17:4:2) (flow rate, 1.2 ml/min), or (C) 10 mM H_3PO_4–10 mM KH_2PO_4–MeCN (9:9:2) (flow rate, 1.0 ml/min). Detection was effected with a Shimadzu SPD-6A spectrophotometer at 280 nm. CPC was performed using a CPC apparatus (model L-90, Sanki Engineering, Nagaoka-kyo), which contains 12 partition cell cartridges (type 1000E).

Isolation of Tannins from Leaves of *Camellia japonica* Fresh leaves (1.8 kg) of *Camellia japonica*, collected at the Herbal Garden of Okayama University in March 1988, were homogenized in 70% acetone (13 l). The concentrated filtrate (1.6 l) from the homogenate was extracted with Et_2O, EtOAc and *n*-BuOH, successively, and each solvent was removed by evaporation at below 40 °C. A portion (20 g) of the *n*-BuOH extract (85 g) was subjected to CPC with *n*-BuOH–*n*-PrOH–H_2O (4:1:5, v/v; normal-phase development→reversed-phase development), to separate six fractions (fr. I—III for the normal-phase development, and fr. IV—VI for the reversed-phase development). Fraction II (1.5 g) was chromatographed on Toyopearl HW-40F with 20% EtOH and then with 40% EtOH, to give **3** (20 mg), **4** (13 mg) and **5** (321 mg). Fraction V (1.1 g) from CPC was chromatographed on MCI-gel CHP-20P with H_2O and then with 20% MeOH. The H_2O eluate (296 mg) was further separated on a column of Toyopearl HW-40F with 40% EtOH→60% EtOH, to give **1** (109 mg) and **6** (25 mg). The 20% MeOH eluate from the column of MCI-gel (378 mg) was further chromatographed on Toyopearl HW-40SF with 70% EtOH, and then on MCI-gel CHP-20P with 10% MeOH→20% MeOH), to give **2** (12 mg).

Camelliatannin A (1) An off-white amorphous powder, $[\alpha]_D$ +68° (c=1.2, MeOH). *Anal.* Calcd for $C_{49}H_{36}O_{27}\cdot 7H_2O$: C, 49.75; H, 4.26. Found: C, 49.77; H, 4.24. Positive-ion FAB-MS: m/z 1057 ($[M+H]^+$). Negative-ion FAB-MS: m/z 1055 ($[M-H]^-$). UV λ_{max}^{MeOH} nm (log ε): 207 (4.99), 232 (sh, 4.83), 280 (sh, 4.34). IR ν_{max}^{KBr} cm^{-1}: 1720, 1610. CD (MeOH): $[\theta]_{285}$ +2.8 × 10^4, $[\theta]_{262}$ −6.1 × 10^4, $[\theta]_{234}$ +2.2 × 10^5, $[\theta]_{206}$ −1.2 × 10^5. ^1H-NMR: see text. ^{13}C-NMR: see Table I.

Camelliatannin B (2) An off-white amorphous powder, $[\alpha]_D$ +138° (c=0.6, MeOH). *Anal.* Calcd for $C_{49}H_{36}O_{27}\cdot 8H_2O$: C, 49.00; H, 4.33. Found: C, 48.50; H, 3.67. Positive-ion FAB-MS: m/z 1057 ($[M+H]^+$). UV λ_{max}^{MeOH} nm (log ε): 207 (4.99), 232 (sh, 4.84), 2.80 (sh, 4.34). IR ν_{max}^{KBr} cm^{-1}: 1720, 1610. CD (MeOH): $[\theta]_{285}$ +2.2 × 10^4, $[\theta]_{263}$ −4.5 × 10^4, $[\theta]_{236}$ +2.3 × 10^5, $[\theta]_{202}$ −1.4 × 10^5. ^1H-NMR: see text. ^{13}C-NMR: see Table I.

Degradation of 1 and 2 1) A solution of **1** (2 mg) in 1 N H_2SO_4 (0.2 ml) in a sealed tube was heated in a boiling-water bath for 12 h. Then, the solution was neutralized with Dia-ion SA-20AP, and evaporated. The presence of glucose in the residue was shown by trimethylsilylation followed by GLC analysis. The liberation of glucose upon the treatment of camellianin B with 1 N H_2SO_4 was also proved in an analogous way.

2) A solution of **1** (1 mg) in a mixture of acetic acid and EtOH (1:4, v/v; 1 ml) in a sealed tube was heated in a boiling-water bath for 36 h, and the reaction mixture was analyzed by HPLC [normal-phase HPLC, t_R (retention time) 2.0 min; reversed-phase HPLC with solvent (A), t_R 29.0 min; reversed-phase HPLC with solvent (B), t_R 5.6 min], resulting in the identification of **9**. The liberation of **9**, upon the treatment of **2** with ethanolic acetic acid for 18 h, was also proved by HPLC in an analogous way.

Methylation of 1 Dimethyl sulfate (10 μl) and potassium carbonate (100 mg) were added to a solution (10 ml) of **1** (10 mg) in acetone. The mixture was stirred overnight at room temperature, and then refluxed for 5 h. After centrifugation, the supernatant was evaporated, and the residue was subjected to preparative thin layer chromatography (PTLC) on Kieselgel 60 PF_{254} (Merck) with benzene–acetone (4:1, developed twice), to give **7** (5 mg), $[\alpha]_D$ −13° (c=0.6, acetone). *Anal.* Calcd for $C_{65}H_{68}O_{27}\cdot 2H_2O$: C, 59.26; H, 5.50. Found: C, 59.01; H, 5.21. ^1H-NMR (500 MHz, in acetone-d_6): δ 7.27 [d, J=2 Hz, H-2′ of the epicatechin (EC) moiety], 7.15 (dd, J=2, 8 Hz, EC H-6′), 6.96 (d, J=8 Hz, EC H-5′), 6.92, 6.73, 6.70 (each s, HHDP H-3, H-3′), 6.22 (s, EC H-6), 5.22 (br s, EC H-2), 5.06 [dd, J=5.5, 7 Hz, H-4 of Glc (glucose)], 4.94 (dd, J=1, 2 Hz, Glc H-2), 4.93 (d, J=1 Hz, Glc H-1), 4.91 (dd, J=2, 5.5 Hz, Glc H-3),

4.45 (dd, $J=2.5$, 12.5 Hz, Glc H-6), 4.34 (m, EC H-3), 4.06, 3.94, 3.88, 3.87, 3.84, 3.83, 3.81, 3.80, 3.80, 3.75, 3.74, 3.66, 3.63, 3.59, 3.58, 3.44 (3H each, s, 16 × OMe).

Transformation of 4 and 9 into 1 and 2 A mixture of **4** (200 mg), **9** (300 mg) and *p*-toluenesulfonic acid (100 mg) in dioxane (17 ml) in a sealed tube was heated in a boiling-water bath for 5 h. Then, the solvent was evaporated off, and the residue was chromatographed over MCI-gel CHP-20P with H_2O (fr. 1)→5% MeOH (fr. 2 and fr. 3)→20% MeOH (fr. 4—6). Fraction 1 (150 mg) was mainly composed of unchanged **4**. Fraction 3 (24 mg) was repeatedly chromatographed over Toyopearl HW-40SF (with 40% EtOH and then with 25% EtOH), to give a product (1.0 mg). Fr. 5 (15 mg) was further purified in an analogous way, to give another product (0.9 mg). These products were respectively identified as **1** and **2** by ^{1}H-NMR and HPLC [normal-phase HPLC: **1**, t_R 9.1 min; **2**, t_R 8.9 min. Reversed-phase HPLC with solvent (C): **1**, t_R 3.6 min; **2**, t_R 5.2 min].

Acknowledgements We thank Prof. K. Takaishi and Dr. H. Kuwajima, Faculty of Pharmaceutical Sciences, Kinki University, for the FAB mass spectra. The 500 MHz ^{1}H-NMR and 125.7 MHz ^{13}C-NMR spectra were recorded on an instrument at the SC-NMR Laboratory of Okayama University. This study was supported in part by a Grant-in-Aid for Scientific Research from the Ministry of Education, Science and Culture. One of us (L. H.) is grateful to the Fujisawa Foundation for a scholarship.

References and Notes

1) For Part II, see T. Yoshida, T. Chou, Y. Maruyama and T. Okuda, *Chem. Pharm. Bull.*, **38**, 2681, (1991).
2) T. Yoshida, Y. Maruyama, M. U. Memon, T. Shingu and T. Okuda, *Phytochemistry*, **24**, 1041 (1985).
3) A part of this work was presented at the 35th Annual Meeting of the Japanese Society of Pharmacognosy, Niigata, September 1988, and the two new tannins are identical with the compounds which we called camellianins A and B at the meeting. As these names have been used for flavonoids of *Camellia sinensis* [G.-R. Chen, J.-L. Jin and Y.-X. Wen, *Yaoxue Xuebao*, **22**, 203 (1987)], we renamed these tannins camelliatannins A and B.
4) T. Okuda, T. Yoshida, T. Hatano, K. Yazaki, Y. Ikegami and T. Shingu, *Chem. Pharm. Bull.*, **35**, 443 (1987).
5) *a*) D. W. Armstrong, *J. Liq. Chromatogr.*, **11**, 2433 (1988); *b*) T. Yoshida, T. Hatano and T. Okuda, *J. Chromatogr.*, **467**, 139 (1989); *c*) T. Okuda, T. Yoshida, T. Hatano, K. Mori and T. Fukuda, *J. Liq. Chromatogr.*, **13**, 3637 (1990).
6) T. Okuda, T. Yoshida, M. Ashida and K. Yazaki, *J. Chem. Soc., Perkin Trans. 1*, **1983**, 1965.
7) O. T. Schmidt, L. Wültele and A. Harrèus, *Justus Liebigs Ann. Chem.*, **690**, 150 (1965).
8) M. K. Seikel and W. E. Hillis, *Phytochemistry*, **9**, 1115 (1970).
9) T. Okuda, T. Yoshida, T. Hatano, T. Koga, N. Toh and T. Kuriyama, *Tetrahedron Lett.*, **23**, 3937 (1982).
10) The facile cleavage of the C–C bond between the epicatechin residue and the glucose residue is considered to occur in a way analogous to the acid-catalyzed cleavage of the interflavan linkages of proanthocyanidins (see, refs. 13*a* and 14). A carbocation centered at C-1 of the glucose residue (benzylic position) is assumed to be formed in the present case.
11) T. Hatano, T. Yoshida, Y. Shingu and T. Okuda, *Chem. Pharm. Bull.*, **36**, 3849 (1988).
12) G. Nonaka, T. Sakai, T. Tanaka, K. Mihashi and I. Nishioka, *Chem. Pharm. Bull.*, **38**, 2151 (1990).
13) *a*) R. S. Thompson, D. Jacques, E. Haslam and R. J. N. Tanner, *J. Chem. Soc., Perkin Trans. 1*, **1972**, 1387; *b*) G. Nonaka, O. Kawahara and I. Nishioka, *Chem. Pharm. Bull.*, **30**, 4277 (1982).
14) E. Haslam, *Phytochemistry*, **16**, 1625 (1977).

Tannins and Related Polyphenols of Euphorbiaceous Plants. VIII.[1] Eumaculin A and Eusupinin A, and Accompanying Polyphenols from *Euphorbia maculata* L. and *E. supina* RAFIN.

Isao AGATA,[a] Tsutomu HATANO,[b] Yoko NAKAYA,[a] Takeshi SUGAYA,[a] Sansei NISHIBE,[a] Takashi YOSHIDA[b] and Takuo OKUDA*,[b]

Faculty of Pharmaceutical Sciences, Higashi Nippon Gakuen University,[a] Ishikari-Tobetsu, Hokkaido 061-02, Japan and Faculty of Pharmaceutical Sciences, Okayama University,[b] Tsushima, Okayama 700, Japan. *Received October 24, 1990*

Two new dimeric hydrolyzable tannins named eumaculin A (1) and eusupinin A (2) have been isolated from *Euphorbia maculata* L. and *Euphorbia supina* RAFIN., and their structures elucidated. Twelve other polyphenolic compounds including five hydrolyzable tannins and five flavonol glycosides have also been isolated.

Keywords tannin; dimeric hydrolyzable tannin; eumaculin A; eusupinin A; geraniin; *Euphorbia maculata*; *Euphorbia supina*; Euphorbiaceae

Some *Euphorbia* species of Euphorbiaceae have been used as remedies in various countries, including China and southeast Asia.[2] Among them, *E. maculata* L. and *E. supina* RAFIN. have been used as folk medicines for wounds in Mexico,[3] and as an antidiarrheal and for wound treatment in China.[4] The chemical constituents of these plants have been little studied, although the presence of geraniin was revealed by chromatographic surveys.[5] We have now isolated two new hydrolyzable tannins, named eumaculin A (**1**) and eusupinin A (**2**), together with several flavonoids and hydrolyzable tannins, from these two plants.

Results and Discussion

The overground part of *Euphorbia maculata* was homogenized in aqueous acetone, and the concentrated filtrate from the homogenate was extracted with Et_2O, EtOAc and *n*-BuOH, successively. Repeated column chromatography of the EtOAc extract yielded eumaculin A (**1**), and also four flavonol glycosides, astragalin,[6] isoquercitrin,[6] kaempferol 3-*O*-(2″-*O*-galloyl)-*β*-D-glucoside[6] and quercetin 3-*O*-(2″-*O*-galloyl)-*β*-D-glucoside,[6] and two hydrolyzable tannins, 1,3,4,6-tetra-*O*-galloyl-*β*-D-glucose (**3**)[7] and geraniin.[8]

The EtOAc extract from the homogenate of the overground part of *E. supina* was separated in an analogous way, to give eusupinin A (**2**), along with nine polyphenolic compounds including three flavonol glycosides, astragalin, isoquercitrin and quercetin 3-*O*-α-L-arabinofuranoside,[9] and four hydrolyzable tannins, geraniin, 1,2,3-tri-*O*-galloyl-*β*-D-glucose (**4**),[10] corilagin (**5**)[11] and rugosin D (**6**).[12]

Eumaculin A (**1**) was obtained as a light-brown amorphous powder. The molecular formula $C_{68}H_{52}O_{44}$ was indicated by the $[M+Na]^+$ ion peak at *m/z* 1595 in the fast-atom bombardment mass spectrum (FAB-MS) and by the microanalytical data. The proton nuclear magnetic resonance (^{1}H-NMR) spectrum of this tannin (in acetone-d_6 + D_2O) showed the presence of five galloyl groups [δ 7.14 (2H, s), 7.10 (4H, s), 7.08 (2H, s), 6.84 (2H, s)], a valoneoyl group [δ 7.05 (1H, s, H_C), 6.83 (1H, s, H_A), 6.19 (1H, s, H_B)] and two glucose cores (see Experimental) in the molecule. The coupling pattern of the glucose protons is typical of $^4C_1$ and $^1C_4$ glucopyranoses.[7,13-15]

The hydroxyl groups on the $^4C_1$ glucose core are fully

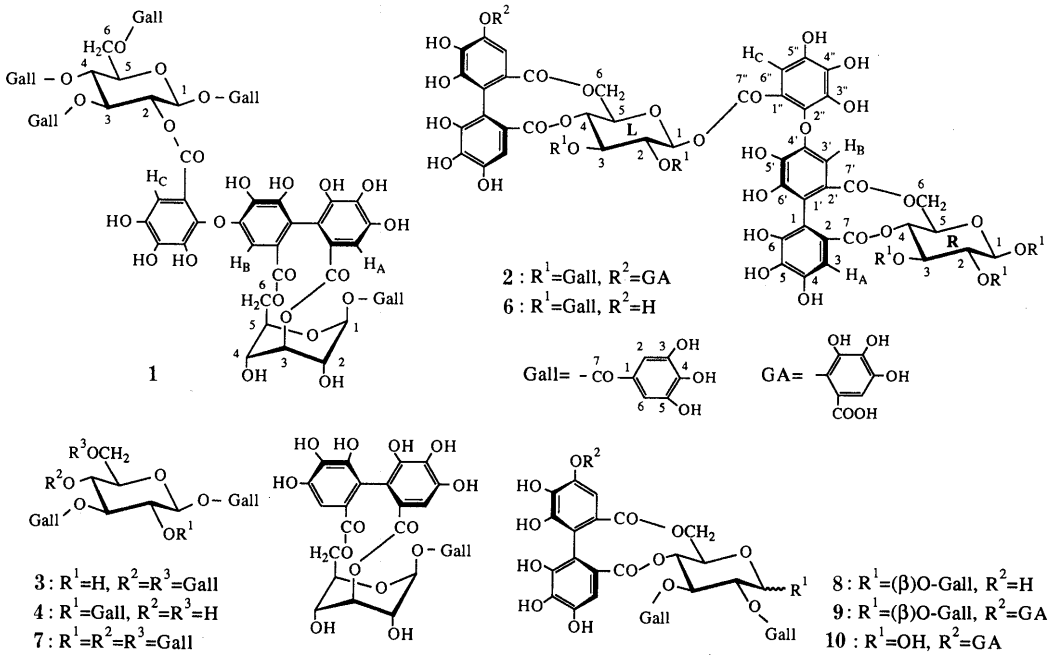

Chart 1

acylated as revealed by the downfield shifts of the protons on the glucose core, while the hydroxyl groups at C-2 and C-4 in the $^1C_4$ glucose core were considered to be unacylated on the basis of the chemical shifts of H-2 (δ 4.07) and H-4 (δ 4.38). Further, the chemical shifts of all of the glucose protons in eumaculin A are almost in agreement with the sum of those of 1,2,3,4,6-penta-*O*-galloyl-β-D-glucose (**7**)[7] and corilagin (**5**).[16] Eumaculin A is therefore a dimeric hydrolyzable tannin composed of these two monomers, and is identical with the product **1**[1,7] derived in two steps from euphorbin A (a dimer isolated from *E. hirta*)[1,7] or with a regio-isomer of **1** concerning the orientation of the valoneoyl group. A direct comparison established the identity of eumaculin A with **1**.

Eusupinin A (**2**) was obtained as a light-brown amorphous powder. The $[M+Na]^+$ ion peak at *m/z* 2065 in the FAB-MS and the microanalytical data indicated its molecular formula to be $C_{89}H_{62}O_{57}$. The ^{1}H-NMR spectrum of eusupinin A (in acetone-d_6+D_2O) indicated the presence of five galloyl and two valoneoyl groups [δ 7.12 (3H, s, galloyl and valoneoyl H_C), 7.10 (valoneoyl H_C), 7.01 (2H, s, galloyl), 6.99 (4H, s, galloyl × 2), 6.96 (2H, s, galloyl), 6.46, 6.45 (1H each, s, valoneoyl H_A × 2), 6.30, 6.20 (1H each, s, valoneoyl H_B × 2)], along with two $^4C_1$ glucopyranose cores (see Experimental). The chirality of both valoneoyl groups in the molecule was determined to be *S*, based on the positive Cotton effect in the short-wavelength region ($[\theta]_{225}$ $+2.3\times10^5$) of its circular dichroism (CD) spectrum (in MeOH).[17]

The large differences in the ^{1}H chemical shifts between the two H-6 protons on each $^4C_1$ glucose core ($\Delta\delta$ 1.49 and 1.49) indicated that the hexahydroxydiphenoyl (HHDP) moieties of the two veloneoyl groups are at O-4/O-6 on each glucose core.[18] Each hydroxyl group at C-1, C-2 and C-3 of the glucose cores is hence esterified with a galloyl group or a galloyl moiety of valoneoyl group, since the chemical shifts of the glucose protons indicate that all hydroxyl groups on the two glucopyranose cores are acylated.

The carbon-13 nuclear magnetic resonance (^{13}C-NMR) spectrum of eusupinin A (in acetone-d_6+D_2O) showed six pairs of glucose carbons [δ 93.64, 93.05 (C-1); 71.70, 71.65 (C-2); 73.20 (2C) (C-3); 70.64, 70.55 (C-4); 72.91 (2C) (C-5); 62.98 (2C) (C-6)] in a pattern similar to that of tellimagrandin II (**8**),[19] and is in agreement with the locations of the acyl groups assigned based on the ^{1}H-NMR spectrum. Although the differences in the ^{13}C chemical shifts between the signals of each pair of glucose carbons are within 0.1 ppm for C-2—C-6, there is a notable difference of the shifts (0.59 ppm) between the two C-1 carbons. This difference, due to an upfield shift of a signal at δ 93.05 (the C-1 signal of **8** is at δ 93.8[19]), is attributable to an effect of the substitution of a valoneoyl group for the galloyl group. One of the two galloyl moieties of the valoneoyl groups is hence assigned to be at C-1.

The orientation of both of the valoneoyl groups in eusupinin A was assigned to be the same as that of rugosin A (**9**),[20] based on the upfield shifts of the valoneoyl H_B signals relative to the HHDP proton (δ 6.63) of the glucose O-6 side of **8**.[20] On the other hand, the chemical shifts of the two valoneoyl H_A signals are in agreement with that of the HHDP proton (δ 6.45) of the glucose O-4 side of **8**.[21]

The structure **2** thus assigned for eusupinin A was substantiated by its partial hydrolysis to form **9** and rugosin B (**10**)[20] (*ca.* 1 : 1 in molar ratio).

Among the oligomeric hydrolyzable tannins hitherto isolated from *Euphorbia* species, those having $^1C_4$ glucose(s) (*i.e.*, euphorbins A—F and tirucallin B) have been found in *E. hirta*,[1,7,22,23] *E. tirucalli*[1] and *E. maculata* (this paper), and not in *E. prostrata*[24] or *E. supina* (this paper). On the other hand, oligomers each consisting solely of monomers with $^4C_1$ glucose (*i.e.*, rugosins D and G, and prostratin B[24]) have been found only in the latter two species.

Experimental

Optical rotations were measured on a JASCO DIP-4 polarimeter. ^{1}H- and ^{13}C-NMR spectra were recorded on a Varian VXR-500 instrument (500 MHz for ^{1}H-NMR and 125.7 MHz for ^{13}C-NMR). Chemical shifts are given in δ values (ppm), based on those of the ^{1}H and ^{13}C signals of acetone-d_6 (δ_H 2.04; δ_C 29.8). CD spectra were recorded on a JASCO J-500A spectrometer, equipped with a DP-501N data processor. FAB-MS were recorded on a VG 70-SE mass spectrometer. High-performance liquid chromatography (HPLC) was performed on a LiChrospher RP-18 cartridge column (4 × 250 mm; Merck) in an oven set at 40 °C, with solvent A (0.01 M H_3PO_4–0.01 M KH_2PO_4–MeOH, 7 : 7 : 6), B (0.01 M H_3PO_4–0.01 M KH_2PO_4–EtOH–EtOAc, 8 : 8 : 3 : 1) or C (0.01 M H_3PO_4–0.01 M KH_2PO_4–MeCN, 21 : 21 : 8). The flow rate was set at 1.0 ml/min.

Isolation of Polyphenols from *Euphorbia maculata* The dried aerial part of *E. maculata* (800 g), collected at the campus of Okayama University, in September, was homogenized in 70% acetone. Concentrated filtrate from the homogenate was extracted with Et_2O, EtOAc and *n*-BuOH, successively. The EtOAc extract (25.2 g) was chromatographed over Sephadex LH-20 with 60% EtOH, to give fractions I—IV. Fraction I was rechromatographed over Sephadex LH-20 (Pharmacia) (50% MeOH) and then on silicic acid (Mallinckrodt) ($CHCl_3$–EtOH, 5 : 1) to yield astragalin (34 mg) and isoquercitrin (58 mg). Purification of fractions II—IV by column chromatography on silicic acid, Sephadex LH-20 and Toyopearl HW-40 (Toso) yielded kaempferol 3-*O*-(2″-*O*-galloyl)-β-D-glucoside (32 mg), quercetin 3-*O*-(2″-*O*-galloyl)-β-D-glucoside (20 mg), geraniin (160 mg) and **3** (124 mg). In a separate experiment, the EtOAc extract from 1 kg of the dried aerial part of this plant was chromatographed over Sephadex LH-20 with 70% EtOH, and a fraction containing **1** was further chromatographed over Toyopearl HW-40 (40% acetone) and then over Sep-Pak C18 (Waters) (25% acetone), to give purified **1** (20 mg).

Isolation of Polyphenols from *Euphorbia supina* The dried aerial part of *E. supina* (1 kg), collected at the campus of Okayama University in September, was treated in a way similar to that described above. The EtOAc extract (58.2 g) was suspended in MeOH, and the insoluble part (4.4 g) was dissolved in 60% EtOH. After removal of the insoluble ellagic acid (1 g), the 60% EtOH soluble part was chromatographed over Sephadex LH-20 (60% MeOH), to give fractions I and II. Fraction I was separated by column chromatography on silicic acid ($CHCl_3$–MeOH, 17 : 3) to give astragalin (10 mg) and quercitrin (1 mg). Fraction II gave **5** (37 mg) after rechromatography over Sephadex LH-20 (MeOH). The MeOH-soluble part (53.8 g) of the EtOAc extract was chromatographed over Sephadex LH-20 with aqueous MeOH (50%→60%→70%) and then with aqueous acetone (35%→50%→70%→100%). Fractions containing polyphenols were further purified by column chromatography on Sephadex LH-20, MCI-gel CHP-20P (Mitsubishi Chemical Industries) and/or Sep-Pak C18, to give gallic acid (25 mg) (from the 50% MeOH eluate), quercetin 3-*O*-α-L-arabinofuranoside (10 mg), **4** (37 mg) (from the 60% MeOH eluate), geraniin (1.5 g) (from the 70% MeOH eluate), **2** (27 mg) (from the 35% acetone eluate) and **6** (30 mg) (from the 50% acetone eluate).

Eumaculin A (1) A light-brown amorphous powder, $[\alpha]_D^{24}$ −22° (*c* = 1.0, acetone). *Anal.* Calcd for $C_{68}H_{52}O_{44}\cdot8H_2O$: C, 47.56; H, 3.99. Found: C, 47.34; H, 3.80. FAB-MS: *m/z* 1595 ($[M+Na]^+$). CD (MeOH): $[\theta]_{290}$ -5.0×10^4, $[\theta]_{260}$ $+3.3\times10^4$, $[\theta]_{245}$ -1.0×10^4, $[\theta]_{228}$ $+5.3\times10^4$, $[\theta]_{213}$ -6.7×10^4. ^{1}H-NMR (acetone-d_6+D_2O): δ 7.14 (2H, s), 7.10 (4H, s), 7.08 (2H, s), 6.84 (2H, s) (galloyl × 5); 7.05 (1H, s, H_C), 6.83 (1H, s, H_A), 6.19 (1H, s, H_B) [valoneoyl (Val)]; 6.27 (1H, d, *J* = 8 Hz, H-1), 5.69 (1H, dd, *J* = 8, 9.5 Hz, H-2), 5.56 (2H, m, H-3 and H-4), 4.40 (1H, m,

H-5), 4.54 (1H, dd, $J=2$, 12.5 Hz, H-6), 4.27 (dd, $J=5$, 12.5 Hz, H-6) ($^4C_1$ glucose); 6.33 (1H, d, $J=2$ Hz, H-1), 4.07 (br s, H-2), 4.81 (br s, H-3), 4.38 (br s, H-4), 4.43 (t-like, $J=9.5$ Hz, H-5), 4.72 (t, $J=11$ Hz, H-6), 4.07 (dd, $J=8$, 11 Hz, H-6) ($^1C_4$ glucose). The identity of eumaculin A with **1** derived from euphorbin A[1,7] was also substantiated by HPLC using solvent A [t_R (retention time) 17.7 min].

Eusupinin A (2) A light-brown amorphous powder, $[\alpha]_D^{24}$ +142° ($c=1.1$, acetone). *Anal.* Calcd for $C_{89}H_{62}O_{57}\cdot 12H_2O$: C, 47.30; H, 3.83. Found: C, 47.18; H, 3.66. FAB-MS: *m/z* 2065 ($[M+Na]^+$). CD (MeOH): $[\theta]_{282}$ $+8.8\times10^4$, $[\theta]_{258}$ -4.4×10^4, $[\theta]_{240}$ $+7.9\times10^4$, $[\theta]_{225}$ $+2.3\times10^5$. ^{1}H-NMR (acetone-d_6+D_2O): δ 7.12 (3H, s, Val H_C and galloyl), 7.10 (Val H_C), 7.01 (2H, s, galloyl), 6.99 (4H, s, galloyl×2), 6.96 (2H, s, galloyl), 6.46, 6.45 (1H each, s, Val H_A×2), 6.30, 6.20 (1H each, s, Val H_B×2). Glucose protons: δ 6.17 (1H, d, $J=8$ Hz, H-1), 5.60 (1H, dd, $J=8$, 10 Hz, H-2), 5.82, (1H t, $J=10$ Hz, H-3), 5.15 (1H, t, $J=10$ Hz, H-4), 4.52 (1H, dd, $J=6.5$, 10 Hz, H-5), 5.27 (1H, dd, $J=6.5$, 13 Hz, H-6), 3.78 (1H, d, $J=13$ Hz, H-6) [the right glucose core (Glu_R) in formula **2**]; 6.05 (d, $J=8$ Hz, H-1), 5.49 (1H, dd, $J=8$, 10 Hz, H-2), 5.74, (1H t, $J=10$ Hz, H-3), 5.09 (1H, t, $J=10$ Hz, H-4), 4.40 (1H, dd, $J=6.5$, 10 Hz, H-5), 5.20 (1H, dd, $J=6.5$, 13 Hz, H-6), 3.71 (1H, d, $J=13$ Hz, H-6) [the left glucose core (Glu_L) in formula **2**]. ^{13}C-NMR (acetone-d_6+D_2O): δ 62.98 (2C) (Glu_L C-6, Glu_R C-6), 70.55 (Glu_L C-4), 70.64 (Glu_R C-4), 71.65 (Glu_L C-2), 71.70 (Glu_R C-2), 72.91 (2C) (Glu_L C-5, Glu_R C-5), 73.20 (2C) (Glu_L C-3, Glu_R C-3), 93.05 (Glu_L C-1), 93.64 (Glu_R C-1), 105.03, 106.19 (Val C-3′), 107.60, 107.63 (Val C-3), 109.87—110.31 (12C) (galloyl C-2, C-6, Val C-6″), 112.76, 115.45, 115.71, 115.93 (Val C-1″, C-1), 117.58, 117.68 (Val C-1′), 119.63, 120.14, 120.23, 120.41, 120.44 (galloyl C-1), 125.40, 125.44, 125.88, 126.09 (Val C-2, C-2′), 136.58, 136.61, 137.13, 137.33, 137.52, 137.71 (Val C-5, C-5′, C-2″), 139.09 (2C), 139.31, 139.34, 139.64, 139.78, 140.30, 140.49, 140.94 (galloyl C-4, Val C-3″, C-4″), 143.09, 143.22 (Val C-5″), 144.56, 144.59, 144.76, 144.80 (Val C-6, C-6′), 145.14, 145.18 (Val C-4), 145.72 (2C), 145.75 (2C), 145.84 (2C), 145.91 (2C), 146.04 (2C) (galloyl C-3, C-5), 146.44, 146.83 (Val C-4′), 162.26 (Val C-7″), 165.11, 165.73, 165.76, 166.30 (3C) (galloyl C-7, Val C-7″), 167.66, 167.71 (Val C-7), 167.80 (2C) (Val C-7′).

Partial Hydrolysis of 2 An aqueous solution (0.5 ml) of **2** (1 mg) in a sealed tube was heated at 90 °C for 1 h, and then the solution was analyzed by HPLC using solvents B and C, to show the formation of **9** [t_R 6.1 min (solvent B); 7.6 min (solvent C)] and **10** {t_R 3.6 and 4.3 min (solvent B); 3.8 and 4.2 min (solvent C) (anomer mixture)[25]} in a molar ratio of *ca.* 1:1.

Acknowledgements The NMR spectra were recorded on an instrument at the SC-NMR Laboratory of Okayama University.

References

1) For Part VII, see T. Yoshida, K. Yokoyama, O. Namba and T. Okuda, *Chem. Pharm. Bull.*, **39**, in press.
2) L. M. Perry, "The Medicinal Plants of East and Southeast Asia," MIT Press, Cambridge, 1987, p. 135.
3) S. v. R. Altschul, "Drug and Foods from Little-known Plants, Notes in Harvard University Herbaria," Harvard University Press, Cambridge, 1973, p. 167.
4) Chiang Su New Medicinal College (ed.), "Dictionary of Traditional Chinese Drugs," Shanghai Scientific Technologic Publishers, Shanghai, 1977, p. 4732.
5) T. Okuda, K. Mori and T. Hatano, *Phytochemistry*, **19**, 547 (1980).
6) K. Kameda, T. Takaku, H. Okuda, Y. Kimura, T. Okuda, T. Hatano, I. Agata and S. Arichi, *J. Nat. Prod.*, **50**, 680 (1987).
7) T. Yoshida, L. Chen, T. Shingu and T. Okuda, *Chem. Pharm. Bull.*, **36**, 2940 (1988).
8) T. Okuda, T. Yoshida and T. Hatano, *J. Chem. Soc., Perkin Trans. 1*, **1982**, 9.
9) T. Ohta, *Hoppe-Seyler's Z. Physiol. Chem.*, **263**, 221 (1940).
10) T. Hatano, N. Ogawa, R. Kira, T. Yasuhara and T. Okuda, *Chem. Pharm. Bull.*, **37**, 2083 (1989).
11) T. Okuda, T. Yoshida and K. Mori, *Phytochemistry*, **14**, 1877 (1975).
12) T. Okuda, T. Hatano and N. Ogawa, *Chem. Pharm. Bull.*, **30**, 4230 (1982).
13) J. C. Jochims, G. Taigel and O. Th. Schmidt, *Justus Liebigs Ann. Chem.*, **717**, 169 (1968).
14) E. A. Haddock, R. K. Gupta, S. M. K. Al-Shafi, E. Haslam and E. Magnolato, *J. Chem. Soc., Perkin Trans. 1*, **1982**, 2515.
15) E. A. Haddock, R. K. Gupta and E. Haslam, *J. Chem. Soc., Perkin Trans. 1*, **1982**, 2535.
16) T. Hatano, T. Yoshida, T. Shingu and T. Okuda, *Chem. Pharm. Bull.*, **36**, 3849 (1988).
17) T. Okuda, T. Yoshida, T. Hatano, T. Koga, N. Toh and K. Kuriyama, *Tetrahedron Lett.*, **23**, 3937 (1982).
18) C. K. Wilkins and B. A. Bohm, *Phytochemistry*, **15**, 211 (1976).
19) T. Yoshida, T. Hatano, T. Okuda, M. U. Memon, T. Shingu and K. Inoue, *Chem. Pharm. Bull.*, **32**, 1790 (1984).
20) T. Hatano, R. Kira, T. Yasuhara and T. Okuda, *Chem. Pharm. Bull.*, **36**, 3920 (1988).
21) T. Hatano, T. Yasuhara, R. Abe and T. Okuda, *Phytochemistry*, **29**, 2975 (1990).
22) T. Yoshida, O. Namba, L. Chen and T. Okuda, *Chem. Pharm. Bull.*, **38**, 86 (1990).
23) T. Yoshida, O. Namba, L. Chen and T. Okuda, *Chem. Pharm. Bull.*, **38**, 1113 (1990).
24) T. Yoshida, O. Namba, L. Chen, Y.-Z. Liu and T. Okuda, *Chem. Pharm. Bull.*, **38**, 3296 (1990).
25) T. Hatano, T. Yoshida and T. Okuda, *J. Chromatogr.*, **435**, 285 (1988).

Tannins and Related Compounds. CIX.[1] Isolation of Alienanins A and B, Novel *C,C*-Linked Ellagitannin Dimers from *Quercus aliena* BLUME

Gen-ichiro NONAKA,*,[a] Takashi SAKAI,[a] Kunihide MIHASHI[b] and Itsuo NISHIOKA[a]

Faculty of Pharmaceutical Sciences, Kyushu University 62,[a] 3-1-1 Maidashi, Higashi-ku, Fukuoka 812, Japan and Faculty of Pharmaceutical Sciences, Fukuoka University,[b] Nanakuma, Jonan-ku, Fukuoka 814-01, Japan. *Received October 25, 1990*

Two novel hydrolyzable tannins, alienanins A (5) and B (13), have been isolated from the leaves of *Quercus aliena* BLUME (Fagaceae), and their structures were elucidated on the basis of chemical and spectroscopic evidence to be dimeric *C*-glycosidic ellagitannins in which the hexahydroxydiphenoyl ester group is linked to the *C*-glycosidic C-1 atom through a carbon to carbon linkage. In addition, the structure elucidation of the monomeric *C*-glycosidic ellagitannin, epipunicacortein A (1), is also described briefly.

Keywords *Quercus aliena*; Fagaceae; *C,C*-linked ellagitannin dimer; *C*-glycosidic ellagitannin; alienanin A; alienanin B; epipunicacortein A; casuarinin; stachyurin; tannin

Recent chemical work has revealed that in some plant species, hydrolyzable tannins are metabolized to much higher-molecular-weight compounds *via* dimerization, trimerization and tetramerization, and such oligomerization almost invariably takes place intermolecularly through the oxidative phenol coupling of two galloyl groups or of galloyl and 3,3′,4,4′,5,5′-hexahydroxydiphenoyl (HHDP) groups attached to the glucose moiety, forming a carbon to oxygen linkage.[2] In this paper, we wish to describe the first isolation from *Quercus aliena* BLUME (Fagaceae) of novel dimeric ellagitannins, alienanins A and B, in which the HHDP group is connected to the *C*-glycosidic C-1 position through a carbon to carbon bond.

Extraction of the fresh leaves of *Q. aliena* with aqueous acetone, followed by repeated chromatographies over Sephadex LH-20 dextran gel, ODS-type reverse-phase gels (Fuji gel ODS G-3, Prep pak 500/C_{18} and Bondapak C_{18}/Porasil B) and a high-porosity polystyrene gel (MCI-gel CHP 20P),[3] yielded alienanins A (**5**) and B (**13**) as major phenolic metabolites, together with five gallotannins (3-*O*-galloyl quinic acid[4] and 1,2,6-tri-*O*-,[3a] 1,2,4,6-tetra-*O*-,[5] 1,2,3,6-tetra-*O*-[6] and 1,2,3,4,6-penta-*O*-galloyl-β-D-glucoses)[7] and ten monomeric ellagitannins [2,3-(*S*)-HHDP-D-glucose (**12**),[2a] pedunculagin (**7**),[8] sanguiin H-5,[2b] praecoxin A,[9] eugeniin,[10] 1(β)-*O*-galloylpedunculagin,[11] casuarinin (**14**),[12] camelliin A,[9] punicacortein A (**2**)[13] and epipunicacortein A (**1**)].

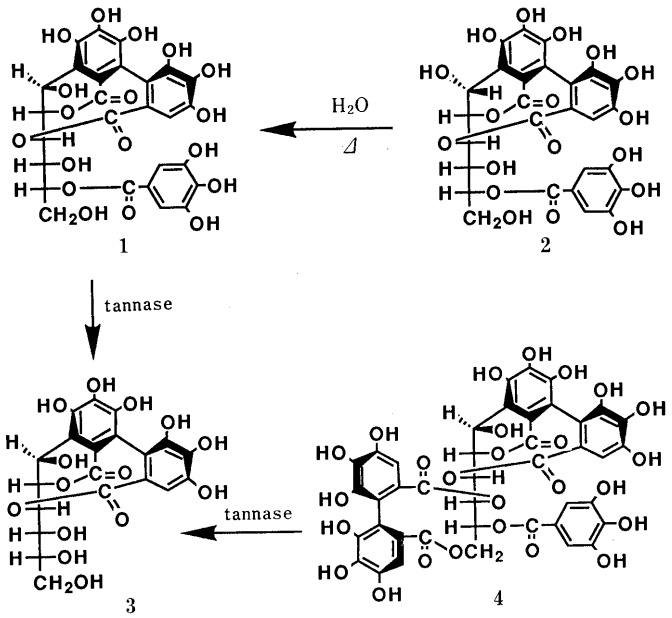

Chart 1

Of the monomeric ellagitannins isolated here, epipunicacortein A (**1**) was found to be new. The proton-nuclear magnetic resonance (^{1}H-NMR) spectrum of **1** showed the presence of one galloyl group (δ 7.07, 2H, s), one isolated aromatic proton (δ 6.42, 1H, s) and seven aliphatic protons. The aliphatic signal pattern was typical of a *C*-glycosidic ellagitannin and similar to that of punicacortein A (**2**).[13] However, the coupling constant between the *C*-glycosidic H-1 and H-2 signals differed from that of **3**, and the small value (J=2 Hz) suggested **1** to be an epimer of **2**.[12] Enzymatic hydrolysis of **1** with tannase afforded gallic acid and a hydrolysate (**3**), which was found to be identical with the product obtained by similar tannase hydrolysis of stachyurin (**4**).[12] Furthermore, refluxing of **2** in water caused epimerization at the C-1 position to give compound **1**.[12] Thus, the structure of epipunicacortein A was established to be as shown by the formula **1**.

The dimeric structure of alienanin A (**5**) was readily deduced from the smaller thin-layer chromatographic *Rf* value than those of the above-mentioned monomeric hydrolyzable tannins and from the observation of the $[M-H]^-$ ion peak at *m/z* 1701 in the negative fast atom bombardment mass spectrum (FAB-MS).[14] The ^{1}H-NMR and carbon-13 nuclear magnetic resonance (^{13}C-NMR) spectra of **5** showed duplicated signal patterns. The appearance of a pair of anomeric carbon signals at δ 92.0 and 95.6 (each d, 1C in total) indicated **5** to be an equilibrium mixture of α- and β-anomers, while the resonances at δ 43.6 and 43.8 (each d, 1C in total) indicated the presence of a methine carbon bearing no oxygen atom.

Methylation of **5** with dimethyl sulfate and potassium carbonate in dry acetone yielded, as a major product, the octacosamethyl ether (**6**) (positive FAB-MS *m/z*: 2095 $[M+H]^+$). The ^{1}H-NMR spectrum of **6** exhibited a two-proton aromatic signal (δ 7.31, s) due to a trimethoxybenzoyl group and six one-proton aromatic singlets (see Experimental). The aliphatic signals were found to consist of two independent systems by proton-proton shift correlation spectroscopy (^{1}H–^{1}H COSY). A series of methine signals at δ 4.05 (d), 4.77 (t), 4.96 (t) and 5.03 (t) (assign-

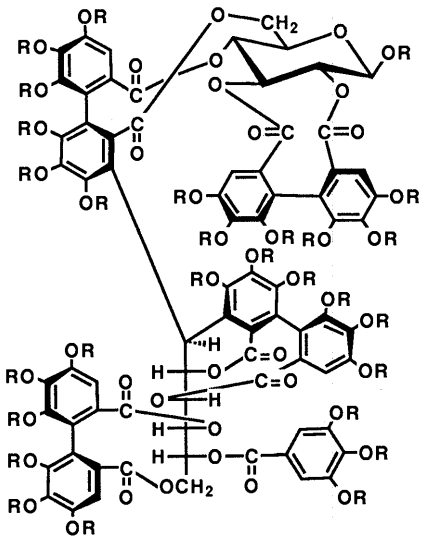

5 : R=H
6 : R=Me

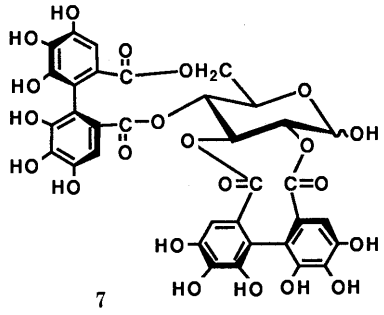

7

Chart 2

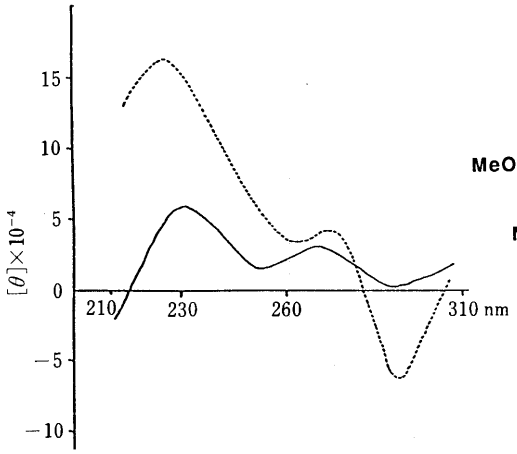

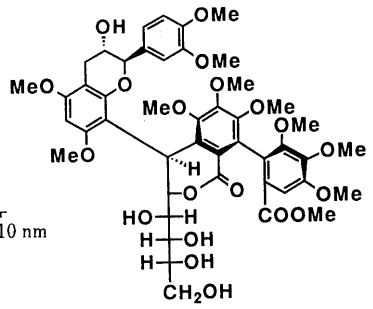

11

Fig. 1. CD Spectra of the Methanolysates (**9** and **11**)
9, ——; **11**, ------.

able to H-1, H-2, H-4 and H-3, respectively), all having a large coupling constant ($J=8$ Hz), was consistent with the presence of a β-glucopyranose ring with a $^4C_1$-conformation. On the other hand, resonances at δ 4.89 (t), 5.39 (d) and 5.58 (d) (assignable to H-2′, H-4′ and H-3′, respectively) with small coupling constants ($J=ca.$ 2 Hz) suggested the presence of an open-chain form of a *C*-glucoside moiety. Furthermore, a small coupling constant ($J=2$ Hz) between the *C*-glycosidic H-1 and H-2 signals indicated that the *C*-glycosidic C-1 atom has the same configuration as that of stachyurin (**4**).[12]

Detailed examination of the ^{13}C-NMR spectrum of **5** revealed that the aliphatic signal patterns were quite similar to the combined signal patterns of stachyurin (**4**) and pedunculagin (**7**), except for the fairly upfield shift (δ 43.6 and 43.8) of the C-1 signal in the stachyurin moiety (δ 65.3). This fact, coupled with the observation of six one-proton aromatic singlets in the ^{1}H-NMR spectrum, implied that **5** consists of stachyurin and pedunculagin moieties linked at the respective C-1 atom and aromatic ring through a carbon to carbon bond.

Alkaline hydrolysis of the methyl ether (**6**), followed by treatment with diazomethane, yielded methyl β-D-glucoside, methyl trimethoxybenzoate, dimethyl 3,3′,4,4′,5,5′-hexamethoxydiphenoate (**8**)[2a] and a hydrolysate (**9**). The measurement of the specific optical rotation (−25.0°, $CHCl_3$) of **8** established the chirality of the biphenyl bond to be in the *S*-series.[15] The positive FAB-MS of **9** showed the $[M+H]^+$ peak at m/z 1031, and the ^{1}H-NMR spectrum of **9** exhibited two one-proton aromatic singlets at δ 7.31 and 7.42, suggesting the presence of two carbon-to-carbon linked HHDP groups. The appearance of the *C*-glycosidic H-2 signal at lower field (δ 5.01, br d) was consistent with the acylation at the C-2 position. The structure of **9** was further confirmed by formation of the tetraacetate (**10**) (positive FAB-MS m/z: 1199 $[M+H]^+$). As for the atropisomerism of the two biphenyl bonds in **9**, comparison of the circular dichroism (CD) spectra (Fig. 1) of **9** and the structurally related compound (**11**) prepared from stenophyllanin A[16] established it to be all in the *S*-series.

When heated in water, **5** gave many partial hydrolysates, of which one was identified as 2,3-(*S*)-HHDP-D-glucose

(**12**),[2a] thus indicating that the stachyurin unit is attached to the 4,6-positioned HHDP group in the pedunculagin moiety. Furthermore, in the ^{1}H–^{13}C long-range COSY spectrum[17] (Fig. 2) of the methyl ether (**6**), the signal at δ 4.96 (t, $J=9$ Hz) assignable to H-4 in the pedunculagin moiety was found to be correlated with the ester carbon signal at δ 168.1, and this carbon signal also showed a correlation with the aromatic proton signal at δ 7.06. This fact clearly indicated that an aromatic proton exists in the ring esterified with the glucopyranose C-4 hydroxyl group, and therefore the stachyurin unit is bonded to the aromatic ring located at the C-6 position in the pedunculagin moiety.

Based on the evidence mentioned above, the structure of alienanin A was concluded to be as shown by the formula **5**.

The ^{1}H-NMR spectrum of alienanin B (**13**) exhibited signals due to two galloyl groups (δ 7.12 and 7.15, each s, 2H) and five one-proton aromatic singlets (see Experimental). The aliphatic signals corresponded to fourteen protons in total, and their coupling modes were analogous to those of stachyurin (**4**) and casuarinin (**14**).[12] The ^{13}C-NMR spectrum more clearly indicated the presence of two *C*-glycosidic cores, showing twelve aliphatic carbon signals, which were found to be in line with those of **4** plus **14**, besides the observation of the highfield shift (δ 40.9) of the C-1 signal in the stachyurin moiety. Thus, taking into account the co-existence of alienanin A (**5**), as well as the appearance of five one-proton aromatic signals, **13** was considered to be a dimeric ellagitannin in which the stachyurin C-1 atom is linked to the aromatic ring in the casuarinin moiety through a carbon to carbon bond. This was supported by the observation of the intense $[M-H]^-$ ion peak at *m/z* 1853 in the negative FAB-MS.

Alkaline hydrolysis of the triacontamethyl ether (**15**) and subsequent diazomethane treatment afforded methyl trimethoxybenzoate, dimethyl (*S*)-hexamethoxydiphenoate (**8**) and the hydrolysates, which were found to be identical

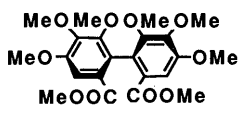

8

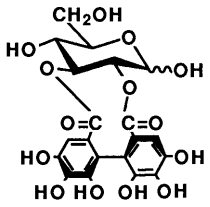

12

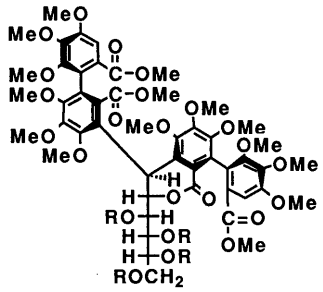

9 : R=H
10 : R=Ac

Chart 3

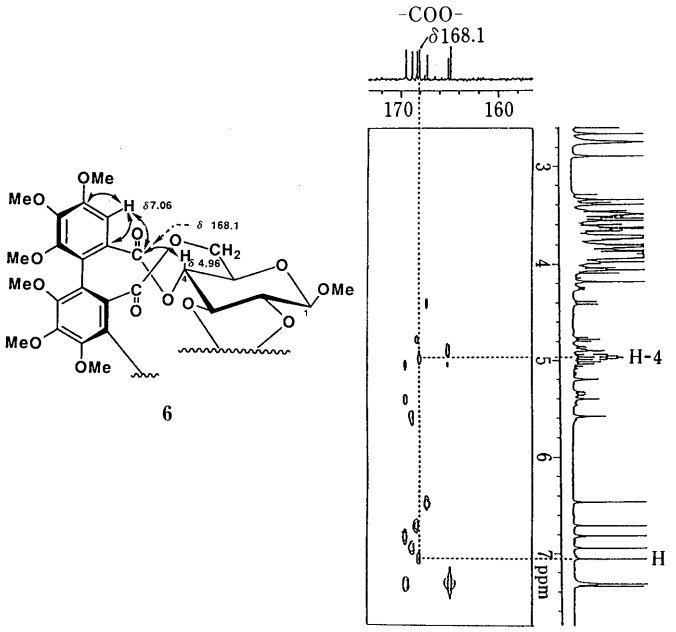

Fig. 2. The ^{1}H–^{13}C Long-Range COSY Spectrum of **6** (in $CDCl_3$, $J_{CH}=10$ Hz)

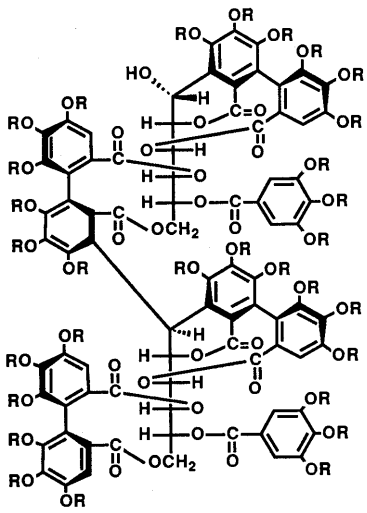

13 : R=H
15 : R=Me

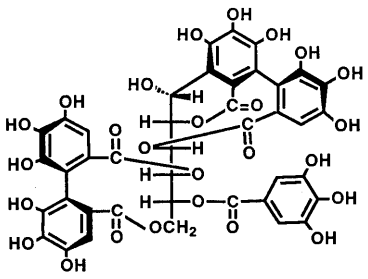

14

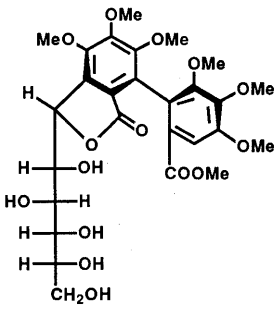

16

Chart 4

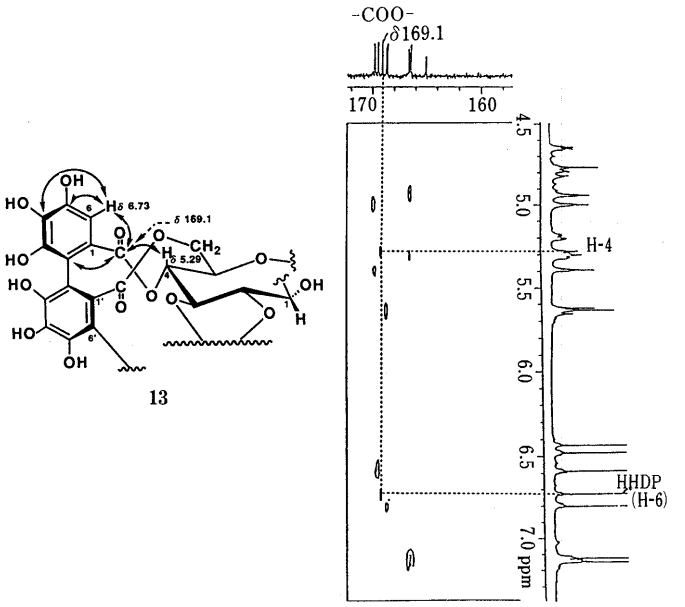

Fig. 3. The ^1H–^{13}C Long-Range COSY Spectrum of **13** (in Me_2CO-d_6+D_2O, $J_{CH}=10$ Hz)

with the products (**9** and **16**) obtained from alienanin A (**5**) and from casuarinin (**14**),[12] respectively.

The location of the linkage between the two hydrolyzable tannin units was determined by examination of the ^1H–^{13}C long-range COSY spectrum (Fig. 3) of **13**. Namely, the signal at δ 5.29 due to H-4 of the casuarinin moiety showed a correlation with the carboxyl carbon signal at δ 169.1, which was further correlated with the aromatic proton signal at δ 6.73. This finding indicated that the aromatic ring located at the casuarinin C-6 position is attached to the stachyurin C-1 position.

From these chemical and spectroscopic results, the structure of alienanin B was established to be as represented by the formula 13.

Alienanins A (**5**) and B (**13**) represent a new class of dimeric *C*-glycosidic ellagitannins, each unit being connected through a carbon to carbon linkage. As mentioned in the introduction, the mode of oligomerization of the previously known hydrolyzable tannins was restricted to oxidative phenol-phenol coupling to form a carbon to oxygen bond, and thus the isolation of the carbon to carbon linked dimeric ellagitannins extends our knowledge of the metabolism of ellagitannins. It should be noted finally that compounds **5** and **13** are the first dimeric *C*-glycosidic ellagitannins to have been isolated from Fagaceous plants.

Experimental

The ^1H- and ^{13}C-NMR spectra were in part measured with a JEOL GX-400 spectrometer, and CD spectra were recorded on a JASCO J-600 spectropolarimeter. Other instruments and chromatographic conditions used throughout this work were essentially the same as described in the preceding paper.[1]

Isolation of Tannins The fresh leaves (19.2 kg) of *Q. aliena*, collected in May, 1988, in Tosu City, Saga Prefecture, were extracted at room temperature with 80% aqueous acetone. The extract, after concentration under reduced pressure at below 40 °C, afforded precipitates, which were removed by filtration through Celite 545. The filtrate was applied to a column of Sephadex LH-20, and elution with water containing increasing proportions of methanol and finally with a mixture of water and acetone (1 : 1) yielded four fractions. Repeated chromatography of fraction I over MCI-gel CHP 20P and Prep Pak 500/C_{18} with a mixture of water and methanol gave 3-*O*-galloyl quinic acid (67 mg), 2,3-(*S*)-HHDP-D-glucose (10 g) and punicacortein A (**2**) (387 mg). Fraction II furnished sanguiin H-5 (25 mg) and epipunicacortein A (**1**) (240 mg) on similar reverse-phase chromatography. Fraction III was rechromatographed over Sephadex LH-20 with a solvent system of ethanol–water–acetone, and four fractions thus obtained were further chromatographed over Fuji gel ODS G-3 and MCI-gel CHP 20P with water and methanol to give 1,2,6-tri-*O*-galloyl-β-D-glucose (4.9 g), alienanin A (**5**) (1.9 g), pedunculagin (**7**) (16 g) and praecoxin A (57 mg). Rechromatography of fraction IV over Sephadex LH-20 with 80% aqueous methanol afforded two fractions, which were separated repeatedly on Bondapak C_{18}/Porasil B, MCI-gel CHP 20P and Fuji gel ODS G-3 with water containing increasing amounts of methanol to give alienanin B (**13**) (1.3 g), casuarinin (**14**) (1.8 g), camelliin A (222 mg), eugeniin (150 mg), 1,2,3,4,6-penta-*O*-galloyl-β-D-glucose (58 mg), 1(β)-*O*-galloylpedunculagin (86 mg), 1,2,4,6-tetra-*O*-galloyl-β-D-glucose (125 mg) and 1,2,3,6-tetra-*O*-galloyl-β-D-glucose (83 mg).

Epipunicacortein A (1) A pale brown amorphous powder, $[\alpha]_D^{13}$ −71.2° ($c=1.0$, MeOH). *Anal.* Calcd for $C_{27}H_{22}O_{18}\cdot 3\frac{1}{2}H_2O$: C, 46.52; H, 4.19. Found: C, 46.15; H, 4.08. Negative FAB-MS *m/z*: 633 $[M-H]^-$. ^1H-NMR (270 MHz, acetone-d_6+D_2O) δ: 3.91 (1H, dd, $J=12$, 4 Hz, H-6), 3.96 (1H, dd, $J=12$, 4 Hz, H-6), 4.29 (1H, dd, $J=8$, 3.5 Hz, H-4), 4.80 (1H, dd, $J=3.5$, 2 Hz, H-3), 4.85 (1H, d, $J=2$ Hz, H-1), 5.03 (1H, dd, $J=8$, 4 Hz, H-5), 5.06 (1H, t, $J=2$ Hz, H-2), 6.42 (1H, s, arom. H), 7.07 (2H, s, galloyl H).

Tannase Hydrolysis of 1 A solution of **1** (20 mg) in water (2 ml) was shaken with tannase at room temperature for 1 h. The reaction mixture was concentrated to dryness, and the residue was treated with ethanol. The insoluble materials were removed by filtration, and the filtrate was subjected to Sephadex LH-20 chromatography. Elution with ethanol yielded gallic acid and a hydrolysate (**3**) (8 mg) as a pale brown amorphous powder, $[\alpha]_D^{22}$ −37.5° ($c=1.0$, MeOH). *Anal.* Calcd for $C_{22}H_{16}O_{14}\cdot 7H_2O$: C, 39.51; H, 5.31. Found: C, 39.55; H, 5.44. ^1H-NMR (100 MHz, acetone-d_6+D_2O) δ: 4.26 (1H, m, H-4), 4.64 (1H, t, $J=2$ Hz, H-3), 4.84 (1H, d, $J=2$ Hz, H-1), 4.95 (1H, m, H-5), 5.09 (1H, t, $J=2$ Hz, H-2), 6.41 (1H, s, arom. H).

Epimerization of 2 A solution of **2** (100 mg) in water (15 ml) was heated under reflux for 30 h. After concentration, the product was separated by Sephadex LH-20 chromatography with water containing increasing proportions of methanol to give **1** (25 mg).

Tannase Hydrolysis of 4 A solution of **4** (30 mg) in water (3 ml) was treated with tannase at room temperature for 2 h. Work-up as described for **1** gave gallic acid and compound **3** (7 mg).

Alienanin A (5) A pale brown amorphous powder, $[\alpha]_D^{17}$ +71.6° ($c=1.0$, MeOH). *Anal.* Calcd for $C_{75}H_{50}O_{47}\cdot 14\frac{1}{2}H_2O$: C, 45.89; H, 4.06. Found; C, 45.53; H, 3.83. Negative FAB-MS *m/z*: 1701 $[M-H]^-$. ^1H-NMR (400 MHz, acetone-d_6+D_2O) δ: 3.55 (d, $J=13$ Hz, α-H-6), 3.81 (d, $J=13$ Hz, β-H-6), 3.95 (dd, $J=5$, 13 Hz, α-H-6′), 4.04 (s, β-H-1′), 4.10 (dd, $J=4$, 12 Hz, β-H-5), 4.12 (d, $J=1$ Hz, α-H-1′), 4.43 (dd, $J=3$, 12 Hz, H-6′), 4.51 (dd, $J=3$, 12 Hz, H-6′), 4.75 (d, $J=8$ Hz, β-H-1), 4.81 (t, $J=8$ Hz, β-H-2), 4.91 (t, $J=8$ Hz, β-H-4), 4.99 (t, $J=8$ Hz, α-H-4), 5.00 (br s, H-2′), 5.02 (dd, $J=6$, 12 Hz, α-H-6′), 5.14 (dd, $J=2$, 8 Hz, α-H-2), 5.16 (t, $J=8$ Hz, β-H-3), 5.26 (dd, $J=4$, 12 Hz, β-H-6), 5.29 (br s, H-3′), 5.38 (m, β-H-5), 5.47 (m, α-H-5), 5.49 (β-H-4′), 5.53 (d, $J=2$ Hz, α-H-1), 5.57 (dd, $J=4$, 12 Hz, α-H-6), 5.69 (t, $J=8$ Hz, α-H-3), 5.71 (dd, $J=2$, 8 Hz, α-H-4), 6.31, 6.42, 6.47, 6.55, 6.61, 6.70, 6.71, 6.72, 6.78, 7.00, 7.13 (each s, HHDP-H), 7.05, 7.07 (each s, galloyl H). ^{13}C-NMR (100 MHz, acetone-d_6+D_2O) δ: 43.6, 43.8 (C-1′), 63.8, 64.5 (C-6), 64.9, 65.1 (C-6′), 68.6, 69.9, 71.6, 72.1, 73.0, 74.0, 74.1, 75.1, 75.5, 76.4, 76.5, 76.9, 78.0, 78.5, 81.5, 81.6 (Glc. C), 92.0 (α-C-1), 95.6 (β-C-1).

Methylation of 5 A mixture of **5** (400 mg), dimethyl sulfate (2 ml) and anhydrous potassium carbonate (2 g) in dry acetone (40 ml) was heated under reflux for 5 h. The inorganic salts were removed by filtration, and the filtrate, after concentration, was subjected to silica gel chromatography. Elution with benzene–acetone (9 : 1) afforded the octacosamethyl ether (**6**) (253 mg) as a pale yellow amorphous powder, $[\alpha]_D^{17}$ −35.8° ($c=0.9$, acetone). *Anal.* Calcd for $C_{103}H_{106}O_{47}$: C, 59.07; H, 5.10. Found: C, 59.23; H, 5.58. Positive FAB-MS *m/z*: 2095 $[M+H]^+$. ^1H-NMR (400 MHz, $CDCl_3$) δ: 3.34, 3.40, 3.48, 3.49, 3.50, 3.53, 3.56, 3.63, 3.65, 3.71, 3.72, 3.73, 3.80, 3.82, 3.83, 3.85, 3.86, 3.88, 3.89, 3.90, 3.91, 3.92, 3.93, 3.94, 3.95, 3.98, 4.06 (each s, OMe), 4.01 (1H, d, $J=14$ Hz, H-6), 4.04 (1H, d, $J=8$ Hz, H-1), 4.24 (1H, dd, $J=9$, 5 Hz, H-5), 4.39 (1H, d, $J=12$ Hz, H-6′), 4.77 (1H, t, $J=8$ Hz, H-2), 4.86 (1H, t, $J=9$ Hz, H-4), 5.03 (1H, t, $J=8$ Hz, H-3), 5.20 (1H, d, $J=4$ Hz, H-5′), 5.34 (1H, dd, $J=14$, 5 Hz, H-6), 5.39 (1H, d, $J=2$ Hz, H-4′), 5.58 (1H, t, $J=2$ Hz, H-3′), 6.46, 6.72, 6.81, 6.98, 7.06, 7.31 (each 1H, s, arom. H),

7.36 (2H, s, arom. H).

Alkaline Hydrolysis of 6, Followed by Methylation A 20% solution of sodium hydroxide in water (3 ml) was added to a solution of **6** (110 mg) in ethanol (5 ml), and the whole was heated at 70 °C for 3 h. The reaction mixture was acidified with 20% hydrochloric acid and extracted with ethyl acetate. The organic layer was washed with water, dried over anhydrous sodium sulfate and concentrated to dryness. The residue was dissolved in methanol and treated with ethereal diazomethane. After evaporation of the solvent, the products were separated by silica gel chromatography with benzene–ethanol (20 : 1—10 : 1) to give dimethyl (*S*)-hexamethoxydiphenoate (**8**) (32 mg), methyl trimethoxybenzoate (12 mg) and a hydrolysate (**9**) (23 mg) as a white amorphous powder, $[\alpha]_D^{12}$ +11.3° (c=0.82, $CHCl_3$). *Anal.* Calcd for $C_{49}H_{58}O_{24}$: C, 57.08; H, 6.13. Found: C, 57.25; H, 6.13. Positive FAB-MS *m/z*: 1031 $[M+H]^+$. ^{1}H-NMR (100 MHz, $CDCl_3$) δ: 3.44—3.98 (OMe), 4.5—4.7 (2H, m, H-1 and H-2), 5.01 (1H, br d, J=7 Hz, H-3), 7.31, 7.42 (each 1H, s, arom. H). CD ($c=1.6\times10^{-2}$, MeOH) $[\theta]^{25}\times10^{-4}$ (nm): +1.81 (267), +0.50 (249), +4.10 (230), −1.19 (216). The aqueous layer was passed through a Sephadex LH-20 column with water, and purification by silica gel chromatography with benzene–ethanol (10 : 1) gave methyl β-D-glucoside (10 mg).

Acetylation of 9 A solution of **9** (10 mg) in dry pyridine (0.5 ml) and acetic anhydride (0.5 ml) was kept at room temperature for 3 h. Usual work-up gave the tetraacetate (**10**) as a white amorphous powder, $[\alpha]_D^{12}$ +9.5° (c=0.2, $CHCl_3$). Positive FAB-MS *m/z*: 1199 $(M+H)^+$. ^{1}H-NMR (270 MHz, $CDCl_3$) δ: 1.94—2.10 (12H, in total, OAc), 3.55—3.95 (OMe), 4.18 (1H, dd, J=12, 4 Hz, H-6), 4.31 (1H, dd, J=12, 2 Hz, H-6), 4.45 (1H, d, J=5 Hz, H-1), 4.66 (1H, d, J=10 Hz, H-3), 4.81 (1H, d, J=5 Hz, H-2), 5.23 (1H, m, H-5), 5.37 (1H, d, J=10 Hz, H-4), 7.36, 7.44 (each 1H, s, arom. H).

Hydrolysis of 5 in Hot Water A solution of **5** (10 mg) in water (3 ml) was heated under reflux for 26 h. The reaction products were directly analyzed by high-performance liquid chromatography (column: Cosmosil 5Ph; solvent: 2% acetonitrile in 50 mM phosphoric acid; flow rate: 0.7 ml/min), and a peak (t_R 15 min) corresponding to 2,3-(*S*)-HHDP-D-glucose was detected.

Alienanin B (13) A pale brown amorphous powder, $[\alpha]_D^{17}$ +73.4° (c=1.0, MeOH), *Anal.* Calcd for $C_{82}H_{52}O_{51}\cdot8H_2O$: C, 49.34; H, 3.43. Found: C, 48.91; H, 3.53. Negative FAB-MS *m/z*: 1853 $[M-H]^-$. ^{1}H-NMR (400 MHz, acetone-d_6) δ: 3.20 (1H, d, J=13 Hz, H-6), 4.05 (1H, dd, J=13, 3 Hz, H-6), 4.07 (1H, d, J=13 Hz, H-6′), 4.64 (1H, dd, J=5, 2 Hz, H-2), 4.76 (1H, d, J=2 Hz, H-1′), 4.80 (1H, dd, J=13, 3 Hz, H-6′), 4.94 (1H, t-like, J=2 Hz, H-2′), 4.99 (1H, t-like, J=2 Hz, H-3′), 5.19 (1H, dd, J=9, 3 Hz, H-5′), 5.29 (1H, dd, J=9, 2 Hz, H-4), 5.31 (1H, dd, J=9, 2 Hz, H-5), 5.39 (1H, t-like, J=2 Hz, H-3), 5.62 (1H, d, J=5 Hz, H-1), 5.64 (1H, dd, J=9, 2 Hz, H-4′), 6.43, 6.47, 6.59, 6.73, 6.80 (each 1H, s, arom. H), 7.12, 7.15 (each 2H, s, galloyl H). ^{13}C-NMR (100 MHz, acetone-d_6) δ: 40.9 (C-1′), 64.9 (C-6′), 66.2 (C-6), 67.9 (C-1), 69.8 (C-3), 70.1 (C-5), 73.9 (C-4′), 75.2 (C-4 and C-3′), 77.6 (C-2), 81.4 (C-2′), 105.8, 106.4 (biphenyl C-6′ and C-6‴), 107.9 (×2) (HHDP C-6′ and C-6‴), 108.3 (HHDP C-6), 109.2 (HHDP C-6″), 110.6, 111.0 (galloyl C-2 and C-2′), 114.2, 115.0, (HHDP C-2′ and C-2‴), 115.9, 116.0, 116.1, 116.4, 116.7, 117.0, (HHDP C-2 and C-2′ and biphenyl C-2, C-2′, C-2″ and C-2‴), 117.1 (HHDP C-6), 117.8 (HHDP C-6″), 121.0, 121.4 (galloyl C-2 and C-2′), 122.4, 124.7 (biphenyl C-1 and C-1′), 125.6, 125.7, 127.0, 127.5, 127.6, 128.2 (biphenyl C-1′ and C-1‴ and HHDP C-2, C-2′, C-2″ and C-2‴), 134.7, 135.4 (biphenyl C-4′ and C-4″), 136.2, 136.6 (HHDP C-4′ and C-4‴), 137.4 (biphenyl C-4″), 139.0 (biphenyl C-4), 139.4, 139,7 (galloyl C-4 and C-4′), 143.8, 144.1, 144.2, 144.4, 144.6, 144.8, 144.9, 145.6, 145.7, 145.8, 145.9, 146.0, 146.1, 146.3, 146.5, 146.7 (HHDP C-3, C-3′, C-3″, C-3‴, C-5, C-5′, C-5″ and C-5‴ and biphenyl C-3, C-3′, C-3″, C-3‴, C-5, C-5′, C-5″ and C-5‴), 146.2, 146.5 (galloyl C-3 and C-3′), 165.0, 166.4, 166.5, 166.7, 168.6, 168.7, 169.1, 169.5, 169.8, 169.9 (–COO–).

Methylation of 13 A mixture of **13** (400 mg), dimethyl sulfate (3 ml) and anhydrous potassium carbonate (3 g) in dry acetone (40 ml) was refluxed for 6 h with stirring. The reaction mixture was worked up as described for **5** to furnish the triacontamethyl ether (**15**) (280 mg) as a white amorphous powder, $[\alpha]_D^{17}$ −15.1° (c=0.88, acetone). *Anal.* Calcd for $C_{112}H_{112}O_{51}\cdot\frac{1}{2}H_2O$: C, 58.97; H, 4.99. Found: C, 58.69; H, 5.35. Positive FAB-MS *m/z*; 2275 $[M+H]^+$. ^{1}H-NMR (100 MHz, $CDCl_3$) δ: 3.30—4.03 (OMe), 6.50, 6.56, 6.73, 6.94, 7.07 (each 1H, s, arom. H), 7.18, 7.30 (each 2H, arom. H).

Alkaline Hydrolysis of 15, Followed by Methylation A solution of **15** (200 mg) in ethanol (5 ml) and 20% aqueous sodium hydroxide (3 ml) was heated on a boiling water bath for 2 h. The reaction mixture was acidified with 20% hydrochloric acid and extracted with ethyl acetate. The organic layer, after concentration, was treated with ethereal diazomethane, and the products were separated by silica gel chromatography. Elution with benzene–ethanol (20 : 1—10 : 1) gave dimethyl (*S*)-hexamethoxydiphenoate (**8**) (32 mg), methyl trimethoxybenzoate (28 mg) and the hydrolysates (**9**, 69 mg and **16**, 42 mg).

Acknowledgements The authors are grateful to Mr. Y. Kuranari, the Experimental Station of Saga Pharmaceutical Industries, for identification of the plant material, and to Dr. M. Kanaoka, Sankyo Co., Ltd., for the gift of tannase. Thanks are due to Mr. Y. Tanaka, Miss Y. Soeda and Mr. R. Isobe for spectral measurements, and to the staff of the Central Analysis Room of this university for elemental analyses.

References

1) Part CVIII: T.-C. Lin, T. Tanaka, G. Nonaka, I. Nishioka and T.-J. Young, *Chem. Pharm. Bull.*, "in press."
2) *a*) G. Nonaka, T. Tanaka and I. Nishioka, *J. Chem. Soc., Perkin Tans. 1*, **1982**, 1067; *b*) T. Tanaka, G. Nonaka and I. Nishioka, *J. Chem. Research (S)*, **1985**, 176; *c*) *Idem, ibid. (M)*, **1985**, 2001; *d*) G. Nonaka, *Pure & Appl. Chem.*, **61**, 357 (1989); *e*) M. Ishimatsu, T. Tanaka, G. Nonaka, I. Nishioka, M. Nishizawa and T. Yamagishi, *Chem. Pharm. Bull.*, **37**, 1735 (1989); *f*) G. Nonaka, S. Nakayama and I. Nishioka, *ibid.*, **37**, 2030 (1989); *g*) J.-H. Lin, T. Tanaka, G. Nonaka, I. Nishoka and I.-S. Chen, *ibid.*, **38**, 2162 (1990).
3) For example, *a*) G. Nonaka, I. Nishioka, T. Nagasawa and H. Oura, *Chem. Pharm. Bull.*, **29**, 2862 (1981); *b*) F. Hashimoto, G. Nonaka and I. Nishioka, *ibid.*, **37**, 3255 (1989).
4) H. Nishimura, G. Nonaka and I. Nishioka, *Phytochemistry*, **23**, 2621 (1984).
5) E. A. Haddock, R. K. Gupta, S. M. K. Al-Shafi and E. Haslam, *J. Chem. Soc., Perkin Trans. 1*, **1982**, 2515.
6) M. Nishizawa, T. Yamagishi, G. Nonaka and I. Nishioka, *J. Chem. Soc., Perkin Trans. 1*, **1983**, 961.
7) M. Nishizawa, T. Yamagishi, G. Nonaka and I. Nishioka, *J. Chem. Soc., Perkin Trans. 1*, **1982**, 2963.
8) O. T. Schmidt, L. Würtele and A. Harreus, *Justus Liebigs Ann. Chem.*, **690**, 150 (1965).
9) Y.-M. Xu, T. Sakai, T. Tanaka, G. Nonaka and I. Nishioka, *Chem. Pharm. Bull.*, **39**, 639 (1991).
10) G. Nonaka, M. Harada and I. Nishioka, *Chem. Pharm. Bull.*, **28**, 685 (1980).
11) R. K. Gupta, S. M. K. Al-Shafi, K. Layden and E. Haslam, *J. Chem. Soc., Perkin Trans. 1*, **1982**, 2525.
12) G. Nonaka, T. Sakai, T. Tanaka, K. Mihashi and I. Nishioka, *Chem. Pharm. Bull.*, **38**, 2151 (1990).
13) T. Tanaka, G. Nonaka and I. Nishioka, *Chem. Pharm. Bull.*, **34**, 656 (1986).
14) R. Isobe, T. Tanaka, G. Nonaka and I. Nishioka, *Chem. Pharm. Bull.*, **37**, 1748 (1989).
15) Y. Ikeya, H. Taguchi, I. Yoshioka and H. Kobayashi, *Chem. Pharm. Bull.*, **27**, 1383 (1979).
16) G. Nonaka, H. Nishimura and I. Nishioka, *J. Chem. Soc., Perkin Trans. 1*, **1985**, 163.
17) M. Ishimatsu, T. Tanaka, G. Nonaka, I. Nishioka, M. Nishizawa and T. Yamagishi, *Chem. Pharm. Bull.*, **37**, 129 (1989); R. Saijo, G. Nonaka and I. Nishioka, *ibid.*, **37**, 2063 (1989).

Studies on the Constituents of *Luffa acutangula* ROXB. II.[1] Structures of Acutosides H and I, Oleanolic Acid Saponins Isolated from the Seed

Tsuneatsu NAGAO, Ryuichiro TANAKA and Hikaru OKABE*

Faculty of Pharmaceutical Sciences, Fukuoka University, Nanakuma 8–19–1, Jonan-ku, Fukuoka 814–01, Japan. *Received November 5, 1990*

From the seeds of *Luffa acutangula* ROXB. (Cucurbitaceae), two 3,28-*O*-bisdesmosidic heptaglycosides of oleanolic acid, named acutosides H and I, were isolated and their structures were elucidated. Acutosides H and I have the same prosapogenin structure, oleanolic acid 3-*O*-[*O*-α-L-arabinopyranosyl-(1→3)-β-D-glucopyranosyluronic acid] and differ in the structures of the ester-linked sugar moieties. Acutoside H is a 28-*O*-[*O*-β-D-xylopyranosyl-(1→3)-*O*-β-D-xylopyranosyl-(1→4)-[*O*-β-D-xylopyranosyl-(1→3)]-*O*-α-L-rhamnopyranosyl-(1→2)-α-L-arabinopyranosyl] ester, and acutoside I is a 28-*O*-[*O*-α-L-arabinopyranosyl-(1→3)-*O*-β-D-xylopyranosyl-(1→4)-[*O*-β-D-xylopyranosyl-(1→3)]-*O*-α-L-rhamnopyranosyl-(1→2)-α-L-arabinopyranosyl] ester.

Keywords *Luffa acutangula*; Cucurbitaceae; oleanolic acid saponin; glucuronide saponin; 3,28-*O*-bisdesmoside; rotating flame Overhauser effect difference spectrum; homodecoupling difference spectrum; one dimentional-hononuclear Hartmann–Hahn

In the preceding paper[1] of this series, we reported the isolation and structure elucidation of seven oleanane-type triterpene saponins, acutosides A—G, from the herb of *Luffa acutangula* ROXB. (Cucurbitaceae). The seed kernels of this plant have been used in traditional Indian medicine as an emetic and an expectorant,[2] and the constituents of the seeds have been investigated by several groups. Cucurbitacin B and a saponin of oleanolic acid were isolated,[3] but the structure of the saponin has not been characterized.

The preliminary investigation of the constituents of the seeds suggested the presence of four acidic saponins. This paper deals with the isolation of the saponins and the structure elucidation of the two major, less polar saponins named acutosides H and I.

The defatted seed powder was extracted successively with MeOH and 50% MeOH. The 50% MeOH extract was passed through a column of Diaion HP-20 and the column was washed with H_2O and 50% MeOH. The saponin fraction was eluted with MeOH. The MeOH eluate showed spots of two major less polar saponins and two minor polar saponins on thin layer chromatography (TLC). They were named acutosides H, I, J and K in order of increasing polarity. The saponin fraction was treated with an ion-exchange resin IRC-84 and the acidic solution was methylated with diazomethane. The methylated product was repeatedly chromatographed on silica gel, reversed-phase material, and acutosides were isolated as their methyl esters.

The methyl ester (I) of acutoside H, obtained as colorless needles, showed in its fast-atom bombardment mass spectrum (FAB-MS) an $[M+Na]^+$ ion at m/z 1475 and an $[M-H]^-$ ion at m/z 1451, indicating the molecular weight to be 1452. The result of elemental analysis by high-resolution FAB-MS was consistent with the molecular formula $C_{68}H_{108}O_{33}$, and I gave L-arabinose, D-xylose, L-rhamnose and D-glucuronic acid on acid hydrolysis.

The ^{1}H-nuclear magnetic resonance (^{1}H-NMR) spectrum of I showed signals of seven tertiary methyl groups (δ 0.83, 0.93, 0.97, 1.01, 1.06, 1.28 and 1.29), one secondary methyl group [δ 1.74 (d, J=6 Hz)], one trisubstituted olefinic proton (δ 5.44, triplet-like) and seven anomeric protons [δ 4.91 (d, J=8 Hz), 5.09 (d, J=7 Hz), 5.15 (d, J=7 Hz), 5.28 (d, J=7 Hz), 5.45 (d, J=8 Hz), 5.67 s and 6.53 (d, J=2 Hz)].

The ^{13}C-nuclear magnetic resonance (^{13}C-NMR) spectrum revealed signals of six C–C bonded quaternary carbons (δ 30.9, 36.9, 39.5, 39.9, 42.1 and 47.3), two ester carbonyl carbons (δ 170.2 and 176.2), a pair of olefinic carbons (δ 122.8 and 144.1) (Table I) and seven anomeric carbons (δ 93.2, 100.7, 104.5, 105.7, 105.85, 105.9 and 106.7). The nuclear magnetic resonance (NMR) signals of the aglycone moiety were quite similar to those of lucyoside H, oleanolic acid 3,28-*O*-bis-β-D-glucoside, isolated from the herb of *Luffa cylindrica* ROEM. (Cucurbitaceae).[4] These spectral data indicated that I is a 3,28-*O*-bisdesmosidic heptaglycoside of oleanolic acid.

On selective cleavage of the ester–glycoside linkage,[5] I

TABLE I. ^{13}C-NMR Chemical Shifts of I and II (Aglycone Moieties)

	Oleanolic acid[a]	I	II
1	39.1	38.6	38.6
2	28.1	26.5	26.5
3	78.2	89.3	89.3
4	39.4	39.5	39.4
5	55.9	55.8	55.7
6	18.9	18.5	18.4
7	33.3	32.7	32.8
8	39.9	39.9	39.8
9	48.2	48.0	47.9
10	37.5	36.9	36.9
11	23.8	23.7	23.6
12	122.6	122.8	122.8
13	144.9	144.1	144.1
14	42.3	42.1	41.9
15	28.4	28.1	28.0
16	23.8	23.7	23.4
17	46.8	47.3	46.9
18	42.1	41.7	41.8
19	46.6	46.3	46.1
20	31.0	30.9	30.8
21	34.4	34.1	33.9
22	33.3	33.1	33.0
23	28.8	28.1	28.0
24	16.5	16.9	16.8
25	15.6	15.5	15.4
26	17.5	17.5	17.1
27	26.2	26.0	26.1
28	180.1	176.2	177.9
29	33.3	33.1	33.1
30	23.8	23.7	23.6
OMe	—	—	51.5

a) NMR data reported by Takemoto *et al.*[4]

gave a prosapogenin and an anomeric mixture of a methyl oligoglycoside.

The methyl ester (II) of the prosapogenin showed an $[M+Na]^+$ ion at m/z 815 in its FAB-MS, and it gave L-arabinose and D-glucuronic acid on acid hydrolysis. From the mass number and NMR signals of anomeric protons [δ 4.93 (d, $J=8$ Hz) and 5.27 (d, $J=7$ Hz)] and anomeric carbons (δ 105.9 and 106.7), it is apparent that II is a glycoside of methyl oleanolate, which has 1 mol each of L-arabinose and D-glucuronic acid methyl ester linked to the C_3-hydroxyl group of the aglycone. The structure of II was determined to be oleanolic acid 3-*O*-[*O*-α-L-arabinopyranosyl-(1→3)-β-D-glucopyranosyluronic acid] dimethyl ester by examination of the NMR spectra. The assignment of the NMR signals of the sugar moiety is shown in Table II.

The anomeric mixture of the methyl oligoglycoside gave L-arabinose, L-rhamnose and D-xylose on acid hydrolysis. The positive FAB-MS showed an $[M+Na]^+$ ion at m/z 729, and its negative FAB-MS showed an $[M-H]^-$ ion at m/z 705 and fragment ions at m/z 573, 441, 309 and 163. These mass data indicate that the methyl oligoglycoside is composed of 4 mol of pentose and 1 mol of L-rhamnose and that it is either a linear MeO-pentose(1)-rhamnose-pentose(2)-pentose(3)-pentose(4) or one of two branched-chain pentaglycosides, one of which has a pentosyl group and a pentobiosyl group at the rhamnosyl unit and the other has three pentosyl groups at the rhamnosyl unit. The anomers were separated by high performance liquid chromatography (HPLC) on a reversed-phase material to give a methyl pentaglycoside (III) and its anomer (IV).

Table II. NMR Chemical Shifts of the Sugar Moiety of II

	Methyl glucuronate		Arabinosyl	
	^{1}H	^{13}C	^{1}H	^{13}C
1	4.93 (d, 8)	106.7	5.27 (d, 7)	105.9
2	4.06 (dd, 8, 9)	74.5	4.47 (dd, 7, 9)	72.8
3	4.28 (t, 9)	85.7	4.15 (dd, 3, 9)	74.4
4	4.35 (t, 9)	71.1	*ca.* 4.27	69.2
5	4.52 (d, 9)	76.7	3.78 (dd, 2, 12)	67.1
			4.34 (dd, 3, 12)	
6	—	170.1		
OCH_3	3.74 (s)	52.0		

Table III. NMR Chemical Shifts of III and IV

		III		IV	
		^{1}H	^{13}C	^{1}H	^{13}C
MeO		3.52 (s)	55.8	3.42 (s)	55.0
Ara(1-OMe)	1	4.54 (d, 7)	103.5	5.29 (d, 3)	101.1
	2	4.46 (dd, 7, 8)	76.9	4.58 (dd, 3, 10)	78.8
	3	4.12 (dd, 8, 4)	74.2	4.47 (dd, 10, 4)	69.0
	4	*ca.* 4.20	69.3	4.27 (br s)	70.6
	5	3.63 (dd, 2, 12)	66.1	3.95 (2H, br s)	63.5
		ca. 4.19			
Rha(1-2Ara)	1	5.97 (d, 2)	102.0	5.62 (d, 1)	104.0
	2	4.90 (dd, 2, 3)	71.8	4.82 (br s)	71.3
	3	4.68 (dd, 3, 9)	82.5	4.63 (dd, 3, 9)	82.4
	4	4.53 (t, 9)	78.4	4.48 (t, 9)	78.2
	5	*ca.* 4.60	68.0	*ca.* 4.42	68.0
	6	1.64 (d, 6)	18.4	1.62	18.6
Xyl(1-3Rha)	1	5.15 (d, 7)	105.8[a]	4.88 (d, 7)	105.5
Xyl(1-4Rha)	1	5.15 (d, 7)	105.9[a]	5.15 (d, 7)	105.9
Xyl(1-3Xyl)	1	5.51 (d, 8)	104.5	5.46 (d, 8)	104.4

a) Assignments are interchangeable. Xyl(1-3Rha) means the xylopyranosyl group which is linked to the C_3-OH group of the rhamnopyranosyl group.

Compound III showed in the ^{1}H-NMR spectrum the signals of five anomeric protons [δ 4.54 (d, $J=7$ Hz), 5.15 (2H, d, $J=7$ Hz), 5.51 (d, $J=8$ Hz) and 5.97 (d, $J=2$ Hz)], while the other anomer (IV) showed the signals at δ 4.88 (d, $J=7$ Hz), 5.15 (d, $J=7$ Hz), 5.29 (d, $J=3$ Hz), 5.46 (d, $J=8$ Hz) and 5.62 (d, $J=1$ Hz). Compound III showed the signals of the axial C_5-protons of the pentosyl units at δ 3.39 (t, $J=10$ Hz), 3.42 (t, $J=10$ Hz), 3.47 (t, $J=10$ Hz) and at 3.63 (dd, $J=2$, 12 Hz), and IV showed the C_5-H signals at δ 3.17 (t, $J=11$ Hz, C_5-Ha), 3.42 (t, $J=10$ Hz, C_5-Ha), 3.47 (t, $J=10$ Hz, C_5-Ha) and 3.95 (2H, br s, C_5-Ha, e). From the coupling constants of the C_5-protons, III and IV were proved to have 1 mol of L-arabinose and 3 mol of D-xylose as the pentosyl units.

In order to identify the pentose(1), the NMR spectra of III and IV were compared and fully examined, and the ^{1}H- and ^{13}C-NMR signals were assigned as shown in Table III by the ^{1}H–^{1}H correlation spectroscopy (COSY) and ^{1}H–^{13}C COSY techniques. The coupling constants of the C_1-H (7 Hz in III, 3 Hz in IV), C_2-H (7, 8 Hz in III, 3, 10 Hz in IV) and C_3-H (8, 4 Hz in III, 10, 4 Hz in IV) showed that the methyl glycosylated sugar is L-arabinose. The ^{13}C-NMR chemical shifts of the C_2 of the arabinosyl groups (δ 76.9 in III and 78.8 in IV) indicate that the rhamnosyl group is linked to C_2-OH of the arabinosyl group.

The NMR chemical shifts of the rhamnosyl group were assigned as shown in Table III. The chemical shifts of the arabinosyl group and rhamnosyl group in III and IV were in good agreement with those of methyl *O*-α-L-arabinopyranosyl-(1→3)-*O*-β-D-xylopyranosyl-(1→4)-[*O*-β-D-xylopyranosyl-(1→3)]-*O*-α-L-rhamnopyranosyl-(1→2)-α-L-arabinopyranoside and its β-anomer, respectively, which were derived from the ester-linked sugar moiety of acutoside G isolated from the herb,[1] suggesting that III and IV are branched-chain pentaglycosides having a xylopyranosyl group and a xylobiosyl group at the C_3-OH and C_4-OH groups of the rhamnopyranosyl unit.

In order to determine the positions of the xylosyl and the xylobiosyl groups at the rhamnosyl unit and the position of the terminal xylosyl group linkage, the assignments of the anomeric protons and carbons of xylosyl units were performed by using the rotating-frame Overhauser effect (ROE) difference spectroscopy (ROEDS) technique (Fig. 1).

On irradiation at the frequency (δ 4.88) of the anomeric proton of the first xylosyl unit (Xa) of IV, NOE was observed on the signals at δ 4.82 (br s, C_2-H), δ 4.63 (dd, $J=3$, 9 Hz, C_3-H), and δ 4.48 (t, $J=9$ Hz, C_4-H) of the rhamnosyl group (Fig. 1C). The intensities of the signals clearly showed that Xa is linked to the C_3-OH group of the rhamnopyranosyl group. Irradiation at the anomeric signal (δ 5.46) of the third xylosyl group (Xc) brought NOE on the signals at δ 4.82 (br s, C_2-H), δ 4.63 (dd, $J=3$, 9 Hz, C_3-H) and δ 4.48 (t, $J=9$ Hz, C_4-H) of the rhamnosyl group. There was also NOE on the signals at δ 4.11 (t, $J=9$ Hz, C_3-H of Xc) and δ 3.42 (t, $J=10$ Hz, C_5-Ha of Xc) (Fig. 1D). The intensities of the NOE signals indicated that Xc is linked to the C_4-OH group of the rhamnosyl unit. Irradiation at the anomeric proton signal (δ 5.15) of the second xylosyl unit (Xb) caused NOE on the triplet signal at δ 4.11 (t, $J=9$ Hz) (Fig. 1E),

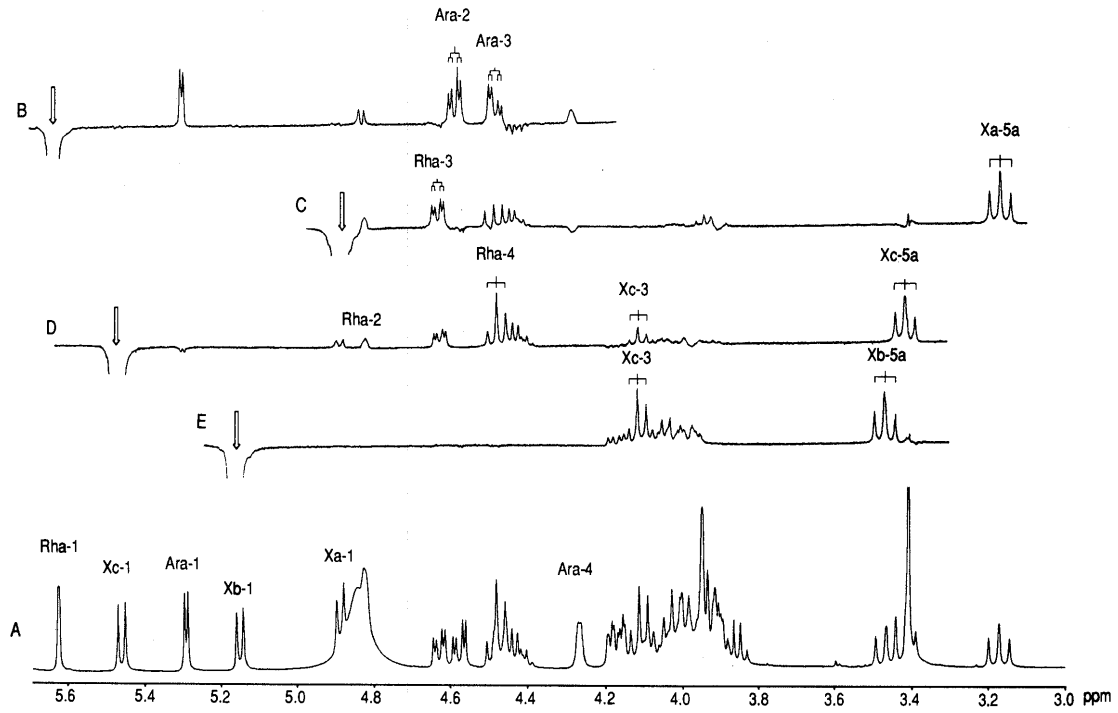

Fig. 1. The ^{1}H-NMR Spectrum (A) and ROEDS Spectra (B—E) of **IV**
Rha-1 means the C_1-H signal of the rhamnopyranosyl group.

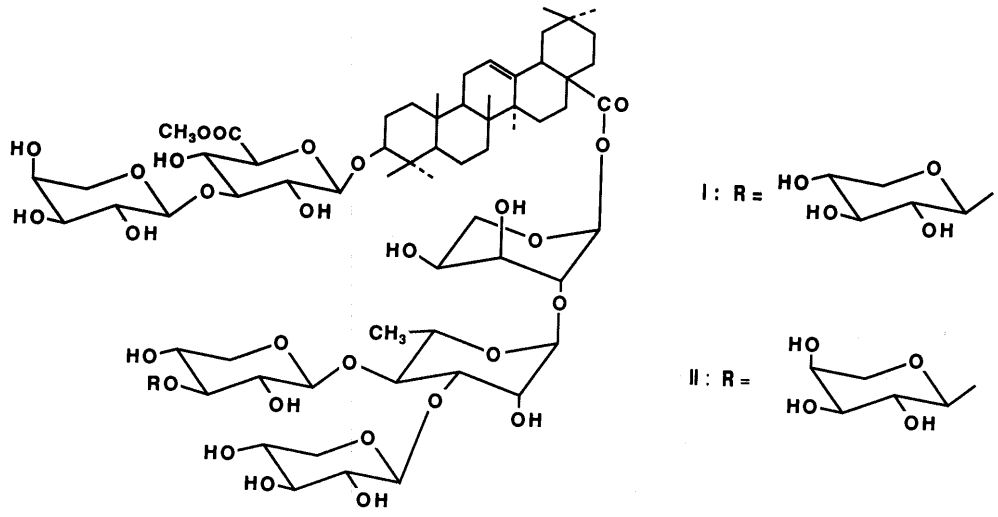

Chart 1

which was proved to be the C_3-H of the Xc by the homonuclear Hartmann–Hahn (HOHAHA) technique. From these ROE difference spectroscopic and HOHAHA techniques, the structure of IV was determined to be methyl *O*-*β*-D-xylopyranosyl(Xb)-(1→3)-*O*-*β*-D-xylopyranosyl-(Xc)-(1→4)-[*O*-*β*-D-xylopyranosyl(Xa)-(1→3)]*O*-*α*-L-rhamnopyranosyl-(1→2)-*β*-L-arabinopyranoside.

Compound IV was fully methylated and methanolyzed. The methanolysis product was acetylated and analyzed by gas chromatography-chemical ionization mass spectrometry (GC-CI-MS). Methyl glycosides of 2,3,4-tri-*O*-methyl-D-xylopyranose, 2,4-di-*O*-methyl-3-*O*-acetyl-D-xylopyranose, 2-*O*-methyl-3,4-di-*O*-acetyl-L-rhamnopyranose and 3,4-di-*O*-methyl-2-*O*-acetyl-L-arabinopyranose were identified, and these results were consistent with the above structure.

The configuration and conformation of the ester-linked L-arabinopyranosyl group in I were determined to be *α* and $^1C_4$ from the J_{C1H1} value (172 Hz)[6] and the coupling constants of the C_1-H (J=2 Hz) and the C_2-H (dd, J=2, 4 Hz) determined by the homodecoupling difference spectroscopy technique. The structure of I is, therefore, concluded to be as shown in the chart.

The methyl ester (V) of acutoside I was obtained as colorless needles, and its FAB-MS showed an $[M+Na]^+$ ion at m/z 1475 and an $[M-H]^-$ ion at m/z 1451. Elemental analysis by high-resolution FAB-MS gave the molecular formula $C_{68}H_{108}O_{33}$.

Compound V gave L-arabinose, L-rhamnose, D-xylose and D-glucuronic acid on acid hydrolysis. The NMR spectra indicated that V is also a 3,28-*O*-bisdesmosidic heptaglyco-

side of oleanolic acid, and V gave a prosapogenin and an anomeric mixture of a methyl pentaglycoside which is composed of L-arabinose, L-rhamnose and D-xylose. The methyl ester of the prosapogenin was proved to be identical with II. The anomers of the methyl glycoside were separated by HPLC on a reversed-phase material. Both methyl glycosides gave L-arabinose, L-rhamnose and D-xylose on acid hydrolysis. The NMR spectra of the faster-eluting anomer (VI) and the other one (VII) were identical with methyl *O*-α-L-arabinopyranosyl-(1→3)-*O*-β-D-xylopyranosyl-(1→4)-[*O*-β-D-xylopyranosyl-(1→3)]-*O*-α-L-rhamnopyranosyl-(1→2)-α-L-arabinopyranoside and its β-anomer, respectively, which were derived from acutoside G isolated from the herb.[1]

The configuration and conformation of the ester-linked L-arabinopyranosyl group in V were determined to be α and $^1C_4$ from the J_{C1H1} value (171 Hz)[6] and the coupling constants of C_1-H ($J=3$ Hz) and the C_2-H (dd, $J=3$, 4 Hz) determined by the homodecoupling difference spectroscopy technique. Therefore, the structure of V was elucidated to be as shown in the chart. Acutosides H and I are contained in the seed as the carboxylate forms.

Acutosides J and K are more polar than H and I, and the NMR data and the molecular weights (1584) suggested that they are 3,28-*O*-bisdesmosidic octaglycosides of oleanolic acid, but their structures could not be determined owing to the small yields of the glycosides.

Experimental[7]

Extraction and Fractionation The seeds (1 kg) of *Luffa acutangula* cultivated in the herbal garden of this university were powdered and extracted first with hexane (15 l). The residue was then percolated with MeOH (10 l) and 50% MeOH (10 l). The 50% MeOH eluate was concentrated to half volume and passed through a column of Diaion HP 20 (1 l). After washing of the column with H_2O (2 l) and 50% MeOH (2 l), MeOH (2 l) was passed through a column to give a crude saponin fraction (9.94 g). The saponin fraction was dissolved in H_2O (100 ml) and passed through the column of Amberlite IRC-84 (100 ml). The acidic solution was concentrated *in vacuo*. The residue was dissolved in 50% MeOH and treated with an ether solution of CH_2N_2 to give a methyl ester of the saponin fraction.

Isolation of Methyl Esters of Acutosides H, I, J and K The methylation product was repeatedly chromatographed on silica gel using $CHCl_3$–MeOH–H_2O (15:6:0.5, 15:6:1) and AcOEt–MeOH–H_2O (8:2:1) and divided into four fractions (fr. I—IV), based on monitoring by TLC (solvent: $CHCl_3$–MeOH–H_2O–AcOH, 21:15:3:1). Fraction I was almost pure acutoside H methyl ester (I) and this fraction was purified by column chromatography on YMC gel (ODS) using 75% MeOH to give a thin-layer-chromatographically homogeneous white powder (2.765 g). Fractions II, III and IV were purified in a same manner to give acutoside I methyl ester (V) (1.892 g), acutoside J methyl ester (337 mg) and acutoside K methyl ester (198 mg), respectively.

Acutoside H Methyl Ester (I): Colorless fine needles from 80% MeOH, mp 235—238 °C, $[\alpha]_D^{24}$ −53.1° ($c=0.58$, 50% MeOH). Positive FAB-MS *m/z*: 1475.6700 ($[C_{68}H_{108}O_{33}Na]^+$). Negative FAB-MS *m/z*: 1451 ($[M-H]^-$). ^{1}H-NMR δ: aglycone moiety: ≥C–CH_3, 0.83, 0.93, 0.97, 1.01, 1.06, 1.28, 1.29; >C=CH–, 5.44 (t-like). Sugar moiety: anomeric H, 4.91 (d, $J=8$ Hz), 5.09 (d, $J=7$ Hz), 5.15 (d, $J=7$ Hz), 5.28 (d, $J=7$ Hz), 5.45 (d, $J=8$ Hz), 5.67 (br s), 6.53 (d, $J=2$ Hz). ^{13}C-NMR δ: aglycone moiety: shown in Table I. Sugar moiety: anomeric C, 93.2, 100.7, 104.5, 105.7, 105.85, 105.9, 106.7.

Acutoside I Methyl Ester (V): Colorless needles from 80% MeOH, mp 234—237 °C, $[\alpha]_D^{24}$ −28.7° ($c=2.0$, 50% MeOH). Positive FAB-MS *m/z*: 1475.6660 ($[C_{68}H_{108}O_{33}Na]^+$). ^{1}H-NMR δ: aglycone moiety: almost the same as those of I. Sugar moiety: anomeric H, 4.92 (d, $J=8$ Hz), 5.11 (d, $J=8$ Hz), 5.17 (d, $J=7$ Hz), 5.28 (d, $J=7$ Hz), 5.44 (d, $J=8$ Hz), 5.67 (br s), 6.52 (d, $J=2$ Hz). ^{13}C-NMR δ: aglycone moiety: almost the same as those of I. Sugar moiety: anomeric C, 93.2, 100.7, 104.6, 105.5, 105.6, 105.9, 106.7.

Identification of the Sugar Species The component sugar species and their absolute configurations were derermined in the same manner as described in the preceding paper[1] of this series. Thus, the glycoside or a saponin (*ca.* 3 mg) was dissolved in 2 N HCl–MeOH (0.5 ml) and the solution was refluxed for 2 h. The acid was neutralized with Ag_2CO_3 and the mixture was filtered. The filtrate was bubbled through with H_2S and concentrated to dryness. Trimethylsilylimidazole (25 μl) was added to the residue. Hexane (0.5 ml) was added to the mixture and washed with water (0.5 ml). The hexane solution was injected into the gas chromatography (GC) column. Authentic sugar samples were treated in the same manner and the retention times were compared with those of the test samples.

Determination of the absolute configurations of the sugars was performed according to the method reported from this faculty.[8] A glycoside (*ca.* 5 mg) was dissolved in 1 N HCl and heated at 90 °C for 1 h. The acid was neutralized in the same manner described above to give the hydrolyzate. A pyridine solution (100 μl) of L-cysteine methyl ester hydrochloride (0.06 mol/l) was added to the hydrolyzate and the mixture was warmed at 60 °C for 1 h. Pyridine was blown off with N_2 and trimethylsilylimidazole (25 μl) was added to the residue. Hexane (0.5 ml) and water (0.5 ml) were added and the mixture was shaken. The hexane solution was injected into the GC column. Authentic sugar samples were treated in the same way and the retention times were compared.

The absolute configuration of the component glucuronic acid was determined as glucose after $NaBH_4$ reduction of the prosapogenin methyl ester followed by hydrolysis.

The GC conditions were as follows: column, Shimadzu capillary column HiCap (0.25 mm i.d. × 50 m); liquid phase, CBP-1; carrier gas, He at 0.7 ml/min (20 cm/s). Temperature: 190 °C for pentose and methylpentose derivatives, and 210 °C for hexose derivatives and for the determination of the absolute configuration. The sugar species identified are cited in the text.

Selective Cleavage of the Ester-Glycoside Linkage Selective cleavage of the ester-linked sugar moiety was performed according to the method reported by Ohtani, *et al.*[5] Acutoside H methyl ester (I) (640 mg) and LiI (815 mg) were added to the mixture of 2,6-lutidine (8 ml) and MeOH (6 ml), and the mixture was heated at 140 °C for 24 h. Then 50% MeOH (35 ml) was added to the reaction mixture and the solution was passed through a column of Amberlite MB-3 (60 ml). The effluent was concentrated to dryness and the residue was dissolved in MeOH and treated with CH_2N_2. After evaporation of the solvent, the residue was redissolved in 50% MeOH and chromatographed on a Diaion HP-20 column eluted with 50% MeOH (100 ml) and MeOH (100 ml). The 50% MeOH eluate (263 mg) was chromatographed on a prepacked Fuji gel (ODS) column (30 cm × 2.5 cm i.d.) using 13% MeOH and finally purified by HPLC on a Shiseido Capcell Pak C18 column (25 cm × 10 mm i.d.) using 15% MeOH (flow rate, 2 ml/min) to give III (33 mg) and IV (52 mg). The MeOH eluate (300 mg) was chromatographed on a silica gel (50 g) column (AcOEt–MeOH–H_2O, 8:1:0.1) to give a prosapogenin methyl ester (II) (184 mg).

Acutoside I methyl ester (V) (800 mg) gave II (300 mg) and an anomeric mixture (299 mg) of a methyl glycoside. The latter was chromatographed on Fuji gel and purified by HPLC in the same manner as described above to give VI (52 mg) and VII (87 mg). The ^{1}H- and ^{13}C-NMR spectra of VI and VII were superimposable on those of methyl *O*-α-L-arabinopyranosyl-(1→3)-*O*-β-D-xylopyranosyl-(1→4)-[*O*-β-D-xylopyranosyl-(1→3)]-*O*-α-L-rhamnopyranosyl-(1→2)-α-L-arabinopyranoside and its β-anomer, respectively.

Prosapogenin Methyl Ester (II): Colorless needles from MeOH, mp 203—207 °C, $[\alpha]_D^{24}$ 23.5° ($c=1.0$, MeOH). Positive FAB-MS *m/z*: 815 ($[M+Na]^+$). ^{1}H-NMR δ: aglycone moiety: ≥C–CH_3, 0.82, 0.85, 0.93, 0.95, 0.97, 1.25, 1.30; >C=CH–, 5.37 (t-like); $COOC\underline{H}_3$, 3.71. Sugar moiety: shown in Table II. ^{13}C-NMR: shown in Tables I and II.

Compound III: An amorphous powder, $[\alpha]_D^{24}$ −58.2° ($c=1.35$, MeOH). Positive FAB-MS *m/z*: 729 ($[M+Na]^+$). Negative FAB-MS *m/z*: 725 ($[M-H]^-$), 573 (725-pentose), 441 (573-pentose), 309 (441-pentose), 163 (309-rhamnose). NMR: shown in Table III.

Compound IV: An amorphous powder, $[\alpha]_D^{24}$ −1.6° ($c=1.6$, MeOH). FAB-MS: same as those of III. NMR: shown in Table III.

Permethylation of IV and Determination of the Component Methylated Sugars of the Permethylate Compound IV (17 mg) was added to dimethylsulfinyl carbanion solution (1 ml) prepared by heating a dimethyl sulfoxide (DMSO) solution of NaH (50 mg) at 80 °C for 20 min. After the mixture had been stirred for 10 min, MeI (1 ml) was added, and the whole was stirred at room temperature for 24 h. Water (5 ml) was added to the reaction mixture and the methylation product was extracted with $CHCl_3$ (5 ml × 3). The $CHCl_3$ layer was separated and dried over Na_2SO_4. After evaporation of $CHCl_3$, the residue was chromatographed on silica gel

(15 g) (solvent: benzene–acetone, 4 : 1) to give the thin-layer-chromatographically homogeneous product (20 mg). The methylation product was heated in 1 N HCl–MeOH (0.5 ml) for 1 h, neutralized with Ag_2CO_3 and filtered. The filtrate was bubbled through with H_2S and concentrated to dryness. The methanolysate was acetylated with Ac_2O–pyridine (1 : 1) (1 ml) at room temperature and checked by GC-CI-MS.

The following methyl glycosides were identified. The numbers in parentheses are retention times. Methyl 2,3,4-tri-*O*-methyl-β-D-xylopyranoside (1.2) and its α-anomer (1.5), methyl 2,4-di-*O*-methyl-3-*O*-acetyl-β-D-xylopyranoside (4.3) and its α-anomer (5.3), methyl 3,4-di-*O*-methyl-2-*O*-acetyl-α-L-arabinopyranoside (5.6) and 2-*O*-methyl-3,4-di-*O*-acetyl-α-L-rhamnopyranoside (7.4).

Acknowledgement The authors are grateful to Ms. Yukiko Iwase, Miss Junko Honda and Mr. Hiroshi Hanazono for measurement of NMR spectra and MS.

References and Notes

1) Part I: T. Nagao, R. Tanaka, Y. Iwase, H. Hanazono and H. Okabe, *Chem. Pharm. Bull.*, **39**, 599 (1991).
2) K. S. Grewal and B. D. Kochhar, *Indian J. Med. Research*, **31**, 63 (1943).
3) A. K. Barua, S. K. Chakraborti and A. K. Ray, *J. Indian Chem. Soc.*, **35**, 480 (1958).
4) T. Takemoto, S. Arihara, K. Yoshikawa, K. Kusumoto, T. Yano and T. Hayashi, *Yakugaku Zasshi*, **104**, 246 (1984).
5) K. Ohtani, K. Mizutani, R. Kasai and O. Tanaka, *Tetrahedron Lett.*, **25**, 4537 (1984).
6) K. Bock and C. Pedersen, *J. Chem. Soc., Perkin Trans. 2*, **1974**, 293.
7) The instruments and materials used in this work were the same as those described in the preceding paper. The NMR spectra were measured in pyridine-d_5.
8) S. Hara, H. Okabe and K. Mihashi, *Chem. Pharm. Bull.*, **35**, 501 (1987).

Evaluation of Effects of Novel Urease Inhibitor, *N*-(Pivaloyl)glycinohydroxamic Acid on the Formation of an Infection Bladder Stone Using a Newly Designed Urolithiasis Model in Rats

Masaru SATOH,*[,a] Keiichi MUNAKATA,[a] Hideo TAKEUCHI,[b] Osamu YOSHIDA,[b] Sachiko TAKEBE[c] and Kyoichi KOBASHI[c]

Eisai Research Laboratories,[a] 4 Koishikawa, Bunkyo-ku, Tokyo 112, Japan, Department of Urology, Faculty of Medicine, Kyoto University,[b] Shogoin, Sakyo-ku, Kyoto 606, Japan and Faculty of Pharmaceutical Sciences, Toyama Medical and Pharmaceutical University,[c] 2630 Sugitani, Toyama-shi, Toyama 930-01, Japan. *Received May 8, 1990*

By using our new infection stone model of a rat, we evaluated the effect of a novel urease inhibitor, *N*-(pivaloyl)glycinohydroxamic acid (P-GHA), on the formation of an infection bladder stone. The oral dosing of P-GHA significantly inhibited the elevation of the urinary ammonia level of rats having the urinary tract infection with *Proteus mirabilis*.

A short term regimen (7 d, 730 ± 38 mg/kg) with P-GHA significantly inhibited the development of the infection bladder stone. Furthermore, a long term combination regimen (11 d) of P-GHA and aminobenzylpenicillin markedly inhibited the development of the infection bladder stone, and also caused a very slight renal impairment to the rats tested in contrast with the method of Vermeulen *et al.*

Our infection stone model in rats, therefore, seems to be useful for the evaluation of therapeutic agents in long term examinations.

Keywords *Proteus species*; urease inhibitor; infection stone; *N*-(pivaloyl)glycinohydroxamic acid; combination

Introduction

It has been well demonstrated that hyperammoniuria and the alkalinization of urine caused by urea-splitting bacteria play an important role in the formation of struvite, so that a urease inhibitor seems to be a promising therapeutic agent for the treatment of an infection stone.[1-3]

We already reported the efficacy of a urease inhibitor, *N*-(pivaloyl)glycinohydroxamic acid (P-GHA) toward the development of struvite in rats using the model of Vermeulen *et al.*[4]

However, the method of Vermeulen *et al.* was not a sufficiently adequate experimental model, because of a relatively high incidence of death, severe renal damage and a considerable decrease in a body weight on the test animals. Consequently, this model appears to be unfavorable for long term examination.

We therefore developed a new infection stone model with a mild urinary tract infection, showing slight renal damage without pyelonephritis and also assuring a stone formation.[5] We investigated the combination effect of P-GHA and aminobenzylpenicillin (ABPC) in a long term examination on the development of an infection bladder stone using our new model.

Materials and Methods

Chemicals P-GHA and acetohydroxamic acid (AHA) were synthesized in our laboratory and purity was more than 99%.[3] ABPC (Meiji Co., Ltd., Japan) was purchased.

Animals Female Spraque–Dawley strain rats (specific pathogen free, 7 weeks old, weighing 180 to 220 g, Charles River Japan Ind.) were used in all experiments.

Bacteria *Proteus mirabilis* (E05106) was isolated from a patient with a urinary tract infection and used after cultivation at 37 °C for 20 h on a Heart Infusion Agar medium (Difco). Urea medium (Eiken Co., Ltd., Japan) was used to detect the urease activity of the bacterium.

The Experimental Procedure in an Animal Model The experimental procedure for infection bladder stone formation was performed according to the method of Satoh *et al.*[5] Namely, a sterile zinc ring (4 mm in diameter) was surgically implanted into the bladder, followed by the administration of ABPC to prevent infection associated with surgery. Seven days after surgery, inoculation of *P. mirabilis* (10^7 cfu/rat) was transuretherally made through a polyethylene tube (PE-10). P-GHA was orally administered by being dissolved in 20 to 30 ml of drinking water containing 5% (w/v) sucrose or 0.01% (w/v) saccharine beginning from 8 h after infection.

Biochemical Findings At the time of sacrifice, the rats tested were anesthetized with sodium pentobarbital and then the peritoneal cavity was opened, followed by sampling the blood of the aorta abdominalis in order to determine the blood urea nitrogen (BUN) which was measured by the method of Seligson and Seligson.[6]

Count of Viable Cells At the time of sacrifice, the bladder urine was aspirated with a tuberculin syringe, and then 0.1 ml of 100-fold diluted urine was inoculated onto an SS agar medium (Eiken Chemical Co., Ltd.). The kidneys were removed for histological studies.

Determination of the Urinary Amount of P-GHA and Ammonia The amount of unchanged P-GHA in urine was determined enzymatically according to the method of Kobashi *et al.*[7] The urinary amount of ammonia was determined by the method of Seligson and Seligson.[6]

Analysis of Stones Formed The disc and associated stones were removed from the bladder at autopsy and dried *in vacuo* at room temperature for 24 h in the presence of P_2O_5, then weighed. The weight of the stones was estimated by subtracting the initial weight of the disc from the weight of the disc and the stones together. Infrared (IR) analysis of the stones was made with a Hitachi-215 spectrophotometer,[8] and the magnesium content of the stones was determined spectroscopically with a Jarrell–Ash atomic absorption and flame emission spectrophotometer AA-855.[9]

Histological Study The kidney specimens prepared for histological studies were fixed in a 10% neutral formalin solution. After fixation, the samples were sectioned and then stained by standard hematoxylin-eosin.

Results

Figure 1 shows that the oral administration of P-GHA significantly inhibited the elevation in urinary ammonia level in the rats tested. When P-GHA was administered orally (100 mg/kg), the cummulative urinary recovery rate of unchanged P-GHA reached about 11.4% within 12 h, representing almost the same recovery rate observed in the non-infected rat. This urinary recovery rate was almost the same as compared with that obtained in the model of Vermeulen *et al.*[4]

Table I indicates the development of the infection bladder stone was significantly prevented by a higher dose (730 ± 38 mg/kg/d) of P-GHA, while such an efficacy could not be observed at the lower dosage level (129 ± 14 mg/kg/d). This result was the same as that observed in the model of Vermeulen *et al.* There was no significant difference in the intake of drinking water, the urine volume or BUN between the P-GHA treated and non-treated groups. Of all the rats

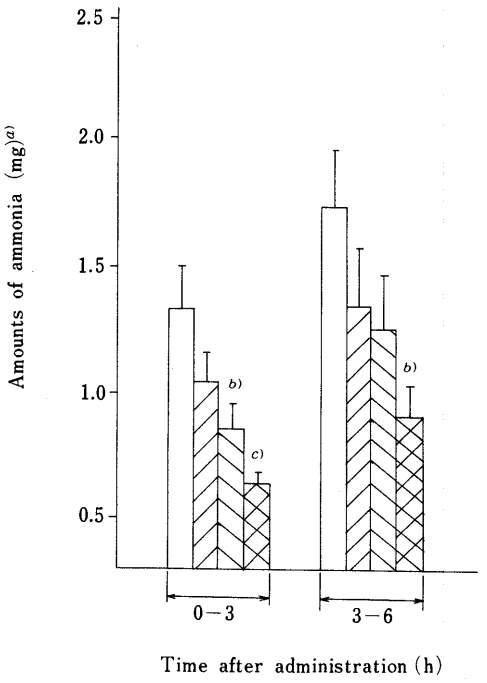

Fig. 1. Effect of P-GHA on the Amounts of Urinary Ammonia in the Rat Infected with *P. mirabilis*

□; non-treated; ▨, P-GHA 50 mg/kg; ▧, P-GHA 100 mg/kg; ▩, P-GHA 200 mg/kg ($n=8$, mean ± S.E.).

a) Total ammonia (mg) was calculated according to the following equation:

$$\text{total ammonia (mg)} = \frac{\text{ammonia concentration (mg/dl)} \times \text{urine volume (ml)}}{100}.$$

Significantly different from the non-treated group by *t*-test, *b*) $p<0.05$; *c*) $p<0.01$.

TABLE I. Preventive Effect of P-GHA on Bladder Stone Formation Caused by *P. mirabilis* in Rats

	Dosage[a] (mg/kg/d)	Number of rats	Stone weight[b] (mg)	BUN (mg/dl)
Exp. 1	730±38[c]	12	5.8±1.6[d]	22.1±1.2
	None (control)	11	20.8±6.0	28.8±6.4
Exp. 2	129±14	8	23.4±3.6	25.4±3.3
	None (control)	8	19.7±5.8	23.5±1.2

a) P-GHA was orally administered by being dissolved in 20 ml of drinking water (5% sucrose solution, w/v) beginning from 8 h after infection and continuing for (exp. 1) or 8 (exp. 2) d. *b*) The stone weight was determined at the 7th (exp. 1) or 8th (exp. 2) d after infection. *c*) Dosage (mg/kg/d) was calculated according to the following equation:

$$\text{dosage (mg/kg/d)} = \frac{\text{daily intake volume (ml)} \times \text{P-GHA concentration (mg/ml)}}{\text{body weight (kg)}}.$$

d) $p<0.05$, significantly different from the control by *t*-test. Values are expressed as mean ± S.E.

with or without the treatment of P-GHA, *P. mirabilis* was detected from the bladder urine ($>10^5$ cfu/ml) at the time of autopsy. On the other hand, in order to compare the efficacy of P-GHA and AHA, P-GHA or AHA was administered orally (500 mg/kg/d) as 1 ml of 5% (w/v) gum arabic suspension *t.i.d.* for 10 d beginning from 8 h after infection. Both P-GHA and AHA treatments exhibited significant inhibitory action, showing 25.4±4.3 mg (mean ± S.E.) and 17.1±4.2 mg of the stone weight, respectively, as compared with 54.1±5.7 mg for the non-treated group. The inhibitory action of P-GHA was the same as that of AHA. There was no significant difference in the value of BUN (mg/dl), indicating 17.7±0.5 (mean ± S.E.) for the P-GHA treated group, 16.8±0.7 for the AHA treated group and 22.5±5.7 for the non-treated group.

TABLE II. Combination Effect of P-GHA and ABPC on Bladder Stone Formation Caused by *P. mirabilis* in Rats

Group	Dosage[a] (mg/kg/d)	Number of rats	Stone weight[b] (mg)	Incidence of kidney abscess (%)
None (control)	None	8	48.6±11.0	25
P-GHA	332±12[c]	8	52.9±10.3	12.5
ABPC	10	7	45.3± 9.0	14.3
P-GHA	309±14			
+	+	9	23.0± 5.3[d]	0
ABPC	10			

a) P-GHA was orally administered by being dissolved in 30 ml of drinking water containing 0.01% (w/v) saccharine, beginning from 8 h after infection and continuing for 14 d. ABPC (10 mg/kg) was also administered orally from the 6th and 12th day after infection for 3 d. *b*) The stone weight was determined at the 15th day after infection. *c*) Dosage (mg/kg/d) was calculated according to the following equation:

$$\text{dosage (mg/kg/d)} = \frac{\text{daily intake volume (ml)} \times \text{P-GHA concentration (mg/ml)}}{\text{body weight (kg)}}.$$

d) $p<0.05$, significantly different from the control by *t*-test. Values are expressed as mean ± S.E.

As shown in Table II, the combination therapy of P-GHA and ABPC manifested marked efficacy in preventing bladder stone formation, while such an efficacy could not be observed with doses of P-GHA or ABPC alone. In addition, kidney abscess formation was completely prevented by this combination therapy.

The main composition of the bladder stone formed was found to be struvite ($MgNH_4PO_4 \cdot 6H_2O$).

Discussion

A relatively high dose of P-GHA (730 mg/kg) was necessary for the prevention of bladder stone formation in the present experimental model, as well as in the model of Vermeulen *et al.*[4] Meanwhile, our *in vitro* examination indicated a urinary level of 34 μg/ml for P-GHA was required to exhibit 80% inhibition of ureolytic activity of intact *P. mirabilis*. After the administration of P-GHA (100 mg/kg) to rats, the urinary level of P-GHA exceeded 34 μg/ml (apparent IC_{80} value) for 6 h, but elevation in the urinary ammonia level was prevented within only 3 h. This finding suggests that a rise in urine pH diminishes the urease inhibitory action of P-GHA. Consequently, this diminished *in vitro* activity of P-GHA might be responsible for the required high dosage of P-GHA to exhibit *in vivo* action.

On the other hand, it is of interest from a clinical viewpoint that the combination of P-GHA and ABPC markedly prevented the formation of an infection bladder stone. This observation suggests that the antibacterial activity of ABPC against *P. mirabilis* produces an advantageous condition for exhibiting the inhibitory action of P-GHA toward bacterial urease, resulting from the inhibition of urine alkalinization by reducing the number of urea-splitting bacteria *P. mirabilis*.

Recently, lithotripsies such as a percutaneous nephrolithotripsy, a transuretheral-lithotripsy and a extracorporeal shock wave lithotripsy have been widely applied in the

treatment of urolithiasis. However, those lithotripsies have caused frequent recurrence of urolithiasis in many cases because of difficulty in completely removing small stones. Under this situation, a concomitant use of a urease inhibitor and/or an antibacterial agent with lithotripsy are thought to be useful for preventing an associated infection and recurrence of the stone. In fact, AHA demonstrated effectiveness in the prevention of the development of a stone in 31 patients with infection stones.[10]

The combination therapy of P-HGA and an antibacterial agent with concurrent use of lithotripsy, therefore, seems to be clinically beneficial in the management of struvite, because P-GHA is estimated to be safer than AHA owing to lack of mutagenicity.[11]

References

1) M. Munakata, K. Kobashi, S. Takebe and J. Hase, *J. Pharmacobio-Dyn.*, **3**, 541 (1980).
2) D. P. Griffith and D. M. Musher, *Invest. Urol.*, **12**, 381 (1975).
3) H. Takeuchi, K. Kobashi and O. Yoshida, *Invest. Urol.*, **18**, 102 (1980).
4) M. Satoh, K. Munakata, K. Kitoh, N. Seto, T. Kanazawa, H. Takeuchi and O. Yoshida, *J. Pharmacobio-Dyn.*, **4**, 469 (1981).
5) M. Satoh, K. Munakata, K. Kitoh, H. Takeuchi and O. Yoshida, *J. Urol.*, **132**, 1247 (1984).
6) E. Seligson and H. Seligson, *J. Lab. Clin. Med.*, **38**, 324 (1951).
7) K. Kobashi, N. Terashima, S. Takebe and J. Hase, *J. Biochem.* (Tokyo), **83**, 287 (1978).
8) E. Takasaki, *Calc. Tiss. Res.*, **7**, 232 (1971).
9) J. Ramirez-Muroz, The Beckman Instrument Company, Fullerton, Calif., **1**, 26 (1966).
10) J. Rodman, 5th International Symposium on Urolithiasis and Related Research, West Germany, 1985.
11) M. Munakata, H. Mochida, S. Kondo and Y. Suzuki, *J. Pharmacobio-Dyn.*, **3**, 557 (1980).

Effects of a Novel Urease Inhibitor, *N*-(Diaminophosphinyl)isopentenoylamide on the Infection Stone in Rats

Masaru SATOH,*[,a] Keiichi MUNAKATA,[a] Hideo TAKEUCHI,[b] Osamu YOSHIDA,[b] Sachiko TAKEBE[c] and Kyoichi KOBASHI[c]

Eisai Research Laboratories,[a] 4 Koishikawa, Bunkyo-ku, Tokyo 112, Japan, Department of Urology, Faculty of Medicine, Kyoto University,[b] Shogoin-Kawaramachi, Sakyo-ku, Kyoto 606, Japan and Faculty of Pharmaceutical Sciences, Toyama Medical and Pharmaceutical University,[c] 2630 Sugitani, Toyama-shi, Toyama 930-01, Japan. *Received May 8, 1990*

We evaluated the effect of a novel potent urease inhibitor, *N*-(diaminophosphinyl)isopentenoylamide (IPA), on the development of an infection bladder stone using our urolithiasis model in rats. IPA was excreted into urine after oral administration to rats, and the cumulative urinary recovery rate of unchanged IPA reached about 29.6% within 24 h (50 mg/kg). The oral administration of IPA (6.25 mg/kg, *b.i.d.*, 5 d) significantly inhibited the development of the infection bladder stone. The present result suggests that IPA is a very promising compound in the prevention of formation and recurrence of an infection stone owing to a high efficacy and a low toxicity of IPA in animals.

Keywords *Proteus* species; urease inhibitor; infection stone; struvite; diaminophosphinylamide

Introduction

The urinary tract infection caused by urea-splitting bacteria, such as a *Proteus* species, is related to the formation of a struvite stone as a result of inducing hyperammoniauria and alkalinization of urine.[1-3] An infection stone comprises 15 to 20% of total urinary stones, and this type of stone is considered to be malignant because of a high incidence of recurrence resulting in renal impairment.[4]

Recently, the introduction of lithotripsies such as percutaneous nephrolithotripsy, transuretheral lithotripsy and extracorporeal shock wave lithotripsy has made great advances in the treatment of urolithiasis.[5-7] However, those lithotripsy regimens are not able to prevent recurrence of urolithiasis in many cases, owing to the difficulty of completely removing small stones. Especially, lithotripsy toward an infection stone relatively easily induces recurrence resulting from the growth of urea-splitting bacteria within residual small stones. Combination therapy using a urease inhibitor and/or an antibacterial agent with lithotripsy is therefore thought to be beneficial in the management of an infection urolithiasis.

Kobashi *et al.* revealed that *N*-(diaminophosphinyl)-isopentenoylamide (IPA) manifested more potent urease inhibitory action than *N*-(pivaloyl)glycinohydroxamic acid (P-GHA), through their *in vitro* investigations.[8-10]

In order to evaluate the possibility of the clinical application of IPA, we conducted the present investigation on the *in vivo* efficacy of IPA using our infection urolithiasis model in rats.[11]

Materials and Methods

Chemicals IPA, *N*-(diaminophosphinyl)benzamide (BPA) and acetohydroxamic acid (AHA) were synthesized in the Eisai Research Laboratory, and those purities were more than 99%.

Animals Female Spraque Dawley strain rats (specific pathogen free, 7 weeks old, weighing 180 to 220 g, Charles River Japan Ind.) were used in all experiments.

Determination of Antibacterial Activity Minimal inhibitory concentrations of IPA and BPA were determined by the agar dilution method using a Mueller Hinton Agar medium (Difco, U.S.A.).

Bacteria *Proteus mirabilis* (E05106) was isolated from a patient with a urinary tract infection and used after cultivation at 37 °C for 18 h on a Heart Infusion Agar medium (Difco).

The Experimental Procedure for the Animal Model The experimental procedure for *in vivo* infection bladder stone formation was performed according to the method of Satoh *et al.*[11] Namely, a sterile zinc ring (4 mm in diameter) was surgically implanted into the bladder, followed by the administration of aminibenzyl-penicillin to prevent infection associated with the surgery. Seven days after surgery, inoculation of *P. mirabilis* (10^7 cfu/rat) was transuretherally performed through a polyethylene tube (PE-10). Test compounds were orally administered as a suspension of 5% gum arabic.

Determination of Urinary Amount of IPA The amount of unchanged IPA in urine was determined enzymatically according to the method of Kobashi *et al.*[12]

Count of Viable Cells At the time of sacrifice, the bladder urine was aspirated with a tuberculin syringe, then 0.1 ml of 100-fold diluted urine was inoculated onto an SS agar medium (Eiken Co., Ltd.).

Analysis of the Stones Formed The disc and associated stones were removed from bladder at the time of autopsy and dried *in vacuo* at room temperature for 24 h in the presence of P_2O_5, then weighed. The weight of the stones was estimated by subtracting the initial weight of the disc from the weight of the stones together. Infrared (IR) analysis of the stones was made with a Hitachi-215 spectrometer.[13]

Results

Both IPA and BPA had no antibacterial activity against *S. aureus*, *S. pneumoniae*, *E. coli*, *P. mirabilis*, *P. vulgaris*, *M. morganii*, *K. pneumoniae*, *P. aeruginosa* and *S. typhimurium* in the agar dilution method. The urinary excretions of unchanged IPA and BPA after oral administration to the infected rats were summarized in Table I. The cumulative recovery rate of unchanged IPA reached 29.5% of the total dosage (50 mg/kg) within 24 h, which was comparable to that of PBA (21.0%). The cumulative recovery rates of unchanged IPA and BPA were almost the same among

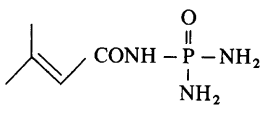

N-(diaminophosphinyl)isopentenoylamide (IPA)

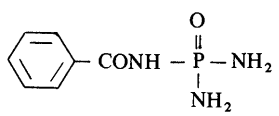

N-(diaminophosphinyl)benzamide (BPA)

Fig. 1. Chemical Structures of Phosphoric Amide Derivatives

TABLE I. Urinary Excretion of Phosphoric Amide Derivatives after Oral Administration to Rats

Compound Dosage[a]	Urine level	Time interval (h) 0—3	3—6	6—9	9—12	12—24	Cumulative (%)
IPA 50 mg/kg	μg/ml	711±288[b]	1247±259	525±156	151±31.6	24.7±10.3	
	%	12.0±3.2	13.6±2.6	1.9±0.5	1.0±0.3	1.0±0.3	29.5±2.1
IPA 5 mg/kg	μg/ml	56.2±5.3	14.7±8.9	12.4±5.1	10.6±3.4	0.9±0.2	
	%	11.7±1.5	1.3±0.7	1.4±0.5	0.7±0.5	0.5±0.2	15.6±2.7
BPA 50 mg/kg	μg/ml	1075±92	484±53	159±45	17.2±5.5	2.8±1.1	
	%	17.1±2.7	2.8±1.1	0.9±0.6	0.1±0.1	0.1±0.1	21.0±2.7

a) Test compounds were orally administered at 4 d after infection as a gum arabic suspension. *b*) Values are expressed as mean±S.E. ($n=3$ to 4).

TABLE II. Preventive Effects of IPA, BPA and AHA on the Formation of an Infection Bladder Stone Caused by *P. mirabilis* in Rats

	Group	Dosage[a] (mg/kg/d)	Number of rats	Stone weight[c] (mg)	Significance[b] (p-values)
Exp. 1	IPA	50	10	10.9±2.8	0.001
		25	9	11.1±3.7	0.001
		12.5	10	15.2±3.2	0.01
	BPA	25	8	13.1±2.8	0.01
		12.5	8	18.0±6.9	0.05
	AHA	200	10	20.9±3.2	0.05
		100	7	21.7±6.3	N.S.[d]
	None (control)	0	10	34.5±2.6	
Exp. 2	IPA	6.25	9	11.8±3.5	0.05
		3.13	9	14.9±6.2	N.S.[d]
	BPA	6.25	7	19.6±9.3	N.S.[d]
	None (control)	0	9	26.3±6.5	

a) Test compounds were orally administered *b.i.d.* at the indicated dosage for 5 d beginning from the 4th day after infection with *P. mirabilis*. *b*) Statistically significant from the control group by *t*-test. *c*) Values are expressed as mean±S.E. *d*) Not significant.

TABLE III. Therapeutic Effects of a Long Term Regimen with IPA on the Development of an Infection Bladder Stone Caused by *P. mirabilis* in Rats

Group	Dosage[a] (mg/kg/d)	Number of rats	Stone weight (mg)
None (control) 7 d	0	29	27.3±3.3[b]
None (control) 21 d	0	27	127.2±9.6
IPA	100	30	37.5±5.7[c]
	25	30	48.1±9.3[c]

a) IPA was orally administered *b.i.d.* at the indicated dosage for 14 d beginning from the 7th day after infection with *P. mirabilis*. *b*) Values are expressed as mean±S.E. *c*) $p<0.001$, statistically significant from the control group (21 d) by *t*-test.

infected and non-infected rats. However, IPA showed a different excretion pattern from BPA, manifesting a more prolonged urinary level than BPA. On the other hand, when IPA was orally administered for a low dosage (5 mg/kg), its cumulative recovery rate was only 15.6% within 24 h. As shown in Table II, the results of 2 separate experiments indicated that IPA significantly prevented the formation of an infection bladder stone at the lower dosage level, which was stronger than both BPA and AHA. The long term regimen of IPA manifested a marked efficacy in preventing the development of an infection bladder stone (Table III). In all the infected rats, *P. mirabilis* ($>10^5$ cfu/ml) was found in the bladder urine at the time of autopsy. There was no significant difference in the abscess formation and blood area nitrogen (BUN) between the treated and non-treated groups. It indicates that the present infection urolithiasis model produced a mild urinary tract infection. The main composition of the bladder stone formed was found to be struvite ($MgNH_4PO_4 \cdot 6H_2O$).

Discussion

Since IPA showed no antibacterial activity toward the *Proteus* species, the preventive effect of IPA on an infection bladder stone may have resulted from its strong inhibitory potency against the ureolytic activity of intact *P. mirabilis*, as reported previously ($I_{50}=3.0$ ng/ml).[8] A higher urinary concentration was necessary to prevent the development of an infection bladder stone *in vivo*, compared to its I_{50} value. After the administration of IPA (5 mg/kg) to rats, the urinary level of unchanged IPA reached about 3000 times higher than the I_{50} value. The urinary recovery rate at the lower dosage (5 mg/kg) of IPA was smaller than that at the higher dosage (50 mg/kg). The reason for the smaller urinary recovery of IPA at the lower dosage may be attributable to the instability of IPA relative to gastric juice. In fact, Millner *et al.* reported that when *N*-(diaminophosphinyl)-4-flurobenzamide was incubated at pH 2.0 at 37 °C, its urease inhibitory activity rapidly diminished.[14] The preventive effect of IPA on the formation of the infection bladder stone was superior to that of BPA, probably resulting from the more prolonged urinary level of IPA than that of BPA, although I_{50} values of IPA and BPA toward intact *P. mirabilis* were almost the same. Meanwhile, the preventive effect of IPA on the formation of the infection bladder stone was estimated to be superior to that of P-GHA reported previously by us.[15]

The long term regimen with IPA exhibited a therapeutic effect on the development of the infection bladder stone, but a dissolving effect with IPA could not be observed in spite of its powerful urease inhibitory activity. This observation suggests that monotherapy with a urease inhibitor such as IPA has limited value for the treatment of an infection urolithiasis.

Since the combination of a urease inhibitor such as P-GHA and an antimicrobial agent markedly prevented the formation of an infection bladder stone, IPA is also though to manifest the combination effect with antibiotic agents.[16,17] Furthermore, IPA is not mutagenic in the Ames test, with or without the S-9 mixture, and less toxic, having an acute LD_{50} of >6000 mg/kg (*p.o.*) in mice, so that IPA seems to be useful for the treatment of an infection stone considering its efficacy and safety.

Recently, lithotripsy has been widely applied for the

treatment of urolithiasis. However, lithotripsy induces a rise in blood pressure and the formation of localized hematomas in many cases because of kidney damage.[18,19] Recurrence of infection stones is also caused inevitably because of the difficulty of a complete removal of small stones. In these situations, in the treatment of urolithiasis, the further combined use of a urease inhibitor and/or an antimicrobial agent with lithotripsy is considered to be more advantageous in the prevention of recurrence of an infection stone and an associated infection.

The present study indicated that IPA was one of the prospective therapeutic agents with promising potential for the treatment of an infection urolithiasis. Further pharmacological and toxicological evaluations are necessary before the clinical application of IPA.

References

1) D. P. Griffith, D. M. Musher and C. Itin, *Invest. Urol.*, **13**, 346 (1976).
2) H. Takeuchi, O. Yoshida, S. Takebe and K. Kobashi, *Acta Urol. Jpn.*, **23**, 637 (1977).
3) D. P. Griffith, P. A. Moskowitz and C. E. Carlton, *J. Urol.*, **121**, 711 (1979).
4) O. Yoshida, *Jpn. J. Urol.*, **70**, 975 (1975).
5) R. V. Clayman, V. Surya and R. D. Miller, *J. Urol.*, **131**, 868 (1984).
6) M. Papadopoulos, M. Figge and L. Weissbach, *Urologe, A.*, **25**, 322 (1986).
7) J. E. Lingeman, D. Newman, J. H. O. Mertz and P. G. Mosbaugh, *J. Urol.*, **135** 1134, (1986).
8) K. Kobashi, K. Sakaguchi, S. Takebe, J. Hase and M. Sato, Abstract of Papers, 12th International Congress of Biochemistry, Australia, 1982, p. 305.
9) K. Kobashi, S. Takebe and A. Numata, *J. Biochem.* (Tokyo), **98**, 1681 (1985).
10) K. Munakata, K. Kobashi, S. Takebe and J. Hase, *J. Pharmacobio-Dyn.*, **3**, 451 (1980).
11) M. Satoh, K. Munakata, K. Kitoh, H. Takeuchi and O. Yoshida, *J. Urol.*, **132**, 1247 (1984).
12) K. Kobashi, N. Terashima, S. Takebe and J. Hase, *J. Biochem.* (Tokyo), **83**, 287 (1978).
13) E. Takasaki, *Cal. Tiss. Res.*, **7**, 233 (1971).
14) O. E. Millner Jr., J. A., Anderson, M. E. Appler, C. E. Benjamin, J. G. Edwards, D. T. Humphrey and E. M. Shearer, *J. Urol.*, **127**, 346 (1982).
15) M. Satoh, K. Munakata, H. Takeuchi, O. Yoshida, S. Takebe and K. Kobashi, *Chem. Pharm. Bull.*, **39**, 894 (1991).
16) J. A. Andersen, *Invest. Urol.*, **12**, 381 (1975).
17) H. Takeuchi, Y. Okada, K. Kobashi and O. Yoshida, *Urol. Res.*, **10**, 217 (1982).
18) R. S. Cole and B. S. I. Montagomery, Abstract of Papers, 7th World Congress on Endourolology and ESWL, Kyoto, 1989, p. 83.
19) B. Saltzman, Abstract of Papers, 7th World Congress on Endourolology and ESWL, Kyoto, 1989, p. 87.

Studies on Cardiotonic Agents. VII.[1] Potent Cardiotonic Agent KF15232 with Myofibrillar Ca^{2+} Sensitizing Effect

Yuji NOMOTO,* Haruki TAKAI, Tetsuji OHNO and Kazuhiro KUBO

Pharmaceutical Research Laboratories, Fuji, Kyowa Hakko Kogyo Co., Ltd., Shimotogari 1188, Nagaizumicho, Shizuoka 411, Japan.
Received August 3, 1990

A series of novel 4,5-dihydro-5-methyl-6-(2 or 4-substituted 7-quinazolinyl)-3(2*H*)-pyridazinones was synthesized and examined for cardiotonic activity in anesthetized dogs. The 4-substituted aminoquinazolines generally showed potent and long-lasting inotropic activity. Fall in the activity was observed on the introduction of substituent at the 2-position of the quinazoline ring. The 3-substituted 4 (3*H*)-quinazolinimines generally exhibited weak activity. Ca^{2+} sensitizing effect of the 4-substituted amino derivatives was also examined in chemically skinned fiber from papillary muscle of guinea pig. The alkylamino derivatives exhibited small sensitizing effect, while the benzylamino derivatives exhibited large effect. Among them, KF15232 (Ix) was found to have the most potent cardiotonic and Ca^{2+} sensitizing activities.

Keywords cardiotonic agent; calcium ion^{2+} sensitizing effect; structure–activity relationship; pyridazinone; quinazoline

The extensive research effort to find a non-glycoside, non-catecholamine digitalis substitute resulted in the discovery of several new cardiotonic agents.[2] Some of these new drugs, including 4,5-dihydro-3(2*H*)-pyridazinone derivatives imazodan (**1**)[3] and indolidan (**2**)[4] showed combined inotropic–vasodilatory properties. These agents demonstrated an inhibitory activity of the cardiac low-Km, cyclic adenosine 3′,5′-monophosphate (c-AMP)-specific phosphodiesterase (PDE III) which was believed to be the principal component of the intropic–vasodilatory action.

Recently, a new mechanism of positive inotropic action was proposed for some 4,5-dihydro-3(2*H*)-pyridazinones, such as pimobendan (**3**) and MCI-154 (**4**).[5,6] These compounds showed a Ca^{2+} sensitizing effect in the contractile protein system, and the effect was responsible, at least in part, for the mechanism of the inotropic action.[7,8] It can be speculated that the risk of arrhythmogenic action of compounds which showed a Ca^{2+} sensitizing effect in addition to a cardiac PDE inhibitory effect might be lower than that of pure PDE inhibitors.[9] Little work has been reported on the structure–activity relationships for Ca^{2+} sensitizing effect.

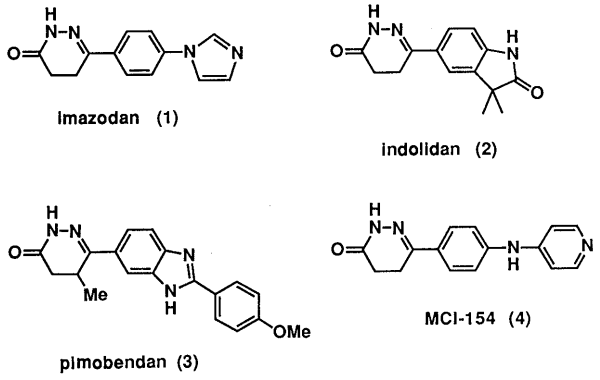

We have recently reported that 4,5-dihydro-5-methyl-6-(4-methylamino-7-quinazolinyl)-3(2*H*)-pyridazinone (Ib)[1] showed potent inotropic activity in anesthetized dogs. As an extension of our studies, we have attempted to modify Ib by replacement of the 4-methylaminoquinazolinyl group with other quinazolinyl groups.

The present paper describes the synthesis and the structure–activity relationships for inotropic and Ca^{2+} sensitizing effect of a series of novel 4,5-dihydro-5-methyl-6-(2 or 4-substituted 7-quinazolinyl)-3-(2*H*)-pyridazinones.

Chemistry Previously,[1] Ib was synthesized from the ethoxymethylenimine (**5**) *via* IIb by the route shown in Chart 1. In order to prepare the compounds which have another amino group at the 4-position of the quinazoline ring, we first attempted the reaction of **5** with various primary amines.

Reaction of **5** with various amines in methanol at 40—60 °C for 0.5—5 h afforded II (method A) and the rearrangement of II[1] in 2 N NaOH and dimethylformamide (DMF) at 60—100 °C for 0.5—5 h afforded I (method B). The results from the experiments are summarized in

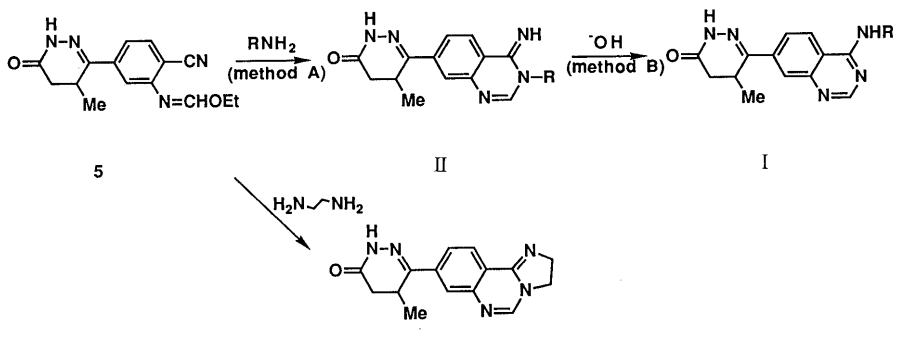

5 II I 6

Chart 1

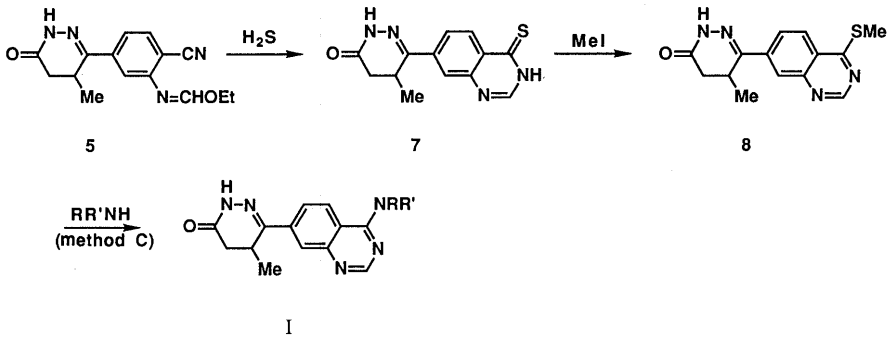

Chart 2

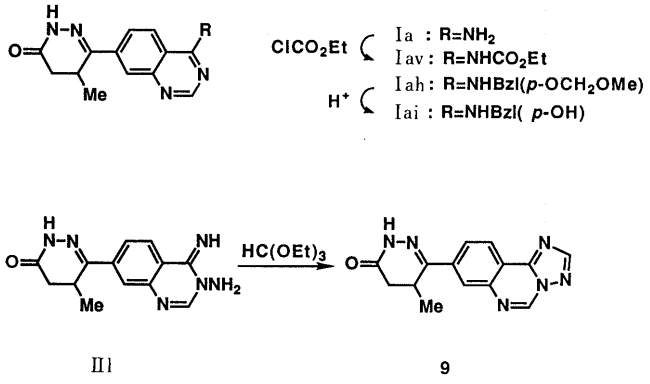

Chart 3

Tables I—II.

Reaction of **5** with *tert*-butylamine was very slow, and the longer reaction time resulted in degradation of **5**. Reaction of **5** with ethylenediamine did not afford IIv but the imidazoquinazoline (**6**).

Rearrangement of II to I proceeded without any unusual occurrence. Consequently, the method shown in Chart 1 is generally applicable for preparation of the compounds which have an amino group at the 4-position of the quinazoline ring.

We also investigated the more generally applicable method for preparation of I. An alternative synthetic route to I is shown in Chart 2. The thione (**7**), which was synthesized from **5** by treatment with H_2S in pyridine in the presence of Et_3N,[10] was converted to the thioether (**8**) by alkylation with MeI. Reaction of **8** with various amines in dimethylsulfoxide (DMSO) or in the absence of solvent at 50—170 °C afforded I (method C). These results are also summarized in Table I.

In the reaction of **8** with cyclopropylamine, the starting **8** was recovered probably due to high volatility of the amine.

Compound Ia reacted with ethyl chloroformate to give the carbamate (Iav). Demethoxymethylation of Iah with 3 N HCl afforded the hydroxybenzyl derivative (Iai). The 3-amino-4(3*H*)-quinazolinimine (III) reacted with triethyl orthoformate to give the triazoloquinazoline (**9**) (Chart 3).

Next, we investigated introduction of the carbon functional group into the 4-position of the quinazoline ring. Treatment of **8** with NaCN in DMF at 100 °C did not afford the desired cyanide (**10**). Sulfur extrusion reaction[11] of **11** prepared from **7** by alkylation with diethyl bromomalonate afforded **12** (Chart 4). The proton nuclear magnetic resonance (^{1}H-NMR) spectrum of **12** at pD 5.6 suggested that **12** was a mixture of tautomeric isomers (**12a** and **12b**) in a ratio of 1 : 1. Compound **12a** showed the proton signals of the 3-position of the quinazoline ring at δ 12.91 ppm and the 2-position of the quinazoline ring at δ 8.22 ppm, while **12b** showed the methine proton of malonic acid group at δ 6.20 ppm and the 2-position of the quinazoline ring at δ 9.30 ppm, respectively. At pD 14.9, the signals due to **12a** were almost non-existent. Therefore, the **12b** form was exclusively dominant at pD 14.9 (see Experimental section).

Hydrolysis under alkaline condition and subsequent acidification gave the 4-methyl derivative (**13**). Reaction of **12** with MeI in the presence of Et_3N followed by hydrolysis did not afford the desired 4-ethyl derivative (**14**) but a complexed mixture (Chart 4).

Desulfurization of **8** with Raney-Ni in DMF afforded the dihydroquinazoline (**15**) which was oxidized with MnO_2 to give the quinazoline (**16**) (Chart 5).

Finally, we investigated the synthesis of 2,4-disubstituted quinazoline derivatives.

The 2-oxo derivatives were synthesized by the method shown in Chart 6. Key intermediate **18** was prepared by reaction of the anthranilonitrile (**17**) with ethyl chloroformate. Reaction of **18** with methylamine in DMSO at 150°C gave the quinazolinimine (**19**), with NH_3 gave the quinazolinone, (**20**) and with ethylenediamine gave no quinazolinimine (**21**) but did give the imidazoquinazoline (**22**).

The synthetic sequences leading to the compounds which have an alkylthio and an alkylamino group at the 2- or 4-position of quinazoline ring are shown in Chart 7. Reaction of **17** with CS_2[12] in pyridine afforded the 2,4-dimercaptoquinazoline (**23**), and followed by alkylation with MeI in basic medium gave the 2,4-bismethylthioquinazoline (**24**). Reaction of **24** with methylamine and propylamine afforded selectively 4-methylamino-2-methylthio and 4-propylamino-2-methylthio derivatives (**25**, **26**), respectively. The structure of **25** was confirmed by the nuclear Overhauser effect (NOE) which was observed between the methyl proton at the 4-position (δ 3.01 ppm as doublet) and the ring proton at the 5-position of quinazoline (δ 8.12 ppm as doublet). In oxidation reaction of **26** with potassium permanganate, a new spot probably due to the formation of the 2-methylsulfonyl-4-propylamino derivative (**27**), was detected on thin layer chromatography analysis. Compound **27** could not be isolated because of its instability. Treatment of the $CHCl_3$ extract of the reaction mixture with methylamine gave the 2-methylamino-4-

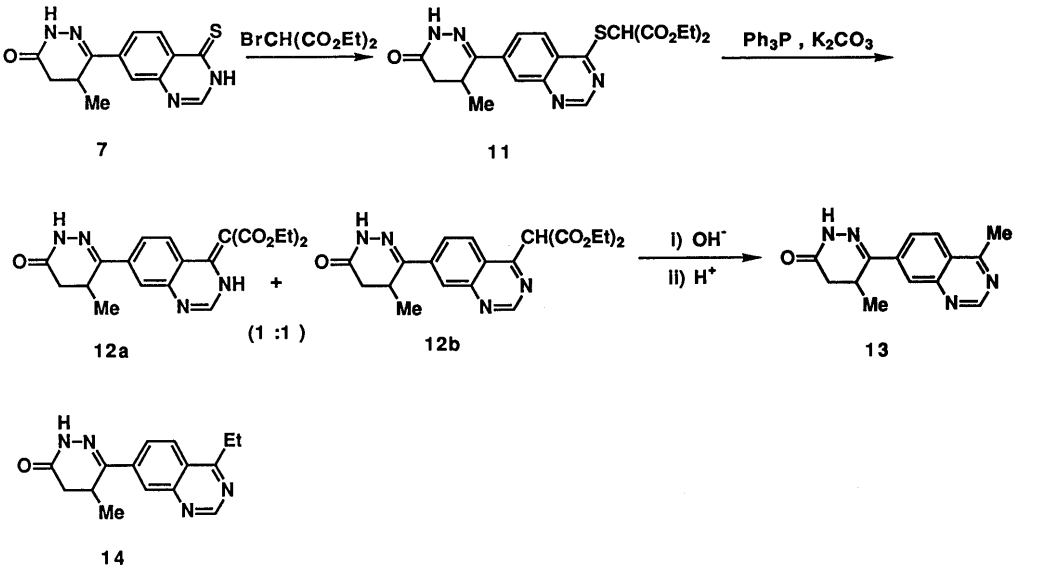

Chart 4

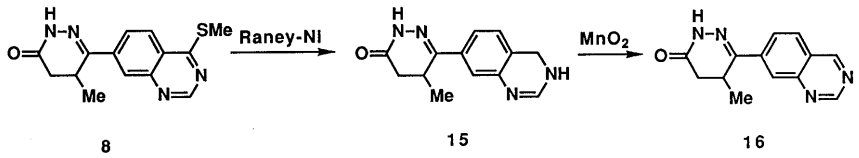

Chart 5

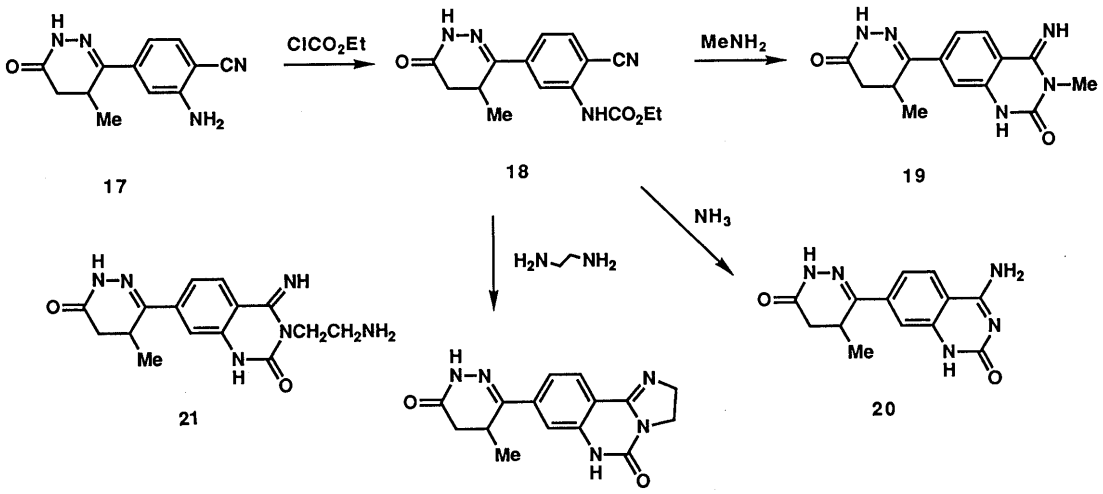

Chart 6

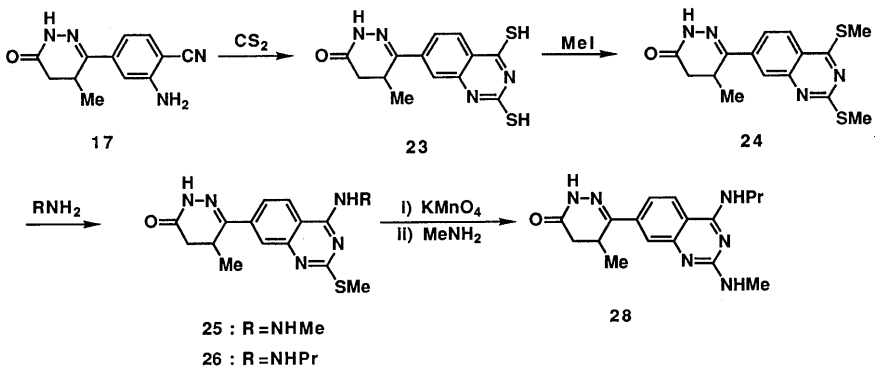

Chart 7

TABLE I.

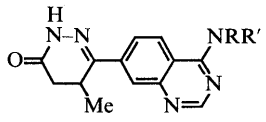

Compd. No.	R, R′	Method Yield (%)	mp (°C) (Crystn.[a] solv.)	Formula	Analysis (%) Calcd (Found)		
					C	H	N
Ia[b]	H, H	B 59	>300	$C_{13}H_{13}N_5O$	61.16 (60.92)	5.13 5.00	27.43 27.15)
Ib[b]	Me, H	B 76	296—302 (DMSO–H_2O)	$C_{14}H_{15}N_5O$	62.44 (62.37	5.61 5.62	26.01 25.62)
Ic	Et, H	B 60	261—266	$C_{15}H_{17}N_5O$	63.59 (63.38	6.05 5.91	24.72 24.69)
Id	Pr, H	B 64	263—269	$C_{16}H_{19}N_5O$	64.63 (64.60	6.44 6.50	23.55 23.55)
Ie	iso-Pr, H	B 71	259—261	$C_{16}H_{19}N_5O$	64.63 (64.73	6.44 6.22	23.55 23.20)
If	cyclo-Pr, H	B 21 C 0	286—287 (dec.)	$C_{16}H_{17}N_5O \cdot 1/2H_2O$	63.14 (63.52	5.96 5.76	23.01 23.26)
Ig	Bu, H	B 21 C 21	225—231	$C_{17}H_{21}N_5O$	65.57 (65.20	6.80 7.12	22.49 22.61)
Ih	iso-Bu, H	C 53	285—286	$C_{17}H_{21}N_5O$	65.57 (65.55	6.80 6.73	22.49 22.32)
Ii	*sec*-Bu, H	C 28	>300	$C_{17}H_{21}N_5O \cdot 1/2H_2O$	63.72 (64.10	6.93 6.90	21.85 21.98)
Ij	*tert*-Bu, H	C 0					
Ik	Pentyl, H	C 57	254—255	$C_{18}H_{23}N_5O$	66.44 (66.53	7.12 7.35	21.52 21.89)
Il	Isopentyl, H	C 46	292—293	$C_{18}H_{23}N_5O$	66.44 (66.59	7.12 7.20	21.52 21.26)
Im	Cyclopentyl, H	C 82	262 (dec.)	$C_{18}H_{21}N_5O$	66.85 (66.80	6.56 6.43	21.65 21.38)
In	Hexyl, H	C 46	254—255	$C_{19}H_{25}N_5O$	67.23 (67.29	7.42 7.53	20.63 20.41)
Io	Cyclohexyl, H	C 65	288—291 ($CHCl_3$–MeOH–Et_2O)	$C_{19}H_{23}N_5O$	67.63 (67.23	6.88 6.92	20.75 20.35)
Ip	Heptyl, H	C 67	234—238	$C_{20}H_{27}N_5O$	67.95 (68.29	7.71 7.75	19.80 19.52)
Iq	Octyl, H	C 71	224—225	$C_{21}H_{29}N_5O$	68.63 (68.80	7.95 8.02	19.06 18.96)
Ir	Cyclooctyl, H	C 31	289—290 (MeOH–H_2O)	$C_{21}H_{27}N_5O \cdot 1/2H_2O$	67.34 (67.53	7.55 7.28	18.69 19.01)
Is	$HOCH_2CH_2$, H	C 43	234—236 (MeOH–H_2O)	$C_{15}H_{17}N_5O_2 \cdot H_2O$	56.77 (56.99	6.03 5.92	22.06 21.83)
It	$Me_2NCH_2CH_2$, H	C 74	243—245	$C_{17}H_{22}N_6O \cdot 1/2H_2O$	60.88 (60.94	6.91 6.75	25.06 24.78)
Iu	3-Morpholinopropyl, H	C 69	234—236	$C_{20}H_{26}N_6O_2 \cdot H_2O$	59.97 (60.30	7.06 6.85	20.97 21.29)
Iw	Allyl, H	C 27	252—255	$C_{16}H_{17}N_5O \cdot 1/2H_2O$	63.14 (63.26	5.97 6.03	23.00 22.95)
Ix	Bzl, H	B 81 C 46	248	$C_{20}H_{19}N_5O \cdot H_2O$	66.10 (66.08	5.82 5.93	19.27 19.44)
Iy	(*o*-Me)Bzl, H	C 12	287 (dec.)	$C_{21}H_{21}N_5O \cdot H_2O$	66.82 (66.95	6.15 6.29	18.55 18.35)
Iz	(*p*-Me)Bzl, H	C 40	268—271	$C_{21}H_{21}N_5O$	70.17 (69.84	5.89 6.00	19.48 19.53)
Iaa	(*p*-F)Bzl, H	C 29	264	$C_{20}H_{18}FN_5O \cdot H_2O$	62.97 (63.31	5.30 5.24	18.35 18.45)
Iab	(*o*-Cl)Bzl, H	C 36	219—224	$C_{20}H_{18}ClN_5O \cdot 1/2H_2O$	61.77 (61.43	4.93 4.89	18.00 17.66)
Iac	(*m*-Cl)Bzl, H	C 68	237—242	$C_{20}H_{18}ClN_5O \cdot H_2O$	60.37 (60.75	5.08 4.95	17.59 17.48)
Iad	(*p*-Cl)Bzl, H	C 34	237—242	$C_{20}H_{18}ClN_5O$	63.24 (63.01	4.78 4.77	18.44 18.40)
Iae	(*o*-MeO)Bzl, H	C 27	>300	$C_{21}H_{21}N_5O_2$	67.18 (67.00	5.64 5.89	18.65 18.48)
Iaf	(*m*-MeO)Bzl, H	C 30	296 (dec.)	$C_{21}H_{21}N_5O_2$	67.18 (66.89	5.64 5.53	18.65 18.57)

TABLE I. (continued)

Compd. No.	R, R′	Method Yield (%)	mp (°C) (Crystn.[a] solv.)	Formula	Analysis (%) Calcd (Found)		
					C	H	N
Iag	(*p*-MeO)Bzl, H	C 46	256—257	$C_{21}H_{21}N_5O_2$	67.18 (67.20)	5.64 5.93	18.65 18.83)
Iah	(*p*-$MeOCH_2O$)Bzl, H	C	192—195	$C_{22}H_{23}N_5O_3$	65.17 (65.25)	5.72 5.43	17.27 17.51)
Iai[c]	(*p*-HO)Bzl, H	[d] 77	187—190	$C_{20}H_{19}N_5O_2 \cdot HCl \cdot 3/2H_2O$	56.54 (56.59)	5.46 5.15	16.48 16.13)
Iaj	(4-Pyridyl)CH_2, H	C 16	284—285	$C_{19}H_{18}N_6O$	65.88 (65.90)	5.24 5.32	24.26 24.37)
Iak	(3-Pyridyl)CH_2, H	C 23	284—285	$C_{19}H_{18}N_6O \cdot 1/2H_2O$	64.21 (64.53)	5.40 5.35	23.64 23.62)
Ial	Ph, H	B 75 C 69	286—289	$C_{19}H_{17}N_5O$	68.87 (68.63)	5.17 5.17	21.13 21.01)
Iam	(*m*-Cl)Ph, H	C 37	293—294	$C_{19}H_{16}ClN_5O$	62.38 (62.26)	4.41 4.33	19.14 18.93)
Ian	(*p*-Cl)Ph, H	C 18	>300	$C_{19}H_{16}ClN_5O$	62.38 (62.40)	4.41 4.37	19.14 18.87)
Iap	$PhCH_2CH_2$, H	C 48	264—265	$C_{21}H_{21}N_5O$	70.17 (70.33)	5.89 5.90	19.48 19.57)
Iaq	(3,4-Di-MeO)$PhCH_2CH_2$, H	C 46	249—250	$C_{23}H_{25}N_5O_3$	65.85 (65.72)	6.02 6.13	16.69 16.90)
Iar	(2-Pyridyl)CH_2CH_2, H	C 20	245—247	$C_{20}H_{20}N_6O$	66.65 (66.64)	5.59 5.63	23.32 22.95)
Ias	Me, Me	C 51	235—237	$C_{15}H_{17}N_5O$	63.59 (63.33)	6.05 6.02	24.72 24.53)
Iat[c]	$-(CH_2)_2-NH-(CH_2)_2-$	C 35	209—211 (MeOH–Et_2O)	$C_{17}H_{20}N_6O \cdot 2HCl \cdot H_2O$	49.16 (48.83)	5.82 6.10	20.23 20.01)
Iau	$-(CH_2)_5-$	C 80	268—270	$C_{18}H_{21}N_5O$	66.85 (66.56)	6.55 6.71	21.66 21.60)
Iav	$EtCO_2$, H	[d] 82	261—265	$C_{16}H_{17}N_5O_3$	58.71 (58.37)	5.23 5.39	21.39 21.18)

a) Recrystallized from DMF–H_2O except where otherwise noted in parentheses. *b*) Ref. 1. *c*) As HCl salt. *d*) See Experimental section.

TABLE II.

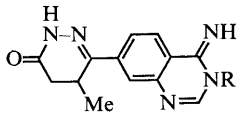

Compd. No.	R	Yield[a] (%)	mp (°C)	Formula	Analysis (%) Calcd			Found		
					C	H	N	C	H	N
IIb[b]	Me	63	253—255	$C_{14}H_{15}N_5O$	62.44	5.61	26.01	62.39	5.55	25.83
IIc	Et	53	238—244	$C_{15}H_{17}N_5O$	63.59	6.05	24.72	63.93	6.18	24.94
IId	Pr	57	239—240	$C_{16}H_{19}N_5O$	64.63	6.44	23.55	64.82	6.44	23.76
IIe	iso-Pr	70	205	$C_{16}H_{19}N_5O$	64.63	6.44	23.55	64.85	6.50	23.54
IIf	cyclo-Pr	65	232 (dec.)	$C_{16}H_{17}N_5O \cdot 1/2H_2O$	63.14	5.96	23.01	63.00	5.82	22.78
IIg	Bu	35	198—200	$C_{17}H_{21}N_5O$	65.57	6.80	22.49	65.52	6.59	22.20
IIj	*tert*-Bu	0								
IIx	$PhCH_2$	82	216	$C_{20}H_{19}N_5O \cdot H_2O$	66.10	5.82	19.27	66.40	5.86	19.34
IIv	$H_2NCH_2CH_2$	0[c]								
IIal	Ph	77	274—275 (dec.)	$C_{19}H_{17}N_5O$	68.87	5.17	21.13	68.78	5.16	20.92
IIao	(4-MeO)Ph	40	268	$C_{20}H_{19}N_5O_2$	66.47	5.30	19.38	66.20	5.32	19.06
IIax	NH_2	70	193	$C_{13}H_{14}N_6O$	57.77	5.22	31.09	57.42	5.01	30.89

a) All compounds were prepared by Method A, and recrystallized from DMF–H_2O. *b*) Ref. 1. *c*) Compound **6** was obtained (see Experimental section).

propylamino derivarive (**28**).

We also investigated the synthesis of the 2-methyl-4-alkylamino derivatives (**30**, **31**). Breukink[13] reported the synthesis of 4-methoxy-2-methylquinazoline by reaction of *o*-acetamidobenzonitrile with sodium methoxide. Acetylation of **17** with acetyl chloride in pyridine, followed by treatment with potassium carbonate in methanol afforded the 4-methoxy-2-methylquinazoline (**29**). Reaction of **29**

TABLE III. Biological Activities of Some Quinazolinylpyridazinone Derivatives

Compd. No.	Cardiotonic activity[a]				Ca^{2+} sensitizing effect[e]	
	Dose (mg/kg i.v.)	LVdP/dt max[b] (Δ%)	Relative[c] potency	Duration[d] (min)	Tension in skinned fiber (Δ%)[f] Drug concn. 10^{-4} M	10^{-5} M
Ia[g]	0.01	56.6±19.8	0.99	>60	7.5±2.3	
Ib[g]	0.01	51.3±9.6	1.31	>60	9.8±1.8	
Ic[g]	0.01	49.5±1.7	1.18	>60	NT[h]	
Id[g]	0.01	55.7±3.9	1.40	>60	NT	
Ie[d]	0.01	40.6±4.3	0.93	>60	20.4±3.3	
If	0.01	41.0±6.3	0.80	>60	35.3±4.8	
Ig	0.01	67.7±10.4	1.56	>60	52.2±8.6 (4)	
Ih	0.01	49.8±10.3	1.03	>60	NT	
Ii	0.01	47.6±6.4	1.41	>60	37.3±2.9	
Ik	0.01	46.9±2.3	0.95	>60	33.6±3.1	
Il	0.01	37.7±12.4	0.93	60	22.8±3.7	
Im	0.01	35.8±11.2	0.95	50	30.5±4.5	
In	0.01	20.2 (2)	0.50	20	16.8±1.0	
Io	0.01	35.5±7.3	1.01	>60	NT	
Ip	0.01	22.2±8.2	0.48	30	NT	
Iq	0.01	8.1 (2)	—	—	NT	
Ir	0.01	21.2 (2)	0.47	>60	NT	
Is	0.01	22.9±5.3	0.68	>60	NT	
It	0.01	4.6 (2)	—	—	NT	
Iu	0.01	28.6 (2)	0.63	>60	16.9±2.0	
Iw	0.01	45.9±8.7	1.05	>60	33.8±2.7	
Ix	0.01	54.5±3.0	1.61	>60	176.4±53.9 (5)	36.7±2.5 (4)
Iy	0.01	59.5±11.0	1.32	>60		16.0±4.2
Iz	0.01	43.0±7.4	1.27	>60		16.8±0.3
Iaa	0.01	42.5±6.8	1.09	>60		27.9±5.5 (4)
Iab	0.01	31.5±3.4	0.87	>50		15.4±2.6 (4)
Iac	0.01	43.5±5.4	1.20	>60		9.4±0.5 (4)
Iad	0.01	33.2±5.0	0.82	>60		10.7±2.6 (4)
Iae	0.01	61.5±10.2	1.45	>60		14.5±2.7
Iag	0.01	44.1±11.0	0.96	>60		10.0±3.1 (4)
Iaj	0.01	21.1±7.4	0.56	>60		14.4±0.8 (4)
Iak	0.01	30.4±3.2	0.69	>60	NT	
Ial	0.01	26.7±8.7	0.63	>60	36.5±5.3	
Iam	0.01	17.2 (2)	0.42	10	NT	
Ian	0.01	10.4 (2)	0.25	10	28.6±1.7	
Iap	0.01	54.1±9.5	1.12	>60		15.0±3.5
Iaq	0.01	2.9 (2)	—	—	NT	
Iar	0.01	39.1±7.9	0.96	>60	NT	
Ias	0.01	38.8±1.4	0.90	>60	19.0±3.2	
Iat[g]	0.01	16.2 (2)	0.35	40	NT	
Iau	0.01	40.3±9.6	0.89	>60	NT	
Iav	0.01	12.9 (2)	0.29	30	NT	
IIb	0.03	12.7 (2)	0.29	15	NT	
IIc	0.01	10.6 (2)	0.22	5	NT	
IId	0.01	3.3 (2)	—	—	NT	
IIe	0.01	4.6 (2)	—	—	NT	
IIg	0.03	42.3±5.1	1.09	>60	NT	
IIx	0.01	9.2±1.9	0.22	5	NT	
IIal	0.01	9.0 (2)	—	—	NT	
IIao	0.01	5.5 (2)	—	—	NT	
6	0.01	11.8 (2)	0.30	30	NT	
7	0.01	9.1 (2)	—	—	NT	
8	0.01	52.0±3.8	1.20	30	NT	
9	0.03	18.8 (2)	0.43	30	NT	
11	0.01	11.0±2.9	0.26	20	NT	
12	0.01	28.7±11.5	0.67	40	NT	
13	0.01	29.0±3.1	0.68	>60	NT	
15	0.01	5.2 (2)	—	—	NT	
16	0.01	64.7±3.1	1.60	30	NT	
19	0.01	4.8 (2)	—	—	NT	
20	0.01	−3.8 (2)	—	—	NT	
22	0.01	3.3 (2)	—	—	NT	
23	0.01	2.4 (2)	—	—	NT	
24	0.01	4.3 (2)	—	—	NT	
25	0.01	9.0 (2)	0.19	10	NT	

TABLE III. (continued)

Compd. No.	Cardiotonic activity[a]				Ca^{2+} sensitizing effect[e]	
	Dose (mg/kg i.v.)	LV$dP/dt$ max[b] (Δ%)	Relative[c] potency	Duration[d] (min)	Tension in skinned fiber (Δ%)[f] Drug concn. 10^{-4} M	10^{-5} M
26	0.01	14.3 (2)	0.30	20	NT	
28	0.01	11.4 (2)	0.25	10	NT	
29	0.01	17.2 (2)	0.50	10	NT	
30	0.01	22.8±5.1	0.56	60	NT	
31	0.01	13.7 (2)	0.40	30	NT	
PM[i]	0.03	8.2±1.6	—	—	68.2±6.8	16.1±1.5
Vehicle					10.1±2.7[j]	6.4±1.8[k]

a) In anesthetized dogs. *b*) Each value represents the mean±standard error of triplicate experiments except where otherwise noted in parentheses. *c*) Compared to the percent increase in LV$dP/dt$ max observed with Milrinone (0.03 mg/kg i.v.) in the same dog. *d*) Time (min) that an agent increases in LV$dP/dt$ more than 10% from the pretreatment control value. *e*) In skinned muscle fibers (see Experimental section). *f*) Each value represents the mean±standard error of triplicate experiments except where otherwise noted in parentheses. *g*) As HCl salt. *h*) NT: not tested. *i*) PM: pimobendan (**3**). *j*) 10 μg/ml of PEG 400. *k*) 5 μg/ml of PEG 400.

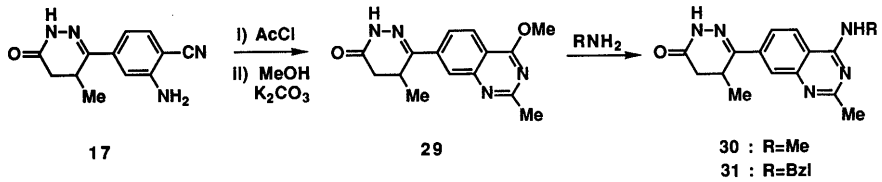

Chart 8

with methylamine and benzylamine gave the 2-methylamino (**30**) and the 2-benzylamino (**31**) derivatives, respectively (Chart 8).

Biological Results We initially examined the cardiotonic activities of these compounds in anesthetized open chest dogs using the procedures previously described.[14] The results of the test are shown in Table III. The cardiotonic activity of the compounds was determined by measuring percent increase in maximum dP/dt left ventricular pressure (LV$dP/dt$ max, Δ%) after i.v. administration (0.01 or 0.03 mg/kg) in anesthetized mongrel dogs of either sex (8—15 kg). The potency of cardiotonic activity of the test compounds was compared with milrinone (0.03 mg/kg).[15] Relative potency was calculated as the LV$dP/dt$ max of each compound to that of milrinone (milrinone = 1) in the same dogs.

The 3-substituted 4(3*H*)-quinazolinimines (II) generally exhibited weak activity except the *n*-butyl derivative (IIg).

We then examined the effects of the substituents at the 4-position of quinazolines on the cardiotonic activity. The methylthio (**8**) and the H (**16**) derivatives showed potent activity with short duration, and the thione (**7**) showed weak activity. Potent and long-lasting activity was observed on introduction of substituted amino groups (I). In a series of alkylamino quinazolines, introduction of an alkyl group having 1—5 carbon atoms (Ib, Ic, *etc.*) into the amino group led to potent and long-lasting activity. The activity of compounds having 6—8 carbon atoms (In, Ip, Iq, Ir) decreased with increasing length of the alkyl chain, except that of the cyclohexyl derivative (Io). The dimethyl derivative (Ias) retained the activity. Marked fall in the activity was observed on introduction of hydrophilic substituents such as hydroxy (Is), dimethylamino (It) and morpholino group (Iu) into the alkyl group. The benzyl derivatives (Ix—Iag) generally showed potent and long-lasting activity. Of these, Ix was one of the most potent (relative potency = 1.61) compounds in the series. The phenethyl (Iap) and pyridylethyl (Iar) derivatives retained the activity. Phenyl (Ial-Ian) and ethoxycarbonyl (Iav) groups led to relatively weak compounds.

Compounds **30** and **31**, which are the 2-methyl analogue of Ib and Ix, respectively, showed weak activity. Generally, introduction of substituents into the 2-position of the quinazoline ring led to diminished activity (**19**, **20**, **22**—**26**, **30**, **31**).

Consequently, the quinazolines having alkylamino and benzylamino groups at the 4-position generally showed potent and long-lasting cardiotonic activity.

Next, we examined the Ca^{2+} sensitizing effect of the quinazolinamines (I) in skinned muscle fibers[16] from guinea pig papillary muscles. The effects of the test (10^{-4} and 10^{-5} M) on the tension development (increased tension, Δ%) induced by pCa ($-\log[Ca^{2+}]$M) 5.8 in chemically skinned fibers are shown in Table III (method D). In this experiment, we used skinned fibers which had been pretreated with 250 μg/ml of saponin. It has been reported[17] that higher concentrations of saponin (> 150 μg/ml) destroy not only the surface membrane but also the sarcoplasmic reticulum (SR) membrane. Therefore, the influence by the Ca^{2+} uptake and release activities of the SR should have been minimal.

Effects of substituents at the 4-position of the quinazoline ring on Ca^{2+} sensitizing effect were also examined. In a series of 4-alkylamino derivatives, introduction of amino (Ia), methylamino (Ib), dimethylamino (Ias) and hexylamino (In) groups led to weak activity. An alkylamino group with 3—5 carbon atoms provided moderately potent compounds (Ie—Ig and Ii—Im). In these compounds, Ig showed the most potent activity, but the activity was weaker than pimobendan. Anilino (Ial, Ian) substituents

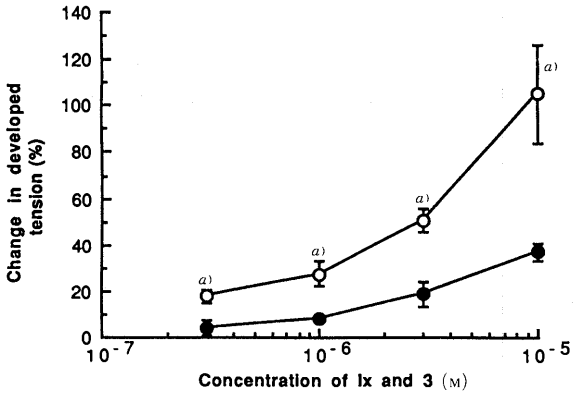

Fig. 1. Concentration–Response Curve for the Effect of Ix and **3** on Developed Tension

pCa = 6.0 (see Experimental section). Results are presented as mean ± SEM. —○—, Ix (KF15232); —●—, **3** (pimobendan). *a*) $p < 0.05$, when compared to **3** (Mann–Whitney U-test, $n = 5$).

also led to moderately active compounds.

The benzylamino derivative (Ix) increased the tension development by about 180% and 40% at the concentration of 10^{-4} and 10^{-5} M, respectively. Decrease of the activity was observed on introduction of substituents on benzyl moiety. Picolyl (Iaj) and phenethyl (Iap) derivatives also showed reduced activity.

The concentration-response curve for the effects of Ix and **3**[5] on the tension development induced by pCa 6.0 is shown in Fig. 1 (method E). The tension development was significantly increased by Ix (3×10^{-7} to 10^{-5} M) in a concentration-dependent manner. The activity of Ix was about 10 times more potent than 3. It seems likely that the concentrations of Ix required for this effect were similar to that for positive inotropic effect.

These results indicated that Ix exhibited the most potent inotropic and Ca^{2+} sensitizing effect. But it must be noted that the compounds which showed potent inotropic activity did not always exhibit potent Ca^{2+} sensitizing effect: there are differences of structural requirement between the two activities. Further studies are necessary to elucidate the definite mechanisms of the positive inotropic action of the compounds.

In summary, this paper has described structure–activity relationships of a novel series of 4,5-dihydro-5-methyl-6-(2- or 4-substituted 7-quinazolinyl)-3(2*H*)-pyridazinones for cardiotonic activity and Ca^{2+} sensitizing effect. Among these compounds, KF-15232 (Ix) was found to have the most potent inotropic and Ca^{2+} sensitizing activities. Further pharmacological and biochemical studies on this compound are in progress and will be reported elsewhere.

Experimental

All melting points were determined on a Büchi 510 micro melting point apparatus and are uncorrected. Infrared (IR) spectra were measured on a JASCO IR810 spectrophotometer. ^{1}H-NMR spectra were measured on a Hitachi R-90H and a JEOL JNM-GX-270 spectrometer using tetramethylsilane (TMS) as an internal standard. Mass spectra (MS) were run on a JEOL-JMS-01SG-2 and a JMS-SX102 spectrometer.

4,5-Dihydro-6-(3,4-dihydro-4-thioxo-7-quinazolinyl)-5-methyl-3(2H)-pyridazinone (7) H_2S gas was passed into a solution of **5**[1] (19.5 g, 68.6 mmol) and Et_3N (25 ml, 179 mmol) in pyridine (250 ml) for 30 min at room temperature with stirring. The precipitated crystals were collected by filtration, washed with water and dried to afford crude **7** (13.0 g, 70%). The crystals were used in the next reaction without further purification. An analytical sample was prepared by recrystallization from DMF–water, mp > 300 °C. *Anal.* Calcd for $C_{13}H_{12}N_4OS$: C, 57.34; H, 4.44; N, 20.57. Found: C, 57.60; H, 4.45; N, 20.60. IR (KBr): 1670, 1590, 1560 cm^{-1}. NMR (DMSO-d_6) δ: 13.89 (1H, br, SH), 11.25 (1H, s, NH), 8.56 (1H, d, J = 9 Hz, Ar-H), 8.20 (1H, s, Ar-H), 8.05 (2H, m, Ar-H), 3.53 (1H, m, CH), 2.80 (1H, dd, J = 7, 17 Hz, CH'H), 2.31 (1H, d, J = 17 Hz, CH'H), 1.11 (3H, d, J = 7 Hz, CH_3). MS *m/z*: 272 (M^+).

4,5-Dihydro-5-methyl-6-(4-methylthio-7-quinazolinyl)-3(2*H*)-pyridazinone (8) A mixture of **7** (13.0 g, 47.7 mmol), MeI (4.0 ml, 64.2 mmol) and 2N NaOH (30.0 ml) in DMF (100 ml) was stirred for 30 min at room temperature. The reaction mixture was concentrated under reduced pressure and mixed with water. The precipitated crystals were collected by filtration, washed with water and dried to afford crude **8** (10.3 g, 75%). The crystals were used in the next reaction without further purification. An analytical sample was prepared by recrystallization from DMF–water, mp 235 °C. *Anal.* Calcd for $C_{14}H_{14}N_4OS$: C, 58.72; H, 4.93; N, 19.57. Found: C, 58.85; H, 5.06; N, 19.80. IR (KBr): 1680, 1610, 1550 cm^{-1}. NMR (DMSO-d_6) δ: 11.12 (1H, s, NH), 8.96 (1H, s, Ar-H), 8.12 (3H, m, Ar-H), 3.55 (1H, m, CH), 2.85 (1H, dd, J = 7, 17 Hz, CH'H), 2.68 (3H, s, SCH_3), 2.28 (1H, d, J = 17 Hz, CH'H), 1.11 (3H, d, J = 7 Hz, $CHCH_3$). MS *m/z*: 286 (M^+).

General Procedure for the Synthesis of 4,5-Dihydro-5-methyl-6-(3-substituted 3,4-Dihydro-4-imino-7-quinazolinyl)-3(2*H*)-pyridazinones. Method A. 4,5-Dihydro-6-(3,4-dihydro-4-imino-3-methyl-7-quinazolinyl)-5-methyl-3(2*H*)-pyridazinone (11b)[1] A mixture of **5** (1.5 g, 5.3 mmol) and 40% $MeNH_2$/MeOH (40 ml) was stirred for 30 min at 50 °C. The precipitated crystals were collected by filtration, washed with MeOH and dried to give crude IIb (0.9 g, 63%) which was recrystallized from DMF–water for analysis.

4,5-Dihydro-6-(2,3-dihydroimidazo[1,2-*c*]quinazolin-8-yl)-5-methyl-3(2*H*)-pyridazinone (6) Compound **6** (0.60 g, 61%) was prepared from **5** (1.0 g, 3.6 mmol) with ethylenediamine (3.0 ml) as described for IIb, mp 280—282 °C. *Anal.* Calcd for $C_{15}H_{15}N_5O \cdot 1/2H_2O$: C, 62.06; H, 5.55; N, 24.12. Found: C, 61.84; H, 5.93; N, 23.97. IR (KBr): 1680, 1620, 1600 cm^{-1}. NMR (DMSO-d_6) δ: 11.20 (1H, s, NH), 8.01 (1H, s, Ar-H), 7.90 (1H, d, J = 8 Hz, Ar-H), 7.78 (1H, d, J = 8 Hz, Ar-H) 7.73 (1H, s, Ar-H), 4.13 (2H, t, J = 8 Hz, CH_2), 3.95 (2H, t, J = 8 Hz, CH_2), 3.47 (1H, m, CH), 2.78 (1H, dd, J = 7, 17 Hz, CHCH'H), 2.30 (1H, d, J = 17 Hz, CHCH'H), 1.12 (3H, d, J = 8 Hz, CH_3). MS *m/z*: 281 (M^+).

General Procedure for the Synthesis of 4,5-Dihydro-5-methyl-6-(4-substituted Amino-7-quinazolinyl)-3(2*H*)-pyridazinones. Method B. 4,5-Dihydro-5-methyl-6-(4-methylamino-7-quinazolinyl)-3(2*H*)-pyridazinone (Ib)[1] A mixture of IIb (0.29 g, 1.1 mmol) and 2N-NaOH (10 ml) was stirred for 5 h at 100 °C. The reaction mixture was neutralized with 1N HCl and the precipitated crystals were collected by filtration, washed successively with water and MeOH and dried to give crude Ib (0.22 g, 76%) which was recrystallized from DMSO–water for analysis.

Method C. 4,5-Dihydro-6-(4-benzylamino-7-quinazolinyl)-3(2*H*)-pyridazinone (Ix) A solution of **8** (0.29 g, 1.0 mmol) and benzylamine (0.33 ml, 3.0 mmol) in DMSO (10 ml) was stirred for 14 h at 170 °C under N_2 atmosphere. Water (20 ml) was added to the mixture and the precipitated crystals were collected by filtration, washed with water and dried to afford crude Ix (0.16 g, 46%) which was recrystallized from DMF–water for analysis. IR (KBr): 1680, 1620, 1580 cm^{-1}. NMR (DMSO-d_6) δ: 11.18 (1H, s, CONH), 8.85 (1H, br, NH), 8.44 (1H, s, Ar-H), 8.29 (1H, d, J = 8 Hz, Ar-H), 7.96 (2H, m, Ar-H), 7.30 (5H, br, benzyl), 4.78 (2H, d, J = 7 Hz, CH_2), 3.55 (1H, m, CH), 2.78 (1H, dd, J = 7, 17 Hz, CHCH'H), 2.25 (1H, d, J = 17 Hz, CHCH'H), 1.12 (3H, d, J = 8 Hz, CH_3). MS *m/z*: 345 (M^+).

4,5-Dihydro-5-methyl-6-(4-ethoxycarbonylamino-7-quinazolinyl)-3(2*H*)-pyridazinone (Iav) Ethyl chloroformate (0.10 ml, 1.6 mmol) was added to a solution of Ia (0.20 g, 0.78 mmol) in pyridine (5 ml) and the resultant solution was stirred for 3 h at room temperature, then concentrated. The residue was mixed with water and the precipitated crystals were collected by filtration, washed with water and dried to afford crude Iav (0.21 g, 82%) which was recrystallized from DMF–water for analysis. IR (KBr): 1690, 1620, 1600 cm^{-1}. NMR (DMSO-d_6) δ: 11.22 (1H, s, NH), 10.73 (1H, s, OCONH), 8.98 (1H, s, Ar-H), 8.36 (1H, d, J = 8 Hz, Ar-H), 8.18 (1H, s, Ar-H), 8.13 (1H, d, J = 8 Hz, Ar-H), 4.27 (2H, q, J = 7 Hz, CH_2CH_3), 3.62 (1H, m, CH), 2.78 (1H, dd, J = 7, 17 Hz, CHCH'H), 2.32 (1H, d, J = 17 Hz, CHCH'H), 1.31 (3H, t, J = 7 Hz, CH_2CH_3), 1.15 (3H, d, J = 8 Hz, CH_3). MS *m/z*: 328 ($M^+ + 1$) (Fast atom bombardment method).

4,5-Dihydro-5-methyl-6-[4-(*p*-hydroxybenzylamino)quinazolin-7-yl]-3-(2*H*)-pyridazinone (Iai) A suspension of Iah (0.40 g, 0.99 mmol) in 3N-HCl (3 ml) was stirred for 8 h at 60 °C. The precipitated crystals were

collected by filtration, washed with water and dried to give crude Iai (0.36 g, 93%) as HCl salt. An analytical sample was prepared by recrystallization from DMF–water. IR (KBr): 1690, 1620, 1600 cm^{-1}. NMR (DMSO-d_6) δ: 11.15 (1H, s, NH), 10.50 (1H, br, OH), 8.88 (1H, s, Ar-H), 8.75 (1H, d, J=8 Hz, Ar-H), 8.08 (1H, d, J=8 Hz. Ar-H), 8.25 (1H, s, Ar-H), 7.22 (2H, d, J=8 Hz, benzyl), 6.73 (2H, d, J=8 Hz, benzyl), 4.80 (2H, br, NHC$\underline{H}_2$), 3.47 (1H, m, CH), 2.78 (1H, dd, J=7, 17 Hz, CHC$\underline{H}$'H), 2.32 (1H, d, J=17 Hz, CHCH'$\underline{H}$), 1.15 (3H, d, J=8 Hz, CH_3). MS m/z: 361 (M^+).

4,5-Dihydro-5-methyl-6-(9-*s*-triazolo[1,5-*c*]quinazolinyl)-3(2*H*)-pyridazinone (9) A suspension of IIax (0.35 g, 1.3 mmol) in triethyl orthoformate (10 ml) was stirred for 3 h at 150 °C, then concentrated. Water was added to the residue and the precipitated crystals were collected by filtration, washed with water and dried to afford crude **9** (0.28 g, 77%), which was recrystallized from DMF–water for analysis, mp 271—273 °C. *Anal.* Calcd for $C_{14}H_{12}N_6O$: C, 59.99; H, 4.32; N, 29.98. Found: C, 60.05; H, 4.40; N, 29.89. IR (KBr): 1700, 1640, 1620 cm^{-1}. NMR (DMSO-d_6) δ: 11.24 (1H, s, NH), 9.68 (1H, s, Ar-H), 8.72 (1H, s, Ar-H), 8.48 (1H, d, J=8 Hz, Ar-H), 8.23 (1H, d, J=8 Hz. Ar-H), 8.32 (1H, s, Ar-H), 3.67 (1H, m, CH), 2.83 (1H, dd, J=7, 17 Hz, C$\underline{H}$'H), 2.38 (1H, d, J=17 Hz, CH'$\underline{H}$), 1.18 (3H, d, J=8 Hz, CH_3). MS m/z: 280 (M^+).

Diethyl [7-(2,3,4,5-Tetrahydro-5-methyl-3-oxo-6-pyridazinyl)-4-quinazolinyl]thiomalonate (11) Diethyl bromomalonate (2.4 ml, 14 mmol) was added to a suspension of **7** (3.7 g, 14 mmol) and Et_3N (13.8 ml, 100 mmol) in DMF (100 ml) and the reaction mixture was stirred for 2 h at room temperature, then concentrated under reduced pressure. The resultant residue was partitioned between water and $CHCl_3$, and the organic layer was washed with water, dried over $MgSO_4$ and evaporated to dryness. The residue was purified by column chromatography (SiO_2, 150 g, 10% MeOH–$CHCl_3$) to afford **11** (3.4 g, 59%). An analytical sample was prepared by recrystallization from DMF–water, mp 164 °C. *Anal.* Calcd for $C_{20}H_{22}N_4O_5S$: C, 55.79; H, 5.16; N, 13.01. Found: C, 56.01; H, 5.35; N, 12.65. IR (KBr): 1740, 1690 cm^{-1}. NMR (DMSO-d_6) δ: 11.30 (1H, s, NH), 9.00 (1H, s, Ar-H), 8.25 (2H, m, Ar-H), 8.18 (1H, d, J=8 Hz, Ar-H), 5.82 (1H, s, COCHCO), 4.26 (4H, q, J=7 Hz, C$\underline{H}_2$CH$_3$), 3.61 (1H, m, CH), 2.80 (1H, dd, J=7, 17 Hz, CHC$\underline{H}$'H), 2.32 (1H, d, J=17 Hz, CHCH'$\underline{H}$), 1.24 (6H, t, J=7 Hz, CH$_2$C$\underline{H}_3$), 1.18 (3H, d, J=8 Hz, CH_3). MS m/z: 430 (M^+).

Diethyl [7-(2,3,4,5-Tetrahydro-5-methyl-3-oxo-6-pyridazinyl)-4-quinazolinyl]malonate (12) A mixture of **11** (2.7 g, 6.3 mmol), Ph_3P (1.9 g, 7.2 mmol) and K_2CO_3 (5.7 g, 41 mmol) in DMF (20 ml) was stirred for 3 h at 120 °C. After cooling, the reaction mixture was partitioned between AcOEt and water, then the water layer was acidified to pH 4.0 with 1 N-HCl. The precipitated crystals were collected by filtration, washed with water and dried to afford crude **12** (1.4 g, 56%) which was recrystallized from EtOH–Et_2O for analysis, mp 173—175 °C. *Anal.* Calcd for $C_{20}H_{22}N_4O_5$: C, 60.29; H, 5.57; N, 14.06. Found: C, 60.66; H, 5.68; N, 14.26. IR (KBr): 1720, 1680 cm^{-1}. NMR (DMSO-d_6) (pD=5.6) δ: 12.91 (0.5H, br s, quinazoline NH of **12a**), 11.30, 11.20 (0.5H, each s, pyridazinone CONH of **12a**, **12b**), 9.30 (0.5H, s, quinazoline 2-H of **12b**), 8.32 (0.5H, s, quinazoline 8-H of **12b**), 8.24, 8.16 (0.5H, each d, J=9 Hz, quinazoline 5, 6-H of **12b**), 8.22 (0.5H, s, quinazoline 2-H of **12a**), 7.89, 7.62 (0.5H, each d, J=9 Hz, quinazoline 5, 6-H of **12a**), 6.20 (0.5H, s, COCHCO of **12b**), 4.24, 4.22 (2H, each q, J=7 Hz, C$\underline{H}_2$CH$_3$), 3.66, 3.49 (0.5H, each m, C$\underline{H}$CH$_3$), 2.82, 2.76 (0.5H, each dd, J=7, 17 Hz, CHC$\underline{H}$'H), 2.33, 2.28 (0.5H each, d, J=17 Hz, CHCH'$\underline{H}$), 1.24, 1.19 (3H each, t, J=7 Hz, CH$_2$C$\underline{H}_3$), 1.15, 1.10 (1.5H, each d, J=7 Hz, CHC$\underline{H}_3$). NMR (DMSO-d_6–D_2O–NaOD) (pD=14.9) δ: 8.88 (1H, s, quinazoline 2-H of **12b**), 8.12 (1H, s, quinazoline 8-H of **12b**), 8.00, 7.98 (1H, d, J=9 Hz, quinazoline 5,6-H of **12b**), 3.94 (4H, q, J=7 Hz, C$\underline{H}_2$CH$_3$ of **12b**), 3.54 (1H, m, CH of **12b**), 2.83 (1H, dd, J=7, 17 Hz, CHC$\underline{H}$'H of **12b**), 2.43 (1H, d, J=17 Hz, CHCH'$\underline{H}$ of **12b**), 1.22 (3H, d, J=7 Hz, CH_3 of 12b), 1.00 (6H, t, J=7 Hz, CH$_2$C$\underline{H}_3$ of **12b**). MS m/z: 398 (M^+).

4,5-Dihydro-5-methyl-6-(4-methyl-7-quinazolinyl)-3(2*H*)-pyridazinone (13) A mixture of **12** (0.77 g, 1.9 mmol) and 2 N NaOH (7.0 ml) in EtOH (20 ml) was stirred for 2 h at 90 °C. The reaction mixture was neutralized with 1 N HCl, then concentrated. The resultant residue was partitioned between $CHCl_3$ and water, then the organic layer was dried over $MgSO_4$ and concentrated to give residual crystals of **13** which were recrystallized from DMF–water to afford pure **13** (0.34 g, 70%), mp 218—221 °C. *Anal.* Calcd for $C_{14}H_{14}N_4O$: C, 66.12; H, 5.55; N, 22.03. Found: C, 66.31; H, 5.71; N, 21.98. IR (KBr): 1690, 1620 cm^{-1}. NMR (DMSO-d_6) δ: 11.14 (1H, s, NH), 9.08 (1H, s, Ar-H), 8.18 (3H, s, Ar-H), 3.60 (1H, m, CH), 2.90 (3H, s, CH_3), 2.78 (1H, dd, J=7, 17 Hz, C$\underline{H}$'H), 2.32 (1H, d, J=17 Hz, CH'$\underline{H}$), 1.15 (3H, d, J=8 Hz, CHC$\underline{H}_3$). MS m/z: 254 (M^+).

4,5-Dihydro-6-(3,4-dihydro-7-quinazolinyl)-5-methyl-3(2*H*)-pyridazinone (15) A mixture of **8** (1.0 g, 3.5 mmol) and Raney-Ni (W-2) (5.0 g) in DMF (10 ml) was stirred for 1 h at 60 °C. After removal of the catalyst by filtration, the mixture was concentrated under reduced pressure. The precipitated crystals were collected by filtration, washed with water and dried to afford crude **15** (0.22 g, 26%) which was recrystallized from DMF–water for analysis, mp 263 °C (dec.). *Anal.* Calcd for $C_{13}H_{14}N_4O$: C, 64.45; H, 5.82; N, 23.12. Found: C, 64.63; H, 5.96; N, 22.98. IR (KBr): 1680, 1600 cm^{-1}. NMR (DMSO-d_6) δ: 10.88 (1H, s, CONH), 8.20 (1H, br s, NH), 7.27 (1H, d, J=8 Hz, Ar-H), 7.12 (2H, s, Ar-H), 6.89 (1H, d, J=8 Hz, Ar-H), 4.48 (2H, s, NHC$\underline{H}_2$), 3.28 (1H, m, CH), 2.68 (1H, dd, J=7, 17 Hz, CHC$\underline{H}$'H), 2.20 (1H, d, J=17 Hz, CHCH'$\underline{H}$), 1.06 (3H, d, J=8 Hz, CH_3). MS m/z: 242 (M^+).

4,5-Dihydro-5-methyl-6-(7-quinazolinyl)-3(2*H*)-pyridazinone (16) A mixture of **15** (0.25 g, 1.0 mmol) and MnO_2 (2.0 g) in $CHCl_3$ (20 ml) was stirred for 1 h at room temperature. The oxidant was filtered off, then the resultant solution was concentrated. The residue was crystallized from Et_2O to afford crude **16** which was recrystallized from DMF–water to give pure **16** (0.20 g, 83%), mp 224—225 °C. *Anal.* Calcd for $C_{13}H_{12}N_4O$: C, 64.98; H, 5.04; N, 23.31. Found: C, 65.23; H, 4.97; N, 23.02. IR (KBr): 1680, 1620 cm^{-1}. NMR (DMSO-d_6) δ: 11.22 (1H, s, NH), 9.60 (1H, s, Ar-H), 9.29 (1H, s, Ar-H), 8.20 (3H, m, Ar-H), 3.62 (1H, m, CH), 2.78 (1H, dd, J=7, 17 Hz, C$\underline{H}$'H), 2.37 (1H, d, J=17 Hz, CH'$\underline{H}$), 1.16 (3H, d, J=8 Hz, CH_3). MS m/z: 240 (M^+).

4-(2,3,4,5-Tetrahydro-5-methyl-3-oxo-6-pyridazinyl)-*N*-(ethoxycarbonyl)anthranilonitrile (18) Ethyl chloroformate (2.3 ml, 24 mmol) was added to a solution of **17** (4.5 g, 20 mmol) in pyridine (40 ml), then the solution was stirred for 30 h at room temperature. The reaction mixture was concentrated and mixed with water. The precipitated crystals were collected by filtrateion to afford crude **18** (3.0 g, 50%). An analytical sample was prepared by recrystallization from DMF–water, mp 178–181 °C. *Anal.* Calcd for $C_{15}H_{16}N_4O_3$: C, 59.98; H, 5.38; N, 18.65. Found: C, 59.72; H, 5.42; N, 18.23. IR (KBr): 2205, 1740, 1680 cm^{-1}. NMR (DMSO-d_6) δ: 11.21 (1H, s, NH), 9.67 (1H, s, NH), 7.90 (1H, s, Ar-H), 7.79 (1H, d, J=7 Hz, Ar-H), 7.68 (1H, d, J=7 Hz, Ar-H), 4.17 (2H, q, J=7 Hz, C$\underline{H}_2$CH$_3$), 3.50 (1H, m, CH), 2.72 (1H, dd, J=7, 17 Hz, C$\underline{H}$'H), 2.30 (1H, d, J=17 Hz, CH'$\underline{H}$), 1.28 (3H, t, J=7 Hz, CH$_2$C$\underline{H}_3$), 1.12 (3H, d, J=8 Hz, CHC$\underline{H}_3$). MS m/z: 300 (M^+).

4,5-Dihydro-5-methyl-6-(1,2,3,4-tetrahydro-4-imino-3-methyl-2-oxo-7-quinazolinyl)-3(2*H*)-pyridazinone (19) To a solution **18** (0.30 g, 1.0 mmol) in DMSO (5 ml) was added dropwise 40% $MeNH_2$–MeOH solution (1.0 ml) within a 2 h period at 150 °C with stirring. After cooling, water (20 ml) was added to the solution and the precipitated crystals were collected by filtration, washed with water and dried to afford crude **19** which was recrystallized from DMF–water to give pure **19** (0.20 g, 74%), mp 271—273 °C. *Anal.* Calcd for $C_{14}H_{15}N_5O_2 \cdot H_2O$: C, 55.43; H, 5.66; N, 23.08. Found: C, 55.68; H, 5.45; N, 23.06. IR (KBr); 1680, 1620 cm^{-1}. NMR (DMSO-d_6) δ: 11.12 (1H, s, NH), 10.81 (1H, br, NH), 8.88 (1H, br, NH), 8.12 (1H, d, J=9 Hz, Ar-H), 7.51 (2H, m, Ar-H), 3.40 (1H, m, CH), 3.34 (3H, s, NCH_3), 2.75 (1H, dd, J=7, 17 Hz, C$\underline{H}$'H), 2.30 (1H, d, J=17 Hz, CH'$\underline{H}$), 1.09 (3H, d, J=7 Hz, CH_3). MS m/z: 285 (M^+).

4,5-Dihydro-6-(1,2-dihydro-4-amino-2-oxo-7-quinazolinyl)-5-methyl-3(2*H*)-pyridazinone (20) Compound **20** (0.20 g, 74%) was prepared from **18** (0.30 g, 1.0 mmol) with ammonia gas (passes into the reaction mixture) as described for **19**, mp 230—236 °C. *Anal.* Calcd for $C_{13}H_{13}N_5O_2 \cdot H_2O$: C, 53.97; H, 5.23; N, 24.21. Found: C, 53.85; H, 5.63; N, 24.01. IR (KBr): 1680, 1620 cm^{-1}. NMR (DMSO-d_6) δ: 11.10 (1H, s, NH), 7.98 (1H, d, J=8 Hz, Ar-H), 7.80 (3H, br, NH_2, NH), 7.50 (1H, s, Ar-H), 7.48 (1H, d, J=8 Hz, Ar-H), 3.40 (1H, m, CH), 2.70 (1H, dd, J=7, 17 Hz, C$\underline{H}$'H), 2.31 (1H, d, J=17 Hz, CH'$\underline{H}$), 1.08 (3H, d, J=8 Hz, CH_3). MS m/z: 271 (M^+).

4,5-Dihydro-5-methyl-6-(2,3,5,6-tetrahydro-5-oxo-8-imidazo[1,2-c]quinazolinyl)-3(2*H*)-pyridazinone (22) Compound **22** (0.20 g, 67%) was prepared from **18** (0.30 g, 1.0 mmol) with ethylenediamine (1.0 ml) at described for **19**, mp >300 °C. *Anal.* Calcd for $C_{15}H_{15}N_5O_2$: C, 60.60; H, 5.09; N, 23.56. Found: C, 60.83; H, 5.25; N, 23.34. IR (KBr): 1700, 1620 cm^{-1}. NMR (DMSO-d_6) δ: 10.88 (1H, s, NH), 7.90 (1H, br s, NH), 7.85 (1H, d, J=8 Hz, Ar-H), 7.50 (2H, m, Ar-H), 3.92 (4H, m, CH_2CH_2), 3.45 (1H, m, CH), 2.68 (1H, dd, J=7, 17 Hz, CHC$\underline{H}$'H), 2.30 (1H, d, J=17 Hz, CHCH'$\underline{H}$), 1.12 (3H, d, J=8 Hz, CH_3). MS m/z: 297 (M^+).

4,5-Dihydro-6-(2,4-dimercapto-7-quinazolinyl)-5-methyl-3(2*H*)-pyridazinone (23) A mixture of **17** (4.5 g, 20 mmol) and CS_2 (5.0 ml) in pyridine (40 ml) was stirred for 4 h at 100 °C. Water (150 ml) was added to the reaction mixture, then precipitated crystals were collected by filtration, washed with water and dried to give crude **23** (5.5 g, 89%). An

analytical sample was prepared by recrystallization from DMF–water, mp > 300°C. *Anal.* Calcd for $C_{13}H_{12}N_4OS_2 \cdot 1/2H_2O$: C, 49.82; H, 4.19; N, 17.87. Found: C, 50.13; H, 4.03; N, 17.85. IR (KBr); 1670, 1620 cm^{-1}. NMR (DMSO-d_6) δ: 13.58 (1H, s, SH), 13.01 (1H, s, SH), 11.22 (1H, s, NH), 8.26 (1H, d, J=8 HZ, Ar-H), 7.73 (1H, s, Ar-H), 7.68 (1H, d, J=8 Hz, Ar-H), 3.40 (1H, m, CH), 2.78 (1H, dd, J=7, 17 Hz, CH'H), 2.34 (1H, d, J=17 Hz, CH'H), 1.14 (3H, d, J=7 Hz, CH_3). MS m/z: 304 (M^+).

4,5-Dihydro-6-(2,4-bismethylthio-7-quinazolinyl)-5-methyl-3(2*H*)-pyridazinone (24) MeI (0.40 ml, 6.4 mmol) was added to a mixture of **23** (0.9 g, 2.9 mmol) and 2N NaOH (2.0 ml) in MeOH (30 ml), then the mixture was stirred for 1 h at room temperature. Water (60 ml) was added to the mixture and the precipitated crystals were collected by filtration, washed with water and dried to give crude **24** (0.87 g, 89%). An analytical sample was preapared by recrystallization from DMF–water, mp 245—246°C. *Anal.* Calcd for $C_{15}H_{16}N_4OS_2$: C, 54.19; H, 4.85; N, 16.85. Found: C, 53.92; H, 4.87; N, 16.68. IR (KBr): 1700, 1610 cm^{-1}. NMR (DMSO-d_6) δ: 11.18 (1H, s, NH), 7.92 (3H, s, Ar-H), 3.50 (1H, m, CH), 2.70 (1H, dd, J=7, 17 Hz, CH'H), 2.62, 2.59 (3H, each s, SCH_3), 2.32 (1H, d, J=17 Hz, CH'H), 1.09 (3H, d, J=8 Hz, $CHCH_3$). MS m/z: 332 (M^+).

4,5-Dihydro-5-methyl-6-(4-methylamino-2-methylthio-7-quinazolinyl)-3(2*H*)-pyridazinone (25) A mixture of **24** (4.9 g, 16 mmol) in 40% $MeNH_2$–MeOH solution (40 ml) was stirred for 30 min at 60°C. The reaction mixture was concentrated under reduced pressure, then the residue was mixed with weter. The precipitated crystals were collected by filtration, washed with water and dried to give crude **25** which was recrystallized from DMF–water to give pure **25** (1.4 g, 29%), mp 137—138°C. *Anal.* Calcd for $C_{15}H_{17}N_5OS \cdot H_2O$: C, 54.04; H, 5.74; N, 21.00. Found: C, 54.35; H, 5.51; N, 21.13. IR (KBr): 1680, 1620 cm^{-1}. NMR (DMSO-d_6) δ: 11.10 (1H, s, NH), 8.35 (1H, br, NH), 8.12 (1H, d, J=8 Hz, 5-H of quinazoline), 7.78 (1H, d, J=8 Hz, 6-H of quinazoline), 7.76 (1H, s, 8-H of quinazoline), 3.51 (1H, m, CH), 3.01 (3H, d, J=6 Hz, $NHCH_3$), 2.74 (1H, dd, J=7, 17 Hz, CH'H), 2.53 (3H, s, SCH_3), 2.30 (1H, d, J=17 Hz, CH'H), 1.12 (3H, d, J=8 Hz, $CHCH_3$), NOE 13% NCH_3 (δ 3.01)—5-H of quinazoline (δ 8.12). MS m/z: 315 (M^+).

4,5-Dihydro-5-methyl-6-(2-methylthio-4-propylamino-7-quinazolinyl)-3(2*H*)-pyridazinone (26) Compound **26** (0.12 g, 39%) was prepared from **24** (0.40 g, 1.2 mmol) with 40% propylamine–MeOH (50 ml) as described for **25**, mp 199°C. *Anal.* Calcd for $C_{17}H_{24}N_5OS$: C, 58.93; H, 6.98; N, 20.21. Found: C, 59.28; H, 6.78; N, 20.19. IR (KBr): 1670, 1620 cm^{-1}. NMR (DMSO-d_6) δ: 11.14 (1H, s, NH), 8.37 (1H, t, J=6 Hz, NH), 8.18 (1H, d, J=9 Hz, Ar-H), 7.83 (1H, d, J=9 Hz, Ar-H), 7.81 (1H, s, Ar-H), 3.50 (3H, m, CH, NCH_2), 2.68 (1H, dd, J=7, 17 Hz, $CHCH'H$), 2.52 (3H, s, SCH_3), 2.28 (1H, d, J=17 Hz, $CHCH'H$), 1.68 (2H, m, CH_2CH_3), 1.12 (3H, d, J=8 Hz, $CHCH_3$), 0.95 (3H, t, J=7 Hz, CH_2CH_3). MS m/z: 343 (M^+).

4,5-Dihydro-5-methyl-6-(2-methylamino-4-propylamino-7-quinazolinyl)-3(2*H*)-pyridazinone (27) A mixture of **26** (0.40 g, 1.2 mmol) and $KMnO_4$ (0.50 g, 3.2 mmol) in 50% AcOH (20 ml) was stirred for 10 min at 5—10°C. Water was added to the mixture, then the mixture was extracted with $CHCl_3$ (20 ml × 5). The extract was added to 40% $MeNH_2$–MeOH solution (50 ml) and the whole was stirred for 10 h at 60°C. The mixture was concentrated under reduced pressure, then the resultant residue was partitioned between $CHCl_3$ and water. The organic layer was washed with water, dried over $MgSO_4$ then evaporated. The residual crystals were recrystallized from DMF–water to give pure **27** (0.27 g, 69%), mp 225—231°C. *Anal.* Calcd for $C_{17}H_{22}N_6O \cdot 1/2H_2O$: C, 60.88; H, 6.91; N, 25.06. Found: C, 61.14; H, 6.98; N, 24.70. IR (KBr): 1680, 1600 cm^{-1}. NMR (DMSO-d_6) δ: 11.13 (1H, s, NH), 7.90 (1H, d, J=8 Hz, Ar-H), 7.75 (1H, s, NH), 7.45 (1H, s, Ar-H), 7.40 (1H, d, J=8 Hz, Ar-H), 6.41 (1H, br, NH), 3.40 (6H, m, CH, $NHCH_3$, $NHCH_2$), 2.67 (1H, dd, J=7, 17 Hz, $CHCH'H$), 2.28 (1H, d, J=17 Hz, $CHCH'H$), 1.63 (2H, m, CH_2CH_3), 1.09 (3H, d, J=8 Hz, $CHCH_3$), 0.90 (3H, t, J=8 Hz, CH_2CH_3). MS m/z: 326 (M^+).

4,5-Dihydro-6-(4-methoxy-2-methyl-7-quinazolinyl)-5-methyl-3(2*H*)-pyridazinone (29) Acetyl chloride (3.0 ml, 42 mmol) was added to a solution of **17** (3.0 g, 14 mmol) in pyridine (30 ml), then the mixture was stirred for 3 h at 80°C. The reaction mixture was concentrated and the residue was partitioned between $CHCl_3$ and water. The organic layer was washed with water, dried over $MgSO_4$ and evporated. A mixture of K_2CO_3 (2.0 g, 14 mmol) in 50% MeOH (100 ml) was added to the residue, then the whole was stirred for 3 h at 80°C. The reaction mixture was concentrated under reduced pressure and the precipitated crystals were collected by filtration, washed with water and dried to give crude **29** (1.1 g, 28%). An analytical sample was prepared by recrystallization from DMF–water, mp 232°C (dec.). *Anal.* Calcd for $C_{15}H_{16}N_4O_2$: C, 63.36; H, 5.68; N, 19.70. Found: C, 63.02; H, 5.73; N, 19.82. IR (KBr): 1690, 1620 cm^{-1}. NMR (DMSO-d_6) δ: 11.22 (1H, s, NH), 8.09 (3H, s, Ar-H), 4.12 (3H, s, OCH_3), 3.58 (1H, m, CH), 2.76 (1H, dd, J=7, 17 Hz, CH'H), 2.64 (3H, s, CH_3), 2.30 (1H, d, J=17 Hz, CH'H), 1.09 (3H, d, J=8 Hz, $CHCH_3$). MS m/z: 284 (m^+).

4,5-Dihydro-6-(4-benzylamino-2-methyl-7-quinazolinyl)-5-methyl-3-(2*H*)-pyridazinone (31) A mixture of **29** (0.76 g, 2.7 mmol) and benzylamine (1.5 ml) in DMSO (15 ml) was stirred for 3 h at 150°C. After cooling, the mixture was concentrated and the residue was partitioned between $CHCl_3$ and water. The organic layer was washed with water, dried over $MgSO_4$ and evaporated. The resultant residue was purified by column chromatography (SiO_2, 100 g, 8% MeOH–$CHCl_3$) to afford **31** (0.31 g, 32%) which was recrystallized from DMF–water for analysis, mp 115°C (dec.). *Anal.* Calcd for $C_{21}H_{21}N_5O \cdot H_2O$: C, 66.82; H, 6.15; N, 18.55. Found: C, 66.53; H, 6.18; N, 18.39. IR (KBr): 1680, 1570 cm^{-1}. NMR (DMSO-d_6) δ: 10.88 (1H, s, NH), 8.67 (1H, br s, NH), 8.22 (1H, d, J=8 Hz, Ar-H), 7.86 (2H, m, Ar-H), 7.31 (5H, br, benzyl), 4.86 (2H, d, J=8 Hz, $NHCH_2$), 3.52 (1H, m, CH), 2.68 (1H, dd, J=7, 17 Hz, CHCH'H), 2.43 (3H, s, CH_3), 2.27 (1H, d, J=17 Hz, CHCH'H), 1.12 (3H, d, J=8 Hz, $CHCH_3$). MS m/z: 359 (M^+).

4,5-Dihydro-5-methyl-6-(2-methyl-4-methylamino-7-quinazolinyl)-3(2*H*)-pyridazinone (30) Compound **30** (0.38 g, 76%) was prepared from **29** (0.50 g, 1.8 mmol) with 40% methylamine–MeOH (20 ml) as described for **31**, mp 151—153°C (dec.). *Anal.* Calcd for $C_{15}H_{17}N_5O \cdot H_2O$: C, 59.79; H, 6.36; N, 23.24. Found: C, 59.75; H, 6.48; N, 22.94. IR (KBr): 1720, 1590 cm^{-1}. NMR (DMSO-d_6) δ: 11.13 (1H, s, NH), 8.23 (1H, br, NH), 8.14 (1H, d, J=8 Hz, Ar-H), 7.88 (1H, s, Ar-H), 7.85 (1H, d, J=8 Hz, Ar-H), 3.52 (1H, m, CH), 3.00 (3H, d, J=6 Hz, $NHCH_3$), 2.74 (1H, dd, J=7, 17 Hz, CH'H), 2.48 (3H, s, CH_3), 2.28 (1H, d, J=17 Hz, CH'H), 1.09 (3H, d, J=8 Hz, $CHCH_3$). MS m/z: 283 (M^+).

Ca^{2+} Sensitizing Effect 1) Method D[16]: Male guinea pigs (Hartley) weighing 300—400 g were killed by a blow on the head, and the hearts were removed. The papillary muscle was isolated from the right ventricle in a bath containing "relaxing solution (Ca^{2+} free)" of the following composition (mM): KSO_3CH_3, 118; Mg $(SO_3CH_3)_2$, 5; ATP-Na_2, 5.3; ethyleneglycolbis (β-aminoethylether)-*N*,*N*'-tetraacetic acid (EGTA), 2; piperazine-*N*,*N*'-bis (2-ethanesulfonic acid) (PIPES), 20; adjusted to pH 7.0 with KOH. The small bundle (about 0.1—0.2 mm in diameter and 2—3 mm in length) was prepared from the papillary muscle, then one end of the bundle was connected to a strain gauge transducer (Nihon Koden TB-611T) for measurement of isometric tension, and the other end was immersed in a bath containing relaxing solution. To obtain skinned fiber, the small bundle was treated with the relaxing solution containing 250 μg/ml of saponin for 30 min. At the beginning of the experiment, the fiber was stretched in relaxing solution until resting tension was 1—2 mg, then the external solution was replaced by "activating solution" (pCa (-log $[Ca^{2+}]_M$) = 5.8, KSO_3CH_3 77, Mg $(SO_3CH_3)_2$ 5, Ca $(SO_3CH_3)_2$, 8.3; ATP-Na_2, 5.4; EGTA, 10; PIPES, 20; (mM) adjusted to pH 7.0 with KOH). The test compounds were added to this solution at a concentration of 10^{-4} or 10^{-5} M, using polyethyleneglycol (PEG) 400 as vehicle. The final concentration of PEG 400 was 10 μl/ml (drug concentration of 10^{-4} M) or 5 μl/ml (drug concentration of 10^{-5} M). The Ca^{2+} sensitizing activity of the compounds was determined by measuring percent increase in the tension development after addition of the test compounds. Experiments were performed at 24—25°C.

2) Method E: The fiber described above was stretched in relaxing solution (KSO_3CH_3, 129; Mg $(CO_3CH_3)_2$, 5.1; ATP-Na_2, 4.2; EGTA, 2; PIPES, 20; (mM), adjusted to pH 7.0 with KOH) until resting tension was 1—2 mg, then the relaxing solution was replaced by activating solution (pCa = 6.0, KSO_3CH_3, 90.2; Mg $(SO_3CH_3)_2$, 5; Ca $(SO_3CH_3)_2$, 7.18; ATP-Na_2, 4.14; EGTA, 10; PIPES, 20; (mM), adjusted to pH 7.0 with KOH) containing PEG 400 (2.5 μl/ml). When the contraction reached a plateau (pre-drug value), the solution was replaced by PEG 400 solution (5 μl) of Ix or **3** in activating solution (2 ml) (drug concentration of 3×10^{-7}, 10^{-6}, 3×10^{-6} and 10^{-5} M). The tension development induced by the compounds was expressed as percent increase from the pre-drug value. Each concentration of one compound was examined in the same skinned fiber.

References and Notes

1) Part VI. Y. Nomoto, H. Takai, T. Ohno and K. Kubo, *Chem. Pharm. Bull.*, **39**, 352 (1991).
2) For a recent review: M. D. Taylor, I. Sircar and R. P. Steffen, *Annu. Rep. Med. Chem.*, **22**, 85 (1987).
3) J. A. Bristol, I. Sircar, W. H. Moos, D. B. Evans and R. E. Weishaar,

J. Med. Chem., **27**, 1099 (1984).
4) D. W. Robertson, J. H. Krushinski, E. E. Beedle, V. Wyss, G. Don Pollock, H. Wilson, R. F. Kauffman and J. S. Hayes, *J. Med. Chem.*, **29**, 1832 (1986).
5) V. Austel, J. Heider, W. Eberlein, W. Diederen and W. Haarmann, U. S. Patent 4361563 (1982) [*Chem., Abstr.*, **98**, 72123*p* (1983)].
6) A. Narimatsu, Y. Kitada, N. Satoh, R. Suzuki and H. Okushima, *Arzneim.-Forsch.*, **37**, 398 (1987).
7) Y. Kitada, A. Narimatsu, R. Suzuki, M. Endoh and N. Taira, *J. Pharmacol. Exp. Ther.*, **243**, 639 (1987).
8) K. Fujino, N. Sperelakis and R. J. Solaro, *J. Pharmacol. Exp. Ther.*, **247**, 519 (1988).
9) B. Mueller-Beckmann, P. Freund, P. Honerjaeger, L. Kling and J. C. Ruegg, *J. Cardiovasc. Pharmacol.*, **11**, 8 (1988).
10) E. C. Taylor, A. McKillop and S. Vromen, *Tetrahedron*, **23**, 885 (1967).
11) M. Roth, P. Dubs, E. Gotschi and A. Eschenmoser, *Helv. Chim. Acta*, **54**, 710 (1971).
12) E. C. Taylor, A. McKillop and R. N. Warrerner, *Tetrahedron*, **23**, 891 (1967).
13) K. W. Breukink, L. H. Krol, P. E. Verkade and B. M. Wepster, *Rec. Trav. Chim.*, **76**, 401 (1957).
14) Part I: Y. Nomoto, H. Obase, H. Takai, T. Hirata, M. Teranishi, J. Nakamura and K. Kubo, *Chem. Pharm. Bull.*, **38**, 1591 (1990).
15) A. A. Alousi, A. Helstosky, M. J. Montenaro and F. Cicero, *Fed. Proc. Fed. Am. Soc. Exp. Biol.*, **40**, 663 (1981).
16) Y. Kitada, A. Narimatsu, N. Matsumura and M. Endo., *J. Pharm. Exp. Ther.*, **243**, 633 (1987).
17) M. Endo and T. Kitazawa, "Biophysical Aspects of Cardiac Muscle," Academic Press, New York, 1978, pp. 307—327.

Synthesis and Antiestrogenic Activity of the Compounds Related to the Metabolites of (*Z*)-4-[1-[4-[2-(Dimethylamino)ethoxy]phenyl]-2-(4-isopropylphenyl)-1-butenyl]phenyl Monophosphate (TAT-59)[1)]

Kazuo OGAWA,* Yoh-ichi MATSUSHITA, Ichiro YAMAWAKI, Manabu KANEDA, Jiro SHIBATA, Toshiyuki TOKO, and Tetsuzi ASAO

Research Laboratory, Taiho Pharmaceutical Co., Ltd., Kawauchi-cho, Tokushima 771-01, Japan. *Received August 20, 1990*

The metabolites of (*Z*)-4-[1-[4-[2-(dimethylamino)ethoxy]phenyl]-2-(4-isopropylphenyl)-1-butenyl]phenyl monophosphate, TAT-59, (1), a potent antitumor agent for hormone-dependent tumors, and derivatives of TAT-59 were synthesized to confirm its proposed structure. The structure and the *Z*-configuration of the metabolites (2a—8a) were confirmed by comparison with synthesized authentic compounds. All of the metabolites and the derivatives of TAT-59 were tested for a binding affinity toward estrogenic receptors *in vitro* and antiuterotrophic activity *in vivo*. Most of the metabolites possessed remarkable binding affinity toward estrogenic receptors as well as fairly good antiuterotrophic activity.

Keywords metabolite; synthesis; hormone-dependent tumor; antitumor agent; binding affinity; estrogen receptor; antiuterotrophic activity

Tamoxifen (TAM),[2)] a nonsteroidal antiestrogenic agent, is currently used as adjuvant in the surgical therapy of breast cancer. Moreover, several derivatives[3)] of TAM have been extensively studied in this field. In the course of a search for a non-steroidal antiestrogenic agent, we identified[4)] a novel non-steroidal antitumor agent, (*Z*)-4-[1-[4-[2-(dimethylamino)ethoxy]phenyl]-2-(4-isopropylphenyl)-1-butenyl]phenyl monophosphate (TAT-59) (**1**), which possesses much stronger antiestrogenic activity than TAM. Furthermore, TAT-59 is currently under study as a promising drug for the treatment of breast cancer. Recently, seven metabolites (**2a—8a**) have been identified in the study of TAT-59 biotransformation in the plasma of rat and dog. Specifically, a dephosphorylated derivative (**2**), three hydroxylated derivatives (**3**, **5** and **6**), an olefinic derivative (**4**), a demethylated derivative (**7**) and a hydroxylated derivative (**8**) with demethylation were proposed. The present study is undertaken to confirm their structure and

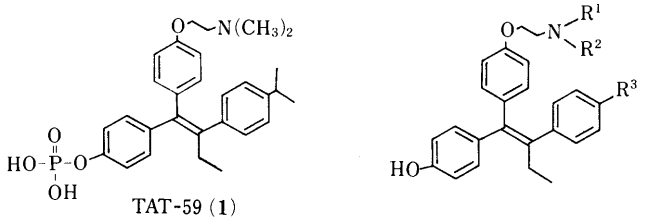

	R^1	R^2	R^3
2	CH_3	CH_3	
3	CH_3	CH_3	OH
4	CH_3	CH_3	
5	CH_3	CH_3	OH, OH
6	CH_3	CH_3	OH
7	H	CH_3	
8	H	CH_3	OH

Chart 1

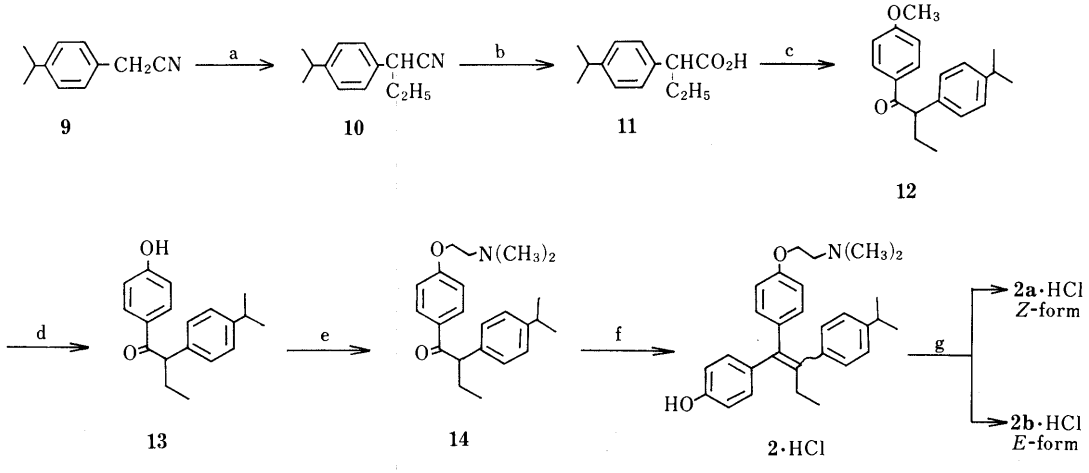

a) C_2H_5Br, aqueous NaOH. b) H_2SO_4, 150°C. c) i) $SOCl_2$, ii) anisole, $AlCl_3$, CH_2Cl_2. d) pyridine hydrochloride, 230°C. e) $ClCH_2CH_2N(CH_3)_2$, NaOH, DMF. f) i) 4-(tetrahydropyran-2-yloxy)phenyl magnesium bromide, THF, ii) HCl-EtOH, reflux. g) recrystallization.

Chart 2

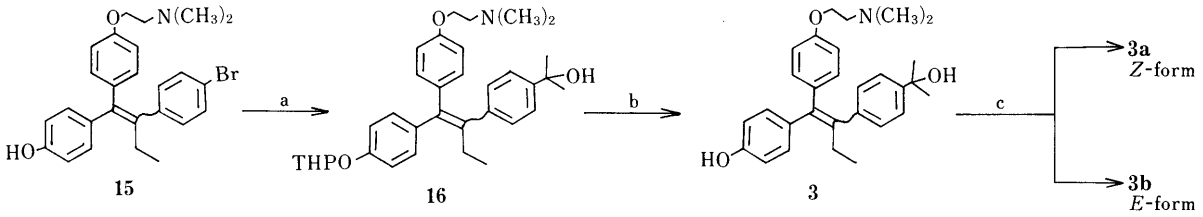

a) i) DHP, *p*-TsOH, DMF, ii) *n*-BuLi, THF, iii) acetone, THF.
b) conc. HCl, THF, room temperature. c) ODS-chromatography.

Chart 3

configuration (*E* or *Z*-form), and to clarify their potency in comparison with TAM and TAT-59 for the binding affinity *in vitro* toward estrogenic receptors and for the antiuterotrophic activity *in vivo*. In this paper, we wish to report on the synthesis of the metabolites (**2a**—**8a**) and related compounds (**2b**—**8b**), and their biological activity.

Synthesis The dephosphorylated compound (**2**) was prepared according to the method shown in Chart 2. *C*-Alkylation of 4-isopropylphenylacetonitrile (**9**)[5] with ethyl bromide resulted in compound (**10**). Compound (**11**) was subjected to chlorination with $SOCl_2$ followed by Friedel–Crafts reaction with anisole to give compounds (**12**) in a fair yield. Compound (**13**), obtained by *O*-demethylation of **12** with pyridinie hydrochloride, was again subjected to *O*-alkylation with 2-(dimethylamino)ethyl chloride to afford compound (**14**).

In accordance with a published method[6] on the synthesis of TAM derivatives, ketone (**14**) was allowed to react with [4-(tetrahydropyran-2-yloxy)phenyl]magnesium bromide,[7] followed by acid-catalytic deprotection of a tetrahydropyranyl moiety and dehydration to afford compound (**2**). The isomeric mixture (**2**) was combined in a ratio of about 1 : 1 (*E*:*Z*) on the basis of proton nuclear magnetic resonance (^{1}H-NMR) spectra. Each isomer could be separated by recrystallization to one isomer (**2a**) and another (**2b**), respectively.

The hydroxylated compound (**3**) was prepared by the method shown in Chart 3. Protection of the hydroxy group on the 4-bromophenyl-4′-hydroxyphenyl derivative (**15**)[6b] with 2,3-dihydropyrane (DHP) in the presence of a catalytic *p*-toluenesulfonic acid successfully resulted in a good yield. The phenyllitium derivative, prepared by treatment of the 4-bromophenyl-4′-(tetrahydropyran-2-yloxy)phenyl derivative with *n*-butyl lithium (*n*-BuLi), was allowed to react with acetone followed by acid-catalytic deprotection of the tetrahydropyranyl moiety to afford the tertiary alcohol derivative (**3**) as an isomeric mixture (*E*:*Z*=1 : 1). The mixture could not be separated by recrystallization but could be separated into the two regio-isomers (**3a** and **3b**) by means of chromatography on an octadecyl-bonded silica gel (ODS) column.

The olefinic (**4**), 1,2-dihydroxylated (**5**) and mono-hydroxylated (**6**) compounds were prepared by the method shown in Chart 4. Deprotection and dehydration of the 4-[(2-hydroxy-2-methyl)ethyl]phenyl-4′-(tetrahydropyran-2-yloxy)phenyl derivative (**16**) proceeded easily on heating in acetic acid to give an olefinic compound (**4**). Oxidation of **4** with osmium tetraoxide (OsO_4)[8] resulted in compound **5** by introducing diol moieties to the 1 and 2-positions on the alkyl chain. On the other hand, oxidation of **4** using

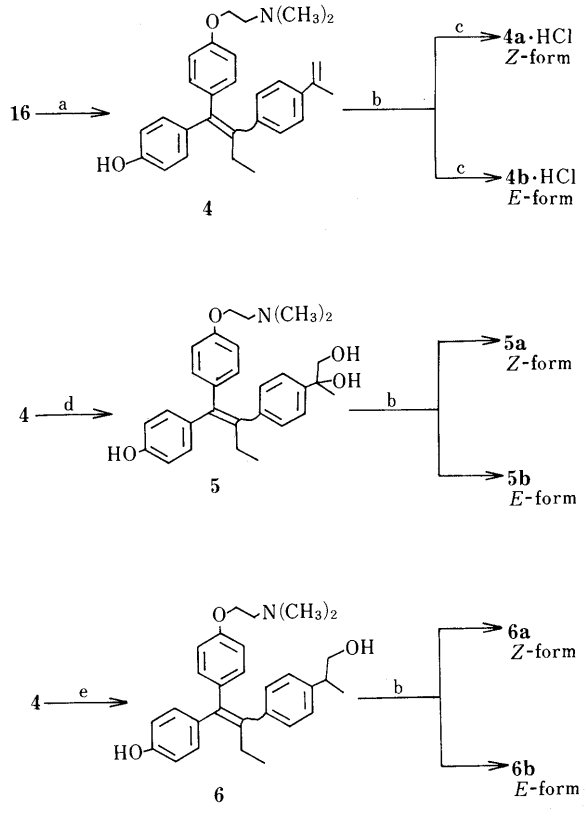

a) AcOH, reflux. b) ODS-chromatography. c) dioxane-HCl
d) OsO_4, pyridine, room temperature. e) i) 9-BBN, benzene, reflux, ii) H_2O_2-$NaOCH_3$, MeOH, 50°C.

Chart 4

9-borabicyclo[3.3.1]nonane (9-BBN)[9] gave compound (**6**), which involved selective introduction of a hydroxyl group to the terminal end of the alkyl chain. These compounds (**4**, **5** and **6**) were independently separated into two regio-isomers (**4a** and **4b**), (**5a** and **5b**), and (**6a** and **6b**), respectively, in the same manner as described for **3**.

The demethylated compounds (**7** and **8**) were prepared by the method shown in Chart 5. In accordance with the known method,[10] compounds (**2** and **6**) were allowed to react with vinyloxycarbonyl chloride followed by acidcatalytic removal of the vinyloxycarbonyl moiety to give the *N*-demethylated compounds (**7** and **8**), respectively. These compounds (**7** and **8**) were separated into the two regio-isomers (**7a** and **7b**) and (**8a** and **8b**), respectively, in the same manner as described for **3**.

Assignment of Configuration (*Z* and *E*) and Determination of Chemical Purity The configurational assignment of the

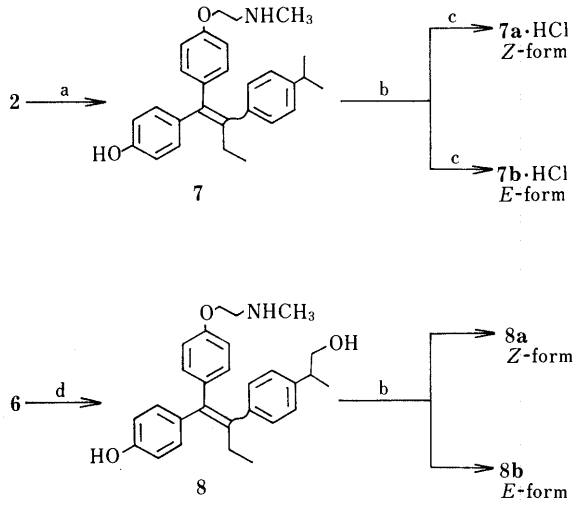

a) i) vinyloxycarbonyl chloride, dioxane, 170°C, ii) HCl-EtOH, 80°C. b) ODS-chromatography. c) dioxane-HCl. d) i) vinyloxycarbonyl chloride, dioxane, ii) 4 N-NaOH, reflux.

Chart 5

TABLE I. Binding Affinity toward Estrogenic Receptor and Anti-uterotrophic Activity of Metabolites (**2a**—**8a**) and Their Isomers (**2b**—**8b**)

Compd. No.	Configuration[a]	Chemical purity[b] (%)	Binding affinity[c]		Antiuterotrophic activity[c]
			RBA	IC_{50} ($\times 10^{-8}$ M)	Inhibition[d] (%)
2a	*Z*	97.0	152.5	0.181	36.2
2b	*E*	97.2	1.7	16.7	10.1
3a	*Z*	99.8	48.5	0.569	11.4
3b	*E*	98.0	0.8	36.4	—[e]
4a	*Z*	95.4	53.8	0.513	38.4
4b	*E*	96.2	0.7	39.0	—[e]
5a	*Z*	99.5	31.5	0.876	29.3
5b	*E*	96.1	0.7	40.1	—[e]
6a	*Z*	99.2	28.9	0.959	36.2
6b	*E*	98.3	3.6	7.72	—[e]
7a	*Z*	95.8	66.2	0.417	37.5
7b	*E*	95.6	1.6	16.8	—[e]
8a	*Z*	98.5	58.5	0.472	15.4
8b	*E*	98.6	2.4	11.4	—[e]
TAT-59 (**1**)			5.1	5.37	42.5
TAM			0.6	45.3	17.8
Estradiol			100.0	0.276	0.0[f]

a) Configurational isomer. *b*) Determined by HPLC-Develosil ODS-5. *c*) See the experimental section. *d*) Dose of 40 μg/kg, i.p. *e*) Not tested. *f*) Dose of 0.5 μg/kg, i.p.

isomers (**2a**—**8a** and **2b**—**8b**) was confirmed on the basis of ^{1}H-NMR chemical shifts in accordance with the literature.[11] Namely, the chemical shift of triplets for the OCH_2 proton in the compounds (**2a** and **2b**) appeared at δ 4.21 and 4.37 ppm, respectively. Shani *et al.*[11] report that the substituents situated *trans* (*E*-form) to a phenyl ring are shifted to lower fields than those in a *Z*-form. On the basis of this observation, the resonance appearing at lower fields was assigned to be *E*-isomer in the compound (**2b**). On the other hand, for **2a**, resonance was considered to be *Z*-isomer. The other isomers (**3a**—**8a**) and (**3b**—**8b**) were confirmed in the same manner as described for **2a** and **2b**. The chemical purity of the regio-isomers was respectively determined by high performance liquid chromatography (HPLC) on Develosil ODS-5 with methanol–phosphate buffer (75 : 25) as an eluant. The data are shown in Table I.

Results and Discussion

All of the metabolites (**2a**—**8a**) were identified to be *Z*-isomers on the bases of ^{1}H-NMR chemical shifts and HPLC properties of the synthesized authentic compounds. During transformation of TAT-59, it was clarified that the double bond configuration of the metabolites did not change. All metabolites (**2a**—**8a**) and the corresponding regio-isomers (**2b**—**8b**) were examined for competitive activity *in vitro* toward estrogenic receptors and for antiuterotrophic activity *in vivo*. The data are shown in Table I. Binding affinity of the *Z*-isomers (**2a**—**8a**) *in vitro* toward estrogenic receptors was remarkably higher than that of the *E*-isomers (**2b**—**8b**) and TAM. In particular, among all of the metabolites (*Z*-isomers), **2a** showed the most potent activity ($IC_{50} = 1.8 \times 10^{-9}$ M). Almost all of the *Z*-isomers showed more potent antiuterotrophic activity *in vivo* in comparison with the *E*-isomers and TAM. On the other hand, the activity of **2a**, **4a**, **6a** and **7a** was as potent as TAT-59 (**1**). Based on pharmacological data, it was suggested that the potent antitumor activity of TAT-59 (parent compound) is mediated by the combination of its metabolites.

Experimental

All melting points were recorded with a Yanagimoto micromelting apparatus and are uncorrected. Spectral data were obtained as follows: mass spectra (MS) with a JEOL LMS-O1G-2 spectrometer; ^{1}H-NMR spectra with a JEOL JMN-FX 100 spectrometer (using tetramethylsilan as an internal standard). Chemical shifts of ^{1}H-NMR signals are given in δ values (ppm).

2-(4-Isopropylphenyl)butyronitrile (10) The title compound (**10**) was prepared from ethyl bromide (49.1 g), 4-isopropylphenylacetonitrile (**9**)[5] (70.0 g), triethylbenzylammonium chloride (TEBAC) (2.0 g) and 50% NaOH solution (60 ml) in accordance with the known method.[12] Yield 63.2 g (78.7%). bp 119—123 °C (5 mmHg). ^{1}H-NMR ($CDCl_3$) δ: 1.06 (3H, t, J=7.3 Hz), 1.24 (6H, d, J=7.1 Hz), 1.70—2.10 (2H, m), 2.70—3.15 (1H, m), 3.70 (1H, t, J=7.1 Hz), 7.23, 7.25 (4H, each s). MS *m/z*: 187 (M^+).

2-(4-Isopropylphenyl)butyric Acid (11) Compound (**10**) (49.0 g) was added to 70% H_2SO_4 (50 ml) and then heated in an oil bath at 150 °C for 3 h. The reaction mixture was cooled to room temperature and then extracted with toluene (100 ml × 2). The organic layer was washed with water, dried over sodium sulfate and evaporated under reduced pressure to give **11** as a crude product, which was purified by distillation. Yield 46.2 g (85.6%). bp 156—160 °C (5 mmHg). (mp 95—96 °C). ^{1}H-NMR ($CDCl_3$) δ: 0.90 (3H, t, J=7.3 Hz), 1.23 (6H, d, J=6.8 Hz), 1.60—2.30 (2H, m), 2.65—3.10 (1H, m), 3.42 (1H, t, J=7.5 Hz), 7.19, 7.20 (4H, each s). MS *m/z*: 206 (M^+). *Anal.* Calcd for $C_{13}H_{18}O_2$: C, 75.69; H, 8.80. Found: C, 75.35, H, 8.60.

2-(4-Isopropylphenyl)-1-(4-methoxyphenyl)-1-butanone (12) Anhydrous aluminium chloride (29.4 g) was gradually added to a solution of anisole (23.0 g) and acid chloride (47.0 g) (prepared by the treatment of **11** with thionyl chloride) in dichloromethane (250 ml) while maintaining the reaction temperature below 0 °C. The reaction mixture was stirred at room temperature for 3 h and then poured into 5% HCl (300 ml). The organic layer was washed with water, then dried over sodium sulfate and evaporated under reduced pressure to give **12**. Yield 60.0 g (82.2%). mp 47—48 °C. ^{1}H-NMR ($CDCl_3$) δ: 0.88 (3H, t, J=7.4 Hz), 1.25 (6H, d, J=7.5 Hz), 1.50—2.50 (2H, m), 2.50—3.20 (1H, m), 3.66 (3H, s), 4.35 (1H, t, J=7.2 Hz), 6.77 (2H, d, J=8.8 Hz), 7.13, 7.16 (4H, each s), 7.92 (2H, d, J=8.8 Hz). MS *m/z*: 296 (M^+). *Anal.* Calcd for $C_{20}H_{24}O_2$: C, 81.04; H, 8.16. Found: C, 81.08; H, 7.92.

1-(4-Hydroxyphenyl)-2-(4-isopropylphenyl)-1-butanone (13) Compound (**12**) (17.3 g) was added to pyridine hydrochloride (20.0 g), and then heated in an oil bath at 230 °C for 2 h. The reaction mixture was poured into ice-water (30 ml) and extracted with dichloromethane (100 ml × 2). The organic layer was dried over sodium sulfate and evaporated under reduced pressure to give **13** as a crude product, which was recrystallized from toluene–hexane. Yield 12.4 g (75.2%). mp 132—133 °C. ^{1}H-NMR ($CDCl_3$) δ: 0.88 (3H, t, J=7.3 Hz), 1.18 (6H, d, J=7.1 Hz), 1.60—2.40 (2H, m), 2.60—3.00 (1H, m), 4.40 (1H, t, J=7.3 Hz), 6.84 (2H, d,

J=8.8 Hz), 7.15, 7.18 (4H, each s), 7.92 (2H, d, J=8.8 Hz). MS m/z: 282 (M^+). *Anal.* Calcd for $C_{19}H_{22}O_2$: C, 80.81; H, 7.85. Found: C, 80.71; H, 7.59.

1-[4-[2-(Dimethylamino)ethoxy]phenyl]-2-(4-isopropylphenyl)-1-butanone (14) Compound (**13**) (12.4 g) was gradually added to a suspension of sodium hydride (about 60%, in oil) (1.8 g) in *N,N*-dimethylformamide (DMF) (50 ml) under stirring at room temperature. The reaction mixture was stirred for 1.5 h at the same temperature and then 2-(dimethylamino)ethyl chloride (5.5 g) [obtained by the treatment of 2-(dimethylamino)ethyl chloride hydrochloride with 10% NaOH solution] was added to the whole mixture. After stirring at 100 °C for 2 h, the reaction mixture was evaporated under reduced pressure, and the resulting residue was extracted with dichloromethane (200 ml), the obtained organic layer was extracted with 2 N HCl (50 ml × 2). The acid layer was adjusted to pH 10 with 10% NaOH solution. The resulting oily product was extracted with dichloromethane (100 ml × 2). The organic layer was dried over sodium sulfate and evaporated under reduced pressure to give **14**. Yield 12.6 g (80.1%). mp 55—56 °C. ^{1}H-NMR ($CDCl_3$) δ: 0.88 (3H, t, J=7.3 Hz), 1.19 (6H, d, J=7.1 Hz), 1.60—2.30 (2H, m), 2.31 (6H, s), 2.71 (2H, t, J=5.6 Hz), 1.70—3.00 (1H, m), 4.07 (2H, t, J=5.6 Hz), 4.38 (1H, t, J=7.3 Hz), 6.88 (2H, d, J=9.0 Hz), 7.15, 7.19 (4H, each s), 7.96 (2H, d, J=9.0 Hz). MS m/z: 353 (M^+). *Anal.* Calcd for $C_{23}H_{31}NO_2$: C, 78.15; H, 8.84; N, 3.96. Found: C, 78.43; H, 8.85; N, 3.97.

(*Z*)- and (*E*)-1-[4-[2-(Dimethylamino)ethoxy]phenyl]-1-(4-hydroxyphenyl)-2-(4-isopropylphenyl)-1-butene Hydrochloride (2a and 2b) A solution of 4-(tetrahydropyran-2-yloxy)phenyl bromide[13] (51.4 g) in tetrahydrofurane (THF) (150 ml) was added dropwise in the presence of a catalytic amount of iodine to a suspension of magnesium (4.9 g) in THF (10 ml) under gentle reflux. The reaction was initiated by heating. After reflux for 2 h, the reaction mixture was cooled below 5 °C, then a solution of compound (**14**) (44.0 g) in THF (100 ml) was added to a solution of its Grignard reagent under ice-cooling. After stirring at room temperature for 1 h, the reaction mixture was refluxed for 2 h and then evaporated under reduced pressure. The resulting residue was poured into ice-water (300 ml) containing a saturated ammonium chloride solution and extracted with dichloromethane (300 ml × 2). The organic layer was dried over sodium sulfate and evaporated under reduced pressure. The obtained black oily product was dissolved in water (200 ml), then the whole was alkalized with ammonium hydroxide and extracted with ether (300 ml × 2). After removal of the solvent, the obtained residue was dissolved in a solution of conc. HCl (20 ml) in ethanol (200 ml). After refluxing for 2 h, the reaction mixture was evaporated under reduced pressure to give **2**·HCl as a crude product (isomeric mixture of E/Z=1/1), which was purified by recrystallization from a mixture of 2-butanone and ether. The yield was 35.2 g (65.8%). The isomeric mixture was separated to *E*- and *Z*-isomer as follows; From the recrystallization, *Z*-isomer (**2a**·HCl) was obtained. mp 200—202 °C. ^{1}H-NMR (DMSO-d_6) δ: 0.84 (3H, t, J=7.1 Hz), 1.15 (6H, d, J=6.8 Hz), 2.20—2.60 (2H, m), 2.60—3.00 (1H, m), 2.77 (6H, s), 3.40 (2H, br t), 4.22 (2H, br t), 6.60—7.30 (12H, m), 9.52 (1H, s), 10.75 (1H, br s). MS m/z: 429 (M^+). *Anal.* Calcd for $C_{29}H_{35}NO_2$·HCl: C, 74.74; H, 7.78; N, 3.01. Found: C, 74.83; H, 7.71; N, 3.10. From the mother liquid, *E*-isomer (**2b**·HCl) was obtained. mp 171—173 °C. ^{1}H-NMR (DMSO-d_6) δ: 0.84 (3H, t, J=6.8 Hz), 1.15 (6H, d, J=6.8 Hz), 2.20—2.60 (2H, m), 2.60—2.95 (1H, m), 2.84 (6H, s), 3.50 (2H, br t), 4.35 (2H, br t), 6.40 (2H, d, J=8.6 Hz), 6.60 (2H, d, J=8.6 Hz), 6.85—7.20 (8H, m), 9.22 (1H, s), 10.52 (1H, br s). MS m/z: 429 (M^+). *Anal.* Calcd for $C_{29}H_{35}NO_2$·HCl: C, 74.74; H, 7.78; N, 3.01. Found: C, 74.90; H, 7.85; N, 3.01.

(*E,Z*)-1-[4-[2-(Dimethylamino)ethoxy]phenyl]-2-[4-(1-hydroxy-1-methylethyl)phenyl]-1-[4-(tetrahydropyran-2-yloxy)phenyl]-1-butene (16) DHP (61.5 g) was added to a solution consisting of DMF (100 ml), *p*-toluenesulfonic acid (6.6 g) and (*E,Z*)-**15** (15.9 g) (prepared starting from 4-bromophenylacetic acid according to the method of Robertson, *et al.*[6b]) After stirring overnight at room temperature, the reaction mixture was neutralized with triethylamine (70 g) under ice-cooling and evaporated under reduced pressure. The residue was dissolved in water (50 ml), adjusted to pH 12—13 with 2 N NaOH and extracted with ether (100 ml × 2). The organic layer was dried over sodium sulfate and evaporated under reduced pressure to give a crude (*E,Z*)-2-(4-bromophenyl)-1-[4-[2-(dimethylamino)ethoxy]phenyl]-1-[4-(tetrahydropyran-2-yloxy)phenyl]-1-butene, which was purified by chromatography on a silica gel column with chloroform–ethanol (10 : 1) as an eluent to give a light brown oil. Yield 13.2 g (70.2%). ^{1}H-NMR ($CDCl_3$) δ: 0.91 (3H, t, J=7.3 Hz), 1.40—2.00 (6H, m), 2.29, 2.34 (6H, each s), 2.45 (2H, q, J=7.3 Hz), 2.65, 2.73 (2H, each t, J=5.9 Hz), 3.40—4.10 (2H, m), 3.94, 4.07 (2H, each t, J=5.9 Hz), 5.27, 5.41 (1H, each br s), 6.50—7.40 (12H, m). MS m/z: 549 (M^+).

A solution of *n*-BuLi in hexane (21.2 ml of 1.6 M) was added dropwise to a solution of the above 4-(tetrahydropyran-2-yloxy)phenyl compound (9.4 g) in THF (50 ml) at −50 °C in a nitrogen atmosphere. After stirring at the same temperature for 0.5 h, acetone (2.53 ml) was added dropwise to the reaction mixture while maintaining the temperature below −50 °C, and stirring was continued at the same temperature for 1 h. The reaction mixture was allowed to warm to room temperature and evaporated under reduced pressure. The residue was dissolved in water (40 ml), and then the solution was adjusted to pH 13 with 2 N NaOH and extracted with ether (100 ml × 2). The organic layer was dried over sodium sulfate and evaporated under reduced pressure to give **16** as a light brown oil (isomeric mixture of E/Z=1/1). Yield 8.2 g (90.9%). ^{1}H-NMR (DMSO-d_6) δ: 0.84 (3H, t, J=6.8 Hz), 1.37, 1.38 (6H, each s), 1.30—1.90 (6H, m), 2.15, 2.22 (6H, each s), 2.53, 2.63 (2H, each t, J=5.6 Hz), 3.30—4.00 (2H, m), 3.89, 4.05 (2H, each t, J=5.6 Hz), 4.90, 4.92 (1H, each s), 5.28, 5.45 (1H, each br s), 6.50—7.40 (12H, m). MS m/z: 529 (M^+). *Anal.* Calcd for $C_{34}H_{43}NO_4$: C, 77.09; H, 8.18; N, 2.64. Found: C, 77.30; H, 8.37; N, 2.81.

(*Z*)- and (*E*)-1-[4-[2-(Dimethylamino)ethoxy]phenyl]-2-[4-(1-hydroxy-1-methylethyl)phenyl]-1-(4-hydroxyphenyl)-1-butene (3a and 3b) Concentrated HCl (4 ml) was added to a solution of (*E,Z*)-**16** (4.46 g) in THF (40 ml). After stirring at room temperature for 15 min, the reaction mixture was neutralized with sodium bicarbonate and extracted with chloroform (50 ml × 2). The organic layer was dried over sodium sulfate and evaporated under reduced pressure to give **3** as a crude product (isomeric mixture of E/Z=1/1), which was purified by chromatography on a silica gel column with chloroform–methanol (5 : 1) as an eluent. The yield was 1.64 g (43.7%). MS m/z: 445 (M^+). The isomeric mixture was separated into *E*- and *Z*-isomers as follows: The compound (**3**) was chromatographed on an ODS column with methanol–phosphate buffer (75 : 25) as an eluent. The first eluate was collected and evaporated under reduced pressure at room temperature. 10% aqueous sodium bicarbonate was added to the residue and the whole was extracted with ether. The organic layer was dried over sodium sulfate and evaporated under reduced pressure to give **3a** (*Z*-isomer). mp 134—136 °C. ^{1}H-NMR (DMSO-d_6) δ: 0.84 (3H, t, J=7.1 Hz), 1.37 (6H, s), 2.16 (6H, s), 3.89 (2H, t, J=6.7 Hz), 4.90 (1H, s), 6.50—7.40 (12H, m), 9.40 (1H, br s). MS m/z: 445 (M^+). *Anal.* Calcd for $C_{29}H_{35}NO_3 \cdot H_2O$: C, 75.13; H, 8.04; N, 3.02. Found: C, 75.27; H, 8.05; N, 3.05. The second eluate was collected, worked-up in the same manner as described for **3a** to give **3b** (*E*-isomer). mp 150—152 °C. ^{1}H-NMR (DMSO-d_6) δ: 0.84 (3H, t, J=7.1 Hz), 1.38 (6H, s), 2.23 (6H, s), 2.63 (2H, t, J=6.7 Hz), 4.05 (2H, t, J=6.7 Hz), 4.93 (1H, s), 6.30—6.40 (12H, m), 9.16 (1H, br s). MS m/z: 445 (M^+). *Anal.* Calcd for $C_{29}H_{35}NO_3$: C, 78.17; H, 7.92; N, 3.14. Found: C, 77.92; H, 8.04; N, 3.12.

(*Z*)- and (*E*)-1-[4-[2-(Dimethylamino)ethoxy]phenyl]-1-(4-hydroxyphenyl)-2-(4-isopropenylphenyl)-1-butene Hydrochloride (4a and 4b) Compound (**16**) (5.76 g) was dissolved in acetic acid (25 ml). After stirring at 90 °C for 5 h, the reaction mixture was poured into saturated sodium carbonate (350 ml) and stirred at room temperature for 0.5 h. The resulting precipitate was collected to give **4** as a crude solid (isomeric mixture of E/Z=1/1), which was purified by chromatography on a silica gel with chloroform–methanol (6 : 1) as an eluent. The yield was 3.9 g (87.1%). The isomeric mixture was separated in the same manner as described for **3a** and **3b**. From the first eluate, the free base of **4a** was obtained and converted into the hydrochloride (**4a**·HCl) by the treatment with dioxane–hydrogen chloride. mp 213—215 °C. ^{1}H-NMR (DMSO-d_6) δ: 0.85 (3H, t, J=6.8 Hz), 2.05 (3H, s), 2.42 (2H, q), 2.79 (6H, s), 4.20 (2H, br t), 5.05 (1H, s), 5.41 (1H, s), 6.60—6.85 (6H, m), 6.98 (2H, d, J=9.0 Hz), 7.08 (2H, d, J=8.4 Hz), 7.34 (2H, d, J=8.4 Hz), 9.47 (1H, s), 10.01 (1H, br s). MS m/z: 427 (M^+). *Anal.* Calcd for $C_{29}H_{33}NO_2$·HCl: C, 75.06; H, 7.38; N, 3.02. Found: C, 74.60; H, 7.34; N, 2.96. From the second eluate, the free base of **4b** was obtained and converted into the hydrochloride (**4b**·HCl) in the same manner as described for **4a**·HCl. mp 128—130 °C. ^{1}H-NMR (DMSO-d_6) δ: 0.85 (3H, t, J=6.8 Hz), 2.06 (3H, s), 2.40 (2H, q), 2.86 (6H, s), 3.52 (2H, br t), 4.36 (2H, br t), 5.05 (1H, s), 5.41 (1H, s), 6.43 (2H, d, J=8.5 Hz), 6.63 (2H, d, J=8.5 Hz), 6.99 (2H, d, J=9.2 Hz), 7.07 (2H, d, J=8.2 Hz), 7.15 (2H, d, J=9.2 Hz), 7.34 (2H, d, J=8.2 Hz), 9.23 (1H, s), 10.25 (1H, br s). MS m/z: 427 (M^+). *Anal.* Calcd for $C_{29}H_{33}NO_2$·HCl: C, 75.06; H, 7.38; N, 3.02. Found: C, 74.61; H, 7.34; N, 2.96.

(*Z*)- and (*E*)-2-[4-(1,2-Dihydroxy-1-methylethyl)phenyl]-1-[4-[2-(dimethylamino)ethoxy]phenyl]-1-(4-hydroxyphenyl)-1-butene (5a and 5b) OsO_4 (1.0 g) was added to a solution of **4** (2.0 g) in pyridine (15 ml). After stirring at room temperature for 5 h, the reaction mixture was added to a solution consisting of sodium sulfite (1.8 g), pyridine (20 ml) and water (30 ml), then stirred at the same temperature for 1 h. The whole was

extracted with chloroform (100 ml × 2), dried over sodium sulfate and the organic layer was evaporated under reduced pressure to give **5** as a crude oil (isomeric mixture of $E/Z=1/1$), which was purified by chromatography on a silica gel column with chloroform–ethanol (5 : 1) as an eluent. The yield was 1.3 g (60.2%). The isomeric mixture was separated in the same manner as described for **3a** and **3b**. From the first eluate, *Z*-isomer (**5a**) was obtained. mp 147—149 °C. ^{1}H-NMR (DMSO-d_6) δ: 0.84 (3H, t, $J=6.8$ Hz), 1.33 (3H, s), 2.15 (6H, s), 3.35 (2H, br s), 3.89 (2H, t, $J=5.8$ Hz), 4.60 (1H, t, $J=5.8$ Hz), 4.76 (1H, s), 6.56 (2H, d, $J=9.3$ Hz), 6.72 (2H, d, $J=9.3$ Hz), 6.74 (2H, d, $J=8.6$ Hz), 6.99 (2H, d, $J=8.6$ Hz), 7.01 (2H, d, $J=8.3$ Hz), 7.25 (2H, d, $J=8.3$ Hz), 9.39 (1H, s). MS *m/z*: 461 (M^+). *Anal.* Calcd for $C_{29}H_{35}NO_4\cdot 1/2H_2O$: C, 74.01; H, 7.71; N, 2.98. Found: C, 73.69; H, 7.67; N, 3.01. From the second eluate, *E*-isomer (**5b**) was obtained. mp 165—167 °C. ^{1}H-NMR (DMSO-d_6) δ: 0.86 (3H, t, $J=6.8$ Hz), 1.34 (3H, s), 2.23 (6H, s), 2.64 (2H, t, $J=5.7$ Hz), 3.35 (2H, br s), 4.05 (2H, t, $J=5.7$ Hz), 4.62 (1H, br t), 4.76 (1H, s), 6.39 (2H, d, $J=8.5$ Hz), 6.61 (2H, d, $J=8.5$ Hz), 6.91 (2H, d, $J=8.5$ Hz), 7.00 (2H, d, $J=8.3$ Hz), 7.08 (2H, d, $J=8.5$ Hz), 7.26 (2H, d, $J=8.3$ Hz), 9.15 (1H, s). MS *m/z*: 461 (M^+). *Anal.* Calcd for $C_{29}H_{35}NO_4\cdot 1/2H_2O$: C, 74.01; H, 7.71; N, 2.98. Found: C, 74.13; H, 7.93; N, 2.90.

(*Z*)- and (*E*)-1-[4-[2-(Dimethylamino)ethoxy]phenyl]-2-[4-(2-hydroxy-1-methylethyl)phenyl]-1-(4-hydroxyphenyl)-1-butene (6a and 6b) Compound (**4**) (2.43 g) was added to a solution of 9-BBN (2.68 g) in benzene (80 ml) under a nitrogen atmosphere. After stirring under reflux for 10 h, the reaction mixture was evaporated under reduced pressure and the residue was dissolved in methanol (60 ml). 28% sodium methoxide–methanol (14.2 ml) followed by 30% hydrogen peroxide (7.9 ml) were carefully added to the above solution under ice-cooling. After stirring at 50 °C for 2.5 h, the reaction mixture was concentrated to 1/3 volume, then added to a 5% aqueous potassium carbonate (100 ml) and extracted with chloroform (100 ml × 2). The organic layer was dried over sodium sulfate and evaporated under reduced pressure to give **6** as a crude oil (isomeric mixture of $E/Z=1/1$), which was purified in the same manner as described for **5**. The yield was 1.12 g (44.3%). The isomeric mixture was separated in the same manner as described for **3a** and **3b**. From the first eluate, *Z*-isomer (**6a**) was obtained. mp 126—128 °C. ^{1}H-NMR (DMSO-d_6) δ: 0.84 (3H, t, $J=7.0$ Hz), 1.14 (3H, t, $J=6.8$ Hz), 2.15 (6H, s), 2.74 (2H, t, $J=5.7$ Hz), 3.10—3.60 (2H, m), 3.89 (2H, t, $J=5.7$ Hz), 4.59 (1H, t, $J=5.6$ Hz), 6.56 (2H, d, $J=8.9$ Hz), 6.71 (2H, d, $J=8.9$ Hz), 6.73 (2H, d, $J=8.6$ Hz), 6.96 (2H, d, $J=8.6$ Hz), 7.01 (4H, s), 9.38 (1H, s). MS *m/z*: 445 (M^+). *Anal.* Calcd for $C_{29}H_{35}NO_3$: C, 78.17; H, 7.92; N, 3.14. Found: C, 78.11; H, 7.75; N, 3.09. From the second eluate, *E*-isomer (**6b**) was obtained. mp 155—157 °C. ^{1}H-NMR (DMSO-d_6) δ: 0.83 (3H, t, $J=7.0$ Hz), 1.14 (3H, d, $J=6.8$ Hz), 2.22 (6H, s), 2.82 (2H, t, $J=5.6$ Hz), 3.10—3.60 (2H, m), 4.04 (2H, t, $J=5.6$ Hz), 4.60 (1H, br t), 6.39 (2H, d, $J=8.6$ Hz), 6.60 (2H, d, $J=8.6$ Hz), 6.90 (2H, d, $J=8.8$ Hz), 7.06 (2H, d, $J=8.8$ Hz), 7.01 (4H, s), 9.16 (1H, s). MS *m/z*: 445 (M^+). *Anal.* Calcd for $C_{29}H_{35}NO_3$: C, 78.17; H, 7.92; N, 3.14. Found: C, 78.09; H, 8.10; N, 3.06.

(*Z*)- and (*E*)-1-(4-Hydroxyphenyl)-2-(4-isopropylphenyl)-1-[4-[2-(methylamino)ethoxy]phenyl]-1-butene Hydrochloride (7a and 7b) Compound (**2**) (3.82 g) was added to a solution of vinyloxycarbonyl chloride (1.81 ml) in dioxane (90 ml) in a sealed tube and heated in an oil bath at 170 °C for 5 h. The reaction mixture was evaporated under reduced pressure and then the residue was dissolved in 5% hydrogen chloride–ethanol solution (40 ml). After stirring at 80 °C for 0.5 h, the whole was evaporated under reduced pressure to give **7** as a crude oil (isomeric mixture of $E/Z=1/1$), which was purified by chromatography on a silica gel column with chloroform–methanol (7 : 1) as an eluent. The yield was 1.96 g (53.1%). The isomeric mixture was separated in the same manner as described for **4a** and **4b**. From the first eluate, the free base of *Z*-isomer (**7a**) was obtained. **7a**·HCl was prepared by working up in the same manner as described for **4a**·HCl or **4b**·HCl. **7a**·HCl: mp 210—212 °C. ^{1}H-NMR (DMSO-d_6) δ: 0.83 (3H, t, $J=6.8$ Hz), 1.15 (6H, d, $J=6.8$ Hz), 2.40 (2H, q, $J=6.8$ Hz), 2.56 (3H, s), 2.80 (1H, m), 3.22 (2H, br t), 4.11 (2H, br t), 6.50—7.00 (8H, m), 7.03 (4H, s), 8.93 (2H, br s), 9.46 (1H, s). MS *m/z*: 415 (M^+). *Anal.* Calcd for $C_{28}H_{33}NO_2\cdot HCl$: C, 74.40; H, 7.58; N, 3.10. Found: C, 74.64; H, 7.48; N, 3.11. From the second eluate, the free base of *E*-isomer (**7b**) was obtained. **7b**·HCl: mp 195—197 °C. ^{1}H-NMR (DMSO-d_6) δ: 0.84 (3H, t, $J=6.8$ Hz), 1.15 (6H, d, $J=6.8$ Hz), 2.38 (2H, q, $J=6.8$ Hz), 2.62 (3H, s), 3.30 (2H, br s), 4.27 (2H, t, $J=5.5$ Hz), 6.40 (2H, d, $J=8.8$ Hz), 6.60 (2H, d, $J=8.8$ Hz), 6.89 (2H, d, $J=8.6$ Hz), 7.03 (4H, s), 7.13 (2H, d, $J=8.6$ Hz), 9.10 (2H, br s), 9.22 (1H, s). MS *m/z*: 415 (M^+). *Anal.* Calcd for $C_{28}H_{33}NO_2\cdot HCl$: C, 74.40; H, 7.58; N, 3.10. Found: C, 74.37; H, 7.28; N, 3.06.

(*Z*)- and (*E*)-2-[4-(2-Hydroxy-1-methylethyl)phenyl]-1-(4-hydroxyphenyl)-1-[4-[2-(methylamino)ethoxy]phenyl]-1-butene (8a and 8b) Compound (**6**) (1.78 g) was added to a solution of vinyloxycarbonyl chloride (1.7 ml) in dichloromethane (40 ml) in a sealed tube and heated in an oil bath at 170 °C for 6 h. The reaction mixture was evaporated under reduced pressure and then the residue was dissolved in ethanol (50 ml) and added to 4 N NaOH (10 ml). After stirring under reflux for 5 h, the whole was evaporated under reduced pressure to give **8** as a crude solid (isomeric mixture of $E/Z=1/1$), which was purified by chromatography on a silica gel with chloroform–methanol–triethylamine (10 : 1 : 1) as an eluent. The yield was 1.06 g (61.5%). The isomeric mixture was separated in the same manner as described for **3a** and **3b**. From the first eluate, *Z*-isomer (**8a**) was obtained. mp 155—157 °C. ^{1}H-NMR (DMSO-d_6) δ: 0.83 (3H, t, $J=7.0$ Hz), 1.14 (2H, d, $J=6.8$ Hz), 2.28 (3H, s), 2.73 (2H, t, $J=5.6$ Hz), 3.10—3.50 (2H, m), 3.85 (2H, t, $J=5.6$ Hz), 4.55 (1H, br s), 6.56 (2H, d, $J=9.1$ Hz), 6.71 (2H, d, $J=9.1$ Hz), 6.73 (2H, d, $J=8.6$ Hz), 6.97 (2H, d, $J=8.6$ Hz), 7.00 (4H, s). MS *m/z*: 431 (M^+). *Anal.* Calcd for $C_{28}H_{33}NO_3$: C, 77.93; H, 7.71; N, 3.25. Found: C, 77.88; H, 7.68; N, 3.13. From the second eluate, *E*-isomer (**8b**) was obtained. mp 180—182 °C. ^{1}H-NMR (DMSO-d_6) δ: 0.84 (3H, t, $J=6.8$ Hz), 1.14 (3H, d, $J=6.8$ Hz), 2.34 (3H, s), 2.82 (3H, t, $J=5.6$ Hz), 3.00—3.50 (2H, m), 4.01 (2H, t, $J=5.6$ Hz), 4.55 (1H, br s), 6.39 (2H, d, $J=8.5$ Hz), 6.61 (2H, d, $J=8.5$ Hz), 6.91 (2H, d, $J=8.7$ Hz), 7.01 (4H, s), 7.05 (2H, d, $J=8.7$ Hz). MS *m/z*: 431 (M^+). *Anal.* Calcd for $C_{28}H_{33}NO_3$: C, 77.93; H, 7.71; N, 3.25. Found: C, 77.97; H, 7.61; N, 3.18.

Binding Affinity toward Estrogenic Receptor (*in Vitro*)[14] Uterus and tumors from female rats were obgained as soon as possible after decapitation, and stored under −80 °C until use. Tissues were homogenized in the buffer (20 mM Tris, 1.5 mM ethylenediaminetetraacetic acid (EDTA), 5% glycerol, 12 μM monothioglycerol, pH 7.8) using a Bitron homogenizer. The homogenate was then centrifuged at 105000 × *g* for 1 h, and the supernatant was subjected to an estrogenic receptor (ER) binding assay. In order to distinguish between specific and non-specific binding capacity, the non-specific binding was measured by using a 100-fold excess of non-radioactive estradiol. Relative binding affinity toward ER of uterine cytosol was determined in the competition experiments (18 h at 4 °C) using 5 nM (^{3}H)-estradiol (105 Ci/mmol) and increasing concentrations of antiestrogens or unlabeled estradiol. Relative binding affinity (RBA) is expressed by the following equation.

$$\mathrm{RBA}=\frac{\mathrm{IC_{50}\ of\ estradiol}}{\mathrm{IC_{50}\ of\ test\ compound}}\times 100$$

Antiuterotrophic Activity (*in Vivo*)[15] Female Sprague-Dawley rats (4 weeks old, 7 rats/group) were used to determine antiuterotrophic activities of the compounds. In order to estimate the value of inhibition without endogenous estrogen, the animals were ovariectomized under ether anesthesia. The rats were injected intraperitoneally for 3 d at daily doses of 40 μg/kg of each metabolite and 0.5 μg/body of estradiol as a control. Animals were sacrificed on the fourth day, and the wet weight of the uterus was measured. Percent inhibition of uterine growth was calculated based on the wet weight of the uterus using the following equation.

$$\text{inhibition }\%=\frac{(\text{control}-\text{tested})}{(\text{control}-\text{ovariectomized})}\times 100$$

References

1) A part of the present work was presented at the 16th International Congress of Chemotherapy, Jerusalem, Israel, June 1989, Abstracts of Papers, p. 281.
2) S. S. Legha. H. L. Davis, and F. M. Muggia, *Ann. Intern. Med.*, **88**, 69 (1978).
3) *a*) L. Kangas, A. L. Nieminen, G. Blanco, M. Gronroos, S. Kallio, A. Karjalainen, M. Perila, M. Södervall, and R. Toivola, *Cancer Chemother. Pharmacol.*, **17**, 109 (1986); *b*) W. Roos, L. Oeze, R. Lösen, and V. Eppenberger, *J. Natl. Cancer. Inst.*, **71**, 55 (1983).
4) T. Asao, T. Toko, Y. Sugimoto, S. Takeda, Y. Yamada, K. Ogawa, and M. Yasumoto, The 16th International Congress of Chemotherapy, Jerusalem, Israel, June 1989, Abstracts of Papers, p. 248.
5) P. K. Yonan, R. L. Novotney, C. M. Woo, K. A. Prodan, and F. M. Hershenson, *J. Med. Chem.*, **23**, 1102 (1980).
6) *a*) P. C. Ruenitz, J. R. Bagley, and C. M. Mokler, *J. Med. Chem.*, **25**, 1056 (1982); *b*) D. W. Robertson and J. A. Katzenellenbogen, *J. Org. Chem.*, **47**, 2387 (1982).
7) A. B. Foster, M. Jarman, O. T. Leung, R. McCague, G. Leclercq, and N. Devleeschouwer, *J. Med. Chem.*, **28**, 1491 (1985).

8) J. S. Baran, *J. Org. Chem.*, **25**, 257 (1960).
9) C. G. Scouten and H. C. Brown, *J. Org. Chem.*, **38**, 4092 (1973).
10) R. A. Olofson, R. C. Schnur, L. Bunes, and J. P. Pepe, *Tetrahedron Lett.*, **1977**, 1567.
11) J. Shani, A. Gazit, T. Livshitz, and S. Biran, *J. Med. Chem.*, **28**, 1504 (1985).
12) M. Makosza and A. Jonczyk, "Organic Syntheses," Coll. Vol. VI, ed. by W. E. Noland, John Wiley and Sons, Inc., New York, 1988, p. 897.
13) W. E. Parham and E. L. Anderson, *J. Am. Chem. Soc.*, **70**, 4187 (1948).
14) A. E. Wakeling, "Steroid Hormones," ed. by B. Green and R. E. Leake, IRL Press Ltd., Washington D.C., 1987, pp. 219—236.
15) V. C. Jordan, M. M. Collins, L. Rowsby, and G. Prestwich, *J. Endocrinol.*, **75**, 305 (1977).

Reduction of 2,3,5-Trimethyl-6-(3-pyridylmethyl)-1,4-benzoquinone by PB-3c Cells and Biological Activity of Its Hydroquinone

Shigenori OHKAWA,*[,a] Takashi TERAO,[a] Morio MURAKAMI,[a] Tatsumi MATSUMOTO,[a] and Giichi GOTO[a]

Chemistry Research Laboratories[a] and Biology Research Laboratories,[b] Research and Development Division, Takeda Chemical Industries, Ltd., 17–85 Jusohonmachi 2-chome, Yodogawa-ku, Osaka 523, Japan. *Received August 27, 1990*

2,3,5-Trimethyl-6-(3-pyridylmethyl)-1,4-benzoquinone (CV-6504) has inhibitory activities on both thromboxane A_2 synthase and 5-lipoxygenase as well as scavenging activity against active oxygen species. The latter two activities are closely related to the quinone moiety, which is reduced to a hydroquinone in the living body. Comparison of these two activities for both the quinone and hydroquinone showed that the hydroquinone form had superior activities. Concerning the reduction mechanism by PB-3c cells we can see that superoxide dismutase (SOD) has no influence on the rate of reduction, but dicumarol almost completely inhibits the reduction at a concentration greater than 1×10^{-6} M. Therefore, it can be concluded that CV-6504 is reduced mainly by two electron donating enzymes without the intermediary of a semiquinone radical and that the resulting hydroquinone inhibits lipid peroxidation as well as 5-lipoxygenase activity.

Keywords quinone derivative; CV-6504; hydroquinone 5-lipoxygenase inhibitor; radical scavenger; thromboxane A_2 synthase inhibitor; biological reduction; PB-3c cell; RBL-1 cell; stopped-flow technic

We reported previously that 2,3,5-trimethyl-6-(3-pyridylmethyl)-1,4-benzoquinone (CV-6504) had inhibiting activities against thromboxane A_2 synthase, 5-lipoxygenase, and lipid peroxidation.[1] This compound is now under phase II clinical investigation for chronic glomerular nephritis in which thromboxane A_2 (TXA_2), leukotrienes (LTs), and active oxygen species (AOS) may play significant roles.[2] The mechanism of inhibition of thromboxane A_2 synthase by pyridine derivatives is well understood from the results of Ulrich *et al.*[3] Although there are many reports that quinone derivatives have an antioxidant activity[4] and an inhibiting activity on 5-lipoxygenase,[5] the mechanism of the quinone moiety involved in these activities is still not clear.

Recently, some important results concerning 5-lipoxygenase activity have been reported which show that hydroperoxides activate the enzyme,[6] whereas antioxidants such as phenols and catechols inhibit it.[7] These mechanisms of action are probably related to the redox of the metal, which is presumably an iron atom, existing in the active center of the enzyme. The hydroperoxides oxidize the ferrous iron (resting state) to the ferric state (active state) for activation of the enzyme.[8] By contrast, antioxidants reduce ferric iron to the ferrous state and also reduce the concentration of hydroperoxides, both of which result in inhibition of the enzyme. Since a reducing ability is necessary for the inhibition of both 5-lipoxygenase and lipid peroxidation, we assumed that the active form of CV-6504 is its hydroquinone form (Fig. 1).

In order to clarify the reaction mechanism of CV-6504, we investigated the inhibitory effects of CV-6504 itself and its hydroquinone form on 5-lipoxygenase and radical scavenging activities. We also tried to examine the reduction of CV-6504 by various cells as a model of the living body and to determine the reduction mechanism involved.

Materials and Methods

Materials CV-6504 was prepared as previously described.[1] CV-6504 hydroquinone was prepared by the reduction of CV-6504 using sodium hydrosulfite. Commercial galvinoxyl 2,2-diphenyl-1-picrylhydrazyl hydrate

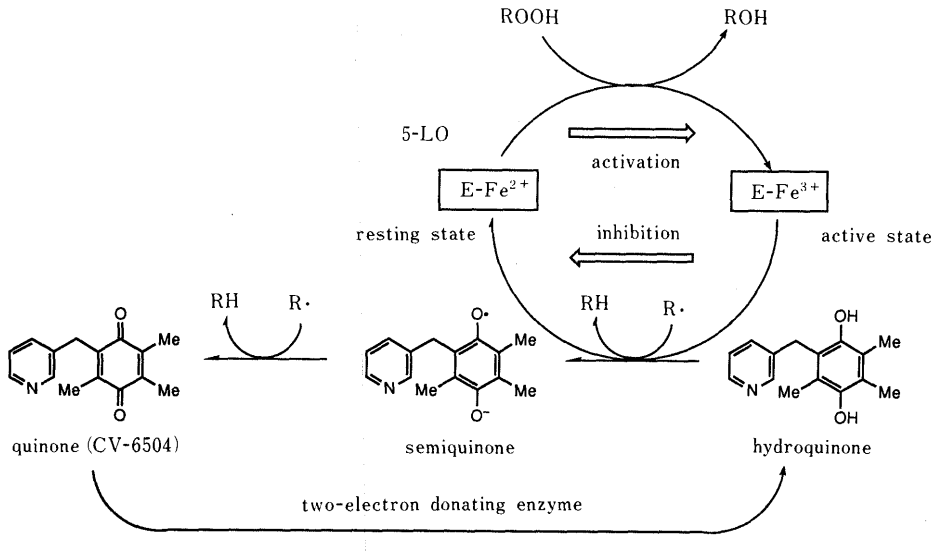

Fig. 1. Redox Cycle of CV-6504

R represents various radicals such as the hydroxy radical, hydroperoxyradical, galvinoxyl and DPPH, ROOH and ROH represent a lipid hydroperoxide and a lipid hydroxide respectively.

(DPPH), dicumarol, and superoxide dismutase (SOD from bovine erythrocytes) were used as received.

Cell Culture RBL-1 cells were kindly supplied by Dr. J. R. Vane. PB-3c cells were kindly supplied by Drs. T. Shimizu and K. Tadokoro.[9] The smooth muscle cells of rat aorta were prepared as previously described.[10] The endothelium of the bovine pulmonary artery was supplied by ATCC (American type culture collection) cell line.

Reactions with Stable Radicals The stopped-flow data were obtained on a Hitachi Double Wavelength Spectrophotometer Model 557 with stopped-flow accessory. Decay plots of DPPH (0.2 mM) in the presence of CV-6504 (0.5 mM) or its hydroquinone (0.063—0.5 mM) were observed at 515 nm (reference: 420 nm) in ethanol. Similarly, decay plots of galvinoxyl (0.01 mM) in the presence of CV-6504 (0.5 mM) or its hydroquinone (0.063—0.5 mM) were observed at 428 nm (reference: 500 nm) in ethanol. The reactions were studied under pseudo-first-order conditions, and the observed rate constants, k_{obsd}, were calculated in the usual way using a standard least-squares analysis. All measurements were performed at 25.0 ± 0.5 °C.

Electron spin resonance (ESR) measurements were carried out using a JEOL JES-RE3X spectrometer.

Preparation of 5-Lipoxygenase The preparation of leucocytes was mainly based on the method of Sbarra and Karnovsky.[11] A sterile 2% casein solution (one-tenth volume of body weight) was injected intraperitoneally to guinea pigs weighing 450—650 g. After 14—16 h, the guinea pigs were killed by bleeding from the carotid artery. The peritoneal exudate was collected. The peritoneal cavity was washed with about 30 ml of physiological saline containing a 10 mM potassium phosphate buffer at pH 7.4. The exudate was filtered through four layers of gauze, followed by centrifugation at $450 \times g$ for 5 min. Cell pellets were suspended in water for 30 s to allow for lysis of the contaminating red cells. After centrifugation at $200 \times g$ for 5 min, the cells were suspended in a 50 mM Hepes buffer at pH 8.0. Analysis of the cell composition indicated that more than 85% of the cells were polymorphonuclear leukocyte (PMNL). The PMNL suspension was subjected to sonic disruption at 20 kHz for 15 s using a Branson sonifier. The sonicate was centrifuged at $10000 \times g$ for 20 min, and the supernatant was referred to as the enzyme preparation.

Assay of 5-Lipoxygenase Activity 5-Lipoxygenase activity was determined by the method of Ueda *et al.*[12] The standard mixture for the 5-lipoxygenase assay contained a 50 mM potassium phosphate buffer at pH 7.4, 2 mM $CaCl_2$, 2 mM adenosin triphosphate (ATP), 25 μM [1-^{14}C] arachidonic acid (50000 cpm, 5 μl of ethanol solution), and 200 μl of enzyme preparation. The reaction was initiated by the addition of [1-^{14}C] arachidonic acid, continued at 25 °C for 3 min, and then terminated by the addition of 0.4 ml of an ice-cold mixture of ethyl ether/methanol/0.2 M citric acid (30/4/1). The organic layer was spotted onto a silica gel plate in a cold room at 4 °C. Thin layer chromatography was carried out with a solvent system of ethyl ether/petroleum ether/acetic acid (85/15/0.1) at −10 °C for 18 min. Radioactivity on the plate was monitored by autoradiography. For quantitative determination of the enzyme activity, the silica gel zones corresponding to authentic arachidonic acid and its metabolite were scraped, and radioactivity was determined using a liquid scintillation counter.

Reduction of CV-6504 by Various Cells The experiments for cell reduction were carried out using RBL-1 cells, PB-3c cells, smooth muscle cells of the rat aorta, and the endothelium of the bovine pulmonary artery. To a suspension of cells (2×10^6/ml) in a phosphate buffer (pH 7.0, 3 ml) was added a solution of CV-6504 (1 mM) in ethanol (100 μl), and the ultraviolet (UV) spectrum was measured on a Hitachi Double Wavelength Spectrophotometer Model 557. In order to investigate the effects of SOD and dicumarol, SOD (60 units) and dicumarol (0.012, 0.024, 0.060, 0.12, 0.30 and 1.20 μM) were added before the addition of CV-6504. The absorbance was monitored at 260 nm.

Results and Discussion

In the reaction of CV-6504 hydroquinone (CV-6504 HQ) with DPPH, the ESR signal of DPPH disappeared on addition of the CV-6504 hydroquinone (Fig. 2A), when the molar ratio of CV-6504 hydroquinone to DPPH was higher than 0.5. The results indicated that 1 mol of CV-6504 hydroquinone could scavenge 2 mol of DPPH. Similar results were obtained in the case of galvinoxyl (Galv) (Fig. 2B). The reaction product of CV-6504 hydroquinone with

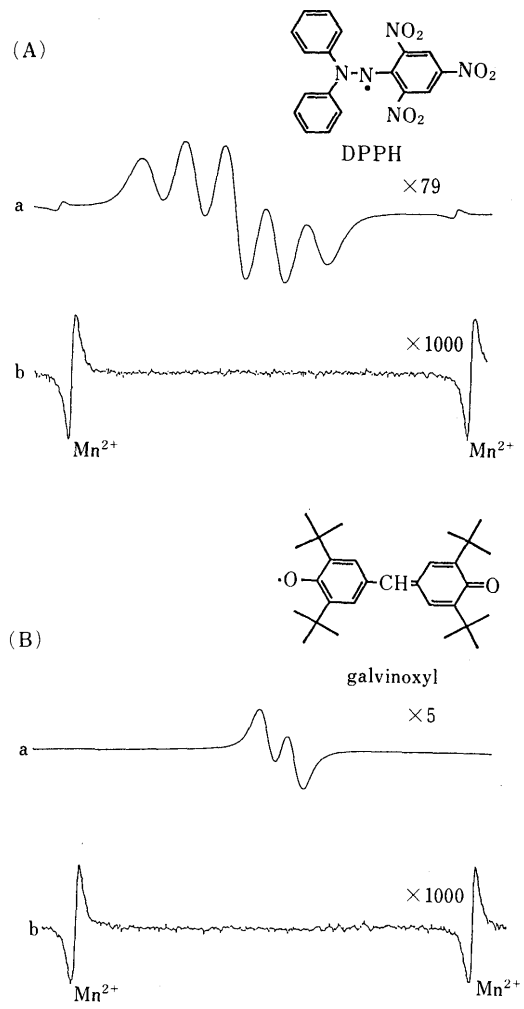

Fig. 2. (A) ESR Spectrum of DPPH (0.52 mM) Before (a) and After (b) the Addition of CV-6504 Hydroquinone (1.0 mM)
(B) ESR Spectrum of Galvinoxyl (0.49 mM) Before (a) and After (b) the Addition of CV-6504 Hydroquinone (1.0 mM)

these radicals were identified as CV-6504 by infrared spectrum. However, CV-6504 itself could not scavenge either DPPH or galvinoxyl. In order to determine the rate constant of the reaction between CV-6504 hydroquinone and DPPH or galvinoxyl, the stopped-flow technic[13] was applied. Figure 3A shows the decay plots of galvinoxyl observed when galvinoxyl (0.01 mM in ethanol) was mixed with CV-6504 hydroquinone (0.063—0.5 mM in ethanol). The pseudo-first-order rate constants, k_{obsd}, obtained by monitoring at 428 nm (reference: 500 nm), were linearly dependent on the concentration of CV-6504 hydroquinone (Fig. 3B). The rate law is expressed as

$$-d[\text{Galv}]/dt = k_{obsd}[\text{Galv}] = k[\text{CV-6504 HQ}][\text{Galv}]$$

where k is the second-order rate constant for oxidation of CV-6504 hydroquinone by galvinoxyl. The values of k calculated from k_{obsd} was 2473 s^{-1} M^{-1}. Similar results were obtained in the case of DPPH, and a rate constant of 385 s^{-1} M^{-1} was determined. These values of rate constant are greater than that of α-tocopherol. (The rate constants for oxidation of α-tocopherol with galvinoxyl and DPPH were determined as 1400 and 242 s^{-1} M^{-1}, respectively, in the same method). Therefore, the hydroquinone form of CV-6504 has sufficient ability to inhibit lipid peroxidation

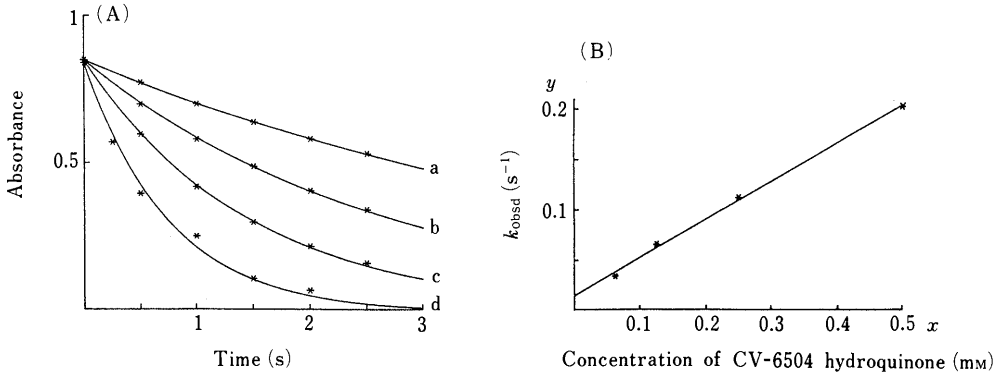

Fig. 3. (A) Decay Plots of Galvinoxyl in the Presence of CV-6504 Hydroquinone

a, 0.063; b, 0.125; c, 0.25; d, 0.50 mM; at 25 °C observed at 428 nm (reference: 500 nm), solvent: ethanol.

(B) The Dependence of the Pseudo-First-Order Rate Constant, $k_{obsd}(y)$, on the Concentration of CV-6504 Hydroquinone (x) in Ethanol

$y=0.0145+0.3768x$, $r^2=0.9976$.

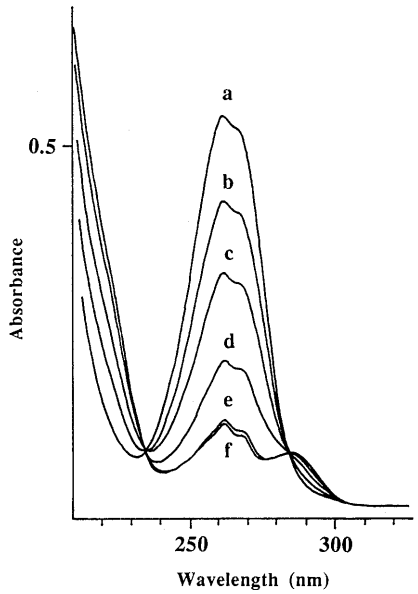

Fig. 4. Spectral Changes of CV-6504 with PB-3c (2×10^6/ml) Cells in a Phosphate Buffer (pH 7.0)

a, 0 min; b, 2 min; c, 4 min; d, 6 min; e, 8 min; f, 10 min.

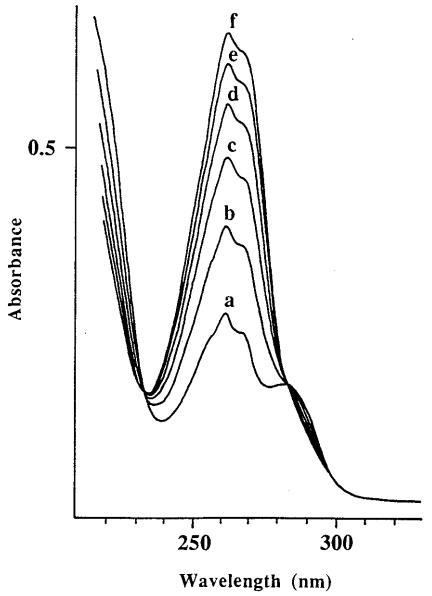

Fig. 5. Spectral Changes of CV-6504 Hydroquinone in Oxidation by Air

a, 0 min; b, 10 min; c, 20 min; d, 30 min; e, 40 min; f, 50 min.

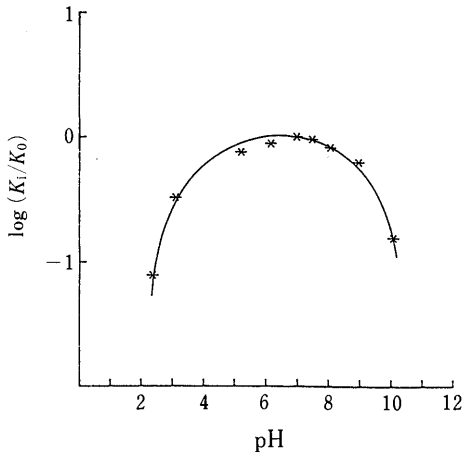

Fig. 6. The Influence of pH on the Rate of Reduction of CV-6504 by PB-3c Cells

K_i, the rate of reduction at each pH; K_0, the rate of reduction at pH 7.0.

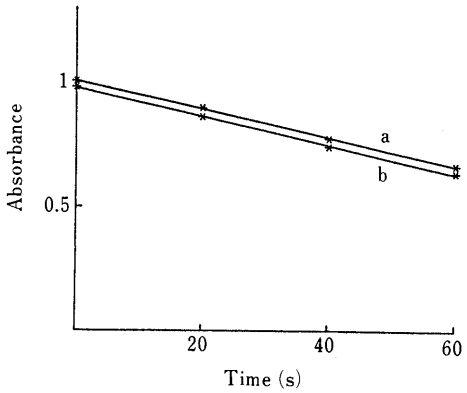

Fig. 7. Effect of SOD (60 Units) on the Reduction of CV-6504 by PB-3c Cells

caused by oxygen radicals.

The inhibitory effects of CV-6504 and its hydroquinone on the activity of 5-lipoxygenase are shown in Table I. 5-Lipoxygenase was prepared from guinea-pig PMN. CV-6504 hydroquinone is superior to CV-6504 alone in inhibiting 5-lipoxygenase. These results suggest that CV-6504 hydroquinone is active in the inhibition of both lipid peroxidation and 5-lipoxygenase activity in the living body.

To model reduction after the living body, we tried

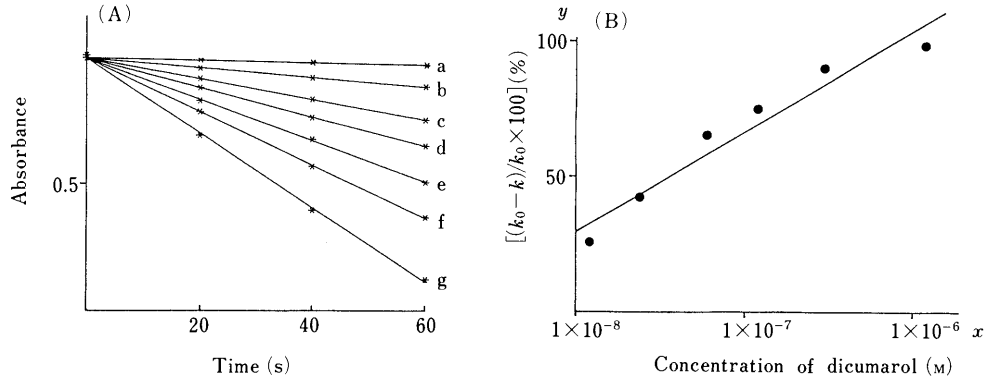

Fig. 8. (A) Effect of Dicumarol

a, 1.2; b, 0.30; c, 0.12; d, 0.060; e, 0.024; f, 0.012; g, 0 μM; on the reduction of CV-6504 (0.03 mM) by PB-3c cells. The absorbance was monitored at 260 nm.

(B) Plots of the Inhibition of the Reduction Rate of CV-6504

$[(k_0-k)/k_0\times100]$ *versus* concentration of dicumarol (k: the rate constant with dicumarol, k_0: the rate constant without dicumarol). $y=326.9+37.19\log x$, $r=0.969$.

TABLE I. 5-Lipoxygenase Inhibitory Activity of CV-6504 and Its Hydroquinone

Compounds	Conc. (M)	No. of expt.	Product[a] (nmol)	Inhibition (%)	IC_{50} (M)
Vehicle		3	2.42±0.07		
	10^{-6}	3	1.78±0.09	26.4	
CV-6504	10^{-5}	3	1.68±0.06	30.6	1.0×10^{-4}
	10^{-4}	3	1.21±0.10	50.0	
CV-6504	10^{-6}	3	1.77±0.10	27.1	
Hydroquinone	10^{-5}	3	0.86±0.07	64.1	4.2×10^{-6}
	10^{-4}	3	0.03±0.01	98.9	

a) Values represent means±SEM.

reduction of CV-6504 using various kinds of cells. Figure 4 shows the spectral change observed when CV-6504 (100 nmol) was added to a suspension of PB-3c cells (2×10^6/ml, 3 ml). A similar spectral change was observed in the case of both RBL-1 cells and the smooth muscle cells of the rat aorta. The reverse spectral change was observed when CV-6504 hydroquinone was oxidized by air (Fig. 5). The endothelium of the bovine pulmonary artery, however, was unable to reduce CV-6504. Therefore, the endothelium seems to have no enzyme which is able to reduce quinone, which is different from the other types of cells. The influence of pH on the rate of reduction of CV-6504 by PB-3c cells was investigated and a pH of 7.0 was found to be optimal, the rate decreasing both above and below this value (Fig. 6).

Thus it seems as though reduction by these cells might involve either reduction in the medium by superoxide anion generated by the cells[14] or reduction by one-electron donating enzymes such as reduced nicotineamide adenine dinucleotide (NADPH)-cytochrome P-450 reductase[15] or reduction by two electron donating enzymes such as DT-diaphorase.[15] In our study, SOD did not affect the spectral change significantly in the case of CV-6504 and PB-3c cells (Fig. 7), but dicumarol, which is known as an inhibitor of DT-diaphorase, reduced the rate of reduction in a dose-dependent manner and almost completely inhibited the reduction at a concentration greater than 1×10^{-6} M (Fig. 8). Therefore, it can be concluded that CV-6504 was reduced mainly by two-electron donating enzymes without intermediation of the semiquinone radical. The resulting hydroquinone inhibits both 5-lipoxygenase activity and lipid peroxidation on the basis of its antioxidative ability. Although the semiquinone radical is generated when the hydroquinone scavenges a reactive radical, it immediately reacts with another reactive radical to afford quinone (Fig. 1). The quinone is efficiently recycled by the enzyme reduction. Since the semiquinone radicals produced by one-electron reduction sometimes cause side effects like adriamycin,[16] these features of CV-6504 seem to be favorable for medicine.

It can thus be concluded that in the living body, 5-lipoxygenase inhibitors and antioxidants having a quinone moiety are rapidly reduced to their hydroquinones by a two-electron donating enzyme, and the resulting hydroquinones exhibit 5-lipoxygenase inhibiting activity and antioxidative activity.

Acknowledgement We are indebted to Drs. T. Shimizu and K. Tadokoro (Faculty of Medicine, University of Tokyo) for providing PB-3c cells. We wish to thank Dr. S. Terao for the insightful discussions on the reduction of quinones by cells. Thanks are also due to Dr. D. Murphy for reviewing the manuscript.

References and Notes

1) S. Ohkawa, S. Terao, Z. Terashita, Y. Shibouta, and K. Nishikawa, *J. Med. Chem.*, **34**, 267 (1991). The IC_{50} values of CV-6504 on thromboxane A_2 synthase (human blood), on 5-lipoxygenase (human blood), and on lipid peroxidation (rat brain homogenate) are 0.33, 0.36, and 1.8 μM respectively.
2) *a*) G. Remuzzi, L. Imberit, M. Rossini, C. Morelli, C. Carminati, G. M. Cattanso, and T. Bertani, *J. Clin. Invest.*, **75**, 94 (1985); *b*) J. Failer, A. Wiemeyer, K. H. Marx, K. Kuhn, K. M. Koch, and J. C. Frolich, *Kidney Int.*, **36**, 46 (1989); *c*) A. Rehan, K. J. Johnson, R. C. Wiggins, R. G. Kunkel, and P. A. Ward, *Lab. Invest.*, **51**, 396 (1984).
3) M. Hecker, M. Haurand, V. Ulrich, and S. Terao, *Eur. J. Biochem.*, **157**, 217 (1986).
4) E. D. Wills, *Biochem. Pharmacol.*, **21**, 1879 (1972).
5) Y. Yoshimoto, C. Yokoyama, K. Ochi, S. Yamamoto, Y. Maki, Y. Ashida, S. Terao, and M. Shiraishi, *Biochim. Biophys. Acta*, **713**, 470 (1982).
6) C. A. Rouzer and B. Samuelsson, *FEBS Lett.*, **204**, 293 (1986).
7) C. Kemal, P. L. Flamberg, R. K. Olson, and A. L. Shorter, *Biochemistry*, **26**, 7064 (1987).
8) R. W. Egan, Abstract from 21st National Medicinal Chemistry Symposium, Minneapolis, June 1988, p. 145.
9) T. Shimizu, T. Izumi, Y. Seyama, K. Tadokoro, O. Radmark, and B. Samuelsson, *Proc. Natl. Acad. Sci. U.S.A.*, **83**, 4175 (1986).
10) R. J. Ross, *Cell Biol.*, **50**, 172 (1971).
11) A. J. Sbarra and M. L. Karnovsky, *J. Biol. Chem.*, **234**, 1355 (1959).
12) N. Ueda, S. Kaneko, T. Yoshimoto, and S. Yamamoto, *J. Biol.*

Chem., **261**, 7982 (1986).
13) K. Mukai, Y. Watanabe, Y. Uemoto, and K. Ishizu, *Bull. Chem. Soc. Jpn.*, **59**, 3113 (1986).
14) K. Sugioka, M. Nakano, H. T. Nakano, H. Minakami, S. T. Kubota, and K. Ikegami, *Biochim. Biophys. Acta*, **936**, 377 (1988). We also confirmed that CV-6504 was reduced by the superoxide anion generated by xanthine–xanthine oxidase systems by monitoring UV spectra.
15) H. Thor, M. T. Smith, P. Hartzell, G. Bellomo, S. A. Jewel, and S. Orrenius, *J. Biol. Chem.*, **257**, 12419 (1982).
16) *a*) C. E. Myers, W. P. McGuire, R. Liss, I. Frim, K. Grotzinger, and R. C. Yound, *Science*, **197**, 165 (1977); *b*) R. D. Olson, R. C. Boerth, J. G. Gerber, and A. S. Nies, *Life Sci.*, **29**, 1393 (1981).

1,5-Benzoxathiepin Derivatives. III.[1] Optical Resolution of Methyl (±)-*cis*-3-Hydroxy-4-[3-(4-phenyl-1-piperazinyl)propyl]-3,4-dihydro-2*H*-1,5-benzoxathiepin-4-carboxylate Hydrochloride ((±)-CV-5197) with Selective 5-Hydroxytryptamine$_2$(5-HT$_2$)-Antagonistic Activity

Masakuni KORI,[a] Kazuhide KAMIYA,[a] Etsuo KURIHARA,[b] and Hirosada SUGIHARA*,[a]

Chemistry Research Laboratories,[a] and Biology Research Laboratories,[b] Takeda Chemical Industries, Ltd., 2–17–85, Jusohonmachi, Yodogawa-ku, Osaka 532, Japan. *Received October 19, 1990*

The selective 5-HT$_2$-receptor antagonist, methyl (±)-*cis*-3-hydroxy-4-[3-(4-phenyl-1-piperazinyl)propyl]-3,4-dihydro-2*H*-1,5-benzoxathiepin-4-carboxylate hydrochloride ((±)-CV-5197) was resolved in high optical purity using (*R*)-(−)- and (*S*)-(+)-1,1′-binaphthyl-2,2′-diyl hydrogen phosphates ((*R*)-(−)- and (*S*)-(+)-BNP). The absolute configuration of (+)-CV-5197 was determined to be 3*S*,4*R* by X-ray crystallographic analysis. In the binding assay, it was demonstrated that (+)-CV-5197 was a more active isomer (IC$_{50}$ = 23 nM ± 6.3) for 5-HT$_2$ receptor binding than the (−)-enantiomer (IC$_{50}$ = 1600 nM ± 82). (+)-CV-5197 completely inhibited the 5-HT-induced contraction of the isolated pig coronary artery at a concentration of 3×10^{-7} M, whereas (−)-CV-5197 showed little antagonistic activity, even at 3×10^{-4} M. Thus, the agreement between the results of the binding assays and the biological activities for the 3*S*,4*R* enantiomer of CV-5197 suggests that its physiological activity is probably exerted through 5-HT$_2$-receptor antagonism.

Keywords 1,5-benzoxathiepin derivative; methyl [3*S*,4*R*]-3-hydroxy-4-[3-(4-phenyl-1-piperazinyl)propyl]-3,4-dihydro-2*H*-1,5-benzoxathiepin-4-carboxylate hydrochloride; (+)-CV-5197; optical resolution; X-ray crystallographic analysis; absolute configuration; 5-HT$_2$-receptor antagonist

Multiple receptor subtypes have been proposed for 5-hydroxytryptamine (5-HT), and it has been established that the contraction of the vascular smooth muscle as well as platelet aggregation is mediated *via* 5-HT$_2$-receptors.[2] In a preceding paper,[1] we reported that a benzoxathiepin analogue, methyl *cis*-3-hydroxy-4-[3-(4-phenyl-1-piperazinyl)propyl]-3,4-dihydro-2*H*-1,5-benzoxathiepin-4-carboxylate hydrochloride (CV-5197) showed potent and selective 5-HT$_2$-receptor-blocking activity, and was chosen as a candidate for clinical trials. In order to clarify the mechanism of action and the pharmacological profile of CV-5197, obtaining the optically active isomer was essential. In this paper, we describe the optical resolution of racemic CV-5197, determination of the absolute stereochemistry of each enantiomer by X-ray crystallographic analysis, and the biological activity results.

Chemistry We aimed to resolve the basic form of CV-5197 with various kinds of optically active acids, and this goal has been achieved efficiently using both (*R*)-(−)- and (*S*)-(+)-1,1′-binaphthyl-2,2′-diyl hydrogen phosphates ((*R*)-(−)- and (*S*)-(+)-BNP). After allowing a mixture of 1 eq of the free base of CV-5197 and 0.78 of an equivalent of (*S*)-(+)-BNP to stand in acetone for 2 d in a refrigerator, a white crystalline solid was deposited. Recrystallization twice from methanol–acetone (2 : 3 v/v) gave the salt of (−)-CV5197 free base and (*S*)-(+)-BNP with a constant optical rotation value, as colorless needles in a 92% yield, mp 224 °C, $[\alpha]_D^{23}$ +173.7° (*c* = 0.985, MeOH). The base liberated from the salt following partitioning between methylene chloride and 1 N NaOH solution was converted into crystalline hydrochloride, which was then recrystallized from ethanol to give (−)-CV-5197

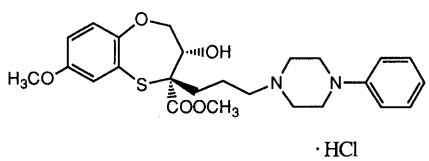

(3*S*,4*R*)-(+)-CV-5197

Chart 1

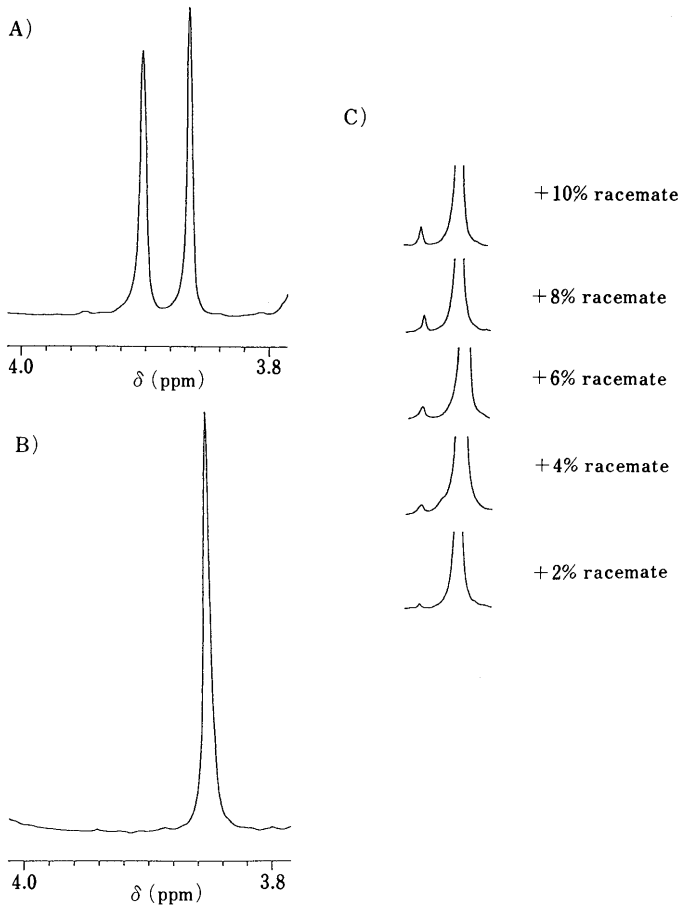

Fig. 1. 400 MHz NMR Spectra (in $CDCl_3$ Containing 4.3 mol% of Eu(hfc)$_3$) of OCH_3 Region of the Free Base of A) (±)-CV-5197, B) (+)-CV-5197, and C) Samples of (+)-CV-5197 Containing 2, 4, 6, 8, and 10% Racemate

as colorless prisms, mp 199—203 °C, $[\alpha]_D^{22}$ −115.4° (c=1.06, MeOH). The mother liquor from the above described separation of the *levo* isomer was worked up with 1 N NaOH solution. Treatment of the resulting *dextro* enantiomer enriched base with (*R*)-(−)-BNP gave a white crystalline salt which was recrystallized twice from methanol–acetone (2 : 3 v/v) to yield colorless needles of the phosphate salt, (+)-CV-5197 free base·(*R*)-(−)-BNP, in 57% yield, mp 224 °C, $[\alpha]_D^{21}$ −173.8° (c=0.925, MeOH). Conversion of this salt into its hydrochloride and recrystallization from ethanol afforded colorless prisms of (+)-CV-5197, mp 199—203 °C, $[\alpha]_D^{22}$ +115.9° (c=1.595, MeOH).

The 400 MHz proton nuclear magnetic resonance (^{1}H-NMR) spectrum of the free base of racemic CV-5197 in $CDCl_3$ showed two signals as sharp singlets at δ 3.751 and δ 3.798 ppm corresponding to two methoxy groups (7-OCH_3 or 4-$COOCH_3$). Addition of 4.3 mol% tris[3-heptafluoropropylhydroxymethylene)-(+)-camphorato], europium(III), [Eu(hfc)$_3$] changed this signal pattern into a singlet peak at δ 3.770 ppm (3H) and a pair of two singlet peaks at δ 3.864 and δ 3.902 ppm (3H). On the basis of the 400 MHz ^{1}H-NMR spectral data of the free base of (+)-CV-5197, and of samples of (+)-CV-5197 containing 2, 4, 6, 8, and 10% racemate, the optical purity of (+)-CV-5197 was estimated to exceed 98% ee (Fig. 1). (−)-CV-5197 was similarly deduced to be obtained with high enantiomeric purity (≧98%).

The absolute stereochemistry of the *dextro* enantiomer ((+)-CV-5197) was determined to be 3*S*,4*R* by X-ray crystallographic analysis of the hydrobromide of (+)-CV-5197 free base. (−)-CV-5197 was then established to possess a 3*R*,4*S* configuration. Stereoscopic drawings of the (+)-CV-5197 molecule are shown in Figs. 2 and 3.

Biological Activity and Discussion Interaction of the enantiomers of CV-5197 with the binding of ^{3}H-5-HT to 5-HT$_1$ sites, and with the binding of ^{3}H-ketanserin to 5-HT$_2$ sites was evaluated in rat brain membranes according to the methods described by Peroutka *et al.*,[3] and Leysen *et al.*,[4] respectively. Biological testing of the optical isomers was carried out in order to determine antagonistic activity against 5-HT-induced contraction in an isolated pig coronary artery using the method described previously.[1]

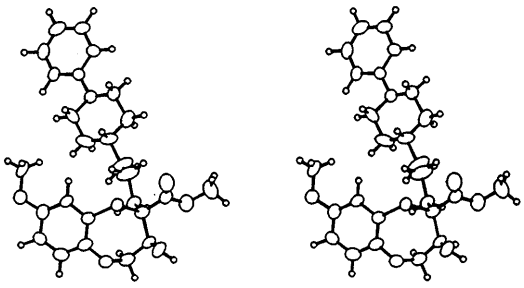

Fig. 2. Stereoscopic View of Molecular Conformation of (3*S*,4*R*)-(+)-CV-5197 Determined by Its Hydrobromide

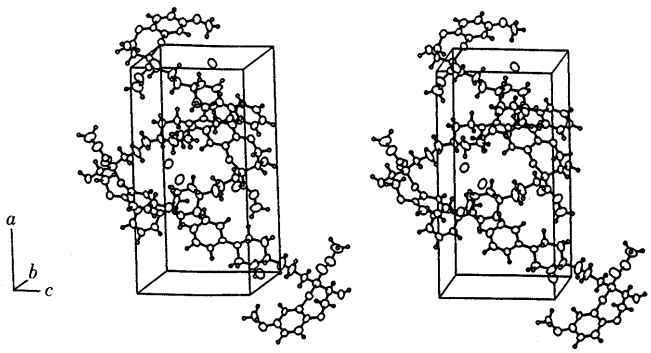

Fig. 3. Stereoscopic View of Molecular Arrangement in the Unit Cell

TABLE I. Positional Parameters ($\times 10^4$) and U_{eq} (Å$^2 \times 10^3$) for Non-hydrogen Atoms, with e.s.d.'s

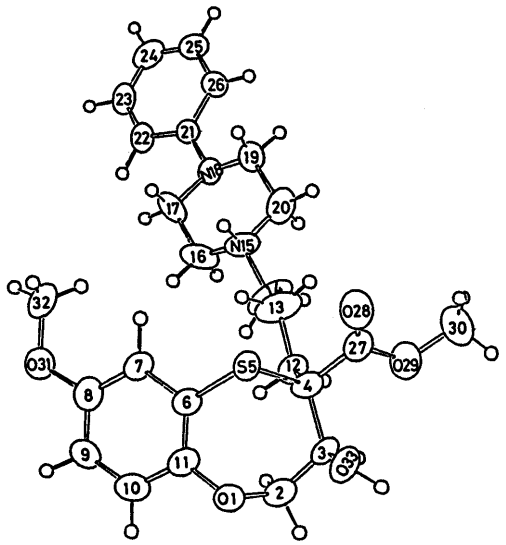

	x/a	y/b	z/c	U_{eq}
Br(1)	4914 (1)	1614 (1)	3642 (2)	69 (1)
O(1)	6546 (4)	3686 (9)	9515 (9)	55 (6)
C(2)	5924 (8)	4068 (13)	9999 (14)	60 (10)
C(3)	5439 (6)	3177 (12)	10178 (11)	47 (8)
C(4)	5172 (7)	2639 (11)	8914 (13)	51 (8)
S(5)	5811 (2)	1900 (3)	8015 (3)	42 (2)
C(6)	6297 (6)	2982 (10)	7417 (12)	40 (7)
C(7)	6430 (6)	2935 (12)	6078 (11)	45 (8)
C(8)	6893 (7)	3652 (12)	5600 (13)	53 (9)
C(9)	7223 (6)	4393 (11)	6397 (15)	51 (8)
C(10)	7086 (7)	4418 (12)	7684 (15)	56 (9)
C(11)	6632 (6)	3698 (11)	8205 (12)	42 (7)
C(12)	4836 (6)	3513 (11)	8076 (11)	48 (8)
C(13)	4545 (9)	3041 (13)	6848 (15)	78 (11)
C(14)	4217 (10)	3856 (15)	6175 (16)	89 (13)
N(15)	4042 (6)	3599 (10)	4780 (11)	54 (7)
C(16)	4241 (8)	4526 (13)	3947 (16)	69 (11)
C(17)	4086 (7)	4297 (13)	2567 (16)	61 (10)
N(18)	3386 (5)	4096 (10)	2415 (11)	47 (7)
C(19)	3171 (7)	3188 (13)	3207 (12)	57 (9)
C(20)	3324 (8)	3377 (15)	4611 (14)	69 (10)
C(21)	3159 (6)	4167 (11)	1136 (13)	41 (7)
C(22)	3446 (6)	4834 (12)	217 (12)	46 (8)
C(23)	3202 (7)	4847 (12)	−1017 (13)	50 (9)
C(24)	2672 (7)	4232 (14)	−1362 (15)	65 (10)
C(25)	2358 (7)	3600 (14)	−474 (14)	60 (9)
C(26)	2599 (7)	3552 (14)	789 (13)	58 (9)
C(27)	4699 (6)	1691 (13)	9254 (12)	50 (8)
O(28)	4736 (5)	771 (9)	8925 (12)	79 (8)
O(29)	4250 (5)	2087 (9)	10043 (11)	74 (7)
C(30)	3764 (8)	1263 (16)	10449 (19)	87 (13)
O(31)	7054 (5)	3694 (9)	4311 (9)	66 (7)
C(32)	6698 (9)	2986 (17)	3447 (14)	90 (13)
O(33)	5690 (5)	2321 (9)	10986 (8)	60 (6)

$U_{eq}=(U_{11}+U_{22}+U_{33})/3$.

Table II. Positional Parameters ($\times 10^3$) for Hydrogen Atoms, with e.s.d.'s

	x/a	y/b	z/c
H(21)	574 (6)	466 (11)	938 (12)
H(22)	597 (6)	448 (11)	1086 (13)
H(31)	506 (6)	357 (10)	1065 (11)
H(71)	621 (6)	230 (11)	549 (12)
H(91)	757 (7)	490 (12)	596 (13)
H(101)	730 (6)	502 (11)	826 (13)
H(121)	515 (6)	412 (10)	781 (12)
H(122)	450 (6)	390 (10)	860 (14)
H(131)	423 (6)	243 (11)	705 (13)
H(132)	490 (6)	274 (9)	626 (12)
H(141)	453 (6)	457 (11)	621 (14)
H(142)	383 (6)	407 (11)	662 (14)
H(151)	430 (6)	291 (11)	445 (12)
H(161)	472 (6)	462 (11)	403 (13)
H(162)	399 (6)	524 (10)	426 (12)
H(171)	437 (6)	362 (10)	225 (12)
H(172)	422 (6)	500 (10)	202 (12)
H(191)	338 (6)	241 (11)	290 (12)
H(192)	266 (6)	309 (10)	314 (11)
H(201)	318 (6)	261 (11)	512 (13)
H(202)	306 (6)	407 (11)	491 (13)
H(221)	386 (6)	531 (11)	47 (13)
H(231)	343 (6)	539 (10)	−170 (13)
H(241)	249 (6)	428 (10)	−229 (13)
H(251)	194 (6)	313 (11)	−70 (12)
H(261)	236 (6)	304 (10)	141 (13)
H(301)	382 (6)	43 (11)	1028 (13)
H(302)	334 (6)	144 (12)	996 (13)
H(303)	368 (6)	132 (12)	1143 (15)
H(321)	690 (6)	214 (10)	339 (13)
H(322)	672 (6)	334 (12)	258 (13)
H(323)	623 (6)	292 (11)	370 (14)
H(331)	546 (6)	264 (11)	1177 (13)

Table III. Bond Lengths (Å) with Standard Deviations in Parentheses

O(1)–C(2)	1.47 (2)	C(14)–N(15)	1.54 (2)
O(1)–C(11)	1.38 (2)	N(15)–C(16)	1.48 (2)
C(2)–C(3)	1.49 (2)	N(15)–C(20)	1.53 (2)
C(3)–C(4)	1.58 (2)	C(16)–C(17)	1.50 (2)
C(3)–O(33)	1.44 (2)	C(17)–N(18)	1.49 (2)
C(4)–S(5)	1.86 (1)	N(18)–C(19)	1.45 (2)
C(4)–C(12)	1.55 (2)	N(18)–C(21)	1.42 (2)
C(4)–C(27)	1.56 (2)	C(19)–C(20)	1.52 (2)
S(5)–C(6)	1.77 (1)	C(21)–C(22)	1.39 (2)
C(6)–C(7)	1.43 (2)	C(21)–C(26)	1.43 (2)
C(6)–C(11)	1.39 (2)	C(22)–C(23)	1.39 (2)
C(7)–C(8)	1.39 (2)	C(23)–C(24)	1.38 (2)
C(8)–C(9)	1.41 (2)	C(24)–C(25)	1.37 (2)
C(8)–O(31)	1.39 (2)	C(25)–C(26)	1.41 (2)
C(9)–C(10)	1.38 (2)	C(27)–O(28)	1.17 (2)
C(10)–C(11)	1.40 (2)	C(27)–O(29)	1.34 (2)
C(12)–C(13)	1.53 (2)	O(29)–C(30)	1.49 (2)
C(13)–C(14)	1.40 (2)	O(31)–C(32)	1.45 (2)

Table IV. Bond Angles (°) with Standard Deviations in Parentheses

C(2)–O(1)–C(11)	117 (1)	C(12)–C(13)–C(14)	110 (1)
O(1)–C(2)–C(3)	114 (1)	C(13)–C(14)–N(15)	117 (1)
C(2)–C(3)–C(4)	116 (1)	C(14)–N(15)–C(16)	110 (1)
C(2)–C(3)–O(33)	111 (1)	C(14)–N(15)–C(20)	112 (1)
C(4)–C(3)–O(33)	109 (1)	C(16)–N(15)–C(20)	110 (1)
C(3)–C(4)–S(5)	112 (1)	N(15)–C(16)–C(17)	111 (1)
C(3)–C(4)–C(12)	110 (1)	C(16)–C(17)–N(18)	110 (1)
C(3)–C(4)–C(27)	110 (1)	C(17)–N(18)–C(19)	112 (1)
S(5)–C(4)–C(12)	112 (1)	C(17)–N(18)–C(21)	115 (1)
S(5)–C(4)–C(27)	102 (1)	C(19)–N(18)–C(21)	119 (1)
C(12)–C(4)–C(27)	111 (1)	N(18)–C(19)–C(20)	112 (1)
C(4)–S(5)–C(6)	103 (1)	N(15)–C(20)–C(19)	110 (1)
S(5)–C(6)–C(7)	115 (1)	N(18)–C(21)–C(22)	123 (1)
C(5)–C(6)–C(11)	123 (1)	N(18)–C(21)–C(26)	118 (1)
C(7)–C(6)–C(11)	121 (1)	C(22)–C(21)–C(26)	118 (1)
C(6)–C(7)–C(8)	117 (1)	C(21)–C(22)–C(23)	120 (1)
C(7)–C(8)–C(9)	122 (1)	C(22)–C(23)–C(24)	122 (1)
C(7)–C(8)–O(31)	123 (1)	C(23)–C(24)–C(25)	121 (1)
C(9)–C(8)–O(31)	116 (1)	C(24)–C(25)–C(26)	119 (1)
C(8)–C(9)–C(10)	119 (1)	C(21)–C(26)–C(25)	120 (1)
C(9)–C(10)–C(11)	120 (1)	C(4)–C(27)–O(28)	127 (1)
O(1)–C(11)–C(6)	121 (1)	C(4)–C(27)–O(29)	108 (1)
O(1)–C(11)–C(10)	119 (1)	O(28)–C(27)–O(29)	125 (1)
C(6)–C(11)–C(10)	120 (1)	C(27)–O(29)–C(30)	114 (1)
C(4)–C(12)–C(13)	113 (1)	C(8)–O(31)–C(32)	117 (1)

Table V. Inhibitory Potencies of Optical Isomers of CV-5197 in ^{3}H-5-HT and ^{3}H-Ketanserin Binding

Compound	Receptor binding: IC_{50} (nM)	
	^{3}H-5-HT	^{3}H-Ketanserin
(±)-CV-5197	>10000 (3)	30±4.1 (4)
(+)-CV-5197	>10000 (3)	23±6.3 (4)
(−)-CV-5197	>10000 (3)	1600±82 (4)
Ketanserin	>10000 (3)	3.2±1.3 (4)

Each value represents the mean±S.E. Number of experiments are given in parentheses.

Table VI. 5-HT_2 Receptor Blocking Activities of Optical Isomers of CV-5197

Compound	5-HT_2 Receptor blocking activity[a]	
	3×10^{-4} M	3×10^{-7} M
(+)-CV-5197	—	99
(−)-CV-5197	0	0
Ketanserin	—	97

a) % Inhibition of contraction of pig coronary artery induced by 10^{-6} M 5-HT.

the results are shown in Tables V and VI.

In the binding assay, it was found that the *dextro* isomer ((+)-CV-5197) was the biologically active isomer with an IC_{50} of 23 nM±6.3 for 5-HT_2 receptors, showing 70 times more potent affinity for 5-HT_2 receptors than its enantiomer ((−)-CV-5197). Neither the stereoisomers nor the racemate showed interaction with 5-HT_1 sites at a concentration of 10^{-4} M.

In vitro experiments showed that (+)-CV-5197 completely inhibited 5-HT-induced contractions of the isolated pig coronary artery at 3×10^{-7} M. However, (−)-CV-5197 did not prevent contraction, even at 3×10^{-4} M.

The agreement between the binding affinity and biological activity of the enantiomers of CV-5197 shows that CV-5197 acts selectively on vascular smooth muscle and/or platelets through 5-HT_2 receptors. Among known 5-HT_2 antagonists such as mianserin[5] and irindalone,[6] it has been demonstrated that the 5-HT_2 receptor binding sites discriminate against the chirality of molecules. The high degree of stereoselectivity displayed by CV-5197 and previous studies of structure–activity relationships of 1,5-benzoxathiepin derivatives[1] in 5-HT_2 receptor blocking activity, suggest the importance in the 5-HT_2 recognition

sites of a particular spacial arrangement between the aromatic rings of 1,5-benzoxathiepin moiety and the *N*-phenylpiperazinyl group, as well as the nitrogen atom attached to the 3-propyl side chain.

Further studies on CV-5197 and its optical isomers are currently being continued.

Experimental

All melting points were determined on a Yanagimoto micro melting point apparatus (hot stage type) and are uncorrected. Infrared (IR) spectra were recorded with a Hitachi 260-01 spectrophotometer. ^{1}H-NMR spectra were recorded in the indicated solvents on Varian XVRD 200 and JEOL JNM-GX 400FT instruments. Chemical shifts are reported as δ-values relative to tetramethylsilane (TMS) as an internal standard. $[\alpha]_D$ values were determined in the indicated solvents on a JASCO DIP-181 4-4822 polarimeter.

Radiolabeled ligands ^{3}H-5-HT and ^{3}H-ketanserin were obtained from Du Pont NEN Research Products. Ketanserin was synthesized in our laboratories according to the method described in Japan Patent unexamined publication No. 55—105, 679 (1980).

Resolution of Racemic CV-5197 A solution of 1 N NaOH (30 ml) was added to a solution of racemic CV-5197 dihydrate (10 g, 18.3 mmol) dissolved in CH_2Cl_2 (50 ml). The mixture was stirred vigorously for 0.5 h, and the organic layer was separated, dried over anhydrous Na_2SO_4 and evaporated *in vacuo*. The residual oil and (*S*)-(+)-BNP (5.0 g, 14.3 mmol) were dissolved in MeOH. The mixture was condensed *in vacuo*. The residue was dissolved in acetone (200 ml) and the mixture was allowed to stand in a refrigerator for 2 d. The resulting white precipitate was filtered off and washed with acetone. The collected crystals were recrystallized twice from a solution of MeOH (150 ml) and acetone (100 ml) to give colorless needles (6.9 g, 92%) of (−)-CV-5197 free base·(*S*)-(+)-BNP, mp 224 °C, $[\alpha]_D^{23}$ +173.7° (c=0.985, MeOH). IR ν_{max}^{KBr} cm^{-1}: 1730, 1710, 1595, 1485, 1255, 1105. *Anal.* Calcd for $C_{25}H_{32}N_2O_5 \cdot C_{20}H_{13}O_4P$: C, 65.84; H, 5.53; N, 3.41. Found: C, 65.59; H, 5.80; N, 3.20.

The combined mother liquor was evaporated *in vacuo*. The residue was suspended in CH_2Cl_2 (200 ml) and mixed with 1 N NaOH (150 ml). The mixture was vigorously stirred for 1 h. The organic layer was separated, washed with 1 N NaOH and subsequently with H_2O, dried over anhydrous Na_2SO_4 and evaporated *in vacuo*. The residual oil (6.4 g) was treated with (*R*)-(−)-BNP (4.0 g, 11.5 mmol) in acetone to yield a crystalline salt of (+)-CV-5197 free base·(*R*)-(−)-BNP. Repeated recrystallization from MeOH–acetone (3:2, v/v) gave colorless needles (4.3 g, 57%) of (+)-CV-5197 free base·(*R*)-(−)-BNP, mp 224 °C, $[\alpha]_D^{21}$ −173.8° (c=0.925, MeOH). IR ν_{max}^{KBr} cm^{-1}: 1730, 1710, 1595, 1485, 1255, 1105. *Anal.* Calcd for $C_{25}H_{32}N_2O_5S \cdot C_{20}H_{13}O_4P$: C, 65.84; H, 5.53; N, 3.41. Found: C, 65.60; H, 5.82; N, 3.16.

Methyl (3*S*,4*R*)-3-Hydroxy-4-[3-(4-phenyl-1-piperazinyl)propyl]-3,4-dihydro-2*H*-1,5-benzoxathiepin-4-carboxylate Hydrochloride ((+)-CV-5197) A suspension of (+)-CV-5197 free base·(*R*)-(−)-BNP (31 g) in CH_2Cl_2 (500 ml) was mixed with 1 N NaOH (100 ml) and vigorously stirred for 1 h. The mixture was filtered off and the filtrate was separated. The organic layer was washed with H_2O, dried over anhydrous Na_2SO_4 and evaporated *in vacuo*. The residual oil was dissolved in EtOH (10 ml) and treated with 1 N HCl (45 ml), and the mixture was allowed to stand overnight in a refrigerator.

The resulting precipitate was collected and recrystallized from EtOH to give colorless prisms (15.6 g, 81%) of (+)-CV-5197, mp 199—203 °C, $[\alpha]_D^{22}$ +115.9° (c=1.595, MeOH). IR ν_{max}^{KBr} cm^{-1}: 3270, 2800—2300, 1725, 1595, 1490, 1435, 1280, 1265, 1250, 1205. 200 MHz ^{1}H-NMR (d_6-DMSO) δ: 1.4—2.3 (3H, m), 2.8—3.6 (11H, m), 3.70 (3H, s, OCH_3), 3.76 (3H, s, OCH_3), 3.7—4.3 (3H, m), 6.8—7.4 (8H, m). *Anal.* Calcd for $C_{25}H_{32}N_2O_5S \cdot HCl$: C, 58.99; H, 6.53; N, 5.50. Found: C, 59.04; H, 6.66; N, 5.48.

Methyl (3*R*,4*S*)-3-Hydroxy-4-[3-(4-phenyl-1-piperazinyl)propyl]-3,4-dihydro-2*H*-1,5-benzoxathiepin-4-carboxylate Hydrochloride ((−)-CV-5197) (−)-CV-5197 was obtained in an 80% yield from (−)-CV-5197 free base·(*S*)-(+)-BNP by a method similar to that described for the (+)-isomer. Colorless prisms, mp 199—203 °C (from EtOH), $[\alpha]_D^{22}$ −115.4° (c=1.06, MeOH). IR ν_{max}^{KBr} cm^{-1}: 3270, 2800—2300, 1725, 1595, 1490, 1435, 1280, 1265, 1250, 1205. 200 MHz ^{1}H-NMR (d_6-DMSO) δ: 1.4—2.3 (3H, m), 2.8—3.6 (11H, m), 3.70 (3H, s, OCH_3), 3.76 (3H, s, OCH_3), 3.7—4.3 (3H, m), 6.8—7.4 (8H, m). *Anal.* Calcd for $C_{25}H_{32}N_2O_5S \cdot HCl$: C, 58.99; H, 6.53; N, 5.50. Found: C, 59.04; H, 6.63; N, 5.46.

The Hydrobromide of (+)-CV-5197 Free Base (+)-CV-5197 free base (1.0 g) was dissolved in acetone (10 ml) and treated with 3 ml of the solution of 47% HBr/MeOH (0.1 g/ml). The mixture was condensed *in vacuo* below 30 °C. The residue was dissolved in H_2O (1 ml) and allowed to stand in a refrigerator overnight. The resulting precipitate was collected and recrystallized from MeOH to give colorless prisms (0.9 g), mp 215—217 °C. $[\alpha]_D^{22}$ +110.9° (c=0.84, MeOH). IR ν_{max}^{KBr} cm^{-1}: 1725, 1595, 1480, 1205. *Anal.* Calcd for $C_{25}H_{32}N_2O_5S \cdot HBr$: C, 54.25; H, 6.01; N, 5.06. Found: C, 54.10; H, 6.14; N, 4.96.

Crystal Data of (+)-CV-5197·HBr $C_{25}H_{32}N_2O_5S \cdot HBr$, M_r=553.518, orthorhombic, $P2_12_12_1$, a=20.817(4), b=12.173(3) c=10.449(3) Å, V=2648(1) Å, D_c=1.38 g·cm^{-3}, Z=4.

X-Ray Analysis Colorless prisms of (+)-CV-5197·HBr were obtained from a MeOH solution. Intensity data was measured on an automated diffractometer (Rigaku AFC-5) with graphite-monochromated MoK_α radiation. In all, 2319 reflections were measured, of which 2055 were judged significant ($|F_O| \geq 3\sigma(F_O)$). The structure was solved by the heavy atom method and refined by the least-squares method with anisotropic temperature factors for all non-hydrogen atoms and with isotropic factors for all hydrogen atoms using the program XRAY.[7] The final R value was 0.073. The final atomic parameters of non-hydrogen and hydrogen atoms are listed in Tables I, II, III, and IV. Bond distances and angles are shown in Figs. 2 and 3, respectively.

Absolute Configuration The absolute configuration was determined using an anomalous dispersion term in the atomic scattering factor of the bromine atom.[8] The R values obtained using two configurations were 0.06917 and 0.08477, and the atomic coordinates shown in Table I were found to be correct, even in the absolute sense.

^{3}H-5-HT Binding Studies Experimental methods were essentially similar to those described previously.[3] The cerebral cortex was removed and homogenized in 10 vol. of ice-cold 0.32 M sucrose. The homogenate was centrifuged at 700 × *g* for 10 min and the resultant supernatant fluid was centrifuged at 50000 × *g* for 10 min. The sedimented P_2 fraction was suspended in a standard assay buffer consisting of 50 mM Tris–HCl (pH 7.7, 25 °C), 4 mM $CaCl_2$, 10 μM pargyline, and 0.1% ascorbic acid. The tissue suspension was incubated for 15 min at 37 °C and then stored on ice until it was used for the binding assay. Reaction tubes consisting of 0.9 ml of tissue suspension, 10 μl of test drugs and 0.1 ml of ^{3}H-5-HT (final concentration: 3 nM) were incubated for 15 min at 37 °C.

Nonspecific binding was estimated in the presence of 10 μM 5-HT.

^{3}H-Ketanserin Binding Studies The binding study was performed according to the method of Leysen *et al.*[4] Briefly, the prefrontal cortex was removed and homogenized in 40 vol. of 50 mM Tris–HCl buffer (pH 7.7, 25°C). The homogenate was then centrifuged at 35000 × *g* for 30 min at 4 °C and the pellet was washed twice more with the same buffer. The final pellet was suspended in the following salt buffer; Tris–HCl 50 mM, pH 7.6 at 25 °C containing 120 mM NaCl, 5 mM KCl, 2 mM $CaCl_2$, 1 mM $MgCl_2$, 10 mM pargyline, and 0.1% of ascorbic acid. The tissue suspension was preincubated for 5 min at 37 °C and then kept on ice until it was used. Test drugs (10 μl) and 0.1 ml of ^{3}H-ketanserin (final concentration: 0.5 nM) were added to 0.9 ml aliquots of membrane suspension, and the mixture was incubated at 37 °C for 15 min. Specific ^{3}H-ketanserin binding was obtained by subtracting the nonspecific binding in the presence of 10 μM methysergide from the total binding.

5-HT Receptor Blocking Activity in Isolated Pig Coronary Artery Pig hearts were obtained from a slaughterhouse under ice-cooling and the left circumflex or the anterior descending coronary artery was dissected out within 3 h of death. The coronary artery was cut into ring preparations 3 mm in width. These vessel preparations were suspended in organ baths containing 20 ml of Krebs–Henseleit solution with a pair of suspending hooks. One of the hooks was fixed to the bottom of the organ bath, while the other was connected to a strain-gauge transducer, and the tension developed by these preparations was isometrically measured. The organ bath was maintained at 37 °C, and the Krebs–Henseleit solution was saturated with a gas mixture of 97% O_2+3% CO_2. As an agonist, 5-HT(10^{-6} M) was used in the porcine coronary preparations.

Acknowledgments The authors are grateful to Dr. T. Imamoto for the biological testing.

References

1) Part II: H. Sugihara, H. Mabuchi, M. Hirata, T. Imamoto, and Y. Kawamatsu, *Chem. Pharm. Bull.*, **35**, 1930 (1987).
2) A. W. Schmidt and S. J. Peroutka, *FASEB J.*, **3**, 2242 (1989).

3) S. J. Peroutka and S. H. Snyder, *Mol. Pharmacol.*, **16**, 687 (1979).
4) J. E. Leysen, C. J. E. Niemegeers, J. M. Van Neuten, and P. M. Laduron, *Mol. Pharmacol.*, **21**, 301 (1982).
5) B. S. Alexander and M. D. Wood, *J. Pharm. Pharmacol.*, **39**, 664 (1987).
6) K. P. Bøgesø, J. Arnt, V. Boeck, A. V. Christensen, J. Hyttel, and K. G. Jensen, *J. Med. Chem.*, **31**, 2247 (1988).
7) J. M. Stewart, P. A. Machin, C. Dickinson, H. Ammon, H. Heck, and H. Flack, "The XRAY System, Version of 1976," Computer Science Center, University of Maryland, College Park, Maryland.
8) International Tables for X-Ray Crystallography, Vol. IV, Kynoch Press, Birmingham, 1974, p. 75.

Phenolic Glycosides from Nuo-Mi-Xang-Cao, a Chinese Acanthaceous Herb

Ryoji KASAI,*[,a] Katsuki OGAWA,[a] Kazuhiro OHTANI,[a] Jing-Kai DING,[b] Pei-Qiong CHEN,[b] Chen-Ji FEI[b] and Osamu TANAKA[a]

Institute of Pharmaceutical Sciences, Hiroshima University School of Medicine,[a] Kasumi, Minami-ku, Hiroshima 734, Japan and Kunming Institute of Botany, Academia Sinica,[b] Kunming, Yunnan, China. *Received September 12, 1990*

From leaves of nuo-mi-xang-cao, a Chinese acanthaceous herb collected at Xi-shuang-ban-na, Yunnan, two new phenolic glycosides called nuomioside A and isonuomioside A were isolated and determined to be composed of 3,4-dihydroxyphenethylalcohol-(3′-*O*-*β*-D-apiosyl-4′-*O*-caffeoyl)-*β*-D-glucopyranoside and 3,4-dihydroxy-phenethylalcohol-3′-*O*-*β*-D-apiosyl-6′-*O*-caffeoyl)-*β*-D-glucopyranoside, respectively. Together with these compounds, known phenolic glycosides, acteoside, isoacteoside, crassifolioside, apigenin 7-*O*-*β*-D-glucuronide and its methyl ester were also identified in the leaves.

Keywords nuo-mi-xang-cao; Acanthaceae; *Strobilanthus* species; Chinese herb; acteoside; isoacteoside; nuomioside; phenethyl alcohol glycoside

Leaves of nuo-mi-xang-cao (糯米香草), an herb growing at Xi-shuang-ban-na (西双版納), South Yunnan, China are well-known to have an odor like glutinous rice and have been used as a flavoring for tea in this district. This plant seems to belong to *Strobilanthus* genus, Acanthaceae, however, due to its sparse blooming pattern to the fact that it blooms very rarely, a scientific species name has yet been proposed. As part of China–Japan joint studies on traditional Chinese plant drugs, we have conducted chemical investigations of this plant and report now the identification of phenolic glycosides.

The leaves were extracted with methanol and an aqueous suspension of the methanolic extract was successively extracted with hexane, ether and then 1-butanol (saturated with water). The butanolic extract was subjected to repeated chromatography to give seven compounds, I—VII. Based on inspection of the proton and carbon-13 nuclear magnetic resonance (^{1}H- and ^{13}C-NMR) spectra, compounds I, II and V were identified as known caffeoyl glycosides of 3,4-dihydroxyphenethyl alcohol: I: acteoside[1] from *Digitalis purpurea*,[2] *Syringa vulgaris*,[3] *Plantago major*,[4] *etc.*, II: isoacteoside[5] from *Leucosesptrum japonicum etc.* and V: crassifolioside[6] from *Plantago crassifolia*. It is noteworthy that certain biological activities such as antiviral activity[4] and enzyme inhibitory activities[7] have been reported for I and/or the congeners.

A new glycoside III, $C_{28}H_{34}O_{15}$ from high resolution fast atom bombardment mass spectrometry (HR-FAB-MS) afforded D-glucose and D-apiose on acid hydrolysis. Inspection of the ^{1}H- and ^{13}C-NMR signals due to sugar moieties indicated the presence of a *β*-D-apiosyl moiety[8,9] in III. All of the carbon and proton signals of I were assigned (Tables I and II) by means of the ^{1}H–^{1}H correlated spectroscopy (^{1}H–^{1}H COSY) and ^{13}C–^{1}H COSY spectra. Comparison of the spectrum of III with that of I revealed that all of the carbon signals due to the caffeoyl, glucosyl and dihydroxyphenethyl moieties of I appeared at almost the same positions in the spectrum of III (Table I). This indicates that III can be formulated as 3,4-dihydroxyphenethylalcohol-(3′-*O*-*β*-D-apiosyl-4′-caffeoyl)-*β*-D-glucopyranoside (=3′-*O*-*β*-D-apiosyl-desrhamno-acteoside). The location of the apiosyl moiety in III was further substantiated as follows. Identification of all of the proton signals of III was established by the ^{1}H–^{1}H COSY spectrum, and the subsequent ^{1}H–^{1}H nuclear Overhauser effect correlated spectroscopy (NOESY) spectrum revealed the presence of NOE between 3-H of the glucosyl moiety and H-1 of the apiosyl moiety (Chart 1). The name nuomioside A is proposed for the new glycoside, III.

Another new glycoside, IV, $C_{28}H_{34}O_{15}$ from HR-FAB-MS (an isomer of III), yielded D-glucose and D-apiose on acid hydrolysis. The carbon and proton signals of IV indicated the presence of a terminal *β*-D-apiosyl moiety (Tables I and II). Comparison of the ^{13}C-NMR spectrum of IV with that of II (Table I) showed that IV can be formulated as 3′,4′-dihydroxyphenethyl-(3′-*O*-*β*-D-apiosyl-6′-*O*-caffeoyl)-*β*-D-glucopyranoside (=3′-*O*-*β*-D-apiosyl-desrhamno-isoacteoside). The name isonuomioside A is proposed for IV. The location of the apiosyl moiety was confirmed by the ^{1}H–^{1}H COSY spectrum and the

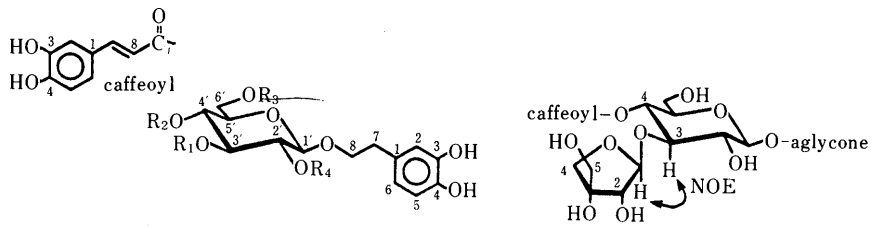

	R_1	R_2	R_3	R_4
I	*α*-L-Rha	caffeoyl	H	H
II	*α*-L-Rha	H	caffeoyl	H
III	*β*-D-Api	caffeoyl	H	H
IV	*β*-D-Api	H	caffeoyl	H
V	*α*-L-Rha	caffeoyl	H	Rha

Chart 1

Table I. ^{13}C-NMR (δ in DMSO-d_6, 100 MHz) of Phenolic Glycosides

C	I	II	III	IV	V
Caffeoyl moiety					
1	125.4	125.4	125.4	125.4	125.4
2	114.5	114.7	114.7	114.8	114.4
3	145.5	145.3	145.5	145.5	145.5
4	148.5	148.2	148.3	148.3	148.4
5	115.7	115.6	115.7	115.7	115.7
6	121.4	121.3	121.2	121.3	121.3
7	145.2	145.1	145.2	145.2	145.3
8	113.4	113.8	113.8	113.2	113.6
9	165.6	166.4	165.6	165.4	165.7
Aglycone					
1	129.1	129.0	129.1	129.1	128.6
2	116.2	116.1	116.2	116.2	116.2
3	144.9	144.8	144.9	144.9	145.0
4	143.5	143.3	143.5	143.5	143.5
5	115.4	115.3	115.4	115.4	115.4
6	119.4	119.4	119.4	119.4	119.4
7	34.9	35.0	35.0	35.1	34.7
8	70.3	70.2	70.3	70.4	70.2
Glucose					
G-1	102.2	102.5	102.9	102.4	100.7
G-2	74.4	74.4	74.4	73.6	79.1
G-3	79.0	80.7	78.9	81.3	78.8
G-4	69.0	68.0	69.0	68.4	69.3
G-5	74.4	73.6	73.6	73.4	74.4
G-6	60.6	63.3	60.7	63.2	60.6
Rhamnose					
R-1	101.1	100.5			101.5
R-2	70.4	70.4			70.4[a]
R-3	70.2	70.2			70.1[b]
R-4	71.6	71.9			71.5
R-5	68.6	68.4			68.7
R-6	18.1	17.3			18.1
Apiose					
A-1			109.5	109.2	
A-2			76.0	76.0	
A-3			78.5	79.0	
A-4			73.6	73.6	
A-5			63.8	63.6	
Rhamnose					
R′-1					101.9
R′-2					70.5[a]
R′-3					70.2[b]
R′-4					71.8
R′-5					69.2
R′-6					18.1

a, b) Interchangeable.

Table II. ^{1}H-NMR (δ in DMSO-d_6; 400 MHz) of III, IV

H	III	IV
Caffeoyl moiety		
2	7.10 (d, 1.4)	7.07 (d, 2.0)
5	6.83 (d, 8.2)	6.76 (d, 8.0)
6	7.05 (dd, 1.4, 8.2)	6.97 (dd, 2.0, 8.0)
7	7.53 (d, 15.8)	7.47 (d, 15.7)
8	6.29 (d, 15.8)	6.29 (d, 15.7)
Aglycone		
2	6.69 (d, 1.9)	6.61 (d, 2.0)
5	6.70 (d, 8.1)	6.58 (d, 8.0)
6	6.57 (dd, 1.9, 8.1)	6.46 (dd, 2.0, 8.0)
7	2.77 (ddd, 7.2, 8.8, 9.0)	2.69 (ddd, 6.8, 8.9, 9.0)
	2.75 (ddd, 7.2, 8.8, 9.0)	2.71 (ddd, 6.8, 8.9, 9.0)
8	3.71 (ddd, 7.2, 8.8, 8.8)	3.61 (ddd, 6.8, 8.9, 9.0)
	3.95 (ddd, 7.2, 8.8, 8.8)	3.79 (ddd, 6.8, 8.9, 9.0)
Glucose		
1	4.36 (d, 7.8)	4.31 (d, 7.7)
2	3.27 (dd, 7.8, 9.3)	3.18 (dd, 7.7, 8.4)
3	3.74 (dd, 9.3, 9.5)	3.41 (dd, 8.4, 9.3)
4	4.68 (dd, 9.5, 9.6)	3.24 (dd, 8.7, 9.3)
5	3.53 (ddd, 1.7, 6.0, 9.6)	3.49 (ddd, 1.6, 6.1, 8.7)
6	3.42 (dd, 6.0, 10.7)	4.20 (dd, 6.1, 12.0)
	3.47 (dd, 1.7, 10.7)	4.39 (dd, 1.6, 12.0)
Apiose		
1	5.26 (d, 1.7)	5.23 (d, 2.1)
2	3.77 (d, 1.7)	3.82 (d, 2.1)
4	3.49 (d, 9.0)	3.63 (d, 9.1)
	3.70 (d, 9.0)	4.01 (d, 9.1)
5	3.25 (d, 10.8)	3.40 (2H, s)
	3.28 (d, 10.8)	

Values in parenthesis are coupling constant in Hz.

subsequent ^{1}H–^{1}H NOESY spectrum in a similar manner to III (Chart 1).

Inspection of the ultraviolet spectrum (UV), infrared spectrum (IR), ^{1}H- and ^{13}C-NMR spectra disclosed that VI and VII are identical to the known flavonoid-glycosides, apigenin 7-*O*-β-D-glucuronide[10] and its methyl ester,[11] respectively. The methyl ester VII might be an artifact which is formed from VI during the process of the extraction with methanol.

Experimental

NMR spectrum were recorded on a JEOL JNM GX-400 spectrometer in deuterio-dimethyl sulfoxide (DMSO-d_6) using tetramethylsilane as an internal standard. FAB-MS spectra were taken on a JEOL JMS SX-102 spectrometer. The plants were collected at Xi-shuang-ban-na, Yunnan, China and identified by the Kunming Institute of Botany, Chinese Academy of Science. A specimen has been deposited in the herbarium of this Institute.

Acid Hydrolysis of Glycosides and Identification of the Resulting Monosaccharides A solution of a few mg of III or IV in 3.5% HCl (in 50% dioxane, 1 ml) was heated at 80 °C for 3 h in a sealed microtube. The mixture was washed with $CHCl_3$ and neutralized with Amberlite MB-3. Monosaccharides in the aqueous layer were identified by comparison of thin layer chromatography (TLC) and gas-liquid chromatography (GC) with a respective authentic sample. TLC: on a silica gel plate with $CHCl_3$–MeOH–H_2O (6:4:1) was visualized with 2,3,4-triphenyltetrazolium chloride. Identification of monosaccharides including absolute configuration was conducted according to Oshima, Kumanotani and Watanabe's procedure.[12] A solution of the reaction product and the L-amine-reagent (*vide infra*) in H_2O (50 μl) was heated at 40 °C for 4 h. After addition of a few drops of AcOH, the mixture was concentrated to dryness. The residue was treated with a few drops of *N*-trimethylsilylimidazole at 40 °C for 8 h and the mixture was extracted with *n*-C_6H_{14}. The product was subjected to GC to compare derivatives prepared from authentic monosaccharides with the L-amine-reagent or the DL-amine-reagent in the same way as above. L-amine-reagent: a solution of L-α-methylbenzylamine (400 mg) and $NaBH_3CN$ (100 mg) in EtOH (2.5 ml), DL-amine-reagent: DL-α-methylbenzylamine (400 mg) and $NaBH_3CN$ (100 mg) in EtOH (2.5 ml). Condition of GC: on a capillary glass column, coated with Carbowax PEG 20M, WCOT type, 0.25 mm × 25 m, carrier gas: He, flow rate 3 ml/min, column temp.: 150 °C, injection and detector temp.: 190 °C, detection: FID.

Isolation and Properties of Glycosides The dried leaves (800 g) were extracted with MeOH. An aqueous suspension of the MeOH extract was successively extracted with *n*-C_6H_{14}, Et_2O and then 1-BuOH (saturated with H_2O). The BuOH extract was chromatographed on silica gel with $CHCl_3$–MeOH–H_2O (30:10:1, 10:5:1, 6:4:1 and then 3:2:1) to give nine fractions, frs. 1—9. Fraction 6 was subjected to chromatography on LiChroprep RP-8 (Merck) with MeOH–H_2O (1:2) followed by high-performance liquid chromatography (HPLC) on TSK gel ODS 120T (Tosoh, 21.5 mm i.d. × 30 cm) with 10% 2-PrOH (in MeOH)–H_2O (1:2) (flow rate: 6 ml/min, detection: RI and UV 254 nm) to give I, II, III and IV in yields of 0.1, 0.005, 0.01 and 0.006%, respectively. Fraction 7 was chromatographed on LiChroprep RP-8 with MeOH–H_2O (3:7) and then with MeOH to give fractions, frs. 7-1 and 7-2. Fraction 7-1 was purified by HPLC on TSK gel ODS 120T (21.5 mm i.d. × 30 cm) with 10% 2-PrOH (in MeOH)–H_2O (1:2), (flow rate: 6 ml/min, detection: RI and UV

254 nm) to afford V in a yield of 0.025%. Fraction 7-2 was subjected to chromatography on silica gel with $CHCl_3$–MeOH–H_2O (10 : 5 : 1) and then on Sephadex LH-20 with MeOH–H_2O (1 : 4) followed by HPLC TSK gel Amide-80 (Tosoh, 21.5 mm i.d. × 30 cm) with CH_3CN–H_2O (9 : 1) (flow rate: 6 ml/min, detection: RI and UV 254 nm) to give VI and VII in yields of 0.008 and 0.004%, respectively.

Compound I: A pale yellow powder. $[\alpha]_D^{25}$ −87.5° (c=0.71, MeOH). UV λ_{max}^{MeOH} nm (log ε): 244 (sh, 4.05), 291 (4.07), 344 (4.19).

Compound II: A pale yellow powder. $[\alpha]_D^{20}$ −52.3° (c=0.58, MeOH). UV λ_{max}^{MeOH} nm (log ε): 245 (sh, 4.05), 290 (4.10), 329 (4.19).

Compound III: A pale yellow powder. $[\alpha]_D^{21}$ −52.3° (c=0.53, MeOH). UV λ_{max}^{MeOH} nm (log ε): 289 (sh, 4.92), 290 (5.00), 329 (4.65). HR-FAB-MS: Calcd for $[C_{28}H_{34}O_{15}+H]^+$ 611.1975. Found: m/z 611.1893.

Compound IV: A pale yellow powder. $[\alpha]_D^{22}$ −54.7° (c=0.53, MeOH). UV λ_{max}^{MeOH} nm (log ε): 291 (sh, 4.92), 338 (5.00), 378 (4.71). HR-FAB-MS: Calcd for $[C_{28}H_{34}O_{15}+H]^+$ 611.1975. Found: m/z 611.1989.

Compound V: A pale yellow powder. $[\alpha]_D^{21}$ −74.9° (c=2.67, MeOH). UV λ_{max}^{MeOH} nm (log ε): 291 (sh, 4.91), 334 (5.07), 379 (4.72). HR-FAB-MS: Calcd for $[C_{35}H_{46}O_{19}+H]^+$ 771.2711. Found: m/z 771.2759.

Compound VI: Pale yellow needles from MeOH. mp 253—254 °C, $[\alpha]_D^{19}$ −64.9° (c=0.60, MeOH). UV λ_{max}^{EtOH} nm (log ε): 269 (4.36), 334 (4.39); $\lambda_{max}^{EtOH+NaOEt}$ nm 269, 392; $\lambda_{max}^{EtOH+NaOAc}$ nm 269, 334; $\lambda_{max}^{EtOH+NaOAc+HBO_3}$ nm 269, 333; $\lambda_{max}^{EtOH+AlCl_3}$ nm 270, 382. ^{1}H-NMR (DMSO-d_6) δ: aglycone moiety 7.92 (2H, d, J=8.5 Hz, H-2′, 6′), 6.95 (2H, d, J=8.5 Hz, H-3′, 5′), 6.86 (1H, s, H-3), 6.84 (1H, d, J=1.5 Hz, H-8), 6.46 (1H, d, J=1.5 Hz, H-6), glucuronide moiety 5.19 (1H, d, J=7.8 Hz, H-1), 3.92 (1H, d, J=7.8 Hz, H-5), 3.2—3.5 (3H, br, H-2, 3, 4).

Compound VII: Pale yellow needles from MeOH. mp 242—244 °C, $[\alpha]_D^{19}$ −72.3° (c=0.30, MeOH). UV λ_{max}^{EtOH} nm (log ε): 269 (4.34), 334 (4.36); $\lambda_{max}^{EtOH+NaOEt}$ nm 269, 392; $\lambda_{max}^{EtOH+NaOAc}$ nm 269, 332; $\lambda_{max}^{EtOH+NaOAc+HBO_3}$ nm 269, 334; $\lambda_{max}^{EtOH+AlCl_3}$ nm 270, 383. ^{1}H-NMR (DMSO-d_6) δ: aglycone moiety 7.95 (2H, d, J=8.8 Hz, H-2′, 6′), 6.94 (2H, d, J=8.8 Hz, H-3′, 5′), 6.86 (1H, s, H-3), 6.85 (1H, d, J=2.2 Hz, H-8), 6.47 (1H, d, J=2.2 Hz, H-6), glucuronide moiety 5.32 (1H, d, J=7.1 Hz, H-1), 3.92 (1H, d, J=9.3 Hz, H-5), 3.67 (3H, s, $-OCH_3$), 4.32 (1H, dd, J=8.4, 9.3 Hz, H-4), 3.35 (1H, dd, J=8.4, 8.4 Hz, H-3), 3.32 (1H, dd, J=7.1, 8.4 Hz, H-2). A solution of VII (30 mg) in 0.5 N aqueous NaOH (5 ml) was allowed to stand at room temperature for 30 min. The reaction mixture was acidified (pH 3.0) with 0.5 N aqueous HCl and extracted with EtOAc. The EtOAc extract was purified by HPLC on TSK gel Amide-80 with CH_3CN–H_2O (9 : 1) (*vide supra*) to give VI (25 mg) which was identified by comparison of ^{13}C-NMR spectrum with that of an authentic sample of VI.

Acknowledgements We are grateful to Professor J. Zhou, Kunming Institute of Botany for his encouragement and to Mr. Guo-da Tao, Xi-shuang-ban-na Tropical Botanic Garden, Academia Sinica for the collection of the plant material.

References

1) M. L. Acarpati and D. M. Monache, *Ann. Chem.* (Rome), **53**, 356 (1963).
2) M. Matsumoto, S. Koga, Y. Shyoyama and I. Nishioka, *Phytochemistry*, **26**, 3325 (1987).
3) L. Birkofer, C. Kaiser and U. Thomas, *Naturforscher.*, **23**, 1051 (1968).
4) H. Raun and L. Birmer, *Phytochemistry*, **27**, 3433 (1988).
5) T. Miyase, Y. Akiyama, A. Koizumi, A. Ueno, T. Noda, M. Kuroyanagi, S. Fukushima and T. Takemoto, *Chem. Pharm. Bull.*, **30**, 2732 (1982).
6) C. Candary, H. Ravn, R. Wylde, A. Heitz and E. M. Florac, *Phytochemistry*, **28**, 288 (1989).
7) H. Sasaki, H. Nishimura, T. Morota, M. Chin, H. Mitsuhashi, Y. Komatsu, H. Maruyama, G. Tu, W. He and Y. Xiong, *Planta Medica*, **55**, 458 (1989); H. Nishimura, T. Yamaguchi, H. Sasaki, T. Morita, T. Yanagisawa, T. Sato, M. Chin and H. Mitsuhashi, Abstracts of Papers, International Joint Symposium of Biology and Chemistry of Active Natural Substances, Bonn, West Germany, July, 1990, p. 201; Y. Kimura, H. Okuda, S. Nishibe and S. Arichi, *Planta Medica*, **53**, 148 (1987).
8) P. Satyanarayana, P. Subrahmanyam, R. Kasai and O. Tanaka, *Phytochemistry*, **24**, 1862 (1985).
9) R. Higuchi, Y. Tokimitsu, T. Fujioka, T. Komori, T. Kawasaki and D. G. Oakenful, *Phytochemistry*, **26**, 229 (1987).
10) S. S. Subtamanlan, A. G. R. Nair and T. N. C. Vedamthana, *Ind. J. Pharm.*, **1973**, 192.
11) E. V. Rao and A. Rao, *Curr. Sci.*, **51**, 1040 (1982).
12) R. Oshima, J. Kumanotani and C. Watanabe, *J. Chromatogr.*, **259**, 159 (1983).

Chem. Pharm. Bull. **39**(4) 930—933 (1991) Vol. 39, No. 4

Inhibition of Adenosine 3′,5′-Cyclic Monophosphate Phosphodiesterase by Flavonoids from Licorice Roots and 4-Arylcoumarins[1)]

Ayumu KUSANO,[a] Tamotsu NIKAIDO,[a] Takashi KUGE,[a] Taichi OHMOTO,*[,a] G. Delle MONACHE,[b] Bruno BOTTA,[b] Maurizio BOTTA,[b] and Tamotsu SAITOH[c]

School of Pharmaceutical Sciences, Toho University,[a] 2–2–1 Miyama, Funabashi, Chiba 274, Japan, Centro Chimica dei Recettori del C.N.R., Universita Cattolica,[b] del, S. Cuore, Roma, Italy, and Faculty of Pharmaceutical Sciences, Teikyo University,[c] Sagamiko, Kanagawa 199–01, Japan.
Received September 18, 1990

Isoliquiritigenin, glabridin, licoarylcoumarin and licoricidin were identified as strong inhibitors of adenosine 3′,5′-cyclic monophosphate (cAMP) phosphodiesterase in waste materials which were obtained during the industrial extraction of glycyrrhizin from licorice roots. The structure–activity relationships of 12 flavonoids from licorice roots and 34 4-arylcoumarins were studied. In 4-arylcoumarins, 5,7-dihydroxy derivatives were generally highly inhibitory towards cAMP phosphodiesterase.

Keywords licorice root; cAMP phosphodiesterase; inhibitor, flavonoid; 3-arylcoumarin;4-arylcoumarin; structure–activity relationship

The relationships between adenosine 3′,5′-cyclic monophosphate (cAMP) and platelet or prostaglandin are well known. Some of the cAMP phosphodiesterase inhibitors also have inhibitory activity on platelet aggregation.[2–5)] A cAMP phosphodiesterase inhibition test was recently introduced for the research of novel cardiotonics.[6,7)] This test provides a useful tool for the screening of biologically active compounds contained in medicinal plants.

We have reported on cAMP phosphodiesterase inhibitors contained in various medicinal plants.[8–15)] The present paper deals with the identification of these inhibitors contained in licorice roots (*Glycyrrhiza* spp., Leguminosae), which is one of the medicines most often used in traditional Chinese herbal therapy. It is reported to contain saponins and many flavonoids.[16)]

Glycyrrhizin, a main component of licorice roots, was isolated by a method of the medicinal industry, and waste materials were obtained in the process. We examined and identified cAMP phosphodiesterase inhibitors from these waste materials and studied the possibility of their utilization.

3-Arylcoumarin with very high inhibitory activity was isolated together with some flavonoids. Some authors have isolated many 4-arylcoumarins from medicinal plants. The structure–activity relationships of these compounds were investigated.

Results and Discussion

Glycyrrhizin was isolated from the method as shown in Chart 1. Samples 1 and 4 showed relatively high inhibitory activity for cAMP phosphodiesterase in the waste materials. These samples were fractionated by column chromatography and centrifugal partition chromatography on silica gel and monitored by thin layer chromatography (TLC) and also by measurement of inhibitory activity against cAMP phosphodiesterase. The active fractions were re-fractionated by preparative TLC, medium-pressure liquid chromatography (MPLC) and high-performance liquid chromatography (HPLC) to give some active flavonoids and 3-arylcoumarins.

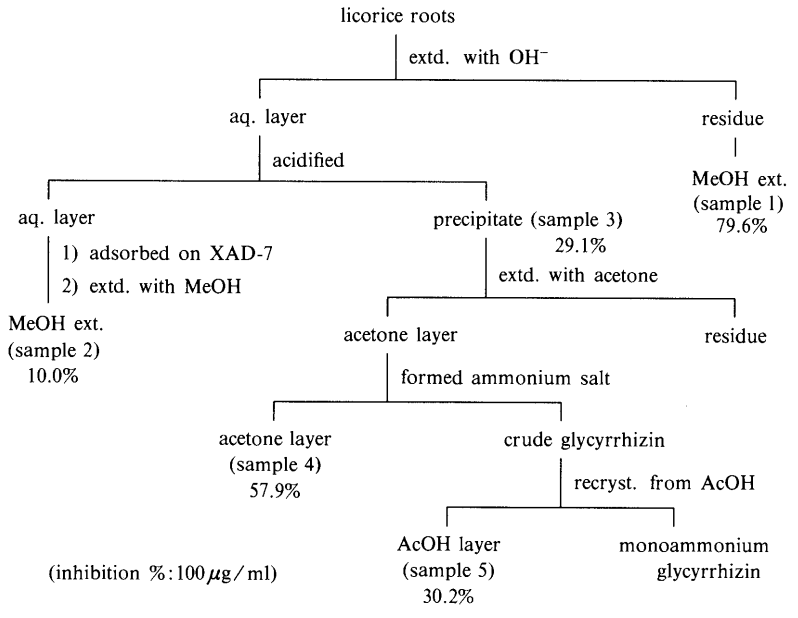

Chart 1

Isoliquiritigenin-4′-*O*-apioglucoside (**1**), isoliquiritigenin (**2**) and liquiritin (**3**) were detected from sample 4. Glabridin (**5**), licoricidin (**6**), licoarylcoumarin (**7**) and glycyrin (**8**) were also detected from sample 1. **2**, **5**, **6** and **7** showed high inhibitory activity but **1** was not so high. **3** and **8** did not show activity. These compounds and some related flavonoids isolated from licorice roots were tested for inhibitory activity against cAMP phosphodiesterase (Table I).

TABLE I. Inhibitory Activity of Flavonoids on cAMP Phosphodiesterase

Sample	IC_{50} ($\times 10^{-5}$ M)
Isoliquiritigenin-4′-*O*-apioglucoside (**1**)	171
Isoliquiritigenin (**2**)	18
Liquiritin (**3**)	>500
Liquiritigenin (**4**)	108
Glabridin (**5**)	8.2
Licoricidin (**6**)	4.9
Licoarylcoumarin (**7**)	1.0
Glycyrin (**8**)	>500
Glycycoumarin (**9**)	0.7
Glycyrol (**10**)	4.4
Isoglycyrol (**11**)	>500
Licoricone (**12**)	2.3
Cf. papaverine	3.0

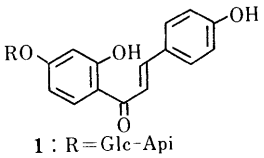

1 : R=Glc-Api
2 : R=H

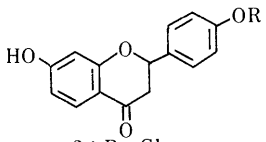

3 : R=Glc
4 : R=H

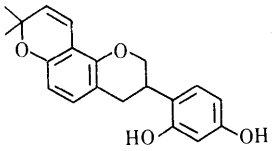

5

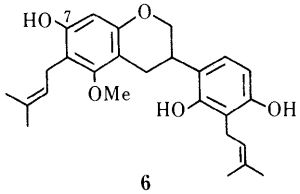

6

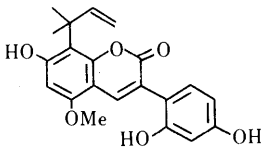

7

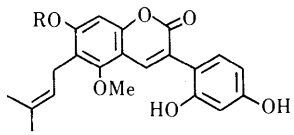

8 : R=Me
9 : R=H

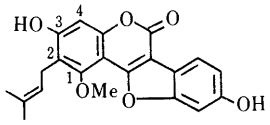

10

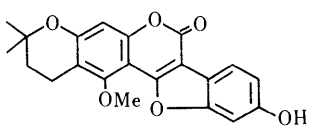

11

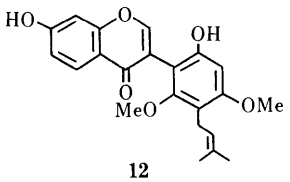

12

Among the 3-arylcoumarin derivatives tested, **6** and glycycoumarin (**9**) which have 7-hydroxy group, showed high inhibitory activity but **8** in which the methoxyl group is located at the 7 position, showed no activity. Similarly, in the case of coumestan derivatives, glycyrol (**10**) with a hydroxyl group at 3 position exhibited high inhibitory activity but isoglycyrol (**11**) which was cyclized between the isoprenoid side chain at C-2 and the hydroxyl group at C-3, showed no activity.

The results so far obtained indiçate that the presence of hydroxyl group at the 7 position of the 3-arylcoumarins (the 3 position of the coumestans) is very important for the cAMP phosphodiesterase inhibitory activity. Both **9** and **10** had similar substitutions, but **9** was more active than **10** in a fixed B-ring. *O*-Glycosides (**1** and **3**) were generally less potent than the corresponding chalcone (**2**) and flavanone (**4**), respectively. This result was similar to flavone.[15] In these compounds, **2** was reported to have aldose reductase inhibitory activity,[17] platelet aggregation inhibitory activity[18] and to be antispasmodic.[19] **5** was reported to have antimicrobial activity.[20] Therefore, it was expected that the strong inhibitors of cAMP phosphodiesterase from licorice roots might have pharmacological application, and it was also suggested that the waste materials resulting from the glycyrrhizin manufacturing process may have some use.

Many 4-arylcoumarins have been found in *Coutarea hexandra* and *C. latiflora* (Rubiaceae). These plants have respectively been used in folk medicine as an antimalarial and an antidiabetic agent.[21] Some authors examined *C. hexandra* in the course of their research of pharmacologically active and insecticidal substances, and isolated many 4-arylcoumarins.[22] Nathanson reported that phosphodiesterase inhibitors could be useful as pesticides.[23] In view of the relation and structure similarity to 3-arylcoumarin which we isolated from licorice roots, we investigated the inhibitory activity on cAMP phosphodiesterase by 4-arylcoumarins. Next, thirty-four 4-arylcoumarins were similarly tested, and the results are summarized in Table II. The structure–activity relationships can be summarized as follows. 1) 5,7-Dihydroxy-4-arylcoumarins (**13**, **17**, **18**, **25** and **26**) have higher inhibitory activity than corresponding 5,7-dimethoxy-4-arylcoumarins (**15**, **19**, **20**, **30** and **39**). 2) 5,7-Dimethoxy-4-arylcoumarins with hydroxyl group or no substitution in 4′ position (**15** and **30**) exhibited potent inhibitory activities, but corresponding 4′-methoxyl derivatives (**20** and **33**) had no inhibitory activity. Similarly, 5,6,7-trimethoxy derivatives having no substitution in 4′ position (**21**) had higher inhibitory activity than corresponding 4′-methoxy derivatives (**31**). 3) Introduction of a methoxyl group at 8 position into 5,7,4′-trimethoxy-(**32**) and 5,7,4′-trimethoxy-3′-hydroxy-(**42**) derivatives caused a remarkable increase of inhibitory activity on cAMP phosphodiesterase. But in the corresponding 4-arylcoumarins having methoxyl (**33**) or acethoxyl (**37**) group at the 3′ position, introduction of a methoxyl group at 8 position did not increase inhibition (**43** and **44**).

Experimental

The following instruments were used to obtain the physical data. The liquid scintillation counter was an Aloka LSC-903 or LSC-3100. Silica gel $60F_{254}$ (Merck, precoated plate, 0.25 mm) was used for TLC and detection was achieved by illumination with an ultraviolet (UV) lamp or by spraying 1 N $FeCl_3$ or 10% H_2SO_4 followed by heating. On preparative TLC (Silica

TABLE II. Inhibitory Activity and on cAMP Phosphodiesterase and Source of 4-Arylcoumarins

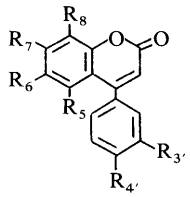

No.	Substituent						IC_{50} ($\times 10^{-5}$ M)	Ref.
	R_5	R_6	R_7	R_8	$R_{3'}$	$R_{4'}$		
13	OH	H	OH	H	H	H	7.0	22*a*[b]
14	OH	H	OMe	H	H	H	53.0	22*a*[c]
15	OMe	H	OMe	H	H	H	69.7	22*a*[c]
16	OAc	H	OAc	H	H	H	>500	un[c]
17	OH	H	OH	H	H	OH	10.1	22*b*[c]
18	OH	H	OH	H	H	OMe	9.0	22*b*[c]
19	OMe	H	OMe	H	H	OH	>500	22*c*[b]
20	OMe	H	OMe	H	H	OMe	>500	22*c*[b]
21	OMe	OMe	OMe	H	H	H	16.5	un[c]
22	OAc	H	OMe	H	OMe	H	8.3	un[c]
23	OMe	H	OMe	H	H	OAc	>500	22*b*[c]
24	OAc	H	OAc	H	H	OAc	>500	un[c]
25	OH	H	OH	H	OMe	OH	1.8	22*b*[c]
26	OH	H	OH	H	OMe	OBz	0.6	22*b*[c]
27	OMe	H	OMe	H	OH	OH	11.7	22*c*[b]
28	OMe	H	OMe	OH	H	OMe	10.4	31[b]
29	OMe	H	OMe	H	OH	OMe	>500	22*c*[b]
30	OMe	H	OMe	H	OMe	OH	6.8	22*c*[c]
31	OMe	OMe	OMe	H	H	OMe	>500	22*d*[c]
32	OMe	H	OMe	OMe	H	OMe	13.3	22*d*[b]
33	OMe	H	OMe	H	OMe	OMe	>500	22*c*[c]
34	H	OMe	OMe	H	OMe	OMe	49.0	un[c]
35	OMe	H	OMe	H	$-OCH_2O-$		>500	22*c*[b]
36	OMe	H	OMe	OEt	H	OMe	>500	22*d*[c]
37	OMe	H	OMe	H	OAc	OMe	>500	22*c*[c]
38	OMe	H	OMe	H	OAc	OAc	8.7	22*c*[c]
39	OMe	H	OMe	H	OMe	OBz	>500	22*b*[c]
40	OMe	H	OMe	OH	OH	OH	3.7	22*e*[b]
41	OMe	H	OMe	OH	OH	OMe	>500	22*e*[b]
42	OMe	H	OMe	OMe	OH	OMe	12.5	22*e*[b]
43	OMe	H	OMe	OMe	OMe	OMe	>500	22*e*[c]
44	OMe	H	OMe	OMe	OAc	OMe	>500	22*d*[c]
45	OMe	H	OMe	OAc	OAc	OMe	98.0	22*e*[c]
46	OMe	H	OMe	OAc	OAc	OAc	42.2	22*e*[c]

Abbreviations: Ac, acetyl; Bz, benzyl: Et, ethyl; Me, methyl; un, unpublished. *a*) To be published. *b*) Natural product. *c*) Synthetic sample.

gel $60GF_{254}$, Merck, 0.5 mm), detection was also achieved by UV illumination. For column chromatography, Silica gel BW-820MH (Fuji Davison), Polyamide C-200 (Wako) and Chromatorex ODS-BU3050MT (Fuji Davison) were used. Centrifugal partition chromatography was performed on a Chromatotron (Harrison Research) with Silica gel $60GF_{254}$ (Merck, 4 or 2 mm) plate. For MPLC, Silica gel type CQ-3 (Fuji gel) was used. Preparative HPLC was performed on a Capcell Pak C_{18} column (10 × 250 mm, Shiseido) with acetonitrile–H_2O (1 : 1) as an eluent. Detection was effected by a Senshu 3000A-II UV detector at 360 nm, and the flow rate was 2 ml/min. UV and infrared (IR) spectra were recorded on a Hitachi 340 spectrophotometer and on a Hitachi 260-30 IR spectrophotometer, respectively. ^{1}H- and ^{13}C-nuclear magnetic resonance (NMR) spectra were recorded on a JEOL JMN-GX400 FT-NMR spectrometer (400 MHz for ^{1}H-NMR and 100 MHz for ^{13}C-NMR) and on a Hitachi R-900 spectrometer (90 MHz for ^{1}H-NMR) with tetramethylsilane as an internal standard. Mass spectra (MS) were recorded on JEOL JMS-D300 (EI-MS) and JEOL JMS-DX303 (FAB-MS, HR-MS) mass spectrometers.

Assay of cAMP Phosphodiesterase Samples were tested for inhibition of cAMP phosphodiesterase activity in duplicate by the method described previously.[8]

Enzymes and Chemicals Beef heart phosphodiesterase was purchased from Boehringer. Snake venom nucleotidase and cAMP were obtained from Sigma, and [^{3}H]cAMP from the Radiochemical Centre. Papaverine, a reference inhibitor, was purchased from Tokyo Kasei Kogyo Co., Ltd.

Extraction and Separation *Glycyrrhiza uralensis* (5 kg), which was purchased from Uchida Pharmacy for Oriental Medicine, was extracted with *n*-hexane, and the *n*-hexane extract when concentrated to dryness *in vacuo* yielded 69 g of the residue. This residue was subjected to centrifugal partition chromatography using $CHCl_3$–acetone (8 : 1) into 10 separate fractions. Fraction 3 was purified by column chromatography on silica gel, and recrystallized from $CHCl_3$ to give licoricidin (**6**) (23 mg). Fraction 7 was chromatographed on silica gel to give several fractions. The fractions 12—20 were purified by preparative TLC, polyamide C-200 column chromatography, ODS column chromatography and preparative HPLC, successively, and recrystallized from MeOH–H_2O to give licoarylcoumarin (**7**) (9.7 mg). Fractions 21—28 were purified by preparative TLC and recrystallized from $CHCl_3$ to give glycyrin (**8**) (52 mg).

Glycyrrhizin was produced from licorice roots by the method as shown in Chart 1. These waste materials were used as samples. The acetone layer as sample 4 (6 g) was chromatographed on silica gel to afford isoliquiritigenin (**2**), liquiritin (**3**) and isoliquiritigenin-4′-*O*-apioglucoside (**1**) (26 mg). The MeOH extract of residue as sample 1 (10 g) was chromatographed on silica gel into 8 separate fractions. The $CHCl_3$–MeOH (4 : 1) eluted fraction was subjected to centrifugal partition chromatography, preparative TLC and MPLC, successively, and recrystallized from acetone to afford glabridin (**5**) (12 mg) and a small amount of licoarylcoumarin (**7**). These samples, fractions and compounds

were tested for their inhibitory effect on cAMP phosphodiesterase.

Isoliquiritigenin-4′-*O*-apioglucoside (**1**): Yellow needles, mp 175—177 °C, FAB-MS *m/z*: 573 $[M+Na]^+$, 551 $[M+H]^+$. The spectroscopic properties (UV, ^{1}H- and ^{13}C-NMR) were in good agreement with those reported.[24]

Isoliquiritigenin (**2**): Yellow needles, mp 197—198 °C. EI-MS *m/z*: 256 (M^+). The spectroscopic properties (UV, ^{1}H- and ^{13}C-NMR) were in good agreement with those reported.[25]

Liquiritin (**3**): Colorless needles, mp 214—216 °C. FAB-MS *m/z*: 418 (M^+). The spectroscopic properties (UV, ^{1}H- and ^{13}C-NMR) were in good agreement with those reported.[26]

Grabridin (**5**): Colorless plates, mp 156—158 °C. EI-MS *m/z*: 324 (M^+), 309, 187, 173. The compound was identified as **5** by comparison with an authentic sample (mixed mp, TLC, UV, MS and ^{1}H-NMR).[27]

Licoricidin (**6**): Colorless needles, mp 158—160 °C. The compound was identified as **6** by comparison with an authentic sample (mixed mp, TLC, UV and ^{1}H-NMR).[28]

Licoarylcoumarin (**7**): Yellow needles, mp 145 °C. The compound was identified as **7** by comparison with an authentic sample (HPLC, UV, ^{1}H- and ^{13}C-NMR).[29]

Glycyrin (**8**): Yellow needles, mp 215—217 °C. The compound was identified as **8** by mixed mp and comparison of UV and IR spectra with those of an authentic sample.[30]

Purified Flavonoids Purified liquiritigenin (**4**), glycycoumarin (**9**), glycyrol (**10**), isoglycyrol (**11**) and licoricone (**12**) were obtained from licorice roots in the course of structural studies.[16]

Purified 4-Arylcoumarins The authentic samples of **13**—**46** used for cAMP phosphodiesterase inhibitory activity test were isolated or prepared during structural studies (Table II).

References and Notes

1) A part of this study was presented at the 110th Annual Meeting of the Pharmaceutical Society of Japan, Sapporo 1990. This paper is Part XVII of "Inhibitors of cAMP Phosphodiesterase in Medicinal Plants". Part XVI: T. Nikaido, T. Ohmoto, T. Kinoshita, U. Sankawa, F. D. Monache, B. Botta, T. Tomimori, Y. Miyaichi, Y. Shirataki, I. Yokoe, and M. Komatsu, *Chem. Pharm. Bull.*, **37**, 1392 (1989).
2) M. Horlington and P. A. Watson, *Biochem. Pharmac.*, **19**, 955 (1970) and references cited therein.
3) R. L. Vigdahl, N. R. Marquis, and P. A. Tavormina, *Biochem. Biophys. Res. Commun.*, **37**, 409 (1969).
4) R. R. Gorman, S. Bunting, and O. V. Miller, *Prostaglandins*, **13**, 377 (1977).
5) S. M. Wolfe and N. R. Shulman, *Biochem. Biophys. Res. Commun.*, **35**, 265 (1969).
6) K. Yoshioka, I. Takayanagi, and T. Hisayama, *J. Pharmacobio-Dyn.*, **12**, 660 (1989).
7) M. Maruyama, J. Kamiya, T. Kaiho, and T. Kobari, *J. Cardiovasc. Pharmacol.*, **12**, 579 (1988).
8) T. Nikaido, T. Ohmoto, H. Noguchi, T. Kinoshita, H. Saitoh, and U. Sankawa, *Planta Medica*, **43**, 18 (1981).
9) T. Nikaido, T. Ohmoto, T. Kinoshita, U. Sankawa, S. Nishibe, and S. Hisada, *Chem. Pharm. Bull.*, **29**, 3586 (1981).
10) T. Nikaido, T. Ohmoto, U. Sankawa, T. Hamanaka, and K. Totsuka, *Planta Medica*, **46**, 162 (1982).
11) T. Nikaido, T. Ohmoto, H. Saitoh, U. Sankawa, S. Sakuma, and J. Shoji, *Chem. Pharm. Bull.*, **30**, 2020 (1982).
12) T. Nikaido, T. Ohmoto, U. Sankawa, O. Tanaka, R. Kasai, J. Shoji, S. Sanada, S. Hiai, H. Yokoyama, H. Oura, and Y. Kawashima, *Chem. Pharm. Bull.*, **32**, 1477 (1984).
13) T. Nikaido, T. Ohmoto, U. Sankawa, S. Kitanaka, and M. Takido, *Chem. Pharm. Bull.*, **32**, 3075 (1984).
14) T. Nikaido, T. Ohmoto, T. Nomura, T. Fukai, and U. Sankawa, *Chem. Pharm. Bull.*, **32**, 4929 (1984).
15) T. Nikaido, T. Ohmoto, U. Sankawa, T. Tomimori, Y. Miyaichi, and Y. Imoto, *Chem. Pharm. Bull.*, **36**, 654 (1988).
16) S. Shibata and T. Saitoh, *J. Indian Chem. Soc.*, **55**, 1184 (1978).
17) K. Aida, M. Tawata, H. Shindo, T. Onaya, H. Sasaki, T. Yamaguchi, M. Chin, and H. Mitsuhashi, *J. Med. Pharmaceut. Soc. WAKAN-YAKU*, **5**, 514 (1988).
18) K. Tawata, K. Aida, H. Shindo, T. Onaya, H. Sasaki, T. Yamaguchi, M. Chin, and H. Mitsuhashi, *J. Med. Pharmaceut. Soc. WAKAN-YAKU*, **5**, 512 (1988).
19) K. Watanabe, *Taisha*, **10**, 626 (1973).
20) K. Okada, Y. Tamura, M. Yamamoto, Y. Inoue, R. Takagaki, K. Takahashi, S. Demizu, K. Kajiyama, Y. Hiraga, and T. Kinoshita, *Chem. Pharm. Bull.*, **37**, 2258 (1989).
21) *a*) J. Martinez del Campo, *An. Inst. Med. Nac.*, **8**, 332 (1906); *b*) J. Terres, *An. Inst. Med. Nac. Mexico*, **12**, 109 (1913).
22) *a*) G. D. Monache, I. Messana, B. Botta, and E. G. Baitz, *Magn. Reson. Chem.*, **27**, 1181 (1989); *b*) G. D. Monache, B. Botta, F. D. Monache, and M. Botta, *Phytochemistry*, **24**, 1355 (1985); *c*) G. D. Monache, B. Botta, A. S. Neto, and R. A. Lima, *ibid.*, **22**, 1657 (1983); *d*) G. D. Monache, B. Botta, F. Menichini, and R. M. Pinheiro, *Bull. Chem. Soc. Ethiopia*, **1**, 65 (1987); *e*) G. D. Monache, B. Botta, V. Vinciguerra, and R. M. Pinheiro, *Phytochemistry* (1990), **29**, 3984 (1990).
23) J. A. Nathanson, *Science*, **226**, 184 (1984).
24) H. Miething and A. Speicher-Brinker, *Arch. Pharm.* (*Weinheim*) **322**, 141 (1989).
25) T. Saitoh, H. Noguchi, and S. Shibata, *Chem. Pharm. Bull.*, **26**, 144 (1978).
26) T. Nakanishi, A. Inada, K. Kambayashi, and K. Yoneda, *Phytochemistry*, **24**, 339 (1985).
27) T. Saitoh, T. Kinoshita, and S. Shibata, *Chem. Pharm. Bull.*, **24**, 752 (1976).
28) S. Shibata and T. Saitoh, *Chem. Pharm. Bull.*, **16**, 1932 (1968).
29) T. Hatano, T. Yasuhara, T. Fukuda, T. Noro, and T. Okuda, *Chem. Pharm. Bull.*, **37**, 3005 (1989).
30) T. Kinoshita, T. Saitoh, and S. Shibata, *Chem. Pharm. Bull.*, **26**, 135 (1978).
31) F. Sanchez-Viesca, *Phytochemistry*, **8**, 1821 (1969).

Chem. Pharm. Bull. **39**(4) 934—936 (1991) Vol. 39, No. 4

Picrodendrins B, G and J, New Picrotoxane Terpenoids from *Picrodendron baccatum*

Kazuo KOIKE, Hiroshi FUKUDA, Katsuyoshi MITSUNAGA and Taichi OHMOTO*

School of Pharmaceutical Sciences, Toho University, 2–2–1 Miyama, Funabashi, Chiba 274, Japan. *Received September 20, 1990*

Three new picrotoxane type terpenoids, picrodendrins B, G and J, were isolated from the bark of *Picrodendron baccatum* KLUG *et* URBAN (Simaroubaceae). The structures were determined by spectroscopic evidence.

Keywords *Picrodendron baccatum*; Simaroubaceae; picrodendrin B; picrodendrin G; picrodendrin J; picrotoxane

We have recently reported on three new picrotoxane terpenoids (picrodendrins A,[1] C and D[2]) from the barks of *Picrodendron baccatum* (L.) KLUG *et* URBAN (Simaroubaceae)[3] collected in Indonesia. Continuing to examine *P. baccatum* extracts, we have now isolated, and report here, on three new picrotoxane terpenoids, picrodendrins B (**1**), G (**2**) and J (**3**).

Results and Discussion

The methanol extract of the bark of *P. baccatum* was partitioned between chloroform and water. The aqueous layer was further extracted successively with ethyl acetate and *n*-butanol. The chloroform-soluble fraction was repeatedly chromatographed on silica gel and further purified by preparative low-pressure liquid chromatography (LC) to give the new picrotoxane terpenoids, picrodendrins B (**1**) and G (**2**). The ethyl acetate soluble fraction was subjected to separation by Diaion HP-20 and further purified by preparative low-pressure LC to afford picrodendrin J (**3**).

Picrodendrin B (**1**) has a molecular formula $C_{20}H_{24}O_{10}$ ([M]$^+$ *m/z* 424.1366, Calcd 424.1370) and picrodendrin G (**2**) has a molecular formula $C_{21}H_{28}O_{10}$ ([M+H]$^+$ *m/z* 441.1768, Calcd 441.1761) derived from high-resolution mass spectrometry (HRMS). Comparisons of the proton and carbon-13 nuclear magnetic resonance (^{1}H- and ^{13}C-NMR) spectral data (Tables I and II) of **1** and **2** with those of picrodendrin A (**4**), whose structure was elucidated by X-ray analysis,[1] indicated that **1** and **2** are picrotoxane terpenoids. In particular, ^{1}H and ^{13}C signals due to the cyclohexane, cyclopentane and γ-lactone systems of **1** and **2** resonanced at almost the same frequencies as the corresponding signals in **4**, while the remaining ^{1}H and ^{13}C signals of a five-membered ring were observed at different major positions.

In picrodendrin B (**1**), the infrared (IR) and ultraviolet (UV) spectra showed absorption bands due to hydroxyls (3510 and 3400 cm^{-1}) and saturated and unsaturated γ-lactones (1785, 1720 cm^{-1} and 231 nm). It formed a monoacetate (**1a**). The long-range ^{1}H–^{13}C correlation spectroscopy (COSY) study of **1** revealed several interesting correlations *via* long-range couplings. Thus, the long-range couplings were observed between formyl proton (H-18, δ 9.23) and both γ-lactone carbonyl carbon (C-17, δ 166.57) and olefinic carbon (C-14, δ 161.18), and between methoxyl proton (OMe-14, δ 3.64) and both the olefinic carbon (C-14) and spiro-carbon (C-13, δ 92.84). These connectivities of long-range ^{1}H–^{13}C established the spiro unsaturated γ-lactone group of the molecule. The difference nuclear Overhauser effect (NOE) experiments of **1** were carried out to determine the relative stereochemistry at various chiral centers (Fig. 1). Thus, the structure of picrodendrin B was proposed to be formula **1**.

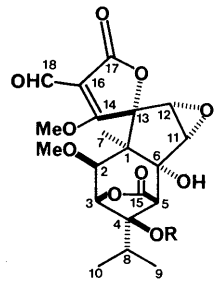

1 : R=H
1a : R=Ac

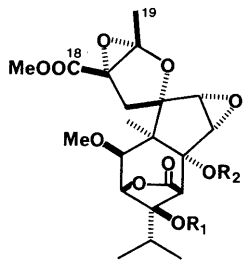

2 : R_1=R_2=H
2a : R_1=H, R_2=Ac
2b : R_1=R_2=Ac

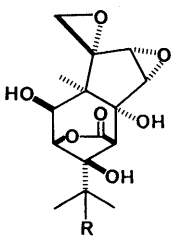

3 : R=OH
5 : R=H

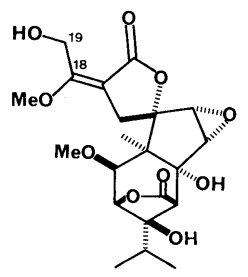

4

Chart 1

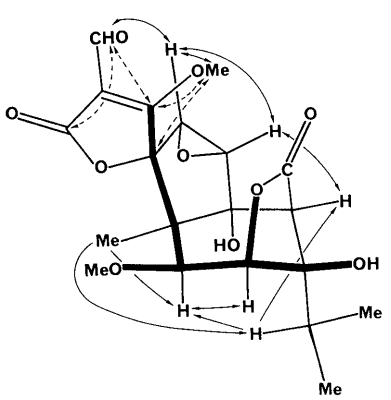

1

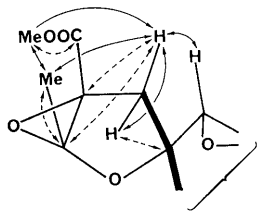

2

Fig. 1. NOEs Observed in NOE Difference Spectra and Long-Range ^{1}H–^{13}C Correlations of Picrodendrins B (**1**) and G (**2**)

⟳, NOE; ·····, long-range ^{1}H–^{13}C coupling.

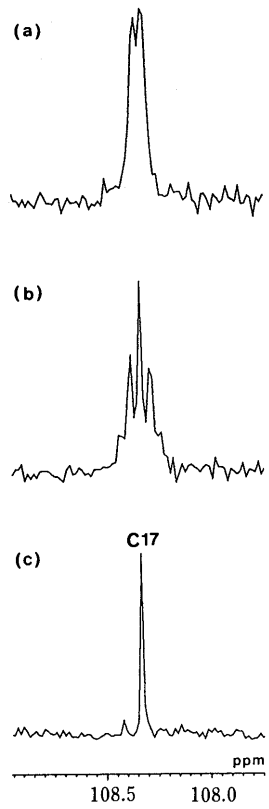

Fig. 2. Complete Decoupled, Nondecoupled and LSPD Spectra of Picrodendrin G (**2**)

a; irradiated at H-19 (Me) (δ 1.96); b, nondecoupled; c, complete decoupled.

TABLE I. ^{1}H-NMR Spectral Data for Compounds **1**—**5**[a,b]

Proton	1	2	4	3	5
H-2	3.65 d (1.2)	3.87 br s	3.70 s	5.56 d (3.6)	4.44 d (5.5)
H-3	5.13 br s	5.14 br s	5.15 d (1.1)	5.26 d (1.3)	5.13 d (1.1)
H-5	3.56 d (1.1)	3.37 d (1.1)	3.47 d (1.1)	3.64 d (1.3)	3.50 d (1.1)
H-7 (Me)	1.88 s	1.92 s	1.89 s	2.00 s	2.06 s
H-8	2.61 sep (6.6)	2.76 sep (6.0)	2.74 sep (6.2)		2.96 sep (6.6)
H-9 (Me)	1.47 d (6.6)	1.43 d (6.0)	1.48 d (6.2)	1.86 s	1.46 d (6.6)
H-10 (Me)	1.20 d (6.6)	1.19 d (6.0)	1.21 d (6.2)	1.68 s	1.11 d (6.6)
H-11	4.32 d (2.5)	4.03 d (3.0)	4.18 d (2.9)	4.36 d (3.1)	4.24 d (2.9)
H-12	3.87 d (2.5)	4.44 d (3.0)	3.66 d (2.9)	3.65 d (3.1)	3.63 d (2.9)
H-14α		4.77 d (15.0)	4.74 d (17.2)	4.99 d (6.2)	4.85 d (6.2)
H-14β		2.96 d (15.0)	3.44 d (17.2)	3.15 d (6.2)	3.11 d (6.2)
H-18	9.23 s				
H-19		1.96 s	5.29 dd (13.2, 4.0)		
			5.37 dd (13.2, 4.0)		
OMe-2	3.26 s	3.50 s	3.96 s		
OMe-14	3.64 s				
OMe-18		3.65 s	3.31 s		
OH-2				7.39 d (3.6)	7.53 d (5.5)
OH-19			7.35 br d (4.0)		

a) The spectra were measured in pyridine-d_5. b) s=singlet, d=doublet, dd=double doublet, sep=septed, br=broad. The figures in parentheses are the coupling constants in Hz.

In picrodendrin G (**2**), the IR spectra showed the absorption bands of hydroxyl (3400 cm^{-1}), γ-lactone (1790 cm^{-1}) and ester (1720 and 1255 cm^{-1}) groups. It formed monoacetate (**2a**) and diacetate (**2b**). For the connectivities of the remaining functional groups of a five-membered ring, long-range ^{1}H–^{13}C COSY and long-range selective proton decoupling (LSPD) experiments were carried out for **2** as illustrated in Figs. 1 and 2. The observation of the ^{1}H and ^{13}C long-range couplings between methyl proton (H-19, δ 1.96) and ketal carbon (C-17, δ 108.32), H-14β (δ 2.96) and both epoxide carbon (C-16, δ 86.77) and the ketal carbon, between carbomethoxyl proton (δ 3.65) and ester carbonyl carbon (δ 172.69) and between H-14α (δ 4.77) and spiro-carbon (C-13, δ 90.63) indicated the existence of a five-membered ring including epoxide, ketal and methoxycarbonyl groups. The location of a methyl group was further supported by the LSPD experiment to be at the ketal position (C-17). Irradiation of the proton giving the methyl signal at δ 1.96 caused the ketal carbon signal at δ 108.32 (quintet) to change into a doublet (Fig. 2). The relative stereochemistry of **2** was also confirmed from observation of the difference NOE experiments (Fig. 1). The NOE experiments showed that the α-epoxide between C-16 and C-17 and the other chiral centers were compatible with those of picrodendrins A (**4**) and B (**2**). Thus, the structure of picrodendrin G was proposed to be formula **2**.

TABLE II. ^{13}C-NMR Spectral Data for Compounds **1**—**5**[a]

C	1	2	4	3	5
1	54.43	53.15	52.99	45.51	45.53
2	86.61	89.86	87.89	75.11	75.35
3	83.25	82.72	83.15	89.59	90.04
4	81.68	82.30	82.21	83.13	82.04
5	57.71	58.00	57.82	58.76	58.34
6	78.11	78.39	78.17	78.37	78.52
7	25.61	25.77	25.12	21.16	21.75
8	30.93	31.04	31.03	72.67	30.91
9	15.85	15.57	15.63	25.19	15.44
10	18.19	18.26	18.24	27.92	18.32
11	62.99	62.61	62.85	61.59	61.82
12	60.83	64.11	63.17	60.70	60.95
13	92.84	90.63	89.33	67.50	66.90
14	161.18	41.73	34.25	52.45	52.35
15	175.99	175.86	175.83	175.55	176.45
16	123.02	86.77	104.27		
17	166.57	108.32	170.99		
18	166.18	172.69	166.34		
19		20.52	53.63		
OMe-2	58.18	58.69	59.08		
OMe-14	52.02				
OMe-18		52.00	55.75		

a) The spectra were measured in pyridine-d_5.

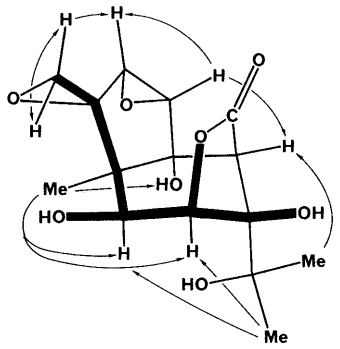

3

Fig. 3. NOEs Observed in NOE Difference Spectra of Picrodendrin J (**3**)

Picrodendrin J (**3**) showed the absorption bands of hydroxyl (3550, 3470 and 3430 cm^{-1}) and γ-lactone (1770 cm^{-1}) group in the IR spectrum. From the elementary analysis, the molecular formula was concluded to be $C_{15}H_{20}O_7$, suggesting that it has one more hydroxyl group

than picrodendrin C (**5**).[2] Comparisons of the ^{1}H- and ^{13}C-NMR spectral data with those of **5** indicated that the isopropyl group at C-4 in **5** was replaced by the hydroxyisopropyl group in **3**. Therefore, the structure of picrodendrin J is presented as 8-hydroxypicrodendrin C. The relative stereochemistry of **3** was ascertained by analysis of the NOE difference spectra of **3** (Fig. 3). These observations indicated that all the chiral centers were compatible with those of picrodendrin C (**5**). Thus, the structure of picrodendrin J was proposed to be formula **3**.

Experimental

Melting points were determined on a Yanagimoto micromelting point apparatus and are uncorrected. The UV and IR spectra were recorded with Hitachi 340 and Hitachi 260-30 spectrophotometers, respectively. The ^{1}H- and ^{13}C-NMR spectra were recorded with a JEOL GX-400 (^{1}H, 400 MHz; ^{13}C, 100 MHz) spectrometer. Chemical shifts are given on the δ-scale (with ppm downfield from tetramethylsilane as an internal standard) and coupling constants (J) in herts (Hz). Electron-impact (EI) MS and HRMS were run on JEOL JMS D-300 and JEOL DX-303 mass spectrometers, respectively. Optical rotations were determined on a JASCO DIP-4 digital polarimeter. Column chromatography was carried out on silica gel (BW-820 MH, Fuji Davison) and Diaion-HP20 (Mitsubishi Kasei). Low-pressure LC was carried out on silica gel (CQ-3, 24 i.d. × 320 mm, Fuji gel).

Extraction and Isolation Dried bark (8 kg) of *Picrodendron baccatum* collected at the Botanical Garden of Bogor, Indonesia, in September, 1986 was extracted with MeOH (49 l) at room temperature. The MeOH extract was concentrated under reduced pressure to give a residue (1.9 kg), to which an equal volume of H_2O was added. The aqueous solution was extracted successively with $CHCl_3$, EtOAc and *n*-BuOH. Each fraction was concentrated to give $CHCl_3$ (80 g), EtOAc (260 g), *n*-BuOH (300 g) and H_2O-soluble fractions (1260 g). The $CHCl_3$-soluble fraction (80 g) was chromatographed on a silica gel column (2.0 kg) and eluted with $CHCl_3$, $CHCl_3$/MeOH and MeOH. The crude picrotoxane terpenoids fraction was obtained by eluting with $CHCl_3$–MeOH (9 : 1) and further purified by low-pressure LC (Silica gel CQ-3, solvent system benzene–EtOAc (9 : 1)) to afford picrodendrin-B (20 mg) and picrodendrin-G (200 mg). The EtOAc fraction (260 g) was chromatographed on Diaion HP-20 (2 kg) and eluted with H_2O, H_2O/MeOH and MeOH. The crude picrotoxane terpenoids fraction was obtained by eluting with H_2O–MeOH (5 : 1) and further purified by low-pressure LC (Silica gel CQ-3, solvent system benzene–EtOAc (9 : 1)) to afford picrodendrin-J (30 mg).

Picrodendrin-B (1) Colorless prisms (MeOH), mp 245 °C, $[\alpha]_D^{25}$ −50.4° (c = 1.8, pyridine). UV λ_{max}^{MeOH} nm (log ε): 231 (4.46). IR ν_{max}^{KBr} cm^{-1}: 3510, 3400, 2960, 1785 (sh), 1760, 1720, 1640, 1270, 1240, 1165, 1105, 1075, 1010. MS m/z (%): 424 [M$^+$, 28], 393 (16), 330 (4), 242 (5), 193 (10), 155 (100), 141 (48), 113 (51), 71 (86), 43 (78). ^{1}H- and ^{13}C-NMR data are given in Tables I and II, respectively. HRMS m/z: 424.1366 (Calcd for $C_{20}H_{24}O_{10}$, 424.1370).

Acetylation of 1 Compound **1** (10 mg) was treated with Ac_2O and pyridine at 80 °C for 10 h. The reaction mixture was worked up as usual and then recrystallization from MeOH gave a monoacetate (**1a**, 8 mg) as colorless prisms, mp 210 °C, $[\alpha]_D^{25}$ −21.5° (c = 0.4, pyridine). IR ν_{max}^{KBr} cm^{-1}: 3480, 2950, 1800, 1790 (sh), 1740, 1645, 1230, 1095, 1060, 1010. MS m/z (%): 466 [M$^+$, 16], 435 (8), 424 (4), 271 (7), 99 (100). ^{1}H-NMR (C_5D_5N) δ: 1.12 (3H, d, J = 7.0 Hz, H-9), 1.32 (3H, d, J = 7.0 Hz, H-10), 1.82 (3H, s, H-7), 2.04 (3H, s, OAc-4), 2.76 (1H, sep, J = 7.0 Hz, H-8), 3.21 (3H, s, OMe-2), 3.59 (1H, d, J = 0.5 Hz, H-2), 3.71 (3H, s, OMe-14), 3.88 (1H, d, J = 2.2 Hz, H-12), 4.11 (1H, d, J = 0.5 Hz, H-5), 4.32 (1H, d, J = 2.2 Hz, H-11).

Picrodendrin-G (2) Colorless prisms (MeOH), mp 211—213 °C, $[\alpha]_D^{26}$ −33.1° (c = 1.5, pyridine). IR ν_{max}^{KBr} cm^{-1}: 3400, 2965, 1790, 1720, 1290, 1255, 1210, 1135, 1090, 1080. MS m/z (%): 441 ([M+H]$^+$, 1), 384 (7), 365 (3), 348 (8), 320 (16), 295 (4), 277 (4), 205 (10), 165 (16), 135 (36), 111 (46), 43 (100). ^{1}H- and ^{13}C-NMR data are given in Tables I and II, respectively. HRMS m/z: 441.1768 (Calcd for $C_{21}H_{29}O_{10}$ [M+H]$^+$, 441.1761).

Acetylation of Compound 2 Compound **2** (15 mg) was treated with Ac_2O and pyridine at 80 °C for 10 h, and the reaction mixture was worked up as usual and then further purified by low-pressure LC (Silica gel CQ-3, solvent system $CHCl_3$–MeOH (20 : 1)) to give monoacetate (**2a**, 8 mg) and diacetate (**2b**, 4 mg).

Monoacetate (**2a**): $[\alpha]_D^{25}$ −33.8° (c = 0.4, pyridine). IR ν_{max}^{KBr} cm^{-1}: 3420 (br), 1760, 1750, 1285, 1260, 1245, 1150, 1115, 1080. MS m/z (%): 440 ([M−Ac]$^+$, 25), 381 (70), 363 (17), 43 (100). ^{1}H-NMR (C_5D_5N) δ: 1.21 (3H, d, J = 7.0 Hz, H-9), 1.47 (3H, d, J = 7.0 Hz, H-10), 1.94 (3H, s, H-7), 1.95 (3H, s, H-19), 2.02 (3H, s, OAc-6), 2.78 (1H, sep, J = 7.0 Hz, H-8), 3.44 (1H, d, J = 1.0 Hz, H-5), 3.53 (3H, s, OMe-2), 3.71 (3H, s, OMe-18), 3.86 (1H, d, J = 3.0 Hz, H-11), 3.93 (1H, s, H-2), 4.13 (1H, d, J = 3.0 Hz, H-12), 3.29, 5.08 (each d, 1H, J = 16.0 Hz, H-14), 5.24 (1H, s, H-3).

Diacetate (**2b**): $[\alpha]_D^{25}$ −34.1° (c = 0.6, pyridine). IR ν_{max}^{KBr} cm^{-1}: 1800, 1770, 1755, 1740, 1260, 1235, 1160, 1145, 1110, 1080. MS m/z (%): 482 ([M−Ac]$^+$, 1), 440 (1), 390 (8), 363 (12), 43 (100). ^{1}H-NMR (C_5D_5N) δ: 1.13 (3H, d, J = 6.0 Hz, H-9), 1.30 (3H, d, J = 6.0 Hz, H-10), 1.87 (3H, s, H-7), 1.93 (3H, s, H-19), 2.01, 2.02 (each 3H, s, OAc-4, 6), 2.93 (1H, sep, J = 6.0 Hz, H-8), 3.50 (3H, s, OMe-2), 3.76 (3H, s, OMe-18), 3.86 (1H, s, H-2), 3.84 (1H, d, J = 3.0 Hz, H-11), 3.89 (1H, s, H-5), 4.11 (1H, d, J = 3.0 Hz, H-12), 3.23, 4.99 (each d, 1H, J = 16.0 Hz, H-14), 5.90 (1H, s, H-3).

Picrodendrin-J (3) Colorless prisms (MeOH), mp 240 °C, $[\alpha]_D^{24}$ −23.4° (c = 2.5, pyridine). IR ν_{max}^{KBr} cm^{-1}: 3550, 3470, 3430, 2990, 1770, 1665, 1170, 1020. MS m/z (%): 310 ([M−H_2O]$^+$, 3), 227 (4), 223 (3), 207 (14), 193 (12), 179 (12), 165 (15), 141 (55), 125 (59), 71 (25), 59 (100), 43 (68). ^{1}H- and ^{13}C-NMR data are given in Tables I and II, respecgively. *Anal.* Calcd for $C_{15}H_{20}O_7 \cdot H_2O$: C, 52.07; H, 6.40. Found, C, 52.35; H, 6.36.

Acknowledgement We are grateful to the P. T. Indonesia Eisai Co., Ltd., and Eisai Co., Ltd., for their kind supply of plant material. We thank the members of the Botanical Garden of Bogor, Indonesia, for their identification of plant material.

References

1) T. Ohmoto, K. Koike, H. Fukuda, K. Mitsunaga, K. Kagei, T. Kawai and T. Sato, *Chem. Pharm. Bull.*, **37**, 1805 (1989).
2) T. Ohmoto, K. Koike, H. Fukuda, K. Mitsunaga, K. Ogata and K. Kagei, *Chem. Pharm. Bull.*, **37**, 2988 (1989).
3) S. Danimibardja and D. Noyodihardjo, "An Alphabetical List of Plant Species, Cultivated in the Hortus Botanicus Bogoriensis," Republic of Indonesia, Indonesia Institute of Sciences, National Biological Institute, Botanic Garden, 1978, p. 193.

Sesquiterpene Glycosides from *Ainsliaea cordifolia* FRANCH. *et* SAV.

Toshio MIYASE,* Hitoshi OZAKI and Akira UENO

School of Pharmaceutical Sciences, University of Shizuoka, 395, Yada, Shizuoka 422, Japan. *Received October 3, 1990*

Three new eudesmane-type sesquiterpene glycosides, ainsliasides C, D and E, have been isolated from *Ainsliaea cordifolia* FRANCH. *et* SAV. (Compositae). Their structures were elucidated on the basis of chemical and spectroscopic data.

Keywords *Ainsliaea cordifolia*; Compositae; sesquiterpene glycoside; eudesmane; ainsliaside C; ainsliaside D; ainsliaside E; taraxinsäure-1′-*O*-*β*-D-glucopyranosid

In connection with a study on the sesquiterpene glycosides of some plants in Compositae, we have also reported on the sesquiterpene glycosides of *Ainsliaea acerifolia* and *A. dissecta*.[1] Now we have also investigated *Ainsliaea cordifolia* FRANCH. *et* SAV. and isolated three new eudesmane-type sesquiterpene glycosides, ainsliasides C, D and E together with a known germacrane-type sesquiterpene glycoside, taraxinsäure-1′-*O*-*β*-D-glucopyranosid. Their structures were elucidated on the basis of chemical and spectroscopic data.

The air dried whole plants of *A. cordifolia* were extracted with hot methanol. The concentrated extract was suspended in water and the suspension was extracted with ether and then *n*-butanol, successively. The resulting butanol extract was subjected to repeated column chromatography on silica gel and semi-preparative high performance liquid chromatography on octadecyl silanized silica (ODS) to give **1**—**4**.

The main compound **1** was identified as taraxinsäure-1′-*O*-*β*-D-glucopyranosid by comparison of the proton nuclear magnetic resonance (^{1}H-NMR) and carbon-13 nuclear magnetic resonance (^{13}C-NMR) spectra with reported data.[2]

The fast atom bombardment mass spectrum (FAB-MS) of ainsliaside C (**2**) exhibited ions at *m/z* 439 $[M+Na]^+$ and 417 $[M+H]^+$. The ^{1}H-NMR spectrum of **2** showed three singlet methyl proton signals at *δ* 1.08, 1.57, 1.58, *exo*-methylene proton signals at *δ* 5.03, 5.17 (each br s), two methine proton signals at *δ* 3.58 (dd, *J*=11, 4 Hz), 4.92 (br t, *J*=5.5 Hz) and an anomeric proton signal at *δ* 5.09 (d, *J*=8.5 Hz). Acetylation of **2** with acetic anhydride–pyridine afforded a pentaacetate **2a** and acid hydrolysis afforded glucose as the sugar moiety, but enzymatic hydrolysis with crude hesperidinase did not proceed. The ^{1}H-NMR spectrum of **2a** exhibited a down-field shifted axial methine proton at *δ* 4.66 (dd, *J*=11.5, 5 Hz). In the ^{13}C-NMR spectrum of **2**, twenty-one carbon signals, including six carbon signals due to a glucopyranosyl residue, were observed. These chemical and spectral data suggested that **2** was a sesquiterpene glucoside which had one secondary-equatorial hydroxyl group in the aglycone moiety. In the ^{1}H-NMR spectrum of **2**, an up-field shifted methyl signal (*δ* 1.08) suggested **2** to be a *trans*-fused eudesmane-type compound.[3] The position of the secondary hydroxyl group was decided to be 1 by comparison of the chemical shifts of A-ring carbons and the coupling constants of the methine proton with those of selin-4 (15)-en-1*β*,11-diol.[4] From the results of the detailed difference nuclear Overhauser effect (NOE) experiments, which results were illustrated in the structure formula by an arrow, and the coupling constants (br t, *J*=5.5 Hz) of the methine proton which was attached to a glucose bearing carbon, the glucosylation position was decided to be 6*β*. Thus, the structure of ainsliaside C was decided to be **2**.

The FAB-MS of ainsliaside D (**3**) exhibited the same ions at *m/z* 439 $[M+Na]^+$ and 417 $[M+H]^+$ as **2**. The ^{1}H-NMR showed four methyl proton signals at *δ* 1.20, 1.49, 1.61, 2.15, two methine proton signals at *δ* 3.78 (dd, *J*=8, 7 Hz), 4.91 (t, *J*=3 Hz), an anomeric proton signal at *δ* 5.15 (d, *J*=8 Hz) and an olefinic proton signal at *δ* 5.43 (br s). The ^{13}C-NMR spectrum showed the presence of a tri-substituted double bond (122.0, 136.3, confirmed by ^{1}H–^{13}C correlation spectroscopy (COSY) spectrum). Acetylation afforded a pentaacetate **3a** and acid hydrolysis afforded glucose as the sugar moiety as **2**. These results and the difference NOE experiments (Chart 1) propose the structure **3** for ainsliaside D.

The ^{13}C-NMR spectrum of ainsliaside E (**4**) showed twenty-one sp^3 carbon signals. The FAB-MS (*m/z* 457 $[M+Na]^+$; 435 $[M+H]^+$) and elemental analysis suggested the molecular formula $C_{21}H_{38}O_9$, which was H_2O more than that of **2** or **3**. The ^{1}H-NMR spectrum of **4** exhibited four singlet methyl signals at *δ* 1.33, 1.47, 1.52, 1.63, two methine proton signals at *δ* 3.63 (dd, *J*=10, 5 Hz); 5.09 (t, *J*=3 Hz) and an anomeric proton signal at *δ* 5.30

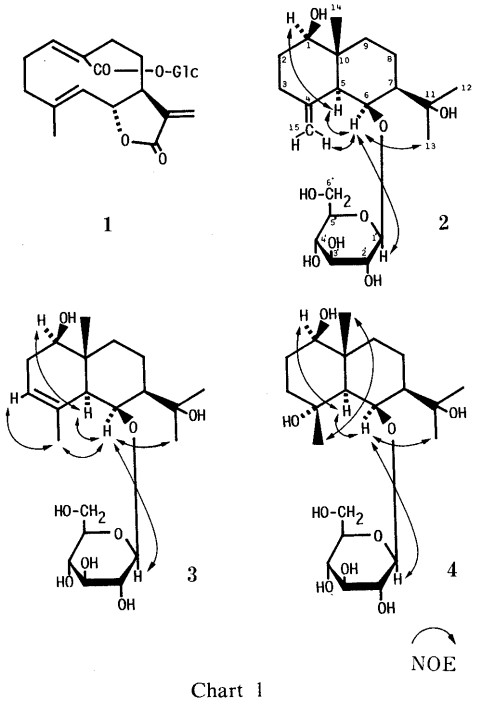

Chart 1

TABLE I. ^{13}C-NMR Spectral Data in Pyridine-d_5

	2	2a	3	3a	4	4a
Aglycone moiety						
1	79.4	81.4	76.6	78.2	79.0	81.6
2	33.3[a]	29.1	34.3	30.4[c]	29.9	25.5
3	33.8[a]	32.8	122.0	121.1	42.5	40.8
4	148.5	147.0	136.3	[g]	72.3[e]	73.5
5	53.2	52.4	53.6	50.0	59.4	52.1
6	78.0	78.0	79.9	78.9	80.9	78.6
7	45.4	44.9	44.8	44.5	45.5	43.6
8	19.8	18.5	17.8	19.1	18.1	20.4
9	36.4	35.4	30.8	30.4[c]	34.6	35.5
10	41.2	39.6	38.8	38.0	40.4	40.4
11	72.9	72.6[b]	72.4	72.2[d]	72.1[e]	72.9[f]
12	29.6	29.4	30.2	30.0	30.4	31.0
13	31.3	29.9	30.7	30.9	30.7	31.5
14	15.7	16.4	12.6	13.2	16.5	15.4
15	107.2	107.5	23.1	23.3	23.8	24.3
Glucose moiety						
1	104.4	100.5	105.6	99.8	105.6	97.4
2	75.2	72.2[b]	74.1	72.5[d]	75.2	71.2
3	78.8	72.2[b]	78.7	72.5[d]	78.8	72.7[f]
4	71.5	69.1	71.8	69.4	72.4	69.6
5	78.3	72.1[b]	78.3	73.7	78.5	72.4[f]
6	62.6	62.3	62.8	62.4	63.0	62.4
Ac						
		20.4 × 2		20.3 × 2		20.4
		20.6		20.4		20.5
		20.8		20.7		20.6
		20.9		20.9		21.0
		169.5 × 2		169.4		21.2
		170.1 × 2		169.5		169.6
		170.3		170.1 × 3		169.8
						170.1
						170.2 × 2

a—*f*) Assignments may be interchanged in each column. *g*) Overlapped with solvent signals.

(d, J=8 Hz). The ^{13}C-NMR spectrum of **4** showed four oxygenated carbons (δ 72.1, 72.3, 79.0, 80.9) other than glucosyl carbons. Acetylation afforded a pentaacetate **4a** suggesting that **4** had one secondary hydroxyl group in the aglycone moiety. In the ^{1}H-NMR spectrum of **4**, NOE was observed between a methyl signal at δ 1.33 and a methyl signal at δ 1.47 which were correlated with a signal at δ 16.5 and 23.8, respectively, in the ^{1}H–^{13}C COSY spectrum (Chart 1). Thus **4** had a 4α-hydroxy-4β-methyl structure.

These three new eudesmane-type sesquiterpenes are closely related to each other in the biosynthesis. The absolute configuration of these eudesmane-type sesquiterpenes could not be decided.

Experimental

Optical rotations were determined with a JASCO DIP-360 digital polarimeter. MS were measured on a JEOL JMS-SX102 mass spectrometer. ^{1}H- and ^{13}C-NMR spectra were recorded on a JEOL FX-90Q, GSX-270 and GSX-500 NMR spectrometers. Chemical shifts are given on the δ scale with tetramethylsilane as an internal standard (s, singlet; d, doublet; t, triplet; m, multiplet; br, broad). Gas chromatography (GC) was done on a Hitachi G-3000 gas chromatograph. High performance liquid chromatography (HPLC) was done on a JASCO system 800 instrument.

Isolation Air dried whole plants (700 g) of *A. cordifolia* FRANCH. *et* SAV. collected in June, in Shizuoka, Japan, were extracted twice with methanol under reflux. The extract was concentrated under reduced pressure and the residue was suspended in water. This suspension was extracted with ether and *n*-butanol, successively. After repeated chromatography of the *n*-butanol-soluble fraction (29 g) using a chloroform–methanol system with silica gel 60 and a water-acetonitrile system with ODS HPLC, taraxinsäure-1′-*O*-β-D-glucopyranosid (**1**) (19.0 g), ainsliaside C (**2**) (100 mg), ainsliaside D (**3**) (20 mg) and ainsliaside E (**4**) (1.0 g) were isolated.

Ainsliaside C (2) Amorphous powder, $[\alpha]_D^{22}$ −22.0° (c=2.00, MeOH). *Anal.* Calcd for $C_{21}H_{36}O_8 \cdot H_2O$: C, 58.05; H, 8.81. Found: C, 58.25; H, 8.65. FAB-MS m/z: 439 $[M+Na]^+$, 417 $[M+H]^+$. ^{1}H-NMR (C_5D_5N) δ: 1.08 (3H, s, H_3-14), 1.57, 1.58 (each 3H, s, H_3-12/H_3-13), 2.84 (1H, d, J=6 Hz, H-5), 3.58 (1H, dd, J=11, 4 Hz, H-1), 3.77 (1H, m, H-5′), 3.96 (1H, t, J=8.5 Hz, H-2′), 4.20 (1H, t, J=9 Hz, H-3′), 4.24 (1H, t, J=9 Hz, H-4′), 4.34 (1H, dd, J=12, 4 Hz, H-6′), 4.37 (1H, dd, J=12, 2 Hz, H-6′), 4.92 (1H, br t, J=5.5 Hz, H-6), 5.03 (1H, br s, H-15a), 5.09 (1H, d, J=8 Hz, H-1′), 5.17 (1H, br s, H-15b). ^{13}C-NMR: Table I.

Ainsliaside D (3) Amorphous powder, $[\alpha]_D^{22}$ −28.4° (c=0.74, MeOH). *Anal.* Calcd for $C_{21}H_{36}O_8 \cdot 1/2H_2O$: C, 59.27; H, 8.76. Found: C, 59.37; H, 8.65. FAB-MS m/z: 439 $[M+Na]^+$, 417 $[M+H]^+$. ^{1}H-NMR (C_5D_5N) δ: 1.20 (3H, s, H_3-14), 1.49, 1.61 (each 3H, s, H_3-12/H_3-13), 2.15 (3H, br s, H_3-15), 3.25 (1H, br s, H-5), 3.78 (1H, dd, J=8, 7 Hz, H-1), 3.92 (1H, m, H-5′), 4.01 (1H, t, J=8.5 Hz, H-2′), 4.20 (1H, t, J=9 Hz, H-4′), 4.25 (1H, t, J=8.5 Hz, H-3′), 4.31 (1H, dd, J=12, 5 Hz, H-6′), 4.42 (1H, dd, J=12, 2 Hz, H-1′), 4.91 (1H, t, J=3 Hz, H-6), 5.15 (1H, d, J=8 Hz, H-1′) 5.43 (1H, br s, H-3). ^{13}C-NMR: Table I.

Ainsliaside E (4) Amorphous powder, $[\alpha]_D^{22}$ −19.0° (c=0.87, MeOH). *Anal.* Calcd for $C_{21}H_{38}O_9 \cdot H_2O$: C, 55.74; H, 8.91. Found: C, 55.96; H, 8.69. FAB-MS m/z: 457 $[M+Na]^+$, 435 $[M+H]^+$. ^{1}H-NMR (C_5D_5N) δ: 1.33 (3H, s, H_3-14), 1.47 (3H, s, H_3-15), 1.52, 1.63 (each 3H, s, H_3-12/H_3-13), 2.66 (1H, d, J=3 Hz, H-5), 3.63 (1H, dd, J=10, 5 Hz, H-1), 3.94 (1H, t, J=9 Hz, H-4′), 4.01 (1H, t, J=8.5 Hz, H-2′), 4.06 (1H, dt, J=8, 2 Hz, H-5′), 4.16 (1H, dd, J=11, 8.5 Hz, H-6′), 4.19 (1H, t, J=9 Hz, H-3′), 4.67 (1H, dd, J=11, 1.5 Hz, H-6′), 5.09 (1H, t, J=3 Hz, H-6), 5.30 (1H, d, J=8 Hz, H-1′). ^{13}C-NMR: Table I.

Acetylation of 2, 3 and 4 **2** (20 mg), **3** (10 mg) and **4** (50 mg) were acetylated in the usual manner using acetic anhydride–pyridine (1 : 1) (1 ml) to give the acetate **2a** (18 mg), **3a** (8 mg) and **4a** (43 mg), respectively. **2a**: Amorphous powder. ^{1}H-NMR (CD_3COCD_3) δ: 0.88 (3H, s, H_3-14), 1.21, 1.30 (each 3H, s, H_3-12/H_3-13), 1.92, 1.98, 2.05 (each 3H, s, OAc), 1.99 (6H, s, OAc × 2), 2.68 (1H, br d, J=5.5 Hz, H-5), 3.81 (1H, ddd, J=10, 4, 2.5 Hz, H-5′), 4.10 (1H, dd, J=12.5, 2.5 Hz, H-6′), 4.20 (1H, dd, J=12.5, 4 Hz, H-6′), 4.63 (1H, dd, J=5.5, 4 Hz, H-6), 4.66 (1H, dd, J=11.5, 5 Hz, H-1), 4.88 (1H, dd, J=9, 8 Hz, H-2′), 4.96, 4.98 (each 1H, br s, H-15a/H-15b), 5.00 (1H, d, J=8 Hz, H-1′), 5.04 (1H, t, J=9 Hz, H-4′), 5.21 (1H, t, J=9 Hz, H-3′). ^{13}C-NMR: Table I. **3a**: Amorphous powder. ^{1}H-NMR (CD_3COCD_3) δ: 0.97 (3H, s, H_3-14), 1.20, 1.32 (each 3H, s, H_3-12/H_3-13), 1.91 (3H, br s, H_3-15), 1.93, 1.99, 2.03 (each 3H, s, OAc), 2.00 (6H, s, OAc × 2), 4.00 (1H, ddd, J=9, 3, 2 Hz, H-5′), 4.15 (2H, m, H_2-6′), 4.67 (1H, dd, J=5, 3 Hz, H-6), 4.75 (1H, dd, J=9, 8 Hz, H-1), 4.95 (1H, dd, J=9, 8 Hz, H-2′), 5.02 (1H, t, J=9 Hz, H-4′), 5.15 (1H, d, J=8 Hz, H-1′), 5.28 (1H, t, J=9 Hz, H-3′), 5.30 (1H, br s, H-3). ^{13}C-NMR: Table I. **4a**: Amorphous powder. ^{1}H-NMR (CD_3COCD_3) δ: 1.08 (3H, s, H_3-14), 1.27, 1.33 (each 3H, s, H_3-12/H_3-13), 1.36 (3H, s, H_3-15), 1.96, 1.97, 1.98, 2.01, 2.05 (each 3H, s, OAc), 2.15 (1H, m, H-7), 2.64 (1H, d, J=10 Hz, H-5), 4.00 (1H, m, H-5′), 4.18 (1H, dd, J=12, 5.5 Hz, H-6′), 4.29 (1H, dd, J=12, 2 Hz, H-6′), 4.53 (1H, dd, J=8, 6 Hz, H-1), 4.80 (1H, dd, J=10, 4 Hz, H-6), 4.94 (1H, dd, J=10, 8 Hz, H-2′), 5.04 (1H, t, J=10 Hz, H-4′), 5.25 (1H, d, J=8 Hz, H-1′), 5.31 (1H, t, J=10 Hz, H-3′). ^{13}C-NMR: Table I.

Acid Hydrolysis of 2, 3 and 4 A solution of a glycoside (*ca.* 0.2 mg) in 5% H_2SO_4 (2 drops) was heated in a boiling water bath for 30 min. The solution was passed through an Amberlite IRA-45 column and concentration to give a residue, which was reduced with $NaBH_4$ (*ca.* 2 mg) for 1 h at room temperature. The reaction mixture was passed through an Amberlite IR-120 column and the eluate was concentrated to dryness. Boric acid was removed by co-distillation with methanol and the residue was acetylated with acetic anhydride–pyridine (1 : 1) (2 drops) at 100 °C for 1 h. The reagents were evaporated off *in vacuo*. From each glycoside, glucitol acetate was detected by GC. Conditions: column, Supelco SP-2380 capillary column, 0.25 mm × 30 m; column temperature, 250 °C; carrier gas, N_2; t_R 12.2 min.

Acknowledgement We thank the staff of the Central Analytical Laboratory of this university for elemental analysis and the measurement of MS.

References

1) T. Miyase and S. Fukushima, *Chem. Pharm. Bull.*, **32**, 3043 (1984).
2) R. Hansel, M. Kartarahardja, J.-T. Huang and F. Bohlmann, *Phytochemistry*, **19**, 857 (1980).
3) D. Adinarayana and K. U. Syamasundar, *Phytochemistry*, **21**, 1083 (1982).
4) K. R. Verma, T. C. Jain and S. C. Battacharyya, *Tetrahedron*, **18**, 979 (1962).

Javanicins N, P and Q, New Quassinoids from *Picrasma javanica*

Kazuo KOIKE, Kiyoshi ISHII, Katsuyoshi MITSUNAGA and Taichi OHMOTO*

School of Pharmaceutical Sciences, Toho University, 2-2-1 Miyama, Funabashi, Chiba 274, Japan. *Received October 5, 1990*

A new quassinoid, javanicin N, was isolated from the woods of *Picrasma javanica* (Simaroubaceae) collected in Indonesia, and two new quassinoids, javanicins P and Q, were also isolated from the leaves of the same plant. Their structures were determined by spectroscopic data.

Keywords *Picrasma javanica*; Simaroubaceae; javanicin N; javanicin P; javanicin Q; des-4-methylpicrasane; quassinoid

We have recently reported on several novel des-4-methylpicrasane type quassinoids[1-5] and quassinoid glucosides[2,6] from *Picrasma javanica* BL. collected in Indonesia. Continuing to examine *P. javanica* extracts, we have now isolated three new quassinoids, javanicins N (**1**), P (**2**) and Q (**3**), which are reported here.

Results and Discussion

Javanicin N (**1**), mp 222—224 °C, was obtained as colorless needles, and its molecular formula was $C_{30}H_{36}O_{10}$ as determined by high-resolution mass spectrometry (HRMS). The infrared (IR) spectrum of **1** indicated the presence of δ-lactone (ν_{max} 1735 cm^{-1}), aromatic (ν_{max} 1610, 1490 and 762 cm^{-1}) and ester (ν_{max} 1700 and 1290 cm^{-1}) groups. Its ultraviolet (UV) spectrum (λ_{max} 220, 262 and 296 nm) was similar to that of javanicin G (**4**),[3] indicating that **1** has an aromatic ring in the molecule. Comparison of the proton and carbon-13 nuclear magnetic resonance (^{1}H- and ^{13}C-NMR) spectral data (Tables I and II) with those of **4** indicated that a methoxyl group (δ 2.84, s) at C-2 in **4** was replaced by an acetoxyl group (δ 1.97, s) in **1**. The relative downfield shift ($\Delta\delta$ = 1.59 ppm) of the H-2 proton in **1** may be attributed to the relief from anisotropic shielding due to the acetyl carbonyl group. The position of the acetoxyl, 3,4-methylenedioxybenzoyloxyl and methoxyl groups were assigned to be C-2, C-11 and C-12, respectively, based on the ^{13}C–^{1}H long-range correlation spectroscopy (COSY) of **1**. A carbonyl carbon at δ 169.89 correlated with H-2 (δ 5.71) and acetyl protons (δ 1.97). A carbonyl carbon at δ 165.58 correlated with H-11 (δ 5.80) and *ortho* protons (δ 7.83 and 8.00, each 1H) of the 3,4-methylenedioxybenzoyl group. A methine carbon at δ 85.85 (C-12) correlated with a methoxyl proton (δ 3.29). The relative stereochemistry of **1** was examined through an extensive series of nuclear Overhauser effect (NOE) experiments. Irradiation of Me-8 at δ 1.15 induced NOEs at H-7 (14%), Me-10 (11%), H-11 (11%), H-13 (10%) and H-14 (7%). Irradiation of Me-10 at δ 1.43 induced NOEs at H-2 (15%), OMe-12 (3%), Me-8 (8%) and H-11 (8%). Irradiation of Me-13 at δ 0.97 induced 7% NOE at H-12. Thus, the proton at C-2 (δ 5.71) was assigned as the β-axial from the coupling constants (J = 12 and 7 Hz), and this was confirmed by the presence of an NOE with C-10 β-axial methyl protons. On the basis of the above data, the structure of javanicin N is proposed to be **1**.

Javanicin P (**2**), mp 150—152 °C, was obtained as colorless needles, and its molecular formula was $C_{21}H_{30}O_7$ as determined by HRMS. The IR and UV spectra of **2** indicated the presence of hydroxyl (ν_{max} 3440 cm^{-1}), δ-lactone (ν_{max} 1725 cm^{-1}) and α,β-unsaturated ketone (ν_{max} 1670, 1633 cm^{-1} and λ_{max} 266 nm) groups. The ^{1}H-NMR spectrum of **2** showed signals due to one secondary methyl at δ 1.09 (d, J = 7 Hz, Me-13), two tertiary methyls at δ 1.15 (s, Me-8) and 1.45 (s, Me-10), two methoxyls at δ 3.60 (s, OMe-2) and 3.65 (s, OMe-12) and an olefinic proton at δ 5.67 (dd, J = 5 and 2 Hz). The ^{1}H- and ^{13}C-NMR spectral data of javanicin P (**2**) and those of javanicin A (**5**)[1] were closely related. From HRMS, **2** contains one oxygen atom more than **5**, and the presence of an extra hydroxyl group was suggested for **2**. The downfield shift of the lactone terminus proton at δ 4.58 (H-7) relative to **5** (H-7, δ 4.10) revealed the extra hydroxyl group was located on C-14 with a β-orientation in **2**, as it had been established for the nigakilactone M (**8**) (H-7, δ 4.76) and nigakilactone A (**9**) (H-7, δ 4.10).[7] A downfield shift (β-effect) was observed for the C-8 ($\Delta\delta$ = 2.9 ppm) and C-15 ($\Delta\delta$ = 7.5 ppm) resonances, and an upfield shift (γ-effect) was experienced by the C-7 ($\Delta\delta$ = 3.7 ppm) resonance in javanicin P (**2**), as compared with the corresponding signals in javanicin A (**5**), which also suggested that the extra hydroxyl group is attached at C-14. The relative stereochemistry of **2** was determined by NOE measurements as follows. Irradiation of H-7 at δ 4.58 induced 12% NOE at Me-8. Irradiation of H-11 at δ 3.77 induced NOEs at Me-8 (9%) and Me-10 (6%). Irradiation of Me-13 at δ 1.09 induced 5% NOE at H-12. Based on the above data, the structure of javanicin P is proposed to be **2**.

Javanicin Q (**3**), mp 243—245 °C, was obtained as

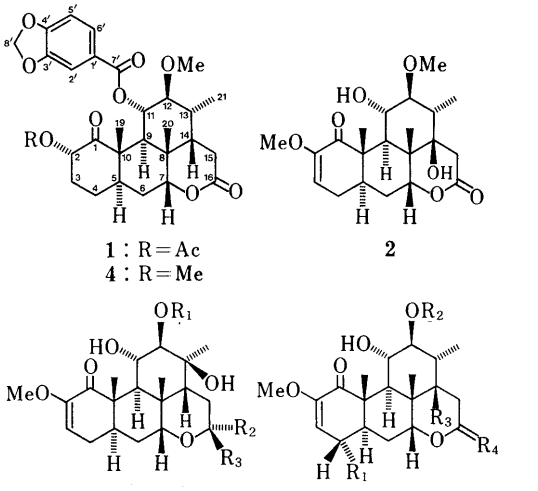

Chart 1

TABLE I. ^{1}H-NMR Spectral Data for Compounds **1**—**6**

Proton	**1**[b]	**4**[a]	**2**[a]	**5**[b]	**3**[b]	**6**[b]
H-2	5.71 dd (12, 7)	4.12 dd (11, 7)				
H-3	1.53 m, 2.10 m	1.49 m, 2.26 m	5.67 dd (5, 2)	5.49 dd (6, 2)	5.51 dd (6, 2)	5.56 dd (5, 2)
H-4	1.25 m, 1.66 m	1.44 m, 1.78 m	2.18 m, 2.37 m	1.86 ddd (18, 6, 4), 2.16 ddd (18, 11, 2)	1.90 m, 2.16 m	1.99 ddd (18, 5, 4), 2.20 ddd (18, 10, 2)
H-5	1.92 m	1.80 m	2.35 m	2.28 m	2.66 m	2.53 m
H-6	1.60 m, 1.88 m	1.73 ddd (14, 3, 3), 1.92 ddd (14, 13, 3)	1.76 ddd (14, 4, 4), 1.93 m	1.55 ddd (14, 3, 3), 1.96 ddd (14, 11, 3)	1.51 ddd (14, 3, 3), 2.04 m	1.38 ddd (14, 5, 3), 2.03 ddd (14, 11, 3)
H-7	4.18 t (3)	4.17 t (3)	4.58 dd (4, 2)	4.10 t (3)	3.31 t (3)	3.96 t (3)
H-9	3.14 d (12)	2.92 d (12)	2.03 d (12)	2.43 d (11)	2.94 d (11)	2.81 d (10)
H-11	5.80 dd (12, 9)	5.50 dd (12, 9)	3.77 ddd (12, 9, 7)	3.96 ddd (11, 9, 8)	4.41 ddd (11, 9, 4)	4.37 dd (10, 9)
H-12	3.43 dd (12, 9)	3.26 dd (11, 9)	2.72 dd (10, 7)	3.08 dd (10, 8)	3.15 d (9)	3.16 d (9)
H-13	2.21 m	2.24 m	1.92 m	2.08 m		
H-14	1.76 m	1.82 m		1.66 ddd (12, 8, 5)	1.85 m	2.16 m
H-15	2.73 dd (19, 7), 2.91 dd (19, 12)	2.62 dd (20, 12), 2.68 dd (20, 8)	2.58 d (19), 2.73 d (19)	2.67 dd (20, 8), 2.76 dd (20, 12)	1.95 m, 2.08 m	1.74 (2H, m)
H-16					5.06 dd (9, 2)	4.82 d (2)
Me-8	1.15 s	1.34 s	1.15 s	1.07 s	1.53 s	1.55 s
Me-10	1.43 s	1.27 s	1.45 s	1.35 s	1.44 s	1.45 s
Me-13	0.97 d (7)	1.05 d (7)	1.09 d (7)	0.99 d (8)	1.34 s	1.23 s
OMe-2		2.84 s	3.60 s	3.45 s	3.48 s	3.48 s
OMe-12	3.29 s	3.30 s	3.65 s	3.71 s		3.72 s
OMe-16					3.67 s	3.33 s
OH-11			4.01 d (9)	4.60 d (9)	4.39 d (4)	
OAc-2	1.97 s					
H-2′	7.83 d (2)	7.53 d (2)				
H-5′	7.03 d (8)	6.82 d (8)				
H-6′	8.00 dd (8, 2)	7.72 dd (8, 2)				
H-8′	6.05 d (1), 6.09 d (1)	6.01 d (1), 6.02 d (1)				

Coupling constants (J in Hz) are given in parentheses. *a*) In $CDCl_3$. *b*) In C_5D_5N.

TABLE II. ^{13}C-NMR Spectral Data for Compounds **1**—**6**

Carbon	**1**[b]	**4**[a]	**2**[a]	**5**[b]	**3**[b]	**6**[b]
C-1	208.21	211.01	204.48	204.75	206.26	206.37
C-2	72.89	79.99	149.16	149.72	149.63	149.61
C-3	33.69	35.32	112.35	112.47	112.35	112.24
C-4	25.16	25.26	27.77	28.08	28.50[c]	28.49
C-5	42.72	42.04	36.06	36.72	37.69[d]	37.52
C-6	29.42	29.19	28.67	29.61	29.89[c]	29.42
C-7	82.40	82.61	78.77	82.42	72.01	69.98
C-8	36.18	34.92	40.86	37.96	39.89[d]	38.98
C-9	36.04	35.80	38.92	37.96	38.84[d]	38.91
C-10	51.26	50.70	47.53	48.16	52.70	48.73
C-11	73.81	73.57	73.07	74.05	76.61	71.94
C-12	85.85	85.74	88.94	88.78	90.88	90.62
C-13	34.94	35.58	42.58	34.95	78.07	76.62
C-14	45.26	45.49	74.27	44.85	48.89	47.18
C-15	28.29	27.93	36.13	28.64	28.87[c]	29.31
C-16	169.16	169.91	170.02	169.99	97.25	98.22
C-19	12.32	12.64	11.24	11.27	11.56	11.45
C-20	21.78	22.24	15.33	21.38	26.87	26.74
C-21	14.36	14.42	10.41	14.68	23.97	24.37
OMe-2		57.44	55.24	55.08	55.05	55.04
OMe-12	60.28	61.00	61.51	61.28		62.36
OMe-16					61.37	54.22
OCOMe-2	20.26					
OCOMe-2	169.89					
C-1′	125.36	123.75				
C-2′	110.81	110.01				
C-3′	148.04	147.73				
C-4′	151.91	151.83				
C-5′	108.05	107.96				
C-6′	126.58	126.16				
C-7′	165.58	165.26				
C-8′	102.33	101.80				

a) In $CDCl_3$. *b*) In C_5D_5N. *c, d*) Values may be interchanged.

colorless prisms, and its molecular formula was $C_{21}H_{32}O_7$ as determined by HRMS. The IR and UV spectra of **3** indicated the presence of hydroxyls (ν_{max} 3557, 3480 and 3420 cm^{-1}) and α,β-unsaturated ketone (ν_{max} 1672, 1628 cm^{-1} and λ_{max} 268 nm) groups. The ^{1}H-NMR spectrum of **3** showed signals due to three tertiary methyls at δ 1.34 (s, Me-13), 1.44 (s, Me-10) and 1.53 (s, Me-8), two methoxyls at δ 3.48 (s, OMe-2) and 3.67 (s, OMe-16), an olefinic proton at δ 5.51 (dd, J=6 and 2 Hz) and a hemiacetal proton at δ 5.06 (dd, J=9 and 2 Hz). The ^{1}H- and ^{13}C-NMR signals of javanicin Q (**3**) showed close correspondence with those of javanicin C (**6**),[1] except that a methoxyl signal was missing at C-12 and replaced by a hydroxyl group. The couplings between the hemiacetal proton at C-16 and methylene protons at C-15 were increased to coupling constants 9 and 2 Hz, suggesting that the hemiacetal proton at C-16 had a β-orientation in **3**, as had been established earlier for the javanicinoside A (**7**) (H-16, J=9 and 2 Hz).[6] The relative upfield shift ($\Delta\delta$=0.65 ppm) of a proton at the lactone terminus (H-7, δ 3.31) in **3** compared with that of the corresponding proton at δ 3.96 in **6**, suggests that methoxyl may be located on C-16 with an α-configuration. The relative stereochemistry of **3** was determined by NOE measurements as follows. Irradiation of H-11 proton at δ 4.41 induced NOEs at Me-8 (5%) and Me-10 (5%). Irradiation of H-7 at δ 3.31 induced NOEs at Me-8 (14%), H-14 (6%) and H-16 (20%). Irradiation of Me-13 protons at δ 1.34 induced 3% NOE at H-12. On the basis of above data, the structure of javanicin Q is proposed to be **3**.

Experimental

All melting points were determined on a Yanagimoto micromelting point

apparatus and are uncorrected. The UV and IR spectra were recorded on Hitachi 340 and Hitachi 260-30 spectrophotometers, respectively. The ^{1}H- and ^{13}C-NMR spectra were recorded with a JEOL JNM GX-400 (^{1}H, 400 MHz; ^{13}C, 100 MHz) spectrometer. Chemical shifts are given on the δ-scale (with ppm downfield from tetramethylsilane as an internal standard) and coupling constants (J) in hertz (Hz). Electron-impact (EI) MS and HRMS were run on JEOL JMS D-300 and JEOL JMS DX-303 mass spectrometers, respectively. Optical rotations were determined on a JASCO DIP-4 digital polarimeter. Column chromatography was carried out on silica gel (BW-820MH, Fuji Davison) and the Diaion HP-20 (Mitsubishi Kasei). Low-pressure liquid chromatography (LC) and high performance LC (HPLC) were carried out on silica gel (CQ-3, 24 mm i.d. × 360 mm, Fuji gel, detector: 254 nm) and silica gel (Senshu Pak SSC-Silica 3251-N, 8 mm i.d. × 250 mm, detector: 254 nm), respectively.

Isolation of Javanicin N (1) The dried stems (3.7 kg) of *Picrasma javanica* collected in Bogor, Indonesia, in July, 1986, were extracted with MeOH (49 l). The MeOH extract was concentrated under reduced pressure to give a residue, to which an equal volume of H_2O was added. The aqueous solution was extracted with $CHCl_3$ (12 l) and then *n*-BuOH (3.6 l). The $CHCl_3$ soluble fraction (73 g) was subjected to repeated column chromatography on silica gel and further purified by low-pressure LC and HPLC to give javanicin N (**1**, 30 mg).

Isolation of Javanicins P (2) and Q (3) The fractionation of the MeOH extract from the leaves of *P. javanica* was described in a previous report.[4] The $CHCl_3$ soluble fraction (200 g) was subjected to repeated column chromatography on a Diaion HP-20 and further purified by low-pressure LC on silica gel with CH_2Cl_2–MeOH (20 : 1, v/v) and HPLC on silica gel with CH_2Cl_2–MeOH (20 : 1, v/v) to give javanicin P (**2**, 13 mg) and javanicin Q (**3**, 11 mg).

Javanicin N (**1**): Colorless needles (MeOH), mp 222—224 °C, $[\alpha]_D^{27}$ −48.0° (c = 3.0, $CHCl_3$). UV λ_{max}^{MeOH} nm (log ε): 220 (4.03), 262 (3.60), 296 (3.54). IR ν_{max}^{KBr} cm^{-1}: 1735, 1700, 1610, 1490, 1290, 1260, 1100, 1040, 762. ^{1}H- and ^{13}C-NMR data are given in Tables I and II, respectively. MS m/z: 556 (M^+, 30%), 390 (19), 365 (11), 330 (54), 261 (11), 166 (14), 149 (100), 121 (9). HRMS m/z 556.2271 $[M]^+$ (Calcd for $C_{30}H_{36}O_{10}$: 556.2298).

Javanicin P (**2**): Colorless needles (MeOH), mp 150—152 °C, $[\alpha]_D^{22}$ +52.0° (c = 1.2, MeOH). UV λ_{max}^{MeOH} nm (log ε): 266 (3.54). IR ν_{max}^{KBr} cm^{-1}: 3440, 1725, 1670, 1633, 1460, 1445, 1265, 1237, 1120, 1038. ^{1}H- and ^{13}C-NMR data are given in Tables I and II, respectively. MS m/z: 394 (M^+, 8%), 376 (9), 331 (36), 287 (22), 269 (100), 155 (30), 234 (78), 203 (37), 191 (24), 159 (37), 151 (28), 139 (52). HRMS m/z: 394.1997 $[M]^+$ (Calcd for $C_{21}H_{30}O_7$: 394.1983).

Javanicin Q (**3**): Colorless prisms (MeOH), mp 243—245 °C, $[\alpha]_D^{21}$ +102.7° (c = 1.1, MeOH). UV λ_{max}^{MeOH} nm (log ε): 268 (3.79). IR ν_{max}^{KBr} cm^{-1}: 3557, 3480, 3420, 1672, 1628, 1430, 1270, 1240, 1100, 1065. ^{1}H- and ^{13}C-NMR are given in Tables I and II, respectively. MS m/z: 396 (M^+, 9%), 378 (64), 360 (67), 290 (66), 262 (32), 232 (52), 205 (40), 191 (56), 180 (40), 163 (63), 139 (76), 127 (40). HRMS m/z 396.2119 $[M]^+$ (Calcd for $C_{21}H_{32}O_7$: 396.2139).

Acknowledgement We are grateful to P. T. Indonesia Eisai Co., Ltd., and Eisai Co., Ltd., for their kind supply of the plant material. We thank the members of the Botanical Garden of Bogor, Indonesia, for the identification of plant material.

References and Notes

1) T. Ohmoto, K. Koike, K. Mitsunaga, H. Fukuda, K. Kagei, T. Kawai and T. Sato, *Chem. Pharm. Bull.*, **37**, 2991 (1989).
2) K. Koike and T. Ohmoto, *Phytochemistry*, **29**, 2617 (1990).
3) K. Koike, K. Mitsunaga and T. Ohmoto, *Chem. Pharm. Bull.*, **38**, 2746 (1990).
4) K. Koike, K. Ishii, K. Mitsunaga and T. Ohmoto, *Phytochemistry*, **30**, 933 (1991).
5) K. Koike, K. Ishii, K. Mitsunaga and T. Ohmoto, *J. Nat. Prod.*, in press (1991).
6) T. Ohmoto, K. Koike, K. Mitsunaga, H. Fukuda, K. Kagei, T. Kawai and T. Sato, *Chem. Pharm. Bull.*, **37**, 993 (1989).
7) T. Murai, A. Sugie, T. Tsuyuki, S. Masuda and T. Takahashi, *Tetrahedron*, **29**, 1515 (1973).

Complete Structures of Breynins A and B

Hiroaki OHKUMA, Takashi TSUNO, Masataka KONISHI,* Takayuki NAITO and Hiroshi KAWAGUCHI

Bristol-Myers Squibb Research Institute, 2–9–3 Shimo-meguro, Meguro-ku, Tokyo 153, Japan. *Received October 9, 1990*

The complete structures of breynins A and B, hypocholesterolemic active compounds isolated from *Breynia officinalis* HEMSL, have been established by spectroscopic analysis and chemical degradation. Breynin A is 3-*O*-[α-L-rhamnopyranosyl-(1→3)-*O*-β-D-glucopyranosyl-(1→2)-*O*-β-D-glucopyranosyl]breynogenin and breynin B is the 17-hydroxy analog.

Keywords *Breynia officinalis*; breynin A; breynin B; NMR; 2D-COSY; FAB-MS; six-membered ketal ring; breynogenin triglycoside; hypocholesterolemic activity

Breynins A and B were isolated as the major hypocholesterolemic active components from an alcoholic extract of *Breynia officinalis* HEMSL (Euphorbiaceae), collected in Taiwan.[1] It was demonstrated that both components significantly reduced the serum cholesterol of rats (by 20—35%) at relatively low dose levels (0.001—0.02 mg/kg/d). We have previously established unique six-membered ketal ring structures of breynogenin and breynolide, the aglycones of breynin A.[2,3] A total synthesis of (+)-breynolide was recently achieved by D. R. Williams *et al.*[4]

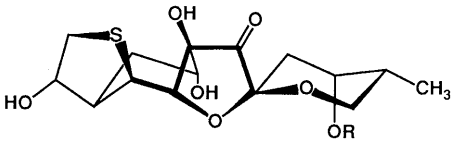

breynolide : R = H

breynogenin : R = -CO-⟨⟩-OH

Although a sugar-containing structure had been deduced for breynin A, and glucose and rhamnose were identified in the hydrolyzate, the complete structure of the compound remained to be elucidated. In our continuing study, we investigated the position and configuration of the sugars in breynin A[1,2] with newly improved spectroscopic techniques, and have established their complete structures. The structure of breynin B[1,2] was resolved by comparative spectroscopic analysis with breynin A. This paper presents the evidence for assigning the structures in Fig. 1 to breynins A and B.

Results and Discussion

The molecular formulae of breynins A (**1**, $C_{40}H_{56}O_{23}S$) and B (**2**, $C_{40}H_{56}O_{24}S$), previously assigned by microanalysis, were confirmed by their quasi-molecular ions ($[M+1]^+$, $[M+Na]^+$, $[M+K]^+$) in high-resolution fast atom bombardment mass spectrometry (HRFAB-MS). Both **1** and **2** responded to the anthrone reagent and showed strong broad absorption at around 3400 and 1070 cm^{-1} in the infrared (IR) spectra, indicating the presence of glycoside substituents. Previous studies showed that, upon acid hydrolysis, **1** was cleaved to give two sugars (glucose and rhamnose) and breynogenin **3** (now named breynogenin A), whose structure had been determined by X-ray crystallography and degradation.[2,3] Optical rotational data of the sugars established that they are D-glucose (Glu) and L-rhamnose (Rha). Proton nuclear magnetic resonance (^{1}H-NMR) of **1** demonstrated proton signals corresponding to two hexose and one deoxyhexose units, in addition to those of **3** (Table I). The proton signals at δ 4.11 (d, J=7.7 Hz), 4.36 (d, J=7.7 Hz) and 4.99 (d, J=1.4 Hz) were assigned to the anomeric protons of the Glu (the first two) and Rha (the last one) by two-dimensional ^{1}H–^{1}H shift correlation spectrometry (^{1}H–^{1}H COSY). The carbon-13 nuclear magnetic resonance spectrum (^{13}C-NMR) and ^{1}H–^{13}C shift correlation spectrometry (^{1}H–^{13}C COSY) showed 40 carbon signals containing two secondary methyl (δ 11.8 and 17.8), one ketal (δ 97.7), three anomeric (δ 100.3 (Rha), 102.1 (Glu-1) and 104.8 (Glu-2)), six aromatic (δ 115.3×2, 120.6, 131.6×2, 162.0) and two carbonyl carbons (δ 165.0 and 212.2). The negative FAB-MS afforded, together with the $(M-1)^-$ ion, the diagnostic fragment ions ($[M-Rha]^-$ at m/z 789, $[M-Rha-Glu]^-$ at m/z 627 and $[M-Rha-2Glu]^-$ at m/z 465) produced by sequential cleavage of the three sugars.

In ^{1}H-NMR of **1**, the splitting of the anomeric protons of the two Glu (Glu-1 and Glu-2, both J=7.7 Hz) was consistent with the β-pyranoside form, while the observed coupling constant of Rha (J=1.4 Hz) could not define the configuration of the sugar. The anomeric carbon, however, resonated at δ 100.3 as a doublet with a $^1J_{C-H}$ value of 170.0 Hz in the non-decoupled INEPT experiment of **1**, which allowed the assignment of an α-pyranosyl structure to the sugar.[5] The assignment was confirmed by nuclear Overhauser effect spectroscopy (NOESY) of **1**. A methine proton H-3 (δ 4.25) of the aglycone exerted a distinct cross peak with the H-1′ anomeric proton (δ 4.36) of Glu-1 in

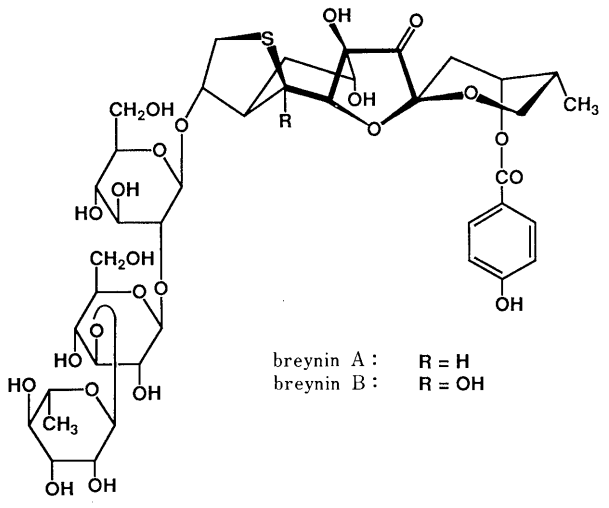

Fig. 1. Structures of Breynin A (**1**) and B (**2**)

TABLE I. ^{1}H-NMR of Breynins and Breynogenins (400 MHz, DMSO-d_6)

Protons	δ in ppm (J in Hz)			
	Breynin A	Breynin B	Breynogenin A	Breynogenin B
2-H	3.00 dd (11.7, 3.5)	3.12 m	2.99 dd (11.1, 4.2)	3.03 dd (14.5, 5.1)
	3.08 dd (11.7, 4.7)	3.18 m	3.51 dd (11.1, 4.3)	3.70 d (14.5)
3-H	4.25 m	4.39 m	4.16 m	4.48 m
4-H	2.73 m	2.97 m	2.46 m	2.77 m
5-H	1.39 dt (15.9, 4.2)	1.22 br d (15.4)	1.27 dt (13.6, 3.8)	1.57 dd (14.1, 2.1)
	1.53 t (15.9)	1.57 br d (15.4)	1.45 t (13.6)	1.62 ddd (14.1, 5.1, 2.1)
6-H	3.82 br	3.82 br	3.80 t (11.1)	3.74 dd (6.4, 1.3)
10-H	1.86 dd (14.1, 5.4)	1.88 dd (14.1, 6.4)	1.87 dd (14.5, 3.8)	1.93 dd (14.5, 3.6)
	1.99 dd (14.1, 3.9)	2.03 dd (14.1, 5.4)	1.95 dd (14.5, 3.5)	2.00 dd (14.5, 3.4)
11-H	5.33 m	5.40 m	5.24 t (3.0)	5.25 dd (6.0, 3.4)
12-H	2.10 m	2.13 m	2.08 m	2.11 m
13-H	3.57 m	3.65 d (11.1)	3.51 dd (11.1, 4.3)	3.56 dd (11.1, 4.5)
	3.77 dd (11.5, 9.0)	3.77 m	3.80 t (11.1)	3.90 t (11.1)
16-H	4.22 s	4.58 s	4.19 s	4.70 s
17-H	3.91 dd (6.8, 1.4)	—	3.93 d (5.1)	—
18-H	0.83 d (7.3)	0.89 d (6.8)	0.77 d (6.8)	0.78 d (6.8)
21-H	7.89 d (8.5)	7.90 d (8.5)	7.90 d (8.5)	7.89 d (8.5)
22-H	6.86 d (8.5)	6.89 d (8.5)	6.88 d (8.5)	6.85 d (8.5)
24-H	6.86 d (8.5)	6.89 d (8.5)	6.88 d (8.5)	6.85 d (8.5)
25-H	7.89 d (8.5)	7.90 d (8.5)	7.90 d (8.5)	7.89 d (8.5)
6-OH	5.12 d (4.7)	5.24 d (4.7)	4.98 d (4.3)	5.17 d (4.7)
7-OH	5.85 s	6.20 s	5.79 s	5.62 s
17-OH	—	5.14 br s	—	5.32 br s
23-OH	10.27 br	10.29 br	10.52 br	10.20 br
Glc				
1′-H	4.36 d (7.7)	4.04 d (7.7)		
2′-H	3.22 m	3.26—3.49 m		
3′-H	3.20 m			
4′-H	3.49 m			
5′-H	3.20 m			
6′-H_2	3.47 m, 3.67 m	3.47 m, 3.65 m		
Glc				
1″-H	4.11 d (7.7)	4.27 d (7.7)		
2″-H	3.07 m	3.16 m		
3″-H	3.22 m	3.3—3.45 m		
4″-H	3.19 m			
5″-H	3.35 m			
6″-H_2	3.37 m, 3.55 m	3.38 m, 3.58 m		
Rha				
1‴-H	4.99 d (1.4)	5.04 br s		
2‴-H	3.69 m	3.69 m		
3‴-H	3.13 m	3.12 m		
4‴-H	3.17 m	3.18 m		
5‴-H	3.86 dd (9.6, 6.4)	3.89 dd (9.4, 6.8)		
6‴-H	1.10 d (6.4)	1.09 d (6.8)		

the NOESY spectrum. Similarly, two cross peaks observed were assigned as those between H-2′ (δ 3.22) of Glu-1 and H-1″ (δ 4.11) of Glu-2, and H-3″ (δ 3.22) of Glu-2 and H-1‴ (δ 4.99) of the terminal Rha. In the ^{13}C-NMR (Table II) of **1**, the C-2′ carbon signal of Glu-1 and C-3″ carbon signal of Glu-2 appeared considerably lower field than the corresponding signals of methyl β-D-glucopyranoside,[6] but practically no down-field shift was observed for all the carbons of Rha.

In comparison with that of **3**, the C-3 carbon signal of **1** appeared at lower field than that of **3** by 10.3 ppm, presumably owing to the attachment of the trisaccharide moiety to the hydroxyl group of **3** (Table II). These results, coupled with the fragmentation pattern in the mass spectrum of **1**, indicate that an α-L-rhamnopyranosyl-(1→3)-*O*-β-D-glucopyranosyl-(1→2)-*O*-β-D-glucopyranoside was linked at C3-OH. Thus, the complete structure of breynin A is established as shown in Fig. 1.

The FAB-MS of **2** exhibited a protonated molecular ion at m/z 953, 16 mass units higher than that of **1**, indicating the presence of one more oxygen than **1**. When hydrolyzed with dilute hydrochloric acid, **2** produced a new aglycone **4** (breynogenin B) together with D-glucose (2 mol) and L-rhamnose. The FAB-MS (positive) spectrum of **4** yielded pseudomolecular ions at m/z 483 (MH^+) and 505 (MNa^+), suggesting that the additional oxygen of **2** is in the aglycone moiety.

In a comparison of their ^{1}H-NMR, **2** showed a very similar spectrum to that of **1**, except for the lack of a methine proton (δ 3.91, dd, J=6.8, 1.4 Hz, 17-H) observed in **1**. Significant down-field shifts were observed for H-4 and H-16 of **2**, which are adjacent to oxygenated C-17.

In addition, comparison of the ^{13}C-NMR spectra indicated that the C-17 methine carbon (δ 45.2, d) of **1**

TABLE II. ^{13}C-NMR of Breynins A and B and Breynogenin A (100 MHz, DMSO-d_6)

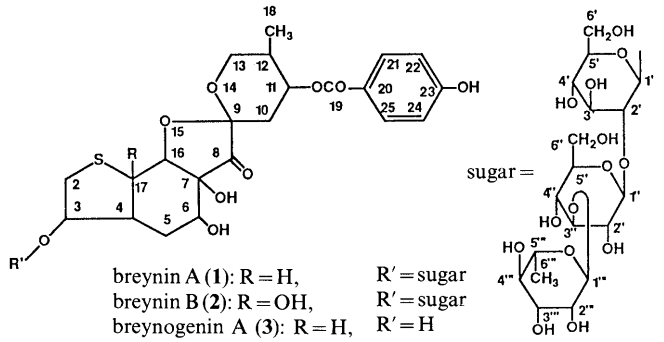

breynin A (**1**): R = H, R′ = sugar
breynin B (**2**): R = OH, R′ = sugar
breynogenin A (**3**): R = H, R′ = H

	δ in ppm, spoltting		
	Breynin A	Breynin B	Breynogenin A
Aglycone moiety			
C-2	35.1 t	56.1 t	37.2 t
C-3	88.7 d	84.6 d	78.4 d
C-4	37.9 d	36.2 d	39.7 d
C-5	26.4 t	28.0 t	26.8 t
C-6	67.2 d	67.7 d	68.0 d
C-7	74.0 s	73.7 s	74.3 s
C-8	212.2 s	211.3 s	212.6 s
C-9	97.7 s	98.2 s	97.7 s
C-10	30.5 t	30.3 t	31.3 t
C-11	67.8 d	68.2 d	68.8 d
C-12	32.2 d	32.1 d	32.3 d
C-13	62.7 t	63.2 t	61.7 t
C-16	76.5 d	76.7 d	75.8 d
C-17	45.2 d	70.5 s	45.3 d
C-18	11.8 q	11.7 q	12.4 q
C-19	165.0 s	165.0 s	165.3 s
C-20	120.6 s	120.5 s	120.9 s
C-21	131.6 d	131.5 d	131.5 d
C-22	115.3 d	115.4 d	115.3 d
C-23	162.0 s	162.1 s	161.8 s
C-24	115.3 d	115.4 d	115.3 d
C-25	131.6 d	131.5 d	131.5 d
Sugar moieties			
C-1′	102.1 d	101.0 d	
C-2′	83.2 d	81.9 d	
C-3′	76.8 d	76.5 d	
C-4′	70.5 d	72.1 d	
C-5′	75.9 d	75.5 d	
C-6′	60.8 t	60.9 t	
C-1″	104.8 d	104.1 d	
C-2″	75.9 d	76.1 d	
C-3″	80.4 d	80.4 d	
C-4″	68.7 d	68.0 d	
C-5″	75.9 d	76.7 d	
C-6″	60.1 t	60.4 t	
C-1‴	100.3 d	100.2 d	
C-2‴	70.6 d	70.5 d	
C-3‴	69.6 d	69.6 d	
C-4‴	72.1 d	73.6 d	
C-5‴	68.1 d	67.7 d	
C-6‴	17.8 q	17.8 q	

appeared at δ 70.5 as a quarternary carbon carrying an oxygen in **2**.

These spectral data are fully consistent with the 17-hydroxybreynin A structure for breynin B (Fig. 1).

Experimental

Melting points were determined on a Yanagimoto micro-melting point apparatus and are uncorrected. Optical rotations were measured with a JASCO DIP-400 automatic digital polarimeter. The IR spectra were recorded with a JASCO IRA-1 spectrometer. The ^{1}H- and ^{13}C-NMR spectra were measured with a JEOL JNM-GX400 NMR spectrometer in deuterio dimethyl sulfoxide (DMSO-d_6) solutions with tetramethylsilane as an internal standard. Multiplicities of ^{13}C-NMR spectra were determined by means of the distortionless enhancement by polarization transfer (DEPT) method. ^{1}H–^{1}H, ^{1}H–^{13}C and long ^{1}H–^{13}C COSY spectra and NOESY were measured by the use of JEOL standard pulse sequences (^{1}H–^{1}H COSY: VCOSYNH; ^{1}H–^{13}C COSY: VBDCHSHF, J=140 Hz; long-range ^{1}H–^{13}C COSY: VCHSHF, J=8 Hz). FAB-MS and HRFAB-MS were taken on a JEOL JMS-AX505H mass spectrometer. Thin layer chromatography (TLC) was performed on precoated silica gel plates (Merck, Kieselgel 60F_{254}) and detection was performed by spraying them with 10% H_2SO_4. High performance liquid chromatography (HPLC) analysis was performed using a reversed phase silica gel column (A301-3S-3-120A ODS, 4.6 i.d. × 100 mm, Yamamura Chemical Lab.) and developing solvent of MeOH–0.15% KH_2PO_4 buffer, pH 3.5 (4 : 6, v/v).

Breynins A and B The isolation of breynins A and B and their major physico-chemical properties were described in the previous paper.[1]

Breynin A (**1**): Positive FAB-MS *m/z*: 937 $(M+1)^+$. Negative FAB-MS *m/z*: 935 $(M-1)^-$. HRFAB-MS $(M+Na)^+$ *m/z*: 959.2833 (Calcd for $C_{40}H_{56}O_{23}SNa$: 959.2835). HPLC (t_R): 8.2 min (flow rate, 1 ml/min).

Breynin B (**2**): Positive FAB-MS *m/z*: 953 $(M+1)^+$. Negative FAB-MS *m/z*: 951 $(M-1)^-$. HRFAB-MS $(M+Na)^+$ *m/z*: 975.2793 (Calcd for $C_{40}H_{56}O_{24}SNa$: 975.2806). HPLC (t_R): 5.0 min (flow rate, 1 ml/min).

Breynogenin A (**3**): Positive FAB-MS *m/z*: 467 $(M+1)^+$. ^{1}H-NMR is shown in Table I. HPLC (t_R): 12.9 min (flow rate, 1 ml/min).

Methanolysis of Breynin A (1) A solution of **1** (67 mg) in 1.0 N HCl–MeOH (5 ml) was refluxed for 1.5 h. The reaction mixture was poured into water (50 ml) and extracted with ethyl acetate (50 ml). The extract was washed with an aqueous $NaHCO_3$ solution and water and then evaporated *in vacuo*. The residue was crystallized from ethyl acetate to afford colorless needles of breynogenin A (**3**, 12 mg). The aqueous layer was neutralized with Amberlite IR-45 (OH^- form) and evaporated *in vacuo* to afford a sugar mixture. This was chromatographed on a silica gel column (1.0 i.d × 43 cm) developed with CH_2Cl_2–MeOH (10 : 1, v/v). Upon monitoring the elution by an anthrone sulfuric acid reaction, two major sugars were isolated. The sugar fractions were desalted using Sephadex LH-20 chromatography with 50% methanol elution.

Methyl α-D-Glucopyranoside: Eluted first in the silica gel chromatography. 19 mg, syrup. $[\alpha]_D^{23}$ +166° (c=1.0, H_2O). Identical with an authentic sample by TLC and NMR.

Methyl α-L-Rhamnopyranoside: 7 mg, syrup, $[\alpha]_D^{23}$ −46.9° (c=0.35, H_2O). Identical with an authentic sample.

Acid Hydrolysis of Breynin B (2) The solution of **2** (14 mg) in 2 N HCl–MeOH (4 ml) was refluxed for 1 h. The mixture was poured into water (20 ml) and extracted three times, each time with 20 ml of ethyl acetate. Removal of the solvent from the extract under reduced pressure gave a crude hydrolyzate. It was purified by preparative TLC (SiO_2, CH_2Cl_2–MeOH (9 : 1, v/v), Rf=0.19) followed by Sephadex LH-20 column chromatography (solvent, MeOH) to afford breynogenin B (**4**, 4.6 mg). The aqueous layer of the above hydrolyzate was shown to contain methyl α-D-glucopyranoside and methyl α-L-rhamnopyranoside by TLC.

Breynogenin B (**4**): White amorphous powder, mp 132—134 °C. $[\alpha]_D^{25}$ +19° (c=0.2, MeOH). Positive FAB-MS *m/z*: 483 $(M+H)^+$. HRFAB-MS $(M+Na)^+$ *m/z*: 505.1124 (Calcd for $C_{22}H_{26}O_{10}SNa$: 505.1103). ^{1}H-NMR is shown in Table I. HPLC (t_R): 13.3 min (flow rate, 1 ml/min).

Acknowledgment The authors are grateful to Prof. M. Ohashi of the University of Electrocommunication for his valuable advice on this work.

References

1) H. Koshiyama, M. Hatori, H. Ohkuma, F. Sakai, H. Imanishi, M. Ohbayashi and H. Kawaguchi, *Chem. Pharm. Bull.*, **21**, 169 (1976).
2) F. Sakai, H. Ohkuma, H. Koshiyama, T. Naito and H. Kawaguchi, *Chem. Pharm. Bull.*, **24**, 114 (1976).
3) K. Sasaki and Y. Hirata, *Tetrahedron Lett.*, **1973**, 2439.
4) D. R. Williams, P. A. Jass, H. L. Allan Tse and R. D. Gaston, *J. Am. Chem. Soc.*, **112**, 4552 (1990).
5) K. Bock, I. Lundt and C. Pedersen, *Tetrahedron Lett.*, **1973**, 1037.
6) A. Philip, J. Gorin and M. Mazurek, *Can. J. Chem.*, **52**, 1212 (1975).

Chemotaxonomy of the Genus *Citrus* Based on Polymethoxyflavones

Mizuo MIZUNO,*[,a] Munekazu IINUMA,[a] Mitsuharu OHARA,[a] Toshiyuki TANAKA[a] and Masao IWAMASA[b]

Department of Pharmacognosy, Gifu Pharmaceutical University,[a] 6–1 Mitahorahigashi 5-chome, Gifu 502, Japan and Department of Horticultural Science, Saga University,[b] Honjo 2, Saga 840, Japan. *Received October 17, 1990*

The contents of seven polymethoxyflavones [5,6,7,8,4′-pentamethoxy- (1), 5,6,7,8,3′,4′-hexamethoxy- (2), 5,7,4′-trimethoxy- (3), 5,6,7,3′,4′-pentamethoxy- (4), 5,7,3′,4′-tetramethoxy- (5), 5,7,8,4′-tetramethoxy- (6) and 5,7,8,3′,4′-pentamethoxyflavones (7)] in the fruit peels of *Citrus* species (Rutaceae) were determined by use of high performance liquid chromatography. On the basis of their composition, relative ratio and the total contents, seven distinct flavone-patterns (types I—VII) were designated. These flavonone-patterns facilitate the chemotaxonomy of the genus *Citrus*. The results obtained in the present study support the morphological classification systems presented by Swingle or Tanaka except several taxa.

Keywords *Citrus* species; Rutaceae; chemotaxonomy; polymethoxyflavone; flavone-pattern

Introduction

The flavone derivatives in citrus peels are characterized as polymethoxyflavones such as tangeritin (ponkanetin), nobiletin and 3,5,6,7,8,3′,4′-heptamethoxyflavone, *etc.* Such lipophilic polymethoxyflavones are sometimes related with bioactivity. For example, nobiletin has a potent inhibitory activity on cyclic adenosin monophosphate (AMP) phosphodiesterase[1] and an antifungal activity against *Deuterophoma tracheiphila* which causes a destructive disease of citrus trees (Mal-seco).[2] UP to the present time, about 40 flavones have been reported in peels. In addition to essential oils, flavanones and their glycosides are also representative chemical constituents. Such flavone derivatives have generally little seasonal fluctuation,[3] while the contents of flavanone glycosides decrease in proportion to the fruit's maturity.[4]

To analyze the flavonoid compounds for the chemotaxonomical study on the genus *Citrus*, thin layer chromatography and paper partition chromatography for the detection of flavanone glycosides[5,6] and of the above flavones,[7,8] and high performance liquid chromatography (HPLC) have been applied.[3] All the flavones occurring in citrus peels, however, are not necessarily detected by these methods because of their contents. When examination of the flavones in the fruit peels of *C. reticulata* was on a large scale (1.2 kg), fifteen polymethoxyflavones were isolated.[9] In contrast, the analytical experiment of the peels by HPLC merely resulted in the detection of six or seven flavones.[3] In the present paper, the chemotaxonomy of the genus *Citrus* based on polymethoxyflavones as a species specific-marker is described.

Materials and Methods

Species and Cultivars *Citrus* species used in this experiment are listed in Table I. Cultivars and other species are as follows; Mandarin hybrids: 'Fremont' (*C. clementia* × *C. reticulata*) [44], 'Anchol' (*C. nobilis* × *C. deliciosa*) [52], 'Kara' (*C. nobilis* × *C. unshiu*) [63]. Tangors: 'Ortanique' [66] and 'Kiyomi' (*C. reticulata* × *C. sinensis*) [69]. Tangelos: 'Allspice,' 'Minneola' (*C. tangerina* × *C. paradisi*) [58], 'San Jacinto' [133]. Tangerine–Tangelos: 'Fairchild' [43], 'Osceola' [45], 'Lee' [51], 'Nova' [54], and 'Clementine' (*C. clementina* × 'Minneola') [46]. Miscellaneous variety: 'Kobayashi-mikan' (*C. unshiu* × *C. natsudaidai*) [86, 113]. *Fortunella japonica* SWINGLE [16] and *F. obovata* TANAKA [117]. In brackets are indicated the herbarium numbers in the Herbarium of Gifu Pharmaceutical University.

Polymethoxyflavones As species specific-marker, seven polymethoxyflavones—5,6,7,8,4′- (tangeritin or ponkanetin) (**1**), 5,6,7,8,3′,4′-pentamethoxy- (nobiletin) (**2**), 5,7,4′-trimethoxy- (apigenin trimethyl ether) (**3**), 5,6,7,3′,4′-pentamethoxy- (sinensetin) (**4**), 5,7,3′,4′-tetramethoxy- (luteolin tetramethyl ether) (**5**), 5,7,8,4′-tetramethoxy- (**6**), and 5,7,8,3′,4′-pentamethoxyflavone (**7**) were used and the structures are shown in Chart 1. These flavones have been isolated from the fruit peels of *C. reticulata* and the structures have been established by means of spectroscopic analysis and synthesis.[9]

HPLC Apparatus and Conditions Liquid chromatograph: Shimadzu LC-6A. Detector: Shimadzu UV spectrophotometric detector SPA 6A. Injector: Reodyne 7215. Recorder: Shimadzu R-11. Conditions: column Si60 (5 μm) (Merck) 250 × 4 mm i.d.; flow rate, 2.0 ml/min, detection, UV 340 nm, chart speed, 2 mm/min; solvent system, the previous systems[3,10,11] for detection of polymethoxyflavones were improved in the present

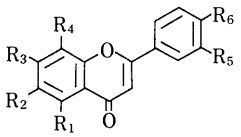

1: $R_1=R_2=R_3=R_4=R_6=OMe$, $R_5=H$
2: $R_1=R_2=R_3=R_4=R_5=R_6=OMe$
3: $R_1=R_3=R_6=OMe$, $R_2=R_4=R_5=H$
4: $R_1=R_2=R_3=R_5=R_6=OMe$, $R_4=H$
5: $R_1=R_3=R_5=R_6=OMe$, $R_2=R_4=H$
6: $R_1=R_3=R_4=R_6=OMe$, $R_2=R_5=H$
7: $R_1=R_3=R_4=R_5=R_6=OMe$, $R_2=H$

Chart 1

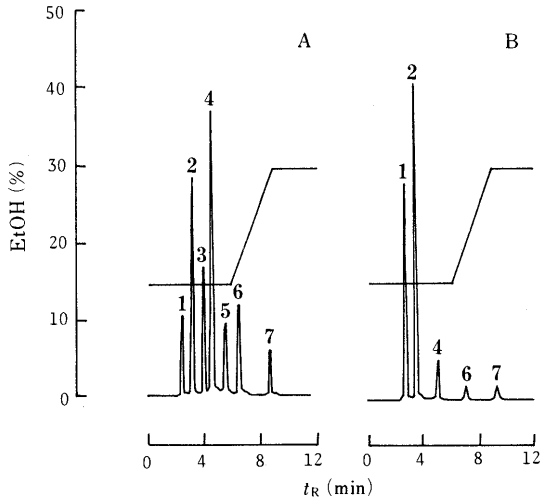

Fig. 1. HPLC Chromatogram of Polymethoxyflavones

A: A mixture of authentic polymethoxyflavones. B: A methanolic extract of *Citrus kinokuni* [No. 36].

TABLE I. Tanaka Systematics and *Citrus* Species Investigated in the Present Study

Subgenus	Section	Subsection	Group	Subgroup	Microgroup	Species	Herbarium No.	Type
Archicitrus	Limonellus	Eulimonellus				*C. aurantifolia* SWING.	248	I
	Citrophorum	Citroides				*C. medica* L.	102, 249	I
		Limonoides				*C. limon* BURM. f.	250	I
		Decumanoides				*C. pyriformis* HASSK.	155	II
	Cephalocitrus	Decumana				*C. grandis* OSBECK	78, 87, 136, 240	II
		Intermedia	Flavicarpa			*C. paradisi* MAEF.	60, 75, 88	II
						C. flavicarpa HORT. ex TANAKA	49, 110	VI
						C. pseudoparadisi HORT. ex Y. TANAKA	83	III
			Aureocarpa			*C. intermedia* HORT. ex TANAKA	9	II
						C. hassaku HORT. ex TANAKA	135, 190	V
	Aurantium	Medioglobosa				*C. natsudaidai* HAYATA	76, 130, 139, 153, 171, 173, 181, 191	III
						C. otachibana HORT. ex Y. TANAKA	81	II
						C. obovoidea HORT. ex TAKAHASHI	82	III
						C. sulcata HORT. ex TAKAHASHI	80	III
		Aurantioides	Racemosa			*C. aurantium* L.	64, 71, 251	IV
						C. myrtifolia RAF.	156	IV
		Sinensioides				*C. sinensis* OSBEK	50, 55, 56, 57, 61, 65, 67, 68, 73, 141, 143, 150, 244, 245, 252	V
						C. tankan TANAKA	149	VII
						C. iyo HORT. ex TANAKA	72, 79	VI
		Osmocitriodes	Tenuicarpa			*C. ujukitsu* HORT. ex TANAKA	96	III
			Compacta			*C. aurea* HORT. ex TANAKA	253	III
			Paranobilis			*C. shunkokan* HORT. ex TANAKA	154	VI
Metacitrus	Osmocitrus	Euosmocitrus				*C. junos* SIEB. ex TANAKA	11	I
						C. hanaju HORT. ex SHIRAI	114, 246	VII
						C. sudachi HORT. ex SHIRAI	106, 109	I
		Pseudo-acrumen				*C. nippokoreana* TANAKA	119, 128	V
	Acrumen	Euacrumen				*C. unshiu* MARC.	108, 131, 132, 134	VI
		Microacrumen	Anisodora			*C. keraji* HORT. ex TANAKA	8, 12, 107, 192	VI
						C. oto HORT. Y. TANAKA	13	VI
			Citriodora	Megacarpa		*C. reticulata* BLANCO	33, 59, 62, 70, 92, 99, 188, 254	VII
				Microcarpa	Angustifolia	*C. tachibana* TANAKA	10, 37, 90, 93, 129	VII
						C. erythrosa HORT. ex TANAKA	118	VII
						C. kinokuni HORT. ex TANAKA	35, 36, 40, 47, 48, 187	VII
					Latifolia	*C. depressa* HAYATA	7, 15, 104	VII
						C. leiocarpa HORT. ex TANAKA	30, 31, 34	VII
	Pseudo-fortunella					*C. madurensis* LOUR.	111	VI

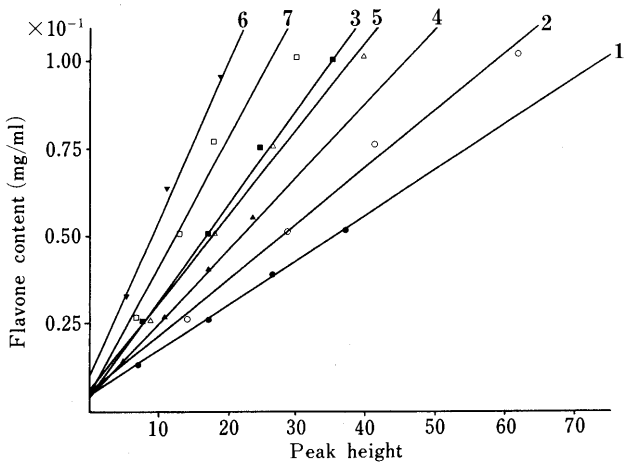

Fig. 2. Calibration Curves for Polymethoxyflavones

1: $Y_1 = 1.30 \times 10^{-3} X_1 + 3.65 \times 10^{-3}$
2: $Y_2 = 1.60 \times 10^{-3} X_2 + 5.22 \times 10^{-3}$
3: $Y_3 = 2.75 \times 10^{-3} X_3 + 3.47 \times 10^{-3}$
4: $Y_4 = 2.12 \times 10^{-3} X_4 + 2.99 \times 10^{-3}$
5: $Y_5 = 2.48 \times 10^{-3} X_5 + 5.24 \times 10^{-3}$
6: $Y_6 = 4.60 \times 10^{-3} X_6 + 8.52 \times 10^{-3}$
7: $Y_7 = 3.67 \times 10^{-3} X_7 + 4.30 \times 10^{-3}$.

experiment. Ethanol concentration in the gradient (heptan–ethanol) is shown by a solid line in Fig. 1.

Sample preparation and quantitative determination: About 200 mg of dry mature peels were weighed accurately, placed in a spit tube (10 ml) and extracted with MeOH (5 ml) under ultrasonification in a water bath (60 °C) for 5 min. The spit tube was removed to a centrifuge apparatus (18000 rpm × 15 min), and the supernatant was filtered with a membrane filter. A filtrate (5.0 ml) was subjected to HPLC. The contents of polymethoxyflavones were calculated by means of the respective calibration curves (Fig. 2).

Results and Discussion

Each relative ratio of flavones (**1**—**7**) is shown by per cent (%) and the total flavone content by mg/g in respective citrus peels were determined. The results are listed in Table II. The total flavone content and its relative ratios have some definite inclinations. For example, the breeds in the subgenus Metacitrus such as *C. keraji*, *C. kinokuni*, *C. depressa*, *C. leiocarpa* are generally rich in polymethoxyflavones. To the contrary, the breeds in the subgenus Archicitrus such as *C. grandis*, *C. paradisi*, *C. sinensis* are poor in flavones. The relative ratio of each flavone is constant within the same species including its breeds. For example, flavones (**5** and **6**) were not detected

TABLE II. Quantitative Determination of Polymethoxyflavones

	Herbarium No.	1	2	3	4	5	6	7 (%)	Total (mg/g)
C. grandis									
Buntan	136	14.7	6.7	2.7	12.0	—	56.0	8.0	0.75
Tosa-buntan	78	14.3	2.4	7.1	9.5	—	64.3	2.4	0.42
Banpeiyu	87	33.3	4.8	9.5	14.3	—	33.3	4.8	0.21
Shatayu	240	22.2	1.9	9.8	14.8	—	44.4	7.4	0.54
C. paradisi									
Mccarty	60	19.2	21.2	11.5	11.5	—	36.5	—	0.52
Marsh seedless	75	18.4	20.4	12.2	10.2	—	38.8	—	0.49
Red Blush	88	15.4	15.4	15.4	12.3	—	41.5	—	0.65
C. natsudaidai									
Natsudaidai	130, 153, 173, 180	32.2	18.4	—	17.1	—	32.3	—	0.63
Kawano-natsudaidai	171, 191	34.8	19.5	—	17.3	—	28.6	—	0.64
C. aurantium									
Sour orange	71, 251	23.1	21.1	4.2	2.5	—	33.6	15.7	0.53
Kaiseito	64	22.6	23.8	8.3	4.8	—	33.3	7.1	0.84
C. sinensis									
Valencia	50	23.2	41.5	7.3	19.5	—	—	8.5	0.82
Hamlin	57	23.9	38.8	7.5	19.4	—	—	10.4	0.67
Salustiana	65	19.1	35.3	10.3	25.0	—	—	10.3	0.68
White siletta	55	21.4	37.5	10.7	19.6	—	—	10.7	0.56
Red siletta	61	21.1	35.2	9.9	23.9	—	—	9.9	0.71
Inshi-kan	143, 150	24.1	36.5	9.4	21.3	—	—	8.9	0.85
Fukuhara No. 1	68, 141	20.7	35.9	11.2	23.6	—	—	8.7	0.76
Touka	244, 245	21.7	33.9	10.7	23.6	—	—	10.1	0.70
Frost Washington	67	22.8	33.3	10.5	21.1	—	—	12.3	0.57
Yoshida navel	73	25.0	31.3	10.4	20.8	—	—	12.5	0.48
Ruby blood	252	30.0	30.0	10.0	22.5	—	—	7.5	0.40
Tarocco	56	18.9	37.1	12.9	25.0	—	—	6.1	1.32
C. iyo									
Miyauchi-iyo	79	32.6	31.5	—	6.5	—	17.4	12.0	0.92
Ohta-iyo	72	25.0	28.8	—	9.6	—	21.2	15.4	0.52
C. unshiu									
Unshiu	131, 132	29.7	30.0	7.2	6.9	—	15.7	10.6	0.72
Jyuman-unshiu	134	35.4	34.4	5.2	5.2	—	12.5	7.3	0.96
Beni-unshiu	108	28.8	28.8	—	7.7	—	21.2	13.5	0.52
Okitsuwase	189	41.3	47.8	—	10.9	—	—	—	0.46
C. keraji									
Keraji	107, 192	44.5	29.0	—	4.6	—	14.3	7.6	1.19
Kabuchii	8, 12	44.8	35.6	—	4.1	—	10.9	4.7	4.59
C. kinokuni									
Kinokuni	35, 40, 48	26.4	54.0	—	5.1	—	8.6	5.8	6.73
Hira-kisyu	36, 47	25.2	52.1	—	5.8	—	10.0	7.1	3.62
Kinokuni-seedless	187	28.7	51.1	1.6	4.9	2.0	7.0	4.8	7.99
C. depressa									
Shiikuwasha	7, 104	29.9	50.6	—	6.0	—	8.5	5.1	5.11
Kugani	15	22.2	54.8	—	7.9	—	8.4	6.7	4.78
C. leiocarpa									
Kohji	34, 34	27.4	50.8	—	5.8	—	10.0	6.1	3.95
Suruga-yukoh	30	30.8	53.0	—	5.7	—	6.7	3.7	3.51

in *C. sinensis* and in its breeds of Valencia, Hamlin, Salustiana *etc.*, while flavone (**2**) predominantly occurred and reached 35% in the average. These results allowed us the conclusion that the species itself and its breeds have a species-dependent flavone ratio and a total content, and the estimation by two factors will characterize the species as well as the breed. To simplify the values within the same species and its breeds, the average numerals were calculated and are shown in Tables III and IV. The patterns based on the relative ratio of flavones and the total content of flavones can be divided into seven different types (types I—VII), the graphic drawing of which is exhibited in Fig. 3. The results of each species, which ever type it is, is shown in Table I.

The first type (type I) is explained as follows: Type I is exclusively composed of **1** and **2** among the seven flavones, and the relative ratios of **1** and **2** are sometimes changeable. In the peels of *C. aurantifolia*, *C. medica*, *C. limom*, and *C. sudachi*, the content of **1** is 2—4 fold that of **2**. On the contrary, the ratios of **1** and **2** are almost the same in *C. junos*, and the other genus of *Fortunella japonica* and *F. obovata*. The total flavone content in type I is the poorest among the genus *Citrus* and reached to only *ca.* 0.17 mg/g in the average. By the investigation utilizing isozyme patterns, *C. aurantifolia* and *C. limon* were suggested to be a hybrid of *Papeda* × *C. medica*, and *C. sinensis* × *C. aurantifolia*,[12] respectively. *C. junos* and *C. sudachi* in the subgenus Metacitrus were also explained as hybrids derived from *C. ichangensis*.[13-15] These species in both the subgenera of Archicitrus and Metacitrus all belong to type I which is regarded as containing the most primitive plants in the genus *Citrus*. *C. medica* among them has been considered as a basic species.[16] The genus of *Fortunella*,

which was differentiated from *Citrus* in a primitive stage, was also included in type I.

The second type (type II) is characterized as having a substantial amount of the flavone (**6**), the ratio of which reached to 50%. The species absent of **7** such as *C. pyriformis* and *C. otachibana* are included in type II. The total flavone content attached to 0.6 mg/g. In spite of the equivocality of the original plant, it has been assumed that *C. grandis* is one of the original species,[12] and *C. paradisi* is a hybrid between *C. grandis* and *C. sinensis*.[12,13,16-21] Type II involved *C. grandis* and its hereditary relatives.

The third type (type III) is summarized as follows: The flavones (**1**, **2**, **4** and **6**) are commonly contained, whilst **3** is characteristically lacking. The relative contents of **1** and **6** are much higher in *C. pseudoparadisi*, *C. natsudaidai* and *C. obovoidea*, and occasionally flavone **7** is detected in some species such as *C. ujukitsu* and *C. aurea*. The total flavone content reached to *ca.* 0.5 mg/g. *C. natsudaidai* is a hybrid of *C. autantium* × *C. grandis*,[18] and other species in type III have been considered to be originally derived more or less from *C. grandis*. The species in type III will be lesser influenced by *C. grandis* than those of type II.

In the fourth type (type IV), all the flavones except **5** are detected such as in the peels of *C. aurantium* and *C. myrtifolia*. The relative ratio of **6** reached to 30%, and that

TABLE III. The Average Contents of Polymethoxyflavones

Species	1	2	3	4 (%)	5	6	7	Total (mg/g)
C. aurantifolia	81.6	18.4	—	—	—	—	—	0.38
C. medica	72.7	27.3	—	—	—	—	—	0.22
C. limon	72.7	27.3	—	—	—	—	—	0.11
C. pyriformis	17.9	17.9	21.4	10.7	—	32.1	—	0.56
C. grandis	20.0	4.0	10.0	10.0	—	50.0	8.0	0.50
C. paradisi	18.2	18.2	12.7	10.9	—	40.0	—	0.55
C. flavicarpa	44.8	35.2	—	4.8	—	9.7	5.5	1.45
C. pseudoparadisi	41.7	18.8	—	10.4	—	29.2	—	0.48
C. intermedia	20.0	17.3	10.7	8.0	—	44.0	—	0.75
C. hassaku	48.7	33.3	—	17.9	—	—	—	0.39
C. natsudaidai	32.8	18.8	—	17.2	—	31.3	—	0.64
C. otachibana	14.3	11.1	11.1	11.1	—	52.4	—	0.63
C. obovoidea	44.6	18.5	—	10.8	—	26.2	—	0.65
C. sulcata	71.4	14.3	—	5.7	—	8.6	—	0.35
C. aurantium	22.6	22.6	6.5	3.2	—	33.9	11.3	0.62
C. myrtifolia	26.2	26.2	7.1	4.8	—	27.4	8.3	0.84
C. sinensis	22.7	36.0	10.7	22.7	—	—	9.3	0.75
C. tankan	33.3	51.9	—	5.2	—	5.2	4.4	2.70
C. iyo	30.1	30.1	—	8.2	—	19.1	12.3	0.73
C. ujukitsu	44.1	22.0	—	6.8	—	16.9	10.2	0.59
C. aurea	50.0	12.5	—	8.3	—	25.0	4.2	0.48
C. shunkokan	36.6	40.7	—	6.5	—	9.8	6.5	1.23
C. junos	50.0	50.0	—	—	—	—	—	0.14
C. hanaju	24.8	41.7	—	8.3	—	12.4	12.8	2.18
C. sudachi	66.7	33.3	—	—	—	—	—	0.09
C. nippokoreana	21.1	26.3	5.3	27.8	—	11.3	8.3	1.33
C. unshiu	29.4	29.4	5.9	7.4	—	17.6	11.8	0.68
C. keraji	44.9	34.5	—	4.2	—	11.8	4.5	2.87
C. oto	28.7	33.5	—	8.4	—	18.6	10.8	1.67
C. reticulata	33.2	49.0	—	4.2	—	8.5	5.1	3.55
C. tachibana	27.8	50.2	1.5	6.7	—	8.3	5.4	8.45
C. erythrosa	32.0	52.7	—	3.0	—	8.2	4.1	3.66
C. kinokuni	26.4	52.8	0.3	5.8	0.6	10.0	6.9	5.91
C. depressa	27.8	51.7	—	6.6	—	8.5	5.6	4.68
C. leiocarpa	29.1	53.6	—	5.7	—	8.9	5.1	3.71
C. madurensis	33.3	34.9	—	7.9	—	15.9	7.9	0.63
F. japonica	50.0	50.0	—	—	—	—	—	0.12
F. obovata	53.8	46.2	—	—	—	—	—	0.13

TABLE IV. The Average Contents of Polymethoxyflavones in *Citrus* Cultvars

	1	2	3	4 (%)	5	6	7	Total (mg/g)
Fremont	17.6	63.2	—	5.8	—	7.9	5.5	3.29
Anchol	26.1	56.0	—	5.0	—	7.0	5.8	6.16
Kara	36.4	39.0	3.9	6.5	—	8.4	5.8	1.54
Ortanique	25.9	36.1	—	12.0	—	16.5	9.5	1.58
Kiyomi	21.3	24.6	8.2	16.4	—	18.0	11.5	0.61
Allspice	36.4	29.5	—	8.0	—	15.9	10.2	0.88
Pearl	32.1	44.6	4.5	3.6	—	9.8	5.4	1.12
Minneola	27.0	40.9	4.3	7.0	—	12.2	8.7	1.15
San Jacinto	35.4	34.4	5.2	5.2	—	12.5	7.3	0.96
Fairchild	29.2	34.5	8.8	11.5	—	9.7	6.2	1.13
Osceola	23.8	41.3	—	9.5	—	15.9	9.5	0.63
Lee	15.7	35.3	5.9	23.0	—	12.3	7.8	2.04
Nova	14.2	31.8	16.5	15.3	—	13.6	8.5	1.76
Clementine	17.8	31.8	10.9	10.1	—	18.6	10.9	1.29
Page	10.4	30.4	13.6	29.2	—	9.6	6.8	2.50
Kobayashi-mikan	32.3	16.9	—	15.4	—	24.6	10.8	0.65

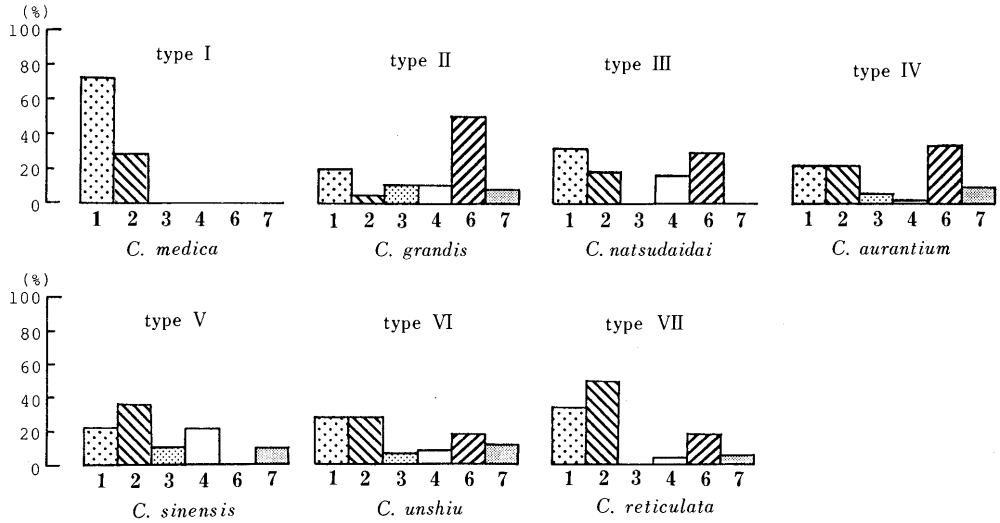

Fig. 3. Representative Types (Types I—VII) Characterized by the Relative Ratio of Polymethoxyflavones (**1**—**7** Except **5**)

of **1** or **2** to 20—25%. The total flavones content is 0.7 mg/g. *C. aurantium* is a hybrid between *C. grandis* and *C. reticulata*,[16] the basis of which was supported by the investigation of isozyme.[12] Therefore, type IV combines two characters of types II and VI.

The fifth type (type V) is distinguished from the others by a higher content of flavone **4**. Flavone **6** is absent in *C. hassaku* and *C. sinensis*, whereas *C. nippokoreana* contains **6** at 11.3%. The feature being rich in **4** was also observed in 'Lee' and 'Page' which belong to Tangerine–Tangelos. It was too difficult to estimate the average content in type V because the highest species of *C. nippokoreana* attached to 1.33 mg/g, in contrast, the lowest of *C. hassaku* was only 0.39 mg/g. *C. sinensis* in type V had been considered a hybrid of *C. grandis* × *C. reticulata*.[17] It is now deduced, however, that *C. sinensis* did not originate in F_1, but broke out after F_2 hybridization.[12]

The sixth type (type VI) is also composed by flavones **1**—**7** except **5**, and alike to type IV. The conspicuous difference from type IV is a lower total of flavone content (1.5 mg/g). Some species in type VI are richer in **1** than **2** (*C. flavicarpa* and *C. keraji*), others have almost the same contents (*C. iyo*, *C. shunkokan*, *C. unshiu*, *C. oto* and *C. madurensis*). An abundance of **1** and **2** or lacking of **3** shows that type VI is closely related with type VII.

Type VII is characterized as follows: flavone **2** is contained about two times richer than **1** such as in *C. tankan*, *C. reticulata*, *C. tachibana*, *C. erythrosa*, *C. kinokuni*, *C. depressa*, *C. leiocarpa* and *C. hanaju*). In *C. tahibana*, and flavone **3** was detected as a minor one, and **3** and **5** were also detected in *C. kinokuni* (Kinokuni-seedless). The marked feature of type VII is the highest content of total flavones (4.3 mg/g). The citrus taxa located at the most evolutionary position in the classification system presented by Swingle[13] and by Tanaka[14,15] belong to type VII.

In the present study, the inheritance problems reflected on the occurrences of polymethoxyflavones are also applied to the respective cultivars. Among three hybrids, 'Fremont' (*C. clementina* × *C. reticulata*) succeeded to both its parent biosynthesis to reveal type VII. 'Anchol' (*C. nobilis* × *C. unshiu*), which is a hybrid of type VI, also inherits type VI. Tangors: 'Ortanique' and 'Kiyomi' (*C. reticulata* × *C. sinensis*) shows both characters of types VII and V. In the case of 'Ortanique,' the chromatogram just indicated the middle-laid profiles between types VII and V, and the latter type sometimes appears in a hybrid which is produced by types VII and V when type VII is superior to type V such as 'Kiyomi.' 'Ortanique' was absent of the flavone **3** and was included into type V. 'Allspice,' 'Pearl' (*C. paradisi* × *C. deliciosa*), 'Minneola' (*C. paradisi* × *C. tangerina*) and 'San Jacinto' are all included in Tagelos. 'Allspice' and 'San Jacinto' showed type VI, while 'Pearl' and 'Minneola' did type VII. In the miscellaneous variety, Kobayashi-mikan (*C. unshiu* × *C. natsudaidai*) showed type III, which will be regarded as a close relation of *C. grandis*.

Conclusion

Types ordering from I to VII are aligned with the evolutionary order in the *Citrus* species presented by Swingle or Tanaka. For example, the sections Limonellus and Citrophorum in the subgenus Archicitrus in addition to the genus *Fortunella* belong to type I, and as the evolution from the section Cephalocitrus to the section Aurantium, type changes from II to VI *via* V. In the same way, the section Acrumen in the subgenus Metacitrus includes two types (VI and VII). The group Anisodora corresponds to type VI and the group Citriodora is type VII. Tentatively divided into seven types based on the relative ratio of flavones and total flavones content, thus, are well-agreed with the morphological classification systems presented by Swingle or Tanaka. Consideration of their types obtained in the present study, the classification of and *C. hassaku* and *C. flavicarpa* (section Cephalocitrus), *C. tankan* (subsection Sinensioides), *C. ujukitsu* and *C. aurea* (subsection Osmocitriodes), and *C. junos* and *C. sudachi* (subsection Euosmocitrus) is out of order despite a lack of enough proof.

Further chemotaxonomical investigation on the genus *Citrus* by use of coumarin derivatives as a marker is now in progress.

References

1) N. Nikaido, T. Ohmoto, U. Sankawa, T. Hamanaka and K. Totsuka, *Planta Medica*, **46**, 162 (1982).
2) J. Pinka, O. Lavie and M. Chorin, *Phytochemistry*, **7**, 169 (1968).
3) M. Mizuno, M. Iinuma, T. Tanaka, Y. Matoba, Y. Fujii, J. Murata, H. Murata and M. Iwamasa, *Chem. Pharm. Bull.*, **35**, 3205 (1987).
4) S. Tosa, S. Ishihara, M. Toyama, S. Yoshida, H. Nakazawa and T. Tomimatsu, *Shoyakugaku Zasshi*, **42**, 41 (1988).
5) M. Nishiura, S. Esaki and S. Kamiya, *Agric. Biol. Chem.*, **33**, 1109 (1969); M. Nishiura, S. Kamiya, S. Esaki and F. Ito, *ibid.*, **35**, 1683 (1971); M. Nishiura, S. Kamiya and S. Esaki, *ibid.*, **35**, 1961 (1971).
6) R. F. Albach and G. H. Redman, *Phytochemistry*, **8**, 127 (1969).
7) H. C. Dass, G. S. Randhawa and D. Prakash, *Indian J. Exp. Biol.*, **16**, 62 (1978).
8) J. H. Tatum, C. J. Hearn and R. E. Berry, *J. Am. Soc. Hort. Sci.*, **103**, 492 (1978).
9) M. Iinuma, S. Matsuura, K. Kurogochi and T. Tanaka, *Chem. Pharm. Bull.*, **28**, 717 (1980).
10) J. P. Bianchini and E. M. Gaydou, *J. Chromatogr.*, **190**, 233 (1980).
11) E. M. Gaydou, J. P. Bianchini and R. P. Randriamiharisoa, *J. Agric. Food Chem.*, **35**, 525 (1987).
12) A. M. Torres, R. K. Soost and U. Diedenhofen, *Am. J. Bot.*, **65**, 869 (1978).
13) W. T. Swingle, "The Botany of *Citrus* and Its Relatives of the Orange Subfamily," ed. H. J. Webber and L. D. Batchelor, The *Citrus* Industry, Vol. 1, Univ. of California Press, Berkeley, 1943, pp. 129—474.
14) T. Tanaka, "Species Problem in *Citrus*," Japanese Society for the Promotion of Science, Tokyo, 1954.
15) T. Tanaka, *Bull. Univ. Osaka Prefect. Ser. B.*, **21**, 139 (1969).
16) R. W. Scora, *Bull. Torry. Bot. Club.*, **102**, 369 (1975).
17) H. C. Barrett and A. M. Rhodes, *Syst. Bot.*, **1**, 105 (1976).
18) T. Tanaka, *Bull. Univ. Osaka Prefect. Ser. B*, **18**, 31 (1966).
19) A. Esen and R. W. Scora, *Am. J. Bot.*, **62**, 1078 (1975).
20) A. Esen and G. Geraci, *Am. J. Bot.*, **63**, 329 (1976).
21) A. Esen and R. W. Scora, *Am. J. Bot.*, **64**, 305 (1977).

Lignified Materials as a Potential Medicinal Resource. IV. Dehydrogenation Polymers of Some Phenylpropenoids and Their Capacity to Stimulate Polymorphonuclear Cell Iodination

Hiroshi SAKAGAMI,[a] Toshinari OH-HARA,[b] Kohfuku KOHDA[b] and Yutaka KAWAZOE*,[b]

1st Department of Biochemistry, School of Medicine, Showa University,[a] Hatanodai, Shinagawa-ku, Tokyo 142, Japan and Faculty of Pharmaceutical Sciences, Nagoya City University,[b] Tanabedori, Mizuho-ku, Nagoya 467, Japan. *Received October 19, 1990*

Based on our recent finding regarding diverse biological activities of natural lignified materials, synthetic dehydrogenation homo- and copolymers were prepared using 3 *p*-hydroxylated cinnamic acids and coniferyl alcohol in order to explore the role of lignin skeleton in the activities displayed by natural lignins. The synthetic polymers stimulated polymorphonuclear cell iodination as potently as the natural lignified materials.

Keywords lignin; phenylpropenoid; cinnamic acid; dehydrogenation polymer; cell iodination

Lignin is a major class of constituents in the land-plant kingdom, amounting to 20—30% of woods and 15—25% of grasses. However, very little attention has been paid to their biological activity,[1] despite the volume of studies on other natural products as potential medicinal resources. Recently, we have demonstrated that water extracts of lignified materials, including the waste from the pulp industry, displayed diverse biological activities such as antiviral,[2-5] antibacterial,[6-8] antitumor,[9] and also immunopotentiating activity.[10-14] It remains a matter of debate which component in the extracts is the active principle, a lignin-related component or certain other appendages included in the extracts.[15,16] Under these circumstances, this study was undertaken to explore the biological activity of purely synthesized dehydrogenation polymers, starting from several phenylpropenoids, some of which are regarded as synthetic lignins. This paper describes the synthesis and spectral characterization of the polymers and their capacity to stimulate polymorphonuclear cell iodination, which might be one of the biological measures for the potentiation of host-defense mechanisms.[11,12]

Materials and Methods

Materials *p*-Coumaric acid (4-hydroxycinnamic acid), ferulic acid (4-hydroxy-3-methoxycinnamic acid), caffeic acid (3,4-dihydroxycinnamic acid), coniferyl alcohol (4-hydroxy-3-methoxycinnamic alcohol), and horseradish peroxidase were purchased from Tokyo Kasei Kogyo Co., Ltd., Tokyo.

Dehydrogenative Polymerization of Phenylpropenoids Four kinds of phenylpropenoids were used for dehydrogenative polymerization; *p*-coumaric acid, ferulic acid, caffeic acid, and coniferyl alcohol. Polymerization procedures were as follows. Solutions A, B, and C were prepared. Solution A: One gram of a phenylpropenoic acid was neutralized with 1 N NaOH and diluted to 200 ml with a 0.05 M Na-phosphate buffer (pH 8.0). For conifery alcohol, neutralization with NaOH was not necessary. Solution B: Ten milligrams of horseradish peroxidase was dissolved in 200 ml of a 0.05 M Na-phosphate buffer (pH 8.0). Solution C: H_2O_2 (*ca.* 30%) was diluted to 0.1% with a 0.05 M Na-phosphate buffer (pH 8.0).

Endwise Polymerization[17]: Solution A and solution C (H_2O_2: 1.5 mol eq to the phenylpropenoid) were introduced dropwise from respective dropping funnels into a flask containing solution B and a magnet bar for stirring for a period of 1 h at 25 °C. The reaction mixture all combined continued to be stirred for 2 h more at 25 °C, and then the pH of the mixture was adjusted to 3.0 by the addition of glacial acetic acid. After being cooled in a refrigerator for 1 h, the precipitates were collected by centrifugation (10^4 *g* for 10 min) and washed twice with 400 ml of dil. HCl (pH 2). The precipitates were dissolved in 80 ml of MeOH or acetone, and filtered through a Toyo filter paper (No. 2). The filtrate was dropped into 800 ml of HCl (pH 2) with stirring. After being cooled in a refrigerator for 30 min, the precipitates were collected by centrifugation. They were dissolved in a small amount of H_2O and lyophilized. When caffeic acid was polymerized, the polymer formed was soluble even in an acidic medium. Therefore, after the reaction mixture was acidified to pH 3.0, it was dialyzed sequentially against dozens of butches of distilled water for 72 h, then evaporated under reduced pressure. The residue was dissolved in 200 ml of EtOH and filtered through a millipore filter. After the filtrate was evaporated to dryness, the residue was dissolved in a small amount of H_2O and lyophilized.

Bulk Polymerization[17]: Solution C (1.5 eq H_2O_2) was added dropwise into a mixture of solution A and solution B for a period of 1 h with stirring at 25 °C. The isolation and purification of dehydrogenation polymers were carried out in the same way as described in the endwise polymerization.

Spectral Measurements Ultraviolet (UV) spectra were taken in an aqueous solution at room temperature with a Shimadzu UV-2100 spectrophotometer. Infrared (IR) spectra were recorded on a Perkin Elmer FT-IR 1600 spectrometer. Electron spin resonance (ESR) spectra were measured in solid state at room temperature with a JEOL JES-RE2X spectrometer. Proton magnetic resonance (^{1}H-NMR) spectra were taken in a dimethyl sulfoxide solution at room temperature with a JEOL EX 270 spectrometer.

Centrifugal Ultrafiltration A phosphate buffer solution (1/15 M PB, pH 7.4) of each sample (*ca.* 25 μg/ml) was centrifuged at 2500 *g* for 20 min using centrifugal ultrafilters Centri Cell™ (Polysciences, Inc., Warrington, PA) with molecular weight limits of 10000 and 30000 dalton, respectively.

Iodination of Human Peripheral Blood Polymorphonuclear Cells Human polymorphonuclear (PMN) cells were obtained from 20 ml of the peripheral blood of normal healthy volunteers after successive centrifugations on Ficoll-Paque and Mono-Poly Resolving Medium as described previously.[11] The purity of the PMN population was above 95%, as judged by morphological examination after staining with May-Grunwald-Giemsa. Iodination was determined by a modified procedure of Klebanoff and Clark.[18] The standard reaction mixture (0.5 ml) contained 1×10^6 PMN, 4 nmol $Na^{125}I$ (0.5 μCi), and a test sample in a serum-free RPMI 1640 medium. The serum was omitted from the reaction mixture because of its inhibitory effect. The reaction was allowed to start by the addition of the cells to the solution containing all the others, and the mixture was incubated at 37 °C for 150 min. The radioactivity incorporated into a trichloroacetic acid (TCA)-insoluble fraction of PMN was measured by a gamma-counter as described previously.[11] A blank containing all the components except the cells was run with each experiment, and the results were subtracted from the experimental measures. Less than 0.5% of the total radioactivity added was recovered in TCA-precipitates in the blank.

Results

Synthetic Phenylpropenoids The polymers synthesized in the present study were homopolymers obtained from *p*-coumaric acid, ferulic acid, and caffeic acid, respectively. A copolymer of ferulic acid and coniferyl alcohol (1 : 1 mixture) was also synthesized. Dehydrogenative polymerization was performed with each starting monomer in two ways; the "endwise" and "bulk" polymerizations[17] as reported for the preparation of synthetic lignins starting from *p*-coumaric, coniferyl, and sinapyl alcohols. A

TABLE I. Synthetically Polymerized Phenylpropenoids

Dehydrogenation polymer (DHP)	pH of medium	Element. analy. (%)		Yield of polymer	OD at 280 nm (50 μg/ml)	Spin (ESR) nmol/mg
		C	H			
Coniferyl alcohol (Con)						
DHP–Con (endwise-pH 6)	6	63.03	5.60	90.1	1.46	0.11
DHP–Con (bulk-pH 6)	6	64.08	5.78	94.5	1.19	0.13
p-Coumaric acid (*p*CA)						
DHP–*p*CA (endwise-pH 6)	6	64.36	3.83	71.1	2.81	0.10
DHP–*p*CA (endwise-pH 8)	8	63.01	3.67	74.2	2.38	0.24
DHP–*p*CA (bulk-pH 8)	8	61.97	3.56	86.2	2.51	0.32
Ferulic acid (FA)						
DHP–FA (endwise-pH 6)	6	61.60	4.35	91.9	1.75	0.11
DHP–FA (endwise-pH 8)	8	59.37	4.25	68.6	1.66	0.29
DHP–FA (bulk-pH 8)	8	59.69	3.97	69.0	1.72	0.29
Caffeic acid (CA)						
DHP–CA (endwise-pH 8)	8	53.29	3.27	59.9	1.92	0.76
DHP–CA (bulk-pH 8)	8	53.05	3.14	70.8	1.86	1.11
Copolymer						
DHP–FA&Con (bulk-pH 8)	8	61.33	4.68	88.4	1.56	0.24
Natural lignins						
Alkali lignin (pulp waste)		51.58	4.28	—	1.20	1.23
Dealkali lignin (pulp waste)		52.36	4.46	—	0.61	0.45
Lignosulfonic acid (pulp waste)		39.38	4.27	—	0.35	0.03
PC (fr. VI) (fr. VI of pine cone)		47.42	3.77	—	1.01	0.94

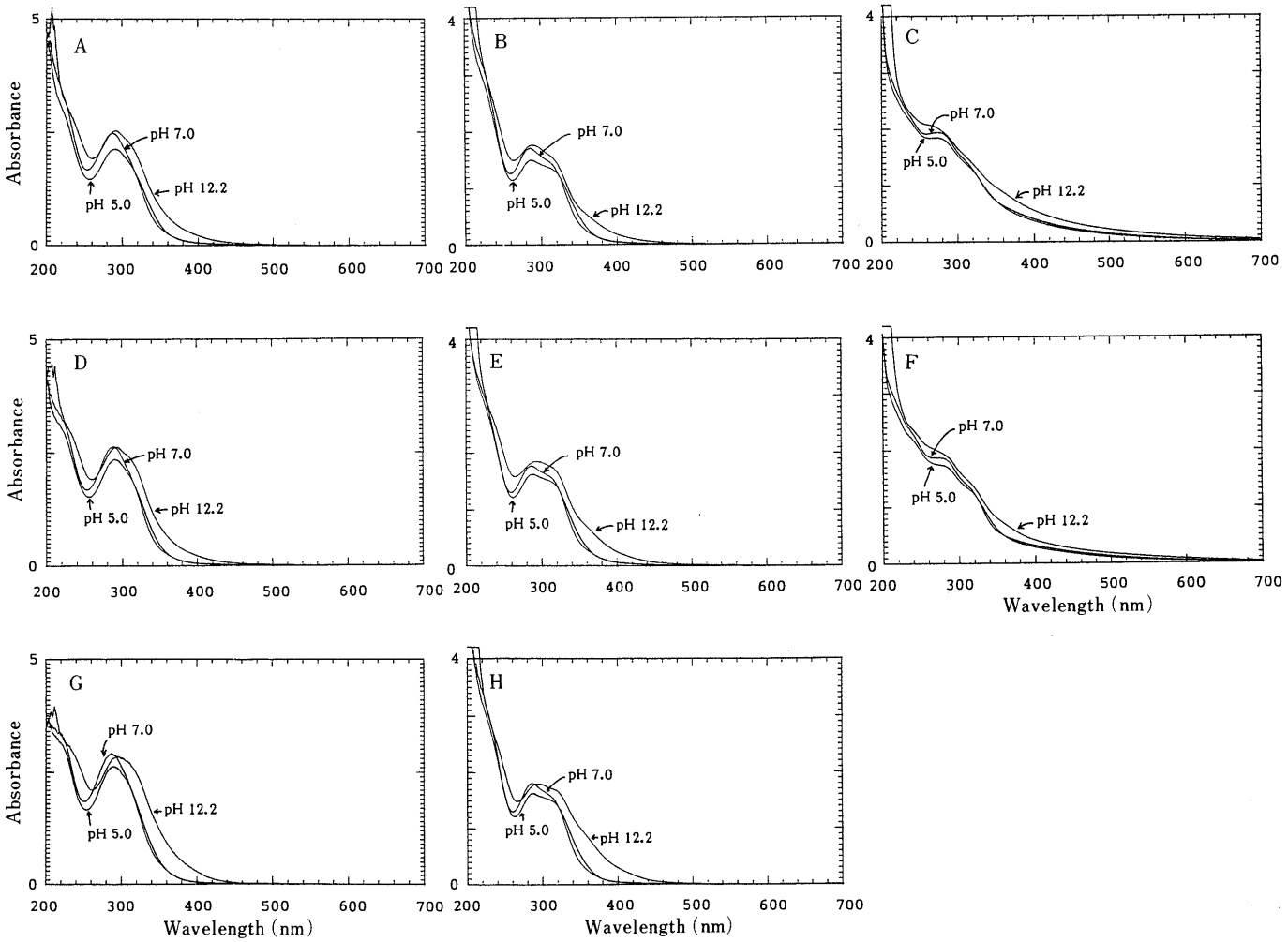

Fig. 1. UV Spectra of Synthesized Polymers in Water

A, DHP–*p*CA(endwise-pH 8); B, DHP–FA(endwise-pH 8); C, DHP–CA(endwise-pH 8); D, DHP–*p*CA(bulk-pH 8); E, DHP–FA(bulk-pH 8); F, DHP–CA(bulk-pH 8); G, DHP–*p*CA(endwise-pH 6); H, DHP–FA(endwise-pH 6). pH was adjusted with aqueous HCl or NaOH as indicated in the figure. Concentration was 50 μg/ml.

synthetic lignin obtained from coniferyl alcohol was also prepared. A list of the polymers synthesized, the reaction yield, and their abbreviations are given in Table I. Each polymer contained a small percentage of inorganic salt which remained contaminated after thorough washing of the precipitates as described in Materials and Methods. The enzyme used for polymerization stayed in the supernatant when the polymer was precipitated by acidification (pH 3) of the reaction mixture. It was confirmed that each polymer showed no nitrogen in its elementary analysis. Polymerized phenylpropenoic acids prepared in this study are all soluble in neutral water, whereas synthetic lignins are in general very poorly soluble. A copolymer of ferulic acid and coniferyl alcohol (1 : 1 mixture) was soluble enough for biological examinations *in vitro*.

UV Spectra Spectra measured in neutral, alkaline, and acidic media are shown in Fig. 1. All the synthesized polymers showed a maximum at *ca.* 280 nm and a minimum at *ca.* 260 nm, accompanied by an end-absorption in the visible region. In an alkaline medium (pH 12), some intensity

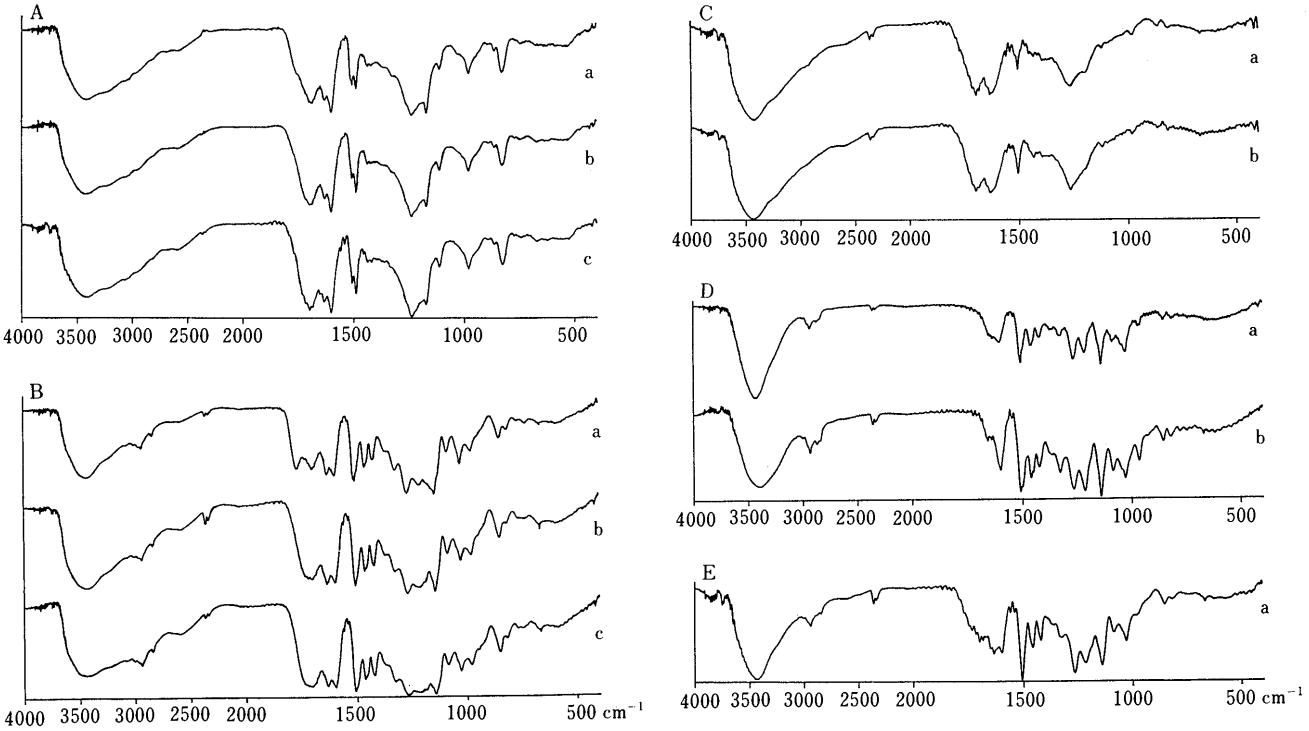

Fig. 2. IR Spectra of Synthesized Polymers in KBr Disk

A: a, DHP–*p*CA(endwise-pH 6); b, DHP–*p*CA(endwise-pH 8); c, DHP–*p*CA(bulk-pH 8). B: a, DHP–Fa(endwise-pH 6); b, DHP–FA(endwise-pH 8); c, DHP–FA(bulk-pH 8). C: a, DHP–CA(endwise-pH 8); b, DHP–CA(bulk-pH 8). D: a, DHP–Con(endwise-pH 6); b, DHP–Con(bulk-pH 6). E: a, DHP–FA & Con(bulk-pH 8). The ordinate is transmittance.

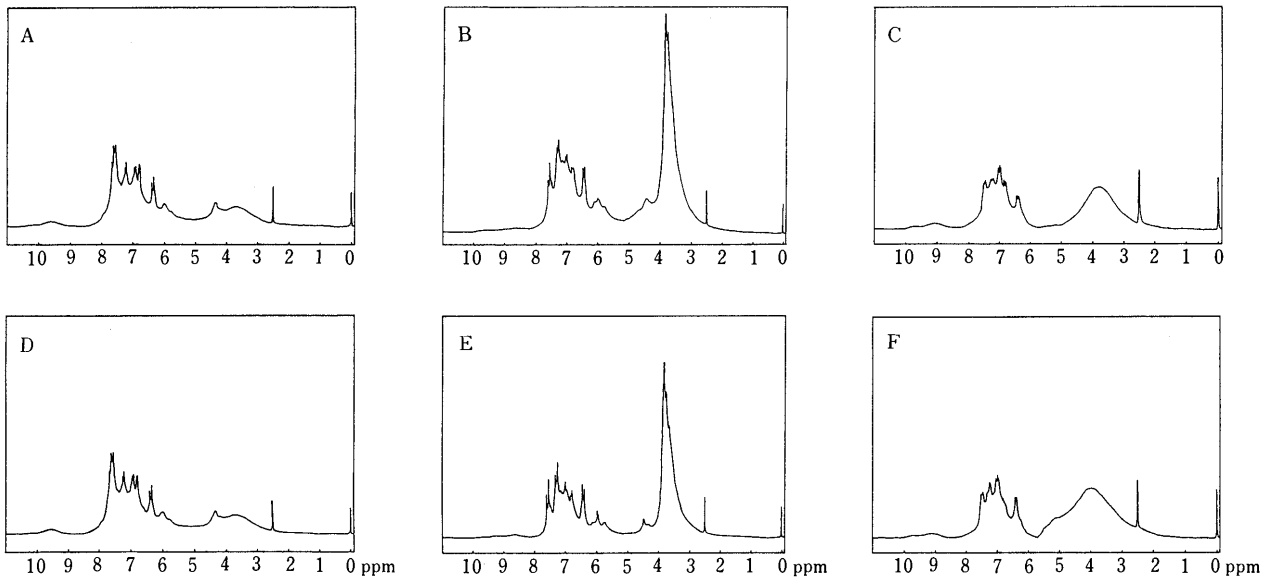

Fig. 3. ^{1}H-NMR Spectra of Synthesized Polymers in Dimethyl Sulfoxide-d_6

A, DHP–*p*CA(endwise-pH 8); B, DHP–FA(endwise-pH 8); C, DHP–CA(endwise-pH 8); D, DHP–*p*CA(bulk-pH 8); E, DHP–FA(bulk-pH 8); F, DHP–CA(bulk-pH 8). The internal standard was tetramethylsilane.

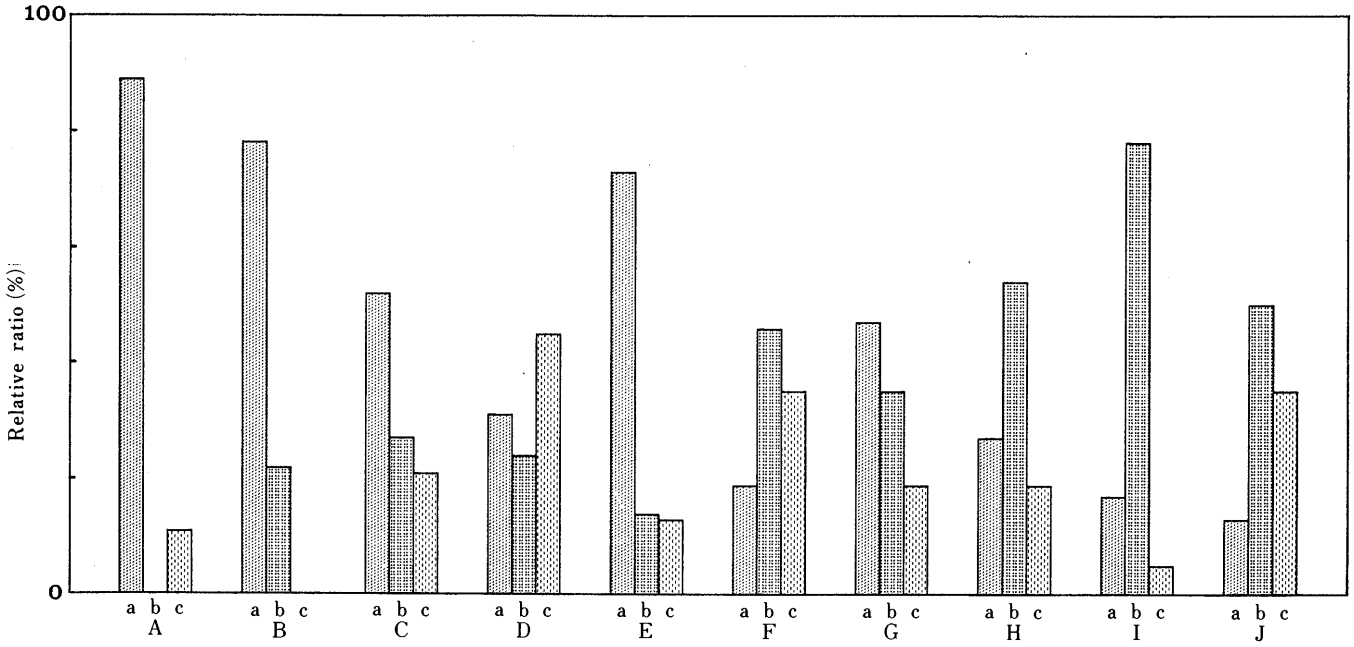

Fig. 4. Distribution of Molecular Weight of Synthesized Polymers and Some Natural Lignins Estimated by Centrifugal Ultrafiltration Method

a, less than 10000 dalton; b, between 10000 and 30000; c, more than 30000.

A, DHP-*p*CA(endwise-pH 6); B, DHP-*p*CA(endwise-pH 8); C, DHP-*p*CA(bulk-pH 8); D, DHP-FA(endwise-pH 6); E, DHP-FA(endwise-pH 8); F, DHP-FA(bulk-pH 8); G, DHP-CA(endwise-pH 8); H, DHP-CA(bulk-pH 8); I, PC(fr. VI); J, alkali lignin.

increase was observed in the longer wave region, probably due to dissociation of the phenolic OH group. These features coincide with those reported for lignins synthesized and also isolated from lignified natural products.[16]

IR Spectra The IR spectra shown in Fig. 2 were taken in a form of KBr-disk. All the spectra show common features: a broad and strong absorption at *ca.* 3600—3000 cm^{-1} due to hydrogen-bonded OH groups, peaks at *ca.* 1750—1600 cm^{-1} due to carbonyl groups of carboxylic acids and esters (or lactones), a set of peaks at *ca.* 1600 and 1500 cm^{-1} due to aromatic double bonds, and peaks at *ca.* 1300—1100 cm^{-1} due to C–O groups. All these features coincide with those reported of lignins, although the absorptions might not all be assigned precisely. It is worth noting that the spectra of each isomeric pair of endwise and bulk homopolymers are very similar to each other, indicating no appreciable structural difference between the isomers.

ESR Spectra As already reported,[16] lignins isolated from lignified natural products give an ESR signal due to organic free radicals in the solid state. The present study revealed that synthesized polymers of phenylpropenoic acids, and a synthetic lignin of coniferyl alcohol as well, give an intense ESR signal at $g=2.003$ in the solid state at room temperature. No signal was given by either the monomeric precursors of polymers, or tannins, which constitute another group of oligomeric phenolic natural products. Free radicals probably initiated by the semiquinone formation must be stabilized through delocalization over a conjugated pi-electron system and also by a shielding effect of steric hindrance involved in the highly hindered structure. The ESR intensity depended slightly on the kind of monomer and the method employed for polymerization. The relative intensity is given in Table I.

^{1}H-NMR Spectra As shown in Fig. 3, the signals appeared as expected from the structural units; acidic protons at 10—9 ppm, aromatic ring protons at *ca.* 8—7 ppm, aliphatic double bond protons at *ca.* 7—6 ppm, CH protons adjacent to the oxygen function at *ca.* 5—3.5 ppm. Ferulic acid polymers showed an additional

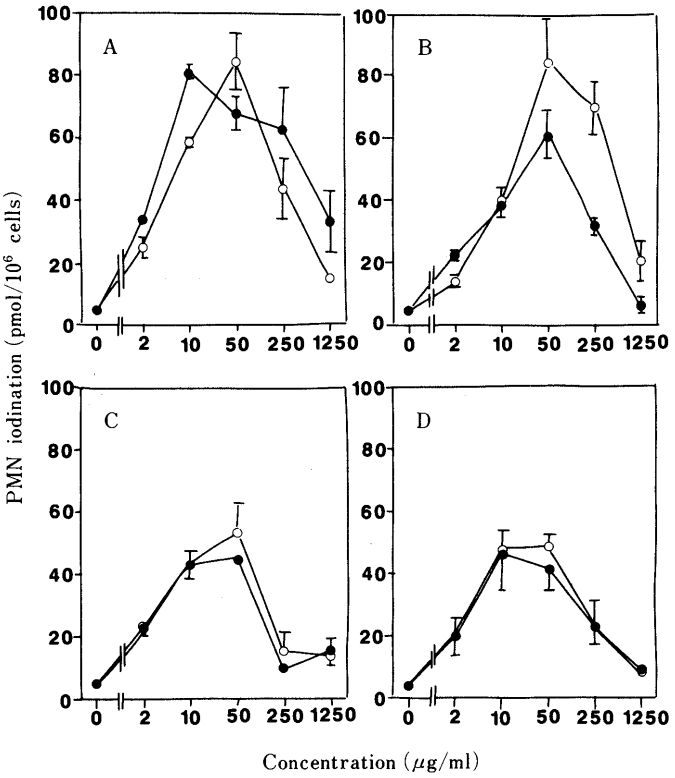

Fig. 5. PMN Iodination Induced by Synthesized Polymers

PMN (1×10^6 cells) were iodinated for 120 min with 4 nmol Na ^{125}I in the presence of a test polymer. Each point is mean ± S.E. from three independent experiments. A, PC(fr. VI) (●) and alkali lignin (○); B, bulk (○) and endwise (●) polymers of DHP-FA(pH 8); C, bulk (○) and endwise (●) polymers of DHP-*p*CA(pH 8); D, bulk (○) and endwise (●) polymers of DHP-CA(pH 8).

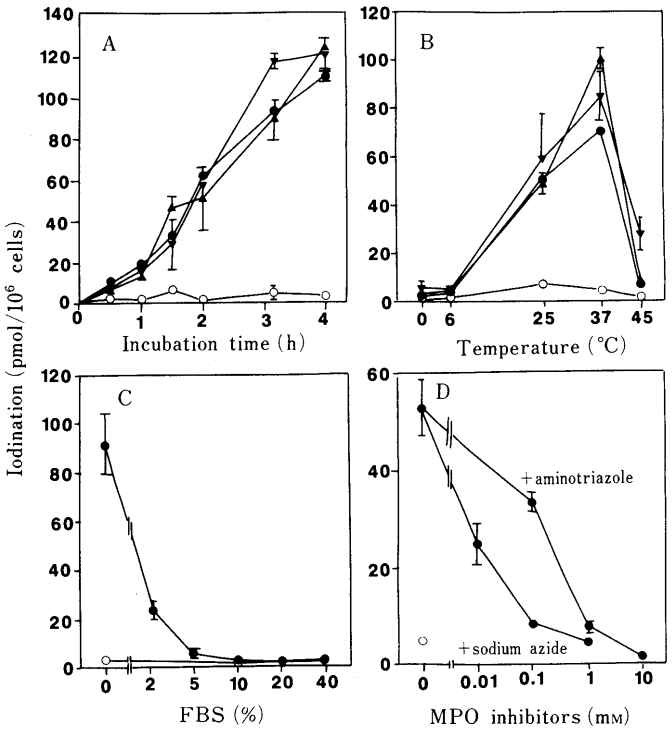

Fig. 6. Dependence of PMN Iodination Rate on Some Assay Conditions

PMN (1×10^6 cells) were iodinated in the presence of 50 μg/ml of each polymer. Symbols for test polymers in figures are: control (saline) (○), DHP–FA(endwise-pH 8) (●), DHP–*p*CA(endwise-pH 8) (▲), and DHP–CA(endwise-pH 8) (▼). Each point is mean ± S.E. from triplicate assays.

A, dependence on incubation time (at 37 °C); B, dependence on incubation temperature (after 2 h incubation); C, dependence on the concentration of FBS (after 2 h incubation at 37 °C); D, inhibitory effect of myeloperoxidase inhibitors, sodium azide and aminotriazole, respectively (after 2 h incubation at 37 °C).

intense signal at *ca.* 3.8 ppm due to OCH_3 protons. It is worth noting that the spectra of an isomeric pair of polymers of each homopolymer were almost superimposed on each other.

Molecular Weight Molecular weights of the major components of synthetic polymers are less than 30000 dalton in most cases, estimated by the centrifugal ultrafiltration method. Thus, each polymer was subfractionated into three: less than 10000, 10000—30000, and more than 30000, as illustrated in Fig. 4. The data of some bioactive natural lignins, the fraction VI of pine cone (PC) and a commercial alkali lignin,[16] are also shown.

Stimulation of PMN Cell Iodination As shown in Fig. 5, a remarkable PMN stimulation was displayed when the cells were treated with any of the synthetic polymers in a wide dose range of *ca.* 2—250 μg/ml. Their optimal concentrations were around 50 μg/ml. The stimulation rate and working dose range are both almost comparable with those shown by bioactive lignin-fractions isolated from lignified natural products[11,12] (Fig. 5A). The PMN iodination increased with an increase in the incubation time (Fig. 6A). Incubation for 2 h was used for the following experiments, since significant PMN aggregation occurred after more prolonged incubations. The synthetic polymer-stimulated PMN iodination strongly depended on incubation temperature; maximum iodination occurred at 37 °C (Fig. 6B). Fetal bovine serum (FBS) was inhibitory; addition of 2% FBS reduced the stimulation rate to 25% (Fig. 6C). The data described in the present study were obtained by incubating the cells in the reaction medium without FBS. As shown in Fig. 6D, PMN iodination was inhibited by two myeloperoxidase (MPO) inhibitors, NaN_3 and aminotriazole[18] in a dose-dependent manner, 50% inhibition yielding at *ca.* 0.01 mM and 0.3 mM, respectively. All the features described here are the same as those shown by PC (fr. VI) and alkali lignin, as we reported.[11,12]

Discussion

As we previously reported,[15] lignin fractions obtained from lignified natural products, including waste from the pulp industry, stimulate PMN iodination to a remarkable extent. Their stimulating capacity increased after drastic acid-hydrolysis of these lignin fractions, indicating that the lignin moiety, but not certain possible appendages such as hemicelluloses, plays a substantial role in this activity. This was further supported by the fact that lignified extracts were almost completely deprived of the stimulating capacity by their $NaClO_2$-treatment that is known to decompose the lignin component of lignified materials. The present study on synthetic polyphenylpropenoids, including a synthetic lignin, gave a decisive conclusion that lignin skeleton itself is the active stimulant for PMN iodination, *i.e.*, to stimulate the PMN cell to potentiate the capacity of the myeloperoxidase-related oxidizing system of the cell.

It seems that much effort in the lignin chemistry has so far been devoted to (i) elucidation of lignin structure, *i.e.*, how to polymerize the lignin precursors in the plant kingdom, and (ii) degradation of lignin moiety, *i.e.*, how to isolate cellulose and hemicelluloses from lignified natural products.[17] The lignin component has been regarded as a cumbersome component of lignified natural products. In addition to natural lignins, synthetic lignins prepared so far have been used mainly for investigations aimed at a better understanding of the structure and a more effective degradation of the lignin component. Very few reports have been published on synthetic polyphenylpropenoids aiming at their medicinal utility, including toxicity. Our recent finding on the diverse biological activities of lignified materials[2-16] have shed light on the promising utility of lignified materials as medicinal resources. The present study proposes synthetic polymers, especially water-soluble polymers of hydroxylated cinnamic acid derivatives, ready to use for biological investigations *in vitro* and *in vivo*. It should be cited that Thiel *et al.* once reported the anti-herpes activity of oxidized polymeric caffeic acid, a model compound of natural humic acid.[19] More attention should be paid to the potential capacity of synthetic lignin-like polymers, in addition to natural lignified materials, in medicinal utility.

Acknowledgments We thank Dr. K. Konno, President of Jonan General Hospital, Tokyo for encouragement, Dr. K. Kikuchi and Ms. S. Kohno, Showa University for secretarial assistance, and Dr. A. Simpson of Showa University for help with the manuscript. This study was supported in part by a Grant-in-Aid for Scientific Research from the Ministry of Education, Research and Culture of Japan, the SHORAI Foundation for Science and Technology, and a U. S. Public Health Service Grant U01 A127280 from the National Institutes of Health.

References

1) *E.g.*, K. Yamafuji and H. Murakami, *Enzymologia*, **35**, 139 (1968).
2) K. Fukuchi, H. Sakagami, M. Ikeda, Y. Kawazoe, T. Oh-hara, K. Konno, S. Ichikawa, N. Hata, H. Kondo and M. Nonoyama,

Anticancer Res., **9**, 313 (1989).
3) K. Nagata, H. Sakagami, H. Harada, M. Nonoyama, A. Ishihama and K. Konno, *Antiviral Res.*, **13**, 11 (1990).
4) P. K. Lai, J. Donovan, H. Sakagami, A. Tanaka, K. Konno and M. Nonoyama, *AIDS Res. Human Retroviruses*, **6**, 205 (1990).
5) H. Sakagami, K. Nagata, A. Ishihama, T. Oh-hara and Y. Kawazoe, *Biochem. Biophys. Res. Commun.*, **172**, 1267 (1990).
6) H. Harada, H. Sakagami, K. Konno, T. Sato, N. Ohsawa, M. Fujimaki and N. Komatsu, *Anticancer Res.*, **8**, 581 (1988).
7) T. Oh-hara, H. Sakagami, Y. Kawazoe, T. Kaiya, N. Komatsu, N. Ohsawa, M. Fujimaki, S. Tanuma and K. Konno, *In Vivo*, **4**, 7 (1990).
8) T. Oh-hara, H. Sakagami, Y. Kawazoe, T. Momoi, T. Kaiya, K. Kohda, N. Komatsu, N. Ohsawa, M. Fujimaki and K. Konno, *In Vivo*, **4**, 221 (1990).
9) H. Sakagami, M. Ikeda, S. Unten, K. Takeda, J. Maruyama, A. Hamada, K. Kimura, N. Komatsu and K. Konno, *Anticancer Res.*, **7**, 1153 (1987).
10) T. Oh-hara, Y. Ikeda, H. Sakagami, K. Konno, T. Kaiya, K. Kohda and Y. Kawazoe, *Chem. Pharm. Bull.*, **38**, 282 (1990).
11) S. Unten, H. Sakagami and K. Konno, *J. Leukocyte Biol.*, **45**, 168 (1989).
12) H. Sakagami, Y. Kawazoe, T. Oh-hara, K. Kitajima, Y. Inoue, S. Tanuma, S. Ichikawa and K. Konno, *J. Leukocyte Biol.*, **46**, in press (1990).
13) Y. Kurakata, H. Sakagami, M. Takeda, K. Konno, K. Kitajima, S. Ichikawa, N. Hata and T. Sato, *Anticancer Res.*, **9**, 961 (1989).
14) A. Hanaoka, H. Sakagami and K. Konno, *Showa Univ. J. Med. Sci.*, **1**, 57 (1989).
15) T. Oh-hara, Y. Kawazoe and H. Sakagami, *Chem. Pharm. Bull.*, **38**, 3031 (1990).
16) H. Sakagami, T. Oh-hara, T. Kaiya, Y. Kawazoe, M. Nonoyama and K. Konno, *Anticancer Res.*, **9**, 1593 (1989).
17) K. V. Sarkanen and C. H. Ludwig, "Lignins," Wiley Interscience, New York, 1971, pp. 150—155.
18) S. J. Klebanoff and R. A. Clark, *J. Lab. Clin. Med.*, **89**, 675 (1977).
19) K. D. Thiel, B. Helbig, M. Sprossig, R. Klocking and P. Wulzler, *Acta Virol.*, **27**, 200 (1983).

Gas Liquid Chromatography–Mass Spectrometry of Paraquat and Diquat Reduction Products.[1] A Reductive Cleavage of Paraquat and Diquat by $NaBH_4$ in the Presence of a Transition Metal Salt (Ni^{2+})

Susumu KANNO,[a] Yuzi TAKEKOSHI,[a] Shozi KAWASE,[a] and Shigeo UKAI*,[b]

Scientific Investigation Research Laboratory, Gifu Prefectural Police Headquarters,[a] 1, Yabuta-1-chome, Gifu 500, Japan and Gifu Pharmaceutical University,[b] 5-6-1, Mitahora-higashi, Gifu 502, Japan. *Received September 17, 1990*

When herbicide preparations paraquat(I) and diquat(II), based on *N*-alkylbipyridylium derivatives, were analyzed by gas liquid chromatography (GLC) with sodium borohydride ($NaBH_4$)–nickel(II) chloride ($NiCl_2$) reduction, the chromatograms showed minor side peaks from slight amounts of by-products appearing in front of the main peaks, arising from the respective perhydrogenated products of I or II.

Reductive cleavage of a C–N bond within each pyridine ring of I or II was suggested in view of the production of trifluoroacetic acid derivatives prepared from these by-products.

The by-products, whose structures were elucidated by GLC–mass spectrometry, were consequently presumed to be *p*-(*N*-methylaminopent-3′-yl)-*N*-methylpiperidine, arising from I, or 1-butyl-2-aza-perhydroquinolizine, arising from II.

Correlation was also observed between the amounts of $NaBH_4$ and $NiCl_2$ and the production of by-products; the less $NaBH_4$ and the more $NiCl_2$ in a given volume of water, the greater the increase in side reaction products.

The side peaks could not be observed on the gas-chromatogram when perhydrogenated products prepared separately from I and II were treated by $NaBH_4$–$NiCl_2$ reduction. The side peaks could be observed, however, when incomplete reduction products with one or two double bonds, obtained by reduction of I and II by $NaBH_4$ alone, were reduced by $NaBH_4$–$NiCl_2$ reduction. It could therefore be presumed that this reductive cleavage at a C–N bond occurred, the intermediate state being the complex between nickel and incomplete reduction products with one or two remaining double bonds in the pyridine ring.

Keywords paraquat; diquat; sodium borohydride–nickel(II) chloride reduction system; GC-MS; mass fragmentation; C–N bond reductive cleavage; trifluoroacetic acid-derivative; deuterium analogue; *p*-(*N*-methylaminopent-3′-yl)-*N*-methylpiperidine; 1-butyl-2-aza-perhydroquinolizine

Introduction

Paraquat(I) and diquat(II), based on *N*-alkylbipyridylium derivatives, have been widely used as non-selective herbicides; it is well known that they are highly lethal to humans and animals when ingested.[2]

In a previous paper,[3] we reported on gas liquid chromatography (GLC) of perhydrogenated products (III, IV) of I and II with reduction *via* $NaBH_4$ and a transition metal salt; *e.g.*, nickel(II) chloride ($NiCl_2$), in aqueous solution, urine and blood. The reduction process is shown in Chart 1.

Minor peaks arising from by-products (V or VI), whose mass numbers were larger by two than those of III or IV, were observed in front of the main peaks arising from III or IV (*trans*) on the chromatogram.

This paper deals with the structural analysis of V and VI on the basis of GLC–mass spectrometer (GLC-MS) of perhydrogenated products, by-products and their derivatives, as well as their deuterium analogues with $NaBH_4$–$NiCl_2$ (or $NaBD_4$–$NiCl_2$) reduction of I and II. In addition, the relationship between the production of V and the amounts of $NaBH_4$ and $NiCl_2$ in a given volume of water, and the mechanism of production of V and VI, are discussed.

Experimental

Materials Aqueous solutions of paraquat dichloride and diquat dibromide were kindly provided by ICI Japan, Ltd. (1-1, 1-chome, Marunouchi, Chiyoda-ku, Tokyo 100, Japan).

Reagents All chemicals were of analytical-reagent grade. Freshly distilled diethyl ether was used in the extraction of reduction products.

Apparatus GLC was performed using a packed glass column (3 mm i.d., 2 m long). The stationary phase and column conditions were 5% Apiezon grease L with 5% KOH on 60—80 mesh Chromosorb W (acid-washed and dimethyldichlorosilane treated (AW, DMCS)) at 212 °C or 170—210 °C (5 °C/min): injection port temperature 250 °C with a nitrogen flow-rate of 50 ml/min. A gas chromatograph (Shimadzu GC-7AG) equipped with a hydrogen flame-ionization detector (HFID) was employed for this experiment. Retention times were measured *via* a

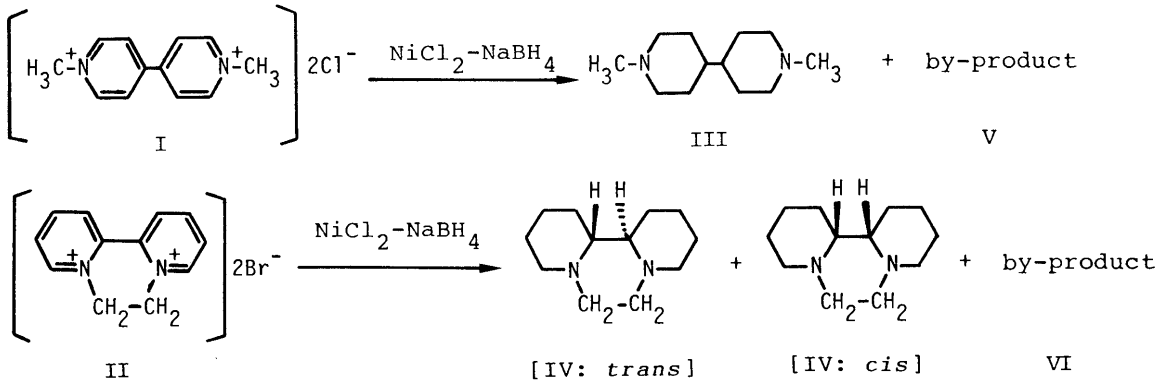

Chart 1. Reduction Process in $NiCl_2$–$NaBH_4$ Reduction of I and II

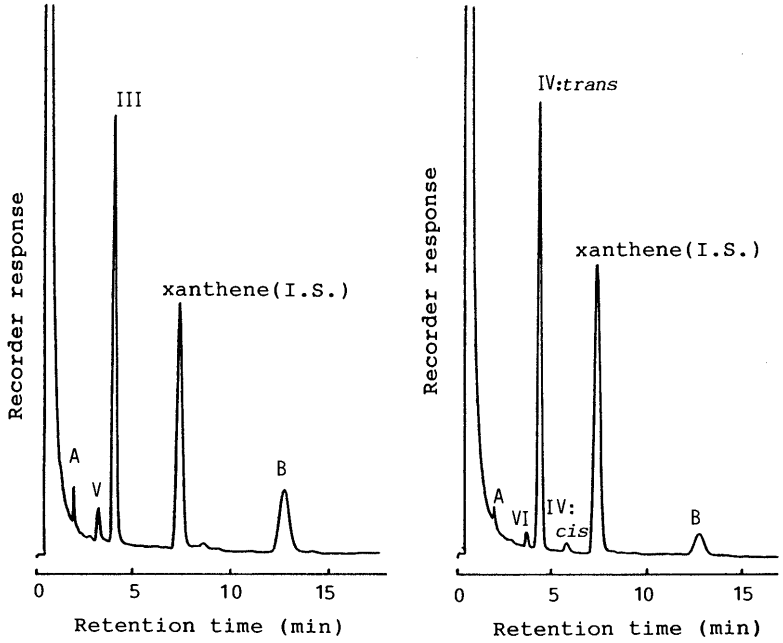

Fig. 1. Gas Chromatogram for Reduction Products Arising from I and II with Two-Step ($NaBH_4$ and $NiCl_2$–$NaBH_4$) Reduction

GLC conditions: column (glass), 5% Apiezon grease L plus 5% KOH 2 m × 3 mm i.d. Chromosorb W (AW, DMCS 60—80 mesh); column temp., 212 °C; inj. temp., 250 °C; carrier gas, N_2 50 ml/min; detection, HFID; attenuation, 16; range, 10. Side peaks A and B are reductants arising from $NaBH_4$ and $NiCl_2$ [*J. Chromatogr.*, **283**, 231 (1984)], but intensity of side peak B is not constant.

Shimadzu Chromatopac C-R2A integrator.

GLC-MS was conducted with a Shimadzu QP-1000 equipped with a packed glass column (3 mm i.d., 2 m long). The stationary phase and conditions were 5% Apiezon grease L with 5% KOH on 60—80 mesh Chromosorb W (AW, DMCS) at 212 °C or 170—210 °C (5 °C/min), injection port temperature 250 °C, separator temperature 250 °C, ion source temperature 250 °C, ion voltage 70 eV, ion current 60 μA and helium flow-rate 40 ml/min.

Preparation of I and II Reduction Products and Their Deuterium Analogues for GLC and GLC-MS Analysis To the aqueous solution (1 ml) containing 100 μg/ml of I or II was added 1.2 ml of 10% $NaBH_4$ solution; the mixture was then allowed to stand for 30 min at room temperature. Five hundred μl of 10% $NiCl_2$ solution was then added.[4] A black precipitate, nickel boride, was immediately formed with the evolution of hydrogen, which continued as the mixture was allowed to stand for 1 h at room temperature.

The deuterium analogues of the reduction products of I and II were prepared by use of sodium borodeuteride, anhydrous $NiCl_2$ and heavy water in a manner similar to the above.

To the reaction mixture were added 5 drops of a 50% sodium hydroxide aqueous solution, followed by extraction four times with 2 ml volumes of diethyl ether. The combined organic solvent layer was dried over anhydrous sodium sulfate, acidified with a few drops of trifluoroacetic acid (TFA)[5] and evaporated to dryness under reduced pressure.

Part of the above residue was dissolved in 50 μl of ethyl acetate containing 0.004% xanthene as an internal standard. To the ethyl acetate solution was added a small amount of anhydrous potassium carbonate. A 1 μl volume of the ethyl acetate solution was injected into the gas chromatograph or the gas chromatograph–mass spectrometer.

Preparation of TFA Derivatives of By-Products of I and II Another part of the above residue was dissolved in 200 μl of ethyl acetate, and 200 μl of trifluoroacetic anhydride was then added. The mixture was allowed to stand for 20 min at 55 °C, and evaporated to dryness under reduced pressure at a bath temperature of 40—50 °C.

The residue was dissolved in 50 μl of ethyl acetate containing 0.004% (or 0.04%) xanthene as an internal standard. A 1—2 μl volume of the ethyl acetate solution was injected into the gas chromatograph or gas chromatograph–mass spectrometer.

Relationship between Production of the By-Product of I and Amounts of $NaBH_4$ and $NiCl_2$ in a Given Volume of Water One-Step $NiCl_2$–$NaBH_4$ Reduction: To an aqueous solution (1 ml) containing 100 μg/ml of I was added 1.0 ml of 1%, 3% or 5% $NiCl_2$ solution. To the mixture was then added 1 ml of 10%, 15% or 20% $NaBH_4$ solution. The mixture was then allowed to stand for 30 min at room temperature. After the evolution of hydrogen ceased, 5 drops of a 50% sodium hydroxide aqueous solution were added. Subsequent operations were carried out in a manner similar to the above.

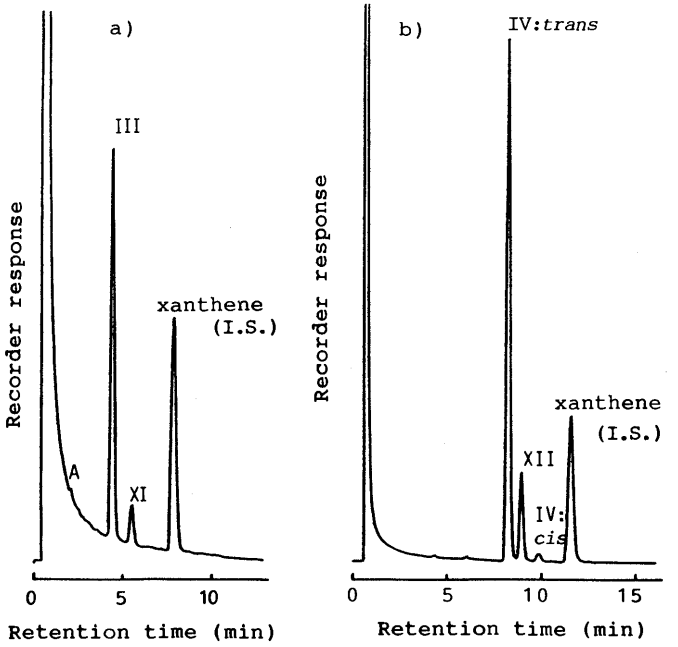

Fig. 2. Gas Chromatogram for III, IV and TFA Derivatives of V and VI Arising from I and II

GLC conditions: a) column temp. 212 °C, b) column temp. 170—210 °C (5 °C/min); attenuation, 16; range, 10^2; other GLC condition same as Fig. 1.

Two-Step $NaBH_4$ and $NiCl_2$–$NaBH_4$ Reduction: To an aqueous solution (1 ml) containing 100 μg/ml of I was added 1.0 ml of 10%, 15% or 20% $NaBH_4$ solution; the mixture was then allowed to stand for 30 min at room temperature; 1.0 ml of 1%, 3% or 5% $NiCl_2$ solution was then added. After the evolution of hydrogen ceased, 5 drops of a 50% sodium hydroxide aqueous solution were added. Subsequent operations were carried out in a manner similar to the above.

Attempts to Produce By-Products by $NaBH_4$–$NiCl_2$ Reduction of Perhydrogenated Products (1,1′-Dimethyl-4,4′-bipiperidine, *trans*-Perhydro-

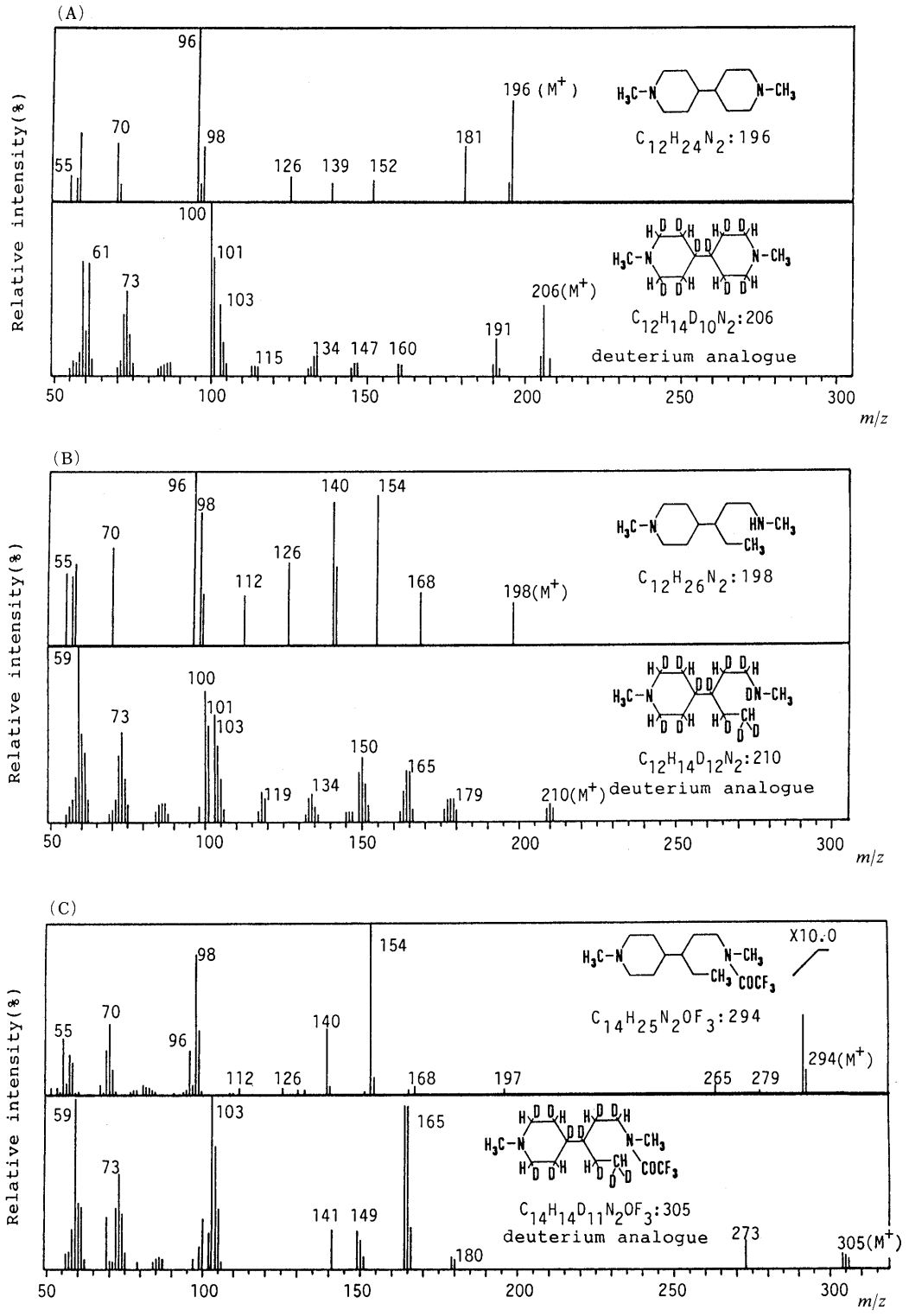

Fig. 3. Mass Spectra (EI) of Perhydrogenated Product III (A), By-Product V (B) and TFA Derivative of By-Product XI (C), and Their Deuterium Analogues of I

8a,10a-diazaphenanthrene) and Dienes(*N,N'*-dimethyl-1,1',2,2',3,3',6,6'-octahydro-4,4'-bipyridyl, *trans*-Octahydro-8a,10a-diazaphenanthrene) Arising from I and II 1,1'-Dimethyl-4,4'-bipiperidine·2HCl,[6] *N,N'*-dimethyl-1,1',2,2',3,3',6,6'-octahydro-4,4'-bipyridyl·2HCl prepared from the free bases[6,7] and *trans*-perhydro-8a,10a-diazaphenanthrene·2HBr,[8] *trans*-octahydro-8a,10a-diazaphenanthrene·2HCl,[8] prepared separately, were used as the starting materials in this experiment.

To an aqueous solution (1 ml) containing 100 μg/ml 1,1'-dimethyl-4,4'-bipiperidine, *trans*-perhydro-8a,10a-diazaphenanthrene *N,N'*-dimethyl-1,1',2,2',3,3',6,6'-octahydro-4,4'-bipyridyl or *trans*-octahydro-8a,10a-diazaphenanthrene was added 1.0 ml of 10% $NaBH_4$ solution. The mixture was then allowed to stand for 30 min at room temperature; 1.0 ml of 5% $NiCl_2$ solution was then added. After the evolution of hydrogen ceased, 5 drops of a 50% sodium hydroxide aqueous solution were added. Subsequent operations were carried out in a manner similar to the above.

Results and Discussion

The results of GLC and GLC-MS of III, IV, V, VI and TFA derivatives of V and VI arising from I and II are shown in Figs. 1, 2, 3 and 4.

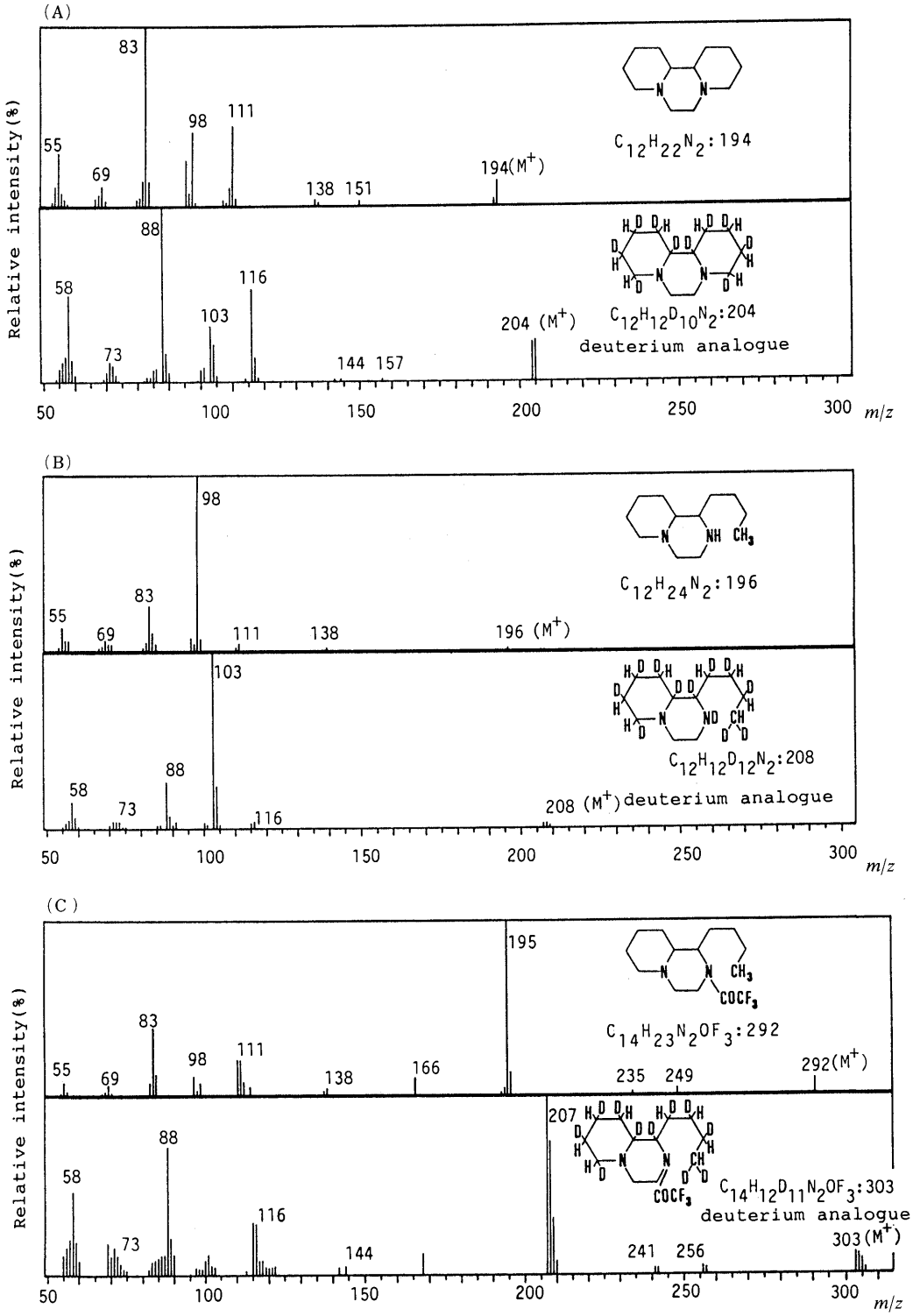

Fig. 4. Mass Spectra (EI) of Perhydrogenated Product IV (A), By-Product VI (B) and TFA Derivative of By-Product XII (C), and Their Deuterium Analogues of II

A slight amount of V or VI appears as a weak peak on the gas chromatogram. The mass numbers of parent ions of V (*m/z* 198) and VI (*m/z* 196) are two abundant portions of mass numbers larger than those of III (*m/z* 196) and IV (*m/z* 194).

It can therefore be presumed that a reductive cleavage occurs at the C–N or C–C bond in the pyridine ring of I and II. First, we examined whether trifluoro acetylation of V and VI proceeded. To this end, trifluoro acetylation of V or VI was conducted by warming the ethyl acetate with trifluoro acetic anhydride, and GLC was carried out for the obtained derivative. The peaks arising from V and VI had disappeared and new peaks appeared behind those arising from III or IV (*trans*). The peak movement was examined by GLC-MS.

The mass numbers *m/z* 294 (M^+ arising from V) and *m/z* 292 (M^+ arising from VI) are 96 abundance portions of mass number larger than those of by-products (V and VI)

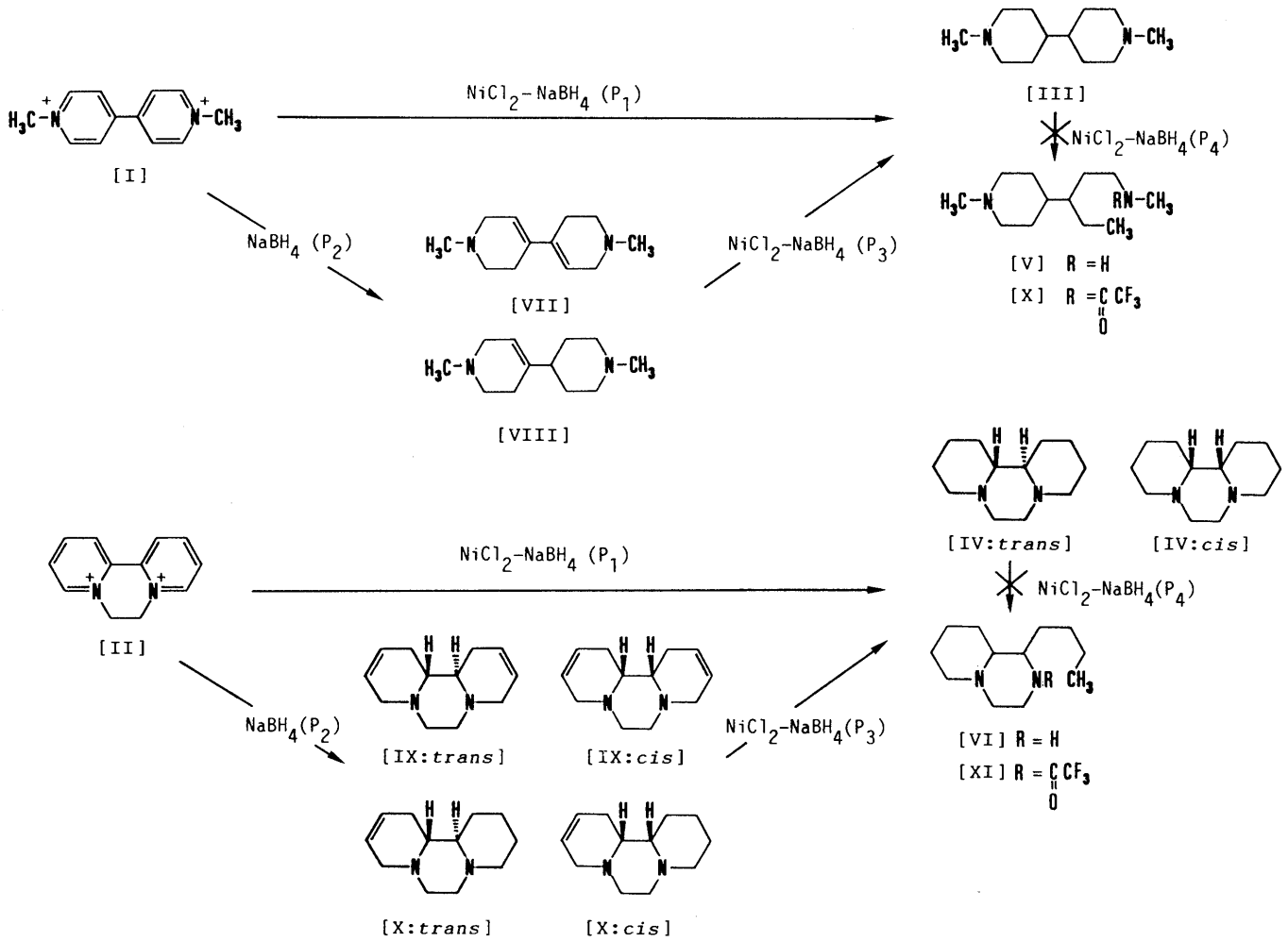

Chart 2. Side Reaction Process in Reduction Process with $NaBH_4$–$NiCl_2$ Reduction of I and II

of I and II. It is clear that TFA derivatives were formed from V and VI. Thus V and VI are secondary amines, *i.e.*, R_1R_2N–$COCF_3$ (R_1, R_2=alkyl) is derived from R_1R_2N–H. This indicates reductive cleavage at the C–N bond in the pyridine ring of I and II; and it negates the possibility of cleavage at the C–C bond in the pyridine ring.

Thus, the structural formulas of V and VI are as shown in Chart 2.

Further, reductive cleavage could occur through the complex with nickel and the intermediate [VII, VIII, IX and X] containing a double bond (see Chart 2; route P_1, P_2+P_3), because the cleavage of III and IV (*trans*) could not occur in $NiCl_2$–$NaBH_4$ reduction (see Chart 2; route P_4).

Detailed descriptions of fragmentations of derivatives of I and II are shown in Figs. 3 and 4.

In paraquat, mass numbers of the base peaks in the spectra of III and V are the same (*m/z* 96), but there are notable differences in the relative intensity of their fragments, especially in the *m/z* 98 to 198 region, as shown in Fig. 3.

A reasonable example of fragmentation was established by comparing the mass spectra of reduction products (III, V) and the TFA derivative of V (XI) with those of their deuterium analogues. An example is shown in Chart 3.

In the fragmentation of III, a significant amount of the parent ion *m/z* 196 (M^+) and ion *m/z* 181 ($=M^+-CH_3$) are detected on the mass spectrum. But intensities of fragment ions *m/z* 152 [$=181-(CH_2+N, H)$], *m/z* 139 ($=152-CH$), *m/z* 126 ($=139-CH$) and *m/z* 98 ($=126-2CH_2$ or $M^+/2$) are weaker than those of fragment ions *m/z* 168 [$=198-(NH+CH_3)$], *m/z* 154 ($=168-CH_2$), *m/z* 140 ($=154-CH_2$), *m/z* 126 ($=140-CH_2$), *m/z* 112 ($=126-CH_2$) and *m/z* 98 ($=112-CH_2$) of V in the relative intensity (see Chart 3; route A, B, C_1+C_2). It is considered that the base peak *m/z* 96 arises from a fragment ion *m/z* 98 (see Chart 3; route G_1).

In addition, it is suggested that there are two kinds of fragment ions *m/z* 96 in route G_1. One *m/z* 96 has 5 deuterium atoms, another has 4 deuterium atoms. These fragment ions further dissociated successively to fragment ion *m/z* 55 (see Chart 3; route G_2 and G_3).

On the other hand, a portion of fragment ion *m/z* 98 further dissociated successively to fragment ions *m/z* 70 ($=98-C_2H_4$) and *m/z* 55 ($=70-CH_3$) (see Chart 3; route F). According to R. A. Saunders' report[9] on methylpiperidines, fragment ion *m/z* 70 is presumed to be a five-membered ring of  .

That is to say, there are notable differences in the relative intensities of fragmentation between III and V, and structural differences exist between the two products.

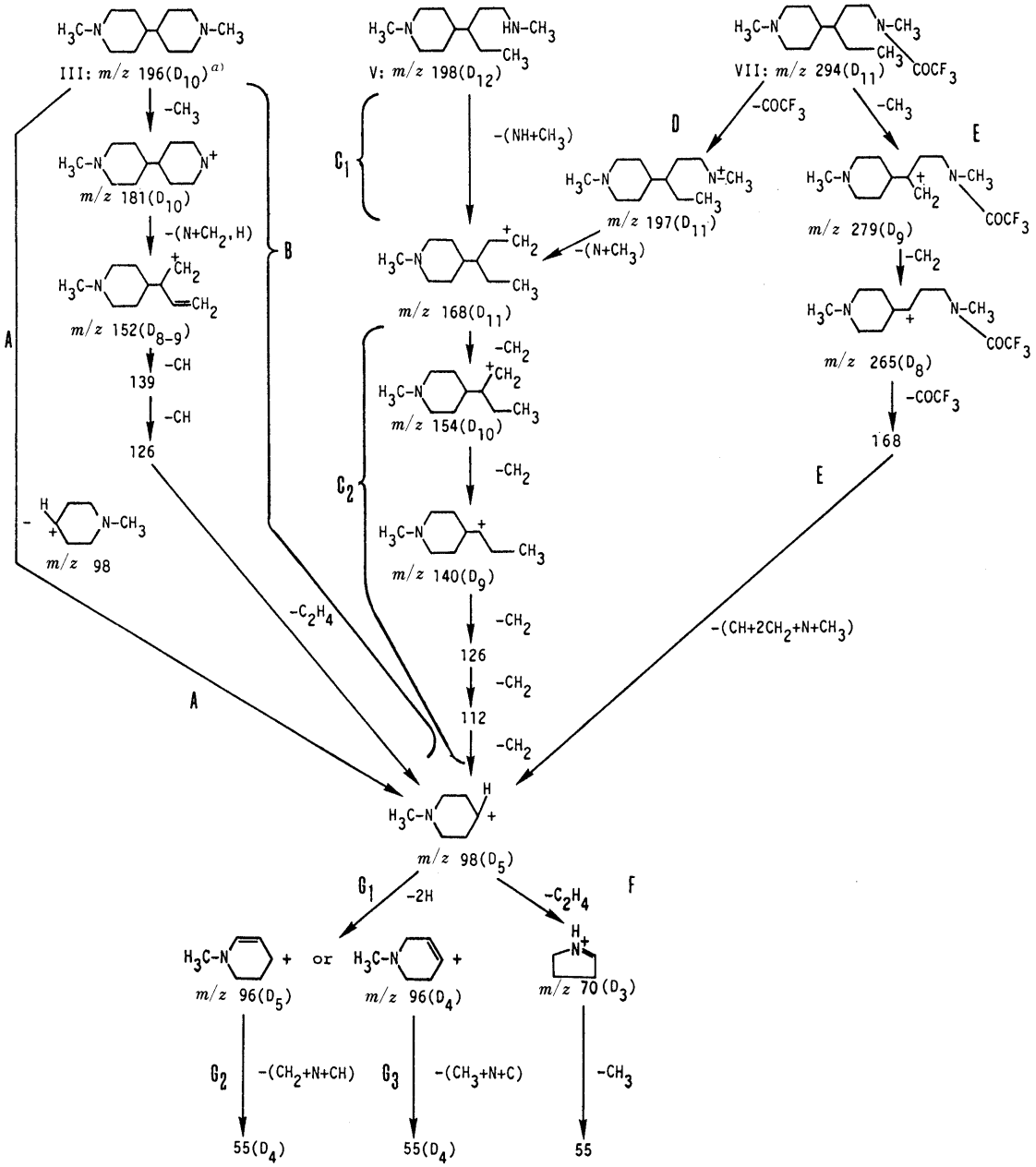

Chart 3. Dissociation Routes of Mass Fragments of Perhydrogenated Product, By-Product and TFA Derivative of By-Product of I

a) Number of residual deuterium atoms assigned from fragment of deuterium analogue.

It is suggested, therefore, that production of V results from reductive cleavage on one side of each pyridine ring of I by a side reaction in this reduction system.

There are two dissociation routes for the TFA derivative(VII) of the by-product of I. Dissociation proceeds successively to *m/z* 294 (M^+), to *m/z* 197 ($=294-COCF_3$), then to *m/z* 168 [$=197-(N+CH_3)$]; or to *m/z* 294 (M^+), to *m/z* 279 ($=294-CH_3$), to *m/z* 265 ($=279-CH_2$), to *m/z* 168 ($=265-COCF_3$) then finally to *m/z* 98 [$=168-(HC+2CH_2+N+CH_3)$] (see Chart 3; route D, E).

Dissociation then proceeds from *m/z* 168 to route C_2+F, $C_2+G_1+G_2$ or $C_2+G_1+G_3$.

In addition, it is suggested that there are two kinds of fragment ion *m/z* 168 on two routes (VII+D+C_2 and VII+E) for the TFA derivative of V. This is because there are 11 deuterium atoms in fragment ion *m/z* 168 on route VII+D+C_2, but only 8 deuterium atoms in pre-fragment ion *m/z* 265 on *m/z* 168 of VII+E.

In diquat, there is a difference in the mass number of base peaks between the perhydrogenated product(IV) and by-product(VI), as shown in Chart 4.

m/z 194 of IV is shown to dissociate through two routes.

On one of the routes, the base peak *m/z* 83 is formed by dissociation from the parent ion *m/z* 194 (M^+) to *m/z* 151 [$=194-(3CH_2, H)$], then to *m/z* 83 [$=151-(CH_2+CH_2+N+C=CH_2)$] (see Chart 4; route H).

Another route proceeds from the parent ion *m/z* 194 (M^+) to *m/z* 138 [$=194(M^+)-4CH_2$], then to *m/z* 83 [$=138-(HCN, CH, CH_3)$] (see Chart 4; route I+L_1+L_2+L_3).

In contrast, VI gives the base peak *m/z* 98. Thus two routes are presumed, one proceeding from the parent ion *m/z* 196 (M^+) to *m/z* 138 [$=196(M^+)-(CH_3+3CH_2, H)$], *m/z* 111 ($=138-HCN$), base peak *m/z* 98 ($=111-CH$)

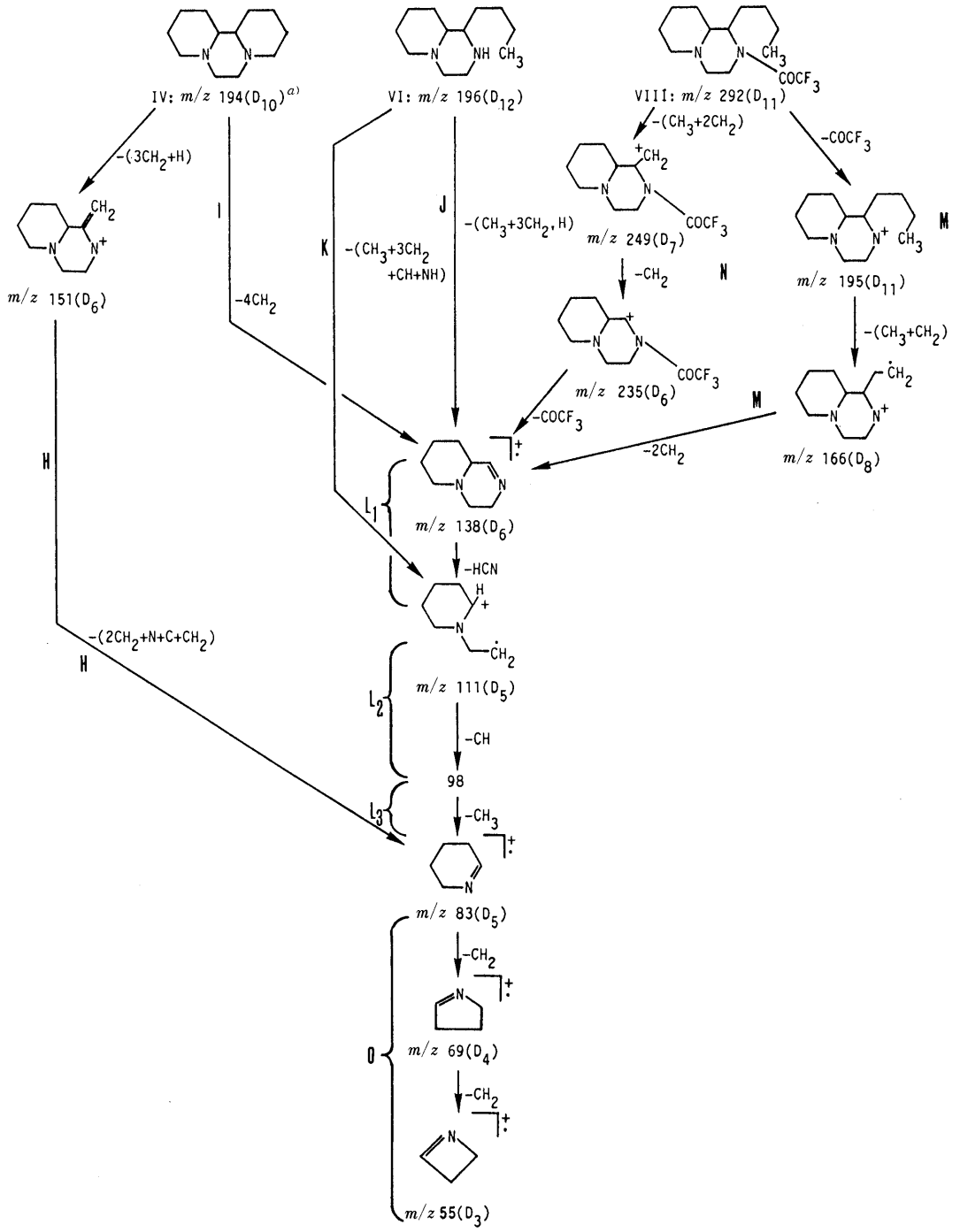

Chart 4. Dissociation Routes of Mass Fragments of Perhydrogenated Product, By-Product and TFA Derivative of By-Product of II

a) Number of residual deuterium atoms assigned from fragment of deuterium analogue.

and *m/z* 83 (=98−CH_3).

Another route is shown to dissociate directly from parent ion *m/z* 196 (M^+) to base peak *m/z* 98 [=196 (M^+)−(CH_3+3CH_2+CH+NH)] (see Chart 4; route K+L_2).

Consequently, from the fragmentation of IV, route H is a main dissociation and route I+L_1+L_2 is a side dissociation.

As mentioned above, there are some notable differences in relative intensities of fragmentation between IV and VI, and there are structural differences between IV and VI.

In TFA derivative(VIII) of by-product(VI) of II, the dissociation proceeds in a manner similar to that of VI along *m/z* 138 (=235−$COCF_3$), namely, to *m/z* 292 (M^+), to *m/z* 195 (=292−$COCF_3$), to *m/z* 166 [=195−(CH_3+CH_2)], then to *m/z* 138 (=166−2CH_2), or, to *m/z* 292 (M^+), to *m/z* 249 [=292−(CH_3+2CH_2)], then to *m/z* 235 (=249−CH_2) (see Chart 4; route M, N). The dissociation proceeds along route L_1+L_2+L_3+O through *m/z* 138.

These results are summarized below. V and VI result from reductive cleavage of their pyridine rings to pass through III and IV, when I or II is reduced with the $NaBH_4$–$NiCl_2$ reduction system. V and VI appear as weak peaks on the gas chromatogram. That is to say, these

TABLE I. Integral Ratio of By-Product of Perhydrogenated Product of Paraquat in One-Step Reduction

$NiCl_2$ (aqueous solution; %)	$NaBH_4$ (aqueous solution; %)		
	10	15	20
1	1 : 0.06[a]	1 : 0.04[a]	1 : 0.02[a]
3	1 : 0.04[a]	1 : 0.04[a]	1 : 0.04[a]
5	1 : 0.03[a]	1 : 0.03[a]	1 : 0.03[a]

a) Integral ratio of perhydrogenated paraquat (III): by-product (V).

TABLE II. Integral Ratio of By-Product of Perhydrogenated Product of Paraquat in Two-Step Reduction

$NiCl_2$ (aqueous solution; %)	$NaBH_4$ (aqueous solution; %)		
	10	15	20
1	1 : 0.14[a]	1 : 0.10[a]	1 : 0.08[a]
3	1 : 0.16[a]	1 : 0.14[a]	1 : 0.09[a]
5	1 : 0.17[a]	1 : 0.16[a]	1 : 0.10[a]

a) Integral ratio of perhydrogenated paraquat (III): by-product (V).

V and VI are presumably *p*-(*N*-methylaminopent-3′-yl)-*N*-methylpiperidine (for V) and 1-butyl-2-aza-perhydroquinolizine (for IV and VI).

In the experiment using 100 μg of I, on the relationship between the production of the by-product of I and the amounts of $NaBH_4$ and $NiCl_2$ in a volume of water, the production of the by-product increased in two-step ($NaBH_4$ and $NiCl_2$–$NaBH_4$) reduction rather than one-step ($NiCl_2$–$NaBH_4$) (see Tables I and II).

In this two-step reduction system, the reductive cleavage reaction is promoted when the $NaBH_4$ aqueous solution concentration is low and the $NiCl_2$ aqueous solution concentration is high.

The reaction, on the contrary, is inhibited when $NaBH_4$ aqueous solution concentration is high and $NiCl_2$ aqueous solution concentration is low.

Based on these results, it is expected that this two-step reduction system will be used for a reductive cleavage reaction at the C–N bond of other cyclic compounds containing nitrogen atoms and double bond, through the optimization of the amounts of reductants $NaBH_4$ and $NiCl_2$.

References and Notes

1) This work was presented in part at The Japanese–United States Congress of Pharmaceutical Sciences, Honolulu, Hawaii, Dec. 1987, Poster Abstract, S 30.
2) L. A. Summers, "The Bipyridinium Herbicides," Academic Press London, 1980; A. Pasi, "The Toxicology of Paraquat, Diquat and Morphamquat," Hans Huber Publishers, Bern, 1978; "Annual Case Reports of Drug and Toxic Poisoning in Japan," No. 30, National Research Institute of Police Science, Tokyo, 1987; *ibid.*, No. 31, 1988; C. M. Bullivant, *Br. Med. J.*, **1966**, 1272; *idem*, *ibid.*, **1967**, 721; E. D. Carson, *J. Forens. Sci. Soc.*, **12**, 437 (1972).
3) S. Kawase, S. Kanno, and S. Ukai, *J. Chromatogr.*, **283**, 231 (1984).
4) When diquat is reduced by one-step reduction of using $NiCl_2$ and $NaBH_4$, *trans* and *cis* stereo isomers as perhydrogenated product are obtained in the integral ratio of 1 : 0.36, respectively. But it has become feasible to simplify to single isomer (*trans* isomer) with a two-step reduction using $NaBH_4$ and $NiCl_2$ in this order. (This work was presented at the 105th Annual Meeting of the Pharmaceutical Society of Japan).
5) The free basic compound has been concentrated with acetic acid, but TFA is superior to acetic acid for prevention of loss due to volatility of reduction products by evaporation of the organic solvent used for the extraction. (This work was presented at the 106th Annual Meeting of the Pharmaceutical Society of Japan).
6) S. Ukai, K. Hirose, and S. Kawase, *Eisei Kagaku*, **23**, 32 (1977).
7) S. Ukai, K. Hirose, and S. Kawase, *Eisei Kagaku*, **19**, 281 (1973).
8) S. Ukai, S. Kawase, S. Kanno, T. Kiho, M. Kido, and I. Miura, *Heterocycles*, **22**, 803 (1984).
9) R. A. Saunders and A. E. Williams, "Advances in Mass Spectrometry" Vol. 3, ed. by W. L. Mead, The Elsevier Publishing Company, Amsterdam, 1966, pp. 681—699.

Detection and Identification of Loline and Its Analogues in Horse Urine[1)]

Akira TAKEDA,*[,a] Etsuko SUZUKI,[a] Katsutoshi KAMEI[a] and Hisao NAKATA[b]

Laboratory of Racing Chemistry,[a] 4–37–6, Kamiyoga, Setagaya-ku, Tokyo 158, Japan and Faculty of Pedagogy, Aichi Kyoiku University,[b] 1, Hirosawa, Igaya-cho, Kariya-shi, Aichi 448, Japan. *Received September 27, 1990*

Several kinds of loline-type alkaloids, norloline, loline, *N*-acetylnorloline, *N*-acetylloline, *N*-formylnorloline, *N*-formylloline and *N*-methylloline were detected in the urine of race-horses. Furthermore, a new compound of the alkaloids, *N*-senecioylnorloline, was also found and identified. These compounds were mainly identified by means of gas chromatography–mass spectrometry (GC-MS) and gas chromatography–fourier transform–infrared spectrometry (GC-FT-IR). A certain plant of Gramineae containing four kinds of loline-type alkaloids was found in a bale of hay used for the horse forage. The taxonomic feature of the plant was different from known plants containing loline-type alkaloids. The common fragmentation of loline-type alkaloids under electron ionization was briefly discussed.

Keywords *Lolium* alkaloid; pyrrolizidine alkaloid; loline; *N*-senecioylnorloline; mass spectrum; infrared spectrum; GC-MS; fragmentation; horse urine

Introduction

Loline-type alkaloids are classified into one type of group of pyrrolizidine alkaloids whose common feature is a unique oxygen bridge. Loline was first isolated from the seeds of *Lolium cuneatum* NEVSKI, Gramineae in 1955.[2a)] Several kinds of loline alkaloids have been isolated and identified from *Lolium cuneatum*[2b–d)]; from tall fescue (*Festuca arundinacea* SCHREB., Gramineae)[3)]; and from *Adenocarpus decorticans* BOISS., Legminosae.[4)] As shown in Table I, twelve kinds of loline analogues, in all, have so far been isolated and identified from three genera of the families described in the above literature.

Tall fescue is widely grown in the United States as a highly adaptable forage for stock farming in poor soil. On the other hand, fescue foot and abdominal fat necrosis have been found in cattle grazing on tall fescue.[5)] Although several reports have showed the relationship of fungal endophyte infection frequency and loline analogues concentration,[6)] the causative substance of toxic tall fescue in cattle is still unclear. Recently, Yates *et al.*[7)] reported on the gas chromatographic analysis of loline analogues in endophyte-infected tall fescue. However, no report on the detection of these alkaloids in biological fluids has been published.

TABLE I. Chemical Structure of Loline-Type Alkaloids

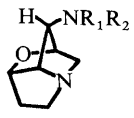

Compound	Formula	M.W.	R_1	R_2	Plant
Norloline	$C_7H_{12}N_2O$	140	H	H	*L., A.*
Loline	$C_8H_{14}N_2O$	154	H	CH_3	*L., F.*
N-Methylloline	$C_9H_{16}N_2O$	168	CH_3	CH_3	*L., F.*
N-Formylnorloline	$C_8H_{12}N_2O_2$	168	CHO	H	*L.*
N-Formylloline	$C_9H_{14}N_2O_2$	182	CHO	CH_3	*L., F.*
N-Acetylnorloline	$C_9H_{14}N_2O_2$	182	$COCH_3$	H	*L., F.*
N-Acetylloline	$C_{10}H_{16}N_2O_2$	196	$COCH_3$	CH_3	*L., F.*
N-Acetylloline-*N*-oxide	$C_{10}H_{16}N_2O_3$	212	$COCH_3$	CH_3	*L.*
N-Propionylnorloline (Decorticasine)	$C_{10}H_{16}N_2O_2$	196	$COCH_2CH_3$	H	*A.*
N-Butyrylnorloline	$C_{11}H_{18}N_2O_2$	210	$CO(CH_2)_2CH_3$	H	*A.*
N-Isobutyrylnorloline	$C_{11}H_{18}N_2O_2$	210	$COCH(CH_3)_2$	H	*A.*
N-Isovaleroylnorloline	$C_{12}H_{20}N_2O_2$	224	$COCH_2CH(CH_3)_2$	H	*A.*

M.W.: molecular weight. *L.*, *Lolium cuneatum* NEVSKI; *F.*, *Festuca arundinacea* SCHREB.; *A.*, *Adenocarpus decorticans* BOISS.

In our study, six kinds of known loline-type alkaloids and a new compound which was estimated as *N*-senecioylnorloline were detected in the urine of race-horses. Further, some plants used as forage were also analyzed for inquiring into the cause of loline-type alkaloids being detected in horse urine. This paper deals with the detection and identification of loline-type alkaloids from horse urine and from plants used for horse feed. Also, the common fragmentation of loline-type alkaloids under electron ionization (EI) with a linked scan at constant B/E and B^2/E and elemental composition data will be briefly discussed.

Experimental

Materials Authentic norloline, loline, *N*-methylloline, *N*-formylloline and *N*-acetylloline were a generous gift from Dr. R. J. Petroski, United States Department of Agriculture. Horse urine samples after our routine dope testing were used. Plant materials were obtained through the courtesy of the Japan Racing Association.

Phenyl senecioate was synthesized from phenol with senecioyl chloride which was prepared from senecioic acid and thionyl chloride by the usual manner. Colorless oily liquid, $bp_{2.5}$ 83 °C. EI-MS *m/z* (rel. int. %): 176 ($M^{+\cdot}$, 11), 94 (4), 83 (100), 77 (2), 65 (4), 55 (26).

N-Senecioylnorloline was derived from norloline with phenyl senecioate using a modified method referred to as a synthetic method of *N*-acetylnorloline by Petroski *et al.*[8)] The compound prepared, EI-MS *m/z* (rel. int. %): 222 ($M^{+\cdot}$, 6), 193 (10), 167 (5), 154 (2), 139 (3), 127 (6), 123 (22), 110 (4), 99 (9), 95 (35), 83 (17), 82 (100), 80 (11), 69 (26), 55 (19).

Other chemicals and reagents were of analytical reagent grade.

Gas Chromatography–Mass Spectrometry (GC-MS) A model AX505H mass spectrometer (JEOL Co., Ltd., Tokyo, Japan) interfaced to a 5890A gas chromatograph (Hewlett Packard, PA, U.S.A.) and a JMA-DA5500 data processing system (JEOL Co., Ltd.) was employed. A bonded-phase fused-silica capillary column (DB-17, 15 m × 0.53 mm i.d., Megabore column; J&W Scientific Inc., CA, U.S.A.) was used. Direct injection was made at an injection temperature of 230 °C; the column was programmed from 130 to 280 °C at 5 °C/min. Helium was used as a carrier gas at the flow rate of 5 ml/min. Isobutane was used as a reagent gas for the chemical ionization (CI). The EI and CI mass spectra were measured at 70 and 200 eV, respectively. Other conditions were: ion accelerating voltage at 3 kV, ion source temperature at 220 °C, and the mass range of total ion chromatogram (TIC) at *m/z* 40—400 for EI and *m/z* 100—400 for CI. The linked scanning data at constant B/E and constant B^2/E were recorded on a model SX102 mass spectrometer (JEOL Co., Ltd.) interfaced to a 5890A gas chromatograph (Hewlett Packard) and JMA-DA6000 data analysis system (JEOL Co., Ltd.).

Gas Chromatography–Fourier Transform–Infrared Spectrometry (GC-FT-IR) A model 5890A gas chromatograph (Hewlett Packard) equipped with a 5965A infrared detector (IRD, Hewlett Packard) was employed. A bonded-phase fused-silica capillary column (DB-17, 30 m × 0.25 mm i.d., 0.25 μm film thickness; J&W Scientific Inc.) was used. A splitless injection

using dry toluene as a solvent was made at a column temperature of 100 °C; 30 s after injection, the split valve was opened and the column oven was programmed up to 280 °C at 10 °C/min. The final temperature of 280 °C was held for 3 min. The IR spectra were recorded at a range between 4000—750 cm^{-1}. The temperature of IRD flow cell and transfer line was 280 °C. Helium was used as the carrier gas at a column head pressure of 100 kPa.

Sample Preparation Twenty ml of horse urine were extracted with 80 ml of chloroform at pH 12 by mechanical shaking. After evaporation of the chloroform layer, the residue was dissolved in 20 ml of 0.125 M sulfuric acid and shaken two times with 40 ml of chloroform for 5 min. The aqueous layer was extracted with 50 ml of chloroform at pH 12 for 5 min. The chloroform layer was dried over anhydrous Na_2SO_4 and evaporated to dryness under reduced pressure. The residual material was applied to GC-MS and GC-FT-IR analyses after being dissolved in dry toluene.

The ground plant (10 g) was wet with 20 ml of 10% (w/v) ammonium hydroxide, and homogenized for 10 min with 150 ml of chloroform. After centrifuging at 8500 rpm for 10 min, the chloroform layer was collected and concentrated to *ca.* 10 ml of the volume under reduced pressure. Then 15 ml of 0.125 M sulfuric acid was added and shaken two times for 5 min. This aqueous layer was extracted three times by mechanically shaking with 30 ml of chloroform at pH 12 for 5 min. The chloroform layer was dried over anhydrous Na_2SO_4 and evaporated to dryness under reduced pressure. The resulting residue was dissolved in dry toluene, then applied to GC-MS analyses.

Results and Discussion

Identification of Loline-Type Alkaloids in Horse Urine

During the screening of equine body fluids for the doping control of race-horses, some substances different from drugs and related compounds are sometimes detected. Among them, the substances concerned in this paper were initially detected in a routine mass chromatographic screening[9] as unusual peaks on the ion trace of *m/z* 82. The same cases were found concentrated especially in the winter of 1984, and in the urine samples from race-courses located in a certain region. To identify the compounds corresponding to the peaks, capillary GC-MS and GC-FT-IR analyses were performed.

Figure 1 shows the TIC of urine extracts containing the substances. The chromatogram was classified into two typical patterns. In most of the cases, the substances corresponding to peaks 1 to 6 were detected simultaneously from each urine samples (Fig. 1(a)). In rare cases, the substance corresponding to peak 7 was detected alone (Fig. 1(b)). This result suggested the presence of at least two different plants related to the compounds found in the horse urine. At first we tried to identify the compounds corresponding to peaks 1 to 6. As shown in Fig. 2, the mass spectral pattern of their major fragment ions was similar to each other. The molecular weights were indicated as 154 (1), 168 (2), 168 (3), 182 (4), 182 (5) and 196 (6), respectively, by CI-MS measurement. The elemental composition data of each molecular ion, except for peak 3, were confirmed to be $C_8H_{14}N_2O$ (1), $C_9H_{16}N_2O$ (2), $C_9H_{14}N_2O_2$ (4), $C_9H_{14}N_2O_2$ (5) and $C_{10}H_{16}N_2O_2$ (6), respectively, by the accurate mass measurement (resolution: *ca.* 7000). It was supposed that the characteristic ions, *m/z* 69, 82 and 95, common in the EI spectrum of each substance originated from a pyrrolizidine ring.[10]

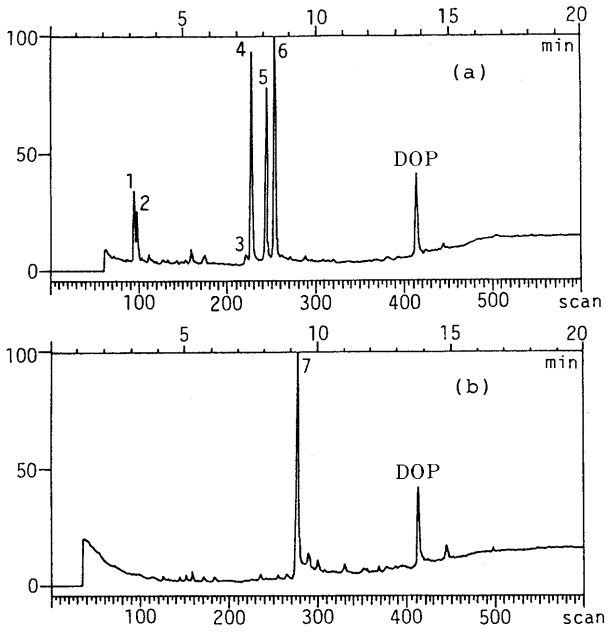

Fig. 1. TIC of Loline-Type Alkaloids Detected in Horse Urine
DOP, dioctylphthalate.

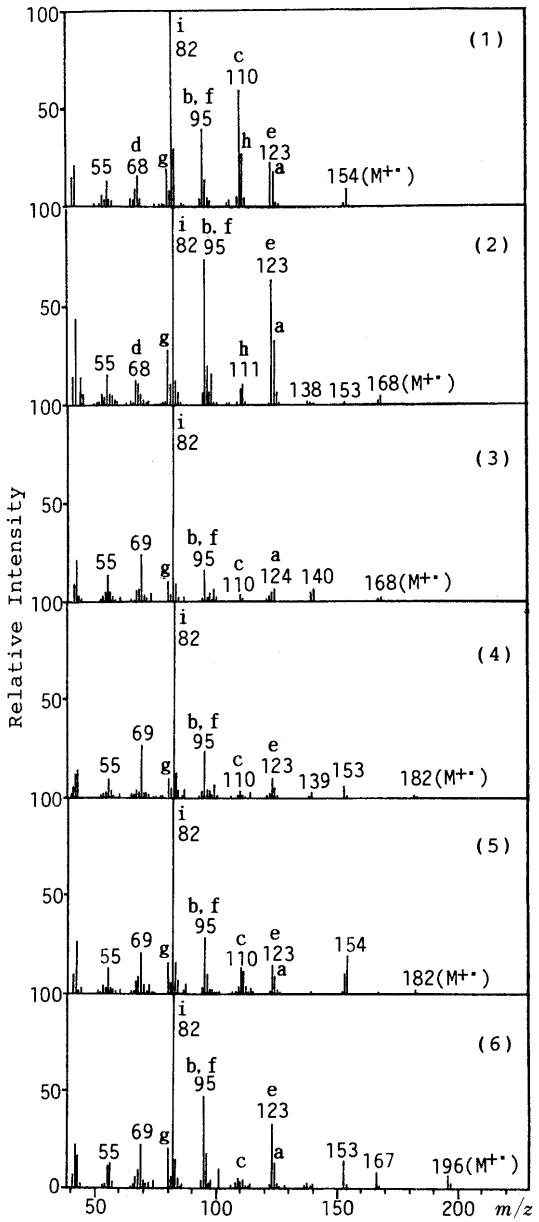

Fig. 2. Mass Spectra of Loline-Type Alkaloids Detected in Horse Urine
Each number of spectra corresponds to the numbers in Fig. 1.

From these data, the most likely substances corresponding to these peaks were estimated to be loline and its related compounds, a small group of pyrrolizidine alkaloids whose common feature is a unique oxygen bridge. To substantiate these findings, the mass and IR spectra were compared with those of the authentic compounds and/or those in the literature. The retention time and EI mass spectral data corresponding to peaks 1, 2, 5 and 6 were identical with those of the authentic compounds of loline, *N*-methylloline, *N*-formylloline and *N*-acetylloline, respectively. The substances corresponding to peaks 3 and 4 were identical with *N*-formylnorloline and *N*-acetylnorloline, respectively, on the mass and IR spectral data.[2c,d,11a]

Common Fragmentation of Loline Analogues Although mass spectra of loline alkaloids under EI were reported,[11] a detailed examination of the fragmentation has not been performed in the literature. The elemental composition data of the prominent ions of loline are shown in Table II. All of the data are consistent with the observed mass within experimental error.

The linked scanning data at constant B/E confirmed the fragmentation of the molecular ion ($M^{+\cdot}$) to give daughter ions at m/z 124 (loss of $\cdot NHCH_3$), 123 (loss of NH_2CH_3), 111 (loss of C_2H_5N) and 110 (loss of $\cdot CH_2NHCH_3$). The constant B/E linked scanning spectra of the ions at m/z 124 and 123 are shown in Fig. 3. Both of these two ions fragment to the ions at m/z 95 as the major pathway. The ion at m/z 123 was observed with low intensity on the B/E constant linked scan spectrum from m/z 124. This result suggests the ions at m/z 95 are formed from each of the ions at m/z 123 and 124. Moreover, the linked scanning data at constant B^2/E from the ion at m/z 95 supported this fragmentation pathway (Fig. 4). The ion at m/z 95 further loses a CH_3 radical to give an ion at m/z 80. The base peak at m/z 82 is formed from the ion at m/z 111 by the loss of a CHO radical. The intermediate ion at m/z 110 further decomposes into the ion at m/z 68 with the loss of CH_2CO molecule.

From data of the elemental composition and of the linked

TABLE II. Elemental Composition of Prominent Ions of Loline

Elemental composition	Accurate mass	
	Observed	Calcd.
C_4H_6N	68.0496	68.0500
C_4H_7N	69.0571	69.0579
C_5H_6N	80.0517	80.0500
C_5H_8N	82.0658	82.0657
C_6H_9N	95.0724	95.0735
C_6H_8NO	110.0604	110.0606
C_6H_9NO	111.0701	111.0684
C_7H_9NO	123.0682	123.0684
$C_7H_{10}NO$	124.0772	124.0762
$C_8H_{14}N_2O$	154.1091	154.1106

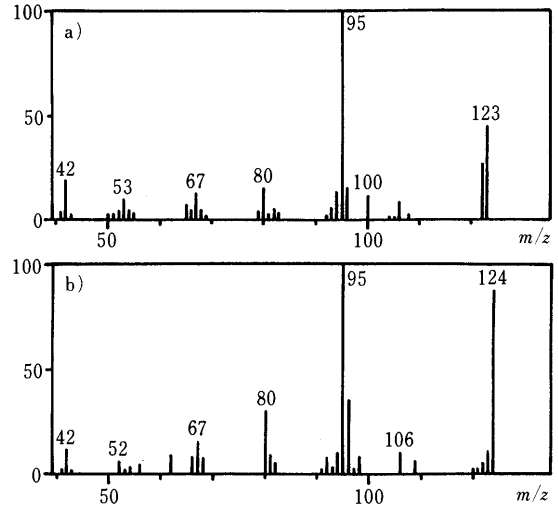

Fig. 3. Linked Scanning Data of Loline at Constant B/E
a) B/E from m/z 123. *b*) B/E from m/z 124.

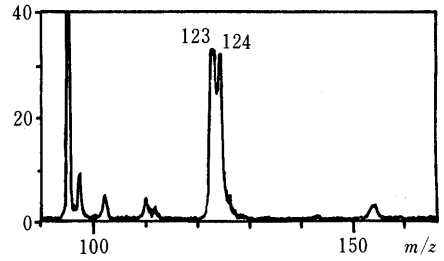

Fig. 4 Linked Scanning Data of Loline at Constant B^2/E from m/z 95

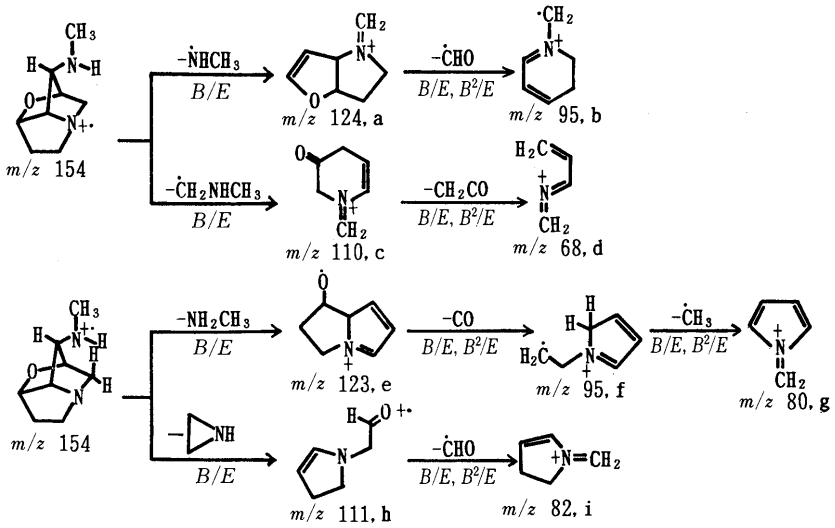

Chart 1

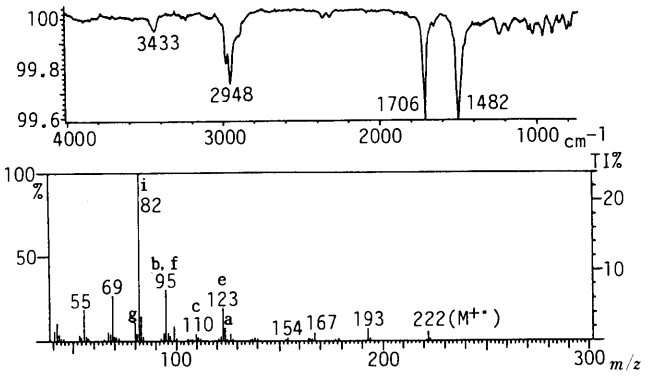

Fig. 5. IR and Mass Spectra of a Compound Corresponding to Peak 7

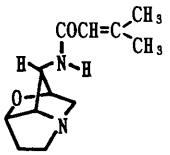

Fig. 6. *N*-Senecioylnorloline

Fig. 7. Plant Containing Loline-Type Alkaloids

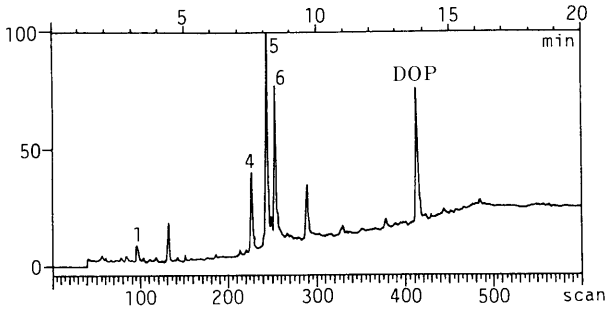

Fig. 8. TIC of Extracts from a Plant

DOP, dioctylphthalate. Each number of peaks corresponds to the numbers in Fig. 1.

scan at constant B/E and/or constant B^2/E, we considered the fragmentation pathway of loline as shown in Chart 1. We tentatively assumed two molecular ionic species by removing one electron from the lone pair of electrons either at N-4 or N-10. Each of the ions marked on the mass spectra of loline analogues in the figures corresponds to the ion marked in Chart 1. It seems that the fragmentation pathway is to be useful for the structural analysis of loline analogues.

Structure of a New Compound of Loline-Type Alkaloid The mass and IR spectra corresponding to peak 7 also gave a similar pattern to other loline-type alkaloids. However, no compound having a molecular weight of 222 among the loline-type alkaloids has been reported. The mass and IR spectra of this compound are shown in Fig. 5. The IR spectrum showed absorption peaks due to amide (NHCO, at 1482 cm^{-1}) and amino (NH, broad band at 3433 cm^{-1}) groups. This result suggested a *N*-acylnorloline structure. The elemental composition of $M^{+\cdot}$ and m/z 193 ions were confirmed to be $C_{12}H_{18}N_2O_2$ and $C_{10}H_{13}N_2O_2$, respectively. From these results, we tried to compare the mass spectral data of norloline-type compounds which were attached with naturally occurring five-carbon enoic acids, senecioic acid, tiglic acid and others. The EI and CI mass spectral data and the retention time corresponding to peak 7 was identical with those obtained from synthetic *N*-senecioylnorloline, a new compound of the loline group whose chemical structure was shown in Fig. 6. However, it is not yet clear whether the compound is a new member of naturally occurring lolines or a urinary metabolite of another compound.

Identification of Loline Alkaloids in a Plant Several kinds of plants contained in forage were examined for inquiring into the cause of loline-type alkaloids being detected in the urine of race-horses. We finally tried to focus on hay because small amounts of loline-type alkaloids were found in a chop of hay which was used as forage at the stable concerned. From the bale of hay produced in Hokkaido, each plant was classified according to kinds and analyzed. A small quantity of a certain plant of Gramineae shown in Fig. 7 existed in pasturage comprised of timothy (*Phleum pratense* L.) and orchard grass (*Dactylis glomerata* L.). It was proved that the plant contained much loline-type alkaloids. A typical TIC of the plant extracts by GC-MS is shown in Fig. 8. The retention time and mass spectral data corresponding to peaks 1, 4, 5 and 6 were identical with those of loline, *N*-acetylnorloline, *N*-formylloline and *N*-acetylloline detected from the urine extracts of race-horses (see Figs. 1 and 2). Therefore, it was concluded that the presence of this plant in hay is one of the causes of lolines being detected in horse urine. The taxonomic feature of this plant (Fig. 7) was different from known plants of Gramineae (*Lolium* and *Festuca*) containing loline-type alkaloids. This plant of Gramineae is grown not as horse forage but as weeds on pasture. The taxonomic identification of the plant is under investigation.

We recently found some other loline-type alkaloids in horse urine besides the alkaloids described in this paper, but the identification and structural analysis of them have not been completed. This study will be continued.

Acknowledgments We gratefully acknowledge Dr. R. J. Petroski, United States Department of Agriculture, for his helpful suggestions and kind supply of the authentic compounds. We are also grateful to the late Mr. S. Araki and Mr. Y. Asai, Japan Racing Association, for providing baits and hay. Moreover, thanks are to Mr. K. Nojima, JEOL Co., Ltd.

for linked scanning MS measurements, and Ms. A. Shimizu, Yokogawa Electric Corporation, for GC-FT-IR measurements.

References and Notes

1) Part of this work was presented at the 109th Annual Meeting of the Pharmaceutical Society of Japan, Nagoya, April 1989 and the Annual Meeting of the Mass Spectroscopy Society of Japan, Osaka, May 1990.
2) *a*) S. Yu. Yunusov and S. T. Akramov, *J. Gen. Chem. U.S.S.R.*, **25**, 1765 (1955); *b*) *Idem*, *ibid.*, **30**, 699 (1960); *c*) É. Kh. Batirov, S. A. Khamidkhodzhaev, V. M. Malikov and S. Yu. Yunusov, *Chem. Nat. Compd.*, **12**, 50 (1976); *d*) É. Kh. Batirov, V. M. Malikov and S. Yu. Yunusov, *ibid.*, **12**, 114 (1976).
3) S. G. Yates and H. L. Tookey, *Aust. J. Chem.*, **18**, 53 (1965); J. D. Robbins, J. G. Sweeny, S. R. Wilkinson and D. Burdick, *J. Agric. Food Chem.*, **20**, 1040 (1972).
4) I. Ribas and M. Pazo, *An. R. Soc. Esp. Fis. Quim., Ser. B*, **63**, 915 (1967) [*Chem. Abstr.*, **68**, 39878*w* (1968)]; M. Ribas, A. Landa and I. Ribas, *An. Quim.*, **64**, 515 (1968) [*Chem. Abstr.*, **69**, 109764*c* (1968)]; M. Ribas and I. Ribas, *ibid.*, **64**, 637 (1968) [*Chem. Abstr.*, **69**, 87265*m* (1968)]; A. Landa and I. Ribas, *ibid.*, **70**, 360 (1974) [*Chem. Abstr.*, **81**, 60849*r* (1974)].
5) D. R. Jacobson, W. M. Miller, D. M. Seath, S. G. Yates, H. L. Tookey and I. A. Wolff, *J. Dairy Sci.*, **45**, 416 (1963); D. J. Williams, D. E. Tyler and E. Papp, *J. Am. Vet. Med. Assoc.*, **154**, 1017 (1969); M. M. Forney, D. J. Williams, E. M. Papp and D. E. Tyler, *ibid.*, **155**, 1603 (1969).
6) T. A. Jones, R. C. Buckner and P. B. Burrus, II, *Can. J. Plant Sci.*, **65**, 317 (1985); D. P. Belesky, J. D. Robbins, J. A. Stuedemann, S. R. Wilkinson and O. J. Devine, *Agron. J.*, **79**, 217 (1987).
7) S. G. Yates, R. J. Petroski and R. G. Powell, *J. Agric. Food Chem.*, **38**, 182 (1990).
8) R. J. Petroski, S. G. Yates, D. Weisleder and R. G. Powell, *J. Nat. Prod.*, **52**, 810 (1989).
9) K. Kamei, M. Murata, A. Takeda, F. Shirai, T. Matsumoto and A. Momose, Proceedings of 4th International Conference on the Control of the Use of Drugs in Racehorses, Melbourne, May 1981, pp. 149—155.
10) H. Budzikiewicz, C. Djerassi and D. H. Williams, "Mass Spectrometry of Organic Compounds," Holden-Day, Inc., San Francisco, 1967, pp. 317—318.
11) *a*) S. T. Akramov and S. Yu. Yunusov, *Chem. Nat. Compd.*, **4**, 252 (1968); *b*) Ya. V. Rashkes, U. A. Abdullaev and S. Yu. Yunusov, *ibid.*, **14**, 121 (1978).

Application of Liquid Particle Extraction to the Purification of Glycyrrhizin

Hideyuki NISHIZAWA,* Sakiko OKIMURA, Yukako WATANABE and Yoshihiro ABE

Kyoritsu College of Pharmacy, 1–5–30, Shibakoen, Minato-ku, Tokyo 105, Japan. *Received October 1, 1990*

Glycyrrhizin on the market (about 90% in purity) contains two major impurities which are difficult to remove by recrystallization. Purification of a commercial sample was carried out by a dual-flow countercurrent extraction method, liquid particle extraction, which was recently introduced. Starting from 72.6 mg of commercial glycyrrhizin, it was purified to a purity of 99.7% with a recovery of 53.9% (35.3 mg).

Keywords purification; extraction; glycyrrhizin; glycyrrhizic acid; liquid particle extraction

Introduction

Glycyrrhizin, a principal triterpenoid present in licorice extract, has been widely investigated for its pharmacological activities.[1] Although glycyrrhizin is commercially available as an ammonium salt in high purity (90%), it contains impurities which are difficult to remove by repeated recrystallization.[2] It is essential to obtain the compound in high purity for analytical or biological studies.

Purification of glycyrrhizin by preparative high performance liquid chromatography (HPLC) was reported,[2] but no detailed description was given of the amount of the sample nor of the recoveries after purification. We recently reported on a liquid particle extraction, a simple and efficient procedure of dual-flow countercurrent extraction.[3] In contrast to chromatography, though the method can separate a mixture into only two fractions, it is advantageous in that it can be carried out continuously over a long period, and can be used to treat a large amount of sample in a single run.

In this article, we describe an application of the liquid particle extraction (LPX) method to the purification of commercial glycyrrhizin. Using LPX, glycyrrhizin in a purity of 99.7% was obtained with a recovery of 53.9%.

Experimental

Apparatus The liquid particle extractor used in this work was reported previously.[3]

HPLC analysis was performed with an HPLC system 800 (JASCO, Tokyo) equipped with a Rheodyne sampling valve (20 μl), a reversed phase column (ODS, Wakosil 5C18, 4 mm i.d. × 15 cm with a precolumn of 4 mm i.d. × 3 cm) and a data processor, Chromatopac CR-6A (Shimadzu, Kyoto). A mixture of 2% acetic acid and acetonitrile (65 : 35)[2] was used as an eluent (1.5 ml/min) with monitoring at 258 nm at room temperature.

Ion-pair chromatography was carried out according to the previous report.[4] Thus, 5 mM tetra-*n*-butylammonium hydroxide in a mixture of methanol and water (55 : 45, v/v) of pH 6.0 adjusted with 1 M phosphoric acid was used as a mobile phase (1.0 ml/min) and monitored at 254 nm. The column used was the same as described above except that it was maintained at 50 °C.

Chemicals Glycyrrhizic acid monoammonium salt (glycyrrhizin, >90%), 1-butanol and *p*-nitrocinnamic acid were purchased from Wako Pure Chemical Industries (Osaka). Formic acid was obtained from Nakarai Kagaku (Kyoto). For the solvents for HPLC, distilled water, methanol and acetonitrile of HPLC grade were also purchased from Wako Pure Chemical Ind. Tetra-*n*-butylammonium hydroxide (10% solution) for ion-pair chromatography was from Tokyo Kasei Kogyo (Tokyo).

Glycyrrhizin was dried under vacuum over phosphorous pentoxide for 15 h at room temperature before use. 1-Butanol was distilled with a small amount of sodium borohydride. Equal volumes of 1-butanol (2 l) and 0.5 M phosphate buffer (pH 5.95, which was prepared by dissolving 105.47 g of potassium dihydrogen phosphate and 80.58 g of disodium hydrogen phosphate (12-hydrate) in deionized water to make 2 l of solution) were mixed in a separatory funnel and the two phases were separated at 25 °C and used for the organic and aqueous solvents, respectively.

Measurement of the Distribution Ratio Five ml of the aqueous phase was placed in a test tube with a glass stopper. A solution of glycyrrhizin in the organic phase (5 ml, 1.0 mg/ml) was overlayered and stirred for 30 s with a tube touch mixer, then was shaken for 16 h in a bath maintained at 25 °C (Circle Shaker, Taiyo Kagaku-Kogyo Co., Tokyo). After separation of the two layers, 1 ml of *p*-nitrocinnamic acid solution (as an internal standard, 0.01 mg/ml in methanol) was added to each 0.5 ml of the two phases. Following removal of the solvents under reduced pressure (< 40 °C), the residue was redissolved in 1 ml of the eluent and was injected into HPLC. The distribution ratio was determined from the peak areas of the chromatograms of the organic and aqueous phases.

Purification of Glycyrrhizin The flow rates of the organic and the aqueous phases were set as 0.97 and 1.26 ml/min, respectively. Under rotation of 500 rpm, a solution of commercial glycyrrhizin (3 mg/ml, 24.2 ml) was fed into the middle of the column at a flow rate of 0.028 ml/min. After 14 h, glycyrrhizin in the organic fraction (934 ml) was twice extracted by a saturated sodium bicarbonate solution (100 ml × 2). After acidification with concentrated formic acid (15 ml), the aqueous solution was back-extracted with 1-butanol (three times; 30, 20 and 10 ml). The 1-butanol extract was washed with 0.01 M formic acid (100 ml), and then was evaporated to dryness under reduced pressure (< 40 °C). Purified glycyrrhizin (35.3 mg) was obtained as colorless powder, and the purity was determined by HPLC.

The aqueous extract (1216 ml) was acidified with conc. formic acid (50 ml), and was extracted with 1-butanol twice (80 and 20 ml). The combined organic layer was washed with 1 M formic acid and then with 0.01 M formic acid. The solvent was removed under reduced pressure (< 40 °C) to obtain 18.1 mg of glycyrrhizin including impurities (*cf.* Fig. 4).

Results and Discussion

Change of Distribution Ratio with pH To determine the optimum condition for extraction, the change of distribution ratio of glycyrrhizin and its impurities (1 and 2 in Fig. 4) was measured by changing the pH of the aqueous phase (Fig. 1).

For separation, pH of 5.96 was chosen, where the distribution ratio of glycyrrhizin became larger than 1.0 while that of impurities was less than 1.0. That is, glycyrrhizin can be extracted to the organic phase, and the impurities to the aqueous phase under nearly equal flow rates with the extractor.

Optimization of Separation Condition Based on the values of the distribution ratio (glycyrrhizin: $D_1 = 1.19$, and impurity 2: $D_2 = 0.87$) obtained at pH 5.96, the flow rate of the aqueous phase (H) was determined as 1.10 by Eq. 1,[3b] under the flow rate of sample feed (a) of 0.028 ml/min and that of the organic phase (S) of 1.07 ml/min.

$$H = S(1 + a/2)\sqrt{D_1 \times D_2} \quad (1)$$

An unexpected result was obtained in the extraction experiment which was planned to separate the impurities into the aqueous phase and to extract glycyrrhizin into the 1-butanol phase under the condition shown above. It

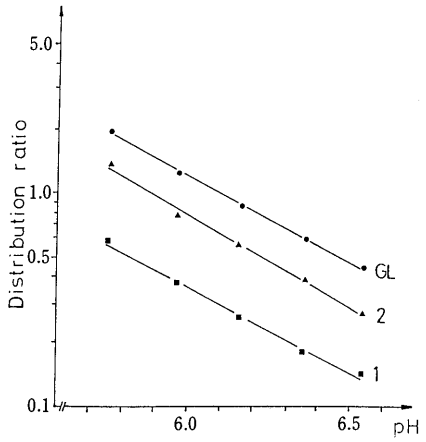

Fig. 1. Change of Distribution Ratio with pH of the Aqueous Phase (25 °C)

Distribution ratio of glycyrrhizin (GL) and impurities (1 and 2, see Fig. 4) in 1-butanol and 0.5 M phosphate buffer system were measured by HPLC. Commercial glycyrrhizin (5 mg) was partitioned between the organic (5 ml) and the aqueous phase (5 ml).

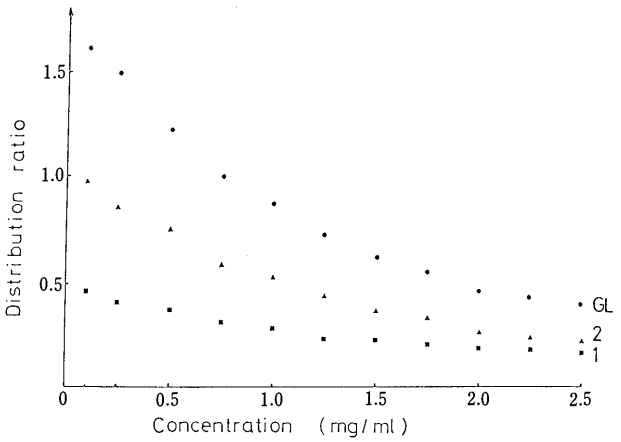

Fig. 2. Changes in Distribution Ratio with the Changes in Concentration (25 °C)

GL, glycyrrhizin; 1, impurity 1; 2, impurity 2 (*cf.* Fig. 4). Concentration is represented as total weight (mg) of commercial glycyrrhizin in 1 ml of a 1 : 1 mixture of the two phases. The acidity of the aqueous phase is pH 5.95.

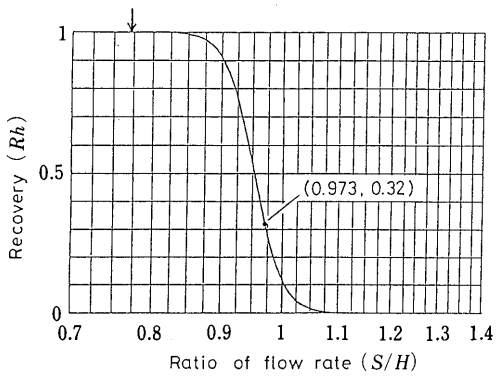

Fig. 3. Correction of Extraction Condition

The curve was obtained by calculation on the assumption that 32% of impurity 2 was extracted into the aqueous phase when the flow rate of the organic (S) and the aqueous phases (H) were set as 1.07 and 1.10 ($S/H=0.973$), respectively, and the flow rate of the sample feed (a) is 0.028 with an apparatus with 100 theoretical plates. When the ratio of the flow (S/H) is changed from 0.973 to 0.77 (indicated by an arrow), impurity 2 should be extracted almost completely into the aqueous phase.

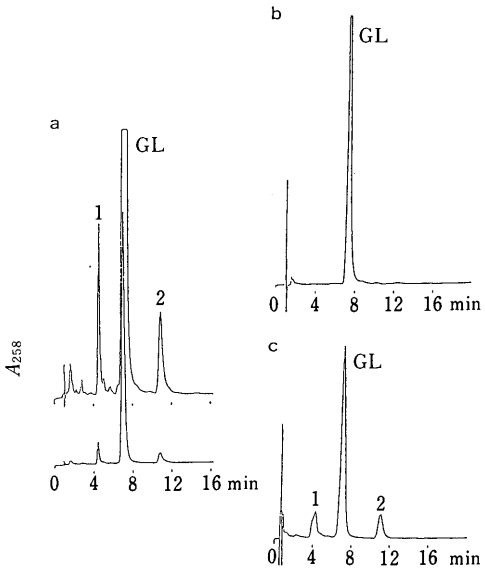

Fig. 4. HPLC Chromatograms after Purification

a, commercial glycyrrhizin; b and c, the organic, and the aqueous extracts after purification by LPX, respectively. Two impurities (1 and 2 in a) were removed to the aqueous phase by extraction (b and c).

was found that a large quantity (68%) of impurity 2, which should be extracted into the aqueous phase, was accompanied by glycyrrhizin in the organic extract contrary to the calculation.

To investigate the cause, the distribution ratio of glycyrrhizin was determined using different concentrations. The distribution ratios of glycyrrhizin and impurities were found to change significantly with the changes of concentrations even in a buffered two-phase system (Fig. 2). On the contrary, in the case of phenyl α- and phenyl β-D-glucoside, concentration dependency on the distribution ratio was negligible.

The distribution ratio of glycyrrhizin and that of impurity 2 were decreased remarkably with the increase in their concentrations. A micelle formation with glycyrrhizin (pH 4.2—5.5) was reported,[5] but apparently no micelle colloid nor emulsion formation was observed throughout the extraction process where "water and oil (1-butanol)" were stirred in the presence of the surfactant, glycyrrhizin. We speculated that association of the molecules may have occurred in the aqueous phase at its hydrophobic portion, resulting in the formation of more hydrophilic associated species.

Correction of the Extraction Condition The flow rates of both phases were, hence, corrected as follows. The relationship between the recovery into the aqueous phase (Rh) and the ratio of the flow rates (S/H) in dual-flow extraction can be depicted as shown in Fig. 3. The curve was obtained on the assumption that 32% of impurity 2 was extracted into the aqueous phase under the condition of $S=1.07$ ml/min, $H=1.10$ ml/min ($S/H=0.973$) and $\alpha=0.026$ ($a/S=0.028$ (ml/min)/1.07 (ml/min)) with an extractor having 100 theoretical plates (50 plates at both the top and bottom). In order to extract most of impurity 2 into the aqueous phase, the flow rate ratio of $S/H\approx0.82$ (where Rh comes to nearly 1.0) was required. But to secure a high purity of glycyrrhizin, S/H of 0.77 (indicated by an arrow in Fig. 3) was chosen. Thus, the flow rates were corrected to $H=1.26$ ml/min and $S=0.97$ ml/min ($S/H=0.77$).

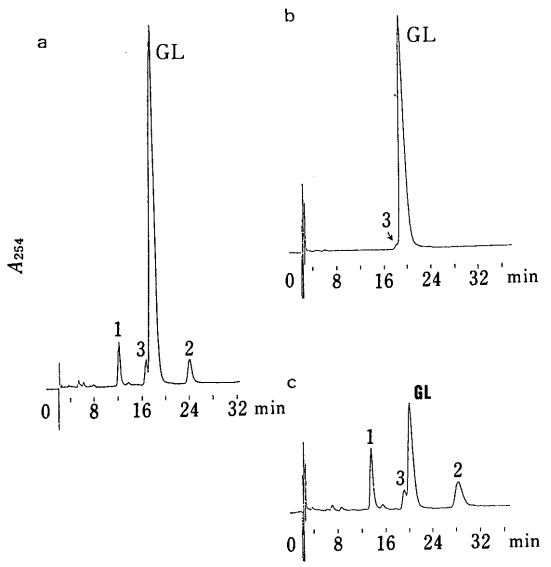

Fig. 5. HPLC Chromatograms after Purification under Ion-Paired Condition

a, the commercial sample; b, the organic extract; c, the aqueous fraction. Almost all impurity 3 in the initial sample was extracted to the aqueous phase by LPX. The sample solutions were the same as used in Fig. 4.

Purification of Glycyrrhizin A solution of glycyrrhizin (72.6 mg in 24.2 ml of the organic phase) was fed into the middle of the extractor at a flow rate of 0.028 ml/min and the extractive separation was carried out under the conditions shown above. After 14 h, 35.3 mg of glycyrrhizin had been isolated from the organic extract in 99.7% purity. From the aqueous extract, 18.1 mg of a mixture of glycyrrhizin and impurities was recovered (Fig. 4). The recovery of materials was 73.6% (most of the remaining materials were left in the column of the apparatus).

An ion-pair chromatographic method was used to separate another impurity (impurity 3) from glycyrrhizin which could not be resolved by the acid suppressed condition.[4] The condition reported for the purification of glycyrrhizin[2] was an acid suppressing one, under which impurity 3 could not be removed. Purification by LPX was performed under different conditions from the acid suppressed solvent system for HPLC. And impurity 3 hidden in the peak of glycyrrhizin under the acid suppressed condition was largely removed by the LPX purification (Fig. 5).

Conclusion

A dual-flow countercurrent extraction technique, LPX, was applied to the purification of commercial glycyrrhizin. Glycyrrhizin of 99.7% purity as calculated from the areas of chromatograms at 258 nm was obtained with a recovery of 53.9%. To date, the previously reported method for optimization of extraction condition[3b] was not applicable directly to the purification of glycyrrhizin, because it changed its partition ratio according to the concentration even in a buffered two-phase system. To surmount this problem, an improved calculation method to obtain the optimum condition in LPX is now under investigation.

An interesting property of glycyrrhizin was found in its partition between the two-phase system, where a hydrophobic interaction might play an important role in the association of the molecules.

References

1) S. Shibata, "New Natural Products and Plant Drugs with Pharmacological, Biological or Therapeutical Activity," ed. by H. Wagner and P. Wolff, Springer–Verlag, Berlin, 1977, pp. 178—180.
2) K. Okada, J. Tanaka, A. Miyashita and K. Imoto, *Yakugaku Zasshi*, **101**, 822 (1981).
3) *a*) H. Nishizawa, S. Okimura, Y. Watanabe and Y. Abe, *Anal. Sci.*, **5**, 399 (1989); *b*) *Idem*, *ibid.*, **5**, 345 (1989).
4) K. Sugawara, Y. Ito, T. Oshima, M. Kawamura and T. Misaki, *Chem. Pharm. Bull.*, **33**, 5364 (1985).
5) A. Otsuka, Y. Yonezawa, K. Iba, T. Tatsumi and H. Sunada, *Yakugaku Zasshi*, **96**, 203 (1976).

20β-Hydroxysteroid Dehydrogenase of Neonatal Pig Testis: Reverse Catalytic (Oxidation) Reaction

Shuji OHNO, Shizuo NAKAJIN,* and Masato SHINODA

Faculty of Pharmaceutical Sciences, Hoshi University, 2–4–41, Ebara, Shinagawa-ku, Tokyo 142, Japan. *Received September 11, 1990*

Neonatal pig testicular 20β-hydroxysteroid dehydrogenase (20β-HSD) catalyzed the oxidation of 20β-hydroxysteroids, 17α,20β-dihydroxypregn-4-en-3-one and 20β-hydroxypregn-4-en-3-one in the presence of β-nicotinamide adenine dinucleotide phosphate (β-NADP$^+$). The behavior of 20β-HSD activity toward the substrate of 17α,20β-dihydroxypregn-4-en-3-one differed from the catalytic reaction for 20β-hydroxypregn-4-en-3-one. The enzyme could catalyze not only 20β-hydroxysteroids but also 20α-hydroxy-5-ene steroids, 20α-hydroxypregn-5-en-3β-ol and 17α,20α-hydroxypregn-5-en-3β-ol with 22.1 and 8.7% of activity relative to 20β-hydroxypregn-4-en-3-one, respectively. The enzyme preferentially required β-NADP$^+$, and also utilized β-nicotinamide adenine dinucleotide β-NAD$^+$ and β-nicotinamide adenine dinucleotide 3′-phosphate (β-3′-NADP$^+$) nonspecifically as the cofactor. The optimum pH was observed at pH 7.5 with the substrate of 20β-hydroxypregn-4-en-3-one. The activation energies obtained from oxidation-reduction reactions of 20β-HSD for the substrate of 20β-hydroxypregn-4-en-3-one, progesterone and 17α-hydroxyprogesterone were estimated at 13.8, 27.0 and 20.0 kcal/mol, respectively.

Keywords 20β-hydroxysteroid dehydrogenase, reverse catalytic reaction, activation energy, neonatal pig testis, oxidoreductase

One of the pyridine nucleotide dependent hydroxysteroid dehydrogenases concerned with steroidogenesis in mammalian species, the 20α-hydroxysteroid dehydrogenase (20α-HSD; EC 1.1.1.149) is known to be present in pig testis[1] and in other organs and species.[2] 20β-Hydroxysteroid dehydrogenase (20β-HSD; EC 1.1.1.53) was also expected to be present in mammalian species because of the detection of some 20β-hydroxysteroids in rat testis,[3] bull testis[4] and human testis;[5] however, 20β-HSD had not been purified except for that from prokaryotic cell of *Streptomyces hydrogenans*.[6]

We earlier reported that a large quantity of 20β-HSD was specifically localized in the cytosol fraction of pig testis at neonatal stage[7] and purified the ennzyme.[8] Some of its properties were studied and compared with pig testicular 20α-HSD and prokaryotic 20β-HSD, and those were fully investigated. The pig testicular 20β-HSD was quite distinct from 20α-HSD from the same origin in enzymological properties, nevertheless similar substrates were utilized by both enzymes. Especially in the stereochemistry of hydrogen transfer from nicotinamide moiety of reduced form of nicotinamide adenine dinucleotide phosphate (NADPH) on the forward reaction (reduction) from 20-carbonyl group to 20-hydroxy group by 20β-HSD, clear differences were observed. In addition, we noticed that there was a marked difference from 20α-HSD on the reverse reaction (oxidation) corresponding to formation of 20-oxo-steroid from 20-hydroxysteroid.

In this paper, we extend our investigations of some properties mentioned in our previous paper, particularly those on the reverse catalytic reaction of 20β-HSD.

Experimental

Chemicals 17α-Hydroxy[4-^{14}C]progesterone (lot; 1767-039, 2.0 GBq/mmol) and [4-^{14}C]progesterone (lot; 1895-013, 2.1 GBq/mmol) were purchased from New England Nuclear Corp., (Boston, Mass., U.S.A.). β-Nicotinamide adenine dinucleotide phosphate (β-NADP$^+$) and its reduced form (β-NADPH), β-nicotinamide adenine dinucleotide (β-NAD$^+$), β-nicotinamide adenine dinucleotide 3′-phosphate (β-3′-NADP$^+$), all sodium salts, and 20β-HSD purified from *Streptomyces hydrogenans* and all non-radioactive steroids used were purchased from Sigma Chemical Co. (St. Louis, Mo., U.S.A.). All other reagents used were of the best grade available and obtained from Iwai Chemicals, Tokyo.

Preparation of Other Radioactive Steroids Two radioactive [4-^{14}C]steroids (20β-hydroxy[4-^{14}C]pregn-4-en-3-one and 17α,20β-dihydroxy[4-^{14}C]pregn-4-en-3-one) were synthesized enzymatically. 20β-Hydroxy[4-^{14}C]pregn-4-en-3-one was prepared from [4-^{14}C]progesterone: [4-^{14}C]progesterone was incubated with 20β-HSD from the mycelium of *Streptomyces hydrogenans* in the presence of reduced form of β-nicotinamide adenine dinucleotide (β-NADH). 17α,20β-Dihydroxy[4-^{14}C]pregn-4-en-3-one was converted from 17α-hydroxy[4-^{14}C]progesterone and its condition was the same as above. Each prepared [4-^{14}C]steroid was purified by thin-layer chromatography (TLC) and high performance liquid chromatography (HPLC),[9] and their radiochemical purity was established by TLC before use.

Purification of 20β-HSD 20β-HSD was purified from neonatal pig testes by the same method described previously.[10] The enzyme preparation in 50 mM KPB (pH 7.4)–0.1 mM ethylenediaminetetraacetic acid (EDTA) (1.3 mg/ml) was stored at −20 °C when not in use, and was stable for at least six months.

Enzyme Activity Enzyme activity of 20β-HSD using radioactive steroid was measured as previously described.[7] This method is based on a conversion of 20β-hydroxy-[4-^{14}C]steroid and 20-oxo-[4-^{14}C]steroid. The substrate and product were separated by TLC developed with benzene : acetone = 8 : 2 (v/v).

The assay of 20β-HSD activities for the substrate specificity, pH optimum and cofactor requirements were carried out spectrophotometrically. This method was based on the production of NADPH from NADP$^+$ by the enzyme. 20β-Hydroxypregn-4-en-3-one (50 nmol/10 μl ethanol) was incubated in a cuvette (1 cm path, 1 ml) with 20β-HSD in the presence of β-NADP$^+$ (250 nmol) in 1.0 ml of 50 mM potassium phosphate buffer (KPB; pH 7.4) at 37 °C, and the increment of absorbance 340 nm was monitored continuously. The molar extinction coefficient used was 6200 (cm·mol)$^{-1}$. Under these conditions, the 20β-HSD activity was obtained with a high rectilineal relationship to the incubation time from 0 to 5 min, and the amount of 20β-HSD from 0 to 184.8 μg with the correlation coefficient of 0.9990.

Enzyme activity obtained by this method was 3.35 nmol/min/mg protein, a rate as almost equal to that using radioactive 20β-hydroxy[4-^{14}C]pregn-4-en-3-one as the substrate.

The final concentration of ethanol, which was added as the solvent of steroids in the assay medium, was standardized to 1%, and no significant decrease in 20β-HSD activity was observed at an ethanol concentration between 1 and 5%.

Results

Oxidation Reaction of 20β-Hydroxy Group of C_{21}-Steroid by 20β-HSD When β-NADP$^+$ was used as a cofactor, the two radioactive 20β-hydroxy-steroids, 17α,20β-dihydroxy-[4-^{14}C]pregn-4-en-3-one and 20β-hydroxy[4-^{14}C]pregn-4-en-3-one, were converted to 20-oxo-steroids, 17α-hydroxy-[4-^{14}C]progesterone and [4-^{14}C]progesterone, by purified 20β-HSD, respectively. Although both 20-oxo-steroids were

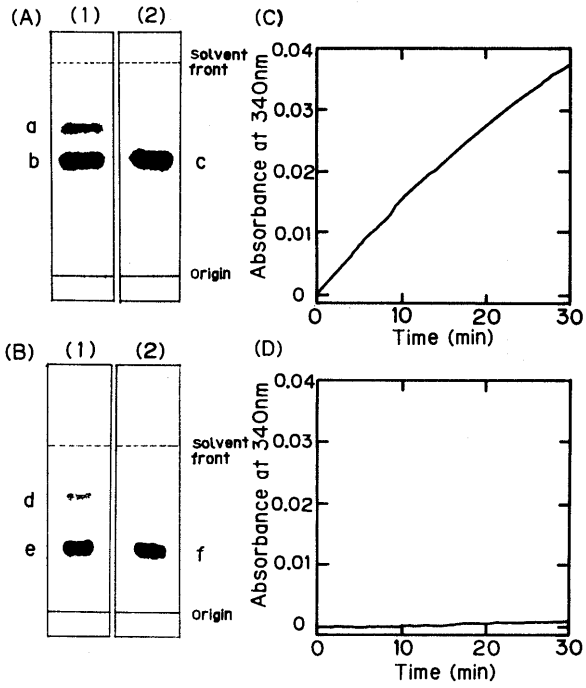

Fig. 1. Reverse Catalytic Activities of 20β-HSD, Detection of the Metabolite on the TLC and Time Course of the Reaction

20β-Hydroxy[4-^{14}C]pregn-4-en-3-one (A) or 17α, 20β-dihydroxy[4-^{14}C]pregn-4-en-3-one (B) (370Bq/20 nmol/10 μl ethanol) was incubated with $NADP^+$ (250 nmol) in the presence (1) or absence (2) of 20β-HSD (44 μg) in 1.0 ml of 50 mM KPB (pH 7.4) for 30 min at 37 °C. TLC was carried out using a silica gel plate (Kodak 13181), and developed with benzene–acetone (8 : 2 v/v). Radioactive metabolites detected by radioautography are indicated as dark spots. Assigned spots are progesterone (a), 20β-hydroxypregn-4-en-3-one (b, c), 17α-hydroxyprogesterone (d) and 17α,20β-dihydroxypregn-4-en-3-one (e, f).

20β-Hydroxypregn-4-en-3-one (C) or 17α,20β-dihydroxypregn-4-en-3-one (D) (20 nmol/10 μl ethanol) was incubated in a quartz cuvette (1 cm path, 1.0 ml) with purified 20β-HSD (89 μg) in the presence of $NADP^+$ (250 nmol) in 1.0 ml of 50 mM KPB (pH 7.4) at 37 °C. The absorbance at 340 nm was monitored continuously for 30 min.

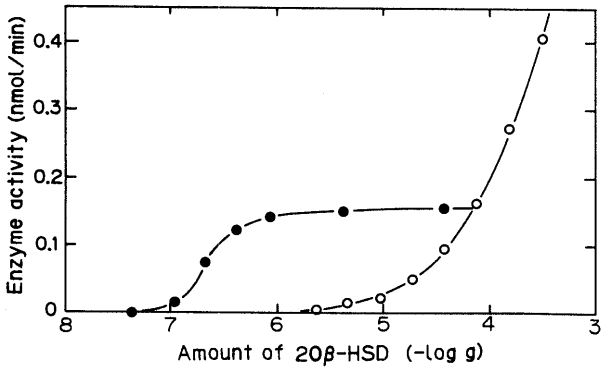

Fig. 2. Reverse Catalytic Reaction (Oxidation) of 20β-HSD as the Amount of Enzyme

17α,20β-Dihydroxy[4-^{14}C]pregn-4-en-3-one (●) or 20β-hydroxy[4-^{14}C]pregn-4-en-3-one (○) (20 nmol/10 μl ethanol) was incubated with various amounts of purified 20β-HSD in the presence of $NADP^+$ (250 nmol) in 1.0 ml of 50 mM KPB (pH 7.4) at 37 °C for 30 min.

produced by oxidation at C_{20} position by 20β-HSD, the amount of 17α-hydroxyprogesterone as a product from 17α,20β-dihydroxypregn-4-en-3-one was less than progesterone from 20β-hydroxypregn-4-en-3-one (Fig. 1). On the other hand, the oxidation behaviors of 20β-hydroxy group by 20β-HSD as a function of the amount of enzyme showed marked difference between the two substrates, 17α,20β-dihydroxypregn-4-en-3-one and 20β-hydroxypregn-4-en-3-one. When 20 nmol of 17α,20β-dihydroxypregn-4-en-3-one was employed as the substrate in the presence of β-$NADP^+$, the 20β-HSD catalyzed the conversion to 20-oxo-steroid with only one-fiftieth the amount of purified 20β-HSD as the minimum concentration for the 20β-hydroxypregn-4-en-3-one; it was found that this activity reached saturation at the amount of 8.7×10^{-4} mg, and the relation of enzyme activity to protein added was minimal (1.09×10^{-4}—4.36×10^{-4} mg). Over the range of 9.6×10^{-3} mg protein, the 20β-HSD activity for the substrate of 20β-hydroxypregn-4-en-3-one was higher than that for 17α,20β-dihydroxypregn-4-en-3-one (Fig. 2). When 20β-hydroxypregn-4-en-3-one was used as the substrate, the kinetic parameters of K_m and V_{max} values obtained from Lineweaver–Burk plot were estimated at 31.4 μM and 11.1 nmol/min/mg protein, respectively.

Activation Energy The maximum rates of 20β-HSD reactions were determined between 15 and 45 °C at pH 7.4. The maximum velocity (V_{max}) values were increased in relation to the incubation temperature of assay. As shown in Table I, activation energies for the 20β-HSD reactions were estimated to be 27000 cal/mol for progesterone, 20000 cal/mol for 17α-hydroxyprogesterone in the presence of β-NADPH and to be 13800 cal/mol for 20β-hydroxypregn-4-en-3-one in the presence of β-$NADP^+$ by Arrhenius plot obtained from V_{max} values and temperature over the range of 15—45 °C.

Table I. Kinetic Parameters and Activation Energies of 20β-HSD

Substrate	(Cofactor)	K_m (μM)	V_{max} (nmol/min/mg)	A.E.[a] (cal/mol)
20β-Hydroxypregn-4-en-3-one	($NADP^+$)	31.4	11.1	13800
Progesterone	(NADPH)	1.54[b]	4.43[b]	27000
17α-Hydroxyprogesterone	(NADPH)	9.42[b]	9.62[b]	20000

a) A.E.: Activation energy. *b*) Data were quoted from previous paper.[8]

Various concentrations of 20β-hydroxy[4-^{14}C]pregn-4-en-3-one were incubated in the presence of $NADP^+$ (250 nmol) in 1 ml of 50 mM KPB (pH 7.4) at 37 °C for 30 min. The Michaelis constant (K_m) and maximum velocity (V_{max}) were obtained by Lineweaver–Burk plot. The correlation coefficient of the Lineweaver–Burk plot was 0.999. For activation energies, various concentrations of [4-^{14}C] substrates were incubated in the presence of $NADP^+$ or NADPH (250 nmol) in 50 mM KPB (pH 7.4) at various temperatures (15—45 °C) for 30 min, and the V_{max} values were obtained by Lineweaver–Burk plots with correlation coefficients from 0.956 to 0.999.

Table II. Substrate Specificity of 20β-HSD

Substrate	(Cofactor)	20β-HSD Activity (nmol/min/mg)	%
20β-Hydroxypregn-4-en-3-one	($NADP^+$)	3.13	100
	(NAD^+)	2.25	71.8
20α-Hydroxypregn-4-en-3-one	($NADP^+$)	N.D.	—
20β-Hydroxypregn-5-en-3β-ol	($NADP^+$)	1.20	38.3
20α-Hydroxypregn-5-en-3β-ol	($NADP^+$)	0.69	22.1
17α,20β-Dihydroxypregn-4-en-3-one	($NADP^+$)	N.D.	—
17α,20α-Dihydroxypregn-4-en-3-one	($NADP^+$)	N.D.	—
17α,20β-Dihydroxypregn-5-en-3β-ol	($NADP^+$)	N.D.	—
17α,20α-Dihydroxypregn-5-en-3β-ol	($NADP^+$)	0.27	8.7

N.D.: not detected. Each substrate (50 nmol/10 μl ethanol) was incubated in a cuvette (1 cm path, 1 ml) with purified 20β-HSD (77 μg) in the presence of $NADP^+$ or NAD^+ (250 nmol) in 1.0 ml of 50 mM KPB (pH 7.4) at 37 °C. The slope of initial linear increase in absorbance at 340 nm as a function of time was determined.

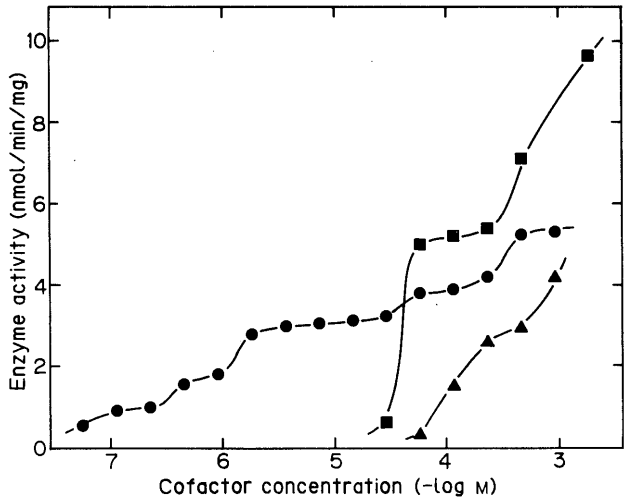

Fig. 3. Cofactor Requirement of 20β-HSD

Enzyme assays were carried out in a quartz cuvette (1 cm path, 1 ml) with 20β-hydroxypregn-4-en-3-one (50 nmol/10 μl ethanol) and 20β-HSD (77 μg) in the presence of various concentrations of β-NADP$^+$ (●), β-3′-NADP$^+$ (■) and β-NAD$^+$ (▲) in 1.0 ml of 50 mM KPB (pH 7.4) at 37°C and absorbance at 340 nm was monitored continuously.

Substrate Specificity Various 20α- or 20β-hydroxypregnane-steroids were examined as substrate in the presence of β-NADP$^+$ and the enzyme activities were measured by spectrophotometrical assay. As shown in Table II, 20β-hydroxypregn-4-en-3-one was considered the preferred substrate for 20β-HSD. Furthermore, not only 20β-hydroxypregn-4-en-3-one but also 20β-hydroxypregn-5-en-3β-ol, 20α-hydroxypregn-5-en-3-β-ol and 17α,20α-dihydroxypregn-5-en-3β-ol were utilized as the substrate by 20β-HSD. However, the ratio of specific enzyme activity for 20β-hydroxypregn-5-en-3β-ol, 20α-hydroxypregn-5-en-3β-ol and 17α,20α-dihydroxypregn-5-en-3β-ol to that for 20β-hydroxypregn-4-en-3-one was only 38.3%, 22.1% and 8.7%, respectively. When 17α,20β-dihydroxypregn-4-en-3-one was used as a substrate, the enzyme activity was not detected under these spectrophotometrical assay conditions, though the radioactive metabolite from 17α,20β-dihydroxy-[4-^{14}C]pregn-4-en-3-one was detected by TLC shown in Fig. 1.

Cofactor Requirement Several oxidized forms of pyridine nucleotide cofactors were examined as the hydrogen acceptor from 20β-hydroxy group of 20β-hydroxypregn-4-en-3-one. As shown in Fig. 3, β-NADP$^+$ was utilized for the oxidation from 20β-hydroxypregn-4-en-3-one to progesterone at the lowest concentration. β-3′-NADP$^+$, β-NAD$^+$ and β-NADP$^+$ were utilized as cofactors in high concentration regions. When β-3′-NADP$^+$ was added to the incubation medium above the range of 60 μM, the enzyme activity obtained was higher than when β-NADP$^+$ was used as a cofactor.

pH Optimum Enzyme activity was examined by two kinds of buffer systems: 100 mM KPB (pH 5.5 to 8.5) and 100 mM Tris–HCl (pH 8.5 to 10.5). Maximum 20β-HSD activity was observed at pH 7.5 in the reaction from 20β-hydroxypregn-4-en-3-one to progesterone, and the specific activity was twice that at pH 6.0.

Discussion

Although the physiological significance of 20β-HSD and 20α-HSD in testis is not yet clear, the 20β- and 20α-hydroxysteroids considered to be catalyzed by these enzymes were reported to inhibit cytochrome P-450 (17α-hydroxylase/C_{17-20}-lyase) activity.[11,12] From this phenomenon, it was believed that these enzymes were concerned with part of the regulation of androgen biosynthesis in testes. The 20β-HSD activity is specifically present in pig testis at neonatal stage, and this activity showed a dependence on the amount of enzyme molecule detected by Western blotting method (S. Ohno *et al.*, unpublished observation); therefore, it was considered that the 20β-HSD had some specific involvement with the androgen metabolism in the testis at neonatal stage.

It was reported that pig testicular 20α-HSD could specifically catalyze the reduction of 17α-hydroxyprogesterone to 17α,20α-dihydroxypregn-4-en-3-one but could not catalyze the reverse (oxidation of steroid) reaction, and that progesterone was converted to only 3% lower than 17α-hydroxyprogesterone by 20α-HSD.[1] In contrast, 20β-HSD catalyzed the reduction of progesterone as well as 17α-hydroxyprogesterone, thus being one of the preferential substrates. Moreover, 20β-HSD could also catalyze the reverse reaction when the 20β-hydroxy-form of both steroids, 17α,20β-dihydroxypregn-4-en-3-one and 20β-hydroxypregn-4-en-3-one, was used as the substrate, though the reverse reaction for 17α,20β-dihydroxypregn-4-en-3-one by 20β-HSD produced lower metabolites than that for 20β-hydroxypregn-4-en-3-one. 20β-HSD sensitively catalyzed the oxidation of 17α,20β-dihydroxypregn-4-en-3-one with a very small amount of enzyme, but the area in which the enzyme activity was increased in proportion to the enzyme amount was very narrow as a function of protein added; further, the quantity of steroid obtained as the metabolite was very small even when the activity reached saturation, compared with the catalytic reaction when 20β-hydroxypregn-4-en-3-one was used as the substrate. This result suggests the following equilibrium of the reaction between 17α-hydroxyprogesterone and 17α,20β-dihydroxypregn-4-en-3-one catalyzed by 20β-HSD: 17α-hydroxyprogesterone + NADPH + H$^+$ ⇄ 17α,20β-dihydroxypregn-4-en-3-one + NADP$^+$, inclines greatly toward the right side of reaction. On the other hand, in the reversible reaction between progesterone and 20β-hydroxypregn-4-en-3-one, the activation energy on reverse (oxidation of steroid) reaction was about half that with the forward reaction, so the reverse (oxidation of steroid) catalytic reaction of 20β-HSD could be regarded as the exergonic reaction. In the forward (reduction) reaction, the activation energy obtained from the substrate of 17α-hydroxyprogesterone was less than that from progesterone, so it was assumed that the reaction which employed 17α-hydroxyprogesterone as the substrate was catalyzed more effectively than the reduction of progesterone by 20β-HSD. In the same way, it was also supposed that in the reverse (oxidation) reaction employing 17α,20β-dihydroxypregn-4-en-3-one as the substrate (data not included), catalyzation would occur more quickly to equilibrium of the reversible reaction that 20β-hydroxypregn-4-en-3-one by 20β-HSD.

From the results of substrate specificity, 20β-hydroxypregn-4-en-3-one was converted as the substrate by 20β-HSD but 20α-hydroxypregn-4-en-3-one was not, among the 4-en-3-one steroids examined. Of further interest was

the confirmation that, although the activity was far less than that from 20β-hydroxypregn-4-en-3-one, the 20β-HSD employed one of 20α-hydroxysteroids only when 5-en-3β-ol steroids were used as the substrate in reverse (oxidation of steroid) reaction, in spite of the 20β-HSD having no 20α-HSD activity in forward reaction. From this finding, it was considered possible that purified 20β-HSD catalyzes the oxidation at positions other than the C_{20}-position of steroid.

References

1) F. Sato, Y. Takagi, and M. Shikita, *J. Biol. Chem.*, **247**, 815 (1972).
2) D. B. Gower, "Biochemistry of Steroid Hormones," ed. by H. L. J. Markin, Blackwell Scientific Publications, Oxford, 1984, pp. 230—292.
3) B. Tamaoki and M. Shikita, "Steroid Dynamics," ed. by G. Pincus, T. Nakao, and J. F. Tait, Academic Press, New York, 1966, pp. 493—530.
4) R. Neher and A. Wettstein, *Helv. Chim. Acta*, **43**, 1628 (1960).
5) H. Oshima, D.-F. Fan, and P. Troen, *J. Clin. Endocrinol. Metab.*, **40**, 426 (1975).
6) H. J. Hübener and C. O. Lehmann, *Z. Physiol. Chem.*, **313**, 124 (1958).
7) S. Nakajin, S. Ohno, M. Takahashi, K. Nishimura, and M. Shinoda, *Chem. Pharm. Bull.*, **35**, 2490 (1987).
8) S. Nakajin, S. Ohno, and M. Shinoda, *J. Biochem.* (Tokyo), **104**, 565 (1988).
9) M. J. O'Hara, E. C. Nice, R. Magee-Brown, and H. Bullman, *J. Chromatogr.*, **125**, 357 (1976).
10) S. Nakajin, S. Ohno, M. Aoki, and M. Shinoda, *Chem. Pharm. Bull.*, **37**, 148 (1989).
11) H. Inano, J. Nakano, M. Shikita, and B. Tamaoki, *Biochim. Biophys. Acta*, **137**, 540 (1967).
12) S. Nakajin, K. Takahashi, and M. Shinoda, *Yakugaku Zasshi*, **108**, 1188 (1988).

Antioxidant Effect of Vitamin K Homologues on Ascorbic Acid/Fe^{2+}-Induced Lipid Peroxidation of Lecithin Liposomes

Takao OHYASHIKI,* Yoshihisa YABUNAKA and Katsuhiko MATSUI

Department of Biochemistry, School of Pharmacy, Hokuriku University, Kanagawa-machi, Kanazawa, Ishikawa 920-11, Japan.
Received September 28, 1990

The effects of vitamin K homologues (K_1, K_2 and K_3) on lipid peroxidation of lecithin liposomes induced by ascorbic acid and ferrous ion were examined. Ubiquinone-10 (UQ-10) was used as a reference in evaluation of the effectiveness of these vitamins. The lipid peroxidation was assessed by measurements of thiobarbituric acid-reactive substance (TBARS) and conjugated diene formation during the reaction. Among them, vitamins K_1 and K_2 inhibited the lipid peroxidation, as did UQ-10, with the order of effectiveness: UQ-10 > K_2 > K_1. By contrast, vitamin K_3 had no inhibitory effect on ascorbic acid/Fe^{2+}-induced lipid peroxidation of the liposomes. The inhibitory effect of vitamins K_1 and K_2 appeared only when these vitamins were incorporated into the liposomes by sonication. Simple mixing of the liposomes with these vitamins or with UQ-10 did not inhibit peroxidation of the liposomes even at high concentrations. From measurements of nitroblue tetrazolium reduction and *p*-nitrosodimethylaniline bleaching of vitamin K_1- or K_2-incorporated liposomes in the presence of ascorbic acid/Fe^{2+}, it was found that these vitamins prevent the formation of hydroxyl radicals, not superoxide anions, during the peroxidation reaction. However, the degree of ascorbic acid/Fe^{2+}-induced TBARS formation of the liposomes was not inhibited by the addition of mannitol to the reaction mixture. From these results, it is suggested that the inhibitory effect of these vitamins is mainly involved in termination of radical-chain reaction. Experimantal results using several radical scavengers and/or antioxidants supported this interpretation. The treatment of vitamin K_2-incorporated liposomes with ascorbic acid/Fe^{2+} resulted in a decrease of the absorbance at 328 nm of the vitamin, depending on the incubation time. In addition, it was found that there is a linear relationship between the degree of the absorbance change at 328 nm and the amount of TBARS formed at different incubation times of the liposomes with ascorbic acid/Fe^{2+}.

Keywords lipid peroxidation; antioxidant; vitamin K homologue; lecithin liposome

In recent years there has been extensive research of lipid peroxidation of biological membranes, and it has been suggested that lipid peroxidation is important in connection with a variety of pathological events including the aging process.[1-3] These pathological consequences of lipid peroxidation may be related to alterations of membrane structure and function.[4]

It has been well recognized[5-7] that phenolic compounds, including α-tocopherol, act as one of the most effective antioxidants *in vivo* and prevent biological membrane components and tissues from oxygen toxicity. In the previous paper, we have reported[8] that α-tocopherol itself induces perturbation of the lipid organization of the porcine intestinal brush-border membranes, and we proposed the possibility that the antioxidant action of α-tocopherol is related to modification of the dynamic properties of lipid bilayers in the membranes.

In addition, ubiquinone[9,10] and derivatives of vitamin A,[11-13] which are also widely distributed in many biological systems, have been reported to possess an antioxidant capacity against lipid peroxidation. However, very little attention has been given to vitamin K as a naturally occurring antioxidant.

In the present study, we examined the effects of several forms of vitamin K on lipid peroxidation of lecithin liposomes in order to evaluate the effectiveness of vitamin K as an antioxidant against oxidative stress *in vivo*.

Experimental

Materials Egg yolk phosphatidylcholine, vitamin K homologues (K_1, K_2 (menatetrenone) and K_3), ubiquinone-10 (UQ-10), xanthine, xanthine oxidase (0.5 U/mg protein), superoxide dismutase (3000 U/mg protein) and catalase (3100 U/mg protein) were purchased from Sigma Co. 2-Thiobarbituric acid, 3(2)-*tert*-butyl-4-hydroxyanisole (BHA) and nitroblue tetrazolium were obtained from Wako Pure Chemical Co. *p*-Nitroso-*N*,*N*-dimethylaniline (*p*-NDA) was obtained from Aldrich Chemical Co. All other chemicals used were of the purest grade commercially obtainable.

Preparation of Lecithin Liposomes A chloroform solution of egg yolk phosphatidylcholine (30 mg/ml) was evaporated to dryness with a stream of nitrogen gas. After the residual solvent completely removed under vacuum, the appropriate amount of 30 mM Tris–HCl buffer (pH 7.4) was added and then sonicated with an Ultra Sonic Disruptor UR-200 P (Tomy Seiko Co., Tokyo) until the dispersion became clear. This clear solution was then centrifuged at 25000 × *g* for 20 min and the supernatant was used in the present study. Incorporation of vitamin K homologues or UQ-10 into the liposomes (15 mg/ml) was carried out by sonication for 1 min with a Bronson 3200 Sonifier (Yamato Scientific Co., Tokyo).

Lipid Peroxidation The lecithin liposomal suspension (0.3 mg/ml) was incubated with 100 μM ascorbic acid and 10 μM $FeSO_4$ in 30 mM Tris–HCl buffer (pH 7.4) for 30 min at 37 °C, unless otherwise specified. After termination of the reaction by the addition of 5 mM BHA (as a final concentration), the reaction mixture (1 ml) was heated for 30 min at 90 °C with 1 ml of 0.67% 2-thiobarbituric acid (50% CH_3COOH) and 1 ml of 10% trichloroacetic acid. After cooling to room temperature, the reaction mixture was then filtered using a Syringe filter (0.2 μm pore size). The amount of thiobarbituric acid-reactive substances (TBARS) in the filtrate was determined by measuring the absorbance at 530 nm using a Hitachi spectrophotometer 100-60. The amount of conjugated diene formed during the reaction was measured by monitoring the absorbance at 233 nm[14] in 10 mM phosphate buffer (pH 7.1).

Assay of Hydroxyl Radicals and Superoxide Anion Production The formation of hydroxyl radicals and superoxide anion during the peroxidation reaction were measured by monitoring the absorbance changes of *p*-NDA at 440 nm[15] and nitroblue tetrazolium at 560 nm,[16] respectively.

Results

Time Course of Lipid Peroxidation The time course of TBARS and conjugated diene formation by treatment of lecithin liposomes with 100 μM ascorbic acid/10 μM Fe^{2+} was examined.

As shown in Fig. 1, the amounts of TBARS and conjugated diene formed during the reaction increased

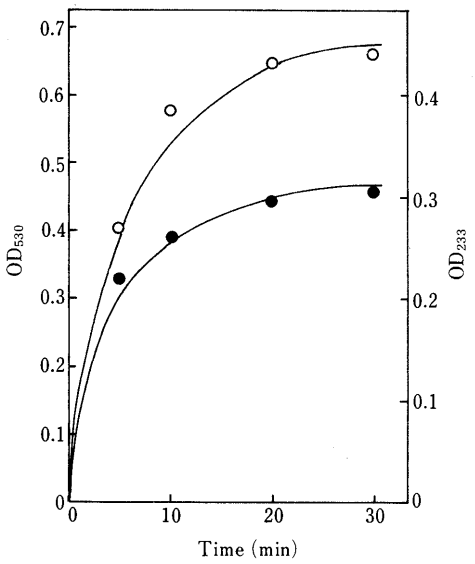

Fig. 1. Time Course of TBARS and Conjugated Diene Formation

The procedure and conditions of lipid peroxidation are described in Experimental. The reaction times were 5, 10, 20 and 30 min. Values are expressed as means of triplicate determinations. Symbols: ○, OD_{530}; ●, OD_{233}.

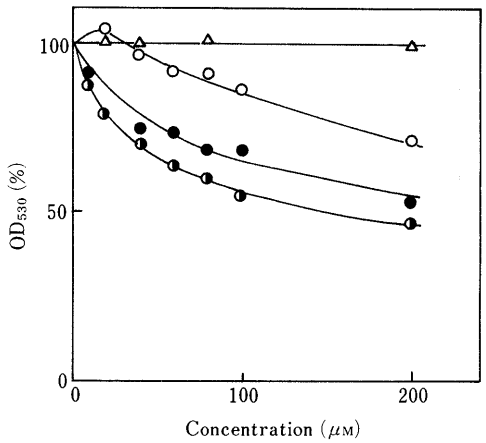

Fig. 2. Concentration Dependence of Vitamin K Homologues or UQ-10 on TBARS Formation

The liposomes were sonicated for 1 min with various concentrations (10—200 μM) of vitamin K homologues or UQ-10 before incubation with ascorbic acid/Fe^{2+}. Other experimental conditions are described in Experimental. Values are expressed as relative to those in the absence of these compounds in each system and represented as means of triplicate determinations. Symbols: ○, vitamin K_1; ●, vitamin K_2; ◑, UQ-10; △, vitamin K_3.

depending on the incubation time and reached almost constant levels within 30 min, indicating that ascorbic acid/Fe^{2+}-induced lipid peroxidation of the liposomes was completed with 30 min.

Effect of Vitamin K Homologues on Lipid Peroxidation The concentration dependence of vitamin K homologues and UQ-10 on TBARS formation of the liposomes by treatment with ascorbic acid/Fe^{2+} was examined. In this experiment, the liposomes were sonicated for 1 min with various concentrations of these compounds before incubation with ascorbic acid/Fe^{2+}.

As shown in Fig. 2, the degree of ascorbic acid/Fe^{2+}-induced TBARS formation of the liposomes was inhibited depending on the concentrations of vitamins K_1 and K_2, and UQ-10. The order of effectiveness in the inhibition of TBARS formation was UQ-10 > K_2 > K_1. By contrast, the

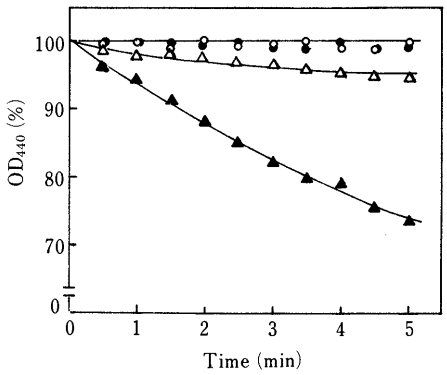

Fig. 3. *p*-NDA Bleaching by Treatment of Lecithin Liposomes with Ascorbic Acid/Fe^{2+} at 25 °C

The reaction was started by the addition of oxidizing agents to the liposomal suspension (0.1 mg/ml) containing 20 μM *p*-NDA in a 10 mM Tris–HCl buffer (pH 7.4). Symbols: ○, control (no addition); ●, 10 μM Fe^{2+} alone; △, 100 μM ascorbic acid alone; ▲, 100 μM ascorbic acid/10 μM Fe^{2+}. Values are expressed as relative to those before addition of oxidizing agents in each system, and represented as means of triplicate determinations.

liposomes with vitamin K_3 did not induce a decrease in TBARS, indicating that vitamin K_3 has no inhibitory effect on the lipid peroxidation.

On the other hand, TBARS formation of the liposomes by exposure to ascorbic acid/Fe^{2+} was not inhibited by simple mixing of the liposomes with vitamin K homologues or UQ-10 (data not shown).

Generation of Superoxide Anions and Hydroxyl Radicals Formation of superoxide anions during the reaction of the liposomes with ascorbic acid/Fe^{2+} or xanthine/xanthine oxidase was examined by measuring the nitroblue tetrazolium reduction.

In this experiment, the reaction mixture contained 0.3 mg/ml of the liposomes, 50 μM nitroblue tetrazolium and 30 mM Tris–HCl buffer (pH 7.4). The reaction was started by the addition of ascorbic acid (100 μM)/Fe^{2+} (10 μM) or xanthine (0.42 mM)/xanthine oxidase (0.1 U/ml) to the liposomal suspension. After 30 min incubation at 37 °C, the number of superoxide anions generated during the reaction was determined using the molar extinction coefficient of the dye at 560 nm ($\varepsilon_{560} = 17.9 \cdot 10^3\ M^{-1}\ cm^{-1}$).[16]

The values of superoxide anions per mg liposomes generated by treatment of the liposomes with ascorbic acid/Fe^{2+} and xanthine/xanthine oxidase were 96.2 ± 0.9 and 106.3 ± 4.2 nmol/30 min ($n = 3$, S. D.), respectively.

Next we measured the formation of hydroxyl radicals by monitoring the absorbance change at 440 nm of *p*-NDA in the reaction medium containing the liposomes.

As shown in Fig. 3, the absorbance at 440 nm of the dye progressively decreased after the addition of ascorbic acid/Fe^{2+} to the reaction mixture. On the other hand, addition of ascorbic acid or Fe^{2+} alone to the liposomal suspension containing *p*-NDA gave little or no change in the absorbance at 440 nm of the dye.

Effects of Antioxidants The effects of several antioxidants or radical scavengers on TBARS formation of the liposomes induced by ascorbic acid/Fe^{2+}-treatment were examined.

As shown in Table I, the TBARS value effectively decreased by the addition of thiourea, BHA or diphenylamine to the reaction mixture. On the other hand, superoxide dismutase and catalase did not induce an appre-

TABLE I. Effects of Antioxidants on Ascorbic Acid/Fe^{2+}-Induced TBARS Formation

Addition	Concentration	OD_{530}
No addition	—	0.276±0.002
SOD	0.1 mg/ml	0.243±0.008
Catalase	0.1 mg/ml	0.239±0.015
Thiourea	30 mM	0.104±0.004
Diphenylamine	1 mM	0.004±0.001
BHA	1 mM	0.060±0.004
Mannitol	10 mM	0.229±0.023
Mannitol	50 mM	0.246±0.021

The experimental conditions and procedures are described in Experimental. Values are expressed as means±S.D. for triplicate determinations.

TABLE II. Effects of Vitamin K Homologues and UQ-10 on the Reduction of Nitroblue Tetrazolium

Addition	OD_{560}	
	A	B
No addition	0.189±0.002	0.190±0.007
Vitamin K_1	0.171±0.001	0.193±0.005
Vitamin K_2	0.181±0.002	0.199±0.013
Vitamin K_3	0.185±0.002	0.195±0.005
UQ-10	0.184±0.011	0.197±0.005

A: Ascorbic acid/Fe^{2+} system. B: Xanthine/xanthine oxidase system. Values are expressed as means±S.D. for triplicate determinations.

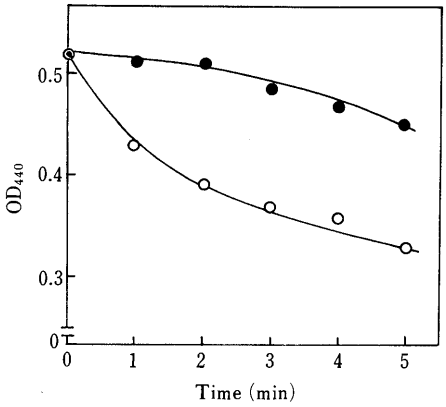

Fig. 4. *p*-NDA Bleaching of Vitamin K_2-Containing Liposomes by Treatment with Ascorbic Acid/Fe^{2+}

The experimental conditions were the same as those described in the legend to Fig. 3. Symbols: ○, without vitamin K_2; ●, with 200 μM vitamin K_2. Values are expressed as means of triplicate determinations.

ciable inhibition of TBARS formation of the liposomes, even at high concentrations.

Effects of Vitamin K Homologues and UQ-10 on Formation of Superoxide and Hydroxyl Radicals Table II shows the effects of vitamin K homologues and UQ-10 on superoxide anion production induced by treatment of the liposomes with ascorbic acid/Fe^{2+} or xanthine/xanthine oxidase.

In both the oxidizing systems, these compounds did not inhibit the formation of superoxide anions, indicating that the inhibitory effect of vitamins K_1 and K_2, and UQ-10 against ascorbic acid/Fe^{2+}-induced lipid peroxidation of the liposomes is not due to quenching superoxide anions generated during the reaction.

On the other hand, the rate of ascorbic acid/Fe^{2+}-induced *p*-NDA bleaching in the liposomes was effectively suppressed by incorporation of vitamin K_2 into the liposomes (Fig. 4).

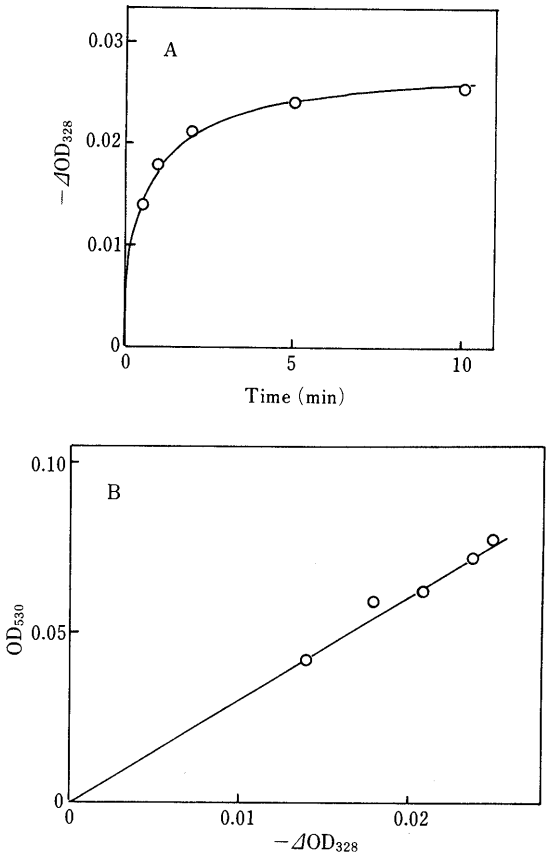

Fig. 5. Absorbance Change in Vitamin K_2 (200 μM) Incorporated into Lecithin Liposomes by Incubation with Ascorbic Acid/Fe^{2+}

(A) Time course of absorbance change. The experimental conditions were the same as those described in the legend to Fig. 2. After termination of the peroxidation reaction by the addition of 5 mM BHA, the absorbance at 328 nm was measured. ΔOD was expressed as the difference in the absorbance between liposomal suspension before and after incubation with ascorbic acid/Fe^{2+} at each time. Values are expressed as means of triplicate determinations.

(B) Relationship between degrees in absorbance change and TBARS formation. The data of the absorbance change at 238 nm was obtained from (A).

Changes in the Absorbance of Vitamin K_2 Treatment of vitamin K_2-incorporated liposomes with ascorbic acid/Fe^{2+} resulted in a decrease of the absorbance at 328 nm of the vitamin, depending on incubation time (Fig. 5A). In this experiment, the absorbance at 328 nm of vitamin K_3 in the liposomal suspension did not change until 10 min after the addition of ascorbic acid/Fe^{2+} (data not shown).

In addition, it was found that there is a good linear relation between the degrees of the absorbance change at 328 nm of vitamin K_2 in the liposomes and the TBARS values at different incubation times (Fig. 5B).

Discussion

In the present study, we examined the effects of three types of vitamin K on ascorbic acid/Fe^{2+}-induced lipid peroxidation of lecithin liposomes.

The results indicated that vitamins K_1 and K_2 possess an antioxidant capacity against lipid peroxidation of the liposomes induced by ascorbic acid/Fe^{2+} (Fig. 2). On the other hand, vitamin K_3 did not exhibit an inhibitory effect on ascorbic acid/Fe^{2+}-induced lipid peroxidation of the

liposomes. This finding is different from that reported by Wills.[17] In that communication, Wills reported that vitamin K_3 caused a marked inhibition of ascorbic acid- or reduced nicotinamide adenine dinucleotide phosphate (NADPH)-induced lipid peroxidation of rat liver microsomes. In the present study, however, the inhibitory effect of vitamin K_3 on ascorbic acid/Fe^{2+}-induced lipid peroxidation of the liposomes was not observed in the concentration range of 10 to 200 μM of the vitamin (Fig. 2). From these results, it is clear that vitamin K_3 has no inhibitory effect on lipid peroxidation, although the exact reason for the discrepancies between vitamin K_3 performance is unclear at present.

The inhibitory effect of vitamins K_1 and K_2, and UQ-10 did not appear by simple mixing of the liposomes with these compounds (data not shown), suggesting that the phytyl side chain may be important in placing these compound at the most suitable position in the lipid layers in the liposomes for inhibition of lipid peroxidation, as reported with α-tocopherol.[18] Therefore, it seems that the lack of a protective effect of vitamin K_3 against ascorbic acid/Fe^{2+}-induced lipid peroxidation is due to the lack of a phytyl side chain in the molecules.

The results with several antioxidants and radical scavengers (Table I) suggested that superoxide anions generated during the reaction are not related to lipid peroxidation of the liposomes, bacause superoxide dismutase produced little effect on TBARS formation induced by treatment of the liposomes with ascorbic acid/Fe^{2+}. Namely, this result suggests that inhibition of the lipid peroxidation by vitamins K_1 and K_2 is not due to quenching superoxide anions. In fact, vitamins K_1 and K_2 have no effect on superoxide anion generation by treatment of the liposomes with ascorbic acid/Fe^{2+} or xanthine/xanthine oxidase (Table II). On the other hand, thiourea, BHA and diphenylamine effectively inhibited ascorbic acid/Fe^{2+}-induced lipid peroxidation of the liposomes (Table I). As is well known, BHA and diphenylamine are terminators of free-radical chain reaction[19,20] and/or scavergers of alkoxyl radicals[21] in lipid peroxidation. On the other hand, thiourea is an excellent scavenger of hydroxyl radicals[22] and it can also scavenge alkoxyl radicals at high concentrations.[21]

The rate of *p*-NDA bleaching in the liposomes was stimulated by treatment with ascorbic acid/Fe^{2+} (Fig. 3), indicating that hydroxyl radicals are produced in a "metal-catalyzed" Harber–Weiss reaction.[23-25] Vitamin K_2 effectively prevented this ascorbic acid/Fe^{2+}-induced *p*-NDA bleaching (Fig. 4). These results suggest that hydroxyl radicals play an important role in the lipid peroxidation of the liposomes induced by ascorbic acid/Fe^{2+}. On the other hand, catalase and mannitol, which are commonly thought of as H_2O_2 and hydroxyl radical scavengers, respectively, had little effect on ascorbic acid/Fe^{2+}-induced TBARS formation of the liposomes (Table I). From these results, it seems that the inhibitory effect of vitamins K_1 and K_2 is related to termination of the radical-chain reaction in the lipid peroxidation by trapping lipid radicals, such as lipid peroxy and/or alkoxyl radicals, which propagate free radical-chain oxidation. However, the possibility that vitamin K homologues also act as scaverngers of hydroxyl radicals cannot be perfectly exclusive, because it seems that catalase and mannitol may react with H_2O_2 and hydroxyl radicals only in the aqueous phase, respectively.

As shown in Fig. 5, A and B, the absorbance at 328 nm of vitamin K_2 incorporated into the liposomes decreased in a linear fashion against the amount of TBARS formed during the reaction of the liposomes with ascorbic acid/Fe^{2+} at different times of incubation. It is well known[26,27] that the interaction of quinones with superoxide anions leads to the formation of quinols. In addition, Landi *et al.*[9] have reported that ultrasonic irradiation of ubiquinone-O solution results in a decrease of the absorbance at 268 nm of the compound, due to reduction of the quinone to quinol. Therefore, it seems that the absorbance change at 328 nm of vitamin K_2 in the liposomes by lipid peroxidation may be related to the formation of a quinol-type compound, although it is difficult at present to explain exactly the mechanisms of the absorbance change. Further detailed studies, including the identification of the reaction products of lipid radicals with vitamin K homologues, could shed additional light on analysis of the mechanism of antioxidant action of vitamins K_1 and K_2.

References

1) B. N. Ames, *Science*, **221**, 1256 (1983).
2) B. Halliwell, *Med. Biol.*, **62**, 71 (1984).
3) G. O. Till, J. R. Hatherill, W. W. Tourtellote, M. J. Lutz and P. A. Ward, *Am. J. Pathol.*, **119**, 376 (1985).
4) V. E. Kagan, "*Lipid Peroxidation in Biomembranes*," CRC Press, Boca Raton, FL., 1988.
5) K. Fukuzawa, S. Takase and H. Tsukatani, *Arch. Biochem. Biophys.*, **240**, 117 (1985).
6) H. Sies, *Angew. Chem. Int. Ed. Engl.*, **25**, 1058 (1986).
7) K. Fukuzawa, T. Tadokoro, K. Kishikawa, K. Mukai and J. M. Gebicki, *Arch. Biochem. Biophys.*, **260**, 146 (1988).
8) T. Ohyashiki, H. Ushiro and T. Mohri, *Biochim. Biophys. Acta*, **858**, 294 (1986).
9) L. Landi, P. Pasquali, P. Bassi and L. Cabrini, *Biochim. Biophys. Acta*, **902**, 200 (1987).
10) L. Landi, D. Fiorentini, L. Cabrini, C. Stefanelli and A. M. Sechi, *Biochim. Biophys. Acta*, **984**, 21 (1989).
11) V. Viti, R. Cicero, D. Callari, L. Guidoni, A. Bullitteri and G. Sichel, *FEBS Lett.*, **158**, 36 (1983).
12) G. W. Burton and K. U. Ingold, *Science*, **224**, 569 (1984).
13) I. Ya. Kon and L. Sh. Gorgoshidze, *Bull. Exp. Biol. Med.*, **99**, 428 (1985).
14) J. A. Buege and S. D. Aust, "Methods in Enzymology," Vol. 52, ed. by S. Fleisher and L. Packer, Academic Press, New York, 1978, pp. 302—310.
15) G. Minotti and S. D. Aust, *J. Biol. Chem.*, **262**, 1098 (1987).
16) C. Beauchamp and I. Fridovich, *Anal. Chem.*, **44**, 276 (1971).
17) E. D. Wills, *Biochem. Pharmacol.*, **21**, 1879 (1972).
18) M. J. Machlin, "Vitamin E," Marcel Dekker, New York, 1980.
19) H. P. Wang and T. Kimura, *Biochim. Biophys. Acta*, **423**, 374 (1976).
20) W. L. Porter, "Autoxidation in Food and Biological Systems," ed. by M. G. Sinic and M. Karel, Plenum Press, New York, 1980, pp. 295—366.
21) W. Bors, C. Michel and M. Saran, *Bull. Eur. Physiopathol. Respir. Suppl.*, **17**, 13 (1981).
22) G. Bartosz and W. Leyko, *J. Radiat. Biol.*, **39**, 39 (1981).
23) J. M. McCord and E. D. Day, *FEBS Lett.*, **86**, 139 (1978).
24) W. Bors, C. Michel and M. Saran, *Eur. J. Biochem.*, **95**, 621 (1979).
25) J. C. Edwards and P. J. Quinn, *J. Lipid Res.*, **25**, 944 (1982).
26) D. T. Sawyer and E. Nanni, "Oxygen and Oxy-radicals in Chemistry and Biology," ed. by M. A. J. Rodgers and E. L. Powers, Academic Press, New York, 1981, pp. 15—44.
27) J. A. Fee, "Oxygen and Oxy-radicals in Chemistry and Biology," ed. by M. A. J. Rodgers and E. L. Powers, Academic Press, New York, 1981, pp. 205—239.

High Paraoxon-Hydrolyzing Activity in Organophosphorous Insecticide-Resistant Mosquitoes

Mamoru WATANABE,[a] Sachiko TAKEBE,[b] and Kyoichi KOBASHI*,[b]

Toyama Institute of Health,[a] Nakataikouyama 17–1, Kosugi-machi, Toyama 939–03, Japan and Faculty of Pharmaceutical Sciences, Toyama Medical and Pharmaceutical University,[b] 2630 Sugitani, Toyama-shi 930–01, Japan. *Received October 11, 1990*

We found a strong paraoxon-hydrolyzing activity (23.4±8.50 nmol/h/individual and 137±86.2 nmol/h/mg protein) in the crude extract from larvae of *Culex tritaeniorhynchus* Toyama 89, which is markedly resistant to organophosphorous insecticides. The activity was higher than those from *Cx. tritaeniorhynchus re-e-ae* (0.175±0.0336 and 1.83±0.651), *Anopheles omorii* (0.112±0.0301 and 1.86±0.746) and *An. stephensi* (0.0651±0.0713 and 0.789±0.910), which are susceptible to organophosphorous insecticides. These facts suggest that the high paraoxon-hydrolyzing activity plays a role in the development of organophosphorous resistance in *Cx. tritaeniorhynchus*. The enzyme preparation obtained from Toyama 89 showed higher activity in the alkaline pH range and its K_m values to paraoxon were 0.67 mM in larvae and 0.50 mM in adults. A calcium ion was strictly required for the hydrolysis of paraoxon. Fenitroxon was also hydrolyzed, in addition to paraoxon. However, it did not degradate parathion and fenitrothion at all. Dichlorvos and phenyl acetate competitively inhibited the enzyme. The phenyl acetate-hydrolyzing activity in the preparation of Toyama 89 was significantly ($p<0.01$) lower than those in susceptible strains, and was irreversibly inhibited by paraoxon. Therefore, the paraoxon-hydrolyzing activity belongs to the class of organophosphate compound hydrolases; it must be thus distinguished from bacterial phosphotriesterase.

Keywords *Culex tritaeniorhynchus*; organophosphorous insecticide-resistance; paraoxon; paraoxonase; arylesterase; phenyl acetate

Introduction

Several mechanisms concerning the development of pesticide-resistance in insects have been reported as follows[1]; an alteration of acetylcholinesterase (AChE: the enzyme targeted by insecticides), an activation and induction of esterase, gene amplification of esterase and/or alteration of mixed-function oxidase *etc.* The *Culex tritaeniorhynchus* Toyama 89 strain was extremely resistant to both organophosphorous and carbamate insecticides.[2] Lethal concentration 50% (LC_{50}) values of dichlorvos, parathion or fenitrothion against the mosquito were 5875-, 2712- or 2541-fold higher than those against the *Cx. tritaeniorhynchus re-e-ae* strain, respectively. The great difference in these LC_{50} values between Toyama 89 and *re-e-ae* has never been reported in any insect of medical importance, and therefore it is very interesting to clarify the mechanism of its development of resistance to organophosphorous insecticides. Acetylcholinesterase from the Toyama strain has a markedly poor affinity to organophosphorous compounds,[3] and is altered from a true- to a pseudo-type.[4] Especially, the weak inhibition of AChE from Toyama with organophosphorous compounds roughly corresponds to an increase of the concentrations for lethality. We therefore suggest that in the Toyama strain, the AChE plays the major role in the development of the acquired resistance to organophosphorous insecticides. Moreover, we[2] and Takahashi and Yasutomi[5] showed that the naphthylacetate-hydrolyzing activity from the resistant strain was higher as compared to that from the susceptible strain, and that a zymogram for the naphthylacetate-hydrolyzing activity in Toyama differed from that in *re-e-ae*. Matsumura and Hogendijk[6] first reported the presence of parathion-hydrolyzing activity *in vitro* from houseflies, but that partially purified enzyme hydrolyzed little paraoxon. Welling *et al.*,[7] and Oppenoorth and Voerman[8] detected a low paraoxon-hydrolyzing activity from parathion-resistant houseflies and aphides, respectively. Kao *et al.*[9] reported that the purified esterase from insecticide-resistant houseflies had low paraoxon-hydrolyzing activity. Konno and Shishido[10] reported that the metabolites produced *in vivo* by hydrolysis of fenitroxon in an organophosphorus-resistant strain of rice stem borers were considerably detectable. In this paper, therefore, we measured a phosphotriester-hydrolyzing activity in a crude extract of the larvae, as well as the adults of *Cx. tritaeniorhynchus* Toyama 89 and *re-e-ae* strain.

Materials and Methods

Mosquitoes *Cx. tritaeniorhynchus* Toyama 89, *re-e-ae*, *Anopheles omorii* and *An. stephensi* were reared in our insectarium at 23±1 °C and a 16:8 (L:D) photoperiod. Lethal concentration 50% of various insecticides on these mosquitoes was reported previously[2] in detail. Larvae were fed on a powdered mixture containing insect food (Oriental Yeast Co., Tokyo, Japan) and dry beer yeast (Asahi Brewery Ltd., Tokyo, Japan) (ratio 1:1). Larvae (final stage) and adult mosquitoes (2 d after emergence) were stored at −30 °C until use.

Chemicals Paraoxon was purchased from Aldrich Chemical Co. Inc., WI, U.S.A., and parathion, fenitrothion, *O,O*-dimethyl-*O*-(2,2-dichlorovinyl)phosphate(dichlorvos) and phenyl acetate were purchased from Wako Pure Chemical Industries Ltd., Osaka, Japan. Fenitroxon was kindly supplied by Sumitomo Chemical Co. Ltd., Takarazuka, Japan. Phenylphosphorodiamidate was synthesized in our laboratory.

Preparation of Crude Extract from Mosquitoes In the case of Toyama 89, five larvae or ten adults were homogenized in 2 ml of 106 mM Tris HCl buffer, pH 8.5, containing 2.1 M sodium chloride, 50 mM calcium chloride and 0.1% Triton X-100 (buffer A) in a glass homogenizer with a Teflon pestle in an ice-bath. The homogenates were centrifuged at 20000×*g* for 30 min and the supernatants were used as a crude extract. In the cases of *re-e-ae*, *An. omorii* and *An. stephensi*, one hundred larvae or twenty adults were used to prepare a crude extract according to the method described above. In the experiment concerning the effect of salts, one hundred larvae of Toyama 89 were homogenized in 10 ml of 10 mM Tris HCl buffer, pH 8.5, containing 0.1% Triton X-100. The supernatants after the centrifugation at 20000×*g* for 30 min were used as a crude extract.

Separation of Hydrolyzed Products with Thin Layer Chromatography (TLC) Fifty larvae were homogenized in 10 ml of buffer A adjusted pH at 7.5 to prepare a crude extract. Paraoxon was incubated with 1.0 ml of the crude extract at 30 °C for the indicated period of time as shown in Table II. Eight hundred μl of the reaction mixture was extracted repeatedly three times with the same volume of ethyl acetate, then the organic layer was evaporated at 45 °C to dryness. The sediment was dissolved in 50 μl of acetone. Five μl of the sample was applied to a Silica gel F_{254} plate and was developed with the solvent system, benzene, ethyl acetate and hexane (ratio 2:2:1) at room temperature until a solvent front was

developed to 7 cm. Ultraviolet (UV) light was used for the detection of the products, and 2% sodium carbonate was sprayed for the coloring of 4-nitrophenol and 3-methyl-4-nitrophenol.

Measurement of Hydrolysis of Paraoxon and Fenitroxon Hydrolysis of paraoxon was measured by the method of Furlong *et al.*[11] with minor modification. Eight hundred μl of the crude extract was incubated at 30 °C for 1 h with 200 μl of 6 mM paraoxon in a 50 mM Tris HCl buffer, pH 8.5, containing 5% acetone. The absorbance at 405 nm was measured after centrifugation at 15000 × *g* for 5 min. The amount of hydrolyzed paraoxon or fenitroxon was calculated based on the molecular extinction coefficient of 4-nitrophenol (18050) or 3-methyl-4-nitrophenol (15100), respectively.

Hydrolysis of phenyl acetate was measured by the method of Lorenz *et al.*[12] with minor modification. One hundred μl of 18.8 mM phenyl acetate was added into 500 μl of buffer A preincubated at 30 °C for 5 min. The crude extract was added within 1 min after adding the substrate. After incubation for a further 10 min, 160 μl of 0.5 M ethylenediaminetetraacetic acid (EDTA) was added to terminate the reaction, then 60 μl of 8.9 mM aminoantipyrine and 30 μl of 213 mM potassium ferricyanide were added into the reaction mixture to measure the amount of produced phenol. The amount of hydrolyzed phenyl acetate was calculated based on the molecular coefficient of (3-benzoquinone-monoimino)-phenazone (8770) at 550 nm in buffer A. The two blanks for hydrolysis of paraoxon, fenitroxon and phenyl acetate were performed as follows: blank 1 omitting the substrate, and blank 2 omitting the crude extract.

The protein of the crude extract was determined with a BCA Protein Assay Reagent (Pierce Chemical Co., IL, U.S.A.) using bovine serum albumin as a standard.

Results

Hydrolysis of Paraoxon by Crude Extracts from Mosquitoes Paraoxon-hydrolyzing activity is found in crude preparations from larvae and adults of *Cx. tritaeniorhynchus* extracted with a buffer containing high concentrations of calcium chloride and sodium chloride. Their activity was extremely elevated as compared with the paraoxon-hydrolyzing activities from houseflies[7] and aphides.[8] The great difference among species of insects may be due to the presence of calcium chloride in a buffer used for homogenizing insects, since the buffer without calcium chloride could extract only a little activity from Toyama 89, and they[7,8] did not use a calcium-containing buffer for the preparation of insect extracts.

As shown in Fig. 1 and Table I, the activities per individual and those per mg protein from Toyama 89 larvae were significantly ($p<0.01$) higher (130- or 75-fold) than those from *re-e-ae* larvae, respectively. The values from Toyama 89 larvae were significantly ($p<0.01$) higher than those from adults of the same strain as shown in Figs. 1 and 2. The average activity per individual from female adults of Toyama 89 was significantly ($p<0.01$) 2.4-fold higher than from the males. Total protein amounts from the whole body of male mosquitoes were significantly ($p<0.01$) less than those of female ones, but there is a significant difference ($p<0.05$) between female and male Toyama 89 in the activity per mg protein. These results show that female mosquitoes possess higher paraoxon-hydrolyzing activity than males. However, no sexual difference in the activity was found in *re-e-ae*, and the activities from adults in a susceptible strain were significantly ($p<0.01$) higher than those from the larvae. These observations in the susceptible strain were inverse to those in the resistant strain.

An. omorii and *An. stephensi* were susceptible to organophosphorous insecticides as well as *Cx. tritaeniorhynchus re-e-ae*. The paraoxon-hydrolyzing activities of these two *Anopheles* and of *re-e-ae* resembled each other in both adults

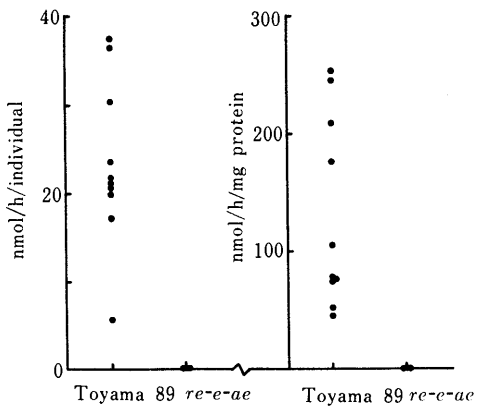

Fig. 1. Hydrolysis of Paraoxon with Larvae of *Cx. tritaeniorhynchus*

One point represents the activity from 5 larvae in Toyama 89 and from 100 larvae in *re-e-ae*.

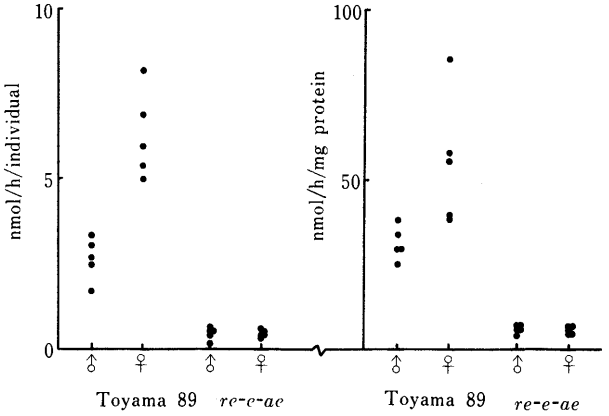

Fig. 2. Hydrolysis of Paraoxon with Adults of *Cx. tritaeniorhynchus*

One point represents the activity from 10 mosquitoes in Toyama 89 and 20 mosquitoes in *re-e-ae*.

TABLE I. Hydrolysis of Paraoxon with Some Mosquitoes

	Produced 4-nitrophenol (nmol/h/individual)				Produced 4-nitrophenol (nmol/h/mg protein)			
	Cx. tritaeniorhynchus		*An. omorii*	*An. stephensi*	*Cx. tritaeniorhynchus*		*An. omorii*	*An. stephensi*
	Toyama 89	*re-e-ae*			Toyama 89	*re-e-ae*		
Larvae	23.4 ±8.50[a]	0.175±0.0336[c]	0.112±0.0301[c]	0.0651±0.0713[c]	137 ±86.2[a]	1.83±0.651[c]	1.86±0.746[c]	0.789±0.910[c]
Adults								
Male	2.65±0.62[b]	0.481±0.131[c]	0.105±0.067[b]	0.240 ±0.153[b]	31.6± 4.85[b]	6.35±1.19[c]	1.03±0.702[b]	2.33 ±1.570[b]
Female	6.30±1.28[b]	0.492±0.080[c]	0.598±0.081[b]	0.418 ±0.197[b]	55.8±19.3[b]	6.23±0.932[c]	1.48±0.268[b]	0.745±0.357[b]

a) Average±S.D. of 10 experiments. *b*) Average±S.D. of 5 experiments. *c*) Average±S.D. of 3 experiments.

and larvae as shown in Table I, and they were significantly ($p<0.01$) lower than those of Toyama 89.

Hydrolysis of Fenitroxon by Crude Extract from Mosquitoes Fenitroxon was also hydrolyzed with the crude extract from both larvae and adults resistant to organophosphorous insecticides. The results shown in Table II were obtained by measuring hydrolysis at pH 7.5, because spontaneous hydrolysis of the substrates occurred at pH 8.5 during prolonged incubation time. The fenitroxon-hydrolyzing activity level in larvae or adults was 72% of the paraoxon-hydrolyzing activity level at the same concentration of substrates. However, parathion and fenitrothion were not hydrolyzed under the assay condition at all. Even though the concentrations of these thiono-compounds and the incubation pH were elevated to 0.5 mM and 8.5, respectively, no hydrolysis was detected. Strain *re-e-ae* also did not exhibit any parathion- or fenitrothion-hydrolyzing activity.

TABLE II. Hydrolysis of Oxo- and Thiono-Organophosphorous Insecticides by *Cx. tritaeniorhynchus*

	mM	Hydrolysis			
		nmol/4 h/larva		nmol/5 d/adult	
		Toyama 89	*re-e-ae*	Toyama 89	*re-e-ae*
Paraoxon	1	26.8	0.153	59.0	1.46
	0.1	4.15	<0.102	3.56	<0.0966
Parathion	0.1	<0.102	<0.102	<0.0966	<0.0966
Fenitroxon	0.1	3.00	<0.125	2.56	<0.115
Fenitrothion	0.1	<0.125	<0.125	<0.115	<0.115

Organophosphorous compounds (10 μl) were incubated with the crude extract (1.0 ml) for the indicated time. The values were calculated based on the molecular extinction coefficients of 4-nitrophenol and 3-methyl-4-nitrophenol at pH 7.5.

Identification of Products of Hydrolysis by TLC The reaction mixture (Table II) was extracted with ethyl acetate and the concentrated organic layer was then analyzed by TLC. The results obtained by using larvae extract were shown in Fig. 3. Three distinct quenching spots were observed: at the origin, at a substrate position and at an upper position in each lane under UV light. The third quenching spot corresponded to authentic 4-nitrophenol or 3-methyl-4-nitrophenol, and these spots were colored in alkaline. The third spot was therefore identified to be 4-nitrophenol or 3-methyl-4-nitrophenol. By incubating either paraoxon or fenitroxon with the crude extract from Toyama 89, the density of the third spot increased

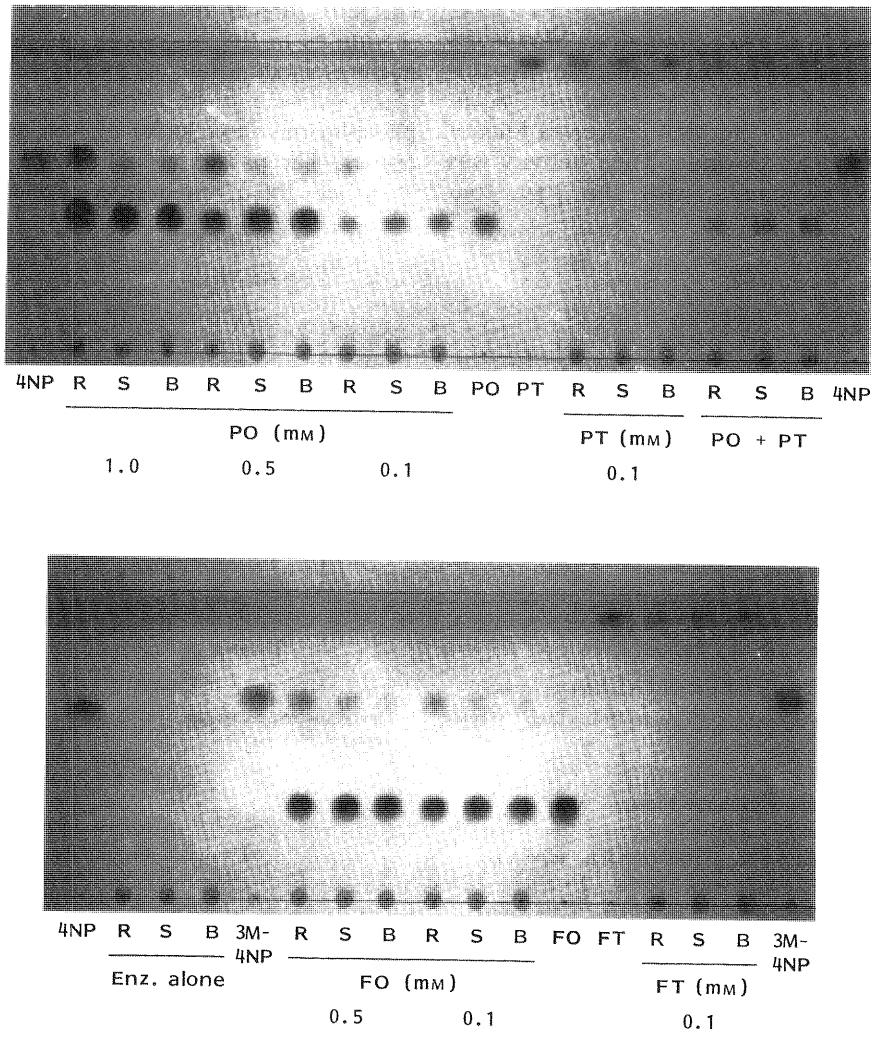

Fig. 3. Detection of 4-Nitrophenol (4NP) and 3-Methyl-4-Nitrophenol (3M4NP) Produced from Paraoxon (PO), Parathion (PT), Fenitroxon (FO) and Fenitrothion (FT)

Details of the method are described in the legend to Table II. R, S and B represent resistant strain extract (Toyama 89 larvae), susceptible strain extract (*re-e-ae* larvae), and a buffer as a control, respectively.

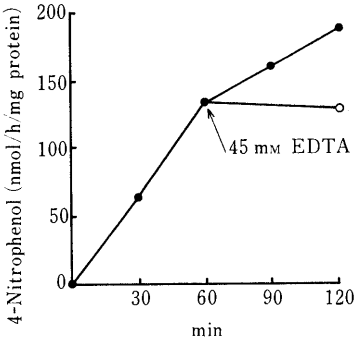

Fig. 4. Time Course of Paraoxon Hydrolysis

The crude extract of Toyama 89 larvae was prepared and the activity was measured at the indicated time according to Materials and Methods. After 60 min incubation, 100 μl of 500 mM EDTA in 50 mM Tris HCl buffer, pH 8.5, was added to the reaction mixture. The open circle represents the activity after a further 60 min incubation with EDTA.

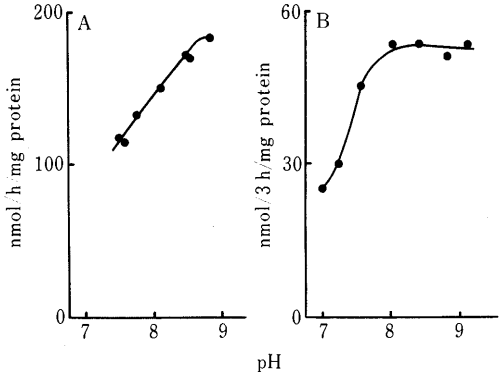

Fig. 5. Paraoxon Hydrolysis at Various pHs by Crude Extract of Toyama 89

A, larvae; B, adults.

The crude extract (170 μl) was incubated with buffer A (830 μl) at various pHs and 1.45 mM paraoxon. The amount of the hydrolyzed paraoxon was calculated based on the molecular extinction coefficient of 4-nitrophenol corrected at the corresponding pHs.

TABLE III. Effect of Divalent Ions on Paraoxon Hydrolysis

Ion	Produced 4-nitrophenol (nmol/h/mg protein)					
	With 2 M NaCl			Without 2 M NaCl		
	1 mM	10 mM	50 mM	1 mM	10 mM	50 mM
Mg^{2+}	9.20	10.9	12.6	13.2	13.5	23.9
Ca^{2+}	17.5	45.2	38.3	39.7	49.6	48.4
Mn^{2+}	7.67	18.9	31.5	19.7	20.4	35.6
Co^{2+}	7.11	16.4	24.5	14.5	14.9	9.29
Ni^{2+}	7.94	7.43	7.23	13.6	20.4	12.1
Zn^{2+}	9.96	30.1	3.83	11.8	18.9	6.68
None		6.01			11.8	

Crude extract (200 μl) from Toyama 89 larvae were incubated with 600 μl of the salt solutions at final concentrations described in the table.

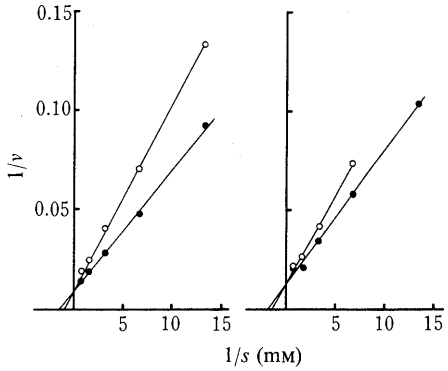

Fig. 6. Competitive Inhibition of Paraoxon Hydrolysis by Dichlorvos and Phenyl Acetate

The crude extract was incubated with 10 μM dichlorvos in the left figure or with 100 μM phenyl acetate in the right figure. The open and closed circles represent the activities in the presence and the absence of test compounds, respectively.

TABLE IV. Effect of Ca^{2+} on Paraoxon Hydrolysis

	Produced 4-nitrophenol (nmol/h/mg protein)
None	6.96
18 mM EDTA	1.21
Ca^{2+} 0.1 mM	12.7
1	35.4
10	89.2
50	114
90	91.0

Six larvae of Toyama 89 were extracted with 1.0 ml of the buffer A without calcium chloride.

dependently on the concentration of the substrate. In this condition, no other spot colored in alkaline was detected except spots of 4-nitrophenol, 3-methyl-4-nitrophenol, paraoxon and fenitroxon, with the result that no derivatives of 4-nitrophenol or 3-methyl-4-nitrophenol were produced. At the position of 3-aminophenol, which was produced by the reduction of 4-nitrophenol, no quenching spot was observed under UV light. These results, obtained from TLC analysis, evidently proved that paraoxon and fenitroxon were hydrolyzed to 4-nitrophenol and 3-methyl-4-nitrophenol, respectively and also that the enzyme(s) could not hydrolyze parathion and fenitrothion at all.

General Properties of Paraoxon-Hydrolyzing Activity When paraoxon was incubated with the crude extract obtained from the larvae of the resistant strain, 4-nitrophenol was progressively produced with time until 1 h, then the rate of production of 4-nitrophenol decreased (Fig. 4). 4-Nitrophenol increased for 1 h of incubation to 20 μM in a final concentration, but the product inhibition at the concentration was not observed. Therefore, the inactivation gradually occurred during long-term incubation at 30 °C. Inactivation was also observed during preincubation for 15 min at 30 °C (88% of the original activity) and at 45 °C (complete loss of activity).

Hydrolysis of paraoxon was terminated by the addition of EDTA (Fig. 4) because little activity was exhibited in the presence of EDTA. Table III showed the effects of sodium chloride and divalent cations on paraoxon-hydrolyzing activity. The highest activity was observed in the presence of Ca^{2+} without sodium chloride. As shown in Table IV, 50 mM Ca^{2+} was required for the maximal activity. Zn^{2+}, Mn^{2+} and Co^{2+} at 10 mM activated the paraoxon hydrolysis as well as Ca^{2+} with sodium chloride. Higher activities with sodium chloride than without the salt were observed with 50 mM Co^{2+} as well as 10 mM Zn^{2+}, but a contrary effect of sodium chloride was shown with 1 mM Ca^{2+}, 10 mM Ni^{2+} and 50 mM Mg^{2+}. We have no explanation for the various effects of sodi-

TABLE V. Hydrolysis of Phenyl Acetate by Crude Extract from Mosquitoes

	Hydrolysis of phenyl acetate	
	μmol/h/individual	μmol/h/mg protein
Cx. tritaeniorhynchus		
Toyama 89	0.368±0.0536	6.39±0.192
re-e-ae	0.666±0.118	6.23±1.46
An. omorii	2.20 ±0.188	8.69±1.24
An. stephensi	5.79 ±1.07	28.3 ±3.60

Twenty larvae were extracted with 2 ml of the buffer A, and the preparation method of the crude extract was described in Materials and Methods. The value is the average±S.D. of 5 experiments.

um chloride on the activation by divalent ions.

The effect of pH on paraoxon hydrolysis as shown in Fig. 5 indicated that the maximal activity in larvae was at around pH 9.0 but that in adults, maximal activity ranged from pH 8 to 9. The K_m values of paraoxon were 0.67 mM in larvae and 0.50 mM in adults. Dichlorvos (10 μM) and phenyl acetate (0.1 mM) competitively inhibited the paraoxon-hydrolyzing activity as shown in Fig. 6. However, 0.1 mM each of parathion, phenylphosphorodiamidate and *O*-cumenyl methylcarbamate did not inhibit this activity at all. One % 1-butanol, 1-propanol or dioxan in the assay mixture for the measurement of paraoxon-hydrolyzing activity decreased it to 46, 81 or 73% of the activity measured in 1% acetone, in that order. The activity observed in the presence of 1% methanol, ethanol or dimethyl sulfoxide was the same value as that in 1% acetone.

Hydrolysis of Phenyl Acetate by Crude Extract of Mosquitoes Phenyl acetate was hydrolyzed with four species of larvae under the same condition as for paraoxon-hydrolyzing activity, as shown in Table V. The highest activity was detected with *An. stephensi*, whose activities per individual and mg protein were 39000- and 89000-fold higher than those of its paraoxon hydrolysis, respectively. The activity per individual from Toyama 89 larvae was significantly ($p<0.01$) lower than those from three species of larvae which were susceptible to organophosphorous insecticides. The phenyl acetate-hydrolyzing activity from Toyama 89 larvae was almost completely inhibited by paraoxon at 1.2 mM, which was the same concentration as a substrate concentration for the measurement of paraoxon-hydrolyzing activity. The inhibited preparation was gelfiltrated though Sephadex G-25 to remove free-paraoxon, but phenyl acetate-hydrolyzing activity was not restored any more even after 1 h of incubation. After this procedure, however, the paraoxon-hydrolyzing activity was kept at half of the original activity, independently, whether the crude extract was preincubated with paraoxon or not. These results therefore suggest that the paraoxon-hydrolyzing enzyme should be distinguished from the phenyl acetate-hydrolyzing enzyme.

Discussion

Cx. tritaeniorhynchus Toyama 89 was a unique strain, having the highest resistance to organophosphorus insecticides among insects of medical importance as reported previously.[2,13] Our results indicated that the larvae of Toyama 89 had a higher phosphotriesterase activity, which was measured by using paraoxon and fenitroxon as substrates. This activity was at least 130-fold higher than that of organophosphate-susceptible strains such as *re-e-ae*, *An. omorii* and *An. stephensi*. A small correlation between the degree of resistance and paraoxon-hydrolyzing activity in houseflies[7] and aphides[8] might be due to a low degree of resistance in these insects. On the other hand, LC_{50} of paraoxon to *Cx. tritaeniorhynchus* was 4.25 ppm, which was similar to that of parathion (5.46 ppm). This similarity agreed with LD_{50} values of fenitrothion and fenitroxon to rice stem borers[14] and planthoppers.[15] Therefore, our results suggested that a rate of conversion of parathion to paraoxon did not participate in the development of resistance to organophosphorous compounds.

The crude extract from Toyama 89 did not hydrolyze parathion and fenitrothion, although Matsumura and Hogendijk[6] reported that the partially purified enzyme from resistant houseflies showed parathion-hydrolyzing activity. It has not been reported whether the homogenates of insecticide-resistant insects showed parathion-hydrolyzing activity, except for their report.[6] Their enzyme might have been contaminated with bacteria, since parathion-hydrolyzing activity has been reported to be present in some bacteria.[16] The paraoxon-hydrolyzing activity shown in insects must be different from phosphotriesterases detected in bacteria, since the purified phosphotriesterases from bacteria hydrolyze parathion as well as paraoxon.[17]

Paraoxon-hydrolyzing activity from the sera of humans was stimulated by adding sodium chloride,[18] while the salt did not affect the activity from Toyama 89 in the presence of calcium chloride. In our experiment, the stimulation of the activity by salt was observed in the presence of 10 mM zinc ion. The requirement for a zinc ion was reported in bacterial phosphotriesterase,[19] which contains one atom per subunit and is irreversibly inactivated by the loss of a zinc ion. In this study, we found that the paraoxon-hydrolyzing enzyme required a calcium ion, but it is not clear how the calcium ion participates in the enzyme–substrate interaction. This problem will be clarified by using the enzyme purified from Toyama 89 in the future.

K_m values of paraoxon were found to be several hundred μM, and these values were extremely higher than those reported in houseflies[7] and aphides,[8] which were several hundred pM and several nM, respectively. Poor affinity of the Toyama 89 enzyme to paraoxon may indicate a low correlation between the expression of resistance and paraoxon-hydrolyzing activities. However, if paraoxon is condensed in some cells or the subcellular particles of insects, it is possible that paraoxon is degraded with the enzyme. Our assumption is supported by the high solubility of parathion and paraoxon in lipid layers.

Phenyl acetate-hydrolyzing activity, classified as arylesterase EC 3.1.1.2 by the Nomenclature Committee, includes A-esterase, namely paraoxonase. The "International Meeting on Esterases Hydrolyzing Organophosphorus Compounds"[20] recommended to the NC-IUB that the paraoxonase is segregated from arylesterases to "Organophosphorus Compound Hydrolase," which is a new category. Phenyl acetate-hydrolyzing activity in our preparation was observed in all four species tested, while the degrees of their activities did not correlate with the

expression of resistance to organophosphorous insecticides. On the contrary, the resistant strain showed lower activity than the susceptible strains. Moreover, phenyl acetate hardly inhibited the paraoxon-hydrolyzing activity, but the phenyl acetate-hydrolyzing activity was irreversibly inhibited by paraoxon. We therefore propose that these two compounds are degraded in insects by different enzymes.

Consequently, we suggest that higher paraoxon-hydrolyzing activity and lower affinity of organophosphorus-insecticides to acetylcholinesterase[3] are related to the development of organophosphorus-resistance in *Cx. tritaeniorhynchus* Toyama 89. But we have not tested the permeability of insecticides into the insect or the conversion from parathion to paraoxon in the present experiment. Further investigations on these points of view will be required in order to prove the mechanism of development of resistance in *Cx. tritaeniorhyncus*.

Acknowledgement We thank Ms. S. Takayanagi for her help in the preparation of the manuscript.

References

1) "Pest Resistance to Pesticides," ed. by G. P. Georghiou and T. Saito, Plenum Press, New York and London, 1983, pp. 175—331.
2) M. Watanabe, S. Takebe, R. Arakawa, K. Kamimura and K. Kobashi, *Jpn. J. Sanit. Zool.*, **42**, 15 (1991).
3) M. Watanabe, S. Takebe, D.-H. Kim, R. Arakawa, K. Kamimura, and K. Kobashi, *Chem. Pharm. Bull.*, **36**, 312 (1988).
4) M. Watanabe, S. Takebe, D.-H. Kim, K. Kobashi, R. Arakawa, and K. Kamimura, *Eisei Kagaku*, **35**, 479 (1989).
5) M. Takahashi and K. Yasutomi, *J. Med. Entomol.*, **24**, 595 (1987).
6) F. Matsumura and C. J. Hogendijk, *J. Agric. Food Chem.*, **12**, 447 (1964).
7) W. Welling, P. Blaakmeer, G. J. Vink, and S. Voerman, *Pestic. Biochem. Physiol.*, **1**, 61 (1971).
8) F. J. Oppenoorth and S. Voerman, *Pestic. Biochem. Physiol.*, **5**, 431 (1975).
9) L. R. Kao, N. Motoyama, and W. C. Dauterman, *Pestic. Biochem. Physiol.*, **23**, 228 (1985).
10) Y. Konno and T. Shishido, *J. Pesticide Sci.*, **12**, 469 (1987).
11) C. E. Furlong, R. J. Richter, S. L. Seidel, and A. G. Motusky, *Am. J. Hum. Genet.*, **43**, 230 (1988).
12) K. Lorentz, B. Flatter, and E. Augustin, *Clin. Chem.*, **25**, 1714 (1979).
13) M. Watanabe, R. Arakawa, and K. Kamimura, *Jpn. J. Sanit. Zool.*, **41**, 51 (1990).
14) Y. Konno, T. Shishido, and F. Tanaka, *J. Pesticide Sci.*, **11**, 393 (1986).
15) T. Miyata and T. Saito, *J. Pesticide Sci.*, **3**, 179 (1978).
16) D. M. Munnecke, *Appl. Environ. Microbiol.*, **32**, 7 (1976).
17) W. J. Donarski, D. P. Dumas, D. P. Heitmeyer, V. E. Lewis, and F. M. Raushel, *Biochemistry*, **28**, 4650 (1989).
18) J. Ortigoza-Ferado, R. J. Richter, S. K. Hornung, A. G. Motulsky, and C. E. Furlong, *Am. J. Hum. Genet.*, **36**, 295 (1984).
19) D. P. Dumas, S. R. Caldwell, J. R. Wild, and F. M. Raushel, *J. Biol. Chem.*, **264**, 19659 (1989).
20) M. I. Mackness, *Biochem. Pharm.*, **38**, 385 (1989).

Mechanism of Immunosuppression by a Murine Non-specific Suppressor T Cell Line, SB-1

Kunio EZAWA, Satoshi TOYOSHIMA and Toshiaki OSAWA*

Division of Chemical Toxicology and Immunochemistry, Faculty of Pharmaceutical Sciences, University of Tokyo, Hongo, Bunkyo-ku, Tokyo 113, Japan. *Received October 11, 1990*

The mechanism of immunosuppression by a murin non-specific suppressor T cell clone (SB-1), which was established from concanavalin A (Con A)-activated murine spleen cells [*Jpn. J. Exp. Med.*, 53, 139 (1983)], was investigated. SB-1-induced decrease of antigen non-specific plaque-forming cell (PFC) response was restored by the addition of 5×10^{-6} M indomethacin, an inhibitor of cyclooxygenase. On the other hand, suppressive activity for antigen non-specific PFC response was found in the culture supernatant of SB-1 cells in the presence of proteose peptone-elicited macrophages. This induction of the suppressive activity was also inhibited by 5×10^{-6} M indomethacin. Furthermore, 10^{-5} M prostaglandine E_2 (PGE_2) was found to induce suppressive activity in the culture supernatant of SB-1 cells. 10^{-5} M PGE_2 did not suppress interleukin-2 (IL-2)-dependent proliferation of SB-1 cells, but increased a small quantity of protein synthesis and deoxyribonucleic acid (DNA) synthesis of SB-1 cells in the absence of IL-2. These results suggest that a cyclooxygenase product(s) such as PGE_2 from macrophages may induce production of soluble suppressor factors in SB-1 cells.

To characterize these suppressor factors, those in the culture supernatant of PGE_2-stimulated SB-1 cells were partially purified by ammonium sulfate fractionation and sequential column chromatographies on diethylaminoethyl (DEAE)-cellulofine and Sephacryl S-200. Suppressor activities were eluted at the positions corresponding to the molecular masses of 10, 30, 70 and over 70 kilodalton (kDa) on Sephacryl S-200 column chromatography. Quite interestingly, the suppressive effects of 10 and 30 kDa factors on non-specific PFC response were reversed by 1 mM *N*-acetyl-galactosamine but not by equimolar concentration of D-glucose, α-methyl-D-mannoside and L-rhamnose. It seemed that these factors had sugar binding activity like lectins.

Keywords non-specific suppressor T cell; macrophage; prostaglandin E_2 (PGE_2); suppressor factor; plaque-forming cell (PFC) response

Introduction

It has been reported that suppressor T cells are generated in many different experimental systems and are related to much of the regulation of the immune response.[1] These cells are classified into two groups, *i.e.*, antigen specific suppressor T cells and antigen-non-specific T cells. A common feature of these suppressor T cells is that their suppressor functions are at least partly mediated by soluble factors. Some of these factors have been already identified.[2-6] However, the mechanism of immunosuppression by suppressor T cells has not been fully elucidated.

As described previously,[7] we established murine antigen-non-specific suppressor T cell lines and showed that the suppressive activity of these cell lines is exerted at least partly *via* soluble factors. In the present study, the mechanism of the suppression of antibody production by one of these cell lines was investigated.

Materials and Methods

Mice Female (C57BL/6 × DBA/2)F_1 (BDF_1) and BALB/c mice were obtained from Charles River Japan (Kanagawa, Japan). They were 8 to 20 weeks old.

Reagents and Media Prostaglandin E_2 (PGE_2), prostaglandin $F_{2\alpha}$ ($PGF_{2\alpha}$), 6-ketoprostaglandin $F_{1\alpha}$ (6-KetoPGF$_{1\alpha}$), prostaglandin B_2 (PGB_2), prostaglandin D_2 (PGD_2) and indomethacin were purchased from Sigma (St. Louis, MO, U.S.A.). Prostaglandins and indomethacin were solubilized in ethanol at a concentration of 10^{-2} M and stored at −80°C. RPMI 1640 medium (Gibco, Grand Island, NY, U.S.A.) was adjusted to pH 7.2 and supplemented with 2 mM glutamine, 60 μg/ml kanamycin (Meiji Seika Co., Tokyo, Japan). Fetal calf serum (FCS) was purchased from M.A. Bioproducts (Walkersville, MD, U.S.A.). Concanavalin A (Con A) and pokeweed mitogen (PWM) were from Honen Oil Co. (Tokyo, Japan) and Gibco, respectively. Proteose peptone was from Difco (Detroit, MI, U.S.A.). *N*-Acetyl-D-galactosamine (GalNAc), D-glucose, α-methyl-D-mannoside (α-MM) and L-rhamnose were obtained from Sigma.

Cloned Non-specific Suppressor T Cells A non-specific suppressor T cell clone, SB-1, was established from Con A activated murine spleen cells.[7] Several other clones with (SE-7) and without suppressive activity (SA-2, SB-5, SF-1, SF-7 and SF-11) were also used in this study. In some experiments, SB-5 cells were used as negative control without suppressive activity.

Cell Cultures To investigate the effect of prostaglandins on SB-1 or SB-5 cells, the cells (10^4—10^5 cells/ml) in 10% FCS–RPMI 1640 medium were cultured with an appropriate concentration of prostaglandins on a tissue culture plate with 96 round-bottomed wells (Nunc, Rockilde, Denmark) in the presence or absence of interleukin-2 (IL-2). After incubation at 37 °C for 48 h, 0.5 μCi [^{3}H]TdR (NEN, Boston, MA, U.S.A.) was added to each well and the cells were subsequently cultured for 17 h at 37 °C. The radioactivity was measured with a liquid scintillation system.

Co-culture of Suppressor Cells with Syngeneic Macrophages Peritoneal exudate macrophages were isolated from BDF_1 mice 3 d after intraperitoneal injection of 1.5 ml of 10% proteose peptone solution. Cells were cultured at a concentration of 2×10^6 cells/ml on a 96 flat-bottomed plate (Falcon, Oxnard, CA, U.S.A.) in 5% FCS–RPMI 1640 medium. After incubation at 37 °C for 90 min, the cultures were washed twice to remove nonadherent cells. The adherent cells were treated with 40 μg/ml of mitomycin C (Kyowa Hakko, Tokyo, Japan) and anti-Thy 1.2 (AKR anti-C3H) plus complement (Cederane, Ontario, Canada). More than 90% of the cells were macrophages, as judged by their ability to take up latex beads and by morphological observations. After incubation at 37 °C for 60 min, 4×10^4 suppressor T cells were added to each well and the co-cultures of suppressor T cells with macrophages were further incubated at 37 °C for 48 h. Twenty μl of the culture supernatant from each well was removed and added to plaque-forming cell (PFC) culture.

Preparation of Culture Supernatant Containing IL-2 To maintain cloned suppressor T cells, culture supernatants of Con A-activated BALB/c mouse spleen cells, which have IL-2 activity, were prepared as described previously.[7] These culture supernatants were used as IL-2.

Hemolytic Plaque Assay Primary polyclonal immunoglobulin M (IgM) response stimulated with PWM was assayed as described by Gronowicz *et al.*[8] For the assay of non-specific suppressive activity of cloned T cells, the cells were cultured as described previously.[7] Briefly, 10^6 murine spleen cells were cultured with 10^3—10^5 suppressor T cells or 20 μl sample solution (culture supernatants or fractions from column chromatographies) in 1 ml of 10% FCS–RPMI 1640 medium supplemented with 5×10^{-5} M 2-mercaptoethanol (20ME) in the presence of PWM (20 μg/ml) at 37 °C

for 72 h and then the number of PFC was determined. To investigate the effect of sugars on the suppressive activity, D-glucose, α-methyl-D-mannoside (α-MM), L-rhamnose or *N*-acetyl-D-galactosamine (GalNAc) was added to the culture of PFC at a final concentration of 1 mM.

Analysis of Arachidonate Metabolites Peritoneal exudate cells (PEC, 2×10^6/ml/well) from BDF_1 mice, suspended in 5% FCS–RPMI 1640 medium, were cultured in a 24-well culture plate for 90 min at 37 °C. After removal of non-adherent cells, 1 ml of RPMI 1640 medium containing 10 μCi of ^{3}H-arachidonic acid (80—120 Ci/mmol, NEN) was added to each well and the cells were incubated for 30 min at 37 °C in the presence or the absence of 10 μM indomethacin. Then the cells were washed with RPMI 1640 medium to remove excess ^{3}H-arachidonic acid and further incubated for 30 min at 37 °C in RPMI 1640 medium. Reaction was stopped by the addition of acetic acid at a final concentration of 1%. Radio-labeled arachidonic acid metabolites were extracted with chloroform–methanol (1 : 1) and developed on a thin layer plate (Silica gel 60 plate, E. Merck, Darmstadt, Germany) with benzene : dioxane : acetic acid (60 : 30 : 3, v/v). Radioactivity in the separated metabolites was measured by a liquid scintillation system.

Metabolic Label of Suppressor Factors SB-1 cells were cultured in 10% FCS–RPMI 1640 medium containing 20% culture supernatant with IL-2 activity on a 96 flat-bottomed well plate. When the cell density reached about 10^4 cells/well, the cells were washed with warmed RPMI 1640 medium and then 0.2 ml of 2% FCS–RPMI 1640 medium containing 0.5 μCi ^{3}H-leucine (45 Ci/mmol, Amersham, UK) and various amounts of prostaglandins were added to the wells. After incubation at 37 °C for 1 h, the supernatants was collected and 1 ml of the supernatant was applied onto a Sephadex G-25 column. Equal volume of 10% trichloroacetic acid was added to void volume fractions eluted from Sephadex G-25 columns and the radioactivity of acid insoluble materials was determined.

Partial Purification of Suppressor Factors SB-1 cells at a concentration of 2×10^4/ml were incubated in a Corning 25 cm^2 flask at 37 °C for 5 d in 10% FCS–RPMI 1640 medium containing 40% culture supernatant with IL-2 activity. After 5 d incubation, SB-1 cells attached firmly to the culture flask were gently washed with warmed RPMI-1640 medium. Then, 10 ml of 10% FCS–RPMI 1640 medium containing 10^{-5} M PGE_2 was added to the flask and the cells were incubated at 37 °C for 24 h. The cell-free supernatant (crude suppressor factor fraction) was collected by centrifugation. To obtain control supernatant, SB-1 cells were incubated in 10% FCS–RPMI 1640 medium without 10^{-5} M PGE_2, and after 27 h of incubation PGE_2 was added to the culture at a final concentration of 10^{-5} M. The suppressive activity in culture supernatant (50 ml) was concentrated by salting-out techniques with saturated ammonium sulfate. Concentrated materials were dialyzed against 10 mM phosphate buffer (pH 7.4) containing 10 mM NaCl and 0.2 mM phenylmethylsulfonyl fluoride (PMSF, Sigma), and applied onto a DEAE-cellulofine column (3 × 30 cm) equilibrated with the same buffer. The elution was carried out with a concentration gradient of NaCl between 10 and 180 mM. Active fractions were collected and concentrated in a collodion bag (S.M. 13200; Sartorious membrane filter GmBH, Göttingen, Germany). Then, suppressor factors were further puriffed by gel permeation chromatography on a Sephacryl S-200 column (1.5 × 95 cm). The column was equilibrated with 10 mM phosphate buffer (pH 7.4) containing 150 mM NaCl. The elution was carried out with the same buffer.

Results

Restoration of SB-1-Induced Decrease of PFC Response by Indomethacin The number of PFC was in inverse proportion to that of SB-1 cells added to PWM-induced primary PFC cultures. When the number of SB-1 cells added to the cultures was 10^4, this decrease of PFC was restored by the addition of indomethacin (Fig. 1). 5×10^{-6} M of indomethacin completely restored the PFC response. The addition of 5×10^{-6} M of indomethacin to the primary PFC cultures without SB-1 cells did not affect the PFC response. Low concentration of indomethacin (1.25×10^{-6} M) induced a slight increase of PFC numbers in the same cultures but it did not seem to be significant. High concentration of SB-1 cells (10^5 cells/well) showed very strong inhibitory effect on the PFC response, and in the presence of 10^5 SB-1 cells, even 5×10^{-6} M indomethacin was not able to restore the response.

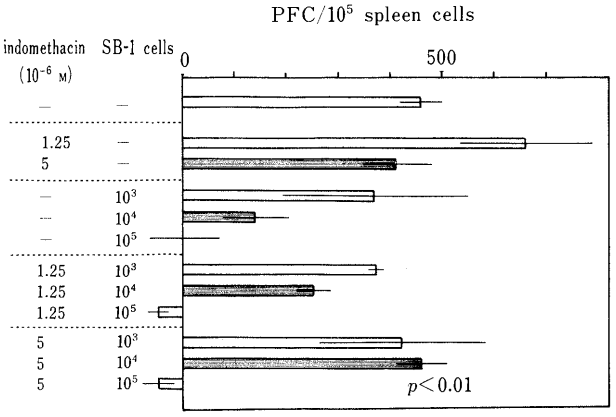

Fig. 1. Restoration of SB-1-Induced Decreases of Primary PFC Response

Indomethacin was added at a concentration of 1.25 or 5×10^{-6} M to the assay culture. The details of hemolytic plaque assay are given in Materials and Methods.

TABLE I. Effect of Supernatants from Co-cultures of Murine Cloned T Cells with Macrophages on Antigen Non-specific PFC Response

T cell clone	Macrophage	PFC/10^5 spleen cells[a] Exp. 1	Exp.2	Exp.2 Indomethacin[b]
—	—	343±22	321±37	ND[c]
—	+	325±41	351±59	372±46
SA-2	+	364±72	ND	ND
SB-1	−	ND	276±41[e]	ND
SB-1	+	199±47[d]	182±38	289±43[f]
SB-5	+	319±41	ND	ND
SE-7	+	287±82	ND	ND
SF-1	+	273±21	ND	ND
SF-7	+	329±77	ND	ND
SF-11	+	319±33	ND	ND

a) Each value is expressed as the mean±S.E. ($n=4$). *b*) 5×10^{-6} M. *c*) Not determined. *d*) $p<0.01$ *vs.* T cell clone −, macrophage −. *e*) $p<0.05$. *vs.* T cell clone −, macrophage −. *f*) $p<0.02$ *vs.* SB-1, macrophage +.

Suppressive Activity in the Culture Supernatant of SB-1 Cells Mixed with Peritoneal Exudated Macrophages The supernatant from co-culture of SB-1 cells with macrophages showed suppressive activity for the primary PFC response. As shown in Table I, significant suppressive activity was observed in the culture supernatant from the co-culture of SB-1 cells and macrophages, but not in those from the co-cultures of other cloned T cells and macrophages. The addition of 5×10^{-6} M indiomethacin, a cyclooxygenase inhibitor, to the culture inhibited the induction of suppressive activity. The supernatant from the culture of SB-1 cells without macrophages also showed weak but meaningful suppressive activity. It seemed that SB-1 cells mainly produced suppressor factors in the presence of macrophages.

Arachidonate Metabolites in the Culture Macrophages Macrophages were prelabeled with ^{3}H-arachidonic acid and the arachidonate metabolites in the culture of macrophages were analyzed. Only PGE_2 was clearly detected among cyclooxygenase products (Fig. 2). The production of PGE_2 was inhibited by indomethacin. The arachidonate metabolites in the co-culture of SB-1 cells and macrophages were also analyzed and were quite similar to

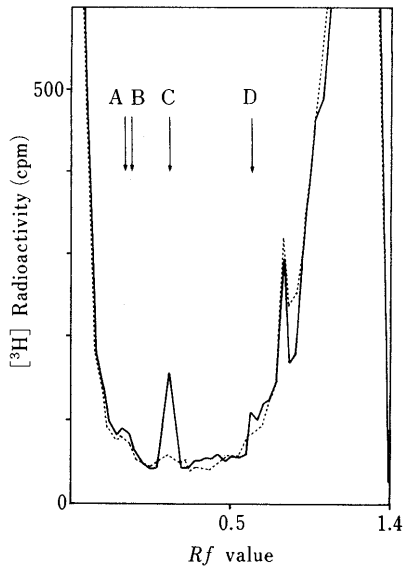

Fig. 2. Production of PGE_2 in Mouse Peritoneal Exudated Cells and its Inhibition by Indomethacin

The details of analysis of arachidonate metabolites are given in Materials and Methods. *Rf* values of 6-ketoPGF$_{1\alpha}$ (A), PGF$_{2\alpha}$ (B), PGE_2 (C) and PGD_2 (D) are indicated by the arrows. —, without indomethacin; ---, with indomethacin.

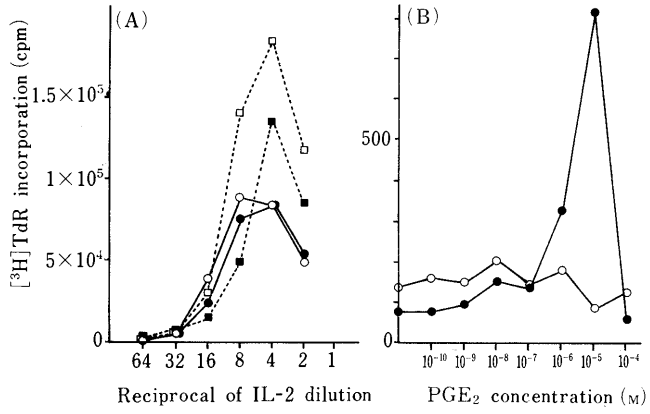

Fig. 3. Effect of PGE_2 on SB-1 Cell Growth

(A) IL-2 dependent growth of a suppressor clone, SB-1 and a non-suppressor clone, SB-5 in the presence or absence of PGE_2. In RPMI-10% FCS supplemented with various concentrations of IL-2, SB-1 or SB-5 cells (2×10^4 cells/well) were cultured with or without PGE_2. After 24 h, 1 μCi of ^{3}H-TdR was added to each well and pulsed for 15 h; then the incorporated radioactivity was determined. ■---■, SB-5 cells with 10 μM PGE_2; ●—●, SB-1 cells with 10 μM PGE_2; □---□, SB-5 cells without PGE_2; ○—○, SB-1 cells without PGE_2. Each symbol represents the mean of triplicate cultures. (B) Effect of PGE_2 on ^{3}H-TdR incorporation in SB-1 cells in the absence of IL-2. SB-1 (●—●) or SB-5 (○—○) cells (2×10^4 cells/well) were cultured with PGE_2 at the concentration indicated. 1 μCi ^{3}H-TdR was added to each well and pulsed for 15 h.

those in the culture of macrophages (data not shown).

Effect of PGE_2 on Deoxyribonucleic Acid (DNA) and Protein Synthesis of SB-1 Cells The above results suggest that a cyclooxygenase product(s), especially PGE_2, plays an important role in the production of suppressor factors in the co-culture of SB-1 cells and macrophages. Therefore, the effects of PGE_2 on ^{3}H-TdR and ^{3}H-leucine incorporation, and the suppressor factor production by SB-1 cells were investigated.

As shown in Fig. 3A, in the presence of IL-2, PGE_2 inhibited ^{3}H-TdR incorporation into SB-5 cells, but had little effect on that into SB-1 cells. On the other hand, in the absence of IL-2, high concentration of PGE_2 (10^{-6} to 10^{-5} M) increased ^{3}H-TdR incorporation into SB-1 cells (Fig. 3B). High concentration of PGE_2 (10^{-5} M) also induced an increase in protein synthesis of SB-1 cells cultured in the absence of IL-2 (Table II). $PGF_{2\alpha}$ did not increase ^{3}H-TdR incorporation into SB-1 cells (data not shown) but increased protein synthesis slightly. Con A and PGB_2 did not affect the protein synthesis of SB-1 cells. Since the culture supernatant from PGE_2-stimulated SB-1 cells suppressed PWM-induced primary PFC response and this induction of the suppressive activity was inhibited by the addition of actinomycin D to the culture (data not shown), it seems that PGE_2 activates SB-1 cells and induces increases in the production and secretion of proteins including suppressor factors.

TABLE II. Effect of PGE_2 on Protein Synthesis in SB-1 Cells

Medium	^{3}H-Leucine incorporated (cpm)[a]
RPMI-2% FCS	869±128[b]
2 μg/ml Con A	1055±139
+20% IL-2	1946±139
+10^{-8} M PGE_2	1141±116
+10^{-5} M PGE_2	1655±143[c]
+10^{-5} M $PGF_{2\alpha}$	1403±141[c]
+10^{-5} M PGB_2	1087±191
+10^{-5} M PGE_2+20% IL-2	1899±244

a) Supernatant containing metabolically labeled proteins with ^{3}H-leucine was applied on a Sephadex G-25 column, and radioactivity in the void volume fraction was determined. *b*) The means ± S.D. (triplicate cultures). *c*) $p<0.05$ *vs.* control.

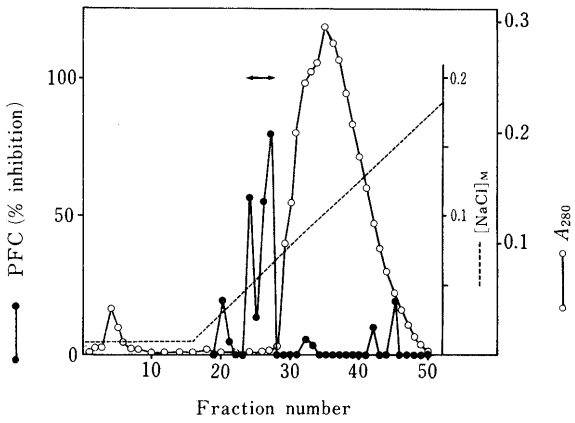

Fig. 4. DEAE-Cellulofine Column Chromatography on Suppressor Factors from SB-1 Cells

Details are given in Materials and Methods. Fractions of 5 ml were collected at 4 °C. For the assay of suppressive activity, 20 μl of each fraction was added to PFC culture. The value of control PFC was 1020±135/10^5 spleen cells.

Fractionation of Suppressor Factors in the Culture Supernatant from PGE_2-Stimulated SB-1 Cells SB-1 cells were cultured in 10% FCS–RPMI 1640 medium with 10^{-5} M PGE_2 at 37 °C for 24 h. Then, the suppressive activity in the culture supernatant was concentrated by ammonium sulfate fractionation (50—80% saturation). Since the suppressive activity was not observed in the 50—80% ammonium sulfate fraction of the control supernatant which contained 10^{-5} M PGE_2, it seemed that the suppressive activity detected in the culture supernatant from PGE_2-stimulated SB-1 cells was not due to contaminated PGE_2. After dialysis, the concentrated materials were applied to a DEAE-cellulofine column. The suppressive activity was

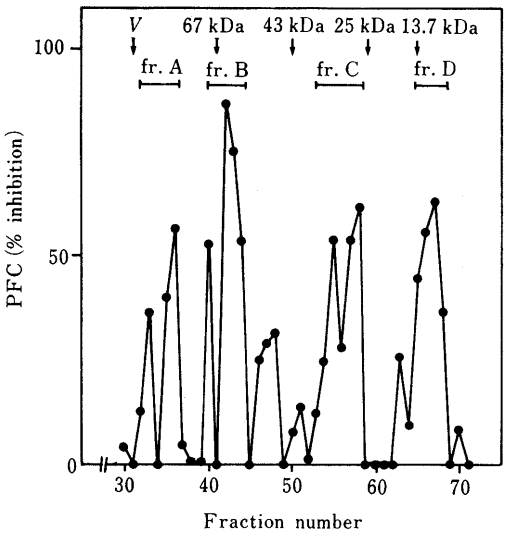

Fig. 5. Sephacryl S-200 Column Chromatography of Suppressor Factors from SB-1 Cells

Details are given in Materials and Methods. Fractions of 1.7 ml were collected. For the assay of suppressive activity, 20 μl of each fraction was added to PFC culture. The value of control PFC was $395 \pm 90/10^5$ spleen cells. Molecular weight markers: 67 kDa, bovine serum albumin; 43 kDa, ovalbumin; 25 kDa, chymotrypsinogen A; and 13.7 kDa, ribonuclease A.

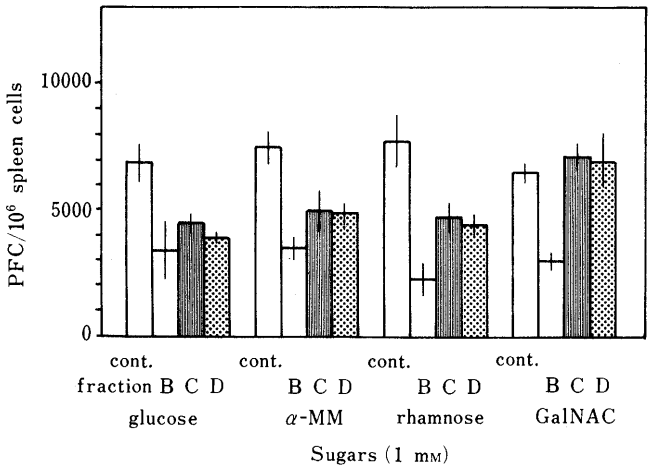

Fig. 6. Effect of Sugars on the Suppressive Activity of Frs. B, C and D from the Gel Filtration Column of Sephacryl S-200

Details of the effect on hemolytic plaque assay inhibition are given in Materials and Methods.

eluted at NaCl concentrations between 0.05—0.07 M (Fig. 4). Then, the active fractions were collected and applied to a Sephacryl S-200 column for further purification. Figure 5 shows the elution profile. Four main peaks (frs. A—D) of the activity were obtained; the activity of fr. A was too labile to study further. Apparent molecular masses of frs. B, C and D were estimated to be about 70, 30 and 10 kDa, respectively. Since the activities of frs. B, C and D were trypsin sensitive, suppressor factors in these fractions might be proteins.

Specific Sugar Reversal of Suppressive Activity To characterize suppressor factors further, the effect of sugars on the suppressive activity of frs. B, C and D from the gel filtration column of Sephacryl S-200 was investigated. The suppressive effect of frs. C and D on PWM-induced PFC response was reversed by 1 mM D-GalNAc but not by equimolar concentrations of D-glucose, α-MM and L-rhamnose (Fig. 6). The suppressive activity of fr. B was not reversed by the sugars used here.

Discussion

The mechanism of immunosuppression by a murine suppressor T cell clone, SB-1, which was established from Con A-stimulated murine T cells,[7] was investigated.

There are several reports suggesting that PGEs play an important role in the expression of immunosuppressive functions.[9-13] In the present study, it was shown that SB-1-induced decrease of antigen non-specific PFC response was restored by the addition of indomethacin to the assay culture (Fig. 1), and that PGE_2 induced the suppressive activity in the culture supernatant of SB-1 cells (Table I). Furthermore, the immunosuppressive function of Con A-stimulated lymphocytes is indicated to be dependent on PGE_2.[13] These results suggest that PGE_2 also has an essential role in the induction of suppressor function of SB-1 cells.

PGE_2 is known to be an inhibitor of proliferation in some kinds of cells. However, it caused a small increase in protein synthesis (Table II) and DNA synthesis of SB-1 cells (Fig. 3). Stobo *et al.*[14] also reported that mitogen responsiveness of human peripheral lymphocytes is enhanced by PGE_2 treatment. It seemed that there was a T cell subset responsive to PGE_2 in peripheral lymphocytes. This PGE_2-dependent suppressor T cell subset has been shown to be radiosensitive and short-lived,[13,15,16] but has not yet been fully identified. In the present study, SB-1 cells were indicated to be PGE_2-dependent suppressor T cells; therefore, SB-1 cells are useful tools to examine properties of PGE_2-dependent suppressor T cells.

Significant amounts of prostaglandins were not detected in Con A or IL-2-stimulated SB-1 cells but were detected in adherent peritoneal exudate cells. Most adherent cells among peritoneal exudate cells were macrophages and, as known well, antigen- or mitogen-stimulated macrophages produce PGE.[17] Furthermore, it has been shown that human peripheral blood monocytes produce PGE_2 and thromboxane A_2 (TXA_2) but T cells do not produce prostaglandins.[18] Thereofore, in our PFC assay culture, macrophages may produce PGE_2 which induces the suppressor function of SB-1 cells.

SB-1 cells incubated with PGE_2 were found to produce suppressor factors (Table I and Fig. 4). By sequential column chromatographies on DEAE-cellulofine and Sephacryl S-200, suppressive activity in the culture supernatant from SB-1 cells was separated into four fractions (frs. A, B, C and D). Quite interestingly, suppressive activity in frs. C and D was inhibited by D-GalNAc. This suggests that suppressor factors in frs. C and D are different from known suppressor factors. To compare with known suppressor factors, further characterization of these factors in the culture supernatant of SB-1 cells is required and this is now under investigation.

Finally, from the present results we suggest that a cyclooxygenase product(s), such as PGE_2, which is produced by macrophages, may induce the production and secretion of suppressor factors in SB-1 cells.

References

1) R. N. Germain and B. Benacerraf, *Scand. J. Immunol.*, **13**, 1

(1981).
2) T. Tadakuma, A. L. Kühner, R. R. Rich, J. R. David and C. W. Pierce, *J. Immunol.*, **117**, 323 (1976).
3) T. M. Aune, D. R. Webb and C. W. Pierce, *J. Immunol.*, **131**, 2848 (1983).
4) M. Nakamura, H. Ogawa and T. Tsunematsu, *J. Immunol.*, **136**, 2904 (1986).
5) C. Grillot-Courvalin, K. Dellagi, A. Chevalier and J. C. Brouet, *J. Immunol.*, **129**, 1008 (1982).
6) O. Se-Kyung and F. L. Moolten, *J. Immunol.*, **127**, 2300 (1981).
7) K. Ezawa, S. Toyoshima and T. Osawa, *Jpn. J. Exp. Med.*, **53**, 139 (1983).
8) R. Gronowicz, A. Coutinho and F. Melchers, *Eur. J. Immunol.*, **6**, 588 (1976).
9) M. S. Kennedy, J. D. Stobo and M. E. Godyne, *Prostaglandins*, **20**, 135 (1980).
10) J. S. Goodwin, A. D. Bankhurst and R. P. Messner, *J. Exp. Med.*, **146**, 1719 (1977).
11) J. S. Goodwin, *Cell Immunol.*, **49**, 421 (1980).
12) D. R. Webb and I. Nowowiejski, *Cell Immunol.*, **63**, 321 (1981).
13) A. Fischer, A. Durandy and C. Griscelli, *J. Immunol.*, **126**, 1452 (1981).
14) J. D. Stobo, M. S. Kennedy and M. E. Goldyne, *J. Clin. Invest.*, **64**, 1188 (1979).
15) D. R. Webb, K. J. Wieder, T. J. Rogers, C. T. Healy and I. Nowowiejski, *Lymphokine Res.*, **4**, 139 (1985).
16) B. Bressnihan and H. E. Jasin, *J. Clin. Invest.*, **59**, 106 (1977).
17) J. L. Hunes, R. J. Bonney, L. Pelus, M. E. Dahlgren, S. J. Sadowski, F. A. Kuehl, Jr. and P. Davies, *Nature* (London), **269**, 149 (1977).
18) M. E. Goldne and J. D. Stobo, *Prostaglandins*, **18**, 687 (1979).

Elevation of Intracellular Cyclic Adenosine 3′,5′-Monophosphate Levels in Macrophages Activated with Lipopolysaccharide for Tumor Cell Killing

Satoshi ONODERA

Department of Clinical Chemistry, Showa College of Pharmaceutical Sciences, Machida, Tokyo 194, Japan. *Received October 18, 1990*

The macrophage activation for tumor cytotoxicity with lipopolysaccharide (LPS) was remarkably inhibited by adding indomethacin (5×10^{-6} M) or 10mM LiCl which is known to inhibit adenylate cyclase activity. The tumor cytotoxicity of macrophages inhibited with these agents was recovered by adding dibutyryl cyclic adenosine 3′,5′-monophosphate (cAMP) (10^{-4} or 10^{-5} M) and furthermore tumor cell killing activity was augmented as compared with LPS-activated macrophage.

Macrophages showed a 5 to 6 times increased intracellular cAMP concentration over the control within 30 min when incubated with LPS. However, the increased intracellular cAMP concentration was decreased by adding LiCl (10 mM).

Thus, these findings indicate that there is an important relation between intracellular cAMP concentration and the mechanism of macrophage activation. One can then conclude that at least the initial enhancement of intracellular cAMP was important for tumor cell killing as a signal transmission in macrophage activated by LPS.

Keywords macrophage activation; tumor cell killing; cyclic AMP; lipopolysaccharide; lithium chloride

Introduction

It is well known that macrophages from peritoneal cavities of mice are activated with substances such as lipopolysaccharide (LPS)[1] and consequently induce tumor cell killing. Recently, various mechanisms for macrophage activation with such substances have been reported.[2-4] In several previous studies, an association between cyclic adenosine 3′,5′-monophosphate (cAMP) and macrophage activation was suggested.[5-10] It is well known that in many cell types cAMP is a second mediator for signal transmission *via* the enzyme adenylate cyclase by interaction of a hormone with a plasma membrane.[11] Incubation of macrophages with lymphocyte mediators was found to increase the adenylate cylase activity and cause morphological and functional changes.[6] The macrophage migration inhibitory factor (MIF), which is a soluble material produced by lymphocytes and inhibits the migration of macrophages *in vitro*, caused a reduction in intracellular cAMP concentration.[7] On the contrary, other workers demonstrated that MIF did not directly affect the level of cAMP.[8] On the other hand, Schultz *et al.*[9] reported that enhancement of intracellular cAMP and exogenous dibutyryl cAMP inhibited the cytotoxicity of interferon-treated macrophages.

In this study, LiCl was used as an agent for the study of the mechanism of macrophage activation, because it is known that LiCl selectively inhibits adenylate cyclase and as a result the cAMP level in cells is reduced.[12] Therefore, we attempted to clarify the role of intracellular cAMP for tumor cell killing in macrophages activated by LPS.

Materials and Methods

Materials C3H/HeSlc, ICR and BALB/c mice (6—8 weeks old) were obtained from Shizuoka Experimental Animal Cooperative. All mice were housed in a specific pathogen free state until use. LPS (phenol extract from *Escherichia coli* 0111: B4), dibutyryl cAMP, indomethacin and LiCl were purchased from the Sigma Chemical Co., St. Louis, Mo. $Na_2{}^{51}CrO_4$ was from New England Nuclear, Boston, Mass. The cAMP assay kit was from the Yamasa Syoyu Co. RPMI 1640 medium was prepared from powdered stock (Nissui Seiyaku Co., Ltd., Tokyo) and supplemented with 100 U of penicillin G potassium (Banyu Seiyaku Co., Ltd., Tokyo) per ml and 100 μg of streptomycin sulfate (Meiji Seika, Yokohama) per ml. Fetal bovine serum (FBS) (Lot 309, GIBCO Laboratories, Grand Island, N.Y.) was inactivated at 56 °C for 30 min before use. RPMI 1640 medium was supplemented with 5% FBS and used as the culture medium unless otherwise noted.

Preparation of Peritoneal Resident Macrophage (PRM) Preparation of macrophages was done as previously described.[13] In brief, animals were sacrified by the dislocation of the cervical vertebra and the peritoneum was immediately exposed. A germ-free peritoneal solution was harvested by aspirating 5 ml of cold saline into the peritoneal cavity. The cells obtained from several mice were pooled, pelleted by centrifugation and suspended in cold RPMI 1640 medium containing 100 U/ml penicillin and 100 μg/ml streptomycin. The cells were seeded into 96-well flat-bottomed tissue culture plates (Falcon) at a density of 2×10^5 cells/well in RPMI 1640 medium. After incubation at 37 °C for 2 h in a humidified 5% CO_2 atmosphere, nonadherent cells were removed by washing the wells twice with saline. Macrophage monolayers were used for the cytotoxicity assay.

Preparation of Target Cells EL_4 cells (murine myeloid leukemia cells) were used as target cells for the ^{51}Cr-release assay.[13] Target cells suspended in RPMI 1640 medium were incubated with 50 μCi of $^{51}Cr(Na_2{}^{51}CrO_4$, 200—500 Ci/g chromium) at 37 °C for 50 min, washed three times in RPMI 1640 medium by centrifugation and resuspended in RPMI 1640 medium at a density of 1×10^5 cells/ml.

Tumor Cytotoxicity Assay of Macrophage[13] After adherence of macrophages to plates, LPS (0.1—10 μg/ml), 10 mM LiCl, dibutyryl cAMP (10^{-5} or 10^{-4} M) or indomethacin (5×10^{-6} M) were added and cultured for 18—20 h at 37 °C in a humidified 5% CO_2 atmopshere. Macrophage monolayers were subsequently washed and EL_4 cells prelabeled with ^{51}Cr were added in a final volume of 0.2 ml to give effector/target cells ratios of 20 : 1. The plates were incubated at 37 °C for 24 h in a humidified 5% CO_2 atmosphere. After incubation, the radioactivity released in the supernatant of each well was counted with a γ-counter. As a control, spontaneous ^{51}Cr release was determined by the supernatant in ^{51}Cr labeled EL_4 cells alone. The percent of cytotoxicity was determined by the following formula:

$$\text{cytotoxicity}(\%) = \frac{\text{experimental release} - \text{spontaneous release}}{\text{maximum release} - \text{spontaneous release}} \times 100$$

All data presented are from triplicate determination with the standard deviation (S.D.) indicated.

Assay of Intracellular cAMP The intracellular level of cAMP was determined using radioimmunoassay of a cAMP assay kit.[14] All samples were assayed in triplicate. PRM from C3H/HeSlc was seeded into 24-well flat-bottomed tissue culture plates (Falcon) at a density of 2×10^6 cells/well in RPMI 1640 medium. After incubation at 37 °C for 2 h in a humidified 5% CO_2 atmosphere, nonadherent cells were removed by washing the well with saline. Each well was separated into five groups. One group was used for the Lowry protein assay.[15] The other four groups were respectively cultured with RPMI 1640 medium alone, 10 mM LiCl alone, LPS (10 μg/ml) alone or in combination with LPS (10 μg/ml) and 10 mM LiCl at 37 °C for 0—24 h in a humidified 5% CO_2 atmosphere. After incubation, the wells

were washed two times with phosphate buffered saline, and then 0.2 ml of cold 0.1 N HCl was added. The cells were scratched with a rubber policeman, sonicated and centrifuged at 10000 rpm for 1 h. 0.1 ml of the supernatant was used for the cAMP assay.

Results

Effects of LiCl on Tumor Cytotoxicity of LPS-Activated Macrophages As shown in Fig. 1, when PRM from C3H/HeSlc mice were cultured in LPS dilution (0.1—10 μg/ml), PRM were activated and induced tumor cell killing. This figure shows a typical pattern of macrophage activation with LPS. However, when PRM were cultured in combination with LPS dilution and 10 mM LiCl, cytotoxicity of the macrophage was remarkably inhibited. Incubation of PRM with 5 mM LiCl also inhibited LPS-activation of PRM, but more than 10 mM LiCl failed to inhibit macrophage killing because the macrophage itself died. In addition, these same results were obtained using PRM from BALB/c and ICR mice (data not shown).

Effects of Dibutyryl cAMP on Lowering of Macrophage Tumor Cytotoxicity by LiCl It has been well known that LiCl inhibited adenylate cyclase activity,[12] therefore the effects of exogenous dibutyryl cAMP were investigated (Figs. 2 and 3). When PRM was incubated in combination with LPS and dibutyryl cAMP, activation of the macrophage was enhanced more than by LPS alone. Furthermore, on lowering of the cytotoxicity by LiCl, when dibutyryl cAMP was added, activation of the macrophage was restored.

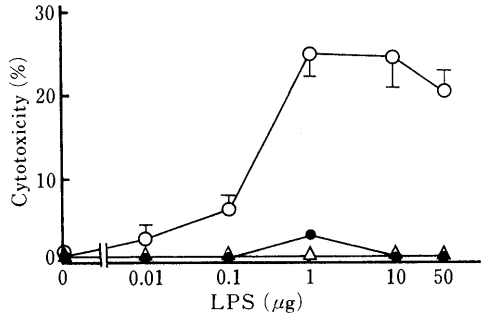

Fig. 1. Effects of LiCl on Tumor Cytotoxicity of LPS-Activated Macrophages

Adherent PRM were cultured in combination with LPS and LiCl for 18—20 h at 37 °C. Macrophage monolayers were subsequently washed. EL_4 cells prelabeled with ^{51}Cr were then added. Cytotoxicity was estimated by the measurement of ^{51}Cr released after 24 h of incubation. The data represent the means ± S.D. of triplicate cultures. ○, medium; ●, LiCl (5 mM); △, LiCl (10 mM).

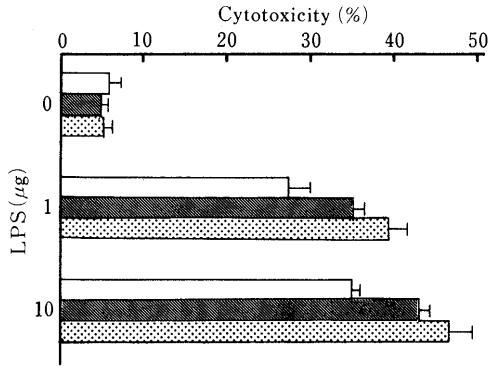

Fig. 2. Effects of Dibutyryl cAMP on Tumor Cytotoxicity

Adherent PRM were cultured in various cAMP concentrations for 18—20 h at 37 °C. Macrophage monolayers were subsequently washed and EL_4 cells prelabeled with ^{51}Cr were then added. Cytotoxicity was estimated by the measurement of ^{51}Cr released after 24 h of incubation. The data represent the means ± S.D. of triplicate cultures. □, medium; ▨, cAMP, (10^{-5} M); ▩, cAMP (10^{-4} M).

Intracellular Levels of cAMP in Macrophages It is conceivable that intracellular levels of cAMP, as cellular messengers, play an important role in regulating the cytotoxicity of the macrophage. Accordingly, in order to know whether LPS and/or LiCl alters the intracellular levels of cAMP in macrophages, the cAMP concentration of PRM treated for 0.5—24 h under various conditions as shown in

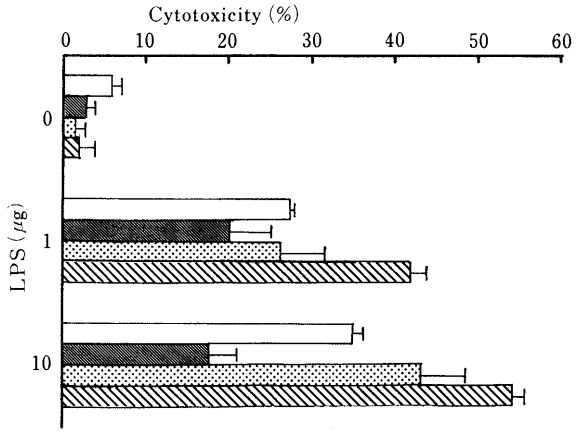

Fig. 3. Effects of Dibutyryl cAMP on Lowering of Macrophage Tumor Cytotoxicity by LiCl

Adherent PRM were cultured in various combinations of LPS, LiCl and dibutyryl cAMP for 18—20 h at 37 °C. Macrophage monolayers were subsequently washed and EL_4 cells prelabeled with ^{51}Cr were then added. Cytotoxicity was estimated by the measurement of ^{51}Cr released after 24 h of incubation. □, medium; ▨, LiCl (10 mM); ▩, LiCl (10 mM) + cAMP (10^{-5} M); ▧, LiCl (10 mM) + cAMP (10^{-4} M). The data represent the means ± S.D. of triplicate cultures.

Table I. Intracellular Levels of cAMP in PRM under Various Conditions

Incubation of cells with	cAMP (pmol/mg protein)				
	0.5 h	1 h	2 h	4 h	24 h
Medium	3.8±0.2	2.7±0.3	2.7±0.2	2.1±0.4	1.8±0.3
LiCl (10 mM)	3.4±0.1	2.8±0.2	2.5±0.05	1.6±0.1	1.7±0.3
LPS (10 μg/ml)	18.0±0.8	16.0±0.4	11.0±0.2	4.6±0.1	2.6±0.1
LPS (10 μg/ml) + LiCl (10 mM)	9.4±0.3	8.0±0.07	5.0±0.1	3.8±0.1	2.5±0.05

PRM were treated for 0.5—24 h under various conditions. After destruction of the cells with a sonicator, the intracellular cAMP was assayed using a radioimmunoassay kit. The results represent the means ± S.D. of triplicate cultures.

Table II. Effects of cAMP on Lowering of Macrophage Tumor Cytotoxicity by Indomethacin

Treatments	LPS (μg/ml)				
	0	0.01	0.1	1	10
Medium	−4.3±0.4[a)]	4.9±0.5	12.9	20.5±3.5	28.1±1.8
cAMP	−1.4±0.2	14.9±1.7	28.3±4.9	34.6±2.3	38.8±2.7
Indomethacin	−6.0±0.9	−5.5±1.3	−5.2±0.5	−4.2	−5.0±2.2
Indomethacin + cAMP	−1.4±0.9	4.1±1.6	5.7±0.1	14.7±1.5	22.7±0.3

Adherent peritoneal resident macrophages were cultured in various concentrations of LPS, dibutyryl cAMP (1×10^{-4} M) and indomethacin (5×10^{-6} M) for 18—20 h at 37 °C. *a)* Cytotoxicity (%) was estimated by measurement of the radiolabel release after 24 h of incubation. The results represent the means ± S.D. of triplicate cultures.

Table I was assayed using a radioimmuno assay kit. Intracellular levels of cAMP of PRM treated with medium (control) or LiCl alone did not change (0.5—24 h). In PRM treated with LPS alone, however, the cAMP concentration increased 5 to 6 times as much as the control and peaked within 30 min. After incubation for 4—24 h, cAMP levels were then the same as in the control. Furthermore, when PRM was incubated in combination with LPS and LiCl, the cAMP levels were lowered as compared with LPS alone.

Effect of Indomethacin on Tumor Cytotoxicity of LPS Activated Macrophages It has been well known that PRM produces prostagrandin E (PGE) by LPS treatment.[16] Generally, PGE activated adenylate cyclase and increased the intracellullar cAMP level. The elevation of the intracellular cAMP level by LPS-treatment was considered to be a reaction of PGE produced by LPS-treatment. In order to clarify the effects previously described, indomethacin, which is an inhibitor of PGE production from arachidonic acid of the cell membrane and a secondary decrease agent for intracellular cAMP levels, was used. The results are shown in Table II. Treatment of PRM with indomethacin alone did not affect the cytotoxic activity of the macrophages. However, when PRM was treated in combination with LPS (1 or 10 μg/ml) and indomethacin (5×10^{-6} M), the cytotoxicity of the macrophages was inhibited as compared with LPS alone. Furthermore, when dibutyryl cAMP (1×10^{-4} M) was added to the reaction system, activation of the macrophages was restored.

Discussion

This paper examined the mechanism of signal transmission in macrophages of LPS-induced activation for tumor cell killing. From the present study, LPS has been shown to elevate the intracellular level of cAMP at the early stage of activation of macrophages, and it is conceivable that activation of the macrophages for tumor cell killing may at least require elevation of the intracellular cAMP levels as a cellular signal transmission. As shown in Table I, it was shown that elevation of the intracellular cAMP within 30 min was important to cause morphological and functional changes. Furthermore, indomethacin, which inhibits the production of PGE, inhibited the cytotoxicity of the LPS-treated macrophages. PRM produced PGE by LPS treatment.[16] Accordingly, elevation of the intracellular cAMP level by LPS-treatment was considered to be a reaction of PGE produced by LPS-treatment. From the results obtained in the present study, it seems likely that PRM are mainly activated by the following scheme: in the first step LPS interacts with cell surface receptors and synthesizes PGE, PGE stimulates adenylate cyclase, and increases intracellular cAMP level and macrophage activation. However, our findings differ from those of Taffet and Russell,[17] who reported that endogeneous PGE produced by LPS-stimulated macrophages inhibited the effect on macrophage-mediated tumoricidal activity. Schultz *et al.*[9] reported that dibutyryl cAMP inhibit tumor cell killing by interferon-activated macrophages. The discrepancy between our findings and those of the above investigations remains to be clarified. The LPS receptor or LPS-binding protein in the first step interaction of LPS with several cell surfaces has been reported,[18-21] but the structure and function of its receptor is not known in detail. There is no consensus about the interaction of LPS with its target cells. However, Akagawa and Tokunaga[22] immunochemically demonstrated that LPS binded to the macrophage cell surface. Furthermore, it was described that mouse lung macrophage, lacking the binding of LPS, restored binding by stimulation with interferon-γ. These results showed that the LPS receptor was included on the cell surface of the macrophage. As shown in Fig. 2, as dibutyryl cAMP alone did not cause macrophage activation, it seems likely that macrophage activation is induced by the action of both cAMP and other unknown substances. Now it is conceivable that the unknown substances are messenger molecules such as calmodulin,[23] protein kinase A,[24] protein kinase C[25,26] and so on. Furthermore, it is important to determine the extent of the role of intracellular cAMP and other mechanisms in the activation of macrophages by LPS.

Acknowledgements The author wishes to thank Drs. K. Akagawa and T. Tokunaga (National Institute of Health, Japan) for their help and guidance in this work.

References

1) H. M. Ögmundsdottir and D. M. Weir, *Clin. Exp. Immunol.*, **40**, 223 (1980).
2) M. S. Meltzer, *J. Immunol.*, **127**, 179 (1981).
3) R. M. Schultz and W. J. Kleinschmidt, *Nature* (London), **305**, 239 (1983).
4) K. Onozaki, T. Takenawa, Y. Homma and T. Hashimoto, *Cell. Immunol.*, **75**, 242 (1983).
5) Y. Katakami, Y. Nakao, T. Koizumi, N. Katakami, R. Ogawa and T. Fujita, *Immunology*, **64**, 719 (1988).
6) O. E. Remold and H. G. Remold, *J. Biol. Chem.*, **249**, 3622 (1974).
7) E. Pick, *Cell. Immunol.*, **32**, 329 (1977).
8) T. J. Higgins, C. T. Winston and J. R. David, *Cell. Immunol.*, **27**, 11 (1976).
9) R. M. Schultz, N. A. Pavlidis, J. N. Stoychkov and M. A. Chirigos, *Cell. Immunol.*, **42**, 71 (1979).
10) E. R. O'Donnell and H. G. Remold, *J. Biol. Chem.*, **249**, 3622 (1974).
11) J. M. Cancedo, M. J. Mazón and P. Eraso, *TIBS*, **5**, 210 (1983).
12) Y. C. Wang, G. N. Pandy, J. Mendels and A. Frazer, *Biochem. Pharm.*, **23**, 845 (1974).
13) K. S. Akagawa, K. Kamosita, S. Onodera and T. Tokunaga, *Jpn. J. Cancer Res.* (*Gann*), **78**, 279 (1987).
14) M. Honma, T. Satoh, J. Takezawa and M. Ui, *Biochem. Med.*, **18**, 257 (1977).
15) O. H. Lowry, N. J. Rosenbrough, A. L. Farr and R. J. Randall, *J. Biol. Chem.*, **193**, 265 (1951).
16) R. M. Schultz, J. N. Stoychkov, N. Paulidis, M. A. Chirigos and Z. L. Olkowski, *J. Reticulo. Soci.*, **26**, 93 (1979).
17) S. M. Taffet and S. W. Russell, *J. Immunol.*, **126**, 424 (1981).
18) G. F. Springer, J. C. Adye, A. Bezkorovainy and B. Jirgenson, *Biochemistry*, **13**, 1379 (1974).
19) K. Yokoyama, T. Terao and T. Osawa, *Japan J. Exp. Med.*, **48**, 511 (1978).
20) K. Yokoyama, J. Mashimo, N. Kasai, T. Terao and T. Osawa, *Hoppe-Seyler's Z. Physiol. Chem.*, **360**, 587 (1979).
21) S. J. C. Warner, N. Savage and D. Mitchell, *Biochem. J.*, **232**, 379 (1985).
22) K. S. Akagawa and T. Tokunaga, *J. Exp. Med.*, **162**, 1444 (1985).
23) J. O. Mecham, M. M. Soong, C. A. Cain, S. Koehm, J. Goff and W. A. Tompkins, *J. Immunol.*, **134**, 3516 (1985).
24) L. B. Justement, W. A. Aldrich, G. D. Wenger, M. S. O'Dorisio and B. S. Zwilling, *J. Immunol.*, **136**, 270 (1986).
25) Y. Nishizuka, *Nature* (London), **308**, 693 (1984).
26) T. A. Hamilton, D. L. Becton, S. D. Somere, P. W. Gray and D. O. Adams, *J. Biol. Chem.*, **260**, 1378 (1985).

Inhibition of Avian Myeloblastosis Virus Reverse Transcriptase by Heterocyclic Quinones: Structure–Activity Correlation

Yoshio INOUYE,*[,a] Hidemi MATSUMOTO,[a] Ryuji MORISHIGE,[a] Yoshiyasu KITAHARA,[b] Akinori KUBO[b] and Shoshiro NAKAMURA[a]

Institute of Pharmaceutical Sciences, Hiroshima University School of Medicine,[a] 1–2–3 Kasumi, Minami-ku, Hiroshima 734, Japan and Department of Organic Chemistry, Meiji College of Pharmacy,[b] 1–35–23 Nozawa, Setagaya-ku, Tokyo 154, Japan. *Received October 26, 1990*

Synthetic heterocyclic quinones (107 samples) consisting of *o*- and *p*-quinoline quinones, *o*-isoquinoline quinones and *p*-quinoxaline quinones as well as *o*- and *p*-naphthoquinones (3 samples) were tested for their inhibitory activities against avian myeloblastosis virus reverse transcriptase (AMV-RT) and cytotoxic activities against mouse lymphoblastoma L5178Y cells. In general, *o*-quinoline quinones (*i.e.*, the 5,6-quinolinedione derivatives) are more potent inhibitors of AMV-RT than *p*-quinoline quinones (the 5,8-quinolinedione derivatives). Furthermore, the growth of L5178/Y cells were significantly refractory to the 8-methoxy-5,6-quinolinedione derivatives whose suppressive effects on AMV-RT function were fairly comparable to those of the other *o*-quinoline quinones. The longer the chain length of 7-alkyl substituent in *o*- or *p*-quinoline quinones, the lower the biological activities.

Keywords heterocyclic quinone; reverse transcriptase; retrovirus; structure–activity correlation; enzyme inhibitor; lymphoblastoma: cytotoxicity

Reverse transcriptase plays an important role in the life cycle of retroviruses and the enzyme is considered to be an excellent target for the chemotherapeutics of retroviral diseases such as human acquired immunodeficiency syndrome (AIDS). Previously, we reported that streptonigrin (STN), a quinoline quinone antibiotic, was one of the most potent inhibitors of avian myeloblastosis virus reverse transcriptase (AMV-RT) in our screening of natural and synthetic compounds.[1] STN was originally reported as an antitumor antibiotic by Rao and Cullen[2] in 1960 and its

TABLE I. Effects of *p*-Quinoline Quinones on Avian Myeloblastosis Virus Reverse Transcriptase Activity and Growth of Mouse Lymphoblastoma L5178Y Cells

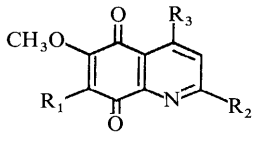

1—44

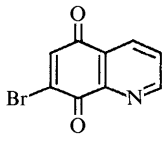

45

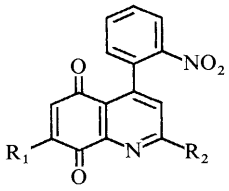

46—48

Compd.	R_1	R_2	R_3	IC_{50} (μg/ml) AMV-RT	IC_{50} (μg/ml) L5178Y
1	H	H	H	1.1	1.21
2	H	Cl	H	1.7	2.63
3	H	CH_3	H	1.8	2.68
4	H	CH_2OCOCH_3	H	1.6	2.50
5	H	H	CH_3	5.1	0.51
6	CH_3	H	H	4.1	0.54
7	CH_3	Cl	H	3.7	0.81
8	CH_3	CH_3	H	6.4	1.16
9	CH_3	CH_2OCOCH_3	H	9.1	1.93
10	CH_3	H	CH_3	12	0.55
11	CH_3	Cl	CH_3	5.9	0.62
12	C_2H_5	H	H	5.5	0.23
13	C_2H_5	Cl	H	4.3	0.61
14	C_2H_5	CH_3	H	5.9	0.55
15	C_2H_5	CH_2OCOCH_3	H	6.6	0.65
16	C_2H_5	H	CH_3	17	1.56
17	C_2H_5	Cl	CH_3	8.3	1.29
18	$(CH_2)_2CH_3$	H	H	8.8	0.42
19	$(CH_2)_2CH_3$	Cl	H	7.4	1.56
20	$(CH_2)_2CH_3$	CH_3	H	11	1.79
21	$(CH_2)_2CH_3$	CH_2OCOCH_3	H	13	1.68
22	$(CH_2)_2CH_3$	H	CH_3	30	0.73
23	$(CH_2)_3CH_3$	H	H	7.4	0.52
24	$(CH_2)_3CH_3$	Cl	H	16	1.16
25	$(CH_2)_3CH_3$	CH_3	H	16	1.23
26	$(CH_2)_3CH_3$	CH_2OCOCH_3	H	6.0	2.03
27	$(CH_2)_3CH_3$	H	CH_3	>40	0.69
28	$(CH_2)_4CH_3$	H	H	13	0.60
29	$(CH_2)_4CH_3$	Cl	H	18	1.85
30	$(CH_2)_4CH_3$	CH_3	H	19	1.13
31	$(CH_2)_4CH_3$	CH_2OCOCH_3	H	25	2.75
32	$(CH_2)_4CH_3$	H	CH_3	>40	2.21
33	$(CH_2)_4CH_3$	Cl	CH_3	>40	3.30
34	$(CH_2)_5CH_3$	H	H	>40	2.02
35	$(CH_2)_5CH_3$	CH_3	H	>40	2.12
36	$(CH_2)_5CH_3$	H	CH_3	>40	2.16
37	$(CH_2)_7CH_3$	H	H	>40	2.65
38	$(CH_2)_7CH_3$	Cl	H	>40	>10
39	$(CH_2)_7CH_3$	CH_3	H	>40	6.37
40	$(CH_2)_7CH_3$	CH_2OCOCH_3	H	>40	5.38
41	$(CH_2)_7CH_3$	H	CH_3	>40	2.58
42	$(CH_2)_7CH_3$	Cl	CH_3	>40	6.71
43	$(CH_2)_{11}CH_3$	H	H	>40	2.72
44	$(CH_2)_{11}CH_3$	CH_3	H	>40	>10
45				3.6	4.55
46	H	Cl		25	2.19
47	H	Br		18	3.03
48	Br	Cl		16	2.12

TABLE II. Effects of *o*-Quinoline Quinones on Avian Myeloblastosis Virus Reverse Transcriptase Activity and Growth of Mouse Lymphoblastoma L5178Y Cells

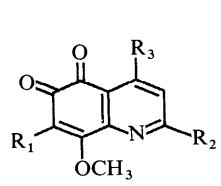
51—67

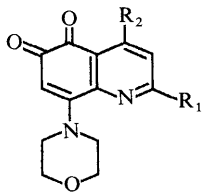
68—70

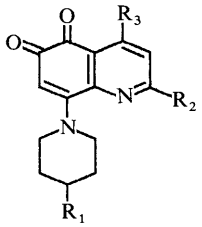
71—76

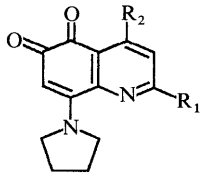
77—79

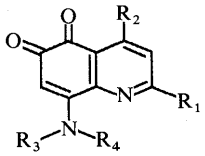
80—84


85—89

Compd.	R_1	R_2	R_3	IC_{50} (μg/ml) AMV-RT	IC_{50} (μg/ml) L5178Y
51	H	H	H	1.4	>10
52	H	Cl	H	1.4	7.47
53	H	CH_3	H	1.2	>10
54	H	CH_2OCOCH_3	H	0.94	>10
55	H	H	CH_3	1.4	>10
56	CH_3	H	H	3.2	>10
57	CH_3	CH_3	H	1.5	>10
58	CH_3	H	CH_3	4.4	>10
59	C_2H_5	H	H	2.5	>10
60	C_2H_5	CH_3	H	1.9	>10
61	C_2H_5	H	CH_3	3.8	>10
62	$(CH_2)_2CH_3$	CH_3	H	2.1	>10
63	$(CH_2)_2CH_3$	H	CH_3	3.8	>10
64	$(CH_2)_4CH_3$	H	CH_3	4.0	>10
65	$(CH_2)_5CH_3$	H	CH_3	11	>10
66	$(CH_2)_7CH_3$	CH_3	H	>40	>10
67	$(CH_2)_7CH_3$	H	CH_3	>40	>10
68	H	H		0.96	2.03
69	CH_3	H		0.97	0.35
70	H	CH_3		1.7	2.26

Compd.	R_1 (R)	R_2	R_3	R_4	IC_{50} (μg/ml) AMV-RT	IC_{50} (μg/ml) L5178Y
71	H	H	H		1.1	0.42
72	H	CH_3	H		1.5	1.29
73	H	H	CH_3		1.4	0.86
74	CH_3	H	H		1.7	0.66
75	CH_3	CH_3	H		1.8	2.10
76	CH_3	H	CH_3		1.6	1.00
77	H	H			6.0	0.55
78	CH_3	H			27	>4
79	H	CH_3			>40	>4
80	H	H	CH_3	CH_3	1.1	0.60
81	CH_3	H	CH_3	CH_3	2.0	1.73
82	H	CH_3	CH_3	CH_3	2.2	1.25
83	H	H	CH_3	$(CH_2)_2CH_3$	1.8	0.37
84	H	H	C_2H_5	C_2H_5	5.8	0.41
85	OCH_3				1.6	0.45
86	C_2H_5				2.5	0.46
87					4.0	1.37
88	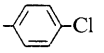				23	5.59
89	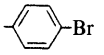				19	>10

remarkable cytotoxic activity seemed to be disadvantageous with respect to a specific inhibitor of retrovirus.[3]

The 6-methoxy-7-amino-5,8-quinolinedione moiety in STN was proved to be the minimum entity to show the inhibition of AMV-RT.[3] The synthetic quinone compounds, 6-methoxy-5,8-quinolinedione (**1**) and 6-methoxy-7-methyl-5,8-quinolinedione (**6**), were as potent as inhibitors of AMV-RT as STN. The inhibition in the growth of mouse lymphoblastoma L5178Y cells by these compounds were not significant when compared with that of STN. The enhanced specificities for AMV-RT shown by these *p*-quinoline quinones were shared by *o*-quinoline quinones and *p*- and *o*-isoquinoline quinones,[4-8] though the IC_{50} values against AMV-RT were still higher than their corresponding values against L5178Y except for two cases of *o*-quinoline quinones, 8-methoxy-5,6-quinolinedione (**51**) and 8-methoxy-7-methyl-5,6-quinolinedione (**56**); their specificity indexes defined as the ratios of IC_{50} values against L5178Y and AMV-RT were higher than 1.

The molecular mechanism of how quinone compounds inactivate AMV-RT is not yet elucidated. However, the inhibitory activities against AMV-RT of individual quinone compounds were closely related with their funcions as electron acceptors demonstrated in such a system as the oxidation of reduced nicotinamide adenine dinucleotide (NADH) by *Clostridium kluyveri* diaphorase (EC 1.6.99).[6,7] Moreover, the reduced quinone compounds are in turn autoxidized to their oxidized forms in couple with the electron transfer to oxygen. The second reaction may not necessarily be required but probably contributes to the inhibition of AMV-RT by increasing the chance of a first reaction.[7] In contrast, the cytotoxic activity of each quinone compound seems not to be related to the electron transfer potency. Therefore, it can be expected to find highly specific inhibitors of AMV-RT such as **51** and **56**.

In this study, approximately 100 quinone compounds were synthesized to be tested for their effects on AMV-RT activity and the growth of L5178Y cells.

Materials and Methods

Materials *p*-Quinoline quinones (**1**—**44** and **46**—**48**), *o*-quinoline quinones (**51**—**67**) and a *p*-quinoxaline quinone (**160**) were synthesized by oxidative demethylation of the corresponding hydroquinone dimethyl ethers with cerium(IV) ammonium nitrate,[9] the details will be published elsewhere. A *p*-quinoline quinone (**45**),[10] *o*-quinoline quinones (**68**—**89**),[11,12] *o*-isoquinoline quinones (**101**—**107**),[13] *p*-quinoxaline quinones (**151**—**159**),[14] quinoxaline hydroquinones (**161**—**163**)[14] and naphthoqui-

nones (**201**—**203**)[15] were prepared as previously described.

AMV-RT was purchased from Seikagaku Kogyo Co., Ltd. Poly(rA) was a product of Sigma Chemical Co. Oligo(dT)$_{12-18}$ was obtained from Pharmacia Fine Chemicals Co. All other chemicals were commercial products of the analytical grade.

Assay Methods Assay procedures for the inhibition of AMV-RT were reported previously.[16,17] The growth inhibition of mouse lymphoblastoma L5178Y cells were evaluated according to the previous method.[16]

Results and Discussion

The IC_{50} values of all compounds against AMV-RT and

TABLE III. Effects of *o*-Isoquinoline Quinones on Avian Myeloblastosis Virus Reverse Transcriptase Activity and Growth of Mouse Lymphoblastoma L5178Y Cells

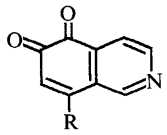

101—**103**

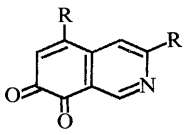

104—**107**

Compd.	R	IC_{50} (μg/ml)	
		AMV-RT	L5178Y
101	$N(CH_3)_2$	1.2	1.19
102	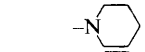	4.8	1.66
103	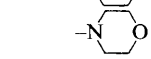	5.0	2.11
104	$N(CH_3)_2$	6.3	>10
105	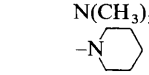	37	4.56
106	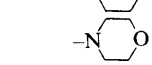	3.8	2.07
107	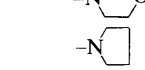	28	>10

TABLE IV. Effects of *p*-Quinoxaline Quinones and Quinoxaline Hydroquinones on Avian Myeloblastosis Virus Reverse Transcriptase Activity and Growth of Mouse Lymphoblastoma L5178Y Cells

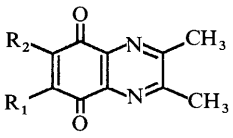

151—**160**

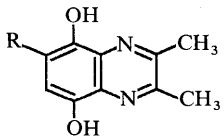

161—**163**

Compd.	R_1 (R)	R_2	IC_{50} (μg/ml)	
			AMV-RT	L5178Y
151	NH_2	H	0.51	2.05
152	$N(CH_3)_2$	H	4.2	1.64
153	$N(C_2H_5)_2$	H	4.5	2.16
154		H	6.5	2.62
155		H	6.9	0.49
156	Br	H	5.7	2.35
157	Cl	H	3.2	1.35
158	Br	NH_2	0.19	0.21
159	Cl	NH_2	0.23	0.15
160	CH_3	OCH_3	4.5	0.32
161	H		2.1	0.59
162	Br		4.0	2.16
163	Cl		4.0	1.59

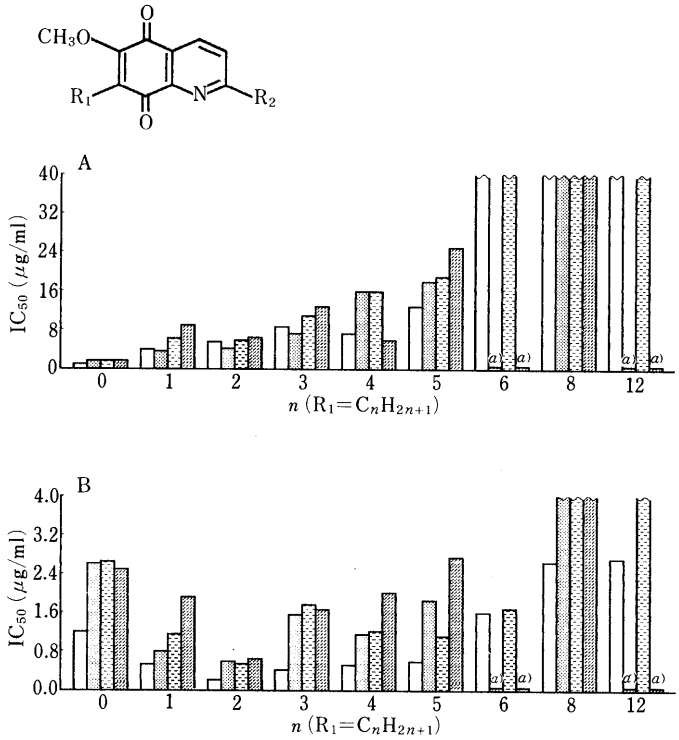

Fig. 1. Effects of 6-Methoxy-5,8-quinolinediones on AMV-RT Activity and Growth of Mouse Lymphoblastoma L5178Y Cells

The IC_{50} values of *p*-quinoline quinones for AMV-RT activity (A) and the growth of L5178Y cells (B) were plotted as functions of the chain length of the 7-alkyl substituent ($R_1=C_nH_{2n+1}$, n=0—12). □, R_2=H; ▨, R_2=Cl; ▩, $R_2=CH_3$; ▤, $R_2=CH_2OAc$. *a*) Not tested.

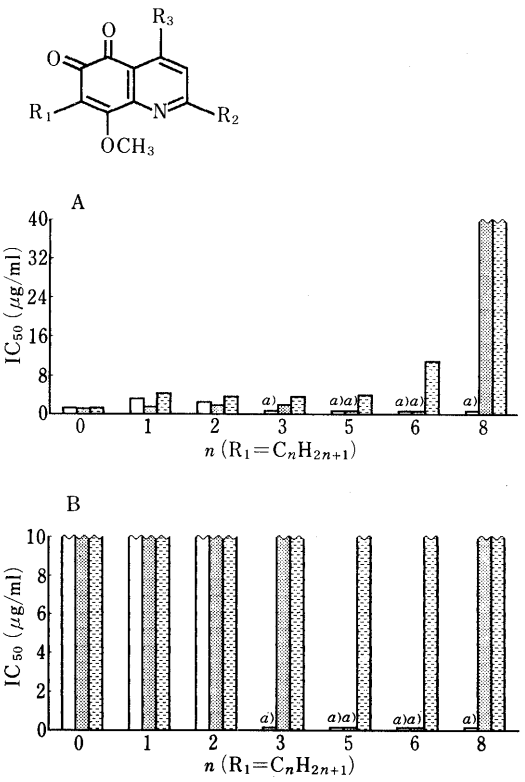

Fig. 2. Effects of 8-Methoxy-5,6-quinolinediones on AMV-RT Activity and Growth of Mouse Lymphoblastoma L5178Y Cells

The IC_{50} values of *o*-quinoline quinones for AMV-RT activity (A) and the growth of L5178Y cells (B) were plotted as functions of the chain length of the 7-alkyl substituent ($R_1=C_nH_{2n+1}$, n=0—8). □, R_2=H, R_3,=H, ▨, $R_2=CH_3$, R_3=H; ▩, R_2=H, $R_3=CH_3$. *a*) Not tested.

L5178Y are given in Tables I (*p*-quinoline quinones), II (*o*-quinoline quinones), III (*o*-isoquinoline quinones), IV (quinoxaline quinones) and V (naphthoquinones).

The biological activities of *p*-quinoline quinones were comparatively depicted in Fig. 1 with special emphasis on the effect of chain length of the alkyl substituent at C-7 (R_1). The inverse correlation between the chain length of R_1 (C_nH_{2n+1}, $n=0$—12) and the inhibitory activity against AMV-RT was clearly shown; the enzyme inhibition was maximum at $n=0$ (or $R_1=H$) irrespective of another substituent at C-2 (R_2) with the IC_{50} values ranging 1.1—1.8 μg/ml. The IC_{50} values were higher than 40 μg/ml at $n \geqq 6$. As for cytotoxic activity, however, the compounds with the 7-ethyl group (*i.e.*, $n=2$) were found to be more potent than any others. The substitutions at C-2 decreased both anti-AMV-RT and cytotoxic activities. The specificity index of compound **1** (1.1) is the highest one among those of *p*-quinoline quinones.

The biological properties of a series of *o*-quinoline quinones are shown in Table II. As in the case of *p*-quinoline quinones, the effect of chain length of the alkyl substituent at C-7 on the biological activities of these compounds was studied and the results are shown in Fig. 2. As well as **51** and **56**, the inhibition of cell growth by *o*-quinoline quinones was not significant; the IC_{50} values were higher than 10 μg/ml (Fig. 2B). In the couple with the enhanced anti-AMV-RT activities (Fig. 2A), *o*-quinoline quinones are, in general, more specific for AMV-RT than *p*-quinoline quinones. The chain length of the alkyl substituent at C-7 (*i.e.*, R_1) is also deeply concerned with the inhibitory activities against AMV-RT. When n is in a range of 0 to 5, the anti-AMV-RT activities did not differ appreciably, though the highest activities were observed at $n=0$ (**51**, **53** and **55**) in each of three different series of compounds: $R_2=H$, $R_3=H$; $R_2=CH_3$, $R_3=H$; and $R_2=H$, $R_3=CH_3$; respectively. The previous findings with **51** and **56** are, therefore, rather general features of *o*-quinoline quinones.

The nitrogen atom in the aromatic ring is also deeply concerned with the cytotoxic activities of heterocyclic quinones. We reported previously that 5-methoxy-7,8-isoquinolinedione was as potent an inhibitor of L5178Y as 7-methoxy-5,8-isoquinolinedione.

The reduced cytotoxic activity with the retention of potent anti-AMV-RT activity observed with *o*-quinoline quinones required the presence of an 8-methoxyl group as was evident from the results shown in Table VI. In the case of *p*-quinoline quinones, however, the effects of either 6- or 7-methoxyl group on the anti-AMV-RT and cytotoxic activities were not significant.[5]

The biological properties of quinoxaline quinones have not yet been reported. Besides quinoline quinone, isoquinoline quinones and naphthoquinones; *p*-quinoxaline quinones are included in the quinone compounds active against AMV-RT. The autoxidation of the reduced

TABLE V. Effects of Naphthoquinones on Avian Myeloblastosis Virus Reverse Transcriptase Activity and Growth of Mouse Lymphoblastoma L5178Y Cells

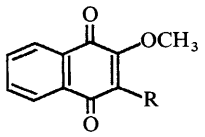

201, 202

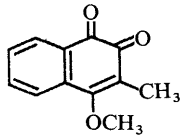

203

Compd.	R	IC_{50} (μg/ml)	
		AMV-RT	L5178Y
201	H	6.5	1.53
202	CH_3	23	1.84
203		1.4	>10

TABLE VI. Role of the 8-Methoxyl Group on Biological Activities of 5,6-Quinolinediones

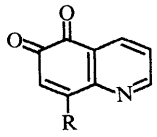

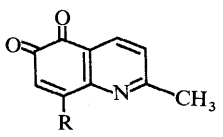

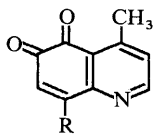

Compd.	R	IC_{50} (μg/ml)		Compd.	R	IC_{50} (μg/ml)		Compd.	R	IC_{50} (μg/ml)	
		AMV-RT	L5178Y			AMV-RT	L5178Y			AMV-RT	L5178Y
51	OCH_3	1.4	>10	**53**	OCH_3	1.2	>10	**55**	OCH_3	1.4	>10
71		1.1	0.42	**72**		1.5	1.29	**73**		1.4	0.86
68		0.96	2.03	**69**		0.97	0.35	**70**		1.7	2.26
74		1.7	0.66	**75**		1.8	2.10	**76**		1.6	1.00
77		6.0	0.55	**78**		27	>4	**79**		>40	>4
80		1.1	0.60	**81**		2.0	1.73	**82**		2.2	1.25
83		1.8	0.37								
84		5.8	0.41								

form to the oxidized one is also the case in *p*-quinoxaline quinones (data not shown) and the biological activities of the reduced forms (**162** and **163**) are fairly comparable to those of their oxidized counterparts (**156** and **157**). The compounds with the 5-amino group (**151**, **158** and **159**) gave the lowest IC_{50} values against AMV-RT, though the significant inhibitions of cell growth were also observed.

Like 8-methoxy-5,6-quinolinediones, 4-methoxy-3-methyl-1,2-naphthoquinone (**203**) shows specificity for AMV-RT. On the other hand, two *p*-napthoquinones **201** and **202** were cytotoxic compounds with poor inhibitory activities against AMV-RT. Further, the requisition of a 4-methoxyl group for the specific inhibition of AMV-RT could be deduced from the role of a 8-methoxyl group in *o*-quinoline quinones.

In conclusion, the specificities for AMV-RT shown by some *o*-quinoline quinones in the previous papers[4-6] proved to be rather common for 8-methoxy-5,6-quinolinediones and probably 4-methoxy-1,2-naphthoquinones.

Acknowledgment This work was partly supported by a Grant-in-Aid for General Scientific Research from the Ministry of Education, Science and Culture, Japan.

References

1) Y. Take, Y. Inouye, S. Nakamura, H. S. Allaudeen and A. Kubo, *J. Antibiot.*, **42**, 107 (1989).
2) K. V. Rao and W. P. Cullen, "Antibiotics Annual 1959—1960," ed. by H. Welch and F. Marti-Ibañz, Medical Encyclopendia Inc., New York, 1960, pp. 950—953.
3) Y. Inouye, Y. Take, K. Oogose, A. Kubo and S. Nakamura, *J. Antibiot.*, **40**, 105 (1987).
4) Y. Take, K. Oogose, T. Kubo, Y. Inouye, S. Nakamura, Y. Kitahara and A. Kubo, *J. Antibiot*, **40**, 679 (1987).
5) Y. Inouye, K. Oogose, Y. Take, T. Kubo and S. Nakamura, *J. Antibiot.*, **40**, 702 (1987).
6) K. Oogose, Y. Hafuri, E. Takemori, E. Nakata, Y. Inouye, S. Nakamura and A. Kubo, *J. Antibiot.*, **40**, 1778 (1987).
7) Y. Hafuri, E. Takemori, K. Oogose, Y. Inouye, S. Nakamura, Y. Kitahara, S. Nakahara and A. Kubo, *J. Antibiot.*, **41**, 1471 (1988).
8) Y. Take, Y. Inouye, S. Nakamura, H. S. Allaudeen and A. Kubo, *J. Antibiot.*, **42**, 107 (1989).
9) A. Kubo, Y. Kitahara, S. Nakahara and R. Numata, *Chem. Pharm. Bull.*, **31**, 341 (1983); A. Kubo and S. Nakahara, *Heterocycles*, **27**, 2095 (1988).
10) V. Petrow and B. Sturgeon, *J. Chem. Soc.*, **1954**, 570.
11) Y. Kitahara, T. Nakai, M. Shimizu and A. Kubo, *Chem. Pharm. Bull.*, **38**, 2841 (1990).
12) Yu. S. Tsizin and M. V. Rubtsov, *Khim. Geterotsikl. Soedin., Sb. 1: Azotsoderzhaschie Geterotsikly*, **1967**, 285 [*Chem. Abstr.*, **70**, 87520*m* (1969)]; F. J. Bullock and J. F. Tweedie, *J. Med. Chem.*, **13**, 261 (1970).
13) Yu. S. Tsizin and B. V. Lopatin, *Khim. Geterotskil. Soedin.*, **1977**, 500 [*Chem. Abstr.*, **87**, 68117*v* (1977)]; Yu. S. Tsizin, *ibid.*, 1974, 1253 [*Chem. Abstr.*, **82**, 43340*w* (1975)]; H. Mishima, H. Fukumi and H. Kurihara, *Heterocycles*, **6**, 1652 (1977).
14) W. F. Gum, Jr. and M. M. Joullie, *J. Org. Chem.*, **32**, 53 (1967).
15) T. Otsuki, *Nippon Kogaku Kaishi*, **47**, 3089 (1974); C. D. Snyder and H. Rapoport, *J. Am. Chem. Soc.*, **94**, 22 (1972).
16) H. Okada, H. Mukai, Y. Inouye and S. Nakamura, *J. Antibiot.*, **39**, 306 (1986).
17) S. Hanajima, K. Ishimaru, K. Sakano, S. K. Roy, Y. Inouye and S. Nakamura, *J. Antibiot.*, **38**, 803 (1985).

Targeting of Mitomycin C to the Liver by the Use of Asialofetuin as a Carrier

Yoshiharu KANEO,* Tetsuro TANAKA and Sadao IGUCHI

Department of Pharmacy & Pharmaceutical Sciences, Fukuyama University, Sanzo, Higashimura-cho, Fukuyama 729-02, Japan. *Received July 23, 1990*

Desialylated fetuin (asialofetuin) was adopted as a carrier for introducing drugs in parenchymal liver cells. Mitomycin C, as a model guest-compound, was covalently attached to asialofetuin through a spacer of the succinyl group. The asialofetuin–mitomycin C conjugate contained 4.4 w/w% of mitomycin C and liberated it gradually at physiological conditions ($t_{1/2}$ = 37 h). The survival time of the conjugate in rat blood circulation was significantly smaller than that of the non-desialylated fetuin conjugate; the elimination half-life was 7.3 min after intravenous injection. At 30 min after injection of the conjugate in rats, 40% of the dose was present in the liver. Parenchymal cells in the liver selectively took up the conjugate, which was highly distributed to the lysosomal fraction in the cell. The greater uptake of the conjugate by hepatocytes reflected the increased excretion in the bile; totally 10.4% of the dose was recovered.

Keywords asialofetuin; asialofetuin–drug conjugate; mitomycin C; plasma level; liver; parenchymal cell; lysosome; biliary excretion

Glycoproteins, after removal of sialic acid and consequent exposure of the galactosyl residue, are selectively taken up by the hepatic asialoglycoprotein receptor.[1,2] The protein–receptor complex is transported into the hepatocytes, where the asialoglycoprotein is digested in lysosomes.[3] The hepatic receptor is not destroyed after internalization, and unoccupied receptor molecules are promptly returned to the cell surface.[4] Consequently, the hepatic uptake of the desialylated glycoproteins remains constant with time.[5]

Fetuin (molecular weight = 48000; isoelectric point = pH 3.3) is an α_1 glycoprotein which has been isolated from fetal calf serum.[6] Desialylated fetuin (asialofetuin) has been previously used to introduce proteins[7] and liposomes[8] into parenchymal cells of the liver. The antiviral agents arabinoside A[9] and trifluorothymidine,[10] coupled to asialofetuin, were selectively delivered to hepatic parenchymal cells, where they inhibited viral deoxyribonucleic acid (DNA) replication. Toxic effects of an asialofetuin–diphtheria toxin fragment A conjugate on cultured rat hepatocytes were mediated by the asialoglycoprotein receptor.[11] It was 1800 times as toxic as diphtheria toxin fragment A. These experiments demonstrated the potential efficacies of drugs conjugated to asialofetuin. However, little is known about the behavior of the conjugated drugs in the body.

In a previous study,[12] mitomycin C-serum albumin conjugates were synthesized. Prior acylation of the protein carrier not only prevented protein polymerization in the presence of carbodiimide, but also increased the extent of conjugation of the drug.[12] We report here the successful construction of an asialofetuin–mitomycin C conjugate. Using mitomycin C as a model compound, the hepatic distribution of the conjugated drug was examined quantitatively in rats.

Experimental Method

Reagents Fetuin was obtained from Sigma Chemical Co. (St. Louis, U.S.A.). Fetuin was purified by dialysis or gel filtration on Sephadex G-150 before use. Neuraminidase was purchased from Marukin Shoyu Co. (Uzi, Japan), CNBr-activated Sepharose 4B from Pharmacia Fine Chemicals (Uppsala, Sweden) and 1-ethyl-3-(3-dimethylaminopropyl)-carbodiimide hydrochloride (EDC) from Nacalai Tesque, Inc. (Kyoto, Japan). Mitomycin C (MMC) was supplied by Kyowa Hakko Kogyo Co. (Tokyo, Japan). All other chemicals and reagents were of the highest grades commercially available.

Preparation of the Conjugates Desialylation of fetuin, *i.e.*, preparation of asialofetuin, was carried out enzymatically with neuraminidase.[13] Briefly, neuraminidase (5 u) was covalently attached to CNBr-activated Sepharose 4B (1 g). The gel was added to a solution of fetuin (1 g) in 30 ml of 0.1 M acetate buffer containing 0.5 M NaCl (pH 5.5). After incubation at 37 °C for 90 min, the gel was removed by filtration. The amount of sialic acid remaining in asialofetuin was estimated to be 20—30% as measured by the method of Jourdian *et al.*[14] The solution containing asialofetuin was dialyzed against 0.9% NaCl at 4 °C for 24 h and lyophilized, giving a water-soluble powder.

MMC was covalently attached to asialofetuin *via* a succinyl group as a spacer, according to the previous method.[12] To a stirred solution of asialofetuin (100 mg in protein equivalent) in 1 M $NaHCO_3$ (10 ml), succinic anhydride (400 mg) was added slowly in small portions. The pH of the reaction mixture was maintained within a range of 7.8—8.2 by the addition of 1 M NaOH for 1 h and gently stirred at 4 °C for 16 h. The reaction mixture was washed repeatedly with a cold 0.9% NaCl solution by pressure dialysis using a Toyo UHP-43 ultrafiltration cell incoporating a UP-20 membrane (Toyo, Tokyo, Japan) and, finally, concentrated to a volume of 20 ml. Excess reagents and low molecular by-products of the reaction were removed by this process. MMC (16 mg) and EDC (40 mg) were added to the solution (20 ml) of succinylated asialofetuin. The pH was maintained at 6.0, and the conjugating reaction was allowed to proceed for 1 h at room temperature. The reaction mixture was applied on a column of Shephadex G-25 (5 × 20 cm) developed with 0.9% NaCl. The asialofetuin conjugate of MMC (AF–MMC) was eluted in the void volume, and free MMC was retarded by the gel. Fractions containing AF–MMC were collected and lyophilized, giving a water-soluble powder. It was further purified by the use of a Sephadex G-150 column (2.5 × 47 cm). A fetuin conjugate of MMC (F–MMC) was also synthesized by the same procedure. The yields in monomeric forms of AF–MMC and F–MMC were 39 and 34%, respectively. The MMC contents of the conjugates were determined spectrophotometrically based on the absorption of MMC at 363 nm. Free amino groups were determined according to the method of Fields[15] described previously.[12]

Electrophoresis Cellulose acetate paper electrophoresis was adopted to examine the molecular charge of the conjugates following the procedure of Kubota and Ueki.[16] The electrophoresis was performed at a constant current of 0.6 mA/cm for 40 min at room temperature. D-Glucose was employed for correcting the migration cuased by electroosmosis. The NaH_2PO_4–Na_2HPO_4 buffer (pH 8.0, μ = 0.1) was used. The conjugates were stained with 0.8% Ponceau 3R containing 6% trichloroacetic acid. The band of D-glucose was detected with 1% of potassium permanganate containing 2% sodium carbonate.

Size Exclusion Chromatography A high performance liquid chromatography (HPLC) system (CCPD, Tosoh, Tokyo, Japan) equipped with a column of TSKgel G-3000SW (4.6 × 600 mm, Tosoh) was used according to the previous method.[12]

***In Vitro* Release Experiment** The release of MMC from AF–MMC was determined in a phosphate buffer system (pH 5.0, 6.0, 7.4, 8.0 and 9.0, μ = 0.3) at 37 °C according to the method desdribed previously.[12,17]

Animal Experiments Male Wistar rats (260—290 g) were obtained from

Japan SLC, Inc. (Shizuoka, Japan). Rats fasted for 24 h were anesthetized with sodium pentobarbital (40 mg/kg, i.p.). Depression of the body temperature was prevented with a heat plate and lamp. A bolus injection of the conjugate (0.5 mg/kg in MMC equivalent in 0.2 ml of 0.9% NaCl) was made through the jugular vein.

(a) Plasma Clearance The femoral artery was cannulated with polyethylene tubing (PE-50, Clay Adams, New Jersey, U.S.A.). After dosing, blood samples (0.5 ml) were drawn through the cannula at appropriate time intervals and were centrifuged immediately to separate the plasma.

(b) Biliary Excretion The bile duct was cannulated with polyethylene tubing (PE-10, Clay Adams). Bile samples were collected through the cannula during 5 h after drug injection.

(c) Liver Distribution At various times after injection, rats were killed by decapitation and livers were removed. The excised liver samples were homogenized (10%) in 0.25 M sucrose containing 1 mM ethylenediaminetetraacetic acid (EDTA).

Cell Separation[18] The liver was perfused *in situ* through the vena cava with 100 ml of 0.1 M NaCl at 37 °C. This was followed by another perfusion at the same temperature with 100 ml of 2 mM ethylene glycol bis(2-aminoethyl ether)-*N,N,N',N'*-tetraacetic acid (EGTA) in 0.15 M NaCl. The liver was then minced and pressed with a carbon steel blade through stainless-steel meshes (100 mesh) immersed in a medium consisting of 10% polyethylene glycol (molecular weight 4000) and 1 mM EGTA. The dispersed cell suspension, which had passed through the meshes, was filtered through a 74 μm nylon screen. The filtrate was centrifuged at $40 \times g$ for 3 min. Hepatocytes were purified by centrifugation of the cell pellets at $40 \times g$ for 3 min (twice). The initial supernatant was centrifuged again at $40 \times g$ for 3 min to remove the remaining hepatocytes and then centrifuged further at $500 \times g$ for 3 min. The resulting cell pellets were designated as the nonparenchymal cell-rich fraction.

Subcellular Fractionation[18] Stainless-steel meshes were used for gentle homogenization of rat liver. Livers were crushed with a wooden spatula through stainless-steel meshes (100 mesh). The disrupted cells were suspended to give 20% homogenate in 0.25 M sucrose containing 0.1 mM EDTA in a Potter–Elvehjem type Teflon homogenizer. The homogenate was fractionated into five subcellular fractions as follows. The homogenate was centrifuged at $60 \times g$ for 5 min, $1500 \times g$ for 10 min, and at $10000 \times g$ for 20 min, and the resulting pellets were designated fractions I, II and III, respectively. Centrifugation of the supernatant at $105000 \times g$ for 60 min yielded a pellet designated as fraction IV and the final supernatant was fraction V. The specific activities of β-glucuronidase in these fractions were determined as lysosomal marker enzymes. One unit was defined as the amount of enzyme required to release 1 nmol of *p*-nitrophenol per min from *p*-nitrophenyl-β-D-glucuronide.[19]

Sample Analysis The concentrations of MMC in the plasma, bile and tissue samples were assayed according to the method of Hashida *et al.*[17] Briefly, the sample solution was added to four volumes of 1 M sodium carbonate buffer (pH 9.0). The mixture was ultrafiltered with a micropartition system (MPS-1, Amicon, Tokyo, Japan), then the filtrate was injected into the HPLC. The mixture was heated at 90 °C for 5 min before ultrafiltration in order to determine the conjugated MMC. The amount of conjugated MMC was estimated by subtracting the amount of free MMC from that of the total MMC obtained from the alkali hydrolysis. The recoveries of both free and conjugated MMC from each biological medium were highly reproducible. The HPLC conditions were identical to those described previously.[12] The protein concentrations of the tissue samples were determined by the method of Lowry *et al.*[20]

Results and Discussion

The conjugation of MMC to the glycoprotein was confirmed by size exclusion chromatography. AF–MMC and F–MMC were eluted slightly faster than the original protein. When MMC and succinylated glycoprotein were simply mixed and applied to the chromatographic system, they were eluted at each position separately. These results indicated that MMC was bound covalently to the succinylated glycoprotein.

Fetuin or asialofetuin was readily polymerized during the carbodiimide reaction because it had both carboxyl and amino groups in its molecule.[6] The prior acylation of the glycoprotein was found to not only prevent the polymerization, but also increase the extent of conjugation of MMC. The conjugates showed a ultraviolet (UV) absorbance spectrum which contained the pattern of free MMC. The MMC contents of AF–MMC and F–MMC were 4.4 ± 0.8 w/w% ($n=11$) and 5.4 ± 1.1 w/w% ($n=10$), respectively, corresponding to 6.3 and 7.7 mol of MMC per mol of the protein (Table I).

TABLE I. Characteristics of AF–MMC and F–MMC

Compound	Acylation[a] (mol/mol protein)	MMC content (mol/mol protein)	MMC content (%(w/w))	Electrophoretic mobility[b] (mm)
AF–MMC	8.9 ± 1.6	6.3 ± 1.1	4.4 ± 0.8	10.2 ± 0.9
F–MMC	9.4 ± 1.5	7.7 ± 1.6	5.4 ± 1.1	11.8 ± 1.1
Asialofetuin	—	—	—	4.6 ± 0.3
Fetuin	—	—	—	10.1 ± 1.4

Each value represents the mean ± S.D. *a*) The number of acyl groups introduced into the protein was estimated by measuring the decrement of free amino residues. *b*) Net migration distance (to the anode) was measured at pH 8.0 on the cellulose acetate paper electrophoresis.

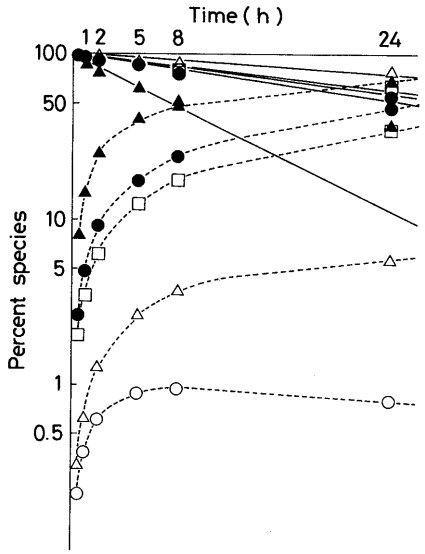

Fig. 1. Stability of AF–MMC (—) and Release of MMC (---) from the Conjugate in 0.1 M Phosphate Buffer Solutions ($\mu=0.3$) of pH 5.0 (○), 6.0 (△), 7.4 (□), 8.0 (●) and 9.0 (▲) at 37 °C

The acylation of the proteins by the use of succinic anhydride caused a marked decrease in the number of free amino residues. Then the number of acyl groups introduced into the protein was estimated by measuring the decrement of the free amino residues. As shown in Table I, nine out of 15 amino residues of the protein (14 ε-amino groups of lysine residue and a terminal amino group) appeared to be substituted by succinic groups.

The electrophoretic mobility of asialofetuin was much smaller than that of fetuin. This indicated that the negative charge was decreased by the removal of sialic acid from fetuin. However, asialofetuin showed an acidic nature because 3—4 out of 14 mol sialic acids contained in fetuin still remained after desialylation by the use of immobilized neuraminidase. The electrophoretic mobility of AF–MMC was similar to that of F–MMC and fetuin. The remaining free carboxyl groups (2.6 ± 1.9 mol/mol protein) which did not participate in bond formation may be responsible for

such a high negative charge of AF–MMC (Table I).

The degradation of AF–MMC was investigated in phosphate buffer solutions (Fig. 1). The release of MMC was observed during the degradation of AF–MMC at the pH range of 5.0—9.0. The disappearance of AF–MMC in buffered solutions followed pseudo first-order kinetics (Fig. 1). The degradation of MMC at each pH followed apparent first-order kinetics, as did AF–MMC.

On the basis of the present results, the overall reactions may be described by Chart 1, where k_1—k_3 are pseudo first-order rate constants for the depicted reactions.[17] Thus, the concentration of the conjugate ([AF–MMC]) and that of MMC released ([MMC]) in the reaction mixture have a time dependence given by the following equations:

$$[\text{AF–MMC}] = [\text{AF–MMC}]_0 \times \exp((-k_2+k_3)t) \quad (1)$$

$$[\text{MMC}] = k_2 \times [\text{MMC}]^*/(k_1-(k_2+k_3)) \times (\exp(-(k_2+k_3)t) - \exp(-k_1 t)) \quad (2)$$

where $[\text{AF–MMC}]_0$ and [MMC]* represent the initial concentration of the conjugate and that of MMC covalently bound to AF–MMC, respectively.

Based on these equations, curve fitting was done using the non-linear least-squares program MULTI.[21] The values of k_1 and k_2 showed good convergence. The degradation of MMC bound to asialofetuin was regarded as negligible ($k_3 \fallingdotseq 0$) because a small negative value of k_3 with an extraordinarily large standard deviation was obtained.

The pH–rate profiles of k_1 and k_2 are shown in Fig. 2. MMC was very stable above neutral pH, but decomposition increased markedly under acidic conditions (k_1, Fig. 2). AF–MMC was markedly stable at low pH contrary to MMC, but it releases predominant MMC at pH 9.0 (k_2, Fig. 2). These results were similar to those obtained in the experiment of the MMC-albumin conjugates.[12] Half-life of the release of MMC from AF–MMC under specific physiological conditions (pH 7.4 and 37 °C) was 36.7 h.

Plasma concentration–time curves of conjugated and released MMC after injection of the conjugates are shown in Fig. 3. Since the MMC attached to the conjugate was determined, the concentrations of the conjugates were expressed as μg equivalent MMC per ml. Elimination of the conjugated MMC after injection of AF–MMC did not follow exponential kinetics, which suggested that capacity-limited elimination processes existed. Therefore, an apparent elimination rate constant was estimated by the slope of the terminal phase by extrapolation in the case of AF–MMC. The elimination rate constants of AF–MMC and F–MMC calculated were 0.0946 ± 0.0033 and $0.0263 \pm 0.0018\ \text{min}^{-1}$ corresponding to the half-lives of 7.3 and 26.3 min, respectively. The asialofetuin conjugate disappeared faster than that of the non-desialylated fetuin conjugate.

However, the plasma survival time of AF–MMC was significantly greater than that of asialofetuin, whose plasma half-life was less than several minutes.[1,22] The rate of uptake by hepatocytes was limited (19.8 μg of asialo-

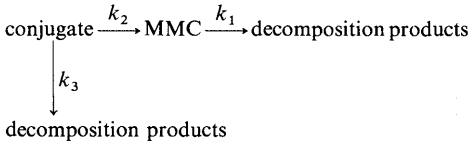

Chart 1

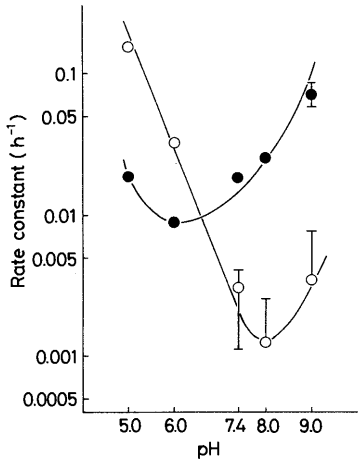

Fig. 2. pH Profiles of the Rate Constants in the Formation of MMC from AF–MMC (k_2) and the Degradation of MMC (k_1) in 0.1 M Phosphate Buffer Solutions ($\mu = 0.3$) at 37 °C

—○—, k_1; —●—, k_2. Vertical bars represent S.D. calculated from 15—20 sets of experimental data by the least-squares method.

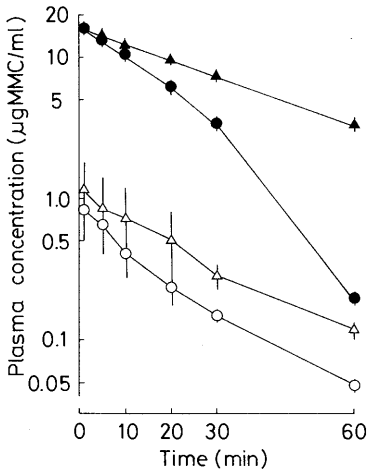

Fig. 3. Plasma Concentrations of Conjugated MMC and Released MMC after Intravenous Injection of 0.5 mg/kg in MMC Equivalent of the Conjugates in Rats

AF–MMC: —●—, conjugated MMC; —○—, released MMC.
F–MMC: —▲—, conjugated MMC; —△—, released MMC.
Each point represents the mean value with S.D. of three rats.

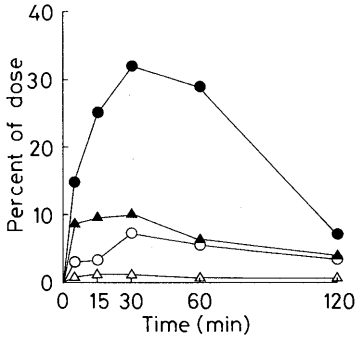

Fig. 4. Hepatic Levels of Conjugated MMC and Released MMC after Intravenous Injection of 0.5 mg/kg in MMC Equivalent of the Conjugates in Rats

AF–MMC: —●—, conjugated MMC; —○—, released MMC.
F–MMC: —▲—, conjugated MMC; —△—, released MMC.

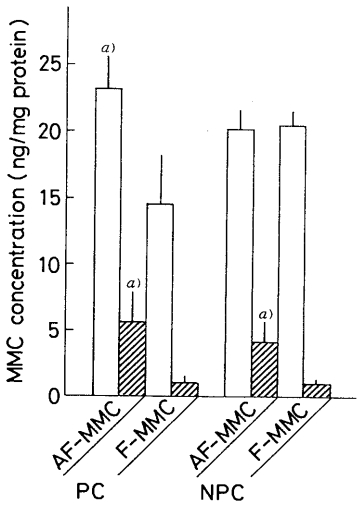

Fig. 5. Distribution of Conjugated MMC (▭) and Released MMC (▨) in Hepatic Cells at 30 min after Intravenous Injection of 0.5 mg/kg in MMC Equivalent of the Conjugates in Rats

PC, parenchymal cells; NPC, nonparenchymal cells.
Each value represents the mean ± S.D. of three rats. *a)* $p < 0.05$ when compared with the value of F–MMC. The Student's *t* test was used.

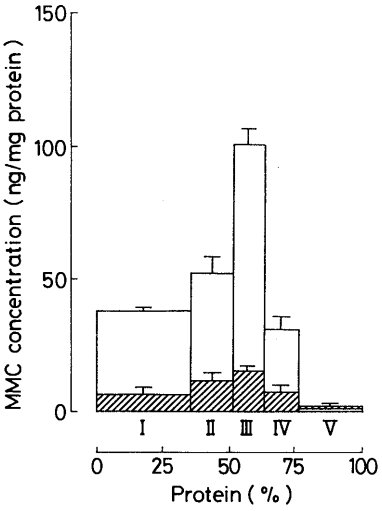

Fig. 6. Distribution Patterns of Conjugated MMC (▭) and Released MMC (▨) in the Liver Subcellular Fractions at 30 min after Intravenous Injection of 0.5 mg/kg in MMC Equivalent of AF–MMC in Rats

Each value represents the mean ± S.D. of three rats. The numbers of I—V designate the subcellular fractions of the liver by the differential centrifugation method (see the text). On the abscissa each fraction is represented as a percentage of the total protein in the homogenate.

fetuin/min per 100 g body weight in rats[5]). This may be the reason why AF–MMC showed the saturable nature of plasma clearance in the initial stage, since the conjugate of 1092 μg in asialofetuin equivalent/100 g body weight was administered to rats.

Figure 4 shows the hepatic levels of conjugated and released MMC after injection of AF–MMC and F–MMC. At 30 min after injection of AF–MMC, 40% of the dose (conjugated MMC + released MMC) was present in the liver. In homologous rats administered F–MMC, the hepatic total MMC was only 10% of the dose at 30 min. These findings suggested that rapid clearance of the conjugate from circulation (Fig. 3) resulted in a prompt uptake by the liver when AF–MMC was administered (Fig. 4). AF–MMC appeared to retain the function of asialofetuin

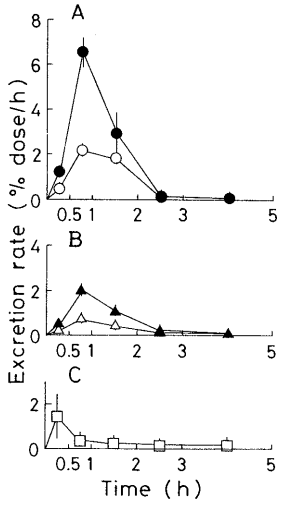

Fig. 7. Biliary Excretions of Conjugated MMC and Released MMC after Intravenous Injection of AF–MMC (A), F–MMC (B) and MMC (C) in Rats

AF–MMC: —●—, conjugated MMC; —○—, released MMC.
F–MMC: —▲—, conjugated MMC; —△—, released MMC.
MMC: —□—.
Each rat was given 0.5 mg/kg in MMC equivalent of AF–MMC, of F–MMC or 1.0 mg/kg of MMC. Each value represents the mean ± S.D. of three rats.

to interact with the specific receptors on the hepatocytes. Similarly, Furuno *et al.* reported that maximally 30% of the dose was detected in the liver when pepstatin–asialofetuin conjugate was administered to rats.[18] However, the extent of the liver accumulation of these conjugates was lower than that of ^{125}I-labelled asialofetuin[3] or ^{3}H-labelled asialofetuin.[22] This may reflect the saturable nature of the receptor-mediated endocytosis and/or negative charge[23] of AF–MMC by the conjugation of succinic acid (Table I). On the other hand, no MMC was detected in the liver when a dose of 1 mg/kg of MMC was administered.

Figure 5 shows the hepatic distributions of conjugated and released MMC at 30 min after injection of AF–MMC and F–MMC. Parenchymal cells selectively took up AF–MMC; a non-selective uptake by nonparenchymal cells was observed in both the conjugates. However, the specific uptake by the parenchymal cells in the liver was accented by taking account of the 27-fold greater cell volume of hepatocytes, compared to sinusoidal cells.[24]

The distribution patterns of conjugated and released MMC in the liver subcellular fractions are depicted in Fig. 6. The liver samples were collected at 30 min after injection of AF–MMC. The highest levels of MMC were observed in fraction III. The subcellular distribution patterns of conjugated and released MMC both paralleled those of the activity of β-gluculonidase, the lysosomal enzyme. The distribution patterns of the conjugate were, therefore, similar to that of native asialofetuin, which was taken up by parenchymal cells and transported into lysosomes. AF–MMC-entered lysosomes might immediately become exposed to an acid milieu, pH most probably between 4 and 5, and to a collection of some 40 or more digestive enzymes.[25]

Biliary excretions of the conjugates were examined in rats (Fig. 7). Excretion rates of both conjugated and released MMC reached a maximum level at the time range of 0.5—1 h after the injection of AF–MMC. The biliary excretion

continued for at least 5 h; totally 10.4% (7.0% conjugated and 3.4% released) of the dose was recovered in the bile (Fig. 7A). Contrary to AF–MMC, the biliary excretions of F–MMC and MMC accounted for only 3.8% (2.6% conjugated and 1.2% released) and 1.6% of the dose, respectively (Fig. 7B, C). The greater uptake of AF–MMC by hepatocytes (Fig. 4) appeared to reflect an increased excretion in bile. On the other hand, lysosomal degradation of asialoglycoprotein, which covalently coupled fluoresceinisothiocyanate (FITC), was shown to be the rate-limiting step in FITC excretion into bile.[26] These findings suggested that at least the part of the conjugated MMC which was excreted into the bile may be low-molecular weight metabolite(s) of AF–MMC leaving the lysosomes.

In the present study, succinylated asialofetuin was found to effectively carry the guest molecule to the hepatocytes. An investigation focusing on the chemical linkage of the guest molecule and its effects on the nature of the conjugate as a site-specific macromolecular prodrug is in progress.

Acknowledgment The authors particularly acknowledge Y. Fujihara, K. Ohno and T. Yokotani for their technical assistance.

References

1) A. G. Morell, G. Gregoriadis, I. H. Shcheinberg, J. Hickman and G. Ashwell, *J. Biol. Chem.*, **246**, 1461 (1971).
2) G. Aschwell and A. G. Morell, *Adv. Enzymol.*, **41**, 99 (1974).
3) J. H. LaBadie, K. P. Chapman and N. N. Aronson, Jr., *Biochem. J.*, **152**, 271 (1975).
4) K. Brridges, J. Harford, G. Ashwell and R. D. Klausner, *Proc. Natl. Acad. U.S.A.*, **79**, 350 (1982).
5) E. Regoeczi, M. T. Debanne, M. W. C. Hatton and A. Koj, *Biochim. Biophys. Acta*, **541**, 372 (1978).
6) R. S. Spiro, *J. Biol. Chem.*, **235**, 2860 (1960).
7) J. C. Rogers and S. Kornfeld, *Biochem. Biophys. Res. Commun.*, **45**, 622 (1971).
8) T. Hara, H. Ishihara, Y. Aramaki and S. Tsuchiya, *Int. J. Pharmaceut.*, **42**, 69 (1988).
9) L. Fiume, A. Mattioli, P. G. Balboni, M. Tognon, G. Barbanti-Brodano, J. D. Vries and T. Wieland, *FEBS Lett.*, **103**, 47 (1979).
10) L. Fiume, A. Mattioli, C. Busi, P. G. Balboni, G. Barbanti-Brodano, J. D. Vries, R. Altoman and T. Wieland, *FEBS Lett.*, **116**, 185 (1980).
11) D. B. Cawley, D. L. Simpson and H. R. Heraschman, *Proc. Natl. Acad. Sci. U.S.A.*, **78**, 3383 (1981).
12) Y. Kaneo, T. Tanaka and S. Iguchi, *Chem. Pharm. Bull.*, **38**, 2614 (1990).
13) P. Cuatrecasac and I. Parikh, *Biochemistry*, **11**, 2291 (1972).
14) G. W. Jourdian, L. Dean and S. Roseman, *J. Biol. Chem.*, **246**, 430 (1971).
15) R. Field, *Methods Enzymol.*, **25**, 464 (1972).
16) Y. Kubota and H. Ueki, *J. Biochem.* (Tokyo), **64**, 405 (1968).
17) M. Hashida, Y. Takakura, S. Matsumoto, H. Sasaki, A. Kato, T. Kojima, S. Muranishi and H. Sezaki, *Chem. Pharm. Bull.*, **31**, 2055 (1983).
18) K. Furuno, N. Miwa and K. Kato, *J. Biochem.* (Tokyo), **93**, 249 (1983).
19) K. Kato, K. Yoshida, H. Tsukamoto, M. Nobunaga, T. Masuya and T. Sawada, *Chem. Pharm. Bull.*, **8**, 239 (1960).
20) O. H. Lowry, M. J. Rosebrough, A. L. Farr and R. I. Randall, *J. Biol. Chem.*, **193**, 265 (1951).
21) K. Yamaoka, Y. Tanigawa, T. Nakagawa and T. Uno, *J. Pharmacobio-Dyn.*, **4**, 879 (1981).
22) Y. Aramaki, A. Inaba and S. Tsuchiya, *Biopharm. Drug Disposit.*, **6**, 389 (1985).
23) S. Nakane, S. Matsumoto, Y. Takakura, M. Hashida and H. Sezaki, *J. Pharm. Pharmacol.*, **40**, 1 (1988).
24) H. A. Krebs, N. W. Cornell, P. Lung and R. Hems, "Regulation of Hepatic Metabolism," ed. by F. Lundquist and N. Tygstrup, Academic Press, New York, 1974, p. 726.
25) C. DeDuve, T. DeBarsy, B. Poole, A. Trouet, P. Tulkens and F. V. Hoob, *Biochem. Pharmacol.*, **23**, 2495 (1974).
26) P. V. D. Sluijs, R. Oosting, J. G. Weitering, M. Hardonk and D. K. F. Meijer, *Biochem. Pharmacol.*, **34**, 1399 (1985).

Targeting of Liposomes Surface-Modified with Glycyrrhizin to the Liver. I. Preparation and Biological Disposition

Hideki TSUJI, Sayoko OSAKA and Hiroshi KIWADA*

Faculty of Pharmaceutical Sciences, University of Tokushima, 1–78–1, Shomachi, Tokushima 770, Japan. *Received August 17, 1990*

We consider glycyrrhizin to be a new ligand for liposomes to the liver because it is known that about 80% of glycyrrhizin is excreted into the bile after intravenous administration in rats. In order to modify the liposomal surface with glycyrrhizin, 30-stearyl glycyrrhizin (GLOSt), one of the lipophilic glycyrrhizin derivatives, was synthesized. The structure of this new compound was identified by nuclear magnetic resonance (NMR), infrared (IR) and mass spectra (MS). Sonicated liposomes were prepared from hydrogenated egg phosphatidylcholine–cholesterol–GLOSt or dicetyl phosphate (DCP) (4:4:1) and were labelled with [^{3}H]inulin as an aqueous marker. It was confirmed by measuring the encapsulation efficiencies and the mean diameters that GLOSt-containing sonicated liposomes (GLOSt-SUV) were SUV-type as well as DCP-containing control liposomes (control-SUV). Four hours after intravenous injection into rats at a dose of 90 μmol as total lipid per kg of rat body weight, GLOSt-SUV showed 4-fold more accumulation (42.4%) in the liver than control-SUV. Therefore, glycyrrhizin is considered to be a useful new ligand on liposomes for targeting to the liver.

Keywords targeting; drug delivery system; liposomes; glycyrrhizin; 30-stearyl glycyrrhizin; liver

Introduction

Liposomes are thought to be the drug carrier for selective delivery to specific tissues or cells. For more than a decade numerous investigations using many kinds of ligands, (glycolipids, lectins, monoclonal antibodies, *etc.*) have been carried out in an attempt to navigate liposomes to target sites.[1] However, it is difficult to apply liposomes *in vivo* since in most tissues the continuous barrier of the vascular endothelial cells prevents liposomes from moving from the intravascular space to the parenchymal cells. The use of liposomes as a tool for active targeting is, therefore, confined to several organs or tissues, such as the liver which has fenestrated endothelium,[2] cancer lesions where the permeability of vasculature is increased in comparison with normal tissues[3] and cells of the reticuloendothelial system resident in the vascular space.[4]

The liver is one of the most important organs in the body but there is to date no effective chemotherapeutic agent to counteract potentially fatal diseases such as chronic virus hepatitis and hepatoma. Several kinds of drugs, for example, cytokines like interferons and interleukin-2, antiviral agents such as adenine arabinoside, and biological response modifiers have been used in clinical trials. But many problems of low therapeutic activity and serious side effect(s) of these drugs remain to be solved. For these reasons, paralleling with development of new drugs, an adequate technique to target drugs to the liver is also necessary.[5]

The liver contains specialized blood capillaries called "sinusoids" are developed. Since these sinusoids are lined with a discontinuous basement membrane and the endothelial lining has many pores called "fenestrations", blood components have easy access to the parenchymal cells through the vascular barrier. The mean diameter of the fenestrations has been estimated at 106 nm and the maximum at 200—300 nm.[6] From this morphological point of view, the liver is also one of the most suitable organs for a drug delivery system such as liposomes.

We selected glycyrrhizin (GL), which is a component of licorice (*Glycyrrhiza glabra*) roots, as the ligand of liposomes for targeting to the liver. It is known that GL demonstrates high accumulation in the liver, and Ichikawa *et al.* reported that when given intravenously to rats, about 80% of the injected dose is excreted into bile.[7] Therefore, it can be assumed that the uptake of GL by the liver is substantial.

In the present study, we examined the ability of liposomes surface-modified with GL to target the liver. We synthesized 30-stearyl glycyrrhizin (GLOSt), which is a novel compound as one of the lipophilic GL derivatives. Small unilamellar liposomes containing GLOSt (GLOSt-SUV) and surface-modified with GL were prepared, and the fate of the liposomes after intravenous injection into rats was investigated.

Experimental

Materials Hydrogenated egg phosphatidylcholine (PC) was a gift from Nippon Fine Chemicals Co., Ltd. (Osaka). Cholesterol (CH) was obtained from Wako Pure Chemicals Co., Ltd. (Osaka), and recrystallized from ethanol. Dicetyl phosphate (DCP) was purchased from Nacalai Tesque Inc. (Kyoto). GL was from Maruzen Chemicals Co., Ltd. (Osaka). All other synthetic chemicals were commercial products of reagent grade or better. [^{3}H(G)]inulin was purchased from New England Nuclear (Boston, MA).

Spectral Analysis Spectral data were obtained with the following instruments: infrared (IR) spectra with a Perkin-Elmer 1720 infrared Fourier transform spectrometer; mass spectra (MS) with a JEOL DX 303 mass spectrometer; ^{1}H- and ^{13}C-nuclear magnetic resonance (^{1}H- and ^{13}C-NMR) spectra with a JEOL GSX-400 spectrometer (400 and 100 MHz, respectively).

Synthesis of GLOSt A solution of *O*-benzyl-*N*,*N*′-dicyclohexylisourea (23.2 g, 73.8 mmol), prepared by the method of Vowinkel,[8] in dimethylformamide (DMF) (40 ml) was added to a solution of GL (30.3 g, 36.8 mmol) in DMF (60 ml) with stirring on an ice-water bath. After continued stirring overnight, the precipitate (dicyclohexylurea) was filtered off and the filtrate was concentrated *in vacuo* to yield a syrup. The syrup was purified by silica gel column chromatography with stepwise elution to obtain 6′,6″-dibenzylglycyrrhizin (I) (10.3 g, 27.8%) with $CHCl_3$–MeOH (8:1, v/v). FAB-MS (NaI) *m/z*: 1025 $[M+Na]^+$.

A solution of I (4.01 g, 4.00 mmol) in DMF (20 ml) was added to melted *O*-*n*-stearyl-*N*,*N*′-dicyclohexylisourea containing CuCl, prepared from *n*-stearylalcohol (1.71 g, 6.32 mmol), dicyclohexylcarbodiimide (1.24 g, 6.05 mmol) and CuCl (5 mg) at 85 °C,[9] and the mixture was stirred at 85 °C for 4 h. The precipitate was filtered off and washed with ethyl acetate and then the filtrate was concentrated *in vacuo* to give a pale green syrup. The syrup was separated by silica gel column chromatography with $CHCl_3$–MeOH (93:7, v/v) to give 6′,6″-dibenzyl-30-stearyl glycyrrhizin (II) (2.90 g, 56.9%). FAB-MS (NaI) *m/z*: 1277 $[M+Na]^+$. ^{1}H-NMR ($CDCl_3$–methanol-d_4 1:1) δ: 1.28 (brs, stearyl-H), 5.27 (m, 4H, Ph-C$\underline{H}_2$–), 5.68 (s, 1H, 12-H), 7.36 (m, 5H, Ph-H).

A solution of II (1.50 g, 1.18 mmol) in 20 ml of isopropanol–AcOEt

(5:1, v/v) was catalytically hydrogenated over 5% Pd–carbon (1 g) at atmospheric pressure for 4 h. Pd–carbon was filtered off and the filtrate was evaporated and dried *in vacuo* to give GLOSt (III) (1.20 g, 99%), which was thin-layer-chromatographically pure. No other signal for impurity was observed in nuclear magnetic resonance (NMR) charts of GLOSt. FAB-MS (NaI) *m/z*: 1097 $[M+Na]^+$, 705 $[M-C_{12}H_{17}O_{13}]^+$. IR ν_{max}^{KBr} cm^{-1}: 3431 (OH), 2926, 2854 ($-(CH_2)_n-$), 1729, 1661 (C=O). ^1H- and ^{13}C-NMR data are compared in Table I with those of authentic GL.

Preparation and Characterization of Liposomes Small unilamellar vesicles (SUV) consisting of PC, CH, and DCP or GLOSt in a molar ratio of 4:4:1 were prepared as follows. A homogeneous lipid solution in chloroform was evaporated to form a dried lipid film in a round-bottomed flask. The lipid film was hydrated with 12 mM NaH_2PO_4–51 mM Na_2HPO_4–77 mM NaCl (pH 7.4, 280 mOsm/kg) containing 0.1 mM [^{3}H]inulin as an aqueous space marker. The total lipid concentration was 45 μmol/ml in the liposomal suspension. The mixture was voltexed and sonicated in a bath type sonicator (Branson ultrasonic cleaner, type-5200, Yamato Science Co., Ltd., Tokyo) until a homogeneous suspension was obtained. The suspension was further sonicated with a probe-type sonicator (ultrasonic disruptor, UR-200P, Tomy Seikou Co., Ltd.) for about 1 h to give SUV.

The vesicles were dialyzed in a flow-type dialysis cell using polycarbonate membranes with a pore size of 0.03 μm against a 200-fold volume of 140 mM phosphate-buffered saline (pH 7.4) at room temperature for 4 d. The phosphate-buffered saline was replaced twice a day.

The encapsulation ratio of [^{3}H]inulin was calculated from the radioactivity in the suspension after dialysis, which was counted with a liquid scintillation counter (Aloka LSC-703, Tokyo) in an emulsifier scintillation cocktail (Scintisol EX-H, Wako Pure Chemicals Co., Ltd., Osaka), and expressed as percentage of the initial radioactivity in the suspension before dialysis.

The incorporation ratio of GLOSt was calculated by measuring the content of GLOSt in the suspension with high performance liquid chromatography (HPLC) after dialysis and expressed as a percentage of the initial content before dialysis. HPLC conditions were as follows: column, μ-Bondapak-C18 (Waters, 15 cm × 3.9 mm i.d.); column temperature, room temperature; flow rate, 1.0 ml/min; detector, UV 254 nm; mobile phase, 2% acetic acid solution (v/v)–MeOH (1:9, v/v).

The mean diameter of the vesicles was measured with a submicron particle analyzer (Coulter N4, Coulter Electronics Inc., U.S.A.).

Animal Experiments Male albino Wistar rats (body weight 300 ± 50 g) anesthetized with ether were cannulated in the femoral vein, femoral artery and bladder and treated as described.[10] Two cannulae were inserted into the bladder, one for sampling and the other for washing. Each operated rat was placed in a Bollman cage. After recovering from anesthesia, liposome suspension was injected into the rat through the femoral vein cannula. At appropriate times after injection, blood and urine samples were collected from the cannulae inserted into the artery and bladder, respectively, without disturbing or anesthetizing the animals. Four hours after injection, rats were anesthetized with pentobarbital and sacrificed by removing blood from the cannula inserted in the femoral artery. Then liver, lung, spleen and kidney were excised and rinsed with 140 mM phosphate-buffered saline (pH 7.4). The radioactivity of each sample was measured as follows.

Determination of Radioactivity Radioactivity in tissues, blood and urine samples after intravenous injection of liposomes encapsulating [^{3}H]inulin as an aqueous marker was determined as described previously with slight modification.[11]

The liver was homogenized in water and the volume was adjusted to 50 ml with water. The urine was diluted with water to 10 ml. Blood samples (0.1 ml), urine samples (0.5 ml) or samples of the liver homogenate (0.5 ml) were treated with a 0.2 ml aliquot of 30% H_2O_2 and 0.2 ml of 2 N KOH solution in isopropanol in a liquid scintillation vial to decolorize and solubilize. The mixture was stirred gently but sufficiently and then left at room temperature overnight. After 0.4 ml of 10% acetic acid was added for neutralization, 10 ml of scintillation cocktail (Scintisol EX-H) was added.

Whole spleen, lung or kidney was solubilized and decolorized by treatment with 2 ml of 2 N KOH solution in isopropanol and 1 or 2 ml of 30% H_2O_2 during incubation at 37 °C overnight. Then, 2.4 ml of 10% (v/v) acetic acid solution was added for neutralization and the volume was adjusted to 10 ml with water. One ml of the mixture was collected in a liquid scintillation vial and then 10 ml of Scintisol EX-H was added.

The mixed scintillator solutions were allowed to stand at room temperature to dissipate chemiluminescence and counted with a liquid scintillation counter (Aloka LSC-703, Tokyo).

Stability of Liposomes in Rat Plasma In this experiment, 5(6)-carboxyfluorescein (CF, Eastman Kodak, N.Y.) solution prepared as described before[12] was used as an aqueous marker of liposomes instead of [^{3}H]inulin. A 0.1 ml aliquot of liposomal suspension (4.5 μmol as total lipid) was incubated with 0.9 ml of fresh rat plasma at 37 °C. At appropriate times after incubation, a 10 μl aliquot was transfered into 5 ml of cold 140 mM phosphate-buffered saline (pH 7.4). A 1 ml aliquot of the diluted mixture was well mixed with 1 ml of 5% Triton X-100 solution and then 2 ml of water was added. The latency of CF in the liposomes was calculated from the fluorescence intensity with and without Triton X-100 treatment and expressed as a percentage of the initial latency.

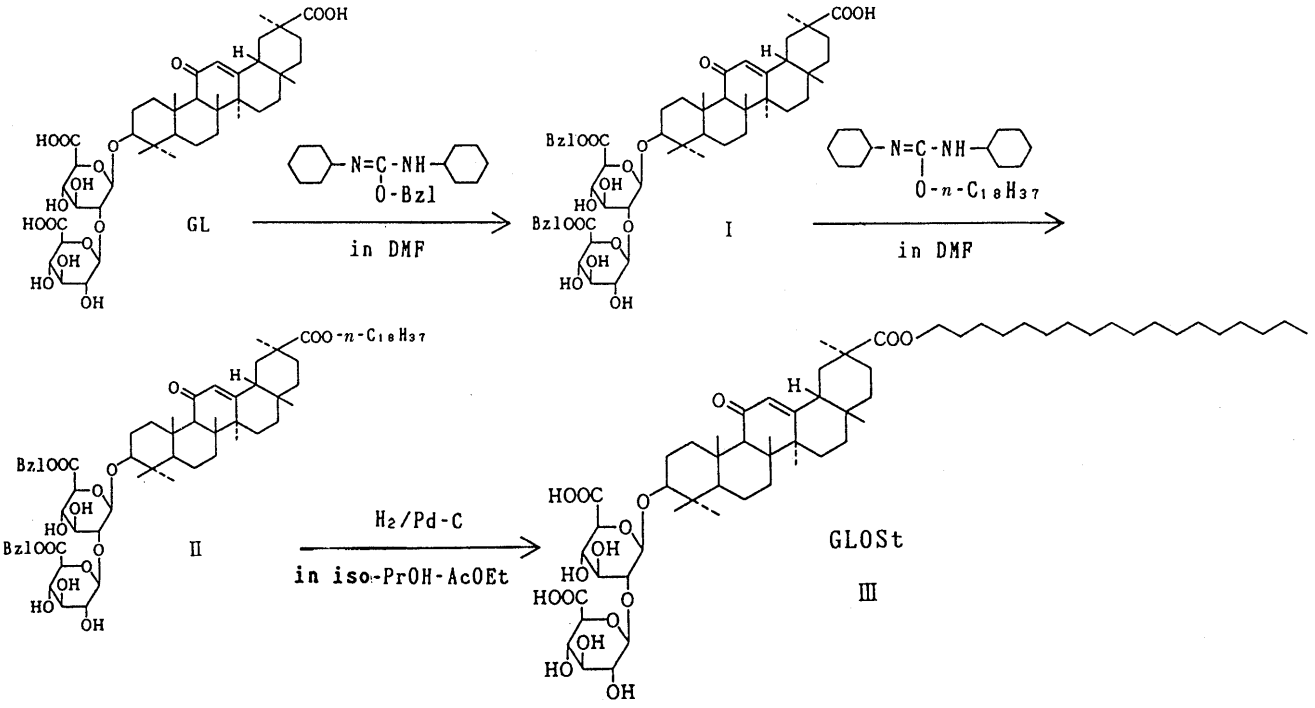

Chart 1. Synthetic Route of GLOSt (Bzl = $-CH_2-C_6H_5$)

Results

Synthesis of GLOSt GLOSt, a novel compound, was synthesized successively by esterification employing isoureas[8,9] according to the process shown in Chart 1. The structure of the new compound was identified by several spectra, *e.g.* NMR, IR, and mass spectra. ^{1}H- and ^{13}C-NMR spectral data of GLOSt are shown in Table I in comparison with those of authentic GL. δ values of GLOSt except for signals based on the stearyl group agreed with those of GL perfectly. No other signal of impurity was observed in NMR charts of GLOSt.

Preparation and Characterization of Liposomes In order to have access to liver parenchymal cells, it is necessary for liposomes to be a size which is smaller than the pore size of the fenestrations, the mean diameter of which has been estimated as 106 nm and the maximum as 200—300 nm.[6] Therefore, SUV-type liposomes were prepared by sonication with a probe-type sonicator for 1 h. CH equimolar with PC was incorporated into liposomes to enhance the *in vivo* stability.[13] DCP was incorporated into control-SUV as an alternative to GLOSt to give a negative charge. The characterization of these liposome preparations is listed in Table II. The encapsulation ratio of [^{3}H]inulin was 2.25% and 2.06% (0.50 and 0.46 μl/μmol as encapsulated volume) for GLOSt-containing liposomes and control-SUV, respectively. The mean diameter of GLOSt-containing liposomes and control-SUV was 60 ± 30 and 54 ± 30 nm, respectively. All these values of GLOSt-containing liposomes were compatible with those of control-SUV. Therefore, it was confirmed that GLOSt-containing sonicated liposomes formed SUV-type liposomes (GLOSt-SUV) as well as control-SUV. Values shown in this table are those of a typical example; deviations in the values of other preparations were less than 5% of each value.

The incorporation ratio of GLOSt obtained by measuring its content in the suspension sampled before and after dialysis was 99.7% (Table II). This result shows that GLOSt was quantitatively incorporated into the liposomal membrane after dialysis.

Blood Disappearance and Urinary Excretion Figure 1 shows the dispositions of [^{3}H]inulin after intravenous injection of the liposomes at a dose of 90 μmol per kg rat body weight. The blood disappearance of [^{3}H]inulin entrapped in liposomes up to 4 h is shown in panel A. The incorporation of GLOSt into SUV induced a substantial increase of the elimination rate. Total body clearances of GLOSt-SUV and control-SUV were 47.4 and 6.6 ml/h/kg,

TABLE I. Spectral Data of ^{1}H- and ^{13}C-NMR for GLOSt Compared with GL

Compound	GLOSt	GL
^{1}H-NMR		
H-1′ (1H, d)	4.50 (J=7.2 Hz)	4.50 (J=7.3 Hz)
H-1″ (1H, d)	4.64 (J=7.2 Hz)	4.61 (J=7.3 Hz)
H-12 (1H, s)	5.63	5.63
CH_3 (3H, s)	0.83, 0.83, 1.06, 1.14, 1.14, 1.19, 1.40	0.83, 0.84, 1.05, 1.13, 1.13, 1.19, 1.40
Stearyl-H	1.27 (–(CH_2)$_n$–, br s) 4.12 (–(CH_2–OCO–, 2H, m)	
^{13}C-NMR		
CH_3	16.3, 16.6, 19.0, 23.6, 27.8, 28.6, 28.9	16.2, 16.5, 18.9, 23.5, 27.6, 28.5, 28.7
CH_2	17.7, 26.3, 26.8, 26.9, 31.5, 33.2, 38.2, 39.6, 41.5	17.6, 26.2, 26.7, 26.8, 31.3, 33.1, 38.1, 39.6, 41.5
CH	48.9, 55.8, 62.3, 72.0, 72.0, 75.0, 75.0, 75.8, 76.0, 76.4, 82.3, 90.3, 104.3, 104,7, 128.6	48.9, 55.7, 62.3, 71.9, 72.0, 75.0, 75.2, 76.0, 76.1, 76.4, 82.9, 90.1, 104.3, 105.2, 128.3
C	32.2, 37.2, 39.8, 43.8, 44.5, 46.0, 171.1, 172.0, 172.3, 177.5, 201.7	32.2, 37.1, 39.8, 43.7, 44.1, 45.9, 171.2, 171.6, 171.7, 179.7, 202.0
Stearyl-C	14.2 (CH_3) 23.0, 26.4, 29.1, 29.5, 29.7, 29.9, 30.0 (overlapped), 32.3, 43.8, 65.1 (CH_2)	

^{1}H-NMR (400 MHz) and ^{13}C-NMR (100 MHz) spectra were recorded on a JEOL GSX-400 spectrometer using $CDCl_3$–methanol-d_4=1:1 as a solvent with tetramethylsilane as an internal standard. Values are chemical shifts given on the δ (ppm) scale with the internal standard. Values of characteristic signals for ^{1}H-NMR and all signals for ^{13}C-NMR are represented in this table. The abbreviations are as follows: s, singlet; d, doublet; t, triplet; q, quartet; m, multiplet; br, broad; J, coupling constant.

TABLE II. Characterization of Control-SUV and GLOSt-SUV

Liposome	Mean diameter (nm)	Encapsulation ratio of [^{3}H]inulin (%)	Incorporation ratio of GLOSt (%)
Control-SUV	54 ± 30	2.25	—
GLOSt-SUV	60 ± 30	2.06	99.7

Liposomes were composed of hydrogenated egg PC, CH and GLOSt or DCP in a 4:4:1 molar ratio and prepared with 140 mM phosphate-buffered saline (pH 7.4, 280 mOsm/kg) containing 0.1 mM [^{3}H]inulin as an aqueous space marker and using a probe-type sonicator to form SUV-type liposomes. Mean diameter was measured with a submicron particle analyzer (Coulter N4) and incorporation of GLOSt was measured with HPLC.

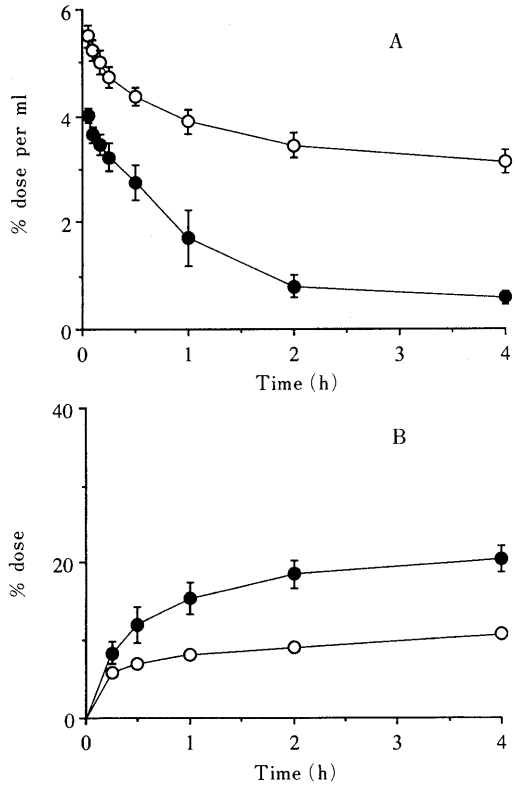

Fig. 1. Time Courses of Blood Levels (Panel A) and Cumulative Urinary Excretions (Panel B) of [^{3}H]Inulin Encapsulated in Control-SUV (○) and GLOSt-SUV (●) after Intravenous Injection into Rats

Liposomes were injected at a dose of 90 μmol as total lipid per kg body weight. Results are expressed as percentage of the injected dose per 1 ml of blood volume (A) and of the injected dose per total urine (B). Values are means $\pm$ S.D. of three animals.

as calculated by area under the plasma concentration (AUC) and dose, respectively (Table IV). Panel B shows the time courses of the cumulative urinary excretion of [^{3}H]inulin which is an aqueous marker of liposomes. The 4 h excretion of [^{3}H]inulin was 20.5% of injected dose after administration of GLOSt-SUV, which was about 2-fold higher than in the case of control-SUV (10.7%). Since the radioactivity found in the urine is considered to be free [^{3}H]inulin, it is concluded that the aqueous marker of GLOSt-SUV, rather than that of control-SUV, tends to leak to some extent *in vivo*.

Stability in Rat Plasma The time courses of leakage of CF, as an aqueous marker, from liposomes during incubation with fresh rat plasma at 37 °C were examined (Fig. 2). Control-SUV was very stable in plasma and the latency of CF was 96%, whereas that of GLOSt-SUV was 70% after 2 h incubation. The instability of GLOSt-SUV in plasma might be one of the reasons that the urinary excretion of GLOSt-SUV was higher than that of control-SUV *in vivo*. In 140 mM phosphate-buffered saline (pH 7.4) no leakage of CF from either SUV preparation was observed during incubation at 37 °C. The latency of control-SUV and GLOSt-SUV respectively was 98% and 99% 2 h after incubation. Therefore, the leakage of [^{3}H]inulin from GLOSt-SUV must be attributable some factor(s) in the plasma.

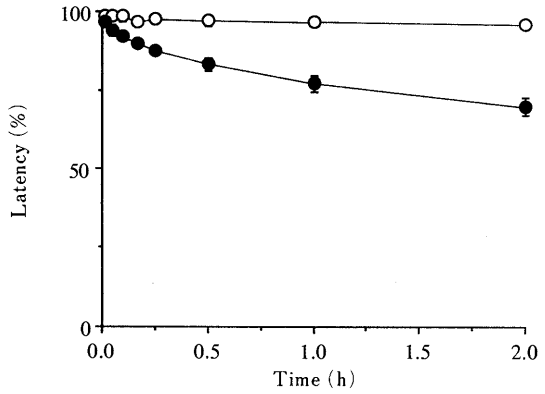

Fig. 2. Time Courses of Latency of CF Encapsulated in Control-SUV (○) and GLOSt-SUV (●) in Fresh Rat Plasma

0.1 ml of liposomal suspension (4.5 μmol as total lipid) was incubated with 0.9 ml of fresh rat plasma at 37 °C. The extent of latency was determined as described in Materials and Methods. Values are means ± S.D. of three animals.

TABLE III. Tissue Distribution of [^{3}H]Inulin Entrapped in Control-SUV and GLOSt-SUV 4 h after Intravenous Injection into Rats

Liposome	Control-SUV	GLOSt-SUV
Blood	51.7±3.0	11.4±2.1[c]
Liver	10.4±0.7	42.4±1.4[c]
Spleen	4.3±0.6	2.0±0.4[a]
Lung	0.5±0.1	0.2±0.1[a]
Kidney	0.9±0.2	0.8±0.1
Urine	10.7±0.5	20.5±1.8[b]
Recovery	78.5±4.1	77.2±3.2

Liposomes were injected at a dose of 90 μmol as total lipid per kg body weight. Values are means ± S.D. of three animals and are expressed as percentage of the initial dose per whole tissues. Blood volume was estimated as 6.5% of total body weight. Significant difference from control-SUV using Student's *t*-test: *a*) $p<0.05$, *b*) $p<0.01$, *c*) $p<0.001$.

TABLE IV. Pharmacokinetic Parameters of [^{3}H]Inulin Entrapped in Control-SUV and GLOSt-SUV

Parameter	Control-SUV	GLOSt-SUV
$AUC^{0\to\infty}$ (% dose·h/ml)	60.5±5.8	7.4±1.1
$AUC^{0\to 4h}$ (% dose·h/ml)	14.8±0.9	5.5±1.0
CL_{total} (ml/h/kg)	6.6±0.5	47.4±6.8
CL_{liver} (ml/h/kg)	2.8±0.2	27.6±5.6
CL_{spleen} (ml/h/kg)	1.2±0.2	1.3±0.04
CL_{lung} (ml/h/kg)	0.1±0.01	0.1±0.02
CL_{kidney} (ml/h/kg)	0.2±0.04	0.5±0.04
CL_{renal} (ml/h/kg)	2.9±0.1	13.3±2.5

Parameters present here were calculated from the values used in Fig. 1 and Table III. AUC was estimated by the trapezoidal rule. Total body clearance (CL_{total}) was calculated by $AUC^{0\to\infty}$ and injected dose. Organ clearance (CL_{organ}) was obtained by dividing the uptake amount for 4 h by $AUC^{0\to 4h}$. Renal clearance (CL_{renal}) was calculated by dividing total urinary excretion for 4 h by $AUC^{0\to 4h}$. Values are mean ± S.D. of three animals.

Tissue Distribution and Organ Clearances Tissue distribution and organ clearances of the liposomes 4 h after intravenous injection are shown in Tables III and IV, respectively. Organ clearance is considered to be a more appropriate parameter than the percent dose distribution commonly used, because clearance represents the ability of tissue uptake independent of blood concentration. In the present study, organ clearance was expressed as the uptake amount for 4 h divided by $AUC^{0\to 4h}$ because the efflux of [^{3}H]inulin from organs can be neglected. A substantial increase was found in the liver uptake as a result of GLOSt incorporation in the SUV. The distribution of GLOSt-SUV to the liver was 42.4% of injected dose, almost 4-fold higher than that of control-SUV. The liver clearance was 10-fold higher. On the other hand, the uptake of GLOSt-SUV by spleen and lung, which are organs rich in reticuloendothelial cells, and by kidney were even lower than that by the liver, confirming that GLOSt-SUV was selectively taken up by the liver.

Discussion

In order to modify the liposomal surface with GL, this ligand was converted into a lipophilic derivative possessing an affinity for liposomal membranes. In this study, GLOSt was synthesized in anticipation of its high incorporation into the liposomal membrane. GLOSt is a single-chain amphiphile having diglucuronide moiety as a hydrophilic head group, a rigid glycyrrhetinate moiety and a flexible tail of alkyl chain as a lipophilic group. It is a favorable structure for incorporation into liposomal membranes.[14] Actually, as shown in Table II, it was confirmed that SUV-type liposomes were also formed in the incorporation of GLOSt as well as control-SUV, and GLOSt was tightly incorporated into the liposomal membrane. It is therefore concluded that GLOSt is appropriate to use for modification of the liposomal surface with GL. In this case, it is assumed that diglucuronide moiety of the GL molecule protrudes from the liposomal surface.

The use of solid liposomes assures maximum efficacy of ligand incorporated into the liposomal membrane.[15] Yoshioka and his colleagues reported that the uptake of lactosylceramide-containing liposomes by hepatocytes was enhanced by decrease in the fluidity of the liposomal membrane.[16] Therefore, in this study we chose hydrogenated egg PC as a liposomal base to maximize the effect of the ligand.

The elimination of GLOSt-SUV from blood after intravenous injection into rats was far more rapid than

that of control-SUV (Fig. 1A), and concomitantly, the GLOSt-SUV showed significantly higher uptake in the liver than the control-SUV (Tables III and IV). The liver uptake of GLOSt-SUV was almost 4-fold that of control-SUV and the liver clearance was 10-fold. The uptake by other organs was low, so that it was confirmed GLOSt-SUV were selectively taken up by the liver. The renal clearance of the GLOSt-SUV was 4-fold higher than that of control-SUV, as calculated from renal excretion of inulin released from liposomes in the body. However, the renal clearance does not reflect the uptake of the liposomes by the kidney but the degradation in the body. Therefore the uptake by the liver is dominant in the biological dispositions of these liposomes. Since the morphology of GLOSt-SUV was the same as that of control-SUV, the difference of biological dispositions is considered to be based on the surface modification with GL. It was also found that the blood clearance and the liver accumulation were dependent on the GLOSt content in liposomal membrane (unpublished data). These results suggest that GLOSt-SUV are accumulated through the affinity site(s) for GL moiety located in the liver.

The urinary excretion data showed that GLOSt-SUV tends to release more of an entrapped aqueous marker than control-SUV *in vivo* (Table II). The results of the latency in plasma suggested that plasma component(s) participates in the instability of GLOSt-SUV *in vivo* (Fig. 3). Cell-surface-binding protein causing instability of liposomes as reported[17] might also take part in the destabilization of the liposomes *in vivo*. It seemed that such instability *in vivo* reduced the targeting efficiency of the liposomes to the liver. The uptake into the liver would be further enhanced if the stability of the liposomes could be enhanced. Indeed, 4 h after intravenous injection to rat, 67% of GLOSt-SUV labeled with [^{3}H]cholesteryl hexadecyl ether, which is a lipophilic and undegradable marker,[18] was found in the liver (urinary excretion was less than 1%). and this was 1.6-fold higher than that of GLOSt-SUV labeled with [^{3}H]inulin (unpublished data). This result shows that GLOSt-SUV leaking an aqueous marker is also taken up by the liver.

In recent years, a number of investigators have attempted to target liposomes to liver parenchymal cells *in vivo*.[2] To increase the uptake into these cells, most of them have exploited the receptor for galactosyl residues on the plasma membrane of liver parenchymal cells[19] and used galactosyl residue as a ligand.[2a,e] However, it has been reported that considerable amounts of galactose-bearing liposomes were also found in Kupffer cells.[20] Therefore, a new ligand for the liver is desired, and GL is one of the candidates. Targeting efficiency of the GLOSt-SUV to the liver was comparable to those of conventional galactose liposomes. The significance of this study is the proposal of a possibility of GL as a targetable ligand on the liposomal surface to liver cells, although the mechanisms of the affinity are not clear at present. The diglucuronide moiety of GL molecule is assumed to protrude from the liposomal surface and to contribute to the affinity of the liposomes to the liver. It is impossible, however, to neglect the contribution of glycyrrhetinate moiety and/or membrane characteristics to the affinity.

From the present study, it is not clear which cell subfraction contributes to the *in vivo* liver uptake of GLOSt-SUV. Since the size of GLOSt-SUV is small enough to pass the fenestrations of liver sinusoids and it is presumed that the uptake of free GL by liver parenchymal cells is very high, it is expected that GLOSt-SUV are preferably taken up by these cells; yet the participation of Kupffer cells cannot be excluded at this time. Surface modification of liposomes may enhance their association with Kupffer cells. Intrahepatic distribution after their intravenous injection is the next subject to be resolved for these liposomes.

Acknowledgement The authors would like to thank Mr. K. Kida (Faculty of Pharmaceutical Sciences, University of Tokushima) for measurement of ^{1}H- and ^{13}C-NMR spectra and Mr. Y. Minami and Mr. R. Azuma (Taiho Pharmaceutical Co., Ltd.) for measurement of mass spectra.

References

1) M. J. Ostro (ed.), "Liposomes: From Biophysics to Therapeutics," Marcel Dekker, Inc., New York, 1987; G. Gregoriadis (ed.), "Liposomes as Drug Carriers: Recent Trends and Progress," John Wiley and Sons, Inc., Chichester, 1988; S. Wright and L. Haung, *Advanced Drug Delivery Rev.*, **3**, 343 (1989).
2) *a*) P. Ghosh, P. K. Das and B. K. Bachhawat, *Arch. Biochem. Biophys.*, **213**, 266 (1982); *b*) H. H. Spanjer and G. L. Scherphof, *Biochim. Biophys. Acta*, **734**, 40 (1983); *c*) P. Soriano, J. Dijkstra, A. Legrand, H. Spanjer, D. Londos-Gagliardi, F. Roerdink, G. Scherphof and C. Nicolau, *Proc. Natl. Acad. Sci. U.S.A.*, **80**, 7128 (1983); *d*) S. Tsuchiya, Y. Aramaki, T. Hara, K. Hosoi and A. Okada, *Biopharm. Drug Disposit.*, **7**, 549 (1986); *e*) T. Hara, Y. Aramaki, S. Tsuchiya, K. Hosoi and A. Okada, *ibid.*, **8**, 327 (1987); *f*) T. Hara, H. Ishihara, Y. Aramaki and S. Tsuchiya, *Int. J. Pharm.*, **42**, 69 (1988); *g*) B. K. Bachhawat, P. K. Das and P. Ghosh, "Liposome Technology," Vol. III, ed. by G. Gregoriadis, CRC Press, Florida, 1984, pp. 117—126.
3) A. Gabizon and D. Papahadjopoulos, *Proc. Natl. Acad. Sci. U.S.A.*, **85**, 6949 (1988); R. K. Jain and L. E. Gerlowski, *Crit. Rev. Oncol. Hematol.*, **5**, 115 (1986).
4) I. J. Fidler, *Cancer Res.*, **45**, 4714 (1985); S. L. Croft, *Pharm. Int.*, **7**, 229 (1986); G. Lopez-Berestein and I. J. Fidler (eds.), "UCLA Symposia on Molecular and Cellular Biology, New Series, Vol. 89: Liposomes in the Therapy of Infectious Diseases and Cancer," Alan R. Liss, Inc., New York, 1989, pp. 59—163.
5) R. J. Fallon and A. L. Schwartz, *Adv. Drug Delivery Rev.*, **4**, 49 (1989).
6) E. Wisse, R. DeZanger and R. Jacobs, "Sinusoidal Liver Cells," ed. by D. L. Knook and E. Wisse, Elsevier Biomedical Press, Inc., Amsterdam, 1982, pp. 61—67.
7) T. Ichikawa, S. Ishida, Y. Sakiya, Y. Sawada and M. Hanano, *J. Pharm. Sci.*, **75**, 672 (1986).
8) E. Vowinkel, *Chem. Ber.*, **99**, 1479 (1966).
9) L. J. Mathias, *Synthesis*, **1979**, 561.
10) H. Kiwada, M. Akimoto, M. Araki, M. Tsuji and Y. Kato, *Chem. Pharm. Bull.*, **35**, 2935 (1987).
11) H. Kiwada, J. Sato, S. Yamada and Y. Kato, *Chem. Pharm. Bull.*, **34**, 4253 (1986).
12) H. Kiwada, I. Nakajima, H. Matsuura, M. Tsuji and Y. Kato, *Chem. Pharm. Bull.*, **36**, 1841 (1988).
13) J. Senior and G. Gregoriadis, *Life Sci.*, **30**, 2123 (1982).
14) T. Kunitake, Y. Okahata, M. Shimomura, S. Yasunami and K. Takarabe, *J. Am. Chem. Soc.*, **103**, 5401 (1981).
15) G. Poste and D. Papahadjopoulos, *Proc. Natl. Acad. Sci. U.S.A.*, **73**, 1603 (1976).
16) Y. Banno, K. Ohki, T. Morita, S. Yoshioka and Y. Nozawa, *Biochem. Int.*, **12**, 865 (1986).
17) L. Huang, "Liposomes," ed. by M. J. Ostro, Marcel Dekker Inc., New York, 1983, pp. 87—124.
18) J. T. P. Derksen, H. W. M. Morselt and G. L. Scherphof, *Biochim. Biophys. Acta*, **971**, 127 (1988).
19) G. Ashwell and A. G. Morell, *Adv. Enzymol.*, **41**, 99 (1974).
20) H. H. Spanjer, H. Morselt and G. L. Scherphof, *Biochim. Biophys. Acta*, **774**, 49 (1984); H. H. Spanjer, T. J. C. van Berkel, G. L. Scherphof and H. J. M. Kempen, *ibid.*, **816**, 396 (1985).

Visible Absorption and Proton Nuclear Magnetic Resonance Studies on the Self-Association of Doxorubicin in Aqueous Solution

Eiji HAYAKAWA,* Kunitoshi FURUYA, Hideo UENO, Tokuyuki KURODA, Masuo MORIYAMA, and Akira KONDO

Pharmaceutical Research Laboratories, Kyowa Hakko Kogyo Co., Ltd., 1188, Shimotogari, Nagaizumi-cho, Sunto-gun, Shizuoka 411, Japan.
Received August 28, 1990

The viscosity of the aqueous solution of doxorubicin increased with the addition of NaCl. Methyl *p*-hydroxybenzoate had a reducing effect on the viscosity of the solution enhanced by the addition of NaCl.

The interaction of doxorubicin with NaCl and methyl *p*-hydroxybenzoate in an aqueous solution was examined by the methods of absorption spectra and proton nuclear magnetic resonance (^{1}H-NMR).

Doxorubicin formed stacked aggregates in concentrated aqueous solutions. The increased ionic strength facilitated the self-association of doxorubicin. The addition of methyl *p*-hydroxybenzoate prevented the self-association of doxorubicin. It is thought that methyl *p*-hydroxybenzoate may interfere with the π–π stacking of doxorubicin molecules in competition with doxorubicin.

On the basis of the results, it is considered that the increase in the viscosity of the aqueous solution of doxorubicin is caused by the self-association of doxorubicin, and methyl *p*-hydroxybenzoate exerts the viscosity reducing effect by the inhibition of the self-association of doxorubicin.

Keywords doxorubicin hydrochloride; visible absorption; ^{1}H-NMR; self-association; stacking interaction; ionic strength; temperature dependence; methyl *p*-hydroxybenzoate

Introduction

Doxorubicin (Fig. 1) is a widely used anthracycline anticancer drug.

We previously studied the interaction of doxorubicin hydrochloride with NaCl in the presence and in the absence of methyl *p*-hydroxybenzoate at 25 °C at pH 5.5 by measuring the dissolution time and viscosity. We found that methyl *p*-hydroxybenzoate had a shortening effect on the dissolution time of doxorubicin hydrochloride freeze-dried product when dissolved in isotonic sodium chloride solution, and we believe that this shortening effect is closely related to the fact that methyl *p*-hydroxybenzoate reduces the viscosity of the aqueous solution of doxorubicin hydrochloride enhanced by the addition of NaCl.[1)]

The self-association of anthracycline compounds such as doxorubicin or daunorubicin in solution has been studied using the ultraviolet/visible (UV/VIS) absorption spectrum[2-4)] and proton nuclear magnetic resonance (^{1}H-NMR),[5,6)] but there is little information about the interaction with additives such as methyl *p*-hydroxybenzoate from the viewpoint of the inhibition of the self-association.

The study of interactions between doxorubicin and methyl *p*-hydroxybenzoate is important in order to understand the ability of methyl *p*-hydroxybenzoate to shorten the dissolution time of doxorubicin hydrochloride freeze-dried product when reconstituted with isotonic sodium chloride solution.

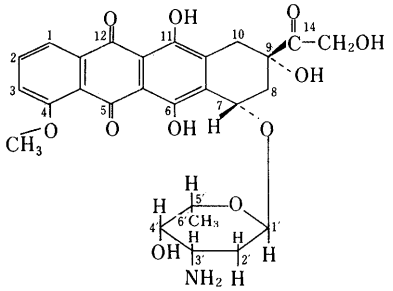

Fig. 1. Chemical Structure of Doxorubicin

The aim of this paper is to investigate the various aspects of doxorubicin by spectroscopy and ^{1}H-NMR, and to discuss the interaction of methyl *p*-hydroxybenzoate.

Experimental

Materials Doxorubicin hydrochloride was supplied by Farmitalia Carlo Erba (Milan, Italy) and used without further purification. D_2O and sodium 3-trimethylsilyl propionate-2, 2, 3, 3-d_4 (TSP-d_4) were obtained from Merck, Sharp and Dohme. Methyl *p*-hydroxybenzoate was obtained from Kanto Chemical Co. (reagent grade). All other materials used for this study were commercial products (reagent grade) and were used without further purification.

Viscosity Measurements The measurement of the solution viscosity was made using a Ubbelohde type viscometer at 25 °C. Methyl *p*-hydroxybenzoate was mixed with an aqueous solution containing doxorubicin and NaCl, and then dissolved completely. The pH of the solutions was about 5.5.

Spectrophotometric Measurements VIS spectra were measured with a Hitachi U-3200 spectrophotometer in aqueous solution at pH 7.0 (Tris buffer) and pH 5.5 (without buffer) at 25 °C using cells of 1-cm path length.

Doxorubicin concentration dependence of the VIS absorption spectra of doxorubicin: The VIS absorption spectra of doxorubicin (1, 10, 100 μg/ml) in solutions of Tris buffer plus NaCl at pH 7.0 were measured. The solutions were prepared by adding NaCl (final concentration 0.15 M) to 0.05 M Tris–HCl buffer, pH 7.0, in order to make the ionic strength 0.196 M.[2)]

NaCl concentration dependence of the VIS absorption spectra of doxorubicin: VIS absorption spectra of doxorubicin (100 μg/ml) in solutions of Tris buffer plus NaCl at pH 7.0 and in solutions of H_2O plus NaCl at pH 5.5 were measured. The solutions of Tris buffer plus NaCl were prepared by adding NaCl (final concentration 0—1.0 M) to 0.05 M Tris–HCl buffer, pH 7.0. After doxorubicin hydrochloride was dissolved with the solutions of H_2O plus NaCl (0—1.0 M), the pH of the solutions was 5.5 ± 0.2.

Methyl *p*-hydroxybenzoate concentration dependence of the VIS absorption spectra of doxorubicin: VIS absorption spectra of doxorubicin (100 μg/ml) were measured in solutions of Tris buffer, NaCl and methyl *p*-hydroxybenzoate at pH 7.0, and in solutions of H_2O, NaCl and methyl *p*-hydroxybenzoate at pH 5.5. When doxorubicin hydrochloride was dissolved with the solutions of H_2O, NaCl and methyl *p*-hydroxybenzoate, the pH of the solutions was 5.5 ± 0.2.

^{1}H-NMR Spectra Measurements ^{1}H-NMR spectra were measured in deuterium oxide solution on a JEOL GX-270 (270 MHz) spectrometer with TSP-d_4 as an internal reference. The conditions for the Fourier transfer measurements were: spectral width, 3000 Hz; pulse width, 10 μs (flip angle, about 45°); acquisition time, 5.5 s; number of data points,

32768; number of scans, 500. NaCl concentration dependence of the chemical shifts of doxorubicin: ^{1}H-NMR spectra of solutions of doxorubicin (5 mg/ml) in D_2O plus NaCl at 30 °C were measured. Solutions of D_2O plus NaCl were prepared by adding NaCl (final concentration 0—0.3 M) to D_2O. Temperature dependence of the chemical shifts of doxorubicin: ^{1}H-NMR spectra of solutions of doxorubicin (5 mg/ml) in D_2O plus NaCl were measured at various temperatures. Methyl *p*-hydroxybenzoate concentration dependence of the chemical shifts of doxorubicin: ^{1}H-NMR spectra of solutions of doxorubicin (5 mg/ml) in D_2O plus NaCl and methyl *p*-hydroxybenzoate at 30 °C were measured. Solutions of D_2O plus NaCl and methyl *p*-hydroxybenzoate were prepared by adding NaCl (final concentration 0.2 M) and methyl *p*-hydroxybenzoate (final concentration 0—10 mg/ml) to D_2O.

Results and Discussion

Viscosity of an Aqueous Solution of Doxorubicin The kinematic viscosity, ν(cSt), of the solution was obtained as a function of the concentration of NaCl in order to investigate the gel formation of the doxorubicin aqueous solution (Fig. 2). The viscosity of the aqueous solution of doxorubicin increased gradually with the concentration of NaCl, but it abruptly increased when the concentration of NaCl exceeded a certain value.

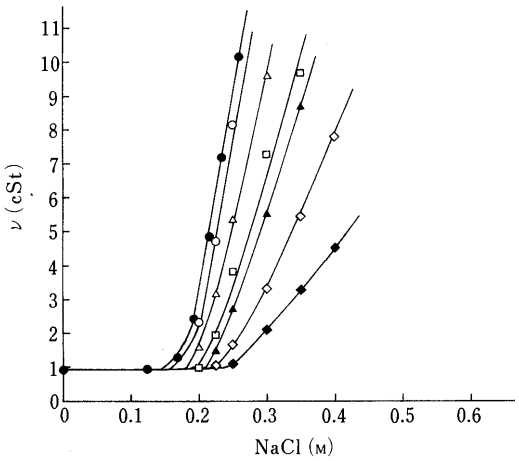

Fig. 2. Effect of NaCl Concentration and Methyl *p*-Hydroxybenzoate Concentration on the Viscosity of Doxorubicin at 25 °C

Doxorubicin conc. = 5 mg/ml. Methyl *p*-hydroxybenzoate conc. = ●, 0 mg/ml; ○, 0.2 mg/ml; △, 0.5 mg/ml; □, 1.0 mg/ml; ▲, 1.5 mg/ml; ◇, 2.0 mg/ml; ◆, 2.5 mg/ml.

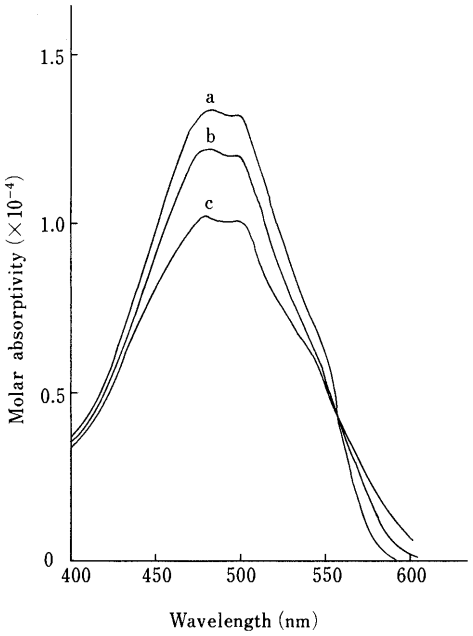

Fig. 3. Visible (VIS) Absorption Spectra of Doxorubicin at Different Concentrations in 0.05 M Tris–HCl Buffer, pH 7.0, Containing 0.15 M NaCl at 25 °C

a, 1.7×10^{-6} M (1 μg/ml); b, 1.7×10^{-5} M (10 μg/ml); c, 1.7×10^{-4} M (100 μg/ml).

The addition of methyl *p*-hydroxybenzoate inhibited the increase in the viscosity of the doxorubicin aqueous solution.

VIS Absorption Spectra of Doxorubicin The dependences of the spectroscopic properties of doxorubicin in aqueous solution on the doxorubicin concentration, NaCl concentration and methyl *p*-hydroxybenzoate concentration were investigated at 25 °C.

Figure 3 shows the differences among the VIS absorption spectra of doxorubicin at various concentrations in Tris buffer, pH 7.0, plus, NaCl. Upon dilution, the molar absorptivity of the doxorubicin solution increased at the absorbance maximums of 480 and 497 nm, which are due to the presence of the dihydroxy anthraquinone chromophore.

The spectra of doxorubicin obtained in this study are in good agreement with the data published by Menozzi *et al.*[2] The concentration-dependent spectra are considered to be due to the self-association of doxorubicin.[4] It was thought that the decrease in the molar absorptivity at 497 nm was more characteristic in the self-association than at 480 nm. The effect of the ionic strength upon the spectra of doxorubicin solutions was investigated. The addition of NaCl resulted in hypochromism (Table I) both at pH 5.5 and pH 7.0. As shown in Table I, the absorbance at pH 7.0 was less hypochromic than at pH 5.5.

The addition of NaCl caused similar effects to those observed when the doxorubicin concentration was increased. This means that increasing the ionic strength facilitates the self-association of doxorubicin.

The absorption band of doxorubicin, which showed hypochromicity with the addition of NaCl, became hyper-

Table I. NaCl Concentration Dependence of 497 nm Absorbance of Doxorubicin at 25 °C

NaCl (M)	OD_{497}	
	pH 5.5	pH 7.0
0	1.949	1.899
0.1	1.873	1.860
0.2	1.849	1.842
0.5	1.806	1.826
1.0	1.786	1.804

Doxorubicin conc. = 100 μg/ml.

Table II. Methyl *p*-Hydroxybenzoate Concentration Dependence of 497 nm Absorbance of Doxorubicin at 25 °C

Methyl *p*-hydroxybenzoate (μg/ml)	OD_{497}	
	pH 5.5	pH 7.0
0	1.806	1.826
10	1.811	1.836
20	1.812	1.837
50	1.820	1.834

Doxorubicin conc. = 100 μg/ml, NaCl conc. = 0.5 M.

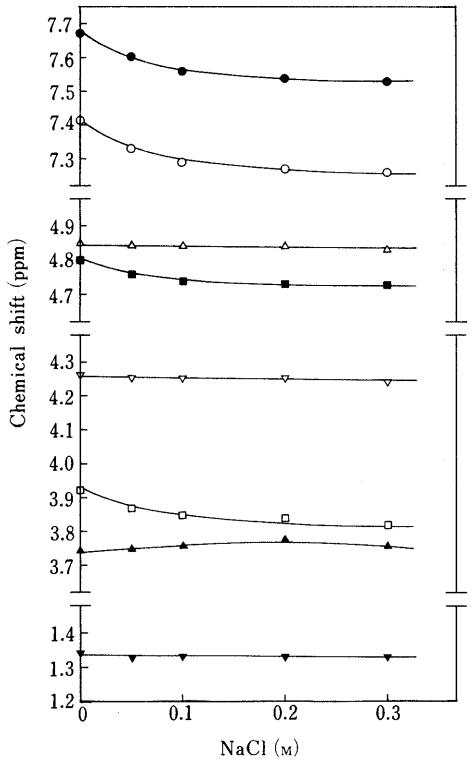

Fig. 4. NaCl Concentration Dependence of Chemical Shifts of Doxorubicin at 30 °C, at Doxorubicin Concentration of 5 mg/ml
○, H1; ●, H2; □, 4OMe; ■, H7; △, H14; ▲, H3′; ▽, H5′; ▼, H6′.

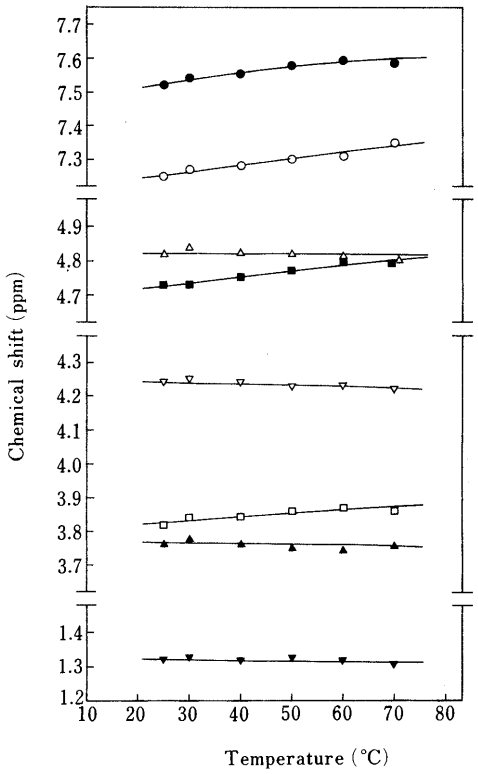

Fig. 5. Temperature Dependence of Chemical Shifts of Doxorubicin at Doxorubicin Concentration of 5 mg/ml, NaCl Concentration of 0.2 M
○, H1; ●, H2; □, 4OMe; ■, H7; △, H14; ▲, H3′; ▽, H5′; ▼, H6′.

chromic with the addition of methyl *p*-hydroxybenzoate both at pH 5.5 and pH 7.0 (Table II). This means that the self-association of doxorubicin is prevented by the addition of methyl *p*-hydroxybenzoate.

^{1}H-NMR Spectra of Doxorubicin Positive evidence of the involvement of the aromatic rings in the self-association of anthracyclines was reported. By increasing the concentration of the anthracyclines in solution, large upfield shifts were found for the aromatic ring protons and the 4 methoxy group as compared with the other protons (H14, and sugar protons) in the molecule.

Therefore, the mechanism of the self-association of anthracyclines is ascribed to the interaction between the planar aromatic rings. This process is called stacking and is based on the interaction between π-electron systems.[4]

Upfield shifts for the aromatic ring protons were also reported with increases in the ionic strength of the doxorubicin solution.[6]

But, there is no report about the inhibition of self-association by the additives such as methyl *p*-hydroxybenzoate with the aim of the shortening effect on the dissolution time of doxorubicin hydrochloride freeze-dried product when reconstituted with isotonic sodium chloride solution.

The dependences of the ^{1}H-NMR spectra of doxorubicin in aqueous solution on NaCl concentration, temperature and methyl *p*-hydroxybenzoate concentration were investigated.

Figure 4 shows the upfield shifts for the aromatic ring protons and the 4 methoxy group with increases in the concentration of NaCl.

The upfield shifts were inhibited by elevating the temperature of the solution (Fig. 5), and by the addition of methyl *p*-hydroxybenzoate to the solution (Table III).

Table III. Methyl *p*-Hydroxybenzoate Concentration Dependence of Chemical Shifts of Doxorubicin at 30 °C, at Doxorubicin Concentration of 5 mg/ml, NaCl Concentration of 0.2 M [δ (ppm from TSP-d_4)]

Position	Methyl *p*-hydroxybenzoate (mg/ml)			
	0	2.48	4.87	9.96
H1	7.27	7.29	7.29	7.31
H2	7.54	7.57	7.57	7.59
H3	7.23	7.26	7.27	7.30
4OMe	3.84	3.86	3.86	3.86
H7	4.73	4.77	4.78	4.80
H8α	2.27	2.28	2.28	2.29
H8β	2.05	2.05	2.05	2.05
H10α	2.88	2.90	2.91	2.92
H10β	2.57	2.60	2.60	2.61
H14	4.84	4.84	4.84	4.85
H1′	5.45	5.47	5.47	5.48
H2′	2.05	2.05	2.05	2.05
H3′	3.78	3.78	3.78	3.78
H4′	3.88	3.88	3.89	3.88
H5′	4.25	4.25	4.26	4.26
H6′	1.33	1.33	1.33	1.33

Therefore, the self-association facilitated by the increase in the NaCl concentration is thought to be inhibited by elevating the temperature and by adding methyl *p*-hydroxybenzoate to the solution.

According to our viscosity experiment, the viscosity of the aqueous solution of doxorubicin, which was enhanced by the addition of NaCl, was reduced by elevating the temperature of the solution,[7] and by the addition of methyl

p-hydroxybenzoate to the solution (Fig. 2).

Our VIS absorption results and ^{1}H-NMR results are consistent with the results obtained from the viscosity experiment. It is considered that the increase in the viscosity of the aqueous solution of doxorubicin is caused by the self-association of doxorubicin, but that methyl *p*-hydroxybenzoate exerts the viscosity reducing effect by the inhibition of the self-association of doxorubicin.

References

1) E. Hayakawa, K. Furuya, T. Kuroda, M. Moriyama, and A. Kondo, *Chem. Pharm. Bull.*, **38**, 3434 (1990).
2) M. Menozzi, L. Valentini, E. Vannini, and F. Arcamone, *J. Pharm. Sci.*, **73**, 6, 766 (1984).
3) H. Porumb, *Prog. Biophys. Mol. Biol.*, **34**, 175 (1978).
4) S. R. Martin, *Biopolymers*, **19**, 713 (1980).
5) J. B. Chaires, N. Dattagupta, and D. M. Crothers, *Biochemistry*, **21**, 3927 (1982).
6) I. J. McLennan, R. E. Lenkinski, and Y. Yanuka, *Can. J. Chem.*, **63**, 1233 (1985).
7) K. Furuya, E. Hayakawa, M. Moriyama, A. Kondo, and T. Kuroda, The 109th Annual Meeting of Pharmaceutical Society of Japan, Nagoya, April 1989.

Determination of End-Point with a Complex Granulation Applying Infrared Moisture Sensor

Satoru WATANO, Keijiro TERASHITA* and Kei MIYANAMI

Department of Chemical Engineering, University of Osaka Prefecture, Mozu-Umemachi, Sakai, 591, Japan. *Received September 17, 1990*

A granulation experiment was conducted in a complex granulator, which was fluidized bed equipped with an agitator blade. An infrared moisture sensor was used to feed back control the moisture content of the granule particles.

Granule properties (mean particle diameter, geometric standard deviation, yield, apparent density and appearance shape) were examined to know the mechanism and the process of moisture feed back control of the complex granulation.

To clear up the factors which determine the mean particle diameter of the granules, the influence of the liquid (binder solution) flow rate, inlet temperature and moisture content were examined to get an experimental equation which expressed the mean particle diameter of the granules. The influence of the moisture content and the rotation speed of the agitator blade on the apparent density was also investigated to get an experimental equation. With the basis of both equations, we established a system which can control the granule mean particle diameter and apparent density using a personal computer, and in addition, a self control system from granulation to drying using an infrared moisture sensor.

Keywords complex granulation; infrared moisture sensor; moisture feed back control; experimental equation; granulation end point

Introduction

Recently, factory automation has been developed in the pharmaceutical and other industries which are dealing with powdered materials.

In keeping abreast of the times, however, demands for automation have gradually changed from mass production to multivariate production with multiitems, thus, there is a great need for a multi system of individual unit operations.

In this paper, we focused our attention on granulation which is carried out with widespread use in many fields. The purpose of granulation had been to control basic components (size, size distribution and yield of granules), however, needs for granules have changed to produce high quality materials with various characteristics like appearance shape, density, hardness and so on.

Many authors have carried out a great deal of investigation to understand the granulation mechanism[1-9] and to detect the process applying different devices.[10-18] These researches, however, were insufficient from the view of factory automation. Therefore, we tried to set up a self system which can be carried out automatically from mixing to drying, and can produce the desired particles with various characteristics. To carry our several operations in one piece of equipment, we adopted a complex granulator which was a fluidized bed equipped with an agitator blade and an infrared moisture self control system. Owing to this blade, this granulator can produce spherical and compact granules which could not be produced by an ordinary fluidized bed, and the moisture content can be continuously measured and feed back controlled by applying the infrared moisture sensor.

To manipulate the granule properties at will, factors which influence the granule properties must be made clear, thus we first investigated the factors which determine the mean particle diameter of the granules by examining the influence of the liquid (binder solution) flow rate, inlet temperature and moisture content to get an experimental equation which expresses the mean particle diameter of the granules. The influence of the moisture content and the rotation speed of the agitator blade on the apparent density was also investigated to get an experimental equation.

Moisture feed back control was conducted by applying an infrared moisture sensor. During the experiment, granule properties (mean particle diameter, geometric standard deviation, yield, apparent density and appearance shape) were examined to know the mechanism and process of moisture feed back control (PID control) of the complex granulation.

As a result, we established a system which can control granule mean particle diameter and apparent density using a personal computer on the basis of the experimental equation, in addition to a self control system from granulation to drying using an infrared moisture sensor.

Experimental

Equipment The measurement theory of the infrared moisture automeasuring system with optical fiber is the same as previously reported.[16-18]

The unit system of complex granulator and infrared moisture sensor is schematically illustrated in Fig. 1. A complex granulator (NQ-LABO, Fuji Paudal, Co., Ltd.) equipped with a binary spray nozzle was used for the granulation experiment. On the bottom of the beds, an agitator blade was equipped for tumbling and compacting the granule particles with fluidization by heated air. This agitator blade is possibly changeable to various types. Powder accompanied with fluidized air was entrapped by a bag filter, and exchanged by pulse jet air. The pulse jet interval selected was 20 s.

The output signals from the transducer of the moisture sensor are both electric current (4—20 mA) and voltage (0—10 mV), and the former is transported to a digital program controller (D/D converter) to be used as a roller pump control signal, the latter is digitalized in a 12 bit A/D converter to be calculated in a personal computer. During the experiment, the moisture content was continuously monitored in a personal computer, and feed back controlled (PID controlled) by a digital program controller (D/D converter).

The sampling interval of this system was 70 ms (14 times/s).

Materials Starting material and its mixing weight are listed in Table I. Starting materials were 0.3 kg of a mixture of lactose and corn starch (mixing weight ratio is 7 : 3, respectively). 0.015 kg of hydroxypropylcellulose was adopted as a binder, which was mixed as a form of dry powder into the starting materials before granulation. Purified water was used as a binder solution.

Method The experiment was conducted as follows. Powder samples penetrated through a 50-mesh (300 μm) sieve were fed into a preheated container, then mixed with fluidized air for 600 s. After the operational conditions were instituted as described in Table II, the binder solution (purified water) was top sprayed by a binary nozzle as a form of mist. After granulation was over, the adding of binder solutions was stopped to shift to the drying process.

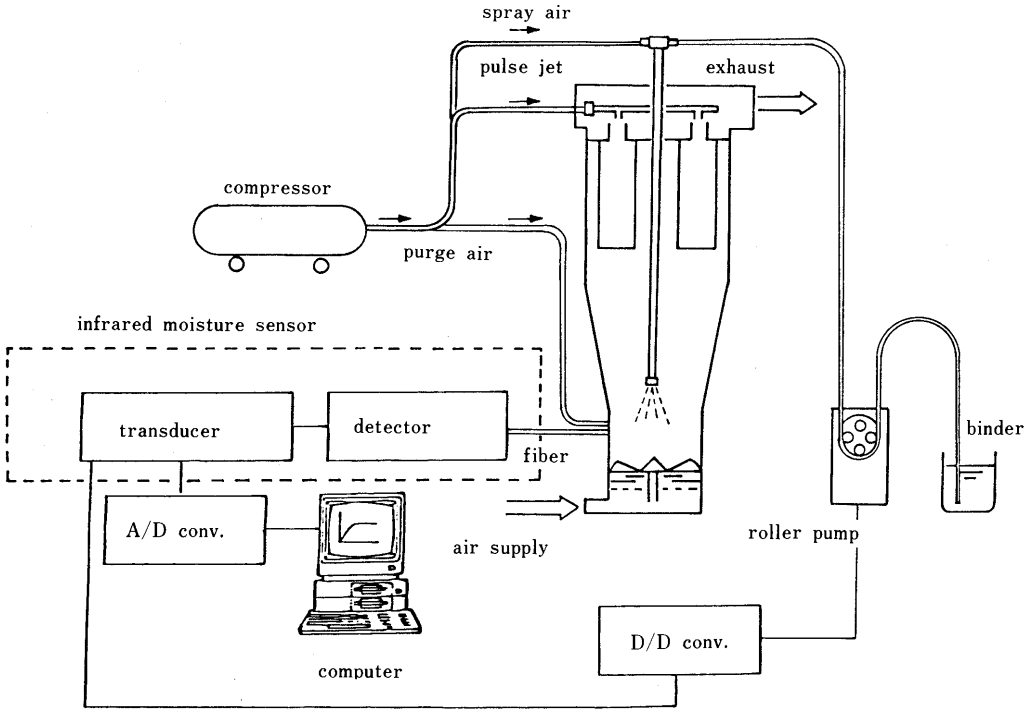

Fig. 1. Schematic Diagram of Apparatus Used for Complex Granulation

TABLE I. Materials and Composition

Materials	Mean particle size (μm)	Mixing weight (kg)
Lactose[a)]	104	0.21
Corn starch[b)]	42	0.09
Hydroxypropylcellulose[c)]	65	0.015
Total		0.315

a) Pharmatose 200M, DMV (crystallized lactose). *b*) Corn Starch W, Nippon Shokuhin Kakou Co., Ltd. *c*) HPC-EFP, Shin-Etsu Chemical Co., Ltd.

TABLE II. Experimental Conditions

Agitating speed	10	rps
Air volume	0.01	m^3/s
Spray nozzle height	0.15	m
Spray pressure	2.0×10^5	Pa
Inlet temperature	333	K
Liquid flow rate	0.25	g/s

Granule size distribution was determined by sieve analysis with a rotating sieve shaker. About 10 g of the granules were shaken for 180 s. After measuring the weight of the granules on each sieve, particle size distribution was calculated by log-normal distribution with computer.

Results and Discussion

Effect of Inlet Temperature and Liquid Flow Rate on Mean Particle Diameter To examine the influence of moisture content on particle diameter of the granules, granulation experiments were carried out at varying liquid (binder solution) flow rates and inlet air temperatures. Figure 2 shows the relation between 50% mean particle diameter, D_{50} and moisture content, W. Here, D_{50} is obtained from the granules sampled out at the random moisture content during the granulation. The relation between 50% mean particle diameter and moisture content could be approximately expressed by two linear equations, thus, the influence of the liquid flow rate and the inlet air temperature on granule size was hardly found. Several authors have shown that an increased liquid flow rate results in increased particle diameter,[2)] whereas in our experiment, the particle diameter was found to be dominated by the moisture content, and moreover, the binder solution was used was water which was of low viscosity so that we could ignore the difference of droplet size.

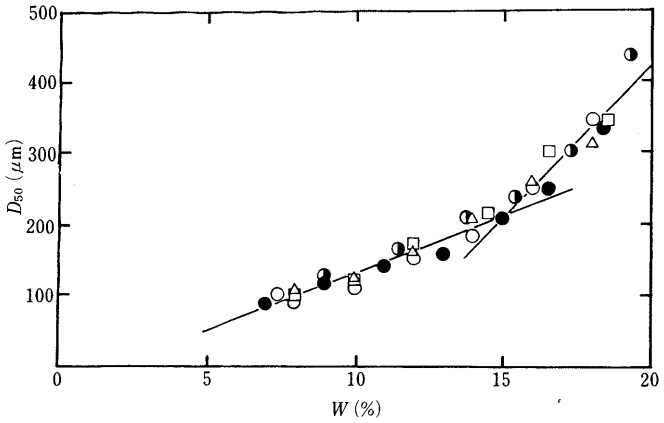

Fig. 2. 50% Mean Particle Diameter D_{50} as a Function of Moisture Content W

Temperature: △, 313K; □, 353K; ○●◑, 333K. Liquid flow rate: △□○, 0.25 g/s; ●, 0.167 g/s; ◑, 0.333 g/s.

From Fig. 2, the mean particle diameter of granules at $W=7$ or 8% were 74μm which was the same size as the material powder, thus it was found that granule growth could not occur until the moisture content was over 7 or 8%. This was because the liquid bridges could not be formulated because the binder solution permeated the powder owing that the materials were porous and the water absorbing power was large. In the regions between $W=8$

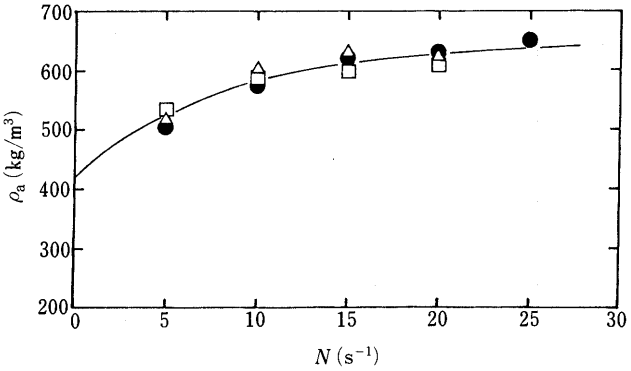

Fig. 3. Apparent Density ρ_a as a Function of Agitator Rotation Speed N

Moisture content: ●, 15%; □, 12.5%; △, 10.0%.

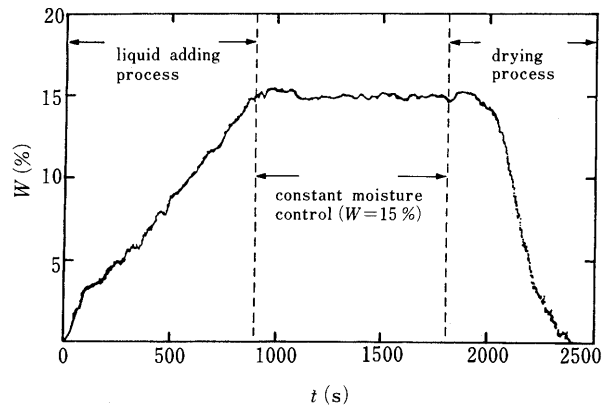

Fig. 4. Relation between Moisture Content W and Granulation Time t

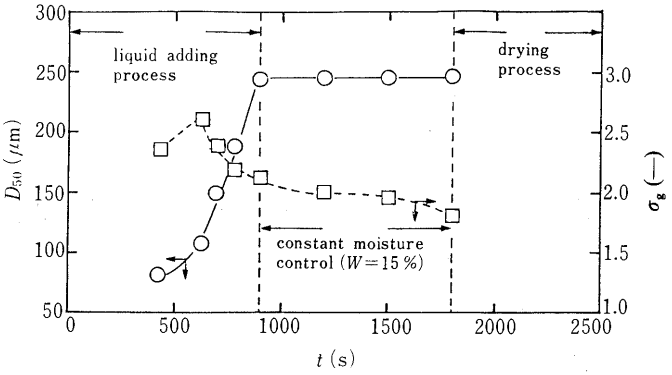

Fig. 5. Relation between 50% Mean Particle Diameter D_{50}, Geometric Standard Deviation σ_g and Granulation Time t

○, 50% mean particle diameter, D_{50}; □, geometric standard deviation, σ_g.

to 15%, binder solutions were partly used for liquid bridges, therefore, gradual growth of granules could be found. At a moisture content was above 15%, the rapid increase of D_{50} was found. It was because that the surface of the particles were saturated with solutions, thus the binding force became large. Therefore $W=15\%$ was the turning point of granule growth. The following experimental equations were obtained using the least squares method;

$$0 \leqq W \leqq 15\%: \quad D_{50}=16.27W(\%)-32.11$$
$$15 \leqq W \leqq 20\%: \quad D_{50}=42.92W(\%)-433.79 \tag{1}$$

Therefore, we can predict approximately the particle diameter by means of monitoring the moisture content of the granules.

Effect of Moisture Content and Agitator Rotation Speed on Apparent Density of Granules To examine the influence of the moisture content and agitator rotation speed on the apparent density of granules, experiments were carried out at varying moisture contents (setting values of constant moisture content were 10.0, 12.5, 15.0%) and rotation speeds.

Figure 3 shows the relation between the apparent density, ρ_a, and rotation speed, N. It was found from Fig. 3 that an increase of rotation speed resulted in an increase of apparent density, which was attributed to the tumbling and shearing effect of the agitator blade. No remarkable influence of moisture content could be found on the apparent density, thus, the apparent density depended on the effect of the agitator blade rather than on the moisture content. D_{50} of the granules here were approximately constant in spite of the variation of rotation speed. From these results, we can predict approximately the apparent density of the granules with a correlation between the apparent density and the agitator rotation speed. The experimental equation which expresses apparent density is as follows:

$0 \leqq N \leqq 25$ (s^{-1}):

$$\rho_a \text{ (kg/m}^3) = 0.016N^3 - 1.10N^2 + 25.45N + 418.58 \tag{2}$$

Granulation Process under Moisture Self-Control Moisture self control of this complex granulator was carried out by means of feed back control (PID control) of the flow rate with the application of an infrared moisture sensor. The binder solution was programmed to spray to the granules at a moisture content less than 15%. After the moisture content had reached 15%, PID control of the flow rate was carried out to keep the moisture content constant for 900 s. At $t=1800$ s, the binder solution was programmed to stop so as to shift to the drying process. The drying process was ended when $W=0\%$.

Figure 4 shows the relation between moisture content, W and granulation time, t while PID control is conducted. Overshoot of the moisture content was only 0.5% and the fluctuation was $\pm 0.3\%$ which is within the permitted limit, thus, it was found that the moisture content was favorably controlled and kept at the preset value.

To examine the change of the granule properties, mean particle diameter, and particle size distribution, the apparent density and shape index were examined. Here, the shape index was indicated the mean ratio of the short/long diameter of 50 granules. Figure 5 shows the relation between mean particle diameter, D_{50}, geometric standard deviation, σ_g and granulation time, t. Figure 6 also shows the relation between the yield of granules and granulation time. An increase of mean particle diameter could not be found from $t=900$ to 1800 s, which attributed to liquid bridges originating from moisture content being kept constant. After $t=900$ s, a slight increase in the yield of large granules (Y_g) and fine granules (Y_s), and a slight decrease of ungranulated fine particles (under 200 mesh (75 μm)) were found. Although the number of liquid bridges were constant, the abrasion of particles was prevented and fine ungranulated particles under 75 μm were made to adhere to the granules, which was resulted in an increase of Y_s, Y_g,

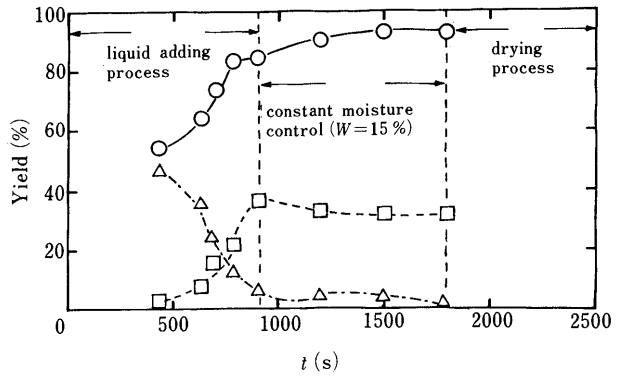

Fig. 6. Relation between Yield of Granule Particle and Granulation Time t

○, yield of fine particles, Y_s ($75<d_p<500\,\mu m$); □, yield of granules, Y_g ($297<d_p<1410\,\mu m$); △, yield of fine particles, Y_f ($d_p<75\,\mu m$).

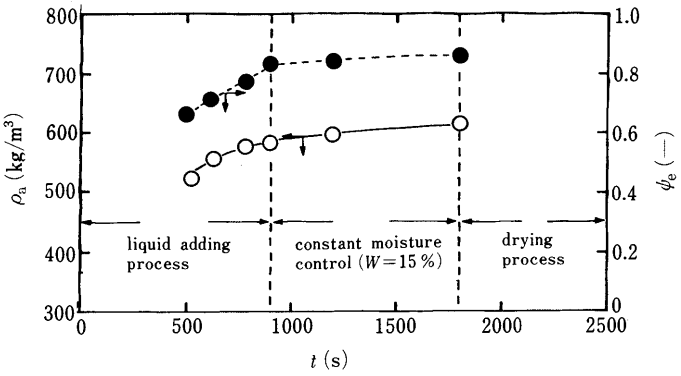

Fig. 7. Relation between Apparent Density ρ_a, Shape Index ψ_e and Granulation Time t

○, apparent density, ρ_a; ●, shape index, ψ_e.

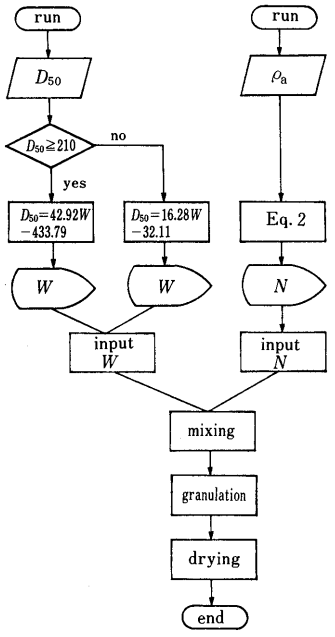

Fig. 8. Flow Sheet Illustrated Determination of Granulation End-Point

and a decrease of Y_f.

Particle size distribution tended to become sharp as granulation time passed.

Figure 7 shows the relation between apparent density ρ_a, shape index ψ_e and granulation time t. Apparent density slightly increased with granulation time passed because the frequency number needed to get a tumbling effect and shearing stress became longer. The shape index ψ_e showed a tendency to increase (becoming spherical) as the granulation time passed. This was also attributed to the tumbling effect of the blade.

It was found that a desired granule diameter corresponding to its moisture content with sharp particle size distribution, a high yield of granules, high density and spherical granules could easily be obtained with the application of moisture control.

Determination of Granulation End-Point A flow sheet which indicating the determination end-point in the complex granulation is illustrated in Fig. 8. By inputting the mean particle diameter and apparent density of the desired granules to Eq. 1 and Eq. 2, a preset value of moisture content, W and agitator rotation speed, N are calculated by the personal computer. By programming the value and granulation time into the controller, control of the process of mixing–granulation–drying is conducted applying feed back control of the moisture content.

By this means, determination of the end-point which selects mean particle diameter and apparent density of the desired granules at one's will is made possible.

Conclusions

Complex granulation was conducted under moisture feed back control and we obtained the following results;

1) If granulation is conducted under a constant value of moisture content, it is found that spherical and compact granules with sharp particle size distribution and high yield can easily be produced.
2) Mean particle diameter was mainly determined by the moisture content, and the correlation between mean particle diameter and moisture content could be expressed by the linear equation.
3) Apparent density of the granules depended on the rotation speed of the agitator blade rather than on the moisture content, thus, we set up the experimental equation which expressed the apparent density with agitator rotation speed.
4) With the basis of both experimental equations, we established a system which can control the granule mean particle diameter and apparent density using a personal computer, and in addition, a self control system from granulation to drying using infrared moisture sensor.

References

1) T. Schœfer and O. Wørts, *Arch. Pharm. Chemi. Sci.*, **5**, 51 (1977).
2) T. Schœfer and O. Wørts, *Arch. Pharm. Chemi. Sci.*, **5**, 178 (1977).
3) T. Schœfer and O. Wørts, *Arch. Pharm. Chemi. Sci.*, **6**, 1 (1978).
4) W. L. Davies and W. T. Gloor, *J. Pharm. Sci.*, **60**, 1869 (1971).
5) W. L. Davies and W. T. Gloor, *J. Pharm. Sci.*, **61**, 618 (1972).
6) W. L. Davies and W. T. Gloor, *J. Pharm. Sci.*, **62**, 170 (1973).
7) A. Y. Gore, D. W. Mcfarland and N. H. Batuyios, *Pharm. Tech.*, **6**, 114 (1985).
8) B. V. Andreev, V. L. Gorodnichev, S. A. Minina and H. M. El-Banna, *Pharm. Ind.*, **42**, 12 (1980).
9) K. Sugimori, S. Mori and Y. Kawashima, *Pharm. Tech. Jpn.*, **4**, 971 (1988).
10) O. Lindberg, L. Leander, L. Wenngren, H. Helgesen and B. Reenstierna, *Acta Pharm. Suec.*, **11**, 603 (1974).
11) N. O. Lindberg, L. Leander, P. G. Nilsson and B. Reenstierna, *Acta*

Pharm. Suec., **14**, 191 (1977).
12) H. Leuenberger, *Pharm. Acta. Helv.*, **57**, 72 (1982).
13) P. Holm, T. Schœfer and H. G. Kristensen, *Pow. Tech.*, **43**, 213 (1985).
14) K. Terashita, M. Katou, A. Ohike and K. Miyanami, *Chem. Pharm. Bull.*, **38**, 1977 (1990).
15) K. Terashita, S. Watano and K. Miyanami, *Chem. Pharm. Bull.*, **38**, 3120 (1990).
16) S. Watano, K. Terashita and K. Miyanami, Abstracts of Papers, 110th Annual Meeting of Pharmaceutical Society of Japan, Hokkaido, Aug. 1990.
17) T. Shibata, *J. Soc. Pow. Tech. Jpn.*, **24**, 10 (1987).
18) A. Miyagijima, Y. Nozawa, Abstracts of Papers, 109th Annual Meeting of Pharmaceutical Society of Japan, Nagoya, Apr. 1989.

Possibility of Heat Sterilization of Liposomes[1)]

Hiroshi KIKUCHI,*[,a] Anders CARLSSON,[b,2)] Kiyoto YACHI[a] and Sadao HIROTA[a,3)]

Pharmaceutical Formulation Research Center, Research Institute, Daiichi Pharmaceutical Co., Ltd.,[a] 16–13, Kita-kasai 1-chome, Edogawa-ku, Tokyo 134, Japan and Department of Applied Chemistry, Faculty of Engineering, Yokohama National University,[b] Tokiwadai, Hodogaya, Yokohama 240, Japan. *Received September 21, 1990*

Several kinds of liposomes were sterilized at 121 °C for 20 min. They tended to aggregate after heat sterilization (HS) in saline, while no aggregation was observed in an isotonized sugar or polyol solution. The dispersions containing egg phosphatidylcholine (EggPC) with a high peroxide value (POV) turned slightly yellowish after HS. This color change was prevented by using EggPC with a low POV, hydrogenated EggPC (H-EggPC) or dipalmitoylphosphatidylcholine (DPPC). Nitrogen gas bubbling at neutral pH also prevented the color change, but vitamin E did not. The particle size of the EggPC liposomes extruded through a 0.4 μm membrane filter did not change significantly after HS, whereas the H-EggPC or DPPC liposomes extruded through a 0.8 μm membrane filter tended to be reduced in size. On this change the type of medium had a considerable influence. The anionic 6-carboxyfluorescein leaked from the negatively charged liposomes (EggPC/cholesterol (Chol)/egg phosphatidylglycerol) during HS, while no leakage was observed from the positively charged liposomes (EggPC/Chol/stearylamine) not only during HS but also during a long period of storage. It was suggested that sterilization of liposomes by heating was practicable as well as that by filtration, if the liposomes were prepared as follows: the charged liposomes made of lipids with low POV's were dispersed in a sugar or polyol solution adjusted to nearly pH 6.5, where the amount of dissolved oxygen was minimized. An ionic water-soluble drug had to be encapsulated in the oppositely charged liposomes.

Keywords heat sterilization; liposome; stability; aggregation; color change; particle size; leakage; electrostatic attraction; electrolyte; storage

It is well recognized that liposomes have great potential as drug carriers in medical applications, *inter alia*, by reducing the toxicity of a drug and achieving targetability to specific cells and organs.[4)] In order to prepare liposomes on a large scale for medical applications, it is necessary to employ techniques which will meet the requirements of the pharmaceutical industry. One of the most important steps in the manufacturing process of injectable liposomes is sterilization. It has been argued that liposomes can only be sterilized by filtration and that any other method involving chemical or physical treatment, especially heating, would destroy the liposomal structure and thereby release the encapsulated drugs.[5)] However, most viruses cannot be removed by filtration, so that intensive microbiological control is required in the plant, and furthermore, the filtering process is so time-consuming that it is preferably avoided when dealing with large batches of the liposomal dispersions. In this report we will show that it is possible to apply an ordinary heat sterilization (HS) technique and obtain liposomes which retain their appearance and bilayer integrity with high encapsulation efficiency after the heat treatment.

Experimental

Materials The lipids were used as received. L-α-dipalmitoylphosphatidylcholine (DPPC), cholesterol (Chol) and stearylamine (SA) were purchased from Sigma Chemical Co. (St. Louis, MO, U.S.A.). Two kinds of egg phosphatidylcholines (EggPC's) were obtained from Nippon Oil and Fats Co., Ltd. (Tokyo, Japan), namely, G-EggPC to indicate EggPC with peroxide values (POV's) of 6.5—7.6 meq/kg and S-EggPC to indicate EggPC with low POV's: 1.0—2.1 meq/kg, respectively. Hydrogenated EggPC (H-EggPC) with iodine value of 2 g/100 g and POV of 0.6 meq/kg, and egg phosphatidylglycerol (EggPG) with POV of 3.0 meq/kg were obtained from Asahi Chemical Ind. Co., Ltd. (Tokyo, Japan). POV's of the phospholipids were kindly determined by Nippon Oil and Fats Co., Ltd. before they were used for the experiments. The purities of the lipids were checked by thin layer chromatography (TLC) on silica gel plates with chloroform–methanol–water (70:30:5 by volume) as the solvent system. 6-Carboxyfluorescein (CF) was purchased from Eastman Kodak Co. (Rochester, NY, U.S.A.) and used as the sodium salt. Polycarbonate membrane filters were purchased from Nuclepore Co. (Pleasanton, CA, U.S.A.). All other chemicals were of reagent grade. The following aqueous isotonic media were used: 0.9% (w/v) NaCl (saline), 5.0% (w/v) glucose, 10.0% (w/v) sucrose, 2.0% (w/v) propylene glycol and 2.6% (w/v) glycerol.

Preparation of Liposomes Multilamellar vesicles were prepared by the conventional method introduced by Bangham *et al.*[6)] The lipids were dissolved in chloroform in a test tube. In order to make a thin lipid film on the wall of the tube, the chloroform was removed by blowing nitrogen gas into the test tube which was warmed in a water bath. The residual solvent was removed in a desiccator under reduced pressure for 1 h. An aqueous isotonic medium was added and the lipids were hydrated. The total lipid concentration was adjusted to 20 mM. Then the test tube was shaken on a Vortex mixer for 15 min above the phase transition temperature (Tc) of the lipid meterials. To attain a more homogeneous size distribution of the liposomes, the liposomal dispersion was extruded once above Tc through a polycarbonate membrane filter with 0.4 or 0.8 μm pore size as described by Olson *et al.*[7)] When CF was used as a model drug, a thin lipid film was hydrated with a 5.0% glucose or 10.0% sucrose aqueous solution containing sodium salt of 0.2 mM CF. After extrusion through a 0.4 μm membrane filter, the liposomal dispersion was centrifuged at 200000 × *g* for 1 h in order to separate the unencapsulated CF. The pellet was resuspended by the same isotonic medium without CF. This centrifugation procedure was repeated and finally the volume of dispersion was adjusted to be the same as that at the beginning.

Heat Sterilization After 2 ml of the dispersion was put into a glass vial, which was then sealed with a rubber stopper and an aluminum cap, the dispersion was heat sterilized at 121 °C for 20 min. In some cases, nitrogen gas was bubbled through before the heat treatment. It was previously confirmed that CF is chemically stable against HS in the pH 3 to 12 region.

Visual Appearance The liposomal dispersions after HS were characterized visually with respect to aggregation and color.

Particle Size The mean particle sizes of liposomes before and after HS were determined by quasi-elastic laser light scattering measurements using a Zetasizer II (Malvern Instruments Ltd., England).

Leakage of Drug In order to estimate the leakage of the model drug from the liposomes during HS, the amount of CF was determined by fluorescence measurements (Hitachi 650-10S fluorescence spectrophotometer; $\lambda_{ex} = 490$ nm, $\lambda_{em} = 519$ nm) on the supernatant obtained after centrifugation (250000 × *g* for 1 h) of the CF-encapsulating liposomes after HS.

Long-Term Stability After the liposomal dispersion was heat sterilized, it was stored for 6 months at about 25 °C in room light. The stability of liposomes during storage was checked in the same way as after HS, by

their visual appearance, their mean particle sizes and the leakage of CF.

Results and Discussion

Factors Affecting the Aggregation of Liposomes after HS When the DPPC liposomes were dispersed in saline, aggregation and subsequent separation of the aggregated mass were observed to occur after HS irrespective of their lipid compositions, as shown in Table I (Rp. 1, 2, 3 and 4). No aggregation was observed when the isotonic solution of sugars or polyols was used instead of saline (Rp. 1a, 3a, 4a and 4b). However, addition of Chol to lecithin without EggPG as a charged lipid led to aggregation of the liposomes after HS, even if the sugar solution was used (Rp. 2a). Replacing DPPC with S-EggPC or H-EggPC led to the same result as above, and no color change was observed in any sample. These results were in agreement with the paper of Nakagaki *et al.* [8] on the colloidal stability of liposomes after preparation. Namely, electrolytes made the uncharged and charged liposomes unstable because of dehydration from hydrophilic colloid and binding of counterions, whereas without added electrolytes, surface charge resulted in enhanced stability of the liposomes. It was therefore suggested that the stabilizing effect of the solution of sugars or polyols was due to the absence of electrolytes. In all the following experiments an isotonic solution of sugars or polyols was used.

TABLE I. Aggregation of Liposomes after HS[a]

Rp.	DPPC[b] (mM)	Chol (mM)	EggPG (mM)	Medium[c]	Aggregation[d] of liposomes after HS
1	20			Saline	Aggregated
1a	20			Glu	Not aggregated
2	10	10		Saline	Aggregated
2a	10	10		Glu	Aggregated
3	18		2	Saline	Aggregated
3a	18		2	Glu	Not aggregated
4	8	10	2	Saline	Aggregated
4a	8	10	2	Glu	Not aggregated
4b	8	10	2	PG	Not aggregated

a) 121 °C for 20 min. The liposomal dispersion was extruded through a 0.8 μm membrane filter and nitrogen gas was not bubbled through before HS. *b*) Replacing DPPC with S-EggPC or H-EggPC led to the same result. *c*) Isotonic aqueous solutions: saline, 0.9% NaCl; Glu, 5.0% glucose; PG, 2.0% propylene glycol. *d*) No color change was observed after HS in any sample.

Factors Affecting the Color of Liposomal Dispersion after HS Each sample in Table II was a milky dispersion before HS, and after HS no aggregation was observed in any sample. If G-EggPC, which has a high POV, was used, the liposomal dispersion turned yellowish after HS (Rp. 5a, 6a, 7a and 7b). This could be partly prevented by bubbling nitrogen gas through the dispersion before HS (Rp. 10a, 10b and 10c), and fully prevented by using either S-EggPC (Rp. 8a), H-EggPC (Rp. 9a and 9b) or DPPC (Rp. 1a, 3a, 4a and 4b). Incorporation of vitamin E as an antioxidant to the liposomal bilayer had no effect on the color change (Rp. 11a), because vitamin E itself was unstable against the heat treatment and turned dark brown after HS. A good reproducibility of the color changes was obtained throughout the experiments.

The effect of pH on the color change was also checked. At pH 3.2 and 7.4 (using *ca.* 30 mM Britton–Robinson buffer solutions composed of H_3PO_4, CH_3COOH, H_3BO_3 and NaOH, which were diluted 6 times with a 5.0% glucose solution), the G-EggPC liposomal dispersion turned yellowish after HS even if nitrogen gas bubbling was performed (Rp. 12a and 15a). At pH 4.9 and 6.6 no color change was observed (Rp. 13a and 14a). When G-EggPC was replaced with S-EggPC, the same effect of pH was obtained, too (a part of the data is shown in Table VI).

Ohta[9] reported that the yellow or brown coloration of lecithins by heat treatment was based on the reaction products of aldehydes (degradation products of unsaturated acyl chains of lecithins *via* peroxide) and amines (inpurities in lecithins), and Frøkjaer *et al.*[10] reported that the hydrolytic degradation rate of distearoylphosphatidylcholine was rapid at both acidic and alkaline pH and was minimum at a pH of 6.5. Though further studies are necessary to clarify the pH dependency of the coloration of lecithins, it is thought that both the amount of dissolved oxygen and the POV of the lipids must be minimized and the pH of the medium adjusted to nearly pH 6.5, in order that the degradation of lipids and the subsequent production of aldehydes might be inhibited during HS.

TABLE II. Color Change of Liposomal Dispersion after HS

Rp.	G-EggPC[a] (mM)	S-EggPC[b] (mM)	H-EggPC[c] (mM)	DPPC (mM)	Chol (mM)	EggPG[d] (mM)	VE[e] (mM)	Medium[f]	Extrusion (μm)	N_2 gas bubbling	Color change[g]
5a	20							Glu	0.8	−	Yellowish
1a				20				Glu	0.8	−	n.c.
6a	18					2		Glu	0.8	−	Yellowish
3a				18		2		Glu	0.8	−	n.c.
7a, b	8				10	2		Glu, PG	0.8	−	Yellowish
8a		8			10	2		Glu	0.8	−	n.c.
9a, b			8		10	2		Glu, PG	0.8	−	n.c.
4a, b				8	10	2		Glu, PG	0.8	−	n.c.
10a, b, c	8				10	2		Glu, PG, Gly	0.8	+	n.c.
11a	8				10	2	0.35	Glu	0.8	−	Brown
12a	8[h]				10	2		Glu (3.2)	0.4	+	Yellowish
13a	8[h]				10	2		Glu (4.9)	0.4	+	n.c.
14a	8[h]				10	2		Glu (6.6)	0.4	+	n.c.
15a	8[h]				10	2		Glu (7.4)	0.4	+	Yellowish

a) POV = 6.5 − 7.6 meq/kg. *b*) POV = 1.0 − 2.1 meq/kg. *c*) Iodine value = 2 g/100 g, POV = 0.6 meq/kg. *d*) POV = 3.0 meq/kg. *e*) Vitamin E (an antioxidant). *f*) Isotonic aqueous solutions: Gly, 2.6% glycerol. The number within parenthesis shows pH of the medium buffered with Britton–Robinson buffer. *g*) Each sample was a milky dispersion before HS; after HS no aggregation was observed in any sample. A good reproducibility of the color changes was obtained throughout the experiments. *h*) Replacing G-EggPC with S-EggPC led to the same result. n.c.: not changed.

Factors Affecting the Particle Size Change of Liposomes during HS Table III shows the influence of the medium and the pore size of the extrusion membrane filter on the particle size change of the liposomes during HS. Chol in concentrations from *ca.* 30 to 50 mol% could be present without any observable aggregation during HS. In the glucose solution, the particle size ratio (particle size after HS/particle size before HS) of the liposomes extruded through a 0.8 μm membrane filter (Rp. 16a, 18a, 7a and 10a) was lower than that of the liposomes extruded through a 0.4 μm membrane filter (Rp. 17a, 19a, 20a and 21a). On the other hand, in the aqueous solution of propylene glycol or glycerol, pore size of the membrane filter did not influence the particle size change of the liposomes during HS. But this apparently better effect of polyols compared with sugars, which is also recognized in Table IV, was thought to result from the initially smaller particle sizes of the liposomes before HS. It can be said that polyols have a tendency to make the particle size of liposomes smaller.

Table IV shows the influence of the type of lecithin and the medium on the particle size change of the liposomes during HS. Prior to HS, the liposomes were extruded through a 0.8 μm membrane filter. Replacing ordinary G-EggPC (Rp. 7a, 7b, 10a and 10b) with hydrogenated H-EggPC or DPPC gave larger liposomal particle size before and after HS, and caused the particle size ratio (after HS/before HS) to be reduced, irrespective of the medium. This apparently better effect of G-EggPC compared with H-EggPC or DPPC was also thought to result from the initially smaller particle sizes of the liposomes before HS. Therefore, it can be said that the phosphatidylcholines which had the unsaturated acyl chains have a tendency to form liposomes of smaller particle size.

At a total lipid concentration of 100 mM, the particle size of liposomes had a tendency to increase after HS (data not shown), perhaps because of a greater number of liposomal collisions. For example, the particle size increased almost 4 times after HS, whereas at a concentration of 20 mM with the same molar ratio, only slight change was observed.

Incidentally, nitrogen gas bubbling had no influence on the particle size change (physical stability) of the liposomes during HS as shown in Tables III and IV, although it had a good effect on the color change (chemical stability) of the liposomal dispersions during HS.

In conclusion, it it thought that any medium (sugars or polyols), any pore size of the membrane filter, any lipid component (type of lecithin) and any lipid concentration

TABLE III. Particle Size Change of Liposomes during HS (I)

Rp.	G-EggPC (mM)	Chol (mM)	EggPG (mM)	Medium	Extrusion (μm)	N_2 gas bubbling	Particle size of liposomes[a]		Ratio (after/before)
							Before HS (nm)	After HS (nm)	
16a	11.5	6.5	2	Glu	0.8	−	538	385[b]	0.72
17a	11.5	6.5	2	Glu	0.4	−	324	290[b]	0.90
18a	9.5	8.5	2	Glu	0.8	−	710	414[b]	0.58
19a	9.5	8.5	2	Glu	0.4	−	388	314[b]	0.81
7a	8	10	2	Glu	0.8	−	579	510[b]	0.88
20a	8	10	2	Glu	0.4	−	364	334[b]	0.92
10a	8	10	2	Glu	0.8	+	500	435	0.87
21a	8	10	2	Glu	0.4	+	331	329	0.99
10b	8	10	2	PG	0.8	+	426	445	1.04
21b	8	10	2	PG	0.4	+	260	278	1.07
10c	8	10	2	Gly	0.8	+	364	405	1.11
21c	8	10	2	Gly	0.4	+	265	298	1.12

a) No aggregation was observed after HS in any sample. *b*) The color of the liposomal dispersion turned yellowish.

TABLE IV. Particle Size Change of Liposomes during HS[a] (II)

Rp.	G-EggPC (mM)	H-EggPC (mM)	DPPC (mM)	Chol (mM)	EggPG (mM)	Medium	N_2 gas bubbling	Particle size of liposomes[b]		Ratio (after/before)
								Before HS (nm)	After HS (nm)	
7a	8			10	2	Glu	−	579	510[c]	0.88
9a		8		10	2	Glu	−	753	584	0.78
4a			8	10	2	Glu	−	882	561	0.64
7b	8			10	2	PG	−	451	443[c]	0.98
9b		8		10	2	PG	−	676	575	0.85
4b			8	10	2	PG	−	675	597	0.88
10a	8			10	2	Glu	+	500	435	0.87
22a		8		10	2	Glu	+	649	564	0.87
23a			8	10	2	Glu	+	730	493	0.68
10b	8			10	2	PG	+	426	445	1.04
22b		8		10	2	PG	+	676	589	0.87
23b			8	10	2	PG	+	675	550	0.81

a) The liposomal dispersion was extruded through a 0.8 μm membrane filter before HS. *b*) No aggregation was observed after HS in any sample. *c*) The color of the liposomal dispersion turned yellowish.

TABLE V. Leakage of CF from Liposomes during HS[a] and during Storage[b]

Rp.	S-EggPC (mM)	H-EggPC (mM)	Chol (mM)	EggPG (mM)	SA (mM)	Medium[c]	Leakage of CF	
							After HS	After 6M
24a		11.5	6.5	2		Glu	>98%	n.s.[d]
25a		8	10	2		Glu	>98%	n.s.
26d	11.5		6.5		2	Suc	< 1%	<1%
27d	8		10		2	Suc	< 1%	<1%

a) The liposomal dispersion was extruded through a 0.4 μm membrane filter and nitrogen gas was not bubbled through before HS. *b*) Stored for 6 months at about 25 °C in room light. *c*) Isotonic aqueous solution: Suc, 10.0% sucrose. *d*) n.s.: not stored, because a considerable amount of CF leaked from the liposomes during HS.

TABLE VI. Long-Term Stability[a] of Liposomes after HS[b]

Rp.	S-EggPC (mM)	Chol (mM)	EggPG (mM)	SA (mM)	Medium[c]	N_2 gas bubbling	Particle size of liposomes[d]		
							Before HS (nm)	After HS (nm)	After 6M (nm)
26d	11.5	6.5		2	Suc	–	197	223	242
27d	8	10		2	Suc	–	252	231	264
28a	8	10	2		Glu (4.9)	+	392	407	335
29a	8	10	2		Glu (6.6)	+	376	323	352
30a	8	10	2		Glu (7.4)	+	363	315[e]	285[f]

a) Stored for 6 months at about 25 °C in room light. *b*) The liposomal dispersion was extruded through a 0.4 μm membrane filter. *c*) The number within parenthesis shows pH of the medium. *d*) No aggregation was observed in any sample. *e*) The color of the liposomal dispersion turned yellowish after HS. *f*) The yellowish color was unchanged after 6 months.

can be used for HS, but the influence of these factors on the particle size change of the liposomes should be very well comprehended.

Leakage of CF from Liposomes during HS and during Storage The CF-encapsulating liposomal dispersion was extruded through a 0.4 μm membrane filter and nitrogen gas was not bubbled through before HS. As shown in Table V, a considerable amount of CF (an anionic water-soluble model drug) leaked from the negatively charged liposomes composed of EggPC/Chol/EggPG (Rp. 24a and 25a) during HS, though the liposomal structure reformed after cooling. However, and most interestingly, almost no leakage of CF was observed during HS in the case of the positively charged liposomes composed of EggPC/Chol/SA (Rp. 26d and 27d). It is thought that a major fraction of the model drug was able to be bound to the liposomal membrane, because the electrostatic attraction between CF and SA was strong enough to overcome the dissipative energy at high temperatures. It is also thought that the absence of the electrolytes such as NaCl had some effect on the electrostatic attraction stability between CF and SA. It is not clear from these experiments alone whether the heat treatment causes the rupture of liposomal structure or changes only the permeability of the liposomal membrane without the rupture of the structure. But it is expected that any ionic water-soluble drug will be effectively encapsulated in the oppositely charged liposomes, which are resistant to the leakage of the drug during HS, provided the drug itself is stable against heat treatment. For instance, anionic X-ray contrast agents such as iotalamate and cationic antibiotics such as gentamicin can be encapsulated in the oppositely charged liposomes, and, of course, the lipophilic drugs such as prostaglandins can be encapsulated in both the positively and the negatively charged liposomes.

It may be because of the same mechanism that almost no leakage of CF was observed after storage for 6 months at about 25 °C in room light, as shown in Table V.

Pellets of the positively charged liposomes redispersed after HS were of almost the same particle size as before HS, and no noticeable changes in size were observed after 6 months at 25 °C in room light, as shown in Table VI (Rp. 26d and 27d).

Long-Term Stability of Liposomes after HS during Storage In addition to the above CF-encapsulating positively charged liposomes (Rp. 26d and 27d), after HS some negatively charged liposomes not containing the model drugs were stored for 6 months at 25 °C in room light. As shown in Table VI, no noticeable changes in particle size or color were observed after 6 months (Rp. 28a, 29a and 30a), though in the case of Rp. 30a the dispersion turned yellowish after HS and this yellowish color was unchanged after 6 months. These results indicate that the liposomal dispersions which are stable against HS are also stable during long-term storage. The factors which affect the stability of the liposomal dispersions during HS are considered to be the same as those which affect the long-term stability of these dispersions during storage. The stability of the liposomes during storage for more than 3 years in an aqueous dispersion state, in a frozen state, in a freeze-dried state or in a spray-dried state will be reported in another paper.[11]

Acknowledgments The authors thank Prof. K. Shinoda, Yokohama National University, for his comments on this work. The stay of Anders Carlsson in Japan was financially supported by the Swedish National Board for Technical Development.

References and Notes

1) A part of this work was presented at the 109th Annual Meeting of Pharmaceutical Society of Japan, Nagoya, April 1989 and at the 4th Princeton Liposome Conference, New Jersey, U.S.A., May 1989.
2) On leave from *Physical Chemistry 1, Chemical Center, Lund University, P. O. Box 124, S-221 00 Lund, Sweden.* Present address: *Kabi Invent AB, Novum, S-141 52 Huddinge, Sweden.*

3) Present address: *School of Pharmaceutical Sciences, University of Shizuoka, Yada, Shizuoka, Japan.*
4) P. Machy and L. Leserman (eds.), "Liposomes in Cell Biology and Pharmacology," John Libbey, Inc., London/Paris, 1987.
5) J. Friese, "Liposome Technology. Volume 1: Preparation of Liposomes," ed. by G. Gregoriadis, CRC Press, Inc., Boca Raton, Florida, 1984, pp. 131—137.
6) A. D. Bangham, M. M. Standish and J. C. Watkins, *J. Mol. Biol.*, **13**, 238 (1965).
7) F. Olson, C. A. Hunt, F. C. Szoka, W. J. Vail and D. Papahadjopoulos, *Biochim. Biophys. Acta*, **557**, 9 (1979).
8) M. Nakagaki, T. Handa, S. Shakutsui and M. Nakayama, *Yakugaku Zasshi*, **102**, 17 (1982).
9) S. Ohta, *Yukagaku*, **19**, 792 (1970).
10) S. Frϕkjaer, E. L. Hjorth and O. Wϕrts, "Liposome Technology. Volume 1: Preparation of Liposomes," ed. by G. Gregoriadis, CRC Press, Inc., Boca Raton, Florida, 1984, pp. 235—245.
11) H. Kikuchi, H. Yamauchi, K. Yachi and S. Hirota, *Chem. Pharm. Bull.*, In preparation.

Diffusion and Reaction of *p*-Nitroaniline and Succinic Anhydride in Controlled Pore Glass[1)]

Etsuo YONEMOCHI, Toshio OGUCHI, Keiji YAMAMOTO and Yoshinobu NAKAI*

Faculty of Pharmaceutical Sciences, Chiba University, 1–33 Yayoicho, Chiba 260, Japan. *Received October 5, 1990*

A multi-layered tablet which consisted of controlled pore glass (CPG) and organic compounds was prepared. Addition reactions between succinic anhydride and *p*-nitroaniline, which were included separately in the CPG layers of the multi-layered tablet, have been studied. The reaction product, succinyl-*p*-nitroanilide, was mainly distributed near the *p*-nitroaniline layer. This can be explained in terms of a higher diffusion rate of succinic anhydride, resulting in its higher vapor pressure. The diffusion rate constant of succinic anhydride in the CPG120 system was evaluated as 6.00×10^{-7} cm^2/s by fitting the diffusion equation to experimental results.

Keywords controlled pore glass; solid state reaction; addition reaction; diffusivity; layered cylindrical tablet; succinic anhydride; *p*-nitroaniline

Introduction

We have already investigated the interaction between medicinals and controlled pore glasses (CPGs).[2–4)] In the previous paper, we reported that the crystalline characteristics of medicinals were changed by mixing them with CPG, and that the solid-state addition reaction between succinic anhydride and *p*-nitroaniline was also accelerated in the CPG mixture.[5)] A possible mechanism was proposed by Pikal *et al.* for the diffusion of medicinals in the mixed powder systems with CPG, *i.e.*, gas-phase diffusion with capillary condensation.[6)] In practice, however, it was difficult to clarify the mechanism of diffusion of medicinals with chemical reactions in the mixture with CPG. The triple (double) layered cylindrical tablet appeared to be a useful model for studying the diffusivity of medicinals in CPG, because of simple geometry and the constant area of interface during the reaction.[7,8)] The present investigation was undertaken to examine the diffusivity of medicinals in CPG with a triple (double) layered cylindrical tablet, and to clarify the mechanism leading to the amorphous state of medicinals in CPG system.

Experimental

Materials Succinic anhydride (Wako Pure Chemical Industries Co., Ltd.) and *p*-nitroaniline (Wako Pure Chemical Industries Co., Ltd.) were of reagent grade and used as received from the supplier. Both crystals were used after sieving (120/250 mesh). CPGs were obtained from Electro-Nucleonics Ltd., CPG120 (mean pore diameter: 117 Å, specific surface area: 119 m^2/g) and CPG1000 (mean pore diameter: 962 Å, specific surface area: 26.1 m^2/g) were used after drying in a vacuum at 120 °C for 3 h.

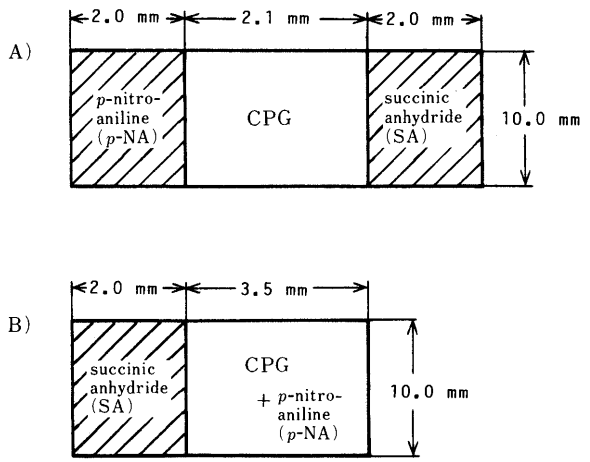

Chart 1. Layered Cylindrical Tablet Systems

A) triple layered system; B) double layered system.

Preparation of Tablets For the *p*-nitroaniline–CPG–succinic anhydride triple layered tablet system (tablet diameter; 10.0 mm, total thickness; 6.1 mm), *p*-nitroaniline (200 mg) and succinic anhydride (200 mg) were compacted at 0.4 ton/cm^2 using die and plane-faced punches, respectively, with a hydraulic press (Riken Seiki, P-1B). A tablet of *p*-nitroaniline was placed in the bottom of the die, then CPG (500 mg) was added on the tablet. A previously cast succinic anhydride tablet was also placed above the CPG layer and compacted using the same pressure (Chart 1A). For the succinic anhydride–CPG double layered tablet system (tablet diameter; 10.0 mm, total thickness; 5.5 mm), first *p*-nitroaniline was mixed with CPG in the mixing ratio of (90% CPG120 + 10% *p*-nitroaniline), or (95% CPG1000 + 5% *p*-nitroaniline). The mixtures were stored for a week in a desiccator at 0% relative humidity (RH) and 50 °C. A tablet of succinic anhydride was first prepared in the bottom of the die, then the mixture of *p*-nitroaniline with CPG was added and compacted under the same pressure (Chart 1B).

Measurement of Concentration of Succinyl-*p*-nitroanilide (Product) in Samples After compression of the tablet, the die without ejection of the tablet was stored in a desiccator at RH 0% and 50 °C. At the appropriate time intervals up to 70 h, the die with tablet was taken out from the desiccator. After ejection of the tablet from the die, the tablet was cut with spacing of 0.5—1.0 mm from the interface and each fraction was collected. To determine the amount of reaction product in each fraction, the powder samples were suspended in a 50% aqueous ethanol solution completely to extract succinyl-*p*-nitroanilide. The concentration of succinyl-*p*-nitroanilide was determined spectrophotometrically at 322 and 384 nm on a Shimadzu double-beam spectrophotometer UV-200S.[5)]

Results and Discussion

Diffusivity Studies The prepared triple layered tablet was stored at 50 °C and RH 0%. In this storage condition, the decomposition rates of organic compounds were negligible. Figure 1 shows the variations of succinyl-*p*-nitroanilide distribution in the CPG120 layer as a function of storage time. The abscissa is the distance from the interface with the *p*-nitroaniline tablet, and the ordinate is the concentration of reaction product in CPG120. Succinic anhydride and *p*-nitroaniline diffused into the CPG120 layer from the right and left sides respectively, and the reaction of succinic anhydride and *p*-nitroaniline was developed in the CPG layer.[5)] The concentration of the reaction product, succinyl-*p*-nitroanilide, increased with the elapse of storage time, and the maximum concentration of the reaction product was observed close to the *p*-nitroaniline interface. Good reproducibility of the concentration profiles of the reactant product was observed for different preparations. This suggests that the diffusivity of succinic anhydride in CPG120 was greater than that of *p*-nitroaniline. The gaseous

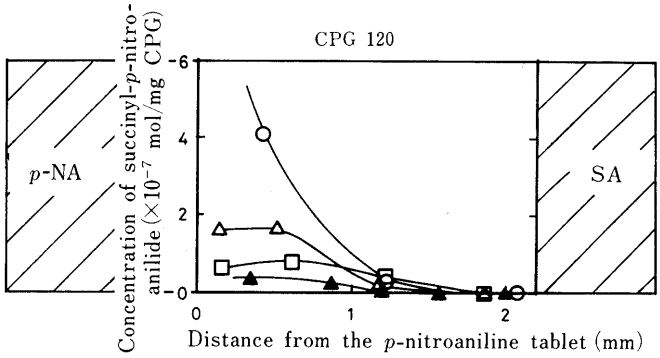

Fig. 1. Plots of Concentration of Reacted Product (Succinyl-*p*-nitroanilide) *vs.* Distance from the Interface between *p*-Nitroaniline and CPG 120

Triple layered tablet was stored at 50 °C, RH 0% for definite time. ▲, 6 h; □, 12 h; △, 22 h; ○, 70 h.

TABLE I. Vapor Pressure of Succinic Anhydride and *p*-Nitroaniline[10]

	Vapor pressure at 100 °C (mmHg)
Succinic anhydride	1.82
p-Nitroaniline	0.0136

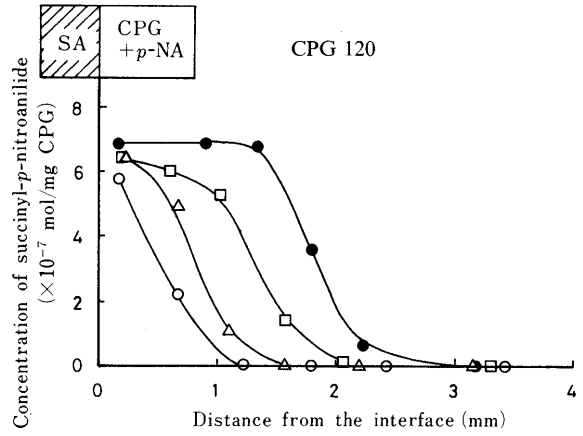

Fig. 2. Plots of Concentration of Reacted Product (Succinyl-*p*-nitroanilide) *vs.* Distance from the Interface between Succinic Anhydride and CPG120 Containing 10% *p*-Nitroaniline

Double layered tablet was stored at 50 °C, RH 0% for definite time. ○, 6 h; △, 12 h; □, 24 h; ●, 48 h.

flux of a sublimating organic compound from the crystal surface depends on many factors such as temperature, vapor pressure and surface area of organic crystals.[9] Table I shows the vapor pressure of succinic anhydride and *p*-nitroaniline crystal at 100 °C.[10] The vapor pressure of succinic anhydride was about 100 times greater than that of *p*-nitroaniline at 100 °C. This should account for the high diffusivity of the succinic anhydride in CPG120. In this experimental system, temperature and surface area of the tablet of succinic anhydride and *p*-nitroaniline were constant, hence the difference of the vapor pressure of the succinic anhydride and *p*-nitroaniline crystal was considered to cause the difference in diffusivity, although the molecular weights and collision cross-section of each compound might also have some effect on the diffusivity.[11,12] To investigate the above results more clearly, we studied a simple system, *i.e.*, a double layered tablet of succinic anhydride and CPG

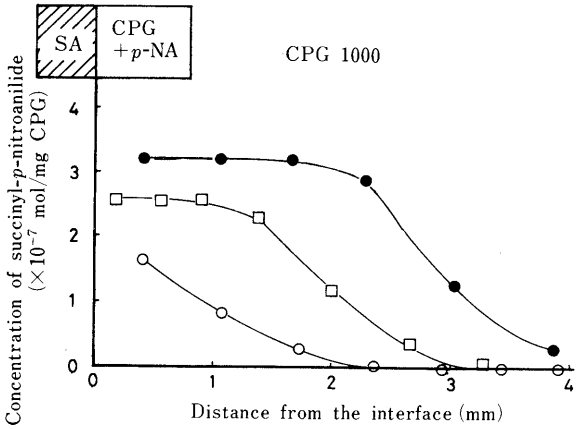

Fig. 3. Plots of Concentration of Reacted Product (Succinyl-*p*-nitroanilide) *vs.* Distance from the Interface between Succinic Anhydride and CPG1000 Containing 5% *p*-Nitroaniline

Double layered tablet was stored at 50 °C, RH 0% for definite time. ○, 6 h; □, 24 h; ●, 48 h.

containing 10 or 5% *p*-nitroaniline. Figure 2 shows the concentration profiles of the reaction product in the CPG120 double layered tablet containing 10% *p*-nitroaniline (Chart 1B) after storage at 50 °C and RH 0%. The concentration of succinyl-*p*-nitroanilide increased with the elongation of storage time, and in the distance within 1.5 mm, the saturated concentration of 7.0×10^{-7} mol/mg of CPG was observed after storage for 48 h. The succinyl-*p*-nitroanilide concentration of this level was reasonable, as the initial concentration of *p*-nitroaniline (one of the reactants) in the mixture was calculated as 7.0×10^{-7} mol/mg of CPG, indicating the completion of an addition reaction between diffused succinic anhydride and *p*-nitroaniline.

The concentration profiles of succinyl-*p*-nitroanilide in the CPG1000 of the double layered tablet (Chart 1B) after storage at 50 °C and RH 0% are shown in Fig. 3. The final concentration saturation level of succinyl-*p*-nitroanilide was just half of the CPG120 mixture, as the initial *p*-nitroaniline concentration was 5% in this case. After storage for 24 h, a high concentration of succinyl-*p*-nitroanilide was observed even at the distance of 1.3 mm. From comparison with Fig. 2, the concentration of succinyl-*p*-nitroanilide at 2.5 mm in the CPG1000 system was significantly higher than that in the CPG120 system. This difference seemed to be consistent with the differences in specific surface area, mean pore diameter of CPGs and adsorption energy of the medicinals on CPGs. Adsorption energy on CPG120 was greater than that on CPG1000, the small mobility of the adsorbed molecules on CPG120 might be associated with a large energy of bonding to the surface, in contrast to the higher mobility of weakly bound molecules on CPG1000.[13] In most meso-porous materials, in which the pore diameter was less than 1000 Å, Knudsen diffusion was important in characterizing the total diffusion of gases. However, in micro-porous materials having pore diameters of less than 100 Å, the effect of the diffusion of adsorbed molecules along the internal surfaces of porous materials on the total diffusion could not be neglected.[14] Therefore, it was suggested that the great adsorption energy on CPG120 correlated with the pore surface diffusion of succinic anhydride.

Calculation of the Diffusivity In the double layered

system, we can regard the addition reaction as a pseudo-first order reaction. If the diffusing substance is immobilized by an irreversible first-order reaction, the equation for diffusion in one dimension becomes[15]:

$$\frac{\partial c}{\partial t}=D\frac{\partial^2 c}{\partial x^2}-k\cdot c \tag{1}$$

where c is the concentration of succinic anhydride, t is the storage time, x is the distance from the interface between succinic anhydride and CPG, D is the diffusivity of succinic anhydride in CPG and k is the reaction rate constant between succinic anhydride and *p*-nitroaniline in CPG. The initial conditions for above system are:

$$c=0, \quad x>0$$

$$c=c_0, \quad x=0$$

Since succinic anhydride does not reach the outer end of the CPG subtablet, the system may be considered as a semiinfinite rod with boundary conditions. The boundary conditions are:

$$c=c_0 \quad \text{at} \quad x=0$$

$$c=0 \quad \text{at} \quad x=+\infty$$

Dimensionless concentration C', time T and distance X' variables, are defined as follows:

$$C'=1/c_0\cdot c \tag{2}$$

$$T=c_0\cdot k\cdot t \tag{3}$$

$$X'=(c_0\cdot k/D)^{1/2}\cdot x \tag{4}$$

Equation 1 can be written in terms of dimensionless parameters as follows:

$$\frac{\partial C'}{\partial T}=\frac{\partial^2 C'}{\partial X'^2}-\frac{1}{c_0}\cdot C' \tag{5}$$

Equation 5 with dimensionless parameters is convenient to calculate by computer. Then, the equation with boundary conditions are numerically solved for C' as a function of X' and T.[15] Since a small net size (ΔT, $\Delta X'$) was necessary to obtain an accurate solution, the value of ΔT was determined as 5.0×10^{-4}.

The concentration ratio of succinyl-*p*-nitroanilide is plotted against the distance from the interface in Fig. 4 and the effect of diffusivity on concentration profiles is demonstrated. The initial concentration of succinic anhydride in CPG120 was calculated as 1.00×10^{-3} mol/cm^3, and the first-order reaction rate constant between succinic anhydride and *p*-nitroaniline in CPG120 at 50 °C was determined as 1.67×10^{-4} cm^3/mol·s respectively.[5] The concentration of reacted product at the distance (x) decreased with the decrease of the diffusivity.

Curves of the concentration ratio (C') *vs.* distance from the interface (x) are shown for assumed values of D in Fig. 5 for comparison with the experimental value. Good agreement between theoretical and experimental concentration profiles is obtained when the diffusivity of succinic anhydride in CPG120 is estimated 6.00×10^{-7} cm^2/s. This value of diffusivity is smaller than the 0.33 cm^2/s observed in gas phase and 0.09 cm^2/s observed in meso-pore (170 Å) by Knudsen diffusion at 1 atm respectively.[16] The

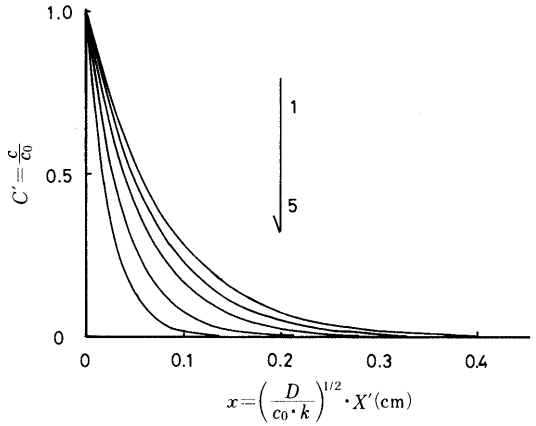

Fig. 4. Effects of Diffusivity on Concentration Profiles of Succinyl-*p*-nitroanilide

$c_0=1.00\times10^{-3}$ mol/cm^3; $t=2.16\times10^4$ s; $k=1.67\times10^{-4}$ cm^3/mol·s; curve 1, $D=1.00\times10^{-6}$ cm^2/s; curve 2, $D=7.50\times10^{-7}$ cm^2/s; curve 3, $D=5.00\times10^{-7}$ cm^2/s; curve 4, $D=2.50\times10^{-7}$ cm^2/s; curve 5, $D=1.00\times10^{-7}$ cm^2/s.

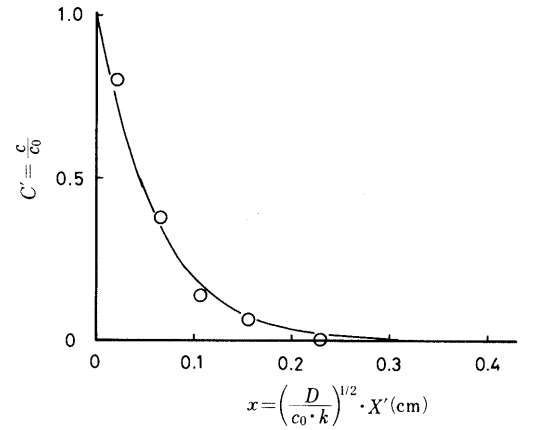

Fig. 5. Plots of Concentration Ratio *vs.* Distance from the Interface

CPG120 double layered tablet was stored at 50 °C, RH 0%.
○, experimental values; $c_0=1.00\times10^{-3}$ mol/cm^3; $t=2.16\times10^4$ s; $k=1.67\times10^{-4}$ cm^3/mol·s; The line assumes a theoretical curve at $D=6.00\times10^{-7}$ cm^2/s.

magnitudes of reported D values of the surface migration range from 1.0×10^{-5} to 1.0×10^{-13} cm^2/s.[17] These results indicated that the diffusion of succinic anhydride on CPG120 might be a pore surface diffusion.

Therefore, the following mechanism could be proposed: vaporization of succinic anhydride and diffusion of the vapors into the pore of the CPGs, followed by the succinic anhydride molecules bring adsorbed on the pore surface; the adsorbed molecules were diffused on the pore surface and reacted with *p*-nitroaniline.

References and Notes

1) This paper is part V of "Interaction of Medicinals and Porous Powder." The previous paper, part IV: E. Yonemochi, T. Oguchi, K. Terada, K. Yamamoto and Y. Nakai, *Chem. Pharm. Bull.*, **37**, 3083 (1989).
2) Y. Nakai, K. Yamamoto, K. Terada and J. Ichikawa, *Chem. Pharm. Bull.*, **32**, 4566 (1984).
3) Y. Nakai, K. Yamamoto, K. Terada and J. Ichikawa, *Yakugaku Zasshi*, **105**, 296 (1985).
4) Y. Nakai, K. Yamamoto and S. Izumikawa, *Chem. Pharm. Bull.*, **37**, 435 (1989).
5) E. Yonemochi, T. Oguchi, K. Terada, K. Yamamoto and Y. Nakai, *Chem. Pharm. Bull.*, **37**, 3083 (1989).
6) M. J. Pikal, A. L. Lukes and L. F. Ellis, *J. Pharm. Sci.*, **65**, 1278

(1976).
7) R. J. Arrowsmith and J. M. Smith, *Ind. Eng. Chem. Fundamental*, **5**, 327 (1966).
8) S. Ramachandran, A. Baradarajan and M. Satyanarayana, *Powder Technol.*, **34**, 143 (1983).
9) Y. Nakai, K. Yamamoto, K. Terada and T. Oguchi, *J. Pharmacobio-Dyn.*, **9**, s-9 (1986).
10) The Chemical Society of Japan (ed.), "Kagakubinran, Fundamental, 3rd Ed.," Maruzen, Tokyo, 1984, Vol. II, pp. 127, 131.
11) T. Konno and K. Kinuno, *Chem. Pharm. Bull.*, **37**, 2481 (1989).
12) S. Ramachandran, *Powder Technol.*, **38**, 7 (1984).
13) Y. Nakai, K. Yamamoto, T. Oguchi, E. Yonemochi, S. Maeda and H. Egawa, *Yakugaku Zasshi*, **110**, 34 (1990).
14) K. Kawazoe, *Kagaku Kogaku*, **44**, 521 (1980).
15) J. Crank, "The Mathematics of Diffusion, 2nd Ed.," Clarendon Press, Oxford, 1976, pp. 137, 329.
16) Catalysis Society of Japan (ed.), "Syokubai To Hannosokudo," Kodansha, Tokyo 1986, p. 266.
17) *a*) E. R. Gilliland, R. F. Baddour, G. P. Perkinson and K. J. Sladek, *Ind. Eng. Chem. Fundamental*, **13**, 95 (1974); *b*) K. J. Sladek, E. R. Gilland and R. F. Baddour, *ibid.*, **13**, 100 (1974).

Stability of Aspirin in Controlled Pore Glass Solid Dispersions[1)]

Etsuo YONEMOCHI, Manabu MATSUMURA,[2)] Toshio OGUCHI, Keiji YAMAMOTO and Yoshinobu NAKAI*

Faculty of Pharmaceutical Sciences, Chiba University, 1–33 Yayoicho, Chiba 260, Japan. *Received October 5, 1990*

Effect of mixing with a controlled pore glass (CPG) on the stability of aspirin was studied under conditions of various relative humidities (RH), pore diameters of CPG and concentrations of aspirin. The crystallinity changes of aspirin in the mixtures with CPG170 or CPG3000 were also studied using the powder X-ray diffraction method and microscopy. The amorphous aspirin in the CPG mixtures showed an extremely fast decomposition rate, and a high rate was obtained when the pore diameter of the CPGs were less than 300 Å. In the mixtures of small pore diameter CPG, the decomposition rate constants were greater at a lower RH. These results can be explained in terms of the catalytic effect of free silanol groups on the surface of the CPG.

Keywords controlled pore glass; stability; amorphous; crystallinity; aspirin; catalytic effect; dispersion; aerosil

Introduction

The hydrolytic decomposition of aspirin has been widely studied in aqueous media, while relatively little is known about the same phenomenon in the solid state.[3)] It has been shown that the rate of hydrolysis of the solid aspirin is proportional to the relative humidity of the strong atmosphere.[4–6)] The effect of additives on this hydrolysis has been investigated, and the presence of additives has been found to affect the decomposition rate of aspirin.[7–10)]

Controlled pore glasses (CPGs) are well known for their large surface area and highly porous structures. We have already investigated the adsorption of medicinal molecules on the pore surface of CPGs, the improvement of benzoic acid dissolution, the retardation of its sublimation, and the accelerated solid state addition reaction between succinic anhydride and *p*-nitroaniline in the CPG mixtures.[11)]

The present study was undertaken to evaluate the chemical stability of aspirin in solid dispersion with CPGs and to elucidate the mechanisms of the interaction of aspirin with the CPGs.

Experimental

Materials CPGs of different mean pore diameters were purchased from Electro-Nucleonics Ltd., and the properties were reported in the previous paper.[12)] Aerosil 200 was purchased from Nippon Aerosil Co., Ltd.; the specific surface area of aerosil 200 was calculated as 198.5 m^2/g from a N_2 gas adsorption isotherm using the BET equation. Potassium hydrogen bisacetylsalicylate (KH-Asp_2) was synthesized by the reported procedure.[13)] Aspirin (Iwaki Seiyaku Co.) used was of JP XI grade.

Powder X-Ray Diffractometry The apparatus and procedures were the same as reported previously.[12)]

Microscopic Study A microscope (Nikon S-keII) equipped with polarizing plate was used to evaluate the mixed state.

Preparation of the Mixtures The mixtures of various aspirin contents (1—5%) were prepared with CPGs or aerosil by manual bottle tumbling of two components or using mortar and pestle at room temperature for 1 min. For the stability studies, we used the mixtures prepared by mortar and pestle.

Stability Studies and Analytical Method Each mixture was stored in a desiccator in which the relative humidity (RH) was controlled at 50 °C. P_2O_5 and aqueous saturated salt solutions were used to get definite RHs. The extent of decomposition of aspirin was monitored periodically by the spectrophotometrical method using a Shimadzu UV-200S spectrophotometer.[14)]

Determination of Adsorbed Water About 1 g of dried CPG170 was stored in a desiccator under the definite RHs (0, 49, 79, 96%) at 50 °C for 1 month. The weight gains were measured by a microbalance.

Results and Discussion

Physicochemical States of Aspirin To investigate the crystallinity changes of aspirin following mixture with CPGs, a 5% aspirin mixture was prepared with CPG170 or CPG3000 by manual tumbling in a bottle. Figure 1 shows the powder X-ray diffraction patterns of the mixtures before and after storage at RH 0% and 50 °C. In the case of the CPG170 mixture, the X-ray diffraction peaked at $2\theta = 16.5°$ due to aspirin crystals disappearing after storage for 2 h. In contrast, for the CPG3000 mixture, the diffraction peak of aspirin crystals was still observed after storage for 24 h. Microscopic observation revealed that aspirin crystals in the CPG170 mixture were no longer detectable after 2 h of storage (Fig. 2 a, b), while the aspirin crystalline particles were clearly observed in the CPG3000 mixture (Fig. 2 c, d). The results indicated that the mixing with CPG of a small pore diameter led the aspirin crystals to be in an amorphous state, and that the pore diameter of the CPG exerted an influence on the crystallinity changes of aspirin.

Since the vapor pressure of solid drugs was reported as a major factor for controlling the crystallinity of the drugs when mixed with porous materials,[15)] the potassium salt of aspirin which had negligible vapor pressure was used for comparison with the behavior of the aspirin crystals. The X-ray diffraction patterns of 5% KH-ASP_2–95% CPG170 mixtures are shown in Fig. 3. KH-ASP_2 had a characteristic X-ray diffraction peak at $2\theta = 7.3°$. Under the same storage condition as that used for the aspirin and CPG170 mixture,

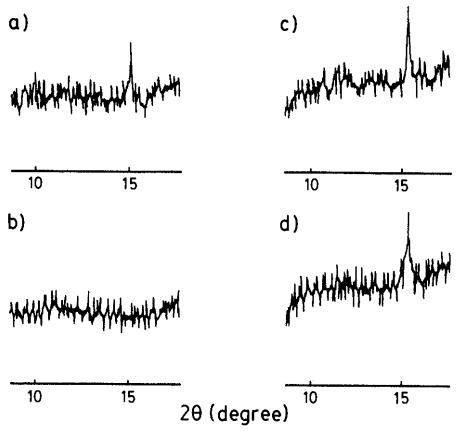

Fig. 1. Powder X-Ray Diffraction Patterns of the Mixture of Aspirin and Either CPG170 or CPG3000

a) 5% aspirin + 95% CPG170; b) sample a) was stored for 2 h at 50 °C and RH 0%; c) 5% aspirin + 95% CPG3000; d) sample c) was stored for 24 h at 50 °C and RH 0%.

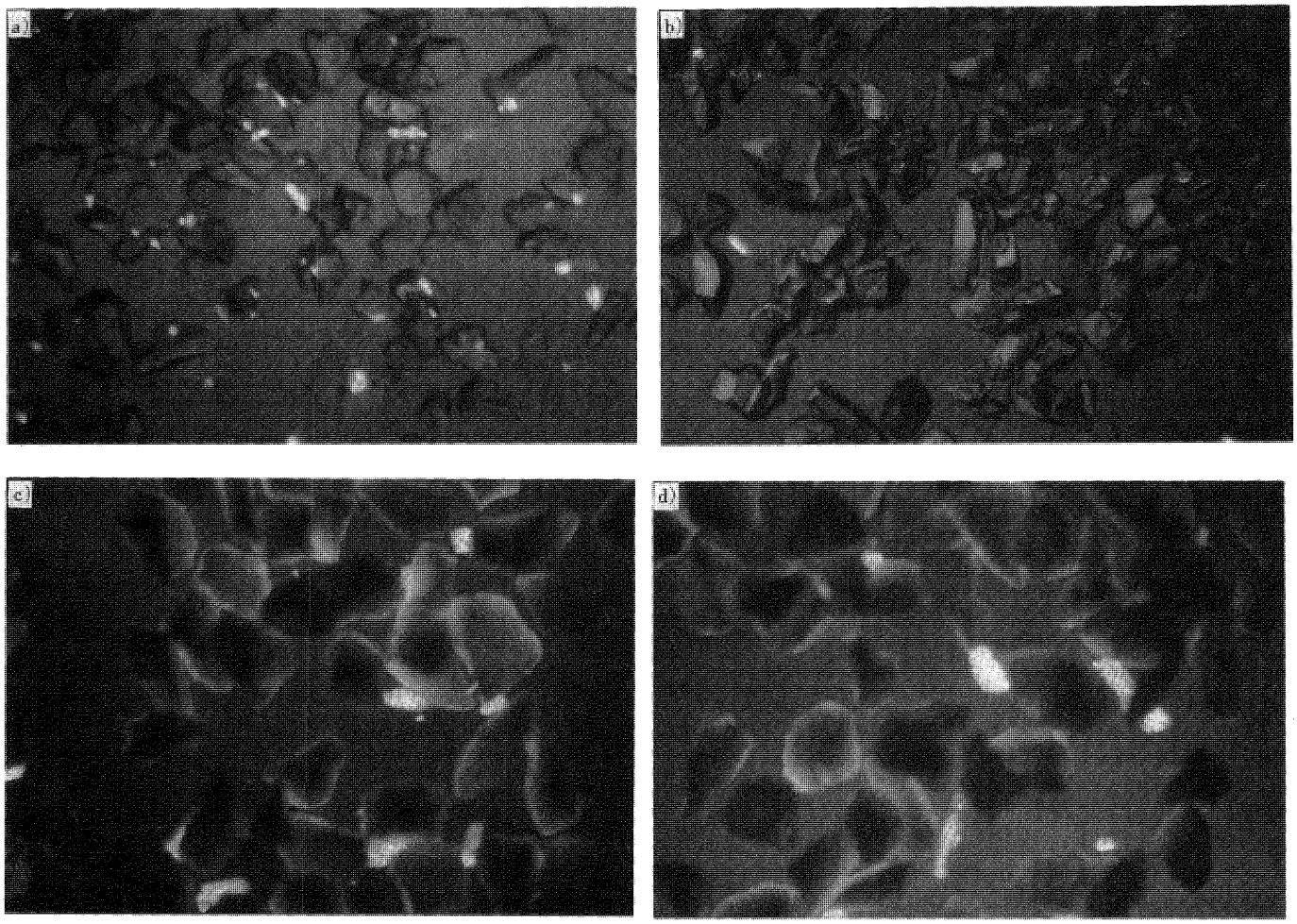

Fig. 2. Polarized Micrographs

Keys are same as Fig. 1.

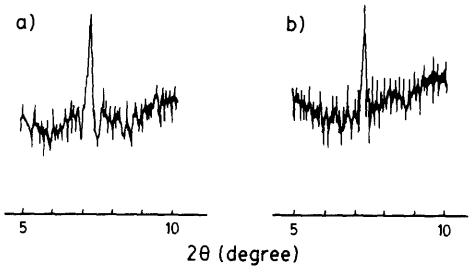

Fig. 3. Powder X-Ray Diffraction Patterns of the Mixture of Potassium Hydrogen Bisacetylsalicylate and CPG170

a) 5% potassium hydrogen bisacetylsalicylate+95% CPG170; b) sample a) was stored for 5 h at 50 °C and RH 0%.

the intensity of this peak was not changed after 5 h. The observed photographs indicate that the KH-ASP_2 crystalline particles remained intact in the CPG170 mixture (Fig. 4). From the X-ray and microscopic studies, no changes in crystallinity of KH-ASP_2 was observed by the mixing with CPG170. According to Konno, the vapor pressure was mentioned as an index to predict the propensity for crystallinity change of a solid drug in a mixture with an adsorbent.[15] The decrease in aspirin crystallinity in the CPG mixture is explained in terms of the transfer of aspirin molecules into CPG particles through a gaseous phase.

Stability of Aspirin in the CPG Mixtures The kinetics of aspirin hydrolysis were studied in the CPG mixtures containing 5% aspirin. The pore diameters of CPGs varied from 75 Å to 3000 Å. Under the conditions used, first-order decomposition patterns were observed as shown in Fig. 5; therefore the first-order rate constants were calculated. In this system, which consisted of only aspirin crystals, no aspirin decomposition was observed after storage at 50 °C for 12 h. Figure 6 shows the plots of the first-order rate constants at 50 °C under the two different RHs *versus* the pore diameter of CPG. In the CPG mixtures where the pore diameter was less than 300 Å, the rate constants of aspirin decomposition were independent of CPG pore diameters in the cases of both 0% RH and 79% RH. However, the rate constants in the mixtures with CPG of large pore size decreased with increasing CPG pore diameter. The pore diameter profiles of the rate constant indicate that the stability of aspirin was closely related to the crystallinity changes of aspirin in the mixtures. That is, greater and similar decomposition rate constants were observed in the mixture of small pore diameter (less than 300 Å) where aspirin was in a completely amorphous state.

Figure 6 also revealed that the decomposition rate constants observed at RH 0% were greater than those at RH 79% in samples from CPG75 to CPG350. In the cases of the CPG1000 and CPG3000 mixtures, the decomposition at RH 79% was faster than that at RH 0%. Although

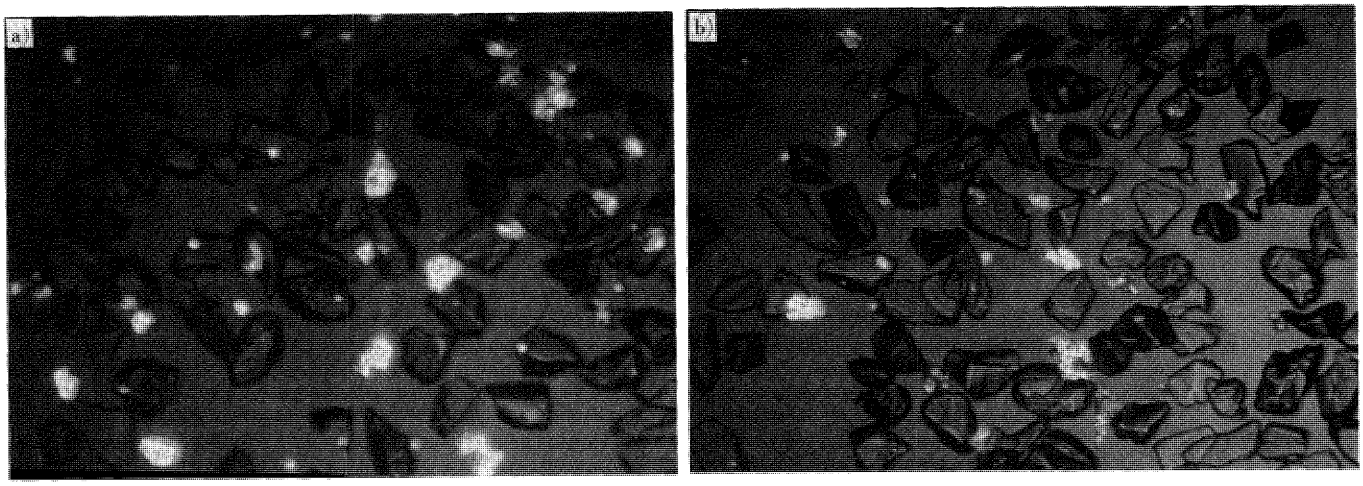

Fig. 4. Polarized Micrographs

Keys are same as Fig. 3.

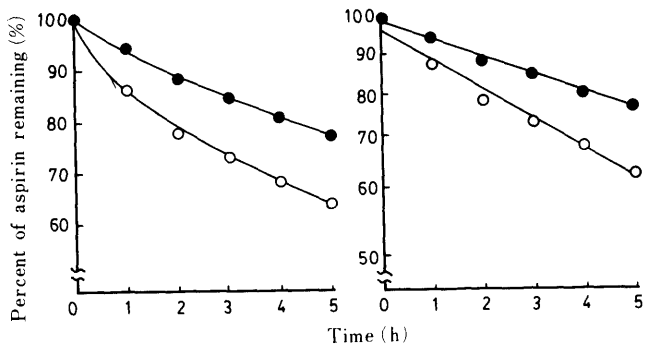

Fig. 5. Decomposition Kinetics of Aspirin in the Mixture of 5% Aspirin and 95% CPG170 at 50 °C

○, RH 0%; ●, RH 79%.

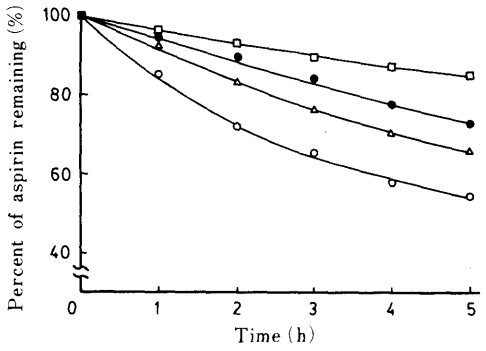

Fig. 7. Effect of RH on the Decomposition of Aspirin Mixed with CPG170 at 50 °C

Aspirin concentration is 1%. ○, RH 0%; △, RH 49%; ●, RH 79%; □, RH 96%.

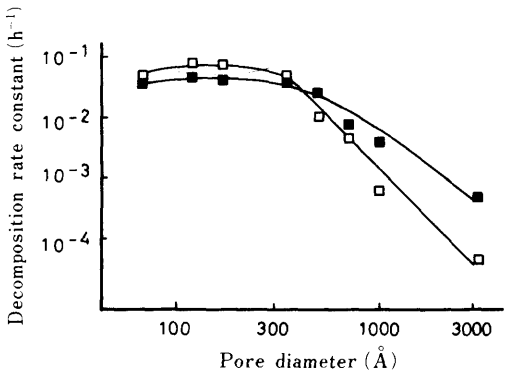

Fig. 6. Effect of CPG's Pore Diameter on the First-Order Rate Constant for the Decomposition of Aspirin at 50 °C

Aspirin concentration is 5%. □, RH 0%; ■, RH 79%.

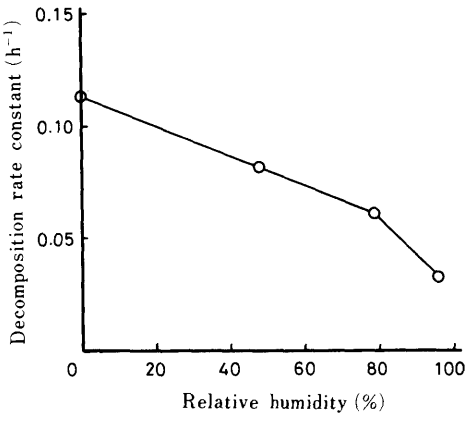

Fig. 8. Effect of RH on the First-Order Rate Constant for the Decomposition of Aspirin Mixed with CPG170 at 50 °C

Aspirin concentration is 1%.

hydrolysis in solid state was accelerated by humidification generally, the opposite situation was observed in the mixtures with small pore CPGs.[3] Especially, the decomposition rate constant in the CPG75 mixture at RH 0% and 50 °C was determined as $4.90 \times 10^{-2}\ h^{-1}$, indicating the half life of aspirin decomposition of 14.1 h.

Effects of RH on Aspirin Decomposition in CPG170 Mixture Kinetic studies in a 1% aspirin–CPG170 mixture were performed at various RH values at 50 °C, as shown in Fig. 7. In this mixture, aspirin was in the amorphous state. Figure 8 illustrates the RH dependency of the first-order rate constants of aspirin decomposition in the CPG170 mixture at 50 °C. An anomalous linear relationship was obtained between the RH and the rate constants, that is, as the RH was raised, the rate constant decreased.

Leeson and Mattocks proposed the aspirin decomposition mechanism in solid state as follows.[4] After the formation of a water layer on aspirin particles, aspirin dissolved into

the water layer, then decomposition occurred in solution. In a crystalline state, the adsorbed amount of water increased at a high RH; therefore, faster aspirin decomposition was observed. On the other hand, the stability of aspirin in the solid dispersed system was affected by many factors such as hygroscopicity of additives, pH on the surface, specific surface area and dispersed state. El-Banna *et al.* reported that aspirin in the coprecipitated samples with povidone or urea had slightly higher degradation rates due to the increased water sorption ability. In the case of urea solid dispersion, urea could also have been dissolved into a thin water layer and imparted a slight alkalinity to this film.[7]

By contrast, Gore and Banker showed a enhanced aspirin stability by addition of colloidal silica at a high RH. They interpreted these results in terms of the action as due to an internal moisture scavenger.[8] The water molecules were entrapped by the silanol groups of colloidal silica. The surface of CPG was also covered by silanol groups as well as by colloidal silica; however, the concentration of aspirin in our experiments was as low as 3%, differing from the high concentration (99—85%) used by Gore and Banker. Therefore, the simple mechanism of preferential water vapor adsorption on the CPG surface should not be applied to the explanation of anomalous behavior of aspirin decomposition in the CPG170 mixtures. The competitive adsorption of aspirin and water molecules on the CPG surface was considered a suitable concept to explain the RH dependence of aspirin decomposition in the CPG mixture.

Water Vapor Adsorption on CPG The adsorption of water vapor by CPGs occurred relatively fast except at 96% RH, where equilibration was attained after 1 month storage. Table I shows the amounts of adsorbed water of CPG170 at various RHs at 50 °C. As the concentration of aspirin was as low as 5%, the differences of adsorption patterns between the CPG–aspirin mixture and CPG alone was very small. The extremely great amount of adsorbed water at 96% RH was explained on the basis of condensation into the pores by water. According to the Kelvin equation, 94.8% RH caused water condensation into the pores of 170 Å diameter. From 0% RH through 79% RH, the amount of adsorbed water increased slightly with an increase of RH. In Fig. 8, decreasing RH caused an acceleration of aspirin decomposition, which disagreed with the results of El-Banna *et al.* and Leeson *et al.*[4,7] Another remarkable feature was that CPG170 contained 2.23% water even at RH 0%. The numbers of silanol groups on the silica surface were estimated to be $5/(10\,\text{Å})^2$.[16] If we assume that one silanol group is bound to one water molecule, 80% of the total silanol groups may be occupied by water molecules and 20% may be in a free state at RH 0%. If all silanol groups are bound to water molecules, the water content of CPG170 must be 25 mg/1 g CPG. Both the competitive adsorption of water and aspirin molecules on the CPG surface and the high coverage of the CPG surface by water molecules at a high RH appear to be corrected by the anomalous linear relationship between decomposition rate constants and RHs shown in Fig. 8. It was known that the silanol groups had high catalytic ability toward the decomposition of ascorbic acid[17]; hence, the obtained results could be explained in terms of the high reactivity of the free silanol groups.

TABLE I. Water Adsorption of CPG170 at Various RH at 50 °C

RH (%)	0	49	79	96
Amount of water adsorbed[a] (mg/1g CPG170)	22.3	29.7	44.1	1030

a) After storage for 1 month.

Stability of Aspirin in the Mixture with Aerosil Aerosil, fine particles of silica, is obtained by the hydrolysis of silicone tetrachloride at a high temperature, and the specific surface area is generally estimated to be more than $100\,\text{m}^2/\text{g}$.[18] Aerosil has no pore structure while it is in amorphous state, similarly to CPG. We used aerosil 200 to investigate the effects of the pore structure of CPG on aspirin decomposition. The concentration of aspirin was 1% in the mixture of aerosil 200. Figure 9 shows the decomposition profiles of aspirin after storage under various conditions. In both cases at 40 and 50 °C, faster decomposition rates were observed at RH 0% in a similar manner as the CPG mixtures. At high RH values, water molecules should completely cover predominantly silanol groups on the aerosil surface, which have a catalytic effect toward aspirin hydrolysis.[17] This seemed to be the reason for slow aspirin decomposition at RH 79%. From Fig. 9, the first-order rate constants of aspirin decomposition under RH 0% and 79% at 50 °C were estimated as $8.10 \times 10^{-3}\,\text{h}^{-1}$ and $2.92 \times 10^{-3}\,\text{h}^{-1}$ respectively, while those in the CPG170 mixtures were determined $1.37 \times 10^{-1}\,\text{h}^{-1}$ and $6.20 \times 10^{-2}\,\text{h}^{-2}$. Aerosil

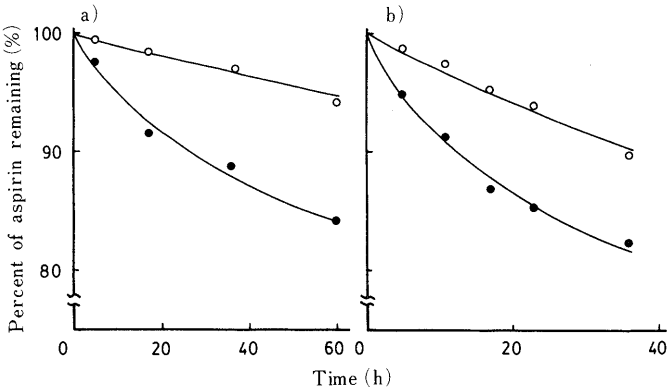

Fig. 9. Decomposition Kinetics of Aspirin in the Mixture of 1% Aspirin and 99% Aerosil 200 at 40 °C (a) and 50 °C (b)
●, RH 0%; ○, RH 79%

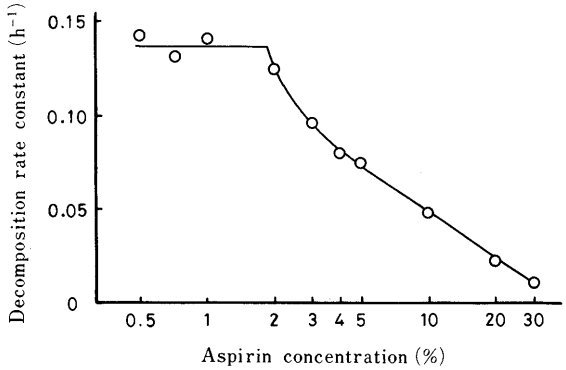

Fig. 10. Effect of Aspirin Concentration on the Aspirin Decomposition Rate Constants in the CPG170 Mixtures at 50 °C and RH 0%.

and CPG170 had a similar surface area and the same functional group on the surface. Also, in the two systems, aspirin was in an amorphous state. Therefore, the differences in decomposition rate constants were attributed to differences in particle morphology. The pore structure of CPG was anticipated to be a definite factor in reducing aspirin stability.

Effects of Aspirin Concentration on the Stability The aspirin concentration in the CPG170 mixture varied from 0.3 to 30%. The condition at 50 °C and RH 0% was used to study aspirin decomposition kinetics. Figure 10 shows the relationship between aspirin concentration in the CPG170 mixture and the decomposition first-order rate constants. In the mixtures in which the concentration was less than 2.0%, the rate constants were great and steady. In other cases, concentrations of more than 2.0%, or increasing concentrations of aspirin caused a decrease in the decomposition rate constant. The linearity of the plots of ln (% remaining of aspirin) *vs.* time also diminished with an increase in the concentration. The regression coefficient for first-order plots for a 30% aspirin mixture was calculated as low as 0.919. In the aspirin concentration range of 0.3—2.0%, both the independency of rate constant with aspirin concentration and good linearity of first-order plots were observed. The results suggest that the aspirin molecules were dispersed homogeneously in CPG170 in low aspirin concentration mixtures and that a sufficient amount of water was adsorbed to hydrolyze aspirin on the CPG170 surface. The decrease of the aspirin deomposition rate in the range of concentration greater than 2.0%, should be ascribed to the remaining crystalline portion of aspirin in the mixture as well as to the time-consuming process of change from crystalline to amorphous aspirin.

References and Notes

1) This paper is part VI of "Interaction of Medicinals and Porous Powder." The previous paper, Part V: E. Yonemochi, T. Oguchi, K. Yamamoto and Y. Nakai, *Chem. Pharm. Bull.*, **39**, 1023 (1991).
2) Present address: *Daiichi Pharmaceutical Co., Ltd., 16–13, Kitakasai 1-Chome, Edogawa-ku, Tokyo 134, Japan.*
3) S. R. Byrn, "Solid-State Chemistry of Drugs," Academic Press, New York, 1982, p. 230.
4) L. J. Leeson and A. M. Mattocks, *J. Am. Pharm. Assoc.*, **47**, 329 (1958).
5) W.-H. Yang and D. Brooke, *Int. J. Pharm.*, **11**, 271 (1982).
6) J. T. Carstensen, F. Attarchi and X.-P. Hou, *J. Pharm. Sci.*, **74**, 741 (1985).
7) H. M. El-Banna, N. A. Daabis and A. Abd El-Fattah, *J. Pharm. Sci.*, **67**, 1631 (1982).
8) A. Y. Gore and G. S. Banker, *J. Pharm. Sci.*, **68**, 197 (1979).
9) P. V. Mroso, A. L. W. Po and W. J. Irwin, *J. Pharm. Sci.*, **71**, 1096 (1982).
10) D. J. Ager, K. S. Alexander, A. S. Bhatti, J. S. Blackburn, D. Dollimore, T. S. Koogan, K. A. Mooseman, G. M. Muhvic, B. Sims and V. J. Webb, *J. Pharm. Sci.*, **75**, 97 (1986).
11) Y. Nakai, K. Yamamoto, K. Terada and J. Ichikawa, *Yakugaku Zasshi*, **105**, 296 (1985).
12) E. Yonemochi, T. Oguchi, K. Terada, K. Yamamoto and Y. Nakai, *Chem. Pharm. Bull.*, **37**, 3083 (1989).
13) L. Manojlovic and J. C. Speakman, *J. Chem. Soc. (A)*, 971 (1967).
14) L. J. Edwards, *Trans. Faraday Soc.*, **46**, 723 (1950).
15) *a)* T. Konno, K. Kinuno and K. Kataoka, *Chem. Pharm. Bull.*, **34**, 301 (1986); *b)* T. Konno and K. Kataoka, *ibid.*, **37**, 2481 (1989); *c)* T. Konno, *ibid.*, **38**, 2003 (1990).
16) V. Y. Davydov, A. V. Kiselev and L. T. Zhuravlev, *Trans. Faraday Soc.*, **60**, 2254 (1964).
17) W.-H. Wu, T.-F. Chin and J. L. Lach, *J. Pharm. Sci.*, **59**, 1122 (1970).
18) E. Wagner and H. Brunner, *Angew. Chem.*, **72**, 744 (1960).

Stability of Forskolin in Lipid Emulsions and Oil/Water Partition Coefficients

Keiko YAMAMURA,[a] Makoto NAKAO,[a] Kohji YANO,[a] Ken-ichi MIYAMOTO[b] and Toshihisa YOTSUYANAGI*,[c]

Hospital Pharmacy, Nagoya University Branch Hospital,[a] Higashi-ku, Nagoya 461, School of Pharmacy, Hokuriku University,[b] Ho-3 Kanagawa-machi, Kanazawa 920-11 and Faculty of Pharmaceutical Sciences, Nagoya City University,[c] Mizuho-ku, Nagoya 467, Japan. *Received October 8, 1990*

Forskolin (FK), a diterpenoid isolated from *Coleus Forskohlii*, underwent base-catalyzed hydrolysis, producing 7-deacetyl forskolin. The half-life at pH 7.0 and 25°C was 16 d. Because of its poor solubility in water and degradation, the drug was incorporated in lipid emulsions (soybean oil/water = 10.9/89.1 v/v, average diameter of the droplets, 204 nm). No degradation of the drug was found in the lipid emulsion up to 30 d. The distribution of FK in the lipid emulsions was investigated based on a three-phase model which assumes that the drug resides in the oil and water phases and at the oil/water interface. From the determination of bulk oil/water and lipid emulsion partition coefficients, the relative percentages of the drug in the oil droplets, in the aqueous phase and at the interface were 43.3, 4.9 and 51.3%, respctively. This distribution profile seems to be consistent with the improved stability of FK in the lipid emulsions where the drug residing in the oil phase and at the interface is well protected from hydrolysis. The FK lipid emulsions should be given more interest in access to preclinical and clinical tests because the drug was well stabilized in the formulation and the excipients used are acceptable to human subjects.

Keywords forskolin; stability; base-catalysis; hydrolysis; lipid emulsion; egg phosphatidylcholine; partition coefficient; phase distribution

Introduction

Forskolin (FK, 7-β-acetoxy-8,13-epoxy-1α,6β,9α-trihydroxylabd-14-en-11-one) is a diterpenoid isolated from *Coleus Forskohlii*.[1] The effects of the drug include positive iontropic and chronotopic responses in isolated guinea pig hearts[2] and hypotensive and vasodilactory actions due to its function as a smooth muscle relaxant.[3] These responses are considered to be due to its activation of adenylate cyclase resulting in a marked increase in levels of intracellular cyclic adenosine monophosphete (AMP) in most tissues and cells.[4,5] Recent studies of FK indicated that the drug enhances the effect of antitumor agents such as mitomycin C and vinblastine in connection with its activating function of adenylate cyclase and cyclic AMP production.[6,7]

Because of its poor solubility in water, FK has been administered after being solubilized by either organic solvents or surface active agents.[6,8] Furthermore, degradation of the drug may be possible at the ester linkage. Thus, such formulation difficulties have to be solved to avoid possible unacceptable effects.

Lipid emulsions attract attention as a promising drug delivery form especially for fat-soluble drugs.[9,10] By partitioning of a drug between the oil phase and the surrounding water, a great fraction of the drug incorporated may be accommodated in the oil phase. In this report we describe the distribution of FK in the lipid emulsion whose composition is equivalent to fat emulsions for clinical nutrition and stability testing of the drug.

Experimental

Materials Forskolin (FK) was purchased from Sigma Chem. Co. and used as received. 7-Deacetyl forskolin was a gift from Nihon Kayaku, Tokyo. Soybean oil and glycerol were obtained from Wako Pure Chem. Co., Osaka. Egg phosphatidylcholine (EPC, Coatsome® NC-10, Nichiyu Liposome Co., Tokyo) was used as an emulsifying agent. Seamless cellulose tubings (18/32, Union Carbide) were used for dialysis. Acetonitrile was of high performance liquid chromatography (HPLC) grade.

Stability Testing of FK in Aqueous Solutions and Lipid Emulsions Solutions (pH 6.0—8.0, phosphate, ionic strength = 0.1 adjusted with NaCl) containing FK (0.48 mM) were used after being filtered with a 0.2 μm filter (Millipore). The temperature was kept at 25 °C by using a thermostated glass cell. Degradation kinetics were followed by an HPLC assay of the remaining FK. An aliquot of the samples (0.4 ml) was dissolved in the HPLC mobile phase (1.6 ml), appropriately diluted with the solvent, if necessarry, and injected to a port (20 μl).

HPLC Assay of FK The chromatography was performed with a Shimadzu LC-6A HPLC apparatus equipped with a UV detector and a reversed-phase column (μ-Bondapak C_{18}, 10 μm, 30 cm × 3.9 mm i.d., Waters Assoc.). The mobile phase was a mixture of acetonitrile and water (6 : 4, v/v). The column eluate was monitored at 309 nm with a sensitivity of 0.005 aufs. All analyses were made at room temperature. The peak of FK did not interfere with the degradation product (7-deacetyl forskolin).

Preparation of FK Lipid Emulsions FK (20 mg) was dissolved in soybean oil (20 g, $d = 0.921$ at 25 °C) to which EPC (2.4 g) was gradually added and dispersed. After the clear solution was obtained, 5 g of glycerol was added. The total volume of the mixture was adjusted to 200 ml by adding water for injection (172.6 ml). The composition was equivalent to commercial products of fat emulsions. Emulsification was conducted using a microfluidizer (M-100N, Tsukishima Kikai, Tokyo). The condition was as follows: the operation pressure was 15000 psi, the maximum pass number 15 and the temperature at the projection orifice 5 °C. This operation gave an emulsion containing 100 μg of FK/ml. Emulsions of 50 and 25 μg of FK/ml were also prepared in the same manner.

Particle Size Determination of Lipid Emulsions Average sizes of FK emulsions and drug-free emulsions, which were prepared at the different pass numbers (5, 10 and 15), were determined with a particlesizer (BI-90, Nikkiso, Tokyo). Size changes of the preparations were followed up to 30 d.

Determination of Partition Coefficients The partition coefficient measurement was made at 5 °C to secure no degradation of FK. Four different systems were as follows: (1) Lipid emulsions: After 10 ml of lipid emulsions (FK, 100 μg/ml) placed in a cellulose tube was dialyzed against water (45 ml) for 24 h, the drug in the aqueous phase was assayed. It was checked in advance that the dialysis time was long enough to attain equilibrium. (2) A soybean oil (1 g)/water (55 ml) system containing FK (100 μg/ml of water), EPC (12% to oil) and glycerol (2.5% to water) at the same ratios as the lipid emulsion was moderately stirred with a magnetic stirrer for 24 h. After the coarsely emulsified content was centrifuged at 3000 rpm for 30 min to separate the layers, the aqueous phase was filtered through a 0.2 μm filter. (3) A soybean oil/water system in which only EPC was excluded from the system (2) was examined in the same manner as described above. (4) An octanol/water system: Eight milligrams of FK was dissolved in 10 ml of water–saturated octanol. Two ml of the solution filtered with a 0.2 μm filter was mixed with water (10 ml) and shaken for 24 h. After being centrifuged at 3000 rpm for 30 min, the aqueous sample was taken and assayed to determine the partition coefficient.

Results and Discussion

Stability of FK in Aqueous Solutions Figure 1 shows first-order plots of the degradation of FK in the pH 6.0—8.0 at 25 °C in addition to that in water at 5 and 25 °C. Glycerol

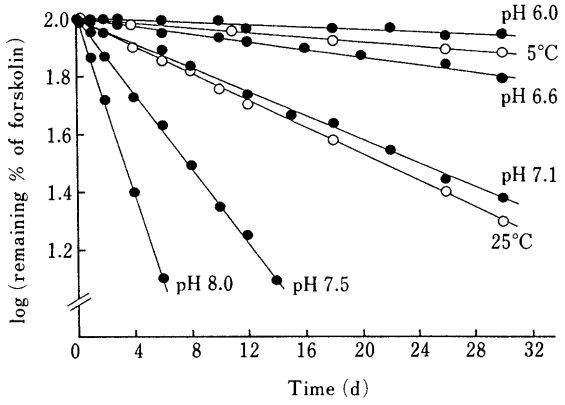

Fig. 1. First-Order Plots of Forskolin Degradation in Water and in Phosphate Buffer (pH 6.0—8.0)

○, water at 5 and 25 °C; ●, phosphate buffer (ionic strength = 0.1, adjusted with NaCl) at 25 °C.

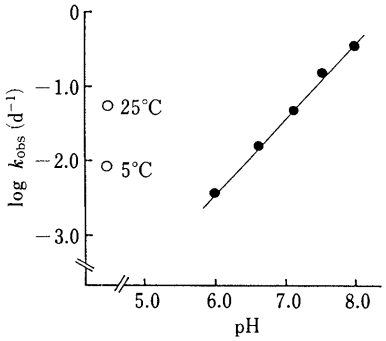

Fig. 2. pH Profiles of Forskolin Degradation in pH 6.0—8.0 Buffers at 25 °C

○, water; ●, phosphate buffer.

TABLE I. Effects of the Pass Time of a Microfluidizer on the Particle Size of Drug Free-Lipid Emulsions and Forskolin–Lipid Emulsions

Drug	Mean diameter (nm) ± S.D. (n = 5)		
	Number of pass time		
	5	10	15
Free	256 ± 12	226 ± 6	202 ± 4
Forskolin (100 μg/ml)	248 ± 15	237 ± 15	204 ± 5

is used to keep the isotonicity of lipid emulsions. Little effect of glycerol (3%, w/v) on the degradation rate was found in water at 25 °C. The degradation product was identified as 7-deacetyl forskolin alone in the present conditions. A thin-layer chromatogram test also revealed one spot of the 7-deacetyl form (data not shown). Although the hydrolytic product also has a hypotensive activity, it is reported to be much lower than that of the parent compound.[11]

Figure 2 shows pH-profiles for the pseudo-first-order rate constant, k_{obs}. It was linear with a slope of about 1, which means that the contribution of specific base-catalysis was predominant in this pH region. The degradation rate of the drug in water at 5 °C was comparable to that at pH 6.4 and the half-life was about 78 d.

Particle Size of Lipid Emulsions Table I shows the average particle sizes of FK-emulsions and drug-free emulsions prepared at the different pass numbers of the microfluidizer setting. As expected, the average particle size decreased as the pass number increased. At the 15 time pass the size was reduced to 0.2 μm, which was comparable to that of commercial products of fat emulsions. At none of the pass times were there any differences between either of the emulsions, indicating no effect of the drug on the emulsification of the oil.

TABLE II. Particle Size Changes of Various Forskolin–Lipid Emulsions[a]

Concentration of forskolin (μg/ml)	Mean diameter (nm) ± S.D. (n = 5)		
	10 d[b]	20 d	30 d
25	210 ± 6	208 ± 7	204 ± 7
50	206 ± 8	211 ± 6	205 ± 4
100	204 ± 5	210 ± 5	203 ± 6

a) The number of pass time was always 15. *b*) Stored at room temperature.

TABLE III. Partition Coefficient of Forskolin and Percent Amount of Its Partitioning Based on a Three Phase Model

Oil/water[a] system	Partition[b] coefficient	Amount distributed (%)[c]		
		Oil	Interface	Water
Lipid emulsions	158	43.3	51.8	4.9
Soybean oil/water with lecithin	90	73.3	18.4	8.3
Soybean oil/water	72	89.8	—	10.2
Octanol/water	1305	99.94	—	0.06

a) Each oil/water system contains glycerol (2.5%, w/v). *b*) Partition coefficients were calculated from the experimentally determined concentrations of the drug in the aqueous phase. *c*) Percent amounts of the drug partitioned are normalized on the basis of the composition of the lipid emulsion, *i.e.* the volume ratio of the oil phase to the aqueous bulk phase, 1.09/8.91.

Table II shows the average sizes of the emulsions in which different amounts of the drug (25—100 μg/ml) were incorporated and the stability of particle size with time. No alteration was observed in the particle size or in visual appearance up to at least 30 d.

Partition Coefficients and Phase Distribution of FK Table III shows the partition coefficients of the drug in the various soybean oil/water systems. It is obvious from these results that EPC added as an emulsifying agent is involved in the partitioning. Accordingly, a three-phase model which assumes that the drug resides to some extent at the lipid-rich interface as well as the oil and water phases may be more reasonable for understanding the distribution of FK in the emulsions, as applied to the prostaglandin partitioning.[12]

The mass balance equations may be given as follows:

$$M_t = V_o C_o + M_i + V_w C_w \quad (1)$$

$$K_{o/w} = C_o / C_w \quad (2)$$

Therefore, we have

$$M_i = M_t - C_w(V_w + K_{o/w} V_o) \quad (3)$$

where M is the amount of a drug, C is the concentration and V is the volume. The subscripts, o, i and w, indicate the oil phase, the oil/water interface and the water phase, respectively. $K_{o/w}$ is the partition coefficient of the drug under the condition of no lipid addition and no adsorption at the interface.

The partition coefficients experimentally obtained are therefore represented by $(C_o + M_i/V_o)/C_w$. The M_i would be determined using Eq. 3, if the M_t, C_w, V_w, V_o and $K_{o/w}$ were known. The partition coefficient, $K_{o/w}$, of FK was separately determined to be 72, where no interfacial absorption of the drug was assumed. The fractions of the drug distributed in each phase and at the interface are shown in Table III. These values are normalized on the basis of the composition of the lipid emulsion, *i.e.* the volume ratio of the oil phase to the bulk aqueous phase is 1.09/8.91.

In the lipid emulsion, about 50% of FK was adsorbed at the lipid-rich interface. 10 ml of the emulsion assumes the following physical dimensions: when the diameter of oil droplets is approximated to be 204 nm;

surface area of each droplet $= 1.3 \times 10^{-9}$ (cm^2)

volume of each droplet $= 4.4 \times 10^{-15}$ (cm^3)

number of oil droplet $= 2.4 \times 10^{14}$

total surface area $= 3.3 \times 10^5$ (cm^2)

Natural phospholipids spread at the air-water interface behave as monolayers with a cross sectional area per molecule of 50—60 $Å^2$ under the "collapse pressure," and as the pressure is released, the area reaches as wide as 100 $Å^2$.[13] Assuming that all the EPC (0.12 g/10 ml, average molecular weight assumed 780) is adsorbed in a similar manner at the interface between the oil and water phases in the emulsion, the total cross sectional area is calculated to be 4.6×10^5 cm^2 where the cross sectional area per molecule is assumed to be 50 $Å^2$ and the total cross sectional area is 9.2×10^5 cm^2 for the other extreme of 100 $Å^2$. The total surface area of droplets was fairly comparable with these values, suggesting that the lipid spreads in a monolayer manner at the interface.

The coase soybean oil/water emulsion containing EPC (system (2)) gave a smaller partition coefficient than that of the lipid emulsion. However, despite a presumably much reduced area of the oil/water interface to one tenth of thousandths of that of the lipid emulsion, the amount of the drug residing at the interface was not always greatly decreased: from 51.8% to only 18.4%. Although the EPC distribution in the oil phase and at the interface is unknown, and furthermore, the lipid may not be arranged in a monolayer fashion at the interface, it may be considered that the drug has a great tendency to interact with EPC regardless of whether it is oriented at the oil/water interface or residing in the oil phase. As characterized by the relatively large partition coefficient of 72 in the plain soybean oil/water system, the drug intrinsically has a lipophilic nature, but, has a much greater affinity to the oil/water interface with the aid of EPC.

TABLE IV. Stability of Forskolin in Lipid Emulsions at 5 °C[a]

Concentration of forskolin (μg/ml)	Remaining (%) ± S.D. ($n=5$)		
	10 d	20 d	30 d
25	101.1 ± 2.3	99.5 ± 1.8	100.5 ± 1.5
50	98.9 ± 1.5	102.3 ± 1.6	99.6 ± 2.0
100	103.0 ± 1.9	99.8 ± 1.1	102.3 ± 2.1

a) Lipid emulsions were always prepared at the pass time number of 15.

The octanol/water partition coefficient of FK was much larger than that of the plain soybean oil/water system. This difference may be primarily due to hydrogen bonding rather than to the hydrophobic squeezing effect.

Stability of FK in Lipid Emulsions Table IV indicates the stability of FK in the emulsion at 5 °C. No degradation of the drug was found up to at least 30 d, while about 23% degradation was seen in water after the same period (see Fig. 1). This is due to the fact that in the emulsion only 4.9% of the drug exists in the aqueous phase. The result also indicates that the drug residing in the oil phase and at the interface little undergoes hydrolysis.

The present data will provide useful information in the preparation of FK lipid emulsions. The FK emulsions will give easier access to preclinical and clinical tests because the drug was well stabilized in the formulation and the excipients used have been widely acceptable to human subjects.

References

1) J. B. Seamon and J. W. Daly, *J. Cyclic Nucleotide Res.*, **7**, 201 (1981).
2) E. Linder, A. N. Dohadwalla and B. K. Bhattacharya, *Arzneim.-Forsch.*, **28**, 284 (1978).
3) M. P. Dubey, R. C. Srimal, S. Nityanano and B. N. Dhawan, *J. Ethnopharmacology*, **3**, 1 (1981).
4) K. B. Seamon, W. Padgett and J. W. Daly, *Proc. Natl. Acad. Sci. U.S.A.*, **78**, 3363 (1981).
5) H. Metzger and E. Linder, *ICRS Med. Sci., Biochem.*, **9**, 99 (1981).
6) K. Miyamoto, T. Matsunaga, R. Koshiura, K. Takagi, T. Satake and T. Hasegawa, *J. Pharmacobio-Dyn.*, **10**, 346 (1987).
7) K. Takagi, T. Satake, T. Hasegawa, K. Miyamoto, S. Wakusawa, T. Matsunaga and R. Koshiura, *Jpn. J. Pharmacol.*, **45**, 69 (1987).
8) M. F. Saettone, S. Burgalassi and B. Giannaccini, *J. Ocular Pharmacol.*, **5**, 111 (1989).
9) Y. Mizushima, *Drugs Exp. Clin. Res.*, **9**, 595 (1985).
10) S. S. Davis, C. Washington, P. West, L. Illum, G. Liversidge, L. Sterson and R. Kirsh, *Ann. N.Y. Acad. Sci.*, **507**, 75 (1987).
11) S. V. Bhat, A. N. Dohadwalla, B. S. Bajwa, N. K. Dadkar, H. Dornauer and N. J. de Souza, *J. Med. Chem.*, **26**, 486 (1983).
12) D. L. Teagarden, B. D. Anderson and W. J. Petre, *Pharm. Res.*, **5** 482 (1988).
13) D. Papahadjopoulos, "Form and Function of Phospholipids," ed. by G. B. Ansell, J. N. Hawthorne and R. M. C. Dawson, Elsevier Scientific Publication Co., Amsterdam, 1973, pp. 145—146.

Synthesis of Fluorinated Retinal: A C_6–C_7 *s-trans* Fixed Retinal Containing a Trifluoromethyl Group at the Terminal Position of the Conjugated System

Yuji HANZAWA, Makoto SUZUKI, Yoshiro KOBAYASHI and Takeo TAGUCHI*

Tokyo College of Pharmacy, 1432–1 Horinouchi, Hachioji, Tokyo 192–03, Japan. *Received October 2, 1990*

For the study of retinal-binding proteins by using fluorine-modified retinals, the all-*trans* bicyclic trifluororetinal (1), whose C_6–C_7 bond is fixed in the *s-trans* form by an ethano bridge, was synthesized. Introduction of a trifluoromethyl group was carried out in 70% yield by photochemical trifluoromethylation of the dienol ether compound (2) with trifluoromethyl iodide. From a comparison of the absorption maximum of 1 with that of the bicyclic retinal (12), it is clear that the electron-withdrawing trifluoromethyl group induces a notable hypsochromic shift (18 nm) of 1.

Keywords trifluoromethyl iodide; bicyclic trifluororetinal; photochemical trifluoromethylation; *s-trans* conformation; hypsochromic shift

The photo-activation process and the structure of retinal-binding proteins—bacteriorhodopsin (bR) and rhodopsin (Rh)—have been studied extensively by many research groups using retinal analogs.[1] Recently, we have reported the synthesis of trifluoro analogs of retinal and an unusual effect of trifluororetinal-binding bR.[2] For further study of the structure and behavior of retinal-binding proteins (bR, Rh), we required a new fluorinated retinal (**1**), which has a fixed *s-trans* C_6–C_7[3] bond. The importance of the *s-trans* C_6–C_7 conformation of the retinal chromophore in native bR has been pointed out by Lugtenburg *et al.* and demonstrated spectroscopically.[4] The retinal analog **1** should be a good analog for studies on the binding site of bR and the unusual effect of the trifluororetinal-binding bR which we have reported.[2] This note describes the synthesis of **1** and the effect of the electronegative trifluoromethyl group in a conjugated system.

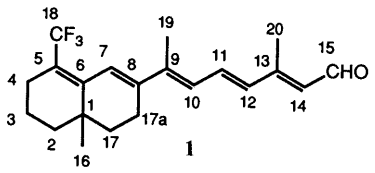

Chart 1

Irradiation of a pyridine solution of **2** and trifluoromethyl iodide in a quartz vessel with a 100 W high-pressure mercury lamp gave the desired trifluoromethylated compound (**3**) in 70% yield along with a trace amount of an iodine-containing compound.[5] Acid treatment (CF_3COOH, yield 60%) of **3** and the subsequent reaction of the enone (**4**) with lithium trimethylsilylacetylide gave a mixture of diastereomers, which was desilylated (n-Bu_4NF, yield 61%) directly to give a diastereomeric mixture of the acetylenic alcohols (**5**). Dehydration (Nafion-H/CCl_4) of the alcohol function of **5** gave a mixture of isomeric products (**6a** and **6b**, yield 28%, ratio 3.8/1) and the ketone (**7**) (10%).[6] The hydration of the triple bond of **6a** (Hg_2O/H_2SO_4) was carried out to give **7** in 51% yield. Horner–Emmons reaction of **7** with diethyl cyanomethylphosphonate afforded a mixture of stereoisomeric cyano compounds (**8**) (53%), which was directly treated with diisobutylaluminum hydride (DIBAL-H) to give the aldehyde as a mixture of stereoisomers (**9a** and **9b**, yield 78%, ratio 4.6/1). After separation of the 9*E*-aldehyde

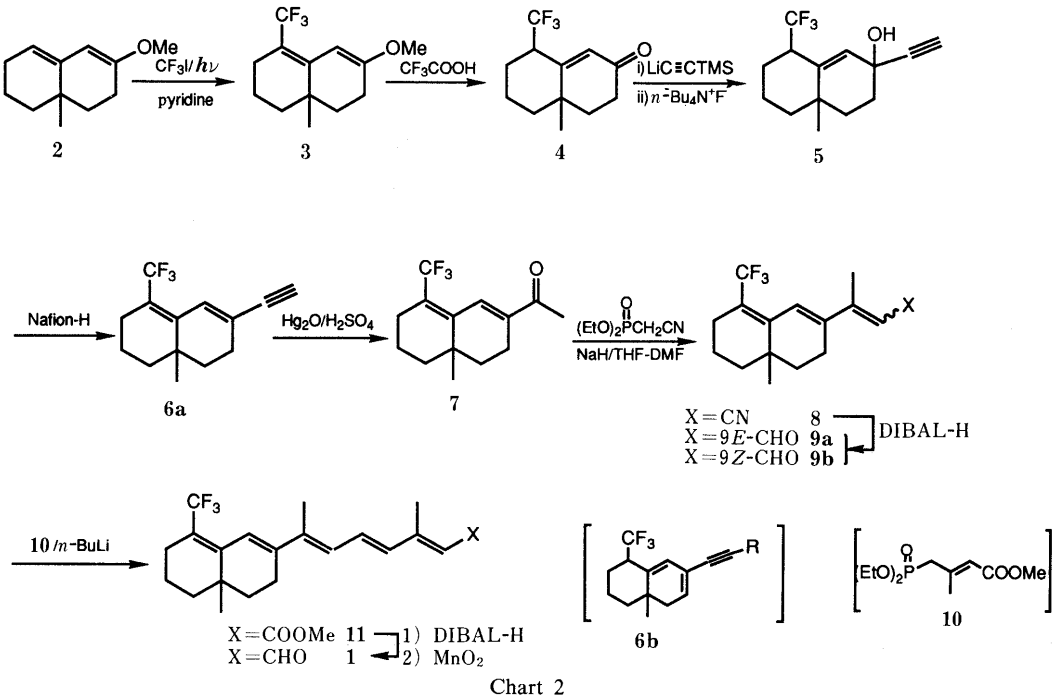

Chart 2

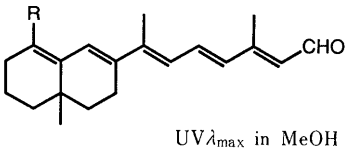

	UVλ_{max} in MeOH
1 : R=CF_3	382 nm
12 : R=CH_3	400 nm[4]

Chart 3

(**9a**) from the 9*Z*-isomer (**9b**),[3] the reaction of **9a** with methyl 4-diethylphosphono-3-methyl-2-butenoate (**10**)[7] gave the all-*trans* ester (**11**) in 98% yield. All-*trans* retinal (**1**) was obtained in 66% yield by reduction (DIBAL-H) of **11** followed by oxidation (MnO_2).

The conformation of **1** is considered to be almost the same as that of the bicyclic retinal (**12**) because the trifluoromethyl group is too far away to affect sterically the rotable C_8—C_{15} side chain[3] of **1**. Therefore, the molecular flattening of the conjugated system should be very similar in the two bicyclic analogs (**1** and **12**). This assumption is also supported by space-filling molecular models and by ^{13}C-nuclear magnetic resonance (^{13}C-NMR) spectral comparison of **1** and **12**. In the ^{13}C-NMR spectrum of **1** (see Experimental), chemical shifts of the side chain carbons (C_8—C_{15}, C_{19} and C_{20})[3] are essentially the same as those of **12** reported by Lugtenburg *et al.*[4] Evaluation of the electronic effect of the trifluoromethyl group in the conjugated system of retinal was done by comparing the absorption maxima of **1** and **12** and a clear hypsochromic shift of **1** was demonstrated. A possible explanation of the notable hypsochromic shift (18 nm) in **1** compared to **12** is the destabilization of the excited state of **1** caused by the electron-withdrawing nature of the trifluoromethyl group. In summary, we could estimate the electronic effect of the trifluoromethyl group at the terminal position of the conjugated system of retinal by preparing **1**. By knowing the electronic effect of trifluoromethyl group, it is significant to study bR using trifluoro analog of retinal. The binding study with the apoprotein will be reported in a separate paper.

Experimental

^{1}H-Nuclear magnetic resonance (^{1}H-NMR) spectra were recorded on a Bruker AM 400 or a Varian EM-390L spectrometer in $CDCl_3$. ^{19}F-Nuclear magnetic resonance (^{19}F-NMR) were recorded at 56.4 MHz on a Varian EM-360L spectrometer in $CDCl_3$, and chemical shifts are reported in ppm relative to benzotrifluoride as an external standard (higher field was assigned as negative). ^{13}C-NMR were recorded at 100.6 MHz on a Bruker AM 400 spectrometer. Infrared (IR) spectra were recorded on a Jasco A302 infrared spectrophotometer. Absorption spectra (ultraviolet (UV)) were recorded on a Hitachi MPF-4 spectrophotometer. The electron impact (EI)- and chemical ionization (CI)-mass spectra (MS) were recorded on a Hitachi M-80. In CI-MS, isobutane was used as the reagent gas. Anhydrous tetrahydrofuran (THF) and ether were distilled from sodium-benzophenone under an argon atmosphere just before use. Anhydrous hexane and *N*,*N*-dimethylformamide (DMF) were distilled from CaH_2 under an argon atmosphere. Medium pressure column chromatography (MPLC) was performed with a silica gel prepacked column (Kusano, HS-101-1), with detection at 320 or 360 nm.

1,2,6,7,8,8a-Hexahydro-3-methoxy-8a-methyl-5-trifluoromethylnaphthalene (3) CF_3I (10 ml) was added to a pyridine solution (10 ml) of 2-methoxy-3,4,4a,5,6,7-hexahydro-4a-methylnaphthalene (**2**) (6.1 g, 34.2 mmol) in a 300 ml quartz tube by using vacuum line and the vessel was sealed with a grease-free stopcock. The resulting solution was irradiated with a 100 W high pressure Hg lamp for 33 h at room temperature. The cooled reaction mixture was diluted with ether and washed with saturated $NaHSO_3$. The separated organic phase was washed with H_2O, 1 N HCl, saturated $NaHCO_3$ and brine successively before drying ($MgSO_4$). The filtrate was concentrated to give a crude oil. Purification by column chromatography on silica gel (hexane–EtOAc=20 : 1) gave **3** (6.6 g, 78%). ^{1}H-NMR δ: 1.06 (3H, s), 1.2—1.8 (6H, m), 2.1—2.5 (4H, m), 3.64 (3H, s), 5.63 (1H, br s). ^{19}F-NMR ppm: 5.83 (s). CI-MS *m/z*: 247 (M+1).

4,4a,5,6,7,8-Hexahydro-4a-methyl-8-trifluoromethyl-2(3*H*)-naphthalenone (4) A solution of **3** (6.5 g, 27 mmol) was treated with 80% CF_3COOH (30 ml) at 0 °C and the mixture was stirred at room temperature for 5 h. The mixture was poured into ice-H_2O and extracted with ether. The organic phase was washed with H_2O, saturated $NaHCO_3$ and brine before being dried ($MgSO_4$). The filtrate was concentrated to give a crude oil, which was purified by flash column chromatography on silica gel (hexane–EtOAc=4 : 1) and subsequent distillation (bp 112 °C/2 mmHg) to give pure **4** (3.75 g, 61%). IR (neat): 1680 cm^{-1}. ^{1}H-NMR δ: 1.25 (3H, s), 1.45—1.95 (6H, m), 2.1—2.5 (4H, m), 6.0 (1H, s). ^{19}F-NMR ppm: −3.83 (d, *J*=9 Hz). EI-MS *m/z*: 232. High-resolution MS *m/z*: Calcd for $C_{12}H_{15}F_3O$: 232.1074. Found: 232.1089.

4,4a,5,6,7,8-Hexahydro-2-ethynyl-4a-methyl-8-trifluoromethyl-2(3*H*)-naphthalenol (5) A hexane solution of *n*-BuLi (16 mmol) was added to a solution of trimethylsilylacetylene (1.6 g, 16 mmol) in THF (15 ml) at −78 °C and the mixture was stirred at room temperature for 1 h. The ketone **4** (3.5 g, 15 mmol) in THF (5 ml) was added to the above solution at −78 °C and the mixture was stirred for 3 h at 0 °C. After addition of saturated NH_4Cl, the mixture was extracted with ether. The combined ether layer was washed with saturated $NaHCO_3$ and brine before being dried ($MgSO_4$). Concentration of the filtrate gave a crude product, which was directly treated with a 1 M solution of *n*-Bu_4NF (12 ml) and the mixture was stirred at room temperature for 1 h. The reaction mixture was then diluted with ether and the solution was washed with H_2O and brine before being dried ($MgSO_4$). The filtrate was concentrated and the residue was purified by flash column chromatography on silica gel (hexane–EtOAc=10 : 1) to give **5** (2.62 g, 61%). IR (neat): 3300 cm^{-1}. ^{1}H-NMR δ: 1.1 (3H, s), 1.5—2.1 (10H, m), 2.5 (1H, s), 5.6 (1H, br s). ^{19}F-NMR ppm: −3.83 (d, *J*=9 Hz). CI-MS *m/z*: 259 (M+1).

1,2,6,7,8,8a-Hexahydro-3-ethynyl-8a-methyl-5-trifluoromethylnaphthalene (6a) 1,5,6,7,8,8a-Hexahydro-3-ethynyl-8a-methyl-5-trifluoromethylnaphthalene (6b) and 1,2,6,7,8,8a-Hexahydro-3-acetyl-8a-methyl-5-trifluoromethylnaphthalene (7) Nafion-H (810 mg) was added to a solution of **5** (2.6 g, 10 mmol) in CCl_4 (5 ml), and the mixture was stirred at room temperature for 17 h. The filtrate was concentrated to give a crude residue, which was purified by column chromatography on silica gel (hexane→hexane–EtOAc=10 : 1). Less polar oil **6a** (370 mg, 15%). IR (neat): 3310 cm^{-1}. ^{1}H-NMR δ: 1.10 (3H, s), 1.4—1.8 (6H, m), 2.25 (4H, br s), 3.0 (1H, s), 6.85 (1H, br s). ^{19}F-NMR ppm: 6.00 (s). CI-MS *m/z*: 241 (M+1). More polar oil **6b** (100 mg, 10%). IR (neat): 3310 cm^{-1}. ^{1}H-NMR δ: 1.1 (3H, s), 1.3—1.7 (6H, m), 2.15 (2H, d, *J*=6 Hz), 2.85 (1H, s), 5.95 (1H, br s), 6.20 (1H, d, *J*=6 Hz). ^{19}F-NMR ppm: −3.16 (d, *J*=9 Hz). The ketone **7** was also isolated as the most polar oil (240 mg, 10%).

Hydration of 6a A hexane solution (2 ml) of **6a** (270 mg, 1.1 mmol) was added to a vigorously stirred solution of Hg_2O (yellow) (30 mg, 0.14 mmol) in H_2O–H_2SO_4 (20/1, 15 ml) and the resulting mixture was stirred at 40 °C for 4 h. The mixture was then extracted with ether and the organic phase was washed with H_2O, saturated $NaHCO_3$ and brine before being dried ($MgSO_4$). Concentration of the filtrate and the purification of the residue by silica gel TLC plate (hexane–EtOAc=20 : 1) gave **7** (150 mg, 51%). IR (CCl_4): 1670 cm^{-1}. ^{1}H-NMR δ: 1.0 (3H, s), 1.2—1.9 (10H, m), 2.3 (3H, s), 7.45 (1H, s). ^{19}F-NMR ppm: 6.0 (s). CI-MS *m/z*: 259 (M+1).

(2*E*)- and (2*Z*)-3-(1,2,6,7,8,8a-Hexahydro-8a-methyl-5-trifluoromethylnaphthalene-3-yl)-2-butenal (9a and 9b) Diethyl cyanomethylphosphonate (102 mg, 0.58 mmol) was added to a suspension of 60% NaH in mineral oil (23 mg, 0.58 mmol) in THF–DMF (7/1, 2.4 ml) at 0 °C. The mixture was stirred for 10 min at the same temperature. To the resulting clear solution was added a solution of **7** (150 mg, 0.58 mmol) in THF (1 ml) at 0 °C and the whole was stirred at room temperature for 1 h. After being quenched with 1 N HCl, the mixture was extracted with ether. The combined organic layer was washed with H_2O, saturated $NaHCO_3$ and brine before being dried ($MgSO_4$). The filtrate was concentrated and the residue was purified by column chromatography on silica gel (hexane–EtOAc=10 : 1) to give a stereoisomeric mixture of **8** (87 mg, 53%). A stereoisomeric mixture of **8** was employed in the next step without further separation. A solution of **8** (40 mg, 0.142 mmol) in hexane (1 ml) was treated with a hexane solution of DIBAL-H (0.21 mmol) and the mixture was stirred at 0 °C for 0.5 h. A mixture of silica gel (260 mg), H_2O (50 μl) and ether–hexane (1/1, 0.6 ml) was added to the reaction mixture. After being

stirred for 30 min at 0 °C, the mixture was filtered through Celite–$MgSO_4$. Concentration of the filtrate and the purification (silica gel TLC plate, hexane–EtOAc = 10 : 1) of the residue gave a mixture of two stereoisomers (**9a** and **9b**, ratio 4.6/1). Less polar oil (**9b**) (6 mg, 14%). ^{1}H-NMR δ: 1.1 (3H, s), 1.2—1.85 (10H, m), 5.9 (1H, dd, J = 1.5, 7.5 Hz), 6.45 (1H, br s), 9.65 (1H, d, J = 7.5 Hz). ^{19}F-NMR ppm: 6.0 (s). EI-MS m/z: 284. High-resolution MS m/z: Calcd for $C_{16}H_{19}F_3O$: 284.1387. Found: 284.1397. More polar oil (**9a**) (26 mg, 64%). ^{1}H-NMR δ: 1.03 (3H, s), 1.2—1.9 (10H, m), 2.3 (3H, s), 6.15 (1H, d, J = 7.5 Hz), 7.0 (1H, br s), 10.2 (1H, d, J = 7.5 Hz). ^{19}F-NMR ppm: 6.0. EI-MS m/z: 284. High-resolution MS m/z: Calcd for $C_{16}H_{19}F_3O$: 284.1387. Found: 284.1412.

Methyl (2*E*,4*E*,6*E*)-3,7-Dimethyl-7-(1,2,6,7,8,8a-hexahydro-8a-methyl-5-trifluoromethylnaphthalene-3-yl)-2,4,6-heptatrienoate (11) A solution of methyl 4-diethylphosphono-3-methyl-2-butenoate (**10**)[7] (45 mg, 0.18 mmol) in THF (0.5 ml) was treated with *n*-BuLi in hexane (0.12 mmol) at −78 °C and the solution was stirred for 10 min at the same temperature. A solution of **9a** (26 mg, 0.09 mmol) in THF (0.5 ml) was added to the above solution and the mixture was stirred at room temperature for 1 h. After addition of saturated NH_4Cl, the mixture was extracted with ether. The organic layer was washed with H_2O, saturated $NaHCO_3$ and brine before being dried ($MgSO_4$). The filtrate was concentrated and the residue was purified by MPLC (hexane–EtOAc = 10 : 1) to give **11** (34 mg, 98%). ^{1}H-NMR[3] δ: 1.03 (3H, s, 1-Me), 2.07 (3H, s, 9-Me), 2.34 (3H, s, 13-Me), 1.2—2.4 (10H, m), 3.71 (3H, s, COOMe), 5.8 (s, 1H, 14-H), 6.36 (1H, d, J = 15 Hz, 12-H), 6.44 (1H, d, J = 11 Hz, 10-H), 6.76 (1H, br s, 7-H), 7.03 (1H, dd, J = 11, 15 Hz, 11-H). EI-MS m/z: 380 (M^+). High-resolution MS m/z: Calcd for $C_{22}H_{27}F_3O_2$: 380.1961. Found: 380.1947.

(2*E*,4*E*,6*E*)-3,7-Dimethyl-7-(1,2,6,7,8,8a-hexahydro-8a-methyl-5-trifluoromethylnaphthalene-3-yl)-2,4,6-heptatrienal (1) A solution of DIBAL-H in hexane (0.28 mmol) was added to a solution of **10** (27 mg, 0.07 mmol) in hexane–ether (1/2, 1 ml) at −78 °C, and the mixture was stirred for 10 min at the same temperature. A mixture of silica gel (300 mg), H_2O (50 μl) and hexane–ether (1/1, 0.2 ml) was added to the reaction mixture at −78 °C and the whole was stirred at room temperature for 1 h. The mixture was then filtered through Celite–$MgSO_4$ and the filtrate was concentrated to dryness to give a residue. The residue was dissolved in ether (5 ml) and stirred with active MnO_2 (170 mg, 1.9 mmol) for 5 min at room temperature. Filtration of the mixture through Celite and concentration of the filtrate gave a crude oil, which was purified by MPLC (hexane–EtOAc = 15 : 1) to give **1** (15 mg, 66%). UV λ_{max}^{MeOH} nm (log ε): 382 (4.62). ^{1}H-NMR[3] δ: 1.03 (3H, s, 1-Me), 2.07 (3H, s, 9-Me), 2.34 (3H, s, 13-Me), 1.2—2.5 (10H, m), 5.99 (1H, d, J = 8 Hz, 14-H), 6.44 (1H, d, J = 15 Hz, 12-H), 6.48 (1H, d, J = 11 Hz, 10-H), 6.8 (1H, br s, 7-H), 7.16 (1H, dd, J = 11, 15 Hz, 11-H), 10.1 (1H, d, J = 8 Hz, 15-H). ^{13}C-NMR ppm: 13.18, 14.32, 17.52, 22.93, 23.27, 25.45, 32.65, 36.59, 36.79, 122.12, 122.45, 126.66, 127.60 (J_{C-F} = 188 Hz), 129.50, 132.60, 136.06, 140.31, 141.53, 144.58, 154.44, 191.09. ^{19}F-NMR ppm: 4.99 (s). EI-MS m/z: 350. High-resolution MS m/z: Calcd for $C_{21}H_{25}F_3O$: 350.1856. Found: 350.1841.

References and Notes

1) R. F. Childs, G. S. Shaw and C. J. L. Lock, *J. Am. Chem. Soc.*, **111**, 5424 (1989) and references cited therein.
2) V. T. Rao, F. Derguini, K. Nakanishi, T. Taguchi, A. Hosoda, Y. Hanzawa, Y. Kobayashi, C. Pande and R. H. Callender, *J. Am. Chem. Soc.*, **108**, 6077 (1986); D. Mead, A. E. Asato, M. Denny, R. S. H. Liu, Y. Hanzawa, T. Taguchi, A. Yamada, N. Kobayashi, A. Hosoda and Y. Kobayashi, *Tetrahedron Lett.*, **28**, 259 (1987) and references cited therein.
3) For convenience, the numbering system for retinoids has been used. See Chart 1.
4) R. Steen, P. L. Biesheuvel, R. A. Mathies and J. Lugtenburg, *J. Am. Chem. Soc.*, **108**, 6410 (1986).
5) W. O. Godfredsen and S. Vangedal, *Acta Chem. Scand.*, **15**, 1786 (1961).
6) G. A. Olah and A. P. Fung, *Synthesis*, **1981**, 473.
7) R. N. Gedye, K. C. Westaway, P. Arora, R. Bisson and A. H. Khalil, *Can. J. Chem.*, **55**, 1218 (1976).

Synthesis of Fluorine and Iodine Analogues of Clorgyline and Selective Inhibition of Monoamine Oxidase A

Yoshiro OHMOMO,*[,a] Masahiko HIRATA,[a] Katsuhiko MURAKAMI,[a] Yasuhiro MAGATA,[b] Chiaki TANAKA,[a] and Akira YOKOYAMA[c]

Osaka University of Pharmaceutical Sciences,[a] 2–10–65 Kawai, Matsubara, Osaka 580, Japan and Kyoto University Hospital[b] and Faculty of Pharmaceutical Sciences,[c] Kyoto University, Sakyo-ku, Kyoto 606, Japan. *Received October 3, 1990*

A series of fluorine and iodine analogues of clorgyline was synthesized and evaluated for inhibitory potency and selectivity toward monoamine oxidase A (MAO-A). Among them, *N*-[3-(2,4-dichloro-6-iodophenoxy)propyl]-*N*-methyl-2-propynylamine (3d), *N*-[3-(4-chloro-2-fluorophenoxy)propyl]-*N*-methyl-2-propynylamine (3f) and *N*-[3-(2-chloro-4-fluorophenoxy)propyl]-*N*-methyl-2-propynylamine (3g) were found to have high inhibitory potency and selectivity toward MAO-A comparable to those of clorgyline itself. Thus, they were considered for advanced development as radiofluorinated and radioiodinated ligands that may be useful for functional MAO-A studies in the living brain with positron emission tomography and single photon emission computer tomography.

Keywords monoamine oxidase; specific inhibitor; clorgyline; fluorine analogue; iodine analogue

Monoamine oxidase (MAO) [E.C.1.4.3.4] catalyzes the oxidative deamination of endogenous neurotransmitter amines as well as exogenous amines. It has been divided into two subtypes, MAO-A and MAO-B, on the basis of substrate and inhibitor selectivity.[1] Both forms appear to be important for neurotransmitter regulation and fluctuations in functional MAO activity may be associated with human diseases such as Parkinson's disease, depression and certain psychiatric disorders.[2]

The development of positron emission tomography (PET) and single photon emission computer tomography (SPECT) has made possible the studies of metabolism and physiological processes in the living human body utilizing organic molecules labeled with positron emitter or single photon emitter. For the direct and non-invasive mapping and functional studies of the MAO activity in the living brain, the carbon-11 labeled suicide inhibitors, pargyline, clorgyline and *l*-deprenyl, have been investigated as positron ligands for PET.[3] Clorgyline and *l*-deprenyl inhibit irreversibly and selectively MAO-A and MAO-B, respectively, by binding covalently to the enzyme itself.[4]

These ^{11}C labeled inhibitors appear to be suitable as the ligands of first approach for PET studies because of their relatively easy preparation. However, the short 20 min half-life time of ^{11}C, among the positron emitting radionuclides, has limited the ability to obtain an understanding of relatively slow ligand kinetics. Fluorine-18 with its half-life time of 110 min may be favored as a longer-lived alternative to the ^{11}C for studies of the kinetic analysis with PET. For SPECT imaging and investigation of the MAO activity in the living human brain, iodine-123 possesses very suitable radiation properties, a half-life time of 13 h and gamma ray energy of 159 keV.

We have explored the feasibility of the fluorinated and iodinated MAO inhibitors as alternatives to clorgyline and *l*-deprenyl themselves for functional MAO studies in the brain with PET and SPECT. This paper describes the synthesis of the fluorine and iodine analogues of clorgyline. The comparative *in vitro* studies on the inhibitory potency and selectivity toward MAO-A and MAO-B of these non-labeled compounds were also evaluated in order to select new ligand candidates for ^{18}F and ^{123}I labeling.

The fluorine and iodine analogues of clorgyline were prepared by the reactions outlined in Chart 1, based on the published procedure for clorgyline itself.[5] The fluorinated and iodinated phenol derivatives (**1a**—**h**) were converted to their corresponding phenoxypropyl bromides (**2a**—**h**). Alkylation of *N*-methylpropargylamine with the phenoxypropyl bromides in the presence of potassium carbonate in acetonitrile gave the required fluorine and iodine analogues (**3a**—**h**) of clorgyline.

The MAO inhibitory potency of the compounds was assayed fluorometrically using kynuramine as a substrate.[6] The MAO-A and MAO-B activity was selectively measured by treating rat liver homogenate with *l*-deprenyl (MAO-B specific inhibitor) and clorgyline (MAO-A specific inhibitor), respectively.[6c,7] The IC_{50} values of these compounds including clorgyline for MAO-A and MAO-B are summarized in Table I.

The 4-chloro-2-fluoro (**3f**) and 2-chloro-4-fluoro (**3g**)

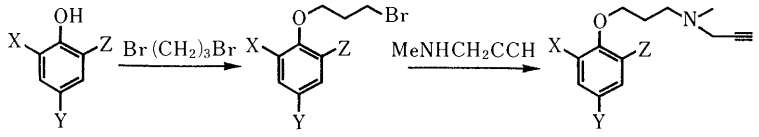

1a–h **2a–h** **3a–h**

a : X=H, Y=I, Z=H
b : X=I, Y=Cl, Z=H
c : X=Cl, Y=I, Z=H
d : X=I, Y=Cl, Z=Cl
e : X=H, Y=F, Z=H
f : X=F, Y=Cl, Z=H
g : X=Cl, Y=F, Z=H
h : X=Cl, Y=Cl, Z=H (clorgyline)

Chart 1

TABLE I. Inhibition of MAO by Fluorine and Iodine Analogues of Clorgyline

Compound	IC_{50} (M)	
	MAO-A (*l*-Deprenyl treated)	MAO-B (Clorgyline treated)
3a	2.7×10^{-8}	9.2×10^{-6}
3b	2.9×10^{-9}	2.0×10^{-5}
3c	6.9×10^{-9}	2.2×10^{-5}
3d	6.3×10^{-11}	3.6×10^{-5}
3e	2.5×10^{-8}	4.0×10^{-6}
3f	3.6×10^{-11}	7.1×10^{-6}
3g	3.4×10^{-11}	6.3×10^{-6}
3h (clorgyline)	3.0×10^{-11}	6.8×10^{-6}

derivatives were found to have high inhibitory potency against MAO-A (IC_{50} 3.6×10^{-11} and 3.4×10^{-11} M, respectively), fully comparable to that of clorgyline (**3h**) (IC_{50} 3.0×10^{-11} M) examined under the same conditions. However, compound **3e** was found to be a relatively weak inhibitor of MAO-A (IC_{50} 2.5×10^{-8} M). The ratio of IC_{50} for MAO-B to that for MAO-A of **3f** and **3g** was 2.0×10^{5} and 1.9×10^{5}, respectively, showing their high specificity for MAO-A. It thus appears that, in the fluorine analogues, one of the two chlorines on the benzene ring of clorgyline is essential for high inhibitory potency and the replacement of another chlorine with a fluorine causes no unfavorable effects on the potency and selectivity toward MAO-A compared to clorgyline itself.

Among the iodine analogues, as shown in Table I, the 2,4-dichloro-6-iodo derivative (**3d**) retained high MAO-A inhibitory potency compared to that of clorgyline (**3h**) (IC_{50} 6.3×10^{-11} M *versus* 3.0×10^{-11} M). The high ratio of IC_{50} for MAO-B to that for MAO-A of **3d**, 5.7×10^{5}, also showed its preferential inhibition toward MAO-A. Other iodine analogues **3a**—**c**, however, were found to be relatively weak MAO-A inhibitors. In the series of iodine analogues, in contrast to fluorine analogues, two chlorines on the benzene ring of clorgyline appear to be indispensable to retain the high potency.

In conclusion, the fluorine and iodine analogues of clorgyline **3d**, **3f** and **3g** were found to have high inhibitory potency and selectivity for MAO-A. They were, therefore, considered to be candidates for further studies as PET and SPECT radiopharmaceuticals for functional MAO-A studies in the brain. Since the present procedure for the preparation of fluorine and iodine analogues of clorgyline involves a rather long reaction period, an alternative short time synthesis of the ^{18}F and ^{123}I labeled counterparts are now in progress.

Experimental

All melting points are uncorrected. Infrared (IR) spectra were recorded on a JASCO IR-700 spectrometer. Proton nuclear magnetic resonance (^{1}H-NMR) spectra were recorded on a Varian Gemini-200 (200 MHz) spectrometer and the chemical shifts are reported in ppm downfield from an internal tetramethylsilane standard. Mass spectra (MS) were obtained on a Hitachi M-80 instrument.

Phenol Derivatives (1a—h) Compounds **1a** and **1e—h** were obtained commercially and used without further purification. Compounds **1b**, **1c** and **1d** were prepared by the reported methods.[8]

Preparation of Clorgyline Analogues (3a—h) A mixture of appropriate phenol derivative **1a—h** (25 mmol), 1,3-dibromopropane (50 mmol) and a solution of sodium hydroxide (1.0 g) in water (4 ml) was stirred at reflux for 1.5 h. A solution of sodium hydroxide (1.0 g) in water (6 ml) was added and the mixture was refluxed for an additional 1.5 h. After cooling, the reaction mixture was extracted with chloroform (50 ml) and washed with water (30 ml × 3). The organic layer was dried over sodium sulfate and evaporated *in vacuo*. Distillation gave the desired phenoxypropyl bromide **2a—h**.

To a solution of phenoxypropyl bromide (10 mmol) in acetonitrile (30 ml) was added a solution of potassium carbonate (11 mmol) in water (3 ml) followed by *N*-methylpropargylamine (20 mmol) and the resulting mixture was stirred at room temperature for 2 d. The acetonitrile solution was decanted and evaporated *in vacuo*. The residue was taken up with ether (50 ml) and washed with water (30 ml × 3). The ether layer was dried over sodium sulfate. Removal of the solvent *in vacuo* gave free base, which was converted to hydrochloride salt. Recrystallization from ethanol–ether afforded the desired product.

N-[3-(4-Iodophenoxy)propyl]-*N*-methyl-2-propynylamine Hydrochloride (**3a**): Yield 73%. mp 151—152 °C. *Anal.* Calcd for $C_{13}H_{17}ClINO$: C, 42.70; H, 4.69; N, 3.83. Found: C, 42.54; H, 4.65; N, 3.77. IR (KBr): 3192, 2926, 2604, 1488, 1469, 1282, 1244 cm^{-1}. ^{1}H-NMR (free base, $CDCl_3$) δ: 1.97 (2H, quintet, J=6.7 Hz, $CH_2C\underline{H}_2CH_2$), 2.23 (1H, t, J=2.3 Hz, C≡C$\underline{H}$), 2.31 (3H, s, NCH_3), 2.58 (2H, t, J=6.7 Hz, $CH_2C\underline{H}_2N$), 3.35 (2H, d, J=2.3 Hz, $C\underline{H}_2C\equiv CH$), 3.95 (2H, t, J=6.7 Hz, OCH_2), 6.66 (2H, d, J=9.0 Hz, aromatics), 7.52 (2H, d, J=9.0 Hz, aromatics). High-resolution MS (free base) Calcd for $C_{13}H_{16}INO$ *m/z*: 329.0275. Found: 329.0269.

N-[3-(4-Chloro-2-iodophenoxy)propyl]-*N*-methyl-2-propynylamine Hydrochloride (**3b**): Yield 66%. mp 141—142 °C. *Anal.* Calcd for $C_{13}H_{16}Cl_2INO$: C, 39.02; H, 4.03; N, 3.50. Found: C, 38.96; H, 4.03; N, 3.56. IR (KBr): 3200, 2928, 2490, 1462, 1286, 1265, 1247 cm^{-1}. ^{1}H-NMR (free base, $CDCl_3$) δ: 1.98 (2H, quintet, J=6.6 Hz, $CH_2C\underline{H}_2CH_2$), 2.22 (1H, t, J=2.4 Hz, C≡C$\underline{H}$), 2.34 (3H, s, NCH_3), 2.67 (2H, t, J=6.6 Hz, $CH_2C\underline{H}_2N$), 3.37 (2H, d, J=2.4 Hz, $C\underline{H}_2C\equiv CH$), 4.04 (2H, t, J=6.6 Hz, OCH_2), 6.72 (1H, d, J=8.8 Hz, aromatic H-6), 7.25 (1H, dd, J=8.8 Hz, 2.5 Hz, aromatic H-5), 7.73 (1H, d, J=2.5 Hz, aromatic H-3). High-resolution MS (free base) Calcd for $C_{13}H_{15}ClINO$ *m/z*: 362.9886. Found: 362.9884.

N-[3-(2-Chloro-4-iodophenoxy)propyl]-*N*-methyl-2-propynylamine Hydrochloride (**3c**): Yield 54%. mp 137—138 °C. *Anal.* Calcd for $C_{13}H_{16}Cl_2INO$: C, 39.02; H, 4.03; N, 3.50. Found: C, 39.19; H, 4.03; N, 3.58. IR (KBr): 3208, 2924, 2618, 1483, 1468, 1286, 1248 cm^{-1}. ^{1}H-NMR (free base, $CDCl_3$) δ: 1.97 (2H, quintet, J=6.6 Hz, $CH_2C\underline{H}_2CH_2$), 2.22 (1H, t, J=2.4 Hz, C≡C$\underline{H}$), 2.32 (3H, s, NCH_3), 2.63 (2H, t, J=6.6 Hz, $CH_2C\underline{H}_2N$), 3.44 (2H, d, J=2.4 Hz, $C\underline{H}_2C\equiv CH$), 4.05 (2H, t, J=6.6 Hz, OCH_2), 6.67 (1H, d, J=8.7 Hz, aromatic H-6), 7.46 (1H, dd, J=8.7 Hz, 2.2 Hz, aromatic H-5), 7.64 (1H, d, J=2.2 Hz, aromatic H-3). High-resolution MS (free base) Calcd for $C_{13}H_{15}ClINO$ *m/z*: 362.9886. Found: 362.9888.

N-[3-(2,4-Dichloro-6-iodophenoxy)propyl]-*N*-methyl-2-propynylamine Hydrochloride (**3d**): Yield 62%. mp 177—178 °C. *Anal.* Calcd for $C_{13}H_{15}Cl_3INO$: C, 35.93; H, 3.48; N, 3.22. Found: C, 35.90; H, 3.34; N, 3.17. IR (KBr): 3208, 2934, 2628, 1467, 1442, 1375, 1244 cm^{-1}. ^{1}H-NMR (free base, $CDCl_3$) δ: 2.04 (2H, quintet, J=6.8 Hz, $CH_2C\underline{H}_2CH_2$), 2.23 (1H, t, J=2.3 Hz, C≡C$\underline{H}$), 2.35 (3H, s, NCH_3), 2.69 (2H, t, J=6.8 Hz, $CH_2C\underline{H}_2N$), 3.39 (2H, d, J=2.3 Hz, $C\underline{H}_2C\equiv CH$), 4.03 (2H, t, J=6.8 Hz, OCH_2), 7.37 (1H, d, J=2.2 Hz, aromatic), 7.66 (1H, d, J=2.2 Hz, aromatic). High-resolution MS (free base) Calcd for $C_{13}H_{14}Cl_2INO$ *m/z*: 396.9496. Found: 396.9498.

N-[3-(4-Fluorophenoxy)propyl]-*N*-methyl-2-propynylamine Hydrochloride (**3e**): Yield 52%. mp 117—118 °C. *Anal.* Calcd for $C_{13}H_{17}ClFNO$: C, 60.58; H, 6.65; N, 5.44. Found: C, 60.59; H, 6.68; N, 5.50. IR (KBr): 3156, 2942, 2490, 1510, 1482, 1242, 1207 cm^{-1}. ^{1}H-NMR (free base, $CDCl_3$) δ: 1.92 (2H, quintet, J=6.8 Hz, $CH_2C\underline{H}_2CH_2$), 2.22 (1H, t, J=2.4 Hz, C≡C$\underline{H}$), 2.33 (3H, s, NCH_3), 2.60 (2H, t, J=6.8 Hz, $CH_2C\underline{H}_2N$), 3.36 (2H, d, J=2.4 Hz, $C\underline{H}_2C\equiv CH$), 3.97 (2H, t, J=6.8 Hz, OCH_2), 6.79—7.00 (4H, m, aromatics). High-resolution MS (free base) Calcd for $C_{13}H_{16}FNO$ *m/z*: 221.1216. Found: 221.1218.

N-[3-(4-Chloro-2-fluorophenoxy)propyl]-*N*-methyl-2-propynylamine Hydrochloride (**3f**): Yield 69%. mp 128—129 °C. *Anal.* Calcd for $C_{13}H_{16}Cl_2FNO$: C, 53.44; H, 5.52; N, 4.79. Found: C, 53.51; H, 5.52; N, 4.87. IR (KBr): 3196, 2950, 2560, 1504, 1470, 1309, 1274 cm^{-1}. ^{1}H-NMR (free base, $CDCl_3$) δ: 1.96 (2H, quintet, J=6.7 Hz, $CH_2C\underline{H}_2CH_2$), 2.24 (1H, t, J=2.3 Hz, C≡C$\underline{H}$), 2.32 (3H, s, NCH_3), 2.61 (2H, t, J=6.7 Hz, $CH_2C\underline{H}_2N$), 3.36 (2H, d, J=2.3 Hz, $C\underline{H}_2C\equiv CH$), 4.06 (2H, t, J=6.7 Hz, OCH_2), 6.85—7.12 (3H, m, aromatics). High-resolution MS (free base) Calcd for $C_{13}H_{15}ClFNO$ *m/z*: 255.0826. Found: 255.0820.

N-[3-(2-Chloro-4-fluorophenoxy)propyl]-*N*-methyl-2-propynylamine Hydrochloride (**3g**): Yield 74%. mp 97—98 °C. *Anal.* Calcd for $C_{13}H_{16}Cl_2FNO$: C, 53.44; H, 5.52; N, 4.79. Found: C, 53.50; H, 5.45; N, 4.86. IR (KBr): 3162, 2910, 2602, 1501, 1479, 1259, 1201 cm^{-1}. ^{1}H-NMR (free base, $CDCl_3$) δ: 1.97 (2H, quintet, J=6.7 Hz, $CH_2C\underline{H}_2CH_2$), 2.22 (1H, t, J=2.4 Hz, C≡CH), 2.33 (3H, s, NCH_3), 2.65 (2H, t, J=6.7 Hz, $CH_2C\underline{H}_2N$), 3.36 (2H, d, J=2.4 Hz, $C\underline{H}_2C{\equiv}CH$), 4.05 (2H, t, J=6.7 Hz, OCH_2), 6.86—7.14 (3H, m, aromatics). High-resolution MS (free base) Calcd for $C_{13}H_{15}ClFNO$ *m/z*: 255.0826. Found: 255.0819.

N-[3-(2,4-Dichlorophenoxy)propyl]-*N*-methyl-2-propynylamine (Clorgyline) Hydrochloride (**3h**): Yield 63%. mp 119—120 °C. (lit. mp 97—99 °C,[5] 115—117 °C[9]). *Anal.* Calcd for $C_{13}H_{16}Cl_3NO$: C, 50.59; H, 5.23; N, 4.54. Found: C, 50.59; H, 5.16; N, 4.58. IR (KBr): 3202, 2930, 2606, 1484, 1466, 1294, 1267 cm^{-1}. ^{1}H-NMR (free base, $CDCl_3$) δ: 1.98 (2H, quintet, J=6.7 Hz, $CH_2C\underline{H}_2CH_2$), 2.22 (1H, t, J=2.4 Hz, C≡CH), 2.33 (3H, s, NCH_3), 2.64 (2H, t, J=6.7 Hz, $CH_2C\underline{H}_2N$), 3.36 (2H, d, J=2.4 Hz, $C\underline{H}_2C{\equiv}CH$), 4.06 (2H, t, J=6.7 Hz, OCH_2), 6.85 (1H, d, J=8.8 Hz, aromatic H-6), 7.16 (1H, dd, J=8.8, 2.5 Hz, aromatic H-5), 7.35 (1H, d, J=2.5 Hz, aromatic H-3). High-resolution MS (free base) Calcd for $C_{13}H_{15}Cl_2NO$ *m/z*: 271.0531. Found: 271.0520.

Assay of MAO Activity Rat liver was homogenized with 10 volumes of 0.25 M sucrose and 2 mM Tris buffer (pH 7.4) under cooling. The homogenates were centrifuged at 1000 ***g*** for 10 min to remove cell debris. The protein content was measured by the biuret method. The MAO activity was assayed fluorometrically using kynuramine as a substrate according to the reported method.[6] Fluorescence was measured at 380 nm with excitation at 315 nm. The activities of MAO-A and MAO-B were assayed in the presence of 1 μM *l*-deprenyl and clorgyline, respectively.[6c,7]

References

1) C. J. Fowler, L. Oreland, and B. A. Callingham, *J. Pharm. Pharmacol.*, **33**, 341 (1981).
2) K. F. Tipton, P. Dostert, and M. S. Benedetti, eds., "Monoamine Oxidase and Disease," Academic Press, New York, 1984.
3) *a*) K. Ishiwata, T. Ido, K. Yanai, K. Kawashima, Y. Miura, M. Monma, S. Watanuki, T. Takahashi, and R. Iwata, *J. Nucl. Med.*, **26**, 630 (1985); *b*) J. S. Fowler, R. R. MacGregor, A. P. Wolf, C. D. Arnett, S. L. Dewey, D. Schlyer, D. Christman, J. Logan, M. Smith, H. Sachs, S. M. Aquilonius, P. Bjurling, C. Halldin, P. Hartvig, K. L. Leenders, H. Lundqvist, L. Oreland, C. G. Stalnacke, and B. Langstrom, *Science*, **235**, 481 (1987).
4) R. R. Rando, *Science*, **185**, 320 (1974).
5) R. R. MacGregor, J. S. Fowler, A. P. Wolf, C. Halldin, and B. Langstrom *J. Labelled Compd. Radiopharm.*, **25**, 1 (1988).
6) *a*) M. Kraml, *Biochem. Pharmacol.*, **14**, 1683 (1965); *b*) T. Yokoyama, N. Iwata, and T. Kobayashi, *Jpn. J. Pharmacol.*, **44**, 421 (1987); *c*) M. Yamazaki, Y. Satoh, Y. Maebayashi, and Y. Horie, *Chem. Pharm. Bull.*, **36**, 670 (1988).
7) *a*) M. Naoi, Y. Hirata, and T. Nagatsu, *J. Neurochem.*, **48**, 709 (1987); *b*) Y. Satoh and M. Yamazaki, *Chem. Pharm. Bull.*, **37**, 206 (1989).
8) *a*) P. S. Varma and K. M. Yashoda, *J. Indian Chem. Soc.*, **16**, 477 (1939); *b*) V. Gold and M. Whittaker, *J. Chem. Soc.*, **1951**, 1184; *c*) S. Buchan and H. McCombie, *ibid.*, **1931**, 137.
9) J. P. Johnston, *Biochem. Pharmacol.*, **17**, 1285 (1968).

A Cytotoxic Substance from Sangre de Grado

Hideji ITOKAWA,* Yoshitatsu ICHIHARA, Miwako MOCHIZUKI, Tamami ENOMORI, Hiroshi MORITA, Osamu SHIROTA, Mutsumi INAMATSU, and Koichi TAKEYA

Tokyo College of Pharmacy, Horinouchi 1432-1, Hachioji, Tokyo 192-03, Japan. *Received September 3, 1990*

Taspine has been isolated as a cytotoxic substance from Sangre de Grado, sap of *Croton palanostigma* (Euphorbiaceae), by bioassay guided fractionation. The cytotoxicity (IC_{50}) of taspine was found to be 0.39 μg/ml against KB cells and 0.17 μg/ml against V-79 cells.

Keywords Sangre de Grado; *Croton palanostigma*; Euphorbiaceae; taspine; alkaloid; cytotoxicity; V-79 cell; KB cell

Sangre de Grado, blood of gladness in Spanish, is red viscous sap produced by several *Croton* species (Euphorbiaceae) growing in the upper Amazon basin in Peru. The species from which it is usually obtained are *Croton erythrochilus*, *C. lechleri*, and *C. palanostigma*, also known as *C. draconoides*. This sap has been largely used by Peruvian natives for several medicinal purposes, including wound healing. Recently, Vaisberg and his collaborators reported the isolation of a potent wound healing substance from Sangre de Grado obtained from *C. lechleri*.[1] Furthermore, Sangre de Grado has been widely used to treat cancer.[2] As part of our continuing efforts to discover the antitumor potential of plant metabolites,[3] Sangre de Grado obtained from *C. palanostigma* was found to be cytotoxic to V-79 cells (IC_{50} = 3.7 μg/ml) *in vitro*. Bioassay directed purification guided by cytotoxicity against V-79 cells led to the isolation of taspine (**1**) as a cytotoxic substance.

Sangre de Grado obtained from *C. palanostigma* was freeze-dried, and chromatographed on a Diaion HP-20 column using stepwise elution [H_2O–MeOH (1:0—0:1) and 80% acetone]. The active fraction eluted with 100% MeOH was purified further by medium-pressure liquid chromatography (MPLC) on a silica gel column (CH_2Cl_2–MeOH, 13:7) to yield taspine (**1**).

Compound **1** was isolated as a white powder, mp >300 °C. Its molecular ion peak (*m/z* 369) in electron impact-mass spectrum (EI-MS) and a positive Dragendorff test suggested an alkaloid for **1**. The elemental analysis of **1** established the molecular formula as $C_{20}H_{19}NO_6$. The proton nuclear magnetic resonance (^{1}H-NMR) spectrum contained the signals due to two N-methyl [δ 2.44 (6H, s)], two methylene [δ 2.68 (2H, m), 3.45 (2H, m)], two methoxy [δ 4.12 (3H, s), 4.13 (3H, s)] and three aromatic protons [δ 7.22 (s), 7.35 (d, *J* = 8.8 Hz), 8.09 (d, *J* = 8.8 Hz)]. These data suggested **1** to be taspine, and the structure was identified in comparison with the published data.[4,5] The carbon-13 nuclear magnetic resonance (^{13}C-NMR) data for **1**, which had not previously been reported, were determined by ^{1}H–^{13}C shift correlation *via* long-range coupling (COLOC) experiments (Table I).

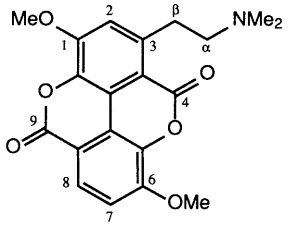

1

Chart 1

The cytotoxic activities of taspine are listed in Table II. Taspine is the alkaloid previously isolated from several families, including Berberidaceae,[6] Euphorbiaceae,[4,7] and Magnoliaceae.[5] The biological activities of Sangre de Grado and/or taspine have been reported with respect to an anti-inflammatory,[4] a reverse transcriptase inhibitory,[8] and wound healing activities.[1] In this study, taspine was revealed to be the cytotoxic substance of Sangre de Grado and showed strong cytotoxicity as a plant metabolite.

Experimental

Melting point (uncorrected) was determined on a Yanagimoto micro melting point apparatus, infrared (IR) spectrum on a Perkin-Elmer 1710 FTIR spectrometer. ^{1}H-NMR (400 MHz) and ^{13}C-NMR (100 MHz) were recorded on a Bruker AM-400 spectrometer in $CDCl_3$–CD_3OD (3:1) with tetramethylsilane (TMS) as an internal standard. Mass spectrum (MS) was obtained on a Hitachi M-80 spectrometer. For column chromatography, Diaion HP-20 (Mitsubishi Chem. Ind. Co., Ltd.) as highly porous synthetic resin was used. MPLC was carried out with a CIG column system (Kusano Scientific Co., Ltd.) on a 10 μm silica gel.

Plant Material Sangre de Grado was obtained in Iquitos, Peru, in August 1987. The material, which was obtained from *C. palanostigma*, was identified by Dr. F. Ayala Flores (Peru Amazon University).

Isolation The freeze-dried sap (70 g) was chromatographed on a Diaion HP-20 with H_2O, 10% MeOH, 20% MeOH, 40% MeOH, MeOH, and 80% acetone. The MeOH eluted material was purified by silica gel MPLC

TABLE I. ^{13}C-NMR Data for Taspine (**1**)

C		C	
1	151.4	9	159.1
2	117.2	10a	136.8
3	143.8	10b	119.2
3a	109.1	10c	118.3
4	158.1	α	60.1
5a	137.7	β	32.6
6	151.6	N-Me × 2	44.8
7	114.2	O-Me × 2	56.8
8	127.2		
8a	111.3		

δ in $CDCl_3$–CD_3OD (3:1).

TABLE II. Cytotoxic Activity of Taspine (**1**)

	IC_{50} (μg/ml)
KB cells	0.39
V-79 cells	0.17

with CH_2Cl_2–MeOH (13:7) to afford taspine (700 mg).

Taspine (**1**): A white powder, mp >300 °C. EI-MS (rel. int.) *m/z*: 369 (7, M^+), 58 (100). IR ($CHCl_3$): 3010, 2943, 2848, 2827, 2786, 1738, 1600, 1472, 1439, 1295, 1135, 1090 cm^{-1}. ^{1}H-NMR δ: 2.44 (6H, s, N-CH_3 × 2), 2.68 (2H, m, H_2-α), 3.45 (2H, m, H_2-β), 4.12 (3H, s, 6-*O*-CH_3), 4.13 (3H, s, 1-*O*-CH_3), 7.22 (1H, s, H-2), 7.35 (1H, d, J=8.8 Hz, H-7), 8.09 (1H, d, J=8.8 Hz, H-8). *Anal.* Calcd for $C_{20}H_{19}NO_6$: C, 65.03; H, 5.18; N, 3.79. Found: C, 64.75; H, 5.12; N, 3.72.

Assay for Cytotoxicity against V-79 Cells See previous paper.[9]

Acknowledgments We would like to thank Dr. F. Ayala Flores, Peru Amazon University, Peru, Mr. T. Shiota, Institute of Andean Resource Discovery, Peru, and Mr. M. Satake, National Institute of Hygienic Science, Japan, for collection of Sangre de Grado, and Dr. M. Tamai, Taisho Pharmaceutical Co., Ltd., for some of the cytotoxic test. This work was financially supported in part by the Ministry of Education, Science, and Culture of Japan.

References and Notes

1) A. J. Vaisberg, M. Milla, M. del Carmen Planas, J. L. Cordova, E. Rosas de Agusti, R. Ferreyra, M. del Carmen Mustiga, L. Carlin, and G. B. Hammond, *Planta Med.*, **55**, 140 (1989).
2) J. L. Hartwell, *Lloydia*, **32**, 153 (1969).
3) The recent paper: H. Morita, E. Kishi, K. Takeya, H. Itokawa, and O. Tanaka, *Chem. Lett.*, **1990**, 749.
4) G. Persinos Perdue, R. N. Blomster, D. A. Blake, and N. R. Farnsworth, *J. Pharm. Sci.*, **68**, 124 (1979).
5) B. Talapatra, P. K. Chaudhuri, and S. K. Talapatra, *Phytochemistry*, **21**, 747 (1982).
6) T. F. Platonova, A. D. Kuzovkov, and P. S. Massagetov, *Zh. Obshch. Khim.*, **23**, 880 (1953).
7) R. Marini Bettolo and M. L. Scarpati, *Phytochemistry*, **18**, 520 (1979).
8) M. L. Sethi, *Can. J. Pharm. Sci.*, **12**, 7 (1977).
9) H. Itokawa, N. Totsuka, K. Nakahara, M. Maezuru, K. Takeya, M. Kondo, M. Inamatsu, and H. Morita, *Chem. Pharm. Bull.*, **37**, 1619 (1989).

Nematocidal Principles in "Oakmoss Absolute" and Nematocidal Activity of 2,4-Dihydroxybenzoates[1)]

Ali Mohammad AHAD,[a] Yoshihisa GOTO,[a] Fumiyuki KIUCHI,[a] Yoshisuke TSUDA,*,[a] Kaoru KONDO,[b] and Toshiya SATO[c]

Faculty of Pharmaceutical Sciences,[a] and School of Medicines,[b] Kanazawa University, 13–1 Takara-machi, Kanazawa 920, Japan and Takasago International Corporation,[c] 5–36–31 Kamata, Ohta-ku, Tokyo 144, Japan. *Received September 20, 1990*

Nematocidal principles obtained from oakmoss absolute were identified as methyl 2,4-dihydroxy-3,6-dimethylbenzoate (2), ethyl 3-formyl-2,4-dihydroxy-6-methylbenzoate (4), and ethyl 5-chloro-3-formyl-2,4-dihydroxy-6-methylbenzoate (7). In relation to their structures, the nematocidal activity of 2,4-dihydroxybenzoates of methyl to tetradecyl was tested and the strongest activity was found in the octyl ester (minimal lethal concentration = 13 μM).

Keywords oakmoss absolute; *Evernia prunastri*; nematocidal activity; *Toxocara canis*; dihydroxybenzoate; octyl 2,4-dihydroxybenzoate; structure–activity relationship

Oakmoss [*Evernia prunastri* (L.) ACH.] is a lichen belonging to the family Usneaceae. Solvent extract of oakmoss has been widely used as an important perfume, industrially producing so-called "absolute" which is the methanol soluble fraction of the hexane extract of oakmoss. A number of qualitative as well as quantitative analyses of *Evernia prunastri* have been reported with identification of a number of phenolic compounds and depsides.[2)]

In the course of our screening work of crude drugs and plant materials effective on visceral larva migrans, we observed[3)] that oakmoss absolute oil shows strong nematocidal activity against the second-stage larvae of dog roundworm, *Toxocara canis*, which is a common pathogenic parasite in visceral larva migrans. In this paper, we report the identification of the active principles and structure–activity relationship of some related compounds.

Materials and Methods

Melting points were taken on a Yanagimoto micro hot-stage melting point apparatus and are uncorrected. Infrared (IR) spectra were taken as chloroform solution on a JASCO A-202 spectrometer and are given in cm^{-1}. Proton nuclear magnetic resonance (^{1}H-NMR) spectra were measured in $CDCl_3$ solution with tetramethylsilane as an internal standard on a JEOL FX-100 or a JNM GX-400 spectrometer and the chemical shifts are given in δ values. Mass spectra (MS) were taken on a Hitachi M-80 spectrometer and M^+ were given by m/z(%). Fuji-Davison BW-820 MH (silica gel) was used for column chromatography.

Assay Method Nematocidal activity was determined according to the method previously described.[4)] For one assay, 20 second-stage larvae of *Toxocara canis* were incubated with a test solution in a Corning cell well at 37 °C and the behavior of the larvae was observed under a microscope at 1, 3, 6, and 24 h. All assays were done in duplicate. The test sample was dissolved in dimethyl sulfoxide (DMSO), which was diluted with 0.75% saline at an appropriate concentration to keep the DMSO concentration in the solution at 2%, and applied to the assay. The nematocidal activity was evaluated in terms of the relative mobility (RM) value[4)]: a smaller RM value indicates a stronger nematocidal activity, and when all larvae die, this value is 0. RM_n indicates the RM value after n hour incubation. Minimal lethal concentration (MLC) was defined as the lowest concentration giving an RM of 0 after 24 h incubation.

Oakmoss Absolute Oakmoss absolute used in this investigation was imported from Etabblissements Arco (France).

Isolation of Active Principles Oakmoss absolute (20.2 g) was fractionated on a silica gel column and eluted with hexane (fraction (fr. 1, 3.12 g), benzene (fr. 2, 12.42 g), chloroform (fr. 3, 0.56 g), chloroform : methanol = 1 : 1 (fr. 4, 3.94 g), and methanol (fr. 5, 34 mg). Nematocidal activities of these fractions are as follows: RM = 0, 30, 78, 100, and 100 at 0.1 mg/ml after 24 h incubation. A portion of fr. 1 (549 mg) was rechromatographed with benzene : hexane = 9 : 1 to give compounds **1** (323 mg), **3** (63 mg), and **4** (33 mg). Another portion of fr. 1 (186 mg) was chromatographed on a recycling preparative high performance liquid chromatograph (HPLC) (LC-908, Japan Analytical Industry Co., Ltd.) with chloroform to give compounds **2** (22 mg), **7** (14 mg), and **8** (11 mg) together with compounds **1**, **3**, and **4**. Fraction 2 (5.03 g) was chromatographed with 2% acetone–benzene to give fr. 2-1 (370 mg) and fr. 2-2 (4.65 g). Fraction 2-1 was rechromatographed with hexane : ethyl acetate = 15 : 1 to give compounds **1** (219 mg), **3** (47 mg), **4** (41 mg), and **5** (60 mg). A portion of fr. 2-2 (598 mg) was rechromatographed on silica gel with hexane : ethyl acetate = 9 : 1 to give compounds **1** (470 mg) and **2** (68 mg). A portion of fr. 3 (0.4 g) was rechromatographed on a silica gel column to give compound **6** (38 mg).

Compound **1** (Diethyl Phthalate): Pale yellow oil. IR: 1717. ^{1}H-NMR: 1.36 (6H, t, J = 7 Hz, $COOCH_2C\underline{H}_3$), 4.36 (4H, q, J = 7 Hz, $COO\underline{CH}_2CH_3$), 7.44—7.77 (4H, m, ArH). MS: 222 (M^+, 5), 177 (31), 149 (100).

Compound **2** (Methyl β-Orcinolcarboxylate): Pale yellow needles from hexane–benzene, mp 146—147 °C (lit. mp 145 °C).[5)] IR: 1700, 1680, 1595, 1545. ^{1}H-NMR: 2.10 (3H, s, Me), 2.42 (3H, s, Me), 3.90 (3H, s, OMe), 5.24 (1H, s, OH), 6.18 (1H, s, ArH), 12.02 (1H, s, OH). MS: 196 (M^+, 54), 164 (100), 136 (92), 107 (12).

Compound **3** (Ethyl Everninate): Colorless needles from hexane, mp 77—78 °C (lit. mp 76—77 °C).[6)] IR: 1644, 1612. ^{1}H-NMR: 1.40 (3H, t, J = 7 Hz, $COOCH_2C\underline{H}_3$), 2.26 (3H, s, Me), 3.80 (3H, s, OMe), 4.40 (2H, q, J = 7 Hz, $COO\underline{CH}_2CH_3$), 6.28 (1H, d, J = 2.8 Hz, ArH), 6.29 (1H, d, J = 2.7 Hz, ArH), 11.72 (1H, s, OH). MS: 210 (M^+, 61), 164 (100), 136 (22).

Compound **4** (Ethyl Hematommate): Colorless needles from hexane, mp 114—115 °C (lit. mp 110—112 °C).[6)] IR: 1644. ^{1}H-NMR: 1.44 (3H, t, J = 7 Hz, $COOCH_2C\underline{H}_3$), 2.48 (3H, s, Me), 4.40 (2H, q, J = 7 Hz, $COO\underline{CH}_2CH_3$), 6.24 (1H, s, ArH), 10.32 (1H, s, CHO), 12.32 (1H, s, OH), 12.88 (1H, s, OH). MS: 224 (M^+, 55), 196 (27), 178 (31), 150 (100), 122 (14).

Compound **5** [(+)-Usnic Acid][7a)]: Yellow needles from hexane–benzene, mp 203—204 °C (lit. mp 203—204 °C).[7b)] $[\alpha]_D^{20}$ = +467° (c = 0.12, $CHCl_3$). IR: 1680, 1624, 1528. ^{1}H-NMR: 1.69 (3H, s, Me), 2.03 (3H, s, Me), 2.59 (3H, s, $COCH_3$), 2.60 (3H, s, $COCH_3$), 5.92 (1H, s, =CH), 10.95 (1H, s, OH), 13.24 (1H, s, OH), 18.76 (1H, s, OH). This was identified with an authentic sample provided by Dr. M. Takani.

Compound **6** (Everninic Acid): Colorless needles from benzene–ether, mp 165—170 °C (lit. mp 165—170 °C).[8)] IR (KBr): 1601, 1583. ^{1}H-NMR: 2.56 (3H, s, Me), 3.84 (3H, s, OMe), 6.32 (1H, d, J = 2.5 Hz, ArH), 6.39 (1H, d, J = 2.5 Hz, ArH). MS: 182 (M^+, 57), 164 (100), 136 (69), 121 (37).

Compound **7** (Ethyl Chlorohematommate)[2b)]: Colorless needles from hexane, mp 98—99 °C. IR: 1642. ^{1}H-NMR: 1.44 (3H, t, J = 7 Hz, $COOCH_2C\underline{H}_3$), 2.68 (3H, s, Me), 4.40 (2H, q, J = 7 Hz, $COO\underline{CH}_2CH_3$), 10.35 (1H, s, CHO), 12.73 (1H, s, OH), 13.11 (1H, s, OH). MS: 260 (M^+ for ^{37}Cl, 9), 258 (M^+ for ^{35}Cl, 28), 212 (19), 186 (34), 184 (100).

Compound **8** (Friedelin): Colorless needles from methanol, mp 259—260 °C (lit. mp 257—261 °C).[9)] IR: 1695. ^{1}H-NMR: eight methyl groups at δ 0.73, 0.87 (d, J = 6.8 Hz), 0.88, 0.96, 1.01 (×2), 1.04, 1.18. MS: 426 (M^+, 26), 125 (100). ^{13}C-NMR: 22.3 (C-1), 41.5 (C-2)*, 213.2 (C-3), 58.2 (C-4), 42.2 (C-5)*, 41.3 (C-6), 18.2 (C-7), 53.1 (C-8), 37.5 (C-9), 59.5 (C-10), 35.6 (C-11), 30.5 (C-12), 39.7 (C-13), 38.3 (C-14), 32.4 (C-15), 36.0 (C-16), 30.0 (C-17), 42.8 (C-18), 35.4 (C-19), 28.1 (C-20), 39.3 (C-21), 32.8 (C-22), 6.8 (C-23), 14.7 (C-24), 18.0 (C-25), 18.7 (C-26), 20.3 (C-27), 32.1 (C-28), 31.8 (C-29), 35.0 (C-30). For the carbons with *, the previous assignment[10)] has been revised based on INEPT experiment.

Demethylation of Ethyl Everninate 3 BBr_3 (186 mg) was added to a stirred mixture of ethyl everninate **3** (21.8 mg) in CH_2Cl_2 (7 ml) at 0 °C, the mixture was allowed to warm at room temperature and stirred for 10 min. The reaction mixture was poured into ice-water and extracted with AcOEt. The organic layer was washed with brine, dried, and concentrated to yield demethylated product **9** which was purified by chromatography

to give colorless needles, mp 134—135 °C, (lit. mp 132 °C).[7]

Alkyl 2,4-Dihydroxybenzoates (β-Resorcylic Acid Esters) Methyl, ethyl, propyl, butyl, pentyl, and hexyl esters were synthesized as follows. 2,4-Dihydroxybenzoic acid (0.2 g) was dissolved in an appropriate alcohol (5 ml) and HCl gas was passed into the solution at room temperature. The mixture was heated under reflux for 5—10 h. The solvent was evaporated and the residue was purified by chromatography.

Heptyl, octyl, nonyl, decyl, and tetradecyl esters were synthesized as follows. The acid **10** (0.2 g), sodium hydrogen carbonate (2 mol eq), and alkyl bromide (1 mol eq) in dimethyl acetamide (2—3 ml) were heated at 50 °C for 6—10 h. The mixture was poured into water and extracted with ether. The organic layer was washed with brine, dried, and concentrated to give the esters which were purified by chromatography.

All of these esters as well as the acid showed, in the 400 MHz ^{1}H-NMR spectra, aromatic proton signals at δ 7.0—7.2 (d, H-6) and 6.24—6.44 (m, H-3 and H-5) with the coupling constants $J_{5,6}=8.2$ Hz, $J_{3,5}=2.3$ Hz, and $J_{3,6}<1$ Hz. The other data are indicated in Table II.

Alkyl 2-Hydroxybenzoates (Salicylic Acid Esters) Butyl, hexyl, and octyl esters were synthesized as follows. Salicylic acid (0.2 g), sodium hydrogen carbonate (2 mol eq) and alkyl bromide (1 mol eq) in dimethyl acetamide (2—3 ml) were heated at 90 °C for 30 min. The mixture was poured into water and extracted with ether. The organic layer was washed with brine, dried, and concentrated to give the esters which were purified by chromatography.

All of these esters were oils and showed the aromatic proton signals at δ 6.80 (dd, $J=8$, 2 Hz, H-3), 7.38 (ddd, $J=8$, 7, 2 Hz, H-5), 6.92—6.94 (ddd, $J=8$, 7, 2 Hz, H-4), and 7.82—7.84 (dd, $J=8$, 2 Hz, H-6). The other data are indicated in Table III.

Hexyl 2,5-Dihydroxy-, 2,6-Dihydroxy-, and 3,5-Dihydroxybenzoates These esters were synthesized from the corresponding acids and hexyl bromide as described above. Physical and spectroscopic data are indicated below and in Table III.

Hexyl 2,5-Dihydroxybenzoate (**25**): Oil. ^{1}H-NMR: 4.32 (2H, t, $J=7$ Hz, $COOCH_2$), 6.04 (1H, dd, $J=9$, 3 Hz, H-4), 6.84 (1H, d, $J=9$ Hz, H-3), 7.30 (1H, d, $J=3$ Hz, H-6).

Hexyl 2,6-Dihydroxybenzoate (**26**): Oil. ^{1}H-NMR: 4.48 (2H, t, $J=8$ Hz, $COOCH_2$), 6.44 (2H, d, $J=8$ Hz, H-3, 5), 7.28 (1H, t, $J=8$ Hz, H-4).

Hexyl 3,5-Dihydroxybenzoate (**27**): Oil. ^{1}H-NMR: 4.22 (2H, t, $J=7$ Hz, $COOCH_2$), 6.54 (1H, t, $J=2$ Hz, H-4), 7.07 (2H, $J=2$ Hz, H-2, 6).

Results and Discussion

Isolation and Identification of Nematocidal Principles of Oakmoss Absolute On chromatography of oakmoss absolute oil over silica gel, nematocidal activity was concentrated in the first three fractions, of which the activity of hexane eluate was the strongest (RM = 0 at 0.1 mg/ml after 24 h incubation). Therefore, fr. 1, fr. 2, and fr. 3 were further fractionated in combination with silica gel column chromatography and recycling HPLC resulting in the isolation of eight compounds (**1**—**8**).

Compound **1** (diethyl phthalate) was the most abundant, but it was a diluent added in the industrial process to liquidize the solid oakmoss absolute. Compound **5** was (+)-usnic acid and compound **8** was friedelin as identified by comparison with the authentic specimens. This is the first time that the presence of friedelin in oakmoss absolute has been indicated. These three compounds were ineffective for nematocidal activity. The other compounds were known phenolics, and identified with methyl β-orcinolcarboxylate (**2**), ethyl everninate (**3**), everninic acid (**6**), ethyl hematommate (**4**), and ethyl chlorohematommate (**7**), by comparison of their respective spectral data with those of the known oakmoss constituents.

The nematocidal activity of compounds **2**, **3**, **4**, **6**, and **7** is shown in Table I, from which we conclude that nematocidal activity of oakmoss absolute is attributed to compounds **2**, **4**, and **7**. Table I also suggests that the compounds of 2,4-dihydroxybenzoate structure exhibited

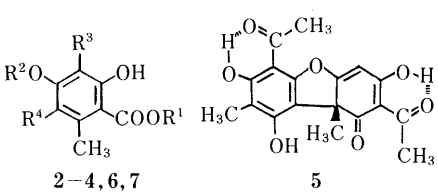

2—4, 6, 7 5 8

	R^1	R^2	R^3	R^4
2	Me	H	Me	H
3	Et	Me	H	H
4	Et	H	CHO	H
6	H	Me	H	H
7	Et	H	CHO	Cl

Chart 1. Structures of Isolated Compounds from Oakmoss Absolute Oil

TABLE I. Nematocidal Activity of Oakmoss Absolute Constituents and Compound **9**

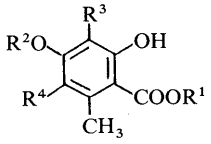

Compd.	R^1	R^2	R^3	R^4	RM (0.1 mg/ml) 6 h	RM (0.1 mg/ml) 24 h	MLC (μM)
2	Me	H	Me	H	—	0	410
3	Et	Me	H	H	100	100	—
4	Et	H	CHO	H	81	0	100
6	H	Me	H	H	100	100	—
7	Et	H	CHO	Cl	98	0	110
9	Et	H	H	H	100	64	—

appreciable nematocidal activity (compounds **2**, **4**, and **7**), while those in which one of the hydroxyl groups was masked by methyl group were inactive. We therefore performed demethylation of ethyl everninate (**3**) by BBr_3. The resulting ethyl 2,4-dihydroxy-6-methylbenzoate (**9**) showed, though it was weak, nematocidal activity as expected. Comparing the activity of compounds **2**, **4** and **9**, it is also suggested that introduction of a substituent between two hydroxyl groups, whether electron attracting or electron donating, enhances the activity.

Nematicidal Activity of β-Resorcylate Esters Since 2,4-dihydroxy-6-methylbenzoates were proved to be responsible for the nematocidal activity of oakmoss absolute oil, the activities of methyl to decyl and tetradecyl esters of 2,4-dihydroxybenzoic acid (β-resorcylic acid) were then examined (Table II). 2,4-Dihydroxybenzoic acid (**10**) showed very weak activity as did its methyl ester **11**. However, the activity (with regard to the MLC) was increased with increase of ester chain length and reached maximum at the octyl ester **18**. The activity then decreased with further increase in ester chain length and became completely ineffective with tetradecyl ester **21**. The activity of the octyl ester **18** (MLC = 13 μM) was stronger than that of the famous anthelmintic 4-hexylresorcinol (MLC = 75 μM).

It must also be noted that, although the octyl (also heptyl and nonyl) ester was most active in the MLC, its activity at 6 h (RM = 33 at 0.1 mg/ml) was weaker than that of propyl to hexyl esters (RM = 0 at 0.1 mg/ml). This suggests that the octyl (and also heptyl and nonyl) ester is slow acting compared to the propyl to hexyl esters, though the activity

TABLE II. Nematocidal Activity and Characterization of Alkyl 2,4-Dihydroxybenzoates

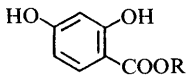

Entry	Compd.	R	RM (0.1 mg/ml) 6 h	RM (0.1 mg/ml) 24 h	MLC (μM)	mp (°C)	^{1}H-NMR (δ) Me[a]	^{1}H-NMR (δ) $COOCH_2$[b]	MS M^+ (%)
1	**10**	H	100	95	—	226—228	—	—	—
2	**11**	CH_3	100	67	—	124—125[c]	3.86	—	168 (65)
3	**12**	C_2H_5	100	0	550	70— 71[d]	1.40	4.38	182 (44)
4	**13**	C_3H_7	0	0	350	Oil	1.02	4.24	196 (32)
5	**14**	C_4H_9	0	0	100	44— 45	0.99	4.30	210 (33)
6	**15**	C_5H_{11}	0	0	78	Oil	0.94	4.30	224 (46)
7	**16**	C_6H_{13}	0	0	35	38— 39	0.92	4.28	238 (28)
8	**17**	C_7H_{15}	10	0	20	38— 39	0.90	4.28	252 (20)
9	**18**	C_8H_{17}	33	0	13	48— 49	0.88	4.29	266 (30)
10	**19**	C_9H_{19}	67	0	26	51— 52	0.86	4.32	280 (28)
11	**20**	$C_{10}H_{21}$	85	15	—	61— 62	0.84	4.28	294 (26)
12	**21**	$C_{14}H_{29}$	100	100	—	74— 75	0.84	4.30	350 (30)
Cf. 13	Hexylresorcinol		0	0	75				

a) Appeared as t, $J=7$ Hz, except for **11** (s). *b*) Appeared as t, $J=7$ Hz, except for **12** (q, $J=7$ Hz). *c*) Lit. mp 121—122 °C (ref. 11). *d*) Lit. mp 69—70 °C (ref. 11).

TABLE III. Nematocidal Activity and Characterization of Hexyl 2-Hydroxy-, 2,5-Dihydroxy-, 2,6-Dihydroxy-, and 3,5-Dihydroxybenzoates and Related Esters

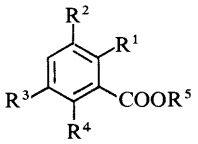

Entry	Compd.	R^1	R^2	R^3	R^4	R^5	RM (0.1 mg/ml) 6 h	RM (0.1 mg/ml) 24 h	MLC (μM)	^{1}H-NMR (δ) Me[a]	MS M^+ (%)
1	**22**	OH	H	H	H	C_4H_9	100	100	—	0.92	194 (22)
2	**23**	OH	H	H	H	C_6H_{13}	100	67	—	0.92	222 (20)
3	**24**	OH	H	H	H	C_8H_{17}	95	67	—	0.88	250 (28)
4	**25**	OH	H	OH	H	C_6H_{13}	14	0	94	0.91	238 (20)
5	**26**	OH	H	H	OH	C_6H_{13}	100	67	—	0.90	238 (23)
6	**27**	H	OH	OH	H	C_6H_{13}	32	12	—	0.87	238 (50)

a) Appeared as t, $J=7$ Hz, except for **26** ($J=8$ Hz).

of the heptyl to nonyl esters in MLC sense is stronger than that of propyl to hexyl esters.

The nematocidal activity of the above esters rapidly decreased when the ester chain length was beyond C-10. Such a cut-off effect was also observed in the nematocidal activity of aliphatic saturated acids and alcohols.[4]

Kiuchi *et al.*[4] showed that, among aliphatic alcohols, tetradecanol exhibits the strongest nematocidal activity (MLC = 20 μM) and this activity decreases with either increase or decrease of the alkyl chain length. Hexanol to nonanol were practically ineffective. Therefore, the strong activity of hexyl to nonyl 2,4-dihydroxybenzoate (**16—19**) must be attributed to the inherent property of these compounds.

Presence of two hydroxy groups at C-2 and C-4 is apparently also necessary to enhance the activity. Table III lists the nematocidal activity of hexyl esters of salicylate and various dihydroxybenzoates. 2-Hydroxybenzoates (entry 1—3) showed very weak or negligible activity. The activity of 2,6- and 3,5-dihydroxybenzoates (entries 5 and 6) was also very weak. Hexyl 2,5-dihydroxybenzoate (entry 4) exhibited a considerably strong activity, but its activity was weaker than that of the 2,4-dihydroxy derivative **16**. Therefore, we conclude that, for nematocidal activity of benzoate esters, presence of a hydroxy group at C-2 is necessary, and that introduction of the second hydroxyl group at C-4 greatly enhances the activity.

Acknowledgements We thank Dr. Masako Takani of this faculty for the sample of (+)-usnic acid. A part of this work was financially supported by the Yamasaki Foundation for Promotion of Spice Research, to which we express our thanks.

References

1) Studies on Crude Drugs Effective on Visceral Larva Migrans. XII. Part XI: N. Nakamura, F. Kiuchi, Y. Tsuda, K. Kondo, and T. Sato *Shoyakugaku Zasshi*, **44**, 183 (1990).
2) *a*) R. ter Heide, N. Provatoroff, P. C. Trass, P. J. de Valois, N. van der Plasse, H. J. Wobben, and R. Timmer, *J. Agric. Food Chem.*, **23**, 950 (1975); *b*) Y. Terajima, H. Ishikawa, K. Tokuda, and S. Nakamura, *Development Food Sci.*, **18**, 685 (1988); *c*) J. Gavin and R. Tabacchi, *Helv. Chim. Acta*, **58**, 190 (1975); *d*) G. Nicollier and R. Tabacchi, *ibid.*, **59**, 2979 (1976); *e*) J. Gavin, G. Nicollier, and R. Tabacchi, *ibid.*, **61**, 353 (1978); *f*) G. Nicollier, M. Rebetez, and R. Tabacchi, *ibid.*, **62**, 711 (1979).
3) see Part XI.
4) F. Kiuchi, N. Miyashita, Y. Tsuda, K. Kondo, and H. Yoshimura, *Chem. Pharm. Bull.*, **35**, 2880 (1987).
5) W. B. Whally, *J. Chem. Soc.*, **1949**, 3278.

6) T. M. Cresp, M. V. Sargent, J. A. Elix, and D. P. H. Murphy, *J. Chem. Soc., Perkin Trans. 1*, **1973**, 340.
7) *a*) C. F. Culberson, *Phytochemistry*, **2**, 335 (1963); *b*) S. Shibata and H. Taguchi, *Tetrahedron Lett.*, **48**, 4867 (1967).
8) Dictionary of Organic Compounds," Vol. II, 5th ed., ed. by J. Buckingham, 1982, D-04664.
9) A. M. Duffield, L. J. Durham, and C. Djerassi, *Tetrahedron*, **24**, 1205 (1968).
10) H. Beierbeck, J. K. Saunders, and J. W. ApSimon, *Can. J. Chem.*, **55**, 2813 (1977).
11) Beilstein, E II, **10**, 252.

Studies on the Nepalese Crude Drugs. XII.[1] On the Phenolic Compounds from the Root of *Scutellaria prostrata* JACQ. *ex* BENTH.[2]

Yuichi KIKUCHI, Yukinori MIYAICHI, Yumi YAMAGUCHI, Haruhisa KIZU and Tsuyoshi TOMIMORI*

School of Pharmacy, Hokuriku University, 3 Ho, Kanagawa-machi, Kanazawa, 920-11, Japan. *Received September 20, 1990*

From the root of *Scutellaria prostrata* JACQ. *ex* BENTH., five compounds (I—V) were isolated, together with three known glycosides of phenylethanoid (VI—VIII) and sixteen known flavonoids (IX—XXIV). On the basis of chemical and spectral evidence, I—V were identified as 5,6,2′,6′-tetrahydroxy-7,8-dimethoxyflavone, 5,6,2′-trihydroxy-7,8,6′-trimethoxyflavone, 5,7,2′-trihydroxy-8-methoxyflavone 7-*O*-β-D-glucuronopyranoside, 2-(3-hydroxy-4-methoxyphenyl)ethyl 1-*O*-β-D-glucopyranoside and 2-(3-hydroxy-4-methoxyphenyl)ethyl 1-*O*-β-D-(4-*O*-feruloyl)glucopyranoside, respectively. Compound II has already been synthesized.

Keywords *Scutellaria prostrata*; Labiatae; phenylethanoid; flavonoid; structure elucidation

Scutellaria prostrata JACQ. *ex* BENTH. is a perennial herb of the Labiatae family, and is widely distributed in China, Nepal, Pakistan and India.[3]

As regards the constituents of this plant, no work has been reported. As part of our studies on Nepalese crude drugs and on the flavonoid constituents of the *Scutellaria* species, we have now examined this plant. As described in the experimental section, five new compounds (I—V) were isolated together with three known phenylethanoids (VI—VIII) and sixteen known flavonoids (IX—XXIV) from the ethanol extract of the root of this plant which was collected in Central Nepal. This paper deals with their structural identification.

Compounds I—III showed positive color reactions to Mg–HCl, and had absorption bands assignable to hydroxyls, conjugated carbonyl groups and aromatic rings in the infrared (IR) spectra.

Compound I was obtained as yellow needles, mp 274—275 °C (dec.), $C_{17}H_{14}O_8$. The ultraviolet (UV) spectrum of I was characteristic of the flavone series and showed a bathochromic shift by the addition of $AlCl_3$/HCl, indicating the presence of a free hydroxyl at the C-5 position.[4] In addition, the proton nuclear magnetic resonance (^{1}H-NMR) spectrum of I showed a signal at 12.45 ppm confirming the presence of a chelated hydroxyl. The ^{1}H-NMR spectrum also showed the presence of two methoxyls (3.82, 3.95 ppm), three hydroxyls (1H, 9.05 ppm; 2H, 9.90 ppm) and one C-3 proton (6.27 ppm). In the aromatic region of the spectrum, the remaining three protons appeared as a doublet (2H, 6.45 ppm, J=8.2 Hz) and a triplet (1H, 7.14 ppm, J=8.2 Hz). These signals could be assigned to C-3′,5′ and C-4′ protons, respectively, from their chemical shifts and coupling patterns.

Compound I was methylated with CH_2N_2 to give a trimethyl ether (Ia), mp 158 °C (dec.), $C_{20}H_{20}O_8$, which was identical with 5-hydroxy-6,7,8,2′,6′-pentamethoxyflavone prepared from skullcapflavone II (5,2′-dihydroxy-6,7,8,6′-tetramethoxyflavone)[5] by partial methylation with CH_2N_2. I is, therefore, a dimethyl ether of 5,6,7,8,2′,6′-hexahydroxyflavone.

In the carbon-13 nuclear magnetic resonance (^{13}C-NMR) spectrum of I, the methoxyl carbon signals appeared down field at 60.8 ppm and 61.6 ppm, indicating that these methoxyls were di-*ortho* substituted by two substituents.[6] This indicated that all the methoxyls were placed in the A-ring. The position of these methoxyls was determined by the long-range selective proton decoupling (LSPD) method[7] in the ^{13}C-NMR spectrum as follows. In the ^{1}H non-decoupling ^{13}C-NMR spectrum of I, one of the carbon singlet when the chelated hydroxyl proton at the C-5 position was selectively irradiated, indicating that the hydroxyl was present at the position *ortho* to the chelated position was selectively irradiated, indicating that the hydroxyl was present at the position *ortho* to the cheleted hydroxyl. The presence of a 5,6-dihydroxy system in I was also supported by the positive $SrCl_2$ test in an ammoniacal methanol solution of I.[8] These results led us to conclude that the methoxyls are present at C-7 and C-8 positions.

From these results, the structure of I was determined to be 5,6,2′,6′-tetrahydroxy-7,8-dimethoxyflavone.

Compound II was obtained as yellow needles, mp 224—225 °C (dec.), $C_{18}H_{16}O_8$, which was identified as 5,6,2′-trihydroxy-7,8,6′-trimethoxyflavone by comparing the physical properties and the ^{1}H-NMR spectral data with those reported by Iinuma *et al.*[9] Compound II has already been synthesized,[9] but this is the first isolation of II from a natural source.

Compound III was obtained as yellow needles, mp 257—259 °C (dec.), $C_{22}H_{20}O_{12}$. The UV spectrum and the diagnostic shifts suggested the presence of a hydroxyl at the C-5 position in the flavone nucleus.[4]

On methanolysis, III yielded scutevulin (5,7,2′-trihydroxy-8-methoxyflavone,[10] IIIa) and a sugar fraction, which was identified as methyl glucuronopyranoside methyl ester and the methyl glycoside of glucurono-6,3-lactone by gas-liquid chromatography (GLC). In the ^{1}H- and ^{13}C-NMR spectra of III, an anomeric proton signal at 5.25 ppm (d, J=7.3 Hz) and a set of carbon signals due to the sugar moiety including an anomeric carbon signal at 99.7 ppm indicated the presence of a β-glucuronopyranosyl unit

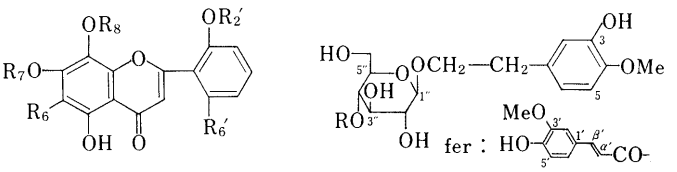

I : R_6=R_6'=OH, R_2'=H, R_7=R_8=Me
II : R_6=OH, R_6'=OMe, R_2'=H, R_7=R_8=Me
III : R_6=R_2'=R_6'=H, R_7=β-D-glu A, R_8=Me
glu A : glucuronopyranosyl

IV : R=H
V : R=fer

Fig. 1

in III. In the ^{13}C-NMR spectrum of III, the A-ring carbon signals coincided well with those of wogonin 7-*O*-glucuronide,[11] suggesting that III is a 7-*O*-glucuronide of IIIa. On methylation with CH_2N_2, III gave a monomethyl ether monomethyl ester, mp 205—206 °C (dec.), $C_{24}H_{24}O_{12}$, which was identified as 5,7-dihydroxy-8,2′-dimethoxyflavone 7-*O*-*β*-D-glucuronopyranoside methyl ester[12] by direct comparison with an authentic specimen.

Hence III was determined to be 5,7,2′-trihydroxy-8-methoxyflavone 7-*O*-*β*-D-glucuronopyranoside.

Compound IV was obtained as an amorphous powder, $[\alpha]_D^{31}$ −12.9° (MeOH), $C_{15}H_{22}O_8$. IV showed the absorption maxima at 219 (sh) and 280 nm in the UV spectrum and showed the absorption bands corresponding to the hydroxyl group and the benzene ring in the IR spectrum. The ^{1}H-NMR spectrum of IV revealed two methylene protons (2H, 2.70 ppm, m; 1H, 3.55 ppm, dt, J=6.6 and 9.2 Hz and 1H, 3.87 ppm, dt, J=7.0 and 9.2 Hz), one methoxyl (3.71 ppm), one hydroxyl (8.43 ppm) and sugar protons (2.92—4.16 ppm). In the aromatic region of the spectrum, there were two doublets (1H, 6.88 ppm, J=1.8 Hz and 1H, 6.79 ppm, J=8.1 Hz) and one broad doublet (1H, 6.60 ppm, J=8.1 Hz).

On enzymatic hydrolysis with *β*-glucosidase, IV afforded an aglycone (IVa), mp 70—71 °C, $C_9H_{12}O_3$, and glucose, which was proved to be the D-form according to the method reported by Oshima and Kumanotani.[13] IVa was identified as 3-hydroxy-4-methoxyphenethyl alcohol[14] by direct comparison with an authentic sample. In the ^{1}H- and ^{13}C-NMR spectra of IV, an anomeric proton signal at 4.16 ppm (d, J=8.1 Hz) and a set of carbon signals due to the sugar moiety including an anomeric carbon signal at 102.8 ppm indicated the presence of a *β*-glucopyranosyl unit in IV.

From these results, the structure of IV was determined to be 2-(3-hydroxy-4-methoxyphenyl)ethyl 1-*O*-*β*-D-glucopyranoside.

Compound V was obtained as an amorphous powder, $[\alpha]_D^{31}$ −31.2° (MeOH), $C_{25}H_{30}O_{11}$, and had absorption bands assignable to hydroxyl, *α*,*β*-unsaturated carbonyl groups and aromatic rings in the IR spectra.

On alkaline hydrolysis with 0.5 N KOH V afforded IV and *trans*-ferulic acid, which suggested V to be a mono-ferulate of IV. In the ^{13}C-NMR spectrum of V, the carbon signals due to the phenethyl alcohol moiety were observed to be almost superimposable on those of IV, suggesting that the acyl group in V was attached to the glucose moiety. In order to clarify the binding site of the acyl group, we used the acylation shifts[15] in ^{13}C-NMR spectroscopy. In the ^{13}C-NMR spectrum of V, the signals

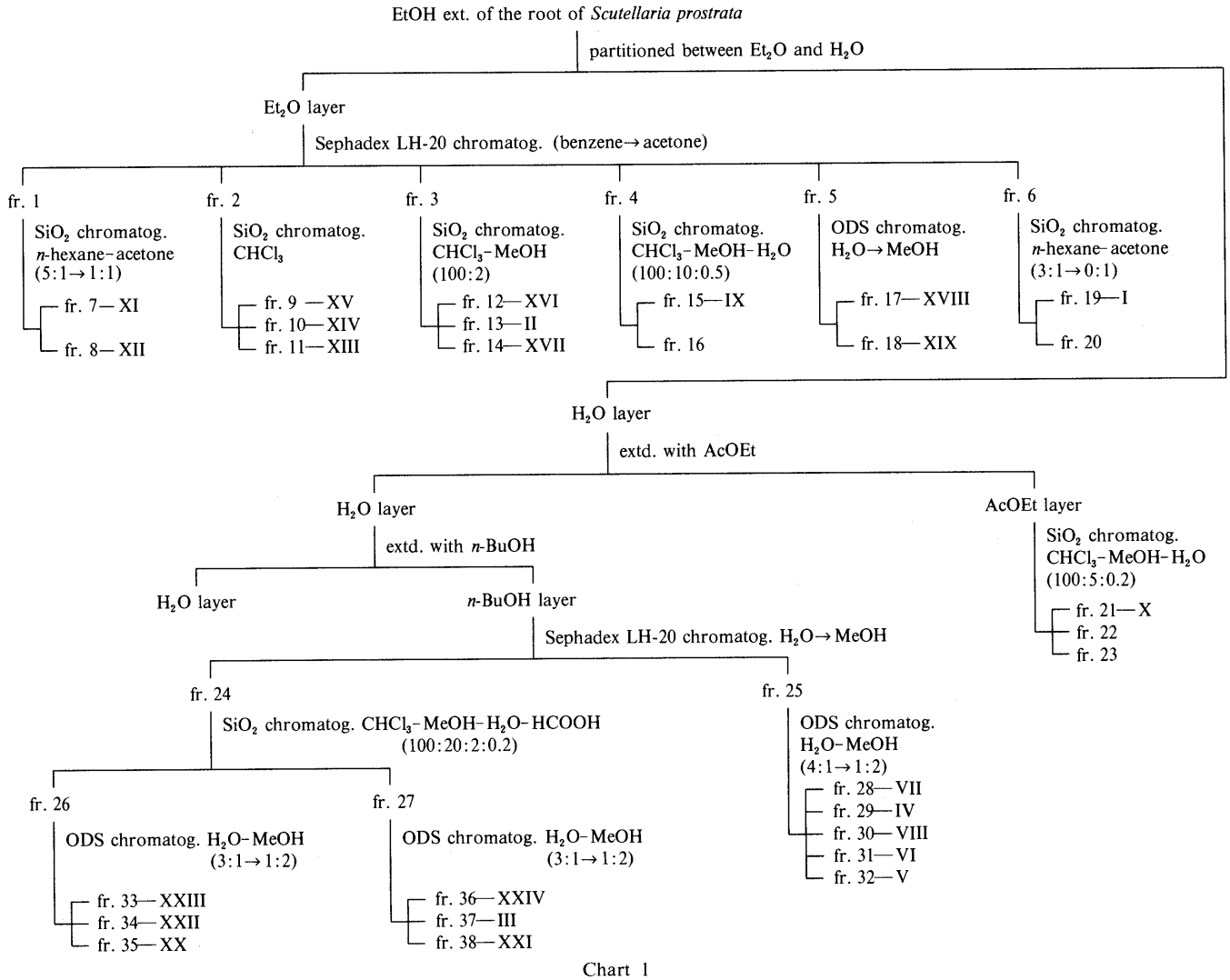

Chart 1

due to the C-3 and C-5 position of glucose were shifted upfield in comparison with those of IV, while other signals remained almost unaffected. These data indicated that the feruloyl group was linked to the C-4 position of glucose.

From these results, the structure of V was determined to be 2-(3-hydroxy-4-methoxyphenyl)ethyl 1-*O*-*β*-D-(4-*O*-feruloyl)glucopyranoside.

Compounds VI—VIII are known glycosides of phenylethanoid and IX—XXIV are known flavonoids, which were identified as martynoside (VI),[16,17] acteoside (VII),[16,18] leucosceptoside A (VIII),[16] 5,7-dihydroxy-2′-methoxyflavone[19] (IX), 5,7-dihydroxy-2′-methoxyflavone 7-*O*-glucuronide[19b,20] (X), oroxylin A[11] (XI), wogonin[11] (XII), rivularin[10] (XIII), skullcapflavone I[21] (XIV), chrysin[22] (XV), baicalein[23] (XVI), 5,7,4′-trihydroxy-8-methoxyflavone[11] (XVII), 5,7,2′-trihydroxyflavone[24] (XVIII), scutevulin[10] (XIX), chrysin 7-*O*-glucuronide[22] (XX), oroxylin A 7-*O*-glucuronide[25] (XXI), wogonin 7-*O*-glucuronide[11] (XXII), baicalin[23] (XXIII) and norwogonin 7-*O*-glucuronide[26] (XXIV), respectively, by direct comparison with authentic samples. Some biological activities of the isolated compounds are under investigation.

Experimental

General Procedures The instruments were the same as described in the previous paper[1] except for the following. NMR spectra were taken in dimethyl sulfoxide-d_6 (DMSO-d_6) on a JNM-GSX-400 spectrometer (^{1}H-NMR at 400 MHz and ^{13}C-NMR at 100 MHz). GLC was run on a Shimadzu GC-6AM unit with a flame ionization detector. GLC-1: column, a glass column (2 m × 4 mm i.d.) packed with 5% SE-30 on Chromosorb W (60—80 mesh); column temperature, programmed from 150 °C (20 min hold) to 240 °C at 5 °C/min. GLC-2: column, a fused-silica WCOT column with Carbowax 20M (Shinwa Kako Co., 25 m × 0.2 mm); column temperature, programmed from 110 °C (1 min hold) to 170 °C (10 min hold) at 2 °C/min (lit.,[13] 158 °C). Thin layer chromatography (TLC) was carried out on Kieselgel 60F-254 (Merck) with the following solvent systems: $CHCl_3$–MeOH–H_2O–AcOH (100 : 10 : 1 : 0.3) (TLC-1), benzene–AcOEt–AcOH (100 : 60 : 0.5) (TLC-2), $CHCl_3$–MeOH–H_2O–HCOOH (25 : 8 : 1 : 0.5) (TLC-3), AcOEt–methyl ethyl ketone–H_2O–HCOOH (6 : 3 : 1 : 1) (TLC-4). Spots were detected by spraying dil. H_2SO_4 followed by heating.

Extraction and Separation As shown in Chart 1, twenty-four compounds, I (50 mg), II (100 mg), III (20 mg), IV (60 mg), V (80 mg), VI (270 mg), VII (150 mg), VIII (230 mg), IX (30 mg), X (30 mg), XI (30 mg), XII (70 mg), XIII (50 mg), XIV (20 mg), XV (40 mg), XVI (200 mg), XVII (20 mg), XVIII (15 mg), XIX (15 mg), XX (30 mg), XXI (20 mg), XXII (50 mg), XXIII (800 mg) and XXIV (20 mg) were obtained from the dried root of *Scutellaria prostrata* (1.5 kg) collected in Nepal in 1986.

I (5,6,2′,6′-Tetrahydroxy-7,8-dimethoxyflavone) Yellow needles (MeOH), mp 274—275 °C (dec.). *Anal.* Calcd for $C_{17}H_{14}O_8$: C, 58.96; H, 4.08. Found: C, 59.03; H, 4.16. EI-MS *m/z* (%): 346 (M^+, 80), 331 ($M^+ - CH_3$, 100), 197 ($C_8H_5O_6$, 65). Mg–HCl (+), $SrCl_2$ (+). *Rf*: 0.28 (TLC-1), 0.30 (TLC-2). UV λ_{max}^{MeOH} nm (log ε): 231 sh (4.26), 278 (4.30), 318 sh (3.93), 372 sh (3.47); $\lambda_{max}^{MeOH-NaOMe}$ nm (log ε): 245 sh (4.20), 288 (4.03), 349 (3.83), 380 sh (3.70); $\lambda_{max}^{MeOH-AlCl_3}$ nm (log ε): 232 sh (4.31), 295 (4.28), 345 (4.08), 420 (3.45); $\lambda_{max}^{MeOH-AlCl_3-HCl}$ nm (log ε): 292 (4.29), 335 (4.05), 420 (3.41); $\lambda_{max}^{MeOH-NaOAc}$ nm (log ε): 278 (4.27), 321 sh (3.89); $\lambda_{max}^{MeOH-NaOAc-H_3BO_3}$ nm (log ε): 279 (4.33), 326 (3.73), 387 sh (3.37). IR ν_{max}^{KBr} cm^{-1}: 3388 (OH), 1662 (conjugated CO), 1626 (arom. C=C). ^{1}H-NMR: 3.82, 3.95 (each 3H, each s, OCH_3 × 2), 6.27 (1H, s, 3-H), 6.45 (2H, d, *J* = 8.2 Hz, 3′,5′-H), 7.14 (1H, t, *J* = 8.2 Hz, 4′-H), 9.90 (2H, s, 2′,6′-OH), 9.05 (1H, s, 6-OH), 12.45 (1H, s, 5-OH). ^{13}C-NMR: 162.6 (C-2), 111.2 (C-3), 182.5 (C-4), 142.9 (C-5), 133.8 (C-6), 147.9 (C-7), 132.7 (C-8), 142.8 (C-9), 106.1 (C-10), 108.2 (C-1′), 156.6 (C-2′,6′), 106.5 (C-3′,5′), 132.7 (C-4′), 60.8, 61.6 (OCH_3 × 2).

Methylation of I: I was methylated with CH_2N_2 to give a trimethyl ether (Ia), yellow needles (MeOH), mp 158 °C (dec.). *Anal.* Calcd for $C_{20}H_{20}O_8$: C, 61.85; H, 5.19. Found: C, 61.73; H, 5.22. EI-MS *m/z* (%): 388 (M^+, 75), 373 ($M^+ - CH_3$, 100), 211 ($C_9H_7O_6$, 30). Mg–HCl (+). *Rf*: 0.80 (TLC-1), 0.60 (TLC-2). UV λ_{max}^{MeOH} nm (log ε): 268 (4.37), 310 sh (3.90), 350 sh (3.63); $\lambda_{max}^{MeOH-AlCl_3}$ nm (log ε): 281 (4.34), 300 sh (4.19), 327 (4.01), 405 (3.64). IR ν_{max}^{KBr} cm^{-1}: 3480 (OH), 1664 (conjugated CO), 1620, 1582 (arom. C=C). ^{1}H-NMR: 3.79 (9H, s, OCH_3 × 3), 3.83, 4.02 (each 3H, each s, OCH_3 × 2), 6.37 (1H, s, 3-H), 6.83 (2H, d, *J* = 8.3 Hz, 3′,5′-H), 7.53 (1H, t, *J* = 8.3 Hz, 4′-H), 12.60 (1H, s, 5-OH). ^{13}C-NMR: 162.0 (C-2), 112.2 (C-3), 182.7 (C-4), 146.4 (C-5), 136.1 (C-6), 152.9 (C-7), 132.8 (C-8), 148.8 (C-9), 106.4 (C-10), 110.2 (C-1′), 158.3 (C-2′,6′), 104.6 (C-3′,5′), 133.2 (C-4′), 56.2 (C-2′,6′-O$\underline{C}$H$_3$), 60.6, 60.8, 61.6 (OCH_3 × 3). Ia was identical (TLC, UV, IR, ^{1}H- and ^{13}C-NMR, mixed fusion) with 5-hydroxy-6,7,8,2′,6′-pentamethoxyflavone prepared from skullcapflavone II (5,2′-dihydroxy-6,7,8,6′-tetramethoxyflavone)[5] by methylation with CH_2N_2.

II (5,6,2′-Trihydroxy-7,8,6′-trimethoxyflavone) Yellow needles (MeOH), mp 224—225 °C (dec.). *Anal.* Calcd for $C_{18}H_{16}O_8$: C, 60.00; H, 4.48. Found: C, 60.12; H, 4.46. EI-MS *m/z* (%): 360 (M^+, 70), 345 ($M^+ - CH_3$, 100), 197 ($C_8H_5O_6$, 50). Mg–HCl (+), $SrCl_2$ (+). *Rf*: 0.45 (TLC-1), 0.36 (TLC-2). UV λ_{max}^{MeOH} nm (log ε): 277 (4.27), 317 sh (3.88), 368 sh (3.44); $\lambda_{max}^{MeOH-AlCl_3}$ nm (log ε): 293 (4.20), 346 (3.96), 418 sh (3.43); $\lambda_{max}^{MeOH-AlCl_3-HCl}$ nm (log ε): 292 (4.22), 338 (3.96), 430 (3.31); $\lambda_{max}^{MeOH-NaOAc}$ nm (log ε): 276 (4.21), 368 sh (3.58); $\lambda_{max}^{MeOH-NaOAc-H_3BO_3}$ nm (log ε): 277 (4.30), 368 sh (3.44). IR ν_{max}^{KBr} cm^{-1}: 3384 (OH), 1662 (conjugated CO), 1622 (arom. C=C). ^{1}H-NMR: 3.75, 3.80, 3.95 (each 3H, each s, OCH_3 × 3), 6.28 (1H, s, 3-H), 6.62 (2H, d, *J* = 8.2 Hz, 3′,5′-H), 7.32 (1H, t, *J* = 8.2 Hz, 4′-H), 9.13 (1H, br s, 6-OH), 10.13 (1H, s, 2′-OH), 12.40 (1H, s, 5-OH). ^{13}C-NMR: 162.0 (C-2), 111.4 (C-3), 182.4 (C-4), 143.0 (C-5), 134.0 (C-6), 148.0 (C-7), 132.8 (C-8), 142.8 (C-9), 106.1 (C-10), 109.0 (C-1′), 156.5 (C-2′), 108.7 (C-3′), 132.3 (C-4′), 102.2 (C-5′), 158.2 (C-6′), 55.8 (C-6′-O$\underline{C}$H$_3$), 60.9, 61.6 (OCH_3 × 2).

III (5,7,2′-Trihydroxy-8-methoxyflavone 7-*O*-*β*-D-Glucuronopyranoside Yellow needles (MeOH), mp 257—259 °C (dec.). $[\alpha]_D^{31}$ −101° (*c* = 0.04, MeOH). *Anal.* Calcd for $C_{22}H_{20}O_{12}$: C, 55.46; H, 4.23. Found: C, 55.38; H, 4.06. EI-MS *m/z* (%): 300 ($C_{16}H_{12}O_6$, 50), 285 ($C_{15}H_9O_6$, 100). FAB-MS *m/z* (%): 477 ($M^+ + 1$, 35), 301 ($C_{16}H_{12}O_6 + 1$, 100). Mg–HCl (+). *Rf*: 0.40 (TLC-3), 0.48 (TLC-4). UV λ_{max}^{MeOH} nm (log ε): 275 (4.26), 342 (3.93); $\lambda_{max}^{MeOH-NaOMe}$ nm (log ε): 233 sh (4.24), 261 sh (4.19), 272 (4.22), 387 (4.07); $\lambda_{max}^{MeOH-AlCl_3}$ nm (log ε): 284 (4.25), 297 (4.22), 353 (4.00), 382 sh (3.81); $\lambda_{max}^{MeOH-AlCl_3-HCl}$ nm (log ε): 284 (4.26), 298 (4.21), 350 (4.10), 383 sh (3.80); $\lambda_{max}^{MeOH-NaOAc}$ nm (log ε): 213 (4.62), 218 sh (4.61), 275 (4.38), 341 (4.04); $\lambda_{max}^{MeOH-NaOAc-H_3BO_3}$ nm (log ε): 214 (4.64), 219 sh (4.63), 275 (4.33), 345 (4.00). IR ν_{max}^{KBr} cm^{-1}: 3456 (OH), 1736 (COOH), 1654 (conjugated CO), 1616 (arom. C=C). ^{1}H-NMR: 3.85 (3H, s, 8-OCH_3), 3.31—3.98 (m, sugar moiety), 5.25 (1H, d, *J* = 7.3 Hz, anomeric H of glucuronic acid unit), 6.69 (1H, s, 6-H), 7.14 (1H, s, 3-H), 7.04 (1H, br t, *J* = 7.4 Hz, 5′-H), 7.08 (1H, br d, *J* = 8.4 Hz, 3′-H), 7.42 (1H, dt, *J* = 1.5, 7.7 Hz, 4′-H), 7.88 (1H, dd, *J* = 1.5, 8.1 Hz, 6′-H), 12.61 (1H, s, 5-OH). ^{13}C-NMR: 161.7 (C-2), 109.0 (C-3), 182.4 (C-4), 155.9 (C-5), 98.4 (C-6), 155.9 (C-7), 129.2 (C-8), 149.2 (C-9), 105.1 (C-10), 117.2 (C-1′), 157.1 (C-2′), 117.1 (C-3′), 133.1 (C-4′), 119.6 (C-5′), 128.3 (C-6′), 99.7 (C-1″), 72.9 (C-2″), 75.2 (C-3″), 71.4 (C-4″), 75.9 (C-5″), 170.4 (C-6″), 61.4 (C-8-O$\underline{C}$H$_3$).

Methanolysis of III: A solution of III (10 mg) in 10% HCl–MeOH (2 ml) was heated under reflux on a water bath for 3 h. The reaction mixture was neutralized with Ag_2CO_3. The precipitates were filtered off and the filtrate was concentrated to give the residue, which was chromatographed on silica gel using benzene as an eluent to give yellow needles (MeOH), mp 278 °C (dec.). This product was identified as scutevulin[10] by direct comparisons (TLC, UV, IR, ^{1}H- and ^{13}C-NMR, mixed fusion) with an authentic specimen. The mother liquor of crystallization was shown to contain methyl glucuronopyranoside methyl ester [t_R 13 min 24 s (both α and β)] and the methyl glycoside of glucurono-6,3-lactone [t_R 6 min 05 s (α, trace), 6 min 48 s (β)] by GLC-1 (as the trimethylsilyl (TMS) ether derivatives).

Methylation of III: III was methylated with CH_2N_2 to give pale yellow needles (MeOH), mp 205—206 °C (dec.), $C_{24}H_{24}O_{12}$, which was identified as 5,7-dihydroxy-8,2′-dimethoxyflavone 7-*O*-*β*-D-glucuronopyranoside methyl ester[12] by direct comparison with an authentic specimen.

IV (2(3-Hydroxy-4-methoxyphenyl)ethyl 1-*O*-*β*-D-Glucopyranoside) Amorphous powder. $[\alpha]_D^{31}$ −12.9° (*c* = 0.33, MeOH). *Anal.* Calcd for $C_{15}H_{22}O_8$: C, 54.54; H, 6.71. Found: C, 54.68; H, 6.83. EI-MS *m/z* (%): 330 (M^+, 2), 137 ($C_8H_9O_2$, 100). FAB-MS *m/z* (%): 353 ($M^+ + Na$, 23), 331 ($M^+ + 1$, 20). *Rf*: 0.45 (TLC-3), 0.27 (TLC-4). UV λ_{max}^{MeOH} nm (log ε): 219 sh (4.30), 280 (3.93). IR ν_{max}^{KBr} cm^{-1}: 3460 (OH), 1596 (arom. C=C). ^{1}H-NMR: 2.70 (2H, m, β-H), 2.92—3.49 (m, sugar moiety), 3.55 (1H, dt, *J* = 6.6, 9.2 Hz, α-H), 3.71 (3H, s, 4-OCH_3), 3.87 (1H, dt, *J* = 7.0, 9.2 Hz, α-H), 4.16 (1H, d, *J* = 8.1 Hz, anomeric H of glucose unit), 6.60 (1H, br d, *J* = 8.1 Hz, 6-H), 6.68 (1H, d, *J* = 1.8 Hz, 2-H), 6.79 (1H, d, *J* = 8.1 Hz, 5-H), 8.43 (1H, br s, 3-OH). ^{13}C-NMR: 131.3 (C-1), 116.3 (C-2), 146.4 (C-3), 146.1 (C-4), 112.9 (C-5), 119.3 (C-6), 69.8 (C-α), 35.1 (C-β), 102.8 (C-1″), 73.5 (C-2″), 76.9 (C-3″), 70.1 (C-4″), 76.8 (C-5″), 61.1 (C-6″), 55.7

(C-4-O$\underline{C}$H$_3$).

Enzymatic Hydrolysis of IV: A solution containing IV (20 mg) and β-glucosidase (20 mg, from almond, Sigma) (pH 5.0 dil. HCOOH, 20 ml) was incubated at 37 °C for 15 h. After cooling, the reaction mixture was extracted with AcOEt. The organic layer was washed with water and concentrated to give the residue, which was recrystallized from MeOH/H_2O to give colorless needles (5 mg), mp 70—71 °C. This product was identical with 3-hydroxy-4-methoxyphenethyl alcohol[14] by direct comparison (UV, IR, ^{1}H- and ^{13}C-NMR). The H_2O layer was concentrated to dryness and extracted with MeOH. The MeOH-soluble portion was concentrated and the residue was passed through an RP-8 column with H_2O to give a syrup, which was shown to contain D-glucose by GLC-2 [as the TMS-MBA-alditol, t_R 25 min 00 s (TMS-MBA-D-glucitol, t_R 25 min 00 s; TMS-MBA-L-glucitol, t_R 24 min 52 s)].

V (2-(3-Hydroxy-4-methoxyphenyl)ethyl 1-*O*-β-D-(4-*O*-Feruloyl)glucopyranoside) Amorphous powder. $[\alpha]_D^{31}$ −31.2° (c=0.33, MeOH). *Anal.* Calcd for $C_{25}H_{30}O_{11}$: C, 59.28; H, 5.97. Found: C, 59.44; H, 6.04. EI-MS m/z (%): 207 ($C_7H_{11}O_7$, 66), 150 ($C_9H_{10}O_2$, 100), 137 ($C_8H_9O_2$, 40). FAB-MS m/z (%): 529 (M^++Na, 8), 507 (M^++1, 15). *Rf*: 0.67 (TLC-3), 0.69 (TLC-4). UV λ_{max}^{MeOH} nm (log ε): 220 sh (4.11), 231 (4.03), 291 sh (3.90), 330 (4.06). IR ν_{max}^{KBr} cm^{-1}: 3470 (OH), 1703 (α,β-unsaturated CO), 1600 (arom. C=C). ^{1}H-NMR: 2.74 (2H, m, β-H), 3.35—3.48 (m, sugar moiety), 3.62 (1H, dt, J=7.0, 9.6 Hz, α-H), 3.73 (3H, s, 4-OCH$_3$), 3.82 (3H, s, 3′-OCH$_3$), 3.91 (1H, dt, J=7.3, 9.6 Hz, α-H), 4.30 (1H, d, J=7.7 Hz, anomeric H of glucose unit), 4.60 (1H, t, J=9.5 Hz, 4″-H), 6.47 (1H, d, J=15.8 Hz, α′-H), 6.63 (1H, dd, J=1.8, 8.1 Hz, 6-H), 6.69 (1H, d, J=1.8 Hz, 2-H), 6.80 (1H, d, J=8.1 Hz, 5′-H), 6.81 (1H, d, J=8.1 Hz, 5-H), 7.12 (1H, dd, J=1.8, 8.1 Hz, 6′-H), 7.33 (1H, d, J=1.8 Hz, 2′-H), 7.55 (1H, d, J=15.8 Hz, β′-H), 8.78 (1H, s, 3-OH), 9.58 (1H, s, 4′-OH). ^{13}C-NMR: 131.1 (C-1), 116.3 (C-2), 146.3 (C-3), 146.1 (C-4), 112.3 (C-5), 119.4 (C-6), 70.0 (C-α), 35.0 (C-β), 102.8 (C-1″), 73.6 (C-2″), 74.1 (C-3″), 71.3 (C-4″), 74.7 (C-5″), 60.9 (C-6″), 125.6 (C-1′), 111.1 (C-2′), 147.9 (C-3′), 149.4 (C-4′), 115.5 (C-5′), 123.2 (C-6′), 145.3 (C-β′), 114.5 (C-α′), 166.0 (CO), 55.7 (C-4, 3′-O$\underline{C}$H$_3$).

Alkaline Hydrolysis of V: A solution of V (20 mg) in 0.5 N KOH was heated on a water bath at 70 °C for 1 min. The reaction mixture was neutralized with dil. HCl and concentrated to give a residue. The residue was chromatographed on silica gel, and successively eluted with $CHCl_3$–MeOH–H_2O–HCOOH (25:4:0.4:0.2) (solvent-1) and (25:6:0.6:0.3) (solvent-2). The solvent-1 eluate was concentrated and recrystallized from MeOH/H_2O to give colorless needles, mp 168 °C. This product was identical with ferulic acid by direct comparison (TLC, UV, IR and mixed fusion). The solvent-2 eluate was concentrated to give colorless amorphous (10 mg); this product was identified as IV by comparison with an authentic sample (TLC, UV, IR, ^{1}H- and ^{13}C-NMR).

Identification of VI—XXIV: VI (amorphous powder), VII (amorphous powder), VIII (amorphous powder), IX (mp 266—267 °C, dec.), X (mp 198—199 °C, dec.), XI (mp 202 °C, dec.), XII (mp 203 °C), XIII (mp 259 °C), XIV (mp 253 °C), XV (mp 285 °C), XVI (mp 255 °C), XVII (mp 302 °C), XVIII (mp 284 °C), XIX (mp 278 °C, dec.), XX (mp 226 °C, dec.), XXI (mp 169—170 °C, dec.), XXII (mp 270 °C, dec.), XXIII (mp 230 °C, dec.), XXIV (mp 245 °C, dec.) were identified as martynoside,[16,17] acteoside,[16,18] leucosceptoside A,[16] 5,7-dihydroxy-2′-methoxyflavone,[19] 5,7-dihydroxy-2′-methoxyflavone 7-*O*-glucuronide,[19b,20] oroxylin A,[11] wogonin,[11] rivularin,[10] skullcapflavone I,[21] chrysin,[22] baicalein,[23] 5,7,4′-trihydroxy-8-methoxyflavone,[11] 5,7,2′-trihydroxyflavone,[24] scutevulin,[10] chrysin 7-*O*-glucuronide,[22] oroxylin A 7-*O*-glucuronide,[25] wogonin 7-*O*-glucuronide,[11] baicalin[23] and norwogonin 7-*O*-glucuronide,[26] respectively, by direct comparison with authentic specimens (UV, IR, ^{1}H- and ^{13}C-NMR).

Acknowledgements We are grateful to Mrs. R. Igarashi and Miss A. Nakashima of this university for elemental analysis and EI and FAB-MS measurements. This work was supported in part by a Grant-in-Aid (No. 61041032) for Scientific Research from the Ministry of Education, Science and Culture of Japan.

References and Notes

1) Part XI: T. Tomimori, Y. Miyaichi, Y. Imoto, H. Kizu and T. Namba, *Chem. Pharm. Bull.*, **36**, 3654 (1988).
2) Presented at the 109th Annual Meeting of the Pharmaceutical Society of Japan, Nagoya, April 1989 and the 36th Annual Meeting of the Japanese Society of Pharmacognosy, Kumamoto, October 1989.
3) Mukerjee, *Rec. B. Surv. Ind.*, **14**, 140 (1940); O. Polunin and A. Stainton, "Flowers of the Himalaya," Oxford University Press, New Delhi, 1984, p. 323.
4) T. J. Mabry, K. R. Markham and M. B. Thomas, "The Systematic Identification of Flavonoids," Springer-Verlag, New York, 1970, Chapter V.
5) T. Tomimori, Y. Miyaichi, Y. Imoto, H. Kizu and Y. Tanabe, *Yakugaku Zasshi*, **104**, 524 (1983).
6) K. S. Dhami and J. B. Stothers, *Can. J. Chem.*, **44**, 2855 (1966); K. Panichpol and P. G. Waterman, *Phytochemistry*, **17**, 1363 (1978).
7) Y. Shirataki, I. Yokoe, M. Endo and M. Komatsu, *Chem. Pharm. Bull.*, **33**, 444 (1985); H. Komura, K. Mizukawa, H. Minakata, H. Huang, G. Qin and R. Xu, *ibid.*, **31**, 4206 (1983); H. Komura, K. Mizukawa and H. Minakata, *Bull. Chem. Soc. Jpn.*, **55**, 3053 (1982).
8) M. Shimizu and N. Morita, *Yakugaku Zasshi*, **88**, 1450 (1968).
9) M. Iinuma and S. Matsuura, *Yakugaku Zasshi*, **99**, 657 (1979).
10) Y. Miyaichi, Y. Imoto, T. Tomimori and C. C. Lin, *Chem. Pharm. Bull.*, **35**, 3720 (1987).
11) Y. Miyaichi, Y. Imoto, T. Tomimori and T. Namba, *Chem. Pharm. Bull.*, **36**, 2371 (1988).
12) T. Tomimori, Y. Imoto and Y. Miyaichi, *Chem. Pharm. Bull.*, **38**, 3488 (1990).
13) R. Oshima and J. Kumanotani, *J. Chromatogr.*, **259**, 159 (1983).
14) H. Sasaki, H. Taguchi, T. Endo, I. Yoshioka, K. Higashiyama and H. Otomasu, *Chem. Pharm. Bull.*, **26**, 2111 (1978).
15) K. Markham, B. Ternai, R. Stanley, H. Geiger and T. Mabry, *Tetrahedron*, **34**, 1389 (1978); T. Yoshida, T. Saito and S. Kadoya, *Chem. Pharm. Bull.*, **35**, 97 (1987); K. Yamasaki, R. Kasai, Y. Masaki, M. Okihara and O. Tanaka, *Tetrahedron Lett.*, **1977**, 1231.
16) T. Miyase, A. Koizumi, A. Ueno, T. Noro, M. Kuroyanagi, S. Fukushima, Y. Akiyama and T. Takemoto, *Chem. Pharm. Bull.*, **30**, 2732 (1982).
17) S. Takagi, M. Yamaki and K. Inoue, *Yakugaku Zasshi*, **101**, 899 (1981).
18) M. Kikuchi and Y. Yamauchi, *Yakugaku Zasshi*, **105**, 542 (1985).
19) *a*) T. P. Popova, V. I. Litvinenko and D. A. Pakaln, *Farm. Zh (Kiev)*, **6**, 49 (1979); *b*) T. P. Popova, V. I. Litvinenko, V. G. Gordienko and D. A. Pakaln, *Khim. Prir. Soedin*, **12**, 730 (1976).
20) J. E. Watkin, *Aspects Plant Phenolic Chem., Proc. Symp., 3rd, Uiniv. of Toronto*, **1963**, 39 (1964).
21) T. Tomimori, Y. Miyaichi, Y. Imoto and H. Kizu, *Shoyakugaku Zasshi*, **38**, 249 (1984).
22) Y. Miyaichi, Y. Imoto, H. Kizu and T. Tomimori, *Shoyakugaku Zasshi*, **42**, 205 (1988).
23) T. Tomimori, Y. Miyaichi, Y. Imoto, H. Kizu and T. Namba, *Chem. Pharm. Bull.*, **33**, 4457 (1985).
24) T. Tomimori, Y. Miyaichi, Y. Imoto and H. Kizu, *Shoyakugaku Zasshi*, **40**, 432 (1986).
25) T. Tomimori, Y. Miyaichi and H. Kizu, *Yakugaku Zasshi*, **102**, 388 (1982).
26) T. Tomimori, Y. Miyaichi, Y. Imoto, H. Kizu and T. Namba, *Chem. Pharm. Bull.*, **34**, 406 (1986).

Studies on the Nepalese Crude Drugs. XIII.[1] On the Flavonoid and Iridoid Constituents of the Root of *Scutellaria grossa* WALL[2]

Yuichi KIKUCHI, Yukinori MIYAICHI and Tsuyoshi TOMIMORI*

School of Pharmacy, Hokuriku University, 3 Ho, Kanagawa-machi, Kanazawa, 920-11, Japan. *Received September 26, 1990*

From the root of *Scutellaria grossa* WALL, three new natural flavonoids (I—III) were isolated, together with fifteen known flavonoids (IV, VIII—XXI), two iridoids (V and VI) and *trans*-cinnamic acid (VII). The structures of I—III were shown to be 5-hydroxy-7,8,2′,6′-tetramethoxyflavone, 5,6,2′-trihydroxy-7,8-dimethoxyflavone and (2*S*)-5-hydroxy-7,8,2′,6′-tetramethoxyflavonone, respectively, on the basis of the chemical and spectral data. Compound I has a already been synthesized.

Keywords *Scutellaria grossa*; Labiatae; flavonoid; iridoid; structure elucidation

Scutellaria grossa WALL is an annual herb of the Labiatae family, and is widely distributed in Nepal, Bhutan and India.[3]

As regards the constituents of this plant, no work has been reported. As part of our studies on the Nepalese crude drugs and on the flavonoid constituents of the *Scutellaria* species, we have now examined this plant. As described in the experimental section, three new natural flavonoids (I—III) were isolated together with fifteen known flavonoids (IV and VIII—XXI), two iridoids (V and VI) and *trans*-cinnamic acid (VII) from the ethanol extract of the root of this plant which was collected in central Nepal. This paper deals with their structural identification.

Compounds I—IV showed positive color reactions to Mg–HCl, and had absorption bands assignable to hydroxyls, conjugated carbonyl groups and aromatic rings in the infrared (IR) spectra.

Compound I was obtained as pale yellow needles, mp 199 °C (dec.), $C_{19}H_{18}O_7$. The ultraviolet (UV) spectrum of I was characteristic of the flavone series, and showed a bathochromic shift by the addition of $AlCl_3$–HCl indicating the presence of a free hydroxyl at the C-5 position.[4] The proton nuclear magnetic resonance (^{1}H-NMR) spectrum of I showed the presence of four methoxyls (each 3H, δ 3.70, 3.92; 6H, δ 3.80), one chelated hydroxyl (δ 12.63) and one C-3 proton (δ 6.32). In the aromatic region of the spectrum, the remaining four protons appeared as a singlet (1H, δ 6.62) for the A-ring proton and a doublet (2H, δ 6.83, J=8.3 Hz) and a triplet (1H, δ 7.52, J=8.3 Hz) for the B-ring protons. The latter two signals could be assigned to C-3′, 5′ and C-4′ protons, respectively, from their chemical shifts and coupling patterns. In the carbon-13 nuclear magnetic resonance (^{13}C-NMR) spectrum of I, the carbon signal of one of the four methoxyls appeared down field at δ 61.0, indicating that the methoxyl was di-*ortho* substituted by two substituents.[5] These data suggested that I was a 5-hydroxy-7,2′,6′-trimethoxyflavone derivative with a methoxyl at the C-6 or C-8 position. The position of the methoxyl was determined by the long-range selective proton decoupling (LSPD) method[6] in the ^{13}C-NMR spectrum as follows. In the ^{1}H non-decoupling ^{13}C-NMR spectrum of I, the signal of the carbon attached to an isolated aromatic hydrogen was observed at δ 96.2 (J=7.4 and 162.5 Hz), which changed to a doublet when the chelated hydroxyl proton at the C-5 position was selectively irradiated, indicating that the isolated aromatic proton was present at the position *ortho* to the chelated hydroxyl, *i.e.*, no substituent was present at the C-6 position. These results led us to conclude that the methoxyl is present at the C-8 position.

I was, therefore, determined to be 5-hydroxy-7,8,2′,6′-tetramethoxyflavone.

This is the first report on the isolation of I from natural sources, although I has already been synthesized by us from rivularin (5,2′-dihydroxy-7,8,6′-trimethoxyflavone)[1] by partial methylation.[7]

Compound II was obtained as yellow needles, mp 249—250 °C, $C_{17}H_{14}O_7$. The UV spectrum and the diagnostic shifts suggested the presence of a hydroxyl at the C-5 position in the flavone nucleus.[4] The ^{1}H-NMR spectrum of II showed the presence of two methoxyls (δ 3.90, 3.96), two hydroxyls (1H, δ 9.11; 1H, δ 10.84), one chelated hydroxyl (δ 12.43) and one C-3 proton (δ 7.09). In the aromatic region of the spectrum, the remaining four protons appeared as a multiplet (2H, δ 7.04), a double triplet (1H, δ 7.42, J=1.8 and 7.9 Hz) and a double doublet (1H, δ 7.87, J=1.5 and 8.1 Hz). These signals could be assigned to C-3′, 5′, C-4′ and C-6′ protons, respectively, from their chemical shifts and coupling patterns. In the ^{13}C-NMR spectrum of II, the methoxyl carbon signals appeared down field at δ 60.9 and 61.8, indicating that these methoxyls were di-*ortho* substituted by two substituents.[5] These data suggested that all the methoxyls were placed in the A-ring. In the ^{1}H non-decoupling ^{13}C-NMR spectrum of II, one of the carbon signals attached to a hydroxyl was observed at δ 134.1 in the form of a doublet (J=4.7 Hz), which changed to a singlet by LSPD as in the case of I. The methoxyls could therefore, be proven to be placed at the C-7 and C-8 positions. The arrangement of substituents in the A-ring was further confirmed by the ^{13}C-NMR spectrum, in which the carbon signals due to the A-ring of II were almost superimposable on those of 5,6,2′,6′-tetrahydroxy-7,8-dimethoxyflavone.[1]

Thus, the structure of II was established as 5,6,2′-trihydroxy-7,8-dimethoxyflavone.

Compound III was obtained as colorless needles, mp 137 °C, $C_{19}H_{20}O_7$. The UV spectrum of III was characteristic of the 5-hydroxyflavanone series.[4] The flavanone nucleus was also confirmed by the ^{1}H-NMR spectrum, in which the signals due to the C-3 and C-2 protons were observed as an AMX type at δ 2.57 (1H, dd, J=3.3 and 17.2 Hz), δ 3.80 (1H, dd, J=13.2 and 17.2 Hz) and δ 5.98

(1H, dd, $J=3.3$ and 13.2 Hz). The ^{1}H-NMR spectrum further showed the presence of four methoxyls (each 3H, δ 3.52, 3.84; 6H, δ 3.78) and one chelated hydroxyl (δ 12.12). In the aromatic region of the spectrum, the remaining four protons appeared as a singlet (1H, δ 6.22) for the A-ring proton and a doublet (2H, δ 6.74, $J=8.4$ Hz) and a triplet (1H, δ 7.37, $J=8.4$ Hz) for the B-ring protons. These signals for the B-ring could be assigned to C-3′, 5′ and C-4′ protons, respectively, from their chemical shifts and coupling patterns. An isolated aromatic hydrogen in the A-ring was confirmed to be present at the C-6 position by the LSPD method as in the case of I. These findings indicated III to be 5-hydroxy-7,8,2′,6′-tetramethoxyflavanone.

It is known that flavanones having (2*S*)-configuration exhibit a positive Cotton effect due to n–π^* transition (*ca.* 330 nm) and a negative Cotton effect due to π–π^* transition (270—290 nm) in the circular dichroism (CD) spectra.[8] The CD curve of III exhibited positive and negative maxima at 307 and 279 nm, respectively, which established the (2*S*)-configuration.

The structure of III was finally confirmed by direct comparison with an authentic sample prepared from (2*S*)-5,2′-dihydroxy-7,8,6′-trimethoxyflavanone[9] by partial methylation with CH_2N_2.

Thus, III was determined to be (2*S*)-5-hydroxy-7,8,2′,6′-tetramethoxyflavanone.

Compound IV was obtained as yellow needles, mp 197 °C (dec.), $C_{21}H_{18}O_{11}$. The UV spectrum of IV was characteristic of the 5-hydroxy flavone series.[4] On methanolysis, IV yielded baicalein[1] (5,6,7-trihydroxyflavone, XIII), and a sugar fraction, which was identified as methyl glucuronopyranoside methyl ester and the methyl glycoside of glucurono-6,3-lactone by gas-liquid chromatography (GLC). In the ^{1}H- and ^{13}C-NMR spectra of IV, an anomeric proton signal at δ 4.94 (d, $J=7.7$ Hz) and a set of carbon signals due to the sugar moiety including an anomeric carbon signal at δ 103.7 indicated the presence of a β-glucuronopyranosyl unit in IV.

The linkage of the sugar to the aglycone was determined by the comparison of the ^{13}C-NMR spectrum of IV with that of XIII. It is known that glycosylation of a phenolic hydroxy group causes a downfield shift of the carbon resonances due to the *ortho*- and *para*-carbons.[10] The ^{13}C-NMR spectrum of IV show that the C-5, C-7 and C-9 signals were lower than the corresponding signals of XIII by δ 5.4—3.1, which can be considered to have been caused by 6-*O*-glycosylation to XIII.

IV was, therefore, identified as baicalein 6-*O*-β-glucuronopyranoside. This compound had already been synthesized[11] and also isolated from the leaves of *Oroxylum indicum*[12] and the metabolites of baicalin and baicalein in rats.[13]

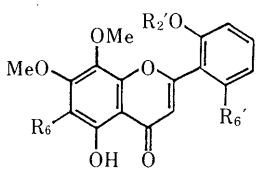

I : R_6=H, R_2'=Me, R_6'=OMe
II : R_6=OH, R_2'=R_6'=H

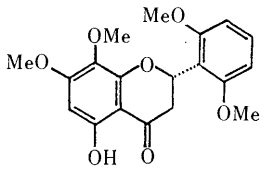

III

Fig. 1

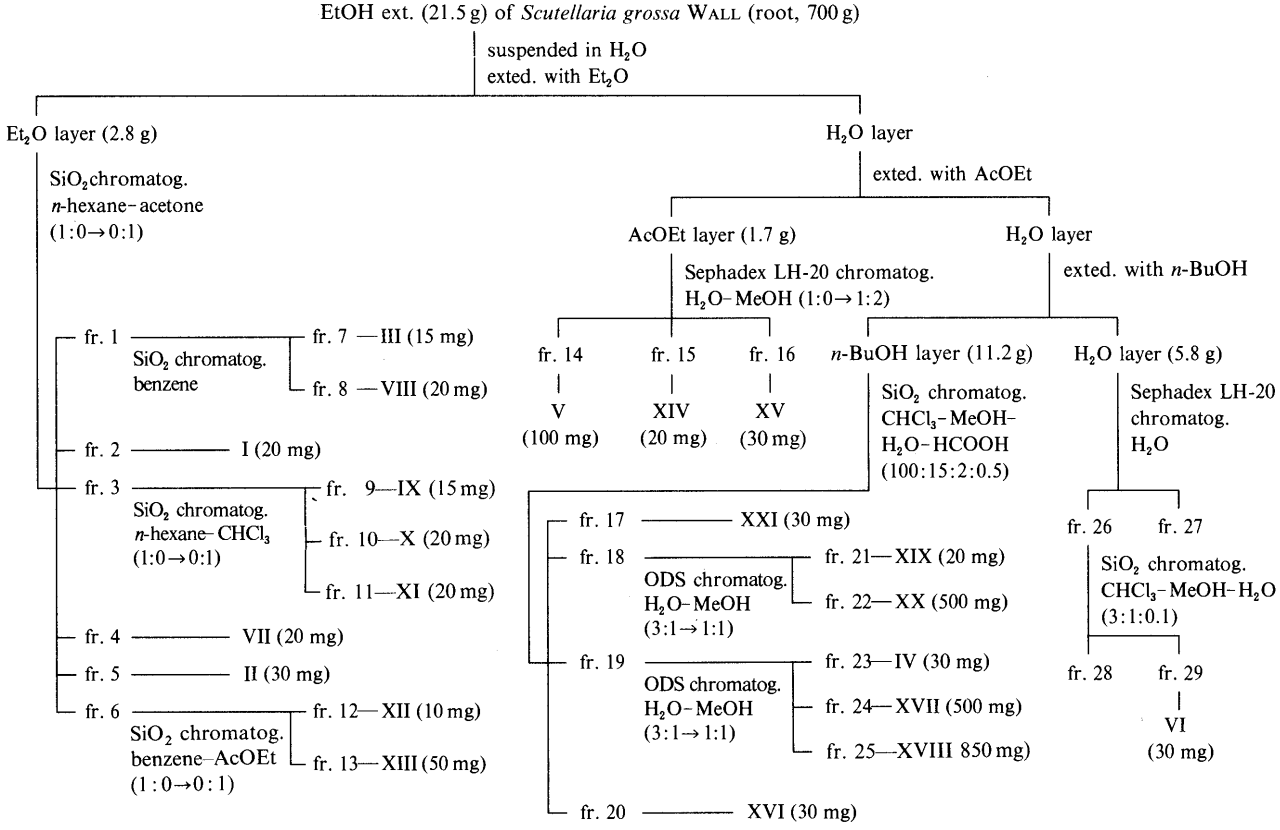

Chart 1

Compound V was obtained as an amorphous powder, $[\alpha]_D^{31}$ −49° (MeOH), $C_{24}H_{28}O_{11}$. V showed the absorption maxima at 204 and 277 nm in the UV spectrum and showed the absorption bands corresponding to hydroxyl, conjugated ester, enol ether groups and benzene ring.

On alkaline hydrolysis V afforded catalpol[14] (VI) and *trans*-cinnamic acid (VII).[14] V is, therefore, a monocinnamate of VI. In order to clarify the site of binding of the acyl groups, we used the acylation shifts[15] in ^{13}C-NMR spectroscopy. In the ^{13}C-NMR spectrum of V, the signals due to the C-8 and C-10 position were shifted downfield by δ 3.2 and upfield by δ 2.0, respectively, in comparison with those of VI, while other signals remained almost unaffected. These data indicated that the cinnamoyl group was linked to the C-10 position of VI.

From these results, the structure of V was identified as 10-cinnamoylcatalpol, which had already been isolated from *Scutellaria altissima* (named scutellariosid-I)[16] and *Globularia alypum* (named globularin).[17]

Compounds VIII—XXI are known flavonoids, which were identified as 5-hydroxy-7,8,2′-trimethoxyflavone[18] (VIII), oroxylin A[1] (IX), wogonin[1] (X), chrysin[1] (XI), norwogonin[19] (XII), baicalein[1] (XIII), scutellarein[19] (XIV), luteolin[20] (XV), oroxylin A 7-*O*-glucuronide[1] (XVI), wogonin 7-*O*-glucuronide[1] (XVII), chrysin 7-*O*-glucuronide[1] (XVIII), norwogonin 7-*O*-glucuronide[1] (XIX), baicalin[1] (XX) and scutellarin[19] (XXI), respectively, by direct comparison with authentic samples.

Experimental

General Procedures The instruments were the same as described in the previous paper[1] except for the following. Nuclear magnetic resonance (NMR) spectra were taken in dimethyl sulfoxide-d_6 (DMSO-d_6) on a JNM-GSX-400 spectrometer (^{1}H-NMR at 400 MHz and ^{13}C-NMR at 100 MHz). GLC was run on a Shimadzu GC-6AM unit with a flame ionization detector. GLC: column, a glass column (2 m × 4 mm i.d.) packed with 5% SE-30 on Chromosorb W (60—80 mesh); column temperature, programmed from 150 °C (20 min hold) to 240 °C at 5 °C/min. Thin layer chromatography (TLC) was carried out on Kieselgel 60F-254 (Merck) with the following solvent systems: $CHCl_3$–MeOH–H_2O–AcOH (100 : 10 : 1 : 0.3) (TLC-1), benzene–AcOEt–AcOH (100 : 60 : 0.5) (TLC-2), $CHCl_3$–MeOH–H_2O–HCOOH (25 : 8 : 1 : 0.5) (TLC-3), AcOEt–methyl ethyl ketone–H_2O–HCOOH (6 : 3 : 1 : 1) (TLC-4). Spots were detected by spraying dil. H_2SO_4 followed by heating.

Extraction and Isolation As shown in Chart 1, twenty-one compounds were obtained from the dried root of *Scutellaria grossa* collected at Kalopani, Nepal in September, 1986.

I (5-Hydroxy-7,8,2′,6′-tetramethoxyflavone)[7] Pale yellow needles (MeOH), mp 199 °C (dec.). *Anal.* Calcd for $C_{19}H_{18}O_7$: C, 63.68; H, 5.06. Found: C, 63.42; H, 5.07. EI-MS *m/z* (%): 358 (M^+, 46), 343 ($M^+ - CH_3$, 100). Mg–HCl (+). *Rf*: 0.81 (TLC-1), 0.66 (TLC-2). UV λ_{max}^{MeOH} nm (log ε): 266 (4.48), 338 (3.84). IR ν_{max}^{KBr} cm^{-1}: 3400 (OH), 1650 (conjugated CO), 1600, 1580 (arom. C=C). ^{1}H-NMR δ: 3.70, 3.92 (each 3H, each s, OCH_3 × 2), 3.80 (6H, s, 2′,6′-OCH_3), 6.32 (1H, s, 3-H), 6.62 (1H, s, 6-H), 6.83 (2H, d, *J* = 8.3 Hz, 3′,5′-H), 7.52 (1H, t, *J* = 8.3 Hz, 4′-H), 12.63 (1H, s, 5-OH). ^{13}C-NMR δ: 161.7 (C-2), 112.2 (C-3), 182.2 (C-4), 157.0 (C-5), 96.2 (dd, *J* = 7.4, 162.5 Hz, C-6), 158.7 (C-7), 128.6 (C-8), 149.9 (C-9), 104.1 (C-10), 110.2 (C-1′), 158.3 (C-2′,6′), 104.6 (C-3′,5′), 133.1 (C-4′), 56.2 (C-2′,6′-O$\underline{C}H_3$), 56.5 (C-7-O$\underline{C}H_3$), 61.0 (C-8-O$\underline{C}H_3$).

This compound was identified by direct comparisons (UV, IR, ^{1}H- and ^{13}C-NMR) with an authentic sample[7] prepared from rivularin[1] by partial methylation with CH_2N_2.

II (5,6,2′-Trihydroxy-7,8-dimethoxyflavone) Yellow needles (MeOH), mp 249—250 °C. *Anal.* Calcd for $C_{17}H_{14}O_7$: C, 61.82; H, 4.27. Found: C, 61.91; H, 4.23. EI-MS *m/z* (%): 330 (M^+, 65), 315 ($M^+ - CH_3$, 100). Mg–HCl (+). *Rf*: 0.47 (TLC-1), 0.39 (TLC-2). UV λ_{max}^{MeOH} nm (log ε): 247 sh (3.98), 283 (4.38), 340 (4.16); $\lambda_{max}^{MeOH-NaOMe}$ nm (log ε): 258 sh (4.15), 291 (4.27), 305 sh (4.18), 404 (4.17); $\lambda_{max}^{MeOH-AlCl_3}$ nm (log ε): 255 sh (3.99), 294 (4.38), 370 (4.28); $\lambda_{max}^{MeOH-AlCl_3-HCl}$ nm (log ε): 255 (4.01), 292 (4.34), 305 sh (4.23), 360 (4.24); $\lambda_{max}^{MeOH-NaOAc}$ nm (log ε): 285 (4.32), 320 sh (4.06), 347 sh (4.01), 410 (3.89); $\lambda_{max}^{MeOH-NaOAc-H_3BO_3}$ nm (log ε): 250 sh (4.02), 285 (4.39), 337 (4.14), 390 sh (3.47). IR ν_{max}^{KBr} cm^{-1}: 3468 (OH), 1664 (conjugated CO), 1612 (arom. C=C). ^{1}H-NMR δ: 3.90, 3.96 (each 3H, each s, OCH_3 × 2), 7.09 (1H, s, 3-H), 7.04 (2H, m, 3′,5′-H), 7.42 (1H, dt, *J* = 1.8, 7.9 Hz, 4′-H), 7.87 (1H, dd, *J* = 1.5, 8.1 Hz, 6′-H), 9.11 (1H, s, 6-OH), 10.84 (1H, s, 2′-OH), 12.43 (1H, s, 5-OH). ^{13}C-NMR δ: 161.1 (C-2), 108.5 (C-3), 182.8 (C-4), 142.4 (C-5), 134.1 (d, *J* = 4.7 Hz, C-6), 148.2 (C-7), 132.9 (C-8), 142.1 (C-9), 106.1 (C-10), 117.4 (C-1′), 156.8 (C-2′), 117.2 (C-3′), 133.0 (C-4′), 119.7 (C-5′), 128.3 (C-6′), 60.9, 61.8 (O$\underline{C}H_3$ × 2).

III ((2*S*)-5-Hydroxy-7,8,2′,6′-tetramethoxyflavanone) Colorless needles (MeOH), mp 137 °C. *Anal.* Calcd for $C_{19}H_{20}O_7$: C, 63.33; H, 5.59. Found: C, 63.26; H, 5.63. EI-MS *m/z* (%): 360 (M^+, 80), 196 ($C_9H_8O_5$, 100). Mg–HCl (+). *Rf*: 0.85 (TLC-1), 0.69 (TLC-2). UV λ_{max}^{MeOH} nm (log ε): 286 (3.87), 342 (3.26); $\lambda_{max}^{MeOH-NaOMe}$ nm (log ε): 286 (3.85), 366 (3.49); $\lambda_{max}^{MeOH-AlCl_3}$ nm (log ε): 310 (3.98), 395 (3.27); $\lambda_{max}^{MeOH-AlCl_3-HCl}$ nm (log ε): 309 (3.96), 395 (3.27); $\lambda_{max}^{MeOH-NaOAc}$ nm (log ε): 286 (3.87), 342 (3.26). IR ν_{max}^{KBr} cm^{-1}: 3400 (OH), 1638 (conjugated CO), 1599 (arom. C=C). ^{1}H-NMR δ: 3.52, 3.84 (each 3H, each s, OCH_3 × 2), 3.78 (6H, s, 2′,6′-OCH_3), 2.57 (1H, dd, *J* = 3.3, 17.2 Hz, *cis* 3-H), 3.80 (1H, dd, *J* = 13.2, 17.2 Hz, *trans* 3-H), 5.98 (1H, dd, *J* = 3.3, 13.2 Hz, 2-H), 6.22 (1H, s, 6-H), 6.74 (2H, d, *J* = 8.4 Hz, 3′,5′-H), 7.37 (1H, t, *J* = 8.4 Hz, 4′-H), 12.12 (1H, s, 5-OH). ^{13}C-NMR δ: 71.1 (C-2), 39.2 (C-3), 197.7 (C-4), 159.1 (C-5), 92.6 (dd, *J* = 7.4, 162.8 Hz, C-6), 160.8 (C-7), 128.5 (C-8), 154.3 (C-9), 102.1 (C-10), 112.8 (C-1′), 158.9 (C-2′,6′), 104.8 (C-3′,5′), 131.0 (C-4′), 56.0 (C-2′,6′-O$\underline{C}H_3$), 56.3 (C-7-O$\underline{C}H_3$), 60.2 (C-8-O$\underline{C}H_3$). CD ($c = 8.3 \times 10^{-5}$, MeOH) $[\theta]^{31}$ (nm): +5225 (307) (positive maximum), −13933 (279) (negative maximum).

(2*S*)-5,2′-Dihydroxy-7,8,6′-trimethoxyflavanone[9] was methylated with CH_2N_2 to give a product, mp 137 °C, which was identical (UV, IR, ^{1}H- and ^{13}C-NMR) with III.

IV (Baicalein 6-*O*-β-Glucuronopyranoside)[11-13] Yellow needles (MeOH), mp 197 °C (dec.). $[\alpha]_D^{31}$ −55° (*c* = 0.11, MeOH). *Anal.* Calcd for $C_{21}H_{18}O_{11}$: C, 56.50; H, 4.06. Found: C, 56.55; H, 4.14. EI-MS *m/z* (%): 270 ($C_{15}H_{10}O_5$, 100). FAB-MS *m/z* (%): 447 ($M^+ + 1$, 10). Mg–HCl (+). *Rf*: 0.55 (TLC-3), 0.54 (TLC-4). UV λ_{max}^{MeOH} nm (log ε): 245 sh (4.01), 271 (4.37), 316 (4.08). IR ν_{max}^{KBr} cm^{-1}: 3400 (OH), 1734 (COOH), 1658 (conjugated CO), 1624, 1588 (arom. C=C). ^{1}H-NMR δ: 3.26—3.64 (m sugar moiety), 4.94 (1H, d, *J* = 7.7 Hz, anomeric H of glucuronic acid unit), 6.64 (1H, s, 8-H), 6.97 (1H, s, 3-H), 7.58 (3H, m, 3′,4′,5′-H), 8.07 (2H, dd, *J* = 1.3, 8.2 Hz, 2′,6′-H), 13.05 (1H, s, 5-OH). ^{13}C-NMR δ: 163.2 (C-2), 104.7 (C-3), 182.3 (C-4), 152.6 (C-5), 128.1 (C-6), 157.8 (C-7), 94.5 (C-8), 153.1 (C-9), 104.1 (C-10), 130.7 (C-1′), 126.4 (C-2′,6′), 129.1 (C-3′,5′), 132.0 (C-4′), 103.7 (C-1″), 73.5 (C-2″), 75.3 (C-3″), 71.3 (C-4″), 75.6 (C-5″), 170.1 (C-6″).

Methanolysis of IV: A solution of IV (10 mg) in 10% HCl–MeOH (2 ml) was heated under reflux on a water bath for 3 h. The reaction mixture was neutralized with Ag_2CO_3. The precipitates were filtered off and the filtrate was concentrated to give the residue, which was chromatographed on silica gel using $CHCl_3$ as an eluent to give yellow needles (MeOH), mp 255 °C (dec.). This product was identified as baicalein[1] by direct comparisons (TLC, UV, IR, ^{1}H- and ^{13}C-NMR) with an authentic specimen. The mother liquor of crystallization was shown to contain methyl glucuronopyranoside methyl ester [t_R 13 min 24 s (both α and β)] and the methyl glycoside of glucurono-6,3-lactone [t_R 6 min 05 s (α, trace), 6 min 48 s (β)] by GLC (as the trimethylsilyl (TMS) ether derivatives).

V (10-Cinnamoylcatalpol)[16,17] Amorphous powder, $[\alpha]_D^{31}$ −49° (*c* = 0.15, MeOH). *Anal.* Calcd for $C_{24}H_{28}O_{11}$: C, 58.53; H, 5.73. Found: C, 58.60; H, 5.69. FAB-MS *m/z* (%): 493 ($M^+ + 1$, 20), 149 ($C_9H_8O_2 + 1$, 90), 103 ($C_8H_6 + 1$, 100). *Rf*: 0.68 (TLC-3), 0.58 (TLC-4). UV λ_{max}^{MeOH} nm (log ε): 204 (4.29), 277 (4.34). IR ν_{max}^{KBr} cm^{-1}: 3400 (OH), 1700 (conjugated ester), 1648 (enol ether), 1580 (arom. C=C). ^{1}H-NMR δ: 5.00 (2H, m, 1,4-H), 6.39 (1H, dd, *J* = 1.7, 6.1 Hz, 3-H), 2.13 (1H, m, 5-H), 3.86 (1H, br t, *J* = 7.0 Hz, 6-H), 5.36 (1H, d, *J* = 5.5 Hz, 6-OH), 3.50 (1H, s, 7-H), 2.48 (1H, dd, *J* = 7.7, 9.5 Hz, 9-H), 4.12, 4.94 (each 1H, each d, *J* = 12.4 Hz, 10-H), 4.58 (1H, d, *J* = 7.7 Hz, 1′-H (anomeric H)), 2.95 (1H, m, 2′-H), 3.15 (1H, m, 3′-H), 2.97 (1H, m, 4′-H), 3.15 (1H, m, 5′-H), 3.41, 3.71 (each 1H, each m, 6′-H), 4.44 (1H, dd, *J* = 5.5, 7.0 Hz, 6′-H), 6.65 (1H, d, *J* = 16.5 Hz, α-H), 7.66 (1H, d, *J* = 16.5 Hz, β-H), 7.43 (3H, m, 3″,4″,5″-H), 7.73 (2H, m, 2″,6″-H). ^{13}C-NMR δ: 93.5 (C-1), 140.4 (C-3), 103.0 (C-4), 37.3 (C-5), 77.0 (C-6), 61.3 (C-7), 61.6 (C-8), 41.9 (C-9), 62.7 (C-10), 98.3 (C-1′), 73.3 (C-2′), 76.5 (C-3′), 70.1 (C-4′), 77.3 (C-5′), 61.5 (C-6′), 134.1 (C-1″), 128.9 (C-2″,6″), 128.4 (C-3″,5″), 130.5 (C-4″), 144.5 (C-β), 118.0 (C-α), 165.8 (CO).

Alkaline Hydrolysis of V: A solution of V (40 mg) in 0.5 N KOH was heated on a water bath at 70 °C for 1 min. The reaction mixture was

neurtralized with dil. HCl and extracted with AcOET. The organic layer was concentrated to dryness, then the residue was recrystallized from MeOH to give colorless needles (7 mg), mp 133 °C; this product was identical with *trans*-cinnamic acid (VII)[14] by direct comparison (TLC, UV, IR and ^{1}H-NMR). The aqueous layer was concentrated to give a residue, which was chromatographed on silica gel with $CHCl_3$–MeOH–H_2O (3:2:0.2) and recrystallized from MeOH to give colorless needles (20 mg), mp 207—208 °C; this product was identical with catalpol (VI)[14] by direct comparison with an authentic sample (TLC, UV, IR, ^{1}H- and ^{13}C-NMR).

Identification of VIII—XXI VIII—XXI were identified as 5-hydroxy-7,8,2′-trimethoxyflavone (VIII, mp 184—186 °C),[18] oroxylin A (IX, mp 202 °C, dec.),[1] wogonin (X, mp 203 °C), chrysin (XI, mp 285 °C),[1] norwogonin (XII, mp 253 °C, dec.),[19] baicalein (XIII, mp 255 °C, dec.),[1] scutellarein (XIV, mp 345 °C, dec.),[19] luteolin (XV, mp 329 °C),[20] oroxylin A 7-*O*-glucuronide (XVI, mp 169—255 °C, dec.),[1] wogonin 7-*O*-glucuronide (XVII, mp 270 °C, dec.),[1] chrysin 7-*O*-glucuronide (XVIII, mp 226 °C, dec.),[1] norwogonin 7-*O*-glucuronide (XIX, mp 245 °C, dec.),[1] baicalin (XX, mp 230 °C, dec.)[1] and scutellarin (XXI, mp 360 °C),[19] respectively, by direct comparison with authentic specimens (TLC, UV, IR and ^{1}H-NMR).

Acknowledgements We are grateful to Dr. G. Murata, Kyoto University for his identification of *Scutellaria grossa* WALL and to Mrs. R. Igarashi and Miss A. Nakashima of this university for elemental analysis and EI and FAB-MS measurement.

This work was supported in part by a Grant-in-Aid (No. 61041032) for Scientific Research from the Ministry of Education, Science and Culture of Japan.

References and Notes

1) Y. Kikuchi, Y. Miyaichi, Y. Yamaguchi, H. Kizu and T. Tomimori, *Chem. Pharm. Bull.*, **39**, 1047 (1991).
2) Presented at the 110 th Annual Meeting of the Pharmaceutical Society of Japan, Sapporo, August 1990.
3) Mukerjee, *Rec. B. Surv. Ind.*, **14**, 140 (1940).
4) T. J. Mabry, K. R. Markham and M. B. Thomas, "The Systematic Identification of Flavonoids," Springer-Verlag, New York, 1970, Chapter V.
5) K. S. Dhami and J. B. Stothers, *Can. J. Chem.*, **44**, 2855 (1966); K. Panichpol and P. G. Waterman, *Phytochemistry*, **17**, 1363 (1978).
6) Y. Shirataki, I. Yokoe, M. Endo and M. Komatsu, *Chem. Pharm. Bull.*, **33**, 444 (1985); H. Komura, K. Mizukawa, H. Minakata, H. Huang, G. Qin and R. Xu, *ibid.*, **31**, 4206 (1983); H. Komura, K. Mizukawa and H. Minakata, *Bull. Chem. Soc. Jpn.*, **55**, 3053 (1982).
7) T. Tomimori, Y. Miyaichi, Y. Imoto, H. Kizu and T. Namba, *Chem. Pharm. Bull.*, **34**, 406 (1986).
8) W. Gaffield, *Tetrahedron*, **26**, 4093 (1970).
9) Y. Miyaichi, Y. Imoto, T. Tomimori and C. C. Lin, *Chem. Pharm. Bull.*, **35**, 3720 (1987).
10) O. Tanaka, *Yakugaku Zasshi*, **105**, 323 (1985).
11) G. M. Vandor, L. Farkas, I. Kanzel and M. Nogradi, *Chem. Ber.*, **113**, 323 (1980).
12) S. S. Subramarian and A. G. R. Nair, *Phytochemistry*, **11**, 439 (1972).
13) K. Abe, O. Inoue and E. Yumioka, *Chem. Pharm. Bull.*, **38**, 208 (1990).
14) I. Kitagawa, K. Hino, T. Nishimura, E. Mukai and I. Yosioka, *Tetrahedron Lett.*, **43**, 3837 (1969).
15) K. Markham, B. Ternai, R. Stanley, H. Geiger and T. Mabry, *Tetrahedron*, **34**, 1389 (1978); T. Yoshida, T. Saito and S. Kadoya, *Chem. Pharm. Bull.*, **35**, 97 (1987); K. Yamasaki, R. Kasai, Y. Masaki, M. Okihara and O. Tanaka, *Tetrahedron Lett.*, **1977**, 1231.
16) K. Weinges, K. Kunstler and G. Schilling, *Justus Liebigs Ann. Chem.*, **1975**, 2190.
17) G. D. Maio and L. Panizzi, *Ric. Sci.*, **36**, 845 (1966).
18) T. Tomimori, Y. Miyaichi, Y. Imoto and H. Kizu, *Shoyakugaku Zasshi*, **38**, 249 (1984); M. E. Ali, K. M. Biswas and S. A. Chowdhury, *Pak. J. Sci. Ind. Res.*, **15**, 33 (1972); M. A. F. Jalal, K. H. Overton and D. S. Rycroft, *Phytochemistry*, **18**, 149 (1979).
19) Y. Kikuchi, Y. Miyaichi, Y. Yamaguchi, H. Kizu, T. Tomimori and K. Vetschera, *Chem. Pharm. Bull.*, **39**, 199 (1991).
20) T. Tomimori, Y. Miyaichi, Y. Imoto and H. Kizu, *Shoyakugaku Zasshi*, **40**, 432 (1986).

Expanded Coagulating Cleanup Procedures for Simultaneous Gas Chromatographic Determination of Organoposphorus Pesticides in Crops and Fruits

Makoto MIYAHARA,* Kumiko SASAKI, Takashi SUZUKI, and Yukio SAITO

National Institute of Hygienic Sciences, Division of Food, 1–18–1 Kamiyoga, Setagaya-ku, Tokyo 158, Japan. *Received July 30, 1990*

A simplified method is described for determining 7 organophosphorus pesticides (mevinphos, phosphamidon, fenamiphos, crufomate, carbophenothion, fenchlorphos, coumaphos) in citrus fruits, banana, soybeans and wheat. Residues were extracted with acetonitrile or acetone, and if necessary, were partitioned with *n*-hexane. Coextractives were coagulated with a solution containing phosphoric acid and ammonium chloride, and were separated by filtration. The filtrate was extracted with dichloromethane. The extract was concentrated and injected into a gas chromatograph equipped with a flame photometric detector and a fused silica capillary column. Recovery data were obtained by fortifying market samples at 0.1 and 0.2 ppm. Recoveries of most organophosphorus pesticides exceeded 80%. The limit of detection ranged from 0.005 to 0.05 ppm, depending on the compound.

Keywords organophosphorus pesticide; cleanup method; coagulation; gas chromatography; simultaneous determination; fruit; grain

Organophosphorus pesticides have been widely used because of their low mammalian toxicity. As a result of their wide spread use, it is necessary to establish a rapid and efficient multiresidue method for monitoring these compounds in domestic and imported products consumed in Japan. Traditional multiresidue analytical methods for organophosphorus pesticides in nonfatty foods, contain cleanup steps such as Florisil column chromatography, sweep codistillation, carbon column chromatography or isolation in an organic phase.[1] Generally, these methods are time consuming and involve difficult analytical steps. However, the less complicated methods, such as the Luke procedure,[2] are not always efficient enough to eliminate interfering materials. For use as standard procedures, simple and efficient cleanup methods which remove interfering compounds, are desirable. The coagulating method is simple, and rapid, but as currently used, is not suitable for the determination of extremely water soluble pesticides such as mevinphos and phosphamidon, and water insoluble pesticides such as crufomate and carbophenothion. In addition, this method is not acceptable for the determination of any pesticides in crops which are rich in fat such as soybean.[3,4]

This paper describes a simple, modified coagulation cleanup procedure used in conjunction with capillary gas chromatography (GC) and flame photometric detection for simultaneous determination of organophosphorus pesticides in fruits and grains. These pesticides, mevinphos, phosphamidon, fenamiphos, crufomate, carbophenothion, fenchlorphos, coumaphos are difficult to cleanup by the charcoal column procedure or by the traditional coagulation method.

Experimental

Materials Organophosphorus pesticide standards for residue analysis (97—100%) were obtained from EPA (Research Triangle Park, NC, U.S.A.). Their chemical structures and ISO names are summarized in Chart 1. Spiking standard solution contained 1 and 2 μg of each compound in 1 ml of acetone. Standard curve solutions contained 0.0625 to 4 μg of each compound in 1 ml of acetone (six steps). Samples (oranges, grapefruits, lemons, bananas, soybeans and wheat) were purchased from retail markets in Tokyo. Celite 545 was obtained from Johns-Manville Co., U.S.A. Charcoal (Darco 60), from Atlas Powder Co., U.S.A., and microcrystalline cellulose (100—200 μm of particle size for chromatography) from Asahikasei Co. All other reagents and solvents were of analytical grade.

Extraction Procedure for Fruits Edible portions of the sample (100 g) were homogenized for 5 min with a waring blender, and a portion of the homogenate (20 g) with 100 ml acetone added was shaken vigorously for 10 min. For the recovery test at 0.1 or 0.2 ppm, 2 ml of the spiking standard solution was added to the homogenate (20 g) before the addition of acetone. The mixture was poured onto a suction funnel packed with a 5 mm layer of Celite 545, and the filtrate and acetone washing (5 ml × 5) were combined. 100 ml of the coagulating solution, which contained 10 g NH_4Cl and 20 ml H_3PO_4 in 800 ml water, and 5 g Celite 545 were added to the filtrate. The mixture stood for 30 min with occasional swirling (once every 10 min). After filtration through filter paper (Toyo Roshi No. 5A) set on a suction funnel, the residual cake was washed twice with 10 ml of 50% aqueous acetone. The filtrate and washing were combined, extracted twice with 100 ml of dichloromethane, and the aqueous layer was discarded. The dichloromethane fraction was dried by passing through about 20 g anhydrous Na_2SO_4 held in a filter funnel with filter paper, and was evaporated to near dryness at 35 °C and under stream nitrogen to complete evaporation. The residue was dissolved in 5 ml of acetone, and 1 μg of the solution was injected to gas chromatograph.

Extraction Procedure for Soybean and Wheat Edible portions of a

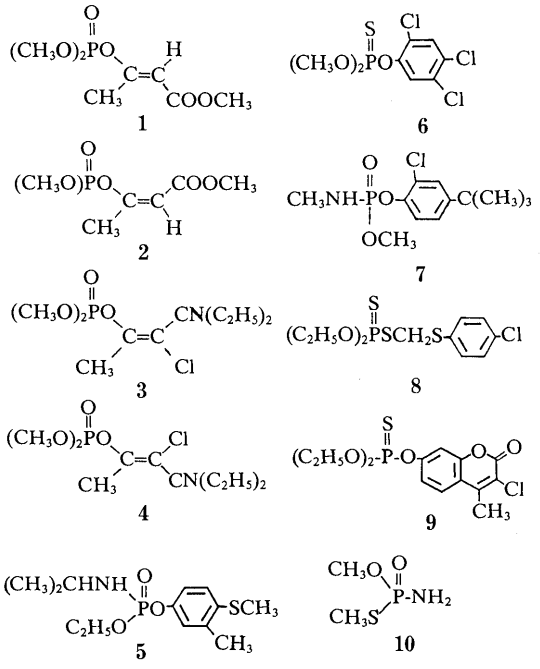

Chart 1. Structures of Pesticide

1, methamidophos; **2**, mevinphos; **3**, *E*-phosphamidon; **4**, *Z*-phosphamidon; **5**, fenchlorphos; **6**, crufomate; **7**, fenamiphos; **8**, carbophenothion; **9**, coumaphos.

sample (100 g) were ground in an ultra centrifugal mill to pass through a 0.5 mm mesh sieve and to a portion of the sieved sample (20 g) 100 ml of acetonitrile was added, and it was shaken vigorously for 10 min. For the recovery test at 0.1 or 0.2 ppm, 2 ml of the spiking standard solution was added to the homogenate (20 g) before the addition of acetonitrile. The mixture was similarly filtered through a 5 mm layer of Celite 545 as described above for the fruits. The filter cake was washed 4 times with 5 ml of acetonitrile. The combined solution of the washings and filtrate was concentrated to about 20 ml at 35 °C under reduced pressure. The concentrated solution was transferred to a graduated test tube with a stopper, to which was added acetonitrile to 30 ml and 15 ml of *n*-hexane. Pesticides in the sample were extracted in the acetonitrile fraction by partitioning it three times with 30 ml of acetonitrile. The combined extracts were concentrated to almost dryness and finally with a stream of dry nitrogen gas to complete evaporation. The residue was dissolved in 50 ml of acetone, and to the solution 50 ml of the coagulating solution and 1 g Celite 545 were added and swirled to mix. The following procedures were the same as those described for the fruits.

Recovery Test from Charcoal Column To make a charcoal column, a chromatographic glass column (21 mm i.d. × 30 cm) was packed with adsorbent mixture slurry containing 0.5 g of charcoal and 4.5 g microcrystalline cellulose in 20 ml of benzene. On top of the column, 5 g of anhydrous sodium sulfate was piled. 1 ml of spiking standard solution was added on top of the column. The column was then eluted with 200 ml of benzene at about 7—10 ml/min. The eluate was collected and evaporated under reduced pressure. The residue was dissolved in 5 ml of acetone and 1 μl of the solution was injected into a gas chromatograph.

Gas Chromatography (GC) The GC used is the one with a flame photometric detector (GC-FPD), Shimadzu Model GC9A or GC15A (Shimadzu, Corp., Kyoto). The capillary column DB-5 (15 m × 0.53 mm, i.d., film thickness, 1.5 μm) was purchased from J & W Scientific, CA. The oven temperature was held initially at 120 °C for 1 min, and then programed to 200 °C at 10 °C/min, held at 200 °C for 12 min, followed by 20 °C/min to 250 °C, and finally 250 °C for 20 min. The temperature of the detector and injector block was kept at 255 °C. The flow rate of carrier gas (helium) was 16 ml/min, and those of air and hydrogen were 60 ml/min, respectively. The flow rate of makeup gas (nitrogen) was 60 ml/min. The optical filter was 526 nm.

Results and Discussion

Validation of the Method In order to evaluate the method described, recovery tests were carried out for several types of samples spiked at the level of 0.1 and 0.2 ppm. The recoveries thus obtained are shown in Table I. Overall recoveries averaged 93—99% for mevinphos, 88—93% for *E*-phosphamidon, 83—105% for *Z*-phosphamidon, and 86—98% for fenchlorphos, 87—98% for crufomate, 80—103% for fenamiphos, 83—96% for carbophenothion, 83—94% for coumaphos. All coefficients of variation (CV%) ranged from 4.6 to 11.3. No control extract contained detectable level pesticides except oranges. The oranges we examined contained *E*- and *Z*-phosphamidon at about 0.02 ppm. The value of recovery was calculated by subtracting the background level from the value of the recovery test.

The limit of detection (LOD), defined as a response 3 times the width of the baseline, was determined for each of the pesticides used in this study. The LOD determined for individual pesticides is of the same level for all samples because interfering peaks due to sample coextractives were few. As shown in Table II, the detection limits for the analysis were 0.01 ng for methamidophos, mevinphos, fenchlorphos, 0.02 ng for *Z*-phosphamidon, crufomate carbophenothion and coumaphos, 0.06 ng for fenamifos, and 0.1 ng for *E*-phosphamidon. These results show that the level of detection depended on the type of compounds. Studies conducted in our laboratory indicated that DB-5 gave a good response and produced a good separation. The detection limits determined in this study correspond to practical limits of detection of 0.02—0.002 ppm.

For the most part, the chromatograms of samples tested were almost free from interfering peaks except for residual organophosphorus pesticide contaminants in some cases. Several varieties of each sample were used for extraction of residues, but significant differences were not noticed in the various chromatograms. Chromatograms for a standard solution and an extract from soybeans, fruits and wheat are shown in Figs. 1 and 2. The straight line calibration curve determined for the detection system appeared to be linear from 0.005 ng up to 4 ng injected for all pesticides tested.

TABLE I. Overall Recovery of 8 Organophosphorus Pesticides at 0.1 and 0.2 ppm

Pesticide	Recovery[a] (%) (CV%)					
	Lemon	Orange	Grapefruit	Banana	Wheat	Soybean
At 0.1 ppm						
Methamidophos	21 (9.2)	17 (6.3)	15 (6.8)	13 (6.0)	16 (7.7)	36 (10.0)
Mevinphos	97 (6.0)	98 (8.5)	95 (4.8)	96 (7.6)	97 (5.6)	99 (6.3)
E-Phosphamidon	94 (10.0)	90 (6.0)	93 (8.2)	91 (6.4)	93 (9.3)	90 (8.4)
Z-Phosphamidon	96 (11.0)	94 (7.9)	89 (6.1)	92 (9.2)	91 (7.8)	95 (8.0)
Fenchlorphos	98 (7.3)	86 (7.0)	96 (4.6)	90 (9.9)	96 (6.0)	94 (6.1)
Crufomate	96 (6.5)	98 (5.7)	95 (7.9)	92 (6.9)	93 (5.3)	95 (7.4)
Fenamiphos	98 (7.5)	88 (11.5)	80 (8.7)	94 (12.2)	96 (9.5)	89 (8.2)
Carbophenothion	104 (9.1)	85 (7.4)	96 (7.8)	91 (5.7)	88 (5.6)	90 (9.2)
Coumaphos	83 (8.4)	87 (8.5)	91 (6.7)	89 (6.8)	91 (5.3)	83 (10.8)
At 0.2 ppm						
Methamidophos	19 (9.5)	20 (7.4)	14 (6.2)	18 (7.1)	22 (8.7)	34 (9.8)
Mevinphos	97 (8.6)	98 (8.4)	93 (5.8)	93 (8.5)	98 (5.3)	94 (6.1)
E-Phosphamidon	86 (11.3)	92 (9.0)	92 (7.6)	89 (7.4)	94 (8.8)	88 (9.7)
Z-Phosphamidon	94 (9.8)	96 (8.6)	91 (6.7)	83 (7.4)	109 (7.9)	91 (5.6)
Fenchlorphos	87 (6.3)	89 (8.1)	98 (4.6)	91 (7.2)	95 (5.9)	96 (6.3)
Crufomate	93 (5.9)	95 (4.9)	87 (6.8)	92 (6.6)	98 (5.0)	97 (5.7)
Fenamiphos	96 (8.3)	87 (6.4)	89 (6.9)	94 (10.2)	103 (5.5)	95 (6.9)
Carbophenothion	96 (8.2)	86 (6.8)	93 (6.8)	88 (5.2)	92 (5.8)	94 (6.4)
Coumaphos	88 (7.3)	91 (7.5)	94 (5.6)	91 (5.8)	94 (4.9)	87 (8.2)

a) The values are means of three determinations.

TABLE II. Relative Retention Time, Solubility, LOD, and Calibration Curve of Organophosphorus Pesticides

Pesticide	Relative retention time[a]			Solubility in water[f]	LOD	Calibration curve ($y=ax+b$)		
	I[b]	II[c]	III[d]	(ppm)	(ng)	r^2	x	y
Methamidophos	0.276	0.10	0.204	Freely	0.005	0.999	29847	−319
Mevinphos	0.523	0.19	0.304	Freely	0.005	0.999	93980	−223
E-Phosphamidon	1.044	0.79	0.846	Freely	0.05	0.999	4559	−471
Z-Phosphamidon	1.147	1.07	0.967	Freely	0.01	0.999	15427	−138
Fenchlorphos	1.220	0.87	0.846	44	0.005	0.999	83474	814
Crufomate	1.413	1.49	1.113	<1	0.01	0.999	28907	645
Fenamiphos	1.838	2.39	1.403	400	0.03	0.991	4179	751
Carbophenothion	2.428	3.12	2.956	<1	0.01	0.999	35795	527
Coumaphos	3.176	ND[e]	ND[e]	1.5	0.01	0.997	26398	656

a) Relative to chlorpyriphos. Retention times were 8.55, 2.85, and 7.22 min on columns I, II, III respectively. *b*) Wide bore column of DB-5. Operating conditions are in text. *c*) Normal bore column (0.25 mm in inner diameter, 25 m in length, 0.25 μm in film thickness) of CBP10. Operating conditions: column temperature, 230 °C; injector and detector, 255 °C; split ratio, 1 : 10; flow rate, 2 ml/min. *d*) Wide bore column of CBP10 (Shimadzu Co.). Detail conditions are in reference 3. *e*) 1 ng was injected and the pesticide was not detected. *f*) Pesticide Manual 1988.

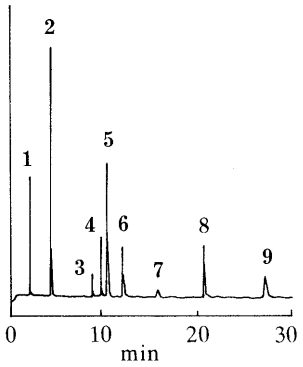

Fig. 1. Gas Chromatogram of 0.4 ng Pesticide Standards

1, methamidophos; 2, mevinphos; 3, *E*-phosphamidon; 4, *Z*-phosphamidon; 5, fenchlorphos; 6, crufomate; 7, fenamiphos; 8, carbophenothion; 9, coumaphos.

r^2, a and b for calibration curves are shown in Table II.

Analysis Condition Acetone and acetonitrile were employed for extraction of organophosphorus pesticides from vegetable and fruits, and from soybeans and wheat, respectively.

The original coagulation method was developed for carbamates in nonfatty foods.[4] No data on application of the coagulation method to fat containing crops were available. Some trials of applying the method to soybean failed. A fat removing process was needed for wheat and soybean because the final solution for GC injection contained large amounts of oily coextractives. Acetonitrile partitioning described in the AOAC method[1] had been shown to be sufficient for pesticides in the crop. The recoveries from the acetonitrile partitioning process at spiking level 0.1 ppm were over 95% for all the pesticides we examined.

The coagulating solution converts coextractives from plant tissue samples into a precipitate which can be removed by filtration. Celite added facilitates the precipitation of the coagulated coextractives. Recovery from the mixture is mainly governed by the solubility of various pesticides. As shown in Table II, the solubility of coumaphos, carbophenothion and fenchlorphos in water at room temperature are 1.5 ppm, below 1 ppm and 44 ppm, respectively. However, it was found that if coagulation was carried out at over 60% acetone, the residue from the dichloromethane extract increased and the cleanup was not efficient.[3] Based on these findings, coagulation at about 50% acetone was chosen.

In carrying out the traditional method, either benzene or hexane is used to extract pesticides from the coagulation mixture. Several solvent combinations including dichloromethane, benzene, and a combination of dichloromethane and 400 ml of 2% aqueous sodium chloride were compared to improve recoveries of fenchlorphos and carbophenothion. Dichloromethane was found to be superior to benzene for recovery of fenchlorphos, 83% *versus* 101%; and carbophenothion, 75% *versus* 85%. The combination of dichloromethane extraction and NaCl dilution reduced the recoveries of all pesticides except crufomate and carbophenothion. Consequently, to maximize recovery of all 8 pesticides, residues were extracted from coagulating the mixture with dichloromethane.

The cleanup effects were evaluated here by the nonvolatile residual weight of a blank sample. Before cleanup, extracts contained 140—195 mg of nonvolatile coextractives of oranges, grapefruits, bananas, and lemons. However, the final residue weights ranged from 6—8 mg for the nonfatty samples. These results show that the cleanup process is very effective for organophosphorus pesticides analysis. As a result, there was no need to cut the precolumn for gas chromatograph every 5 injections in order to eliminate accumulated coextractives from the gas chromatographic separation system.[5]

The final residue weights after the overall process were 26 mg for wheat and 95 mg for soybean. The cleaning effects were poor in comparison with residues from nonfatty crops, but there were no problems on the gas chromatograms.

Several types of columns for GC were tried for the determination of the organophosphorus pesticides. Table II shows relative retention times of pesticides on three types of capillary columns. A wide bore capillary column with 14% cyanopropyl phenyl and 86% dimethyl polysiloxane film (CBP-10) which gave poor sensitivity for phosphamidon (both *E* and *Z* types), crufomate and carbophenothion, and poor separation of *Z*-phosphamidon and fenchlorphos. A capillary column (0.2 mm in inner diameter, 30 m in length, 0.25 μm in film thickness) with the same liquid phase as above, gave good separation but very low sensitivity for fenamifos. This column may result in

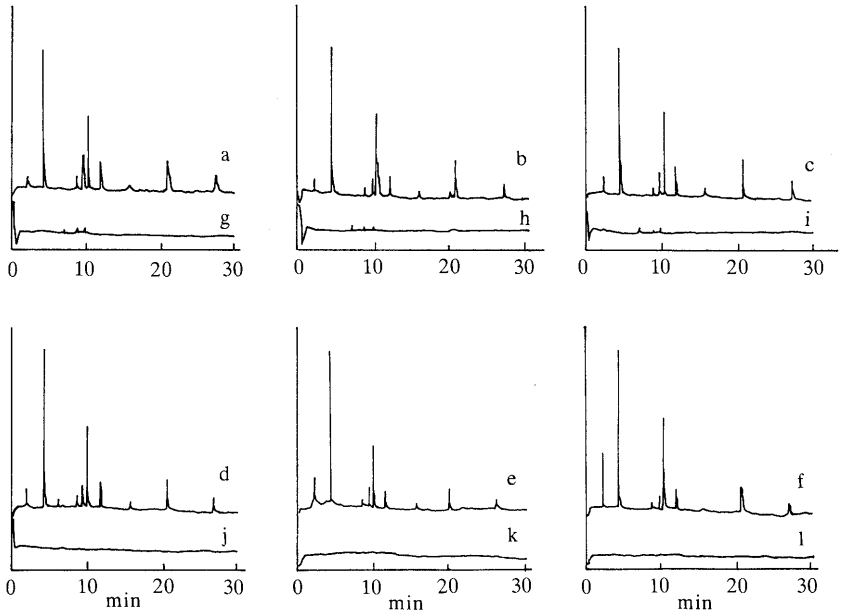

Fig. 2. Gas Chromatograms of 0.1 ppm Fortified Extract with 7 Organophosphorus Pesticides (a—f) and of Control Extract after Coagulation (g—l)

Orange (a, g), grapefruit (b, h), lemon (c, i), banana (d, j), wheat (e, k), and soybeans (f, l).

instability of the pesticides and/or adsorption of pesticides to the capillary column wall. And a wide bore capillary column (0.53 mm in inner diameter, 15 m in length, 1.5 μm in film thickness) with a liquid phase consisting of 5% diphenylmethyl and 95% dimethyl polysiloxane which gave good responses and good separation for all pesticides. Based on the results of this study, the wide bore capillary column of DB-5 was chosen to conduct subsequent analysis.

The traditional coagulation method[3] was employed to analyze grapefruits and bananas. Overall recoveries of 8 organophosphorus pesticides ranged from 0—92% for grapefruits and from 0—89% for bananas. Especially for methamidophos (0% and 0% for grapefruit and banana, respectively), fenchlorphos (50% and 37%) and carbophenothion (50% and 18%), the recoveries were poor.

For the comparison, recovery tests through a charcoal column alone were undertaken. This cleanup procedure is preferred, over the Florisil column cleanup, because organophosphorus pesticides are lost on the column[1,6] can be eluted from the charcoal column. Recoveries of the 6 pesticides ranged from 44—94% and 56—100%, respectively. These results show that the charcoal column cleanup step does not always give satisfactory results. On the other hand, there are some limitations to the coagulation cleanup procedure also. Acid-soluble pesticides which may have one or more amino groups in the structure, such as methamidophos, were not recovered. For these pesticides, the charcoal cleanup procedure still remains as an alternative method.

The results presented demonstrate the applicability of a modified coagulation procedure for the extraction and GC analysis of 7 organophosphorus pesticides with water solubilities ranging from below 1 μg/ml to freely soluble in nonfatty foods (fruits) and fat containing crops (soybean and wheat). The procedure in conjunction with flame photometric detection with whole injection without splitting into wide bore capillary columns, provides a highly sensitive and more selective approach for quantitation or confirmation of the organophosphorus pesticide residues in crops.

Acknowledgment We express our thanks to Dr. Frank. L. Joe, Jr, Food and Drug Administration (U.S.A.), for his helpful advice.

References

1) "Official Methods of Analysis," 14th Ed., AOAC, Arlington, VA, 1984, sec 29.001—29.072.
2) M. A. Luke, H. T. Matumoto, T. Cairns, and H. K. Hundly, *J. Assoc. Off. Anal. Chem.*, **71**, 415 (1988).
3) K. Sasaki, T. Suzuki, and Y. Saito, *J. Assoc. Off. Anal. Chem.*, **70**, 460 (1987).
4) E. R. Holden, *J. Assoc. Off. Anal. Chem.*, **56**, 713 (1973).
5) G. C. Mattern, G. M. Singer, J. Louis, M. Bobson, and J. D. Rosen, *J. Arg. Food. Chem.*, **38**, 403 (1990).
6) Y. Kawamura, A. Takeda, M. Uchiyama, and Y. Saito, *Eisei Shikensho Hokoku*, **104**, 147 (1986).

Presence of the Basement Membrane Component—Heparan Sulfate Proteoglycan—in Bovine Lens Capsules

Satoshi ONODERA

Department of Clinical Chemistry, Showa College of Pharmaceutical Sciences, Machida, Tokyo 194, Japan. *Received October 9, 1990*

Heparan sulfate proteoglycan was extracted from bovine lens capsules by 0.45 M NaCl/2 M urea and purified using ion-exchange chromatography and gel filtration. The proteoglycan was found to consist of protein and carbohydrate in a ratio of 75 to 25. The estimated average molecular weight of the heparan sulfate proteoglycan eluted by 0.2 M NaCl on a diethylaminoethyl (DEAE)-cellulose column was 400 kilodaltons (kDa) and that of its glycosaminoglycan was 18.8 kDa. The amino acid composition of the proteoglycan was quite similar to that of the bovine glomelular basement membrane.

Keywords proteoglycan; heparan sulfate proteoglycan; basement membrane; lens capsule; glycosaminoglycan; collagen

Introduction

It is well known that basement membranes are thin extracellular matrices that underlie endotherial and epithelial cells in various connective tissues.[1] The molecular components of a basement membrane are predominantly composed of heparan sulfate proteoglycan (HSPG), type IV collagen[1] and laminin.[2] HSPG is mainly distributed in the basal lamina of the basement membrane.

HSPG is difficult to isolate from the basement membrane because it is a small component of tissues and is virtually insoluble due to interaction with components such as laminin, type IV collagen and other macromolecules.[1] However, the isolation of HSPG has been recently attempted from some tissues such as Engelbreth–Holm–Swarm (EHS) sarcoma,[3-5] glomerular basement membrane[6,7] and other tissues.[8,9] From these results, the estimated molecular weights of HSPG and its heparan sulfate side chain were in the broad range of 71000—750000 and 14000—40000, respectively. However, the biological function of HSPG in tissues remains obscure at present.

In the present paper, bovine lens capsules were used for the isolation of HSPG because it is easy to deal with and contains few other components except for basement membrane components as compared with renal glomeruli.[10] Therefore, to elucidate whether or not HSPG from lens capsules shares a common structure with HSPG in the other tissues previously described, I tried to characterize HSPG from lens capsules, which will enable me to gain further insight into the role of HSPG in the basement membrane.

Materials and Methods

Materials Fresh normal bovine eyes were obtained from a local slaughterhouse. Phenylmethanesulfonyl fluoride (PMSF), *N*-ethylmaleimide (NEM), pepstatin A and pronase E were purchased from Sigma Chemical Co. Dermatan sulfate (DS, from hog skin), chondroitin-4-sulfate (CS, from whale cartilage), hyaluronic acid (HA, from hog skin), heparin (HP, from hog intestine), heparan sulfate (HS, from bovine kidney), chondroitinase ABC (from *Proteus vulgaris*) and AC II (from *Arthrobacter aurescens*) and heparitinase (from *Flavobacterium heparinum* were from Seikagaku Kogyo Co., Tokyo. Cellulose acetate membrane (Separax) was from Jookoo Sangyo Co., Ltd., Tokyo.

Isolation of HSPG from Bovine Lens Capsules All procedures for the extraction of proteoglycan were carried out at 4 °C. Fresh normal lens capsules (30 g wet weight) obtained from 500 bovine eyes immediately after sacrifice were washed three times with 50 mM Tris–HCl buffer, pH 7.6, containing proteinase inhibitor.[11] After washing, the residue was extracted six times with 0.45 M NaCl, 2 M urea and 50 mM Tris–HCl buffer, pH 7.6, containing proteinase inhibitors. The extracts were diluted with 2 M urea, 50 mM Tris–HCl buffer, pH 7.6, to obtain a final NaCl concentration of 0.05 M. They were directly applied to a diethylaminoethyl (DEAE)-cellulose column (3 × 10 cm) equilibrated with 2 M urea, 0.05 M NaCl in 50 mM Tris–HCl buffer of pH 7.6. After washing the column with the same buffer, the proteoglycan was eluted with 0.3 M NaCl in the same buffer. For a further purification, the 0.3 M NaCl eluate was dialyzed against 7 M urea in 50 mM Tris–HCl of pH 7.6 and was rechromatographed on a DEAE-cellulose (1 × 13 cm) with 7 M urea in 50 mM Tris–HCl buffer of pH 7.6, and then eluted with a stepwise increase in the NaCl concentration. Alcian blue positive fractions were recovered from fractions eluted with 0.15 M and 0.2 M NaCl elutions.

Gel Filtration HS obtained from alkali and pronase-treated[8] HSPG was dissolved in 1.0 M NaCl containing 50 mM Tris–HCl buffer or pH 7.6. The solution was applied to a Sephadex G-200 column (1.25 × 65 cm) and then eluted with 1.0 M NaCl containing the above mentioned buffer. The molecular weight of HS was estimated using the calibration curve reported by Wasteson.[12]

Electrophoresis Polyacrylamide gel electrophoresis in the presence of sodium dodecyl sulfate (SDS-PAGE) using 5% gels was performed as previously reported.[13] After electrophoresis, the gels were stained with 0.1% coomassie brilliant blue in 5% methanol–10% acetic acid for protein with 0.1% toluidine blue in 3% acetic acid for glycosaminoglycans (GAG)[14] or with periodic acid Schiff's reagent (PAS) for glycoprotein.[15] The reduction of the samples was done with 0.1 M dithiothreitol. The determination of the GAG components was carried out by two-dimensional electrophoresis on cellulose acetate membrane[16] and then stained with alcian blue 8 GX to identify the HS component in combination with heparitinase and nitrous acid.[17]

Analytical and Chemical Procedure Amino acid analysis was performed by a JEOL-6AS autoanalyzer after the hydrolysis of a sample of protein with 6 M HCl in an evacuated sealed tube at 110 °C for 24 h.[18] Uronic acid was measured by a carbazole method with D-glucuronolactone as the standard.[19] The protein content was determined using a modification of Lowry's method with bovine serum albumin as the standard.[20] Hexosamine analysis was performed by a JEOL-6AS autoanalyzer after the hydrolysis of a sample of GAG with 5 M HCl at 110 °C for 5 h.

Results and Discussion

The whole of the lens is enclosed by a homogenous capsule rich in glycoprotein which represents a specialized remnant of the epithelial basement membrane. The lens capsules (30 g wet weight) from 500 bovine eyes were treated according to the procedures described in Materials and Methods. The yields of proteoglycan were 2.57 mg of 0.15 M NaCl fraction and 5.08 mg of 0.2 M NaCl fraction from DEAE-cellulose rechromatography. Fig. 1 shows SDS-PAGE patterns of the subfractions eluted with a stepwise increase in the NaCl concentration from DEAE-cellulose chromatography, and then stained with coomassie brilliant blue. The broad band stained with a dye is one of the typical features of proteoglycan. Furthermore, both gel 4 and gel 5

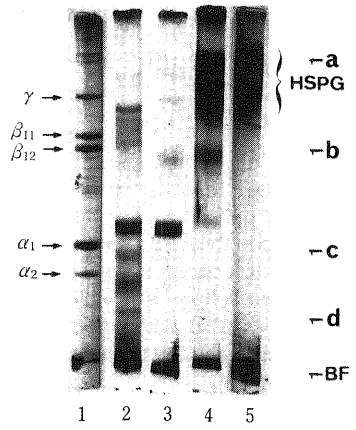

Fig. 1. SDS-PAGE Pattern of HSPG from Bovine Lens Capsules

SDS-PAGE (5% gel) was performed according to the method of Laemmli.[13] 1, bovine type I collagen; 2, 0.05 M NaCl fraction from the second DEAE-cellulose column; 3, 0.1 M NaCl fraction; 4, 0.15 M NaCl fraction; 5, 0.2 M NaCl fraction. The molecular weight markers were: fibronectin (440000 (a) and 220000 (b)), β-galactosidase (116000 (c)), bovine serum albumin (66000 (d)), BF (buffer front).

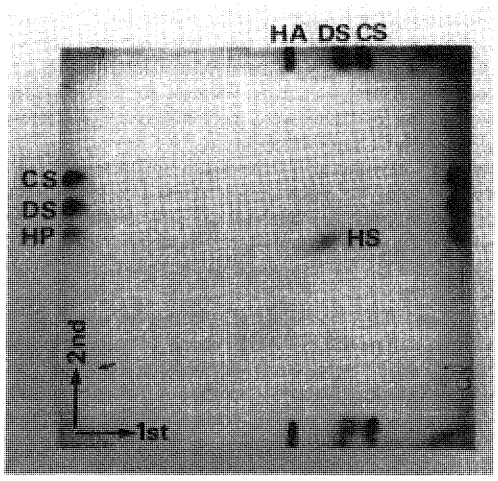

Fig. 2. The Two-Dimensional Electrophoresis Pattern of a GAG Component in 0.2 M NaCl Eluate

A GAG preparation from the 0.2 M NaCl eluate was subjected to two-dimensional electrophoresis on a cellulose acetate membrane and was stained with 0.1% alcian blue. Small arrow indicates the spot position of the sample.

were stained as the same broad bands of macromolecules with toluidine blue for GAG (data not shown).

The GAG component of the 0.2 M NaCl fraction was determined by two-dimensional electrophoresis on a cellulose acetate membrane (Fig. 2). The GAG released with alkali and pronase treatment was electrophoresed in the position of HS used as the standard. Furthermore, the GAG was digested with heparitinase and deaminated with sodium nitrite but not with chondroitinase ABC. From these results, I have concluded that the proteoglycan of the 0.2 M fraction may have only the HS chain as the GAG. The 0.15 M fraction was also entirely composed of HS (data not shown).

The estimated average molecular weight of the 0.2 M NaCl fraction (HSPG) was 400 kilodaltons (350—450 kDa) on the basis of SDS-PAGE and was similar to that of anterior capsules from calf lens.[10] However, the sugar content (Table II) differed from that previously reported.[21] The reason for these differences are not known. The sugar composition of

Table I. Amino Acid Composition of Subfractions from Bovine Lens Capsules

Amino acid[a]	0.15 M NaCl fraction	0.2 M NaCl fraction	Bovine glomerular basement membrane[b]
Hydroxyproline	—	—	6
Aspartic acid	80	70	82
Threonine	55	54	49
Serine	83	86	79
Glutamic acid	124	122	116
Proline	71	93	100
Glycine	131	138	120
Alanine	70	77	80
1/2 Cystine	21	24	61
Valine	69	65	57
Methionine	15	11	11
Isoleucine	34	22	21
Leucine	79	67	64
Tyrosine	23	20	20
Phenylalanine	27	28	25
Histidine	28	30	20
Hydroxylysine	—	6	2
Lysine	25	19	25
Arginine	65	68	62

a) The values of amino acid residues are given per 1000 amino acid residues. *b*) Quoted from reference 5.

Table II. The Proteoglycan Composition of the 0.2 M NaCl Fraction from DEAE-Cellulose Chromatography

Components	μmol/mg[a]
Glucosamine[b]	0.12
Galactosamine[b]	0.02
Hexuronic acids[c]	0.15
Total amino acids[d]	1.18

a) Values are expressed per dry weight of proteoglycan. *b*) Determined by the amino acid analyzer.[11] *c*) Determined by the carbazole method.[19] *d*) Determined from amino acid residues (Table I).

the GAG of the HSPG was notable for its high content of glucosamine. HSPG was found to consist of protein and carbohydrate in a ratio of about 75 to 25. The SDS-PAGE pattern of HSPG did not change with or without a reduction of the samples with dithiothreitol. Recently, the isolation of HSPG has been tried from other tissues. Accordingly, the molecular weight of proteoglycan from tetracarcinoma derived endodermal cells,[22,23] which are known to synthesize an extracellular matrix containing the basement membrane molecules, is 400 kDa and quite similar to that of the HSPG obtained from the lens capsules. It has been recently reported that the molecular weight of HSPG from EHS sarcoma was estimated to be 7.5×10^5 Da.[3]

In order to determine the molecular weight of the HS chain of HSPG, its GAG released with alkali and pronase treatment was applied to a Sephadex G-200 column equilibrated with 1.0 M NaCl/50 mM Tris–HCl buffer of pH 7.6. The average molecular weight of the lens capsule-HS chain was estimated to be 18800 using the calibration curve reported by Wasteson.[12]

The results presented in Table I summarize the amino acid compositions of the two proteoglycan subfractions eluted with 0.15 and 0.2 M NaCl on a DEAE-cellulose column and that of HSPG from the bovine glomerular basement membrane.[6] The amino acid compositions of

both fractions from the lens capsules were quite similar to that of the HSPG of the bovine glomerular basement membrane, showing high contents of glutamic acid and glycine, but different from those reported for other basement membrane components such as laminin,[2] type IV collagen[1] and nidogen.[24]

The biological function of HSPG is not well understood at present. However, it seems most likely that HSPG may serve as a regulator of the penetration of charged macromolecules in the basement membranes. Furthermore, it has been recently reported that HSPG is often present at the junction of the attachment fibrils and the matrix network[25,26] and that a basal lamina proteoheparan sulfate on the surface of skeletal muscle fibers associates with aggregates of acetylcholine receptors.[27] Now it is very interesting how HSPG contributes to the transparency of the lens capsule.

References

1) R. Timpl and G. R. Martin, "Immunochemistry of the Extracellular Matrix," Vol. II, ed. by H. Furthmayr, CRS Press, Florida, 1982, pp. 119—150.
2) R. Timpl and H. Rohde, *J. Biol. Chem.*, **254**, 9933 (1979).
3) J. R. Hassel, P. G. Robey, H. J. Barrach, J. Wilczek, S. I. Rennard and G. R. Martin, *Proc. Natl. Acad. Sci. U.S.A.*, **77**, 4494 (1980).
4) H. K. Kleiman, M. L. McGarvey, L. A. Liotta, P. G. Robey, K. Tryggvason and G. R. Martin, *Biochemistry*, **21**, 6188 (1982).
5) M. Kato, Y. Koike, S. Suzuki and K. Kimata, *J. Cell Biol.*, **106**, 2203 (1988).
6) N. Parthasarathy and R. G. Spiro, *J. Biol. Chem.*, **259**, 12749 (1984).
7) D. J. Klein, D. M. Brown, T. R. Oegema, P. E. Brenchley, J. C. Anderson, M. A. J. Dickinson, E. A. Horigan and J. R. Hassel, *J. Cell Biol.*, **106**, 963 (1988).
8) W. C. J. Branford and J. F. Hardy, *FEBS Lett.*, **78**, 229 (1977).
9) B. Radhakrishnamurthy, F. Smart, E. R. Dalferes and G. S. Brenson, *J. Biol. Chem.*, **255**, 7575 (1980).
10) P. S. Mohan and R. G. Spiro, *J. Biol. Chem.*, **261**, 4328 (1986).
11) S. Onodera and Y. Nagai, *Biochem. Biophys. Res. Commun.*, **129**, 95 (1985).
12) A. Wasteson, *J. Chromatogr.*, **59**, 87 (1971).
13) U. K. Laemmli, *Nature* (London), **222**, 680 (1970).
14) C. A. McDevitt and H. Muir, *Anal. Biochem.*, **44**, 612 (1971).
15) R. M. Zacharius and T. E. Zell, *Anal. Biochem.*, **30**, 148 (1969).
16) S. Onodera, *Chem. Pharm. Bull.*, **36**, 4881 (1988).
17) R. Hata and Y. Nagai, *Biochem. Biophys. Acta*, **304**, 408 (1973).
18) N. Fujii and Y. Nagai, *J. Biochem.*, **90**, 1249 (1981).
19) T. Bitter and H. M. Muir, *Anal. Biochem.*, **4**, 303 (1962).
20) O. H. Lowry, N. G. Rosebrough, A. L. Farr and R. J. Randall, *J. Biol. Chem.*, **193**, 265 (1951).
21) N. Parthasarathy and R. G. Spiro, *Arch. Biochem. Biophys.*, **213**, 504 (1982).
22) A. Oohira, T. N. Wight, J. McPherson and P. Bornstein, *J. Cell Biol.*, **92**, 357 (1982).
23) J. R. Couchman, *J. Cell Biol.*, **105**, 1901 (1987).
24) R. Timpl, M. Dziadesk, S. Fujiwara, H. Nowack and G. Wick, *Eur. J. Biochem.*, **137**, 455 (1983).
25) I. Leivo, *J. Histochem. Cytochem.*, **31**, 35 (1983).
26) J. Laterra, J. E. Silbert and L. A. Culp, *J. Cell Biol.*, **96**, 112 (1983).
27) M. J. Anderson and D. M. Fambrough, *J. Cell Biol.*, **97**, 1396 (1983).

Inhibitory Effects of Catechol Derivatives on Arachidonic Acid-Induced Aggregation of Rabbit Platelets

Shuji KITAGAWA,*[,a] Hiroko FUJISAWA,[b] Satoko BABA[b] and Fujio KAMETANI[b]

Niigata College of Pharmacy,[a] 5–13–2, Kamishin'ei-cho, Niigata 950–21, Japan and Faculty of Pharmaceutical Sciences, University of Tokushima,[b] 1–78, Sho-machi, Tokushima 770, Japan. *Received October 15, 1990*

Pyrocatechol and other non-substituted dihydric phenols, which have strong redox power, inhibited arachidonic acid-induced aggregation of rabbit platelets at much lower concentrations than those at which these phenols inhibited stable prostaglandin endoperoxide, U46619-induced aggregation. Among non-substituted dihydric phenols, pyrocatechol was most potent. In order to clarify the physicochemical properties of the phenolic compounds which control the inhibitory potencies of dihydric phenols, we observed the inhibitory effects of 3- and 4-substituents of pyrocatechol on arachidonic acid-induced platelet aggregation. Among seven derivatives tested, the inhibitory effect of 4-C_6H_5-substituent was strongest and 4-COOH-substituent was weakest. Inhibitory effects of the catechol derivatives were well correlated with the quotients of their hydrophobicities and oxidation-reduction potentials. Inhibitory effects of hydroquinone and resorcinol were also on the same correlation line. These results suggest that the inhibitory effects of catechol derivatives and other dihydric phenols are controlled by two physicochemical properties: oxidation–reduction potential and hydrophobicity.

Keywords catechol derivative; arachidonic acid; platelet aggregation; structure–activity relationship; oxidation–reduction potential

We earlier reported that monohydric phenols with simple substituents which do not have strong redox power inhibit platelet aggregation by non-specific interaction with platelet membranes.[1,2] The increase in membrane fluidity seems to be involved in their inhibitory process.[2] The inhibitory potencies of these phenols were well correlated with their hydrophobicities. This correlation is a common feature for aggregation inhibitors which exhibit their activities by non-specific interaction with platelet membrane.[1–6] Among phenolic compounds di- and poly-hydric phenols are known to have prominent redox power. Therefore, due to their antioxidant activities they are likely to interact with arachidonate cascade in addition to the non-specific interaction with membrane. In fact, it has been reported that various phenolic compounds such as quercetin inhibit platelet cyclooxygenase.[7–10] However, the physicochemical properties which control the activities of these phenolic compounds, as well as the molecular mechanism of their inhibition are still unknown. In this paper we report observation of the inhibitory effects of non-substituted dihydric phenols and mono-substituents of pyrocatechol whose oxidation–reduction potentials ranged from 0.680 to 1.179 V. We attempted to clarify the physicochemical properties of these derivatives which control the inhibitory potencies on arachidonic acid-induced platelet aggregation.

Experimental

Materials Dihydric phenols were obtained from Wako Pure Chemical Industries (Osaka, Japan) and Nakarai Tesque, Inc. (Kyoto, Japan). Arachidonic acid, bovine serum albumin (essentially fatty acid free) and bovine fibrinogen were obtained from Sigma Chemical Co. (St. Louis, MO, U.S.A.). U46619 was from Funakoshi Chemicals (Tokyo, Japan).

Preparation of Platelets Fresh rabbit blood anti-coagulated with one-tenth volume of acid citrate dextrose (ACD) (74.8 mM sodium citrate/38.1 mM citric acid/122 mM dextrose) was centrifuged at $230 \times g$ at room temperature for 13 min to obtain platelet-rich plasma. The plasma was then centrifuged at $1000 \times g$ for 8 min and the platelets were suspended in a solution of Na,K,Mg-Tris (137 mM NaCl, 5.4 mM KCl, 1 mM $MgCl_2$, 11 mM dextrose, 25 mM Tris–HCl adjusted to pH 7.4) containing 1 mg/ml albumin and fibrinogen. Spontaneous platelet aggregation during preservation was prevented by adding 129 mM citrate (adjusted to pH 7.4) to this suspension at a volume ratio of 1 : 9.

Measurement of Platelet Aggregation The platelet suspension was mixed with 9 vol. of the Na,K,Mg-Tris medium mentioned above. The final platelet concentration was about $7 \times 10^4/\mu l$. After preincubation with phenolic compounds for 2 min, $CaCl_2$ at a final concentration of 2 mM and stimulants were added, and aggregation was measured at 37 °C in an RAM-11 aggregometer (Rikadenki Kogyo Co., Tokyo, Japan). The effects of phenolic compounds on aggregation were expressed as the maximum aggregation with the reagents relative to that without reagents, as described previously.[4]

Results and Discussion

We first observed the effects of non-substituted dihydric phenols on arachidonic acid-induced aggregation. As shown in Fig. 1a, pyrocatechol inhibited arachidonic acid-induced platelet aggregation at micromolar concentration ranges. At 10 μM it almost completely inhibited the aggregation. Since pyrocatechol is more hydrophilic than phenol, its non-specific interaction with membrane lipid bilayer is expected to be less than that of phenol[1] (logarithm values of partition coefficient between *n*-octanol and H_2O for phenol and pyrocatechol are 1.48 and 1.01, respectively).[11] However, pyrocatechol inhibited arachidonic acid-induced aggregation at much lower concentration than phenol as

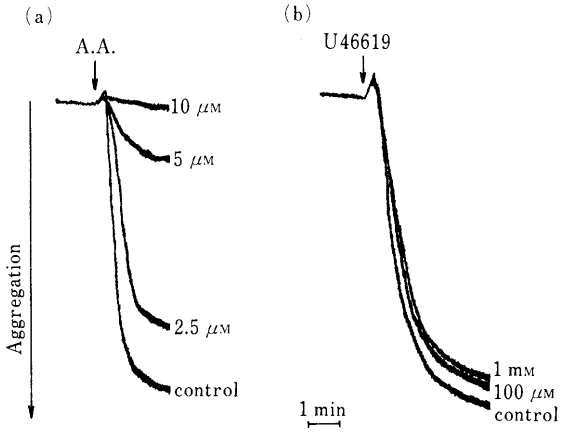

Fig. 1. Effects of Pyrocatechol on 10 μM Arachidonic Acid (A.A.)-Induced Platelet Aggregation (a) and 10 μM U46619-Induced Aggregation (b)

The concentrations of pyrocatechol are shown in the figure.

TABLE I. Concentrations of Phenol and Non-substituted Dihydric Phenols Causing 50% Inhibition, IC_{50} Values on Arachidonic Acid-Induced Platelet Aggregation

Compound	IC_{50} (μM)[a]
Phenol	216 ±56
Pyrocatechol	3.94± 0.41
Resorcinol	24.2 ± 7.5
Hydroquinone	21.6 ± 5.9

a) Data are means±S.D. of four experiments.

TABLE II. Concentrations of Substituted Catechols Causing 50% Inhibition, IC_{50} Values on Arachidonic Acid-Induced Platelet Aggregation, Hydrophobic Parameters, π, of Catechol Substituents and Oxidation–Reduction Potentials, E_0

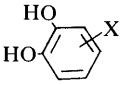

Substituent (X)	IC_{50} (μM)[a]	π[b]	E_0 (V)[c]
4-COO^-	7100 ±640	−4.36	0.833
3-OH	22.5 ±8.5	−0.67	0.680
4-NO_2	6.20 ±0.57	−0.28	—[d]
4-CH_3	5.00 ±1.28	0.56	0.753
H	3.94 ±0.41	0.00	0.795
4-Cl	1.63 ±0.15	0.71	0.801
4-C_6H_5	0.310±0.014	1.96	0.778

a) Data are means±S.D. of four experiments. b) Data cited are from Ref. 11. c) Data cited are from Ref. 15. d) Unknown under these experimental conditions.

shown in Table I. Moreover, pyrocatechol did not inhibit stable prostaglandin endoperoxide, U46619-induced aggregation significantly even at 1 mM, as shown in Fig. 1b. These results suggest that pyrocatechol inhibits arachidonic acid-induced platelet aggregation by inhibiting prostaglandin synthesis due to its redox power. These phenomena were generally found for di- and poly-hydric phenols. As shown in Table I for the IC_{50} values (concentrations causing 50% inhibition of aggregation), among the three non-substituted dihydric phenols, pyrocatechol, whose hydrophobicity was largest,[11] was most potent.

In order to find the physicochemical properties which control the inhibitory potencies of dihydric phenols, we next investigated the inhibitory effects of 3- and 4-substituents of pyrocatechol. As shown in Table II, inhibitory effect of 4-C_6H_5-substituent, which is the most hydrophobic among seven substituents tested, was strongest and that of 4-COOH-substituent, which is present as carboxylate anion at pH 7.4 ($pK_a = 4.40$),[12] was weakest. These results suggest that hydrophobicities of the compounds are also important for their inhibitory activities in addition to their redox power. As shown in Eq. 1 for the relation between IC_{50} values and the quotients of the logarithm values of partition coefficients and the oxidation–reduction potentials, there was good correlation for six derivatives whose oxidation–reduction potentials, E_0(V), are known under this experimental condition:

$$\log(1/IC_{50})(\mu M^{-1}) = 0.558(\log P_{est})/E_0 - 1.573 \quad (1)$$
$$(n=6, r=0.992)$$

where n is the number of compounds tested, r is the correlation coefficient and P_{est} is the estimated partition coefficient of each derivative, obtained by adding its π value to the partition coefficient of pyrocatechol between n-octanol and H_2O. It is shown that even the inhibitory effect of trihydric phenol, pyrogallol, and that of anionic 4-COO^- derivative were on this correlation line. Moreover, as shown in Fig. 2 and Eq. 2, inhibitory effects of other dihydric phenols, hydroquinone and resorcinol were on the same regression line:

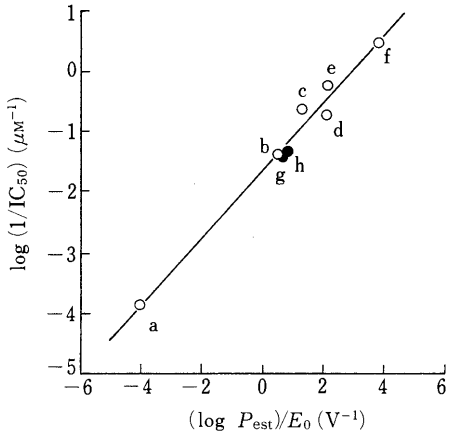

Fig. 2. Relation between Quotients of Logarithm Values of Estimated Partition Coefficients, P_{est}, and Oxidation–Reduction Potentials, E_0, and Inhibitory Effects on 10 μM Arachidonic Acid-Induced Aggregation, Expressed as Logarithm Values of $1/IC_{50}$ for Mono-substituents of Pyrocatechol and Other Non-substituted Dihydric Phenols

○, substituents of pyrocatechol: a, 4-COO^-- (protocatechuic acid); b, 3-OH- (pyrogallol); c, H (pyrocatechol); d, 4-CH_3-; e, 4-Cl-; f, 4-C_6H_5-substituents. ●, other non-substituted dihydric phenols: g, resorcinol; h, hydroquinone. Logarithm value of partition coefficient of each mono-substituted pyrocatechol was estimated by adding each π value to that of pyrocatechol between n-octanol and H_2O. Reported logarithm values of partition coefficients were used for resorcinol and hydroquinone (0.80 and 0.59, respectively).[11] Oxidation–reduction potentials of resorcinol and hydroquinone were obtained from refs. 15 and 16 (1.179 and 0.700V, respectively).

$$\log(1/IC_{50})(\mu M^{-1}) = 0.560(\log P_{est})/E_0 - 1.627 \quad (2)$$
$$(n=8, r=0.988)$$

The results obtained here indicate that not only redox power (small E_0 value) but also hydrophobicity (large P_{est} value) is important for the inhibitory potencies of catechol derivatives and other dihydric phenols. The differences of the activities of three non-substituted dihydric phenols are well explained by this analysis. The dependency of the inhibitory effects of catechol derivatives and other dihydric phenols on their hydrophobicities in addition to their redox power is probably because hydrophobicities are essential for the activities to enter into hydrophobic domain near the reaction sites where prostaglandin synthesis is taking place.

The dependency of the inhibitory potencies on hydrophobicity revealed here for catechol derivatives is also found for other drugs. For example, inhibitory effects of arylalkanic acids on collagen-induced platelet aggregation depend on hydrophobicity. These acids inhibit the aggregation due to the inhibition of cyclooxygenase by a different mechanism.[13] Although antioxidant activities of the catechol derivatives and other dihydric phenols seem to be involved in the inhibitory process, the molecular mechanism of the inhibitory effects is still not clear. These derivatives may inhibit prostaglandin synthesis due to the termination of the cyclooxygenase-catalyzed radical chain

reaction.[14] Further work is now in progress.

References

1) S. Kitagawa, Y. Ito, Y. Oda and F. Kametani, *Biochim. Biophys. Acta*, **1011**, 52 (1989).
2) S. Kitagawa, F. Kametani, K. Tsuchiya and H. Sakurai, *Biochim. Biophys. Acta*, **1027**, 123 (1990).
3) S. Kitagawa, T. Shinohara and F. Kametani, *J. Membrane Biol.*, **79**, 97 (1984).
4) S. Kitagawa, H. Nishitama and F. Kametani, *Biochim. Biophys. Acta*, **775**, 197 (1984).
5) S. Kitagawa, M. Ishida, K. Kotani and F. Kametani, *Biochim. Biophys. Acta*, **905**, 75 (1987).
6) T. Fujii, T. Sato, A. Tamura, M. Kometani, K. Nakao, K. Fujitani, K. Kodama and M. Akasu, *Eur. J. Pharmacol.*, **146**, 285 (1988).
7) J. A. Lindgren, H-E. Claesson and S. Hammarstrom, *Prostaglandins*, **13**, 1093 (1977).
8) K. Sekiya, H. Okuda and S. Arichi, *Biochim. Biophys. Acta*, **713**, 68 (1982).
9) R. Landolfi, R. L. Mower and M. Steiner, *Biochem. Pharmacol.*, **33**, 1525 (1984).
10) Y. Kimura, H. Okuda, T. Nomura, T. Fukai and S. Arichi, *Chem. Pharm. Bull.*, **34**, 1223 (1986).
11) A. Leo, C. Hansch and D. Elkins, *Chem. Rev.*, **71**, 525 (1971).
12) T. Ishimitsu, S. Hirose and H. Sakurai, *Chem. Pharm. Bull.*, **27**, 247 (1979).
13) M. Kuchar and V. Rejholec, *Drugs of the Future*, **11**, 689 (1986).
14) W. E. M. Lands and A. M. Hanel, *Prostaglandins*, **24**, 271 (1982).
15) L. Horner and E. Geyer, *Chem. Ber.*, **98**, 2016 (1965).
16) L. F. Fieser, *J. Am. Chem. Soc.*, **52**, 5204 (1930).

Evidence of Superoxide Dismutase in *Lactobacillus acidophilus*

Silvia N. González,[a,b] Carlos A. Nadra Chaud,[a] María C. Apella,[a] Ana M. Strasser de Saad,[a,b] and Guillermo Oliver*[,a,b]

Centro de Referencia para Lactobacilos [CERELA],[a] Chacabuco 145, 4000 Tucumán, Argentina, and Facultad de Bioquímica, Química y Farmacia, Universidad Nacional de Tucumán,[b] Argentina. *Received November 5, 1990*

Superoxide dismutase was prepared from *Lactobacillus acidophilus* CRL 358. An approximately 191-fold increase in the specific activity of the enzyme was achieved. The extract purified to apparent homogenity and exihibited a single band following polyacrylamide gel electrophoresis which detected superoxide dismutase activity. The apparent molecular weight determined by filtration was about 160000 dalton (Da).

Keywords superoxide dismutase; *Lactobacillus acidophilus*; enzyme activity; purification

Lactobacilli can grow either with or without oxygen; however, the presence or absence of superoxide dismutase (SOD) activity in these bacteria is still in question.[1] There is reason to suspect that metal salts might induce superoxide dismutase.

Yano and Nishie observed a three-fold induction of superoxide dismutase in *E. coli* B when the growth medium was aerated, but a five-fold induction when the aerated medium was enriched with Mn^{2+}.[2] Furthermore, Yamakura,[3] working with *Pseudomonas ovalis*, noted an increase in Fe-SOD when the medium was enriched with iron, and an increase in Mn-SOD when the medium was enriched with manganese. The same results were obtained by Pugh *et al.*,[4] working with *E. coli*. Preliminary experiments in our laboratory with some *lactobacilli* strains showed that a dyalized cell-free extract obtained from a culture enriched with manganese possessed superoxide dismutase activity.[5]

The results presented in this work provide the first evidence of the presence of SOD activity in the *lactobacillus* strain, and also describes a procedure for obtaining the purified form of that enzyme in *L. acidophilus* CRL 358.

Experimental

Xanthine, xanthine oxidase, nitroblue tetrazolium (NBT), and ethylenediaminetetraacetic acid (EDTA) were obtained from Sigma. All other materials were obtained from commercial sources at the highest available purity.

L. acidophilus CRL 358 (obtained from the Centro de Referencia para Lactobacilos) was grown in the medium described by De Man *et al.*[6] The initial pH was 6.5. After culturing for 18 h at 37 °C, the cells were harvested by centrifugation at 8000 *g* for 15 min at 4 °C in an International Equipment Cimoany B-20 centrifuge.

SOD was assayed by an indirect method based on the fact that SOD inhibits the reduction of NBT by superoxide radical ($O_2^{\cdot-}$) generated by the action of xanthine oxidase.[7]

The assay was performed in 3.0 ml of a solution containing 0.1 ml of 3 mM xanthine; 0.1 ml of 0.75 mM NBT; 0.1 ml of 3 mM EDTA; 0.1 ml of 1.5 mg/ml bovine serum albumin; 0.5 ml of dialized cell-free extract and 2.0 ml of a 0.05 M carbonate buffer (pH 10.2). After preincubation for 10 min at 25 °C, 0.1 ml of adequately diluted xanthine oxidase was added and the mixture was incubated for 20 min at 25 °C. The reaction was stopped by the addition of 0.1 ml of 6 mM $CuCl_2$ and the absorbance of this solution at 560 nm was measured and compared with that of the control, to which the cell-free extract had not been added.

Under the specified conditions, 1 unit of superoxide dismutase was considered that amount which gave a 50% decrease in the rate of reduction NBT.

Water that had been redistilled in glassware was used throughout in order to avoid interference with enzyme action by contaminating metal ions.

The protein content of the samples was determined by the method of Lowry *et al.*[8] using bovine serum albumin as a standard.

All spectrophotometric assays were performed with a Gilford spectrophotometer model 2000 UV/vis absorbance.

Results

Cells were washed three times in a 0.05 M phosphate buffer, pH 7.8 containing EDTA at the concentration of 10 mM. The washed cells were suspended in 15 ml at the same buffer and lysed by two passages through a French press at 28000 psi and at −30 °C. Cell debris was removed by centrifugation at 30000 *g* for 30 min at 4 °C. The supernatant was a cell-free extract which was treated with 5 ml of a 20% solution of streptomycin sulfate. After stirring for 1 h at 4 °C, the precipitate was discarded. The supernatant was precipitated with solid ammonium sulfate at 35 and 75% saturation and separated by centrifugation at 20000 *g* for 30 min at 4 °C. The precipitate fraction was suspended in a 0.05 M phosphate buffer, pH 7.8, and dialyzed against the same buffer for 24 h at 4 °C. During dialysis the buffer was replaced every 8 h. The dialyzed fraction was applied to a 2.6 × 40 cm diethylaminoethyl (DEAE)-cellulose column, equilibrated with the same buffer as that used for dialysis, and eluted using a 0.05—0.5 M linear gradient of that buffer. Fractions of 7.5 ml were collected at a flow rate of 30 ml/h. The elution profile obtained from this column, which was monitored at 280 nm is shown in Fig. 1. The fractions that showed SOD activity were pooled and the suspension was applied to a Sepharose 6B column (2 × 50 cm) which was equilibrated and eluted as mentioned above (Fig. 2).

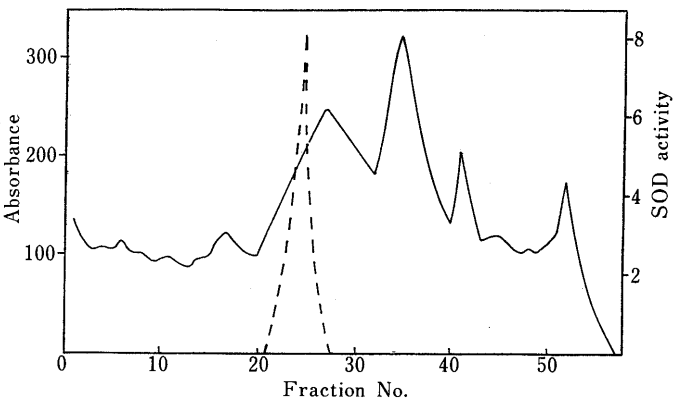

Fig. 1. Chromatography on DEAE Cellulose

L. acidophilus preparation, after dialysis for 24 h as described in the text, was applied to a column (2.6 × 40 cm) of DEAE cellulose equilibrated at 4 °C with a 0.05 M phosphate buffer, pH 7.8, and eluted using a 0.05—0.5 M linear gradient of the same buffer. ——, absorbance at 280 nm; – – –, SOD activity of the fraction collected. Tubes 21 to 26 were pooled.

TABLE I. Purification of SOD from *L. acidophilus* CRL 358

Purification step	Volume (ml)	Protein (mg/ml)	Specific activity (units/mg)	Recuperation (%)	Purification (fold)
Cell-free extract	20.0	21.300	0.400	100.00	1.00
Ammonium sulfate 35—75%	16.5	16.800	0.421	69.46	1.05
DEAE-cellulose	22.5	0.440	5.680	34.58	14.20
Sepharose 6B	14.0	0.018	76.790	11.51	191.70

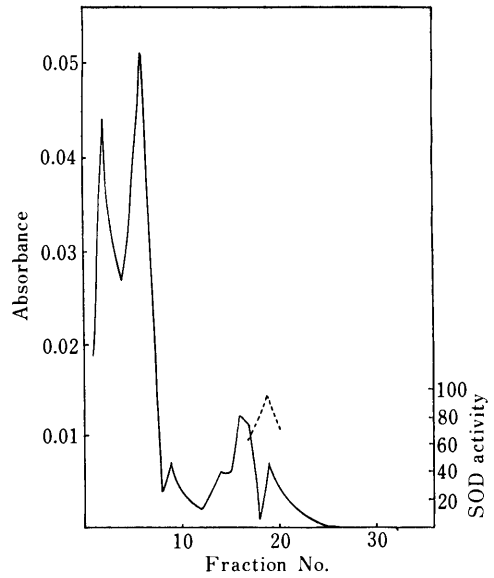

Fig. 2. Chromatography on Sepharose 6B

The active fractions obtained as described in the text were applied to a column (2 × 50 cm) of Sepharose 6B equilibrated at 4 °C with a 0.05 M phosphate buffer, pH 7.8 and eluted using a 0.05—0.5 M linear gradient of the same buffer. ——, absorbance at 280 nm; – – –, SOD activity of the fractions collected. Tubes 18 to 20 were pooled.

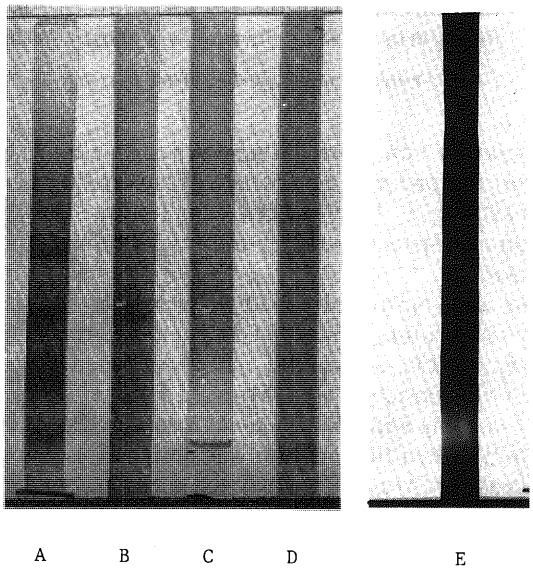

Fig. 3. Polyacrylamide Gel Electrophoresis Patterns of Fractions at Different Steps of the Purification of SOD Enzyme

A, cell-free extract; B, 35—75% ammonium sulfate fraction; C, peak fraction eluted on DEAE-cellulose column chromatography; D, peak fraction eluted on Sepharose 6B column chromatography; E, SOD activity.

Fractions containing the highest specific activity (tubes) were pooled and concentrated by ultracentrifugation over a PM 50 membrane (American Corporation, Cambridge, Massachusetts). A summary of the purification scheme appears in Table I; the overall purification was about 191-fold. The fractions obtained from the purification procedure analyzed by electrophoresis in standard polyacrylamide gels (7.8% gel porosity) as described by Ornstein and Davis[9] are shown in Fig. 3.

SOD activity was detected in polyacrylamide gel that exposed only one protein band when the method of Beauchamp and Fridovich[10] was used (Fig. 3).

The molecular weight was estimated to be approximately 160000 dalton (Da) using a calibrated column with a known molecular weight protein mixture. The molecular weight standards used were ferritine 440000 Da; catalase 232000, and lactate dehydrogenase (LDH) 140000 Da.

Discussion

Reduced nicotinamide adenine dinucleotide (NADH) oxidase,[11,12] reduced nicotinamide adenine dinucleotide phosphate (NADPH) oxidase,[12] NADH peroxidase,[12,13] and NADPH peroxidase[12] were found in the cell-free extracts of *lactobacilli*, suggesting that $O_2^{\cdot-}$ or H_2O_2 might have been formed in the cytosol of aerobically grown *lactobacilli*, and consequently they should have some defense systems against oxygen toxicity. For many years it has been known that $MnSO_4$ or *L. plantarum* cell extracts[1] don't scavenge $O_2^{\cdot-}$ stoichiometrically with an accumulation of Mn^{3+} accompanied by a reaction rate approaching zero as Mn^{2+} is exhausted. Following the appearance of Mn^{3+} it can be seen that, indeed, initially all the Mn^{2+} is oxidized to Mn^{3+}, but that catalytic $O_2^{\cdot-}$ scavenging continues. This fact could be explained if SOD activity is present in lactic acid bacteria. However, there has been controversy about the presence of SOD in *lactobacilli*.[14,15] These are very interesting organisms from an evolutionary viewpoint in that some obligated anaerobes first became tolerant to oxygen and finally became able to utilize oxygen as an effective electron acceptor.

In the present paper we describe the isolation and some properties of a SOD obtained from *L. acidophilus*. The purified SOD seems to possess Mn as an essential metal ion in its molecules because it was resistent to cyanide and azide ions.[16,17] The molecular weight of Mn-SOD isolated from *E. coli*,[18] *S. mutans*,[19] *B. subtilis*,[20] *A. laidlawii*,[21] *B. stearothermophilus*,[22] *S. faecalis*,[23] was found to be about 40000 Da, but the Mn-containing mitochondrial SOD from *S. cervisiae*[24] exhibited a molecular weight of about 80000 Da. The enzyme isolated from *L. acidophilus* has a molecular weight higher than those of the previously described Mn-containing SOD. Mn-SOD found in mitochondria and prokaryotes are either a dimer or tetramer

with a subunit molecular weight of about 20000 Da.

Similar SOD activity was obtained in our laboratory when working with *L. acidophilus* ATCC 4356 (data not shown); however, in order to clarify the aerotolerant nature of these microorganisms, further studies concerning other *lactobacilli* strains are required and this is what we are engaged in at present.

Acknowledgments This work was partially supported by grants from Secretaría de Ciencia y Tecnología, República Argentina, 1985—1986, and PID No. 3-09100/86 from CONICET.

References

1) R. Archibald, *CRC Crit. Rev. Microbiol.*, **13**, 63 (1986).
2) K. Yano and H. Nishie, *J. Gen Appl. Microbiol.*, **24**, 333 (1978).
3) F. Yamakura, *Biochim. Biophys. Acta*, **422**, 280 (1976).
4) S. Y. R. Pugh, J. L. Diguiseppi, and I. Fridovich, *J. Bacteriol.*, **160**, 137 (1984).
5) S. N. González, M. C. Apella, N. C. Romero, A. P. de Ruiz Holgado, and G. Oliver, *Chem. Pharm. Bull.*, **37**, 3026 (1989).
6) J. C. De Man, M. Rogosa, and M. E. Sharpe, *J. Appl. Bacteriol.*, **23**, 130 (1960).
7) T. Imanari, M. Hirota, M. Miyazaki, K. Hayakawa, and Z. Tamura, *Igaku No Ayumi*, **101**, 496 (1977).
8) O. H. Lowry, N. J. Rosebrough, A. L. Farr, and R. J. Randall, *J. Biol. Chem.*, **193**, 265 (1951).
9) L. Ornstein and B. J. Davis, *Ann. N.Y. Acad. Sci.*, **121**, 321 (1964).
10) G. Beauchamp and I. Fridovich, *Anal. Biochem.*, **44**, 276 (1971).
11) C. F. Strittmatter, *J. Biol. Chem.*, **234**, 2789 (1959).
12) L. P. Brown and P. S. Van Demark, *Can. J. Microbiol.*, **14**, 829 (1968).
13) A. A. Yousten, J. L. Johnson, and M. Salim, *J. Bacteriol.*, **123**, 242 (1975).
14) Y. I. Iwamoto and I. Mifuchi, *Chem. Pharm. Bull.*, **30**, 237 (1982).
15) F. Götz, E. T. Elstner, B. Sedewitz, and E. Lengjelder, *Arch. Microbiol.*, **125**, 215 (1980).
16) I. Fridovich, *J. Biol. Chem.*, **245**, 4053 (1970).
17) H. P. Misra and I. Fridovich, *Arch. Biochem. Biophys.*, **189**, 317 (1978).
18) B. B. Keele, J. M. McCord, and I. Fridovich, *J. Biol. Chem.*, **245**, 6176 (1970).
19) P. G. Vance and B. B. Keele, *J. Biol. Chem.*, **247**, 4782 (1972).
20) K. Tsukuda, T. Kido, Y. Shimasue, and K. Soda, *Agric. Biol. Chem.*, **47**, 2865 (1983).
21) R. Reinards, R. Altdorf, and H. D. Ohlenbusch, *Hoppe-Seyler's Z. Physiol. Chem.*, **365**, 577 (1984).
22) C. J. Brock and J. I. Harris, *Biochem. Soc. Trans.*, **5**, 1537 (1977).
23) L. Britton, D. P. Malinowsk, and I. Fridovich, *J. Bacteriol.*, **134**, 229 (1978).
24) C. Diltow and J. T. Johanensen, *Carlsberg Res. Comm.*, **47**, 71 (1982).

Effect of L-Cysteine on Plasma Concentration and Urinary Excretion of 1-(Tetrahydro-2-furanyl)-5-fluorouracil Metabolites[1)]

Nobuo KAWABATA,* Kenichi YANO, Hiromitsu OHNO, and Toshiaki NAKASHIMA

Central Research Laboratory, SS Pharmaceutical Co., Ltd., 1143 Nanpeidai, Narita, 286, Japan. *Received September 25, 1990*

Effects of L-cysteine (CySH) on the plasma concentrations and the urinary excretion of 1-(tetrahydro-2-furanyl)-5-fluorouracil (FT) and its metabolites were studied by high performance liquid chromatography in rats.

Significantly higher plasma concentrations of FT, 5-fluorouracil (5-FU) and *cis*-4′-OH-FT were obtained after an oral administration of FT (500 mg/kg) combined orally with CySH (500 mg/kg) when compared to FT alone. The urinary excretions of 5-FU, *trans*-3′-OH-FT, *cis*-4′-OH-FT, *trans*-4′-OH-FT and 4′,5′-dehydro-FT significantly decreased up to 12 h but that of α-fluoro-β-alanine significantly increased up to 24 h by the combined administration of CySH. Furthermore, the plasma concentration of 5-FU significantly increased at 0.5 h and its urinary excretion significantly decreased up to 4 h after an intraperitoneal administration of 5-FU (10 mg/kg) combined orally with CySH (500 mg/kg) when compared to 5-FU alone. The urinary pH significantly changed to acidic and the urinary volume significantly increased by the combined administration of CySH, so it was thought that the reabsorption of 5-FU through renal tubules from urine could increase and the increment of the urinary excretion of α-fluoro-β-alanine was caused by this. Then it was suggested that the increase of the plasma concentrations of 5-FU and *cis*-4′-OH-FT could be attributed to the decrease of their urinary excretions after an administration of FT combined with CySH when compared to FT alone.

Keywords 1-(tetrahydro-2-furanyl)-5-fluorouracil; cysteine; rat; metabolite; plasma concentration; urinary excretion

1-(Tetrahydro-2-furanyl)-5-fluorouracil (FT) is considered a prodrug of 5-fluorouracil (5-FU) and exerts antitumor activity through metabolic activation.[2,3)] FT is metabolized to some metabolites by liver microsome and cytosol as shown in Fig. 1.[4–9)] Among these metabolites, *trans*-3′-OH-FT, *cis*-4′-OH-FT, *trans*-4′-OH-FT and 4′,5′-dehydro-FT exhibit antitumor activities as well as 5-FU.[10,11)] However, the antitumor activities of these metabolites are lower than that of 5-FU.[11)]

Many efforts have been made to increase the antitumor activity of FT by obtaining a high plasma concentration of 5-FU.[12,13)] In the previous paper,[1)] we reported that the plasma and liver concentrations of FT and 5-FU increased after the administration of FT (500 mg/kg, *p.o.*) combined with L-cysteine (CySH, 500 mg/kg, *p.o.*) when compared to FT alone in rats.

In this study we tried to obtain some clue for elucidating the mechanism of the CySH effect in the previous study,[1)] in terms of metabolic and excretory aspects, by examining the plasma concentrations and the urinary excretions of FT and its metabolites after the oral administration of FT alone or combined with CySH in rats.

Experimental

Materials FT and 5-FU were purchased from Aldrich Chemical Co. (Milwaukee, WI) and Sigma Chemical Co. (St. Louis, MO), respectively. α-Fluoro-β-alanine was obtained from Tokyo Kasei Kogyo Co. (Tokyo). CySH was purchased from Nippon Rikagakuyakuhin Co. (Tokyo). All other reagents and solvents were of reagent grade. FT (150 mg/ml) was dissolved in 1 M Na_2CO_3. 5-FU (5 mg/ml) and CySH (100 mg/ml) were dissolved in physiological saline. These solutions were administered immediately after preparation.

Animals Male Wistar rats weighing 135—170 g were used. Rats were fasted overnight before drug administration and during the experiment, and were given water *ad libitum*.

Preparation of Plasma and Urine Rats were orally given FT alone at

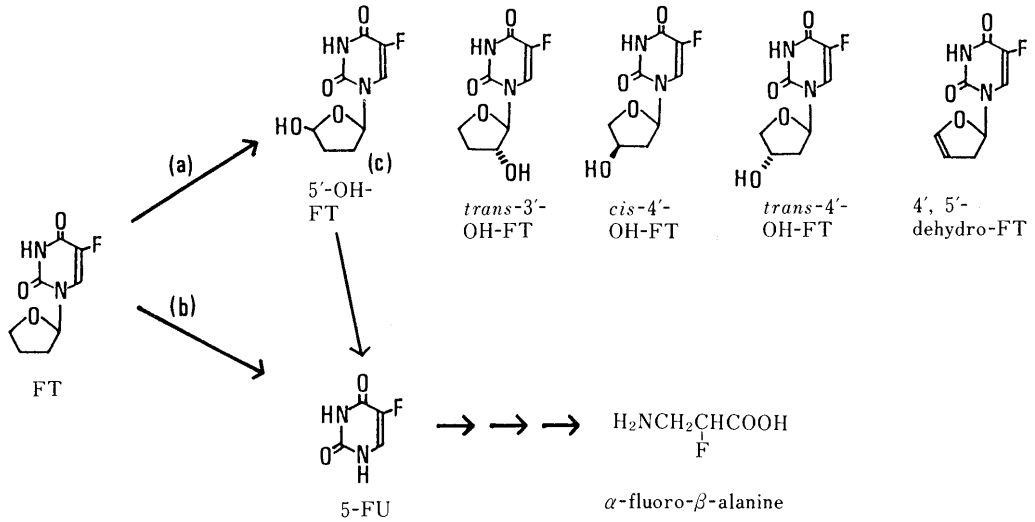

Fig. 1. Postulated Metabolic Pathways of FT

(a) Liver microsome (cytochrome P-450). (b) Liver cytosol (dehydrogenase, *etc.*). (c) Absolute configuration remains undetermined.

a dose of 500 mg/kg or combined with CySH at the same dose, 0, 3 and 6 h after the administration of FT. Rats were lightly anesthetized with diethyl ether at definite times after the administration of FT. Blood was drawn from the inferior vena cava into heparinized tubes after laparotomy. After centrifugation at 2500 rpm for 10 min the resulting plasma was collected. After the administration of FT alone or combined with CySH, urine was sampled up to 12 and 24 h by using metabolic cages and urine up to 4 h was used immediately after collection to determine the pH value.

In a separate experiment, other groups of rats were intraperitoneally given 5-FU at a dose of 10 mg/kg alone or combined orally with CySH at a dose of 500 mg/kg at 0 and 4 h before the administration of 5-FU. Plasma at 0.5 h and urine up to 4 h after the administration of 5-FU were prepared as described above.

The plasma and urine samples were frozen for subsequent analyses.

Determination of FT and Its Metabolites in Plasma and Urine FT and its metabolites except α-fluoro-β-alanine were extracted from plasma and urine according to the method of Wu *et al.*[14] The volume of samples (0.1—1 ml) of plasma or urine was adjusted to 1 ml with water, and mixed with 0.1 ml of 0.5 M NaH_2PO_4. The mixture was extracted with 8 ml of ethyl acetate. After centrifugation at 2500 rpm for 10 min the organic layer was removed and evaporated to dryness under vacuum at room temperature. The residue was dissolved in 100 μl of methanol, and a 5—10 μl aliquot of this solution was injected into a Hitachi Model 635 high performance liquid chromatograph with a JASCO Model UVIDEC-100-V absorbance detector under the following conditions as previously reported[15,16]: analytical column, Nucleosil C_{18} (5 μm, octadecyl, 250 × 4.6 mm i.d., Gasukuro Kogyo Inc., Tokyo); mobile phases, 15% methanol in 0.01 M acetate buffer (pH 4.2) for analyzing FT and 5-FU, 0.01 M acetate buffer (pH 4.0): acetonitrile (95 : 5) for other metabolites; flow rate, 1 ml/min; column temperature, 50 °C; detector, UV, 280 nm. *Trans*-3′-OH-FT, *cis*-4′-OH-FT, *trans*-4′-OH-FT and 4′,5′-dehydro-FT were identified by comparing their retention times with the ones in the previous report.[15] They were quantitated using a standard curve of FT assuming identical chromatographic properties and extinction coefficients of 280 nm.[7]

For the determination of α-fluoro-β-alanine in urine, urine samples (0.1 ml) were added to 0.4 ml water and 0.5 ml of 2% sulfosalicylic acid. After shaking for 15 min and subsequent centrifugation at 3000 rpm for 10 min, a 250 μl aliquot of the supernatant was injected into a Hitachi Model 835 amino acid analyzer under the following conditions: analytical column, 2619 F (ion exchange resin, 150 × 2.6 mm i.d., Hitachi, Tokyo); mobile phase, citrate buffer (pH 3.0, 35 mM lithium citrate, 50 mM lithium chloride, 160 mM citric acid, 5% ethyl alcohol, 50 mM β-thiodiglycol, 0.8 mM polyoxyethylene (23) lauryl ether and 0.8 mM capric acid); flow rate, 0.37 ml/min.

Statistics Data were evaluated by the Student's *t*-test and the difference was considered significant at $p < 0.05$.

Results and Discussion

The plasma concentrations of FT and its metabolites could be measured by using 0.01 M acetate buffer (pH 4.0): acetonitrile (95 : 5) as a mobile phase (Fig. 2). Separation of 5-FU from an endogenous component was achieved by using 15% methanol in 0.01 M acetate buffer (pH 4.2) instead as a mobile phase. The concentrations of FT, 5-FU and *cis*-4′-OH-FT significantly increased after the administration of FT combined with CySH when compared to FT alone (Fig. 3) as reported in the previous study.[1] In the case of the other metabolites, no significant difference was observed for *trans*-3′-OH-FT and *trans*-4′-OH-FT except at 8 and 24 h, respectively.

The urinary excretions of FT metabolites, except α-fluoro-β-alanine, were significantly suppressed up to 12 h and 5-FU was still significantly less excreted up to 24 h after the administration of FT combined with CySH when compared to FT alone (Fig. 4). The pH of urine obtained up to 4 h significantly changed to acidic and the urinary volume significantly increased (Table I).

On the other hand, CySH is metabolized to acidic compounds in rats.[17] It is thought that due to these formations the urinary pH might then change to acidic by the combined administration of CySH. 5-FU is a weakly acidic compound, and has a pK_a value of 8.0.[18] It is reported that 5-FU is reabsorbed from renal tubules in rats.[19] It is

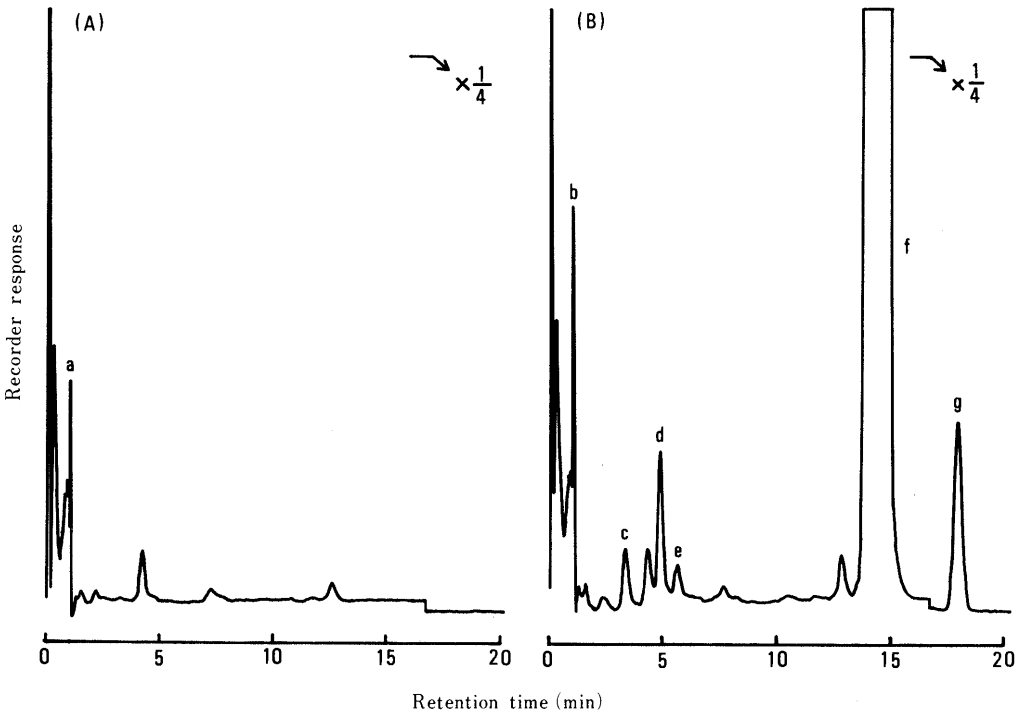

Fig. 2. Chromatograms Obtained from Rat Plasma

(A) Blank plasma, (a) endogeneous component. (B) Plasma at 4 h after oral administration of FT (500 mg/kg); (b) 5-FU, 0.74 μg/ml; (c) *trans*-4′-OH-FT, 0.66 μg/ml; (d) *cis*-4′-OH-FT, 1.34 μg/ml; (e) *trans*-3′-OH-FT, 0.41 μg/ml; (f) FT, 127.6 μg/ml; (g) 4′,5′-dehydro-FT, 6.62 μg/ml. Mobile phase; 0.01 M acetate buffer (pH 4.0): acetonitrile (95 : 5). The sensitivity of the instrument was lowered to 1/4 for 4′,5′-dehydro-FT after other metabolites were detected. Other conditions are described in Experimental.

well known that the renal tubular reabsorption of weakly acidic compounds is greatly enhanced by the decline of urinary pH causing an increase in the concentration of their undissociated forms. Therefore, it is possible to consider that the tubular reabsorption of 5-FU increased due to the decline of the urinary pH caused by the combined administration of CySH. Furthermore, the plasma concentrations of 5-FU significantly increased from 1.53 to 1.88 μg/ml at 0.5 h and concomitantly its urinary excretion significantly decreased from 2.1 to 1.6% in the percentage of the dose after the administration of 5-FU (10 mg/kg, i.p.) combined with CySH (500 mg/kg, *p.o.*) when compared to 5-FU alone. Accordingly, it was suggested that the increase of the plasma concentrations of 5-FU might be attributed, at least partially, to the decrease of its urinary excretion. And also, the increase of the plasma concentrations of *cis*-4′-OH-FT might be caused by the decrease of its urinary excretion in the same manner as 5-FU.

The distinct effect of CySH was not observed in FT metabolites other than 5-FU and *cis*-4′-OH-FT. In the case of these metabolites, the significant increase of their plasma concentrations may not have been distinctly observed in spite of the decrease of their cummulative urinary excretions (Fig. 4A).

The plasma concentrations of the FT metabolites did not decrease, but those of *cis*-4′-OH-FT as well as 5-FU (Fig. 3), significantly increased. Furthermore, the excreted amount of α-fluoro-β-alanine significantly increased (Fig. 4B), and was thought to be caused by the increase of the plasma concentrations of 5-FU. T_{max} of 5-FU was 8 h in plasma (Fig. 3). Some processes are needed for its metabolism[9] and then an appearance of significant increase in the excreted amount of α-fluoro-β-alanine might be observed not up to 12 h, but from 12 h after the ad-

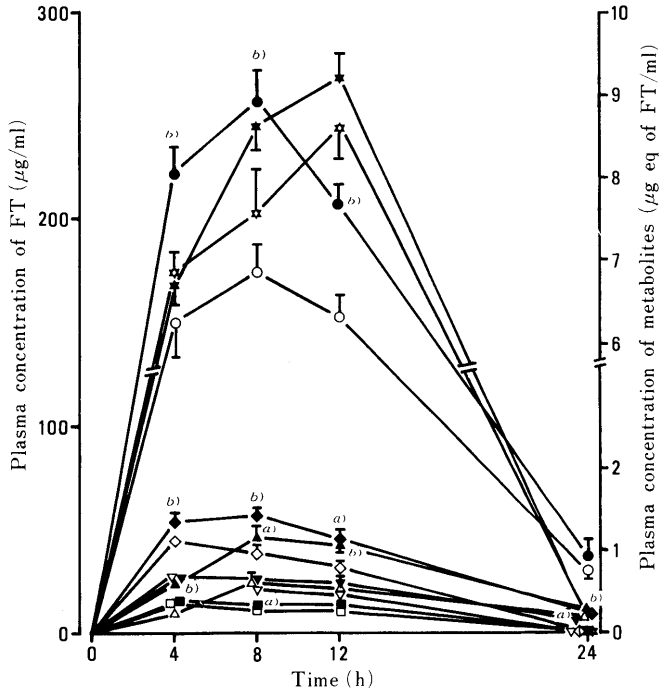

Fig. 3. Plasma Concentrations of FT (○, ●), 5-FU (△, ▲), *trans*-3′-OH-FT (□, ■), *cis*-4′-OH-FT (◇, ◆), *trans*-4′-OH-FT (▽, ▼) and 4′,5′-Dehydro-FT (☆, ★) after Oral Administration of FT (500 mg/kg) Alone (Open Symbol) or Combined with CySH (500 mg/kg, Closed Symbol)

Each point represents the mean ± S.E. for five rats. *a*) $p<0.05$ and *b*) $p<0.01$ when compared to FT alone.

TABLE I. Urinary pH and Urinary Volume Obtained after Oral Administration of FT (500 mg/kg) Alone or Combined with CySH (500 mg/kg)

	FT alone	FT + CySH
Urinary pH	7.87 ± 0.09	6.76 ± 0.22[a)]
Urinary volume (ml)	3.94 ± 0.43	5.70 ± 0.11[a)]

Each value represents the mean ± S.E. for five rats. *a*) $p<0.01$ when compared to FT alone.

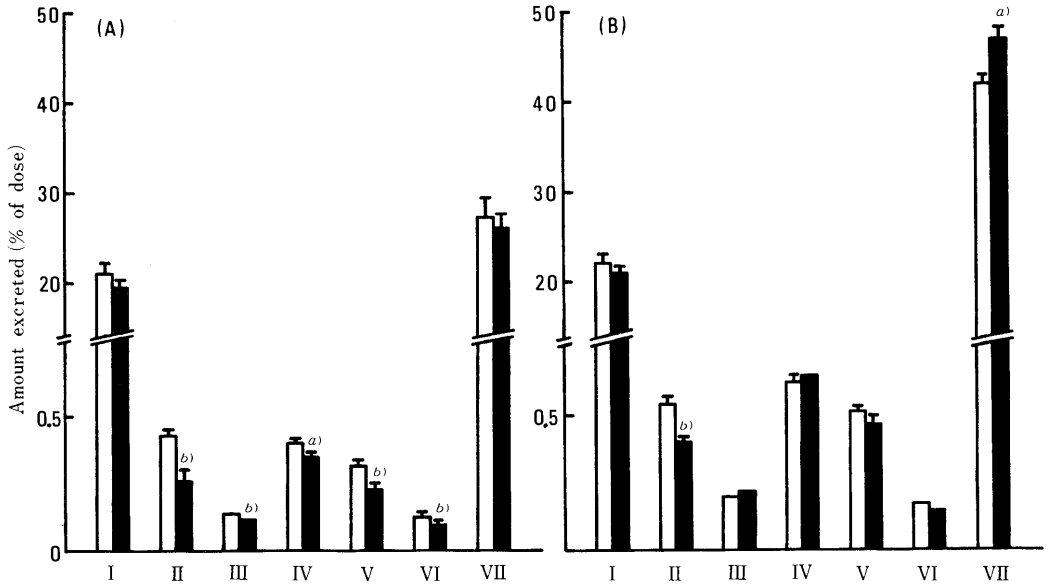

Fig. 4. Cumulative Urinary Excretions of FT (I), 5-FU (II), *trans*-3′-OH-FT (III), *cis*-4′-OH-FT (IV), *trans*-4′-OH-FT (V), 4′,5′-Dehydro-FT (VI) and α-Fluoro-β-alanine (VII) after Oral Administration of FT (500 mg/kg) Alone (Open Symbol) or Combined with CySH (500 mg/kg Closed Symbol)

(A) and (B) show up to 12 and 24 h, respectively, after administration of FT alone or combined with CySH. Each column represents the mean ± S.E. for five rats. *a*) $p<0.05$ and *b*) $p<0.01$ when compared to FT alone.

ministration of FT combined with CySH. It was suggested that FT and 5-FU metabolism was not inhibited by the combined administration of CySH *in vivo*.

On the other hand, we obtained the result that CySH did not have any effect on FT absorption from the digestive tract *in situ* in the previous study.[1] And there was no difference in the amount of FT remaining in the digestive tract after the administration of FT (500 mg/kg, *p.o.*) combined with CySH (500 mg/kg, *p.o.*) when compared to FT alone (data not shown).

Based on these results, it seems that other mechanisms (*e.g.*, an effect of CySH on FT and/or its metabolite distribution) for 5-FU and *cis*-4′-OH-FT, besides the one obtained in this study, might also be responsible for the increase of the plasma concentrations of FT (Fig. 3). In fact, the urinary volume significantly increased by the combined administration of CySH (Table I). And in relation to this, we obtained the preliminary result that a volume of distribution of FT significantly decreased when accompanied by the decrease of body fluid volumes, which is thought to be caused by an increase of urinary volume, after the administration of FT (100 mg/kg, i.v.) combined with CySH (500 mg/kg, *p.o.*) when compared to FT alone in rats (data not shown).

In conclusion, it was suggested that the decrease of urinary excretion of 5-FU and *cis*-4′-OH-FT might result, at least partially, in the increase of their plasma concentrations after the administration of FT combined with CySH when compared to FT alone. But, we could not successfully account for the mechanism of the increase in the plasma concentrations of FT. Further work is in progress on the aspects of FT and its metabolite distribution.

References

1) N. Kawabata, S. Sugiyama, T. Kuwamura, T. Satoh, and H. Kitagawa, *Jpn. J. Pharmacol.*, **33**, 735 (1983).
2) A. M. Cohen, *Drug Metab. Dispos.*, **3**, 303 (1975).
3) S. Fujimoto, T. Akao, B. Itoh, I. Koshizuka, K. Koyano, Y. Kitsukawa, M. Takahashi, T. Minami, H. Ishigami, Y. Nomura, and K. Itoh, *Cancer Res.*, **36**, 33 (1976).
4) Y. M. EI Sayed and W. Sadee, *Biochem. Pharmcol.*, **31**, 3006 (1982).
5) Y. M. EI Sayed and W. Sadee, *Cancer Res.*, **43**, 4039 (1983).
6) S. Kawata, Y. Minami, S. Tarui, T. Marunaka, M. Okamoto, and T. Yamano, *Jpn. J. Pharmacol.*, **36**, 43 (1984).
7) A. T. Wu, J. L. Au, and W. Sadee, *Cancer Res.*, **38**, 210 (1978).
8) T. Marunaka, Y. Minami, Y. Umeno, A. Yasuda, T. Sato, and S. Fujii, *Chem. Pharm. Bull.*, **28**, 1795 (1980).
9) K. L. Mukherjee and C. Heidelberger, *J. Biol. Chem.*, **235**, 433 (1960).
10) A. J. Lin, R. S. Benjamin, P. N. Rao, and T. L. Loo, *J. Med. Chem.*, **22**, 1096 (1979).
11) S. Fujii, *Eksp. Klin. Farmakoter.*, **12**, 84 (1983).
12) G. A. Belitsky, V. M. Bukhman, and I. A. Konopleva, *Cancer Chemother. Pharmacol.*, **6**, 183 (1981).
13) K. Tatsumi, M. Fukushima, T. Shirasaka, and S. Fujii, *Jpn. J. Cancer Res.*, **78**, 748 (1987).
14) A. T. Wu, H.-J. Schwandt, C. Finn, and W. Sadee, *Res. Commun. Chem. Pathol. Pharmacol.*, **14**, 89 (1976).
15) J. L. Au, A. T. Wu, M. A. Friedman, and W. Sadee, *Cancer Treat. Rep.*, **63**, 343 (1979).
16) J. L. Au and W. Sadee, *Cancer Res.*, **40**, 2814 (1980).
17) K. Yamaguchi, I. Ueda, T. Nakashima, Y. Kakimoto, M. Kizumi, E. Hasegawa, and H. Nakagawa, "Biochemical Experimental Lecture 11, Amino Acid Metabolism and Biogenic Amines," ed. by Y. Nishizuka, O. Hayaishi and H. Wada, Tokyokagakudojin, Tokyo, 1976, pp. 431–466.
18) I. Wempen, R. Duschinsky, L. Kaplan, and J. J. Fox, *J. Am. Chem. Soc.*, **83**, 4755 (1961).
19) J. L. Au, J. S. Walker, and Y. Rustum, *J. Pharmacol. Exp. Ther.*, **227**, 174 (1983).

Acid-Induced and Calcium-Induced Gelation of Alginic Acid: Bead Formation and pH-Dependent Swelling

Toshihisa YOTSUYANAGI,* Isamu YOSHIOKA, Naoki SEGI and Ken IKEDA

Faculty of Pharmaceutical Sciences, Nagoya City University, Mizuho-ku, Nagoya 467, Japan. *Received November 7, 1990*

The bead formation of alginic acid in the acidic medium (pH 1.0) was investigated in comparison with that of calcium-induced gel beads. The acid-induced gel beads could be visually observed in a few minutes as the transparent spherical figures were detected with a clear boundary between the gel bead and the bulk aqueous phase. The weight change of acid-induced curing beads was as fast as that of the calcium-induced during the initial several hours. But the acid-induced bead lost 15% of its weight at the full stage of gelation, while the calcium-induced lost 37%. The respective beads were incubated at various pHs of 1.0 to 5.0. In the acidic region up to 2.5, the physical integrity of both beads was well maintained. As the pH was raised, they swelled in a sigmoid manner with an inflexion point at about pH 3.2 for the acid-induced beads and at pH 2.8 for the calcium-induced. However, the acid-induced bead disintegrated at a pH of more than 3.5, while the calcium-induced was kept well. The acid-induced beads would be advantageous for some drugs to be incorporated that calcium ions used for alginate gelation might cause undesirable effects such as insoluble salt formation and inactivation due to metal–drug chelation.

Keywords alginic acid; gel bead; calcium-induced gel; acid-induced gel; swelling; pH-dependent disintegration

Introduction

Alginic acid is a binary heteropolymer consisting of β-D-mannuronic acid (M) and α-L-guluronic acid (G) residues at different proportions of MM-, GG- and MG-blocks.[1] It is well known that the GG blocks have a surpassing affinity to divalent metal ions, being responsible for the gelation.[2] The gelation involves the cooperative binding of the metal ions, which is described in terms of an "egg box" junction model.[3] Calcium association with alginates in the gel-forming reaction has been extensively studied.[4-6]

Alginate gel beads contract to a great extent as the medium pH is lowered because of its decreased solubility due to the increasing fraction of unionized carboxy groups and water discharge.[6,7] This leads us to the possibility of forming of gel beads without the aid of calcium ions. The calcium-free gel beads would be advantageous for incorporation in some drugs because calcium ions used for gelation might offer undesirable effects such as salt formation and inactivation caused by metal–drug chelation. It is useful, in this respect, to explore the physico-chemical properties of calcium-free gel beads as a possible drug gel vehicle.

The present study is concerned with the gelation behavior and pH-dependent disintegration of acid-induced gel beads in contrast to that of calcium-induced gel beads.

Experimental

Materials Na-alginate (Lot No. AR01, Tokyo Kasei Kogyo, Tokyo) was used after being dialyzed against distilled water using a Visking cellulose tube (36/32) for 3 d (three water replacements/d) followed by lyophilization. The proportions of GG-, MM- and MG-blocks of the polymer were 24.8, 37.9 and 37.8%, respectively, and the M/G ratio was 1.28.[7] Calcium chloride, dihydrate (special grade, Wako Pure Chem., Osaka) was used. All other chemicals were of reagent grade.

Preparation of Calcium-Induced and Acid-Induced Alginate Gel Beads Calcium-induced beads were prepared by the method previously described.[6] Briefly, an alginate solution (4%, w/w in distilled water) was allowed to fall in drops into 0.1 M $CaCl_2$. One droplet of the alginate solution has an average weight of 12.9 mg ($n=20$) with a water content of 96.4%. The resulting gel beads were left in the salt solution for 3 d to become cured; they were then referred to as fully-cured beads. Since the gel beads formed contained excess calcium ions which were not associated with the gelation, the excess calcium was washed out once a day for 2 d with freshly distilled water. These beads were referred to as washed gel beads. Acid-induced gel beads were prepared in a KCl–HCl buffer (pH 1.0) in the same manner. The beads were also cured in the buffer for 3 d.

Weight Changes of Curing Alginate Gel Beads Ten curing beads were taken out from the salt solution or from the acidic buffer solution at appropriate time intervals and weighed immediately after the removal of surface moisture on a filter paper. The weight fraction of curing beads was expressed as the ratio between the weight of the curing beads and the 10 original droplets of alginate solution assumed at $t=0$.

Determination of Water Content in Alginate Gel Beads Samples of gel beads were dried by heating in an oven at 110 °C overnight. The weight difference before and after drying was assumed to be attributed to the amount of water in the beads, represented as the volume of water assuming $d=1.0$.

Determination of the Size of Alginate Gel Beads The size of the fully-cured beads was determined by taking a photograph of each bead (×20, 10 beads) and measuring its diameter at three different positions. The average value was taken. Because of the deformed figures of the bead bodies, the volume of the acid-induced bead was measured as follows: 50 beads were placed in a test tube connected with a graduated pipette (1 ml, a minimal graduation 0.01 ml) which was appropriately filled with a buffer (pH 1.0). The difference of the volume with and without the beads was assumed to be the volume of the beads. The average value of two runs was taken.

Results and Discussion

Figure 1 shows the weight changes of curing gel beads in the acidic buffer (pH 1.0) and in 0.1 M $CaCl_2$. When a droplet of the alginate solution contacted the acidic buffer solution, the gelation seemed to occur instantly on the surface of the droplet, as observed in the $CaCl_2$ solution.[8] The average diameter of the droplet calculated from its weight (assuming the density of the alginate solution 4%, w/w = 1) was 2.91 mm. In a few minutes, the gel formation could be visually observed as transparent spherical bodies appeared with a distinct boundary between the gel bead and the bulk phase. The results of weight changes indicate that during the initial several hours the interior water is rapidly squeezed out and the curing gradually reaches its full stage in about 1 d in the acid-induced beads and in 2 d in the calcium-induced beads. Thus, the intrinsic rate of acid-induced gelation is likely to be as fast as that of calcium-induced gelation. However, the apparent curing rate of gel beads should be controlled by the penetration rate of calcium ions or hydrogen ions into the interior of

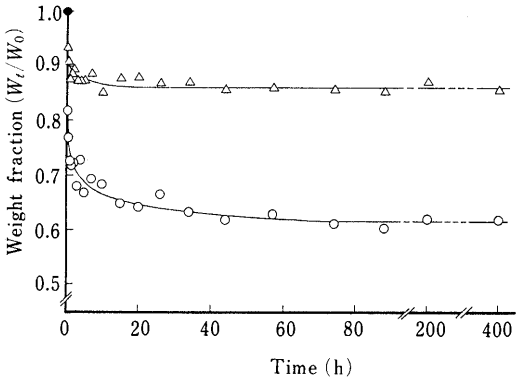

Fig. 1. Weight Fraction Changes of Curing Alginate Gel Beads at 25 °C

△, KCl–HCl (pH 1.0); ○, 0.1 M $CaCl_2$. W_0, weight of 10 droplets of initial alginate solution (● assumes $t=0$); W_t, weight of 10 beads at time t. Initial alginate concentration was 4% (w/w).

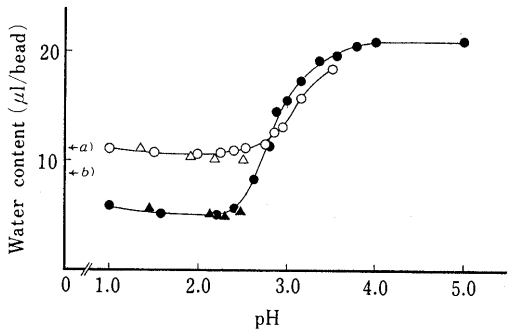

Fig. 2. Water Content Changes of Alginate Gel Beads Incubated at Different pHs at 25 °C

Acid-induced beads: ○, acetate–HCl; △, KCl–HCl. Calcium-induced beads (washed): ●, acetate–HCl; ▲, KCl–HCl. The water contents of original beads: *a*) acid-induced beads; *b*) calcium-induced (washed) bead. Beads were incubated in buffers for 3 d. Each plot represents an average value of 2–3 runs. Initial alginate concentration was 4% (w/w).

TABLE I. Physical Dimensions of Gel Beads Formed in 0.1 M $CaCl_2$ and in KCl–HCl Buffer (pH 1.0)

Bead[a]	Radius[b] (×10 cm)	Volume (×10^3 cm^3)	Weight[b] (mg/bead)	Water reserve[c] (g/g)	Density (g/cm^3)	M_i[b,d] (×10^7 mol)
Calcium-induced						
Fully-cured	1.20	7.15	7.71	12.6	1.08	16.7
Washed	1.28	8.88	9.41	17.5	1.06	11.0
Acid-induced	1.51 (0.99)[e]	10.9[f]	11.6	26.8	1.06	—

a) Gel beads were always prepared with 4% w/w alginate solution. *b*) Average value of 10 beads. *c*) g of water/g of dried residue. *d*) M_i is the total amount of calcium in a single bead. *e*) The thickness of flat-shaped beads. *f*) See Experimental.

the droplets. Therefore, the curing time would depend on the droplet size of the alginate solution used. It should be noted that calcium-induced beads lose 37% of their weight at the full stage of gelation, while the weight loss of the acid-induced bead is only 15%.

While calcium-induced gelation produced almost complete spheres,[7,8] acid-induced gelation produced a disc-like bead with a diameter of 1.51 mm and a thickness of 0.99 mm. This indicates that the calcium-induced gel structure which instantly formed on the immediate surface of the droplets is physically strong enough to maintain the spherical figure of droplets. In the mean time, the acid-induced beads seem to gain only a physically frail support of the immediate surface, so that the droplets are deformed by their dead weight. Spherical gel beads could be formed if the droplet size of the polymer solution were reduced.

Table I shows the physical dimensions of the acid-induced and calcium-induced gel beads. The acid-induced gel beads hold more water than the calcium-induced beads, as typically shown in the volume and water reservation data.

Figure 2 shows the changes of water content, *i.e.* swelling behavior, of the acid-induced and calcium-induced washed gel beads incubated at various pHs of 1.0 to 5.0 for 3 d. The original water content level of both types of the beads before being incubated are pointed out on the ordinate. In the acidic region up to pH 2.5, the physical integrity of the respective beads was well maintained, regardless of the buffer components. As the medium pH was raised, the beads swelled in a sigmoid manner with an inflexion point at about pH 3.2 for the acid-induced bead, assuming that the maximal water content was comparable to that of the calcium-induced bead. However, the acid-induced bead disintegrated at a pH of more than 3.5, while the calcium-induced was maintained up to at least pH 5.0 with an inflexion point at pH 2.8.[7] The inflexion points observed in both types of the beads, which seem to reflect the pK_a values of the carboxy acid residues in the respective beads, were only slightly different from each other, suggesting that the dissociation behavior of the acidic residues was not largely affected by the calcium association. The fully-cured bead incubated at pH 2.8 suffered from a decrease in the associated calcium to 1.36×10^{-7} mol/bead from 8.93×10^{-7} mol/bead obtained before incubation.[6] The swelling of the gel body is most probably due to the dissociation of carboxy acid residues, which results in more dissolution, namely more water migration into the body. Electrostatic repulsion among the charged residues in the beads is also a possible reason for the swelling.

As previously reported,[6] no associated calcium remained in the beads when the calcium-induced beads, whether fully-cured or washed were, incubated at pH 1.0. Such a complete discharge of the metal ion was interpreted in a way that the carboxy groups shifted to an unionized form which was thermodynamically favorable in the acidic environment. It is noted that despite no associated calcium in both the beads at pH 1.0, the water content of acid-induced beads was about twice as high as that of calcium-induced beads. These results could be explained as follows: the acid-induced bead was formed with a rather random gel structure as the result of the conversion of uronic acid residues, regardless of M or G, to an unionized form. In contrast, as the calcium-induced bead showed a massive water discharge on its gelation (about one-third in weight), calcium-induced gelation with GG blocks built a very compact and entangled gel structure, which seems to be too strong to be unraveled for expansion, even if the associated calcium were removed.

The acid-induced gel beads are likely to have a disadvantage regarding acid-susceptible drugs when they are incorporated in the beads. However, the beads can maintain their physical integrity up to about pH 3.5, which could allow for a replacement of the original interior water with a lower pH, with water or a drug solution having a

higher pH at which the drug is stable. A primary advantage of acid-induced gel beads is that they are formed under calcium-free conditions and may be useful in avoiding an undesirable calcium-drug interaction.

References

1) D. A. Rees and J. W. B. Samuel, *J. Chem. Soc.*, **1967**, 2295.
2) O. Smidsrod, *Faraday Discuss. Chem. Soc.*, **57**, 263 (1974).
3) D. A. Rees, E. R. Morris, D. Thom and J. K. Maddem, "The Polysaccharides," Vol. 1, ed. by G. O. Aspinall, Academic Press, New York, 1982, pp. 224—235.
4) E. R. Morris, D. A. Rees and D. Thom, *Carbohydr. Res.*, **66**, 145 (1978).
5) D. Thom, G. T. Grant, E. R. Morris and D. A. Rees, *Carbohydr. Res.*, **100**, 29 (1982).
6) T. Yotsuyanagi, I. Yoshioka, N. Segi and K. Ikeda, *Chem. Pharm. Bull.*, **38**, 3124 (1990).
7) N. Segi, T. Yotsuyanagi and K. Ikeda, *Chem. Pharm. Bull.*, **37**, 3092 (1989).
8) T. Yotsuyanagi, T. Ohkubo, T. Ohhashi and K. Ikeda, *Chem. Pharm. Bull.*, **35**, 1555 (1987).

Inhibitory Effects of Non-steroidal Anti-inflammatory Drugs on Superoxide Generation

Yasukatsu YUDA,*[,a] Junko TANAKA,[a] Koukichi SUZUKI,[a] Kazuei IGARASHI,[b] and Tetsuo SATOH[b]

Pharmaceutical Research Laboratories, Meiji Seika Kaisha, Ltd.,[a] Morooka-cho, Kohoku-ku, Yokohama 222, Japan and Faculty of Pharmaceutical Sciences, Chiba University,[b] 33, Yayoi-cho, 1-chome, Chiba 260, Japan. *Received August 15, 1990*

Effects of non-steroidal anti-inflammatory drugs (NSAID: amfenac sodium, diclofenac sodium, indomethacin and ketoprofen) on the generation of superoxide anion (O_2^-) by isolated rat polymorphonuclear leukocytes (PMN) were studied spectrophotometrically using cytochrome c. The effects of these drugs were also studied on O_2^- production by the xanthine–xanthine oxidase and reduced nicotinamide adenine dinucleotide phosphate (NADPH)–NADPH oxidase systems.

Amfenac sodium, at 0.1 mM, inhibited significantly O_2^- generation in rat PMN induced by opsonized zymosan. At 0.5 mM, diclofenac sodium and indomethacin inhibited the O_2^- generation in rat PMN. All of the above drugs slightly inhibited O_2^- production by the xanthine–xanthine oxidase system. On the other hand, O_2^- production by the NADPH–NADPH oxidase system was significantly inhibited by the addition of amfenac sodium, ketoprofen or indomethacin. These results suggest that non-steroidal anti-inflammatory drugs do not work as an O_2^- scavenger and block O_2^- production by the NADPH–NADPH oxidase system of rat PMN. It is concluded that amfenac sodium and the other drugs are able to inhibit granulocyte O_2^- production by blocking the activation of NADPH-oxidase.

Keywords superoxide generation; polymorphonuclear leucocyte; reduced nicotinamide adenine dinucleotide phosphate-oxidase; xanthine–xanthine oxidase; anti-inflammatory drugs

Introduction

Active oxygen species have been known to be implicated in a variety of pathophysiological phenomena such as inflammation, aging, hepatotoxicity and ischemic brain and myocardium damage. Such active, oxygen species include superoxide radical (O_2^-), hydroxyl radical ($\cdot OH$), singlet oxygen ($^1O_2$) and H_2O_2.[1]

The importance of oxygen free radicals and related activated oxygen intermediates in the pathogenesis of rheumatoid arthritis (RA) is increasingly recognised.[2-4] In RA and in other inflammatory diseases polymorphonuclear leucocytes (PMN) and macrophages are stimulated, which results in the secretion of inflammatory mediators, including large amounts of superoxide and hydrogen peroxide. These cells produce O_2^- by the reduced nicotinamide adenine dinucleotide phosphate (NADPH)-oxidase, an enzyme complex located in the plasma membrane and phagosome.[5]

Oyanagui[6] demonstrated that non-steroidal anti-inflammatory drugs (NSAIDs) inhibited O_2^- production of paraffin-oil-induced macrophages but not those of the xanthine oxidase system; this suggests that NSAIDs block O_2^- production and do not work as O_2^- scavengers.

We studied the inhibitory activity of NSAIDs (amfenac sodium, diclofenac sodium, indomethacin and ketoprofen) against the generation of O_2^- by isolated rat PMN. The effects of these drugs on O_2^- production by the xanthine–xanthine oxidase and NADPH–NADPH oxidase systems were also studied.

Experimental

Animals Male Wistar rats (200—250 g) were used. The animals obtained from Nippon SLC Inc., Hamamatsu, Japan.

Materials Xanthine oxidase solution was obtained from Boehringer Mannheim Yamanouchi, Tokyo. Xanthine, NADPH, zymosan and ferricytochrome c (horse heart type III) were obtained from Sigma, U.S.A. The other chemicals were of reagent grade and were used without purification.

Preparation of Cell Suspension Wistar rat peritoneal cells were obtained 18 to 20 h after the peritoneal injection of 0.15% sterile oyster glycogen solution in 0.9% NaCl. The cells were freed of erythrocytes by hypotonic lysis and washed twice in Krebs–Ringer phosphate buffer (KRP), pH 7.4. The proportion of PMN obtained in this manner averaged 85%.

Measurements of O_2^- Generation The generation of O_2^- was measured by the reduction of ferricytochrome c (horse heart type III) as described by Goldstein and his coworkers.[7]

Leucocytes (1×10^7) and 0.1 mM ferricytochrome c were incubated in the presence of opsonized zymosan for 30 min at 37 °C. The final volume of the reaction mixture was adjusted to 2.0 ml. Opsonized zymosan was prepared by incubating 50 mg zymosan in 1 ml of freshly prepared normal rat serum for 40 min at 37 °C. After centrifuging this at $1700 \times g$ for 15 min, the opsonized particles were suspended again at a concentration of 50 mg/ml in phosphate buffered saline. This was stored at −80 °C before use.

Incubation was terminated by placing the tubes in an ice-water bath; they were then centrifuged at $700 \times g$ for 10 min at 4 °C. The absorbance of the supernatants was read at 550 nm with a spectrophotometer.

Preparation of NADPH Oxidase The oxidase was obtained from zymosan-activated neutrophils by a modification of the method of Hohn and Lehrer.[8] Opsonized zymosan was suspended in Dulbecco's phosphate buffered saline (pH 7.4) containing 2 mM NaN_3 at a concentration of 25 mg/ml. Two ml of zymosan suspension prewarmed to 37 °C was mixed with 2 ml of a prewarmed suspension of PMN in Ca-free KRP ($2-5 \times 10^7$ cells/ml). The mixture was incubated for 10 min at 37 °C with gentle shaking. The incubation was stopped with 4 ml of ice-cold KRP, and the cells were centrifuged at $250 \times g$ for 5 min at 4 °C. The cell pellet was resuspended in 6 ml of ice-cold 0.34 M sucrose containing 1 mM $NaHCO_3$ and the cells were disrupted at 0 °C by sonication. After disrupting the cells, the preparation was centrifuged at $250 \times g$ for 5 min at 4 °C to remove zymosan, nuclei and unbroken cells. The supernatant was then centrifuged at $30000 \times g$ for 30 min at 4 °C. The pellet, which contains the O_2^--forming activity, was resuspended in sucrose at 1 mg protein/ml.

Measurement of NADPH Oxidase The oxidase activity was assayed by measuring the rate of O_2^- formation in the presence of NADPH. The method was based on the spectrophotometric determination of superoxide-mediated ferricytochrome c reduction as originally described by Babior *et al.*[9]

To a tube containing 1.0 ml of 65 mM KRP (pH 7.4) was added 0.2 mM fravin-adenine dinucleotide (FAD) (0.2 ml), 1.0 mM NADPH (0.2 ml), 0.2% Triton X-100 solution (0.2 ml), 0.1 mM cytochrome c (0.2 ml) and 10 μl of a solution which contains a drug or superoxide dismutase (SOD) solution. This mixture was incubated for 5 min at 37 °C. To this solution 0.2 ml of O_2^--forming particles was added, and this was incubated for 10 min at 37 °C. The reaction was stopped by adding 10 μl SOD solution. The amount of reduced cytochrome c was measured spectrophotometrically.

Measurement of SOD-like Activity The activity of O_2^- scavengers was assayed according to the nitrite method described by Oyanagui.[10]

0.5 mM hypoxanthine (0.2 ml), 10 mM hydroxylamine plus 8.85 mM

hydroxylamine *o*-sulfonic acid solution (0.1 ml), 0.1 ml of the sample, and 0.2 ml of water were added to a tube containing 0.2 ml of buffer solution (final concentrations of 13 mM KH_2PO_4 and 7 mM $Na_2B_4O_7$) containing 0.5 mM ethylenediaminetetraacetic acid (EDTA)–2Na (pH 8.2). The reaction was started by adding 0.2 ml of 1 mU/ml xanthineoxidase (XOD). This mixture (1.0 ml) was incubated for 30 min at 37 °C. 2.0 ml of a coloring reagent which contained 30 μM *N*-1-naphthylethylenediamine, 3 mM sulfanilic acid and 25% acetic acid were added. The optical absorption was measured at 550 nm.

Measurements of Protein The amount of protein was determined by the method of Lowry *et al.*

Statistical Method The results were calculated as mean values ± standard deviation (mean ± S.D.) and the probability for significance of the differences was determined by analysis of the variance.

Results

The inhibition of the generation of superoxide anion (O_2^-) by NSAID (amfenac sodium, diclofenac sodium, indomethacin and ketoprofen) in isolated rat PMN is shown in Table I.

Amfenac sodium at 0.1 mM significantly inhibited the O_2^- generation in rat PMN induced by opsonized zymosan. At 0.5 mM, indomethacin and diclofenac sodium inhibited significantly the O_2^- generation. At 0.05 mM, all of the above drugs only slightly inhibited the O_2^- generation (data not shown).

Table II shows the inhibitory effect of the NSAIDs on the generation of O_2^- by NADPH-dependent oxidase. At 0.1 mM, amfenac sodium and indomethacin significantly inhibited the O_2^- generation. At 0.5 mM, amfenac sodium, ketoprofen and indomethacin caused significant inhibition. At 1 mM, diclofenac sodium slightly inhibited the O_2^- generation, while the other drugs did not inhibit it.

All of the above drugs, from 0.1 to 1 mM, only slightly inhibited the generation of O_2^- by the XOD system and did not inhibit the production of uric acid.

TABLE I. Effects of Anti-inflammatory Agents on O_2^- Production in Rat PMN

Compounds	Conc. (μM)	Superoxide generation (μM/min)	Inhibition (%)
Control		0.613 ± 0.052	
Diclofenac Na	100	0.609 ± 0.058	0.65
	500	0.509 ± 0.112[a]	16.97
Ketoprofen	100	0.592 ± 0.096	3.43
	500	0.530 ± 0.052	13.54
Indomethacin	100	0.611 ± 0.048	0.32
	500	0.502 ± 0.068[a]	18.11
Amfenac Na	100	0.504 ± 0.038[a]	17.78
	500	0.560 ± 0.045	8.65

PMN was preincubated with or without a test compound for 5 min and incubations were performed in the presence of opsonized zymosan for 30 min at 37 °C. Each value is the mean ± S.D. of 5 separate experiments. 0.5% carboxymethyl cellulose (CMC) solution was used as a control. *a*) Significantly different ($p < 0.001$) from control.

TABLE II. Effects of Anti-inflammatory Agents on O_2^- Production by NADPH Oxidase

Compounds	Conc. (μM)	Superoxide generation (μM/min)	Inhibition (%)
Control		0.257 ± 0.093	
Diclofenac Na	100	0.264 ± 0.102	−2.7
	500	0.233 ± 0.112	9.3
	1000	0.179 ± 0.120	30.4
Ketoprofen	100	0.222 ± 0.022	13.6
	500	0.132 ± 0.073[b]	48.6
	1000	0.114 ± 0.100[b]	55.6
Indomethacin	100	0.084 ± 0.051[b]	67.3
	500	0.121 ± 0.057[b]	52.9
	1000	0.207 ± 0.072	19.5
Amfenac Na	100	0.042 ± 0.023[a]	83.7
	500	0.095 ± 0.052[b]	63.0
	1000	0.208 ± 0.069	19.1

Each value represents mean ± S.D. of 5 separate experiments. The oxidase activity was assayed by measuring the rate of O_2^- formation in the presence of NADPH. *a*) Significantly different ($p < 0.001$) from control. *b*) Indicates $p < 0.05$. 0.5% CMC solution was used as a control.

Discussion

There are a number of reports which deal with the effects of NSAIDs on O_2^- generation. However, the results regarding the effects of certain drugs vary depending upon cell types and stimuli used. In addition, the mechanism by which NSAIDs retard the chemotactic factor-induced PMN responses remains conjectural. With regard to the O_2^- generation of PMN, Kitagawa *et al.*[11] proposed that chymotrypsin-like serine proteases are essential for these cells to initiate and maintain the O_2^- generation in response to the stimuli. The suggested also that, these proteases might be involved in the activation of NADPH oxidase, which has been known to be the primary enzyme for O_2^- production.

Here we have shown that the anti-inflammatory drugs such as amfenac sodium, diclofenac sodium and indomethacin significantly inhibit the generation in PMN induced by opsonized zymosan. However, the above drugs scarcely inhibit O_2^- generation by xanthine oxidase system. From this, it is evident that these drugs do not have O_2^- scavenger activity. Oyanagui[6] suggested that NSAIDs did not inhibit O_2^- production of the xanthine oxidase system. This agrees with our results. On the other hand, it has been speculated that the inhibitory effect of NSAIDs on the generation of O_2^- is based on the inhibition of NADPH oxidase activity. In the present study, amfenac sodium and indomethacin at 0.1 mM significantly inhibit the generation of O_2^- induced by the NADPH oxidase system. However, concentrations of NSAIDs as high as 1 mM scarcely inhibit the generation of O_2^- induced by the NADPH oxidase system. This shows that amfenac sodium and indomethacin have two different actions; at low concentrations they inhibit the generation of O_2^-, while at high concentrations they activate it. Recently, Dale *et al.*[12] suggested that indomethacin increased O_2^- production from human neutrophils when used in concentrations of 10^{-6}—10^{-4} M. They further reported that some other NSAIDs have effects similar to indomethacin and that the same drugs increase O_2^- production by aggregated immunoglobulin G (IgG) and opsonized zymosan. And then, Mibu *et al.*[13] or Oda *et al.*[14] suggested that the NSAIDs had a weak effect on O_2^- generation and scarcely inhibited it. However, amfenac sodium and the other NSAIDs have the capacity to inhibit NADPH oxidase. This activity may be regarded as the anti-inflammatory mechanism of these NSAIDs. In addition, it may be considered that these NSAIDs decrease the phagocytic function of PMN by non-specifically stabilizing the biological membrane and inhibiting the generation of O_2^- from PMN by NADPH oxidase.

Acknowledgements We are grateful to Dr. M. Nishio for valuable discussions and a critical reading of the manuscript. We thank Drs. S. Inoue and S. Fukatsu for the encouragement.

References

1) H. Sies (ed.), "Oxidative Stress," Academic Press, Inc., London, 1985.
2) B. Halliwell and J. M. C. Gutteridge, *Biochem. J.*, **219**, 1 (1984).
3) J. Lunec, S. P. Halloran, A. G. White, and T. L. Dormandy, *J. Rheumatol.*, **8**, 233 (1981).
4) R. M. Tate and J. E. Repine, "Free Radicals in Biology," Vol. VI, ed. by W. A. Pryer, Academic Press, Inc., New York, 1984, pp. 199—209.
5) P. Biemond, A. J. G. Swaak, J. M. A. Penders, C. M. Beindorff, and J. F. Koster, *Ann. Rheum. Dis.*, **45**, 249 (1986).
6) Y. Oyanagui, *Biochem. Pharmacol*, **25**, 1473 (1976).
7) G. Witz, N. J. Lawrie, M. A. Amoruso, and B. D. Goldstein, *Chem. Biol. Interact.*, **53**, 13 (1985).
8) D. C. Hohn and R. I. Lehrer, *J. Clin. Invest.*, **55**, 707 (1975).
9) M. Markert, P. C. Andrews, and B. M. Babior, *Methods Enzymol.*, **105**, 358 (1984).
10) Y. Oyanagui, *Anal. Biochem.*, **142**, 290 (1984).
11) S. Kitagawa, F. Takaku, and S. Sakamoto, *J. Clin. Invest.*, **65**, 74 (1980).
12) M. M. Dale and A. Penfield, *Br. J. Pharmacol.*, **92**, 63 (1987).
13) M. Oda, M. Ogihara, T. Sato, M. Kurumi, and M. Iwaki, *Nippon Yakurigaku Zasshi*, **87**, 521 (1986).
14) H. Mibu, J. Hasegawa, M. Niwa, M. Nozaki, K. Tsurumi, and H. Fujimura, *Nippon Yakurigaku Zasshi*, **83**, 355 (1984).

Studies on an Enzymatically Synthesized Antitumor Polysaccharide SPR-901

Hisao KADO,* Yasuo YONETA, Suguru TAKEO, Masaru MITSUI, and Nobuhiro WATANABE

Pharmaceutical Research Laboratories, Sapporo Breweries Ltd., 10, Okatohme, Yaizu, Shizuoka 425, Japan. *Received January 14, 1991*

An antitumor polysaccharide SPR-901 was found in a fermented broth of a kind of lactic acid bacteria isolated from rice bran. SPR-901 is a high molecular α-glucan and its linkages are almost linear α-1,6 glucosidic ones with a small amount (*ca.* 5%) of branches at C-3 positions. It is a highly purified α-glucan and it contains no protein and no inorganic salts. SPR-901 showed significant antitumor activities against murine allogeneic and syngeneic tumors by both intraperitoneal and oral administration, and enhanced carbon clearance ability in mice, while it showed no direct cytotoxicities *in vitro*. The mechanism of antitumor activities of SPR-901 is supposed to be a host-mediated one, and this substance is classified as one of the biological response modifiers. These properties of SPR-901 were identical to those of RON, which was obtained from rice bran, therefore we concluded that these two polysaccharides were the same substance.

Keywords RBS; RON; dextran; α-glucan; polysaccharide; SPR-901; *Leuconostoc mesenteroides* subsp. *dextranicum*; antitumor; Meth-A; BRM

In previous papers we reported on the antitumor polysaccharides RBS[1] (rice bran saccharide) and RON.[2] RBS is obtained from the hot water extract of rice bran and RON is a purified main fraction of RBS. Their antitumor and immunomodulating activities were studied well.[3,4] Recently, we found that a certain polysaccharide produced by a kind of lactic acid bacteria, isolated from rice bran, possessed antitumor activities.[5] Therefore we studied the physico-chemical properties and biological activities of this polysaccharide, comparing it with those of RON.

Materials and Methods

Preparation of SPR-901 SPR-901 is enzymatically synthesized by the extracellular enzyme of such bacteria as *Leuconostoc mesenteroides* subsp. *dextranicum* using sucrose as a substrate, purified by the alcohol precipitation method several times, and then dried and recovered as a white powder (Fig. 1).

Measurement of Antitumor Activities Ten mice (6 weeks, female) were used in each group. Tumor cells were inoculated subcutaneously on day 0. SPR-901 was administered on days 1—10 (30 mg/kg/d) and only saline for the control group. Tumor weight or area was measured on day 33 or day 21, respectively, and the inhibition ratio was calculated from the average tumor growth of the test group *vs.* the control group. Statistical significance was evaluated by applying Student's *t*-test.

Carbon Clearance Test Ten mice (BALB/c, 7 weeks female) were used in each group. SPR-901 was administered orally on days 1—10 (30 mg/kg/d). Lipopolysaccharide (LPS) (Difco, *E. coli* 055:B5) was administered intraperitoneally on day 8 (1 mg/kg) as a positive control. Mice of the control group were administered with only saline orally for 10 d. Phagocytic ability against carbon particles was measured on day 11, and phagocytic index was calculated with the method of Biozzi *et al.*[6]

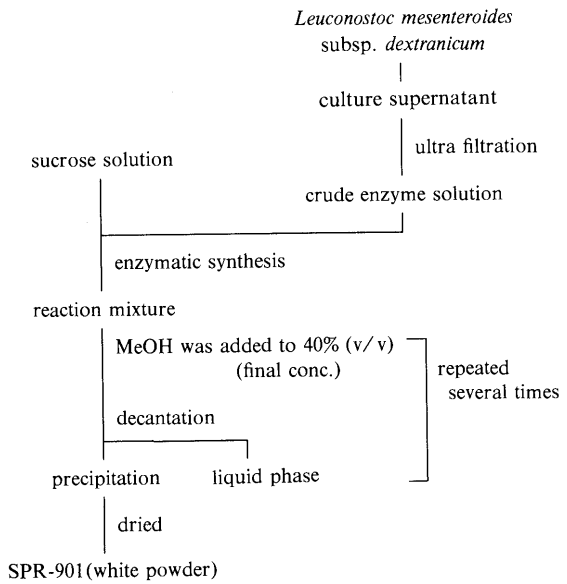

Fig. 1. Process of Synthesis and Purification of SPR-901

Results

The physico-chemical properties of SPR-901 are as follows: it is a pure α-glucan composed solely of glucose and contains no protein and no inorganic salts; its linkages are almost linear α-1,6 glucosidic ones and a small amount of branches (*ca.* 5%) at C-3 positions; infrared (IR) spectrum and ^{13}C nuclear magnetic resonance (^{13}C-NMR)

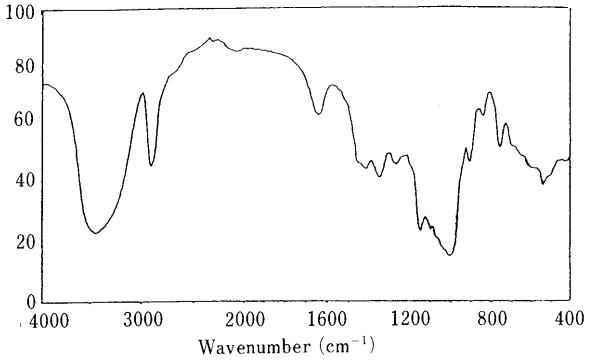

Fig. 2. IR Spectrum of SPR-901

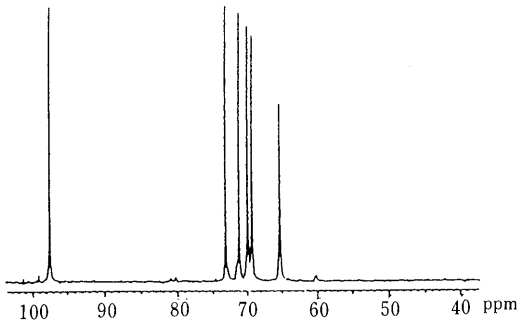

Fig. 3. ^{13}C-NMR Spectrum of SPR-901

TABLE I. Antitumor Effect of SPR-901 on Murine Allogeneic and Syngeneic Tumors

Tumor	Inoculum size	Mice	Route[a]	Tumor growth (mean±S.D.)		Inhibition ratio (%)
				Control group	Test group	
S-180	1×10^7	ICR (CRJ)	i.p.	6.7±3.3 (g)	2.5±2.1 (g)	63[c]
Ehrlich	1×10^6	ddY (SLC)	i.p.	5.7±1.6	3.1±2.0	46[c]
Meth-A	6×10^4	BALB/c (CRJ)	i.p.	3.8±0.9	1.9±0.9	50[d]
Meth-A	6×10^4	BALB/c (CRJ)	*p.o.*	277±46 (mm^2)	101±58 (mm^2)	64[c]
3LL	1×10^5	BDF1 (CRJ)	*p.o.*	414±73	267±93	36[c]
Colon 26	1×10^4	BALB/c (CRJ)	*p.o.*	397±55	297±45	25[c]
B-16	25 mg[b]	BDF1 (CRJ)	*p.o.*	549±87	498±31	9

a) Administration route of SPR-901. *b*) B-16 melanoma cells (25 mg/kg) were inoculated subcutaneously. Significant difference from the control. *c*) $p<0.01$, *d*) $p<0.001$.

TABLE II. Effect of SPR-901 on Carbon Clearance Ability in Normal and Tumor Bearing Mice

Sample	Normal mice		Tumor bearing mice[a]	
	Phagocytic index mean±S.D. ($\times10^2$)	Activation rate[b]	Phagocytic index mean±S.D. ($\times10^2$)	Activation rate[b]
Control	3.48±0.65[c]		3.50±0.86	
SPR-901	4.53±0.78	130[d]	4.21±0.83	120[c]
LPS	5.57±1.75	160[d]	5.88±0.69	168[d]

a) Meth-A cells (6×10^4) were inoculated subcutaneously into mice on day 0. *b*) *Versus* control (%). Significant difference from the control; *c*) $p<0.05$, *d*) $p<0.01$.

spectrum are shown in Figs. 2 and 3, respectively; $[\alpha]_D^{20}$ is *ca.* +185° (H_2O), *ca.* +210° (formamide); intrinsic viscosity is 1.6—2.4 (25 °C, H_2O); molecular weight is approximately 1×10^7 daltons (lightscattering method). Although its molecular weight is high, it is soluble in water giving a viscous solution. The contamination of LPS is less than 1 ng/mg.

SPR-901 showed antitumor activities against murine allogeneic tumors such as sarcoma 180 (S-180) and Ehrlich carcinoma, moreover, it showed significant antitumor activities against murine syngeneic tumors such as Meth-A fibrosarcoma (Meth-A) and Lewis lung carcinoma (3LL) not only by intraperitoneal administration (i.p.) but also by oral administration (*p.o.*) (Table I). Its effective doses were 10—300 mg/kg/d, and an optimum dose was supposed to be around 30 mg/kg/d. Moreover, orally administered SPR-901 enhanced the reticuloendothelial system in both normal and tumor bearing mice (Table II). But SPR-901 showed no direct cytotoxicities against several tumor cell lines including Meth-A tumor cells *in vitro* (data not shown). These results suggest that the mechanism of antitumor activity of SPR-901 is to be a host mediated one, and the substance is classified as one of the biological response modifiers (BRMs).

Discussion

From these results, since both the physico-chemical and the biological properties of SPR-901 are identical to those of RON reported previously,[2] we concluded that these two polysaccharides were the same substance. Also, it is presumed that RON had been produced in the intact rice bran microbiologically by existing lactic acid bacteria and then extracted with hot water.

Recently, some polysaccharides are being used for clinical purposes as anticancer drugs based on their immunomodulating activities, for example lentinan,[7] schizophyllan,[8] and so on. These polysaccharides are all β-glucan and the relationship between their structures and biological activities has been studied.[9] But in the case of SPR-901, its structure is not a β-glucan but an α-glucan, and its linkages are almost linear α-1,6 glucosidic ones with a small amount of branches at C-3 positions. There are few reports on the antitumor and immunomodulating activities of dextrans.[10] Such dextrans are, however, all highly branched ones and no report could be found on antitumor or immunomodulating activities of almost linear dextran like SPR-901. The structure of SPR-901 is very similar to that of NRRL B-512 dextran whose structure and general properties have been well studied,[11] and its down-sized substances are now being used clinically as a plasma expander. But NRRL B-512 dextran shows neither antitumor activities nor immunomodulating activities in our assay systems. The difference between these two dextrans, though still not clear, is very interesting and worthy of investigation. The active site of the antitumor action of SPR-901 and the mode of action are currently being studied.

References and Notes

1) E. Ito, S. Takeo, H. Kado, H. Yamamoto, N. Watanabe, M. Kamimura, E. Soma, K. Uchida, Y. Mori, and T. Morinaga, *Yakugaku Zasshi*, **105**, 188 (1985).
2) S. Takeo, H. Kado, H. Yamamoto, M. Kamimura, N. Watanabe, K. Uchida, and Y. Mori, *Chem. Pharm. Bull.*, **36**, 3609 (1988).
3) S. Takeo and N. Watanabe, Proceedings of the Japanese Cancer Association, Annual Meeting, Tokyo, September 1987, p. 476.
4) Y. Takeda, Y. Yoshikai, S. Ohga, and K. Nomoto, *Int. J. Immunopharmac.*, **12**, 373 (1990).
5) H. Kado, Y. Yoneta, S. Takeo, and N. Watanabe, Proceedings of the Japanese Cancer Association, Annual Meeting, Sapporo, July 1990, p. 344.
6) B. N. Halpern, B. Benacerraf, and G. Biozzi, *Brit. J. Exp. Pathol.*, **34**, 426 (1953).
7) H. Saito, T. Ohki, N. Takasuka, and T. Sasaki, *Carbohydr. Res.*, **58**, 293 (1977).
8) T. Norisuye, T. Yanaki, and H. Fujita, *J. Polym. Sci. Polym. Phys. Ed.*, **18**, 547 (1980).
9) T. L. Bluhm and A. Sarko, *Can. J. Chem.*, **55**, 293 (1977).
10) M. E. Preobrazhenskaya and E. L. Rosenfeld, *Carbohydr. Res.*, **66**, 213 (1978).
11) T. Kobayashi and Y. Tsukano, *Nippon Nougeikagaku Kaishi*, **25**, 421 (1951).

GLYCATION OF HUMAN SERUM ALBUMIN IN LONG-TERM INCUBATION WITH LOW AND HIGH CONCENTRATIONS OF GLUCOSE

Kunio KOBAYASHI,* Naomi OGASAHARA and Akira MATSUOKA

Department of Clinical Pathology and Clinical Laboratories, Hyogo College of Medicine, 1-1, Mukogawa-cho Nishinomiya 663, Japan

Glycated albumin levels of incubation mixtures with high (25.8 mM) and low (8.2 mM) concentrations of glucose when measured by the nitroblue tetrazolium (NBT) reducing method, showed similar values at day 20-25. But when tested by thiobarbituric acid (TBA) colorimetry, the levels with high concentrations of glucose were about twice that with low concentration of glucose.

KEYWORDS human serum albumin; glycation; glycated albumin; nitroblue tetrazilium (NBT) reducing method; thiobarbituric acid (TBA) colorimetry; hyperglycemia; diabetes mellitus

We reported a method using agarose gel electrophoresis with nitroblue tetrazolium (NBT) coloration (NBT-reducing activity) to determine lipoproteins and glycated albumin in serum from diabetics.[1] Conventional methods based on thiobarbituric acid (TBA),[2] furosine,[3] affinity chromatography[4] and immunological methods[5] gave higher levels (1.6-2.0-fold) of glycated albumin in hyperglycemics than that in euglycemics. However, in our method which is based on essentially on an NBT reducing method, the glycated albumin did not increase in diabetics in proportion to the hyperglycemia.[1]

To explain this unexpected finding, we compared changes in the glycated albumin levels in the incubation mixture determined by the NBT reducing method[6] and TBA colorimetry.[2] The solution (66 mM phosphate buffer, pH 7.4) containing human serum albumin (fraction V, fatty acid-free, 40 g/l), glucose (25.8 or 8.2 mM) and sodium azide (3 mM) was incubated at 37°C for 25 days. A portion of the incubation mixture was taken to measure the NBT-reducing activity (fructosamine value, glycated albumin) and TBA coloration (OD_{443}) on the days indicated in Fig. 1, followed by dialysis against the phosphate buffer as described above at 4°C for 48 h.

As shown in Fig. 1, the TBA coloration of both incubation mixtures (with low (8.2 mM) and high (25.8 mM) concentrations of glucose) increased linearly with incubation time. The TBA coloration of the incubation mixture with 25.8 mM glucose was 1.7-1.9-fold of that with 8.2 mM glucose at day 20-25. But the NBT-reducing activity of the incubation mixture with 25.8 mM glucose had risen rapidly by day 5, then remained at at a constant level (about 3 mM) until day 25, while the NBT-reducing activity of the incubation mixture with 8.2 mM glucose increased slowly up to about 3 mM at day 20-25.

The glycated albumin levels at day 20-25 can be compared to those in sera from euglycemics and hyperglycemics because the half-life of circulation serum albumin is 12-20 days.[7] Thus, the fructosamine values (glycated albumin levels) of incubation mixtures with high and low concentrations of glucose, which were measured by the NBT-reducing method, showed similar values at day 20-25. Hyperglycemia-induced glycated albumin may change to advanced Maillard products,[8, 9] which does not show NBT-reducing activity but does show TBA coloration when heated with acid, in long-term incubation.

Schleicher *et al.* demonstrated that the steady-state production of glycated albumin which was determined by the furosine method was reached at day 40.[7] In the present study, the production of glycated albumin having NBT-reducing activity seems to reach the steady-state at by day 5 in the hyperglycemics. A higher fructosamine value (4-5 mM), which is clinically observed in serum from poorly controlled diabetic patients, may be caused by the glycation of serum proteins other than albumin, *e.g.*, lipoproteins which are known to increase in diabetes mellitus.[1]

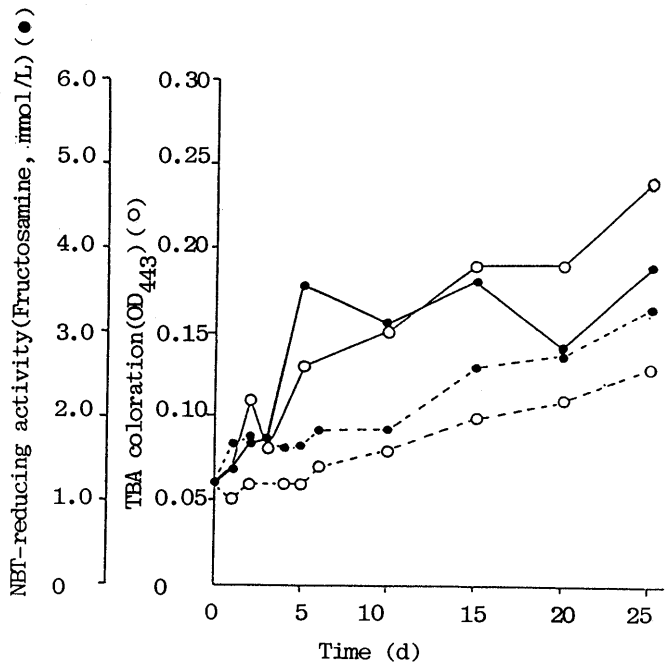

Fig. 1. Glycation of Human Serum Albumin

——, 25.8 mM glucose; ----, 8.2 mM glucose. Each point is the mean of two separate experiments. Fructosamine value (mM) is expressed in terms of 1-deoxy-1-morpholino fructose (DMF)

REFERENCES AND NOTES

1) K.Kobayashi, N. Ogasahara, T. Sakoguchi, M. Kimura, K. Taniuchi and A. Matsuoka, Clin. Chem., 36, 65-69 (1990).
2) R. Dolhofer and O.H. Wieland, Diabetes, 29, 417-422 (1980).
3) E. Schleicher, L. Scheller and O.H. Wieland, Biochem. Biophys. Res. Commun., 99, 1011-1019 (1981).
4) M. Rendell, G. Kao, P. Mecherikunnel, B. Duhaney, J. Nierenberg, K. Rasbold, D. Klenk and P.K. Smith, Clin. Chem., 31, 229-234 (1985).
5) E. Hud and M.P. Cohen, Clin. Chim. Acta, 185, 157-164 (1989).
6) R.N. Johnson, P.A. Metcalf and J.R. Baker, Clin. Chim. Acta, 127, 87-95 (1983).
7) E. Schleicher and O.H. Wieland, Biochim. Biophys. Acta, 884, 199-205 (1986).
8) R. Dolhofer and K.D. Gerbitz, Biol. Chem. Hoppe-Seyler, 371, 693-697 (1990).
9) S. Ponger, P.C. Ulrich, F.A. Bencsath and A. Cerami, Proc. Natl. Acad. Sci. USA, 81, 2684-2688 (1984).

(Received January 18, 1991)

STABILITY CONSTANTS OF (RS)-1-ISOPROPYL CITRATE METAL COMPLEXES AND PHASE TRANSITION OF ZINC (RS)-1-ISOPROPYL CITRATE

Sumiko TSUJI,*,[a] Tadashi SHIBATA,[a] Yoshio ITO,[a] Satoshi FUJII[b] and Ken-ichi TOMITA[b]

Osaka Branch, National Institute of Hygienic Sciences,[a] 1-1-43 Hoenzaka, Chuo-ku, Osaka 540, and Faculty of Pharmaceutical Sciences, Osaka University,[b] 1-6 Yamadaoka, Suita, Osaka 565, Japan

The dissociation constants of (RS)-1-isopropyl dihydrogen citrate and the stability constants of its metal complexes with Cu(II), Ca(II) and Zn(II) have been determined in the aqueous state by a potentiometry. The solid-solid phase transition of its Zn(II) complex has been studied by the thermogravimetry/differential thermal analysis (TG/DTA), IR spectrometry and X-ray powder analysis. It was found that the physical properties, this is, the contents of the water molecule of crystallization, the coordination geometries and the crystal structures before and after the transition, were changed.

KEYWORDS dissociation constant; potentiometry; 1-isopropyl dihydrogen citrate; metal complex; phase transition; zinc 1-isopropyl citrate; stability constant; TG/DTA; IR; X-ray powder analysis

Since 1983 isopropyl citrate (IPCit) has been used in Japan as a synergistic antioxidant. IPCit as a food additive is a mixture of citric acid , 1-isopropyl, 2-isopropyl, 1,2-isopropyl, 1,3-isopropyl, and tri-isopropyl citrates.[1] Each component has been purified and its chemical structure been determined.[2] Of these components, the (RS)-1-isopropyl dihydrogen citrate (1-IPCit), a staple component of isopropyl citrate, has been obtained with high purity. In this communication, its dissociation constants together with the stability constants of its metal complexes are elucidated. Moreover, the phase transition between zinc (RS)-1-isopropyl citrate (Zn(1-IPCit)) mono- and tetra-hydrates was studied by the thermogravimetry/differential thermal analysis (TG/DTA), IR spectrometry and X-ray powder analysis.

Zn(1-IPCit) was prepared from a mixture of zinc acetate and 1-IPCit in 90% methanol, and crystallized as tetrahydrate from the dilute acetic acid solution.[3] The pure 1-IPCit was extracted from its zinc complex with ethyl acetate in aqueous hydrogen chloride solution.[4]

From the potentiometric titration curve in the pH range 2.9~5.5 (Fig. 1. A.), the dissociation constants of 1-IPCit at 25±0.1°C, μ = 0.1(KNO_3) were calculated, using Schwarzenbach's equation,[5] as pK_{a1} = 3.24±0.02, pK_{a2} = 5.05±0.03, whereas the

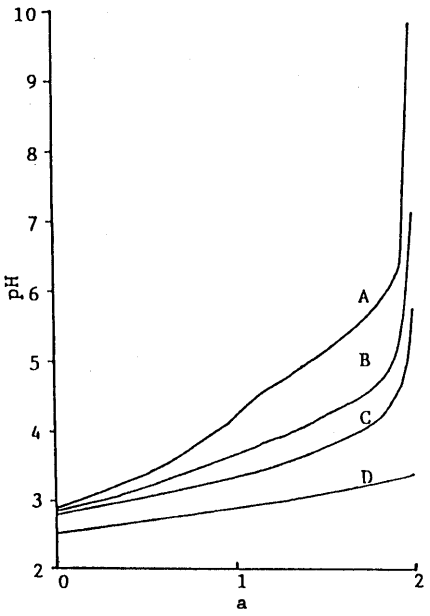

Fig.1. Potentiometric Titration of the 1-IPCit:M = 1:1 Systems by 0.1N NaOH

A:without metal. B:$Ca(NO_3)_2$. C:$Zn(NO_3)_2$. D:$Cu(NO_3)_2$. Concn. of metal:0.004M. Each soln. containes 0.004M 1-IPCit and 0.1N KNO_3. Symbol"a" represents neutralized degree.

corresponding values for citric acid are pK_{a1} = 2.87 and pK_{a2} = 4.35.[6] Probably, the steric interaction between the carboxyl and isopropyl groups in 1-IPCit causes its weaker acidity than that in citric acid.

Then the stability constants, $\log K_{MA}$, of its metal complexes with Cu(II), Ca(II) and Zn(II) were also calculated using their potentiometric titration curves (Fig. 1. B~D), and Schwarzenbach's equation. As shown in Table I, it seems likely that the stability constants of the 1-IPCit metal complexes are very similar to those of the citrate metal complexes even at different ionic strength. This indicates that the isopropyl group of 1-IPCit does not participate in the metal coordination as a ligand. This is also supported by the X-ray structural studies[9] of Zn(1-IPCit) tetrahydrate showing that the 1-IPCit chelates to zinc atoms in a tridentate manner similar to the zinc citrate complex.[10]

Table I. Stability Constants of (RS)-1-Isopropyl Citrate Complexes with Various Metals

Metal	pH range	log K_{MA} (log K_{MA} of Cit)
Cu^{2+}	2.54~2.85	5.51±0.05 (5.2, μ=1*)
Ca^{2+}	3.40~4.52	3.28±0.06 (3.16, μ=0.16**)
Zn^{2+}	2.88~3.47	4.31±0.02 (4.69, μ=0.16**)

μ=0.1
*Ref. 7).
**Ref. 8).

The weight of Zn(1-IPCit) tetrahydrate decreases gradually with increasing temperature as shown in Fig. 2. The weight losses (TG) at 50°C~110°C and at 120°C~180°C are 15% and 5%, respectively. The weight losses indicate the liberation of the water molecules of crystallization from the crystal. Therefore, Zn(1-IPCit) tetrahydrate loses three water molecules at 100.1°C and the remaining one at 164.5°C. Then it is finally decomposed at 200°C. On the other hand, Zn(1-IPCit) monohydrate[11] loses only one water molecule at 164.5°C. By Karl Fischer's method, the moisture contents (%) were : for tetrahydrate, calcd.,19.5 and found, 19.6 and for monohydrate, calcd., 5.7 and found, 7.3 by drying at 100°C for 3 h, or 6.5 by drying together with silicagel for 24 h. The discrepancy may indicate the high hygroscopic character of the monohydrate.

In the IR spectra as shown in Fig. 3, the ν(OH) of free water at 3560 cm^{-1} found in Zn(1-IPCit) tetrahydrate is not detected in the monohydrate. And each of the peaks, ν_{as}(C=O) at 1728 cm^{-1} and ν(C-O) at 1223 cm^{-1} assigned as the esterified carboxyl group in the tetrahydrate was split into two peaks in the monohydrate (the former at 1744 cm^{-1} and 1730 cm^{-1}, and the latter at 1222 cm^{-1} and 1195 cm^{-1}). That is, the (R)- and (S)-isomers in the 6-coordinated octahedral complex polymer are related to each other by the glide plane in the crystal of the tetrahydrate.[9] The (R)- or (S)-isomers in the monohydrate may chelate with different aquazinc ions and form independnt 4-coordinated tetrahedral complexes. This indicates the appearence of two stereochemically complex molecules in the monohydrate crystals.

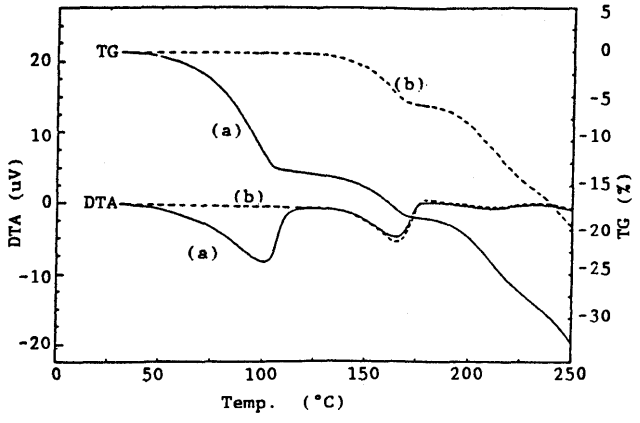

Fig.2. TG/DTA Patterns of Zinc (RS)-1-Isopropyl Citrate

(a) Zn(1-IPCit) tetrahydrate ——
(b) Zn(1-IPCit) monohydrate -----
TG/DTA patterns were determinated by Seiko TG/DTA220. Heating rate: 5°C/min, gas flow: N_2 at 200 ml/min, pseudo-sealed sample.

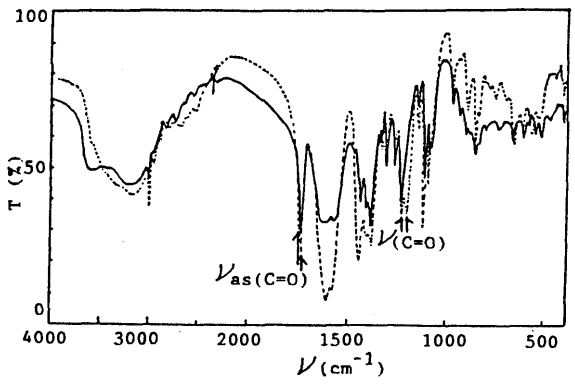

Fig.3. IR Spectra of Zinc (RS)-1-Isopropyl Citrate

(a) Zn(1-IPCit) tetrahydrate ——
(b) Zn(1-IPCit) monohydrate -----
Arrows represent the separated peaks in its monohydrate.
IR spectra (KBr) were determinated using JASCO IR-700.

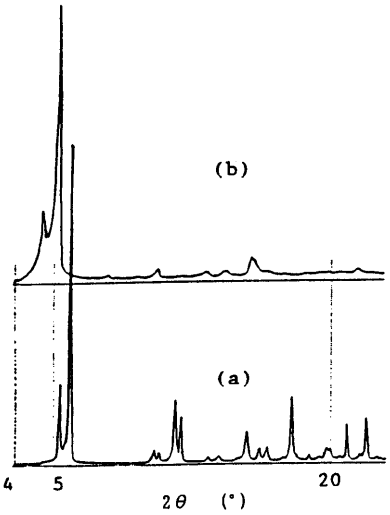

Fig.4. X-Ray Diffraction Patterns of Zinc (RS)-1-Isopropyl Citrate
(a) Zn(1-IPCit) tetrahydrate
(b) Zn(1-IPCit) monohydrate
Rigaku RINT 1100 was used.
Cu Kα_1 1.54056Å, 40KV, 40mA,
scanning rate: 4°/min.

Table II. X-Ray Diffraction Peaks of Zinc (RS)-1-Isopropyl Citrate

2θ(°)	d(Å)	I/I$_o$	h k l (Single crystal data)*	d(Å)	2θ(°)	d(Å)	I/I$_o$
Zn($C_9H_{12}O_7$)4H_2O (tetrahydrate)					Zn($C_9H_{12}O_7$)1H_2O (monohydrate)		
5.35	16.50	24	-----	---	4.78	18.47	24
5.90	14.97	100	0 2 0	14.85	5.30	16.66	100
10.45	8.46	3	-1 1 1	8.48	8.00	11.04	2
10.75	8.22	3	-----	---	10.68	8.28	5
11.55	7.66	14	-1 2 1	7.60	12.71	6.96	2
11.90	7.43	12	0 4 0	7.42	13.23	6.69	4
13.35	6.63	1	-1 3 1	6.60	14.30	6.19	2
13.90	6.37	3	-----	---	15.70	5.64	4
14.90	5.94	2	0 5 0	5.94	19.81	4.48	1
15.40	5.75	14	1 0 0	5.73			
16.10	5.50	4	1 1 0	5.63			
16.50	5.37	8	1 2 0	5.35			
17.40	5.10	2	0 1 1	5.08			
17.85	4.97	17	1 3 0	4.96			
18.85	4.70	1	0 2 1	4.87			
19.35	4.58	2	0 3 1	4.58			
19.80	4.48	4	-2 1 1	4.47			

*Ref.9)

The X-ray diffraction patterns of Zn(1-IPCit) tetra- and mono-hydrate are different from each other as shown in Fig. 4. The reflection angles (2θ), the spacings (d) and the Miller indices (h k l) of the X-ray diffractions of both hydrates are summarized in Table II. The strongest peak at d = 14.97 Å of the tetrahydrate corresponds to the (0 2 0) reflection of its single crystal, and the d (0 2 0) is just the distance between the Zn atoms related by the screw axis in the tetrahydrate crystal. After the release of three water molecules from the tetrahydrate crystal, the rearrangement of molecules in the monohydrate crystal occurs, where the zinc atom coordinates to one 1-IPCit and also to one water molecule, thus forming a 1:1:1 (Zn:1-IPCit:H_2O) complex. Probably this rearrangement makes the Zn-Zn distance longer (from 14.97 Å to 16.66 Å), because these reflections having these interplanar spacings show the strongest intensities in the tetra- and monohydrate crystals, respectively, as indicated in Fig. 4 and Table II.

ACKNOWLEDGEMENTS We thank Dr. K. Andoh, Osaka Prefectural Institute of Public Health, for his technical assistance in the X-ray powder analysis and Miss. Y. Sako, Elemental Analysis Room, Department of Applied Chemistry, Faculty of Technical Sciences, Osaka University, for the elemental analysis.

REFERENCES AND NOTES

1) S.Tsuji, Y.Tonogai, Y.Ito and M.Harada, J. Food Hyg. Soc. Japan, **26**, 357 (1985).
2) S.Tsuji, Y.Tonogai, Y.Ito and M.Fukuoka, Eisei Kagaku, **32**,185 (1986).
3) Mp decomp.>200°C.Anal. Calcd. for Zn(II)$C_9H_{12}O_7(H_2O)_2]2H_2O$:C,29.25;H,5.45;N,0.00. Found:C,29.16;H,5.09;N,0.00.
4) Mp 122°C. Anal. Calcd. for $C_9H_{14}O_7$:C,46.15;H,6.03;N,0.00. Found:C,45.95;H,6.03;N,0.00.
5) G.Schwarzenbach, Helv.Chim.Acta, 33, 947 (1950).
6) "Chemical Handbook,Basic II", ed. Chem.Soc.Japan, p.340(1984).
7) J.Lefebrve, J.Chim.Phys., 601 (1957).
8) Y.Matsushima, Chem.Pharm.Bull., 11, 566 (1963).
9) S.Tsuji, T.Shibata, Y.Ito, S.Fujii and K.Tomita, Acta Crystllogr., in press.
10) R.Swanson, W.H.Ilsley and A.G.Stanislowski, J.Inorg.Biol., **18**, 187 (1983).
11) Mp decomp.>200°C. Anal. Calcd. for [Zn(II)$C_9H_{12}O_7(H_2O)$]:C,34.25;H,4.33;N,0.00. Found:C,34.00;H,4.37;N,0.00

(Received February 4, 1991)

SYNTHESIS OF AXIALLY DISSYMMETRIC BIPHENYLBISPHOSPHINE LIGANDS, BIMOPS AND ASYMMETRIC HYDROGENATIONS OF β-KETO ESTER AND α,β-UNSATURATED CARBOXYLIC ACID CATALYZED BY THEIR RUTHENIUM (II) COMPLEXES[1)]

Naoko YAMAMOTO, Masanao MURATA, Toshiaki MORIMOTO, and Kazuo ACHIWA*
School of Pharmaceutical Sciences, University of Shizuoka, 395 Yada, Shizuoka 422, Japan

Axially dissymmetric biphenylbisphosphine ligands, BIMOP (**1a**) and *p*-MeO-BIMOP (**1b**) have been newly designed and prepared. The ruthenium (II) complexes of (*R*)-**1a** and **1b** proved to be excellent catalysts in asymmetric hydrogenations of methyl 3-oxobutanoate and tiglic acid affording (*R*)-methyl 3-hydroxybutanoate of 95-99 % ee and (*R*)-2-methylbutyric acid of 86-91 % ee, respectively.

KEYWORDS chiral bisphosphine ligand; axially dissymmetric biphenylbisphosphine; ruthenium (II) complex; catalyst; asymmetric hydrogenation; β-keto ester; α,β-unsaturated carboxylic acid

To date, many chiral bisphosphine ligands for rhodium (I)-catalyzed asymmetric hydrogenation have been developed, and some of them showed almost complete enantioselectivity in the hydrogenations of *N*-acyldehydroamino acids. Recently, it has been found that BINAP (**2**) could be utilized also for the ruthenium (II)-catalyzed system.[2)] The BINAP (**2**)-ruthenium (II) complex is an unparalleled highly efficient catalyst in asymmetric hydrogenations of various olefins and ketones, although most of the hydrogenations needed to be carried out under conditions of relatively higher pressures and temperatures. On the other hand, the ruthenium (II) complexes of other chiral bisphosphines do not work well as the catalyst in those reactions.

BINAP (**2**) has a binaphthyl moiety, and its asymmetric source is derived from the carbon (1)-carbon (1') axiality. The steric and electronic characteristics based on its skeleton are remarkably different from those of other chiral bisphosphine ligands. We anticipated that it was necessary to possess an axially dissymmetric biaryl skeleton for the ligand which was successfully applicable for both rhodium (I)- and ruthenium (II)-catalyzed asymmetric hydrogenations. Moreover, we expected that it was also necessary to introduce electron donating substituents such as methoxy and methyl groups into the biaryl moiety in order to increase the catalytic efficiency of both its rhodium (I) complex and ruthenium (II) complex under mild reaction conditions. In the previous communications, we reported BPPM and DIOP analogues, MOD-BPPM [3)] and MOD-DIOP [4)] bearing 4-methoxy and 3,5-dimethyl groups on each phenyl group, and their rhodium (I) complexes were excellent catalysts which exhibited much higher catalytic activities and enantioselectivities in asymmetric hydrogenations of *N*-acyldehydroamino acids and itaconic acids than the complexes of BPPM and DIOP. These results were considered to be caused by the electronic effects of both 4-methoxy and 3,5-dimethyl groups and the steric effects of 3,5-dimethyl groups.

In this communication, we describe the preparation of 6,6'-bis(diphenylphosphino)-3,3'-dimethoxy-2,2',4,4'-tetramethyl-1,1'-biphenyl (**1a**) (abbreviated to BIMOP) and its derivative (**1b**) (abbreviated to *p*-MeO-BIMOP), and the asymmetric hydrogenation of β-keto ester and α,β-unsaturated carboxylic acid catalyzed by the ruthenium (II) complexes of optically pure **1a** and **1b**.

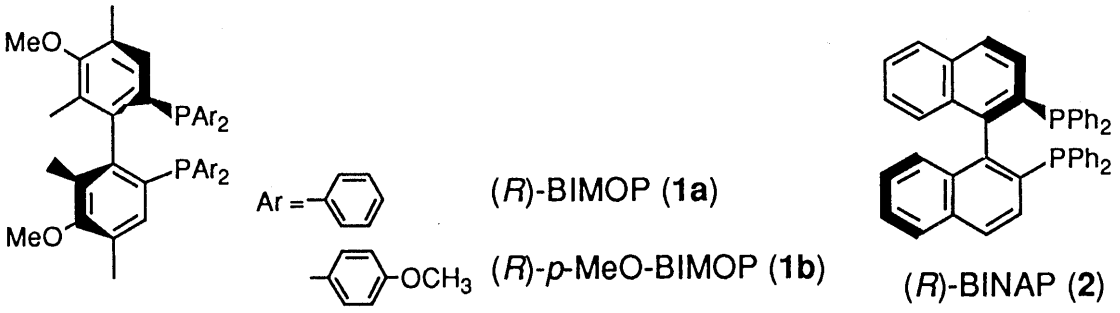

Optically pure BIMOPs (**1a** and **1b**) were synthesized by a procedure shown in Chart 1. Starting from iodination of 2,6-dimethylnitrobenzene, a methoxy group was introduced in good yield by reduction of the nitro group followed by diazotization of the resulting amino group, and methanolysis. Compound **5** was converted to the coupling product (**6**) by Ullmann reaction, and then bromination of **6** afforded the racemic dibromide (**7**). After dilithiation of **7** with *tert*-butyllithium in tetrahydrofuran at -70 °C, phosphination with diphenylphosphinyl chloride furnished BIMOPO (**8a**). *p*-MeO-BIMOPO (**8b**) was also obtained by treatment with chlorodi(4-methoxyphenyl)phosphine followed by oxidation of the phosphino groups. Optical resolution of the racemic **8a** and **8b** was achieved by using optically active (2*R*,3*R*)-(-)-2,3-O-dibenzoyltartaric acid as a resolving agent. The optical purity of the resolved **8a** and **8b** was determined to be 100% ee by HPLC analysis (Waters:Opti-Pak TP). Finally, the phosphinyl groups of optically active **8a** and **8b** were reduced by heating with trichlorosilane in the presence of triethylamine in chlorobenzene to yield the corresponding BIMOP (**1a**) [5] and *p*-MeO-BIMOP (**1b**) [6] without racemization. The absolute configuration of optically pure **1a** and **1b** was determined to be *R* by comparison of their CD spectra with that of (*R*)-(-)-BIPHEMP [7] whose absolute configuration was already determined by X-ray crystallography.

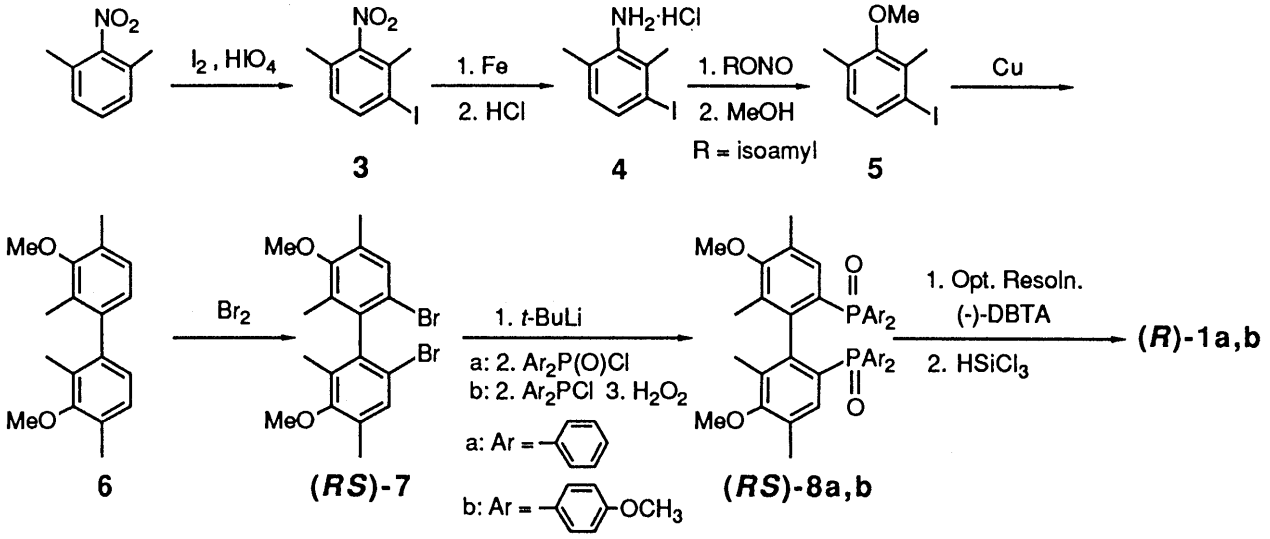

Chart 1

The ruthenium (II)-catalyzed asymmetric hydrogenation of ß-keto ester, methyl 3-oxobutanoate [8] was first chosen as a model reaction for evaluation of the capability of the newly synthesized ligands, BIMOPs (**1a** and **1b**) and for comparison with BINAP (**2**). The cationic ruthenium (II) complexes of (*R*)-**1a**, **1b**, and **2** were prepared just prior to use by mixing and heating ruthenium diiodide *p*-cymene complex and each ligand for 10 min in methanol-dichloromethane (1:1) under an argon atmosphere. All the reactions were carried out by using the substrate to the catalyst molar ratio (S/C) of 1000 at 30-40 °C for 20 h in methanol-dichloromethane (1:1) under an initial hydrogen pressure of 30 atm. The results are summarized in Table I. All the hydrogenations proceeded smoothly to give (*R*)-methyl 3-hydroxybutanoate in nearly quantitative yields. The (*R*)-BIMOP (**1a**)-ruthenium (II) complex showed extremely high (99% ee) enantioselectivity, and the (*R*)-*p*-MeO-BIMOP (**1b**)-ruthenium (II) complex was revealed to have superior chiral recognition ability as well, although slightly lower optical yields (95% ee) was obtained than using the ruthenium (II) complex of **1a** as the catalyst. Next, asymmetric hydrogenation of α,β-unsaturated carboxylic acid, tiglic acid [8b, 9] was carried out in a 0.5 M methanol-dichloromethane (4:1) solution of the substrate in the presence of the ruthenium (II) complex catalyst (0.1 mol%) at 50-60 °C for 24 h under an initial hydrogen pressure of 5 atm. As summarized in Table II, all the hydrogenations proceeded to completion, and both the complexes of **1a** and **1b** gave (*R*)-2-methylbutyric acid in nearly quantitative yields with high enantioselectivity (86-91% ee). Thus, BIMOPs (**1a** and **1b**) proved to be efficient ligands as well as BINAP (**2**) with respect to the enantioselectivity in the hydrogenations of methyl 3-oxobutanoate and tiglic acid.

Further investigaions along this line are in progress, and application to asymmetric hydrogenation catalyzed by their rhodium (I) complexes will be reported in the near future.

Table I. **Asymmetric Hydrogenation[a] of β-Keto Ester**

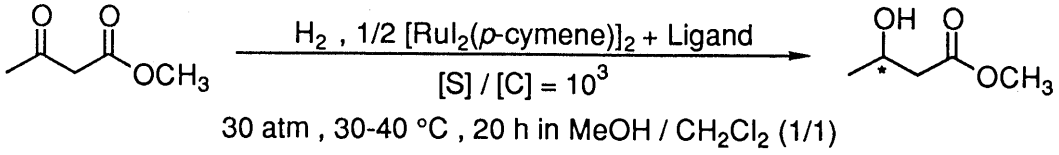

Ligand	Convn.(%)[b]	e.e.(%)[c]	Confign.[d]
(*R*)-BINAP	100	98	*R*
(*R*)-BIMOP	100	99	*R*
(*R*)-*p*-MeO-BIMOP	100	95	*R*

a) All hydrogenations were carried out in 0.5 M solution of the substrate. b) Determined by GLC analysis. c) Determined by HPLC analysis on Chiralcel OB (Daicel) of the ester derived from the product and benzoyl chloride. d) Determined by the sign of optical rotation.

Table II. **Asymmetric Hydrogenation[a] of α,β-Unsaturated Carboxylic Acid**

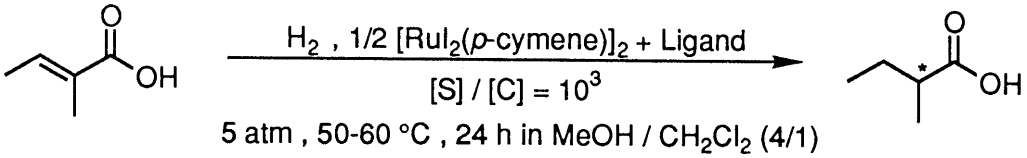

Ligand	Convn.(%)[b]	e.e.(%)[c]	Confign.[d]
(*R*)-BINAP	100	87	*R*
(*R*)-BIMOP	100	91	*R*
(*R*)-*p*-MeO-BIMOP	100	86	*R*

a) All hydrogenations were carried out in 0.5 M solution of the substrate. b) Determined by NMR analysis. c) Determined by HPLC analysis on Chiralcel OD (Daicel) of the amide derived from the product and (*S*)-1-(1-naphthyl)ethylamine. d) Determined by the sign of optical rotation.

REFERENCES AND NOTES

1) Asymmetric Reactions Catalyzed by Chiral Metal Complexes, XLIV.
2) R. Noyori and H. Takaya, *Kagaku,* **43**, 146 (1988); R. Noyori and M Kitamura, "Modern Synthetic Methods", Vol. 5, ed. R. Scheffold, Springer-Verlag, Berlin Heidelberg, **1989**, pp.116-138; R. Noyori, *Chem. Soc. Rev.*, **18**, 187 (1989).
3) H. Takahashi and K. Achiwa, *Chem. Lett.*, **1989**, 305.
4) T. Morimoto, M. Chiba, and K. Achiwa, *Tetrahedron Lett.*, **30**, 735 (1989).
5) (*R*)-(+)-BIMOP: $[\alpha]_D$ +37.4 °, mp 265-266 °C, ^{1}H-NMR ($CDCl_3$) δ: 1.24 (6H, s, CH_3), 2.21 (6H, s, CH_3), 3.48 (6H, s, OCH_3), 6.84 (2H, s, arom.H), 7.24-7.27 (20H, m, arom.H).
6) (*R*)-(-)-*p*-MeO-BIMOP: $[\alpha]_D$ -2.4 °, mp 276-277 °C, ^{1}H-NMR ($CDCl_3$) δ: 1.26 (6H, s, CH_3), 2.22 (6H, s, CH_3), 3.51 (6H, s, OCH_3), 3.78 (12H, s, OCH_3), 6.77-6.82 (10H, m, arom.H), 7.12-7.21 (8H, m, arom.H).
7) R. Schmid, M. Cereghetti, B. Heiser, P. Schonholzer, and H. Hansen, *Helv. Chim. Acta*, **71**, 897 (1988).
8) a) R. Noyori, T. Ohkuma, M. Kitamura, H. Takaya, N. Sayo, H. Kumobayashi, and S. Akutagawa, *J. Am. Chem. Soc.*, **109**, 5856 (1987); b) K. Mashima, K. Kusano, T. Ohta, R. Noyori, and H. Takaya, *J. Chem. Soc., Chem. Commun.*, **1989**, 1208.
9) T. Ohta, H. Takaya, M. Kitamura, K. Nagai, and R. Noyori, *J. Org. Chem.*, **52**, 3174 (1987).

(Received February 19, 1991)

FLUORINATION REACTIONS AT C-4 OF METHYL 2-O-BENZYL-3,6-DIDEOXYHEXOPYRANOSIDES WITH DIETHYLAMINOSULFUR TRIFLUORIDE (DAST) AND WITH TRIS(DIMETHYLAMINO)SULFONIUM DIFLUOROTRIMETHYLSILICATE (TASF)

Yoko MORI and Naohiko MORISHIMA*
School of Nursing, Kitasato University, 2-1-1 Kitasato, Sagamihara 228, Japan

Fluorination at C-4 of methyl 2-O-benzyl-3,6-dideoxy-α-D-ribo- and α-D-arabino-hexopyranosides(1 and 5) using diethylaminosulfur trifluoride(DAST) proceeded with exclusive retention of configuration. But treating the triflates of 1 and 5 with tris(dimethylamino)sulfonium difluorotrimethylsilicate(TASF) afforded mostly the configurationally inverted fluorides.

KEYWORDS fluorination; 3,6-dideoxyhexopyranose; fluorinated carbohydrate; DAST; TASF; F-H coupling constant; ideal trans-diaxial system

In our studies on the incorporation of monofluorinated 3,6-dideoxyhexopyranose moieties into the artificial antigens structurally related to O-antigens of Salmonella typhi and paratyphi, we have found that the reactions of the equatorial 4-hydroxyl groups of methyl 2-O-benzyl-3,6-dideoxy-α-D-ribo- and α-D-arabino-hexopyranosides(1 and 5) with DAST gave the 4-deoxy-4-fluoro derivatives (2 and 6, respectively) with exclusive retention of configuration.

Although DAST has been widely used to introduce fluorine into carbohydrates,[1-3] the reaction mechanisms are not easily rationalized.[4,5] It was first believed that the direct replacement of the hydroxyl group by a fluorine atom using DAST proceeded via the S_N2 mechanism,[6] but some instances of fluorination with configurational retention have been reported.[4,7-9] We now report another instance in comparison with the fluorination using TASF.[10]

When methyl 2-O-benzyl-3,6-dideoxy-α-D-ribo-hexopyranoside(1) was treated[11] with 3 molar equivalents of DAST in dichloromethane at -13℃ for 2.5 h, methyl 2-O-benzyl-3,4,6-trideoxy-4-fluoro-α-D-ribo-hexopyranoside(2) was obtained in 62% yield but no xylo-isomer 3 was isolated. However, the reaction[12] of the triflate of 1, prepared from 1 by use of trifluoromethanesulfonic anhydride in dichloromethane-pyridine, with 4.5 molar equivalents of TASF in dichloromethane at room temperature for 1.5 h afforded both 2 and 3 in yields of 13 and 54%, respectively (Chart 1).

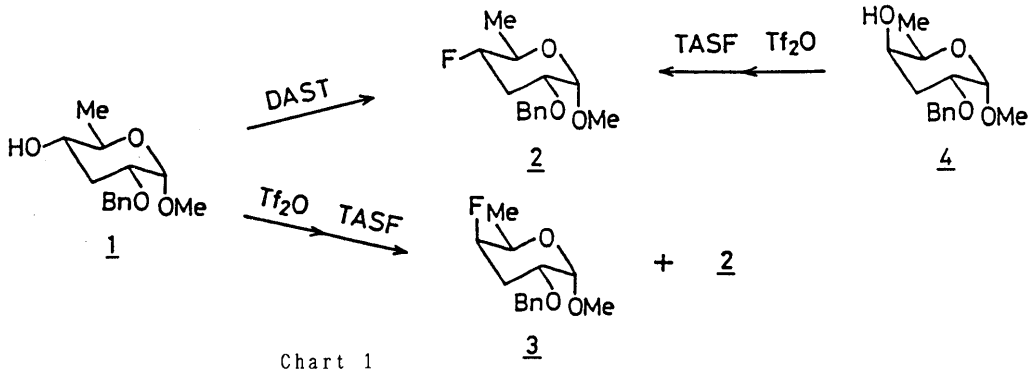

Chart 1

Similarly, 5 was treated with 3 molar equivalents of DAST at -13℃ for 2 h to form methyl 2-O-benzyl-3,4,6-trideoxy-4-fluoro-α-D-arabino-hexopyranoside(6) in 39% yield without isolation of the lyxo-isomer 7. As for the fluorination of the triflate of 5 with TASF in the same manner as that of 1, only the configurationally inverted fluoride 7 was obtained, in 21% yield, accompanied with a 24% yield of the 3,4-unsaturated compound 8 (Chart 2).

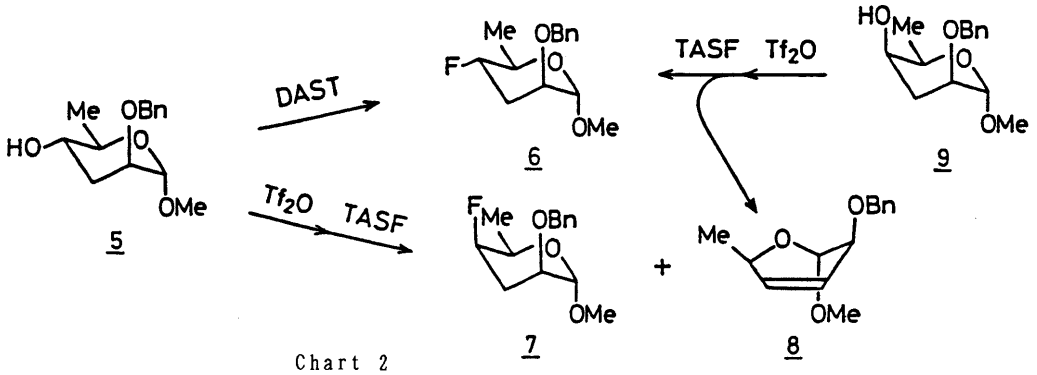

Chart 2

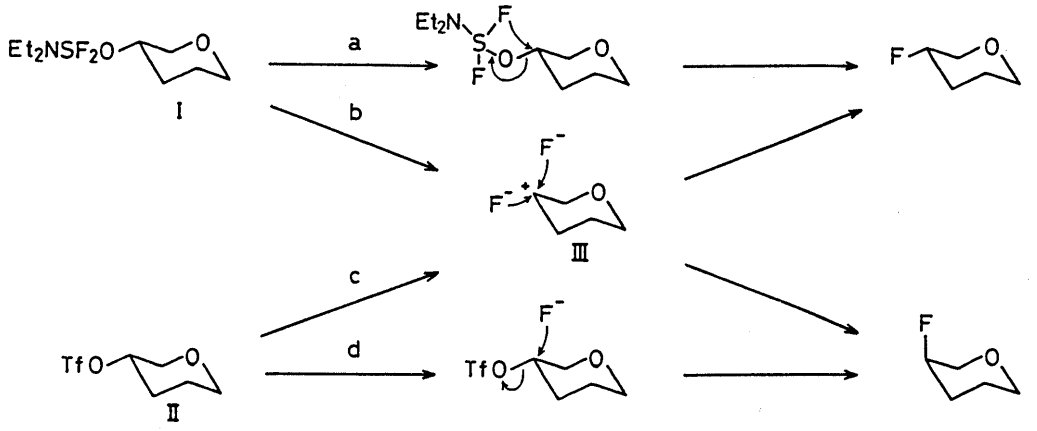

Chart 3

In the fluorination with DAST, the S_N2 reaction of the intermediate I in Chart 3 is negligible because no configurationally inverted fluoride was produced. The fact that even the reaction of 1 with 1.2 equivalents of DAST at -13℃ for 0.5 h with post-stirring at room temperature for 1.5 h gave only 2 in 66% yield implies the higher plausibility of the S_Ni mechanism (pathway a). However, pathway b *via* carbocation III cannot be neglected, as the attack of fluoride anion against C-4 from the β-side of the pyranose ring must be interfered with the repulsive effect of ring oxygen.

In contrast, the fact that inversion of configuration at C-4 predominantly occurred in the fluorination with TASF suggests that the reaction of triflate II is likely to proceed through pathway d (Chart 3). Minor production of the configurationally retained fluoride 2 from the triflate of 1 indicates that pathway c *via* III also contributed to the reaction, but only in part, because, if it were the main course, repulsion between fluoride anion and ring oxygen would have allowed the dominant attack on III from the α-side of the pyranose ring to give 2 as the major product.

The lower yields of fluorides for the reactions of 5 in both methods than those of 1 are considered to be due to the steric and electric hindrance by the axial benzyloxyl group at C-2.

The fluorides, 2 and 6, were also prepared from methyl 2-O-benzyl-3,6-dideoxy-α-D-*xylo*-[13] and *lyxo*-hexopyranosides(4 and 9) by the reactions of their triflates with TASF in yields of 19 and 13%, respectively. In the reaction of 9, compound 8 was isolated in 42% yield as the major product. The treatment of 4 and 9 with DAST gave some unidentified products, but no fluorides were included therein. The synthesis of 1, 4, 5, and 9 are to be published elesewhere.

The F-H coupling constants observed in ^{1}H-NMR spectra of methyl 2-O-benzyl-3,4,6-trideoxy-4-fluoro-α-D-*ribo*-, *arabino*-, *xylo*-, and *lyxo*-hexopyranosides(2, 3, 6, and 7) are depicted in Fig. 1. The diaxial $^3J_{F,H-3}$ of 44.8 Hz and 43.7 Hz observed for 3 and 7, respectively, are very close to the unperturbed value of 43.5 Hz for diaxial $^3J_{F,H}$.[14] This indicates that the axial H on deoxygenated carbon(C-3) and the axial F on C-4 in vicinal disposition of methyl 3,6-dideoxy-α-D-hexopyranoside are in ideal *trans*-diaxial relationship.[15]

The ^{13}C-NMR data shown in Table I are satisfactory for the structures of the fluorides 2, 3, 6, and 7.

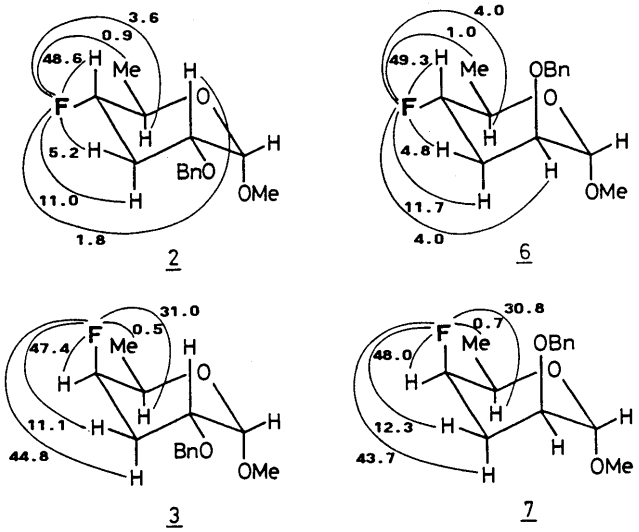

Fig. 1. F-H Coupling Constants for 2, 3, 6, and 7 (in Hz, Measured at 300 MHz in $CDCl_3$)

Table I. ^{13}C-NMR Data for 2, 3, 6, and 7 (Measured at 75.4 MHz in $CDCl_3$)

Compound	δ (ppm) ($J_{C,F}$ (Hz))					
	C-1	C-2	C-3	C-4	C-5	C-6
2	96.9	73.5	30.9	90.3	65.8	17.1
		(11.1)	(19.2)	(180.2)	(24.5)	
3	97.8	70.4	29.9	90.2	64.7	15.7
			(21.0)	(177.5)	(19.5)	(6.5)
6	98.0	75.4	30.2	89.4	66.8	17.4
		(11.9)	(19.2)	(174.6)	(24.5)	
7	99.3	70.3	27.8	87.1	64.8	16.1
			(20.1)	(181.6)	(19.9)	(7.2)

ACKNOWLEDGMENT This work was partly supported by a Sasakawa Scientific Research Grant from The Japan Science Society to Y. Mori.

REFERENCES AND NOTES

1) T. Tsuchiya, Yuki Gosei Kagaku Kyokai Shi, 42, 544 (1984).
2) P. J. Card, J. Carbohydr. Chem., 4, 451 (1985).
3) N. F. Taylor(ed.), "Fluorinated Carbohydrates; Chemical and Biochemical Aspects," ACS Symp. Ser. 374, American Chemical Society, Washington, D. C., 1988.
4) T. Torii, T. Tsuchiya, and S. Umezawa, Carbohydr. Res., 116, 289 (1983).
5) J. D. Moyer, O. Reizes, N. Malinowski, C. Jiang, and D. C. Baker, Chapter 4 of Ref. 3.
6) T. J. Tewson and M. J. Welch, J. Org. Chem., 43, 1090 (1978).
7) S. Castillon, A. Dessinges, R. Faghih, G. Lukacs, A. Olesker, and T. T. Thang, J. Org. Chem., 50, 4913 (1985).
8) S. S. Yang, T. R. Beattie, and T. Y. Shen, Synth. Commun., 16, 131 (1986).
9) C. Jiang, J. D. Moyer, and D. C. Baker, J. Carbohydr. Chem., 6, 319 (1987).
10) B. Doboszewski, G. W. Hay, and W. A. Szarek, Can. J. Chem., 65, 412 (1987).
11) The procedure using DAST is that slightly modified from P. J. Card and G. S. Reddy, J. Org. Chem., 48, 4734 (1983).
12) The procedure using TASF is according to that described in Ref. 10.
13) C. L. Stevens, K. W. Schultz, D. J. Smith, and P. M. Pillai, J. Org. Chem., 40, 3704 (1975).
14) The observed value for cyclohexyl fluoride in R. J. Abraham and L. Cavalli, Mol. Phys., 9, 67 (1965).
15) L. Phillips and V. Wray, J. Chem. Soc., B, 1971, 1618.

(Received March 4, 1991)